

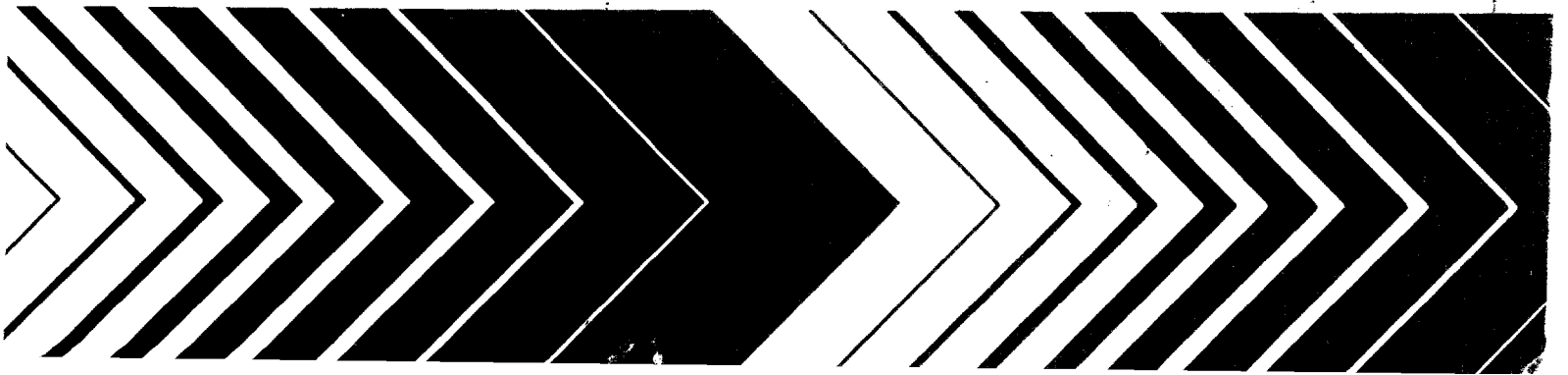
Research and Development

---



# Water Quality Assessment:

A Screening  
Procedure for Toxic and  
Conventional Pollutants in  
Surface and Ground  
Water—Part I  
(Revised—1985)



WATER QUALITY ASSESSMENT:  
A Screening Procedure for Toxic  
and Conventional Pollutants  
in Surface and Ground Water  
(Revised  
Part

by

W. B. Mills, D. B. Porcella, M. J. Unga, S. A. Gherini, K. V. Summers,  
Lingfung Mok, G. L. Rupp, and G. L. Bowie  
Tetra Tech, Incorporated  
Lafayette, California 94549

and

D. A. Hai th  
Cornell University  
Ithaca, New York 14853

Produced by:

JACA Corporation  
Fort Washington, Pennsylvania 19034

Contract No. 68-03-3131

Prepared in Cooperation with U. S. EPA's

Center for Water Quality Modeling  
Environmental Research Laboratory  
Athens, Georgia

Monitoring and Data Support Division  
Office of Water Regulations and Standards  
Office of Water  
Washington, D. C.

Technology Transfer  
Center for Environmental Research Information  
Cincinnati, Ohio

ENVIRONMENTAL RESEARCH LABORATORY  
OFFICE OF RESEARCH AND DEVELOPMENT  
U. S. ENVIRONMENTAL PROTECTION AGENCY  
ATHENS, GEORGIA 30613

DISCLAIMER

Mention of trade names or commercial products does not constitute endorsement or recommendation for use by the U.S. Environmental Protection Agency.

## ABSTRACT

New technical developments in the field of water quality assessment and a reordering of water quality priorities prompted a revision of the first two editions of this manual. The utility of the revised manual is enhanced by the inclusion of methods to predict the transport and fate of toxic chemicals in ground water, and by methods to predict the fate of metals in rivers. In addition, major revisions were completed on Chapter 2 (organic toxicants), Chapter 3 (waste loadings), and Chapter 5 (impoundments) that reflect recent advancements in these fields.

Applying the manual's simple techniques, the user is now capable of assessing the loading and fate of conventional pollutants (temperature, biochemical oxygen demand-dissolved oxygen, nutrients, and sediments) and toxic pollutants (from the U.S. EPA list of priority pollutants) in streams, impoundments, estuaries, and ground waters. The techniques are readily programmed on hand-held calculators or microcomputers. Most of the data required for using these procedures are contained in the manual.

Because of its size, the manual has been divided into two parts. Part I contains the introduction and chapters on the aquatic fate of toxic organic substances, waste loading calculations, and the assessment of water quality parameters in rivers and streams. Part II continues with chapters on the assessment of impoundments, estuaries, and ground water and appendices E, H, I, and J. Appendices D, F, and G are provided on microfiche in the EPA-printed manual. Appendices A, B, and C, which appeared in the first two editions, are now out of date and have been deleted.

This report is submitted in fulfillment of Contract No. 68-03-3131 by JACA Corp. and Tetra Tech, Inc. under the sponsorship of the U.S. Environmental Protection Agency. Work was completed as of May 1985.

TABLE OF CONTENTS

<u>Chapter</u>		<u>Page</u>
PART I		
	DISCLAIMER . . . . .	ii
	ABSTRACT . . . . .	iii
	LIST OF FIGURES (Part I). . . . .	xii
	LIST OF TABLES (Part I). . . . .	xix
	ACKNOWLEDGEMENTS . . . . .	xxvi
1	INTRODUCTION . . . . .	1
	1.1 BACKGROUND . . . . .	1
	1.2 PURPOSE AND SCOPE . . . . .	1
	1.3 METHODOLOGY APPLICATION . . . . .	3
	1.3.1 Base Maps. . . . .	3
	1.4 LIMITATIONS . . . . .	3
	REFERENCES. . . . .	4
2	AQUATIC FATE OF TOXIC ORGANIC SUBSTANCES . . . . .	5
	2.1 INTRODUCTION. . . . .	5
	2.1.1 Background. . . . .	5
	2.1.2 Comparison of Conventional and Toxic Pollutants . . . . .	5
	2.1.3 Water Quality Criteria. . . . .	5
	2.1.4 Frequency of Discharge of Toxic Substances from Industries. . . . .	7
	2.1.5 Physical and Chemical Characteristics of Toxic Organic Compounds . . . . .	18
	2.1.6 Scope and Organization of Chapter . . . . .	18
	2.2 SCREENING METHODS FOR TOXIC ORGANIC COMPOUNDS . . . . .	24
	2.2.1 Modeling the Fate of Toxic Organics . . . . .	29
	2.2.2 Use of Assessment Techniques as Screening Tools . . . . .	29
	2.3 SPECIATION PROCESSES . . . . .	41
	2.3.1 Acid-Base Effects . . . . .	41
	2.3.2 Sorption on Suspended Sediments . . . . .	46
	2.4 TRANSPORT PROCESSES . . . . .	58
	2.4.1 Volubility Limits . . . . .	58
	2.4.2 Volatilization. . . . .	59

<u>Chapter</u>		<u>Page</u>
	2.5 TRANSFORMATION PROCESSES. . . . .	77
	2.5.1 Biodegradation. . . . .	77
	2.5.2 Photolysis. . . . .	95
	2.5.3 Hydrolysis. . . . .	129
	REFERENCES . . . . .	137
3	WASTE LOADING CALCULATIONS. . . . .	142
	3.1 INTRODUCTION. . . . .	142
	3.2 BACKGROUND POLLUTION LOADS. . . . .	142
	3.3 NONPOINT SOURCE MODELS . . . . .	150
	3.4 RURAL RUNOFF LOADS . . . . .	151
	3.4.1 Source Areas. . . . .	151
	3.4.2 Runoff. . . . .	152
	3.4.3 Erosion and Sediment . . . . .	160
	3.4.4 Chemical Loading Functions for Rural Runoff . . . . .	178
	SALT LOADS IN IRRIGATION RETURN FLOWS . . . . .	207
	3.5.1 Description. . . . .	207
	3.5.2 Estimation of Return Flows. . . . .	209
	3.6 URBAN RUNOFF LOADS. . . . .	215
	3.6.1 Annual Urban Runoff and Combined Sewer Loads. . . . .	215
	3.6.2 Event Loads in Urban Runoff. . . . .	219
	3.7 GROUND WATER WASTE LOADS. . . . .	231
	3.7.1 Characteristics . . . . .	231
	3.7.2 Water Balance. . . . .	233
	3.7.3 Nitrate Loads to Ground Water from Waste Application Sites. . . . .	233
	3.7.4 Leaching of Organic Chemicals . . . . .	239
	3.8 ATMOSPHERIC WASTE LOADS. . . . .	245
	3.8.1 Dry Deposition. . . . .	245
	3.8.2 Wet Deposition (Precipitation Scavenging) . . . . .	253
	3.9 POINT SOURCE WASTE LOADS. . . . .	253
	3.9.1 Municipal Waste Loads. . . . .	254
	3.9.2 Industrial Waste Loads. . . . .	262
	REFERENCES . . . . .	273
4	RIVERS AND STREAMS . . . . .	278
	4.1 INTRODUCTION. . . . .	278
	4.1.1 Scope. . . . .	278
	4.1.2 Significance of Problem Areas . . . . .	279
	4.1.3 Applicability to Other Problems . . . . .	282
	4.1.4 Sources of Pollutants . . . . .	283
	4.1.5 Assumptions . . . . .	283
	4.1.6 Data Requirements . . . . .	286
	4.1.7 Selection of Season . . . . .	287
	4.1.8 River Segmentation. . . . .	289

<u>Chapter</u>		<u>Page</u>
4.1.9	Mixing Zones . . . . .	294
4.1.10	Water and Pollutant Balances. . . . .	296
4.1.11	Hand Held Calculator Programs . . . . .	306
4.2	CARBONACEOUS AND NITROGENOUS OXYGEN DEMAND. . . . .	306
4.2.1	Introduction. . . . .	306
4.2.2	BOD Decay Rate. . . . .	310
4.2.3	Mass Balance of BOD. . . . .	313
4.2.4	Typical Solutions. . . . .	315
4.2.5	Other Simplifying Procedures. . . . .	317
4.2.6	Interpretation of Results . . . . .	321
4.3	DISSOLVED OXYGEN. . . . .	321
4.3.1	Introduction. . . . .	321
4.3.2	Dissolved Oxygen Mass Balance . . . . .	323
4.3.3	Reaeration Rate. . . . .	323
4.3.4	Effect of Dams on Reaeration. . . . .	330
4.3.5	Dissolved Oxygen Saturation . . . . .	331
4.3.6	DO-BOD Interactions . . . . .	333
4.3.7	Dissolved Oxygen Calculations . . . . .	335
4.3.8	General Dissolved Oxygen Deficit Equation . . . . .	340
4.3.9	Photosynthesis and Respiration. . . . .	341
4.3.10	Benthic Demand. . . . .	345
4.3.11	Simplifying Procedures in Dissolved Oxygen Calculations. . . . .	347
4.4	TEMPERATURE. . . . .	354
4.4.1	Introduction. . . . .	354
4.4.2	Equilibrium Temperature . . . . .	355
4.4.3	Calculation of Equilibrium Temperature. . . . .	358
4.4.4	Screening of Thermal Discharges . . . . .	371
4.4.5	Longitudinal Temperature Variation. . . . .	381
4.4.6	Diurnal Temperature Variation . . . . .	383
4.4.7	Low Flow and Temperature. . . . .	383
4.4.8	Interrelationships Between Temperature Prediction Tools. . . . .	385
	NUTRIENTS AND EUTROPHICATION POTENTIAL. . . . .	387
4.5.1	Introduction. . . . .	387
4.5.2	Basic Theory. . . . .	388
4.5.3	Estimating Instream Nutrient Concentrations . . . . .	390
4.5.4	Nutrient Accounting System. . . . .	392
4.6	TOTAL COLIFORM BACTERIA . . . . .	395
4.6.1	Introduction. . . . .	395
4.6.2	Mass Balance for Total Coliforms. . . . .	396
4.7	CONSERVATIVE CONSTITUENTS . . . . .	400
4.7.1	Introduction. . . . .	400
4.7.2	Mass Balance for Conservative Constituents. . . . .	400
4.8	SEDIMENTATION. . . . .	402
4.8.1	Introduction. . . . .	402
4.8.2	Long-Term Sediment Loading from Runoff. . . . .	405
4.8.3	Bed Material Load . . . . .	405

<u>Chapter</u>		<u>Page</u>
4.9	TOXIC SUBSTANCES . . . . .	417
4.9.1	Methods of Entry of Toxic Pollutants into Rivers. . . . .	417
4.9.2	Vertical Distribution of Sorbate Within Rivers. . . . .	420
4.9.3	Transport and Transformation Expressions for Toxicants in Rivers. . . . .	426
4.10	METALS. . . . .	457
4.10.1	Introduction. . . . .	457
4.10.2	Water Quality Criteria, Background Concentrations, and Case Studies. . . . .	458
4.10.3	Analytical Models for Fate Prediction of Metals in Rivers. . . . .	480
4.10.4	Speciation of Metals and Equilibrium Modeling . . . . .	525
4.10.5	Execution of Limited Field Reconnaissance and Sampling Program. . . . .	597
	REFERENCES. . . . .	602

PART II

5	IMPOUNDMENTS. . . . .	1
5.1	INTRODUCTION. . . . .	1
5.2	IMPOUNDMENT STRATIFICATION. . . . .	2
5.2.1	Discussion. . . . .	2
5.2.2	Prediction of Thermal Stratification. . . . .	6
5.3	SEDIMENT ACCUMULATION. . . . .	19
5.3.1	Introduction. . . . .	19
5.3.2	Annual Sediment Accumulation. . . . .	20
5.3.3	Short-Term Sedimentation Rates. . . . .	23
5.3.4	Impoundment Hydraulic Residence Time. . . . .	43
5.3.5	Estimation of Sediment Accumulation . . . . .	43
5.4	EUTROPHICATION AND CONTROL. . . . .	49
5.4.1	Introduction. . . . .	49
5.4.2	Nutrients, Eutrophy, and Algal Growth . . . . .	50
5.4.3	Predicting Algal Concentrations . . . . .	51
5.4.4	Mass Balance of Phosphorus. . . . .	52
5.4.5	Predicting Algal Productivity, Secchi Depth, and Biomass . . . . .	60
5.4.6	Restoration Measures . . . . .	64
5.4.7	Water Column Phosphorus Concentrations. . . . .	64
5.5	IMPOUNDMENT DISSOLVED OXYGEN. . . . .	71
5.5.1	Simulating Impoundment Dissolved Oxygen . . . . .	73
5.5.2	A Simplified Impoundment Dissolved Oxygen Model . . . . .	74
5.5.3	Temperature Corrections . . . . .	85
5.6	TOXIC CHEMICAL SUBSTANCES . . . . .	97
5.6.1	Overall Processes . . . . .	99
5.6.2	Guidelines for Toxics Screening . . . . .	104
5.7	APPLICATION OF METHODS AND EXAMPLE PROBLEM. . . . .	109
5.7.1	The Occoquan Reservoir. . . . .	110



<u>Chapter</u>	<u>Page</u>	
5.7.2	Stratification . . . . .	111
5.7.3	Sedimentation . . . . .	115
5.7.4	Eutrophication . . . . .	123
5.7.5	Hypolimnetic DO Depletion . . . . .	128
5.7.6	Toxicants . . . . .	133
	REFERENCES. . . . .	136
	GLOSSARY OF TERMS. . . . .	139
6	ESTUARIES. . . . .	142
6.1	INTRODUCTION. . . . .	142
6.1.1	General . . . . .	142
6.1.2	Estuarine Definition . . . . .	143
6.1.3	Types of Estuaries. . . . .	143
6.1.4	Pollutant Flow in an Estuary. . . . .	145
6.1.5	Estuarine Complexity and Major Forces . . . . .	149
6.1.6	Methodology Summary . . . . .	151
6.1.7	Present Water-Quality Assessment. . . . .	153
6.2	ESTUARINE CLASSIFICATION. . . . .	155
6.2.1	General . . . . .	155
6.2.2	Classification Methodology. . . . .	155
6.2.3	Calculation Procedure . . . . .	155
6.2.4	Stratification-Circulation Diagram Interpretation . . . . .	157
6.2.5	Flow Ratio Calculation. . . . .	163
6.3	FLUSHING TIME CALCULATIONS. . . . .	165
6.3.1	General . . . . .	165
6.3.2	Procedure. . . . .	165
6.3.3	Fraction of Fresh Water Method. . . . .	170
6.3.4	Calculation of Flushing Time by Fraction of Freshwater Method. . . . .	171
6.3.5	Branched Estuaries and the Fraction of Freshwater Method. . . . .	176
6.3.6	Modified Tidal Prism Method . . . . .	176
6.4	FAR FIELD APPROACH TO POLLUTANT DISTRIBUTION IN ESTUARIES. . . . .	184
6.4.1	Introduction. . . . .	184
6.4.2	Continuous Flow of Conservative Pollutants. . . . .	185
6.4.3	Continuous Flow Non-Conservative Pollutants . . . . .	197
6.4.4	Multiple Waste Load Parameter Analysis. . . . .	204
6.4.5	Dispersion-Advection Equations for Predicting Pollutant Distributions . . . . .	207
6.4.6	Pritchard's Two-Dimensional Box Model for Stratified Estuaries. . . . .	216
6.5	POLLUTANT DISTRIBUTION FOLLOWING DISCHARGE FROM A MARINE OUTFALL. . . . .	226
6.5.1	Introduction. . . . .	226
6.5.2	Prediction of Initial Dilution. . . . .	227
6.5.3	Pollutant Concentration Following Initial Dilution. . . . .	248
6.5.4	pH Following Initial Dilution . . . . .	250
6.5.5	Dissolved Oxygen Concentration Following Initial Dilution. . . . .	255

<u>Chapter</u>		<u>Page</u>
6.5.6	Far Field Dilution and Pollutant Distribution . . . . .	257
6.5.7	Farfield Dissolved Oxygen Depletion . . . . .	263
6.6	THERMAL POLLUTION. . . . .	266
6.6.1	General . . . . .	266
6.6.2	Approach. . . . .	267
6.6.3	Application. . . . .	269
6.7	TURBIDITY. . . . .	274
6.7.1	Introduction . . . . .	274
6.7.2	Procedure to Assess Impacts of Wastewater Discharges on Turbidity or Related Parameters. . . . .	276
6.8	SEDIMENTATION. . . . .	282
6.8.1	Introduction. . . . .	282
6.8.2	Qualitative Description of Sedimentation. . . . .	282
6.8.3	Estuarine Sediment Forces and Movement. . . . .	283
6.8.4	Settling Velocities . . . . .	287
6.8.5	Null Zone Calculations. . . . .	291
	REFERENCES. . . . .	295
7	GROUND WATER . . . . .	300
7.1	OVERVIEW . . . . .	300
7.1.1	Purpose of Screening Methods. . . . .	300
7.1.2	Ground Water vs. Surface Water. . . . .	301
7.1.3	Types of Ground Water Systems Suitable for Screening Method. . . . .	302
7.1.4	Pathways for Contamination. . . . .	303
7.1.5	Approach to Ground Water Contamination Problems . . . . .	305
7.1.6	Organization of This Chapter. . . . .	309
7.2	AQUIFER CHARACTERIZATION. . . . .	310
7.2.1	Physical Properties of Water. . . . .	310
7.2.2	Physical Properties of Porous Media . . . . .	310
7.2.3	Flow Properties of Saturated Porous Media . . . . .	319
7.2.4	Flow Properties of Unsaturated Porous Media . . . . .	323
7.2.5	Data Acquisition or Estimation. . . . .	329
7.3	GROUND WATER FLOW REGIME. . . . .	345
7.3.1	Approach to Analysis of Ground Water Contamination Sites. . . . .	345
7.3.2	Water Levels and Flow Directions. . . . .	346
7.3.3	Flow Velocities and Travel Times. . . . .	353
7.4	POLLUTANT TRANSPORT PROCESSES . . . . .	363
7.4.1	Dispersion and Diffusion. . . . .	363
7.4.2	Chemical and Biological Processes Affecting Pollutant Transport . . . . .	374
7.5	METHODS FOR PREDICTING THE FATE AND TRANSPORT OF CONVENTIONAL AND TOXIC POLLUTANTS . . . . .	382
7.5.1	Introduction to Analytical Methods. . . . .	382
7.5.2	Contaminant Transport to Deep Wells . . . . .	390
7.5.3	Solute Injection Wells: Radial Flow. . . . .	396

<u>Chapter</u>	Page
7.5.4 Contaminant Release on the Surface with 1-D Vertical Downward Transport. . . . .	403
7.5.5 Two-Dimensional Horizontal Flow with a Slug Source. . . . .	410
7.5.6 Two-Dimensional Horizontal Flow with Contiguous Solute Line Sources . . . . .	417
7.6 INTERPRETATION OF RESULTS . . . . .	423
7.6.1 Appropriate Reference Criteria. . . . .	423
7.6.2 Quantifying Uncertainty . . . . .	424
7.6.3 Guidelines for Proceeding to More Detailed Analysis . . . . .	429
REFERENCES. . . . .	435
References Cited . . . . .	435
Additional References on Ground Water Sampling . . . . .	444
APPENDIX A. . . . .	A-1
APPENDIX B. . . . .	B-1
APPENDIX C. . . . .	C-1
APPENDIX D IMPOUNDMENT THERMAL PROFILES. . . . .	D-1
APPENDIX E MODELING THERMAL STRATIFICATION IN IMPOUNDMENTS . . . . .	E-1
APPENDIX F RESERVOIR SEDIMENT DEPOSITION SURVEYS . . . . .	F-1
APPENDIX G INITIAL DILUTION TABLES . . . . .	G-1
APPENDIX H EQUIVALENTS BY COMMONLY USED UNITS OF MEASUREMENTS. . . . .	H-1
APPENDIX I ADDITIONAL AQUIFER PARAMETERS . . . . .	I-1
APPENDIX J MATHEMATICAL FUNCTIONS. . . . .	J-1

## LIST OF FIGURES

### PART I

Figure		<u>Page</u>
II-1	Environmental Fate of a Toxic Pollutant. . . . .	6
II-2	Speciation, Transport and Transformation Processes in the Aquatic Environment. . . . .	25
II-3	Flow System Representations. . . . .	27
II-4	Isotherms for Adsorption of a Hydrophobic Pollutant on Sediments. . . . .	49
II-5	Relationship between $K_{oc}$ and Octanol-water Partition Coefficient ( $K_{ow}$ ) of Energy-related Organic Pollutants . . . . .	52
II-6	Correlation of Aqueous Volubility with Octanol-water Partition Coefficient . . . . .	53
II-7	Relationship Between $K_{oc}$ and $K_{ow}$ for Coarse Silt . . . . .	54
II-8	Range of Validity of Henry's Law . . . . .	63
II-9	Schematic Representation of Volatilization from Solution Phase to Liquid Phase. . . . .	65
11-10	Microbial Transformations of Phenoxy Herbicides. . . . .	80
11-11	Ultraviolet Absorption Spectrum of Naphthacene . . . . .	98
11-12	Spectral Distribution of Solar Energy Outside the Earth's Atmosphere and At the Earth's Surface. . . . .	99
11-13	Solar Radiation in the United States . . . . .	101
11-14	Photochemical Pathways of an Excited Molecule. . . . .	107
11-15	Direct Photochemical Reactions of 2,4-D Ester, Benz(a)anthracene, and Pentachlorophenol . . . . .	108
11-16	Comparison of Solar Irradiance with the Absorption Spectra of a Compound Which Does Not Directly Photolyze, a Compound Which Does Directly Photolyze, and a Substance Which Initiates Indirect Photochemical Reactions . . . . .	110
11-17	Chromophoric Groups which Absorb Sunlight. . . . .	114
11-18	Major Processes which Influence Photolysis of Pollutants in Natural Waters. . . . .	115
11-19	pH Dependence of Hydrolysis Rate Constants . . . . .	131
III-1	Background Concentrations of Nitrate-Nitrogen, BOD, Total Phosphorus, and Dissolved Solids . . . . .	144

<u>Figure</u>	<u>Page</u>	
III-2	Background Levels of pH, Suspended Sediment, Total Coliforms, and Sulfate . . . . .	145
III-3	Background Concentrations of Chloride, Iron + Manganese, Total Heavy Metals, and Arsenic + Copper + Lead + Zinc . . . . .	146
III-4	Relationships between Streamflow Nitrogen Concentrations and Land Use from the National Eutrophication Survey . . . . .	147
III-5	Relationships between Streamflow Phosphorus Concentrations and Land Use from the National Eutrophication Survey . . . . .	148
III-6	Average Annual Streamflow in Inches. . . . .	149
III-7	The Nonpoint Source Loading Process. . . . .	151
III-8	SCS Curve Number Runoff Equation . . . . .	154
III-9	Mean Annual Row Crop Runoff in Inches for Selected Curve Numbers. . . . .	159
111-10	Average Annual Erosivity Indices for Eastern Us. . . . .	162
111-11	Average Annual Erosivity Indices for Western Us. . . . .	163
111-12	Values of "a" for Equation 111-14. . . . .	175
111-13	Sediment Delivery Ratio as a Function of Watershed Drainage Area. . . . .	
111-14	Nitrogen in Surface Foot of Soil . . . . .	182
111-15	Phosphorus (as P <sub>2</sub> O <sub>5</sub> ) in the Surface Foot of Soil . . . . .	182
111-16	Components of an Irrigation System . . . . .	209
111-17	Collection of Irrigation Drainage. . . . .	210
111-18	Mean Annual Pan Evaporation in Inches. . . . .	211
111-19	Mean Annual Precipitation in Inches. . . . .	217
111-20	Conceptual Model of Depression Storage . . . . .	224
111-21	Pollutant Transport to an Aquifer. . . . .	232
III-22	Mean Annual Potential Evapotranspiration Minus Precipitation in Inches. . . . .	234
III-23	Nitrogen Dynamics at a Land Application Site . . . . .	236
III-24	Downward Movement of a Chemical in Soil. . . . .	243
III-25	Nitrogen (NH <sub>4</sub> -N and NO <sub>3</sub> -N) in Precipitation. . . . .	247
III-26	Influent Cadmium Loading to Plant During Study . . . . .	254

<u>Figure</u>		<u>Page</u>
III-27	Influent Copper Concentrations to Wastewater Treatment Plants as a Function of Percent Industrial Flow. . . . .	262
IV-1	Illustration of River Segmentation Procedure on the James River. . . . .	291
IV-2	Hypothetical River Having a Variety of Pollutant Sources and Sinks. . . . .	292
IV-3	River Segmentation for BOD Distribution. . . . .	293
IV-4	Pollutant Discharge where Initial Mixing Occurs a Fractional Distance Across the River. . . . .	295
IV-5	Illustration of Water Balance. . . . .	300
IV-6	Sketch of Snake River from Heise to Neelley, Idaho. . . . .	302
IV-7	Example of Flow Rate Information Tabulated in U.S. Geological Survey's Water Data Report. . . . .	304
IV-8	Example Set of User's Instructions for Hand-Held Calculator Programs. . . . .	307
IV-9	The BOD Curve for Oxidation of Carbonaceous Matter and Curve Showing Influence of Nitrification . . . . .	310
IV-10	Mechanisms of BOD Removal from Rivers. . . . .	311
IV-11	Deoxygenation Coefficient as a Function of Depth . . . . .	312
IV-12	Example of Computation of $K_L$ from Stream Data. . . . .	313
IV-13	Hypothetical BOD Waste Loadings in a River . . . . .	318
IV-14	Variability of Dissolved Oxygen by Season for 22 Major Waterways, 1968-72. . . . .	322
IV-15	Reaeration Coefficient as a Function of Depth. . . . .	325
IV-16	Reaeration Coefficient for Shallow Streams, Owen's Formulation . . . . .	326
IV-17	Reaeration Rate Versus Depth and Velocity. . . . .	327
IV-18	Characteristic Dissolved Oxygen Profile Downstream from a Point Source of Pollution. . . . .	335
IV-19	Flow Process of Solution to Dissolved Oxygen Problem in Rivers. . . . .	336
IV-20	Daily Dissolved Oxygen Variation in Two Rivers . . . . .	343
IV-21	Flow Process in Reach by Reach Solution to Critical Dissolved Oxygen Values. . . . .	349
IV-22	Hypothetical River Used in Example IV-9. . . . .	353

<u>Figure</u>		<u>Page</u>
IV-23	Mechanisms of Heat Transfer Across a Water Surface . . . . .	356
IV-24	Schematic of Site No. 3 Cooling Lake . . . . .	357
IV-25	Observed Temperatures, Site No. 3, July 18-July 24, 1965 . . . . .	358
IV-26	Comparison of Computed Equilibrium and Ambient Temperatures with Observed Mean Diurnal Temperature Variations for Site No. 3, July 18-July 24, 1966. . . . .	359
IV-27	Mean Daily Solar Radiation Throughout the U.S. for July and August. . . . .	361
IV-28	Mean Dewpoint Temperature Throughout the United States for July and August. . . . .	368
IV-29	Mean Daily Wind Speeds (mph) Throughout the United States for July and August. . . . .	369
IV-30	Idealization of a Run-of-the-River Power Plant . . . . .	372
IV-31	Downstream Temperature Profile for Completely Mixed Stream, $T-E/T_{m-E}$ vs. $r$ . . . . .	382
IV-32	Measured Air and Water Temperatures for the Santa Ana River near Mentone, California, in June 1979 . . . . .	384
IV-33	Measured Dissolved Oxygen Concentration and Predicted Satur- ation Concentration for the Santa Ana River near Mentone, California in June 1979. . . . .	385
IV-34	Flow Duration Curve, Hatchie River at Bolivar, Term. . . . .	386
IV-35	Frequency of Lowest Mean Discharges of Indicated Duration, Hatchie River at Bolivar, Term. . . . .	387
IV-36	Three River Temperature Profiles . . . . .	388
IV-37	Total Coliform Profiles for the Willamette River . . . . .	397
IV-38	Salinity Distribution in a Hypothetical River. . . . .	401
IV-39	Division Between Wash Load and Bed Material Load . . . . .	404
IV-40	$\Psi$ and $\tau$ for DuBoys Relationship as Functions of Median Size of Bed Sediment . . . . .	406
IV-41	Hydraulic Radii for Different Channel Shapes . . . . .	409
IV-42	User Instructions for Yang's Sediment Transport Equation . . . . .	412
IV-43	Program Listing and Sample Input/Output for Yang's Sediment Transport Equation . . . . .	413
IV-44	Sediment Discharge as a Function of Water Discharge for the Colorado River at Taylor's Ferry . . . . .	416

<u>Figure</u>		<u>Page</u>
IV-45	Sediment Discharge as a Function of Water Discharge for the Niobrara River at Cody, Nebraska . . . . .	416
IV-46	Toxicant Concentrations Following Initiation and Cessation of Point Source. . . . .	421
IV-47	Vertical Equilibrium Distribution of Suspended Solids in a River. . . . .	422
IV-48	Vertical Distribution of Relative Solute Concentration, $K_p S_a = 10$ . . . . .	424
IV-49	Vertical Distribution of Relative Solute Concentration, $K_p S_a = 100$ . . . . .	424
IV-50	Instream Transformation Processes Analyzed for Toxicants . . . . .	430
IV-51	Location Map of Hudson River, New York . . . . .	437
IV-52	Hypothetical Concentration Distributions of Finitely Soluble and Infinitely Soluble Toxicants . . . . .	440
IV-53	Hypothetical Distribution of Toxicant at Various Locations Following a Spill. . . . .	443
IV-54	Illustration of Hypothetical Spill Incident. . . . .	447
IV-55a	Chloroform Concentration in Water Column for First 60 Hours Following a Spill 16.3 Miles Upstream. . . . .	453
IV-55b	Chloroform Concentration in the Mississippi River at a Location 16.3 Miles Below the August 19, 1973 Spill . . . . .	454
IV-56	Summary of Screening Procedures for Metals in Rivers . . . . .	459
IV-57	Measured Total and Dissolved Copper Concentrations in Flint River, Michigan, During August 1981 Survey . . . . .	470
IV-58	Extent of Priority Pollutant Contamination in Chattanooga Creek Waters . . . . .	471
IV-59	Comparison of Observed and Predicted Mercury Concentration Calculated from a Dilution Model for the North Fork Holston River. . . . .	474
IV-60	Station Locations on Coal Creek and Slate River, Colorado. . . . .	476
IV-61	Physical Processes Influencing the Fate of Metals in Rivers. . . . .	483
IV-62	Relationship Between Stream Velocity, Particle Size, and the Regimes of Sediment Erosion, Transport, and Deposition . . . . .	486
IV-63	Comparison of Predicted and Observed Total Metal Concentrations in Flint River, Michigan (August 1981) . . . . .	490
IV-64	Total Zinc, Copper, and Cadmium in the Flint River . . . . .	491



<u>Figure</u>	<u>Page</u>	
IV-65	Framework for River Model MICHRIV. . . . .	493
IV-66	Suspended Solids and Total Metal Concentrations in the Flint River, Michigan, (March 1982). . . . .	504
IV-67	Suspended Solids and Total Metal Concentrations in Flint River, Michigan (August 1981) . . . . .	508
IV-68	Definition Sketch of Idealized Reservoir . . . . .	511
IV-69	Definition Sketch Used in Example IV-23. . . . .	514
IV-70	Relationship Between Metal Concentration in Water Column and in Bedded Sediments During a Nonequilibrium Adsorption Period. . . . .	517
IV-71	River System for Example IV-24 . . . . .	521
IV-72	Speciation of Metals in the Aquatic Environment. . . . .	526
IV-73	Relative Characterizations of Environments by pe and pH. . . . .	527
IV-74	Activity Coefficient and Ionic Strength Relationships for Typical Ions and Specific Ions . . . . .	529
IV-75	Ionic Strength Versus Specific Conductivity for Surface Waters . . . . .	530
IV-76	Typical Adsorption Curves for Metal Cations and Anions for a Range of pH and Adsorbent Levels . . . . .	534
IV-77	Partition Coefficient for Copper in Streams. . . . .	538
IV-78	Periodic Table of the Elements . . . . .	540
IV-79	pe/pH Stability Field Diagram for Arsenic at 25°C. . . . .	542
IV-80	Cadmium Speciation as a Function of pH in the Presence of $1.55\text{m}^2/\text{l SiO}_2(\text{s})$ , $C_{\text{dt}}=10^{-6}\text{M}$ . . . . .	544
IV-81	pe/pH Diagram Showing Stability of Chromium Species for $C_{\text{rt}}=10^{-5}\text{M}$ . . . . .	545
IV-82	pe/pH Diagram Showing Areas of Dominance of Five Species of Copper at Equilibrium at 25°C and 1 atm. . . . .	546
IV-83	Copper Speciation in the Presence of Inorganic Ligands; and in the Presence of Inorganic Ligands and an Adsorbing Surface, $1.55\text{m}^2/\text{l SiO}_2(\text{s})$ . . . . .	547
IV-84	Effect of Humic Acid on Partitioning of Copper . . . . .	549
IV-85	Lead Speciation in the Presence of Inorganic Ligands; and in the Presence of Inorganic Ligands and a Solid Adsorbing Surface, $1.55\text{m}^2/\text{l SiO}_2(\text{s})$ . . . . .	550
IV-86	The pe-pH Diagram for Hg, Showing Predominant Species in Solution for Concentrations of Total Hg Greater than $5\ \mu\text{g}/\text{l}$ . . . . .	551

<u>Figure</u>	<u>Page</u>
IV-87 Nickel Carbonate and Nickel Hydroxide Volubility phase Diagram	553
IV-88 Zinc Speciation in the Presence of Inorganic Ligands and an Adsorbing Surface . . . . .	554
IV-89 Zinc Solubility: Zinc Hydroxide; Zinc Carbonate; and Zinc Silicate. . . . .	555
IV-90 Water Resources Regions of the United States . . . . .	557
IV-91 Example Procedure for Superposition of Adsorption. . . . .	592

# LIST OF TABLES

## PART I

<u>Table</u>		<u>Page</u>
II-1	Brief Comparison of Conventional and Toxic Pollutants. . . . .	6
II-2	Proposed Criteria for Toxic Substances Designated to Protect Aquatic Life. . . . .	8
II-3	EPA List of 129 Priority Pollutants and the Relative Frequency of These Materials in Industrial Wastewaters . . . . .	16
II-4	Most Commonly Discharged Priority Pollutants . . . . .	17
II-5	Selected Characteristics of Various Aliphatic Hydrocarbons . . . . .	19
II-6	Various Characteristics of Selected Pesticides . . . . .	20
II-7	Selected Characteristics of Polychlorinated Biphenyls and Related Compounds . . . . .	21
II-8	Selected Characteristics of Monocyclic Aromatic Hydrocarbons . . . . .	22
II-9	Selected Characteristics of Various Polycyclic Aromatic Hydrocarbons . . . . .	23
11-10	Expressions for Toxic Pollutant Levels in Various Water Bodies . . . . .	30
11-11	Relative Importance of Processes Influencing Aquatic Fate of Organic Priority Pollutants. . . . .	33
11-12	Occurrence of Acids and Bases in Neutral and Charged Forms as a Function of pH, $pK_a$ , and $pK_b$ . . . . .	44
11-13	$pK_a$ and $pK_b$ Values for Selected Toxic Organic Acids and Bases and Values of $pK_w$ for Water . . . . .	45
11-14	Procedure for Calculating Fraction of a Compound which is in the Neutral (Non-Charged) Form . . . . .	47
11-15	Procedure for Calculating Partition Coefficient. . . . .	55
11-16	Relationship of Dissolved and Sorbed Phase Pollutant Concentrations to Partition Coefficient and Sediment Concentration. . . . .	56
11-17	Henry's Law Constant for Selected Hydrocarbons . . . . .	62
11-18	Henry's Law Constants for Selected Compounds . . . . .	69
11-19	Typical Values of Pollutant Volatilization Rates in Surface Waters . . . . .	69
11-20	Comparison of Tabulated and Predicted Values of Diffusion Coefficients for Selected Pollutants . . . . .	70
11-21	Volatilization Rates of Several Priority Pollutants in 12 Rivers. . . . .	73

<u>Table</u>	<u>Page</u>
II-22	Procedure for Predicting Volatilization Rate . . . . . 74
II-23	Relative Volatilization Mass Fluxes of Several Chemicals in Saturated Solutions . . . . . 77
II-24	Size of Typical Bacterial Populations in Natural Waters. . . . . 84
II-25	Summary of the Characteristics of the Two General Types of Biodegradation: Metabolism and Cometabolism . . . . . 85
II-26	Potential Biodegradability of Organic Pollutants in an Aerobic Environment. . . . . 88
II-27	Biodegradation Rate Constants under Aerobic Conditions . . . . . 90
II-28	Calculated Solar Radiant Energy Flux to a Horizontal Surface under a Clear Sky. . . . . 100
II-29	Calculated Solar Irradiance in a Water Body Just Beneath the Surface, Annual Mean at 40°N. . . . . 102
II-30	Contributions to Light Attenuation Coefficient . . . . . 105
II-31	Disappearance Quantum Yields, $\Phi_d$ For Direct Photolysis . . . . . 109
II-32	Near-Surface Direct Photolysis Rate Constants. . . . . 118
II-33	Summary of Near Surface Approach . . . . . 121
II-34	<b>Range of <math>1-e^{-K(\lambda^*)Z}/K(\lambda^*)Z</math> . . . . . 122</b>
II-35	Direct Prediction of Near Surface Rate . . . . . 123
II-36	Procedure for Calculating Direct Photolysis Rate Constant for a Reference Light Intensity of 540 Langley/Day. . . . . 124
II-37	Direct Prediction of Depth-Averaged Photolysis Rate. . . . . 125
II-38	Estimated Half-Lives for Indirect Photolysis of Organics in Okefenokee Swamp Water. . . . . 126
II-39	Generalized Hydrolytic Reactions of Organic Compounds. . . . . 130
II-40	Hydrolysis Rate Parameters and Estimated Environmental Hydrolysis Rates. . . . . 134
II-41	Procedure for Calculating Hydrolysis Rate Constant . . . . . 135
III-1	Runoff Curve Numbers for Average Antecedent Moisture Conditions. 155
III-2	Antecedent Moisture Limits for Curve Number Selection. . . . . 156
III-3	Soil Erodibility, K. . . . . 165
III-4	Generalized Values of the Cover and Management Factor, C, in the 37 States East of the Rocky Mountains. . . . . 166
III-5	C Factor Values for Construction Sites . . . . . 168

<u>Table</u>	<u>Page</u>	
III-6	C Factor Values for Permanent Pasture, Range and Idle Land . . . . .	169
III-7	C Factor Values for Undisturbed Forest Land. . . . .	170
III-8	C Factor Values for Mechanically Prepared Woodland Sites . . . . .	171
III-9	Practice Factors (P) Used in Universal Soil Loss Equation. . . . .	172
III-10	Expected Magnitudes of Single-Storm Erosivity Indices. . . . .	173
III-11	Heavy Metal Concentrations in Surficial Materials in the United States . . . . .	183
III-12	Representative Dissolved Nutrient Concentrations in Rural Runoff. . . . .	188
III-13	Mean Bulk Densities and Available Water Capacities . . . . .	195
III-14	Organic Carbon Partition Coefficients for Selected Pesticides. . . . .	195
III-15	Octanal-Water Partition Coefficients for Selected Pesticides . . . . .	197
III-16	Mean First Order Decay Coefficients for Selected Pesticides. . . . .	198
III-17	First Order Pesticide Decay Coefficients for Selected Pesticides and Soil Conditions . . . . .	199
III-18	Mean Daylight Hours per Day. . . . .	213
III-19	Saturation Vapor Pressure as Function of Temperature . . . . .	214
III-20	Pollutant Concentration Factors for Annual Loading Functions . . . . .	218
III-21	Runoff Curve Numbers (Antecedent Moisture Condition II) for Urban Areas . . . . .	222
III-22	Urban Sediment (Solids) Accumulation Rates . . . . .	226
III-23	Concentrations of Conventional Pollutants in Urban Sediment. . . . .	228
III-24	Concentrations of Metal in Urban Sediment. . . . .	228
III-25	Concentrations of Mercury and Organic Compounds in Urban Sediment . . . . .	229
III-26	Typical Values of Crop Nitrogen Uptake . . . . .	238
III-27	Mean Soil Properties. . . . .	241
III-28	Atmospheric Contributions of Nitrogen and Phosphorus in Precipitation. . . . .	246
III-29	Field-Measured Dry Deposition Velocities . . . . .	249
111-30	Average Monthly Atmospheric Levels of Four Pesticides at Stoneville, Mississippi . . . . .	252

<u>Table</u>	<u>Page</u>
111-31 Typical Influent Municipal Waste Concentrations. . . . .	255
III-32 Municipal Wastewater Treatment System Performance. . . . .	256
III-33 Median and Mean Phosphorus and Nitrogen Concentrations and Median Loads in Wastewater Effluents Following Four Conventional Treatment Processes . . . . .	257
111-34 Yearly Average Phosphorus Removal Performance. . . . .	259
III-35 Metal Concentrations and Removal Efficiencies in Treatment Plants at Selected Cities. . . . .	260
III-36 Influent Variability Analysis at Moccasin Bend Wastewater Treatment Plant. . . . .	263
III-37 Selected Pollutant Mass Percent Removals at Meccasin Bend Wastewater Treatment Plant . . . . .	264
III-38 1981 Effluent Concentrations from Five Southern California Wastewater Treatment Plants. . . . .	265
III-39 Occurrence of Priority Pollutants in POTW Influent and Effluents for Pollutants Detected in at Least 10 Percent of the Samples. . . . .	266
111-40 Median Percent Removals of Selected Pollutants through POTW Treatment Processes. . . . .	269
111-41 Industrial Categories and Frequently Detected Priority Pollutants by Category . . . . .	271
IV-1 Reference Level Values of Selected Water Quality Indicators for U.S. Waterways . . . . .	279
IV-2 Condition of Eight Major Waterways . . . . .	280
IV-3 Water Quality Problem Areas Reported by States . . . . .	282
IV-4 Example River Water Quality Standards. . . . .	283
IV-5 Water Quality Parameters Commonly Monitored by States. . . . .	284
IV-6 Annual Phosphorus and Nitrogen Load for Selected Iowa River Basins. . . . .	285
IV-7 Major Waterways: Seasonal Flow Analysis, 1968-72. . . . .	288
IV-8 Water Quality Analyses for River Screening Methodology . . . . .	289
IV-9 Experimental Measurements of Transverse Mixing in Open Channels with Curves and Irregular Sides. . . . .	297
IV-10 Suggested Configuration for Water and Nutrient Balance Table . . . . .	299
IV-11 Solution to Snake River Water and Phosphorus Balance Problem . . . . .	305

<u>Table</u>	Page	
IV-12	Municipal Waste Characteristics Before Treatment . . . . .	308
IV-13	Comparison of Predicted and Observed Reaeration Rates on Small Streams in Wisconsin. . . . .	328
IV-14	Typical Hydraulic Properties, Patuxent River . . . . .	329
IV-15	Volubility of Oxygen in Water. . . . .	332
IV-16	Dissolved Oxygen Saturation Versus Temperature and Altitude. . . . .	333
IV-17	$D_c/L_0$ Values Versus $D_o/L_o$ and $k_a/K_L$ . . . . .	338
IV-18	$k_a t_c$ Versus $D_o/L_o$ and $k_a/K_L$ . . . . .	339
IV-19	Some Average Values of Gross Photosynthetic Production of Dissolved Oxygen. . . . .	342
IV-20	Average Values of Oxygen Uptake Rates of River Bottoms . . . . .	347
IV-21	Compilation of Information in Example IV-8 . . . . .	350
IV-22	Critical Travel Time Results . . . . .	352
IV-23	Net Long Wave Atmospheric Radiation, Han . . . . .	362
IV-24	Saturated Water Vapor Pressure, $e_s$ , Versus Air Temperature, $T_a$ , and Relative Humidity. . . . .	363
IV-25	B and C(B) as Functions of Temperature . . . . .	364
IV-26	Summary of Solar-Radiation Data for Mineola, Brookhaven, and the Connetquot Riversides . . . . .	365
IV-27	Data Needed for Thermal Discharge Screening. . . . .	374
IV-28	Eutrophication Potential as a Function of Nutrient Concentrations . . . . .	390
IV-29	Regional Stream Nutrient Concentration Predictive Models . . . . .	393
IV-30	Total Nitrogen Distribution in a River in Response to Point and Non-Point Source Loading . . . . .	395
IV-31	Total Coliform Analysis. . . . .	397
IV-32	Salinity Distribution in a Hypothetical River. . . . .	402
IV-33	Relationship of Total Suspended Sediment Concentration to Problem Potential. . . . .	404
IV-34	Sediment Grade Scale. . . . .	407
IV-35	Computing D/T for Determining the Hydraulic Radius of a Parabolic Section. . . . .	408

<u>Table</u>	<u>Page</u>
IV-36 Relationship Between Width to Depth Ratio of a Graded Stream and the Suspended and Bed Load Discharge . . . . .	409
IV-37 Characteristics of the Colorado and Niobrara Rivers. . . . .	415
IV-38 Methods of Introduction of Toxic Organic Compounds Into Rivers, and Fate in Terms of Volatilization and Sorption . . . . .	418
IV-39 Mass of Contaminated Sediments and Equivalent Water Depth as a Function of Depth of Contamination . . . . .	436
IV-40 Water-Soluble, High Density ( $\rho > 1$ ), Immiscible Chemicals. . . . .	445
IV-41 Water Quality Criteria for Selected Priority Metals for Protection of Freshwater Aquatic Life. . . . .	460
IV-42 Typical Concentrations of Metals in Several Soils and in the Earth's Crust. . . . .	462
IV-43 Average Concentration of Metals in Various Types of Rock and Deep Ocean Sediments . . . . .	463
IV-44 Ranges of Concentrations of Dissolved Minor Elements Measured at NASQAN Stations During the 1975 Water Year, Summarized by Water Resources Regions. . . . .	465
IV-45 Ranges of Total Concentrations of Minor Elements Measured at NASQAN Stations During the 1975 Water Year, Summarized by Water Resources Regions. . . . .	466
IV-46 Summary of Case Studies. . . . .	468
IV-47 Summary of Metal and Suspended Solids Concentrations in Flint River, Michigan. . . . .	469
IV-48 Inorganic Priority Pollutants Detected in Chattanooga Creek, September 1980. . . . .	472
IV-49 Mercury Concentrations in Water, Suspended Matter, and Bed Sediments Immediately Upstream and Downstream of Former Chloralkali Plant on North Fork Holston River. . . . .	473
IV-50 Streams Selected for 1980 U.S. EPA Field Surveys and Metals Anticipated to be Present in Excess of U.S. EPA Recommended Aquatic Life Criteria. . . . .	475
IV-51 Comparison of Mean Total Concentrations of Selected Metals in the Slate River Versus U.S. EPA Calculated Acute Water Quality Criteria for Aquatic Life. . . . .	477
IV-52 Metal Concentrations in Bottom Sediments of Saddle River, New Jersey, and in Adjacent Soils. . . . .	478



<u>Table</u>	<u>Page</u>	
IV-53	Average Heavy Metal Concentrations by Particle Size for Sediments of the Saddle River, New Jersey. . . . .	479
IV-54	Lead Concentrations in Streams Tributary to Cayuga Lake, New York . . . . .	480
IV-55	Summary of Cadmium, Zinc, and Copper in Particulate Carried by Tributary Streams of Cayuga Lake. . . . .	481
IV-56	Summary of Soluble Cadmium, Zinc, and Copper in Tributary Streams of Cayuga Lake . . . . .	482
IV-57	Boundary Conditions and Point Sources to Flint River for August 4-7, 1981. . . . .	489
IV-58	Summary of Screening Procedures for Metals in Rivers and Lakes .	499
IV-59	Source Data Required for Example IV-24 . . . . .	521
IV-60	Summary of Results of Example IV-24. . . . .	522
IV-61	Linear Partition Coefficients for Priority Metals in Streams and Lakes. . . . .	536
IV-62	Speciation of Priority Metals Between Dissolved and Adsorbed Phases as a Function of Suspended Solids Concentrations in Streams. . . . .	537
IV-63	Summary of Metal Speciation in Oxidizing and Reducing Environments, Solids Controlling Volubility, and pH-pe Combinations Conductive to Metal Mobilization. . . . .	541
IV-64	Characteristics of River Waters Chosen for Analysis. . . . .	558
IV-65	Metal Speciation in the Hudson River . . . . .	560
IV-66	Metal Speciation in the Ogeechee River . . . . .	562
IV-67	Metal Speciation in the Muskegon River . . . . .	564
IV-68	Metal Speciation in the Ohio River . . . . .	567
IV-69	Metal Speciation in the Mississippi River. . . . .	569
IV-70	Metal Speciation in the Missouri River . . . . .	572
IV-71	Metal Speciation in the Brazes River . . . . .	575
IV-72	Metal Speciation in the Columbia River . . . . .	577
IV-73	Metal Speciation in the Sacramento River . . . . .	579
IV-74	Metal Speciation in the Colorado River . . . . .	581
IV-75	Metal Speciation in Woods Lake Outlet. . . . .	584
IV-76	Metal Speciation in Penobscot River, Maine . . . . .	585

<u>Table</u>		<u>Page</u>
IV-77	Metal Speciation in St. Marys River, Florida. . . . .	587
IV- 78	Metal Speciation in Grand River, South Dakota. . . . .	588
IV-79	Metal Speciation in Pecos River, New Mexico. . . . .	589
IV-80	Summary of Data Requirements for Screening of Metals in Rivers .	599

## ACKNOWLEDGEMENTS

This publication is the result of the labors of a number of individuals who contributed to both this document and the previous editions. Major contributors to previous editions are David Dean (waste loadings), Walter Frick (estuaries), Kendall Haven (estuaries), Robert Hudson (organic toxicants), and Stanley Zison (lakes). JACA Corporation designed a new, condensed format and prepared all text and artwork for this third edition.

In addition, all of the individuals in the U.S. EPA who supported this work, especially Mr. Tom Barnwell, Ms. Carol Grove, Mr. Bill Vocke, Dr. James Falco, Mr. Orville Macomber, and Mr. Robert Ambrose, must be thanked for their input, consideration, and patience.

CHAPTER 1  
INTRODUCTION

1.1 BACKGROUND

In 1977, the United States Environmental Protection Agency published Water Quality Assessment: A Screening Method for Nondesignated 208 Areas (Zison, et al., 1977). This document was intended as a simplified methodology that water quality planners in nondesignated 208 areas could use to perform preliminary assessments of surface water quality. The methods addressed both point and nonpoint sources of pollutants including nutrients, sediments, dissolved oxygen deficits, temperature, salinity, and coliforms in rivers, lakes, and estuaries. The methodology was applied to the Sandusky River in northern Ohio, to the Ware, Patuxent, and Chester Rivers in Virginia and Maryland, and to the Occoquan Reservoir in Virginia. Test results were favorable (Dean et al., 1981). and some urban pollutants in streams, lakes and estuaries.

In 1982 the screening methods were revised and updated to include toxic organic chemicals in surface waters (Mills et al., 1982). The methods were demonstrated for a formaldehyde spill in the Russian River, California (Mills and Porcella, 1983), and for synfuel contamination of rivers (Mills and Porcella, 1984).

1.2 PURPOSE AND SCOPE

Due to increased emphasis on contaminant transport in ground waters and on contamination by heavy metals in all natural waters, the screening methods have been expanded to address these issues. This report contains a simplified methodology which can be used by planners or engineers to perform preliminary assessments of toxic and conventional pollutants in surface and ground waters. Conventional pollutants include suspended sediments, nitrogen, phosphorus, coliform bacteria, BOD, temperature, and dissolved oxygen deficits. The 129 EPA priority pollutants are included in the sections on toxic chemicals. Much data are supplied by figures and tables in the text and appendices. An additional source of data for many rate constants used in this manual is Bowie et al., 1985. All the algorithms are intended to be used on desk-top calculators, or on microcomputers. Many of the environmental chemistry, ground water, and river algorithms have been put on microcomputer (Mills et al., 1985).

Where instructive, introductory material has preceded the actual presentation of water quality assessment methodologies. This is done to orient the planner toward pertinent background material, as well as to clearly state limitations of the methodologies due to assumptions and simplifications. Further, example calculations are included to illustrate the ideas being presented. These examples are designed to unify the theory that has preceded it, as well as in some cases to introduce new but related ideas.

The units most commonly used in this report are those that historically appear in the literature. Often, the units are not metric. Consequently an English-metric-conversion appendix is included at the end of this report. Many equations are presented with both English and metric constants.

The report is divided into six major chapters (two through seven). A brief description of the content of each chapter is presented in the following paragraphs:

- Chapter 2 deals with the environmental chemistry of toxic organic chemicals. Processes considered include photolysis, hydrolysis, volatilization, biodegradation and adsorption. The purpose of the chapter is to provide an understanding of the processes and to provide procedures for estimating associated rate and equilibrium constants.
- Chapter 3 addresses methods to estimate pollutant loads from nonpoint and point sources for both toxic and conventional pollutants. Procedures include load estimation for single events and annual loads from agricultural, forested, and urban areas.
- In Chapter 4, impacts of point and nonpoint sources of conventional and toxic pollutants in rivers are addressed. Conventional pollutants include BOD-D<sub>0</sub>, temperature, coliform bacteria, nutrients, and sediment transport. Fate of toxic organic chemicals is assessed with consideration being given to the importance of volatilization, sorption and first order degradation. Metals are also assessed, and emphasis is given to nine priority metals. MINEQL is used to predict aqueous solubility and speciation of the metals in natural waters around the country. Methods are also presented to handle large spills of toxic chemicals having density the same as or different from the receiving waters.
- Chapter 5 contains methods for assessing water quality in impoundments. The topics covered are sediment accumulation, thermal stratification, BOD-D<sub>0</sub> interactions, eutrophication, and fate of toxic materials. The physical/chemical processes governing the fate of toxicants as well as biological uptake and bioconcentration are considered.
- In Chapter 6, methods are presented for estuary classification, flushing time prediction, and transport of conservative and non-conservative pollutants and dissolved oxygen in well-mixed estuaries. For stratified estuaries, Pritchard's box model is used to determine the distribution of conservative materials. Additionally, methods are presented to calculate initial dilution from a waste water discharge and pollution distribution at the completion of and subsequent to initial dilution.
- Chapter 7 presents the methodology necessary to predict the transport and fate of ground water contamination from typical sources. Sets of

tables are provided to give representative values and methods of measurement for the required ground water hydrology and transport parameters. In addition, five analytical models are presented with worked out examples to show how contaminant sources such as solute injection wells, leaky ponds, landfills, and spills can be handled.

### 1.3 METHODOLOGY APPLICATION

For each category in the methodology, the six conceptual steps shown below can be followed to screen a river basin:

- Obtain necessary tools and data to make calculations
- Identify problems that are obvious from inspection of the data base
- Determine the state variables which will be screened
- Apply procedures and compare where possible to observed data
- Consider consequences of errors
- Reevaluate and make recommendations for further analyses or remedial actions.

The techniques in the screening procedure are designed to interact which makes them ideal for use as an analytical tool for river basin surface waters which may include rivers, lakes, and/or estuaries. Although the procedures may interact, they can be applied individually and with identified data sets for specific case studies.

#### 1.3.1 Base Maps

The first step in the screening process can be to obtain large scale topographic maps of the study area. These can be used to determine which water bodies are to be examined and to establish an order of study. Once this has been done, selected small scale (7 1/2-minute or 15-minute series) topographic sheets can be obtained. On these, the planner can locate and mark point source discharges, regions of specific kinds of land use, population centers, and industrial complexes. Use of overlays or push pins may be helpful in preparing these displays.

### 1.4 LIMITATIONS

The processes which govern the fate of pollutants in the environment are complex. Any methodology, particularly one designed for hand calculation or microcomputer applications, cannot be inclusive of all of these processes. An attempt has been made in each chapter to cover the assumptions under which algorithms are developed. Users should be aware of the assumptions, potential errors, and limitations of the tools presented. When deficiencies are noted or the methods deemed inappropriate, the user should be prepared to use a higher level analytical tool.

## REFERENCES

- Bowie, G.L., W.B. Mills, D.B. Porcella, C.L. Campbell, J.R. Pagenkopf, G.L. Rupp, K.M. Johnson, P.W.H. Chan, S.A. Gherini. 1985. Rates, Constants, and Kinetics Formulations in Surface Water Quality Modeling (Edition 2). For U.S. Environmental Protection Agency, Athens, GA.
- Dean, J.D., W.B. Mills and D.B. Porcella. 1981. A Screening Methodology for Basin Wide Water Quality Management. Symposium on Unified River Basin Management. R.M. North, L.B. Dworsky and D.J. Allee, eds. May 4-7, 1980, Gatlinburg, TN.
- Mills, W.B., V. Kwong, L. Mok, and M.J. Unga. 1985. Microcomputer Methods for Toxicants in Ground Waters and Rivers. Proceedings on the 1985 Conference on Environmental Engineering. American Society of Civil Engineers.
- Mills, W.B. and D.B. Porcella. 1984. Screening Methods for Synfuel Chemicals in Aquatic Environments. Journal of Environmental Management, Vol. 18, pp 297-307.
- Mills, W.B. and D.B. Porcella. 1983. Screening for Organic Toxicants in Aquatic Environments. Proceedings of the 1983 National Conference on Environmental Engineering. American Society of Civil Engineers.
- Mills, W.B., J.D. Dean, D.B. Porcella, S.A. Gherini, R.J.M. Hudson, W.E. Frick, G.L. Rupp, and G.L. Bowie. 1982. Water Quality Assessment: A Screening Procedure for Toxic and Conventional Pollutants. Prepared for U.S. Environmental Protection Agency Center for Water Quality Modeling, Environmental Research Laboratory, Athens, Georgia and Monitoring and Data Support Division, Office of Water Regulations and Standards, Washington, DC. Volumes I and II. EPA-600/6-82-004a, b, c.
- Zison, S.W., K. Haven, and W.B. Mills, 1977. Water Quality Assessment: A Screening Methodology for Nondesignated 208 Areas. U.S. Environmental Protection Agency, Athens, GA. EPA-600/9-77-023.

## AQUATIC FATE OF TOXIC ORGANIC SUBSTANCES

## 2.1 INTRODUCTION

2.1.1 Background

Today's technological society generates enormous quantities of chemicals both as products for consumption and as waste. As the volume and number of chemicals has increased, numerous unintended adverse effects of these chemicals have been observed in the environment. Because of the potential hazard that exposure to these compounds poses to biota, the levels of toxic and carcinogenic substances in the environment have become important criteria for evaluating environmental quality.

The level, or concentration, of a toxic compound in the environment depends on the quantity added to the environment and the processes which influence its fate. "Transport" processes tend to distribute chemicals between the atmospheric, aquatic, and soil environments depending on the affinity of the compound for each phase. "Transformation" processes within each phase chemically alter pollutants to forms of lesser, equivalent, or sometimes greater toxicity. These processes occur at rates which are specific to each chemical and to each environmental compartment. The sum of these processes and their interactions, as Figure II-1 illustrates, determines the environmental fate and consequent exposure of biota to a toxic pollutant. The fate of toxic substances in the aquatic environment is the concern of this chapter. The algorithms presented in this chapter have recently been programmed on microcomputers (Mills *et al.*, 1985).

2.1.2 Comparison of Conventional and Toxic Pollutants

Toxic substances frequently exhibit properties which are quite different from the properties of conventional aquatic pollutants. It is worthwhile to compare these differences in order to better appreciate the problems of analyzing impacts of toxicants in surface water systems. Table II-1 shows some of the more important differences.

Typically, one to two dozen pollutants and water quality parameters are classified as "conventional". Until the past several years, these parameters (e.g. BOD, nutrients) have received most of the attention of water quality planners. In contrast to the small number of conventional pollutants there are thousands of toxicants and many more synthetic chemicals are continually being developed. Potentially, any of these toxicants could enter the environment.

Even though there are relatively few types of conventional pollutants, numerous sources combine to routinely discharge large quantities. However, because many surface water bodies have a capacity to assimilate conventional pollutants (e.g. BOD) without apparent adverse effects, this practice is, within limits, both acceptable and pragmatic. Toxic substances, on the other hand, can cause adverse effects



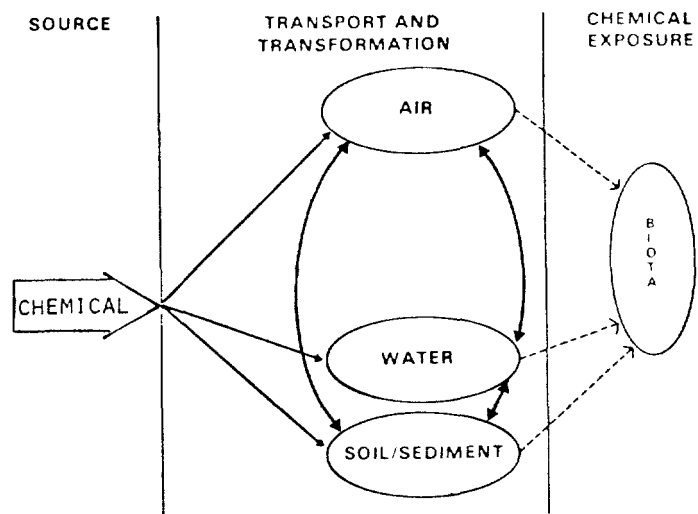


Figure II-1 Environmental Fate of a Toxic Pollutant (After Haque, 1980)

TABLE II-1  
BRIEF COMPARISON OF CONVENTIONAL AND TOXIC POLLUTANTS

Conventional	Toxic
One to two dozen pollutants fall into this category	Thousands fall into this category; many more being synthesized
Often large quantities required to produce impact (e.g. thousands lbs/day)	Small quantities can produce impact (e.g. few lbs/day)
Concentrations often expressed as ppm (mg/l)	Concentrations often expressed as ppb ( $\mu\text{g/l}$ ), or in smaller units
Often travel in dissolved form	May be highly sorbed to suspended and bedded sediments
Mean residence time within water bodies often equal to or less than the mean residence time of moving waters	Can reside in bedded sediments for years
Many biodegrade into harmless substances	Many are transformed to chemicals which are also toxic; others are resistant to degradation and bioconcentrate

even at low discharge rates.

Concentrations of conventional pollutants are most often expressed in units of ppm (or mg/l). Because of the small quantities of toxicants which are typically released, concentrations are often expressed in the ppb (or  $\mu\text{g/l}$ ) range, or in even smaller units. This represents at least a thousandfold difference relative to concentrations of conventional pollutants. However, because toxic substances present in small amounts can adversely impact the environment, these small concentrations can not always be ignored.

Many conventional pollutants are transported in dissolved form. The mean residence times of dissolved, conservative pollutants in a system is equivalent to the mean residence time of water in the system, which is:

- The hydraulic detention time for freshwater lakes
- The travel time for freshwater rivers
- The flushing time for estuaries.

Many toxic chemicals strongly sorb to suspended and bedded sediments and consequently can become a part of the immobile sediments in the bed. The residence time of such chemicals can be on the order of years. Therefore, depending on the properties of the toxicant the period of impact can greatly exceed the period of discharge (e.g., a PCB spill may occur in a few minutes, but quantities of the PCB may remain in immobile, bedded, sediments for years). Consequently the recovery period of a system can be years.

### 2.1.3 Water Quality Criteria

As previously indicated, toxicants are presented in the environment in quantities which are often measured in the ppb range. Such small concentrations are often foreign to many workers in the field. When data or model predictions contain concentrations in the ppb range, the significance of the toxicant level is not always obvious (i.e., there is no "feel" as to whether the concentration is large or small). Proposed criteria for toxic substances can serve as a basis to gauge the significance of observed or predicted levels. Table II-2 shows proposed criteria for numerous toxicants. Since proposed criteria evolve over time the criteria shown in the table are not necessarily the most current. Nevertheless, their function remains: to provide a comparison with levels observed or predicted in real systems. The data in these tables come from the "Red Book" (U.S. EPA, 1976) and the Federal Register, March 15, 1979; July 25, 1979; October 1, 1979; and November 28, 1980. Criteria designed to protect human health, for levels of toxicants in domestic water supplies, are available from these same sources as well.

### 2.1.4 Frequency of Discharge of Toxic Substances from Industries

Numerous organizations, including the U.S. Department of Transportation and the U.S. Environmental Protection Agency, continually collect and analyze data on the

TABLE II-2  
 PROPOSED CRITERIA FOR TOXIC SUBSTANCES DESIGNATED  
 TO PROTECT AQUATIC LIFE

	Freshwater			Saline Water		
	24 Hour Average μg/l	Maximum μg/l	"Red Book" μg/l	24 Hour Average μg/l	Maximum μg/l	"Red Book" μg/l
Acenaphthene	LD <sup>a</sup>	1700 <sup>b</sup>		710 <sup>c</sup>	970 <sup>b</sup>	
Acrolein	21 <sup>c</sup>	68 <sup>b</sup>		LD	55 <sup>b</sup>	
Acrylonitrile	2600 <sup>c</sup>	7550 <sup>b</sup>		LD	LD	
Aldrin/Dieldrin	0.0019	2.5	0.003	0.0019	0.71	0.003
Antimony	1600	9000		LD	LD	
Arsenic	40 <sup>c</sup>	440 <sup>b</sup>		LD	508 <sup>b</sup>	
Asbestos	LD	LD		LD	LD	
Benzene	LD	5300 <sup>b</sup>		700 <sup>c</sup>	5100 <sup>b</sup>	
Benzidine	LD	2500		LD	LD	
Beryllium	5.3 <sup>c</sup>	130 <sup>b</sup>	11.-1100	LD	LD	
Cadmium	d	e	0.4-1.2 <sup>f</sup> 4.0-12.0 <sup>g</sup>	4.5	59	5.0
Carbon Tetrachloride	620	1400		2000	4000	
Chlordane	0.0043	2.4	0.01	0.0040	0.09	0.004
Chlorinated benzenes						
Chlorobenzene	1500 <sup>h</sup>	3500 <sup>h</sup>		120 <sup>h</sup>	280 <sup>h</sup>	
1,2,4 - Trichlorobenzene	210 <sup>h</sup>	470 <sup>h</sup>		3.4 <sup>h</sup>	7.8 <sup>h</sup>	
1,2,3,5 - Tetrachlorobenzene	170 <sup>h</sup>	390 <sup>h</sup>		2.6 <sup>h</sup>	5.9 <sup>h</sup>	
1,2,4,5 - Tetrachlorobenzene	97 <sup>h</sup>	220 <sup>h</sup>		9.6	26	
Pentachlorobenzene	16 <sup>h</sup>	36 <sup>h</sup>		1.3 <sup>h</sup>	2.9 <sup>h</sup>	

TABLE II-2  
(Continued)

	Freshwater			Saline Water		
	24 Hour Average μg/l	Maximum μg/l	"Red Book" μg/l	24 Hour Average μg/l	Maximum μg/l	"Red Book" μg/l
<b>Chlorinated Ethanes</b>						
1,2 - Dichloroethane	3900 <sup>h</sup>	8000 <sup>h</sup>		880 <sup>h</sup>	2000 <sup>h</sup>	
1,1,1 - Trichloroethane	5300 <sup>h</sup>	12000 <sup>h</sup>		240 <sup>h</sup>	540 <sup>h</sup>	
1,1,2 - Trichloroethane	310 <sup>h</sup>	710 <sup>h</sup>		LD	LD	
1,1,1,2 - Tetrachloroethane	420 <sup>h</sup>	960 <sup>h</sup>		LD	LD	
1,1,2,2 - Tetrachloroethane	170 <sup>h</sup>	380 <sup>h</sup>		70 <sup>h</sup>	160 <sup>h</sup>	
Pentachloroethane	440 <sup>h</sup>	1000 <sup>h</sup>		38	87	
Hexachloroethane	62 <sup>h</sup>	140 <sup>h</sup>		7.0 <sup>h</sup>	16 <sup>h</sup>	
Chlorinated Naphthalenes	29	67		2.8	6.4	
<b>Chlorinated Phenols</b>						
4 - Chlorophenol	45	180		LD	LD	
2,4,6 - Trichlorophenol	52	150		LD	LD	
Chloroalkyl Ethers	LD	LD		LD	LD	
Chloroform	500	1200		620 <sup>h</sup>	1400 <sup>h</sup>	
2 - Chlorophenol	60	180		LD	LD	
Chromium (Hexavalent)	0.29	21	100	18	1260	
Copper	5.6	i	j	4.0	23	j
Cyanide	3.5	52	5.0	LD	LD	5.0
DDT	0.00023	0.41	.001	0.0067 <sup>h</sup>	0.021 <sup>h</sup>	.001

TABLE II-2  
(Continued)

	Freshwater			Saline Water		
	24 Hour Average $\mu\text{g/l}$	Maximum $\mu\text{g/l}$	"Red Book" $\mu\text{g/l}$	24 Hour Average $\mu\text{g/l}$	Maximum $\mu\text{g/l}$	"Red Book" $\mu\text{g/l}$
<b>Dichlorobenzenes</b>						
1,2 - Dichlorobenzene	44	99		15h	34h	
1,3 - Dichlorobenzene	310h	700h		22h	49h	
1,4 - Dichlorobenzene	190h	440h		15h	34h	
3,3' - Dichlorobenzidine	LD	LD		LD	LD	
<b>Dichloroethylenes</b>						
1,1 - Dichloroethylene		11600		224000		
1,2 - Dichloroethylene		11600		224000		
2,4 - Dichlorophenol	0.4	110		LD	LD	
<b>Dichloropropanes and Dichloropropenes</b>						
1,1 - Dichloropropane	410	930		LD	LD	
1,2 - Dichloropropane	920	2100		400h	910h	
1,3 - Dichloropropane	4800	11000		79	180	
1,3 - Dichloropropene	18	250		5.5h	14h	
2,4 - Dimethylphenol	38	86		LD	LD	
<b>Dinitrotoluenes</b>						
2,3 - Dinitrotoluene	12	27		4.4h	10h	
2,4 - Dinitrotoluene	620	1400		LD	LD	
1,2 - Diphenylhydrazine	17	38		LD	LD	
Endosulfan	0.042	0.49	0.003	LD	LD	0.001

TABLE II-2  
(Continued)

	Freshwater			Saline Water		
	24 Hour Average μg/l	Maximum μg/l	"Red Book" μg/l	24 Hour Average μg/l	Maximum μg/l	"Red Book" μg/l
Endrin	0.0023	0.18	0.004	0.0023	0.037	0.004
Enthylbenzene	LD	LD		LD	LD	
Fluoranthene	250 <sup>h</sup>	560 <sup>h</sup>		0.30	0.69	
Haloethers						
4 - bromophenylphenyl ether	6.2	14		LD	LD	
Halomethanes						
Chloromethane	7000	16000		3700 <sup>h</sup>	8400 <sup>h</sup>	
Bromomethane	140	320		170 <sup>h</sup>	380 <sup>h</sup>	
Dichloromethane	4000 <sup>h</sup>	9000 <sup>h</sup>		1900 <sup>h</sup>	4400 <sup>h</sup>	
Tribromomethane	840 <sup>h</sup>	1900 <sup>h</sup>		180	420	
Heptachlor	0.0038	0.52	0.001	0.0036	0.053	0.001
Hexachlorobutadiene	LD	LD		LD	LD	
Hexachlorocyclohexane						
Lindane	0.080	2.0		LD	0.16	
Other isomers	LD	LD		LD	LD	
Hexachlorocyclopentadiene	0.39	7.0		LD	LD	
Isophorone	2100	4700		97	220	
Lead	k	1	m	25 <sup>b</sup>	668 <sup>b</sup>	
Mercury (total)	0.2	4.1	0.05	0.10	3.7	0.10

TABLE II-2  
(Continued)

	Freshwater		Saline Water	
	24 Hour Average $\mu\text{g/l}$	Maximum $\mu\text{g/l}$	24 Hour Average $\mu\text{g/l}$	Maximum $\mu\text{g/l}$
Naphthalene	LD	LD	LD	LD
Nickel	n	o	7.1	140
Nitrobenzene	480	1100	53	120
Nitrophenols				
2 - Nitrophenol	2700 <sup>h</sup>	6200 <sup>h</sup>	LD	LD
4 - Nitrophenol	240 <sup>h</sup>	550 <sup>h</sup>	53	120
2,4 - Dinitrophenol	79 <sup>h</sup>	180 <sup>h</sup>	37 <sup>h</sup>	84 <sup>h</sup>
2,4 - Dinitro-6-methylphenol	57 <sup>h</sup>	140 <sup>h</sup>	LD	LD
2,4,6 - Trinitrophenol	1500 <sup>h</sup>	3400 <sup>h</sup>	150 <sup>h</sup>	340 <sup>h</sup>
N-Nitrosodiphenylamine	LD	LD	LD	LD
Pentachlorophenol	6.2	14	3.7	8.5
Phenol	600	3400	LD	LD
Phthalate esters	LD	LD	LD	LD
Polychlorinated biphenyls	0.014	2.0 <sup>b</sup>	0.030	10 <sup>b</sup>
Polynuclear aromatic hydrocarbons	LD	LD	LD	LD
Selenium	35	260	54	410
Silver	0.0090	1.9	0.26	2.3
2,3,7,8 - Tetrachlorodibenzo-p-dioxin	LD	LD		
Tetrachloroethene	310	700	79	180

TABLE II-2  
(Continued)

	Freshwater			Saline Water		
	24 Hour Average μg/l	Maximum μg/l	"Red Book" μg/l	24 Hour Average μg/l	Maximum μg/l	"Red Book" μg/l
Thallium	LD	LD	LD	LD	LD	LD
Toluene	2300h	5200h		100	230	
Toxaphene	0.013	1.6	0.005	LD	0.07	0.005
Trichloroethene	1500	3400		LD	LD	
Vinyl chloride	LD	LD		LD	LD	
Zinc	47	q	p	58	170	

Source: The criteria in this Table are from the following sources:

- "Red Book" (U.S. EPA 1976)
- Federal Register on these dates:  
March 15, 1979 - July 25, 1979 - October 1, 1979 - November 28, 1980

aLD denotes lack of data.

bAcute toxicity level.

cChronic toxicity level.

dThe value in μg/l should not exceed exp [1.05 ln (hardness) -8.53] where hardness is expressed in mg/l as CaCO<sub>3</sub>.

eThe value in μg/l should not exceed exp [1.05 ln (hardness) -3.73] where hardness is expressed in mg/l as CaCO<sub>3</sub>.

f0.4 mg - 1.2 mg/l for cladocerans and salmonid fishes.

g4.0 mg - 12.0 mg/l for other, less sensitive aquatic life.

hValues derived using procedures other than the guideline.



TABLE II-2

(Continued)

- i The value in  $\mu\text{g/l}$  should not exceed  $\exp [0.94 \ln (\text{hardness}) - 1.23]$ , where hardness is expressed in  $\text{mg/l}$  as  $\text{CaCO}_3$ .
- j For freshwater and marine aquatic life, 0.1 times a 96 hr LC50 as determined through nonaerated bioassay using a sensitive aquatic resident species.
- k The value in  $\mu\text{g/l}$  should not exceed  $\exp [2.35 \ln (\text{hardness}) - 9.48]$  where hardness is expressed in  $\text{mg/l}$  as  $\text{CaCO}_3$ .
- l The value in  $\mu\text{g/l}$  should not exceed  $\exp [1.22 \ln (\text{hardness}) - 0.47]$  where hardness is expressed in  $\text{mg/l}$  as  $\text{CaCO}_3$ .
- m 0.01 times the 96 hour LC50 value, using the receiving or comparable water as the diluent and soluble lead measurements (using an 0.45 micron filter) for sensitive freshwater resident species.
- n The value in  $\mu\text{g/l}$  should not exceed  $\exp [0.76 \ln (\text{hardness}) + 1.06]$  where hardness is expressed in  $\text{mg/l}$  as  $\text{CaCO}_3$ .
- o The value in  $\mu\text{g/l}$  should not exceed  $\exp [0.76 \ln (\text{hardness}) + 4.02]$  where hardness is expressed in  $\text{mg/l}$  as  $\text{CaCO}_3$ .
- p For marine and/or fresh water aquatic life, 0.01 of the 96 hour LC50 as determined through bioassay using a sensitive resident species.
- q The value in  $\mu\text{g/l}$  should not exceed  $\exp [0.83 \ln (\text{hardness}) + 1.95]$  where hardness is expressed in  $\text{mg/l}$  as  $\text{CaCO}_3$ .

discharge of toxic substances. Table II-3 summarizes the results of a study reported by Keith and Telliard (1979) which shows the frequency of detection of the 129 priority pollutants in industrial wastewaters. A total of 32 industrial categories were analyzed for organics and 28 for metals. The number of samples ranged from 2532 to 2988. Table II-4 summarizes the most commonly discharged priority pollutants. Table III-53, shown in the next chapter, provides a breakdown by industry of the occurrence of priority pollutants in industrial effluent.

It is common in this country for numerous industrial plants to release their effluents into a single water body. Because of this situation a question that naturally arises is: Based on the number and type of industries located on the water body, what kinds of toxic chemicals are likely to be discharged there? If the industrial categories of each plant are known, the probability that a particular pollutant is discharged from at least one of the plants is:

$$P_j = 1 - \prod_{i=1}^n \left( 1 - \frac{f_{ij}}{100} \right) \quad j = 1, M \quad (II-1)$$

where

$f_{ij}$  = relative frequency of discharge of pollutant type  $j$  from plant type  $i$ , expressed as a percent

$P_j$  = probability that pollutant type  $j$  is discharged from at least one of the  $n$  plants located on the water body

$M$  = number of toxic substances being analyzed.

If the industrial categories of the plants are not known, then the probability that a particular pollutant is discharged can be estimated using Table II-3 together with the following formula:

$$P_j = 1 - \left( 1 - \frac{g_j}{100} \right)^n \quad j = 1, M \quad (II-2)$$

where

$g_j$  = percent of samples containing pollutant  $j$

$P_j$  = probability that pollutant  $j$  is detected in at least one of the  $n$  discharges.

Equation II-1 is obviously the more accurate of the two formulae, because it is based on a knowledge of the types of industries which discharge. Although the above equations provide information on the likelihood that different chemicals are discharged into the environment, and thus can be used to prioritize investigative efforts, they do not predict quantities of pollutants which are discharged. Chapter III can be used to generate that type of information.

TABLE II-3  
EPA LIST OF 129 PRIORITY POLLUTANTS AND THE RELATIVE FREQUENCY OF  
THESE MATERIALS IN INDUSTRIAL WASTEWATERS  
(After Keith and Telliard, 1979)

Percent of Samples <sup>a</sup>	Number of Industrial Categories <sup>b</sup>		Percent of Samples <sup>a</sup>	Number of Industrial Categories <sup>b</sup>	
<u>Purgeable Organics</u>					
1.2	5	Acrolein	2.1	5	1,2-Dichloropropane
2.7	10	Acrylonitrile	1.0	5	1,3-Dichloropropane
29.1	25	Benzene	34.2	25	Methylene chloride
29.3	28	Toluene	1.9	6	Methyl chloride
16.7	24	Ethylbenzene	0.1	1	Methyl bromide
7.7	14	Carbon tetrachloride	1.9	12	Bromoform
5.0	10	Chlorobenzene	4.3	17	Dichlorobromomethane
6.5	16	1,2-Dichloroethane	6.8	11	Trichlorofluoromethane
10.2	25	1,1,1-Trichloroethane	0.3	4	Dichlorodifluoromethane
1.4	8	1,1-Dichloroethane	2.5	15	Chlorodibromomethane
7.7	17	1,1-Dichloroethylene	10.2	19	Tetrachloroethylene
1.9	12	1,1,2-Trichloroethane	10.5	21	Trichloroethylene
4.2	13	1,1,2,2-Tetrachloroethane	0.2	2	Vinyl chloride
0.4	2	Chloroethane	7.7	18	1,2-trans-Dichloroethylene
1.5	1	2-Chloroethyl vinyl ether	0.1	2	bis(Chloromethyl)ether
40.2	28	Chloroform			
<u>Base/Neutral Extractable Organic Compounds</u>					
6.0	9	1,2-Dichlorobenzene	5.7	11	Fluorene
		1,3-Dichlorobenzene	7.2	12	Fluoranthene
		1,4-Dichlorobenzene	5.1	9	Chrysene
0.5	5	Hexachloroethane	7.8	14	Pyrene
0.2	1	Hexachlorobutadiene	10.6	16	Phenanthrene
1.1	7	Hexachlorobenzene			Anthracene
1.0	8	1,2,4-Trichlorobenzene	2.3	6	Benzo(a)anthracene
0.4	3	bis(2-Chloroethoxy)methane	1.6	6	Benzo(b)fluoranthene
10.6	18	Naphthalene	1.8	6	Benzo(k)fluoranthene
0.9	9	2-Chloronaphthalene	3.2	8	Benzo(a)pyrene
1.5	13	Isophorone	0.8	4	Indeno(1,2,3-c,d)pyrene
1.8	9	Nitrobenzene	0.2	4	Dibenzo(a,h)anthracene
1.1	3	2,4-Dinitrotoluene	0.6	7	Benzo(g,h,i)perylene
1.5	9	2,6-Dinitrotoluene	0.1	2	4-Chlorophenyl phenyl ether
0.04	1	4-Bromophenyl phenyl ether	0	0	3,3'-Dichlorobenzidine
41.9	29	bis(2-Ethylhexyl)phthalate	0.2	4	Benidine
6.4	12	Di-n-octyl phthalate	1.1	4	bis(2-Chloroethyl)ether
5.8	15	Dimethyl phthalate	0.8	7	1,2-Diphenylhydrazine
7.6	20	Diethyl phthalate	0.1	1	Hexachlorocyclopentadiene
18.9	23	Di-n-butyl phthalate	1.2	5	N-Nitrosodiphenylamine
4.5	12	Acenaphthylene	0.1	1	N-Nitrosodimethylamine
4.2	14	Acenaphthene	0.1	2	N-Nitrosodi-n-propylamine
8.5	13	Butyl benzyl phthalate	1.4	6	bis(2-Chloroisopropyl)ether
<u>Acid Extractable Organic Compounds</u>					
26.1	25	Phenol	1.9	8	p-Chloro-m-cresol
2.3	11	2-Nitrophenol	2.3	10	2-Chlorophenol
2.2	9	4-Nitrophenol	3.3	12	2,4-Dichlorophenol
1.6	6	2,4-Dinitrophenol	4.6	12	2,4,6-Trichlorophenol
1.1	6	4,6-Dinitro-o-cresol	5.2	15	2,4-Dimethylphenol
6.9	18	Pentachlorophenol			
<u>Pesticides/PCB's</u>					
0.3	3	α-Endosulfan	0.3	3	Heptachlor
0.4	4	β-Endosulfan	0.1	1	Heptachlor epoxide
0.2	2	Endosulfan sulfate	0.2	4	Chlordane
0.6	4	α-BHC	0.2	2	Toxaphene
0.8	6	β-BHC	0.6	2	Aroclor 1016
0.2	4	δ-BHC	0.5	1	Aroclor 1221
0.5	3	γ-BHC	0.9	2	Aroclor 1232
0.5	5	Aldrin	0.8	3	Aroclor 1242
0.1	3	Dieldrin	0.6	2	Aroclor 1248
0.04	1	4,4'-DDE	0.6	3	Aroclor 1254
0.1	2	4,4'-DDD	0.5	1	Aroclor 1260
0.2	2	4,4'-DDT	-	-	2,3,7,8-Tetrachlorodibenzo-p-dioxin (TCDD)
0.2	3	Endrin			
0.2	2	Endrin aldehyde			

TABLE II-3 (continued)

Percent of Samples <sup>a</sup>	Number of Industrial Categories <sup>b</sup>		Percent of Samples <sup>a</sup>	Number of Industrial Categories <sup>b</sup>	
		<u>Metals</u>			
18.2	20	Antimony	16.5	20	Mercury
19.9	19	Arsenic	34.7	27	Nickel
14.1	18	Beryllium	18.9	21	Selenium
30.7	25	Cadmium	22.9	25	Silver
53.7	28	Chromium	19.2	19	Thallium
55.5	28	Copper	54.6	28	Zinc
43.8	27	Lead			
		<u>Miscellaneous</u>			
33.4	19	Total cyanides	Not available		Asbestos (fibrous)
			Not available		Total phenols

<sup>a</sup> The percent of samples represents the number of times this compound was found in all samples in which it was analyzed for divided by the total as of 31 August 1978. Numbers of samples ranged from 2532 to 2998 with the average being 2617.

<sup>b</sup> A total of 32 industrial categories and subcategories were analyzed for organics and 28 for metals as of 31 August 1978.

TABLE II-4

MOST COMMONLY DISCHARGED PRIORITY POLLUTANTS

Pollutant	Percent of Samples	Percent of Industries
Non-Metals		
Bis (2-Ethyl hexyl) Phthalate	41.9	91
Chloroform	40.2	88
Methylene Chloride	34.2	78
Total Cyanides	33.4	59
Toluene	29.3	88
Benzene	29.1	78
Phenol	29.1	78
Di-n-Butyl Phthalate	18.9	72
Ethyl benzene	16.7	75
Naphthalene	10.6	56
Phenanthrene and Anthracene	10.6	50
Metals		
Copper	55.5	100
Zinc	54.6	100
Chromium	53.7	100
Lead	43.8	96
Nickel	34.7	96

### 2.1.5 Physical and Chemical Characteristics of Toxic Organic Compounds

The most intensively investigated toxic pollutants, as a group, are the priority pollutants. Because of the greater availability of data on priority pollutants from such sources as Callahan *et al.* (1979), Dilling *et al.* (1975) and Mackay and Leinonen (1975), data are presented for organic priority pollutants in the following categories:

- Halogenated Aliphatic Hydrocarbons (Table II-5)
- Pesticides (Table II-6)
- Polychlorinated Biphenyls (Table II-7)
- Monocyclic Aromatic Hydrocarbons (Table II-8)
- Polycyclic Aromatic Hydrocarbons (Table II-9).

The properties of the pollutants tabulated in Tables II-5 through II-9 are:

- Vapor pressure, Torr (1 Torr = 1 mm-Hg)
- Volubility
- Octanol-water partition coefficient ( $K_{ow}$ )
- Volatilization half-life
- Qualitative statement of the importance of sorption.

Specific information is included in the tables for volatilization and sorption because of the demonstrated importance of these processes in governing the fate of many pollutants. In particular, for the approximately 103 organic priority pollutants:

- Sorption processes are important for 60
- Sorption is not important for 28
- It is not certain if sorption is important for the remaining 15
- Volatilization is important for 52
- Volatilization is not important for 44
- It is uncertain if volatilization is important for the remaining 7.

The volatilization half-lives presented in the tables were typically measured under a specific set of laboratory conditions, and consequently are shorter than in most natural systems. Other useful properties such as molecular weight and specific gravity are available in standard references such as Perry and Chilton (1973).

### 2.1.6 Scope and Organization of Chapter

The complexity of the transport and transformation processes which influence fate of toxicants require additional analytical tools beyond those required for conventional pollutants. This chapter develops these analytical tools in a general way that is applicable to rivers, lakes, and estuaries. Individual chapters on the various surface water types refine these tools further and provide a framework within which to use them. When used together, the various chapters in this document should help the user to both understand and quantitatively represent the processes influencing the aquatic fate of a pollutant.

This chapter presents both a general overview of the screening approach for

TABLE II-5  
SELECTED CHARACTERISTICS OF VARIOUS ALIPHATIC HYDROCARBONS

Halogenated Aliphatic Hydrocarbons	Vapor Pressure (Torr) at 20°C	Volubility	K <sub>OW</sub>	Volatilization Half-Life	Sorption Important?
Chloromethane	3700	6450-7250 mg/l at 20°C	8	27 minutes <sup>a</sup>	No
Dichloromethane	362	13000-20000 mg/l at 25°C	20	21 minutes <sup>a</sup>	Probably Not
Trichloromethane (chloroform)	150	8200 mg/l at 20°C	93	21 minutes <sup>a</sup>	Probably Not
Tetrachloromethane (carbon tetrachloride)	90	785 Mg/l at 20°C	400	29 minutes <sup>a</sup>	Uncertain
Chloroethane	1000	5740 mg/l at 20°C	35	21 minutes <sup>a</sup>	Probably Not
1,1-Dichloroethane	180	5500 mg/l at 20°C	60	22 minutes <sup>a</sup>	Probably Not
1,2-Dichloroethane	61	8690 mg/l at 20°C	30	29 minutes <sup>a</sup>	Probably Not
1,1,1-Trichloroethane	96	440-4400 mg/l at 20°C	150	20 minutes <sup>a</sup>	Probably Not
1,1,2-Trichloroethane	19	4500 mg/l at 20°C	150	21 minutes <sup>a</sup>	Uncertain
1,1,2,2-Tetrachloroethane	5	2900 mg/l at 20°C	360	56 minutes <sup>a</sup>	Uncertain
Hexachloroethane	0.4	50 mg/l at 22°C	2200	45 minutes <sup>a</sup>	Uncertain
Chloroethene (vinyl chloride)	2660	60 mg/l at 10°C	4	26 minutes <sup>a</sup>	Probably Not
1,1-Dichloroethene	591	400 mg/l at 20°C	30	22 minutes <sup>a</sup>	Probably Not
1,2-trans-Dichloroethene	200	600 mg/l at 20°C	30	22 minutes <sup>a</sup>	Probably Not
Trichloroethene	57.9	1100 mg/l at 20°C	200	21 minutes <sup>a</sup>	Probably Not
Tetrachloroethene	14	150-200 mg/l	760	26 minutes <sup>a</sup>	Probably Not
1,2-Dichloropropane	42	2700 mg/l	190	<50 minutes <sup>a</sup>	Probably
1,3-Dichloropropene	25	2700 mg/l	95	31 minutes <sup>a</sup>	Uncertain
Hexachlorobutadiene	0.15	2	5500	-	Probably
Hexachlorocyclopentadiene	0.081 at 25°C	0.8 mg/l	10 <sup>d</sup>	-	Probably
Bromomethane	1420	900 mg/l	10	~30 minutes	Probably Not
Bromodichloromethane	50	-	75	-	Uncertain
Dibromochloromethane	15	-	120	-	Uncertain
Tri bromomethane	10	3000 mg/l	200	-	Uncertain
Dichlorodifluoromethane	4306	280 mg/l	145	few minutes	Probably
Trichlorofluoromethane	667	1100 mg/l	3400	few minutes	Uncertain

a Stirring in an open container of depth 65 mm at 200 RPM (Dining *et al.*, 1975)

TABLE II-6  
 VARIOUS CHARACTERISTICS OF SELECTED PESTICIDES

Pesticide	Vapor Pressure (Torr)	Solubility	K <sub>ow</sub>	Volatilization Half-Life	Sorption Important?
Acrolein	220 at 20°C 330 at 30°C	20.8% at 20°C	0.8	Uncertain	No
Aldrin	2.3x10 <sup>-5</sup> at 20°C 6x10 <sup>-6</sup> at 25°C	17-180 ppb at 25°C	≈410	Few hours to few days	Yes
Chlordane	1x10 <sup>-5</sup> at 25°C	0.056-1.85 ppm	600	Several weeks	Probably
DDD	10.2-18.9x10 <sup>-7</sup> at 30°C	20-100 ppb at 25°C	10 <sup>6</sup>	1 day to 1 month	Yes
DDE	6.2-6.5x10 <sup>-6</sup> at 20°C	1.2-140 ppb at 20°C	5x10 <sup>5</sup>	1 to 10 hours	Yes
DDT	1.5x10 <sup>-7</sup> at 20°C 1.9x10 <sup>-7</sup> at 25°C	2-85 ppb	10 <sup>4</sup> -10 <sup>6</sup>	4 hours-1 week	Yes
Dieldrin	1.8x10 <sup>-7</sup> to 2.9x10 <sup>-7</sup> at 20°C	186-200 ppb at 25°C	-	Few hours to few days	Probably
Endosulfan	1x10 <sup>-5</sup> at 25°C	100-260 ppb at 20°C	4x10 <sup>3</sup>	11 days-1 year	Yes
Endrin	2x10 <sup>-7</sup>	220 ppb at 25°C	4x10 <sup>5</sup>	-	Uncertain
Heptachlor	3x10 <sup>-4</sup>	56-180 ppb at 25°C	-	-	Probably
Heptachlor Epoxide	-	200-350 ppb at 25°C	-	-	Probably
Hexachlorocyclohexane	10 <sup>-5</sup> -10 <sup>-7</sup>	0.70-21.3 ppm at 25°C	10 <sup>4</sup>	-	Probably
Lindane	10 <sup>-4</sup> -10 <sup>-6</sup>	5-12 ppm at 25°C	5x10 <sup>3</sup>	100-200 days	Probably
Isophorone	0.38	12000 ppm	50	Probably great	No
TCDD	-	0.2 ppb	-	-	Yes
Toxaphene	0.2-0.4	0.7-3. ppm	2000	-	Yes

<sup>a</sup> Conditions described in Callahan et al. (1979).

TABLE II-7  
 SELECTED CHARACTERISTICS OF POLYCHLORINATED BIPHENYLS AND RELATED COMPOUNDS

PCBs and Related Compounds	Percent Chlorine	Density (gm/cm <sup>3</sup> )	Vapor Pressure at 25 C°(Torr)	Solubility mg/l	K <sub>OW</sub>	Volatilization	
						Half-Lives in laboratory (hrs) <sup>a</sup>	Loss in Natural Systems <sup>b</sup>
Aroclor 1016	41	1.33	4x10 <sup>-4</sup>	0.42	2x10 <sup>4</sup> -3x10 <sup>5</sup>	9.9	3.6% after 24 hours
Aroclor 1221	21	1.15	6.7x10 <sup>-3</sup>	15.	600-10 <sup>4</sup>	-	4.2% after 24 hours
Aroclor 1232	32	1.24	4x10 <sup>-3</sup>	1.45	1.5x10 <sup>3</sup> -3x10 <sup>4</sup>	-	-
Aroclor 1242	42	1.35	4x10 <sup>-4</sup>	0.1-0.3	10 <sup>4</sup> -4x10 <sup>5</sup>	12.1	-
Aroclor 1248	48	1.41	4.9x10 <sup>-4</sup>	0.054	~10 <sup>6</sup>	9.5	-
Aroclor 1254	54	1.50	7.7x10 <sup>-5</sup>	0.01-0.06	~10 <sup>6</sup>	10.3	-
Aroclor 1260	60	1.58	4x10 <sup>-5</sup>	0.0027	>10 <sup>6</sup>	10.2	34%-67% after 12 weeks
2-chloronaphthalene	-	-	0.017	6.47	10 <sup>4</sup>	-	-

<sup>a</sup>At 25°C in 1 m<sup>3</sup> of water, 1 m deep (MacKay and Leinonen, 1975).

<sup>b</sup>Conditions described in Callahan et al. (1979).



TABLE II-8  
 SELECTED CHARACTERISTICS OF MONOCYCLIC AROMATIC HYDROCARBONS

Monocyclic Aromatics	Vapor Pressure (Torr)	Solubility	K <sub>ow</sub>	Volatilization Half-Life	Sorption Important?
Benzene	95. at 25°C	1800 mg/l at 25°C	100	4.8 hrs at 25°C <sup>a</sup>	Uncertain
Chlorobenzene	~10 at 20°C	~500 mg/l	700	0.5-9 hrs	Probably
1,2-Dichlorobenzene	1.5 at 25°C	145 mg/l	2400	8-9 hours <sup>a</sup>	Probably
Hexachlorobenzene	10 <sup>-5</sup> at 20°C	~20 µg/l	~10 <sup>6</sup>	8 hours <sup>a</sup>	Yes
Ethylbenzene	7	152 mg/l	1400	5-6 hours <sup>a</sup>	Probably
Toluene	29 at 25°C	535 mg/l	500	5 hours <sup>a</sup>	Probably
2,4-Dinitrotoluene	0.001 at 59°C	270 mg/l at 22°C	100	~100 days	Yes
2,6-Dinitrotoluene	low	~300 mg/l	100	~100 days	Yes
Pentachlorophenol	0.0001	14 mg/l	10 <sup>5</sup>	>100 days	Yes
2-Nitrophenol	1.0 at 49°C	2100 mg/l at 20°C	60	-	Yes
4-Nitrophenol	2.2 at 146°C	16000 mg/l at 25°C	80	-	Yes
2,4-Dinitrophenol	-	5600 mg/l	34	-	Yes
4,6-Dinitro-o-cresol	-	-	700	-	Yes

<sup>a</sup>Mackay and Leinonen (1975). Calculated based on water depth of 1 m, and using mass transfer coefficients of 20 cm/hr and 3000 cm/hr for the liquid and gas transfer phases, respectively.

TABLE II-9  
SELECTED CHARACTERISTICS OF VARIOUS POLYCYCLIC AROMATIC HYDROCARBONS

Polycyclic Aromatics	Vapor Pressure (Torr)	Solubility	K <sub>ow</sub>	Volatilization Important?	Sorption Important?
Acenaphthene	10 <sup>-3</sup> -10 <sup>-2</sup> at 20°C	3.4 mg/l at 25°C	21,000	Less than sorption	Yes
Acenaphthylene	10 <sup>-3</sup> -10 <sup>-2</sup> at 20°C	3.93 mg/l	12,000	Less than sorption	Yes
Fluorene	10 <sup>-3</sup> -10 <sup>-2</sup> at 20°C	1.9 mg/l	15,000	Less than sorption	Yes
Naphthalene	.0492	32. mg/l	2,300	Less than sorption	Yes
Anthracene	2x10 <sup>-4</sup> at 20°C	0.05-0.07 mg/l at 25°C	28,000	Probably	Yes
Fluoranthene	10 <sup>-6</sup> to 10 <sup>-4</sup> at 20°C	0.26 mg/l at 25°C	340,000	Probably Not	Yes
Phenanthrene	6.8x10 <sup>-4</sup> at 20°C	1.0-1.3 mg/l at 25°C	29,000	Probably Not	Yes
Benzo[a]anthracene	5x10 <sup>-9</sup> at 20°C	0.01 mg/l at 25°C	4x10 <sup>5</sup>	No	Yes
Benzo[b]fluoranthene	11 <sup>-11</sup> to 10 <sup>-6</sup> at 20°C	-	4x10 <sup>6</sup>	Probably Not	Yes
Benzo[k]fluoranthene	9.6x10 <sup>-11</sup> at 20°C	-	7x10 <sup>6</sup>	Probably Not	Yes
Chrysene	10 <sup>-11</sup> to 10 <sup>-6</sup> at 20°C	0.002 mg/l at 25°C	4x10 <sup>5</sup>	Probably Not	Yes
Pyrene	6.9x10 <sup>-7</sup> at 20°C	0.14 mg/l at 25°C	2x10 <sup>5</sup>	Probably Not	Yes
Benzo[ghi]perylene	~10 <sup>-10</sup>	0.00026 mg/l at 25°C	10 <sup>7</sup>	Probably Not	Yes
Benzo[a]pyrene	5x10 <sup>-9</sup>	0.0038 mg/l at 25°C	10 <sup>6</sup>	Probably Not	Yes
Dibenzo[a]anthracene	~10 <sup>-10</sup>	0.0005 mg/l at 25°C	10 <sup>6</sup>	Probably Not	Yes
Indeno[1,2,3-cd]pyrene	~10 <sup>-10</sup>	-	5x10 <sup>7</sup>	Probably Not	Yes

toxics and a detailed description of the processes included in the screening methodology. The various topics are organized as follows:

Screening methods for toxic organic substances

Speciation processes

1) Acid-base effects

2) Sorption

Transport processes

1) Volubility limits

2) Volatilization

Transformation processes

1) Biodegradation

2) Photolysis

3) Hydrolysis.

Lyman et al. (1982) and Mabey et al. (1984) provide additional information that can be used to evaluate the importance of these processes.

## 2.2 SCREENING METHODS FOR TOXIC ORGANIC COMPOUNDS

### 2.2.1 Modeling the Fate of Toxic Organics

The goal of this screening methodology for toxic pollutants is to help the user identify surface water bodies where toxicants could reach hazardous levels. Multiple approaches for identifying pollution problems are possible, e.g. extensive field measurements, statistical correlations of discharges and pollutants detected in rivers, computer simulation models, etc. The approach taken here is to present simple methods for assessing the fate of toxicants.

The application of any method necessitates the use of judgment on the part of those applying it. In almost every case, the user must estimate many of the methods' input parameters on the basis of limited data. Consequently, even the projections of detailed computer models such as EXAMS (Burns, et al., 1981) and PEST (Park, et al., 1980) are only as good as the accuracy of the assumptions made by their developers and users. Thus, the goal of the materials presented herein is twofold: to present simple methods and to provide the background necessary to make knowledgeable judgments.

Predicting aquatic fate of pollutants involves several steps. The steps described in the remainder of this section include:

- Determination of Fate-Influencing Processes
- Delineation of Environmental Compartments
- Representation of Hydrologic Flow
- Mathematical Representation of Speciation Processes
- Mathematical Representation of Transport and Transformation Processes
- Determination of Pollutant Load and Mode of Entry into the Aquatic Environment.

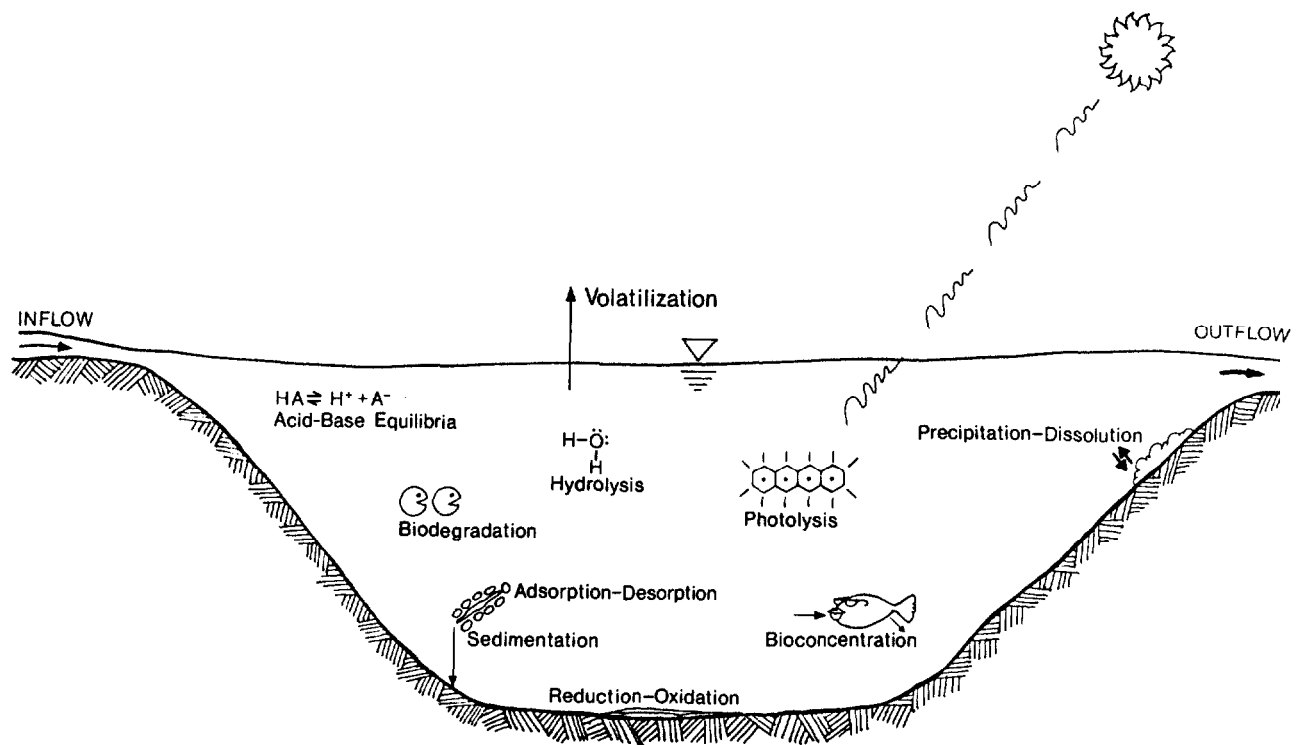


FIGURE 11-2 SPECIATION, TRANSPORT AND TRANSFORMATION PROCESSES IN THE AQUATIC ENVIRONMENT

Prediction of the fate of toxic pollutants requires the user to know which processes act on the toxicant. Figure 11-2 illustrates the transport and transformation processes which are of potential importance in a lake or other surface water body. The processes fall into four categories as follows:

Loading Processes.

The rates at which waste discharges, atmospheric deposition, and land runoff introduce toxicants into natural waters influence resulting pollutant levels.

Speciation Processes

Acid-Base Equilibria. The pH of a natural water determines the fraction of an organic acid or base in neutral or ionic states, and therefore influences volatility.

Sorption. Hydrophobic organic compounds sorb to suspended matter; their subsequent fate is influenced by the fate of the suspended matter.

Transport Processes

Precipitation-Dissolution. Volubility limits of both organic and inorganic pollutants can cause a pure pollutant phase to form restricting its availability to transport and transformation processes or substantially changing the transport route.

Advection. Hydraulic flows transport pollutants which are dissolved or sorbed on suspended sediments into and out of particular aquatic habitats.

Volatilization. Organic pollutants may enter the atmosphere from a water body, thereby reducing aquatic concentrations.

Sedimentation. Deposition of suspended sediments containing sorbed pollutants, as well as direct sorption onto or resorption from bottom sediments can alter pollutant concentrations.

#### Transformation Processes

Biodegradation. Microbial organisms metabolize pollutants, altering their toxicity in the process.

Photolysis. The absorption of sunlight by pollutants causes chemical reactions which affect their toxicity.

Hydrolysis. The reaction of a compound with water frequently produces smaller, simpler organic products.

Reduction-Oxidation. Reactions of organic pollutants and metals which involve the subtraction or addition of electrons strongly influence their environmental properties. For organics, nearly all significant redox reactions are microbially mediated.

#### Bioaccumulation

Bioconcentration. Uptake of toxic pollutants into biota via passive means, e.g. absorption through fish gills.

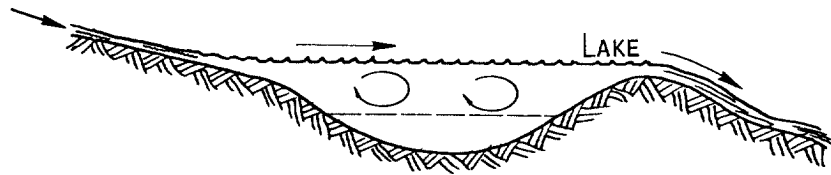
Biomagnification. Uptake of toxicants into biota via consumption of contaminated food.

Once the pertinent processes have been identified, the physical compartments of the environment between which the transport processes act must be delineated. For most water bodies, compartments representing the atmosphere, bottom sediments, and one or more water elements are sufficient. These methods are capable of representing transport of pollutants between the atmosphere and a water body. But rather than calculating atmospheric concentrations of a pollutant, these methods generally assume them to be close to zero unless available data indicate otherwise. Bottom sediments, however, frequently accumulate high levels of organic pollutants. Because of the difficulty of modeling the behavior of toxicants in sediments, usually assumptions which approximate only the removal or addition of a pollutant to the water column are made. These approximations are presented in the individual chapters on each water body.

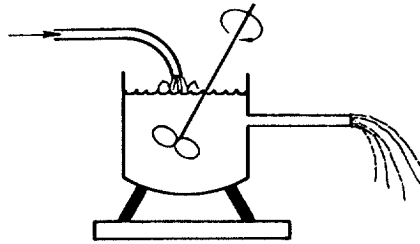
The next step in assessing the aquatic fate of toxic pollutants is to represent the advection or flow of water. Figure 11-3 illustrates a representation of rivers as a segregated flow system and lake layers as completely mixed flow systems. Although these models are simple, they serve as adequate first-approximations of real

COMPLETELY MIXED FLOW

NATURAL SYSTEM:



IDEALIZATION:



MIXED FLOW

SEGREGATED FLOW

NATURAL SYSTEM:



IDEALIZATIONS:

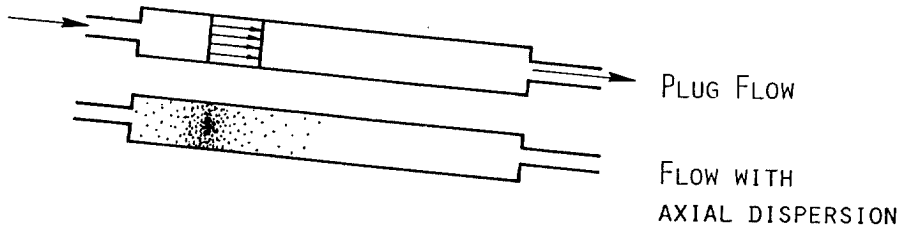


FIGURE 11-3 FLOW SYSTEM REPRESENTATIONS

systems. Refinements and limitations of these flow system models are considered in the individual chapters on rivers, lakes, and estuaries.

The transport and transformation processes responsible for the removal of a pollutant from the water column are considered next. First-order rate expressions adequately represent all of the processes considered here. The first-order decay of

a pollutant by a process is represented as follows:

$$\text{Rate of Pollutant Removal} = k_i \cdot C_T \quad (11-3)$$

where

$k_i$  = first-order rate constant for process  $i$

$C_T$  = total concentration of pollutant.

The rate constant for a process is specific to both the chemical it acts upon and the local environment in which it acts.

When all the first-order processes act independently, the total rate of pollutant removal is:

$$\text{Total Rate of Removal} = k_T \cdot C_T \quad (11-4)$$

where

$$k_T = k_{vm} + k_s + k_b + k_p + k_h \quad (11-5)$$

and

$k_{vm}$  = specific mixed-body volatilization rate constant

$k_s$  = specific rate constant for removal to bottom sediment

$k_b$  = specific rate constant for biodegradation

$k_p$  = specific rate constant for photolysis

$k_h$  = specific rate constant for hydrolysis.

The additivity of processes which are first-order with respect to pollutant concentration is particularly convenient for analysis.

Many of the decay processes are influenced by the chemical state of the toxicant. For example, sorbed pollutants cannot volatilize. Mathematical representations of equilibria between two species of a chemical can be reduced to the following type of equation. This type of equation serves well at the low solute concentrations encountered in waste waters and natural waters:

$$C_i = K_{ij} C_j \quad (11-6)$$

where

$C_i$  = concentration of form  $i$

$K_{ij}$  = equilibrium constant

$C_j$  = concentration of form  $j$ .

It is also convenient to know the fraction of the total pollutant concentration which is in a given state:

$$\alpha_i = \frac{C_i}{C_T} \quad (11-7)$$

where

$C_j$  = concentration in state  $i$

$C_T = C + C_s$

$C$  = total dissolved phase pollutant concentration

$C_s$  = total sorbed phase pollutant concentration.

To complete the assessment of the aquatic fate of a pollutant the mode of entry into the aquatic environment must be considered. Many pollutants enter in dissolved or sorbed form from a point source. In this case, a simple mixing computation is sufficient to determine the initial concentration of a pollutant in the water body. Other cases include spills, non-point sources, and resorption from sediments.

Chapter 4 presents methods for dealing with these cases.

The user may now reckon the concentration of a pollutant in a given water body. The equations which yield the desired results are specific to each surface water type and are developed in the individual chapters on lakes, rivers, and estuaries. An equation representative of those in each chapter is presented in Table 11-10. The individual chapters go into greater detail about factors influencing rate processes and interactions with other important phenomena in each water body (See Sections 4.9, 5.6, 6.4.3, and 6.4.5).

## 2.2.2 Use of Assessment Techniques as Screening Tools

### 2.2.2.1 Making Conservative Assumptions

With the computational methods presented in this document, the user could produce a relatively complete analysis of the aquatic fate of a pollutant. The goal of this screening method, however, is to determine--with a minimum of effort--whether toxicants are likely to reach problem levels in surface water bodies for either existing or projected loading rates. The user can minimize the effort expended in screening a pollutant by starting with a simple approach which incorporates conservative assumptions about the fate of a pollutant. Conservative assumptions are designed to yield higher calculated environmental concentrations than probably exist in the real system. If these higher concentrations are below the water quality criterion under consideration, a violation of the standard is unlikely. If the initial predictions are higher than the standard, the user may successively refine the approach until it becomes apparent that either the standard will be met or that a more detailed study is necessary.

Three levels of refinement in assessing the aquatic fate of a pollutant are considered here. In order of increasing complexity, they are:

- 1) Treating the pollutant as a conservative substance
- 2) Considering transport and speciation processes
- 3) Considering transformation, transport, and speciation processes.

Each approach has advantages and limitations which the user should consider. By



TABLE II-10

EXPRESSIONS FOR TOXIC POLLUTANT LEVELS  
IN VARIOUS WATER BODIES

Water Body	Expression for Steady-State Pollutant Concentration
Rivers (Chapter IV)	$C = C_0 \exp \left[ \frac{-k'_v - \sum K_i}{1 + K_p S} \cdot \frac{x}{U} \right] \quad (IV-115)$ <p>where <math>x</math> = distance downstream  <math>U</math> = river velocity  <math>C</math> = total dissolved phase concentration</p>
Impoundments (Chapter V)	$C = C_{irr} / (1 + T_w \times k) \quad (V-47)$ <p>where <math>T_w</math> = hydraulic residence time  <math>C</math> = total dissolved and sediment phase concentration</p>
Estuaries	$C_i = C_{i=1} \frac{f_i}{f_{i-1}} B_i \quad (VI-33)$ $B_i = \frac{r_i}{1 - (1 - r_i)e^{-kt}} \quad (VI-34)$ <p>where <math>C_i</math> = concentration in segment <math>i</math>  <math>f_i</math> = fraction of fresh water in segment <math>i</math>  <math>r_i</math> = segment <math>i</math> exchange ratio  <math>t</math> = time expressed in tidal cycles</p>

following this sequence of refinements, the user should be able to eliminate cases where water quality problems are unlikely with a minimum of time and effort.

#### 2.2.2.2 Treating the Pollutant as a Conservative Substance

The simplest approach to estimating the concentration of a toxic pollutant is to assume it behaves conservatively (i.e. does not undergo reaction):

$$k_T = 0$$

Unless an internal source of the pollutant exists, this approach will yield the highest possible pollutant levels since pollutant decay and removal processes are neglected. The obvious advantage of this approach is that it requires no chemical or environmental data to evaluate rate and equilibrium constants. The only data needed are pollutant loads and hydrological parameters. Its major drawback is that it neglects the possibility of a compound accumulating in another environmental compart-

ment, especially bedded sediments. This could result in the underestimation of the duration of the exposure of an aquatic habitat to a chemical. Although the duration of exposure may be underestimated, water column concentrations would not exceed the upper limits predicted by this approach at any time during the exposure period. The fate of conservative pollutants in rivers, impoundments, and estuaries is discussed in Sections 4.1.9, 5.6.1, and 6.4.

### 2.2.2.3 Considering Transport and Speciation Processes

This refinement incorporates those processes which influence pollutant transport out of the aquatic environment but neglects those processes which chemically alter the compound. Transport processes strongly depend upon chemical speciation, which therefore must be included. The rate constant for first-order pollutant attenuation in this approach is:

$$k_T = k_S + k_{vm} \quad (11-8)$$

where

$k_S$  = specific rate constant for removal to bottom sediment

$k_{vm}$  = specific mixed body volatilization rate constant.

This approach requires more information on the properties of the toxicant and the environment than when the pollutant is assumed to behave conservatively, but the necessary data are much more readily available than those required to characterize transformation processes. Nearly all the chemical data necessary to characterize acid-base equilibria, sediment sorption, volatility limitations, and volatilization for the organic priority pollutants are presented in tables in Sections 2.1.5, 2.3.1, and 2.4.2. The necessary environmental data can usually be obtained or estimated with a minimal amount of effort. Because of the demonstrated importance of transport processes and the relative simplicity of assessing them, this is a good intermediate step between the simplest and most complicated approaches.

Transport and speciation processes are applied specifically to rivers, impoundments, and estuaries in Sections 4.9, 5.6, 6.4.3, and 6.4.5.

### 2.2.2.4 Considering Transformation, Transport, and Speciation Processes

The most complex model which the user can employ using these screening methods includes consideration of transformation, transport, and speciation processes. With this approach, the rate constant for first-order attenuation of a pollutant is:

$$k_T = k_S + k_{vm} + k_B + k_P + k_H \quad (11-9)$$

where

$k_B$  = specific rate constant for biodegradation.

$k_P$  = specific rate constant for photolysis.

$k_H$  = specific rate constant for hydrolysis.

The inclusion of the degradative processes (i.e. biodegradation, photolysis, and hydrolysis), considerably increases the chemical and environmental data required to model a compound's fate. Rather than accurately determining all the constants for speciation, transport, and transformation, the user should first ascertain which processes are the most significant for a compound. As a first step the user should obtain data on the properties of the chemical which influence its aquatic fate from this document or other sources. From compound specific data, it is usually possible to eliminate some processes from consideration. For organic priority pollutants, consulting the ratings of the relative importance of aquatic processes for the fate of each compound, Table 11-11, may aid the user in eliminating unimportant processes. Once the most significant processes have been identified, the user should collect the environmental data necessary to determine site specific constants. These site specific constants are then applied in the appropriate equation for each water body type to obtain the best estimate of the actual pollutant concentrations in the environment that these methods are capable of making. (See Sections 4.9, 5.6, 6.4.3, and 6.4.5).

Frequently, kinetic and equilibrium constants will depend on the values of parameters which the user must estimate (e.g., pH). In such cases, assuming conservative values is the best policy. However, calculations using a range of values may identify processes for which a more careful determination of the key environmental and chemical parameters is warranted.

Example 11-1 is an overall example for this chapter. It demonstrates the initial steps a user would take in applying these methods to assess the fate of a particular organic pollutant. The example follows the three level analysis described above and also draws upon some of the procedures for specific environmental processes which are developed later in this chapter. This example can serve as a guide to evaluating the importance of the various fate influencing processes for a particular pollutant.

TABLE 11-11

RELATIVE IMPORTANCE OF PROCESSES INFLUENCING  
AQUATIC FATE OF ORGANIC PRIORITY POLLUTANTS (After Callahan et al., 1979)

Compound	Process					
	<u>Sorption</u>	<u>Volatilization</u>	<u>Biodegradation</u>	<u>Photolysis-Direct</u>	<u>Hydrolysis</u>	<u>Bioaccumulation</u>
<u>PESTICIDES</u>						
Acrolein	-	+	+	+	-	-
Aldrin	+	+	?	-	-	+
Chlordane	+	+	?	-	-	+
DDD	+	+	-	-	-	+
DDE	+	+	-	+	-	+
DDT	+	+	-	-	+	+
Dieldrin	+	+	-	+	-	+
Endosulfan and Endosulfan Sulfate	+	+	+	?	+	-
Endrin and Endrin Aldehyde	?	?	?	+	-	+
Heptachlor	+	+	-	?	+	+
Heptachlor Epoxide	+	-	?	?	-	+
Hexachlorocyclohexane ( $\alpha, \beta, \delta$ isomers)	+	?	+	-	-	-
-Hexachlorocyclohexane (Lindane)	+	-	+	-	-	-
Isophorone	-	-	?	+	-	-
TCDD	+	-	-	?	-	+
Toxaphene	+	+	+	-	-	+
<u>PCBs and RELATED COMPOUNDS</u>						
Polychlorinated Biphenyls	+	+	+ <sup>a</sup>	?	-	+
2-Chloronaphthalene	-	?	+	+	-	-
<u>HALOGENATED ALIPHATIC HYDROCARBONS</u>						
Chloromethane (methyl chloride)	-	+	-	-	-	-
Dichloromethane (methylene chloride)	-	+	?	-	-	-
Trichloromethane (chloroform)	-	+	?	-	-	-
Tetrachloromethane (carbon tetrachloride)	?	+	-	-	-	?
Chloroethane (ethyl chloride)	-	+	?	-	+	-
1,1-Dichloroethane (ethylidene chloride)	-	+	?	-	-	-
1,2-Dichloroethane (ethylene dichloride)	-	+	?	-	-	-
1,1,1-Trichloroethane (methyl chloroform)	-	+	-	-	-	-
1,1,2-Trichloroethane	?	+	-	-	-	?
1,1,2,2-Tetrachloroethane	?	+	-	-	-	?
Hexachloroethane	?	?	?	?	?	+
Chloroethene (vinyl chloride)	+	-	-	-	-	-
1,1-Dichloroethene (vinylidene chloride)	?	+	?	-	-	?
1,2- <u>trans</u> -Dichloroethene	-	+	?	-	-	-
Trichloroethene	-	+	?	-	-	-
Tetrachloroethene (perchloroethylene)	-	+	+	-	-	-
1,2-Dichloropropane	?	+	-	?	+	?
1,3-Dichloropropane	?	+	-	?	+	-
Hexachlorobutadiene	+	+	?	-	?	+
Hexachlorocyclopentadiene	+	+	-	+	+	+
Bromomethane (methyl bromide)	-	+	-	-	+	-

TABLE 11-11 (continued)

Compound	Process					
	<u>Sorption</u>	<u>Volatilization</u>	<u>Biodegradation</u>	<u>Photolysis-Direct</u>	<u>Hydrolysis</u>	<u>Bioaccumulation</u>
Bromodichloromethane	?	?	?	?	-	+
Dibromodichloromethane	?	+	?	?	-	+
Tri bromomethane (bromoform)	?	+	?	?	-	+
Dichlorodifluoromethane	?	+	-	?	-	?
Trichlorofluoromethane	?	+	-	-	-	?
<u>HALOGENATED ETHERS</u>						
Bis(chloromethyl) ether	-	-	?	-	++	-
Bis(2-chloroethyl) ether	-	+	-	-	-	?
Bis(2-chloroisopropyl) ether	-	+	-	-	-	?
2-Chloroethyl vinyl ether	-	+	?	-	+	-
4-Chlorophenyl phenyl ether	+	?	?	+	-	+
4-Bromophenyl phenyl ether	+	?	?	+	-	+
Bis(2-chloroethoxy) methane	-	-	?	-	+	?
<u>MONOCYCLIC AROMATICS</u>						
Benzene	+	+	-	-	-	-
Chlorobenzene	+	+	-	-	-	+
1,2-Dichlorobenzene (o-dichlorobenzene)	+	+	-	?	-	+
1,3-Dichlorobenzene (m-dichlorobenzene)	+	+	?	?	?	+
1,4-Dichlorobenzene (p-dichlorobenzene)	+	+	-	?	-	+
1,2,4-Trichlorobenzene	+	+	-	?	-	+
Hexachlorobenzene	+	-	-	-	-	-
Ethyl benzene	?	+	?	-	-	-
Nitrobenzene	+	-	-	+	-	-
Toluene	+	+	?	-	-	-
2,4-Dinitrotoluene	+	-	-	+	-	?
2,6-Dinitrotoluene	+	-	-	+	?	?
Phenol	-	+	+	-	-	-
2-Chlorophenol	-	-	?	+	-	-
2,4-Dichlorophenol	-	-	++	-	-	-
2,4,6-Trichlorophenol	?	-	?	?	-	-
Pentachlorophenol	+	-	+	+	-	+
2-Nitrophenol	-	-	-	++ <sup>b</sup>	-	-
4-Nitrophenol	+	-	-	++ <sup>b</sup>	-	-
2,4-Dinitrophenol	+	-	-	++ <sup>b</sup>	-	-
2,4-Dimethyl phenol (2,4-xyleneol)	-	-	?	+	-	-
p-chloro-m-cresol	-	-	?	++	-	-
4,6-Dinitro-o-cresol	+	-	-	++	?	?
<u>PHTHALATE ESTERS</u>						
Dimethyl phthalate	+	-	+	-	-	+
Diethyl phthalate	+	-	+	-	-	+
Di-n-butyl phthalate	+	-	+	-	-	+
Di-n-octyl phthalate	+	-	+	-	-	+
Bis(2-ethylhexyl) phthalate	+	-	+	-	-	+
Butyl benzyl phthalate	+	-	+	-	-	+

TABLE 11-11 (continued)

Compound	Process					
	<u>Sorption</u>	<u>Volatilization</u>	<u>Biodegradation</u>	<u>Photolysis-Direct</u>	<u>Hydrolysis</u>	<u>Bioaccumulation</u>
<u>POLYCYCLIC AROMATIC HYDROCARBONS</u>						
Acenaphthene <sup>c</sup>	+	-	+	+	-	-
Acenaphthylene <sup>c</sup>	+	-	+	+	-	-
Fluorene <sup>c</sup>	+	-	+	+	-	-
Naphthalene	+	-	+	+	-	-
Anthracene	+	+	+	+	-	-
Fluoranthene <sup>c</sup>	+	+	+	+	-	-
Phenanthrene <sup>c</sup>	+	+	+	+	-	-
Benzo(a)anthracene	+	+	+	+	-	-
Benzo(b)fluoranthene <sup>c</sup>	+	-	+	+	-	-
Benzo(k)fluoranthene <sup>c</sup>	+	-	+	+	-	-
Chrysene <sup>c</sup>	+	-	+	+	-	-
Pyrene <sup>c</sup>	+	-	+	+	-	-
Benzo(ghi)perylene <sup>c</sup>	+	-	+	+	-	-
Benzo(a)pyrene	+	+	+	+	-	-
Di benzo(a, h)anthracene <sup>c</sup>	+	-	+	+	-	-
Indeno(1, 2, 3-cd)pyrene <sup>c</sup>	+	-	+	+	-	-
<u>NITROSAMINES AND MISCELLANEOUS COMPOUNDS</u>						
Dimethylnitrosamine	-	-	-	++	-	-
Diphenylnitrosamine	+	-	?	+	-	?
Di-n-propylnitrosamine	-	-	-	++	-	-
Benzidine	+	-	?	+	-	-
3, 3'-Dichlorobenzidine	++	-	-	+	-	-
1, 2-Diphenylhydrazine (Hydrazobenzene)	+	-	?	+	-	+
Acrylonitrile	-	+	?	-	-	+

Key to Symbols:

- ++ predominate fate determining process
- + Could be an important fate process
- Not likely to be an important process
- ? Importance of process uncertain or not known

Notes

a Biodegradation is the only process known to transform polychlorinated biphenyls under environmental conditions, and only the lighter compounds are measurably biodegraded. There is experimental evidence that the heavier polychlorinated biphenyls (five chlorine atoms or more per molecule) can be photolyzed by ultraviolet light, but there are no data to indicate that this process is operative in the environment.

b Based on information for 4-nitrophenol.

c Based on information for PAH's as a group. Little or no information for these compounds exists.

## Pentachlorophenol in the Aurum Mirth Watershed

Pentachlorophenol enters the Aurum Mirth River from a continuous point source. The river is the sole tributary to Lake Castile. After mixing at the point of entry, the concentration of pentachlorophenol in the river is  $20 \mu\text{g}/\text{l}$ . The travel time from the point of contamination with pentachlorophenol to Lake Castile is about 6 days. The mean hydraulic residence time in Lake Castile is 10 days.

Use the screening methods to determine which chemical and environmental parameters are of the greatest importance for predicting the fate of pentachlorophenol in the watershed's surface waters.

## 1) TREATING PENTACHLOROPHENOL AS A CONSERVATIVE SUBSTANCE

The first step in the screening method is to assess the fate of pentachlorophenol treating it as a conservative substance. Sections 4.1.9, 5.6.1, and 6.4 discuss the fate of conservative pollutants in rivers, lakes, and estuaries. In this case, we assume no further dilution of the pentachlorophenol occurs in either the lake or the river. Consequently, the conservative pollutant approach predicts a mean concentration in the river and lake of  $20 \mu\text{g}/\text{l}$ .

Table 11-2 lists a proposed water quality standard for pentachlorophenol. The 24 hour mean concentration must be less than  $6.2 \mu\text{g}/\text{l}$ . Since  $20 \mu\text{g}/\text{l}$  exceeds this standard, a second level assessment is in order.

Prior to applying the next two levels of analysis it is worthwhile to check Table 11-11 for the relative importance of the different transformation and transport processes. Table 11-11 summarizes the influence of the aquatic processes on pentachlorophenol as follows:

- Sorption - Important process
- Volatilization - Not an important process
- Biodegradation - Important process
- Direct Photolysis - Important process
- Hydrolysis - Not an important process
- Bioaccumulation - Important process.

It will be instructive to compare these statements to the results of the screening methodology.

## 2) CONSIDERING TRANSPORT AND SPECIATION PROCESSES

To analyze transport and speciation processes, first examine each process for its potential influence on the fate of pentachlorophenol.

### Speciation Processes

Acid-Base Effects (Section 2.3.1). The chemical and environmental parameters governing acid-base effects are:

- Chemical Parameters:
  - $pK_a$  or  $pK_b$  - Acid or base equilibrium constants
- Environmental Parameters:
  - pH - Hydrogen ion concentrations.

The  $pK_a$  of pentachlorophenol is 4.74, as shown in Table 11-13. According to Table 11-12, at least 90 percent of the pentachlorophenol will be in the anionic state at pH's greater than 5.74. As long as the pH in the Aurum Mirth River and Lake Castile remain above 5.74, the properties of pentachlorophenol as measured for neutral waters will remain unaffected. But, because pH's below 5.74 could significantly alter the behavior of the compound, it is important to determine actual surface water pH values.

Sorption (Section 2.3.2) The key environmental and chemical parameters which influence sorption are:

- Chemical parameters:
  - $K_{ow}$  - Octanol-water coefficient
  - $S_w$  - solubility in water
- Environmental Properties:
  - Suspended sediment concentration
  - Organic carbon content of the suspended sediment.

Table 11-8 lists the solubility and octanol-water coefficient of pentachlorophenol as:

$$S = 14 \text{ mg/l}$$

$$K_{ow} = 10^5$$

Assuming an organic carbon content of 2 percent for the suspended sediments, calculate  $K_p$  using Equations 11-18 and 11-16:

$$K_p = (.02) (.63) (10^5) = 1300$$

According to Table 11-16, greater than 10 percent of the pentachlorophenol will be in the sorbed state at suspended sediment concentrations exceeding 100 mg/l. The relatively strong sorption of pentachlorophenol dictates that the suspended sediment concentration in the Aurum Mirth River and the sediment trapping efficiency of Lake Castile be investigated further. Sorption of pentachlorophenol potentially affects both its speciation and its transport rates.

### Transport Processes

Solubility Limitations (Section 2.4.1). The most important chemical



and environmental factors which influence volatility of a compound are:

- Chemical Parameters:
  - SW - Aqueous equilibrium volatility
- Environmental Parameters:
  - T - Temperature
  - Salinity.

Table II-8 lists the volatility limit for pentachlorophenol as 14 mg/l (14000  $\mu\text{g/l}$ ). At no point in the Aurum Mirth watershed should the volatility of pentachlorophenol restrict the ability of the aqueous phase to transport it.

Volatilization (Section 2.4.2). The most significant chemical and environmental properties which influence volatilization are:

- Chemical Parameters:
  - $K_H$  - Henry's Law Constant
- Environmental Parameters:
  - $k_a$  - Reaeration constant
  - V - Wind speed
  - Z - Mixed depth of water body.

It is possible to estimate the Henry's Law Constant for pentachlorophenol from its vapor pressure and aqueous volatility using Equation 11-32. However, it is simpler to rule out volatilization as a significant transport process on the basis of the volatilization half-life of 100 days given in Table II-8. Because laboratory volatilization half-lives are shorter than the true environmental values, it is safe to assume the environmental half-life will be much greater than 100 days. Given a total system mean hydraulic residence time of only 16 days (6 + 10), volatilization can be safely neglected.

### Summary

Acid-base equilibria and sorption significantly influence the transport and speciation of pentachlorophenol in the aquatic environment. Acid-base effects do not influence the near-neutral volatilization and photolysis rate constants presented in this document as long as pH's remain above 5.7. Sorption is a potentially important speciation process. Consequently, the pH values and suspended sediment concentrations should be determined in order to accurately evaluate these processes.

The strong tendency of pentachlorophenol to sorb on sediments may result in sedimentation serving as a significant removal process in Lake Castile. The absence of net sediment deposition in the river implies that transport processes do not reduce pentachlorophenol concentrations in the Aurum Mirth. Thus, the second level analysis predicts a total concentration of **20  $\mu\text{g/l}$**  of pentachlorophenol in the Aurum Mirth River with lower levels possible in the lake. Because the

predicted river concentrations exceed the standard, the third level model is necessary.

### 3) CONSIDERING TRANSFORMATION, TRANSPORT, AND SPECIATION PROCESSES

To consider transformation, transport, and speciation processes, the transformation processes which were neglected in the level two analysis must be examined for their potential importance in influencing the rate of pentachlorophenol degradation.

#### Transformation Processes

Biodegradation (Section 2.5.1). The key chemical and environmental variables which influence biodegradation are:

Chemical Parameters:

Metabolic Pathway (growth or co-metabolism)

$k_B$  - Biodegradation rate constant

Environmental Parameters:

Bacterial population size

State of adaptation

Inorganic nutrient concentrations - Phosphorus

Dissolved oxygen

Temperature

Pollutant concentration.

According to Table II-26, pentachlorophenol is potentially biodegradable, although adaptation may be slow. The reported specific rate constant values, 0.1 to 1.0 per day, in Table II-27 are in the same range as the 0.05 to 0.5 per day values suggested in Table II-26. Although both rate constants were determined under laboratory rather than environmental conditions, they do indicate that pentachlorophenol can degrade very rapidly.

Table II-27 also indicates that pentachlorophenol is used by bacteria as a growth substrate. Thus, the time required for adaptation is of primary concern. The most important environmental factors for determining whether microorganisms in the Aurum Mirth watershed will adapt to degrade pentachlorophenol are previous exposure, time, and the actual concentrations of pentachlorophenol in the surface waters (too low--no enzyme induction; too high--may have toxic effect on microbiota).

Photolysis (Section 2.5.2). The key chemical and environmental characteristics influencing the rate of photolysis are:

● Chemical Properties:

$k_{do}$  - Near-surface rate constant

$\epsilon(\lambda)$  - Light absorption coefficient of pollutant

$\phi$  - Quantum yield

- Environmental Properties:

- I - Solar radiant flux

- Z - Mixed depth of water body

- K - Diffuse light attenuation coefficient

- a)  $Z_{sd}$  - Secchi disc depth

- b)  $C_{ss}$  - Suspended sediment concentration

- $C_{doc}$  - Dissolved organic carbon concentration

- $C_a$  - Chlorophyll pigment concentration

According to Table 11-32, the near-surface photolysis rate constant for pentachlorophenol is .46/day. The size of the rate constant implies that photolysis would be an important factor if the water bodies are not too deep or too turbid. Thus, it is important to gather information on the water depths, and to estimate the light attenuation coefficients and the solar radiant flux in the Aurum Mirth watershed.

Hydrolysis (Section 2.5.3). The important parameters influencing the rate of hydrolysis are:

Chemical Parameters:

- $k_a, k_n, k_b$  - Acid, neutral, and base catalyzed hydrolysis rate constants

Environmental Properties:

- pH - Concentration of hydrogen ion in the water bodies.

Table 11-40 gives acid and base hydrolysis rate constants for pentachlorophenol of  $1.1 \times 10^4$  and  $3.3 \text{ liter mole}^{-1} \text{ day}^{-1}$ . The neutral rate constant is  $5.8 \times 10^{-3}$  per day. The same table lists a half life of 100 days at pH = 7. Because the acid catalyzed rate constant is large, significantly higher rates could occur at lower pH's. Using Equation 11-85, the rate constant for pH = 5 is:

$$k_H = 1.1 \times 10^4 (10^{-5}) + 5.8 \times 10^{-3} + 3.3 (10^{-9}) \\ = .23 \text{ day}^{-1}$$

At this lower pH, degradation by abiotic hydrolysis would be very rapid. Thus, determining the pH in the Aurum Mirth River and Lake Castile is very important.

### Summary

The consideration given to transformation, transport, and speciation processes indicates the following processes are of potential importance to the fate of pentachlorophenol in the Aurum Mirth watershed:

- Acid-base effects
- Sorption
- Biodegradation
- Photolysis
- Hydrolysis.

Since the three transformation processes are potentially important, there is a good possibility that the initial pentachlorophenol concentration of  $20 \mu\text{g/l}$  will be reduced below the  $6.2 \mu\text{g/l}$  standard. Therefore further analysis as presented in the specific water body sections is warranted.

The results of this example agree with the summary of rate processes given in Table 11-11 except for the case of hydrolysis. This demonstrates that the process summary table can serve as a useful guide but should be supplemented with actual data whenever possible.

----- END OF EXAMPLE 11-1 -----

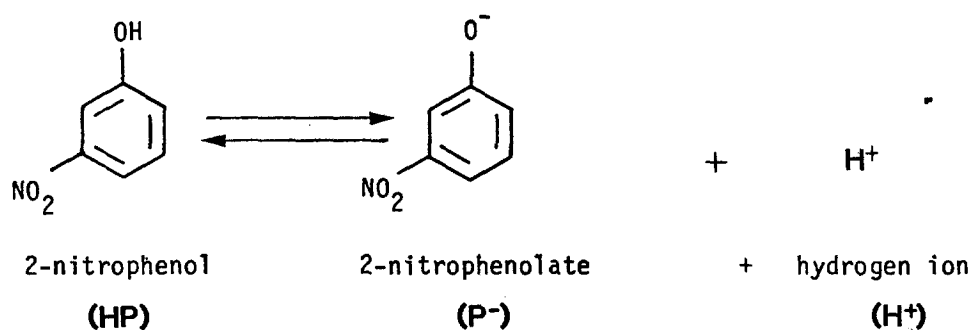
## 2.3 SPECIATION PROCESSES

### 2.3.1 Acid-Base Effects

The fate of toxic organics which are either acids or bases can be strongly affected by the concentration of hydrogen ions in a water body. It is therefore necessary to have a means for estimating this influence. This section will first present a brief review of acid-base equilibria and then will give a technique for quantifying the influence of hydrogen ion concentration on the behavior of toxicants.

#### 2.3.1.1 Acid-Base Equilibria

Acids by definition donate hydrogen ions,  $\text{H}^+$ , to solution. Bases, by definition, accept hydrogen ions from solution. 2-Nitrophenol, one of the 129 priority pollutants, is an acid and donates hydrogen ions as shown by the following reaction:



Acid-base reactions are extremely fast and can be represented by equilibrium expressions. For the above reaction the expression would be:

$$\frac{[H^+][P^-]}{[HP]} = K_a \quad (11-10)$$

where

- [H<sup>+</sup>] = concentration of hydrogen ions, moles/liter
- [P<sup>-</sup>] = concentration of nitrophenolate ions, moles/liter
- [HP] = concentration of undissociated nitrophenol, moles/liter
- [K<sub>a</sub>] = an equilibrium constant for acid dissociation (also called an acidity constant).

The extent to which any acid will donate hydrogen ions to the solution depends on how many hydrogen ions are in solution (the concentration of hydrogen ions) and on the strength of the acid.

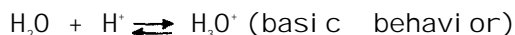
The concentration of free hydrogen ions in natural waters can range from about 10<sup>-4</sup> to 10<sup>-10</sup> moles per liter. Hydrogen ion concentrations are normally expressed in pH units. In dilute solutions, such as natural waters, pH is defined as the negative logarithm of the molar hydrogen ion concentration (pH = -log<sub>10</sub> [H<sup>+</sup>]). For the above two concentrations the pH values are 4 and 10.

The strength of an acid is quantified by the equilibrium constant, K<sub>a</sub>. For very strong acids (those which most readily donate hydrogen ions) the value of this constant is greater than unity. Included in this group are strong acids such as hydrochloric and nitric acid. Toxic organic acids, though, are generally weak acids and have K<sub>a</sub> values between 10<sup>-3</sup> and 10<sup>-9</sup>. K<sub>a</sub> values are typically expressed in terms of negative base ten logarithms. When this approach is used the equilibrium constants are called "pK<sub>a</sub>" (pK<sub>a</sub> = -log<sub>10</sub> K<sub>a</sub>).

When the pH of a solution is the same as the pK<sub>a</sub> value of an acid (i.e., pH = pK<sub>a</sub>), 50 percent of the acid will have donated its hydrogen ions to the solution and will exist as a charged anionic species. For pH values greater than the pK<sub>a</sub> value by one or more units, the acid will have donated essentially all of its hydrogen ions to the solution and will exist in the anionic form (i.e., P<sup>-</sup>).

The extent to which any base will extract hydrogen ions from solution depends upon the concentration of hydrogen ions in solution (pH) and on the strength of the base. The strength of a base is quantified by an equilibrium constant, K<sub>b</sub>. For very strong bases (those that most readily extract hydrogen ions from solution) the value of K<sub>b</sub> is of the order of 1. Toxic organic bases are generally weak and have K<sub>b</sub> values between 10<sup>-3</sup> and 10<sup>-10</sup>. In a manner similar to acids, K<sub>b</sub> is typically expressed in terms of negative base ten logarithms and is called "pK<sub>b</sub>" (pK<sub>b</sub> = -log<sub>10</sub> K<sub>b</sub>).

Water itself can behave as a weak acid or a weak base:



Note that  $[\text{H}^+] \cdot [\text{OH}^-] = K_w$

where  $[\text{OH}^-]$  = the concentration of hydroxide ion, moles/l

$$K_w \cong 10^{-14}, \text{ at } 20^\circ\text{C}$$

$$\text{p}K_w \cong 14, \text{ at } 20^\circ\text{C}.$$

When the pH of a solution equals the value  $(\text{p}K_w - \text{p}K_b)$  of a base, 50 percent of the base has accepted hydrogen ions and will exist as a charged cationic species. For pH values greater than one unit above the value of  $(\text{p}K_w - \text{p}K_b)$ , essentially all of the base will exist in electrically neutral form (e.g.  $\text{NH}_3$ ). For pH values less than the value of  $(\text{p}K_w - \text{p}K_b)$  by 1 or more units, the base will essentially exist in the electrically charged cationic form (e.g.,  $\text{NH}_4^+$ ).

Table 11-12 summarizes the behavior described above for acids and bases. Values for  $\text{p}K_a$  and  $\text{p}K_b$  for selected toxic organic acids and bases and values of  $\text{p}K_w$  are given in Table 11-13. Additional  $\text{p}K_a$  values can be found in Doniganet *et al.* (1983).

Since toxic organics almost always exist in very low concentrations and are at best only weak acids or weak bases, they will have little influence, if any, on the pH values of the water. The hydrogen ion concentration of the water will, however, determine whether acids or bases exist in neutral or ionic forms.

Values of pH for natural waters can be obtained from the USGS, the U.S. EPA, and state and local agencies. Waters with low alkalinities (e.g.,  $\leq 50$  mg/l as  $\text{CaCO}_3$ , or 1 milliequivalent/liter) are quite susceptible to changes in pH due to natural processes such as photosynthesis and respiration and even to relatively small additions of strong acid or base. Selection of representative pH values for such waters will require more data than for systems with higher alkalinities where less change in pH can be anticipated.

### 2.3.1.2 Quantifying the Influence of pH on Toxicant Volatilization

Only electrically neutral species are directly volatile. Volatilization rate expressions must therefore use as the concentration of toxicant only that fraction which is electrically neutral (non-ionic). The fraction of an acid or base which is in the non-ionic form can be determined by use of the expressions given below:

For organic acids:

$$\alpha_{A_0} = \frac{A_0}{A} = \frac{1}{1 + 10^{(\text{pH} - \text{p}K_A)}} \quad (\text{II-11})$$

TABLE 11-12

OCCURRENCE OF ACIDS AND BASES IN NEUTRAL AND CHARGED FORMS AS A FUNCTION OF pH,  $pK_a$ , AND  $pK_b$ 

Acids			Bases		
Definition:	Hydrogen ion donors		Definition:	Hydrogen ion acceptors	
Example:	$\text{HNO}_3 \longrightarrow \text{H}^+ + \text{NO}_3^-$		Example:	$\text{NH}_3 + \text{H}^+ \longrightarrow \text{NH}_4^+$	
General Reaction:	$\text{HP} \longrightarrow \text{H}^+ + \text{P}^-$		General Reaction:	$\text{B} + \text{H}^+ \longrightarrow \text{BH}^+$	
<u>Speciation:</u>			<u>Speciation:</u>		
<u>pH</u>	<u>Fraction in Neutral Form</u>	<u>Fraction in Ionic Form</u>	<u>pH</u>	<u>Fraction in Neutral Form</u>	<u>Fraction in Ionic Form</u>
$pK_a+3$	0.001	0.999	$pK_w-pK_b+3$	0.999	0.001
$pK_a+2$	0.01	0.99	$pK_w-pK_b+2$	0.99	0.01
$pK_a+1$	0.09	0.91	$pK_w-pK_b+1$	0.91	0.09
$pK_a$	0.5	0.5	$pK_w-pK_b$	0.5	0.5
$pK_a-1$	0.91	0.09	$pK_w-pK_b-1$	0.09	0.91
$pK_a-2$	0.99	0.01	$pK_w-pK_b-2$	0.01	0.99
$pK_a-3$	0.999	0.001	$pK_w-pK_b-3$	0.001	0.999

For organic bases:

$$\alpha_{\text{Bo}} = \frac{\text{Bo}}{\text{B}} = \frac{1}{1 + 10^{(pK_w - pK_b - \text{pH})}} \quad (11-12)$$

where

$\alpha_{\text{Ao}}$  = the decimal fraction of the organic acid which is in the electrically neutral (non-ionic) form

$\alpha_{\text{Bo}}$  = the decimal fraction of the organic base which is in the electrically neutral (non-ionic) form

A = the total dissolved concentrations of the toxic organic acid (e.g.,  $\text{HP} + \text{P}^-$ ), also called the analytical concentration of A

B = the total dissolved concentration of the toxic organic base (e.g.,  $\text{BH}^+ + \text{B}$ ), also called the analytical concentration of B.

The rate expressions then become in general form:

TABLE 11-13

pK<sub>a</sub> AND pK<sub>b</sub> VALUES FOR SELECTED TOXIC ORGANIC  
ACIDS AND BASES AND VALUES OF pK<sub>w</sub> FOR WATER

<u>Acids</u>	<u>p K<sub>a</sub><sup>a</sup></u>
Phenol	10.0
2-Chlorophenol	8.52
2, 4-Dichlorophenol	7.85
2, 4, 6-Trichlorophenol	5.99
Pentachlorophenol	4.74
2-Nitrophenol	7.21
4-Nitrophenol	7.15
2, 4-Dinitrophenol	4.09
2, 4-Dimethylphenol	10.6
4, 6-Dinitro-o-cresol	4.35
<u>Bases</u>	<u>pK<sub>b</sub><sup>b</sup></u>
Benzidine	9.34, 10.43
<u>Water</u>	<u>p K<sub>w</sub><sup>c</sup></u>
Freshwater	14.63 at 5°C 14.53 at 10°C 14.35 at 15°C 14.17 at 20°C 14.00 at 25°C 13.82 at 30°C
Seawater	14.03 at 5°C 13.81 at 10°C 13.60 at 15°C 13.40 at 20°C 13.20 at 25°C 13.00 at 30°C

## Notes:

<sup>a</sup> All pK<sub>a</sub> values from Callahan et al (1979).

<sup>b</sup> All pK<sub>b</sub> values from Weast and Astle (1980).

<sup>c</sup> pK<sub>w</sub> values from Stumm and Morgan (1981) and from Dickson and Riley (1979).



$$R = k_v \alpha_{A_0} A \quad (11-13d)$$

and

$$R = k_v \alpha_{B_0} B \quad (11-13b)$$

where

$R$  = rate of volatilization

$k_v$  = specific rate constants for volatilization.

Table 11-14 summarizes the procedure.

----- EXAMPLE 11-2 -----

2-nitrophenol has been detected in the Alchandra Estuary, which has a pH of 8, at concentrations of 20  $\mu\text{g/l}$  (total dissolved form). Determine the volatilization flux on a per unit area basis. Assume the volatilization rate constant,  $k_v$ , is 2 cm/hr.

From Table 11-13, the  $pK_a$  of 2-nitrophenol is 7.21. The fraction present in the electrically neutral (non-ionic) form is:

$$\begin{aligned} \alpha_{A_0} &= \frac{1}{1 + 10^{(\text{pH} - pK_a)}} \\ &= \frac{1}{1 + 10^{(8.0 - 7.2)}} \\ &= 0.14 \end{aligned}$$

From Equation 11-13 the volatilization flux is:

$$R_v = 2 \text{ cm/hr} (0.14) \left(\frac{20 \mu\text{g}}{\text{l}}\right) \left(\frac{1000 \text{ l}}{\text{m}^3}\right) \left(\frac{1 \text{ m}}{100 \text{ cm}}\right) = 56 \mu\text{g} \cdot \text{hr}^{-1} \cdot \text{m}^{-2}$$

----- END OF EXAMPLE 11-2 -----

### 2.3.2 Sorption on Suspended Sediments

#### 2.3.2.1 Introduction

Sorption refers to the accumulation of a chemical in the boundary region of a solid-liquid interface. Sorption occurs when the net sorbate-sorbent attraction overcomes the solute-solvent attraction, where solute and sorbate refer to the sorbing species in solution and sorbed at the interface, respectively.

Sorption of chemicals in the natural environment is significant because the

TABLE 11-14

PROCEDURE FOR CALCULATING FRACTION OF A COMPOUND  
WHICH IS IN THE NEUTRAL (NON-CHARGED) FORM

1. Decimal fraction of a compound which is in the neutral (non-charged) form:

For Organic Acids  $\alpha_{A_0} = \frac{A_0}{A} = \frac{1}{1 + 10^{(pH-pK_A)}} \quad (1)$

For Organic Bases  $\alpha_{B_0} = \frac{B_0}{B} = \frac{1}{1 + 10^{(pK_w-pK_B-pH)}} \quad (2)$

2. Procedure

- a) Find the pH value of the water, pH = \_\_\_\_\_.
- a) For an organic acid, use Table 11-13 to find the  $pK_A$  value of the organic acid,  $pK_A =$  \_\_\_\_\_.
- c) For an organic base use Table 11-13 to find the  $pK_B$  value of the organic base,  $pK_B =$  \_\_\_\_\_.
- d) Also use Table 11-13 to find the  $pK_w$  value for water,  $pK_w =$  \_\_\_\_\_.

3. Substitute: For organic acids substitute pH and  $pK_A$  into equation 1.  $\alpha_{A_0} =$  \_\_\_\_\_.

For organic bases substitute pH,  $pK_B$ , and  $pK_w$  into equation 2.  $\alpha_B =$  \_\_\_\_\_.

Note:  $10^0 = 1$  (any number to the zero power equals 1)

4. For approximations of the decimal fraction of a compound which is in the neutral form use Table 11-12.

fates of sorbates and solutes can be significantly different. Sorbates are transported along with sediments, and can be deposited in river or lake beds to remain indefinitely. Sorbates are in many ways protected from transformation processes which would otherwise affect the solute. For example:

- Microbial degradation rates can be reduced. Steen et al. (1978) performed tests which showed that sorption of toxicants to suspended sediments renders some compounds unavailable for biodegradation in the adsorbed state.
- Volatilization is diminished. Since volatilization of a chemical occurs from the dissolved phase, the sorbate is not directly available for volatilization. Rather, the sorbate first desorbs before it volatilizes. Example 11-4 will show the significant influence of sorption on volatilization.
- Direct photolysis of pollutants adsorbed on suspended particles is inhibited in some cases. Further, suspended solids deposited on the bed of a river, lake, or estuary, receive very little radiation for photolytic reactions.

The net interaction between the surface of a solid and sorbate can result from a variety of forces, including coulombic attraction, Van der Waals forces, orientation energy, induction forces, hydrogen bonding, and chemical forces (Reinhold et al., 1979). In the case of many organic compounds, the solute-solvent interaction is often weak so that even a weak sorbate-sorbent attraction can result in sorption. This type of sorption is referred to as hydrophobic sorption because of the importance of the weak solute-solvent attraction. Hydrophobic sorption will be the topic of much of the following discussion, but it is preceded by brief discussions of equilibrium isotherms and sorption kinetics.

#### 2.3.2.2 Adsorption Isotherms

Adsorption isotherms describe the relationship between the amount of chemical sorbed and the equilibrium solution concentration. The most commonly used isotherms are:

- Langmuir Adsorption Isotherm. This equation was originally developed to describe adsorption of a gas to a solid surface, but has been used to describe solid-liquid sorption.
- Freundlich Adsorption Isotherm. This empirical equation is based on surface-free energy and monolayer capacity.
- Linear Adsorption Isotherm. This equation assumes that there is a linear relationship between the concentrations of solute and sorbate at equilibrium. It is valid for dilute solutions.

Figure 11-4 shows example comparisons between the three isotherms, and includes the equations which describe each isotherm. The quantity  $X$  is the amount of sorbed chemical per mass of sediment, and  $C_w$  is the amount of dissolved chemical per

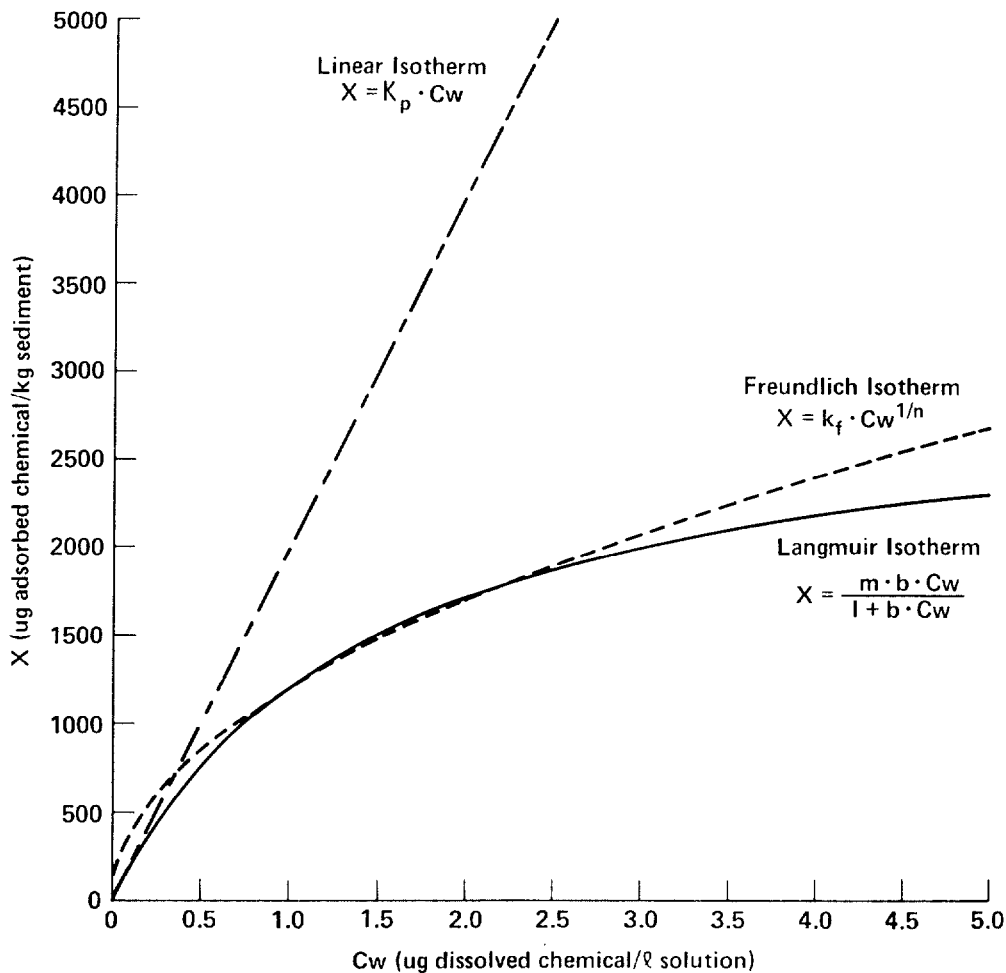


Figure II-4 ISOTHERMS FOR ADSORPTION OF A HYDROPHOBIC POLLUTANT ON SEDIMENTS

volume of solution. The remaining variables are unknown parameters required to define the relationship between X and  $C_w$ . The linear isotherm has one unknown parameter ( $K_p$ ), while both the Freundlich and Langmuir isotherms have two unknown parameters ( $k_f, n$  and  $m, b$ , respectively).

For the purposes of this document, analyses will mostly deal with dilute aqueous solution in the range where the linear isotherm is generally valid. This approach has the advantage of requiring that one unknown parameter ( $K_p$ ) be evaluated, rather than two, and of being easier to manipulate mathematically. Section 2.3.2.4 will present methods of predicting the unknown parameter  $K_p$ .

### 2.3.2.3 Kinetics of Adsorption

Sorption of organic pollutants is often treated as a process which achieves rapid equilibrium so that expressions of kinetics are not needed. The equilibrium approach will be used in the remaining chapters of this document. However, a brief

introduction will be given of sorption kinetics.

Studies of sorption kinetics are apparently few, with the result that parameters required in rate expressions are ill defined and applicable only under a specific set of conditions. Under these constraints, kinetics expressions become less attractive unless the user can determine values of the rate constants which apply to the specific system being investigated.

Most typically, kinetics expressions for sorption and desorption are chosen to be first order. Specifically:

$$\frac{\partial C_w}{\partial t} = -k_d C_w \quad (11-14)$$

express the kinetic expression for the sorbate and

$$S \frac{\partial X}{\partial t} = -k_d X \quad (11-15)$$

for the sorbate. The concentrations  $X$  and  $C_w$  are not necessarily equilibrium concentrations. In these two equations, the rate constant for adsorption is  $k_a$  and for desorption is  $k_d$ . When the rates of adsorption and desorption are equal, Equations 11-14 and 11-15 can be equated, with the result that  $X = K_p C_w$ , where  $K_p = k_a/k_d$ .

Karickhoff (1979) investigated the sorption and desorption of organic pollutants and found that a very rapid component of adsorption preceded a much slower component of adsorption, and that first order kinetics were obeyed during each of the two periods. For the fast process, the time constant was found to range from 4 to 30 per hour, while for the slow process the time constant ranged from 0.06 to 1.5 per hour. Approximately half of the sorptive equilibrium was realized within minutes, while the slower component required days or weeks to complete. The slower second period was visualized as diffusive transfer to sorption sites that were inaccessible directly to the bulk water. Thus, equilibrium conditions are more likely to be rapidly attained when the number of easily accessible surface sites exceeds the amount of available sorbate, e.g. when suspended sediment concentrations are high.

#### 2.3.2.4 Partition Coefficients for Organic Chemicals Obeying Linear Isotherms

The single unknown parameter,  $K_p$ , which relates the sorbate and solute for linear isotherms is called the partition coefficient. A number of studies have been completed which develop empirical relationships for partition coefficients in natural sediments. Several of these studies will be summarized here. Theoretically based methods of estimating partition coefficients exist, such as a thermodynamic approach described in Pavlou (1979); however, these will not be discussed here.

Karickhoff et al. (1979) examined the sorption of aromatic hydrocarbons and chlorinated hydrocarbons on natural sediments. They found it convenient to relate the partition coefficient directly to organic carbon content of the sediments as follows:

$$K_p = K_{oc} x_{oc} \quad (11-16)$$

where

$K_{oc}$  = partition coefficient expressed on an organic carbon basis

$x_{oc}$  = mass fraction of organic carbon in sediment.

These workers were able to expand this relationship to segregate the influence of particle size as follows:

$$K_p = K_{oc} [0.2(1-f)x_{oc}^s + fx_{oc}^f] \quad (11-17)$$

where

$f$  = mass fraction of fine sediments ( $d < 50 \mu m$ )

$x_{oc}^s$  = organic carbon content of coarse sediment fraction

$x_{oc}^f$  = organic carbon content of fine sediment fraction.

Karickhoff et al. (1979) were able to relate  $K_{oc}$  to the octanol-water partition coefficient and to the water volatility by the following relationships:

$$K_{oc} = 0.63 K_{ow} \quad (11-18)$$

where

$K_{ow}$  = octanol-water partition coefficient (concentration of chemical in octanol divided by concentration of chemical in water, at equilibrium)

and

$$K_{oc} = -0.54 \log S_w + 0.44 \quad (11-19)$$

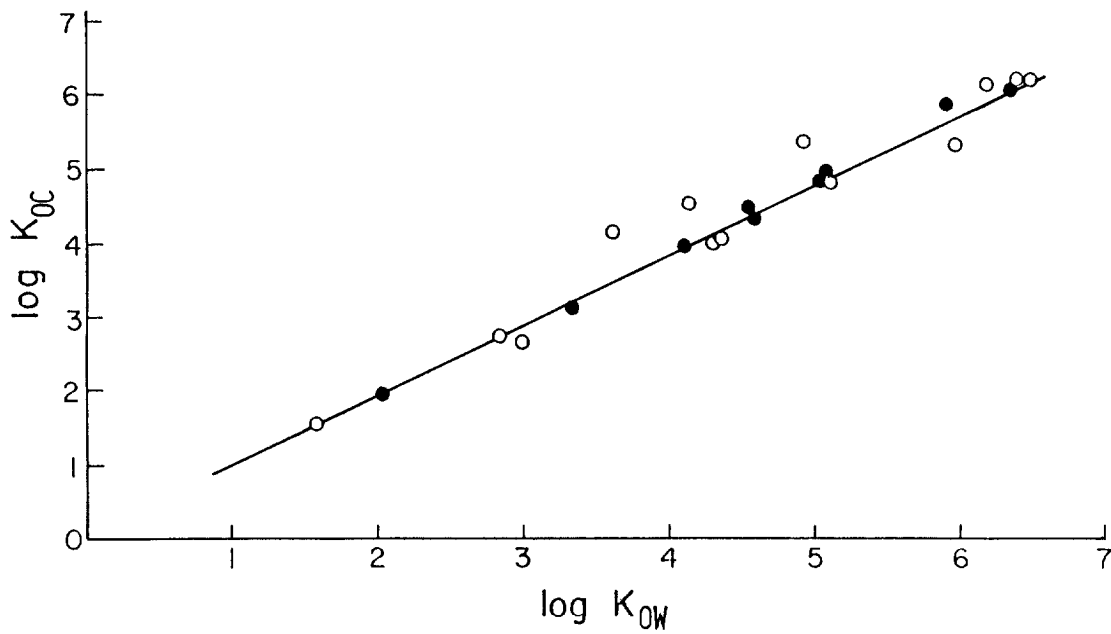
where

$S_w$  = water volatility of sorbate, expressed as a mole fraction.

The water solubilities of the compounds examined ranged from 1 ppb to 1000 ppm.

Hassett et al. (1980) found a similar relationship between  $K_{oc}$  and  $K_{ow}$  for organic energy-related pollutants. Figure 11-5 shows the relationship. Data from Karickhoff et al. are included in the plot for comparison.

Prior to the work of Karickhoff et al., Chiou et al. (1977) investigated the relationship between octanol-water partitioning and aqueous solubilities for a wide variety of chemicals including aliphatic and aromatic hydrocarbons, aromatic



REFERENCE: HASSETT ET AL. (1980)

FIGURE II -5 RELATIONSHIP BETWEEN  $K_{OC}$  AND OCTANOL-WATER PARTITION COEFFICIENT ( $K_{OW}$ ) OF ENERGY-RELATED ORGANIC POLLUTANTS

acids, organochlorine and organophosphate pesticides, and polychlorinated biphenyls. Their results, shown in Figure II-6, cover more than eight orders of magnitude in volatility and six orders of magnitude in the octanol-water partition coefficient. The regression equation based on this figure is:

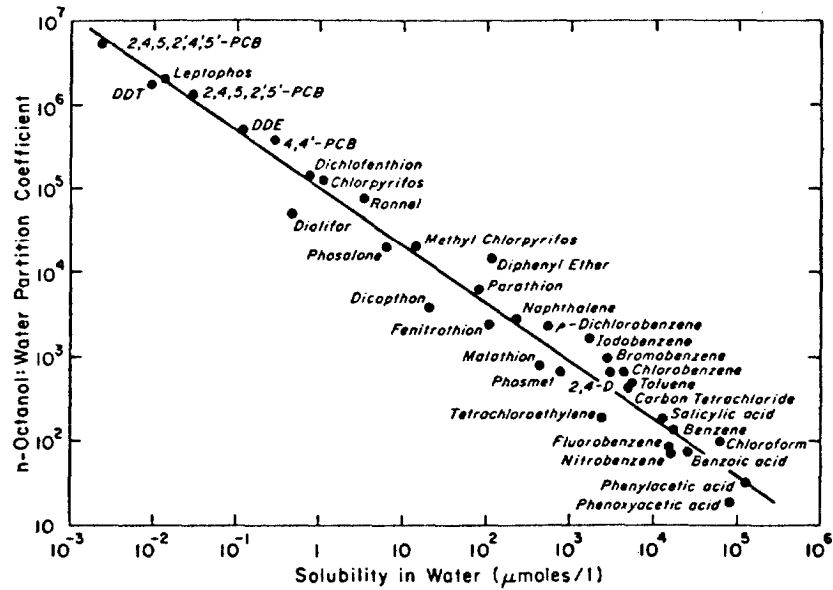
$$\log K_{ow} = 5.00 - 0.670 \log S_w \quad (11-20)$$

where

$$S_w = \text{volubility, in } \mu\text{mol/l.}$$

Bowman and Saris (1983) report additional  $K_{ow}$  versus  $S_w$  relationships. Leo et al. (1971) have tabulated  $K_{ow}$  values for thousands of organics. Subsequent to their work in 1971, they have determined  $K_{ow}$  values for many additional compounds.

Brown and Flagg (1981) have extended the work of Karickhoff et al. by developing an empirical relationship between  $K_{ow}$  and  $K_{oc}$  for nine chloro-s-triazine and dinitroaniline compounds. They plotted their results, along with those of Karickhoff et al., as shown in Figure II-7. The combined data set produces the following correlation:



REFERENCE: CHIOU ET AL. (1977)

FIGURE 11-6 CORRELATION OF AQUEOUS VOLUBILITY WITH OCTANOL-WATER PARTITION COEFFICIENT

$$\log K_{oc} = 0.937 \log K_{ow} - 0.006 \quad (11-21)$$

The linear correlation between  $K_{oc}$  and  $K_{ow}$  for the compounds studied by Brown and Flagg has a larger factor of uncertainty than those studied by Karickhoff et al. Other relationships between  $K_{oc}$  and  $K_{ow}$  for specific groups of compounds are reported in Karickhoff (1984).

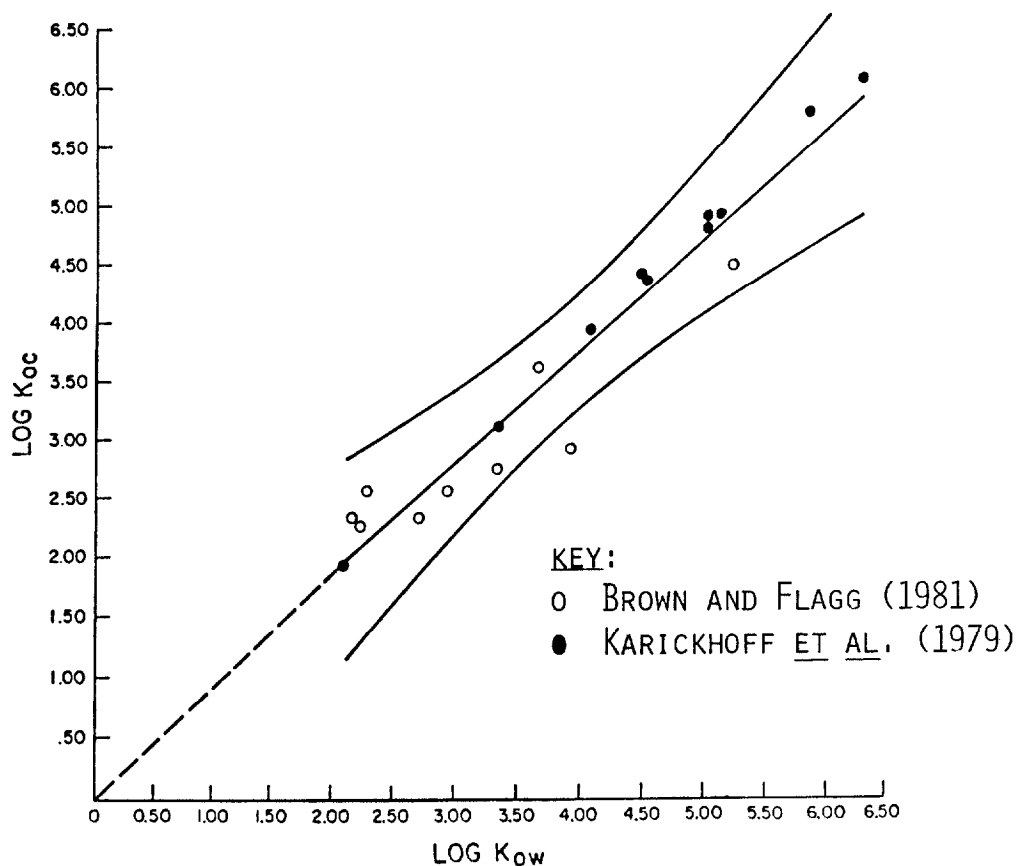
The previous paragraphs have shown how the partition coefficient  $K_p$  can be predicted for organic hydrophobic compounds which obey a linear isotherm relationship. First,  $K_{oc}$  is predicted based on either water volubility or the octanol-water partition coefficient. Tables 11-5 through 11-9 shown earlier contain  $K_{ow}$  values for a number of compounds. Then based on an estimate of organic carbon fraction in the fine and coarse sediments,  $K_p$  can be estimated from Equation 11-17. This procedure is summarized in Table 11-15.

### 2.3.2.5 Solute and Sorbate Fractions

The relative amount of pollutant sorbed and dissolved depends on both the suspended sediment concentration and the partition coefficient, and at equilibrium is given by:

$$\alpha_w \equiv \frac{C_w}{C_T} = \frac{1}{1 + K_p S} \quad (11-22)$$





Note: The actual error bands for this figure are probably greater than indicated here due to error in the measurement of  $K_{ow}$ .

FIGURE II-7 RELATIONSHIP BETWEEN  $K_{oc}$  AND  $K_{ow}$  FOR COARSE SILT

where

$C_w$  = total dissolved phase concentration

$C_T = C_w + C_s$

$C_s = XS$

$K_p$  = partition coefficient

$S$  = suspended sediment concentration, on a part per part basis

$X$  = mass of sorbed pollutant per mass of suspended sediment.

Equation II-22 can be illustrated more vividly by tabulating ranges of  $K_p$  and  $S$  values. Table 11-16 shows this information. Partition coefficients and suspended sediment concentrations range from  $10^0$  to  $10^4$ . For the lowest value of the partition coefficient nearly all of the pollutant is present in the dissolved form, regardless of the suspended sediment concentration. Also, for low suspended sediment concentrations, nearly all of the pollutant is dissolved, unless the partition coefficient is extremely large. When relatively high partition coefficients and sediment concentrations occur simultaneously, then most of the

TABLE II-15

PROCEDURE FOR CALCULATING PARTITION COEFFICIENT

1. Partition Coefficient

$$K_p = K_{oc} \left[ 0.2 (1-f) x_{oc}^S + f x_{oc}^f \right] \quad (1)$$

2. Procedure

a. Find  $K_{ow}$  (octanol-water partition coefficient)

(1) Use Tables II-5 through II-9

for priority pollutants.  $K_{ow} =$    
 OR, If the value is not tabulated:

(2) Estimate  $K_{ow}$  by:

$\log K_{ow} = 5.00 - 0.670 \log S_w =$    
 where  $S_w =$  solubility,  $\mu\text{mole/l}$

$$S_w (\mu\text{mole/l}) = \frac{S_w (\text{mg/l})}{\text{molecular weight}} \times 10^3$$

Use Tables II-5 through II-9 to find  $S_w$  (mg/l)

b. Find  $K_{oc}$ :

$$K_{oc} = 0.63 K_{ow} = \text{_____}$$

(2)

c. Estimate:

(1)  $f$  (mass fraction of silt or clay) = \_\_\_\_\_, ( $0 \leq f \leq 1$ ;

$f = 1$ , if all suspended solids are silts and clays

$f = 0$ , if all suspended solids are sands)

(2)  $x_{oc}^S$  (organic carbon content of sand, 0.00-0.05 typically) = \_\_\_\_\_

(3)  $x_{oc}^f$  (organic carbon content of silt-clay, 0.03 - 0.10 typically) = \_\_\_\_\_

3. Substitute:  $K_{oc}$ ,  $f$ ,  $x_{oc}^f$ ,  $x_{oc}^S$  into Equation (1).

$$K_p = \text{_____}$$

4. Typical Value for  $K_p = 0.01 K_{ow}$

Maximum Value for  $K_p = 0.065 K_{ow}$

TABLE II-16  
RELATIONSHIP OF DISSOLVED AND SORBED PHASE POLLUTANT  
CONCENTRATIONS TO PARTITION COEFFICIENT AND  
SEDIMENT CONCENTRATION

$K_p$	S (ppm)	$C_w/C_T$	If $C_T = 100$ ppb		
			$C_w =$	$X =$	$C_s =$
$10^0$	1	1.0	100.	100.	0.0
	10	1.0	100.	100.	0.0
	100	1.0	100.	100.	0.0
	1000	1.0	100.	100.	0.0
	10000	1.0	99.	99.	1.0
$10^1$	1	1.0	100.	$1 \times 10^3$	0.0
	10	1.0	100.	$1 \times 10^3$	0.0
	100	1.0	99.9	999.	0.1
	1000	1.0	99.0	990.	1.0
	10000	0.9	90.9	909.	9.1
$10^2$	1	1.0	100.	$1 \times 10^4$	0.0
	10	1.0	99.9	$1 \times 10^4$	0.1
	100	1.0	99.0	$9.9 \times 10^3$	1.0
	1000	0.9	90.9	$9.1 \times 10^3$	9.1
	10000	0.5	50.	$5 \times 10^3$	50.
$10^3$	1	1.0	99.9	$1 \times 10^5$	0.1
	10	1.0	99.0	$9.9 \times 10^4$	1.0
	100	0.9	90.9	$9.1 \times 10^4$	9.1
	1000	0.5	50.	$5 \times 10^4$	50.
	10000	0.1	9.1	$9 \times 10^3$	90.9
$10^4$	1	1.0	99.0	$9.9 \times 10^5$	1.0
	10	0.9	90.9	$9.1 \times 10^5$	9.1
	100	0.5	50.	$5 \times 10^5$	50.
	1000	0.1	9.1	$9.1 \times 10^4$	90.9
	10000	0.0	1.0	$9.9 \times 10^3$	99.0

pollutant present exists as sorbate. For all the cases shown, X is high which indicates that the mass sorbed per unit mass of sediment present can be high while  $C_s$  is simultaneously low.

----- EXAMPLE 11-3 -----

Determine the fraction of benzo(a)pyrene that is dissolved in a system containing 300 ppm suspended solids. The suspended sediments are 70 percent fines ( $d < 50 \mu\text{m}$ ) and the weight fraction of organic carbon is 10 percent of the fines and 5 percent of the sand fraction.

From Table 11-9, the volatility of benzo(a)pyrene is 0.0038mg/l, and the octanol-water partition coefficient is  $10^6$ . If, for the moment, the octanol-water partition coefficient is ignored, Equation 11-20 can be used to predict  $K_{ow}$  based on volatility. The volatility of 0.0038mg/l must be converted to mole/l:

$$\begin{aligned} S_w &= (0.0038 \text{ mg/l}) (10^{-3} \text{ g/mg}) \left(\frac{1 \text{ mole}}{252 \text{ gm}}\right) (10^6 \frac{\mu\text{mole}}{\text{mole}}) \\ &= 0.015 \mu\text{mole/l} \end{aligned}$$

From Equation 11-20, the predicted octanol-water partition coefficient is:

$$\begin{aligned} \log K_{ow} &= 5.00 - 0.670 \log (.015) \\ &= 6.22 \end{aligned}$$

so  $K_{ow} = 10^{6.22}$ , which is acceptably close to the tabulated value of  $10^6$ .

Using the tabulated  $K_{ow}$ ,  $K_{oc}$  is computed from Equation 11-18:

$$\begin{aligned} K_{oc} &= 0.63 \times 10^6 \\ &= 630,000 \end{aligned}$$

From Equation 11-17, the partition coefficient becomes:

$$\begin{aligned} K_p &= 630,000 [0.2 (1-.7) (.05) + 0.7 (.10)] \\ &= 46,000 \end{aligned}$$

The suspended sediment concentration for the system is 300 ppm, or  $300 \cdot 10^{-6}$  parts per part. Using Equation 11-22, the fraction of benzo(a)-pyrene which is dissolved is:

$$\begin{aligned} \frac{C_w}{C_T} &= \frac{1}{1 + 300 \cdot 10^{-6} \cdot 46,000} \\ &= 0.067 \text{ or about 7 percent} \end{aligned}$$

Consequently, most of the benzo(a)pyrene is present as sorbate.

----- END OF EXAMPLE 11-3 -----

## 2.4 TRANSPORT PROCESSES

### 2.4.1 Volubility Limits

The concentration of a compound in a natural water, and therefore the rate of transport by that water, can be limited by its equilibrium volubility. The aqueous volubility of organic compounds ranges widely:

<u>Compound</u>	Aqueous Volubility at 25°C (mass which will dissolve in 1 liter of water)	
	<u>(in milligrams)</u>	
Sucrose	2,000,000	
Benzene	2,000	
Toxaphene	2	
Chrysene	0.002	

Non-polar compounds have limited solubilities in polar solvents such as water. The volubility of toxic organic compounds is generally much lower than for inorganic salts. Equilibrium solubilities for toxic organic compounds are given in Tables II-5 through II-9. Volubility increases with temperature for most organic compounds, typically by a factor of about 3 from 0°C to 30°C.

Organics are generally less soluble in sea water than in fresh water as can be seen in the tabulations below (Rossi and Thomas, 1981):

<u>Compound</u>	Volubility at 25°C	
	<u>Distilled Water</u> (mg/l)	<u>Sea Water</u> (mg/l)
Toluene	507	419
Acenaphthene	2.41	1.84
Pyrene	0.13	0.09

In the absence of colloids or micelles, the maximum amount of a toxic organic substance which can be held in the water column under equilibrium conditions is just the aqueous equilibrium volubility  $S_w$ , plus the equilibrium amount of solute sorbed on suspended matter:

$$C_T = S_w + f_s(S_w) \quad (II-23)$$

where

$C_T$  = total amount of compound which can be held in a natural water at equilibrium conditions,  $\mu\text{g liter}^{-1}$

$S_w$  = equilibrium aqueous volubility,  $\mu\text{g liter}^{-1}$

$f_s(S_w)$  = equilibrium amount of sorbate on suspended matter; a function of  $S_w$ .  $f_s$  is the sorption isotherm function.

If a linear sorption isotherm is used, as is commonly the case for trace constituents (see Section 2.3.2), the above expression becomes:

$$C_T \leq S_w (1 + K_p S) \quad (11-24)$$

where

$K_p$  = linear partition coefficient (see Section 2.3.2.4), liter  $\text{Kg}^{-1}$

$S$  = the "concentration" of suspended matter (sorber),  $\text{Kg liter}^{-1}$

The inequality results in the above equation because at high solute concentrations linear isotherms overpredict the amount of solute sorbed. The use of linear sorption isotherms (a common practice for trace constituents) is adequate at pollutant concentrations which are equal to, or less than, one half of the equilibrium volatility. When linear sorption isotherms are used, e.g. those with the simple partition coefficient approach ( $K_p$ ) presented in Section 2.3.2, one must then check to insure that the aqueous pollutant concentration is less than or equal to one-half of its equilibrium volatility.

## 2.4.2 Volatilization

### 2.4.2.1 Introduction

Volatilization is defined as the transfer of matter from the dissolved to the gaseous phase. A considerable number of toxic substances volatilize in the natural environment. Volatilization rates depend on the properties of the toxicant and on the characteristics of the water body. If a toxicant is "highly volatile", then obviously volatilization is an important process affecting the fate of the toxicant. However, even for toxicants which are considerably less volatile, volatilization cannot always be ignored. This is because the fate of a toxicant is governed by a variety of processes. If volatilization proceeds as fast as other competing mechanisms, even though all the rates might be slow, then volatilization will influence the fate of the toxicant.

Methods will be provided in this section to predict the volatilization rate for toxic organic substances, which volatilize according to the following relationship:

$$\frac{\partial C}{\partial t} = \frac{k_v}{Z} \left( C - \frac{P}{K_H} \right) = -k'_v \left( C - \frac{P}{K_H} \right) \quad (11-25)$$

where

$C$  = concentration of toxicant in dissolved phase (concentration of solute)

$k_v$  = volatilization rate constant in units of length/time

$k'_v$  = volatilization rate constant in mixed water body in units of time<sup>-1</sup>

Z = mixed depth of water body

P = partial pressure of toxicant in atmosphere above the water body being investigated

$K_H$  = Henry's Law constant.

For many applications the partial pressure of the compound in the atmosphere is zero, so that Equation 11-25 simplifies to:

$$-\frac{\partial C}{\partial t} = -k'_v C \quad (11-26)$$

An alternate form of Equation 11-26 is in terms of the total pollutant concentration,  $C_T$ , and the site specific volatilization rate constant,  $k_{vm}$ :

$$\frac{\partial C_T}{\partial t} = -k_{vm} C_T \quad (11-27)$$

where

$$k_{vm} = \frac{k_v \alpha_w}{Z} \quad (11-28)$$

where

$\alpha_w$  = fraction of toxicant present in dissolved phase.

The following sections will illustrate how to predict the volatilization rate for toxicants of either low or high volatility. But first, a brief discussion of Henry's Law is required.

#### 2.4.2.2 Henry's Law

Henry's Law is an expression which relates the concentration of a chemical dissolved in the aqueous phase to the concentration (or pressure) of the chemical in the gaseous phase when the two phases are at equilibrium with each other. One common method of expressing Henry's Law is:

$$P = K_H C_w \quad (11-29)$$

where

P = equilibrium partial pressure of pollutant in atmosphere above the water, atm

$C_w$  = equilibrium concentration of pollutant in the water, mole/m<sup>3</sup>

$K_H$  = Henry's Law constant, atm m<sup>3</sup>/mole.

Henry's Law in this form is valid for pollutants present in concentrations up to 0.02 expressed as a mole fraction. For compounds with molecular weights greater than 50 g/mole, a mole fraction of 0.02 represents a concentration of at least 55,000 mg/l.

Typically toxic pollutants in the environment are present at levels far below this concentration.

Table 11-17 contains values of Henry's Law constants for a number of selected hydrocarbons. In the table, Henry's Law constant is expressed in units of atm m<sup>3</sup>/mole. However, in the literature Henry's Law constant can be defined in numerous ways. A second, widely used method of defining Henry's Law constant is:

$$K'_H = \frac{C_a}{C_w} \quad (11-30)$$

where

$C_a$  = molar concentration in air, mole/m<sup>3</sup>

$K'_H$  = alternate form of Henry's Law constant, dimensionless.

Equations 11-29 and 11-30 are related as follows:

$$K'_H = \frac{K_H}{R_u T_k} = \frac{K_H}{8.2 \times 10^{-5} T} = 41.6 K_H \text{ at } 20^\circ\text{C} \quad (11-31)$$

where

$T_k$  = temperature of water, °K.

$R_u$  = universal gas constant.

This relationship is based on the ideal gas law. Equation 11-31 is useful because of the frequent necessity to convert literature data from one set of units to another.

Henry's Law constant can be estimated for slightly soluble compounds (mole fraction  $\leq 0.02$ ) by the following expression:

$$K_H \text{ (atm}\cdot\text{m}^3\text{/mole)} = \frac{P_s \times MW}{760 \times S_w} \quad (11-32)$$

where

$P_s$  = saturation vapor pressure of pure compound in Torr

MW = molecular weight

$S_w$  = solubility in water in ppm.

Figure 11-8 illustrates the limits of Henry's Law for an acetone-water mixture. Henry's Law is obeyed by acetone in region B (mole fraction of acetone  $\leq 0.1$ ) and by water in region A (mole fraction of acetone  $\geq 0.95$ ). Notice that the generally accepted limit of validity of Henry's Law (mole fraction  $\leq 0.02$ ) corresponds to concentrations of 34,000 mg/l to 227,000 mg/l for compounds with molecular weights between 30 to 200. Thus Henry's Law is likely to be applicable in nearly all cases of concern in the natural environment. For pollutants which happen to be largely soluble, however, care must be taken to calculate Henry's Law by some method other than Equation 11-32.



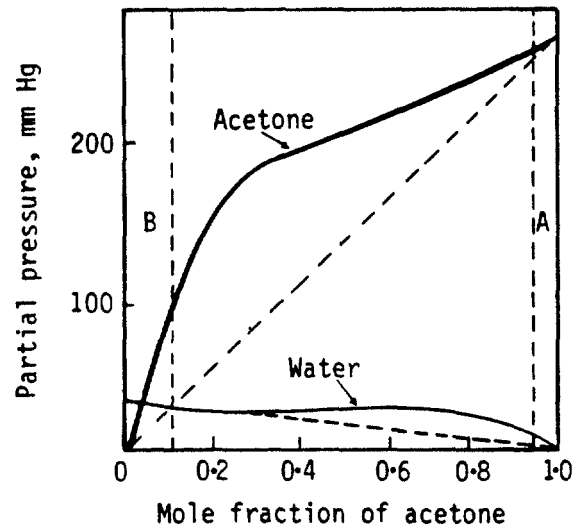
TABLE II-17

## HENRY'S LAW CONSTANT FOR SELECTED HYDROCARBONS

Olefins and Acetylenes	Henry's Law Constant (atm. m <sup>3</sup> /mole)	k <sub>v</sub> (cm/hr) <sup>a</sup>	Aromatics	Henry's Law Constant (atm. m <sup>3</sup> /mole)	k <sub>v</sub> (cm/hr) <sup>a</sup>
Ethene (g)	0.214	20.	Benzene (L)	5.49x10 <sup>-3</sup>	19.4
Propene (g)	0.232	20.	Toluene (L)	6.66x10 <sup>-3</sup>	19.5
1-Butene (g)	0.268	20.	Ethyl benzene (L)	8.73x10 <sup>-3</sup>	19.6
1-Pentene (L)	0.398	20.	<i>o</i> -Xylene (L)	5.27x10 <sup>-3</sup>	19.4
1-Hexene (L)	0.412	20.	Isopropyl benzene (L)	1.45x10 <sup>-2</sup>	19.8
2-Heptene (L)	0.418	20.	Naphthalene (s)	4.25x10 <sup>-4</sup>	14.5
1-Octene (L)	0.905	20.	Biphenyl (s)	6.36x10 <sup>-4</sup>	16.0
propyne (g)	0.0110	19.8	Acenaphthene (s)	2.28x10 <sup>-4</sup>	11.7
1-Butyne (g)	0.0194	20.	Fluorene (s)	2.35x10 <sup>-4</sup>	11.9
			Anthracene (s)	1.65x10 <sup>-7</sup>	18.2
			Phenanthrene (s)	1.48x10 <sup>-4</sup>	9.6
Cycloalkanes Branched-Chain Alkanes			<i>n</i> -Alkane		
Cyclopentane (L)	0.187	20.	Methane (g) <sup>a</sup>	0.665	20.
Cyclohexane (L)	0.196	20.	Ethane (g)	0.499	20.
Methyl cyclopentane (L)	0.362	20.	Propane (g)	0.707	20.
Methyl cyclohexane (L)	0.428	20.	<i>n</i> -Butane (g)	0.947	20.
Propyl cyclopentane (L)	0.893	20.	<i>n</i> -Pentane (L)	1.26	20.
Isobutane (g)	1.24	20.	<i>n</i> -Hexane (L)	1.85	20.
Isopentane (L)	1.364	20.	<i>n</i> -Heptane (L)	2.07	20.
2-Methyl pentane (L)	1.73	20.	<i>n</i> -Octane (L)	3.22	20.
2-Methyl hexane (L)	3.42	20.	<i>n</i> -Nonane (L)	3.29	20.
2,2-Dimethyl pentane (L)	3.15	20.	Decane (L)	4.93	20.
3-Methyl heptane (L)	3.71	20.	Dodecane (L)	7.12	20.
2,2,4-Tri methyl pentane (L)	3.04	20.	Tetradecane (L)	1.14	20.
4-Methyl octane (L)	9.936	20.			
Polychlorinated Biphenyls			Pesticides		
Aroclor 1242	5.7x10 <sup>-4</sup>	15.6	DDT	3.9x10 <sup>-5</sup>	3.9
Aroclor 1248	3.5x10 <sup>-3</sup>	18.9	Lindane	4.9x10 <sup>-7</sup>	0.06
Aroclor 1254	2.8x10 <sup>-3</sup>	18.9	Dieldrin	2.0x10 <sup>-7</sup>	0.02
Aroclor 1260	7.1x10 <sup>-3</sup>	19.6	Aldrin	1.4x10 <sup>-5</sup>	0.60
			Endrin	4.6x10 <sup>-7</sup>	0.06
			Heptachlor	1.5x10 <sup>-3</sup>	18.
			Chlordane	5x10 <sup>-5</sup>	4.8
			Toxaphene	0.1	19.8

<sup>a</sup> These are estimated values based on k<sub>1</sub> = 20 cm/hr and k<sub>2</sub> = 3000 cm/hr.

- Consider acetone-water mixture



- Henry's Law is obeyed:
  - by acetone when mole fraction of acetone  $\leq 0.1$  (Region B)
  - by water when mole fraction of acetone  $\geq 0.95$  (Region A)
- General range of validity: mole fraction  $\leq 0.02$

MW	Concentration when mole fraction = 0.02
30	34000 mg/l
75	85000 mg/l
100	113000 mg/l
200	227000 mg/l

FIGURE 11-8 RANGE OF VALIDITY OF HENRY'S LAW



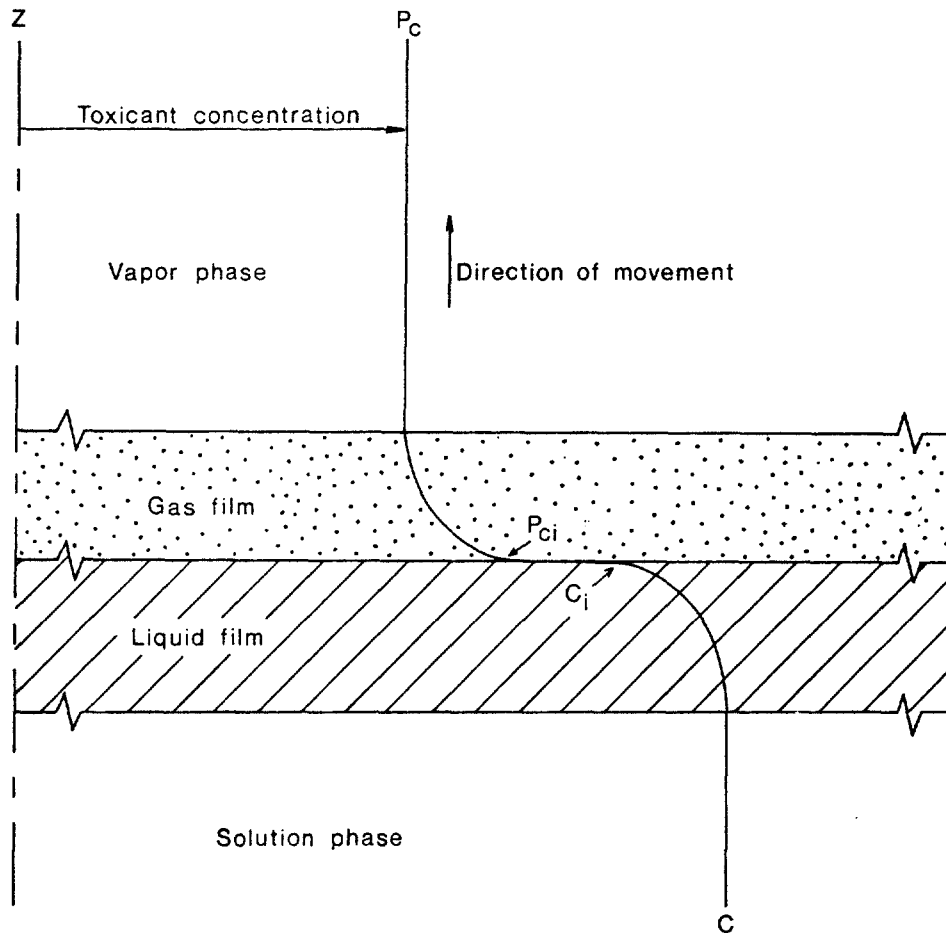


FIGURE 11-9 SCHEMATIC REPRESENTATION OF VOLATILIZATION FROM SOLUTION PHASE TO LIQUID PHASE

representation of the process. The concentration of the chemical is  $C$  in the bulk liquid solution. As the chemical moves upward in the bulk solution it moves through a thin "liquid film" where a concentration gradient develops because the transfer rate is limited by diffusion. The dissolved chemical then volatilizes and passes through a thin "gas film", where again transfer may be limited, before reaching the bulk vapor phase.

At the interface between the gas and liquid films the concentrations in the liquid ( $C_i$ ) and in the gas ( $P_{ci}$ , expressed as partial pressure) are assumed to be in equilibrium and to obey Henry's Law:

$$P_{ci} = K_H C_i \quad (11-34)$$

In the absence of net accumulation at the interface the mass flux from one phase must equal the mass flux from the other, or:

$$F_z = \frac{-k_{gi}}{R_u T} (P_c - P_{ci}) = k_{li} (C - C_i) \quad (11-35)$$

where

$F_z$  = flux of chemical in z direction

$k_{gi}$  = mass transfer coefficient in the gas phase across "gas film"

$k_{li}$  = mass transfer coefficient in the liquid phase across "liquid film"

$P_c, P_{ci}, C, C_i$  are defined in Figure 11-9.

Since it is not convenient to measure the partial pressure and concentration at the interface, it is worthwhile to develop expressions for bulk transfer coefficients, given by:

$$F_z = \frac{-k_{vg}}{R_u T} (P_c - P'_c) = k_{vl} (C - S_p) \quad (11-36)$$

where

$k_{vg}$  = overall volatilization rate defined for the gaseous phase

$k_{vl}$  = overall volatilization rate defined for the liquid phase

$S_p$  = saturation concentration of chemical in equilibrium with  $P_c$

$P'_c$  = partial pressure in equilibrium with  $C$ .

Combining Henry's Law equilibrium expressions with Equations 11-35 and 11-36 the overall volatilization rates become:

$$\frac{1}{k_{vg}} = \frac{1}{R_u T} \cdot \frac{K_H}{k_{li}} + \frac{1}{k_{gi}} \quad (11-37)$$

and

$$\frac{1}{k_{vl}} = \frac{1}{k_{li}} + \frac{R_u T}{K_H k_{gi}} \quad (11-38)$$

Of the two expressions, normally Equation 11-38 is more useful for the purposes of this document because the pollutants being analyzed are in the aqueous phase. To simplify terminology Equation 11-38 will be rewritten as:

$$\frac{1}{k_v} = \frac{1}{k_l} + \frac{R_u T}{K_H k_g} \quad (11-39a)$$

or

$$\frac{1}{k_v} = \frac{1}{k_l} + \frac{1}{K'_H k_g} \quad (11-39b)$$

where the second subscripts to each variable have been dropped. The volatilization rate,  $k_v$ , is the same as shown earlier in Equation 11-25 and depends on  $k_g$ ,  $K_H'$ , and  $k_l$ .

There are two special cases of Equation 11-39, depending on the value of Henry's Law constant. They are:

$$k_v = \begin{cases} k_l, & \text{for large } K_H' \text{ (liquid-phase limited)} & (11-40a) \\ K_H' k_g, & \text{for small } K_H' \text{ (gas-phase limited)} & (11-40b) \end{cases}$$

To make Equation 11-40 usable, "large" and "small" values of  $K_H'$  have to be defined. For cases when the liquid phase is limiting the transfer rate, a large fraction,  $R$ , of the total resistance exists in the liquid phase, or:

$$\frac{1}{k_l} = R \left( \frac{1}{k_v} \right) = R \left( \frac{1}{k_l} + \frac{1}{K_H' k_g} \right) \quad (11-41)$$

Similarly when the gas phase is limiting:

$$\frac{1}{K_H' k_g} = R \left( \frac{1}{k_v} \right) = R \left( \frac{1}{k_l} + \frac{1}{K_H' k_g} \right) \quad (11-42)$$

Equations 11-41 and 11-42 can be rearranged to express Henry's Law constant explicitly:

$$K_H' = \begin{cases} \frac{k_l}{k_g} \frac{R}{1-R}, & \text{for liquid-phase limited} & (11-43a) \\ \frac{k_l}{k_g} \frac{1-R}{R}, & \text{for gas-phase limited} & (11-43b) \end{cases}$$

At this point values for  $R$ ,  $k_l$ , and  $k_g$  must be specified. "Typical" values of  $k_g$  and  $k_l$  for surface waters are in the range of 20 cm/hr and 3,000 cm/hr, respectively. For  $R$  values of 0.83, 0.90, and 0.95, the phase limiting values of Henry's Law constants, converted to units of atm·m<sup>3</sup>/mole using Equation 11-31, are as follows:

<u>R</u>	<u>Henry's Constant (atm·m<sup>3</sup>/mole)</u>	
	<u>Liquid-phase Limited</u>	<u>Gas-phase Limited</u>
0.83	7.8 X 10 <sup>-4</sup>	3.3 x 10 <sup>-5</sup>
0.90	1.4 x 10 <sup>-3</sup>	1.8 X 10 <sup>-5</sup>
0.95	3 x 10 <sup>-3</sup>	8.4 X 10 <sup>-6</sup>

Hence, for Henry's Law constants larger than about  $1.0 \times 10^{-3}$  atm m<sup>3</sup>/mole most of the resistance to volatilization lies in the liquid phase, and for Henry's Law constants less than about  $1.0 \times 10^{-5}$  atm m<sup>3</sup>/mole, most of the resistance lies in the gas phase. When either of the two phases controls the volatilization rate, then the simplified Equation 11-40 can be used in lieu of Equation 11-39. The data in the tables presented earlier can be used to predict Henry's Law constant and then to decide whether the gas or liquid phase limits volatilization.

Based on the two-film model there are two methods which can be used to estimate volatilization rates. One approach is considerably more simple than the other. The simpler approach is based on the following reasoning. Using "typical" values of  $k_l$  and  $k_g$ ,  $k_v$  can be estimated based solely on  $K_H$  as the independent variable, where  $K_H$  is allowed to vary over its potential range of values. As Table 11-18 shows,  $K_H$  can vary by at least seven orders of magnitude. Based on this variability of Henry's Law constant, Table 11-19 presents the associated volatilization rates. As Henry's Law constant increases, the volatilization rate approaches 20 cm/hr, the liquid phase limiting rate. As Henry's Law constant decreases, so does the volatilization rate, with the lower limit being zero.

The second method of predicting  $k_v$  is based on finding  $k_g$  and  $k_l$  individually, rather than assuming typical values. The gas-phase transfer rate can be found based on the evaporation rate of water as outlined in Mills (1981). Mills showed that:

$$k'_g = 700 V \quad (11-44)$$

where

$k'$  = gas transfer rate for water vapor, cm/hr

$V$  = wind speed, m/sec.

This expression was derived from an empirical relationship shown in Linsley et al. (1979) for the evaporation of water. Liss (1973) conducted measurements in an experimental basin and found that:

$$k'_g = 1000 V \quad (11-45)$$

where the units are the same in Equation 11-44. Considering that the approaches used to develop Equations 11-44 and 11-45 are different, their agreement is good. Still other relationships exist between  $k'_g$  and  $V$  (e.g. Rathbun and Tai, 1983).

The values of  $k_g$  and  $k'_g$  are related by penetration theory (Bird et al. 1960) as follows:

$$k_g = \left( \frac{D_a}{D_{wv}} \right)^{1/2} k'_g \quad (11-46)$$

TABLE 11-18

HENRY'S LAW CONSTANTS FOR SELECTED COMPOUNDS

Compound	Henry's Law Constant ( $\text{atm}\cdot\text{m}^3/\text{mole}$ )
Vinyl Chloride	3.7
Carbon Tetrachloride	$2 \times 10^{-2}$
Toluene	$6.7 \times 10^{-3}$
Aroclor 1254	$2.8 \times 10^{-3}$
Flourene	$2.4 \times 10^{-4}$
DDT	$3.9 \times 10^{-5}$
Dieldrin	$2.0 \times 10^{-7}$

TABLE 11-19

TYPICAL VALUES OF POLLUTANT VOLATILIZATION RATES  
IN SURFACE WATERS

$K_H(\text{atm}\cdot\text{m}^3/\text{mole})$	$K_H'(\text{dimensionless})$	$k_v(\text{cm/hr})^*$	$k_v(\text{l/day})^{**}$	
$10^0$	41.6	201	4.8	Liquid-film limited
$10^{-1}$	4.2	20.	4.8	
$10^{-2}$	$4.2 \times 10^{-1}$	19.7	4.7	
$10^{-3}$	$4.2 \times 10^{-2}$	17.3	4.2	
$10^{-4}$	$4.2 \times 10^{-3}$	7.7	1.8	
$10^{-5}$	$4.2 \times 10^{-4}$	1.2	0.3	
$10^{-6}$	$4.2 \times 10^{-5}$	0.1	0.02	Gas-film limited
$10^{-7}$	$4.2 \times 10^{-6}$	0.01	0.002	

\*Using  $k_g = 3000 \text{ cm/hr}$   
 $k_l = 20 \text{ cm/hr}$ .  
 \*\*For water depth = 1 m.



where

$D_a$  = diffusion coefficient of pollutant in air

$D_{wv}$  = diffusion coefficient of water vapor in air.

Diffusion coefficient data can be found in such references as Perry and Chilton (1973), or estimated using the Wilke-Chang method, also in Perry and Chilton. If an analytical method is used to estimate diffusion coefficients, note that it is easier to predict the ratio of two diffusion coefficients than to predict each coefficient individually because some of the required information cancels out of the ratio, and consequently is not needed at all.

In many cases it is acceptable to approximate the ratio of diffusion coefficients as follows:

$$\frac{D_a}{D_{wv}} = \left( \frac{18}{MW} \right)^{1/2} \quad (11-47)$$

where

MW = molecular weight of pollutant.

Table 11-20 illustrates the difference between calculating the diffusion coefficient ratio by using tabulated data from Perry and Chilton and by using Equation 11-47. The percent differences between the ratios range from 1 to 27 percent and average 15 percent. This agreement is acceptable for screening purposes. Combining Equations 11-46, 11-44, and 11-47, the final expression for  $k_g$  (in units of cm/hr) is:

TABLE 11-20  
COMPARISON OF TABULATED AND PREDICTED VALUES OF DIFFUSION  
COEFFICIENTS FOR SELECTED POLLUTANTS

Pollutant	Molecular Weight	Diffusion Coefficient		Perry & Chilton	Predicted	Percent Difference
		& Chilton (cm <sup>2</sup> /sec)	Predicted (cm <sup>2</sup> /sec)	$\left( \frac{D_a}{D_{wv}} \right)^{1/2}$	$\left( \frac{D_a}{D_{wv}} \right)^{1/2}$	
Chlorobenzene	113	0.075	0.088	.58	.63	9
Toluene	92	0.076	0.097	.59	.66	12
Chloroform	119	0.091	0.086	.64	.63	1
Naphthalene	128	0.051	0.083	.48	.61	27
Anthracene	178	0.042	0.070	.44	.56	27
Benzene	78	0.077	0.106	.59	.69	17

$$k_g = 700 \left( \frac{18}{MW} \right)^{1/4} v \quad (11-48)$$

This expression is valid for rivers, lakes, and estuaries.

The liquid phase transfer coefficient  $k_l$  can be predicted based on the reaeration rate,  $k_a$ , for the system. The relationship proposed by Smith et al. (1981) is:

$$k_l = \left( \frac{D_w}{D_{O_2}} \right)^n k_a', \quad 0.5 \leq n \leq 1 \quad (11-49)$$

where

- $D_w$  = diffusion coefficient of pollutant in water
- $D_{O_2}$  = diffusion coefficient of dissolved oxygen in water
- $k_a'$  = surface transfer rate of dissolved oxygen, expressed in the same units as  $k_l$ .

In other chapters of this report, the reaeration rate is presented as  $k_a$ , defined as:

$$k_a = k_a' / Z \quad (11-50)$$

where

- $Z$  = mixed depth of water body.

For rivers the mixed depth is the total depth, while for estuaries the mixed depth is the total depth only if the estuary is well mixed. Otherwise, it is the depth to the pycnocline. Similarly for lakes, the mixed depth can be less than the total depth and can be chosen to be the depth of the epilimnion.

The exponent  $n$  varies as a function of the theoretical approach used to develop Equation 11-49. If film theory is used, i.e., the film is considered to be a laminar sublayer, then  $n = 1$ . If penetration or surface renewal theory is used,  $n = 0.5$ . Using experimental approaches, researchers have found  $n$  to vary from 0.5 to 1.0. Since the movement of water in natural water bodies is generally turbulent, the parameter  $n$  can be chosen to be 0.5.

Perry and Chilton (1973) provide data and methods to predict the diffusion coefficient of a pollutant in water. The Othner-Thakor relationship, described in Smith et al. (1981) can also be used. As an approximate approach, by using the square root of the molecular weights the following expression results:

$$k_l = \left( \frac{32}{MMW} \right)^{1/2} k_a' \quad (11-51)$$

A recent study (Rathbun and Tai, 1981) used a tracer technique to predict the volatilization rates of four priority pollutants from 12 different rivers. That

study provides an opportunity to compare, even if only to a limited degree, some of the methods presented here against field results. Table 11-21 briefly summarizes the results of Rathbun and Tai (1981). As shown by the values of Henry's Law constant for the four pollutants, each pollutant is liquid phase limited, since all Henry's Law constants exceed  $1.0 \times 10^{-3} \text{ atm m}^3/\text{mole}$ . The study results were unable to predict differences in volatilization rates for the four pollutants, and found that the best predictive expression was:

$$k_v = 0.655 k'_a$$

Based on Equation 11-51 the screening methods predict:

$$k_v = 0.7 k'_a \text{ to } 0.8 k'_a$$

where the range reflects the variability in molecular weight among the four pollutants.

If the default value of 20 cm/hr, suggested earlier in this section were used as a rough estimate of the volatilization rate for liquid phase limited pollutants, this value would fall within the observed range of 1.5 to 24 cm/hr. It appears that the screening methods presented here generate acceptable estimates of volatilization rates.

Table 11-22 summarizes the two methods presented in the manual for calculating the volatilization rate constant  $k_v$ . The first approach is more simplified and is based on typical values of  $k_g$  and  $k_l$ . In the second approach,  $k_g$  and  $k_l$  are calculated rather than assumed.

#### 2.4.2.4 Volatilization Half-Life

Numerous researchers have in the past calculated the volatilization half-life of toxicants under controlled laboratory conditions. The result of some of this work was shown earlier in Tables 11-5 through 11-9. Typically, researchers have used the following expression to calculate the half-life:

$$t_{1/2} = \frac{0.693 Z}{k_v} \quad (11-52)$$

where

$t_{1/2}$  = half-life (time required for the concentration of the contaminant to decrease by half).

It is important to understand that the volatilization half-life of a toxicant varies according to the environmental conditions. Under controlled laboratory

TABLE 11-21  
VOLATILIZATION RATES OF SEVERAL PRIORITY POLLUTANTS IN 12 RIVERS<sup>a</sup>

Pollutant	Henry's Constant (atm·m <sup>3</sup> /mole)	Molecular Weight
Benzene	5.5 x 10 <sup>-3</sup>	119
Chloroform	2.9 x 10 <sup>-3</sup>	78
Methylene Chloride	2.7 x 10 <sup>-3</sup>	85
Toluene	6.7 X 10 <sup>-3</sup>	92

Study results showed:  $k_v = 0.655 k'_a$

Range of values for 12 rivers: 1.5 to 24 cm/hr

Screening method predicts:  $k_v = 0.7 k'_a$  to  $0.8 k'_a$

---

<sup>a</sup>Rathbun, R. E. and D. Y. Tai. 1981. Techniques for Determining the Volatilization Coefficients of Priority Pollutants in Streams. Water Research, Volume 15, pp. 243-250.

---

conditions, where the depth of water is extremely small,  $t_{1/2}$  can be extremely small. If the water depth increases by 100 fold, for example, so does  $t_{1/2}$ .

The volatilization half-life is affected by suspended solids in the system. When suspended solids are present, Equation 11-52 should be modified to:

$$t_{1/2} = \frac{0.693 Z}{k_v} (1 + SK_p) \quad (11-53)$$

where

S = suspended solids concentration

K<sub>p</sub> = partition coefficient.

The partition coefficient is the ratio of the sorbed pollutant concentration to the dissolved phase concentration. A method to predict K<sub>p</sub> was discussed earlier in Section 2.3.2. Since the toxicant which sorbs to the sediments is not directly available for volatilization, the total flux of volatilizing particles decreases. The following example illustrates how sorption can influence the half-life.

TABLE 11-22

PROCEDURE FOR PREDICTING VOLATILIZATION RATE

I: Simplified Approach

1. Input Henry's Law Constant (Table 11-17)
2. Procedure: Use Table 11-19
3. Result:  $k_v$  (cm/hr) = \_\_\_\_\_

To convert to units of per day:

$$k_v \text{ (per day)} = k_v \text{ (cm/hr)} \times \frac{24}{100Z} = \text{_____}$$

where

$z$  = depth of mixed surface layer, meters

II: Two-Film Theory Approach

$$\frac{1}{k_v} = \frac{1}{k_1} + \frac{1}{K_H k_g} \quad (1)$$

1. Input: Henry's Law Constant ( $K_H$ , atm x m<sup>3</sup>/mole) = \_\_\_\_\_  
 Wind speed ( $V$ , m/sec) = \_\_\_\_\_  
 Molecular weight of compound (MW) = \_\_\_\_\_  
 Reaeration rate ( $k'_a$ , cm/hr, or  $k_a$ , per day) = \_\_\_\_\_  
 Water temperature ( $T$ , °C) = \_\_\_\_\_  
 Water depth ( $Z$ , meters) = \_\_\_\_\_

2. Procedure

a. Find:  $K_H'$  (unitless) =  $\frac{K_H \text{ (atm x m}^3\text{/mole)}}{8.2 \times 10^{-5} (T + 273)}$  = \_\_\_\_\_ (2)

b. Find:  $k_g$  (cm/hr) =  $700 \left(\frac{18}{MW}\right)^{1/4} V$  =  (3a)

OR

$k_g$  (per day) =  $700 \left(\frac{18}{MW}\right)^{1/4} V \times \frac{24}{100Z}$  =  (3b)

c. Find:  $k_1$  (cm/hr) =  $\left(\frac{32}{MW}\right)^{1/4} k'_a$  =  (4a)

OR

$k_1$  (per day) =  $\left(\frac{32}{MW}\right)^{1/4} k_a$  =  (4b)

d. Find  $k_v$  (cm/hr):

$$\frac{1}{k_v} = \frac{1}{k_1} + \frac{1}{K_H' k_g} \Rightarrow k_v = \text{_____}, \text{ answer}$$

OR

Find  $k_v$  (per day):

$$\frac{1}{k_v} = \frac{1}{k_1} + \frac{1}{K_H' k_g} \Rightarrow k_v = \text{_____}, \text{ answer}$$

----- EXAMPLE 11-5 -----

The following data for hexachlorobenzene were obtained from Table 11-8:

$$\text{Volubility} = 20 \mu\text{g/l}$$

$$\text{Vapor pressure} = 10^{-5} \text{ Torr at } 20^\circ\text{C}$$

$$K_{ow} \approx 10^6.$$

Under the conditions reported in the work of Mackay and Leinonen (1975):

$$L = 1 \text{ m}$$

$$k_v = 8 \text{ cm/hr} = 8 \times 10^{-2} \text{ m/hr. m/hr.}$$

Hence:

$$t_{1/2} = \frac{0.693 \times 1}{8 \times 10^{-2}} = 8.7 \text{ hours}$$

Note that the half-life is small even though the vapor pressure is only  $10^{-5}$  Torr. The results indicate that the vapor pressure is, by itself, not necessarily a good indicator of the importance of volatilization.

Now, consider the following conditions which might be encountered in a river:

$$k_a \text{ (reaeration rate)} = 0.5/\text{day}$$

$$\text{Suspended sediment concentration} = 550 \text{ ppm}$$

$$K_p = 5 \times 10^4$$

$$\text{Depth} = 1 \text{ m.}$$

The expression of volatilization half-life modified to account for the presence of the suspended solids is:

$$t_{1/2} = \frac{0.693 Z}{k_v} (1 + S K_p)$$

From Equation 11-51, the liquid-phase transfer rate for hexachlorobenzene is:

$$k_1 = \left( \frac{32}{285} \right)^{1/2} \times 0.5 \times 1 = 0.29 \text{ m/day} = 0.01 \text{ m/hr} = 1 \text{ cm/hr}$$

Henry's Law constant can be estimated based on Equation 11-32. Using the data presented earlier:

$$K_H = \frac{10^{-5} \times 285}{760 \times .02} = 1.9 \times 10^{-4} \text{ atm}\cdot\text{m}^3/\text{mole}$$

or

$$K'_H = 7.8 \times 10^{-3}, \text{ dimensionless}$$

Using a default value of 3,000 cm/hr for  $k_g$ , the volatilization rate is:

$$\frac{1}{k_v} = \frac{1}{1} + \frac{1}{3000 \times 7.8 \times 10^{-3}} = 1.04 \text{ cm/hr}$$

so

$$k_v \approx 1.1 \text{ cm/hr}$$

The half-life becomes:

$$t_{1/2} = \frac{0.693 \times 1}{1 \times 10^{-2}} \left( 1 + \frac{550}{10^6} \times 5 \times 10^4 \right) = 1800 \text{ hr} = 75 \text{ days}$$

A comparison of half-lives shows that:

$$t = 8.7 \text{ hours under laboratory conditions}$$

$$t = 75 \text{ days under instream conditions.}$$

This example illustrates that half-lives are not always extrapolatable from one type of system to another due to the combined difference in sorption effects and volatilization rates.

----- END OF EXAMPLE II-5 -----

#### 2.4.2.5 Flux of Volatilizing Pollutants

The preceding sections have provided techniques for predicting volatilization rates of pollutants. Obviously, if the volatilization rate of one pollutant exceeds that of a second pollutant, then the first pollutant is more volatile than the second. However, this criterion alone does not determine whether volatilization is important in a specific situation. The volatilization flux is the rate at which mass is transferred to the gaseous phase from the liquid phase and is given by the following expression:

$$\text{Flux} = k_v C - \frac{P}{K_H} \quad (11-54)$$

$$= k_v C, \text{ when } P = 0 \quad (11-55)$$

where

C = concentration of pollutant in water as solute

P = partial pressure of pollutant in atmosphere.

Hence both the volatilization rate and the dissolved phase concentration have to be considered jointly to predict the flux being volatilized. Table II-23 illustrates

TABLE 11-23

## RELATIVE VOLATILIZATION MASS FLUXES OF SEVERAL CHEMICALS IN SATURATED SOLUTIONS

Chemical	Henry's Law Constant (atm·m <sup>3</sup> /mole)	Volatilization Rate Constant (cm/hr)	Volubility (ppm)	K <sub>ow</sub>	Flux Ratio <sup>a</sup>
Carbon Tetrachloride	2.3 × 10 <sup>-2</sup>	20.	785	400	1
DDT	3.9 × 10 <sup>-5</sup>	3.9	.002-.085	10 <sup>4</sup> -10 <sup>6</sup>	5×10 <sup>4</sup> -2×10 <sup>6</sup>
Dieldrin	2.0 × 10 <sup>-4</sup>	0.02	0.2		4 × 10 <sup>6</sup>
Phenanthrene	1.5 × 10 <sup>-3</sup>	9.6	1.0	29,000	2 × 10 <sup>3</sup>

<sup>a</sup>This is the ratio of volatilization flux of a saturated solution of carbon tetrachloride to the volatilization of the specified chemical,

these principals for several chemicals. The volatilization rates for these pollutants range from a high of 20 cm/hr for carbon tetrachloride to a low of 0.02 cm/hr for dieldrin. Anthracene has a volatilization rate constant of 18 cm/hr, 90 percent as high as the volatile carbon tetrachloride. However, the volubility of anthracene in water is much lower (0.06 ppm versus 785 ppm). Hence if each of these two chemicals were to volatilize from saturated solutions, the flux of carbon tetrachloride would be 15,000 times as great. The same type of comparison can be made for DDT and carbon tetrachloride. The volatilization rate constant for DDT is relatively high (about 20 percent that of carbon tetrachloride), but the volubility is so low that the ratio of volatilization flux would be about 100,000:1.

These comparisons have not considered the relative differences in sorption characteristics of the pollutants. Since only the solute volatilizes, the volatilization flux of a pollutant which is mostly sorbed to suspended material is lower than in the absence of suspended material, all other factors remaining the same. Tables 11-5 through 11-9 show the octanol-water partition coefficient, which provides a measure of relative importance of sorption for the four pollutants. Because both DDT and anthracene have higher octanol-water partition coefficients than does carbon tetrachloride, the ratio of volatilization of mass fluxes is likely to be even greater than calculated above for natural systems containing suspended material.

## 2.5 TRANSFORMATION PROCESSES

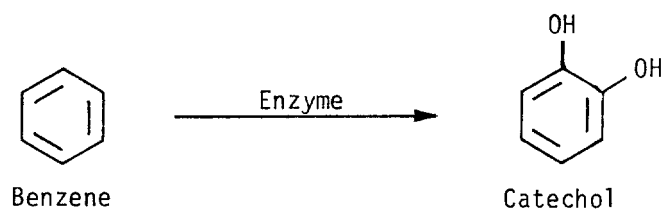
### 2.5.1 Biodegradation



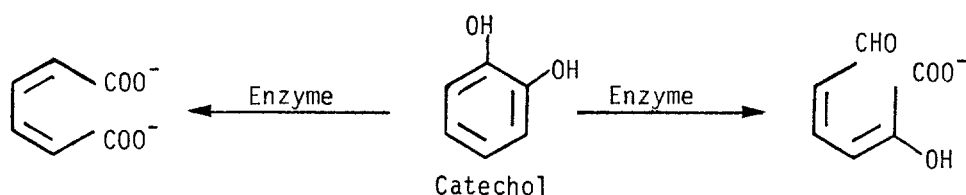
### 2.5.1.1 Introduction

Microorganisms are ubiquitous in the aquatic environment. Microbes are also very active chemically due to their ability to supply energy for reactions through normal metabolic processes and to catalyze reactions through enzymatic activity. Chemical reactions which proceed very slowly or not at all in the absence of biota occur at rates of up to eleven orders of magnitude faster in the presence of biological enzymes. Some of the reactions catalyzed by microorganisms transform or degrade organic pollutants. Frequently, microbial degradation, or biodegradation, is the most important, if not the only process which can decompose an organic pollutant in the aquatic environment.

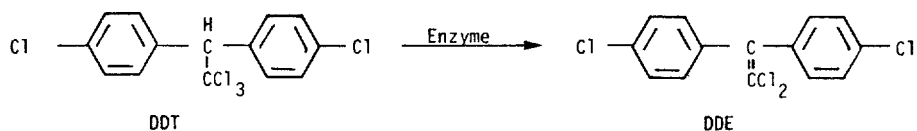
Although microbial communities catalyze countless reactions, many of them fall into a few classes of important reactions. Oxidative reactions make up one very important class of biochemical reactions. The hydroxylation of aromatic compounds, such as benzene, is an example of an oxidative reaction which generates polar compounds from non-polar ones:



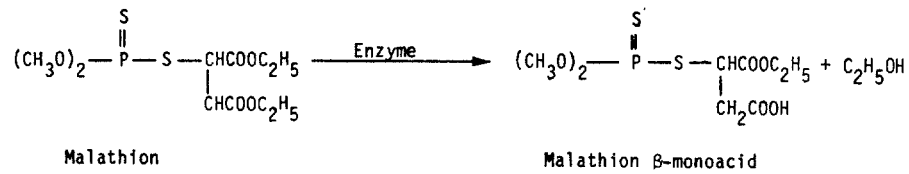
An extremely important oxidative reaction unique to microbial organisms is aromatic ring fission:



Microbes also catalyze reductive reactions. A notorious example is the dehydrochlorination of DDT to produce DDE:

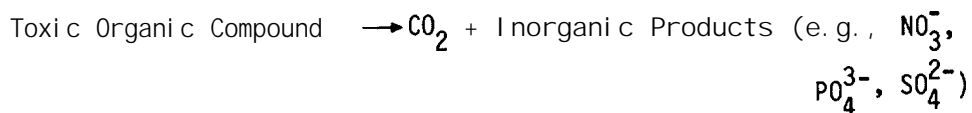


Enzymes can catalyze otherwise slow hydrolytic reactions as well:



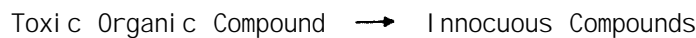
The term "biodegradation" encompasses these and other biologically mediated processes which chemically alter a pollutant. Although each reaction causes the disappearance or primary degradation of a compound, different reactions affect the toxicity of a compound in markedly different ways (Alexander, 1980).

"Mineralization" refers to the complete degradation of an organic compound to inorganic products:



In many reactions, however, organic products remain.

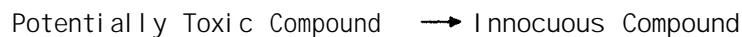
"Detoxification" reactions produce innocuous metabolites from a toxic substance:



In "activation" reactions, microbes convert an innocuous compound into a toxic compound:



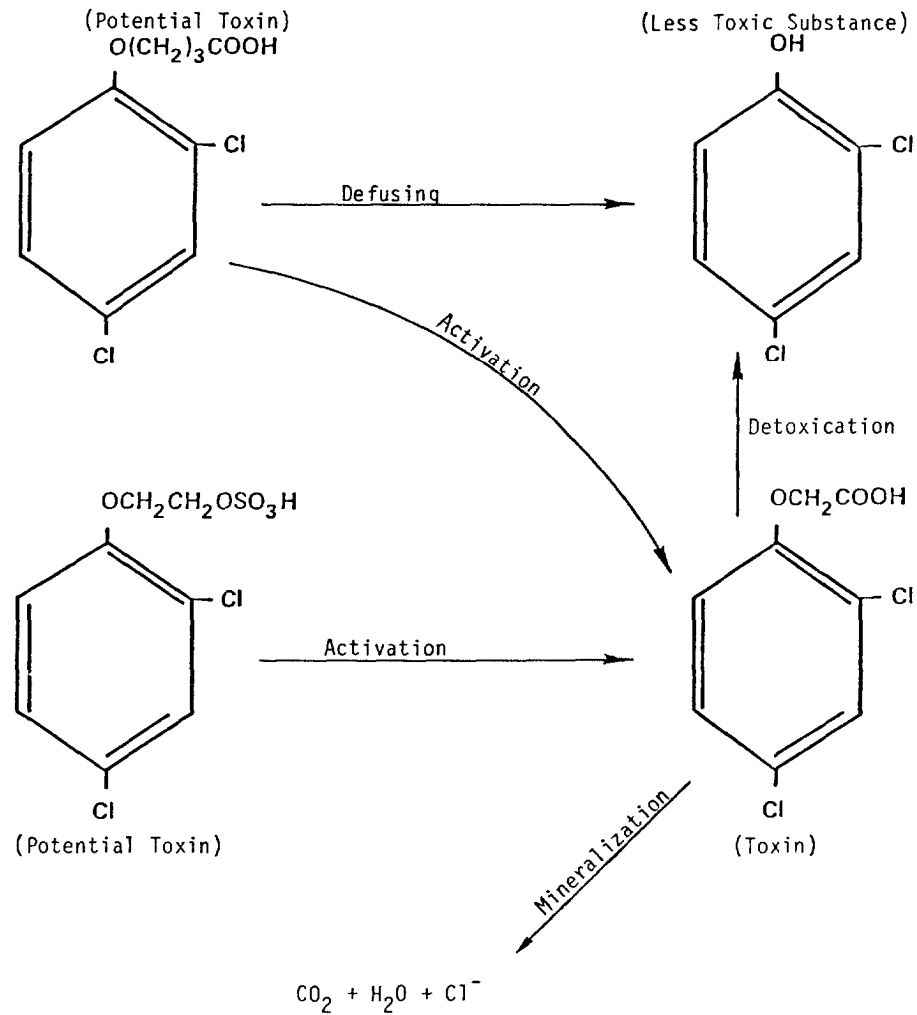
The "defusing" of potentially hazardous compounds occurs when biota produce an innocuous compound before the parent compound's harmful form is generated.



Finally, a toxic compound may be transformed chemically but still retain its toxicity. Figure 11-10 illustrates some of these types of reactions as they occur among the phenoxy herbicides.

Because of the wide variety of toxicological effects metabolic transformations may have, evaluating the impact of a compound on the environment requires a knowledge of the potential products which form. However, for the purposes of estimating the concentration of a pollutant in a natural water body, the user may simply consider biodegradation to be a decay process. Methods of estimating the rates of biodegradation constitute the subject matter of the remainder of this section.

MICROBIAL TRANSFORMATIONS OF TOXIC CHEMICALS



Source: Alexander (1980)

FIGURE 11-10 MICROBIAL TRANSFORMATIONS OF PHENOXY HERBICIDES

2.5.1.2 Rates of Biodegradation in the Environment

The rate at which a compound biodegrades in the aquatic environment depends on its role in microbial metabolism. Some organic pollutants serve as food sources which provide energy and carbon for growth and cell maintenance when metabolized by a microorganism. In other cases, microorganisms transform the pollutant, but are unable to derive energy for growth from the reaction. These two metabolic patterns, growth metabolism and cometabolism, exhibit distinct characteristics and rates of degradation. Because of the important differences between these two types of biodegradation, they are treated separately in the following discussion.

#### 2.5.1.2,1 Metabolism of Growth Substances

Heterotrophic bacteria degrade certain organic compounds to provide the energy and carbon required for their growth. Many toxic substances function as growth substrates for bacteria in a manner similar to naturally occurring organic compounds. These growth substrates are identifiable by their ability to serve as the sole carbon source for a bacterial culture. The metabolic transformation of these growth substrates generally results in relatively complete degradation or mineralization, thus detoxifying toxic growth substrates. The detoxifying effect and relatively rapid rates of growth metabolism imply that potential growth substrates pose a lesser threat to the environment than compounds which cannot be used in this way (Tiedje, 1980).

Before the utilization of a compound can begin, the microbial community must adapt itself to the chemical. Investigations of biodegradation of a compound to which the biota have not been recently exposed, both in the field (Spain *et al.* 1980) and in the laboratory (Shamat and Maier, 1980) have shown the existence of a lag time (lag phase) of 2 to 50 days before the microbial community acclimates. Since the degradation of a growth substrate is relatively rapid once a microbial population has adapted to it, Tiedje (1980) has suggested that the primary concern in assessing biodegradation of such substances should be the conditions and time period required for adaptation or acclimation.

The lag time depends on several biological and environmental constraints. The primary constraint is the development of a sufficiently large bacterial population which is capable of utilizing the pollutant as a growth substrate. Frequently, specific organisms with specific enzymes are required to metabolize a pollutant. The processes of species selection and enzyme induction by which a microbial community adapts itself to a pollutant require time. The adaptation time is influenced both by prior exposure of the community to a pollutant and the initial numbers of suitable species. Spain *et al.* (1980) have demonstrated that prior exposure to a compound reduces or eliminates the adaptation period. Thus, lag times in pristine environments should be much longer than in locations which have been chronically exposed to a compound. In addition, Ward and Brock (1976) have shown that lag time preceding the onset of petroleum degradation depends on the initial size of the bacterial population. Water with larger microbial communities should require relatively shorter times to develop a viable population of degraders. High microbial biomass levels are associated with higher  $BOD_5$  concentrations.

The presence of more easily degraded carbon sources may delay the adaptation of a microbial community to the metabolism of a pollutant. Ward and Brock (1976) found that microorganisms in lake water metabolized added glucose completely before degrading hydrocarbons. This diauxic pattern may result in longer lag times.

A final factor which influences lag time is the concentration of the pollutant

in the water. There may be concentration thresholds below which adaptation does not take place. (For example, no adaptation for metabolism of 4-nitrophenol occurred at concentrations below about 40 µg/l (Spain et al , 1981). Too high a pollutant concentration, on the other hand, may be toxic to the microbes (Tabak et al ., 1981). The user should be aware of these possibilities when extremely low or high concentrations are involved.

Once the microbial community has adapted to the organic pollutant, it is of interest to know the rate at which biodegradation occurs. Kinetic expressions for compounds used as a growth substrate can be relatively complicated since both the substrate and bacterial concentrations change with time. The Monod equation has been used to describe the degradation rate of a compound which serves as a sole carbon source:

$$-\frac{dC}{dt} = \frac{1}{Y} \cdot \frac{dB}{dt} = \frac{\mu_{max}}{Y} \cdot \frac{B \cdot C}{K_s + C} \quad (11-56)$$

where

- C = pollutant concentration
- B = bacterial concentration
- Y = biomass produced per unit C consumed
- $\mu_{max}$  = maximum specific growth rate
- $K_s$  = half-saturation constant.

Frequently, the Monod equation is reduced to a second-order biodegradation expression by assuming  $C \ll K_s$ , in which case:

$$-\frac{dC}{dt} = k_{B2} \cdot B \cdot C \quad (11-57)$$

where

$$k_{B2} = \text{second-order biodegradation rate constant} \\ = \frac{\mu_{max}}{Y \cdot K_s}$$

Although Monod kinetics accurately describe some laboratory results, they are inapplicable in the environment due to the presence of other carbon sources. As a simple alternative, first order kinetics are frequently applied:

$$-\frac{dC}{dt} = k_B \cdot C \quad (11-58)$$

where

$$k_B = \text{first-order biodegradation rate constant.}$$

This first-order expression is analogous to the equation commonly used for the decay of BOD (see Chapter 4). Larson (1981) has shown that first-order kinetics which include a lag phase (lag time) represent the degradation of growth substrates reasonably well at initial bacterial concentration of  $10^6$  cells/ml or less, a condition which is usually met in the environment.

#### 2.5.1.2.2 Cometabolism

Microorganisms also degrade compounds which they cannot use as a nutrient or growth substrate through cometabolism. Cometabolism is thought to occur when enzymes of low specificity alter a compound to form products which the other enzymes in the organism cannot utilize. The metabolites formed in the process are structurally similar to their parent molecules and frequently retain their toxicity. In some cases, the product of cometabolism can be used as nutrients by other organisms, but often these intermediate products accumulate (Alexander, 1980).

The kinetics of microbial cometabolism differ significantly from that of growth metabolism. Often no lag occurs before cometabolism begins. The degradation rates, though, are generally slower than the fully adapted rates of growth metabolism (Tiedje, 1980). Since cometabolism does not provide the microbes with any energy, it has no effect on the population size. The rate of cometabolism, however, is directly proportional to the size of the microbial population. Paris *et al.* (1981) showed that a second-order rate law described microbially catalyzed hydrolytic reactions:

$$-\frac{dC}{dt} = k_{B2} \cdot B \cdot C \quad (11-59)$$

Since the bacterial population,  $B$ , is independent of the rate of cometabolism, it is possible to reduce Equation 11-59 to a first-order law by making the following substitution:

$$k_B = k_{B2} \cdot B \quad (11-60)$$

In order to use literature values of the second-order biodegradation rate constant in Equation 11-60, it is necessary to make an estimate of the size of the bacterial population. Since different techniques of bacterial enumeration can yield results which vary over several orders of magnitude, it is important to use estimates of  $B$  based on the same method used to calculate  $k_{B2}$ . Table 11-24 lists bacterial densities which are typical of lakes and rivers. Obviously, large uncertainties in environmental rates of cometabolism exist due to the wide range of possible bacterial densities. Generally, the user should make conservative assumptions unless other data, e.g., a high BOD, indicate larger bacterial densities.

TABLE II-24

## SIZE OF TYPICAL BACTERIAL POPULATIONS IN NATURAL WATERS

Water Body Type	Bacterial Numbers (cells/ml)	Ref.
Oligotrophic Lake	50- 300	a
Mesotrophic Lake	450- 1,400	a
Eutrophic Lake	2000-12,000	a
Eutrophic Reservoir	1000-58,000	a
Dystrophic Lake	400- 2,300	a
Lake Surface Sediments	$8 \times 10^9$ - $5 \times 10^{10}$ cells/g dry wt	a
40 Surface Waters	$500-1 \times 10^6$	b
Stream Sediments	$10^7-10^8$ cells/g	c
Rur River (winter)	$3 \times 10^4$	d

<sup>a</sup>Wetzel (1975). Enumeration techniques unclear

<sup>b</sup>Paris et al . (1981). Bacterial enumeration using plate counts.

<sup>c</sup>Herbes & Schwall (1978). Bacterial enumeration using plate counts.

<sup>d</sup>Larson et al . (1981). Bacterial enumeration using plate counts.

### 2.5.1.2.3 Summary

Table II-25 summarizes some of the major differences between growth metabolism and cometabolism. Although the exceptions to the generalizations about each process are numerous and some compounds can undergo both processes, the distinction between the metabolic processes can serve a useful function in a screening method. The generalizations about each process suggest the following approaches when the user has some knowledge of a compound's metabolic pathway:

#### Cometabolism

- a) Find a second-order rate constant and estimate biomass density.  
Apply Equations II-59, 60.
- b) When a) is not possible, assume cometabolism is negligible, i.e.,  
 $k_B = 0$ .

TABLE II-25

SUMMARY OF THE CHARACTERISTICS OF THE TWO GENERAL TYPES OF BIODEGRADATION: METABOLISM AND COMETABOLISM (After Tiedje, 1980)

Topics	Metabolism for Growth	Cometabolism*
Distinguishing characteristics	Organism will grow on substance as sole C source. Generally ultimate degradation.	Organism will not grow on substance as sole C source. Accumulation of intermediate products likely.
Degradation rates	High rates.	Generally slow rates.
Behavior at low pollutant concentrations	Possible anomalous behavior due to threshold for enzyme induction.	No anomalous behavior, rates are first order in pollutant concentration.
Acclimation	Major effect: lag may be quite variable or lengthy due to low initial density of degraders, and perhaps starvation state of organisms in natural sample.	Often no effect; rarely causes induction, may increase tolerance to toxic chemical.
Relation of degradation kinetics to total biomass, e.g. decay rate = $k_{B2} \cdot B \cdot C$	Likely not valid, use first-order kinetics.	May be valid since activity of interest is often proportional to general biomass.
Extrapolation	General: expect eventual degradation in nature. Quantitative: difficult to be precise because of growth kinetics and acclimation effects, but may not be important problem because of generally fast rates.	Measure kinetic parameters accurately: because of the generally slower rates, extrapolations will be made over longer times, and thus measured parameters need to be accurate. Also environmental influence factors, e.g. temperature, pH, play a more important role.
Effect of added carbon	Diauxic pattern--more easily metabolized substrates are used first.	Generally effect is proportional to microbial population unless specific carbon source happens to induce or inhibit activity of interest.

\*Alteration of a substrate, for purposes other than growth, e.g. for detoxification.



### Growth Metabolism

- a) Find a first- or second-order rate constant.
- b) Estimate a range of lag times. For chronically exposed water bodies, assume that no lag time ( $t_L$ ) occurs. For water bodies not recently exposed (within 200 days), proceed as follows:
  1. Estimate lag time using available information. If no information is available use a range of 2-20 days.
  2. Assume adaptation occurs as follows:

Rivers - At travel times  $< t_L$ ,  $k_B = 0$   
At travel times  $\geq t_L$ ,  $k_B \neq 0$

Lakes - For well mixed lakes, first determine C at time =  $t_L$ ,  $C_{t_L}$  due to all processes except biodegradation. Then using  $C_{t_L}$  as  $C_0$  solve for  $C_t$  with a modified time,  $t_m$ , ( $t_m = t - t_L$ ). (Use equations in Section 5.6.1)  
For stratified lake use only the volume through which the inflow passes (e.g., the hypolimni on volume) in calculating the hydraulic residence time ( $\tau_w$ ) Then proceed as above.

Estuaries - Consider all processes except biodegradation through that downstream segment for which  $\tau_w$ , as measured from the injection point, becomes greater than  $t_L$ . Thereafter include biodegradation.

When no data on which metabolic pathway a compound follows are available, the user should apply any available kinetic information and allow for the possibility of a lag phase prior to the onset of degradation.

#### 2.5.1.3 Chemical Properties Influencing Biodegradation

The chemical properties of a compound determine whether microbes can potentially utilize it as a growth substrate or not. Compounds which serve as bacterial growth substrates usually decay more rapidly than those which microbes cometabolize. Thus, significant differences in the aquatic fate of pollutants can arise depending on which degradation process takes place.

Unfortunately, it is not possible at this time to predict whether a toxic compound is a potential source of energy and carbon solely on the basis of its chemical structure. Rather, the biodegradability of a compound is usually investigated in laboratory tests (Gilbert and Lee, 1980). Compounds which are growth substrates should be able to serve as sole carbon sources for a microbial community. Compounds which cometabolize should degrade only in the presence of another carbon

source. A systematic study of the metabolic pathways of the priority pollutants is desperately needed.

Table II-26 contains the results of a preliminary degradation test on the organic priority pollutants (Tabak *et al.* , 1981). Because the experimental conditions were so favorable for biodegradation, the tests serve as a good indicator of a compound's potential biodegradability. Since the pollutants were not the sole carbon sources, no conclusions can be reached about their metabolic pathways. Some information on the rates of adaptation and decay, through, can be extracted from the results.

The adaptation summary results may be used as follows:

- Rapid Adaptation (D) - Use a range of adaptation times from zero days upward depending upon conditions described above
- Gradual Adaptation (A) - Use a range of adaptation times from 7 days to more than 20 depending upon the conditions described above.

The rate summary results represent estimates of the biodegradation rate constants assuming the compounds decay according to first-order kinetics. General values presented at the bottom of the table are gross estimates and should only be used if no better data is available. The rate constants should represent an upper limit for biodegradation rates by adapted populations observed in the environment.

Table II-27 contains literature values of biodegradation rate constants. Where possible, the likely metabolic pattern has been indicated. Some of these constants were measured under environmentally relevant conditions. In general, rate constants should be compared with those in Table II-27 before use.

#### 2.5.1.4 Environmental Influences on Biodegradation Rates

Environmental conditions strongly influence the metabolic activity of a microbial population. The environment affects the types of metabolic reactions microbes are able to carry out, the availability of nutrients for these reactions, and the rates at which these reactions occur. The environmental variables which are responsible for these effects are discussed in the following sections.

##### 2.5.1.4.1 Temperature

In general, a molecule must have an energy greater than a threshold or activation level in order for it to react chemically. Since increasing the temperature increases the number of molecules which have this minimum energy, both biotic and abiotic reactions generally proceed more rapidly at higher temperatures. However, because enzymes catalyze most biochemical reactions and microbial populations can adapt to changes in ambient temperatures, the temperature dependence of microbially mediated reactions is complicated.

TABLE II-26

POTENTIAL BIODEGRADABILITY OF ORGANIC POLLUTANTS  
IN AN AEROBIC ENVIRONMENT  
(After Tabak et al., 1981)

<u>Test Compound</u>	<u>Adaptation Summary</u>	<u>Rate Summary</u>	<u>Test Compound</u>	<u>Adaptation Summary</u>	<u>Rate Summary</u>
<u>Pesticides</u>					
Aldrin	N	0	Endrin	N	0
Di el drin	N	0	Heptachlor	N	0
Chlordane	N	0	Heptachlor epoxide	N	0
DDT p.p'	N	0	Hexachlorocyclohexane α-BHC-α	N	0
DDE p.p'	N	0	Hexachlorocyclohexane γ-BHC-β	N	0
DDD p.p'	N	0	Hexachlorocyclohexane δ-BHC-δ	N	0
Endosulfan-α	N	0	Hexachlorocyclohexane λ-BHC-γ (lindane)	N	0
Endosulfan-β	N	0	Acrolein	D	2
Endosulfan sulfate	N	0			
<u>PCB's and Related Compounds</u>					
PCB-1016	N	0	PCB-1248	N	0
PCB-1221	D	2	PCB-1254	N	0
PCB-1232	D	2	PCB-1260	N	0
PCB-1242	N	0	2-Chloronaphthalene	D	2
<u>Halogenated Aliphatic Hydrocarbons</u>					
Chloroethanes			Chloroethylenes		
1,1-Dichloroethane	A	1	1,1-Dichloroethylene	A	2
1,2-Dichloroethane	B	1	1,2-Dichloroethylene-cis	B	1
1,1,1-Trichloroethane	B	1	1,2-Dichloroethylene-trans	B	1
1,1,2-Trichloroethane	C	1	Trichloroethylene	A	1
1,1,2,2-Tetrachloroethane	N	0	Tetrachloroethylene	A	1
Hexachloroethane	D	2	Chloropropanes		
Halomethanes			1,2-Dichloropropane	A	1
Methylene chloride	D	2	Chloropropylenes		
Bromochloromethane	D	2	1,3-Dichloropropylene	A	1
Carbon tetrachloride	D	2	Chlorobutadienes		
Chloroform	A	2	Hexachloro-1,3-butadiene	D	2
Dichlorobromomethane	A	1	Chloropentadienes		
Bromoform	A	1	Hexachlorocyclopentadiene	D	2
Chlorodibromomethane	N	0			
Trichlorofluoromethane	N	0			
<u>Halogenated Ethers</u>					
Bis-(2-chloromethyl) ether	D	2	4-Bromodiphenyl ether	N	0
2-Chloroethyl vinyl ether	D	2	Bis-(2-chloroethoxy) methane	N	0
4-Chlorodiphenyl ether	N	0	Bis-(2-chloroisopropyl) ether	D	2

TABLE II-26 (Continued)

Test Compound	Adaptation Summary	Rate Summary	Test Compound	Adaptation Summary	Rate Summary
<u>Monocyclic Aromatics</u>					
Benzene	D	2	Hexachlorobenzene	N	0
Chlorobenzene	D	2	Nitrobenzene	D	2
1,2-Dichlorobenzene	T	1	Ethylbenzene	D	2
1,3-Dichlorobenzene	T	1	Toluene	D	2
1,4-Dichlorobenzene	T	1	2,4-Dinitrotoluene	T	1
1,2,4-Trichlorobenzene	T	1	2,6-Dinitrotoluene	T	1
<u>Phenolic Compounds</u>					
Phenol	D	2	p-Chloro-m-cresol	D	2
2-Chlorophenol	D	2	2-Nitrophenol	D	2
2,4-Dichlorophenol	D	2	4-Nitrophenol	D	2
2,4,6-Trichlorophenol	D	2	2,4-Dinitrophenol	D	2
Pentachlorophenol	A	1	4,6-Dinitro-o-cresol	N	0
2,4-Dimethylphenol	D	2			
<u>Phthalate Esters</u>					
Dimethyl phthalate	D	2	Bis-(2-ethylhexyl) phthalate	A	1
Diethyl phthalate	D	2	Di-n-octyl phthalate	A	1
Di-n-butyl phthalate	D	2	Butyl benzyl phthalate	D	2
<u>Polycyclic Aromatic Hydrocarbons</u>					
Naphthalene	D	2	Fluorene	A	1
Acenaphthene	D	2	Fluoranthene	A*	2
Acenaphthylene	D	2	1,2-Benzanthracene	N	0
Anthracene	A	1	Pyrene	D*	2
Phenanthrene	D	2	Chrysene	A*	1
<u>Nitroso Amines and Miscellaneous Compounds</u>					
Nitrosamines			Substituted benzenes		
N-Nitroso-di-n-propylamine	N	0	Isophorone	D	2
N-Nitrosodiphenylamine	D	2	1,2-Diphenylhydrazine	T	1
			Acrylonitrile	D	2

Results of Tabak *et al.* (1981) using Bunch and Chambers screening test. Results reflect potential biodegradability under favorable conditions. The test measures disappearance rather than mineralization of a compound. A domestic sewage inoculum was used. Test duration = 28 days.

Key to Test Summary

- N Not significantly degraded under conditions of test method.
- D Significant degradation with rapid adaptation; < 7 days.
- D\* Same as D except slower adaptation at higher pollutant concentration.
- A Significant degradation with gradual adaptation; 7-21 days.
- A\* Same as A except no degradation evident at higher pollutant concentration.
- B Slow degradation.
- C Very slow degradation with long adaptation period required; > 28 days.
- T Significant degradation with gradual adaptation followed by readaptation (toxicity).

Key to Rate Summary

Very crude estimates of first-order biodegradation rate constants may be made from the information given in Tabak *et al.*

- 0 No significant degradation rate
- 1  $.05 \text{ day}^{-1} < k_B < .5 \text{ day}^{-1}$ ; use  $.05 \text{ day}^{-1}$
- 2  $k_B > .5 \text{ day}^{-1}$ ; use  $.5 \text{ day}^{-1}$

TABLE II-27

## BIODEGRADATION RATE CONSTANTS UNDER AEROBIC CONDITIONS

Compound	$k_{R2}$ Second-Order Rate Constant ( $\text{ml cell}^{-1} \text{day}^{-1}$ )	$k_B$ First-Order Rate Constant (1/day)	$t_{1/2}$ Half-Life (days)	$T_0$ Reference Temperature (°C)	Compound Used as a Growth Substrate?	Experimental Conditions	Ref
<u>Pesticides</u>							
2,4-D Butoxyethyl ester	1.2x1	1.3x10 <sup>-2</sup> (1)	53	20	?	Natural surface water samples	a
Malathion	1.1x10 <sup>-6</sup> (3)	1.1x10 <sup>-3</sup> (1)	6.3x10 <sup>2</sup>	20	?	Natural surface water samples	a
Chlorpropham	6.2x10 <sup>-10</sup> (3)	6.2x10 <sup>-7</sup> (1)	1.1x10 <sup>6</sup>	20	?	Natural surface water samples	a
Furadan	2.4x10 <sup>-8</sup>	2.4x10 <sup>-5</sup> (1)	3 x 10 <sup>4</sup>	?	?	?	b
Atrazine	2.4x10 <sup>-8</sup>	2.4x10 <sup>-5</sup> (4)	3 x 10 <sup>4</sup>	?	?	?	b
<u>Polychlorinated Biphenyls</u>							
Aroclor 1221	-	.8 <sup>(2)</sup>	.9	?	?	Acclimated activated sludge	c
Aroclor 1016	-	.2 <sup>(2)</sup>	3.5	?	?	Acclimated activated sludge	c
Aroclor 1242	-	.15 <sup>(2)</sup>	4.5	?	?	Acclimated activated sludge	c
Aroclor 1254	-	.1 <sup>(2)</sup>	7.	?	?	Acclimated activated sludge	c
<u>Halogenated Ethers</u>							
4-Chlorophenyl phenyl ether	-	.011-.016 <sup>(2)</sup>	43-63	?	?	River water; Log = 5-13 days	c
	-	3.8 <sup>(4)</sup>	.2	?	?	Activated sludge	c
<u>Monocyclic Aromatics</u>							
Nitrobenzene	-	.7 <sup>(2)</sup>	1.	20	Yes	Adapted activated sludge; COD decay	d
2-Chlorotoluene	6.5x10 <sup>-8</sup> (3)	6.5x10 <sup>-4</sup>	1.1x10 <sup>3</sup>	?	?	Natural surface water sample	e
<u>Phenolic Compounds</u>							
Phenol	-	4. <sup>(2)</sup>	.2	20	Yes	Adapted activated sludge; COD decay	d
	-	6. <sup>(2)</sup>	.1	?	?	Polluted river water	c
	-	1. <sup>(2)</sup>	.7	20	Yes	Adapted activated sludge	d
	-	.3	2.3	?	?	Soil suspension	c
2,4-Dichlorophenol	-	.5 <sup>(2)</sup>	1.4	20	Yes	Adapted activated sludge; COD decay	d
	-	.1 <sup>(4)</sup>	6	25	?	Natural lake waters	c
Pentachlorophenol	-	.1 <sup>(2)</sup>	7	25	Yes	Unadapted; Nutrient Broth	f
	-	1. <sup>(2)</sup>	.7	25	Yes	Adapted; Nutrient Broth	f
2,4-Dimethylphenol	-	1. <sup>(2)</sup>	.7	20	Yes	Adapted activated sludge	d
2,4-Dinitrophenol	-	.2 <sup>(2)</sup>	3.5	20	Yes	Adapted activated sludge	d
2,4,6-Trinitrophenol	-	0		20	No	Activated sludge	d
<u>Phthalate Esters</u>							
Dimethyl	1.2x10 <sup>-4</sup>	.12 <sup>(1)</sup>	5.6	?	?	?	g
Di-ethyl	7.7x10 <sup>-8</sup>	7.7x10 <sup>-5</sup> (1)	9.0x10 <sup>3</sup>	?	?	?	g
Di-n-butyl	7.0x10 <sup>-7</sup>	7.0x10 <sup>-4</sup> (1)	1.0x10 <sup>3</sup>	?	?	?	g
Di-n-octyl	7.4x10 <sup>-9</sup>	7.4x10 <sup>-6</sup> (1)	9.3x10 <sup>4</sup>	?	?	?	g
Di-(2-ethyl hexyl)	1.0x10 <sup>-10</sup>	1.0x10 <sup>-7</sup>	6.9x10 <sup>6</sup>	?	?	?	g
	-	2.5x10 <sup>-2</sup> (4)	28	?	?	River Water	c
Butyl Benzyl	-	>.35 <sup>(4)</sup>	<2	?	?	River Water	c

TABLE II-27 (Continued)

Compound	$k_B^2$ Second-Order Rate Constant (ml/cell l/day)	$k_B$ First-Order Rate Constant (l/day)	$t_{1/2}$ Half-Life (days)	$T_o$ Reference Temperature (°C)	Compound Used as a Growth Substrate?	Experimental Conditions	Ref.
<u>Polycyclic Aromatic Hydrocarbons</u>							
Naphthalene	-	.14	5.0	12	Yes	Contaminated stream sediments	h
	-	$< 4 \times 10^{-4}$	$1.7 \times 10^3$	12	?	Pristine stream sediments	h
Anthracene	-	.0025	$2.8 \times 10^2$	12	Yes	Contaminated stream sediments	h
	-	$2.5 \times 10^{-4}$	$2.8 \times 10^3$	12	?	Pristine stream sediments	h
	-	1.5	.5	?	?	Contaminated stream	c
Benz(a)anthracene	-	1.	$6.9 \times 10^3$	12	Yes	Contaminated stream sediments	h
	-	$4 \times 10^{-6}$	$1.7 \times 10^5$	12	?	Pristine stream sediments	h
Benz(a)pyrene	-	$< 3 \times 10^{-5}$	large	12	?	Contaminated stream sediments	h
	-	$< 3 \times 10^{-5}$	large	12	?	Pristine stream sediments	h
Phenanthrene	$3.8 \times 1$	$3.8 \times 10^{-3(1)}$	$1.8 \times 10^2$	?	?	?	e

## Notes:

- 1) First-order rate constant computed using Equation II-60 and  $B = 10^3$  cells/ml.
- 2) First-order constant calculated from percent disappearance and elapsed time.
- 3) Bacterial enumeration using plate count technique.
- 4) First-order rate constant computed from reported half-life

## References:

- a) Paris *et al.* (1981)
- b) Schnoor (1981)
- c) Callahan *et al.* (1979)
- d) Pitter (1976)
- e) Paris *et al.* (1980)
- f) Kirsch and Etzel (1973)
- g) Wolfe *et al.* (1980)
- h) Herbes & Schwall (1978)

It is common practice to represent the temperature dependence of biodegradation using the following empirical formula:

$$k_B(T) = k_B(T_0) \cdot \theta_B^{(T-T_0)} \quad (11-61)$$

where

- $k_B(T)$  = specific biodegradation rate constant at temperature = T
- $k_B(T_0)$  = specific biodegradation rate constant at temperature =  $T_0$
- T = ambient temperature, °C
- $T_0$  = reference temperature, °C
- $\theta_B$  = temperature coefficient for biodegradation.

The results of Larson et al. (1981) and Ward and Brock (1976) show that the rates of nitrilotriacetate and hydrocarbon biodegradation increased approximately two-fold over a ten degree temperature range ( $\theta_B = 1.072$ ). Either this value or the standard value of 1.047 for BOD decay is adequate for screening purposes.

#### 2.5.1.4.2 Nutrient Limitation

Microbes require nutrient such as nitrogen and phosphorus in order to metabolize an organic substrates. Several researchers have suggested that inorganic nutrient limitation is a significant factor influencing biodegradation rates in the aquatic environment (Ward and Brock, 1976; Roubel and Atlas, 1978; Herbes and Schwall, 1978). Ward and Brock (1976) found a high correlation between hydrocarbon degradation rates and phosphorous concentrations in natural waters. The data fit a saturation relationship of the Michaelis-Menten type:

$$k_B(C_p) = k_B(C_p^*) \cdot \frac{.0277 \cdot C_p}{1 + .0277 \cdot C_p} \quad (11-62)$$

where

- $k_B(C_p)$  = specific biodegradation rate constant at dissolved inorganic phosphorus concentration,  $C_p$
- $C_p$  = dissolved inorganic phosphorus concentration,  $\mu\text{g/l}$
- $k_B(C_p^*)$  = non-nutrient limited biodegradation rate constant.

This relationship should serve as a good indicator of possible phosphorus limitation of biodegradation in the environment. Generally surface waters downstream of domestic sewage treatment plants are not limited in either nitrogen or phosphorus. Equation 11-62 should be applied only when other nutrients such as carbon and nitrogen are not limiting.

#### 2.5.1.4.3 Sorption of Substrates

Many organic pollutants adsorb strongly on sediments, (See Section 2.3.2. The difference in the physical and chemical environments between sorbed and dissolved pollutants is likely to influence their availability to microbial organisms. Baughman *et al.* (1980) showed that the dissolved fraction of the compounds studied was available to biota for degradation while the sorbed fraction was not. In such cases, the rate of disappearance of the pollutant is:

$$\frac{dC_T}{dt} = k_B \cdot C_W = \alpha_W \cdot k_B \cdot C_T \quad (11-63)$$

where

$C_W$  = the pollutant concentration in the aqueous phase

$\alpha_W$  = the decimal fraction of the total analytical pollutant concentration which is in the aqueous phase ( $\alpha_W = 1 - \text{fraction sorbed}$ ).

It is well known, however, that bacteria grow very readily on surfaces and that increasing available surface area in the form of clays and sediments can increase rates of microbial metabolism. If specific information regarding the effects of sorption on the rates of biodegradation are not available for a compound, it is best to assume that sorption does not change this rate.

#### 2.5.1.4.4 Solubility

Wodzinski and Bertalini (1972) have shown that in the dissolved state, naphthalene and biphenyl were degradable while in the pure crystalline state they were not. Thus, sparingly soluble compounds could degrade slowly for this reason alone. The extent to which this phenomenon applies to other biodegradation reactions has not been established. The user may assume that only dissolved chemicals are degraded.

#### 2.5.1.4.5 pH

The hydrogen ion concentration also influences rates of biodegradation. Each bacterial species has a pH range for which it is best suited. Thus, at different pH values, different species may exist, or a given species may metabolize the pollutant at a different rate. Hambrick *et al.* (1980) found that the mineralization rate of naphthalene in oxidizing sediments varied in the proportions 1:6:5 at pH 5, 6.5, and 8. The same study found that the mineralization rates of octadecane varied in the proportions 4:5:7 at the same three pH's. Until more general rules for predicting pH effects are available, the user should assume biodegradation rates are independent of pH in the pH range 5-9 and decrease outside this range.

#### 2.5.1.4.6 Anoxic Conditions

As the concentration of dissolved oxygen in natural water is depleted, metabolic pathways shift. When the dissolved oxygen concentration drops to about 1 mg/l, the rate of biodegradation becomes dependent on oxygen concentration in addition to



substrate concentration and the rate of degradation starts to decrease. At a dissolved oxygen concentration of about 0.5 to 1.0 mg/l nitrate begins to substitute for molecular oxygen as an oxidant.

When oxygen is depleted, anaerobic metabolism prevails with its generally lower energy yields and growth rates. Most organic substances are biodegraded more slowly under anaerobic conditions. Rate constants derived for oxygenated systems are no longer appropriate; their use may overpredict the amount of degradation.

Exceptions do exist to the rule of slower degradation under anoxic conditions. Reactions such as dehydrochlorinations and reductive dechlorination lead to much higher degradation rates for many chlorinated hydrocarbons. Example compounds include lindane, heptachlor, pentachlorophenol, and some one and two carbon chlorinated alkanes.

EXAMPLE 11-6

Biodegradability of Naphthalene

Evaluate the biodegradability of naphthalene discharged into the Lepidoptera River by a point source just upstream from Northville's sewage treatment plant. Assume the following water quality parameters at the upstream discharge:

Temperature = 10°C  
Suspended sediment = 10 mg/l  
Inorganic phosphorus = 5 µg/l  
Dissolved oxygen = 5 mg/l.

First, check the potential biodegradability of naphthalene in Table 11-26. The table indicates that naphthalene degrades rapidly,  $k_B = .5 \text{ day}^{-1}$ , and that bacteria adapt quickly to it.

Next, examine Table 11-27 for further information on naphthalene's biodegradability. Naphthalene is a potential growth substrate. In addition, the data in this table concur with the rapid degradation rates suggested by Table 11-26. In sediment, which had been previously exposed to naphthalene, a biodegradation rate constant of  $0.14 \text{ day}^{-1}$  was measured. As one would expect for a growth substrate, degradation rates are much lower, e.g.,  $k_B < 4 \times 10^{-4} \text{ day}^{-1}$ , in sites not previously exposed to naphthalene.

Since naphthalene is a growth substrate, estimating the adaptation time in the Lepidoptera River is a primary issue. Because the point source continuously discharges naphthalene into the Lepidoptera River, it is safe to assume that the bacterial populations have adapted.

In a complete analysis, the user would check whether the oxygen is depleted

from the river. If so, degradation could be neglected until dissolved oxygen levels exceed 1.0 mg/l again.

Sorption by suspended sediment could potentially reduce the rate at which naphthalene biodegrades. Table 11-9 gives a  $K_{ow}$  for naphthalene of 2,300. Using Equations 11-16 and 11-18 and assuming a suspended sediment organic carbon content of 2 percent, the partition coefficient is:

$$\begin{aligned}K_p &= (.02) (.63) (2,300) \\ &= 29\end{aligned}$$

At the suspended sediment levels in the Lepidoptera River 10mg/l, Table 11-16 shows that sorption will not significantly reduce water column concentrations of naphthalene. Although phosphorus levels are low, assume carbon is the growth-limiting substrate.

Finally, the degradation rate is adjusted to the river water temperature using Equation 11-61:

$$\begin{aligned}k_B &= 0.14 \cdot 1.072^{(10-12)} \\ &= 0.12 \text{ day}^{-1}\end{aligned}$$

----- END OF EXAMPLE 11-6 -----

## 2.5.2 Photolysis

### 2.5.2.1 Introduction

The sun provides the aquatic environment with a large supply of energy. Substances which absorb sunlight transform much of its radiant energy into thermal energy. But, molecules which absorb sunlight in the ultraviolet and visible portion of the spectrum may gain sufficient energy to initiate a chemical reaction. Plants use very specific photochemical reactions to provide energy for the synthesis of sugar from carbon dioxide. In other photochemical reactions, the absorption of light leads to the decomposition of a molecule. The latter type of reaction, known as photolysis, strongly influences the fate of certain pollutants in the aquatic environment.

Photolysis is truly a pollutant decay process since it irreversibly alters the reacting molecule. However, the products of the photochemical decomposition of a toxic compound may still be toxic. For example, irradiated 2,4-D esters form 2,4-D acid, a priority pollutant, in aerated waters (Zepp *et al.*, 1975). Upon irradiation, DDT reacts to form DDE, which persists in the environment longer than DDT (Tinsley, 1979). Thus, even though the methods in this section assume that pollutants irreversibly decay through photolysis, the planner should remember that the decomposition of a pollutant does not imply the detoxification of the environment.

The rate at which a pollutant photolyzes depends on numerous chemical and environmental factors. The light absorption properties and reactivity of a compound,

the light transmission characteristics of natural waters, and the intensity of solar radiation are some of the most important factors influencing environmental photolysis. These factors will be covered by the following discussion. Understanding these factors facilitates the computation of rate constants and the identification of pollutants likely to photolyze - the final two topics of this section.

#### 2.5.2.2 Factors Influencing Photolysis in the Aquatic Environment

##### 2.5.2.2.1 Photochemical Reactions

All chemical reactions which occur at finite rates require the reacting molecule to gain sufficient energy to become "activated" or form a reactive intermediate. In dark or thermal reactions, the thermal energy of the environment supplies the activation energy. In photochemical reactions, the absorption of light provides the activation energy.

The "activated" molecules in photochemical reactions differ in important respects from those of thermal reactions. Thermally activated molecules usually remain in the normal or "ground" electronic energy state, whereas photochemically activated molecules exist in higher, "excited" electronic states. Because of the excess energy and the alteration of the chemical bonds of photoactivated molecules, the range of potential reaction products is much greater than that for thermally activated molecules.

The mechanism by which photoactivated molecules form and react is divided into three steps: 1) the absorption of light to produce an electronically excited molecule, 2) the "primary photochemical processes" which transform or de-excite the excited molecule, and 3) the secondary or "dark" thermal reactions which the intermediates produced in step 2 undergo (Turro, 1978).

The mechanism of photochemical reactions provides a convenient structure for a discussion of the factors which influence photolysis in the aquatic environment. Environmental factors affecting the absorption of light, step 1, will be considered first. Then, the factors influencing the fate of molecules which become excited by the absorption of light, steps 2 and 3, are discussed.

##### 2.5.2.2.2 Light Absorption

"Only that light which is absorbed by a system can produce chemical changes (Grotthaus-Draper Law)."

(Glasstone, 1946)

As this "first law of photochemistry" implies, it is necessary to know the rate at which reacting molecules absorb light in order to determine the rate of a photo-

chemical reaction in the environment. The following factors which influence light absorption in the aquatic environment are discussed here: 1) molecular absorption of light, 2) solar radiation, and 3) light attenuation in natural waters.

#### 2.5.2.2.2.1 Molecular Absorption of Light

Both light and molecules have quantized energies. Light interacts with matter as quanta with energies inversely proportional to their wavelengths. A molecule has quantized internal energy states associated with the configuration of its electrons and the rotation and vibration of its chemical bonds. Since a molecule can absorb light only as a whole photon, light absorption is possible only if the energy of the photon corresponds to the energy change of an allowed transition between the molecule's internal energy states. Consequently, the probability of a photon being absorbed varies strongly with wavelength of the light in a way that is unique to every chemical species.

To initiate a chemical reaction, the absorbed light must be sufficiently energetic to cause a change in the absorbing molecule's electronic structure. Generally, radiation with wavelengths in the ultraviolet-visible range, or shorter, has sufficient energy to initiate photochemical reactions while radiation with wavelengths in the infrared range, or longer, does not. Thus, the ultraviolet-visible light absorption properties of a chemical are of primary interest in photochemistry.

Photochemical reactions in the aquatic environment depend on the rate at which molecules in aqueous solution absorb light. According to Beer's Law, the rate of light absorption by a single compound ( $I_a$ ) in a cross-section of solution with infinitesimal thickness ( $\Delta z$ ) is proportional to the concentration of the light absorbing specie (C), i.e.,

$$I_a(z) = I(z) \cdot 2.3 \cdot \epsilon \cdot C \cdot \Delta z \quad (11-64)$$

where

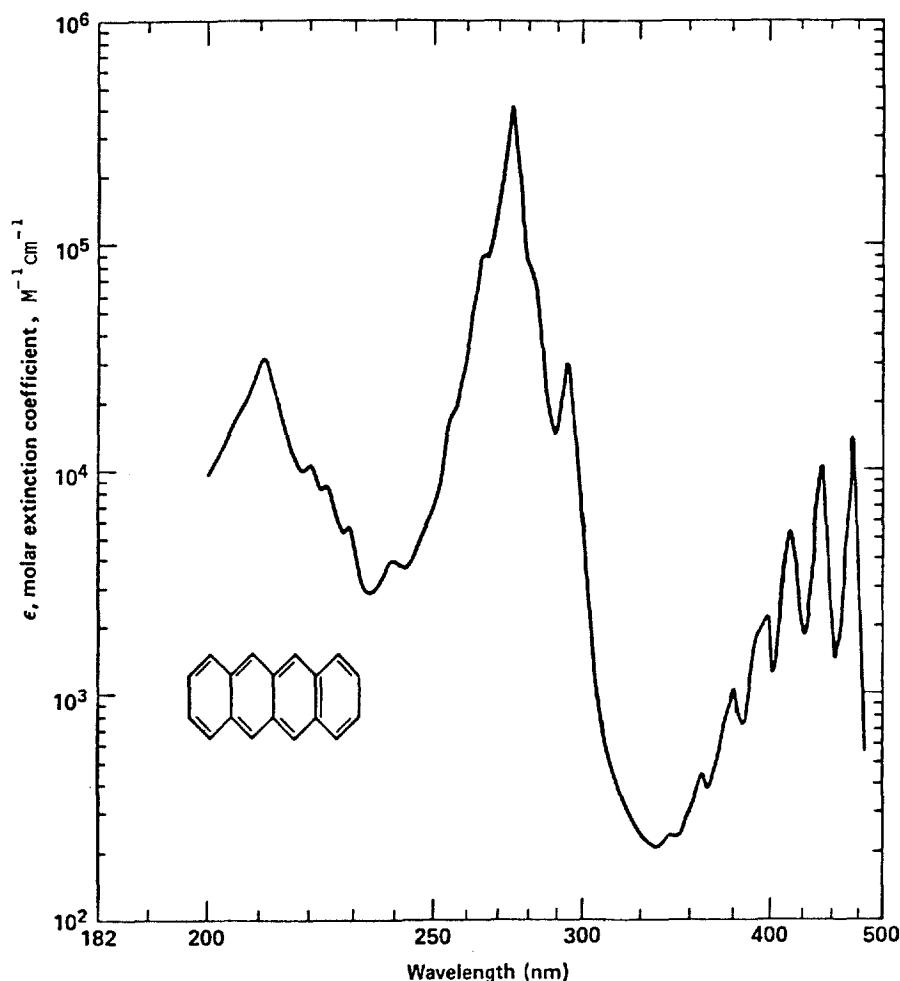
$I(z)$  = intensity of the light at a depth  $z$  in the solution

$\epsilon$  = base 10 molar extinction coefficient.

$\epsilon$  reflects the probability of the light being absorbed by the dissolved molecules and therefore varies with the wavelength of the incident light as shown in Figure 11-11. Absorption spectra, such as shown here, contain information necessary to compute the rate at which pollutants absorb radiation available in the environment.

#### 2.5.2.2.2.2 Solar Radiation

The only radiant energy available for absorption by pollutants in the aquatic environment comes from the sun. The sun emits radiation of nearly constant intensity

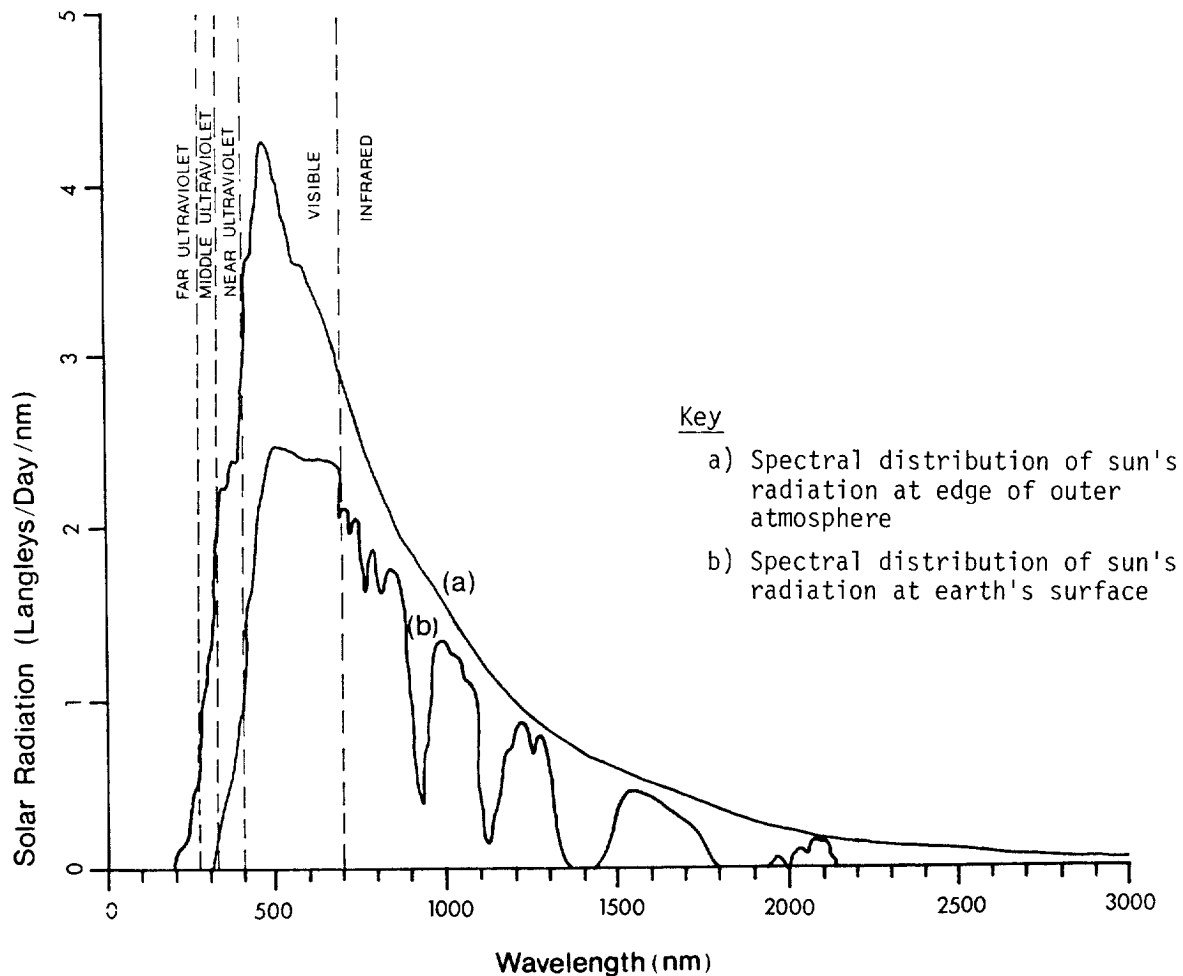


Source: U.V. Atlas of Organic Compounds.

FIGURE II -11 ULTRAVIOLET ABSORPTION SPECTRUM OF NAPHTHACENE

and spectral distribution. But, gases and particles in the earth's atmosphere alter the incoming solar radiation through scattering and absorption. Scattering of the direct solar beam creates the diffuse or sky radiation visible at the earth's surface. Absorption of both diffuse and direct radiation reduces the intensity of solar radiation reaching the earth. Since the strength of absorption and scattering depends strongly on the wavelength of the light involved, the interaction of sunlight with the atmosphere alters the spectral distribution of solar radiation as well, as Figure 11-12 shows.

The composition of the earth's atmosphere and the geometrical relationship of the sun and earth change over time causing the solar radiation incident upon the earth's surface to vary as well. A comparison of the total solar irradiance under clear skies at various times, seasons, and latitudes (Table II-28) to the extra-



Sources: (a) Weast and Astle (1980); (b) Moon (1940).

FIGURE 11-12 SPECTRAL DISTRIBUTION OF Solar Energy  
 (A) OUTSIDE THE EARTH'S ATMOSPHERE, AND  
 (B) AT THE EARTH'S SURFACE

atmospheric solar flux of 2800 Langley's/day demonstrates the effects of changes in earth-sun geometry. The composition of the atmosphere differs greatly from place to place and, of the factors influencing the total solar flux, is the most difficult to accurately quantify. Historical records of the solar radiation, such as shown in Figure 11-13, are the best way to estimate the mean solar energy flux at a given locale. However, care should be taken to account for the influence of riparian vegetation on incoming radiation. Section 4.4.3 discusses how to approximate the effects of shading.

Information concerning the variability of the spectral distribution of solar energy incident upon the earth's surface is not as readily available. It is known

TABLE II-28

CALCULATED SOLAR RADIANT ENERGY FLUX TO A HORIZONTAL SURFACE UNDER A CLEAR SKY  
(l ang l eys/day)

Latitude	Time Of Day	Season				Annual Mea n
		Spring	Summer	Fall	Winter	
30°N	Mean <sup>1</sup>	680	750	530	440	600
	Mid-Day <sup>2</sup>	2100	2200	1700	1400	1900
40°N	Mean	650	740	440	320	540
	Mid-Day	1900	2100	1400	1000	1600
50°N	Mean	590	710	330	190	460
	Mid-Day	1700	1900	1000	650	1300

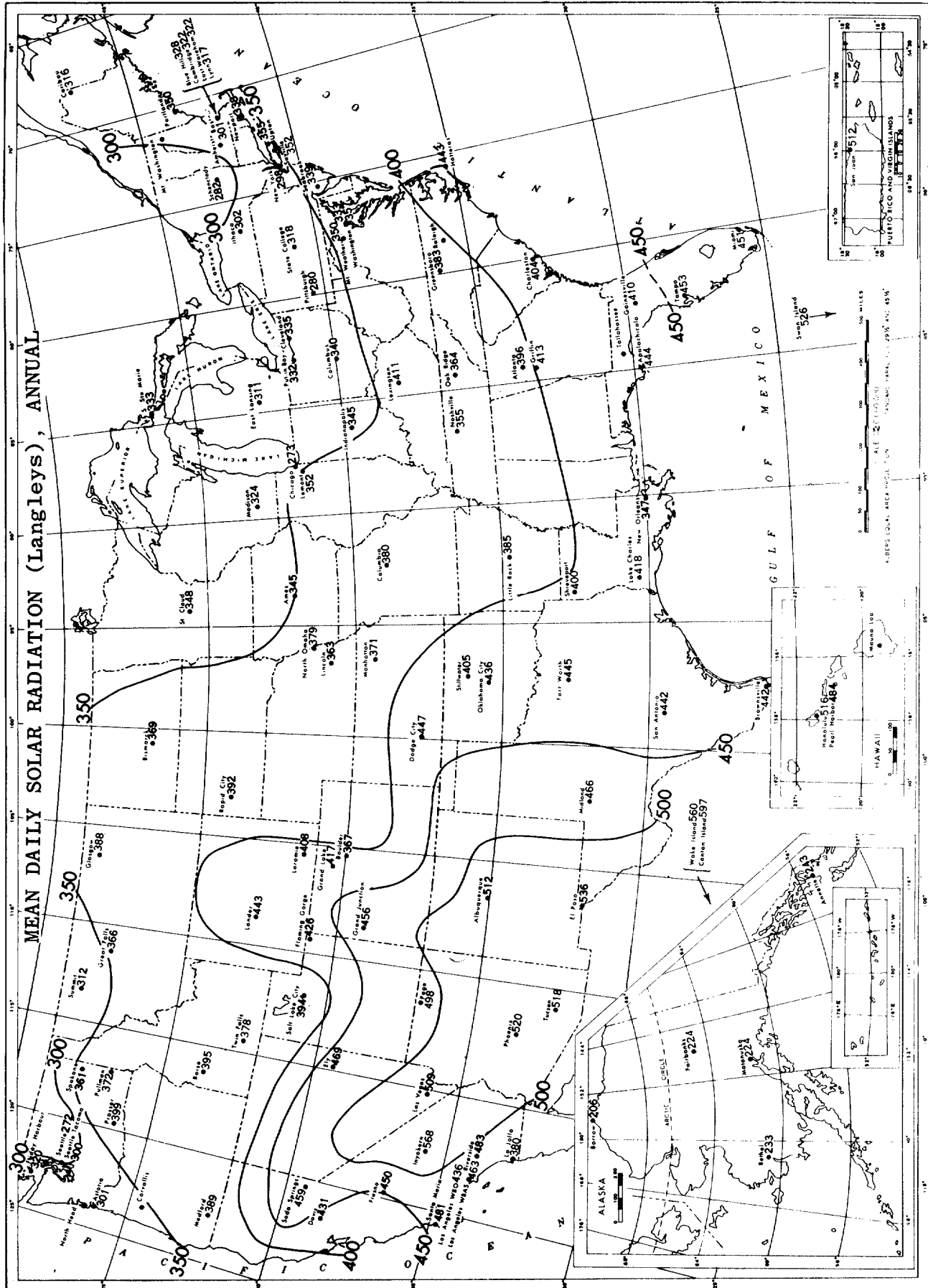
1 Mean values represent calculated seasonal means under a clear sky. These should represent upper limits for solar radiant energy at sea level. Reference: Weast and Astle (1980).

2 Mid-Day values represent mid-day flux extended over a 24-hour period. These assume an atmospheric turbidity of 0, precipitable water content of 2 cm, and an atmospheric ozone content of .34 cm NTP. Reference: Robinson (1966).

that the fraction of the solar energy in the ultraviolet region decreases with increased attenuation of light by the atmosphere. The fraction of the energy which is visible remains relatively constant. For the purpose of this document, it is sufficiently accurate to assume that the reduction in UV-visible radiation is proportional to the reduction in the total flux.

#### 2.5.2.2.2.3 Light Attenuation in Natural Waters

Just as the earth's atmosphere reduces the intensity of solar radiation reaching the earth's surface, natural waters reduce the intensity of radiation available for absorption by aquatic pollutants. The first process which reduces the availability of light in the water column is reflection. In most cases, the surface of the water reflects less than 10 percent of solar radiation (Zepp and Cline, 1977). Reflection also alters the solar spectrum slightly. A calculated spectral distribution of solar radiation, expressed in photons, immediately below the surface of a water body is presented in Table II-29.



Ref: US Dept. Comm. (1968)

FIGURE II-13 SOLAR RADIATION IN THE UNITED STATES



TABLE II-29

CALCULATED SOLAR IRRADIANCE IN A WATER BODY JUST BENEATH  
THE SURFACE, ANNUAL MEAN AT 40°N

Wavelength <sup>b</sup> (nm)	Photon Spectral Irradiance <sup>a</sup>	
	$w(\lambda)^c$ ( $10^{14}$ photons $\text{cm}^{-2} \text{sec}^{-1} \text{nm}^{-1}$ )	$w'(\lambda)^d$ ( $10^{14}$ photons $\text{cm}^{-2} \text{sec}^{-1}$ )
300	.00303	.0303
310	.0388	.388
320	.113	1.13
330	.181	1.81
340	.211	2.11
350	.226	2.26
360	.241	2.41
370	.268	2.68
380	.294	2.94
390	.366	3.66
400	.526	5.26
410	.692	6.92
420	.712	7.12
430	.688	6.88
440	.814	8.14
450	.917	9.17
460	.927	9.27
470	.959	9.59
480	.983	9.83
490	.930	9.30
500	.949	9.49
510	.962	9.62
520	1.00	10.0
550	1.04	52.0
600	1.07	53.5
650	1.08	54.0
700	1.07	53.6
750	1.03	51.5
800	.988	49.4

<sup>a</sup>Estimated reference solar flux,  $I_0 = 540$  langley/day.  $D_0 = 1.0$

<sup>b</sup>Centric wavelength of waveband X nm in width,  
for  $300 < \lambda \leq 520$ ,  $X=10$  nm. For  $\lambda \geq 550$ ,  $X=50$  nm

<sup>c</sup>Mean irradiance over wavelength interval of width X.

<sup>d</sup>Integrated irradiance over wavelength interval of width X.  
 $w'(\lambda) = w(\lambda) \cdot \Delta\lambda = w(\lambda) \cdot X.$

Reference: Burns et al. (1981).

As solar radiation penetrates deeper into natural waters, it is absorbed and scattered by particulate, dissolved substances, and water itself. Measurements of light attenuation in natural waters have been based on the decrease of solar irradiance, which includes both collimated and scattered light. Lambert's Law expresses the decrease in the irradiance,  $I(z)$ , i.e., the total flux incident upon an element of surface divided by its area, with depth  $z$ , as follows:

$$-\frac{dI(z)}{dz} = K \cdot I(z) \quad (11-65)$$

where

$K$  = diffuse light attenuation coefficient.

The diffuse attenuation coefficient can be expressed as a sum of terms accounting for absorption,  $a$ , and backward scattering of light,  $s_b$  (Smith and Tyler, 1976):

$$K = Da + s_b \quad (11-66)$$

where

$D$  = radiance distribution function.

Usually,  $s_b$  is small compared to the absorption term. The absorption term constitutes part of the beam attenuation coefficient,  $\alpha$ , which can be measured in a spectrophotometer:

$$\alpha = a + s_b + s_f \quad (11-67)$$

where

$s_f$  = the forward scattering coefficient of the solution.

The inclusion of the distribution function,  $D$ , in Equation (11-66) accounts for the difference in mean light pathlength of collimated and diffuse light. Perfectly diffuse light has a mean path through an element of water which is twice as long as that of a beam of light. The distribution function, generally increases asymptotically with depth due to the increasing fraction of the total light which is scattered. In water bodies where scattering can be ignored,  $D$  has a value of 1.2. Miller and Zepp (1979) reported that the mean value of  $D$  for six sediment laden waters was 1.6.

The diffuse light attenuation coefficient of natural waters differs greatly due to variations in the types and amounts of particles and dissolved substances in the water. Miller and Zepp (1979), Zepp and Schlotzhauer (1981), and Smith and Baker (1978) have investigated the contributions of suspended sediments, dissolved organic carbon, and chlorophyll pigments to the light attenuation coefficient. By using Equation (11-66) to integrate the results of these investigations, and assuming

backscattering to be negligible, Burns et al. (1981) derived the following expression to estimate the diffuse light attenuation coefficient:

$$K = D \cdot \left[ a_w + (a_a \cdot \text{chl } a) + (a_{\text{DOC}} \cdot \text{DOC}) + (a_{\text{SS}} \cdot \text{SS}) \right] \quad (11-68)$$

where

- $a_w$  = absorptivity of water
- $a_a$  = absorptivity of chlorophyll-a pigment
- chl a = concentration of chlorophyll-a pigment
- $a_{\text{DOC}}$  = absorptivity of dissolved organic carbon
- DOC = concentration of dissolved organic carbon
- $a_{\text{SS}}$  = absorptivity of suspended sediments
- SS = concentration of suspended sediments.

Each absorptivity term varies with the wavelength of light, as shown in Table II-30.

Diffuse light attenuation coefficients can also be estimated using turbidity indicators such as Secchi disc depth. Empirical studies have shown that the diffuse light attenuation coefficient is inversely proportional to the Secchi disc depth,

$Z_{\text{sd}}$ :

$$K = \frac{R}{Z_{\text{sd}}} \quad (11-69)$$

The proportionality constant, R, has a value between 1.44 and 1.7 for visible light, i.e. 400-800 nm. In the middle ultraviolet portion of the spectrum, i.e. near 312 nm, R has a value of 9.15 (Zepp, 1980).

#### 2.5.2.2.3 Fate of Excited Molecules

"Each molecule taking part in a chemical reaction which is a direct result of the absorption of light takes up one quantum of radiation (Stark-Einstein Law)." (Glasstone, 1946)

According to this "second law of photochemistry", the extent to which a photochemical reaction progresses depends on the number of quanta of light absorbed. Each absorbed photon produces an electronically excited molecule which can undergo numerous processes, including reaction. Factors which influence the fraction of excited molecules which undergo reaction, called the quantum yield, comes first in the following discussion of the fate of excited molecules. Then, the two major classes of environmental photolysis reactions, direct and sensitized, are discussed.

##### 2.5.2.2.3.1 The Quantum Yield

Although all photochemical reactions are initiated by the absorption of a photon, not every absorbed photon induces a chemical reaction. Besides chemical

TABLE 11-30

CONTRIBUTIONS TO LIGHT ATTENUATION COEFFICIENT

Waveband Center (nm)	$a_w^a$ ( $m^{-1}$ )	$a_a^b$ [(mg/l) $^{-1}$ m $^{-1}$ ]	$a_{DOC}^c$ [(mg/l) $^{-1}$ m $^{-1}$ ]	$a_{SS}^d$ [(mg/l) $^{-1}$ m $^{-1}$ ]
300	.141	69. *	6.25	.35
310	.105	67. *	5.41	.35
320	.0844	63. *	4.68	.35
330	.0678	61. *	4.05	.35
340	.0561	58. *	3.50	.35
350	.0463	55.	3.03	.35
360	.0379	55.	2.62	.35
370	.0300	51.	2.26	.35
380	.0220	46.	1.96	.35
390	.0191	42.	1.69	.35
400	.0171	41.	1.47	.35
410	.0162	39.	1.27	.35
420	.0153	38.	1.10	.35
430	.0144	35.	0.949	.35
440	.0145	32.	0.821	.35
450	.0145	31.	0.710	.35
460	.0156	28.	0.614	.35
470	.0156	26.	0.531	.35
480	.0176	24.	0.460	.35
490	.0196	22.	0.398	.35
500	.0257	20.	0.344	.35
510	.0357	18.	0.297	.35
520	.0477	16.	0.257	.35
550	.0638	10.	0.167	.35
600	.244	6.	0.081	.35
650	.349	8.	-	.35
700	.650	3.	-	.35
750	2.47	2.	-	.35
800	2.07	0.	-	.35

<sup>a</sup>Source: Smith and Baker (1981)

<sup>b</sup>Source: Smith and Baker (1978) Calculated using  $a_a = K_2/D$ ,  
D = 1.2

<sup>c</sup>Source: Zepp and Schlotzhauer (1981)

<sup>d</sup>Source: Miller and Zepp (1979). Calculated using  $a_{SS} = K_S/D$ .

\* Denotes extrapolated values.

reactions, possible processes which excited molecules may undergo include the reemission of light through fluorescence and phosphorescence, the internal conversion of the photons' energy into heat, and the excitation of other molecules, as shown in Figure 11-14. The fraction of absorbed photons which cause the desired reaction(s) is termed the quantum yield,  $\phi$

$$\phi \equiv \frac{\text{moles of a given species formed or destroyed}}{\text{moles of photons absorbed by the system}} \quad (11-70)$$

The quantum yields for photochemical reactions in the solution phase exhibit two properties which greatly simplify their use:

- The quantum yield is less than or equal to one
- The quantum yield is independent of the wavelength of the absorbed photons.

Although exceptions to these rules exist, they are rare for photochemical reactions in the aquatic environment.

Environmental conditions influence photolysis quantum yields. Molecular oxygen acts as a quenching agent (see Figure 11-14) in some photochemical reactions, reducing the quantum yields (Wolfe *et al.*, 1978). In other cases, it has no effect or may even be a reactant. In any case, rate constant and quantum yield measurements should be performed in water with oxygen concentrations representative of environmental conditions.

Suspended sediments also influence rates of photolysis. Not only do suspended sediments increase light attenuation, but they change the reactivity of compounds sorbed on them (Miller and Zepp, 1979). Sorption may either increase or decrease a compound's reactivity depending on the reaction it undergoes. This effect, however, is of secondary importance in comparison to the increase in light attenuation by the suspended sediments (Burns *et al.*, 1981). Thus, the effects of sorption will be neglected.

Chemical speciation also affects rates of photolysis. Different forms of an organic acid or base may have different quantum yields, as well as absorptivities, causing the apparent photolysis rate of the compound to vary with pH. The possibility of this should be kept in mind when the  $pK_a$  of a photolyzing compound is  $7 \pm 2$ . Except where stated otherwise, data contained herein may be assumed independent of pH over the range of values observed in natural waters.

Photochemically initiated reactions may show a temperature effect depending upon the actual mechanisms involved. General methods for predicting this effect have yet to be developed. Users of this screening manual should assume thermal effects on photolysis to be negligible.

Quantum yields vary over several orders of magnitude depending on the nature of the molecule which absorbs light and the reactions it undergoes. The two major

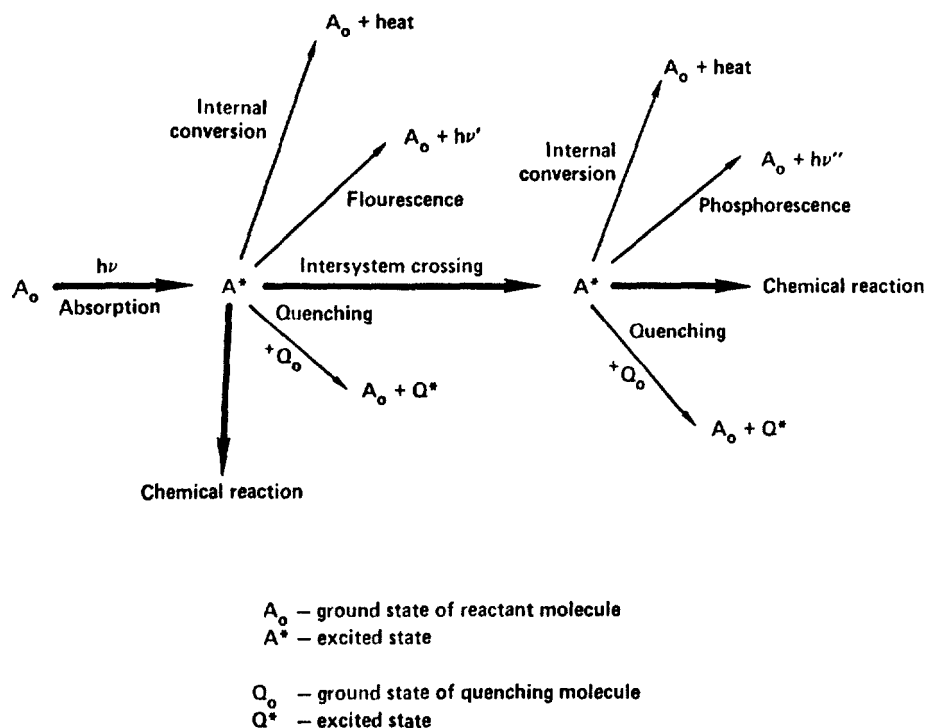


FIGURE 11-14 PHOTOCHEMICAL PATHWAYS OF AN EXCITED MOLECULE, EXCITED MOLECULES DO NOT ALWAYS CHEMICALLY REACT.

classes of photochemical reactions of interest in the aquatic environment are direct and sensitized photolysis. A closer examination of each reaction type follows.

#### 2.5.2.2.3.2 Direct Photolysis

Direct photolysis occurs when the reacting molecule itself directly absorbs light. The excited molecule can undergo various types of reactions, including fragmentation, reduction, oxidation, hydrolysis, acid-base reaction, addition, substitution, isomerization, polymerization, etc. Figure 11-15 shows examples of the reactions undergone by three toxic substances which directly photolyze.

The quantum yield for the direct photolysis,  $\phi_d$ , of a compound is a constant defined as follows:

$$\phi_d = \frac{-dC}{dt} / I_{ad} \quad (11-71)$$

where

$C$  = concentration of the compound

$I_{ad}$  = rate at which the compound absorbs light.

Table 11-31 lists several disappearance quantum yields for direct photolysis of

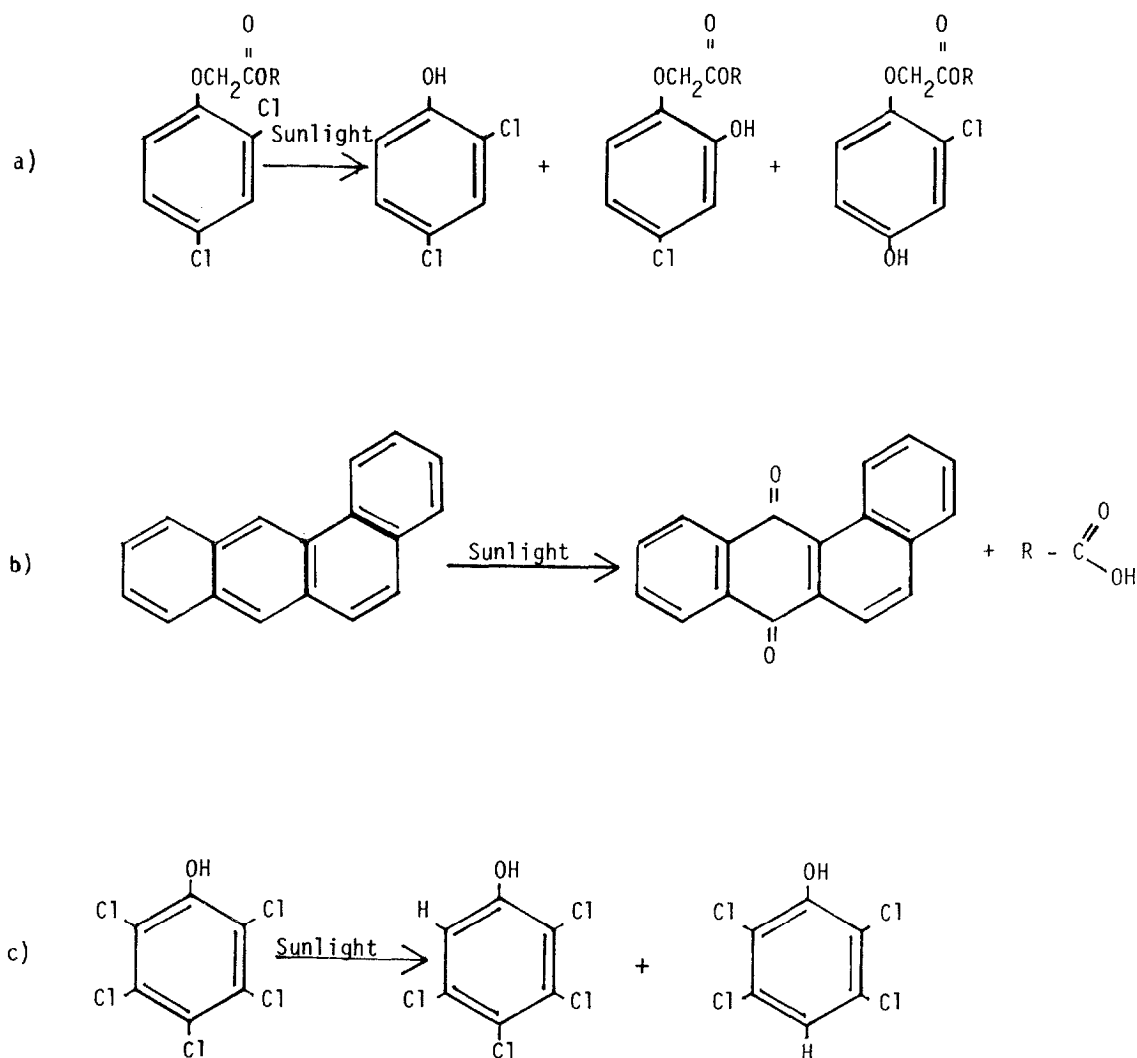


FIGURE 11-15 DIRECT PHOTOCHEMICAL REACTIONS OF (A) 2,4-D ESTER, (B) BENZ(A)ANTHRACENE, AND (C) PENTACHLOROPHENOL,

aquatic pollutants.

By comparing molecular absorption spectra with the spectral distribution of sunlight, it is possible to determine whether or not a compound may directly photolyze. Benzene, as shown in Figure II-16a, does not directly photolyze because it does not absorb light above 275 nm. Naphthacene, shown in Figure II-16b, does directly photolyze because of its strong absorptivity in the sunlight region of the spectrum. Humic acids, Figure II-16c, by virtue of their absorption of sunlight may initiate indirect, or sensitized, photochemical reactions.

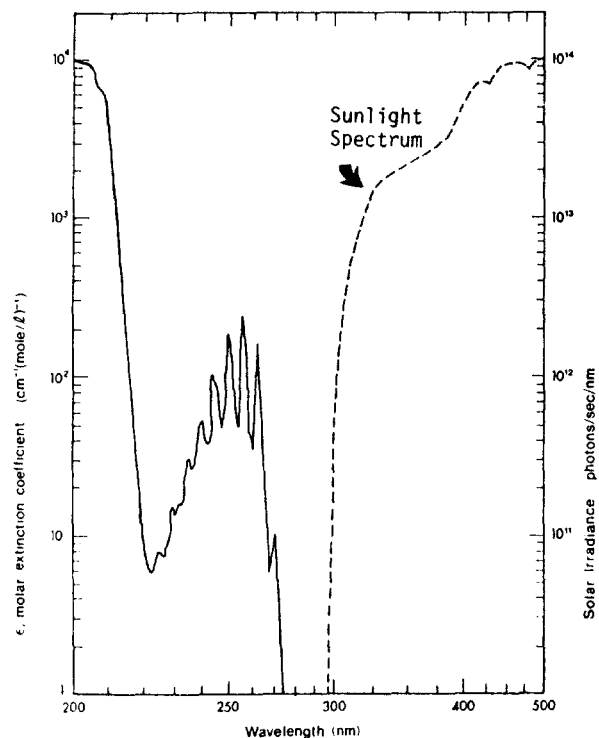
TABLE 11-31

DI SAPPEARANCE QUANTUM YIELDS,  $\phi_d$  FOR DIRECT PHOTOLYSIS

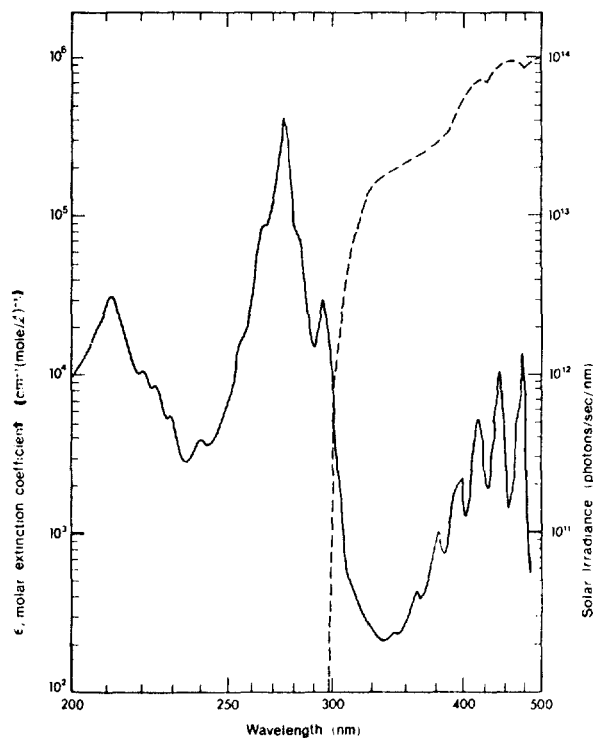
Compound	$\phi_d$	Reference
<u>Polycyclic Aromatic Hydrocarbons</u>		
Naphthalene	.015	a
1-Methyl naphthalene	.018	a
2-Methyl naphthalene	.0053	a
Phenanthrene	.010	a
Anthracene	.0030	a
9-Methyl anthracene	.0075	a
9, 10-Di methyl anthracene	.0040	a
Pyrene	.0021	a
Fluoranthrene	(313 nm) .00012	a
	(366 nm) .000002	a
Chrysene	.0028	a
Naphthacene	.013	a
Benz(a)anthracene	.0033	a
Benz(a)pyrene	.00089	a
<u>2, 4-D Esters</u>		
Butoxyethyl ester	.056	b
Methyl ester	.031	b
Carbaryl	.0055	c
N-Nitrosoatrazine	.30	d
Tri flural in	.0020	d
DMDE	.30	d
<sup>a</sup> Zepp and Schlotzhauer (1979)		<sup>c</sup> Wolfe et al . (1978)
<sup>b</sup> Zepp et al . (1975)		<sup>d</sup> Zepp and Cline (1977)



(a) BENZENE



(b) NAPHTHACENE



(c) HUMIC ACID

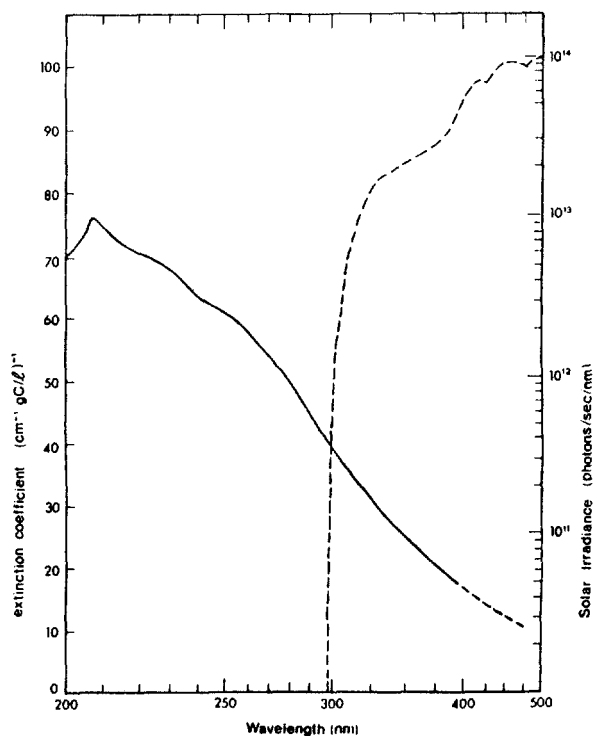


FIGURE 11-16

COMPARISON OF SOLAR IRRADIANCE WITH THE ABSORPTION SPECTRA OF (A) A COMPOUND WHICH DOES NOT DIRECTLY PHOTOLYZE, (B) A COMPOUND WHICH DOES DIRECTLY PHOTOLYZE, AND (C) A SUBSTANCE WHICH INITIATES INDIRECT PHOTOCHEMICAL REACTIONS

References: Sunlight spectrum, Burns et al. (1981); Benzene and naphthalene spectra, U.V. Atlas of Organic Compounds; Humic acid spectrum, Schnitzer (1971).

### 2.5.2.2.3.3 Sensitized Photolysis

Sunlight can cause the degradation of aquatic pollutants by means other than direct photolysis. A light-absorbing molecule can transfer its excess energy to an acceptor molecule causing the acceptor to react as if it had absorbed the radiant energy directly. This reaction mechanism, known as photosensitization, contributes to the degradation of aquatic pollutants when suitable light absorbing substances, or photosensitizers, are present. 2,5-Dimethylfuran is an example of a compound which degrades by sensitized photolysis. It does not react when exposed to sunlight in distilled water but degrades rapidly in waters containing natural humic acids (Zepp *et al.* 1981a).

Numerous substances, including humic acids, titanium dioxide, and synthetic organic compounds, can sensitize photochemical reactions. But, most potential sensitizers occur at such low environmental concentrations that they have negligible effects on photolysis rates. Humic acids, the naturally occurring by-products of plant matter decay, frequently attain concentrations of 1-10mg as carbon per liter in natural systems. Humic acids strongly absorb sunlight with wavelengths shorter than 500 nm, as the absorption coefficients for dissolved organic carbon,  $a_{DOC}$ , in Table II-27, indicate.

The quantum yield for photosensitized reactions,  $\phi_s$ , is defined in a manner similar to the quantum yield for direct photolysis:

$$\phi_s = \frac{-dC}{dt} / I_{as} \quad (II-72)$$

where

$c$  = concentration of the pollutant

$I_{as}$  = rate of light absorption by the sensitizing molecule.

The quantum yield for sensitized photolysis, however, is not constant but depends on the pollutant concentration, such that:

$$\phi_s = Q_s \cdot C \quad (II-73)$$

where

$Q_s$  = a constant.

This is due to the fact that the probability of the sensitized molecule donating its energy to a pollutant molecule is proportional to the concentration of the pollutant molecule. Published values of  $Q$  are very rare. Zepp *et al.* (1981b) report a  $Q$  of  $19 \text{ (mol/l)}^{-1}$  for the photosensitized oxidation of 2,5-dimethylfuran.

#### 2.5.2.2.4 Preliminary Screening of Direct Photolysis

As the preceding discussion indicates, a number of environmental parameters influence photolysis. The following sections show that the procedure for calculating the photolysis rate can be quite involved. Therefore, a preliminary screening which attempts to determine whether photolysis rates are likely to be significant or insignificant (without actually calculating the rate itself) is useful.

If  $\epsilon = 0$  (i.e. if the molecule does not absorb solar radiation) for  $290 < \lambda < 700$  nm, then direct photolysis does not occur. References which show  $\epsilon$  versus  $\lambda$  relationships include Lyman *et al.* (1982), Sadtler (undated), and Schnitzer (1971). Numerous other references contain  $\lambda^*$  values (i.e. the wavelength of maximum absorption.) If  $\lambda^* < 270$  nm or  $\lambda^* > 730$  nm, then direct photolysis is probably unimportant. References which contain  $\lambda^*$  values (in addition to Table II-32 of this document) include Lyman *et al.* (1982), Friedel and Orchin (1951), Hershenson (1966) and Kamlet (1960). The Kamlet reference is a series of 20 volumes from 1960 to present and contains  $\lambda^*$  values for many thousands of organics.

It should be recognized that small  $\phi_d$  or small  $\epsilon_{max}$  are not good indicators of the importance of photolysis. For example, consider the tabulations below:

$$\phi_d \text{ (benzo[a]pyrene)} = 0.00089 \text{ at } \lambda = 313 \text{ nm}$$

but

$$\epsilon_{max} = 13,000; \lambda = 347 \text{ nm}$$

$$\epsilon_{max} = 24,000; \lambda = 364 \text{ nm}$$

$$\epsilon_{max} = 29,000; \lambda = 384 \text{ nm}$$

and

$$k_{do} \text{ (near surface photolysis rate)} = 17. / \text{day}$$

The quantum yield for benzo[a]pyrene is small (0.00089) considering that quantum yields can be as high as 1.0. However, the near surface photolysis rate (i.e. the photolysis rate in a very thin layer of clear water) is 17./day, a very large rate. This result is caused by the high extinction coefficients for benzo[a]pyrene, and it is evident that photolysis can be important for this compound.

Now consider the case of small  $\epsilon_{max}$

For naphthalene:

$$\epsilon_{max} = 250 \text{ at } \lambda = 311 \text{ nm}$$

but

$$\phi_d = 0.015$$

and

$$k_{do} = 0.2 / \text{day}$$

For the small  $\epsilon_{\max}$  (250), the near surface photolysis rate is 0.2/day. While this is not an extremely large rate, it may also not be negligible either, depending on the particular environmental condition.

Certain categories or groups of chemicals are likely to be poor absorbers of sunlight. A number of these groups are shown below:

<u>Group</u>	<u>Examples</u>
alcohols	R-OH: ethyl alcohol
ethers	R-O-R': diphenyl ether
amines	<b>R-NH<sub>2</sub>(primary)</b> : methyl amine
nitriles (cyanides)	R-CN: hydrogen cyanide

For these groups, photolysis is likely to be unimportant. Other groups, however, do tend to absorb sunlight. Figure 11-17 shows a number of these groups.

A final preliminary screening is to compare an estimated upper limit photolysis rate (e.g., using  $\phi_d = 1$ ) against other first-order rates which have already been calculated. If these rates are high enough, the photolysis rate, even under optimal light-absorbing conditions, may be relatively small and therefore negligible. For example, an upper limit photolysis rate which is calculated to be 20 percent as large as a hydrolysis rate is relatively insignificant.

### 2.5.2.3 Computing Environmental Photolysis Rates

The overall rate at which a pollutant photolyzes in the aquatic environment is the sum of the rates of direct and sensitized photochemical reactions. At the low pollutant concentrations observed in the environment, the rates of both direct and sensitized photolysis are proportional to the concentration of the pollutant. Thus, photolysis follows a first-order rate law:

$$\frac{dC}{dt} = -k_p \cdot C \quad (11-74)$$

where

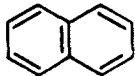
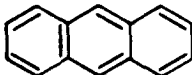

$$k_p = \text{overall photolysis rate constant, day}^{-1}$$

$$= k_d + k_s$$

$$k_d = \text{direct photolysis rate constant, day}^{-1}$$

$$k_s = \text{sensitized photolysis rate constant, day}^{-1}$$

Due to the complexity of the units for the parameters in the photolysis section, it is essential that the user employ the specified units in each equation. All resulting first-order photolysis rate constants have units of  $\text{day}^{-1}$ .

Group	$\lambda_{\max}$ (nm)	Molar Absorptivity, $\epsilon$ (L/mol-cm)
$\text{>C=O}$ (aldehyde, ketone)	295	10
$\text{>C=S}$	460	weak
$\text{-N=N-}$	347	15
$\text{-NO}_2$	278	10
	311 270	250 5000
	360	6000
	440 300	20 1000
$\text{>C-C-C=O}$ 	330	20

SOURCE: CALVERT AND PITTS

FIGURE II-17 CHROMOPHROIC GROUPS WHICH ABSORB SUNLIGHT

The determination of rate constants for direct and sensitized photolysis is the subject of the remainder of this section. Section 2.5.2.3.1 includes a derivation of the equations for  $k_d$  and  $k_s$ . Sections 2.5.2.3.2 and 2.5.2.3.3 describe how to calculate these constants on the basis of near surface rate constants or molecular absorption spectra.

#### 2.5.2.3.1 Derivation of Rate Constant Equations

##### 2.5.2.3.1.1 Direct Photolysis

Figure II-18 shows the major processes which influence direct photolysis of pollutants in natural waters and indicates data requirements. This figure can be translated into mathematics as follows:

Light absorption within a small wavelength band  $\Delta\lambda$ :

$$\epsilon_{\lambda} W_{\lambda} \Delta\lambda$$

Light absorption in a water body of depth Z:

$$\frac{1-e^{-KZ}}{KZ} \epsilon_{\lambda} W_{\lambda} \Delta\lambda$$

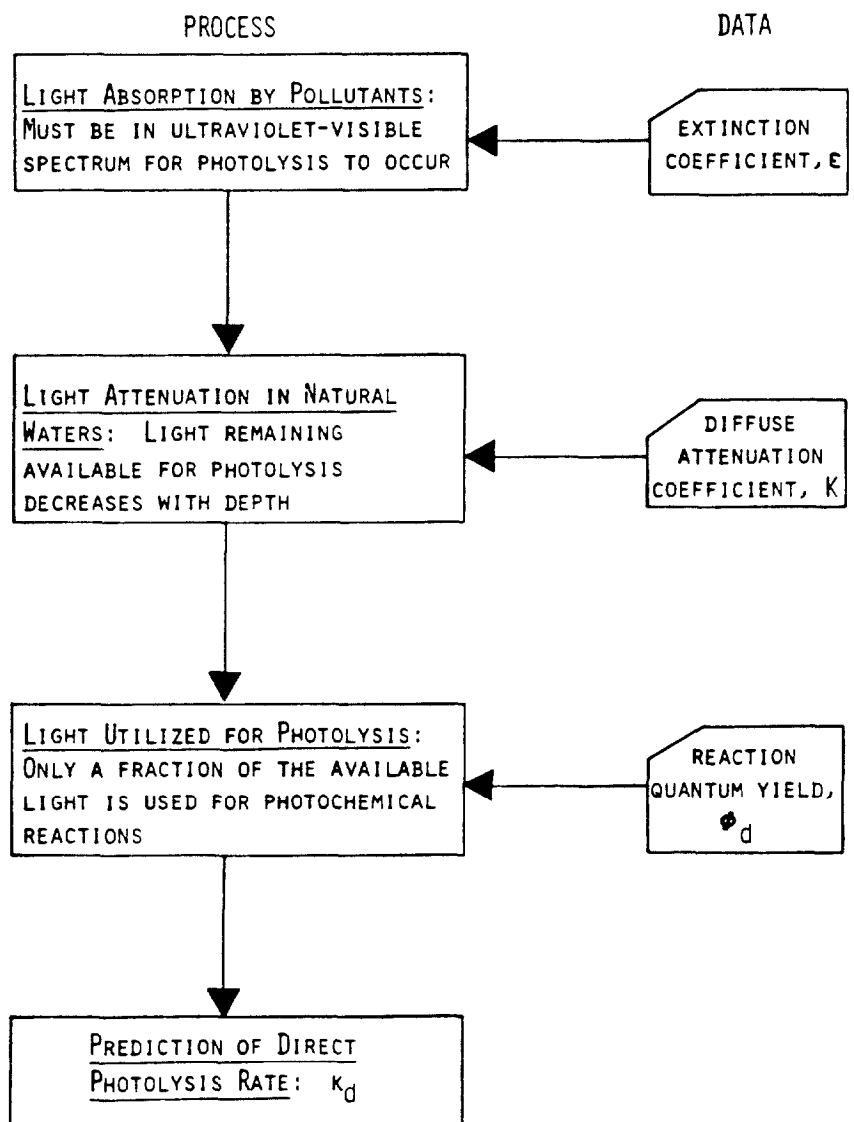


FIGURE 11-18 MAJOR PROCESSES WHICH INFLUENCE PHOTOLYSIS OF POLLUTANTS IN NATURAL WATERS

Photolysis rate for wavelength band  $\Delta\lambda$ :

$$\phi_{\lambda} \epsilon_{\lambda} W_{\lambda} \frac{1-e^{-KZ}}{KZ} \Delta\lambda$$

The equation for direct photolysis becomes:

$$k_d = 2.3 j \phi_d D \int_{\lambda_0}^{\lambda_1} \epsilon W \frac{1-e^{-K \cdot Z}}{K \cdot Z} d\lambda \quad (11-75)$$

where

Z = mixed depth of water body, m

$\lambda_1$  = 700 nm

$\lambda_0$  = 300 nm

j = conversion factor =  $1.43 \times 10^{-16} \text{ mole} \cdot \text{cm}^3 \cdot \text{sec} \cdot \text{l}^{-1} \cdot \text{day}^{-1}$

$\epsilon$  = base 10 molar extinction coefficient of pollutant,  $1 \text{ mol}^{-1} \text{cm}^{-1}$

C = concentration of pollutant, mol/l

D = radiance distribution function

W = photon irradiance near the surface, photons  $\text{cm}^{-2} \text{sec}^{-1} \text{nm}^{-1}$

K = diffuse light attenuation coefficient of the water,  $\text{m}^{-1}$

Equation 11-75 can be written in summation notation as:

$$k_d = 2.3 j \phi D \sum_{\lambda=290}^{700} \epsilon_{\lambda} W_{\lambda} \frac{1-e^{-KZ}}{KZ} \Delta\lambda \quad (11-76)$$

Equation (11-75) incorporates the assumption that C, K, and D are independent of depth.

#### 2.5.2.3.1.2 Sensitized Photolysis

The rate at which a compound decays through sensitized photolysis is proportional to the rate at which sensitizing molecules absorb light. The rate at which sensitizers absorb light in the aquatic environment is:

$$I_{as} = \frac{1}{Z} \int_0^Z \int_{\lambda_0}^{\lambda_1} j \cdot a_s(\lambda) \cdot C_s(z) \cdot D(z) \cdot W(\lambda) \cdot e^{-K(\lambda)z} d\lambda dz \quad (11-77)$$

where

$I_{as}$  = rate of light absorption by sensitizers, einstein  $\text{l}^{-1} \text{day}^{-1}$

$a_s$  = base e absorption coefficient of the sensitizer, e.g.,  $1 \text{ mg-DOC}^{-1} \text{cm}^{-1}$

$C_s$  = concentration of sensitizer, e.g., mg-DOC/l.

The rate constant for sensitized photolysis of a compound,  $k_s$ , is then:

$$k_s = j \cdot C_s \cdot D \cdot Q_s \cdot \int_{\lambda_0}^{\lambda_1} a_s \cdot W \cdot \frac{1 - e^{-K \cdot Z}}{K \cdot Z} \cdot d\lambda \quad (11-78a)$$

Equation 11-78a includes the assumptions that  $C_s$ ,  $K$ , and  $D$  are independent of depth and that  $Q_s$  is independent of wavelength.

In terms of summation notation, this equation becomes:

$$k_s = j \cdot Q_s \cdot D \cdot C_s \cdot \sum_i a_s \cdot W_i \cdot \frac{1 - e^{-K \cdot Z}}{K \cdot Z} \quad (11-78b)$$

### 2.5.2.3.2 Use of Near Surface Rate Constants

Experimental data for direct photolysis are generally reported as near surface rate constants, as in Table 11-32. Near the surface of a water body ( $K \cdot z < 0.2$ ), the mean irradiance is approximately equal to the surface irradiance. This fact permits Equation 11-75 to be simplified to the following expression which defines the near surface rate constant,  $k_{do}$ :

$$k_{do} = 2.3 \cdot \phi_d \cdot D_o \cdot j \cdot \int_{\lambda_0}^{\lambda_1} \epsilon \cdot W \cdot d\lambda \quad (11-79)$$

where

$k_{do}$  = near-surface direct photolysis rate constant,  $\text{day}^{-1}$   
 $D_o$  = radiance distribution near the surface (approximate value = 1.2).

According to Equation (11-79), the near surface rate constant is independent of the properties of the water it is measured in, except for the small variation in  $D_o$ . Thus, when the difference in solar irradiance between the experimental and environmental conditions is accounted for, the user can apply a near surface rate constant to other bodies of water using the following expression:

$$\frac{k_d}{k_{do}} = \frac{2.3 \cdot j \cdot \phi \cdot D \cdot \sum_{\lambda=290}^{700} \epsilon_{\lambda} \cdot W_{\lambda} \cdot \frac{1 - e^{-KZ}}{KZ} \cdot \Delta\lambda}{2.3 \cdot j \cdot \phi \cdot D_o \cdot \sum_{\lambda=290}^{700} \epsilon_{\lambda} \cdot W_{\lambda_0} \cdot \Delta\lambda} \quad (11-80a)$$



TABLE II-32  
NEAR-SURFACE DIRECT PHOTOLYSIS RATE CONSTANTS

Compound <sup>1</sup>	$k_{do}$ <sup>1</sup> (day <sup>-1</sup> )	$I_o$ <sup>2</sup> (1angleys/day)	$\lambda^*$ <sup>3</sup> (nm)	Ref.
<u>Polycyclic Aromatic Hydrocarbons</u>				
Naphthalene	.23	2100	310	a
1-Methyl naphthalene	.76	2100	312	a
2-Methyl naphthalene	.31	2100	320	a
Phenanthrene	2.0	2100	323	a
Anthracene	22.0	2100	360	a
9-Methyl anthracene	130.0	2100	380	a
9, 10-Dimethyl anthracene	48.0	2100	400	a
Pyrene	24.0	2100	330	a
Fluoranthrene	.79	2100	-	a
Chrysene	3.8	2100	320	a
Naphthacene	490.0	2100	440	a
Benzo(a)pyrene	31.0	2100	380	a
Benzo(a)anthracene	28.0	2100	340	a
<u>Carbamate Pesticides</u>				
Carbaryl	.32	2100	313	b
Propham	<.003	740	-	c
Chlorpropham	<.006	740	-	c
<u>Phthalate Esters</u>				
dimethyl ester	$5 \times 10^{-3}$	600	-	d
diethyl ester	$5 \times 10^{-3}$	600	-	d
di-n-butyl ester	$5 \times 10^{-3}$	600	-	d
di-n-octyl ester	$5 \times 10^{-3}$	600	-	d
di-(2-ethyl hexyl)	$5 \times 10^{-3}$	600	-	d
<u>2,4-D Esters</u>				
butoxyethyl ester	.050	420	-	e
methyl ester	.030	420	-	e
Hexachlorocyclopentadiene	94.	540	-	f
Pentachlorophenol (anion)	.46	600	318*	f
3,3'-dichlorobenzidine	670.	2000	280-330*	f
N-nitrosodiazine	300.	1800	-	g
Triuralin	30.	1800	-	g
DMDE(1,1-bis(p-methyl phenyl)-2,2-dichloroethane)	17.	2200	-	g

Notes:

- 1 Parenthetic comments after name of compound indicate when the form of the compound undergoing photolysis is something other than the neutral form.
- 2 Estimated Solar Flux - usually high estimates to give conservative photolysis rates.
- 3 Wavelength of maximum sunlight absorption.
- \* Indicates the maximum of the absorption spectrum is used.

References:

- a) Zepp and Schlotzhauer (1979)
- b) Zepp (1978)
- c) Wolfe *et al.* (1978)
- d) Wolfe *et al.* (1980)
- e) Zepp *et al.* (1979)
- f) Callahan *et al.* (1979)
- g) Zepp and Cline (1977)

$$= \frac{D \sum_{\lambda=290}^{700} \epsilon_{\lambda} \alpha_{\lambda} I \frac{1-e^{-KZ}}{KZ} \Delta\lambda}{D_0 \sum_{\lambda=290}^{700} \epsilon_{\lambda} \alpha_{\lambda} I_0 \Delta\lambda} \quad (11-80b)$$

$$\approx \frac{DI}{D_0 I_0} \frac{1-e^{-K(\lambda^*)Z}}{K(\lambda^*)Z} \quad (11-80c)$$

so:

$$k_d = k_{d0} \cdot \frac{I}{I_0} \cdot \frac{D}{D_0} \cdot \frac{1-e^{-K(\lambda^*)Z}}{K(\lambda^*)Z} \quad (11-80d)$$

where

$I$  = total solar radiation (langley/day)

$I_0$  = total solar radiation under conditions at which  $k_{d0}$  was measured (langley/day)

$\lambda^*$  = wavelength of maximum light absorption, i.e. wavelength where the product  $\epsilon(\lambda) \cdot H(\lambda)$  is greatest.

This approximate expression is valid if the following assumptions are sufficiently accurate: 1) the solar irradiance at a wavelength is a constant fraction of the total solar irradiance (Park **et al.**, 1980) and 2) the light attenuation coefficient,  $K$ , is constant over the range of wavelength that the compound absorbs solar radiation at high rates (Burns **et al.**, 1981).

Although it is possible to derive a similar expression for sensitized photolysis, variation in the absorptivity and reactivity of natural humic substances make extrapolations based on the concentration of dissolved organic carbon subject to large errors. An approach taken by Zepp (1980) was to correlate the sensitized photolysis rate constant with the absorbance of a solution at 366nm. Such an empirical relationship was found for 2,5-dimethyl furan

$$\log k_{s0} = .67 \log a_{366} - 1.15 \quad (11-81)$$

where

$a_{366}$  = absorbance of solution at 366nm

$k_{s0}$  = near surface rate constant,  $\text{day}^{-1} \text{cm}^{-1}$  ( $I_0 = 1$  langley/day).

At present, data on sensitized photolysis are difficult to obtain. The planner should be aware of its potential significance even if it is not possible to estimate rates at this time.

### 2.5.2.3.3 Evaluation of Direct Photolysis Rate

The simplest and preferred method of calculating the direct photolysis rate is

shown in a step-wise fashion in Table II-33. Note that the effects of water depth and light attenuation can be estimated based on water-body characteristics from Table II-34. Thus the method essentially consists of multiplying several numbers together to find  $k_d$ .

If  $k_{do}$ , which is required to use the method outlined in Table II-33, is not directly obtainable, it can be calculated from Table II-35 and then used in conjunction with the near-surface approach described above. One advantage of using the near-surface approach (in addition to its simplicity) is that the photolysis rate in different classes of natural waters can be readily evaluated using Table II-33, once  $k_{do}$  has been calculated a single time.

In some cases, the near-surface approach may not be applicable. Equations II-80a through II-80c show some of the simplifications required to develop a near-surface approach. Photolysis rates for chemicals which have multiple  $\epsilon_{max}$  values within the wavelength range  $290 \text{ nm} < \lambda < 700 \text{ nm}$  should not be calculated using the near-surface approach. Rather, the direct approach outlined in Table II-37 should be used in conjunction with the procedure shown in Table II-36.

Very little emphasis is given here on rates of indirect photolysis because little data are available on indirect photolysis rates. Table II-38 summarizes the pertinent work of Zepp (1977). Zepp found that the near-surface half-life for indirect photolysis for several chemicals in Okefenokee Swamp waters was very short: from 0.02 hr to 7 hrs. The near-surface rate constant translates to between 2.4/day to 830./day. However, on a depth-averaged basis, four of the five photolysis rates are below 0.06/day. Only for pentacene is the depth-averaged photolysis rate high (5.8/day). Thus, the same factor (humic material) that is responsible for the high near-surface rate constants, is also responsible for the small depth-averaged values because much of the sunlight is rapidly absorbed near the water surface. For this reason, and because of the lack of data, indirect photolysis is ignored in these assessment procedures.

TABLE II-33

SUMMARY OF NEAR SURFACE APPROACH

1. Predictive Equation:

$$k_d = k_{do} \frac{DI}{D_o I_o} \frac{1 - e^{-K(\lambda^*)Z}}{K(\lambda^*)Z}$$

2. Find:

$$k_{do} = \underline{\hspace{2cm}}$$

- See Table II-32, or
- See Table 8-12, p. 8-38, Lyman et al., where half-lives are given:

$$k_{do} = \frac{0.693}{t_{1/2}}$$

$$D = \underline{\hspace{2cm}} \quad (1.2-1.6)$$

$$D_o = \underline{\hspace{2cm}} \quad (1.2)$$

$$I = \underline{\hspace{2cm}} \quad (500-700 \text{ langley/day})$$

$$I_o = \underline{\hspace{2cm}} \quad (500-2100 \text{ langley/day; see Table II-29})$$

$$\lambda^* = \underline{\hspace{2cm}}$$

- Table II-32
- Table 8-5, p. 8-14, of Lyman et al.
- Friedel and Orchin, 1951.
- Hershenson, 1966.
- Kamlet (ed.), 1960.

3. Knowing  $\lambda^*$  and Depth of Water body, Z, Find

$$\frac{1 - e^{-K(\lambda^*)Z}}{K(\lambda^*)Z}$$

Table II-34 shows some typical values of this expression.

4. Find  $k_d$  using equation shown in step 1.

5. Suppose  $k_{do}$  is not known from experimental studies. It can be calculated from the procedure shown in Table II-35.

TABLE II-34

$$\text{RANGE OF } \frac{1 - e^{-K(\lambda^*)Z}}{K(\lambda^*)Z}$$

$\lambda^*$ (nm)	Water Type <sup>a</sup>	Depth of Water (m)				
		1	2	3	5	10
300	A	0.9	0.8	0.8	0.6	0.4
	B	0.5	0.4	0.2	0.14	0.07
	C	0.1	0.06	0.04	0.03	0.01
	D	0.03	0.01	0.009	0.005	0.003
340	A	0.9	<b>0.9</b>	0.9	0.8	0.7
	B	0.7	<b>0.5</b>	0.4	0.2	0.1
	C	0.2	0.08	0.06	0.03	0.02
	D	0.04	0.02	0.01	0.007	0.004
380	A	<b>1.0</b>	1.0	1.0	0.9	0.9
	B	<b>0.8</b>	<b>0.6</b>	0.5	<b>0.3</b>	0.2
	C	<b>0.2</b>	<b>0.1</b>	0.07	<b>0.04</b>	0.02
	D	<b>0.05</b>	0.02	0.02	0.009	0.005
420	A	<b>1.0</b>	1.0	1.0	1.0	0.9
	B	<b>0.8</b>	0.6	0.5	0.4	0.2
	C	<b>0.3</b>	0.1	0.09	0.05	0.03
	D	<b>0.06</b>	0.03	0.02	0.01	0.006
460	A	1.0	1.0	1.0	1.0	0.9
	B	0.8	0.7	<b>0.6</b>	0.4	0.2
	C	0.3	0.2	<b>0.1</b>	0.06	0.03
	D	0.07	0.3	0.02	0.01	0.007
500	A	1.0	1.0	1.0	0.9	0.9
	B	0.8	0.7	<b>0.6</b>	<b>0.4</b>	0.2
	C	<b>0.3</b>	0.2	<b>0.1</b>	<b>0.07</b>	0.03
	D	<b>0.07</b>	0.4	0.02	0.01	0.007

<sup>a</sup> Water Type	chl a (mg/l)	DOC (mg/l)	SS (mg/l)
A	0.0	0.0	0.0
B	0.001 (Lake Tahoe)	0.1	0.5
C	0.01 (eutrophic)	0.5	5.0
D	0.1 (highly eutrophic)	2.0	20.0

TABLE II-35

## DIRECT PREDICTION OF NEAR SURFACE RATE

- Predictive Equation:

$$k_{do} = 2.3 j \phi_d D_o \sum_{\lambda=290}^{700} \epsilon_{\lambda} W_{\lambda} \Delta \lambda$$

- Data Required:

1.  $\phi_d$  (quantum yield for direct photolysis):
  - Table 11-31, or
  - Table 8-11, p. 8-37, in Lyman et al.
2.  $D_o$  (~1.2)
3.  $\epsilon_{\lambda}$  versus  $\lambda$  relationship
  - Table 8-7, p. 8-20, in Lyman et al.
  - Sadtler, undated.
  - Schnitzer, 1971.
4.  $W$  versus  $\lambda$  (typical values for central U.S.A. are given in Table II-36 for  $I = 540$  langley/day)

- Approach

Use procedure shown in Table II-36

- a) Enter  $\epsilon_{\lambda}$  versus  $\lambda$  values in column 5 and appropriate rows.
- b) Find each  $\epsilon W \Delta \lambda$  in column 6.
- c) Find  $\sum \epsilon W \Delta \lambda$  at bottom of column 6.
- d) Use Equation 3 on right-hand side of table to find  $k_{do}$ .

TABLE II-36  
 PROCEDURE FOR CALCULATING DIRECT PHOTOLYSIS RATE CONSTANT  
 FOR A REFERENCE LIGHT INTENSITY OF 540 LANGLEYS/DAY

1	2	3	4	5	6	7	8	9	10	11	12	13	14	15
Wavelength(m)	$\frac{W}{h}$ photons/(cm <sup>2</sup> -sec-nm)	$\frac{dA}{nm}$ photons/(cm <sup>2</sup> -sec)	WDA photons/(cm <sup>2</sup> -sec)	$\frac{1}{V(m^2-cm)}$ - eUDA	eUDA	$b \cdot \left[ \frac{dW}{(m^{-1})} + \frac{1}{V(m^2-cm)} \right] \cdot \frac{C_{112}}{(mg/l-m)}$ (mg/l)	$\frac{C_{112} \cdot C_{112}}{V(m^2-cm)}$ (mg/l)	$\frac{C_{112} \cdot C_{112}}{V(m^2-cm)}$ (mg/l)	$\frac{C_{112} \cdot C_{112}}{V(m^2-cm)}$ (mg/l)	$\frac{C_{112} \cdot C_{112}}{V(m^2-cm)}$ (mg/l)	$\frac{C_{112} \cdot C_{112}}{V(m^2-cm)}$ (mg/l)	$\frac{C_{112} \cdot C_{112}}{V(m^2-cm)}$ (mg/l)	eMAX	P
300	.00303·10 <sup>14</sup>	10	0.03·10 <sup>14</sup>			.141 49.	6.25	0.35						
310	.0368·10 <sup>14</sup>	10	0.368·10 <sup>14</sup>			.105 47.	5.41	0.35						
320	.113·10 <sup>14</sup>	10	1.13·10 <sup>14</sup>			.0844 43.	4.64	0.35						
330	.181·10 <sup>14</sup>	10	1.81·10 <sup>14</sup>			.0678 41.	4.05	0.35						
340	.211·10 <sup>14</sup>	10	2.11·10 <sup>14</sup>			.0561 38.	3.50	0.35						
350	.226·10 <sup>14</sup>	10	2.26·10 <sup>14</sup>			.0463 35.	3.03	0.35						
360	.241·10 <sup>14</sup>	10	2.41·10 <sup>14</sup>			.0379 33.	2.62	0.35						
370	.268·10 <sup>14</sup>	10	2.68·10 <sup>14</sup>			.0300 31.	2.26	0.35						
380	.294·10 <sup>14</sup>	10	2.94·10 <sup>14</sup>			.0220 28.	1.96	0.35						
390	.366·10 <sup>14</sup>	10	3.66·10 <sup>14</sup>			.0181 27.	1.69	0.35						
400	.528·10 <sup>14</sup>	10	5.28·10 <sup>14</sup>			.0171 41.	1.47	0.35						
410	.692·10 <sup>14</sup>	10	6.92·10 <sup>14</sup>			.0162 39.	1.27	0.35						
420	.712·10 <sup>14</sup>	10	7.12·10 <sup>14</sup>			.0153 38.	1.10	0.35						
430	.688·10 <sup>14</sup>	10	6.88·10 <sup>14</sup>			.0144 35.	0.949	0.35						
440	.814·10 <sup>14</sup>	10	8.14·10 <sup>14</sup>			.0145 32.	0.821	0.35						
450	.917·10 <sup>14</sup>	10	9.17·10 <sup>14</sup>			.0145 31.	0.710	0.35						
460	.927·10 <sup>14</sup>	10	9.27·10 <sup>14</sup>			.0156 28.	0.614	0.35						
470	.959·10 <sup>14</sup>	10	9.59·10 <sup>14</sup>			.0166 26.	0.531	0.35						
480	.983·10 <sup>14</sup>	10	9.83·10 <sup>14</sup>			.0176 24.	0.460	0.35						
490	.930·10 <sup>14</sup>	10	9.30·10 <sup>14</sup>			.0196 22.	0.398	0.35						
500	.949·10 <sup>14</sup>	10	9.49·10 <sup>14</sup>			.0257 20.	0.344	0.35						
510	.962·10 <sup>14</sup>	10	9.62·10 <sup>14</sup>			.0357 18.	0.297	0.35						
520	1.00·10 <sup>14</sup>	10	10.0·10 <sup>14</sup>			.0477 16.	0.257	0.35						
550	1.04·10 <sup>14</sup>	50	52.0·10 <sup>14</sup>			.0838 10	0.167	0.35						
600	1.07·10 <sup>14</sup>	50	53.5·10 <sup>14</sup>			.244 6.	0.081	0.35						
650	1.08·10 <sup>14</sup>	50	54.0·10 <sup>14</sup>			.349 6.	-	0.35						
700	1.07·10 <sup>14</sup>	50	53.6·10 <sup>14</sup>			.650 3.	-	0.35						

1. Calculate  $k_p$ :  
 $k_p = 2.3 \cdot \phi_e \cdot J \cdot 0.47 \cdot EP$   
 $= 3.3 \cdot 10^{-16} \cdot \phi_e \cdot 0.47$   
 = \_\_\_\_\_, per day

2. For a light intensity other than  $I_0 = 540$  langley/day:  
 $k_p' = k_p \cdot \frac{I}{I_0}$  = \_\_\_\_\_, per day

Values of  $I$ :  
 Fig. II-12, p. 132 (Annual)  
 Fig. IV-28, p. 431 (July, August)

3. Calculate  $k_{ps}$  (near-surface rate)  
 $k_{ps} = 3.3 \cdot 10^{-16} \cdot \phi_e \cdot 0.47 \cdot EP$   
 = \_\_\_\_\_, per day

TABLE 11-37

## DIRECT PREDICTION OF DEPTH-AVERAGED PHOTOLYSIS RATE

- Predictive Equation:

$$k_d = 2.3 j \phi_d D \sum_{\lambda=290}^{\lambda=700} \epsilon_{\lambda} W_{\lambda} \frac{1-e^{-KZ}}{KZ} \Delta\lambda$$

- Data Required:

1.  $\phi_d$
2. D
3.  $\epsilon_{\lambda}$  versus  $\lambda$
4.  $W_{\lambda}$  versus  $\lambda$
5. Water body characteristics: depth, chl a, DOC, SS

- Approach: Use Table 11-36

- a) Enter  $\lambda$  versus  $\epsilon$  in column 5 and appropriate rows, and calculate  $\epsilon W \Delta\lambda$  in column 6.
- b) Enter D (column 7), chl a (column 9), DOC (Column 10), and SS (column 11) in appropriate rows.
- c) Calculate K (column 12) for appropriate rows.
- d) Knowing water depth Z, calculate appropriate values for column 13.
- e) Transfer column 6 entries to column 14.
- f) Multiply column 13 entries by column 14 entries and record in column 15.
- g) Sum column 15 entries and use Equation 1 on RHS of sheet to find  $k_d$ .



TABLE 11-38

ESTIMATED HALF-LIVES FOR INDIRECT PHOTOLYSIS OF  
ORGANICS IN OKEFENOKEE SWAMP WATER<sup>a</sup>

Organic	Half-Life (hr) <sup>b</sup>	Near-Surface Rate Constant (1/day) <sup>b</sup>	Depth-Averaged Rate Constant (1/day) <sup>c</sup>
Naphthalene	7	2.4	0.01
Pentacene	0.02	830.	5.8
Histidine	2	8.3	0.06
Tryptophan	2	8.3	0.06
Methionine	3	5.5	0.04

<sup>a</sup>Zepp, R. G. *et al.*, 1977. Singlet Oxygen in Natural Waters. Nature, Vol. 267.

<sup>b</sup>Near-Surface (1 cm) rate constant

<sup>c</sup>Depth-averaged rate constant. Assume humic materials 12 mg/l, depth = 3m.

EXAMPLE 11-7

Computation of Photolysis Rate Constants

Compute the mean annual photolysis rate constant for the pesticide carbaryl in a hypothetical river near Fresno, California. Use both the evaluation of integral and near surface rate constant methods described above. Assume the following physical and chemical parameters apply to the river:

- Mean depth = 2 m
- Suspended sediments = 10 mg/l
- Humic acid = 2 mg-DOC/l
- Chlorophyll  $\bar{a}$  = 0 mg/l

Zepp (1978) reported a quantum yield,  $\phi_d$ , of .0060 and the following absorptivities,  $\epsilon$ , for carbaryl:

Wavelength (nm)	Absorptivity ( $M^{-1}cm^{-1}$ )
300	918
310	356
320	101
330	11

#### Near Surface Rate Constant Method

Table II-32 contains the following information regarding carbaryl:

$$k_d = .32 \text{ day}^{-1}$$

$$I_o = 2100 \text{ langley/day}$$

$$\lambda^* = 313 \text{ nm.}$$

According to Figure II-13, the mean annual solar irradiance at Fresno, California is 450 langley/day.

Assume that the radiance distribution function under reference,  $D_o$ , and environmental,  $D$ , conditions have values of 1.2 and 1.6 respectively.

To calculate the light attenuation coefficient at the wavelength of maximum light absorption, 313 nm, we use Equation 11-68 and the data in Table 11-30, at 310 nm:

$$K = 1.6(.105 + 67 \cdot 0 + 5.41 \cdot 0 + 5.41 \cdot 2 + 2 + .35 \cdot 10)$$

$$= 23.1m^{-1}$$

When the water absorbs nearly all of the incident radiation, i.e.,  $KZ \gg 1$ , the following approximation is valid:

$$\frac{1 - e^{-KZ}}{KZ} \approx \frac{1}{KZ}$$

approximation can be applied to Equation II-76 and Equation II-80d. It both simplifies the calculations and eliminates the dependence of the rate constant on the radiance distribution function,  $D$ , in cases where the light attenuation coefficient is calculated from  $D$ , as in this example. In such a case, the user's choice of a value of  $D$  does not affect the result.

Using this approximation in Equation (II-80d), the mean photolysis rate constant is computed to be:

$$k_d = .32 \text{ day}^{-1} \cdot \frac{450}{2100} \cdot \frac{1.6}{1.2} \cdot \frac{1}{23.1 \cdot 2}$$

$$= 2.0 \times 10^{-3} \text{ day}^{-1}$$

This example demonstrates the significant difference, 100 fold in this case, which may exist between near surface and mean photolysis rate constants. The strong attenuation of light by the river water was the primary cause of the reduction in rates.

## B. Evaluation of Integrals

The absorption data for carbaryl indicate that we need to concern ourselves only with light of wavelength 300-330nm in order to determine a mean rate constant.

First, we assume that D has the same value as above, ~1.6. Then, we compute the light attenuation coefficients using Equation II-68 and the data in Table II-36.

$\lambda$ (nm)	D	$a_w$ ( $m^{-1}$ )	$(a_{doc} \cdot C_{doc})$ [(mg/l) $^{-1}m^{-1}$ ]	$C_{doc}$ (mg/l)	$(a_{ss} \cdot C_{ss})$ [(mg/l) $^{-1}m^{-1}$ ]	$C_{ss}$ (mg/l)	K ( $m^{-1}$ )
300	1.6	.141	6.25	2	.35	10	25.8
310	1.6	.105	5.41	2	.35	10	23.1
320	1.6	.0844	4.68	2	.35	10	20.7
330	1.6	.0678	4.05	2	.35	10	18.7

Table II-36 lists the photon spectral irradiance,  $W'$ , at a reference total solar flux, I., of 540 langley/day. The local solar flux, as in part A, is 450 langley/day.

Next, evaluate the sum indicated in Equation II-76.

Since  $KZ > 3$  for all wavelengths of interest, use the approximation discussed in part A.

$\lambda$ (nm)	$\epsilon$ ( $M^{-1}cm^{-1}$ )	$W' \times 10^{-14}$ (photons/ $cm^2/s$ )	(K·Z)	$\frac{\epsilon \cdot W'}{K \cdot Z}$
300	918	.0303	51.6	$.539 \times 10^{-14}$
310	356	.388	46.2	$2.99 \times 10^{-14}$
320	101	1.13	41.4	$2.76 \times 10^{-14}$
330	11	1.81	37.4	$.532 \times 10^{-14}$
				$\sum_i = 6.82 \times 10^{-14}$

Given that the quantum yield is .006, the mean photolysis rate constant can be computed using Equation II-82 and the above information:

$$k_d = 2.3 \cdot 1.43 \times 10^{-16} \cdot \frac{450}{540} \cdot .0060 \cdot 1.6 \cdot 6.82 \times 10^{-14}$$

$$= 1.8 \times 10^{-3} \text{ day}^{-1}$$

The small difference between the rate constants calculated in parts A and B is due to the difference in the reference solar intensities. The assumption made here that the spectral distribution of solar energy is independent of intensity

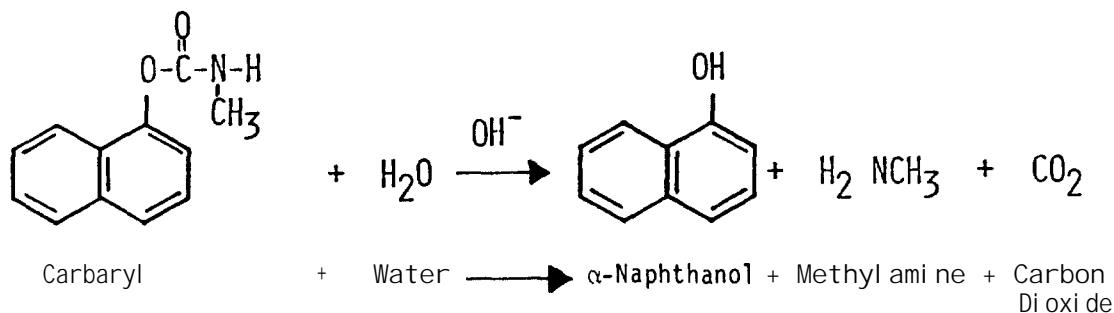
is only approximately true. Consequently, the greater the discrepancy between the reference and local solar intensities, the greater the error in rate constants that can be expected. When the local exceeds the reference intensity, the actual rate constant is probably higher than the calculated value. When the reference exceeds the local intensity, the actual rate constant is probably lower than calculated.

----- END OF EXAMPLE 11-7 -----

### 2.5.3 Hydrolysis

Some toxic compounds can be altered by direct reaction with water. The chemical reaction of a compound with water is called hydrolysis. Typically in hydrolysis reactions hydroxide replaces another chemical group.

An example hydrolysis reaction for a toxic organic compound is given below:



Generalized hydrolytic reactions of organic compounds are presented in Table 11-39.

Hydrolysis reactions alter the reacting molecules but do not always produce less noxious products. For example the more toxic 2,4-D acid is produced from the hydrolysis of certain 2,4-D esters. Alternatively the hydrolysis of carbaryl (shown above) produces less toxic products, i.e.  $\alpha$ -naphthanol and methyl amine.

Hydrolysis products may be more or less volatile than the original compound. Hydrolysis products which ionize may have essentially zero volatility depending upon pH. Hydrolysis products are generally more readily biodegraded than the parent compounds, although there are some exceptions.

Hydrolysis reactions are commonly catalyzed by hydrogen or hydroxide ions. This produces the strong pH dependence often observed for hydrolysis reactions. Examples of this dependency are shown in Figure 11-19, where the logarithms of reaction rate constants ( $k_H$ ) are plotted versus pH. The hydrolysis rate of carbaryl can be seen to increase logarithmically with pH. The rate at pH = 8 is ten times that at pH = 7 and 100 times that at pH = 6. The hydrolysis rate of parathion is high at low pH

TABLE II-39  
GENERALIZED HYDROLYTIC REACTIONS OF ORGANIC COMPOUNDS

REACTANT	REACTION CONDITIONS	PRODUCTS
CARBOXYLIC ACID ESTERS $\begin{array}{c} \text{O} \\ \parallel \\ \text{R}-\text{C} \\ \backslash \\ \text{O}-\text{R}' \end{array}$	ACIDIC, NEUTRAL, BASIC	CARBOXYLIC ACID + ALCOHOL $\begin{array}{c} \text{O} \\ \parallel \\ \text{R}-\text{C} \\ \backslash \\ \text{OH} \end{array} + \text{R}'\text{OH}$
AMIDES $\begin{array}{c} \text{O} \\ \parallel \\ \text{R}-\text{C} \\ \backslash \\ \text{N}-\text{R}' \\   \\ \text{H} \end{array}$	ACIDIC, BASIC	CARBOXYLIC ACID + AMINE $\begin{array}{c} \text{O} \\ \parallel \\ \text{R}-\text{C} \\ \backslash \\ \text{OH} \end{array} + \begin{array}{c} \text{H} \\ \backslash \\ \text{N}-\text{R}' \\ / \\ \text{H} \end{array}$
CARBAMATES $\begin{array}{c} \text{H} \\   \\ \text{R}-\text{N} \\ \backslash \\ \text{C}-\text{O}-\text{R}' \\ \parallel \\ \text{O} \end{array}$	ACIDIC, BASIC	AMINE + ALCOHOL + CARBON DIOXIDE $\begin{array}{c} \text{H} \\ \backslash \\ \text{R}-\text{N} \\ / \\ \text{H} \end{array} + \text{R}'\text{OH} + \text{CO}_2$
ORGANOPHOSPHATES (AND DERIVATIVES) $\begin{array}{c} \text{O} \\ \parallel \\ \text{RO}-\text{P}-\text{OR} \\   \\ \text{OR} \end{array}$	BASIC (ACIDIC, NEUTRAL)	PHOSPHATE DIESTER + ALCOHOL $\begin{array}{c} \text{O} \\ \parallel \\ \text{RO}-\text{P}-\text{OH} \\   \\ \text{OR} \end{array} + \text{ROH}$
HALOGENATED ALKANES $\begin{array}{c} \text{R} \\   \\ \text{C}-\text{X} \\ / \quad \backslash \\ \text{R}' \quad \text{R}'' \end{array}$	NEUTRAL, BASIC	ALCOHOL + HALIDE Ion $\begin{array}{c} \text{R} \\   \\ \text{R}'-\text{C}-\text{OH} \\   \\ \text{R}'' \end{array} + \text{X}^-$

SOURCE: I. J. TINSLEY, CHEMICAL CONCEPTS IN POLLUTANT BEHAVIOR, J. WILEY, NEW YORK (1979).

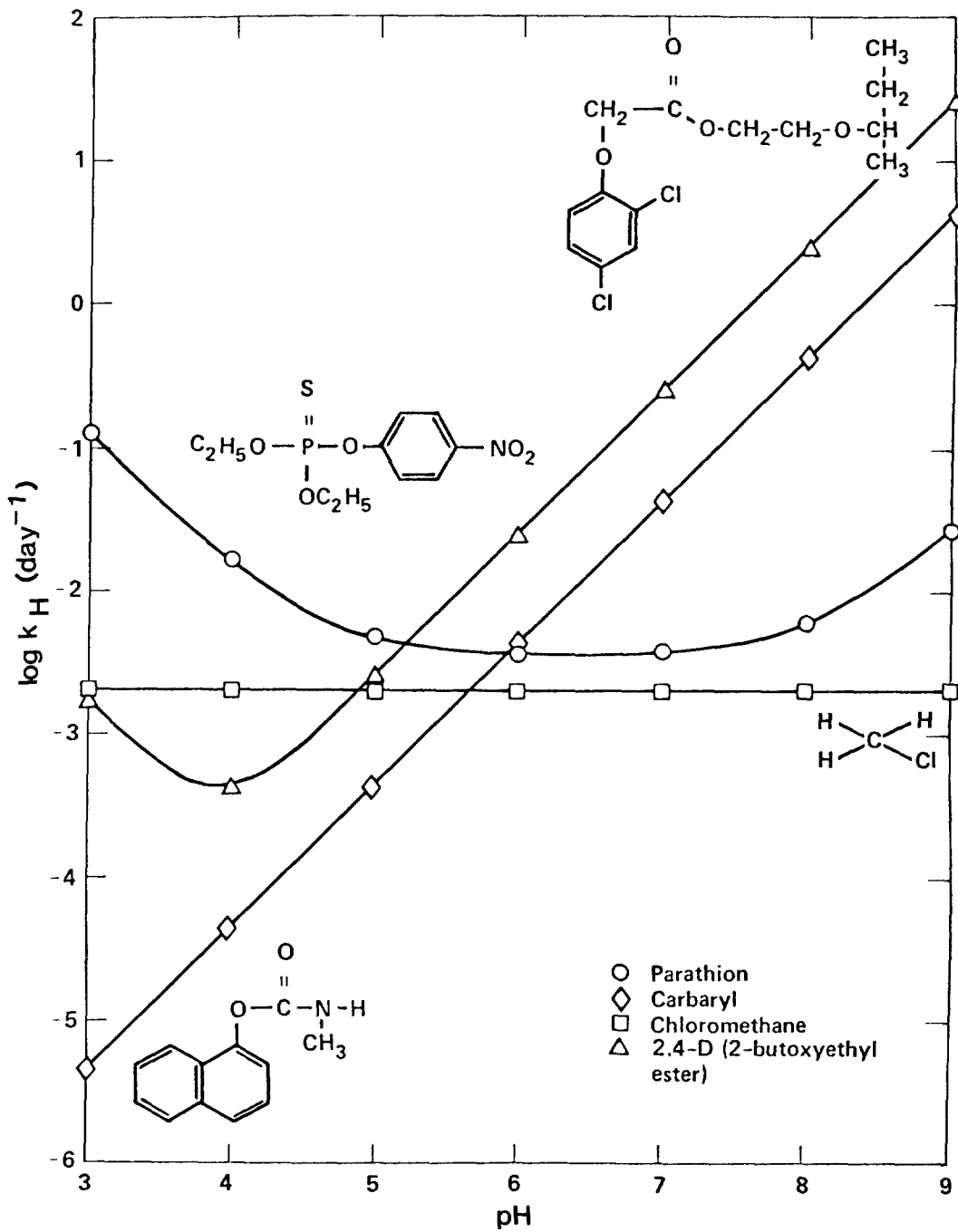


FIGURE 11-19 pH DEPENDENCE OF HYDROLYSIS RATE CONSTANTS

values, reaches a minimum at pH = 6, and then increases with increasing pH. The hydrolysis rate of chloromethane shows minimal dependence on pH over the range presented.

Adsorption can also influence hydrolysis rates. Adsorption of an organic molecule protects it from acid or base catalyzed hydrolysis (Wolfe, 1981). The amount of adsorption can be predicted using the principles presented in Section 2.3.2.

Microbially mediated hydrolysis reactions are responsible for the breakdown of many complex molecules, including natural polymers such as cellulose. Microorganisms catalyze hydrolysis reactions in the process of using organic compounds as energy and/or carbon sources. In cometabolism microbes may hydrolyze toxic organic compounds to hasten their removal from cell protoplasm. Microbially mediated processes are covered under the general heading of biodegradation in Section 2.5.1. Here only abiotic hydrolysis is treated.

Abiotic hydrolysis reactions are represented by rate expressions which are first order in the concentration of the compound being hydrolyzed:

$$R = \frac{\partial C}{\partial t} = -k_H C_T \quad (\text{II-82})$$

where

$R$  = the rate of hydrolysis,  $\text{mole liter}^{-1} \text{sec}^{-1}$  or  $\mu\text{g liter}^{-1} \text{sec}^{-1}$

$k_H$  = specific hydrolysis rate constant,  $\text{sec}^{-1}$

$C_T$  = the dissolved plus sorbed phase concentration of compound C  
 $\text{mole liter}^{-1}$  or  $\mu\text{g liter}^{-1}$ .

In the literature  $k_H$  is typically defined as:

$$k_H = k_n + k_a [H^+] + k_b [OH^-] \quad (\text{II-83})$$

In this document the specific hydrolysis rate constant,  $k_H$ , is defined to include the effects of adsorption:

$$k_H = \left[ k_n + \alpha_w (k_a [H^+] + k_b [OH^-]) \right] \quad (\text{II-84})$$

where

$k_n$  = the neutral hydrolysis rate constant,  $\text{sec}^{-1}$

$\alpha_w$  = the decimal fraction of the total amount of compound C which is dissolved (Calculation procedures in Section 2.3.2)

$k_a$  = the acid catalyzed hydrolysis rate constant,  $\text{liter mole}^{-1} \text{sec}^{-1}$

$[H^+]$  = the molar concentration of hydrogen ion, mole liter<sup>-1</sup>  
 $([H^+] \cong 10^{-pH})$

$k_b$  = the base catalyzed hydrolysis rate constant, liter mole<sup>-1</sup> sec<sup>-1</sup>

$[OH^{-1}]$  = the concentration of hydroxide ion, mole liter<sup>-1</sup>  
 $[OH^-] = 10^{(pH-pK_w)} \cong 10^{(pH-14)}$

Equation 11-84 is a convenient definition of  $k_H$  because specific rate constants which act on the dissolved and total concentrations do not have to be used separately.

Values for the three rate constants  $k_n$ ,  $k_a$ ,  $k_b$  for selected compounds are presented in Table 11-40. Additional values can be found in the literature (e.g. Mabey and Mill, 1978). The three constants can also be determined by simple laboratory tests.

Water body pH values must be obtained for hydrolysis reactions which are pH dependent (i.e. those for which  $k_a \neq 0$  and/or  $k_b \neq 0$ ). It should be noted that in poorly buffered waters (alkalinity  $\leq 50$  mg/l as  $CaCO_3$ ), pH values may change by 1-2 units daily due to natural processes alone. In these cases either additional data must be gathered to characterize the system's pH regime or conservatively low values of  $k_H$  must be used. Table 11-41 summarizes the procedures.

EXAMPLE 11-8

A biodegradation rate constant,  $k_b$  for the fungicide Captan has been given as 0.5 per day. Compare this with the abiotic hydrolysis rate constant,  $k_H$ , at pH = 8.4, a temperature of 25°C, and with 90 percent of the compound adsorbed on suspended matter. Values for  $k_a$ ,  $k_b$ , and  $k_n$  can be found in Table 11-31.

$$\begin{aligned} k_a &= 0 \\ k_b &= 4.9 \times 10^7 \text{ day}^{-1} \\ k_n &= 1.6 \text{ day}^{-1} \end{aligned}$$

$$k_H = \left[ \alpha_w (k_a [H^+] + k_b [OH^-]) \right] + k_n$$

$$[OH^-] \cong 10^{pH-14} = 10^{8.4-14} = 10^{-5.6} = 2.51 \times 10^{-6}$$

thus

$$\begin{aligned} k_H &= \left[ (1.0-0.9) \cdot (4.9 \times 10^7 \times 2.5 \times 10^{-6}) \right] + 1.6 \\ &= 12.3 + 1.6 = 13.9 \text{ day}^{-1} \end{aligned}$$



TABLE II-40

HYDROLYSIS RATE PARAMETERS AND ESTIMATED ENVIRONMENTAL  
HYDROLYSIS RATES

Compound	Hydrolysis Rate Parameters			Environmental Hydrolysis Rates (pH=7)		Ref. Temp. (°C)	Ref.
	$k_a$ (l·m <sup>-1</sup> ·day <sup>-1</sup> )	$k_n$ (day <sup>-1</sup> )	$k_b$ (l·m <sup>-1</sup> ·day <sup>-1</sup> )	$k_H$ (day <sup>-1</sup> )	$t_{1/2}$ (days)		
<u>Pesticides</u>							
Endosulfon	-	-	$3.3 \times 10^5$	$3.5 \times 10^{-2}$	21	27	a
Heptachlor	?	?	?	.7	1.	30	a
Carbaryl	-	-	$4.3 \times 10^5$	$4.3 \times 10^{-2}$	16.	27	b
Propham	-	-	.66	6.6	$1.1 \times 10^7$	27	b
Chlorpropham	-	-	1.7	1.7	$4.0 \times 10^6$	27	b
2,4-D(2-Butoxyethyl ester)	1.7	-	$2.6 \times 10^6$	.26	2.7	28	c
2,4-D(Methyl ester)	-	-	$1.5 \times 10^6$	.15	4.6	28	c
Parathion	$1.3 \times 10^2$	$3.6 \times 10^{-3}$	$2.46 \times 10^3$	3.9	$1.8 \times 10^2$	?	d
Phosmet	?	?	?	2.3	.30	20	e
Dialifor	?	?	?	1.2	.58	20	e
Malathion	?	?	?	6.6	11.	20	e
Captan	-	1.6	$4.9 \times 10^7$	5.6	.13	27	f
Atrazine	3.4	6.6	-	6.6	.10	25	f
Methoxychlor	-	$2.6 \times 10^{-3}$	31.	$2.6 \times 10^{-3}$	$2.7 \times 10^2$	25	f
<u>Halogenated Hydrocarbons</u>							
Chloromethane	-	$2.1 \times 10^{-3}$	.53	$2.1 \times 10^{-3}$	$3.4 \times 10^2$	25	f
Bromomethane	-	$3.5 \times 10^{-2}$	12.	$3.5 \times 10^{-2}$	20.	25	f
Chloroethane	-	$1.8 \times 10^{-2}$	-	$1.8 \times 10^{-2}$	38.	25	f
Dichloromethane	-	$2.8 \times 10^{-6}$	$1.8 \times 10^{-3}$	$2.8 \times 10^{-6}$	$2.6 \times 10^5$	25	f
Trichloromethane	-	-	6.0	6.	$1.3 \times 10^6$	25	f
Bromodichloromethane	-	-	$1.4 \times 10^3$	$1.4 \times 10^{-5}$	$5.0 \times 10^4$	25	f
Dibromochloromethane	-	-	69.	$6.9 \times 10^{-6}$	$1.0 \times 10^5$	25	f
Tri bromomethane	-	-	28.	$2.8 \times 10^{-6}$	$2.5 \times 10^5$	25	f
Hexachlorocyclopentadiene	-	$4.8 \times 10^{-2}$	-	$4.8 \times 10^{-2}$	14.	25	a
<u>Halogenated Ethers</u>							
Bis(chloromethyl) ether	-	$1.6 \times 10^3$	-	$1.6 \times 10^3$	$4.5 \times 10^{-4}$	20	a
2-Chloroethyl vinyl ether	$3.8 \times 10^2$	-	-	$3.8 \times 10^{-5}$	$1.8 \times 10^4$	25	a
<u>Phthalate Esters</u>							
Dimethyl ester	1.	-	$6.0 \times 10^3$	6	$1.2 \times 10^3$	30	g
Diethyl ester	1.	-	$1.9 \times 10^3$	1.9	$3.7 \times 10^3$	30	g
Di-n-butyl ester	1.	-	$9.1 \times 10^2$	9.1	$7.6 \times 10^3$	30	g
Di-n-octyl ester	1.	-	$1.4 \times 10^3$	1.4	$4.9 \times 10^3$	30	g
Di(2-ethylhexyl) ester	1.	-	9.6	9.6	$7.2 \times 10^5$	30	g
<u>Monocyclic Aromatics</u>							
Pentachlorophenol	$1.1 \times 10^4$	$5.8 \times 10^{-3}$	3.3	$6.9 \times 10^{-3}$	$1.0 \times 10^2$	?	d

## Notes

"?" denotes rate parameter not given and not estimable from data in reference  
 "-" denotes zero or very small rate parameter

## References:

- a Callahan *et al.* (1979)  
 b Wolfe *et al.* (1978)  
 c Zepp *et al.* (1975)  
 d Park *et al.* (1980)  
 e Tinsley (1979)  
 f Mabey and Mill (1978)  
 g Wolfe *et al.* (1980)

TABLE 11-41

## PROCEDURE FOR CALCULATING HYDROLYSIS RATE CONSTANT

1. Hydrolysis Rate Constant

$$k_H = \left[ k_n + \alpha_w \left( k_a [H^+] + k_b [OH^-] \right) \right] \quad (1)$$

2. Procedure

- a) Find the hydrolysis rate parameters. Use Table 11-40.

$$k_n = \text{_____} \frac{1}{\text{day}}, k_a = \text{_____} \frac{\text{liters}}{\text{mole day}}, k_b = \text{_____} \frac{\text{liters}}{\text{mole day}}$$

- b) Does the compound sorb? (Table 11-11, Column 1)

If it does, find,  $\alpha_w$ , the fraction of the total amount of compound which is not sorbed

$$\alpha_w = \frac{C_w}{C_T} = \frac{1}{1 + K_p S} \quad (\text{See Section 2.3.2})$$

If it does not sorb set  $\alpha_w = 1$

- c) If the hydrolysis is
- acid catalyzed
- (a
- $k_a$
- value exists) determine the hydrogen ion concentration,
- $[H^+]$
- .

$$[H^+] = 10^{-\text{pH}} = 10^{-\text{---}}$$

- d) If the hydrolysis is
- base catalyzed
- (a
- $k_b$
- value exists) determine the hydroxide ion concentration,
- $[OH^-]$
- .

$$[OH^-] = 10^{(\text{pH} - \text{p}K_w)} = 10^{(-\text{---})} = 10^{-\text{---}}$$

Note:  $\text{p}K_w = 14.2$  for freshwater at  $20^\circ\text{C}$   
 $= 13.4$  for seawater at  $20^\circ\text{C}$

(More precise values for  $\text{p}K_w$  are given in Table 11-13)

- 3.
- Substitute
- $k_n$
- ,
- $\alpha_w$
- ,
- $k_a$
- ,
- $[H^+]$
- ,
- $k_b$
- ,
- $[OH^-]$
- into equation (1) above.

$$K_H = \text{_____}$$

Comparing  $k_H$  to  $k_B$ :

$$\frac{k_H}{k_B} = \frac{13.9}{0.5} = 27.8$$

Comparison of  $k_H$  with  $k_B$  for the above situation shows that the abiotic hydrolysis rate is about 28 times faster than the biodegradation rate. Biodegradation could be neglected here with minimal effect on the results.

----- END OF EXAMPLE II-8 -----

## REFERENCES

- Alexander, M. 1980. Biodegradation of Toxic Chemicals in Water and Soil. In: Dynamics, Exposure, and Hazard Assessment of Toxic Chemicals, ed. R. Haque. Ann Arbor Science, Ann Arbor, MI.
- Baughman, G.L., D.F. Paris, and W.C. Steen. 1980. Quantitative Expression of Biodegradation Rate. In: Biotransformation and Fate of Chemicals in the Environment, ed. A.W. Maki, K.L. Dickson, and J. Cairns, Jr. American Soc. Microbiol., Washington, DC. pp. 105-111.
- Bird, R.B., W.E. Stewart, and E.N. Lightfoot. 1960. Transport Phenomena. John Wiley and Sons, New York.
- Bowman, B.T. and W.W. Saris. 1983. Determination of Octanol-Water Partitioning Coefficients of 61 Organophosphorus and Carbamate Insecticides and Their Relationship to Respective Water Volubility Values. Jour. Envir. Sci. Health. B18(6), pp. 667-683.
- Brown, D.S., and E.W. Flagg. 1981. Journal Environmental Quality 10(3):382-386.
- Burns, L.A., D.M. Cline, and R.R. Lassiter. 1981. Exposure Analysis Modeling System (EXAMS): User Manual and System Documentation. Draft. Environmental Research Laboratory, U.S. Environmental Protection Agency, Athens, GA. 443 PP.
- Callahan, M.A., M.W. Slimak, N.W. Gable, I.P. May, C.F. Fowler, J.R. Freed, P. Jennings, R.L. Durfee, F.C. Whitmore, B. Maestri, W.R. Mabey, B.R. Holt, and C. Gould. 1979. Water-Related Environmental Fate of 129 Priority Pollutants, Volumes I and II. Prepared for EPA by Versar, Inc., Springfield, VA. NTIS PB80-204373.
- Calvert, J.G. and J.N. Pitts. 1966. Photochemistry. John Wiley & Sons, New York.
- Chiou, C.T., V.H. Freed, D.W. Schmedding, and R.L. Kohnert. 1977. Partition Coefficient and Bioaccumulation of Selected Organic Compounds. Environ. Sci. Tech. 11:475-478.
- Dickson, A.G., and J.P. Riley. 1979. The Estimation of Acid Dissociation Constants in Seawater Media from Potentiometric Titrations with Strong Base. I. The Ionic Product of Water  $-K_w$ . Mar. Chem. 7:89-99.
- Dining, W.L., N.B. Terfertiller, and G.J. Kallos. 1975. Evaporation Rates and Reactivities of Methylene Chloride, Chloroform, 1,1,1-Trichloroethane, Trichloroethylene, Tetrachloroethylene and Other Chlorinated Compounds in Dilute Aqueous Solutions. Environ. Sci. Tech. 9:833-838.
- Donigian, A.S., T.Y.R. Lo, and E.W. Shanahan. 1983. Rapid Assessment of Potential Ground-Water Contamination Under Emergency Response Conditions. EPA Report.
- Friedel, R.A. and M. Orchin. 1951. Ultraviolet Spectra of Aromatic Compounds. John Wiley & Sons, New York.
- Gilbert, P.A. and C.M. Lee. 1980. Biodegradation Tests: Use and Value. In: Biotransformation and Fate of Chemicals in the Aquatic Environment, ed. A.W. Maki, K.L. Dickson and J. Cairns, Jr. American Society for Microbiology, Washington, D.C. pp. 34-45.
- Glasstone S. 1946. The Elements of Physical Chemistry. D. Van Nostrand, New York.

- Hambrick, G. A., R.D. DeLaune and W.H. Patrick, Jr. 1980. Effect of Estuarine Sediment pH and Oxidation-Reduction Potential on Microbial Hydrocarbon Degradation. *Applied and Environmental Microbiology* 40(2): 365-369.
- Haque, R. 1980. Dynamics, Exposure and Hazard Assessment of Toxic Chemicals in the Environment: An Introduction. In: *Dynamics, Exposure and Hazard Assessment of Toxic Chemicals*, ed. R. Haque. Ann Arbor Science, Ann Arbor, MI.
- Hassett, J.J., J.C. Means, W.L. Bonwart, and S.G. Wood. 1980. Sorption Properties of Sediments and Energy-Related Pollutants. U.S. Environmental Protection Agency, Athens, Georgia. EPA-600/3-80-041.
- Herbes, S.E., and L.R. Schwall. 1978. Microbial Transformation of Polycyclic Aromatic Hydrocarbons in Pristine and Petroleum-Contaminated Sediments. *Applied and Environmental Microbiology*, 35(2): 306-316.
- Hershenson, H.M. 1966. *Ultraviolet and Visible Adsorption Spectra*. Academic Press.
- Kamlet, M.J. (editor). 1960. *Organic Electronic Spectra Data, Volume 1*, Intersciences Publishers.
- Karickhoff, S.W., D.S. Brown, and T.A. Scott. 1979. Sorption of Hydrophobic Pollutants on Natural Sediments. *Water Res.* 13: 241-248.
- Keith, L.H., and W.A. Telliard. 1979. Priority Pollutants. I. A Perspective View. *Env. Sci. Tech.* 13(4): 416-423.
- Kirsch, E.J., and J.E. Etzel. 1973. Microbial Decomposition of Pentachlorophenol. *Journal Water Pollution Control Federation* 45(2): 359-364.
- Larson, R.J. 1980. Role of Biodegradation Kinetics in Predicting Environmental Fate. In: *Biotransformation and Fate of Chemicals in the Aquatic Environment*, ed. A.W. Maki, K.L. Dickson and J. Cairns, Jr. American Society for Microbiology, Washington, D.C. pp. 67-86.
- Larson, R.J., G.G. Clinckemillie, and L. VanBelle. 1981. Effect of Temperature and Dissolved Oxygen on Biodegradation of Nitrotriacetate. *Water Research* 15: 615-620.
- Leo, A., C. Hansch, and D. Elkins. 1971. Partition Coefficients and Their Uses. *Chemical Reviews*. Volume 71, No. 6.
- Linsley, R.K., M.A. Kohler, and J.L.H. Paulus. 1979. *Hydrology for Engineers*. McGraw-Hill, New York.
- Liss, P.S. 1973. *Deep-Sea Research* 20: 221-238.
- Lyman, W.J., W.F. Reehl, and D.H. Rosenblatt. 1982. *Handbook of Chemical Property Estimation Methods: Environmental Behavior of Organic Compounds*. McGraw-Hill Book Company.
- Mabey, W.R., T. Mill, and R.T. Podoll. 1984. Estimation Methods for Process Constants and Properties Used in Fate Assessments. EPA-600/3-84-035
- Mabey, W., and T. Mill. 1978. Critical Review of Hydrolysis of Organic Compounds in Water Under Environmental Conditions. *J. Phys. Chem. Ref. Data* 7(2): 383-415.
- Mackay, D., and P.J. Leinonen. 1975. Rate of Volatilization of Low-Volatility Contaminants from Water to Atmosphere. *Environ. Sci. Tech.* 9: 1178-1180.

- Miller, G.C. and R.G. Zepp. 1979. Effects of Suspended Sediments on Photolysis Rates of Dissolved Pollutants. *Water Research* 13:453-459.
- Mills, W.B., V. Kwong, L. Mok, M.J. Unga. 1985. Microcomputer Methods for Toxicants in Groundwaters and Rivers. Proceedings of National Conference on Environmental Engineering. Boston, MA.
- Mills, W.B. 1981. Workshop Notes: Screening Analysis of Toxic and Conventional Pollutants in Rivers. Washington, D.C.
- Moon, P. 1940. Proposed Standard Solar-Radiation Curves for Engineering Use. *JFI* 230 (1379-23).
- Paris, D.F., W.C. Steen, J.T. Barnett, and E.H. Bates. 1980. Kinetics of Degradation of Xenobiotics by Microorganisms. *ACS, Division of Environmental Chemistry* 20(2):55-56.
- Paris, D.F., W.C. Steen, G.L. Baughman, and J.T. Barnett, Jr. 1981. Second-order Model to Predict Microbial Degradation of Organic Compounds in Natural Waters. *Applied and Environmental Microbiology* 41(3):603-609.
- Park, R.A., C.I. Connolly, J.R. Albanese, L.S. Clesceri, G.W. Heitzman, H.H. Herbrandson, B.H. Indyke, J.R. Loehe, S. Ross, D.D. Sharma, and W.W. Shuster. 1980. Modeling Transport and Behavior of Pesticides and Other Toxic Organic Materials in Aquatic Environments (PEST). Report No. 7. Center for Ecological Modeling, Rensselaer Polytechnic Institute, Troy, NY. 163 pp.
- Pavlou, S.P. 1980. Thermodynamic Aspects of Equilibrium Sorption of Persistent Organic Molecules at the Sediment-Seawater Interface: A Framework for Predicting Distributions in the Aquatic Environment. In: *Contaminants and Sediments, Volume 2*, ed. R.A. Baker. Ann Arbor Science, Ann Arbor, MI. pp. 323-332.
- Perry, R.H., and C.H. Chilton. 1973. *Chemical Engineers Handbook*. McGraw-Hill, New York.
- Pitter, P. 1976. Determination of Biological Degradability of Organic Substances. *Water Research* 10:231-235.
- Rathbun, E.R. and D. Y. Tai. 1983. Gas Film Coefficients for Streams. *Journal of Environmental Engineering Division, ASCE*. Volume 109, No. 5, pp. 1111-1127.
- Rathbun, R.E., and D.Y. Tai. 1981. Technique for Determining the Volatilization Coefficients of Priority Pollutants in Streams. *Water Research* 15(2).
- Reinbold, K.A., J.J. Hassett, J.C. Means, and W.L. Banwart. 1979. Adsorption of Energy-Related Organic Pollutants: A Literature Review. Environmental Research Laboratory, U.S. Environmental Protection Agency, Athens, Georgia. 178 pp. EPA-600/3-79-086.
- Robinson, N., ed. 1966. *Solar Radiation*. Elsevier Publishing, Amsterdam, London, and New York. 347 pp.
- Rossi, S.S., and W.H. Thomas. 1981. Volubility Behavior of Three Aromatic Hydrocarbons in Distilled Water and Natural Seawater. *Environmental Science and Technology* 15(6):715-716.
- Roubal, G., and R.M. Atlas. 1978. Distribution of Hydrocarbon-Utilizing Microorganisms and Hydrocarbon Biodegradation Potentials in Alaskan Continental Shelf Areas. *Applied and Environmental Microbiology* 35(5):897-905.
- Sadtler Research Laboratories. Sadtler Standard Spectra: Ultraviolet Spectra.

- Schnitzer, M. 1971. In: Soil Biochemistry, Volume 2. Marcel Dekker, New York.
- Schnoor, J.L. 1981. Assessment of the Exposure, Fate and Persistence of Toxic Organic Chemicals to Aquatic Ecosystems in Stream and Lake Environments, Part I. Lecture notes, Water Quality Assessment of Toxics and Conventional Pollutants in Lakes and Streams, a workshop sponsored by U.S. Environmental Protection Agency, June 23-25, 1981 in Arlington, Virginia. Civil and Environmental Engineering, Energy Engineering Division, University of Iowa, Iowa City, IA. 31 pp.
- Shamat, N.A., and W.J. Maier. 1980. Kinetics of Biodegradation of Chlorinated Organics. *Journal Water Pollution Control Federation* 52(8):2158-2166.
- Singer, S.J., and G.L. Nicholson. 1972. *Science* 175:723.
- Smith, J.H., D.C. Bomberger, Jr., and D.L. Haynes. 1981. Volatilization Rates of Intermediate and Low Volatility Chemicals from Water. *Chemosphere* 19:281-289.
- Smith, R.C., and K.S. Baker. 1978. Optical Classification of Natural Waters, *Limnology and Oceanography* 32(2):260-267.
- Smith, R.C., and K.S. Baker. 1981. Optical Properties of the Clearest Natural Waters (200-800 nm). *Applied Optics* 20(2):177-184.
- Smith, R.C., and J.E. Tyler. 1976. Transmission of Solar Radiation into Natural Waters, *Photochemical and Photobiological Reviews*, Volume 1, ed. K.C. Smith. Plenum Press, New York. pp. 117-155.
- Spain, J.C., P.H. Pritchard, and A.W. Bourquin. 1980. Effect of Adaptation on Biodegradation Rates in Sediment/Water Cores from Estuarine and Freshwater Environments. *Applied and Environmental Microbiology* 40(4):726-734.
- Steen, W.C., D.F. Paris, and G.L. Baughman. 1980. Effect of Sediment Sorption on Microbial Degradation of Toxic Substances. In: *Contaminants and Sediments*, Volume 1, ed. R.A. Baker. Ann Arbor Science, Ann Arbor, MI. pp. 477-482.
- Stumm, W., and J.J. Morgan. 1981. *Aquatic Chemistry*, 2nd edition. John Wiley and Sons, New York. 780 pp.
- Tabak, H.H., S.A. Quave, C.I. Mashni, and E.F. Barth. 1981. Biodegradability Studies with Organic Priority Pollutant Compounds. *Journal Water Pollution Control Federation* 53(10):1503-1518.
- Tiedje, J.M. 1980. Fate of Chemicals in the Aquatic Environment: Case Studies, Biotransformation and Fate of Chemicals in the Aquatic Environment, ed. A.W. Maki, K.L. Dickson, and J. Cairns, Jr. American Society for Microbiology, Washington, D.C. pp. 114-119.
- Tinsley, I.J. 1979. *Chemical Concepts in Pollutant Behavior*. A Wiley - Interscience Publication. John Wiley and Sons, New York. 265 pp.
- Turro, N.J. 1978. *Modern Molecular Photochemistry*. Benjamin/Cummings Publishing Menlo Park, CA. 628 pp.
- U.S. Department of Commerce. 1968. *Climatic Atlas of the United States*. U.S. Department of Commerce, Environmental Sciences Services Administration, Environmental Data Service, Washington, D.C.
- U.S. Environmental Protection Agency. 1976. *Quality Criteria for Water*.
- U.V. Atlas of Organic Compounds, Volumes 1-4. 1966-1971. Collaboration of Photoelectric Spectrometry Group, London, and Institut Fur Spektrochemie und Angewandte Spektroskopie, Dortmund. Plenum Press, New York.

- Ward, D.M., and T.D. Brock. 1976. Environmental Factors Influencing the Rate of Hydrocarbon Oxidation in Temperate Lakes, *Applied and Environmental Microbiology* 31(5):764-772.
- Weast, R.C., and M.J. Astle, ed. 1980. *CRC Handbook of Chemistry and Physics*. CRC Press, Boca Raton, FL.
- Wetzel, R.G. 1975. *Limnology*. W.B. Saunders, Philadelphia, PA. 743 pp.
- Wodzinski, R.S., and D. Bertolini. 1972. Physical State in Which Naphthalene and Bibenzyl Are Utilized by Bacteria. *Applied Microbiology* 23(6):1077-1081.
- Wolfe, N.L., R.G. Zepp, and D.F. Paris. 1978. Carbaryl, Protham, and Chloroprotham: A Comparison of the Rates of Hydrolysis and Photolysis with the Rate of Biolysis. *Water Research* 12:565-571.
- Wolfe, N.L. 1980. Determining the Role of Hydrolysis in the Fate of Organics in Natural Waters. In: *Dynamics, Exposure, and Hazard Assessment of Toxic Chemicals*, ed. R. Hague. Ann Arbor Science, Ann Arbor, MI.
- Wolfe, N.L. 1981. Personal Communication.
- Zepp, R.G. 1977. Singlet Oxygen in Natural Waters. *Nature*, Volume 67.
- Zepp, R.G. 1978. Quantum Yields for Reaction of Pollutants in Dilute Aqueous Solution. *Environmental Science and Technology* 12(3):327-329.
- Zepp, R.G. 1980. Assessing the Photochemistry of Organic Pollutants in Aquatic Environments. In: *Dynamics, Exposure, and Hazard Assessment of Toxic Chemicals*, ed. R. Hague. Ann Arbor Science, Ann Arbor, MI. pp. 69-110.
- Zepp, R.G., G.L. Baughman, and P.F. Schlotzhauer. 1981a. Comparison of Photochemical Behavior of Various Humic Substances in Water: I. Sunlight Induced Reactions of Aquatic Pollutants Photosensitized by Humic Substances. *Chemosphere* 10:109-117.
- Zepp, R.G., G.L. Baughman, and P.F. Schlotzhauer. 1981b. Comparison of Photochemical Behavior of Various Humic Substances in Water: II. Photosensitized Reactions. *Chemosphere* 10:119-126.
- Zepp, R.G. and D.M. Cline. 1977. Rates of Direct Photolysis in Aquatic Environment. *Environ. Sci. Tech.* 11:359-366.
- Zepp, R.G., and P.F. Schlotzhauer. 1979. Photoreactivity of Selected Aromatic Hydrocarbons in Water. In: *Polynuclear Aromatic Hydrocarbons*, ed. P.W. Jones and P. Leber. Ann Arbor Science, Ann Arbor, MI. pp. 141-158.
- Zepp, R.G., and P.F. Schlotzhauer. 1981. Comparison of Photochemical Behavior of Various Humic Substances in Water: III. Spectroscopic Properties of Humic Substances, *Chemosphere* 10(5):479-486.
- Zepp, R.G., N.L. Wolfe, J.A. Gordon, and G.L. Baughman. 1975. Dynamics of 2,4-D Esters in Surface Waters. *Environmental Science and Technology* 9(13):1144-1150.



## CHAPTER 3

### WASTE LOADING CALCULATIONS

#### 3.1 INTRODUCTION

Receiving water bodies are subject to waste loads from point sources, nonpoint sources and atmospheric deposition. Point sources are identifiable discrete discharges from municipal, institutional and industrial waste water collection and treatment systems. Nonpoint sources (also known as diffuse or distributed sources) are associated with land drainage which enters a water body through dispersed and often poorly-defined pathways. Atmospheric waste loads are chemicals and particulate matter which settle from the atmosphere or are scavenged by precipitation. These distinctions are not absolute. For example, municipal waste water may be applied to the land and become nonpoint source pollution in runoff and percolation. Similarly, chemicals in precipitation may become a portion of a nonpoint source runoff load.

This chapter describes computational methods or "loading functions" for estimating waste loads to both surface waters and aquifers. These methods share several attributes:

- Required computations are relatively straightforward.
- Necessary data for the functions are generally available. Much of these data are provided in this chapter.
- Notwithstanding computational ease and data availability, use of the functions is not trivial. Considerable information regarding the physical characteristics of the study area must often be compiled.
- The accuracy of loading functions is not high. In general, the best results are obtained when input parameters are based on local pollutant data, such as chemical concentrations in sediment, runoff and wastewater.

The loading functions presented in this chapter are appropriate for water quality screening studies in which the approximate magnitudes of waste loads are needed. In situations requiring higher precision, waste loads must be based on monitoring programs and detailed process modeling.

The chapter places major emphasis on nonpoint sources. Point source loads can often be obtained from available water quality monitoring data. Atmospheric loads are also best determined by monitoring; reliable computational methods are not available to handle such major problems as acid rain. By contrast, monitoring of nonpoint sources is often infeasible and as a result, a number of procedures have been developed and tested for calculation of nonpoint source loads.

#### 3.2 BACKGROUND POLLUTION LOADS

Background water quality "represents the chemical and biological composition of surface waters which would result from natural causes and factors" (Novotny and

Chesters, 1981). A comparable definition could be given for groundwater. The concept of background water quality or pollution is somewhat artificial. Few, if any, water bodies in the United States remain unaffected by human activity. For example, synthetic organic compounds are routinely found in streams and lakes far from any obvious source. In spite of this ambiguity, estimation of background loads is a useful component of water quality planning. These loads represent a baseline or minimum level of water pollution which cannot be eliminated by local or area-wide water quality management.

Background pollution levels can be measured by water quality sampling of surface waters in upstream portions of watersheds which are free of human activity and in aquifers in undeveloped areas. In the absence of such local data, very crude estimates can be determined from the information given in Figures III-1, 2, and 3. These figures show mean surface water concentrations of selected water quality parameters obtained from the U.S. Geological Survey's Hydrologic Benchmark Network (McElroy et al., 1976). The concentrations are based on water quality samples from 57 monitoring locations considered free of human disturbance. More accurate concentration data for nutrients are available from the U.S. National Eutrophication Survey (Omernik, 1977). Nitrogen and phosphorus concentrations in streamflow are grouped according to land use and location in Figures III-4 and 5. Concentrations for the "90% Forest" category can be assumed to represent background concentrations.

Annual mass background loads to surface waters are obtained by multiplying concentrations by streamflow values. Average annual streamflow values for the United States are shown in Figure III-6. Obviously, when local streamflow data are available they are preferable to the regional values given in Figure III-6.

----- EXAMPLE III-1 -----

Background Loading Estimates

Determine the annual background loads of BOD and total phosphorus from a 50 km<sup>2</sup> watershed in northern Illinois.

Solution:

From Figure III-1(b), background BOD concentration is 3.0 mg/l in northern Illinois. Total phosphorus concentrations can be determined from the National Eutrophication Survey data in Figure III-5. Northern Illinois is in the eastern area shown in Figure III-5, and the total phosphorus concentration for the 90 percent Forest category is 0.011 mg/l. Average annual streamflow for the area is 10 in (Figure III-6) or 0.254 m.



FIGURE III-1 BACKGROUND CONCENTRATION (MG/L) OF (A) NITRATE-NITROGEN, (B) BOD, (C) TOTAL PHOSPHORUS AND (D) DISSOLVED SOLIDS (McELROY ET AL., 1976)

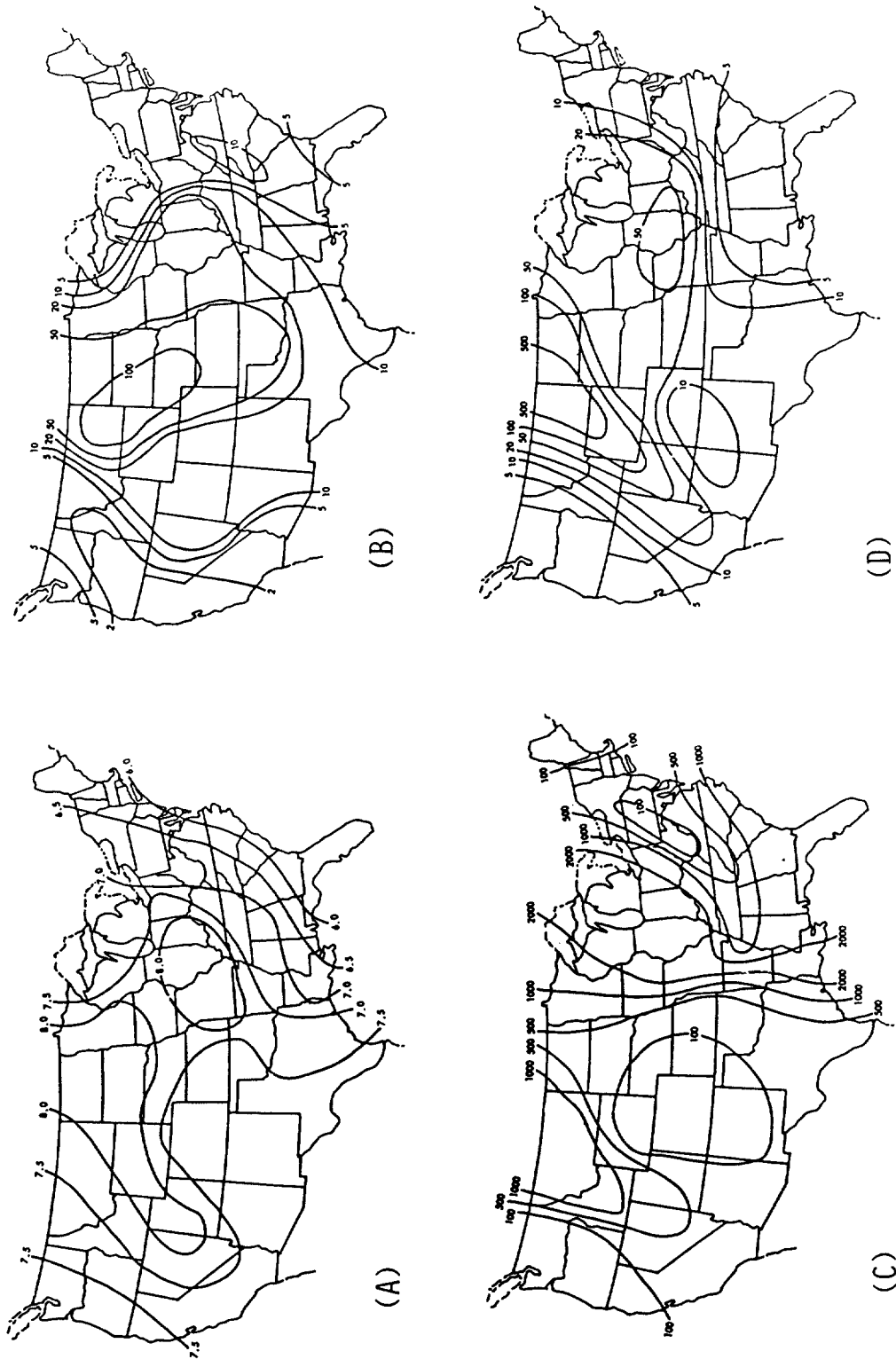


FIGURE III-2 BACKGROUND LEVELS OF (A) PH, (B) SUSPENDED SEDIMENT (MG/L) (C) TOTAL COLIFORMS (MPN/100 ML) AND (D) SULFATE (MG/L) (McELROY ET AL, 1976)

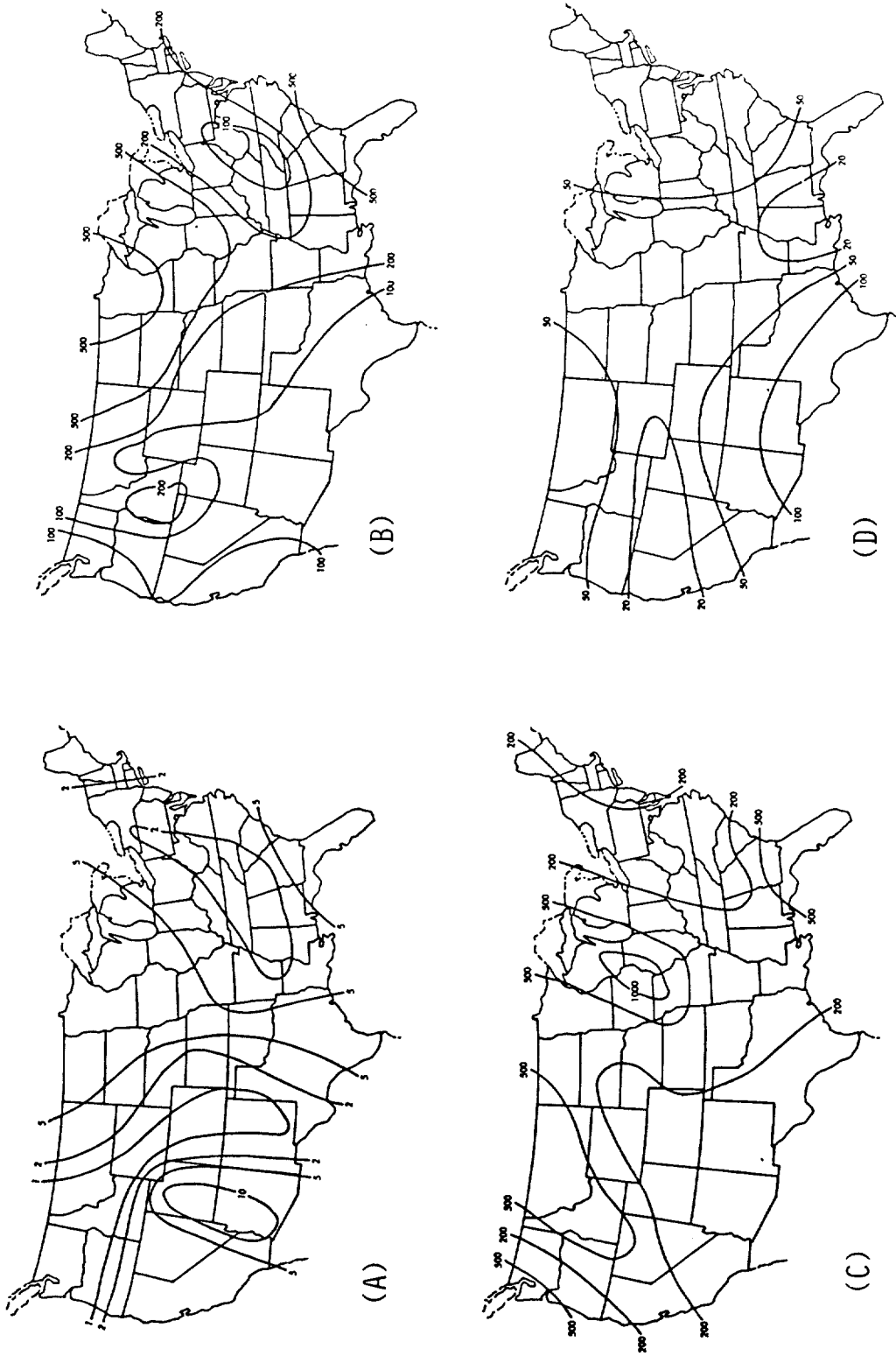


FIGURE III-3 BACKGROUND CONCENTRATIONS OF (A) CHLORIDE (MG/L), (B) IRON + MANGANESE (UG/L), (C) TOTAL HEAVY METALS (UG/L) AND (D) ARSENIC + COPPER + LEAD + ZINC (UG/L) (McELROY ET AL, 1976)

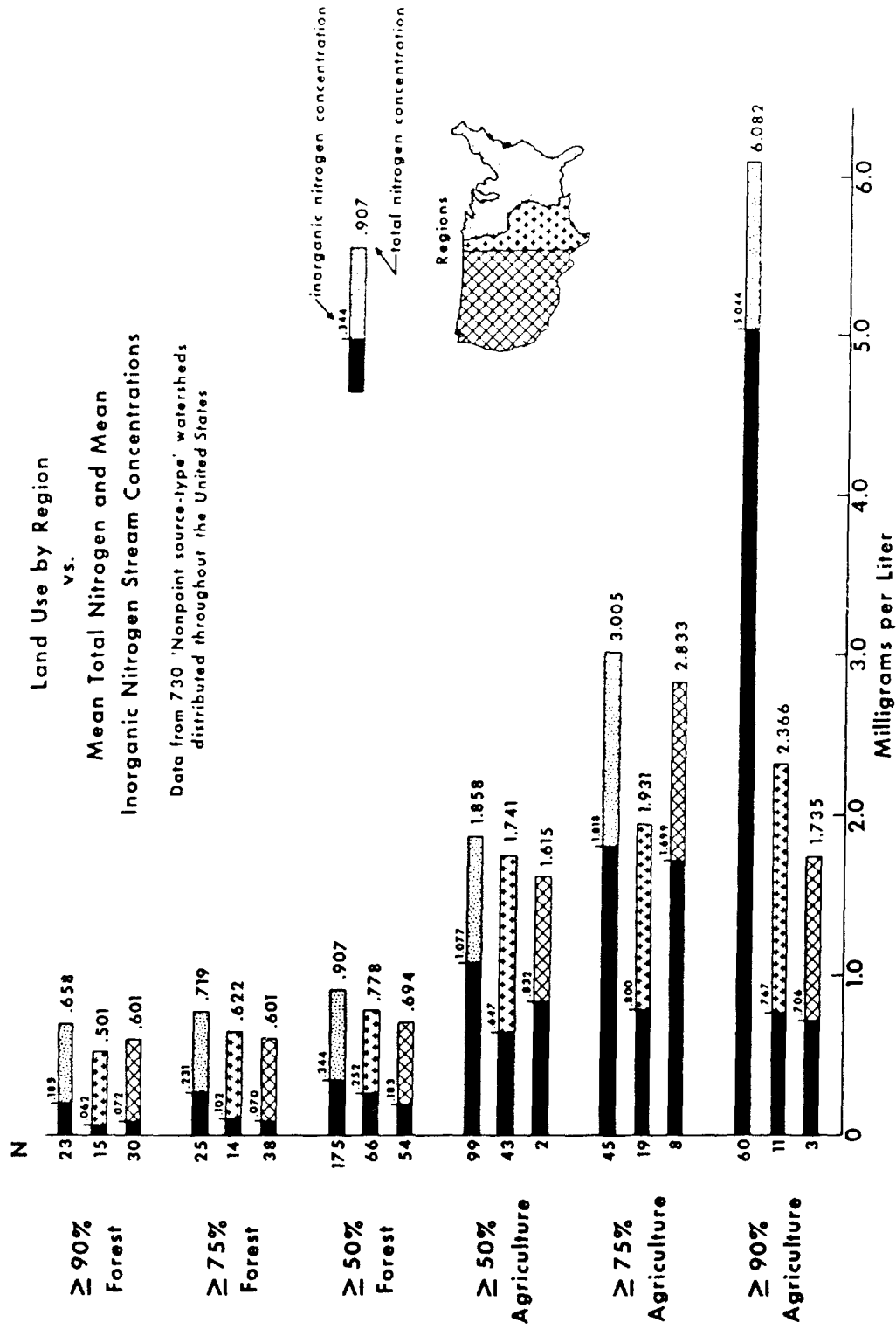


FIGURE III-4 RELATIONSHIPS BETWEEN STREAMFLOW NITROGEN CONCENTRATIONS AND LAND USE FROM THE NATIONAL EUTROPHICATION SURVEY (OMERNIK, 1977)

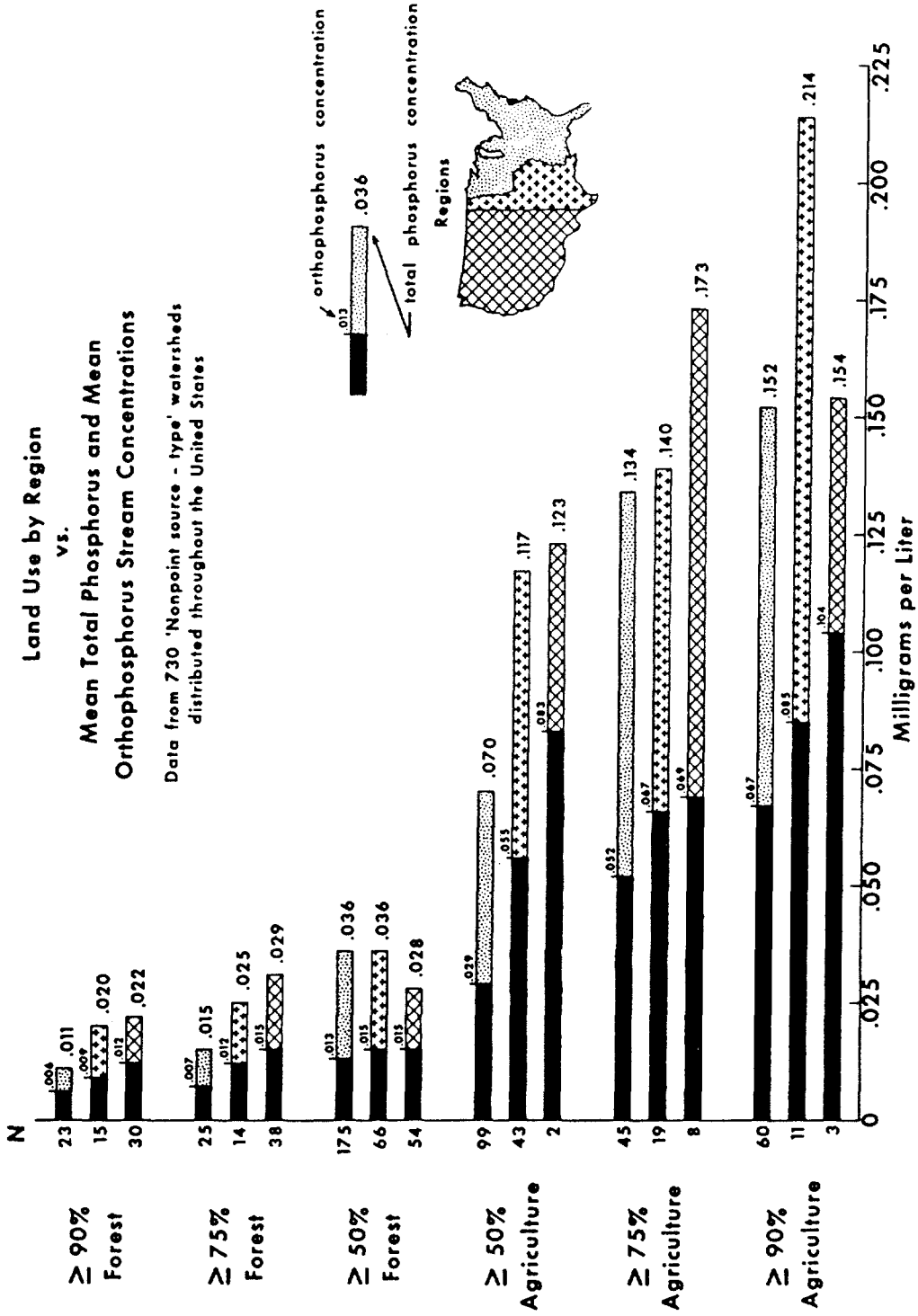


FIGURE III-5 RELATIONSHIPS BETWEEN STREAMFLOW PHOSPHORUS CONCENTRATIONS AND LAND USE FROM THE NATIONAL EUTROPHICATION SURVEY (UMERNIK, 1977)

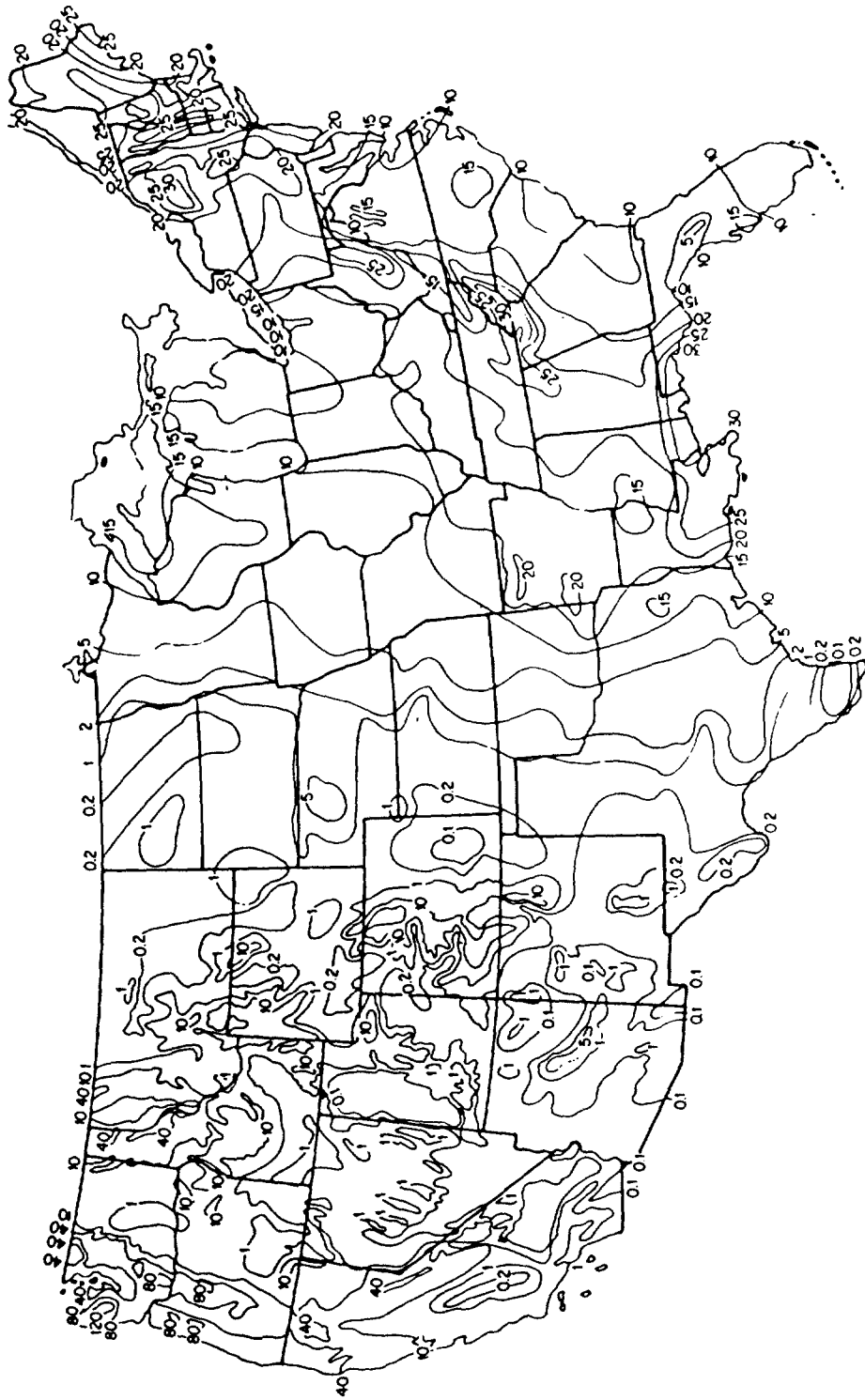


FIGURE III-6 AVERAGE ANNUAL STREAMFLOW IN INCHES (1 IN = 2.54CM )  
 (LANGBEIN ET AL, 1949)



Noting that:

$$1 \text{ mg/L} = 0.001 \text{ kg/m}^3$$
$$1 \text{ km}^2 = 10^6 \text{ m}^2$$

annual runoff is

$$0.254 (50) 10^6 = 12.7 10^6 \text{ m}^3.$$

Background loads are

$$\text{BOD :} \quad 3 (0.001)(12.7) 10^6 = 38,100 \text{ kg/yr}$$

$$\text{Phosphorus:} \quad 0.011(0.001)(12.7) 10^6 = 140 \text{ kg/yr.}$$

----- END OF EXAMPLE III-I -----

### 3.3 NONPOINT SOURCE MODELS

The nonpoint source loading process is illustrated in Figure III-7. Precipitation, in the form of rain or snowmelt, comes in contact with a "waste" product located on the land surface or within the soil. Portions of the waste are transported in runoff and percolation to streams and groundwater aquifers. Nonpoint source wastes are any potential pollutant which comes in contact with drainage. Examples include chemicals in urban dust and road litter, agricultural fertilizers, pesticides and animal manures, road de-icing salts, sanitary landfill wastes, eroded soil, mining slag piles, septic tank effluents, lawn chemicals and toxic wastes in lagoons and land disposal facilities.

Nonpoint source pollution is associated with random hydrologic events. Combined with the dispersed nature of drainage patterns, this randomness produces waste loads which are difficult to monitor, and hence most loading estimates are obtained from mathematical models. The foundations of all nonpoint source models, including the loading functions discussed herein, are equations to predict water movement, especially runoff and percolation. These equations are supplemented by methods to calculate sediment movement, and together the two components describe nonpoint source transport, since pollutants are either dissolved in a water flux or attached to sediment. The third model component is a procedure to estimate the dissolved and solid-phase (sediment-attached) concentrations of the pollutant. "In the loading functions, these concentrations are obtained empirically or derived from simple mass balances. In more analytical, and hence complex models, concentrations are obtained from mechanistic descriptions of chemical and biological processes.

Both average annual and single event loads can be estimated by nonpoint source loading functions. The former are useful when the effects of pollution are determined by long-term mass loads to a water body. Groundwater quality problems are often of this type. Also, several simple lake eutrophication models require annual phosphorus loads as input. Conversely, major storm events exert the most significant impacts on streams and rivers, and estimates of single event nonpoint source loads are necessary.

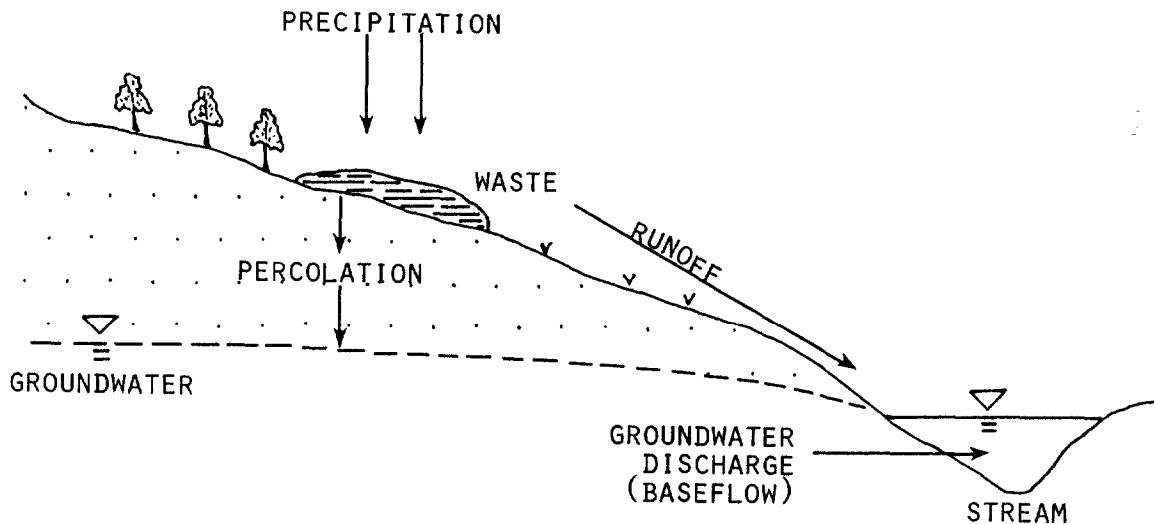


FIGURE III-7 THE NONPOINT SOURCE LOADING PROCESS

The most comprehensive estimates of nonpoint source loads are obtained from continuous simulation models such as HSPF, STORM, SWMM and CREAMS which have been developed under sponsorship of the U.S. Environmental Protection Agency, Army Corps of Engineers and Department of Agriculture. Since these models require computer facilities and extensive data structures, they are beyond the scope of this manual. Nevertheless, the simulation models are based on the same computational concepts presented in this chapter, particularly those used for single event loading functions.

Succeeding sections of this chapter present loading functions for rural runoff, irrigation return flows, urban runoff and groundwater.

### 3.4 RURAL RUNOFF LOADS

Nonpoint source waste loads to surface waters in rural areas include runoff from cropland (including pasture and range), forests, barnyards and feed lots, waste land application and storage facilities, construction sites and mining operations. Cropland and forest runoff are emphasized in this section, since these nonpoint sources are widespread, and their associated loading functions have been most extensively developed. Runoff loads from the other sources can in principle be estimated by procedures similar to the loading functions used for cropland and forest, but data are often lacking to implement the calculations.

#### 3.4.1 Source Areas

Nonpoint source waste loads in runoff can be estimated for several different spatial scales. The most fundamental unit of analysis is a source area, which is a land area with sufficiently homogeneous soil and pollutant characteristics so that

runoff loads can be considered uniform. A farmer's field is often considered a single source area and associated runoff loads are sometimes referred to as "edge-of-field" loads. Larger scales of analysis consist of aggregations of source areas or watersheds. Waste loads are transported from source areas by rivulets, ditches, streams and other drainage paths to eventually exit the watershed in streamflow. During this transit, portions of the wastes may be removed from the water flux by settling, adsorption, filtering or biochemical processes. The total watershed waste load in streamflow consists of these attenuated runoff sources plus waste loads from groundwater discharge.

Pollutants in runoff may be in dissolved and solid-phase forms, with the latter consisting of particulate material, or pollutants that are attached to sediment. The general loading function forms are:

$$\text{Dissolved pollutant waste load} = \text{Runoff water volume} \times \text{Dissolved pollutant concentration} \quad (\text{III-1})$$

$$\text{Solid-phase pollutant wasteload} = \text{Sediment flux} \times \text{Solid-phase pollutant concentration (concentration in sediment)} \quad (\text{III-2})$$

Sections 3.4.2, 3.4.3 and 3.4.4 describe methods for computing runoff volumes, sediment flux and pollutant concentrations, respectively.

### 3.4.2 Runoff

#### 3.4.2.1 SCS Curve Number Equation

The U.S. Soil Conservation Service's curve number equation (CNE) is a standard procedure for estimating storm runoff (Mockus, 1972; Ogrosky and Mockus, 1964). The equation is:

$$Q = (P - 0.2) \quad \text{for} \quad P \geq 0.2S \quad (\text{III-3})$$

where

Q = runoff (cm)

P = precipitation (rainfall + snowmelt, cm)

S = water retention parameter (cm).

The 0.2S is an initial precipitation "abstraction", and hence if  $P < 0.2S$ , Q is assumed to be zero.

The retention parameter S is computed from dimensionless curve numbers (CN) which are functions of soils, cover, management and antecedent moisture:

$$S = (2540/CN) - 25.4 \quad (111-4)$$

The general form of the equation is shown in Figure 111-8.

Although the CNE is most frequently applied to rainfall runoff, it may be used for snowmelt conditions. Snowmelt water can be estimated by the degree-day equation:

$$M = 0.45T \quad (111-5)$$

where

M = snowmelt water (cm)

T = mean air temperature (°C).

If  $T < 0$ ,  $M = 0$ . Also, M must not exceed the water content of the accumulated snowpack. The degree-day factor (0.45) is an average value (Stewart et al. , 1976) and should be replaced by a location-specific value when available.

Since daily weather data are used for Equations 111-3 and 111-5, calculated runoff is the total runoff for a specific day.

#### 3.4.2.2 Curve Number Selection

Curve numbers describe the hydrologic condition of land surface at the time of a precipitation event. The combined effects of soils, management and cover are shown in Table 111-1 for "average" antecedent moisture conditions. Most soils in the United States have been classified in one of four hydrologic groups. Listings are available in Mockus (1972) Ogrosky and Mockus (1964) and Soil Conservation Service (1975). The qualifiers "good," "fair" or "poor" in Table 111-1 indicate the extent to which cover and soil management conditions will minimize runoff. For example, continuous growth of a corn silage on the same site every year will deplete soil organic matter and encourage runoff. Conversely, corn grain in a rotation with hay or under no-till conditions will minimize runoff. Similarly, clear-cutting of woods accompanied by extensive disturbance of the soil surface by log skidding is a "poor" management practice.

The "woods" category in Table 111-1 may be used for vegetated forest areas. Runoff for roads, logging trails and landings should be based on curve numbers for the "roads and right-of-way" category. Those curve numbers are also appropriate for construction sites.

The fourth, and most important factor in curve number selection is the wetness of the soil. If precipitation falls on soil that has been inundated by previous storms, infiltration is much less and runoff is much greater than would be the case for dry soil. Three different antecedent moisture conditions are specified for the CNE: I (dry), II (average), and III (wet). Antecedent moisture is approximated by the five-day antecedent precipitation, which is the total precipitation (rain +

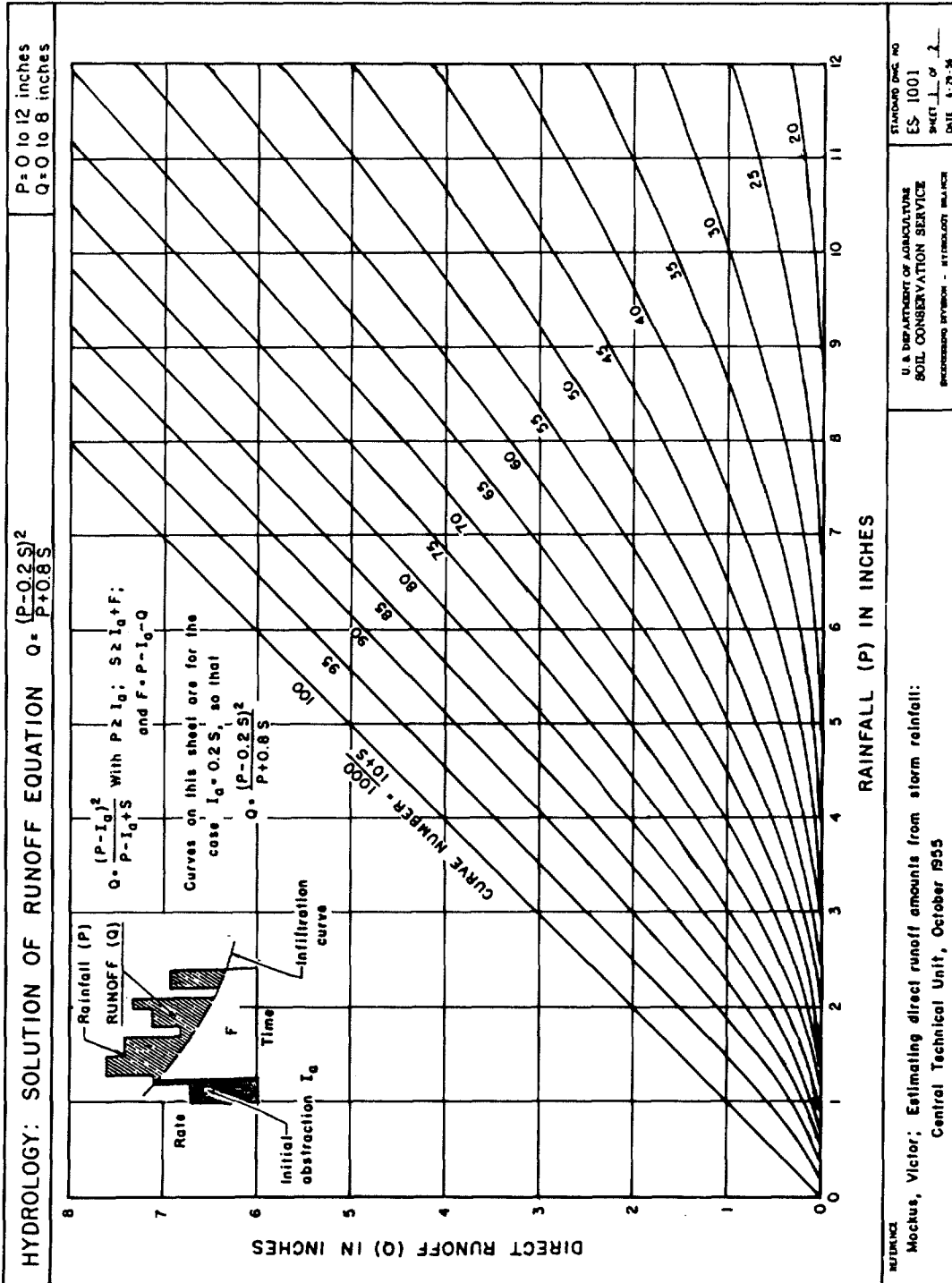


FIGURE III-8 SCS CURVE NUMBER RUNOFF EQUATION (1 IN = 2.54 CM)

TABLE III-1

## RUNOFF CURVE NUMBERS FOR AVERAGE ANTECEDENT MOISTURE CONDITIONS

(Mockus, 1972)

Land Use or Cover	Treatment or Practice	Hydrologic Condition	Hydrologic Soil Group*			
			A	B	C	D
Fallow	Straight row	--	77	<b>86</b>	91	94
Row crops	Straight row	Poor	<b>72</b>	<b>81</b>	88	<b>91</b>
	Straight row	Good	<b>67</b>	<b>78</b>	85	<b>89</b>
	Contoured	Poor	<b>70</b>	<b>79</b>	84	88
	Contoured	Good	<b>65</b>	<b>75</b>	82	86
	Terraced	Poor	<b>66</b>	<b>74</b>	80	<b>82</b>
	Terraced	Good	<b>62</b>	<b>71</b>	78	<b>81</b>
Small grain	Straight row	Poor	65	<b>76</b>	84	<b>88</b>
	Straight row	Good	63	<b>75</b>	83	<b>87</b>
	Contoured	Poor	63	<b>74</b>	<b>82</b>	85
	Contoured	Good	61	<b>73</b>	<b>81</b>	84
	Terraced	Poor	61	<b>72</b>	<b>79</b>	<b>82</b>
	Terraced	Good	59	<b>70</b>	<b>78</b>	<b>81</b>
Close-seeded legumes or rotation meadow	Straight row	Poor	<b>66</b>	<b>77</b>	85	89
	Straight row	Good	<b>58</b>	<b>72</b>	81	<b>85</b>
	Contoured	Poor	<b>64</b>	<b>75</b>	83	<b>85</b>
	Contoured	Good	<b>55</b>	<b>69</b>	78	83
	Terraced	Poor	<b>63</b>	<b>73</b>	80	83
	Terraced	Good	<b>51</b>	<b>67</b>	76	80
Pasture or range		Poor	<b>68</b>	<b>79</b>	86	89
		Fair	<b>49</b>	<b>69</b>	79	84
		Good	<b>39</b>	<b>61</b>	74	80
	Contoured	Poor	<b>47</b>	<b>67</b>	81	88
	Contoured	Fair	<b>25</b>	<b>59</b>	<b>75</b>	83
	Contoured	Good	<b>6</b>	<b>35</b>	<b>70</b>	79
Meadow (permanent)		Good	<b>30</b>	<b>58</b>	71	78
Woods		Poor	45	<b>66</b>	77	83
		Fair	36	<b>60</b>	73	<b>79</b>
		Good	25	<b>55</b>	70	<b>77</b>
Farmsteads		--	59	74	82	86
Roads and right-of-way (hard surface)		--	74	84	90	92

\*Soil GroupDescription

- A Lowest Runoff Potential: Includes deep sands with very little silt and clay, also deep, rapidly permeable loess.
- B Moderately Low Runoff Potential: Mostly sandy soils less deep than A, and loess less deep or less aggregated than A, but the group as a whole has above-average infiltration after thorough wetting.
- C Moderately High Runoff Potential: Comprises shallow soils and soils containing considerable clay and colloids, though less than those of group D. The group has below-average infiltration after presaturation.
- D Highest Runoff potential: Includes mostly clays of high swelling per cent, but the group also includes some shallow soils with nearly impermeable subhorizons near the surface.

snowmelt) in the five days preceding a storm. Approximate limits for the three antecedent moisture conditions are given in Table III-2. Different limits are specified for growing and dormant season since evapotranspiration dries the soil much more rapidly during the growing season. In absence of more specific information, the growing season may be assumed to consist of months for which average air temperature is 10°C or above. Antecedent precipitation is an inadequate criterion during snowmelt, however, and for such events condition III is always assumed (Haith and Tubbs, 1981).

The curve numbers for condition II, or CN2 are given in Table III-1. The curve numbers for the other two conditions, I and III respectively, can be obtained from the equations given by Hawkins (1978):

$$CN1 = CN2 / (2.334 - 0.01334CN2) \quad (III-6)$$

$$CN3 = CN2 / (0.4036 + 0.0059CN2) \quad (III-7)$$

TABLE III-2

ANTECEDENT MOISTURE LIMITS FOR CURVE NUMBER SELECTION  
(Ogrosky and Mockus, 1964)

Antecedent Moisture Condition	5-Day Antecedent Precipitation (cm)	
	Dormant Season*	Growing Season
I	<1.3	<3.6
II	1.3-2.8	3.6-5.3
III	>2.8	>5.3

\*During snowmelt, condition III is always assumed regardless of antecedent precipitation.

- - - EXAMPLE III-2 - - -

Cropland Runoff

A three-day rainstorm falls on a 30-ha soybean field during early August. The crop is continuously grown (no rotation) in straight rows. The soil is in hydrologic group B. The relevant precipitation is as follows:

Date	August	1	2	3	4	5	6	7	8	9
Rain (cm)	0	0	0	0	0	3.8	5.1	0.3	0	

Determine the runoff from this storm.

Solution:

The crop is a row crop planted in straight rows and in poor hydrologic condition. From Table III-1, the curve number for condition 2 is  $CN_2 = 81$  for soil group B. Solving Equations III-6 and III-7 for  $CN_1$  and  $CN_3$ , we have  $CN_1 = 64.6$  and  $CN_3 = 91.9$ .

The three-day storm begins on August 6. On that day, 5-day antecedent precipitation is 0; hence the soil is in the driest antecedent moisture condition.

Thus :

$$CN = CN_1 = 64.6$$

and from Equation III-4:

$$\begin{aligned} S &= (2540/64.6) - 25.4 \\ &= 13.9 \text{ cm.} \end{aligned}$$

Since precipitation exceeds initial abstraction,  $0.2S = 2.78$  cm, runoff occurs as predicted by Equation III-3:

$$\begin{aligned} Q &= (3.8 - 2.78^2 / (3.8 + 0.8(13.9))) \\ &= 0.07 \text{ cm.} \end{aligned}$$

On August 7, 5-day antecedent precipitation is 3.8 cm, which during the growing season corresponds to  $CN = CN_2 = 81$  (Table III-2). Thus:

$$\begin{aligned} S &= (2540/81) - 25.4 \\ &= 5.96 \text{ cm.} \end{aligned}$$

Rain exceeds  $0.2S = 1.19$  cm, and

$$\begin{aligned} Q &= (5.1 - 1.19)^2 / (5.1 + 0.8(5.96)) \\ &= 1.55 \text{ cm.} \end{aligned}$$

On the final day, 5-day antecedent precipitation is  $3.8 + 5.1 = 8.9$  cm,  $CN = CN_3 = 91.9$  and  $S = 2.24$  cm. Since the 0.3 cm of rain does not exceed the initial abstraction of  $0.2(2.24) = 0.45$  cm, no runoff occurs.



The storm summary is as follows:

Day	Rainfall (cm)	Runoff (cm)
8/6	3.8	0.07
8/7	5.1	1.55
8/8	0.3	0
Total	9.2	1.62

The 1.62 cm of runoff over the 30-ha field can be converted to runoff volume ( $m^3$ ) by noting that 1 ha = 10,000  $m^2$ , and hence 1 cm on 1 ha = 0.01 (10,000) = 100  $m^3$ . This runoff volume is 1.62(30)(100) = 4860  $m^3$ .

This example illustrates three important characteristics of runoff:

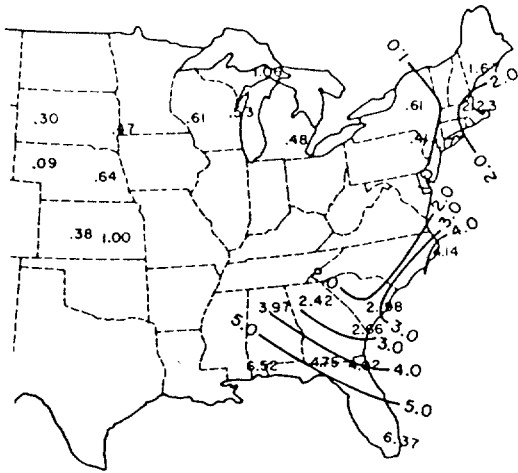
- Runoff is a nonlinear function of precipitation; i.e., runoff is not a constant portion of precipitation.
- Runoff is generally a small fraction of precipitation, particularly during the growing season.
- Runoff is dramatically dependent on antecedent moisture conditions.

----- END OF EXAMPLE III-2 -----

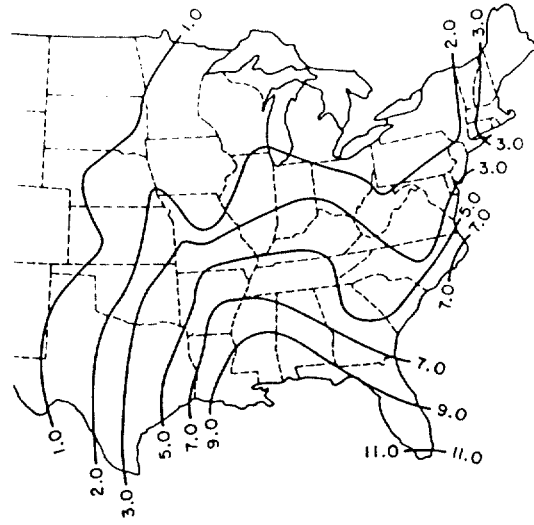
#### 3.4.2.3 Annual Runoff

The CNE is only applicable to individual storm events, and this is a limitation in nonpoint source studies for which annual waste loads are required. In such cases annual runoff estimates are necessary. The only way to produce such estimates is to use Equation III-3 to calculate runoff for each storm in a year, and sum the resulting values for the year. If an average annual runoff is needed, the process must be repeated for each of a number of years. The repeated use of Equation III-3 for all storms in a multi-year period is not difficult (see for example Hai th and Tubbs, 1981), but it is a continuous simulation modeling process that can only be implemented on a computer.

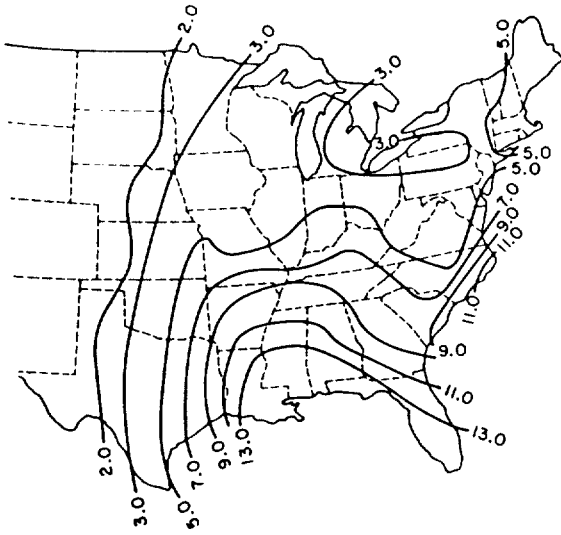
Average annual runoff for row crops has been calculated by Stewart et al. (1976) for the eastern United States. A simulation model based on the CNE was run using 10-25 years of daily weather data from 52 locations. The simulation runs were based on straight row corn in good hydrologic condition on the four different soil groups. Fallow or bare soil conditions were assumed during the spring. Results of the simulations are shown in Figure III-9. The four soil groups correspond to CN2 = 67, 78, 85 and 89. These runoff values should generally be appropriate for any row crop. Runoff for situations with curve numbers falling between any two curve numbers can be determined by linear interpolation.



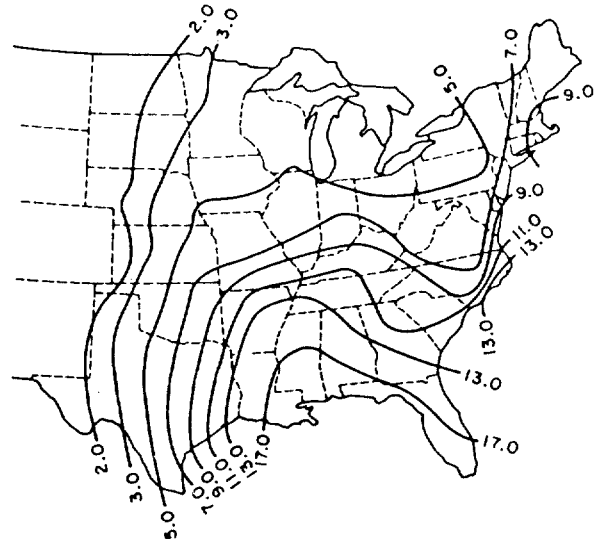
(A)



(B)



(C)



(D)

Figure III-9 MEAN ANNUAL ROW CROP RUNOFF IN INCHES  
 FOR SELECTED CURVE NUMBERS. A; CN2=67,  
 B; CN2=78; C; CN2=85; D: CN2=89. (1 IN  
 = 2.54cm) (STEWART ET AL , 1976)

#### 3.4.2.4 Watershed Runoff

Runoff from a source area such as a farmer's field or logging road is given by Equation III-3. Runoff from an entire watershed is the sum of runoff from all source areas within the watershed. If we define:

$Q_k$  = runoff from source area k (cm)

$A_k$  = area of source area k (ha)

AT = total watershed area (ha)

$a_k$  = fraction of watershed covered by source area k =  $A_k/AT$

then watershed runoff  $Q$ (cm) is:

$$Q = \sum_k a_k Q_k \quad (III-8)$$

Watershed runoff volume  $V(m^3)$  is:

$$\begin{aligned} V &= 100 \sum_k A_k Q_k \\ &= 100 AT \sum_k a_k Q_k \end{aligned} \quad (III-9)$$

Equation III-8 or III-9 require computation of runoff  $Q_k$  from each source area. An alternative and simpler procedure is to determine a weighted average curve number:

$$CN = \sum_k a_k CN_k \quad (III-10)$$

and compute watershed runoff directly from Equations III-3 and III-4. In Equation III-10  $CN_k$  is the curve number for source area k.

The second procedure (average curve number) generally produces slightly lower watershed runoff estimates than Equation III-8 due to the nonlinear nature of the CNE. In any case, note that watershed runoff is only one component of streamflow. Additional components include groundwater discharge and point sources.

#### 3.4.3 Erosion and Sediment

Erosion is the removal of soil particles by wind and water, and sediment is the particulate matter which is carried and eventually deposited by wind and water. Our concern here is with water pollution, and the prediction of sediment loads or yields in streamflow. Upstream erosion of soil surfaces and stream channels is the source of streamflow sediment yields. However, watershed sediment yield, as measured in streamflow at the outlet of the watershed, is generally substantially less than the

total upstream erosion since much of the transported sediment has been deposited or filtered from the water. Near a sediment source, nearly all eroded soil becomes a sediment mass flux. For example the sediment yield in runoff from a corn field is approximately equal to the eroded soil mass from the field. However, as the runoff travels from the field in drainage ditches and stream channels, portions of the sediment are removed, until only a fraction remains to exit the watershed.

Erosion of the land surface by sheet and rill erosion is the major source of solid-phase pollutants in surface waters, and most of this section is accordingly devoted to prediction of this sediment source. Although channel erosion may also be a significant component of sediment yield, it is not generally considered a pollution hazard and will not be considered in the following discussion.

### 3.4.3.1 The Universal Soil Loss Equation

The Universal Soil Loss Equation (USLE) is an empirical equation which was developed to predict average annual soil loss by sheet and rill erosion from source areas (Wischmeier and Smith, 1978). The equation, which was obtained by statistical analyses of over 10,000 plot-years of erosion field research data is:

$$X = 1.29 \quad ECU \quad (III-11)$$

where

X = soil loss (t/ha; 1 t = 1 tonne = 1000 kg = 2205 lb)

E = rainfall/runoff erosivity index ( $10^2$  m-tonne-cm/ha-hr)

K = soil erodibility (t/ha per unit of E)

Is = topographic factor

C = cover/management factor

P = supporting practice factor.

The three factors Is, C, P are dimensionless. The 1.29 is a conversion constant to obtain metric units.

The USLE is an important component of loading functions for runoff waste loads because its parameters have been evaluated for a wide range of conditions and many important pollutants are transported on eroded soil. For example, most organochlorine pesticides are very strongly adsorbed to soil particles. Procedures for determining the USLE parameters are presented in the following subsections.

#### 3.4.3.1.1 Rainfall/Runoff Erosivity

The erosivity term E is related to rainfall intensity. Average annual values for the United States have been computed by Wischmeier and Smith (1978) and are given in Figures 111-10 and 11. The values of E in these figures are in English units ( $10^2$  ft-tons-in/ac-hr) and can be converted to the metric units of Equations 111-11 by multiplying by 1.735; i.e. E (metric) = 1.735 E (English, Figures 111-10,

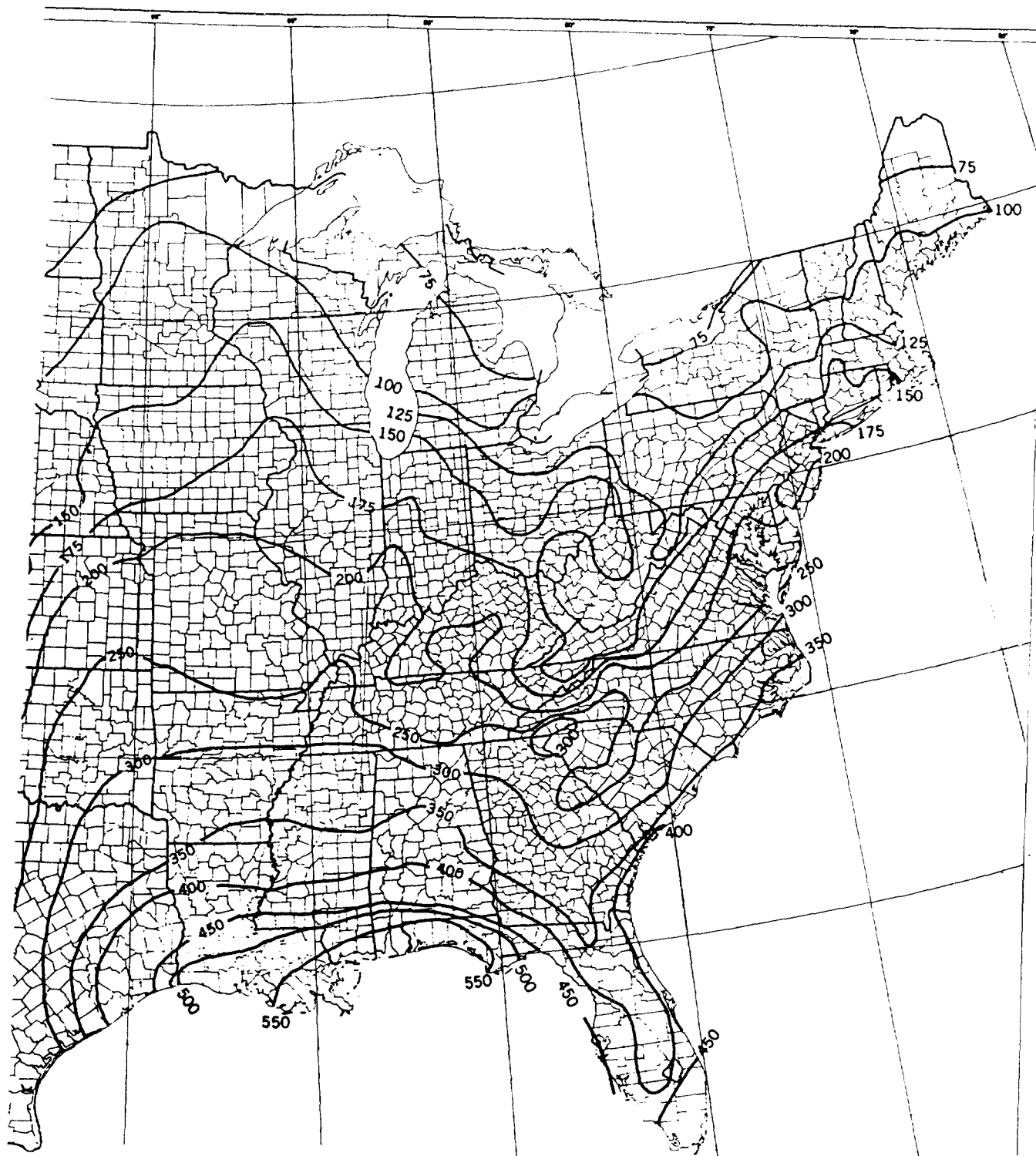


FIGURE 111-10 AVERAGE ANNUAL EROSIIVITY INDICES (ENGLISH UNITS)  
 FOR EASTERN U. S. (WISCHMEIER AND SMITH, 1978)

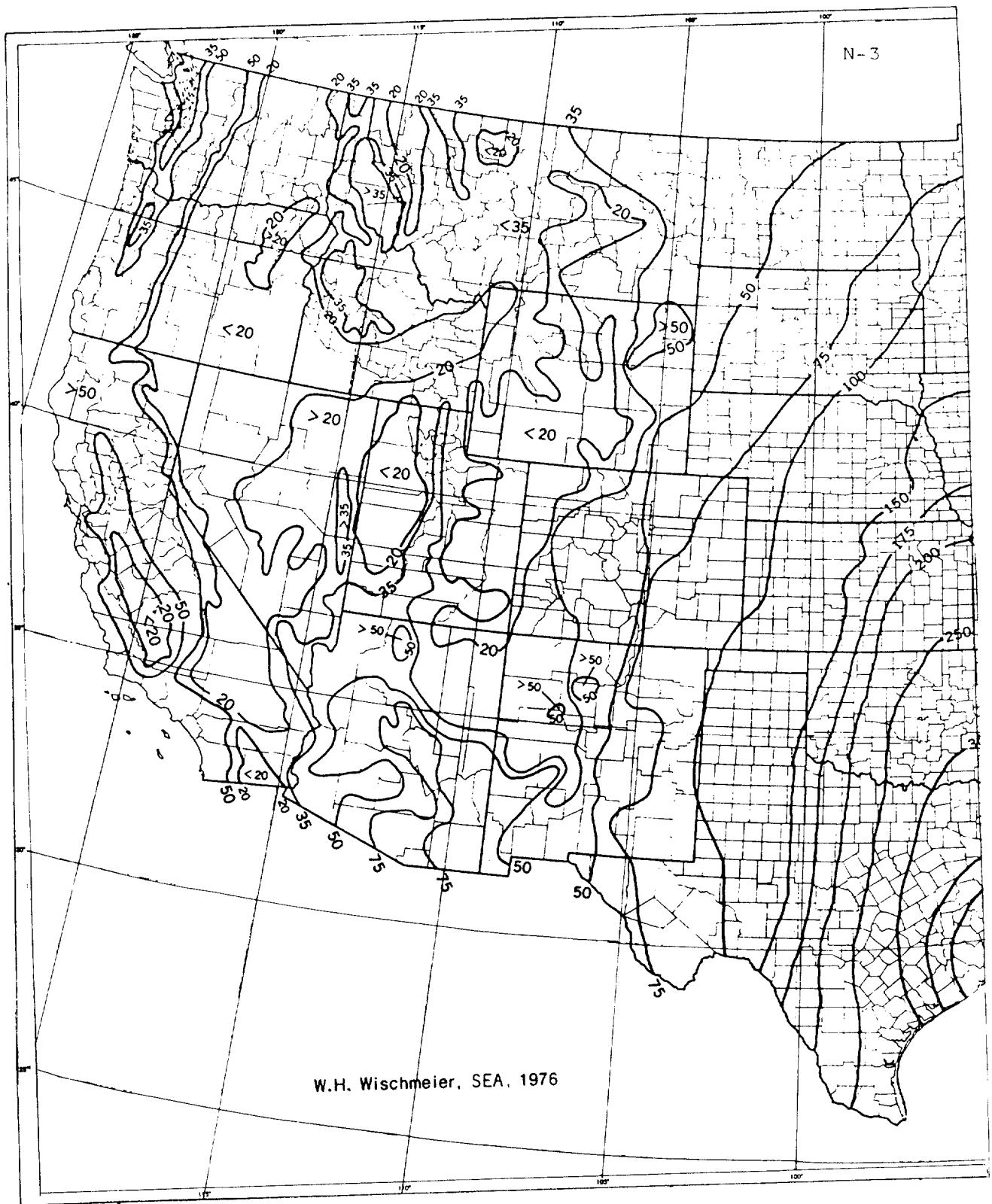


FIGURE III-11 AVERAGE ANNUAL EROSIIVITY INDICES (ENGLISH UNITS)  
FOR WESTERN U. S. (WISCHMEIER AND SMITH, 1978)

11). For example the erosivity for northern Maine is  $E = 1.735 (75) = 130$ .

It can be seen from Figure III-10 that the intense rainstorms of the Southeast produce the highest levels of erosivity in the United States. In contrast, erosivity in much of the western mountain region (Figure III-11) is less than 10 percent of the southeast values.

#### 3.4.3.1.2 Soil Erodibility

Typical values of K are given in Table III-3 as a function of soil texture and organic matter content. Values for specific soils are available from local Soil and Water Conservation Districts and state offices of the Soil Conservation Service.

#### 3.4.3.1.3 Topographic Factor

The topographic factor  $I_s$  is related to the angle of slope  $\theta$  and slope length  $x$  (m) by:

$$I_s = (0.045x)^b (65.41 \sin^2 \theta + 4.56 \sin \theta + 0.065) \quad (\text{III-12})$$

The slope angle  $\theta$  is obtained from percent slope,  $s$  by:

$$\theta = \tan^{-1}(s/100) \quad (\text{III-13})$$

For example, a slope of  $s = 8$  percent has a slope angle of  $\theta = 4.6^\circ$ . The exponent in Equation III-12 is given by  $b = 0.5$  for  $s > 5$ ,  $b = 0.4$  for  $3.5 \leq s \leq 4.5$ ,  $b = 0.3$  for  $1 \leq s \leq 3$ , and  $b = 0.2$  for  $s \leq 1$  (Wischmeier and Smith, 1978).

Research data support Equation III-12 for  $x \leq 100$  m and  $s \leq 18$ , although in practice it is often applied beyond these limits.

#### 3.4.3.1.4 Cover/Management Factor

The cover/management factor  $C$  describes the protection of the soil surface by plant canopy, crop residues, mulches, etc. The maximum  $C$  value is 1.0, corresponding to no protection. Cropland  $C$  values change dramatically during the year in response to planting operations, crop growth and harvest. Although  $C$  values have been determined for each of these stages (Wischmeier and Smith, 1978), generalized annual values such as those given in Table III-4 are more suitable for loading functions.

Wischmeier and Smith (1978) have also developed  $C$  factors for construction sites; pasture, range and idle land; undisturbed forests; and mechanically prepared woodland sites. These  $C$  values are given in Tables III-5 through III-8. Note that cover factors are so small for undisturbed forest and pasture or range with good ground cover that these erosion sources can generally be neglected in water quality studies.

TABLE III-3

SOIL ERODIBILITY, K  
(Stewart et al , 1975)

Texture	Organic Matter		
	0.5%	2%	4%
Sand	0.05	0.03	0.02
Fine sand	0.16	0.14	0.14
Very fine sand	0.42	0.36	0.28
Loamy sand	0.12	0.10	0.08
Loamy fine sand	0.24	0.20	0.16
Loamy very fine sand	0.44	0.38	0.30
Sandy loam	0.27	0.24	0.19
Fine sandy loam	0.35	0.30	0.24
Very fine sandy loam	0.47	0.41	0.33
Loam	0.38	0.34	0.29
Silt loam	0.48	0.42	0.33
Silt	0.60	0.52	0.42
Sandy clay loam	0.27	0.25	0.21
Clay loam	0.28	0.25	0.21
Silty clay loam	0.37	0.32	0.26
Sandy clay	0.14	0.13	0.12
Silty clay	0.25	0.23	0.19
Clay		0.13-0.29	



TABLE 111-4

GENERALIZED VALUES OF THE COVER AND MANAGEMENT FACTOR, C,  
IN THE 37 STATES EAST OF THE ROCKY MOUNTAINS (Stewart *et al* , 1975)

Line no.	Crop, rotation, and management	Productivity level <sup>2</sup>	
		High	Mod.
		C value	
Base value: continuous fallow, tilled up and down slope		1.00	1.00
<b>CORN</b>			
1	C, RdR, fall TP, conv (1)	0.54	0.62
2	C, RdR, spring TP, conv (1)	.50	.59
3	C, RdL, fall TP, conv (1)	.42	.52
4	C, RdR, wc seeding, spring TP, conv (1)	.40	.49
5	C, RdL, standing, spring TP, conv (1)	.38	.48
6	C, fall shred stalks, spring TP, conv (1)	.35	.44
7	C(silage)-W(RdL, fall TP) (2)	.31	.35
8	C, RdL, fall chisel, spring disk, 40-30% rc (1)	.24	.30
9	C(silage), W wc seeding, no-till pl in c-k W (1)	.20	.24
10	C(RdL)-W(RdL, spring TP) (2)	.20	.28
11	C, fall shred stalks, chisel pl, 40-30% rc (1)	.19	.26
12	C-C-C-W-M, RdL, TP for C, disk for W (5)	.17	.23
13	C, RdL strip till row zones, 55-40% rc (1)	.16	.24
14	C-C-C-W-M-M, RdL, TP for C, disk for W (6)	.14	.20
15	C-C-W-M, RdL, TP for C, disk for W (4)	.12	.17
16	C, fall shred, no-till pl, 70-50% rc (1)	.11	.18
17	C-C-W-M-M, RdL, TP for C, disk for W (5)	.087	.14
18	C-C-C-W-M, RdL, no-till pl 2d & 3rd C (5)	.076	.13
19	C-C-W-M, RdL, no-till pl 2d C (4)	.068	.11
20	C, no-till pl in c-k wheat, 90-70% rc (1)	.062	.14
21	C-C-C-W-M-M, no-till pl 2d & 3rd C (6)	.061	.11
22	C-W-M, RdL, TP for C, disk for W (3)	.055	.095
23	[-C-W-M-M, RdL, no-till pl 2d C (5)	.051	.094
24	C-W-M-M, RdL, TP for C, disk for W (4)	.039	.074
25	C-W-M-M-M, RdL, TP for C, disk for W (5)	.032	.061
26	C, no-till pl in c-k sod, 95-80% rc (1)	.017	.053
<b>COTTON</b> <sup>4</sup>			
27	Cot, conv (Western Plains)(1)	0.42	0.49
28	Cot, conv (South) (1)	.34	.40
<b>MEADOW</b>			
29	Grass & Legume mix	0.004	0.01
30	Alfalfa, lespedeza or Sericea	.020	
31	Sweet clover	.025	
<b>SORGHUM, GRAIN (Western Plains)</b> <sup>4</sup>			
32	RdL, spring TP, conv (1)	0.43	0.53
33	No-till pl in shredded 70-50% rc	.11	.18

TABLE III-4 (Continued)

Line no.	Crop, rotation, and management <sup>3</sup>	Productivity level <sup>2</sup>	
		High	Mod.
		C value	
<b>SOYBEANS<sup>4</sup></b>			
34	B, RdL, spring TP, conv (1)	0.48	0.54
35	C-B, TP annually, conv (2)	.43	.51
36	B, no-till pl	.22	.28
37	C-B, no-till pl, fall shred C stalks (2)	.18	.22
<b>WHEAT</b>			
38	W-F, fall TP after W (2)	0.38	
39	W-F, stubble mulch, 500 lbs rc (2)	.32	
40	W-F, stubble mulch, 1000 lbs rc (2)	.21	
41	Spring W, RdL, Sept TP, conv (N & S Dak) (1)	.23	
42	Winter W, RdL, Aug TP, conv (Kans) (1)	.19	
43	Spring W, stubble mulch, 750 lbs rc (1)	.15	
44	Spring W, stubble mulch. 1250 lbs rc (1)	.12	
45	Winter W, stubble mulch. 750 lbs rc (1)	.11	
46	Winter W, stubble mulch. 1250 lbs rc (1)	.10	
47	W-M, conv (2)	.054	
48	W-M-M, conv (3)	.026	
49	W-M-M-M, conv (4)	.021	

<sup>1</sup> This table is for illustrative purposes only and is not a complete list of cropping systems or potential Practices. Values of C differ with rainfall pattern and planting dates. These generalized values show approximately the relative erosion-reducing effectiveness of various crop systems, but Vocationally derived C values should be used for conservation planning at the field level. Tables of local values are available from the Soil Conservation Service.

<sup>2</sup> High level is exemplified by long-term yield averages greater than 75 bu. corn or 3 tons grass-and-legume hay; or cotton management that regularly provides good stands and growth.

<sup>3</sup> Numbers in parentheses indicate number of years in the rotation cycle. No. (1) designates a continuous one-crop system.

<sup>4</sup> Grain sorghum, soybeans or cotton may be substituted for corn in lines 12, 14, 15, 17-19, 21-25 to estimate C values for sod-based rotations.

Abbreviations defined:

B	- soybeans	F	- fallow
c	- corn	M	- grass& legume hay
c-k	- chemically killed	pl	- plant
conv	- conventional	W	- wheat
cot	- cotton	wc	- winter cover

lbs rc - pounds of crop residue per acre remaining on surface after new crop seeding

%rc - percentage of soil surface covered by residue mulch after new crop seeding

70-50% rc - 70%, cover for C values in first column; 50% for second column

RdR - residues (corn stover, straw, etc. ) removed or burned

RdL - all residues left on field (on surface or incorporated)

TP - turn plowed (upper 5 or more inches of soil inverted, covering residues)

TABLE III-5

## C FACTOR VALUES FOR CONSTRUCTION SITES

(Wischmeier and Smith, 1978)<sup>1</sup>

Type of mulch	Mulch rate	Land slope	Factor C	Length limit
	<i>Tons per acre</i>	<i>Percent</i>		<i>Feet</i>
None	0	all	1.0	—
Straw or hay,	1.0	1-5	0.20	200
tied down by	1.0	6-10	.20	100
anchoring and				
tacking	1.5	1-5	.12	300
<b>equipment<sup>3</sup></b>	1.5	6-10	.12	150
Do.	2.0	1-5	.06	400
	2.0	6-10	.06	200
	2.0	11-15	.07	150
	2.0	16-20	.11	100
	2.0	21-25	.14	75
	2.0	26-33	.17	50
	2.0	34-50	.20	35
Crushed stone,	135	< 16	.05	200
$\frac{1}{4}$ to $1\frac{1}{2}$ in	135	16-20	.05	150
	135	21-33	.05	100
	135	34-50	.05	75
Do.	240	< 21	.02	300
	240	21-33	.02	200
	240	34-50	.02	150
Wood chips	7	< 16	.08	75
	7	16-20	.08	50
Do.	12	< 16	.05	150
	12	16-20	.05	100
	12	21-33	.05	75
Do.	25	< 16	.02	200
	25	16-20	.02	150
	25	21-33	.02	100
	25	34-50	.02	75

<sup>1</sup> Developed by an interagency workshop group on the basis of field experience and limited research data.

<sup>2</sup> **Maximum** slope length for which the specified mulch rate is considered effective. When this limit is exceeded, either a higher application rate or mechanical shortening of the effective slope length is required.

<sup>3</sup> **When** the straw or hay mulch is not anchored to the soil, C values on moderate or steep slopes of soils having K values greater than 0.30 should be taken at double the values given in this table.

TABLE III-6

## C FACTOR VALUES FOR PERMANENT PASTURE, RANGE AND IDLE LAND

(Wischmeier and Smith, 1978)<sup>1</sup>

Vegetative canopy		Cover that contacts the soil surface						
Type and height <sup>2</sup>	Percent cover <sup>3</sup>	Type <sup>4</sup>	Percent ground cover					
			0	20	40	60	80	95+
No appreciable canopy		G	0.45	0.20	0.10	0.042	0.013	0.003
		w	.45	.24	.15	.091	.043	.011
Tall weeds or short brush with average drop fall height of 20 in	25	G	.36	.17	.09	.038	.013	.003
		w	.36	.20	.13	.083	.041	.011
	50	G	.26	.13	.07	.035	.012	.003
		w	.26	.16	.11	.076	.039	.011
	75	G	.17	.10	.06	.032	.011	.003
		w	.17	.12	.09	.068	.038	.011
Appreciable brush or bushes, with average drop fall height of 6½ ft	25	G	.40	.18	.09	.040	.013	.003
		w	.40	.22	.14	.087	.042	.011
	50	G	.34	.16	.08	.038	.012	.003
		w	.34	.19	.13	.082	.041	.011
	75	G	.28	.14	.08	.036	.012	.003
		w	.28	.17	.12	.078	.040	.011
Trees, but no appreciable low brush. Average drop fall height of 13 ft	25	G	.42	.19	.10	.041	.013	.003
		w	.42	.23	.14	.089	.042	.011
	50	G	.39	.18	.09	.040	.013	.003
		w	.39	.21	.14	.087	.042	.011
	75	G	.36	.17	.09	.039	.012	.003
		w	.36	.20	.13	.084	.041	.011

<sup>1</sup> The listed C values assume that the vegetation and mulch are randomly distributed over the entire area.

<sup>2</sup> **Canopy** height is measured as the average fall height of water drops falling from the canopy to the ground. Canopy effect is inversely proportional to drop fall height and is negligible if fall height exceeds 33 ft.

<sup>3</sup> **Portion** of total-area surface that would be hidden from view by canopy in a vertical projection (a bird's-eye view).

<sup>4</sup> **G**: cover at surface is grass, grasslike plants, decaying corn-patted duff, or litter at least 2 in deep.

**W**: cover at surface is mostly broadleaf herbaceous plants (as weeds with little lateral-root network near the surface) or undecayed residues or both.

TABLE 111-7

## C FACTOR VALUES FOR UNDISTURBED FOREST LAND

(Wischmeier and Smith, 1978)

Percent of Area Covered by Canopy of Trees and Undergrowth	Percent of Area Covered by Duff (litter) at least 5 cm deep	Factor C
100-75	100-90	0.0001-0.001
70-45	85-75	0.002-0.004
40-20	70-40	0.003-0.009

3.4.3.1.5 Supporting Practice Factor

The supporting practice factor P measures the effect of traditional soil conservation practices on cropland erosion. Values of the P factor are given in Table 111-9. Note that two different types of practice factors apply to terracing. For example, for a double terrace (n=2) on a 6 percent slope,  $P = 0.5/\sqrt{2} = 0.35$ . The value indicates the amount of erosion from the soil surface. However, approximately 80 percent of the eroded soil is trapped in the terraces channel and does not leave the source area. Hence, for purposes of estimating nonpoint source loads, the practice factor is  $0.2(0.35) = 0.07$ .

3.4.3.2 Single Event Erosion Estimates

Although the USLE was developed for average annual erosion estimates, nonpoint source studies often require waste loads for specific storm events. When this is the case, the erosivity term E in Equation 111.11 must be determined for the storms in question. Three different methods may be used to obtain these erosivities.

Method 1: Direct computation from rainfall intensities.

The most analytical approach involves the use of rainfall intensity data directly to compute storm kinetic energy and maximum intensities. This procedure, as described in Wischmeier and Smith (1978) is generally too cumbersome for screening studies.

Method 2: Design storms.

Wischmeier and Smith (1978) have analyzed rainfall data throughout the United States to determine frequencies of E values. The results are given in Table 111-10, and may be used to determine the soil erosion associated with storms of various

TABLE III-8  
 C FACTOR VALUES FOR MECHANICALLY PREPARED WOODLAND SITES  
 (Wischmeier and Smith, 1978)

Site preparation	Mulch cover <sup>1</sup>	Soil condition <sup>2</sup> and weed cover <sup>3</sup>															
		Excellent		Good		Fair		Poor		Excellent		Good		Fair		Poor	
		NC	WC	NC	WC	NC	WC	NC	WC	NC	WC	NC	WC	NC	WC	NC	WC
<i>Percent</i>																	
Disked, raked, or bedded <sup>4</sup>	None	0.52	0.20	0.72	0.27	0.85	0.32	0.94	0.36								
	10	.33	.15	.46	.20	.54	.24	.60	.26								
	20	.24	.12	.34	.17	.40	.20	.44	.22								
	40	.17	.11	.23	.14	.27	.17	.30	.19								
	60	.11	.08	.15	.11	.18	.14	.20	.15								
Burned <sup>5</sup> . . . .	80	.05	.04	.07	.06	.09	.08	.10	.09								
	None	.25	.10	.26	.10	.31	.12	.45	.17								
	10	.23	.10	.24	.10	.26	.11	.36	.16								
	20	.19	.10	.19	.10	.21	.11	.27	.14								
	40	.14	.09	.14	.09	.15	.09	.17	.11								
Drum chopped <sup>5</sup>	60	.08	.06	.09	.07	.10	.08	.11	.08								
	80	.04	.04	.05	.04	.05	.04	.06	.05								
	None	.16	.07	.17	.07	.20	.08	.29	.11								
	10	.15	.07	.16	.07	.17	.08	.23	.10								
	20	.12	.06	.12	.06	.14	.07	.18	.09								
	40	.09	.06	.09	.06	.10	.06	.11	.07								
	60	.06	.05	.06	.05	.07	.05	.07	.05								
	80	.03	.03	.03	.03	.03	.03	.03	.04								

<sup>1</sup> Percentage of surface covered by residue in contact with the soil.  
<sup>2</sup> Excellent soil condition—Highly stable soil aggregates in topsoil with fine tree roots and litter mixed in.  
 Good—Moderately stable soil aggregates in topsoil or highly stable aggregates in subsoil (topsoil removed during raking), only traces of litter mixed in.  
 Fair—Highly unstable soil aggregates in topsoil or moderately stable aggregates in subsoil, no litter mixed in.  
 Poor—No topsoil, highly erodible soil aggregates in subsoil, no litter mixed in.  
<sup>3</sup> NC—No live vegetation.  
 WC—75 percent cover of grass and weeds having an average drop fall height of 20 in. For intermediate percentages of cover, interpolate between columns.  
<sup>4</sup> Modify the listed C values as follows to account for effects of surface roughness and aging:  
 First year after treatment: multiply listed C values by 0.40 for rough surface (depressions > 6 in); by 0.65 for moderately rough; and by 0.90 for smooth (depressions < 2 in).  
 For 1 to 4 years after treatment: multiply listed factors by 0.7.  
 For 4+ to 8 years: use table 6.  
 More than 8 years: use table 7.  
<sup>5</sup> For first 3 years: use C values as listed.  
 For 3+ to 8 years after treatment: use table 6.  
 More than 8 years after treatment: use table 7.

TABLE 111-9

PRACTICE FACTORS (P) USED IN UNIVERSAL SOIL LOSS EQUATION

(Stewart et al , 1975)

Practice	Land slope (percent)				
	1.1-2	2.1-7	7.1-12	12.1-18	18.1-24
(Factor P)					
Contouring ( $P_c$ )	0.60	0.50	0.60	0.80	0.90
Contour strip cropping ( $P_{sc}$ )					
R-R-M-M <sup>1</sup>	0.30	0.25	0.30	0.40	0.45
R-W- M-M	0.30	0.25	0.30	0.40	0.45
R-R-W-M	0.45	0.38	0.45	0.60	0.68
R-W	0.52	0.44	0.52	0.70	0.90
R-O	0.60	0.50	0.60	0.80	0.90
Contour listing or ridge planting ( $P_{cl}$ )	0.30	0.25	0.30	0.40	0.45
Contour terracing ( $P_t$ ) <sup>2</sup>	<sup>3</sup> $0.6/\sqrt{n}$	$0.5/\sqrt{n}$	$0.6/\sqrt{n}$	$0.8/\sqrt{n}$	$0.9/\sqrt{n}$
No support practice	1.0	1.0	1.0	1.0	1.0

<sup>1</sup> R = rowcrop, W = fall-seeded grain, O = spring-seeded grain. M = meadow. The crops are grown in rotation and so arranged on the field that rowcrop strips are always separated by a meadow or winter-grain strip.

<sup>2</sup> These  $P_t$  values estimate the amount of soil eroded to the terrace channels and are used for conservation planning. For prediction of off-field sediment, the  $P_t$  values are multiplied by 0.2.

<sup>3</sup> n = number of approximately equal-length intervals into which the field slope is divided by the terraces. Tillage operations must be parallel to the terraces.

return periods. Note that the English units E values given in Table 111-10 must be multiplied by 1.735 to obtain the metric E used in Equation 111-11.

Method 3 : Erosivities from daily rainfall data.

Richardson et al . (1983) developed a regression equation for erosivity based on daily rainfall data. Converting their results to the units of E in Equation 111-11, the expected values of E for a daily rainfall R (cm) is:

$$E = 6.46a R^{1.81} \tag{111-14}$$

The coefficient "a" varies with location and season. Richardson et al . (1983) determined cool season (October-March) and warm season (April-September) coefficients for the locations shown in Figure 111-12.

TABLE III-10

## EXPECTED MAGNITUDES OF SINGLE-STORM EROSION INDICES (ENGLISH UNITS)

(Wischmeier and Smith, 1978)

Location	Index values normally exceeded once in—					Location	Index values normally exceeded once in—				
	year 1	years 2	years 5	years 10	years 20		year 1	years 2	years 5	years 10	years 20
Alabama:						Kansas:					
Birmingham	54	77	110	140	170	Burlington	37	51	69	83	100
Mobile	97	122	151	172	194	Coffeyville	47	69	101	128	159
Montgomery	62	86	118	145	172	Concordia	33	53	86	116	154
Arkansas:						Dodge City	31	47	76	97	124
Fort Smith	43	65	101	132	167	Goodland	26	37	53	67	80
Little Rock	41	69	115	158	211	Hays	35	51	76	97	121
Mountain Home	22	46	68	87	105	Wichita	41	61	93	121	150
Texarkana	51	73	105	132	163	Kentucky:					
California:						Lexington	28	46	80	114	151
Red Bluff	13	21	36	49	65	Louisville	31	43	59	72	85
San Luis Obispo	11	15	22	28	34	Middlesboro	28	38	52	63	73
Colorado						Louisiana:					
Akron	22	36	63	87	118	New Orleans	104	149	214	270	330
Pueblo	17	31	60	88	127	Shreveport	55	73	99	121	141
Springfield	31	51	84	112	127	Maine:					
Connecticut						Carrabou	14	20	28	36	44
Hartford	23	22	50	64	79	Portland	16	27	48	66	88
New Haven	31	47	73	96	122	Skowhegan	18	27	40	51	63
District of Columbia						Maryland:					
Florida:						Baltimore	41	59	86	109	133
Apalachicola	87	124	180	224	272	Massachusetts:					
Jacksonville	92	123	166	201	236	Boston	17	27	43	57	73
Miami	92	134	200	253	308	Washington	29	35	41	45	50
Georgia:						Michigan:					
Atlanta	49	67	92	112	134	Alpena	14	21	32	41	50
Augusta	24	50	74	94	118	Detroit	21	31	45	56	68
Columbus	61	81	108	131	152	East Lansing	19	26	36	43	51
Macon	53	72	99	122	146	Grand Rapids	24	28	34	38	42
Savannah	12	128	203	272	358	Minnesota:					
Watkinsville	52	71	98	120	142	Duluth	21	34	53	72	93
Illinois:						Fasston	17	26	39	51	63
Cairo	29	63	101	135	173	Mineapolis	25	35	51	65	78
Chicago	33	49	77	101	129	Rochester	41	58	85	105	129
Dixon Springs	29	56	82	105	130	Springfield	24	37	60	80	102
Molina	39	50	89	116	145	Mississippi:					
Rantoul	27	39	56	69	82	Meridian	69	92	125	151	176
Springfield	36	52	75	94	117	Oxford	48	64	86	103	120
Indiana:						Vicksburg	57	78	111	136	161
Evansville	24	38	56	71	86	Missouri:					
Fort Wayne	24	33	45	56	65	Columbia	43	58	77	93	107
Indianapolis	29	41	60	75	90	Kansas City	30	43	63	78	93
South Bend	26	41	65	86	111	McCredie	35	55	89	117	151
Terre Haute	42	57	78	96	113	Rolla	43	63	91	115	140
Iowa:						Springfield	37	51	70	87	102
Burlington	37	48	62	72	81	St. Joseph	45	62	86	106	126
Charles City	33	47	68	85	103	Montana:					
Clairinda	35	48	66	79	94	Great Falls	4	8	14	20	26
Des Moines	31	45	67	86	105	Miles City	7	12	21	29	38
Dubuque	43	63	91	114	140	Nebraska:					
Rockwell City	31	49	76	101	129	Antioch	19	26	36	45	52
Sioux City	40	58	64	105	131	Lincoln	36	51	74	92	112
						Lynch	26	37	54	67	82
						North Platte	25	38	59	78	99
						Scribner	38	53	76	96	116
						Valentine	18	28	45	61	77



TABLE III-10 (Continued)

Location	Index values normally exceeded once in—				
	year 1	years 2	years 5	years 10	years 20
<b>New Hampshire:</b>					
Concord	18	27	45	62	79
<b>New Jersey:</b>					
Atlantic City	39	55	77	97	117
Marlboro	29	57	85	111	136
Trenton	29	48	76	102	131
<b>New Mexico:</b>					
Albuquerque	4	6	11	15	21
Roswell	10	21	34	45	53
<b>New York:</b>					
Albany	18	26	38	47	56
Binghamton	14	24	36	47	58
Buffalo	15	23	36	49	61
Marcellus	14	24	38	49	62
Rochester	13	22	38	54	75
Salamanca	15	21	32	40	49
Syracuse	15	24	38	51	65
<b>North Carolina:</b>					
Asheville	28	40	58	72	87
Charlotte	41	63	100	131	164
Greensboro	37	51	74	92	113
Raleigh	53	77	110	137	168
Wilmington	59	87	129	167	206
<b>North Dakota:</b>					
Devils Lake	19	27	39	49	59
Fargo	20	31	54	77	103
Williston	11	16	25	33	41
<b>Ohio:</b>					
Cincinnati	27	36	48	59	69
Cleveland	22	35	53	71	86
Columbiana	20	26	35	41	48
Columbus	27	40	60	77	94
Coshocton	27	45	77	108	143
Dayton	21	30	44	57	70
Toledo	16	26	42	57	74
<b>Oklahoma:</b>					
Ardmore	46	71	107	141	179
Cherokee	44	59	80	97	113
Guthrie	47	70	105	134	163
McAlester	54	82	127	165	209
Tulsa	47	69	100	127	154
<b>Oregon:</b>					
Portland	6	9	13	15	18
<b>Pennsylvania:</b>					
Franklin	17	24	35	45	54
Harri sburg	19	25	35	43	51
Philadelphia	28	39	55	69	81
Pittsburgh	23	32	45	57	67
Reading	28	39	55	68	81
Scranton	23	32	44	53	63
<b>Puerto Rico:</b>					
San Juan	57	87	131	169	216
<b>Rhode Island:</b>					
Providence	22	34	52	68	83
<b>South Carolina:</b>					
Charleston	74	106	154	196	240
Clemson	51	73	106	133	163
Columbia	41	59	85	106	132
Greenville	44	65	96	124	153
<b>South Dakota:</b>					
Aberdeen	23	35	55	73	92
Huron	19	27	40	50	61
Isabel	15	24	38	52	67
Rapid City	12	20	34	48	64
<b>Tennessee:</b>					
Chattanooga	34	49	72	93	114
Knoxville	25	41	68	93	122
Memphis	43	55	70	82	91
Nashville	35	49	48	83	99
<b>Texas:</b>					
Abilene	31	49	79	103	138
Amarillo	27	47	80	112	150
Austin	51	80	125	169	218
Brownsville	73	113	181	245	312
Corpus Christi	57	79	114	146	171
Dallas	53	82	126	166	213
Del Rio	44	67	108	144	182
El Paso	6	9	15	18	24
Houston	82	127	208	275	359
Lubbock	17	29	53	77	103
Midland	23	35	52	69	85
Nocodoches	77	103	138	164	194
San Antonio	57	82	122	155	193
Temple	53	78	123	162	206
Victoria	59	83	116	146	178
Wichita Falls	47	63	86	106	123
<b>Vermont:</b>					
Burlington	15	22	35	47	58
<b>Virginia:</b>					
Blacksburg	23	31	41	48	56
Lynchburg	31	45	66	83	103
Richmond	46	63	86	102	125
Roanoke	32	33	48	61	73
<b>Washington:</b>					
Spokane	3	4	7	8	11
<b>West Virginia:</b>					
Elkins	23	31	42	51	60
Huntington	18	29	49	69	89
Parkersburg	20	31	46	61	76
<b>Wisconsin:</b>					
Green Bay	18	26	38	49	59
LaCrosse	46	67	99	125	154
Madison	29	42	61	77	95
Milwaukee	25	35	50	62	74
Rice Lake	39	45	70	92	119
<b>Wyoming:</b>					
Casper	4	7	9	11	14
Cheyenne	9	14	21	27	34



FIGURE III-12 VALUES OF "A" FOR EQUATION III-14  
(RICHARDSON *ET AL*, 1983)

When cropland erosion estimates are made for single storm events, the cover/management factor should in principle be selected for the crop stage corresponding to the time of year in which the storm occurs. The procedures for estimating seasonal C values as described in Wischmeier and Smith (1978) require crop development information which is usually not available in screening studies, and hence the annual C values given in Table III-4 are often used for single event estimates.

----- EXAMPLE III-3 -----

Soil Erosion Computations

Compare annual soil erosion values in central Michigan and southern Louisiana for a corn field with the following characteristics:

- Soil: silt loam, 4% organic matter
- Slope: 6%, 100 m length
- Moderate productivity, residues left, fall turn-plowed conventional management

For both locations, determine annual soil erosion with no conservation practices and with contouring.

Solution:

Soil erosion is determined by Equation III-11:

$$X = 1.29 E (K) (I_s) C (P)$$

From Figure 111-10, erosivities (in English units) for the two locations are approximately 100 (Michigan) and 500 (Louisiana). Multiplying by the metric conversion 1.735, we have  $E = 174$  and  $868$ . Other parameters are:

$$K = 0.33 \text{ (Table III-3)}$$

$$C = 0.52 \text{ (Table III-4, line 3).}$$

From Table III-9,  $P = 0.5$  for contouring and  $1.0$  with no practices.

The 6 percent slope corresponds to  $\theta = \tan^{-1}(0.06) = 3.43^\circ$  (Equation 111-13) and the  $I_s$  factor from Equation 111-12 is:

$$I_s = [0.045(100)]^{0.5} (65.41 \sin^2 3.43 + 4.56 \sin 3.43 + 0.065) = 1.21.$$

Thus  $1.29 (K)(I_s)C(P) = 0.268$  without contouring and  $0.134$  with contouring.

Soil erosion for the two locations and practices:

	<u>No practice</u>	<u>Contouring</u>
Michigan	46.6 t/ha	23.3 t/ha
Louisiana	232.6 t/ha	116.3 t/ha

----- END OF EXAMPLE III-3 -----

### 3.4.3.3 Watershed Sediment Yield

#### 3.4.3.3.1 Annual Yields

Watershed sediment yield due to surface erosion is:

$$Y = S_d \sum_k X_k A_k \quad (III-15)$$

where

$Y$  = annual sediment yield (tonnes/yr)

$X_k$  = erosion from source area  $k$  as given by Equation III-11 (t/ha)

$A_k$  = area of source area  $k$  (ha)

$S_d$  = watershed sediment delivery ratio.

The sediment delivery ratio  $S_d$  is a factor which accounts for the attenuation of sediment through deposition and filtering as it travels from source areas to the watershed outlet. Although a number of different relationships have been proposed for  $S_d$ , the simple function of watershed drainage area given in Figure III-13 remains the most generally accepted procedure.

#### 3.4.3.3.2 Seasonal Yields

Equation III-15 is appropriate for annual sediment yields and should not be used to determine event or seasonal watershed sediment yields. Large watershed sediment yields often do not coincide with major erosion periods. For example, in the eastern United States, most soil erosion is caused by late spring and summer intense rainstorms, but most sediment discharge occurs during late winter and early spring runoff. The reason for this is that runoff during erosive periods is often insufficient to transport eroded soil far from a source area. Subsequent large events "flush" portions of the accumulated sediment from the watershed drainage network.

Although general procedures are not available for estimating seasonal sediment yields, the following approach produced satisfactory results for an 850 km<sup>2</sup> watershed in upstate New York (Haith **et al.**, 1984).

Sediment yield in month  $m$ ,  $Y_m$  (tonnes), is assumed to be proportional to  $Q_m^{1.2}$  where  $Q_m$  is the watershed runoff (cm) during month  $m$ . The annual sediment yield  $Y$ , as given in Equation III-15, is likewise proportional to  $QT$ , where

$$QT = \sum_{m=1}^{12} Q_m^{1.2} \quad (III-16)$$

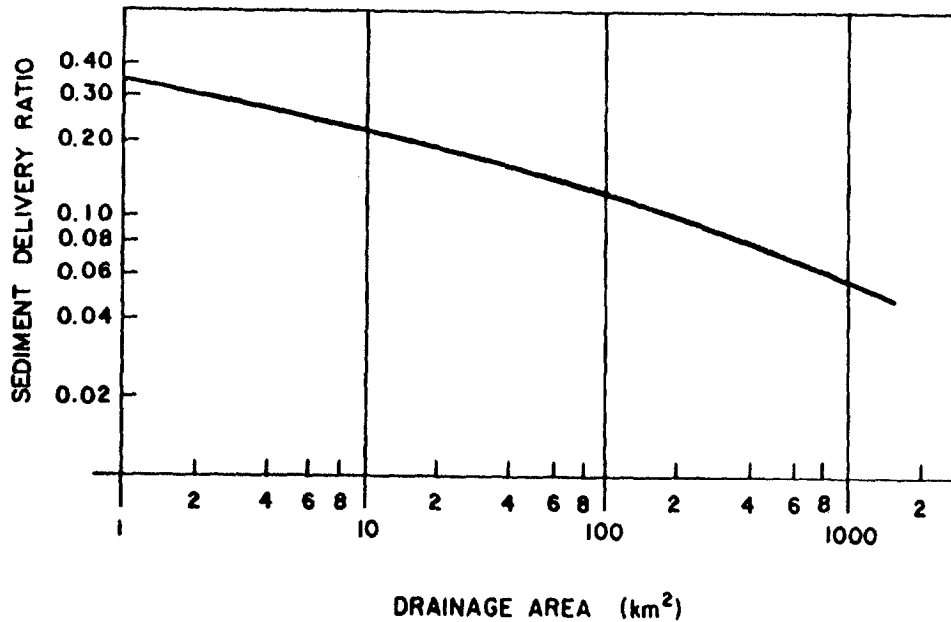


FIGURE III-13 SEDIMENT DELIVERY RATIO AS A FUNCTION OF WATERSHED DRAINAGE AREA (VANONI, 1975)

Thus :

$$Y_m/Y = Q_m^{1.2}/QT$$

or

$$Y_m = Q_m^{1.2} Y/QT \quad (III-17)$$

Equation III-17 was used to estimate monthly sediment yields over a 25-month period for the 850 km<sup>2</sup> West Branch Delaware River Basin in upstate New York. Comparisons with measured sediment yields indicated that the estimated mean monthly sediment yield was within 12 percent of the observed value. Based on correlations between monthly estimated and observed sediments yields, Equation III-17 explained 92 percent of the observed monthly variations (Haith *et al.* , 1984).

#### 3.4.4 Chemical Loading Functions for Rural Runoff

As suggested in Section 3.4.1, loading functions for rural runoff are equations that multiply dissolved and solid-phase pollutant concentrations by volume or mass fluxes of runoff water or sediment, respectively (Equations III-1 and III-2). Procedures for calculating runoff and sediment yield were described in Sections 3.4.2 and 3.4.3. It now remains to outline procedures for determining pollutant concentrations in runoff and sediment.

The principal pollutants in rural runoff are nutrients (nitrogen and phosphorus), heavy metals and synthetic organic pesticides. Although most of these chemicals have both solid and dissolved phases it is convenient to divide them into three categories, based on their main transport phase in runoff:

- Solid phase; chemicals which are strongly associated with sediment.
- Dissolved phase; chemicals which are dissolved in runoff.
- Distributed phase; significant chemical quantities are transported in both solid-phase and dissolved forms.

Loading functions for the first two categories are straightforward; empirical estimates are used for the chemical concentrations. Runoff of distributed-phase chemicals is more difficult to model since dissolved and solid-phase concentrations are influenced by adsorption equilibrium phenomena.

Solid-phase chemicals include organic nitrogen, particulate phosphorus and heavy metals. The assignment of metals to this category is arbitrary, since dissolved forms are often present under acidic conditions. However, it is assumed here that the primary sources of metals in rural runoff are metal-based pesticides which are tightly bound to soil particles (Weber, 1975).

The dissolved chemical group includes only inorganic nitrogen and soluble phosphorus. Inorganic nitrogen in drainage is mostly nitrate-nitrogen, and this ion does not adsorb to soil particles. Phosphorus is a special case. Most phosphorus in runoff is solid-phase, but dissolved phosphorus is directly available to plants and algae and hence cannot be neglected in eutrophication studies. The loading functions for solid-phase and dissolved phosphorus are operational means of describing complex soil chemistry. There is a continuous set of reactions that relate fixed, adsorbed and soluble phosphorus forms. Although it is possible to model this behavior (Donigan and Crawford, 1976; Knisel, 1980; Tubbs and Hai th, 1981), such models are neither simple nor especially accurate.

Distributed-phase chemicals include most organic pesticides. Models for runoff of these chemicals are considerably more complex than the solid-phase and dissolved chemical loading functions. Indeed, the term "loading function" is used advisedly, since models of these adsorbed chemicals are comparable to the continuous simulation models discussed in Section 3.3.

#### 3.4.4.1 Loading Functions for Solid-Phase Chemicals (Organic Nitrogen, Particulate Phosphorus, Heavy Metals)

The loading function for solid-phase chemicals in runoff from a source area is:

$$LS = 0.001 C_s X \quad (III-18)$$

where

LS = solid-phase chemical load in runoff (kg/ha)

Cs = concentration of chemical in eroded soil (sediment) (mg/kg)

X = soil loss (t/ha).

The "0.001" in Equation 111-18 is a dimensional conversion constant. Soil loss is given by the Universal Soil Loss Equation (Equation III-11) on either an annual or single event basis. In determining a source area's contribution to watershed chemical loading, LS must be modified by a sediment delivery ratio (Section 3.4.4.1.2).

Equation III-18 is often considered to be an estimate of total chemical load rather than just the solid-phase portion. The assumption is essentially correct for heavy metals since they are tightly bound to soil particles. Moreover since most soil nitrogen is in the solid-phase organic form and most soil phosphorus is particulate, solid-phase nutrient loads will generally be a very large portion of total loads.

#### 3.4.4.1.1 Solid-Phase Chemical Concentrations

The concentration Cs is best determined by direct measurement. Samples may be taken of sediment depositions in fields and drainage ditches. These samples are subsequently analyzed for total concentrations of heavy metals, organic nitrogen or particulate phosphorus in the sediment. Streamflow suspended solids samples in rural watersheds free of point sources and urban drainage may also be used. When sediment sampling is infeasible, procedures described in the following subsections may be used to obtain approximate concentration estimates.

##### 3.4.4.1.1.1 Organic Nitrogen and Particulate Phosphorus

Nitrogen and phosphorus concentrations in eroded soil are generally larger than comparable concentrations in uneroded or in situ soil. This is due to the selective nature of the erosion process. Lighter organic matter and clay particles are more readily eroded than heavier sand and silt. Since nutrients tend to be associated with these light particles, sediment is "enriched" with nutrients compared to the soil from which it originates. A sediment nutrient concentration can thus be related to the comparable concentration in soil by an enrichment ratio:

$$C_s = e_n C_i \quad (\text{III-19})$$

where

$e_n$  = nutrient enrichment ratio

$C_i$  = nutrient concentration in in situ soil (mg/kg).

Soil nutrient concentrations are sometimes available from soil surveys or extension specialists. Nitrogen concentrations may be inferred from soil organic

matter percentages by assuming that organic matter is 5 percent nitrogen (Brady, 1974). Thus, for nitrogen  $C_i \approx 0.05(\% \text{ OM}/100)10^6 = 500 (\% \text{ OM})$ , where % OM is percent organic matter in the soil.

Very rough estimates of soil nutrient concentrations can be obtained from the general maps shown in Figures 111-14 and 15. Figure 111-15 indicates soil content of  $P_2O_5$  which is 44 percent phosphorus. To use Figures 111-14 and 15, we note that 1% = 10,000mg/kg, and hence for

$$\begin{aligned} \text{Nitrogen: } C_i &= (\% \text{ N})10^4 \\ \text{Phosphorus: } C_i &= 0.44 (\% P_2O_5)10^4. \end{aligned}$$

Although these nutrient concentrations are for total nitrogen and phosphorus, they may be used for organic nitrogen and particulate phosphorus since these nutrient forms are so dominant in the soil.

Nutrient enrichment ratios are in principle event-specific, since they are related to the degree of erosion which occurs during a storm. With very small storms, only the finest soil particles are eroded, and the enrichment ratio is high. Conversely, large storms erode all soil particles, and the enrichment ratio approaches one. Based on analyses of many field studies of nutrient transport, Menzel (1980) suggested the relationship:

$$en = 7.39/\text{Sed}^{0.2} \quad (111-20)$$

in which Sed is the sediment discharge (kg/ha) during the storm event. Equation 111-20 gives values of en ranging from 2.94 at Sed = 100 kg/ha to 1.35 at Sed = 5000 kg/ha.

Equation 111-20 can be used directly for single storm loading estimates by letting Sed = 1000 X, since the units of soil loss X are tonnes/ha. The equation is not suitable for annual loads. For these loads, a midrange value of en = 2.0 is appropriate (Hait h and Tubbs, 1981). In summary:

$$en = \begin{cases} 2.0 & \text{for annual loads} \\ 7.39/(1000 X)^{0.2} & \text{for single event loads} \end{cases} \quad (111-21)$$

For very large soil losses ( $X > 22 \text{ t/ha}$ ), Equation 111-21 will give  $en < 1.0$  for an event. When this occurs, en should be set equal to 1.0.

#### 3.4.4.1.1.2 Heavy Metals

The U. S. Geological Survey has analyzed soil samples from 863 sites in the United States for heavy metals. The results, as summarized by McElroy et al. (1976), are given in Table III-11. These concentrations may be used directly as Cs in Equation III-18 since 1 ppm = 1 mg/kg, and it may be assumed that no metals enrichment of sediment occurs (McElroy et al. , 1976).



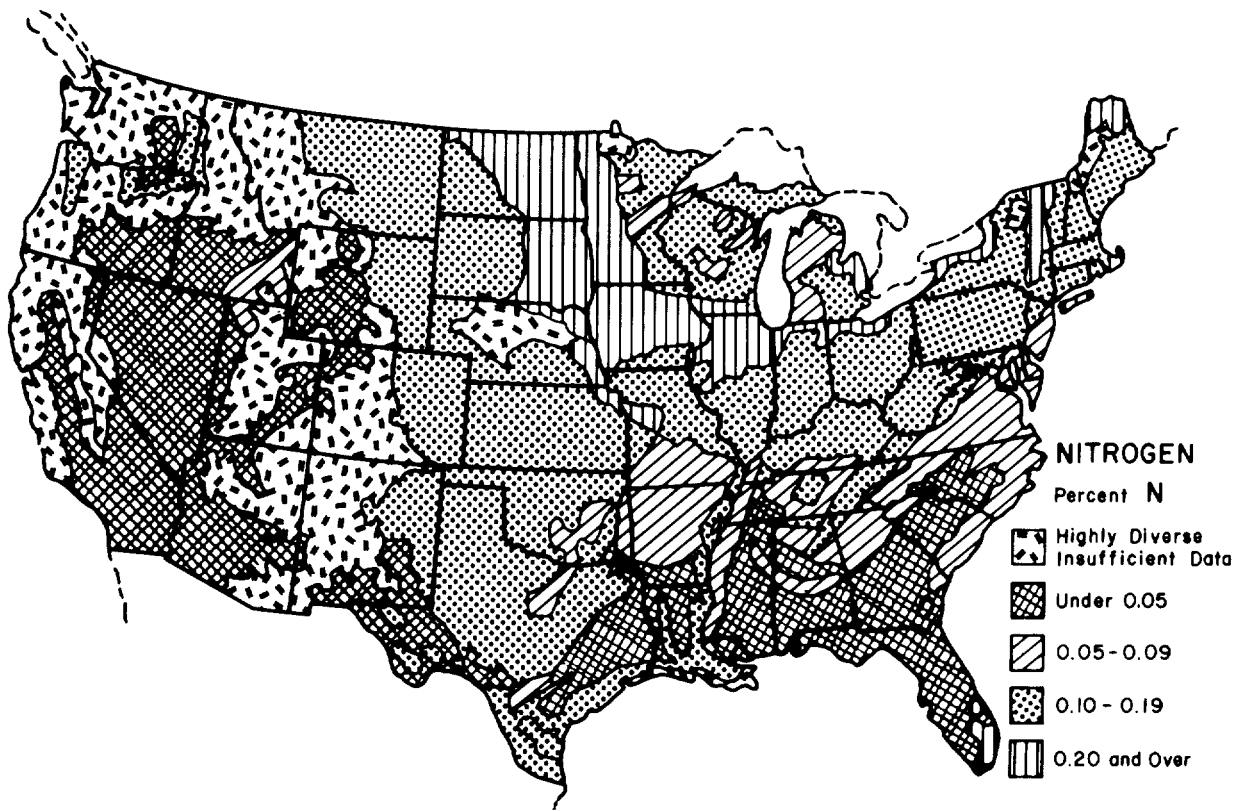


FIGURE III-14 NITROGEN IN SURFACE FOOT OF SOIL (PARKER, ET AL , 1946)

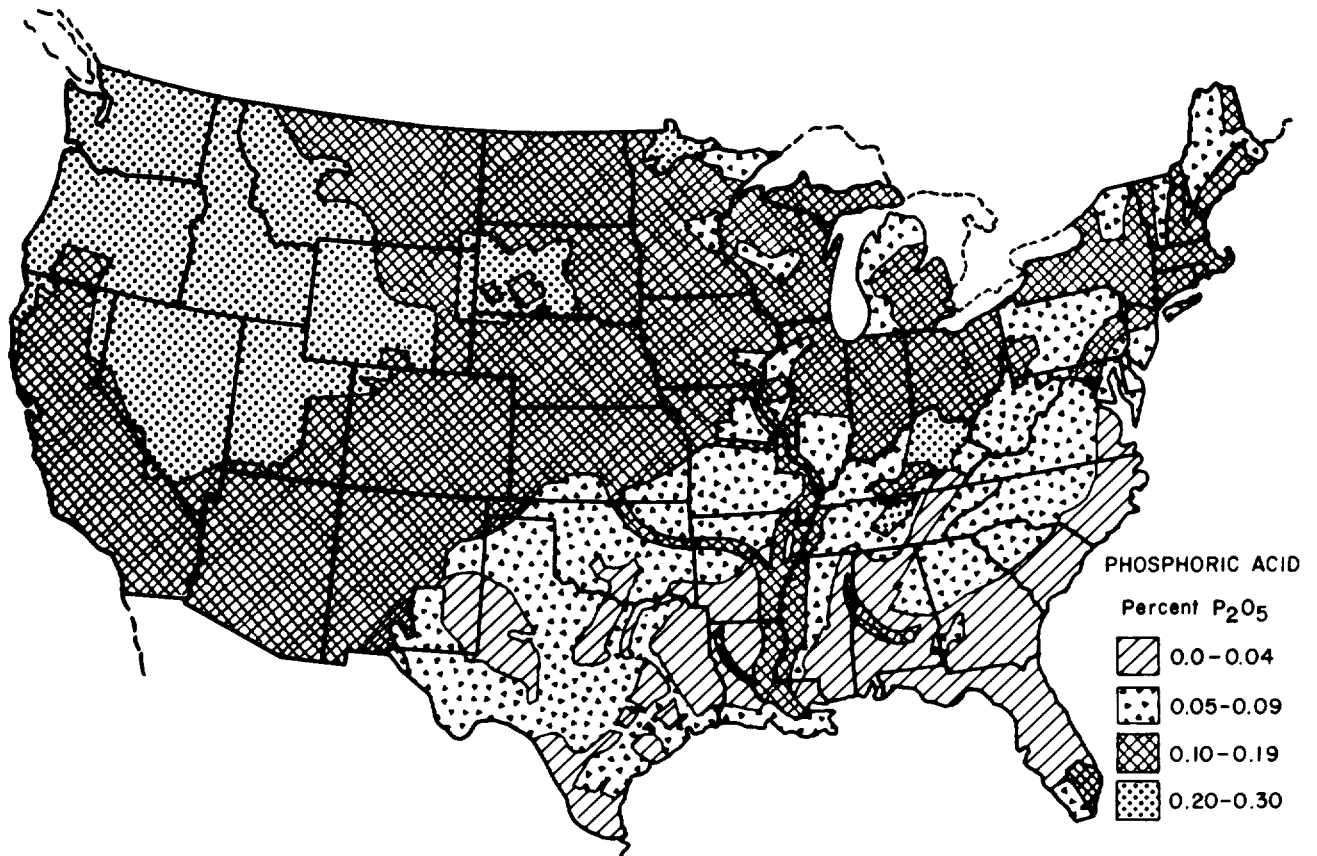


FIGURE III-15 PHOSPHORUS (AS  $P_2O_5$ ) IN THE SURFACE FOOT OF SOIL  
(NOTE:  $P_2O_5$  IS 44% PHOSPHORUS) (PARKER ET AL , 1946)

TABLE III-11

## HEAVY METAL CONCENTRATIONS IN SURFICIAL MATERIALS IN THE UNITED STATES

(McElroy *et al.*, 1976)

Element	Arithmetic analysis		Geometric means		
	Average	Range	Conterminous	West of 97th	East of 97th
	(ppm)	(ppm)	U. S. (ppm)	meridian (ppm)	meridian (ppm)
Arsenic	--	< 1,000	--	--	--
Barium	554	15-5,000	430	560	300
Cadmium	--	< 20	--	--	--
Cerium	86	< 150-300	75	74	78
Chromium	53	1-1,500	37	38	36
Cobalt	10	< 3-70	7	8	7
Copper	25	< 1-300	18	21	14
Iron	25,000	100-100,000	18,000	20,000	15,000
Gallium	19	< 5-70	14	18	10
Germanium	--	< 10	--	--	--
Gold	--	< 20	--	--	--
Hafnium	--	< 100	--	--	--
Iridium	--	< 10	--	--	--
Lanthanum	41	< 30-200	34	35	33
Lead	20	< 10-700	16	18	14
Manganese	560	< 1-7,000	340	389	285
Molybdenum	< 3	< 3-7	--	--	--
Neodymium	45	< 70-300	39	36	44
Nickel	20	< 5-700	14	16	13
Niobium	13	< 10-100	12	11	13
Palladium	--	< 1	--	--	--
Platinum	--	< 30	--	--	--
Rhenium	--	< 30	--	--	--
Scandium	10	< 5-50	8	9	7
Strontium	240	< 5-3,000	120	210	51
Tantalum	--	< 200	--	--	--
Tellurium	--	< 2,000	--	--	--
Thallium	--	< 50	--	--	--
Thorium	--	< 200	--	--	--
Titanium	3,000	300-15,000	2,500	2,100	3,000
Uranium	--	< 500	--	--	--
Vanadium	76	< 7-500	56	66	46
Ytterbium	4	< 1-50	3	3	3
Yttrium	29	< 10-200	24	25	23
Zinc	54	< 25-2,000	44	51	36
Zirconium	<u>240</u>	< 10-2,000	<u>200</u>	<u>170</u>	<u>250</u>
Total	30,099		21,991	23,858	19,263

Note: "--" indicates all analyses showed element to be below detectable limits.

### 3.4.4.1.2 Watershed Loads of Solid-Phase Chemicals

The annual watershed load of a solid-phase chemical in rural runoff is the sum of the attenuated runoff loads from all source areas in the watershed. Since these chemicals travel with sediment, attenuation (i.e., transport loss) is described by the sediment delivery ratio,  $S_d$ :

$$\begin{aligned} WLS &= S_d \sum_k LS_k A_k \\ &= 0.001 S_d \sum_k Cs_k X_k A_k \end{aligned} \quad (III-22)$$

where

- $WLS$  = annual watershed solid-phase chemical load in rural runoff (kg/yr)
- $LS_k$  = solid-phase chemical load in runoff from source area  $k$  (kg/ha)
- $A_k$  = area of source area  $k$  (ha)
- $Cs_k$  = solid-phase chemical concentration in eroded soil (sediment) from source  $k$  (mg/kg)
- $X_k$  = soil loss from source area  $k$  (t/ha).

Single event loads cannot be estimated by Equation III-22 due to the sediment transport variations discussed in Section 3.4.3.3.2. However, seasonal loads may be calculated by assuming them to be proportional to seasonal sediment yields. From Equation III-17, we know that the ratio of monthly watershed sediment yield  $Y_m$  to annual yield  $Y$  is:

$$Y_m/Y = Q_m^{1.2}/QT \quad (III-17)$$

where  $Q_m$  is watershed runoff in month  $m$  (cm) and  $QT$  is given by Equation 111-16. Thus if  $WLS$  is the annual chemical load given by Equation III-22, then  $WLS_m$ , the load (kg) in month  $m$ , is:

$$WLS_m = (Y_m/Y)WLS \quad (III-23)$$

In many watersheds, the concentration of a chemical in sediment is relatively uniform, and hence  $Cs_k$  the same for all source areas. For this case, Equation III-23 reduces to:

$$\begin{aligned} WLS_m &= (Y_m/Y) 0.001 S_d Cs \sum_k X_k A_k \\ &= (Y_m/Y) 0.001 Cs Y \end{aligned}$$

or

$$WLS_m = 0.001 Cs Y_m \quad (III-24)$$

Thus when soil chemical concentrations are uniform, monthly chemical loads can be obtained directly from monthly sediment loads.

EXAMPLE III-4

Watershed Sediment and Phosphorus Loads

The West Branch Delaware River is an 85,000 ha watershed in south-central New York that drains into Cannonsville Reservoir. Soil erosion is a major phosphorus source to the reservoir. Major land uses contributing erosion are as follows:

<u>Land Use</u>	<u>Area (ha)</u>	<u>Mean K(Is)CP</u>
Corn	3,430	0.214
Hay	13,085	0.012
Pasture	5,093	0.016
Inactive Agricultural	3,681	0.017
Logging Roads	20	0.217

Determine:

- Average annual sediment yield (tonnes/yr)
- Average annual solid-phase phosphorus input to the reservoir (kg/yr)

Solution:

- Average annual sediment yield is given by Equations III-15 and III-11:

$$Y = S_d \sum_k X_k A_k \quad (III-15)$$

$$X_k = 1.29 E (K) (Is) C (P) \quad (III-11)$$

There are five different source areas, each with their associated K (Is) C (P) values. Rainfall/runoff erosivity is approximately 125 (Figure III-10).

Converting to metric units:

$$E = 1.735(125) = 217.$$

Soil erosion  $X_k$ , from each source area is:

- Corn:  $1.29(217) 0.214 = 59.9 \text{ t/ha}$
- Hay:  $1.29(217) 0.012 = 3.4 \text{ t/ha}$
- Pasture:  $4.5 \text{ t/ha}$
- Inactive Agriculture:  $4.8 \text{ t/ha}$
- Logging Roads:  $60.7 \text{ t/ha}$

The sediment delivery ratio  $S_d$  is approximately 0.065 for an  $850 \text{ km}^2$

watershed (Figure III-13). Sediment yield is:

$$Y = 0.065 [59.9(3430) + 3.4(13,085) + 4.5(5,093) + 4.8(3681) + 60.7(20)]$$

$$= 18,960 \text{ tonnes/yr}$$

b) Phosphorus load is:

$$LS = 0.001 S_d \sum_k C_{s_k} X_k A_k \quad (III-22)$$

Since no other information is available, phosphorus concentrations are obtained from Figure 111-15. New York soils are 0.10 - 0.19 percent  $P_{205}$ . Using a mid-range value of 0.15 percent and recalling that  $P_{205}$  is 44 percent phosphorus, we obtain a soil phosphorus level of:

$$C_i = 0.44(0.15) 10^4$$

$$= 660 \text{ mg/kg}$$

Using an enrichment ratio of 2.0 (Equation III-21),  $C_s = 2.0 (660) = 1320$  mg/kg.

We must assume that  $C_s$  is the same for all source areas and hence:

$$LS = 0.001 C_s S_d \sum_k X_k A_k$$

$$= 0.001 C_s Y$$

$$= 0.001(1320)(18,960) = 25,000 \text{ kg/yr.}$$

END OF EXAMPLE III-4

#### 3.4.4.2 Loading Functions for Dissolved Chemicals (Inorganic Nitrogen and Soluble Phosphorus)

The loading function for dissolved nutrients in runoff from a source area is:

$$LD = 0.1 C_d Q \quad (III-25)$$

where

LD = dissolved chemical load in runoff (kg/ha)

$C_d$  = concentration of dissolved chemical in runoff (mg/l)

$Q$  = runoff from source area (cm).

The "0.1" in Equation III-25 is a dimensional conversion constant. For event loads,  $Q$  is given by Equation III-3. The loading function may also be used for annual loads provided annual runoff values such as those shown in Figure III-9 are available.

### 3.4.4.2.1 Dissolved Nutrient Concentrations

Concentrations of dissolved nutrients in runoff vary with soil cover. Representative concentrations are given in Table III-12. Concentrations for fallow, corn, small grains, hay and pasture are flow-weighted average concentrations measured in runoff over several years from large field sites in South Dakota (Dornbush, et al., 1974). Forest concentrations are the National Eutrophication Survey values for inorganic nitrogen and orthophosphorus given in Figures III-4 and 5 for 90% forested watersheds.

In the northern U.S., cropland which has manure left on the soil surface, particularly during snowmelt, is likely to have significantly higher dissolved nutrient concentrations in runoff than unmanured cropland. The concentrations for manured fields given in Table III-12 should be used for snowmelt runoff from fields which have received winter applications of manure,

Although the representative concentrations given in Table III-12 should be replaced by local data whenever possible, such data are unavailable in most water quality screening studies. However, since the concentrations in Table III-12 are comparable to other values reported in the literature (see for example Baker, 1980), it is unlikely that use of the representative concentrations would produce large errors in loading estimates.

#### EXAMPLE III-5

##### Single Event Runoff, Sediment and Nitrogen Load

During the growing season a 7.0 cm rainstorm falls on the Louisiana cornfield described in Example III-3. The field has an area of 10 ha and is planted in straight rows. The soil is in hydrologic Group B and is in poor hydrologic condition. This storm was preceded by 5.5 cm of rain four days previously. From Example III-3, the soil has an organic matter content of 4 percent and the USLE parameters for this field are:

$$K = 0.33, \quad I_s = 1.21, \quad C = 0.52 \quad \text{and} \quad P = 1.0$$

Determine:

- a) Storm runoff (cm)
- b) Soil loss (tonnes)
- c) Solid-phase and dissolved nitrogen in runoff (kg).

Solution:

- a) Runoff is given by the Curve Number Equation (Equation III-3). The curve number for straight row, poor hydrologic condition, soil B is  $CN_2 = 81$  (Table III-1). According to Table III-2, the preceding 5.5 cm of

TABLE III-12

## REPRESENTATIVE DISSOLVED NUTRIENT CONCENTRATIONS IN RURAL RUNOFF

Soil Cover	Nitrogen (mg/l)	Phosphorus (mg/l)
Fall	2.6	0.10
Corn <sup>a</sup>	2.9	0.26
Small Grains <sup>a</sup>	1.8	0.30
Hay <sup>a</sup>	2.8	0.15
Pasture <sup>a</sup>	3.0	0.27
Inactive Agriculture <sup>b</sup>		
Eastern U. S.	1.6	0.14
Midwest	1.5	0.14
West	1.5	0.14
Forest		
Eastern U. S.	0.19	0.006
Midwest	0.06	0.009
West	0.07	0.012
Snowmelt Runoff from Manured Fields <sup>d</sup>		
Fallow	12.2	1.9
Corn	12.2	1.9
Small Grains	25.0	<b>5.0</b>
Hay	36.0	<b>8.7</b>

<sup>a</sup>Dornbush *et al.* (1974)

<sup>b</sup>Average of pasture and forest

<sup>c</sup>Omernik (1977). See Figures III-4,5

<sup>d</sup>Gilbertson *et al.* (1979). These concentrations are associated with winter manure spreading.

rain places the field in antecedent moisture condition III, and hence the relevant curve number is  $CN = CN_3$ . From Equation III-7:

$$CN_3 = 81/[0.4036 + 0.0059(81)] = 91.9$$

The retention parameter (Equation III-4) is:

$$S = 2540/91.9 - 25.4 = 2.24 \text{ cm}$$

Runoff  $Q$  is:

$$Q = [7 - 0.2(2.24)]^2/[7 + 0.8(2.24)] \\ = 4.9 \text{ cm}$$

b) Soil loss is given by the USLE:

$$X = 1.29(K)(I_s)C(P) \quad (III-11)$$

where in this case E is the event erosivity given by Equation 111-14:

$$E = 6.46 a R^{1.81}$$

The nearest location for the "a" value is State College, Mississippi (Figure 111-12), which has a warm season value of a = 0.51. Erosivity is thus:

$$E = 6.46(0.51)(7)^{1.81} = 112$$

Soil loss is:

$$\begin{aligned} X &= 1.29(112)0.33(1.21)0.52(1) \\ &= 30 \text{ t/ha} \end{aligned}$$

Over 10 ha, the loss is 30(10) = 300 tonnes.

c) Solid-phase nitrogen loss (kg/ha) is:

$$LS = 0.001 CsX \quad (111-18)$$

where

$$Cs = en Ci \quad (111-19)$$

and

$$en = 7.39/(1000X)^{0.2} \quad (111-21)$$

As described in Section 3.4.4.1.1.1, soil nitrogen concentration Ci (mg/kg) can be estimated by assuming that organic matter is 5 percent nitrogen. The field's 4 percent organic matter gives a nitrogen concentration of:

$$Ci = 0.05(0.04)10^6 = 2000 \text{ mg/kg}$$

The enrichment ratio for the storm is:

$$en = 7.39/[1000(30)]^{0.2} = 0.94$$

Since this is less than 1.0, we set en = 1.0, and the solid-phase nitrogen concentration in sediment is:

$$Cs = 1.0 Ci = 2000 \text{ mg/kg}$$

The solid-phase nitrogen load is:

$$\begin{aligned} LS &= 0.001(2000)(30) = 60 \text{ kg/ha} \\ &\text{or } 600 \text{ kg for the } 10 \text{ ha field.} \end{aligned}$$

The dissolved nitrogen load is:



$$LD = 0.1 CdQ \quad (III-25)$$

where from Table 111-12,  $Cd = 2.9$  mg/l for corn. Hence:

$$LD = 0.1(2.9)(4.9) = 1.4 \text{ kg/ha}$$

or 14 kg for the 10-ha field,

----- END OF EXAMPLE III-5 -----

#### 3.4.4.2.2 Watershed Loads of Dissolved Chemicals

Since all runoff from watershed source areas is transported to the watershed outlet (see Section 3.4.2.4), it is assumed that dissolved nutrient loads are not attenuated. Watershed load is thus the sum of the source area loads:

$$WLD = 0.1 \sum_k Cd_k Q_k A_k \quad (III-26)$$

where

$WLD$  = annual or event watershed dissolved chemical load in rural runoff (kg)

$Cd_k$  = dissolved chemical concentration in runoff from source area k (mg/l)

$Q_k$  = runoff from source area k (cm)

$A_k$  = area of source area k (ha).

#### 3.4.4.3 Loading Functions for Distributed Phase Chemicals (Pesticides)

Runoff of pesticides can be described by the same general loading functions used for nutrients and metals (Equations III-18 and III-25). However, the estimation of dissolved and solid-phase concentrations is more difficult for pesticides. All pesticides are adsorbed to some extent by soil particles, and hence dissolved and solid-phase concentrations cannot be determined independently. Also, these concentrations are dynamic, since pesticides are decomposed or decayed by photochemical, chemical, and microbiological process. Decay rates are often sufficiently high that most of a pesticide will have decomposed within several weeks of application. A final complicating factor is the large number of pesticide compounds currently in use, each with its own properties and characteristic behavior in the soil.

It follows that pesticide concentrations in runoff cannot be estimated by simple empirical methods, since they depend on the relative timing of applications and storm events, and the specific adsorption and degradation properties of the pesticide. However relatively simple equations can be used to describe the adsorption and decay phenomena, and calculations can be made for each storm event following a pesticide application. The following subsections describe such a model and also provide model

parameters for a large number of pesticides. The model estimates pesticide load runoff events from a source area; i.e., a small catchment with uniform soil, hydrologic and chemical characteristics. Methods are not available to aggregate these source area loads into total watershed load.

#### 3.4.4.3.1 Pesticide Runoff Model

The pesticide runoff model developed by Hai th (1980) is based on a pesticide mass balance of the surface centimeter of soil. On day  $t$  after a pesticide application  $P_0$  (g/ha) to the surface soil layer, the pesticide content is:

$$P_t = P_0 \exp(-k_s t) + \Delta P_t \quad (III-27)$$

where

- $P_t$  = pesticide in surface centimeter on day  $t$  (g/ha)
- $k_s$  = pesticide decay rate ( $\text{day}^{-1}$ )
- $\Delta$  = additional pesticide application (if any) on day  $t$  (g/ha)

Equation III-27 is a standard exponential or first-order decay model.

If a previous storm and/or pesticide application was made on some day  $\tau$  prior to day  $t$ , then:

$$P_t = P_\tau^+ \exp [k_s (t-\tau)] + \Delta P_t \quad (III-28)$$

where

- $P_\tau^+$  = pesticide content after storm event or application on day  $\tau$  (g/ha).

Total pesticide  $P_t$  is divided into adsorbed (solid-phase) and dissolved forms based on a linear adsorption equilibrium relationship.

$$P_t = A_t + D_t \quad (III-29)$$

and

$$a_t = K_D d_t \quad (III-30)$$

where

- $A_t$  = adsorbed (solid-phase) pesticide in surface centimeter on day  $t$  (g/ha)
- $D_t$  = dissolved pesticide in surface centimeter on day  $t$  (g/ha)
- $a_t$  = adsorbed pesticide concentration on soil particles (mg/kg)
- $d_t$  = dissolved pesticide concentration in solid water (mg/l)
- $K_D$  = pesticide partition or distribution coefficient (l/kg).

If a rainfall or snowmelt event sufficient to fill the surface layer's volumetric

available water capacity  $w$  (cm/cm) occurs on day  $t$ , then  $D_t$  is given by  $100 w d_t$  and  $A_t$  is  $100b a_t$  where  $b$  is the surface soil bulk density ( $\text{g/cm}^3$ ). Substituting these relationships into Equations III-29 and III-30 produces:

$$A_t = [1/(1 + w/K_D b)] P_t \quad (III-31)$$

and

$$D_t = [1/(1 + K_D b/w)] P_t \quad (III-32)$$

If runoff occurs on day  $t$ , portions of  $A_t$  and  $D_t$  will be removed by water and sediment movement. The solid-phase loss is the product of adsorbed concentration and soil loss. Since  $a_t = A_t/100b$ , we have

$$PX_t = (A_t/100b) X_t \quad (III-33)$$

where

$PX_t$  = solid-phase pesticide in runoff on day  $t$  (g/ha)

$X_t$  = soil loss (sediment) in runoff on day  $t$  (t/ha).

Dissolved pesticide losses are distributed into runoff, percolation and a residual which remains in the surface layer after a storm. These components are assumed proportional to the distribution of rainfall  $R_t$  (cm) plus snowmelt  $M_t$  (cm) into runoff, percolation, and available soil water. Considering only events for which  $R_t + M_t > w$ , runoff loss of dissolved pesticide is:

$$PQ_t = [Q_t/(R_t + M_t)] D_t \quad (III-34)$$

where

$PQ_t$  = dissolved pesticide in runoff on day  $t$  (g/ha)

$Q_t$  = runoff on day  $t$  (cm).

Assuming that the surface layer is dry prior to the event, percolation loss of dissolved pesticide from the layer is  $[(R_t + M_t - Q_t - w)/(R_t + M_t)] D_t$ , and dissolved pesticide remaining in the soil after the event is  $[w/(R_t + M_t)] D_t$ . Pesticide remaining in the surface layer is:

$$P_t^+ = P_t - PX_t - [1 - w/(R_t + M_t)] D_t \quad (III-35)$$

Equations III-33 and III-34 are the basic loading functions for solid-phase and dissolved pesticide in runoff. For the solid-phase loads,  $X_t$  in Equation III-33 is the eroded soil from the source area as given by the Universal Soil Loss Equation, (Equation III-11). The remainder of Equation III-33,  $A_t/100b$ , is

the pesticide concentration in eroded soil or sediment. In the dissolved pesticide loading function, Equation III-34,  $Q_t$  is runoff from the source area determined by the Curve Number Equation (Equation III-3), and  $D_t/(R_t + M_t)$  is the dissolved pesticide in runoff. These loading functions are of the same form as the solid-phase and dissolved chemical loading functions of Sections 3.4.4.1 and 3.4.4.2.

#### 3.4.4.3.2 Computational Steps

The pesticide runoff model is implemented by a set of sequential computations:

1. The day of initial pesticide application is designated  $t = 0$  and  $P_0$  is set equal to the application to the surface centimeter (g/ha).
2. On each day  $t = 1, 2, \dots$  following application, a check is made to see if an "event" occurs. An event is either (i) a new pesticide application or (ii) a precipitation (rain + melt) amount exceeding the soil's available water capacity. If no event occurs, the computations proceed to the next day. If there is an event, the current pesticide content of the soil is determined by Equation III-28.
3. If  $R_t + M_t > w$ , then pesticide leaching will occur, and the following steps are required:
  - a. Dissolved pesticide  $D_t$  is obtained from Equation III-32.
  - b. Runoff  $Q_t$  is computed by Equation III-3. If  $Q_t = 0$ , go to step e.
  - c. Dissolved pesticide runoff  $PQ_t$  is determined from Equation III-34.
  - d. Adsorbed (solid-phase) pesticide runoff  $PX_t$  is obtained from Equation III-33 with soil loss  $X_t$  given by Equation III-11 and adsorbed pesticide  $A_t$  given by Equation III-31.
  - e. Soil pesticide level is updated to  $P_t^+$  by Equation III-35. Note that Equation III-35 may predict substantial pesticide losses in percolation even if no runoff occurs and hence  $PX_t$  and  $PQ_t$  are both zero.

These computational steps are repeated for subsequent days following a storm until the surface pesticide level  $P_t$  becomes negligible. Often the combined effects of decay and leaching will remove virtually all pesticide from the surface layer within several weeks of application.

#### 3.4.4.3.3. Data for the Pesticide Runoff Model

Four types of data are required for pesticide runoff calculations: daily weather records, Universal Soil Loss Equation parameters and runoff curve numbers, soil properties and pesticide parameters. The first two categories have been discussed in previous sections. The soil properties needed are available water capacity ( $w$ ) and bulk density ( $b$ ). These parameters are often given in county soil surveys.

Representative values of  $w$  and  $b$  for several soil textures are given in Table 111-13. These data are mean bulk densities for 207 soils and mean available water capacities for 154 soils reported by Baes and Sharp (1983).

Pesticide application rates, timing, and mode of application cannot be generalized. This information can only be obtained from local or regional pest control specialists. Mode of application refers to surface applied versus soil incorporated pesticide. The model describes pesticide behavior into the surface centimeter of soil and hence the application  $P_0$  or  $\Delta P_t$  are the chemical additions to that surface layer. For example, if 3000 g/ha of pesticide is applied to the soil and incorporated to a depth of 5 cm (2 in.), the application rate for the surface layer is  $3000/5 = 600$  g/ha (assuming complete mixing in the soil). Conversely, if the pesticide is left on the soil surface, the entire 3000 g/ha is contained in the surface centimeter.

#### 3.4.4.3.3.1 Pesticide Partition Coefficients

Pesticide adsorption is generally considered to be related to soil organic matter. A general relationship given by Rao and Davidson (1980) is:

$$K_D = K_{OC} (\%OC/100) \quad (111-36)$$

where

$K_{OC}$  = pesticide partition coefficient for organic carbon  
 $\%OC$  = organic carbon of the soil, measured as a %.

Table 111-14 lists  $K_{oc}$  values which have been summarized by Rao and Davidson (1982) from a number of studies. The table entries are means and coefficients of variation (standard deviation/mean, as a percent). The mean values can be used to estimate a partition coefficient for any soil. For example, the  $K_D$  value for atrazine in a soil with 2 percent organic carbon is:

$$K_D = 163 (2/100) = 3.26$$

Soil organic matter percentage,  $\%OM$ , is often more readily available than  $\%OC$ . In such cases,  $\%OC$  may be estimated as 59 percent of organic matter (Brady, 1974):

$$\%OC = 0.59 (\%OM) \quad (111-37)$$

When  $K_{OC}$  values are unavailable, they may be indirectly measured by the octanol-water partition coefficient  $K_{OW}$ . Rao and Davidson (1980) derived the regression equation:

$$\log K_{OC} = 1.029 \log K_{OW} - 0.18$$

or

TABLE III-13

## MEAN BULK DENSITIES AND AVAILABLE WATER CAPACITIES

(Bass and Sharp, 1983)

Soil Type	Bulk Density (g/cm <sup>3</sup> )	Available Water Capacity (cm/cm)
Silt Loam	1.33	0.22
Clay and Clay Loam	1.30	0.14
Sandy Loam	1.50	0.14
Loam	1.42	0.19

TABLE III-14

## ORGANIC CARBON PARTITION COEFFICIENTS FOR SELECTED PESTICIDES

(Rao and Davidson, 1982)

Pesticide	Number of Soils	$K_{oc}$		Pesticide	Number of Soils	$K_{oc}$	
		Mean	(%CV)			Mean	(%CV)
AMETRYNE	32	388.4	(57.1)	LI NURON	33	862.8	(72.3)
AMIBEN	12	189.6	(149.7)	MALATHI ON	20	1796.9	(65.9)
ATRAZI NE	56	163.0	(49.1)	METHYL PARATHI ON	7	5101.5	(113.6)
BROMACIL	2	72.0	(102.1)	METHYL UREA	5	58.8	(15.1)
CARBOFURAN	5	29.4	(30.0)	METOBROMURON	4	271.5	(37.1)
CHLOROBROMURON	5	995.6	(55.1)	MONOLI NURON	10	284.3	(55.2)
CHLORONEB	1	1652.9	(--)	MONURON	18	183.5	(60.8)
CHLOROXURON	5	4343.3	(28.8)	NEBURON	5	3110.5	(23.5)
CHLOROPROPHAM	36	816.3	(--)	p-CHLOROANI LI NE	5	561.5	(33.6)
CHLORTHI AMI D	6	98.3	(27.5)	PARATHI ON	4	10650.3	(74.6)
CI ODRI N	3	74.8	(59.1)	PHENYL UREA	5	76.3	(12.3)
DDT	2	243118.0	(65.0)	PI CLORAM	26	25.5	(138.5)
DI CAMBA	5	2.2	(73.5)	PROMETONE	29	524.3	(143.6)
DI CHLOBENI L	34	224.4	(77.4)	PROMETRYNE	38	614.3	(99.1)
DI METHYL AMI NE	5	434.9	(19.8)	PROPАЗI NE	36	153.5	(37.0)
DI PROPETRYNE	5	1180.8	(74.9)	SIMAZI NE	147	138.4	(12.6)
DI SULFOTON	20	1603.0	(144.2)	TELONE (ci s)	6	798.1	(44.3)
DI URON	84	382.6	(72.4)	TELONE (trans)	6	1379.0	(45.4)
FENURON	10	42.2	(84.7)	TERBACI L	4	41.2	(42.2)
LI NDANE	3	1080.9	(13.0)	THI MET	4	3255.2	(49.5)
				TRI THI ON	4	46579.7	(80.2)
2,4-D	9	19.6	(72.4)				
2,4-D AMI NE	3	109.1	(30.2)				
2,4,5-T	4	80.1	(45.3)				

$$K_{OC} = 0.66 K_{OW}^{1.029} \quad (III-38)$$

Values of  $K_{OW}$  for selected pesticides are given in Table III-15.

#### 3.4.4.3.3.2 Pesticide Decay Rates

Pesticide decomposition in the soil is related to moisture, temperature and pH. Unfortunately, the only information usually available is a simple pesticide half-life, which is the mean number of days required for 50% of the original pesticide to decompose in the soil. Decay rate  $k_s$  can be obtained from half-life using Equation III-27 (with  $\Delta P_t = 0$ ). Since at  $t = \text{half-life}$ ,  $P_t = 0.5 P_0$ :

$$P_t = 0.5 P_0 = P_0 \exp(-k_s t)$$

and half-life is given by:

$$t = -\ln(0.5)/k_s$$

or

$$k_s = 0.69/\text{Half-life (days)} \quad (III-39)$$

Mean decay coefficients from Rao and Davidson (1982) are given in Table III-16 for 32 pesticides. Three different rates are given for many of these chemicals. When available, the "field" coefficient should be used, since it in principle most closely corresponds to actual runoff conditions. The starred (\*) lab rates are the second choice, since they also measure decomposition of the original compound. The remaining lab rates attempt to describe the complete decay of the pesticide and its decomposition products. These "total decay" rates may be used if a very conservative runoff estimate is described, but the nature, toxicity and fate of most intermediate pesticide decomposition products are so poorly understood that it is probably misleading to model them with a simple first-order decay rate.

The mean decay coefficients given in Table III-16 are supplemented by the specific  $k_s$  values given in Table III-17. The latter were summarized from a large number of decay studies by Nash (1980). Since the coefficients in Table III-17 are often unique to specific soil types, pH and organic matter contents, they are perhaps less useful in screening studies than the mean values in Table III-16. However, many commonly-used pesticides are not listed in Table III-16, and in such cases the data in Table III-17 may be the best available information.

TABLE III-15

## OCTANOL-WATER PARTITION COEFFICIENTS FOR SELECTED PESTICIDES

(Rao and Davidson, 1982)

Pesticide	$K_{ow}$	Pesticide	$K_{ow}$
<u>A. INSECTICIDES</u>		<u>B. HERBICIDES</u>	
ALDI CARB	5.0000E+00	PROPOXUR	2.8000E+01
ALTOSID	1.7600E+02	RONNEL	7.5858E+04
CARBARYL	6.5100E+02	TERBUFOS	1.6700E+02
		TOXAPHENE	1.6950E+03
CARBOFURAN	2.0700E+02		
CHLORDANE	2.1080E+03	ALACHLOR	4.3400E+02
CHLORPYRIFOS	2.0590E+03	ATRAZINE	2.1200E+02
CHLORPYRIFOS	6.6000E+04	ATRAZINE	2.2600E+02
CHLORPYRIFOS	1.28825E+05	BI FENOX	1.7400E+42
CHLORPYRIFOS, METHYL	1.9700E+03	BROMACIL	1.0400E+02
CHLORPYRIFOS, HETHYL	2.0417E+04	CHLORAMBEN	1.3000E+01
DDD	1.1500E+05	CHLOROPROPHAM	1.1600E+03
DDE	7.3445E+04	DALAPON	5.7000E+00
DDE p,p	4.89779E+05	DALAPON, NA SALT	1.0000E+00
DDT	3.7000E+05	DI CAMBA	3.0000E+00
DDT p,p	1.54882E+06	DI CHLOBENIL	7.8700E+02
DDVP	1.9500E+02	DI URON	6.5000E+02
DI ALIFOR	4.8978E+04	MONURON	1.3300E+02
DI AZINON	1.0520E+03	MSMA	8.0000E-04
DI CHLOFENTHON	1.38038E+05	NI TROFEN	1.2450E+03
DI CIFOL	3.4610E+03	PARAQUAT .2HCL	1.0000E+00
DI ELDRI N	4.9300E+03	PI CLORAM	2.0000E+00
DI NOSEB	1.9800E+02	PROPACHLOR	4.1000E+01
ENDRI N	1.6190E+03	PROPANIL	1.0600E+02
ETHOXYCHLOR	1.1800E+03	SIMAZINE	8.8000E+01
FENITROTHION	2.2990E+03	TERBACIL	7.8000E+01
HCB	1.6600E+06	TRIFLURALIN	1.1500E+03
HEPTACHLOR	7.3660E+03	2,4-D	4.1600E+02
LEPTOFOS	4.1220E+03	2,4-D	4.4300E+02
LEPTOPHOS	2.04174E+06	2,4-D	6.4600E+02
LINDANE	6.4300E+02	2,4,5-T	7.0000E+00
MALATHION	2.3000E+02	2,4,5-T, BUTYL ESTER	6.4000E+04
MALATHION	7.7600E+02	2,4,5-T OCTYL ESTER	9.0900E+02
METHOMYL	1.2000E+01		
METHOXYCHLOR	2.0500E+03	<u>C. FUNGICIDES</u>	
METHOXYCHLOR	1.2000E+05	BENOMYL	2.6400E+02
METHYL PARATHION	2.0760E+03	CAPTAN	3.3000E+01
PARATHION	6.4550E+03	PCP	1.4290E+04
PERMETHRIN	7.5300E+02		
PHORATE	8.2300E+02		
PHOSALONE	1.9953E+04		
PHOSMET	6.7600E+02		



TABLE 111-16

## MEAN FIRST ORDER DECAY COEFFICIENTS FOR SELECTED PESTICIDES

(Rao and Davidson, 1982)

Pesticide		Rate Coeff. ( $\text{day}^{-1}$ )		Pesticide		Rate Coeff. ( $\text{day}^{-1}$ )	
		Mean	%CV			Mean	%CV
<u>A. HERBICIDES</u>				<u>B. INSECTICIDES</u>			
2,4-D	Lab. *	0.066	74.2	PARATHION	Lab. *	0.029	48.3
	Lab.	0.051	23.5		Field	0.057	101.8
	Field	3.6	83.3	METHYL PARATHION	Lab. *	0.16	-
2,4,5-T	Lab.	0.029	51.7	Field	0.046	-	
	Lab. *	0.035	82.9	DIAZINON	Lab. *	0.023	108.7
ATRAZINE	Lab. *	0.019	47.4	Lab.	0.022	-	
	Lab.	0.0001	70.4	FONOFOS	Lab. *	0.012	-
	Field	0.042	33.3	MALATHION	Lab. *	1.4	71.4
SIMAZINE	Lab. *	0.014	71.4	PHORATE	Lab. *	0.0084	-
	Field	0.022	95.5	Field	0.01	30.0	
TRIFLURALIN	Lab. *	0.008	65.5	CARBOFURAN	Lab. *	0.047	87.2
	Lab. * (anaerobic)	0.025	-		Lab.	0.0013	-
	Lab. (chain)	0.0013	-		Lab. * (anaerobic)	0.026	50.0
BROMACIL	Field	0.02	65.0	Field	0.016	87.5	
	Lab. *	0.0077	49.4	CARBARYL	Lab. *	0.037	56.8
	Lab.	0.0024	116.2	Lab. (Chain)	0.0063	101.6	
TERBACIL	Field	0.0038	100.0	Field	0.10	79.2	
	Lab. *	0.015	33.3	DDT	Lab. *	0.00013	130.8
	Lab.	0.0045	124.0	Lab. * (anaerobic)	0.0035	82.9	
FIELD	Field	0.006	55.0	ALDRIN and			
	Lab. *	0.0096	19.8	DIELDRI N	Lab. *	0.013	-
LI NURON	Field	0.0034	41.2	Field	0.0023	100.0	
	Lab.	-	-	ENDRI N	Lab. *		
DI URON	Field	0.0031	58.1	(anaerobic)	0.03	53.3	
	Lab. *	0.022	80.2	Field (aerobic)	0.0015	-	
	Lab. (ring)	0.0022	-	Field (anaerobic)	0.0053	-	
DI CAMBA	Lab. (chain)	0.0044	-	CHLORDANE	Field	0.0024	104.2
	Field	0.093	16.1	HEPTACHLOR	Lab. *	0.011	-
	Lab. *	0.0073	58.9	Field	0.0046	119.6	
PI CLORAM	Lab.	0.0008	111.3	LI NDANE	Lab. *	0.0026	-
	Field	0.033	51.5	Lab. (anaerobic)	0.0046	-	
	Lab. *	0.047	-	<u>C. FUNGICIDES</u>			
DALAPON	Lab. *	0.059	103.4	PCP	Lab. *	0.02	60.0
TCA	Field	0.073	-	Lab. (anaerobic)	0.07	44.3	
	Lab. *	0.1	121.0	Field	0.05	-	
GLYPHOSATE	Lab.	0.0086	93.0	CAPTAN	Field	0.231	
	Lab. *	0.0016	-				
PARAQUAT	Field	0.00015	-				

\*These rates are based on the disappearance of solvent-extractable parent compound under aerobic incubation conditions, unless stated otherwise.

TABLE III-17

FIRST ORDER PESTICIDE DECAY COEFFICIENTS FOR  
SELECTED PESTICIDES AND SOIL CONDITIONS

(Nash, 1984)

Pesticide	Soil			Crop or conditions	Application rate	k <sub>s</sub>
	Type	pH	OM/			
			(%)		(kg/ha)	
FUNGICIDES						
BAS 3460F-----	Potting Soil			Agonis Flexuosa		0.0822
Benomyl-----	Potting Soil			Agonis Flexuosa		.1486
Benomyl	sl					.0058
Benomyl	l					.0023
HERBICIDES						
Alachlor						.0384
Amirol						.0768
Arsenic acid						<.0064
Asulam-----	Regina	c	7.7	4.2	14 May	.0986
Asulam-----	Regina	c			12 July	.0619
Asulam-----	Regina	c	7.7	4.2	30 July	.0310
Atrazine	sl		4.8	1.0		.0131
Atrazine-----	Regina	c	6.5	2.0		.0063
Atrazine						.0064
Atrazine-----	Norfolk	sl	<b>6.8</b>		-5.2	.0133
<b>Atrazine-----</b>	<b>Decatur</b>	cl	<b>6.4</b>		-5.2	.0149
<b>Benflin</b>						.0053-
Benflin						.0077
Benflin						.0077-
Benflin						.0070
Bi Fenox-----	Potting soil mixture			Various	1.7	.142
Butralin						.0128
Butralin						.0077
Cyanazine						.0064
Di-Al late-----	Weyburn	l	6.5	6.5	None	2.8 .0138
Di-Al late-----	Weyburn	l	<b>7.0</b>	<b>4.5</b>	Laboratory	.65 .0248
Di-Al late-----	Regina	c	<b>7.5</b>	<b>4.0</b>	<b>Laboratory</b>	<b>.65 .0180</b>
Di-Al late-----	Regina	c	7.8	4.2	<b>None</b>	<b>2.2 .0110</b>
Di camba-----	Asqui thse		7.5	3.2	5% moisture	<b>.25 .0197</b>
Di camba-----	Asqui thse		7.5	<b>3.2</b>	10% moisture	<b>.25 2/ .2140</b>
Di camba-----	Mel tfort	si c	5.2	<b>11.7</b>	Various moisture	<b>.25 2/ &gt;.2140</b>
Di camba-----	Regina	c	7.7	4.2	25% moisture	.25 .0486
Di camba-----	Regina	c	7.7	4.2	35% moisture	.25 .0902
Di camba-----	Ouachi ta	cl		3.3	Forest	.3 .0217
HERBICIDES						
Di camba-----	Ouachi ta	cl		2.8	Grass	.3 .0407
Di camba-----	Cross Timbers	l		3.8	Forest	.3 .0267
2,4-D-----	Cross Timbers	l		3.8	Forest	.6 .1733
2,4-D acid-----	Cross Timbers	l				>.0768
2,4-D-----	Cross Timbers	l		3.3	Forest	.6 .1386
2,4-D salt						.0768
2,4-D-----	Ouachi ta	cl		<b>2.8</b>	Grass	.6 .1733
2,4-D ester						<b>&gt;.0768</b>
2,4-D isooctyl Naff ester.	sl		3.2	Laboratory 30°C	15	<b>.2546</b>
2,4-D-----	Naff	sl	3.2	<b>Laboratory</b> 10°C	15	.2731
2,4-D amine-----	Naff	sl	3.2	<b>Laboratory</b>	32.5	.1457
2,4-D amine-----	Naff	sl	3.2	<b>Laboratory</b>	12.5	.1008
2,4-D isooctyl Naff ester a amine.	sl		3.2	<b>Laboratory</b>	12.5	.0951
2,4-D isooctyl Naff ester a amine.	sl		3.2	<b>Laboratory</b>	12.5	.0555
2,4-D isooctyl ester a amine.	sl		<b>3.2</b>	<b>Laboratory</b>	12.5	.0852
<b>ester a amine.</b>				<b>Ring<sup>14</sup>C</b>		

TABLE III-17 (Continued)

Pesticide	Soil		OM <sup>1</sup> / pH	Crop or conditions	Application rate	k <sub>s</sub>
	Type	pH				
			(%)	HERBICIDES	(kg/ha)	
2,4-D isooctyl ester amine.			<b>3.2</b>	Laboratory Ring- <sup>14</sup> C	12.5	0.0257
Di chloroprop-----Ouachita	sl		3.3	Forest	.6	.0578
Di chloroprop-----Ouachita	sl		2.8	Grass	<b>.6</b>	.0866
Di chloroprop-----Cross Timbers	l		3.8	Forest	<b>.6</b>	.0693
Di ni trami ne						.0193
Di ni trami ne						.0193
Di uron-----Norfolk	cl	<b>6.8</b>			~5.2	.0064
Di uron-----Decatur	cl	<b>6.4</b>			~5.2	.0072
EPTC-----Regina	c	7.5	4.0	Laboratory	.65	.0220
EPTC-----Weyburn	l	7.0	4.5	Laboratory	.65	<b>.0248</b>
Fl uchl oral in						<u>2/</u> .0070
Fl uchl oral in						<u>2/</u> .0045
I sopropal in-----Daummer	si c	6.7	5.1	Vari ous		<b>.0023-</b>
I sopropal in-----El sne	si l	7.2	1.6			<b>.0036</b>
						<u>2/</u> .0054
						.0040
I sopropal in-----Ochley	si l	4.7	2.9	Sorghum	<b>1.68</b>	.0304
I sopropal in-----Ochley	si l	4.7	2.9	Sorghum	<b>3.36</b>	.0214
I sopropal in-----Bl oomfi el d	fs	6.3	<b>.6</b>	Sorghum	1.12	.0275
Karbuti late-----cl		6.3	<b>2.2</b>	Rangel and		.0057-
						<b>.0282</b>
Karbuti late-----l c		6.2	1.1	Rangel and		<b>.0118</b>
Li nuron				Cropped		<u>3/</u> .0104-
						<b>.0231</b>
Li nuron-----l s				Non-cropped		.0047
Li nuron-----l s		<b>7.0</b>	<b>2.0</b>	carrots	.85	<u>3/</u> .0280
Li nuron-----cl		<b>7.0</b>	<b>2.0</b>	None	<b>3.4</b>	<u>3/</u> .0039
Li nuron-----0-5 cm		7.0	<b>2.0</b>	None	<b>3.4</b>	<u>3/</u> .0061
MCPA-----Coarse cl		<b>7.0</b>	<b>2.0</b>	Barley	<b>1.7</b>	<u>3/</u> .1221
MCPA-----Coarse cl		<b>7.0</b>	<b>2.0</b>	None	<b>3.4</b>	<u>4/</u> .1070
Metri buzi n						<u>4/</u> .0298
Metobromuron-----sl		4.8	<b>1.0</b>			.0231
Metobromuron-----sl		6.5	<b>2.0</b>			.0248
Monol i nuron						.00216
Monuron-----Romona sl				Vari ous	2.24	<b>.0060</b>
Monuron-----Romona sl					4.48	<b>.0075</b>
Meburon-----Romona sl				Vari ous	2.24	.0073
Meburon-----Romona sl				Vari ous	4.48	.0059
Ni tral in						.0062-
						<b>.0086</b>
Ni tral in						<b>.0096-</b>
						<b>.0086</b>
Ni tral in-----Ochley si l		4.7	2.9	Sorghum	1.12	<b>.0110</b>
Ni tral in-----Ochley si l		<b>4.7</b>	2.9	Sorghum	1.12	.0079
Ni tral in-----Ochley si l		<b>4.7</b>	2.9	Sorghum	2.24	.0090
Ni tral in-----Ochley si l		<b>4.7</b>	2.9	Sorghum	2.24	.0024
Ni tral in-----Bl oomfi el d fs		<b>6.3</b>	.6	Sorghum	<b>.56</b>	.0155
Ni tral in-----Bl oomfi el d fs		6.3	.6	Sorghum	<b>1.12</b>	<b>.0091</b>
Oryzal in-----Bl oomfi el d fs						<u>2/</u> .0054-
						.0083
Oryzal in						.0144-
						<b>.0056</b>
Pebul ate-----Regina c		7.5	4.0	Laboratory	.65	<b>.0396</b>
Pebul ate-----Weyburn l		7.0	4.5	Laboratory	.65	<b>.0396</b>
Pi cloram-----Scot l. oxbows cl				Vari ous		<b>.0025</b>
						<u>2/</u> .0083
						<u>2/</u> .0056

TABLE III-17 (Continued)

Pesticide	soil		Crop or conditions	Application rate	k <sub>s</sub>	
	Type	pH				OM
		(%)	HERBICIDES	(kg/ha)		
Pebulate-----Regina c		<b>7.5</b>	4.0	Laboratory	.65	0.0396
Pebulate-----Weyburn l		<b>7.0</b>	4.5	Laboratory	.65	.0396
Picloram-----Scot l. oxbows cl				Various		<b>.0025</b>
Picloram-----Various						<b>2/.00772</b>
Picloram-----Nova Scotia cl					4.8	.0044
Picloram-----Somerset sl		<b>4.8</b>	2.9	Fallow	4.48	.0050
Picloram-----fari n cl		<b>6.3</b>	<b>1.9</b>	Orchard grass	2.24	.0354
Picloram-----chandl er f sl		<b>5.5</b>	<b>1.7</b>	Orchard grass	2.24	.0258
Picloram-----Chester l		5.8	1.9	Orchard grass	2.24	.0268
Picloram-----Chester l		5.8	1.9	Orchard grass	4.48	.0269
Picloram-----Various		Various			.05	<b>2/.004</b>
Picloram-----Ouachi ta cl			<b>3.3</b>	Forest	.6	<b>3/.0019</b>
Picloram-----Ouchi ta cl			<b>2.8</b>	Grass	.6	.0048
Picloram-----Cross Timbers l			<b>3.8</b>	Forest	.6	<b>.0028</b>
Profluralin						<b>2/.0047</b>
Profluralin						<b>2/.0051</b>
Pometryne-----sl		<b>7.0</b>	<b>2.0</b>			<b>.0238</b>
Propazine-----sl		<b>4.8</b>	<b>1.0</b>			.0108
Propazine		<b>6.5</b>	<b>2.0</b>			.0056
Propyzamide-----c to sl				Lettuce		<b>.0061-</b>
						<b>4/.0158</b>
Silvex-----Ouachi ta sl			<b>3.3</b>	Forest	.6	.0330
Silvex-----Ouachi ta sl			<b>2.8</b>	Grass	.6	.0495
Silvex-----Cross Timbers l			<b>3.8</b>	Forest	.6	<b>.0462</b>
Simazine		<b>7</b>	<b>2</b>	None	<b>3.4</b>	<b>4/.0074</b>
Simazine-----0 to 5 cm		<b>7</b>	<b>2</b>	None	<b>3.4</b>	<b>.0083</b>
Simazine-----sl		<b>4.8</b>	<b>1.0</b>			<b>.0116</b>
Simazine-----sl		<b>6.5</b>	<b>2.0</b>			.0082
Simazine				Cropped		.0539
Simazine				Noncropped		.062
Simazine-----sl		<b>7.0</b>	<b>2.0</b>			.0187
Tebuthiuron-----Various				Corn	.025	.0024
<b>Tebuthiuron-- Houston Black c, Udic Pellustert</b>				In surface runoff water.	2.24	.0060
<b>Tebuthiuron-- Houston Black Udic Pellustert</b>				In surface pellets.	2.24	.0427
<b>Tebuthiuron-- Houston Black Udic Pellustert</b>				<b>In surface broadcast spray.</b>	<b>2.24</b>	.0201
<b>Tebuthiuron-- Houston Black Udic Pellustert</b>				In pellets	2.24	.0517
<b>Tebuthiuron-- Houston Black Udic Pellustert</b>				In surface band pellets.	2.24	.0624
<b>Tebuthiuron-- Houston Black Udic Pellustert</b>				Broadcast in soil spray.	2.24	.0069
Triallate-----Regina c		<b>7.5</b>	<b>4.0</b>	Laboratory	.65	.0090
Triallate-----Weyburn l		<b>7.0</b>	<b>4.5</b>	Laboratory	.65	.0110
Triallate-----Coarse sl		<b>7.0</b>	<b>2.0</b>	Barley	1.7	<b>3/.0144</b>
Triallate-----Coarse sl		<b>7.0</b>	<b>2.0</b>	None	3.4	<b>3/.0067</b>
Triallate-----Weyburn l		<b>6.5</b>	<b>6.5</b>	None	2.8	.0088
Triallate-----Regina c		<b>7.8</b>	<b>4.2</b>	None	<b>2.2</b>	.0053
2, 4, 5-T-----Ouachi ta sl			<b>3.3</b>	Forest	<b>.6</b>	.0289
2, 4, 5-T-----Ouachl ta sl			<b>2.8</b>	Grass	.6	.0330
2, 4, 5-T-----Cross Timbers l			<b>3.8</b>	Forest	.6	.0330
2, 4, 5-T-----Fani n cl		<b>6.3</b>	<b>1.9</b>	Orchard grass	2.24	<b>3/.0508</b>
2, 4, 5-T-----Chandl er fl s		<b>5.5</b>	<b>1.7</b>	Orchard grass	2.24	.0495

TABLE III-17 (Continued)

Pesticide	soil		Crop or condi ti ons	Appl i cation rate	k <sub>z</sub>	
	Type	pH				OM
HERBI C I D E S						
2, 4, 5-T-----Chester I		5. 8	1. 9	Orchard grass	2. 24	<u>3/</u> .0416
2, 4, 5-T-----Chester I		5. 8	1. 9	Orchard grass	4. 48	.0414
Tri fl u r a l i n						<u>2/</u> .0037-
Tri fl u r a l i n						.0047
Tri fl u r a l i n						<u>2/</u> .0051-
						.0044
Tri fl u r a l i n----Cecil sl		6. 5	. 6	Soybeans		.0175
Tri fl u r a l i n----Wet soil				None		.0956
Tri fl u r a l i n----Dry soil				None		<u>4/</u> .0189
Tri fl u r a l i n-----0chley sil		4. 7	2. 9	<b>Sorghum</b>	.84	.0145
Tri fl u r a l i n-----0chley sil		4. 7	2. 9	Sorghum	.84	.0117
Tri fl u r a l i n-----0chley sil		4. 7	2. 9	Sorghum	1. 68	.0104
Tri fl u r a l i n-----0chley sil		4. 7	2. 9	<b>Sorghum</b>	<b>1.68</b>	.0026
Tri fl u r a l i n-----Bl oomfi el d fs		6. 3	. 6	<b>Sorghum</b>	<b>.56</b>	.0155
Tri fl u r a l i n-----Bl oomfi el d fs		<b>6.3</b>	<b>.6</b>	Sorghum	1. 12	.0091
Vernol ate-----Regi na c		<b>7.5</b>	<b>4.0</b>	Laboratory	.65	.03%
Vernol ate-----Weyburn I		7. 0	4. 5	Laboratory	.65	.03%
I N S E C T I C I D E S						
Al di carb-----Beaumont c		5. 4			130	.00273
Al di carb-----Houston c		7. 8			130	.0087
Al di carb-----Houston cl		<b>7.5</b>	<b>.25</b>	Shendl	<b>.5</b>	<u>3/</u> .0991
Al di carb-----Houston cl		<b>7.5</b>	<b>.25</b>	Shendl	<b>1.0</b>	.0420
Al di carb-----Houston cl		7. 5	. 25	Orange	2. 8-22. 4	.0322 -
Al dri n						< .0032
Al dri n-----Ul ysses sil				Fal low	2. 24	.0264
Al dri n-----Knox sil				Fal low	2. 24	.0259
Al dri n-----Cel eryvil le muck				Fal low	2. 24	<u>4/</u> .0014
Al dri n-----Mari etta sl				Fal low	2. 24	.0136
Al dri n-----Fox fs				Fal low	2. 24	.0256
Al dri n-----Mi ami sil				Fal low	2. 24	.0258
Al dri n-----Muck				Fal low	2. 24	<u>4/</u> .0066
Al dri n-----Carri ngton sil		Nondi sked		Fal low	<b>4.5</b>	<u>2/</u> .0101
Al dri n-----Carri ngton sil		Di sked		Fal low	<b>4.5</b>	<u>2/</u> .0136
Al dri n-----Udai pur cl		7. 8	1. 6	Vari ous	3. 0	.0149
						$\bar{x}$ of 19
Al dri n-----Jobner		8. 6	. 26	Vari ous	3. 0	.0165
						$\bar{x}$ of 19
Al dri n-----Muck					22. 4	.0061
Al dri n-----Mi ami sil					22. 4	.0096
Al dri n-----Composi te					22. 4	.0038
Al dri n						
(Dieldrin)----Carri ngton sil		Nondi sked			4. 5	<u>4/</u> .0006
<b>Aldr in</b>						
(Dieldrin)----Carri ngton sil		Di sked			4. 5	<u>4/</u> .0008
<b>Aldr in</b>						
(Dieldrin)----Carri ngton sil		Di sked		Granul es	5. 6	<u>4/</u> .0012
<b>Aldr in</b>						
(Di el dri n)----Carri ngton sil				Spray		<u>4/</u> .0017
Akton-----Sul tan sil		6. 3	3. 4	3. 4 granul es	2. 24	.0032
Azi nphosmethyl		<b>8.4</b>				.0239
Azi nphosmethyl --Orchard sl		<b>6.6-7.8</b>	3. 4			<u>4/</u> .5/.0026
Azi nphosmethyl --Orchard sl		6. 6-7. 8	3. 4			<u>4/</u> .5/.0014
Azi nphosmethyl --Gi la sil					. 018	.0533
Azi nphosmethyl --Mocho sil						.0273
Azi nphosmethyl --Li nne c						.0516
Azi nphosmethyl --Madera sl						.0086
Azi nphosmethyl --Laveen sl						.0119
Azi nphosmethyl --Santa Lucia sil						.0235

TABLE III-17 (Continued)

Pesticide	Soil			Crop or conditions	Application rate	kg
	Type	pH	OM			
			(%)	I N S E C T I C I D E S	(kg/ha)	
Azinphosmethyl ----Windy I						0.0074
Azinphosmethyl -----fsl						.0101
Azinphosmethyl -----sicl						.0458
Azinphosmethyl -----c						.0505
Azinphosmethyl -----sl						.0211
BHC						.0021
BHC-----Udai pur	7.8		1.6	Vari ous	5.0	.0140
BHC						$\bar{x}$ of 19
BHC-----Jobner sl	8.6		.26	Vari ous	5.0	.0098
BHC al pha-----Berwick sl				Vegetabl es	7.4 BHC	$\bar{x}$ of 19 5/.0006
BHC beta-----Berwick sl				Vegetabl es	7.4 BHC	2/.00015
BHC gamma-----Berwick sl				Vegetabl es	7.4 BHC	2/.00042
BHC del ta-----Berwick sl				Vegetabl es	7.4 BHC	2/.00036
Bromophos-----Composi te						.0198
Cabaryl						.0768
Carbaryl -----Udai pur cl	7.8		1.6	Vari ous	15.0	.11%
Carbaryl -----Jobner sl	8.6		.26	Vari ous	15.0	$\bar{x}$ of 8 .0969
Carbofuran						.0768
Carbofuran-----Take sil	8.5				10.0	.0079
CGA-12223-----sil	<b>4.8</b>		<b>1.0</b>			.0385
CGA12227/-----sil	<b>6.5</b>		<b>2.2</b>			.0693
Chlordane-----Berwick sl					2.0	2/.00072
Chlordane-----Composi te						.0020
Chlorfenvinphos						.0055
Di azinon-----Composi te						.0330
Di azinon-----Sul tan sil	6.7		3.1	25°C		.0151
Di azinon-----Sul tan sil	6.7		<b>3.1</b>	15°C		.0067
Di azinon-----Sul tan sil	4.3		<b>3.1</b>			.0242
Di azinon-----sl	<b>4.8</b>		1.0			.0239
Di azinon-----sl	<b>6.5</b>		2.0			.0239
Di azinon-----sl	<b>6.5</b>		<b>2.0</b>			.0248
Di azinon-----Puyal l up sl	<b>5.0</b>		<b>2.1</b>			.0189
Di azinon-----Puget sil	<b>5.4</b>		<b>3.0</b>			.0260
Di azinon-----Chehal is cl	<b>5.6</b>		<b>7.2</b>			.0166
Di azinon-----Organi c	5.4		40			.0171
Di el dri n-----Carri ngton sil				Fal l ow	4.5	2/.0142
Di el dri n-----Carri ngton sil				Fal l ow	4.5	2/.0187
Di el dri n						3/.0003
Di el dri n-----Imperi al sc	7.8		1.0		20.0	.0002
Di el dri n-----Hol tvil l e fsl	7.8		.5		20.0	.0001
Di el dri n-----Composi te						.0008
Di oxacarb-----sl	<b>4.8</b>		1.0			.0248
Di oxacarb-----sl	<b>6.5</b>		2.0			.3465
Di oxathi on-----fsl						.0156
Di oxathi on-----sicl						.0128
Di oxathi on-----c						.0141
Di oxathi on-----sl						.0229
p, p' -DDT-----Ul ysses sil	6.9		1.8	<b>Fal l ow</b>	9.4	3/.0008
p, p' -DDT-----Knox sil	6.8		<b>.8</b>	<b>Fal l ow</b>	9.4	3/.0005
p, p' -DDT-----Cel eryvil l e muck	4.9		<b>74.5</b>	Fal l ow	9.4	.0021
p, p' -DDT-----Mari etta sl	<b>6.0</b>		<b>2.0</b>	Fal l ow	9.4	3/.0014
p, p' -DDT-----Fox fsl	<b>7.2</b>		<b>.8</b>	Fal l ow	9.4	.0009
p, p' -DDT-----Mi ami sil	<b>7.1</b>		<b>3.6</b>	Fal l ow	9.4	3/.0004
p, p' -DDT-----Muck	<b>6.8</b>		<b>40.0</b>	Fal l ow	<b>1.0</b>	.0009
p, p' -DDT-----Commer ce sil					<b>24.4</b>	.0037

TABLE III-17 (Continued)

Pesticide	Soil			Crop or conditions	Application rate	k <sub>s</sub>
	Type	pH	OM (%)			
					(kg/ha)	
				I N S E C T I C I D E S		
p, p' -DDT-----Carri ngton sil		Nondisked			4.5	<u>2/</u> .0024
p, p' -DDT-----Carri ngton sil		Disked		Fallow	<b>4.5</b>	<u>2/</u> .0048
p, p' -DDT-----Mi ami sil					<b>11.6</b>	.0003
p, p' -DDT-----Carri ngton sil		Disked/non-disked		Fallow	4.5	<u>4/</u> .0002
p, p' -DDT-----Muck					11.2	.0011
p, p' -DDT-----Mi ami sil					11.2	.0029
p, p' -DDT-----Berwick sil				37 DDT		<u>2/</u> .00016
p, p' -DDT-----Composi te						.0007
o, p' -DDT-----Berwick sil						<u>2/</u> .00029
Di methoate-----Composi te						.0990
Di sul foton				Various		.1604
Endosul fan-----Various					1.3	.0162
Ethi on-----Mocho sil						.0014
Ethi on-----Linne c						.0012
Ethi on-----Madera sil						.0009
Ethi on-----Laveen sil						.0015
Ethi on-----Santa Lucia sil						.0014
Ethi on-----Windy l						.0015
Ethi on-----Fsl						<u>3/</u> .0009
Ethi on-----sil						.0022
Ethi on-----c						.0032
Ethi on-----sil						.0025
Feni trothi on-----sil	<b>4.8</b>	<b>1.0</b>				.0578
Feni trothi on-----sil	<b>6.5</b>	<b>2.0</b>				.1155
Fonofos-----Take sil	<b>8.5</b>				10	.0158
Heptachl or-----Composi te						.0021
Heptachl or-----Composi te						.0025
Heptachl or-----Composi te						.0028
Hexachol obenzene--Chevada				<b>Zoysia</b>		<u>3/</u> .0006
I sobenzan-----Composi te						.0050
Li ndane-----Imperi al sc	<b>7.8</b>	1.0			<b>20</b>	.0022
Li ndane-----Hol tville fsl	<b>7.8</b>	.5			<b>20</b>	.0026
Li ndane-----Composi te						.0017
Li ndane-----Gila sil	7.7	.6		None		<u>2/</u> .0046
Li ndane-----Mi ami sil					11.6	.0011
Li ndane-----Muck					11.2	.0014
Li ndane-----Mi ami sil					11.2	.0048
Li ndane-----Ul ysses sil				<b>Fallow</b>	1.12	.0147
Li ndane-----Knox sil				<b>None</b>	11.2	.0264
Li ndane-----Cel eryville muck				<b>None</b>	11.2	.0074
Li ndane-----Mari etta sil				<b>None</b>	11.2	.0263
Li ndanes-----Fox fsl				<b>None</b>	11.2	.0264
Li ndane-----Mi ami sil				<b>None</b>	11.2	.0139
Li ndane-----Muck				<b>None</b>	11.2	<u>3/</u> .0059
Mal athi on-----Poygan sil	7.2			<b>None</b>		2.9173
Mal athi on-----Kewaune c	<b>6.4</b>			<b>None</b>		2.4618
Mal athi on-----El la ls	<b>3.8</b>			<b>None</b>		1.2681
Mal athi on-----Freestone sil	<b>5.3</b>	<b>1.1</b>		<b>None</b>		.4152
Mal athi on-----Okolona c	<b>7.4</b>	<b>3.1</b>		<b>None</b>		1.9832
<b>Malathion-----Trinity I</b>	7.2	<b>4.7</b>		<b>None</b>		1.9026
<b>Mecarbam-----Composite</b>						.0495
Methi dathi on-----sil	<b>4.8</b>	<b>1.0</b>				.0108
Methi dathi on-----sil	<b>6.5</b>	<b>2.0</b>				.0495
Methoxychl or	<b>4.8</b>	<b>1.0</b>				.0046
Methoxychl or	<b>6.5</b>	<b>2.0</b>				.0033
Methyl Purathi on-Carri ngton l				Radi shes	5.6	.2207
Mevi nphos-----Sacramento s	5.4	.4			13	.2936
Parathi on-----Carri ngton l				Radi shes	5.6	.0248
Parathi on						.056
Parathi on-----Mocho sil	>7	<b>.6</b>		None		<u>2/</u> .0046
Parathi on-----Udai pur cl	7.8	<b>1.6</b>		Various	10	.1239

TABLE III-17 (Continued)

Pesticide	soil		Crop or conditions	Application rate	k <sub>s</sub>	
	Type	pH				OM (%)
INSECTICIDES						
Parathion-----Jobner sil		8.6	.26	Vari ous	10	$\bar{x}$ of 8 0.0727
Parathion-----Mocho sil						$\bar{x}$ of 7 <u>3/</u> .1371
Parathion-----Linne c						.1306
Parathion-----Madera sil						<u>3/</u> .0944
Parathion-----Laveen sil						<u>3/</u> .1150
Parathion-----Santa Lucia sil						.0866
Parathion-----fsl		6.8	0.8			.0654
Parathion-----sil		<b>7.3</b>	<b>2.1</b>			<u>3/</u> .0891
Parathion-----c		<b>7.3</b>	<b>2.3</b>			.2962
Parathion-----sil		<b>7.6</b>	1.8			.2614
Phenthoate-----fls		<b>6.8</b>	.8			.2865
Phenthoate-----sil		<b>7.3</b>	<b>2.1</b>			.0156
Phenthoate-----c		<b>7.3</b>	<b>2.3</b>			.0141
Phenthoate-----sil		7.6	1.8			.0229
Phorate----- Sacramento muck					<b>13</b>	.0040
Phorate----- Sacramento peat					<b>13</b>	<u>2/</u> .0043
Phorate----- Sacramento peat					<b>13</b>	<u>2/</u> .0001
Phorate-----Take sil		8.5			<b>10</b>	<u>3/</u> .0363
Phorate----- Sacramento s					13	<u>4/</u> .0078
Phorate----- Sacramento c					13	.0277
Zinophos-----Sul tan sil		6.7	3.1	25°C		<u>3/</u> .0223
Zinophos-----Sul tan sil		<b>6.7</b>	<b>3.1</b>	15°C		.0164
Zinophos-----Sul tan sil		<b>5.5</b>	<b>3.1</b>			.0144
Zinophos-----sul tan sil		8.1	3.1			.0244
Zinophos-----Sul tan sil						.0096
Zinophos						.0133
Zinophos						.0206
Zinophos						.0075
NEMATOCIDES						
Di chl ofenthi on--Composi te						.0031
Tri chl oronate---Composi te						.0050

- 1/ Organic matter.
- 2/ Unknown.
- 3/ r = <-0.9.
- 4/ r = <-0.8.
- 5/ Emulsi fi able concentrate formulati on.
- 6/ Wettable powder formulati on,
- 7/ Di ethyl (1-i so-propyl -5-chl oro-1, 2, 4-tri azol yl -3) phosphorothi oate.



EXAMPLE III-6

Pesticide Runoff

Two pesticides, carbofuran and atrazine, have been applied to a cornfield at planting time. Carbofuran is an insecticide used to control corn rootworm and atrazine is a herbicide for weed control. Three days after each pesticide has been applied at 4000 g/ha, a 4.5 cm storm occurs which produces 0.2 cm of runoff and 0.6 t/ha of sediment. The soil has an organic matter content of 3%, bulk density of  $b = 1.3 \text{ g/cm}^3$  and available water capacity of  $w = 0.2$ . Determine the runoff losses of each pesticide.

Solution:

Partition coefficients  $K_D$  are determined from  $K_{OC}$  values in Table 111-14 (Atrazine,  $K_{OC} = 163$ ; Carbofuran,  $K_{OC} = 29.4$ ):

$$K_D = K_{OC} (\%OC/100) \quad (111-36)$$

where

$$\%OC = 0.59 \%OM \text{ (Equation 111-37), or } \%OC = 0.59(3) = 1.77$$

$$K_D = 163(.0177) = 2.89 \text{ (Atrazine)}$$

$$K_D = 29.4 (0.0177) = 0.52 \text{ (Carbofuran)}$$

Decay coefficients  $k_s$  (field values) are given in Table 111-16:

$$k_s = 0.042 \text{ (Atrazine)}$$

$$k_s = 0.016 \text{ (Carbofuran)}$$

Total adsorbed and dissolved pesticide in the surface centimeter are given by Equations 111-27, 111-31, and 111-32. Assuming the pesticide is left on the soil surface, initial levels for both pesticides are  $P_0 = 4000 \text{ g/ha}$ . For day  $t = 3$ :

Atrazine:

$$P_3 = 4000 \exp [-0.042(3)] = 3526 \text{ g/ha}$$

$$w/K_D b = 0.2/2.89(1.3) = 0.0532$$

$$A_3 = [1/(1 + 0.0532)] 3526 = 3348 \text{ g/ha}$$

$$D_3 = [1/(1 + 1/0.0532)] 3526 = 178 \text{ g/ha}$$

Similarly, for Carbofuran:

$$P_3 = 3813 \text{ g/ha}$$

$$A_3 = 2942 \text{ g/ha}$$

$$D_3 = 871 \text{ g/ha}$$

Solid-phase and dissolved losses are given by:

$$PX_3 = (A_3/100b)X_3 \quad (III-33)$$

$$PQ_3 = [Q_3/(R_3 + M_3)]D_3 \quad (III-34)$$

where

$$X_3 = 0.6 \text{ t/ha}$$

$$Q_3 = 0.2 \text{ cm}$$

$$R_3 = 4.5 \text{ cm}$$

$M_3$ , snowmelt, is obviously zero.

Atrazine:

$$PX_3 = [3348/1.3(100)]0.6 = 15.5 \text{ g/ha}$$

$$PQ_3 = (0.2/4.5)178 = 7.9 \text{ g/ha}$$

Carbofuran:

$$PX_3 = [2942/1.3(100)]0.6 = 13.6 \text{ g/ha}$$

$$PQ_3 = (0.2/4.5)871 = 38.7 \text{ g/ha}$$

In summary:

Losses in Runoff (g/ha)	Atrazine	Carbofuran
Solid-phase	15.5	13.6
Dissolved	<u>7.9</u>	<u>38.7</u>
Total	23.4	52.3

----- END OF EXAMPLE III-6 -----

### 3.5 SALT LOADS IN IRRIGATION RETURN FLOWS

#### 3.5.1 Description

Pollution of surface waters by salty irrigation drainage water is a problem in many arid regions. As shown in Figure III-16, water may be diverted from a river to water crops in an irrigation district. Portions of the diverted water are lost from the diversion canal through seepage and evaporation, and most of the remaining water is applied to crops in the irrigation district. Much of this applied water is consumed by plant evapotranspiration (ET) and the excess passes through the soil to be collected by tile drainage and returned to the river. This drainage water has a much higher salt concentration than the irrigated water. As the water moves through the soil, it retains its salt mass, but due to ET, the water volume is diminished.

Return flow salinity can be computed by assuming a steady-state condition in which:

Salts applied in irrigation = Salts removed in drainage

$$s_0 I = sR$$

or

$$s = s_0 I/R \quad (111-40)$$

where

- $s_0$  = irrigation water salinity (mg/l)
- $s$  = return flow salinity (mg/l)
- $I$  = irrigation application ( $m^3/day$ )
- $R$  = return flow ( $m^3/day$ ).

Salt concentration or salinity is measured either as dissolved solids (mg/l) or electrical conductivity ( $\mu mho/cm$  or  $mmho/cm$ ). In the Western U.S., an average conversion factor is  $1000 \mu mho/cm = 640 mg/l$ . Water fluxes, such as  $I$  and  $R$  refer to total water movement over the irrigation season and can be measured in length or volume units. For example, if  $I$  is given in centimeters, it is converted to cubic meters by  $I(m^3) = I(cm) 100 A$ , where  $A$  = irrigated area (ha).

When the irrigation diversion is taken from a river, as in Figure 111-16, so is the salinity of the river water. The return flow salinity given by Equation 111-40 obviously exceeds  $s_0$  since  $R < I$ . The river salinity after the return flow is:

$$s'_0 = s_0 \frac{(Q - D) + sR}{Q - D + R} \quad (111-41)$$

where

- $s'_0$  = river salinity after return flow (mg/l)
- $Q$  = river flow prior to diversion ( $m^3/day$ )
- $D$  = irrigation diversion ( $m^3/day$ ).

Since  $s'_0 > s_0$  the river is saltier for the next downstream user. As successive irrigation districts withdraw and return water, the river becomes progressively saltier until it is no longer suitable for municipal or agricultural use.

Variations of the salinity problem include pumping of irrigation water from aquifers and unsteady-state or transient leaching of soil salts. In the former case, so is the aquifer salinity. The salty drainage flow might be discharged to surface waters as in Figure 111-16 or allowed to percolate through the soil, thus producing saltier groundwater. Transient salt leaching often occurs when soils are initially irrigated or reclaimed. Until a steady-state situation is reached, the

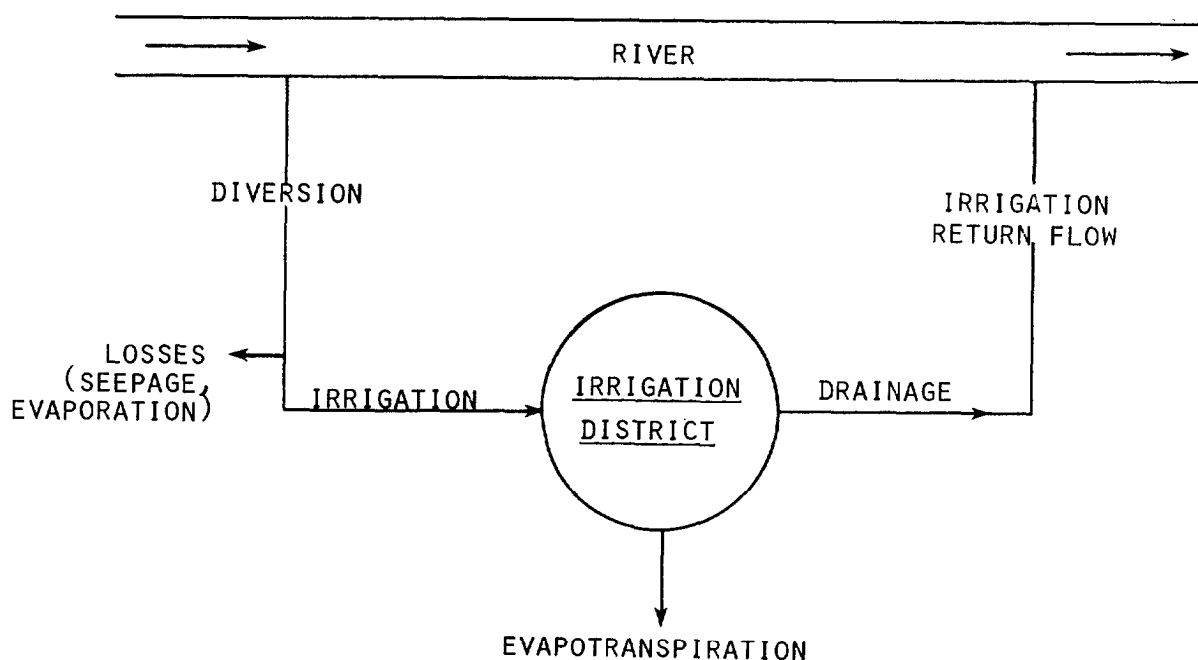


FIGURE III-16 COMPONENTS OF AN IRRIGATION SYSTEM

salt load in return flow may exceed the salts applied in irrigation.

### 3.5.2 Estimation of Return Flows

Equations III-40 and III-41 may be used directly when return flow volumes  $R$  are known. However, accurate return flow measurements are often unavailable and indirect estimates are necessary. A general procedure for computing return flows is shown in Figure III-17.

Design factors for irrigation systems include irrigation efficiencies, diversions, leaching fractions and ET. Water losses in the diversion system are indicated by a delivery efficiency,  $E_d$ :

$$I = E_d D \quad (III-42)$$

To prevent salt buildup in soil which would injure plants, irrigation applications must exceed crop water needs so that applied salts may be washed from the soil in drainage. The Leaching fraction is the fraction of irrigation application which is used to control salinity, or the ratio of drainage to irrigation. As shown in Figure III-17:

$$LF = (I - E)/I \quad (III-43)$$

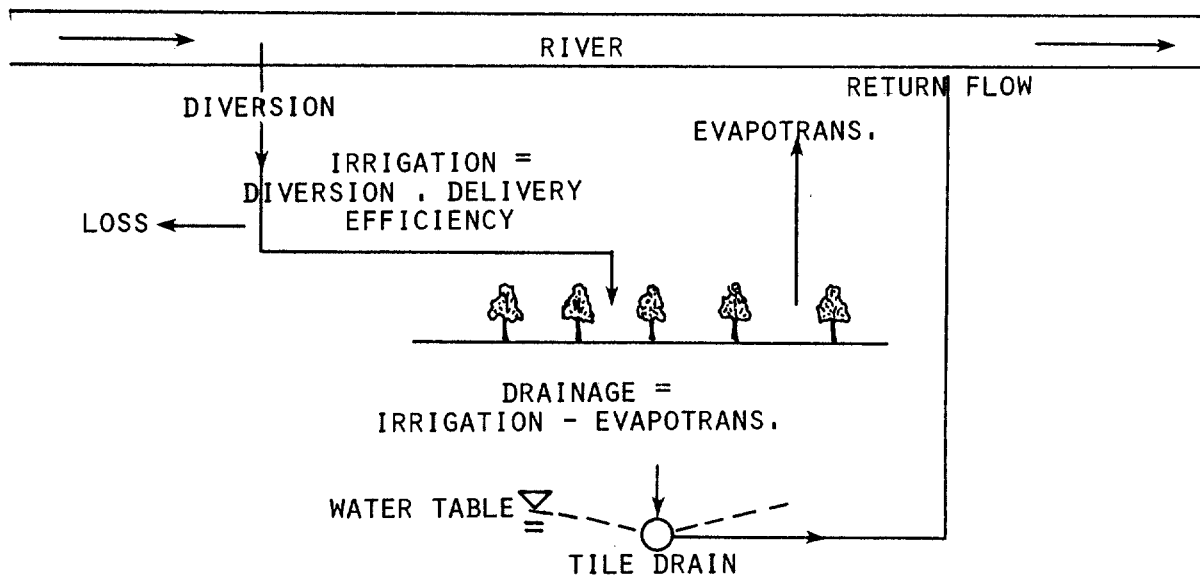


FIGURE III-17 COLLECTION OF IRRIGATION DRAINAGE

where

LF = irrigation leaching fraction

E = crop ET ( $m^3/day$ )

Since return flow (R) consists of the drainage water collected in tile drains,

$R = I - E$  and  $LF = R/I = R/E_d D$ . Thus:

$$R = (LF)E_d D \quad (III-44)$$

and rearranging Equation 111-40:

$$s = s_o / LF \quad (III-45)$$

If irrigation diversion  $D$ , delivery efficiency  $E_d$  and leaching fraction  $LF$  are known, return flow volume and salinity can be estimated by Equations III-44 and III-45. If  $LF$  is unknown, it can be determined from Equation III-43, provided  $E$ , crop ET, is available. Since  $E$  depends on crop mixture and local weather conditions, it is best obtained from local irrigation specialists. In the absence of such data,  $E$  may be estimated from potential ET. Potential ET, or  $PE$ , is a maximum ET which occurs when the soil is covered with a dense cover such as alfalfa and water is not limiting. Thus potential ET is a function of the atmosphere's ability to absorb water. Actual ET is generally less than  $PE$ , but by letting  $E = PE$ , we obtain a conservative overestimate of return flow salinity.

Potential ET can be determined from pan evaporation data or empirical equations. Figure III-18 shows average annual pan evaporation for the U.S. Potential ET is

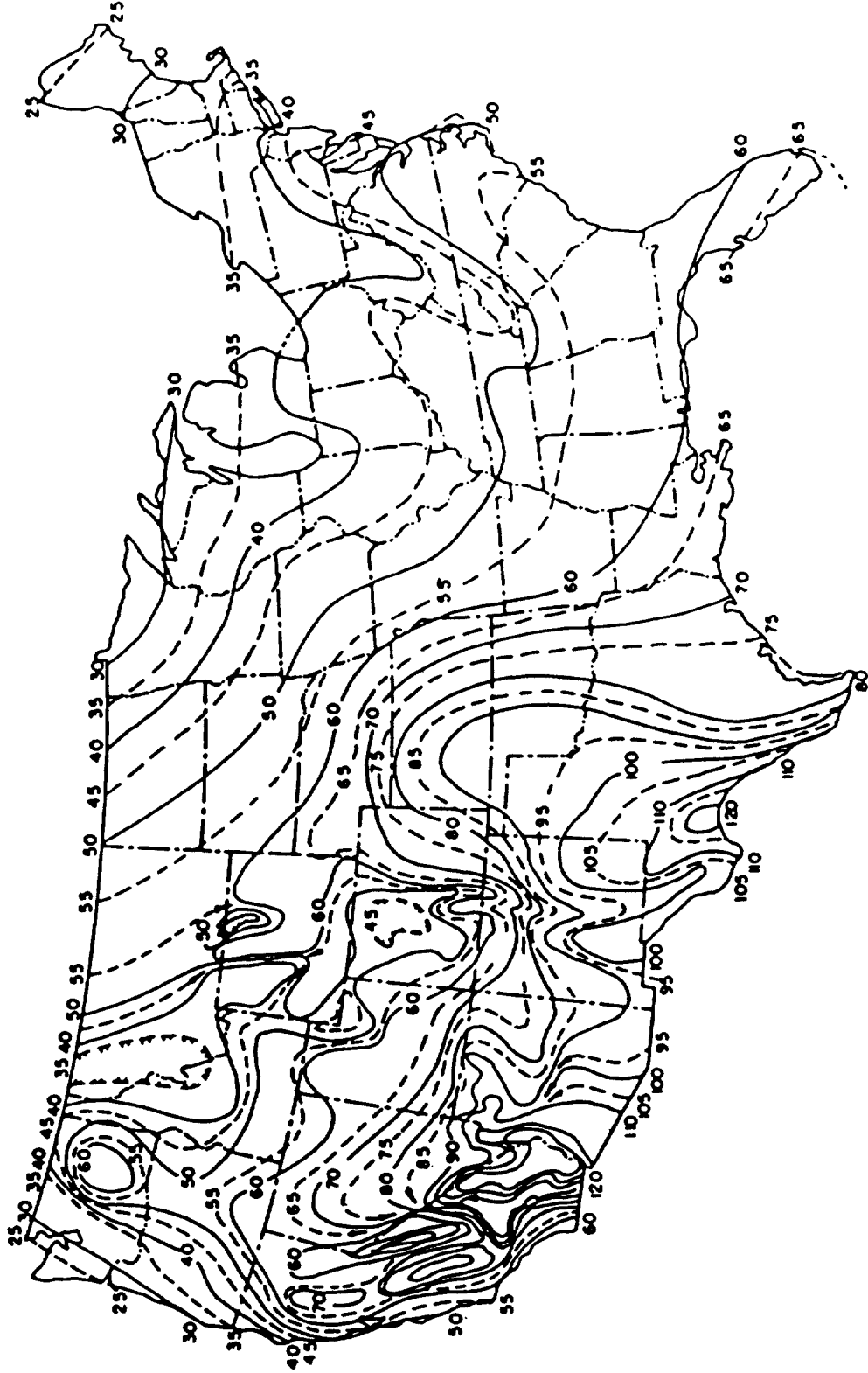


FIGURE III-18 MEAN ANNUAL PAN EVAPORATION IN INCHES (1IN = 2.54CM) (KOHLE ET AL, 1959)

approximately 70% of pan evaporation. To use the data from Figure III-18, we must assume that all annual PE occurs in the growing season. Growing season PE may also be estimated from Hamon's (1961) equation:

$$PE = (0.021 H^2 p)/(T + 273) \quad (III-46)$$

where

PE = potential ET (cm/day)

H = mean number of daylight hours per day during period of interest

T = mean air temperature during period of interest (°C)

P = saturation water vapor pressure at temperature T (millibars).

Values of H and p are given in Tables III-18 and 19. The "period of interest" for irrigation studies is the irrigation season.

#### EXAMPLE III-7

##### Irrigation Return Flows

A 2000 ha irrigation district diverts an average of 350,000 m<sup>3</sup>/day of water from a river in the irrigation season. During this time, the mean river flow is 1,000,000 m<sup>3</sup>/day. The delivery system is 80 percent efficient and the district operates at an average leaching fraction of 0.3. The river water salinity is 200 mg/l.

Determine:

- a) Return flow volume and salinity
- b) River salinity downstream of the return flow.

Solution:

Data for the problem:

$$D = 350,000 \text{ m}^3/\text{day}$$

$$Q = 1,000,000 \text{ m}^3/\text{day}$$

$$s_o = 200 \text{ mg/l}$$

$$E_d = 0.8$$

$$LF = 0.3$$

- a) From equation III-44, return flow is:

$$\begin{aligned} R &= 0.3(9.8)(350,000) \\ &= 84,000 \text{ m}^3/\text{day} \end{aligned}$$

with salinity given by Equation III-45:

$$s = 200/0.3 = 667 \text{ mg/l}$$

TABLE III-18

## MEAN DAYLIGHT HOURS PER DAY

Latitude North	Jan	Feb	Mar	Apr	May	Jun	Jul	Aug	Sep	Oct	Nov	Dec
48	8.7	10.0	11.7	13.4	14.9	15.7	15.3	14.0	12.3	10.6	9.1	8.3
46	8.9	10.2	11.7	13.3	14.7	15.4	15.0	13.8	12.3	10.7	9.3	8.5
44	9.2	10.3	11.7	13.2	14.5	15.2	14.8	13.7	12.3	10.8	9.5	8.8
42	9.3	10.4	11.7	13.1	14.3	15.0	14.6	13.6	12.3	10.9	9.7	9.0
40	9.5	10.5	11.8	13.0	14.1	14.7	14.4	13.6	12.2	11.0	9.8	9.2
38	9.7	10.6	11.8	13.0	14.0	14.5	14.3	13.4	12.2	11.0	10.0	9.4
36	9.9	10.7	11.8	12.9	13.8	14.3	14.1	13.3	12.2	11.1	10.1	9.6
34	10.0	10.8	11.8	12.8	13.7	14.2	14.0	13.2	12.2	11.2	10.2	9.8
32	10.2	10.9	11.8	12.8	13.6	14.0	13.8	13.3	12.2	11.2	10.4	10.0
30	10.3	11.0	11.8	12.7	13.5	13.9	13.7	13.0	12.2	11.3	10.5	10.1
28	10.5	11.1	11.8	12.7	13.4	13.7	13.5	13.0	12.1	11.3	10.6	10.3
26	10.6	11.1	11.8	12.6	13.2	13.6	13.4	12.9	12.1	11.4	10.7	10.4
24	10.7	11.2	11.9	12.6	13.1	13.4	13.3	12.8	12.1	11.4	10.9	10.6



TABLE III-19

## SATURATION VAPOR PRESSURE AS FUNCTION OF TEMPERATURE

(Jensen, 1973)

---

Temperature (°C)	Saturation Water Vapor Pressure (millibars)
0	6.1
2	7.1
4	8.1
6	9.4
8	10.7
10	12.3
12	14.0
14	16.0
16	18.2
18	20.6
20	23.4
22	26.4
24	29.8
26	33.6
28	37.8
30	42.4
32	47.5

---

b) Downstream salinity is computed by Equation III-41:

$$s_o' = \frac{200(1,000,000 - 350,000) + 677(84,000)}{1,000,000 - 350,000 + 84,000}$$
$$= 255 \text{ mg/l}$$

----- END OF EXAMPLE III-7 -----

### 3.6 URBAN RUNOFF LOADS

Nonpoint source pollution from urban runoff differs in several ways from its rural counterpart. Runoff rates are usually much higher in urban areas due to the distribution of impervious surfaces (pavements, roofs, etc.). Urban runoff is collected in separate storm sewers or combined sewers. The latter collect both runoff and sanitary wastewater. During a large runoff event, storm flow may exceed sanitary flows by one or more orders of magnitude. To avoid flooding from surcharged combined sewers, combined sewer "overflows" are discharged directly to receiving waters. These overflows are highly polluting since they contain runoff pollutants, raw sanitary sewage, and scoured wastewater solids which were previously deposited in the sewers.

Urban runoff quality is influenced by human activities; important determinants are land uses and population density. Land uses may be considered the "source areas" in an urban watershed; the total runoff load is the sum of runoff loads from each land use.

Sections 3.6.1 and 3.6.2 describe equations for determining annual and event pollutant loads. The annual loading functions are highly empirical, but provide estimates of pollutant loads from both separate storm sewers and combined sewer overflows. Conversely, the event loading functions are more analytical, but describe only runoff (i.e., separate storm sewer load).

Urban runoff and combined sewer overflow data are summarized by Huber, et al. (1979) and E. C. Jordan Co. (1984). Additional references on urban runoff computations include Novotny and Chesters (1980) and Kibler (1982).

#### 3.6.1 Annual Urban Runoff and Combined Sewer Loads

General urban loading functions have been proposed by Heaney, et al. (1977), and Heaney and Huber (1979) of the form:

$$L_k = \alpha_k F_k Y_k P \quad (III-47)$$

where

- $L_k$  = annual load of pollutant due to runoff from land use k (kg/ha)
- $\alpha_k$  = pollutant concentration factor (kg/ha-cm)
- $F_k$  = population density function
- $Y_k$  = street cleaning factor
- $P$  = annual precipitation (cm).

Total pollutant load from the urban area is:

$$L = \sum_k L_k A_k \quad (III-48)$$

where

- $L$  = annual pollutant load due to runoff (kg)
- $A_k$  = area of land use k (ha).

Equation III-47 can be interpreted as a general loading function which multiplies a water flux ( $F_k P$ ) by a concentration ( $\alpha_k$ ) and an attenuation ratio ( $Y_k$ ).

Annual precipitation is obtained from local weather data or the general map shown in Figure III-19. Concentration factors for separate and combined sewer land uses are given in Table III-20.

The population density function is as follows:

$$F_k = \begin{cases} 1.0, & \text{commercial and industrial} \\ 0.142 + 0.134 PD^{0.54}, & \text{residential} \\ 0.142, & \text{other} \end{cases} \quad (III-49)$$

where

PD = population density (persons/ha).

The street cleaning factor  $Y_k$  is based on street cleaning interval  $N_s$  (days) :

$$Y_k = N_s / 20 \text{ for } N_s < 20 \quad (III-50)$$

For  $N_s > 20$  days, no street cleaning effects are apparent and  $Y_k = 1.0$ .

Because most pollution load in combined sewers is due to raw wastewater and sewer scour, street cleaning will not significantly reduce loads, and  $Y_k = 1.0$  for combined sewers areas.

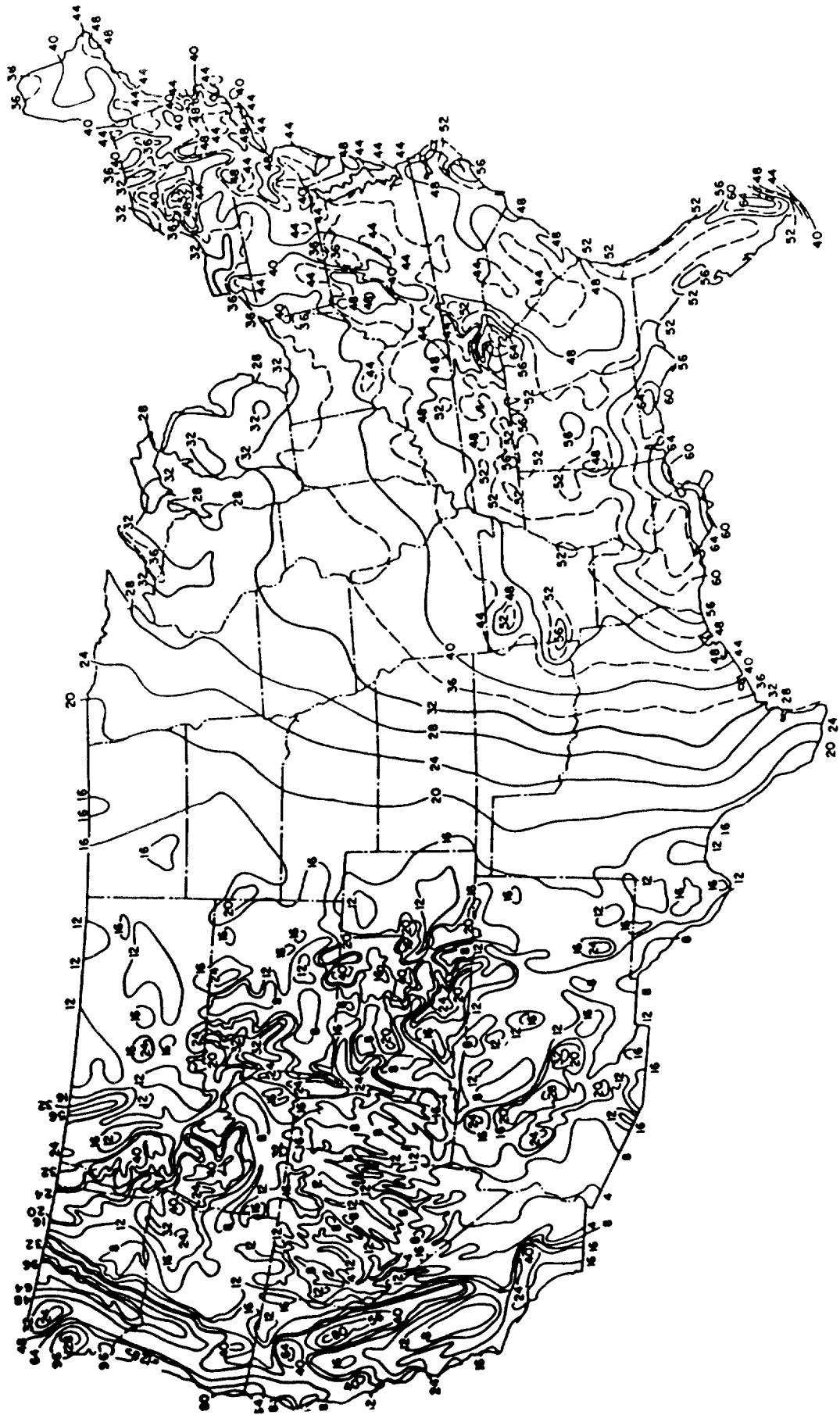


FIGURE III-19 MEAN ANNUAL PRECIPITATION IN INCHES (1IN = 2.54CM) (GILMAN, 1964)

TABLE III-20

POLLUTANT CONCENTRATION FACTORS FOR ANNUAL LOADING  
FUNCTIONS (HEANEY AND HUBER, 1979)

Land Use	Pollutant (kg/ha-cm)				
	BOD <sub>5</sub>	SS	VS	O <sub>4</sub>	N
<u>Separate Sewers</u>					
Residential	0.35	7.2	4.2	0.015	0.058
Commercial	1.41	9.8	6.2	0.033	0.131
Industrial	0.53	12.9	6.3	0.031	0.122
Other Developed	0.05	1.2	1.2	0.004	0.027
<u>Combined Sewers</u>					
Residential	1.45	29.7	17.2	0.061	0.239
Commercial	5.83	40.6	25.6	0.138	0.539
Industrial	2.21	53.0	26.2	0.291	0.504
Other Developed	0.21	4.9	4.8	0.018	0.066

EXAMPLE III-8

Estimation of Annual Urban Pollutant Loads

Consider a city of 4000 hectares of which 20 percent is commercial, 10 percent industrial, 65 percent residential and 5 percent is in other developed areas. The residential population density is 25 persons/ha. Most of the city has separate sewers but approximately 30 percent of the residential area still has combined sewers. The streets are swept every five days in the commercial and industrial areas and are not swept in the residential areas. The mean annual precipitation is 105 cm. Determine the average annual loads of nitrogen and phosphate.

Solution:

The land use areas are:

- Commercial: 800ha
- Industrial: 400ha
- Residential: 780ha, combined  
1820ha, separate
- Other: 200ha

Loads from each land use are given by Equation III-47, with  $F_k$  from Equation III-49. The street cleaning factor is:

$$Y_k = 5/20 = 0.25$$

in commercial/industrial areas and  $Y_k = 1.0$  in all other areas. The population function for residential areas is:

$$F_k = 0.142 + 0.134(25)^{0.54}$$
$$= 0.904$$

Loading calculations are summarized in the following table.

Land Use	$F_k$	$Y_k$	$\alpha_k$ (kg/ha-cm)		$L_k$ (kg/ha)	
			N	PO <sub>4</sub>	N	PO <sub>4</sub>
Residential combined	0.904	1.0	0.239	0.061	22.69	5.79
Residential separate	0.904	1.0	0.058	0.015	5.51	1.42
Commercial	1.0	0.25	0.131	0.033	3.44	0.87
Industrial	1.0	0.25	0.122	0.031	3.20	0.81
Other	0.142	1.0	0.027	0.004	0.40	0.06

Total annual loads are obtained by multiplying each load  $L_k$  by its respective area as in Equation III-48.

Nitrogen:

$$780(22.69) + 1820(5.51) + 800(3.44) + 400(3.20) + 200(0.40)$$
$$= 31,800 \text{ kg/yr}$$

Phosphate:

$$780(5.79) + 1820(1.42) + 800(0.87) + 400(0.81) + 200(0.06)$$
$$= 8100 \text{ kg/yr}$$

Over half the pollution load comes from the 780-ha combined sewer residential area.

----- END OF EXAMPLE III-8 -----

### 3.6.2 Event Loads in Urban Runoff

Event loading functions for urban runoff are based on general procedures proposed by Any et al . (1974), many of which were incorporated in the U.S. Army Corps of

Engineers urban runoff model STORM (Hydrologic Engineering Center, 1977). The basic loading function is similar to that used for solid-phase rural runoff loads (Equation III-18). Sediment (also referred to as "dirt and dust" or simply "solids") in runoff is multiplied by a pollutant concentration:

$$L = 10^{-6} C Y \quad (III-51)$$

where

L = pollutant load in urban runoff (kg/ha)

Y = sediment washed off the urban area during a runoff event (kg/ha)

C = pollutant concentration in sediment (ppm:  $\mu\text{g/g}$ , or mg/kg).

Although Equation III-51 is often used for both dissolved and solid-phase pollutants, we would expect it to be more accurate for the latter.

Sediment washoff is limited by the total sediment which has accumulated on land surfaces:

$$Y = W X \quad (III-52)$$

where

X = accumulated sediment at the time of the storm (kg/ha)

W = fraction of X which washes off during the storm.

The washoff function is derived by assuming that washoff rate is a linear function of runoff rate and accumulated sediment (Amy et al. ., 1974; Alley, 1981) :

$$\frac{dX(h)}{dh} = -uqX(h) \quad (III-53)$$

or

$$X(h) = X(0) \exp \left[ -u \int_0^h q dh \right] \quad (III-54)$$

where

X(h) = sediment remaining on the land surface at hour h after the beginning of a storm (kg/ha)

X(0) = accumulated sediment at the beginning of a storm (kg/ha)

q = runoff rate (cm/hr)

u = washoff coefficient ( $\text{cm}^{-1}$ ).

The integral in Equation III-54 is the total storm runoff up to hour h. If we let h equal storm duration then:

$$X(h) = X(0) \exp(-uQ) \quad (III-55)$$

where

$Q$  = total storm runoff (cm).

The washoff coefficient is determined by assuming 90% of accumulated sediment will be washed off with 1.27cm (0.5in) of runoff (Amy et al., 1974). Hence  $0.1 X(0) = X(h) \exp[-1.27u]$  or  $u = 1.8 \text{ cm}^{-1}$ . The fraction of sediment washed off is:

$$W = \frac{X(0) - X(h)}{X(0)} = 1 - \exp(-1.8Q) \quad (III-56)$$

and Equation III-51 can be written:

$$L = 10^{-6} [1 - \exp(-18Q)] CX \quad (III-57)$$

When this loading function is applied to an area with multiple land uses, either loads are weighted from each area:

$$L = \sum_k a_k L_k \quad (III-58)$$

or weighted average concentrations and sediment accumulations are used:

$$CX = \left[ \sum_k a_k X_k \right] \left[ \sum_k a_k C_k \right] \quad (III-59)$$

where

- $a_k$  = fraction of total area in land use k
- $L_k$  = pollutant load from land use k (kg/ha) as given by Equation III-57
- $X_k$  = accumulated sediment on land use k (kg/ha)
- $C_k$  = pollutant concentration in sediment on land use k (mg/kg).

### 3.6.2.1 Runoff

Two alternative procedures are used in STORM to compute storm runoff. The first is the U.S. Soil Conservation Service's Curve Number Equation (Equation III-3) as described in Section 3.4.2. Appropriate urban curve numbers for average antecedent moisture conditions (CN2) are given in Table III-21.

The second option is based on runoff coefficients and depression storage:

$$Q = CR(P - DS) \quad (III-60)$$



TABLE III-21

RUNOFF CURVE NUMBERS (ANTECEDENT MOISTURE CONDITION II)  
FOR URBAN AREAS (SOIL CONSERVATION SERVICE, 1975)

Land Use Description	Hydrologic Soil Group			
	A	B	C	D
Open spaces, lawns, parks, golf courses, cemeteries, etc.				
Good condition: grass cover on 75% or more of the area	39	61	74	80
Fair condition: grass cover on 50% to 75% of the area	49	69	79	84
Commercial and business area (85% impervious)	89	92	94	95
Industrial districts (72% impervious)	81	88	91	93
Residential:				
Average lot size				
Average % impervious				
1/8 acre or less	65	77	85	90
1/4 acre	38	61	75	83
1/3 acre	30	57	72	81
1/2 acre	25	54	70	80
1 acre	20	51	68	79
Paved parking lots, roofs, driveways, etc.	98	98	98	98
Streets and roads:				
Paved with curbs and storm sewers	98	98	98	98
Gravel	76	85	89	91
Dirt	72	82	87	89

where

$P$  = storm precipitation (rainfall + snowmelt, cm)

$DS$  = depression storage (cm)

$CR$  = runoff coefficient.

Equation 111-60 (which applies only for  $P > DS$ ) suggests that precipitation must satisfy the available depression storage on plant surfaces and in mud puddles, pot holes, etc., before runoff will occur.

A conceptual view of this runoff process is shown in Figure 111-20. Depression storage  $DS$  is at a maximum value  $DS^*$  when the land surface is completely dry, and the depression shown in Figure 111-20 is empty. However, previous events may have partially filled depressions so that as in the figure, only a portion of  $DS^*$  remains to be filled.

Depressions are assumed to be emptied by evaporation, and a general mass balance is:

$$DS_{t+1} = DS_t + E_t - P_t \quad (111-61)$$

for

$$0 \leq DS_{t+1} \leq DS^* \quad (111-62)$$

where

$DS_t$  = depression storage on day  $t$  (cm)

$P_t$  = precipitation on day  $t$  (rain + snowmelt, cm)

$E_t$  = evaporation on day  $t$  (cm)

$DS^*$  = maximum depression storage (cm).

Evaporation may be assumed equal to potential evapotranspiration and determined as in Section 3.5.2.

The depression storage computation (Equations 111-61,62) is a procedure for describing antecedent moisture conditions. When the Curve Number Equation is used, antecedent moisture is a function of 5-day antecedent precipitation. In Equation 111-60, the water in storage on the land surface is the indicator of antecedent moisture.

Both maximum depression storage  $DS^*$  and the runoff coefficient  $CR$  are functions of the urban area's impervious surfaces:

$$CR = cr_i I + cr_p (1-I) \quad (111-63)$$

$$DS^* = ds_i I + ds_p (1-I) \quad (111-64)$$

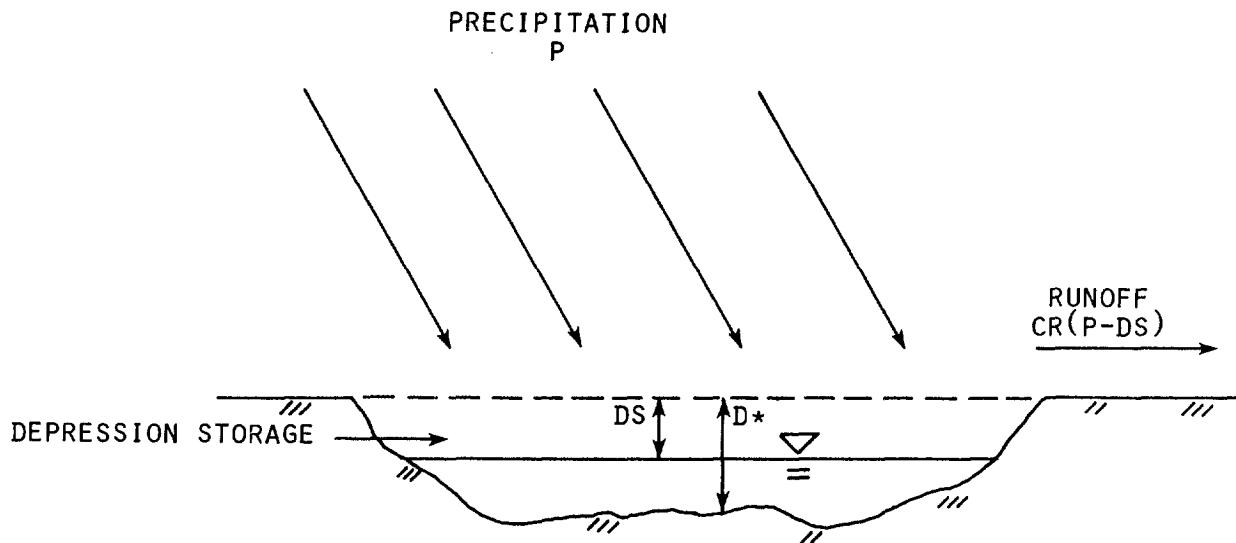


FIGURE III-20 CONCEPTUAL MODEL OF DEPRESSION STORAGE

where

- $I$  = fraction of the urban area which is impervious
- $cr_i, cr_p$  = runoff coefficients for impervious and pervious areas
- $ds_i, ds_p$  = maximum depression storage (cm) for impervious and pervious areas.

Default runoff coefficients used in STORM are  $cr_i = 0.90$  and  $cr_p = 0.15$  (Hydrologic Engineering Center 1977). Typical depression storage coefficients are  $ds_i = 0.15\text{cm}$  and  $ds_p = 0.60\text{cm}$  (Aron, 1982; Novotny and Chesters, 1980). These values may be used when more specific local data are unavailable.

Impervious fractions are best estimated directly from aerial photographs or land-use maps. When these are not available, regression equations based on population density are sometimes used. The equation given by Heaney and Huber (1979) can be approximated by:

$$I = 0.069 PD^{0.48} \quad (III-65)$$

where

$PD$  = population density (persons/ha).

### 3.6.2.2 Sediment

Sediment and pollutant accumulation in urban areas is a complex process which depends on daily deposition from the atmosphere and other sources, removal by street

cleaning and washoff by runoff. In order to estimate C and X in Equation III-57, we must begin by determining the sediment or solids accumulation. This rate may be measured by monitoring of storm sewer suspended solids data. When these data cannot be obtained, average values from previous urban monitoring programs must be used.

Urban sediment data are often normalized with respect to the length of street curbing. This is because most of the dirt and dust which constitutes urban sediment collects in street gutters. Daily sediment buildup is:

$$x = z \text{ cl} \quad (III-66)$$

where

$x$  = daily sediment buildup (kg/ha-day)

$z$  = sediment accumulation rate (kg/km of curb per day)

$Cl$  = curb length density (km/ha).

Curb length may be estimated as twice the total street lengths, and  $Cl$  is obtained by dividing curb length by area. Alternatively, the regression equation given by the American Public Works Association (1974) may be used (converted to metric units):

$$Cl = 0.31 - 0.27(0.93)^{PD} \quad (III-67)$$

Urban sediment accumulation rates from several sources are given in Table III-22. The rates given by Amy et al. , (1974) and Sartor and Boyd (1972) are mean values based on data from a number of urban areas. The STORM rates are suggested default values for that model. Although the Sartor and Boyd (1972) rates are larger than the other two sets, they are generally comparable with the Amy et al. , (1974) data. The Sartor and Boyd rates are recommended for use in Equation III-66 because they are conservative and consistent.

Sediment will accumulate at a daily rate  $x$  until the streets are cleaned or a runoff event occurs. The daily sediment mass balance is:

$$X_{t+1} = X_t + x - Y_t - S_t \quad (III-68)$$

where

$X_t$  = accumulated sediment at beginning of day  $t$  (kg/ha)

$Y_t$  = sediment removed in runoff on day  $t$  (kg/ha)

$S_t$  = sediment removed by street cleaning on day  $t$  (kg/ha).

If a runoff event occurs on day  $t$ , then from Equations III-52 and 56:

TABLE III-22

## URBAN SEDIMENT (SOLIDS) ACCUMULATION RATES

Land Use	Amy et al (1974)	Sartor & Boyd (1972) <sup>a</sup>	STORM <sup>b</sup>
	(all in kg/curbs-l km-day)		
Residential	42	-	-
Single-family residential	-	48*	10
Multi-family residential	-	66*	34
Commercial	21	69*	49
Industrial	-	127*	68
Light industry	110	-	-
Heavy industry	57	-	-
Parks	-	-	22
Open space	3.4	-	-

\*Recommended values

<sup>a</sup>Cited in Novotny and Chesters (1980)

<sup>b</sup>Hydrologic Engineering Center (1977)

$$Y_t = [1 - \exp(-1.8Q_t)] X_t \quad (III-69)$$

where

$Q_t$  = runoff on day t (cm).

Conversely, if the streets are cleaned on day t:

$$S_t = e X_t \quad (III-70)$$

where

$e$  = street cleaning efficiency (fraction removed by cleaning).

It is assumed that streets are not cleaned on the same day that a runoff event occurs.

Sediment accumulations and removal are illustrated in the following example.

EXAMPLE III-9

Urban Sediment Accumulation and Removal

A storm occurs on May 31 which removes all sediment from an urban area. Subsequent storms occur on June 9 and June 15 which produce 0.5cm and 1.1cm of runoff, respectively. On June 6, the streets are cleaned with an efficiency  $e = 0.4$ . The daily sediment buildup is  $x = 80$  kg/ha. How much sediment is contained in the runoff from the June 15 storm?

Solution:

Letting May 31 be day  $t = 0$ , the next event is the cleaning on day 6 (June 6). Accumulated sediment is  $X_6 = 6(80) = 480$  kg/ha. Cleaning removes:

$$S_6 = 0.4(480) = 192 \text{ kg/ha}$$

and on June 7, remaining sediment is:

$$\begin{aligned} X_7 &= X_6 - S_6 + x \\ &= 480 - 192 + 80 = 368 \text{ kg/ha.} \end{aligned}$$

For the June 9 runoff event,  $X_9 = 368 + 2(80) = 528$  kg/ha. Sediment washoff from Equation III-69 is:

$$\begin{aligned} Y_9 &= [1 - \exp(-1.8(0.5))] 528 \\ &= 313 \text{ kg/ha.} \end{aligned}$$

On the following day:

$$\begin{aligned} X_{10} &= X_9 - Y_9 + 80 \\ &= 528 - 313 + 80 \\ &= 295 \text{ kg/ha.} \end{aligned}$$

On June 15,  $X_{15} = 295 + 5(80) = 695$  kg/ha, and sediment washoff in the 1.1 cm of runoff is:

$$\begin{aligned} Y_{15} &= [1 - \exp(-1.8(1.1))] 695 \\ &= 599 \text{ kg/ha} \end{aligned}$$

END OF EXAMPLE III-9

### 3.6.2.3 Pollutant Concentrations

Pollutant concentrations in sediment can be obtained from sampling of sediment accumulations in street gutters or sampling of storm sewer flows. General values for conventional pollutants are given in Table III-23. Concentrations of metals and organic compounds are given in Tables III-24 and 25.

TABLE III-23

CONCENTRATIONS OF CONVENTIONAL POLLUTANTS  
IN URBAN SEDIMENT (SARTOR AND BOYD, 1972,  
CITED IN NOVOTNY AND CHEATERS, 1980)

Pollutant	Land Use		
	Residential (mg/kg)	Commercial (mg/kg)	Industrial (mg/kg)
<b>BOD<sub>5</sub></b>	9,200	8,300	7,500
COD	20,800	19,400	35,700
Kjeldahl Nitrogen	1,700	1,100	1,400
Nitrate-Nitrogen	50	500	60
Phosphate-Phosphorus	900	800	1,200

TABLE III-24

CONCENTRATIONS OF METAL IN URBAN SEDIMENT  
(AMY, et al, 1974)

	Residential (mg/k)	Commercial (mg/k)	Industrial		Weighted Mean (mg/kg)
			Light (mg/kg)	Heavy (mg/kg)	
Cd	3.0	4.2	4.0	3.9	3.4
Cr	192	225	288	278	211
Cu	93	133	128	107	104
Fe	20,600	23,300	21,800	28,600	22,000
Pb	1,430	3,440	2,780	1,160	1,810
Mn	392	397	490	570	418
Ni	28	48	41	37	35
Sr	21	18	27	23	21
Zn	350	520	368	317	370

TABLE III-25

CONCENTRATIONS OF MERCURY AND ORGANIC COMPOUNDS  
IN URBAN SEDIMENT (AMY, et al , 1974)

Pollutant	Concentration (mg/kg)
Hg	0.083
Endrin	0.0002
Dieldrin	0.028
PCB	0.770
Methoxychlor	0.500
DDT	0.076
Lindane	0.0029
Methyl Parathion	0.002
DDD	0.082

#### 3.6.2.4 Loading Computations

The basic loading function for pollutants from urban runoff events (Equation III-57) is deceptively simple. Storm runoff and sediment accumulation, which are required by the loading function, depend on dynamic processes and are not easily computed. If the Curve Number Equation (Equation III-3) is used for runoff, curve numbers must be selected based on antecedent precipitation. Conversely, the runoff coefficient/depression storage runoff equation (Equation III-60) requires the daily moisture calculations indicated by Equations III-61 and 62. Sediment accumulation is determined using Equations III-66, 68, 69, and 70.

Event-based urban runoff loading computations are too complex to be routinely done by hand. Although the following example demonstrates that hand calculations are possible, loading estimates are most efficiently done by computer. Indeed, the equations described in this section are the basis of the STORM computer model of urban runoff waste loads.



EXAMPLE III-10

Lead in Urban Runoff From a Storm Event

Estimate the washoff of lead from a 200-ha urban area during a 2-cm rain-storm. The area has a population density of 25 persons/ha and is 60% residential and 40% commercial. The previous storm 20 days ago washed the area clean. Streets were cleaned 9 days ago with an efficiency of 55%. Daily evaporation rate during the 20-day period was 0.2 cm/day.

Solution:

Since this is a multi-land use area, we will use weighted loads as in Equations 111-59 and 57. Equation 111-60 will be used to compute runoff:

$$Q = CR(P - DS)$$

To obtain runoff and depression storage coefficients from Equations III-63 and 64, the impervious fraction  $I$  must be calculated from Equation III-65:

$$\begin{aligned} I &= 0.069 PD^{0.48} \\ &= 0.069 (25)^{0.48} = 0.32 \end{aligned}$$

Using the typical coefficients for impervious and pervious areas given in Section 3.6.2.1:

$$CR = 0.90(0.32) + 0.15(0.68) = 0.039$$

$$DS^* = 0.15(0.32) + 0.60(0.68) = 0.46\text{cm}$$

Since maximum depression storage is 0.46cm, and daily evaporation is 0.2 cm/day, depressions will dry within three days. Therefore, on the day of the storm  $DS = 0.46\text{cm}$ , and runoff is:

$$Q = 0.39(2 - 0.46) = 0.60\text{cm}$$

From Equation III-57:

$$\begin{aligned} L &= 10^{-6} [1 - \exp(-1.8(0.60))] CX \\ &= 0.66(10)^{-6} CX \end{aligned}$$

Thus 66% of the accumulated lead ( $CX$ ) is washed off by the storm.

Daily sediment accumulation rates can be obtained from Table III-22.

Assuming that the residential area is divided equally between single-family and multi-family residences, rates are  $(48+66)/2 = 57$  kg/km-day for the residential area (60%) and 69 kg/km-day for the commercial Portion (40%). The weighted average is:

$$z = 0.60(57) + 0.40(69) = 61.8 \text{ kg/km-day}$$

Curb length density from Equation III-67 is:

$$Cl = 0.31 - 0.27(0.93)^{25} = 0.266 \text{ km/ha}$$

and daily loading is:

$$x = 0.266(61.8) = 16.4 \text{ kg/ha.}$$

On day 11, when streets are cleaned,  $X = 11(16.4) = 180.4 \text{ kg/ha}$ . Cleaning removes 55%, leaving 81.2 kg/ha. On the storm day:

$$X = 81.2 + 9(16.4) = 229 \text{ kg/ha.}$$

Lead concentrations, from Table III-24, are 1430 mg/kg and 3440 mg/kg for residential and commercial areas, respectively, producing a weighted average of:

$$C = 0.60(1430) + 0.40(3440) = 2234 \text{ mg/kg.}$$

Substituting these values of X and C in the loading function produces the lead load in runoff:

$$L = 0.66(10)^{-6} 2234(229) = 0.34 \text{ kg/ha}$$

or, over the 200-ha area:

$$200(0.34) = 68 \text{ kg.}$$

END OF EXAMPLE III-10

### 3.7 GROUNDWATER WASTE LOADS

#### 3.7.1 Characteristics

Groundwater pollution is of major concern because it endangers water supplies. Organic chemicals, nuclear wastes, nitrates and other compounds may leach from such sources as waste land application sites, storage lagoons, landfills, croplands, lawns, gardens and construction sites. The general characteristics of the problem are shown in Figure III-21. The figure shows a "waste" which has been buried beneath the soil surface. This waste could be contaminants such as PCBs in a landfill, septic tank drainage, fertilizers, pesticides, or toxic compounds in abandoned waste dumps. In other situations the wastes may be on the soil surface or contained in a storage lagoon. Chemicals are leached from wastes by percolation, and this leachate moves through the unsaturated soil zone to an underlying aquifer or saturated zone.

Groundwater pollution is often much more difficult to manage than pollution of surface waters. Since the water supply is beneath the soil surface, pollution effects are seldom visible. When contamination is detected in samples from monitoring wells or water systems, it is usually too late to eliminate the pollution source. Chemical movement through the unsaturated zone is relatively slow in the absence of fractures or other irregularities which channelize flows. In many soils, pollutants may move less than a meter per year. A chemical which is detected in a well may have begun its transit from an abandoned waste dump 20 years ago. Even if the dump is subsequently excavated, a 20-year supply of the chemical remains in the groundwater

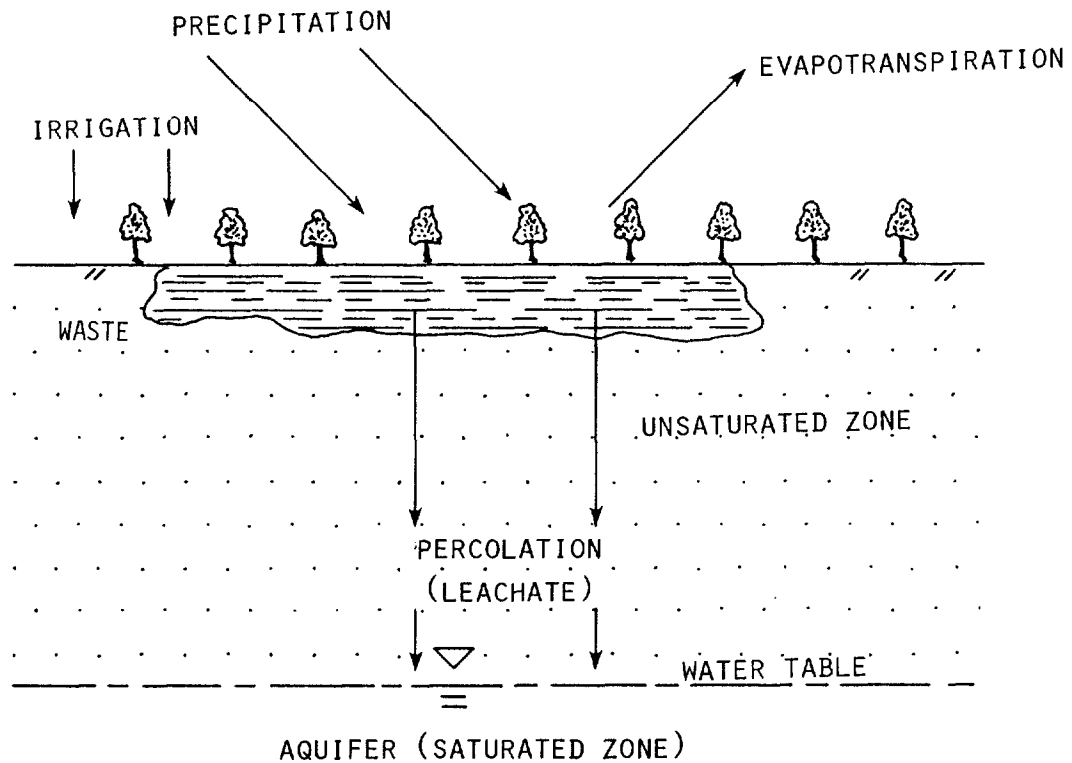


FIGURE III-21 POLLUTANT TRANSPORT TO AN AQUIFER

transport "pipeline". Compared to surface waters, the "flushing time" of aquifers is very long.

A further complication is the conservative nature of many pollutants in aquifers. Aquifers lack much of the self-purifying or assimilative capacity of surface waters. During transport through the aerated unsaturated zone, chemicals may be removed from leachate by plant uptake, volatilization, biochemical decay and adsorption. However, these removal mechanisms are often greatly reduced or eliminated once a chemical reaches the saturated zone.

Groundwater pollution problems are complex, and they are often analyzed by computer models based on the differential equations describing water and solute movement through porous media (Bachmat *et al.*, 1980). These models are well beyond the scope of this screening manual. The discussion in this section is limited to simple procedures to estimate pollution loads to the saturated zone. Pollutant movement in the aquifer is not considered and steady-state, uniform one-dimensional flow is assumed. Since the time scale of groundwater pollution is measured in years, the loading estimates are annual values.

Succeeding subsections discuss water balances, nitrate loads from land application sites and leaching of organic chemicals.

### 3.7.2 Water Balance

Little downward movement of a chemical is possible in the absence of percolation. Although some movement due to diffusion is possible, convection and dispersion associated with a water flux are the major transport mechanisms in the unsaturated zone. Based on the processes shown in Figure III-21, percolation is given by:

$$Q = P + I - E \quad \text{(III-71)}$$

where

- Q = annual percolation (cm)
- I = annual irrigation (cm)
- P = annual precipitation (cm)
- E = annual evapotranspiration (cm).

Equation III-71 applies to a waste source in or on the soil surface which is not contained within an impermeable layer or storage lagoon. In the latter cases, percolation is equal to seepage or leakage through the layer or lagoon bottom.

Mean annual potential evapotranspiration minus precipitation is shown in Figure III-22. For a vigorous plant cover, ET is approximately equal to potential ET and the values in Figure III-22, converted to centimeters, can be used in Equation III-71 to provide a simple screening device for groundwater pollution. In the absence of irrigation, negative values of E-P (i.e.  $P > E$  and hence  $Q > 0$ ) identify areas of potential groundwater pollution. Conversely, nonirrigated areas with positive E-P, and hence negligible percolation, are less likely to have contaminated groundwater.

These conclusions apply only when a vigorous plant cover is maintained on the waste site to maximize ET. A denuded or fallow site will produce little ET and maximize opportunities for percolation.

### 3.7.3 Nitrate Loads to Groundwater From Waste Application Sites

Municipal sewage and sewage sludges are often applied to land. Land application may thus eliminate a major surface-water pollution source, but it may also create a groundwater pollution problem. A major concern is the leaching of inorganic nitrogen, in the form of nitrate, from the wastes and subsequent transport to the saturated zone. Nitrate is extremely mobile in soils, and since it is toxic to infants and livestock, it is often considered the most critical pollutant from land application systems.

This subsection presents a simple nitrate loading calculation procedure adapted from Hai th (1983). The procedure estimates nitrate concentrations as nitrogen in percolation from the root zone of a land application site.

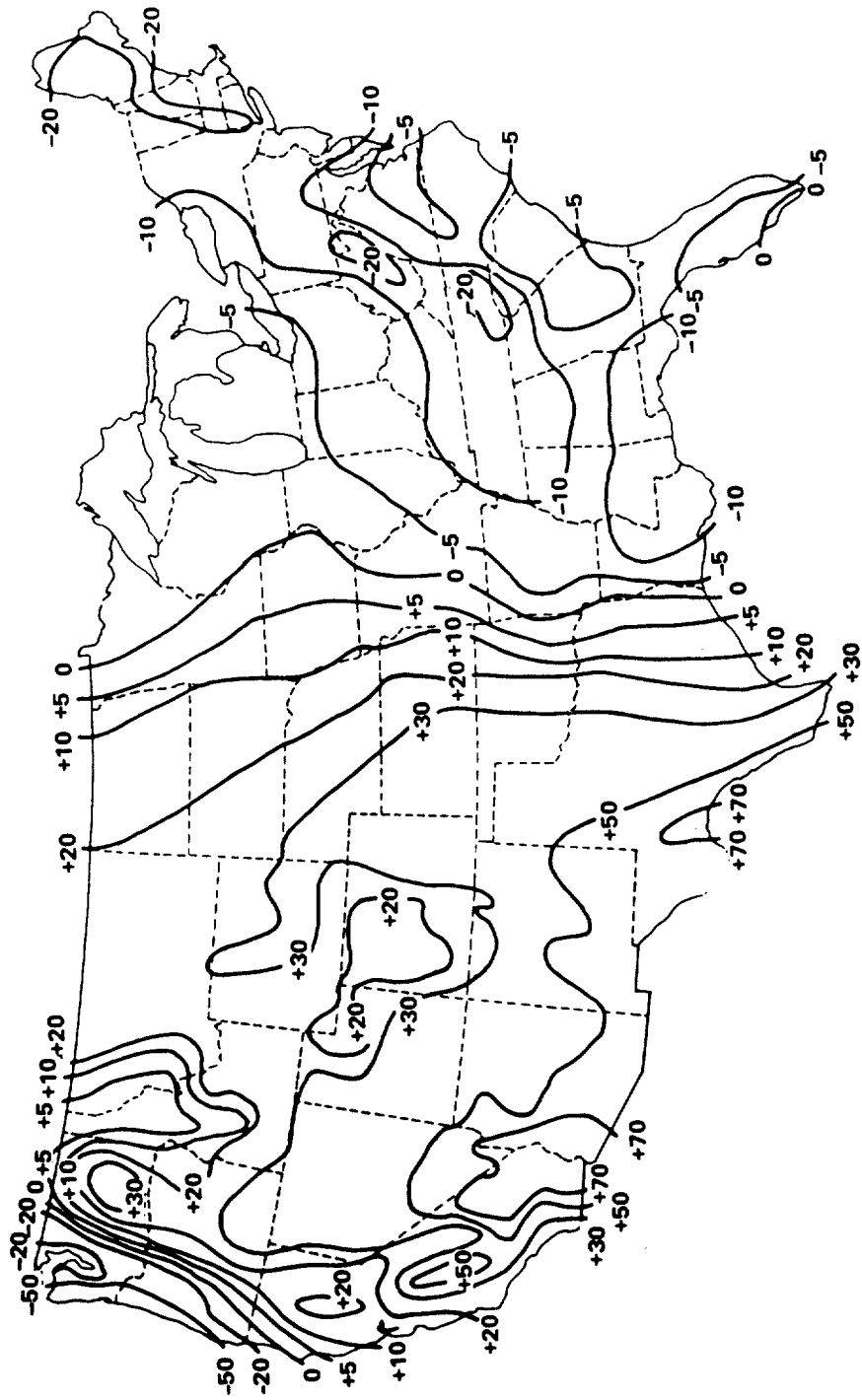


FIGURE III-22 MEAN ANNUAL POTENTIAL EVAPOTRANSPIRATION MINUS PRECIPITATION IN INCHES  
(1 IN = 2.54 CM) (POUND ET AL., 1976)

### 3.7.3.1 Model Description

Components of the model are shown in Figure III-23. An annual application of nitrogen in waste is divided into organic and inorganic forms. Inorganic nitrogen is subject to volatilization losses, and the remainder is considered available for plant or crop uptake and leaching. Waste organic nitrogen consists of two components, a labile or readily mineralizable fraction which is available for plants and leaching during the first year following application, and a stabilized fraction which mineralizes at rates comparable to other forms of soil organic nitrogen. The available nitrogen supply thus consists of sludge inorganic nitrogen, rapidly mineralized sludge organic nitrogen and slowly mineralized soil and sludge organic nitrogen. Since inorganic nitrogen in the soil is rapidly oxidized to nitrate, it is assumed that all available nitrogen is nitrate.

Annual mass balances for soil organic nitrogen and available nitrogen are:

$$O_{t+1} = O_t(1-m) + (1-a)1000 NX_t \quad (III-72)$$

$$\begin{aligned} A_t &= mO_t + (1-v)1000 N(1-F)X_t + a1000 NX_t \\ &= mO_t + 1000 N [(1-v)(1-F) + aF] X_t \end{aligned} \quad (III-73)$$

where

$O_t$  = soil organic nitrogen (including stabilized waste organic nitrogen) at beginning of year t (kg/ha)

$X_t$  = waste application of dry solids in year t (t/ha)

$m$  = annual mineralization rate for soil nitrogen

$a$  = fraction of waste organic nitrogen mineralized during year of application

$N$  = nitrogen fraction of solids

$F$  = organic fraction of waste solids

$A_t$  = available nitrogen (nitrate-nitrogen) in year t (kg/ha)

$v$  = fraction of waste inorganic nitrogen which is volatilized.

Nitrogen loss by leaching is the difference between available nitrogen and crop uptake:

$$L_t = A_t - Cn_t \quad (III-74)$$

where

$L_t$  = nitrate-nitrogen leachate in year t (kg/ha)

$Cn_t$  = crop nitrogen uptake in year t (kg/ha).

Since there are no additional removal mechanisms for nitrate once it passes

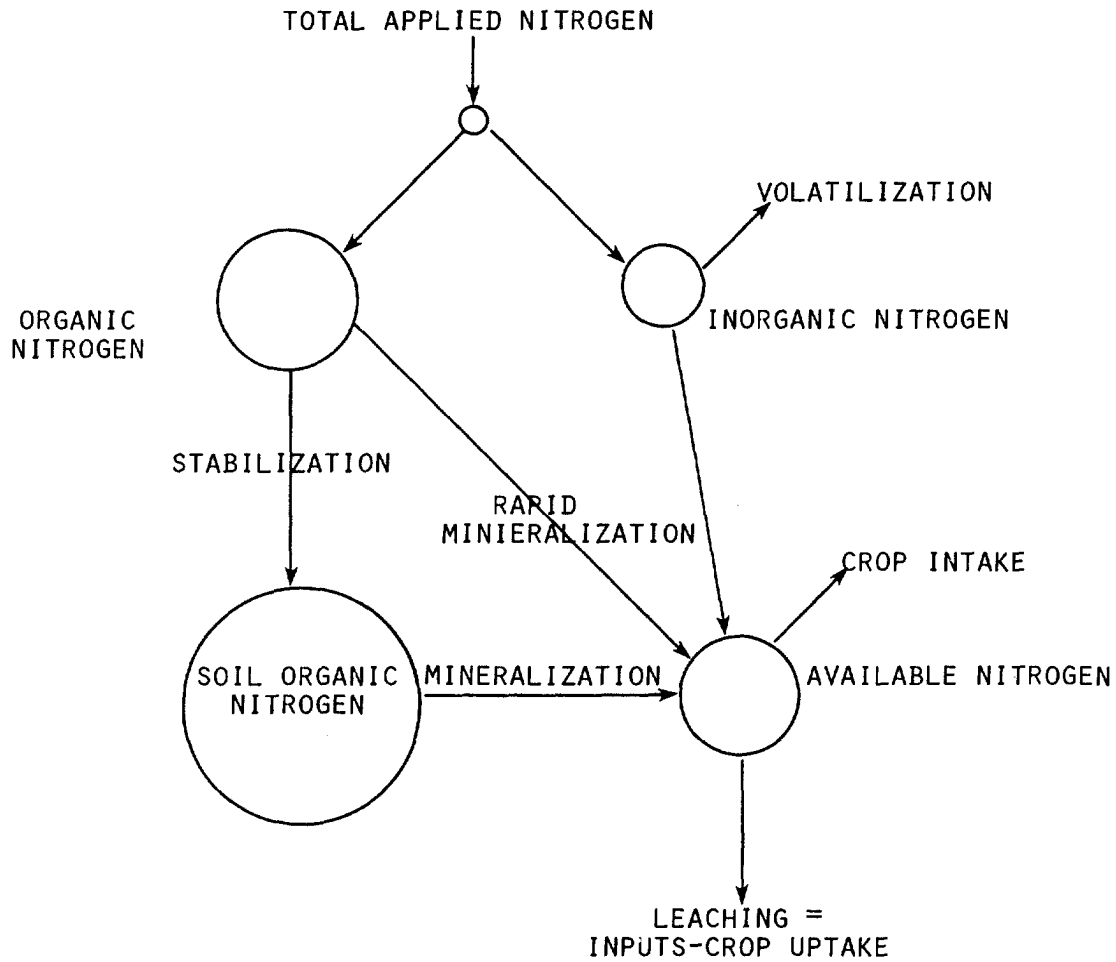


FIGURE III-23 NITROGEN DYNAMICS AT A LAND APPLICATION Site

below the root zone,  $L_t$  is also the nitrate-nitrogen waste load to the saturated zone, although if the water table is well below the soil surface, the load may not reach the aquifer for several years.

### 3.7.3.2 Steady-State Loading Function

The loading calculation given by Equation III-74 is complicated somewhat by the need for sequential computations for soil organic nitrogen by Equation III-72. However, after many years of waste application at an average rate  $X$  (t/ha):

$$\begin{aligned}
 O_t &= O_0(1-m)^t + BX [1 + (1-m) + (1-m)^2 + \dots] \\
 &\approx O_0(1-m)^t + BX/m
 \end{aligned}
 \tag{III-75}$$

where

$B = (1-a) 1000 N F$ , and  $\theta_0$  is the initial soil organic nitrogen level. The steady-state organic nitrogen level  $\bar{\theta}$  is  $BX/m$  or:

$$\bar{\theta} = (1-a)1000 N F X/m \quad (III-76)$$

Substituting  $\bar{\theta}$  into Equations III-73 and 74 produces the steady-state loading function:

$$L = 1000X [1 - v(1-F)] - Cn \quad (III-77)$$

where

- L = annual steady-state nitrate-nitrogen load to groundwater (kg/ha)
- x = average annual solids application rate (t/ha)
- N = nitrogen fraction of solids
- F = organic fraction of waste nitrogen
- v = fraction of waste inorganic nitrogen which is volatilized
- Cn = average crop nitrogen uptake.

### 3.7.3.3 Loading Function Data

Typical values for crop nitrogen uptake are given in Table III-26. Volatilization rates (v) are based on the ammonium content of the waste and the method of application. If the waste is sprayed or spread on the soil surface, all ammonia can be assumed to volatilize. For example, if 70% of the inorganic nitrogen in the waste is in the ammonium form, then  $v = 0.70$ . Conversely, when wastes are injected or otherwise directly incorporated in the soil, there is little opportunity for volatilization and  $v = 0$ .

Waste properties (X, N, F) will depend on the specific waste and the operation of the disposal site.

#### EXAMPLE III-11

##### Nitrate-Nitrogen Load from a Sludge Land Application Site

Determine the steady-state loading of nitrate-nitrogen from a land application site for sewage sludge in central Florida. The sludge is spread on fescue at an annual rate of 10t/ha. The sludge solids are 5% nitrogen and 70% of the nitrogen is organic. The inorganic nitrogen is 90% ammonia nitrogen. Also estimate the average nitrate-nitrogen concentration in percolation entering the saturated zone.



TABLE III-26

## TYPICAL VALUES OF CROP NITROGEN

UPTAKE (POWELL, 1976)

Crop	Annual Nitrogen Uptake (kg/ha)
Forage Crops	
Coastal Bermuda Grass	540-670
Reed Canary Grass	250-400
Fescue	300
Alfalfa	160-250
Sweet Clover	180
Red Clover	90-140
Lespedeza Hay	150
Field Crops	
Corn	170
Soybeans	100-110
Potatoes	220
Cotton	70-110
Wheat	60-90
Sugar Beets	80
Barley	70
Oats	60
Forest	
Young Deciduous ( $\leq 5$ yrs)	110
Young Evergreen ( $\leq 5$ yrs)	70
Medium and Mature Deciduous	30-60
Medium and Mature Evergreen	20-30

Solution:

Equation III-76 is used to determine steady-state loading:

$$L = 1000NX [1 - v(1-F)] - Cn$$

where  $X = 10$ ,  $N = 0.05$ ,  $F = 0.7$ . Also, since the inorganic nitrogen is 90% ammonia and the sludge is spread on the soil surface,  $v = 0.9$ . Crop uptake  $Cn$  is 300 kg/ha from Table III-26.

$$\begin{aligned} L &= 1000(0.05)10 [1 - 0.9(0.3)] - 300 \\ &= 65 \text{ kg/ha} \end{aligned}$$

To determine the nitrate-nitrogen concentration, percolation  $Q$  must be estimated. From Figure III-22,  $E-P = -5i_n = -12.7\text{cm}$  for central Florida. Neglecting water in the sludge, Equation III-71 indicates percolation

$$Q = P - E = 12.7\text{cm}$$

Since 1cm over 1 ha is  $100 \text{ m}^3$ , total percolation is  $1270 \text{ m}^3$ , and the nitrate-nitrogen concentration is

$$65/1270 = 0.051 \text{ kg/m}^3 = 51 \text{ mg/l}$$

which greatly exceeds the drinking water standard of 10 mg/l.

----- END OF EXAMPLE III-11 -----

### 3.7.4 Leaching of Organic Chemicals

The potential for groundwater pollution from an organic chemical is determined by adsorption and degradation processes. Organic chemicals are partially adsorbed by soil particles, and movement of a chemical is retarded or slowed compared to the movement of the percolation water. Degradation of organic compounds by biochemical processes and volatilization in the unsaturated zone will reduce the quantity of the chemical so that only a fraction of the original compound will remain to enter an aquifer. If the chemical is strongly adsorbed and rapidly degraded, and the water table is well below the soil surface, there is minimal chance of groundwater contamination. Conversely, pollution is favored by any of the following conditions: weak adsorption, slow degradation, or high water table.

#### 3.7.4.1 Adsorption

Simple procedures for modeling movement of adsorbed chemicals are based on the concept of a retardation factor,  $R$  (Freeze and Cherry, 1979) which is defined as:

$$R = u/u_s \quad \text{(III-78)}$$

where

$u$  = mean water velocity (cm/yr)

$u$  = mean chemical (solute) velocity (cm/yr).

Harley and Graham-Bryce (1980) have shown that  $R$  is equivalent to the ratio of total to dissolved chemical. Consider a soil element with volume one  $\text{cm}^3$  containing an organic chemical which is both dissolved in soil water and adsorbed to soil particles. Total chemical in the element is:

$$C = fd + ba \quad (111-79)$$

where

$c$  = total chemical ( $\mu\text{g}/\text{cm}^3$ )

$d$  = concentration of chemical in the soil water ( $\mu\text{g}/\text{cm}^3$ )

$f$  = soil water content ( $\text{cm}^3/\text{cm}^3$ )

$a$  = concentration of chemical on soil particles ( $\mu\text{g}/\text{g}$ )

$b$  = soil bulk density ( $\text{g}/\text{cm}^3$ ).

If we assume a linear equilibrium adsorption relationship:

$$a = K_D d \quad (111-80)$$

where

$K_D$  = adsorption partition or distribution coefficient ( $\text{cm}^3/\text{g}$ )

then the ratio of total to dissolved chemical is  $(fd + bK_D d) / fd$ , or:

$$R = 1 + (bK_D/f) \quad (111-81)$$

The retardation factor is thus a function of a chemical property ( $K_D$ ) and two soil properties ( $b$  and  $f$ ). For flow in the unsaturated zone, the moisture content  $f$  is generally assumed to be field capacity. Typical field capacities and bulk densities are given in Table III-27. The partition coefficient  $K_D$  may be estimated from the octanol-water partition coefficient  $K_{OW}$  using Equations III-38 and III-36 as explained in Section 3.4.4.3.3.1. Values of  $K_{OW}$  for many organic compounds are given in Chapter 2 of this manual.

The retardation factor provides a general indication of a chemical's mobility in the soil. For nonadsorbed ions such as chloride and nitrate,  $R$  approaches unity and the chemical moves at approximately the same velocity as the percolation. For strongly adsorbed chemicals,  $R$  is much larger than one and movement through the soil is slow compared to the percolation velocity ( $u_s \ll u$ ).

The retardation factor also is used to estimate the distance which a chemical moves in  $t$  years. Thus,  $Z/X = ut/u_s t = R$ , or:

$$X = Z/R \quad (111-82)$$

where

Z = water displacement during time t (cm)

X = chemical displacement during time t (cm).

Assuming plug flow, annual water displacement (cm/yr) due to percolation is:

$$Z = Q/w \quad (III-83)$$

where

Q = annual percolation (cm)

w = available water capacity (cm).

Available water capacity is used in Equation III-83 rather than field capacity or porosity since unsaturated soils drain to field capacity during percolation, and soil water held below wilting point does not participate in the flow process. Mean values of w are given in Table III-13 or may be computed from Table III-27 as w = field capacity - wilting point.

Equations III-83, 82 and 81 can be combined to estimate the mean annual downward movement of an organic chemical:

$$X = \frac{Q/w}{1 + bK_D/f} \quad (III-84)$$

TABLE III-27

MEAN SOIL PROPERTIES (BAES AND SHARP, 1983)

Soil Type	Bulk Density (g/cm <sup>3</sup> )	Field Capacity cm <sup>3</sup> /cm <sup>3</sup>	Wilting Point cm <sup>3</sup> /cm <sup>3</sup>	Porosity cm <sup>3</sup> /cm <sup>3</sup>
Silt loam	1.33	0.35	0.13	0.49
Clay and clay loam	1.30	0.36	0.22	0.51
Sandy loam	1.50	0.22	0.08	0.43
Loam	1.42	0.32	0.13	0.46

Due to dispersion, portions of the chemical will be displaced greater or lesser distances than  $X$ . If a chemical is initially at the soil surface, the location of its center mass after percolation  $Q$  is given by  $X$  (see Figure III-24).

The time required for the chemical center of mass to reach the aquifer, and hence the mean travel time of the chemical through the unsaturated zone is:

$$T = 100H/X \quad (III-85)$$

where

$T$  = mean time for a chemical to reach the water table (yr)

$H$  = depth to the water table (m),

#### 3.7.4.2 Degradation

In the absence of chemical decomposition, even strongly adsorbed chemicals will eventually reach aquifers. The degree of groundwater pollution by an organic chemical is very much influenced by degradation or decay rates. Degradation of organic compounds is discussed in detail in Chapter 2 of this manual. A first order process is generally assumed such that:

$$c(t) = C(0) \exp(-k_s t) \quad (III-86)$$

where

$C(t)$  = chemical in the soil at time  $t$  (g/ha)

$k_s$  = decay rate ( $yr^{-1}$ ).

Equation III-86 may be used to estimate the chemical mass entering the saturated zone. From Equation III-85, the average travel time to the water table is  $T$  and hence the chemical entering the saturated zone is:

$$C(T) = C(0) \exp(-k_s T) \quad (III-87)$$

where

$C(T)$  = chemical mass entering the water table  $T$  years after leaching begins (g/ha)

$C(0)$  = initial chemical mass at the soil surface (g/ha).

Equation III-87 is only approximate because due to dispersion, portions of the chemical will require more or less time than  $T$  to reach the aquifer. Moreover, decay rates ( $k_s$ ) are uncertain for most chemicals. Although representative values are

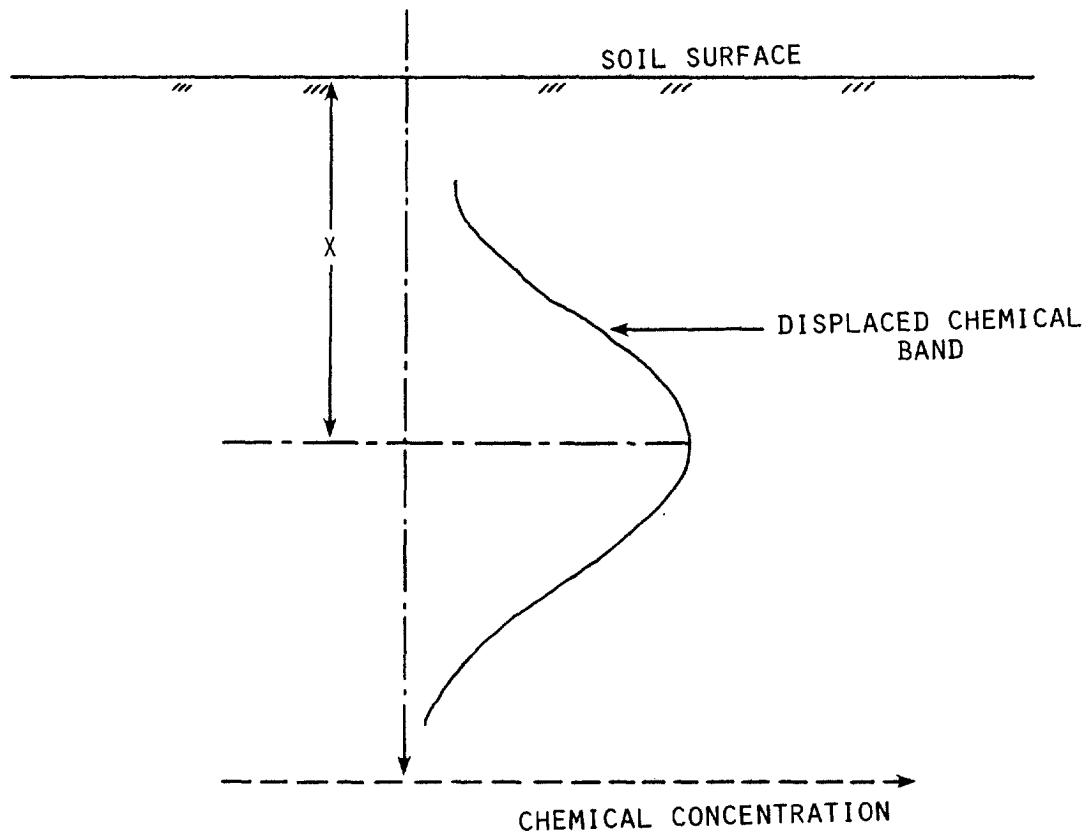


FIGURE III-24 DOWNWARD MOVEMENT OF A CHEMICAL IN SOIL

given in Chapter 2, most reported rates were measured in waste treatment systems and surface waters. Few data are available for estimation of decay rates in the subsoil.

#### 3.7.4.3 Groundwater Loads of Organic Chemicals

Equations III-84, 85 and 87 may be used to estimate organic chemical loads to aquifers. Due to the limitations of the equations (linear adsorption, first order decay, dispersion, uncertain rates, homogeneous porous media), the calculated loads should only be considered "order-of-magnitude" estimates.

#### EXAMPLE III-12

##### Napthalene Leaching from a Waste Storage Site

50,000 g/ha of napthalene is leaching from an abandoned waste disposal site. The site is on a sandy loam with 1% organic matter. Water table depth is 1.5m. Mean annual percolation is 40cm. Based on the information in Chapter 2, napthalene has an octanol-water partition coefficient of  $K_{ow} = 2300$  and a

half-life of 1700 days.

How much naphthalene will reach the aquifer and what will be the resulting naphthalene concentration at the water table surface?

Solution:

Equations III-36, 37 and 38 must be used to estimate the partition coefficient  $K_D$ :

$$K_D = K_{oc} (\%OC/100) \quad (III-36)$$

$$\%OC = 0.59 (\%OM) \quad (III-37)$$

$$K_{oc} = 0.66 K_{ow}^{1.029} \quad (III-38)$$

The organic carbon partition coefficient is:

$$K_{oc} = 0.66(2,300)^{1.029} = 1900$$

$$\%OC = 0.59(1) = 0.59$$

$$K_D = 1900(0.59/100) = 11.2$$

Bulk density (b), field capacity (f) and available water capacity (w) may be estimated from the data in Table III-27 for sandy loams:

$$b = 1.5 \text{ g/cm}^3$$

$$f = 0.22 \text{ cm}^3/\text{cm}^3$$

$$w = 0.22 - 0.08 = 0.14 \text{ cm}^3/\text{cm}^3$$

Annual naphthalene movement is given by Equation III-84:

$$X = \frac{40/0.14}{1 + 1.5(11.2)/0.22} = 3.7 \text{ cm/yr} \quad (III-84)$$

Average time to reach the water table is:

$$T = 100 H/X \quad (III-85)$$

or

$$T = 100(1.5)/3.7 = 40.5 \text{ yr.}$$

To use Equation III-87 to calculate the naphthalene remaining after 40.5 years, we must first determine the decay rate  $k_s$ . From Equation III-86, when  $t = \text{half-life} = 1700/365 = 4.66 \text{ yr}$ ,  $C(t) = 0.5C(0)$ . Hence:

$$0.5 = \exp(-4.66k_s)$$

or

$$k_s = -\ln(0.5)/4.66 = 0.149$$

Using Equation III-87:

$$\begin{aligned} C(T) &= 50,000 \exp [-0.149(40.5)] \\ &= 120 \text{ g/ha} \end{aligned}$$

Thus approximately 120 g/ha of the original 50,000 g/ha will eventually leach into the aquifer. The center of mass of the naphthalene will reach the aquifer in a little over 40 years.

To determine the naphthalene concentration in water at the aquifer surface, we must first divide the 120 g/ha into dissolved and adsorbed components. The retardation factor R is the ratio of total to dissolved chemical. Equation III-81 gives:

$$\begin{aligned} R &= 1 + bK_D/f \\ &= 1 + 1.5(11.2)/0.22 = 77 \end{aligned}$$

The dissolved naphthalene mass is 120/R:

$$120/77 = 1.56 \text{ g/ha}$$

Assuming this mass is dissolved in one year's percolation flow, 40cm = 4000m<sup>3</sup>/ha, the concentration is 1.56/4000 = 0.00039 g/m<sup>3</sup> = 0.39 µg/l.

END OF EXAMPLE III-12

### 3.8 ATMOSPHERIC WASTE LOADS

Atmospheric waste loads are direct mass inputs of pollutants from the atmosphere to surface waters. These loads occur as a result of both dry deposition and scavenging by precipitation. For the purposes of water quality screening studies, atmospheric loads are often considered constant, and are best determined by monitoring. The sum of atmospheric and background waste load (see Section 3.3), generally constitutes the minimum pollution input to a surface water body.

Regional data are available for a limited number of pollutants. Figure III-25 and Table III-28 indicate atmospheric nutrient loads for regions in the U.S.

#### 3.8.1 Dry Deposition

Pollutants occur in the atmosphere as 1) particulate; 2) gases; or 3) dissolved in water vapor. Cautreels and Van Cauwenberghe (1978) give distribution coefficients between the gas and particulate phases for 55 aliphatic hydrocarbons, polycyclic aromatic hydrocarbons, phthalic acid esters, fatty acid esters, aromatic acids and basic compounds.

Both particulate and gases may settle out onto receptor surfaces. For particles



TABLE III-28

## ATMOSPHERIC CONTRIBUTIONS OF NITROGEN AND PHOSPHORUS IN PRECIPITATION

	N Contribution in Kg/ha/yr				P Contribution in Kg/ha/yr			
	NO <sub>3</sub> -N+NH <sub>4</sub> -N		Total N		Inorganic P		Total P	
	Low	High	Low	High	Low	High	Low	High
Northeastern U.S.	5.7	12.1	5.7	12.1	-	-	-	-
Southeastern U.S.	1.5	12.3	-	-	-	-	-	-
Midwestern U.S.	0.2	20.9	1.7	20.9	-	-	-	-
West/Southwestern U.S.	1.7	5.7	9.0	14.6	-	-	-	-
United States	-	-	-	-	0.18	0.18	0.08	0.80

Source: Weiner, et al. (1976)

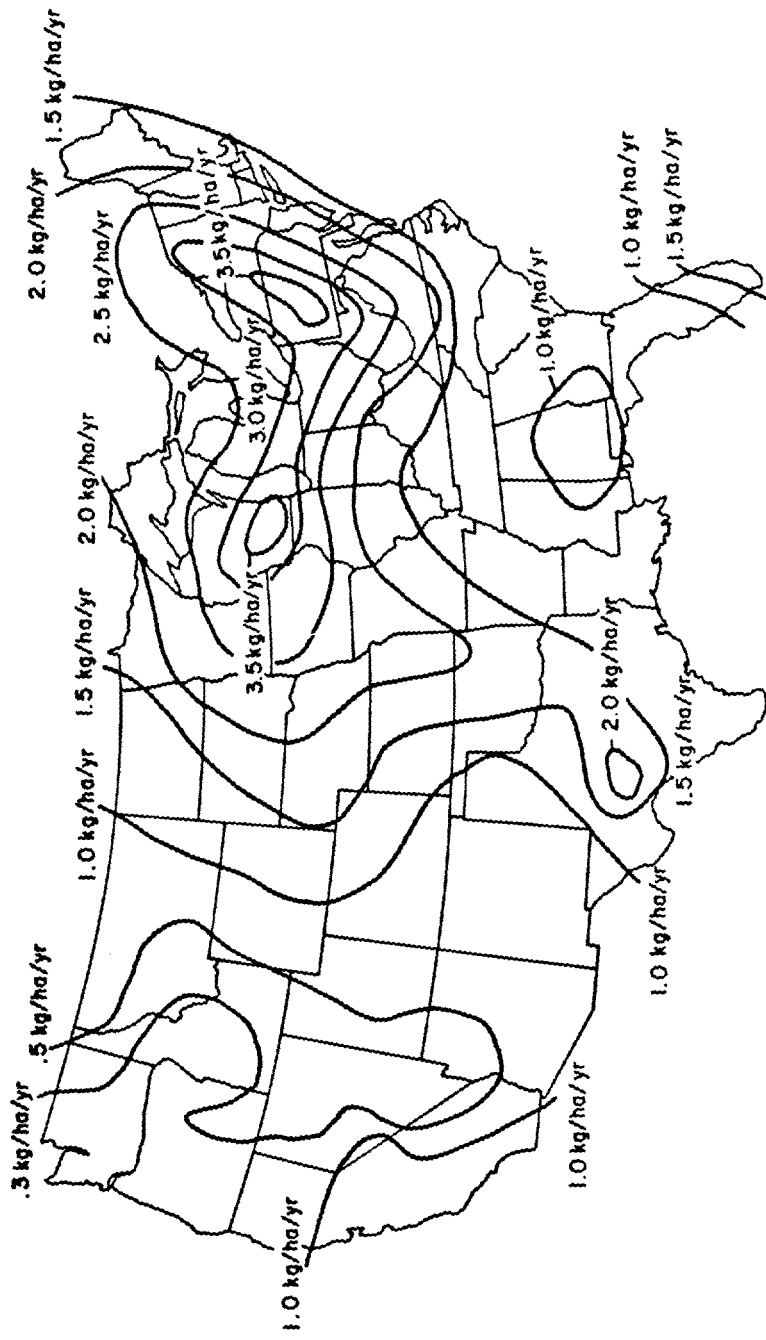


FIGURE III-25 NITROGEN ( $\text{NH}_4\text{-N}$  AND  $\text{NO}_3\text{-N}$ ) IN PRECIPITATION, (PERSONAL COMMUNICATION WITH MRI, J.H. CRAVENS, REGIONAL FORESTER, U.S.D.A-FS EASTERN REGION, 1974)

< 0.3  $\mu\text{m}$  in diameter, the major process is Brownian diffusion. For diameters 0.5 to 5  $\mu\text{m}$  inertial impaction-interception governs and for diameters > 5  $\mu\text{m}$ , gravitational settling is dominant. For gravitational settling, Stokes' Law may be used to predict the settling velocity. Since Stokes' Law is applicable only to quiescent media, it should give an upper bound for  $V_d$  (the deposition velocity). It is stated as:

$$V_d = \frac{g (ad)^2 (\rho - \rho_a)}{18\mu} \quad (\text{III-88})$$

where

- $V_d$  = settling velocity (cm/sec)
- $a$  = conversion factor ( $10^{-4}$ )
- $g$  = acceleration of gravity, 981.46 ( $\text{cm/sec}^2$ )
- $\mu$  = viscosity of air, 0.000177 ( $\text{g/cm-sec}$ ) at  $10^\circ\text{C}$
- $\rho$  = particle density,  $\sim 2$  ( $\text{g/cm}^3$ )
- $\rho_a$  = density of air, 0.001243 ( $\text{g/cm}^3$ ) at  $10^\circ\text{C}$
- $d$  = particle diameter (microns).

For particles < 5  $\mu\text{m}$  in diameter Stokes Law is not applicable and experimental values for the deposition velocity should be used. Eisenreich et al. (1981) suggest values of  $V_d = 0.1$  to 0.5 cm/sec for trace organics. Some experimental values are shown in Table III-29.

Once the settling velocity is known, the following procedure can be used to predict the dry deposition loadings:

$$L = V_d C_p A f \quad (\text{III-89})$$

where

- $L$  = load of the pollutant delivered to the receptor surface as dry deposition (mass/see)
- $V_d$  = particle settling velocity (m/sec)
- $C_p$  = concentration of atmospheric particulate (mass/ $\text{m}^3$ )
- $A$  = projected receptor area ( $\text{m}^2$ )
- $f$  = fraction (by mass) of the pollutant in the particulates.

Normally, smaller size particles are more chemically and physically reactive than larger particulate, and therefore pollutants will be associated with these smaller particles. Obviously the particle size to which pollutants are adsorbed affects their atmospheric residence time and, hence, loadings. According to Neff (1979), most polycyclic aromatic hydrocarbons are associated with particulate in the 1 to 2 micron range. Cautreels and Cauwenberghe (1978) have shown that aerosol

TABLE III-29

## FIELD-MEASURED DRY DEPOSITION VELOCITIES

Compound	$v_d$ (cm/s)	Collection Surface
PCB (Aroclor 1242, 1254)	0.5	---
PCB	0.3-3	Mineral-oil-coated plates
PCB, DDT (gas phase)	0.19	Estimated
PCB, DOT	1.0	Estimated
PCB (total)	0.14	Glycerol-coated plates
PCB (Aroclor 1016)	0.04	Glycerin-water, Al pans
PCB	0.43	---

Source: Eisenreich et al., 1981

polycyclic aromatic hydrocarbons are associated with particles of median diameter from 0.7 to 1.4  $\mu\text{m}$ . In addition, they give the concentrations of 50 trace organic compounds associated with different size particles. Higher weight polycyclic aromatic hydrocarbons, alkanes, and carboxylic acids had significant mass fractions associated with  $>1 \mu\text{m}$  diameter particles.

EXAMPLE III-13

Dry Atmospheric Deposition of Pollutants  
Adsorbed to Particulate

Estimate the maximum daily loading of pyrene to a watershed having an area of  $10^6 \text{m}^2$  overlain by an air mass having a mean daily particulate concentration of  $50 \mu\text{g}/\text{m}^3$ . The average pyrene content of the particulates is  $1.0 \times 10^{-4} \mu\text{g-pyrene}/\mu\text{g}$ . Assume a deposition velocity of 0.1 cm/sec.

Solution:

Compute the daily dry deposited load of pyrene, using Equation III-89:

$$\begin{aligned}
 L &= V_d C_p A F \\
 &= 0.001 \frac{\text{m}}{\text{sec}} \frac{50 \mu\text{g}}{\text{m}^3} 10^6 \text{m}^2 1.0 \times 10^{-4} \frac{\mu\text{g pyrene}}{\mu\text{g}} \frac{86400 \text{ sec}}{\text{day}} \\
 &= 4.32 \times 10^5 \mu\text{g/day}
 \end{aligned}$$

END OF EXAMPLE III-13

Gas phase pollutants may also be deposited directly to the watershed surface. In this case the loading equation is:

$$L = V_d C A \quad (\text{III-90})$$

where

- L = dry deposited load (mass/sec)
- $V_d$  = gas deposition velocity (m/sec)
- A = receptor area ( $\text{m}^2$ )
- C = ambient concentration of the gas phase pollutant ( $\text{mass}/\text{m}^3$ ).

EXAMPLE III-14

Dry Atmospheric Deposition of Gaseous Pollutants

Estimate the annual deposition of toxaphene to a 1 ha area at Stoneville, MS during 1974. The mean monthly atmospheric concentrations are shown in Table III-30. Assume an average deposition velocity of 0.2 cm/sec for the entire year.

Solution:

$$L = \sum_{n=1}^{12} V_d C_n A t_n$$

Month n	$V_d$ (m/sec)	$C_n$ (ng/m <sup>3</sup> )	A (m <sup>2</sup> )	$t_n$ (sec)	L (ng)
1	.002	10.9	10 <sup>4</sup>	31 x 86400	5.84 x 10 <sup>8</sup>
2	.002	9.7	10 <sup>4</sup>	28 x 86400	4.69 x 10 <sup>8</sup>
3	.002	19.1	10 <sup>4</sup>	31 x 86400	1.02 x 10 <sup>9</sup>
4	.002	27.7	10 <sup>4</sup>	30 x 86400	1.43 x 10 <sup>9</sup>
5	.002	44.3	10 <sup>4</sup>	31 x 86400	2.37 x 10 <sup>9</sup>
6	.002	38.6	10 <sup>4</sup>	30 x 86400	2.00 x 10 <sup>9</sup>
7	.002	175.0	10 <sup>4</sup>	31 x 86400	9.37 x 10 <sup>9</sup>
8	.002	903.6	10 <sup>4</sup>	31 x 86400	4.84 x 10 <sup>10</sup>
9	.002	524.6	10 <sup>4</sup>	30 x 86400	2.72 x 10 <sup>10</sup>
10	.002	114.8	10 <sup>4</sup>	31 x 86400	6.15 x 10 <sup>9</sup>
11	.002	32.9	10 <sup>4</sup>	30 x 86400	1.71 x 10 <sup>9</sup>
12	.002	12.6	10 <sup>4</sup>	31 x 86400	6.75 x 10 <sup>8</sup>
					1.01 x 10 <sup>11</sup> ng/year

or 101.4 g/year

TABLE III-30

AVERAGE MONTHLY ATMOSPHERIC LEVELS OF  
FOUR PESTICIDES AT STONEVILLE, MISSISSIPPI

	<u>Endrin (<math>\text{ngm}^{-3}</math>)</u>			<u>Toxaphene (<math>\text{ngm}^{-3}</math>)</u>		
	1972	1973	1974	1972	1973	1974
January	1.1	0.1	0.2	0.0	0.0	10.9
February	1.1	0.1	9.2	13.0	0.0	9.7
March	2.1	0.7	0.6	68.0	16.8	19.1
April	3.1	0.7	0.5	67.4	10.8	27.7
May	1.0	1.2	0.7	32.4	46.8	44.3
June	0.9	3.8	0.7	44.2	109.9	38.6
July	5.2	0.7	9.3	400.7	41.1	175.0
August	10.1	5.0	27.2	1540.0	268.8	903.6
September	8.9	8.4	18.8	827.9	322.6	524.6
October	4.0	5.0	4.3	97.9	161.1	114.8
November	0.5	1.1	1.0	9.3	0.0	32.9
December	0.0	0.2	0.5	0.0	9.9	12.6
Average	3.2	2.3	5.3	258.4	82.3	159.5

	<u>Methyl Parathion (<math>\text{ngm}^{-3}</math>)</u>			<u>Total DDT (<math>\text{ngm}^{-3}</math>)</u>		
	1972	1973	1974	1972	1973	1974
January	0.0	0.0	1.0	10.8	3.9	3.0
February	0.0	0.0	0.3	12.6	4.8	3.6
March	0.0	0.0	0.3	32.6	11.1	7.6
April	0.0	0.0	0.6	34.1	11.4	7.7
May	0.0	0.0	0.6	17.2	18.6	15.6
June	1.6	22.8	0.9	16.2	49.5	12.8
July	61.4	4.5	40.9	117.3	9.6	24.3
August	216.9	129.3	341.1	515.3	25.6	37.9
September	111.7	791.1	167.9	378.8	24.6	19.4
October	1.4	17.1	2.0	37.6	18.9	5.1
November	0.0	0.0	0.0	14.8	11.9	3.3
December	0.0	0.1	0.0	6.3	2.4	2.1
Average	32.8	80.4	46.3	99.5	16.0	11.9

Source: Arthur et al (1976)

END OF EXAMPLE III-14

### 3.8.2 Wet Deposition (Precipitation Scavenging)

Precipitation falling through the atmosphere tends to scavenge particulate and absorb gases so that it contains a variety of substances. Because of the volume of precipitation which generally occurs, it may constitute a significant pollutant loading. Load calculation for wet deposition is given by:

$$L = 10 C P A \quad (III-91)$$

where

L = load of the pollutant delivered to the receptor as wet deposition (mass/see)

C = concentration of the pollutant in precipitation (mass/liter)

P = precipitation rate (cm/sec)

A = projected receptor area (m<sup>2</sup>).

### 3.9 POINT SOURCE WASTE LOADS

The purpose of this section is to help users estimate waste loadings of toxic and conventional pollutants from municipal and industrial point sources. Removal efficiencies and discharge concentrations are both provided.

When possible site-specific data should be used in lieu of the guidance presented here. Since permitted dischargers are required to routinely monitor their discharges, often the point source data required are available.

When only a few measurements of effluent quality are available, those data may not be representative of long-term averages. Long-term averages are typically required for most of the steady-state analyses contained in this document. Figure III-26, for example, shows influent cadmium loading to the Kokomo, Indiana, wastewater treatment plant (Yost et al. , 1981). Cadmium loading appears to exhibit a weekly cycle, with loadings the lowest on Sundays. For this case, seven-day averages would be appropriate for preliminary analyses.

When using the data presented in the following sections, users should keep in mind the variability of removal efficiencies and influent and effluent pollutant concentrations between point sources. The following factors all contribute to effluent quality variability:

- Geographic location
- Climate
- Mixture of influent sources (industrial/domestic)
- Size of community
- Design flow rate versus actual flow rate.



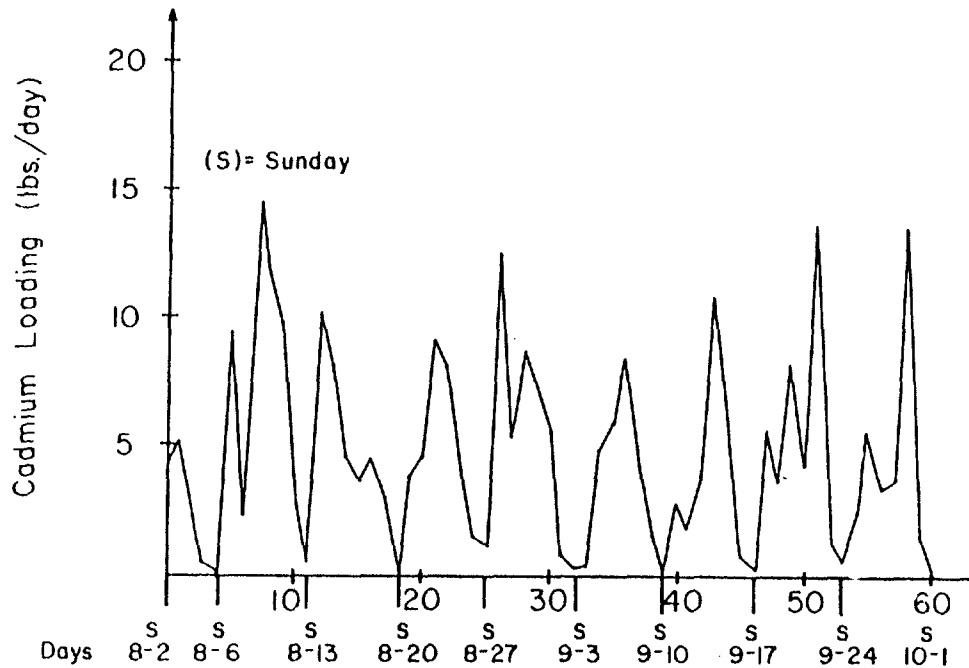


Figure III-26 INFLUENT CADMIUM LOADING TO PLANT DURING STUDY  
(FROM YOST ET AL., 1981)

### 3.9.1 Municipal Waste Loads

Table III-31 summarizes typical influent concentrations of conventional pollutants for wastewater treatment plants. Concentration ranges are shown for strong, medium, and weak wastewater. Table III-32 summarizes typical removal efficiencies of common conventional pollutants from a variety of wastewater treatment plant types. Scheme number 0 in the table denotes the raw wastewater characteristics. The table shows both percent removal and effluent concentrations based on the characteristics of the raw wastewater chosen. The removal efficiencies can be used for the range of concentrations shown previously in Table III-31, assuming the plant is operating within design conditions.

Table III-33 summarizes effluent phosphorus and nitrogen concentrations for 662 primary treatment plants, trickling filters, activated sludge plants, and stabilization ponds. The data were collected as part of the National Eutrophication Survey initiated by the U.S. Environmental Protection Agency in 1972 (Gakstatler *et al.*, 1978). The user can cross-compare effluent nutrient levels predicted based on joint use of Tables III-31 and III-32 against the values in Table III-33 to help get a typical range of values. Table III-33 also shows per capita flow rates, per capita total phosphorus loads, and per capita total nitrogen loads for each treatment type. These

TABLE III-31

## TYPICAL INFLUENT MUNICIPAL WASTE CONCENTRATIONS

Constituent	Concentration mg/L		
	Strong	Medium**	Weak
Solids, total	1,200	720	350
Dissolved, total	850	500	250
Fixed	525	300	145
Volatile	325	200	105
Suspended, total	350	220	100
Fixed	75	55	20
Volatile	275	165	80
Settleable solids, (ml/liter)	20	10	5
Biochemical oxygen demand, 5-day, 20° (BOD <sub>5</sub> -20°)	400	220	110
Total organic carbon (TOC)	290	160	80
Chemical oxygen demand (COD)	1,000	500	250
Nitrogen, (total as N)	85	40	20
Organic	35	15	8
Free ammonia	50	25	12
Nitrites	0	0	0
Nitrates	0	0	0
Phosphorus (total as P)	15	8	4
Organic	5	3	1
Inorganic	10	5	3
Chlorides*	100	50	30
Alkalinity (as CaCO <sub>3</sub> )*	200	100	50
Grease	150	100	50

\*Values should be increased by amount in carriage water.

\*\*In the absence of other data use medium strength data for planning purposes.

Source: Metcalf and Eddy, 1979

TABLE III-32

## MUNICIPAL WASTEWATER TREATMENT SYSTEM PERFORMANCE

Influent: see Scheme Number 0 for assumed characteristics.

Scheme Number**	Effluent Concentrations (mg/l), (% Total Removal			Efficiencies*)	
	<u>BOD<sub>5</sub></u>	<u>COD</u>	<u>SS</u>	<u>P<sub>T</sub>, (mgP/l)</u>	<u>N<sub>T</sub>, (mgN/l)</u>
0 Raw waste water	200(0%)	500(0%)	200(0%)	10(0%)	40(0%)
1	130(35%)	375(25%)	100(25%)	9(10%)	32(20%)
2	40(80%)	125(75%)	30(85%)	7.5(25%)	26(35%)
3	25(88%)	100(80%)	12(94%)	7(30%)	24(40%)
4	18(91%)	70(86%)	7(96%)	1(90%)	22(45%)
5	18(91%)	70(86%)	7(96%)	1(90%)	4(90%)
6	13(94%)	60(88%)	1(99.5%)	1(90%)	3(92%)
7	2(99%)	15(97%)	1(99.5%)	1(90%)	2(95%)

\*Efficiencies for wastewater treatment are for the approximate concentration range, as measured by BOD<sub>5</sub>, of  $100 \leq \text{BOD}_5 \leq 400$ , (mg/l).

**Scheme No.	Process
0	No treatment
1	Primary
2	Primary, plus Activated Sludge (Secondary Treatment)
3	Primary, Activated Sludge, plus <u>Polishing Filter</u> (High Efficiency Or Super Secondary)
4	Primary, Activated Sludge, <u>Polishing Filter</u> , plus <u>Phosphorus Removal and Recarbonation</u>
5	Primary, Activated Sludge, <u>Polishing Filter</u> , Phosphorus Removal, plus <u>Nitrogen Stripping and Recarbonation</u>
6	Primary, Activated Sludge, <u>Polishing Filter</u> , Phosphorus Removal, <u>Nitrogen Stripping Recarbonation</u> , plus <u>Pressure Filtration</u>
7	Primary, Activated Sludge, <u>Polishing Filter</u> , Phosphorus Removal, <u>Nitrogen Stripping Recarbonation</u> , <u>Pressure Filtration</u> , plus <u>Activated Carbon Adsorption</u>

Source: Meta Systems, 1973

TABLE III-33  
 MEDIAN AND MEAN PHOSPHORUS AND NITROGEN CONCENTRATION AND  
 MEDIAN LOADS IN WASTEWATER EFFLUENTS FOLLOWING FOUR  
 CONVENTIONAL TREATMENT PROCESSES (Gakstatter *et al.* , 1978)

		Treatment Type			
		Primary	Trickling Filter	Activated Sludge	Stabilization Pond
Number of Sampled Plants		55	244	244	119
Total Population Served		1,086,784	3,459,893	4,357,138	270,287
Ortho-P Conc. (mg/l)	Median	3.5 ± 0.29*	5.1 ± 0.21	4.6 ± 0.24	3.9 ± 0.34
	Mean	4.0 ± 0.62	5.4 ± 0.38	5.3 ± 0.40	4.87 ± 0.62
Total -P Conc. (mg/l)	Median	6.6 ± 0.66	6.9 ± 0.28	5.8 ± 0.29	5.2 ± 0.45
	Mean	7.7 ± 1.19	7.2 ± 0.50	6.8 ± 0.51	6.6 ± 0.81
Total -P Load (kg/cap·y)	Median	1.1 ± 0.10	1.2 ± 0.05	1.0 ± 0.06	0.9 ± 0.10
Total -N Load (kg/cap·y)	Median	3.7	2.9	2.4	2.0
Inorganic-N Conc. (mg/l)	Median	6.4 ± 1.00	7.1 ± 0.38	6.5 ± 0.45	1.3 ± 0.29
	Mean	8.3 ± 1.40	8.2 ± 0.60	8.4 ± 0.69	5.5 ± 1.95
Total -N Conc. (mg/l)	Median	22.4 ± 1.30	16.4 ± 0.54	13.6 ± 0.62	11.5 ± 0.84
	Mean	23.8 ± 3.48	17.9 ± 1.23	15.8 ± 1.16	17.1 ± 3.59
Total -N Load	Median	4.2 ± 0.40	2.9 ± 0.17	2.2 ± 0.15	2.0 ± 0.26
TN: TP Ratio	Median	3.4	2.4	2.4	2.2
Per Capita Flow (l/cap·d)	Median	473 ± 72	439 ± 19	394 ± 26	378 ± 38

\*Value ± 1 standard error.

can be used to generate loadings based on population served. The typical per capita flow ranges between 378 and 473  $\ell/(\text{cap-d})$ .

Table III-34 summarizes phosphorus removal from plants that use chemical addition for phosphorus removal. The phosphorus removal efficiencies vary from 71 percent to 98 percent, and average 85 percent. This is only 5 percent lower than the percent phosphorus removals shown earlier in Table III-32 for process types 4 through 7 (which included phosphorus removal processes).

Barth and Stensel (1981) also summarize nitrogen removal performance of single-stage and two-stage activated sludge nitrification plants, but do not report removal efficiencies for the nitrification augmented processes.

Removal of metals and toxic organics from municipal wastewater treatment plants has been monitored over a considerably shorter historical time span than for the conventional pollutants. Table III-35 summarizes influent metal concentrations, effluent metal concentrations, and removal efficiencies for treatment plants at selected cities (Yost *et al.*, 1981). From the table, it is clearly seen that there is a wide variability in influent metal concentrations, effluent concentrations, and removal efficiencies (even for the same type of treatment process). The variability of influent concentrations is not unexpected due to the variety of sources that contribute to municipal wastewater. Minear *et al.* (1981) have shown that the correlation between influent metal concentrations and percent industrial flow is very poor. Figure III-27 illustrates for copper. However, for a single treatment plant with fixed industrial sources, the correlation should be better.

E. C. Jordan Co. (1982) documents a 30-day study of priority pollutants at the Moccasin Bend wastewater treatment plant in Chattanooga, Tennessee. The plant is a 42 MGD conventional-activated sludge treatment plant that treats an average dry weather flow of 42 MGD. Approximately 50 percent of the flow originates from industry. Table III-36 summarizes the variability of influent priority pollutants, BOD, and TSS. Table III-37 summarizes the removal efficiencies for the primary and secondary units. Note the generally poor removal efficiencies associated with primary treatment. A number of the pollutants do not appear to be removed at all.

Table III-38 summarizes effluent concentrations in five Southern California wastewater treatment plants. Note that these are generally very large dischargers (four are over 100 MGD), and may not be typical of smaller plants. The effluent trace metal concentrations are, in many cases, higher than the influent concentrations at the Moccasin Bend plant.

The most comprehensive study to date on priority pollutants in publicly owned treatment plants was completed by Burns and Roe (1982). They collected data from 40 POTWs. Table III-39 summarizes the occurrence of priority pollutants in the influents and effluents of the 40 plants for pollutants detected in at least 10 percent of the samples. Note the high occurrence of metals in both influent and effluent samples.

TABLE III-34

## YEARLY AVERAGE PHOSPHORUS REMOVAL PERFORMANCE (Barth and Stensel, 1981)

Plant	Design Capacity (mgd)	Flowsheet	Chemical & Addition Point	Performance, mg/l		Phosphorus Removal Efficiency
				BOD <sub>5</sub>	Total P	
Angola, N.Y.	3.1	Extended aeration--solids contact--tertiary filter	FeCl <sub>3</sub> + polymer to solids contact	Infl. Effl. 130 2	264 2	6.8 0.9 87%
Ely, Minn.	1.0	Primary--rock trickling filter--solids contact--tertiary filter	Alum + polymer before secondary clarifier	Infl. Effl. 180 15	123 13	3.8 0.6 84%
Roanoke, Va.	35	Primary--2-stage activated sludge--nitrification--flocculation--tertiary filter	Pickle liquor to 1st stg. aeration and alum/polymer before flocculation basin	Infl. Effl. 220 2	340 1	11.9 0.2 98%
Rochester, N.Y.	20	Primary--activated sludge	Alum before final clarifier	Infl. Effl. 186 16	165 9	6.3 0.8 87%
Gladstone, Mich.	1.0	Primary--rotating biological contactor	Alum prior to RBC	Infl. Effl. 129 12	118 16	3.5 0.9 74%
Grand Haven, Mich.	3.2	Primary--activated sludge (domestic & tannery)	Pickle liquor before primary	Infl. Effl. 389 16	432 19	5.0 0.6 88%
Blue Plains, D.C.	330	Primary--2-stage activated sludge--nitrification	FeCl <sub>3</sub> to secondary	Infl. Effl. 140 28	135 28	6.2 1.8 71%
Lima, Ohio	18.5	Primary--activated sludge--nitrification towers	FeCl <sub>3</sub> + polymer prior to primaries	Infl. Effl. 157 5	126 9	5.1 0.8 84%
Marlborough, Mass.	5.5	Primary--2-stage activated sludge--nitrification	Alum or FeSO <sub>4</sub> to 1st-stg. aeration	Infl. Effl. 159 3	306 8	6.8 0.6 91%

TABLE III-35

METAL CONCENTRATIONS AND REMOVAL EFFICIENCIES  
IN TREATMENT PLANTS AT SELECTED CITIES

City	Treatment Received		Cd	Cr	Cu	Ni	Zn	Fe	Pb
Anderson, Indiana	Secondary Treatment	Influent, µg/l	9.5	1180	2820	2790	1500	-	160
		Effluent, µg/l	3.9	142	395	885	375	-	40
		Removal Efficiencies, %	59	88	86	41	75	-	75
Buffalo, New York	Secondary Treatment	Influent, µg/l	18	208	137	50	337	-	99
		Effluent, µg/l	11.2	78.6	53.4	44.5	704	-	25.9
		Removal Efficiencies, %	37.7	62.2	61.0	11.0	41.3	-	73.8
Dayton, Ohio	Trickling Filters	Influent, µg/l	27	-	-	-	-	-	-
		Effluent, µg/l	16	-	-	-	-	-	-
		Removal Efficiencies, %	40.7	-	-	-	-	-	-
Grand Rapids, Michigan	Secondary Treatment	Influent, µg/l	-	400	500	500	1200	-	-
		Effluent, µg/l	-	136-325	215-435	295-410	588-780	-	-
		Removal Efficiencies, %	-	19-66	13-57	18-41	35-51	-	-
Muddy Creek, Ohio	Conventional Activated Sludge	Influent, µg/l	8	-	-	-	-	-	-
		Effluent, µg/l	62.5	-	-	-	-	-	-
		Removal Efficiencies, %	3	-	-	-	-	-	-
Muncie, Indiana	Secondary Treatment	Influent, µg/l	-	240	260	140	1150	-	930
		Effluent, µg/l	-	53	83	140	345	-	167
		Removal Efficiencies, %	-	78	68	0	70	-	82

TABLE III-35  
(Continued)

City	Treatment Received		Cd	Cr	Cu	Ni	Zn	Fe	Pb
Pittsburgh, Pennsylvania	Secondary Treatment	Influent, µg/l	21	95	127	78	648	-	119
		Effluent, µg/l	7	31	56	70	227	-	23
		Removal Efficiencies, %	67	67	56	10	65	-	81
Hawaii, Hawaii	Step Aeration	Influent, µg/l	5-65	12-18	62-90	60-70	200-320	1000-1180	40-70
		Effluent, µg/l	2-27	8-12	16-23	35-41	53-93	150-177	11-19
		Removal Efficiencies, %	59	32	74	42	71	85	73
Winnipeg, Man.	Pure Oxygen	Influent, µg/l	-	166	210	32	329	-	117
		Effluent, µg/l	-	53	48	32	66	-	60
		Removal Efficiencies, %	-	68	77	0	80	-	49
Burlington, Ontario	Conventional Activated Sludge	Influent, µg/l	6	290	310	330	2400	1540	230
		Effluent, µg/l	1	61	84	277	552	416	16
		Removal Efficiencies, %	80	79	73	16	77	73	93
Average of 6 Cities near Kansas City	-	Influent, µg/l	20.2	220	146	-	733	-	210
		Effluent, µg/l	-	-	-	-	-	-	-
		Removal Efficiencies, %	16	37	49	-	47	-	49
Survey of 20 Plants in Ontario	-	Influent, µg/l	20	970	300	110	1120	6580	170
		Effluent, µg/l	-	-	-	-	-	-	-
		Removal Efficiencies, %	19	62	54	42	56	69	51



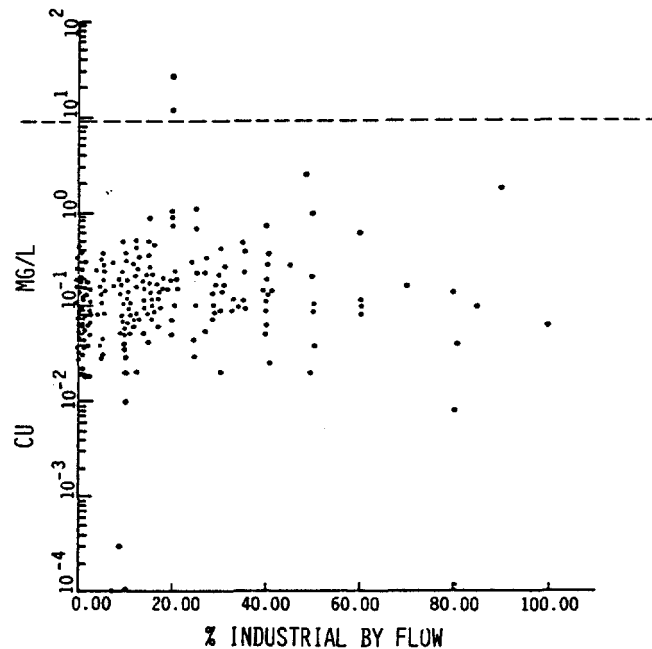


FIGURE III-27 INFLUENT COPPER CONCENTRATIONS TO WASTEWATER TREATMENT PLANTS AS A FUNCTION OF PERCENT INDUSTRIAL FLOW

Table III-40 summarizes removal efficiencies of a number of the pollutants as a function of different types of treatment. There is a significant increase in percentage removal between primary treatment plants and secondary activated sludge treatment plants for each of the pollutants in the table.

### 3.9.2 Industrial Waste Loads

Compared to municipal discharges, effluent levels from industrial sources are less easily predictable because of the variety of categories and treatment processes used. Table III-41 shows 35 major industrial categories and frequently detected priority pollutants associated with the categories. Keith and Telliard (1979) have estimated the frequency of occurrence of the priority pollutants in industrial wastewater. Their results were shown previously in Table II-3. If industrial wastes are thought to contribute a significant percentage of pollutants to the water body being analyzed, the user should try to obtain more specific data on the industries present. Local agencies can provide effluent data for the industries in question. However, the industries may not be required to monitor for the specific pollutant(s) of concern. The Effluent Guidelines Division of the U.S. EPA can also provide guidelines for specific categories of pollutants. They have developed extensive documentation for each major industrial category. The "treatability manual" (USEPA, 1982a, b, c, d) is one such source that contains data related to approximately 200 pollutants associated with industrial processes. The manual contains the following information:

TABLE III-36

## INFLUENT VARIABILITY ANALYSIS AT MOCCASIN BEND WASTEWATER TREATMENT PLANT

Parameter(1)	30-Day Study		Six-Day Study	
	Mean ( $\mu\text{g}/\text{L}$ )	Standard Deviation ( $\mu\text{g}/\text{L}$ )	Mean ( $\mu\text{g}/\text{L}$ )	Standard Deviation ( $\mu\text{g}/\text{L}$ )
<u>Volatiles</u>				
Benzene	18	12	14	8
1, 1, 1-Tri chloroethane	20	49	43	49
Chloroform	73	36	77	59
1, 2-Trans-Di chloro- ethyl ene	1	1	2	1
Ethyl benzene(2)	23	18	20	17
Methyl ene Chlori de(2)	88	86	40	30
Tolu ene(2)	321	325	378	236
Tri chloroethyl ene	26	51	10	12
Tetrachl oroethyl ene	52	87	81	52
<u>Acids</u>				
Phenol	201	155	448	209
2, 4-Di chlorophenol	5	7	2	2
<u>Base/Neutrals</u>				
1, 2, 4-Tri chlorobenzene	17	22	100	45
1, 3-Di chlorobenzene	2	6	1	1
1, 4-Di chlorobenzene	5	8	4	3
Naphthal ene	11	11	55	45
Bis(2-Ethyl hexyl ) Phthal ate	12	15	14	7
Di -N-Butyl Phthal ate	5	14	4	2
Di ethyl Phthal ate	4	8	6	3
Phenanthrene	1	2	3	1
<u>Metals</u>				
Chromi um	225	527	226	160
Copper	77	25	123	24
Cyani de	83	84	4747	1664
Mercury(ng/l )	303	270	333	816
Ni ckel	73	76	98	37
Si lver	5	2	21	7
Zi nc	332	164	486	132
<u>Conventional</u>				
<b>BOD<sub>5</sub></b>	303	115	435	112
TSS	232	93	327	95

1 Influent variability analysis conducted on priority toxic pollutants detected 50 percent of the time or greater in addition to lead and cadmium for combined 36-day period.

2 Outlier values were removed from data base.

TABLE III-37

SELECTED POLLUTANT MASS PERCENT REMOVALS AT  
MOCCASIN BEND WASTEWATER TREATMENT PLANT

<b>Pollutant</b> <sup>1</sup>	<u>Percent Removal</u>		
	Primary Treatment	Secondary Treatment <sup>2</sup>	Overall Treatment
<u>Metals</u>			
Cadmium	25	42	56
Chromium	0	95	79
Copper	21	75	80
Cyanide	0	15	11
Lead	12	69	69
Mercury	21	100	100
Nickel	0	49	49
Silver	17	83	86
Zinc	18	70	75
<u>Volatiles</u>			
Benzene	7	78	80
1, 1, 1-Trichloroethane	13	80	82
Chloroform	1	56	56
1, 2-Trans-Dichloroethylene	0	100	100
Ethylbenzene	0	89	87
Methylene Chloride	16	47	55
Tetrachloroethylene	25	88	91
Toluene	10	86	87
Trichloroethylene	42	78	87
<u>Acids</u>			
Phenol	0	92	91
2, 4-Dichlorophenol	2	46	47
<u>Base/Neutrals</u>			
1, 2, 4-Trichlorobenzene	12	79	82
1, 3-Dichlorobenzene	14	30	40
1, 4-Dichlorobenzene	0	88	88
Naphthalene	0	92	91
Bis(2-Ethylhexyl) Phthalate	0	77	57
Di-N-Butyl Phthalate	40	6	44
Diethyl Phthalate	0	36	0
Phenanthrene	0	36	0
<u>Conventional /Non-Conventional</u>			
<b>BOD<sub>5</sub></b>	10	86	88
TSS	30	82	87

<sup>1</sup> Priority toxic pollutants listed were detected in the influent wastewater 50 percent of the time or greater (with the exception lead and cadmium which were detected 46 percent of the time).

<sup>2</sup> Percent removal based on mass removal, in activated sludge treatment units alone.

TABLE III-38

1981 EFFLUENT CONCENTRATIONS FROM FIVE SOUTHERN  
CALIFORNIA WASTEWATER TREATMENT PLANTS

	Hyperion			Orange County	Point Loma	Oxnard
	JWPCP	5 mile	7 mile (Sludge)			
Flow MGD	364	369	4.72	212	130	17.7
General Constituents (mg/l)						
Suspended Solids	167	77	7,100**	119	114	56.9
Settled Solids	0.3	0.9		1.1	0.95	<0.1
BOD	202	169		151	161	114
Oil + Grease	23.3	22	353	21.1	29.3	12.2
NH <sub>3</sub> -N	39.3	16.1	-	25.7	27.7	17.0
Organic-N	14.0	7.3	266	-	-	5.09
Total -P	9.2	6.9	214	-	-	-
MBAS	5.37	4.12	-	-	4.38	-
CN	0.08	0.08	0.442	0.04	0.013	0.001
Phenols	2.85	0.06	0.37	0.09	0.073	0.10
Turbidity	79	63	-	79	53	44
Toxicity (T.U.)	4.2	0.81	-	1.0	1.3	2.1
Trace Metals ( $\mu\text{g/l}$ )						
Ag	8.0	25.0	739.0	13.0	13.0	3.0
As	<b>5.0</b>	12.0	183.0	3.0	5.0	20.0
Cd	<b>16.0</b>	17.0	892.0	26.0	8.0	3.0
Cr	11.0	54.0	3,340.0	82.0	43.0	0.1
Cu	154.0	200.0	9,320.0	248.0	133.0	93.0
Hg	1.8	0.7	36.0	0.4	0.8	0.05
Ni	148.0	108.0	2,400.0	69.0	7.5	6.0
Pb	0.0	50.0	2,000.0	74.0	136.0	11.0
Se	29.0	1.0	44.0	-	-	-
Zn	500.0	217.0	11,800.0	220.0	190.0	91.0
Chlorinated Hydro- carbons ( $\mu\text{g/l}$ )						
DDT	0.84	0.050	0.58	0.02	0.084	Not de- tected
PCB	0.54	0.76	3.05	1.55	0.665	<0.033
TI CH	1.61	0.94	4.68	1.56	0.816	<0.033
*except as noted						
**Total solids						

TABLE III-39

OCCURRENCE OF PRIORITY POLLUTANTS IN POTW  
INFLUENTS AND EFFLUENTS FOR POLLUTANTS DETECTED  
IN AT LEAST 10 PERCENT OF THE SAMPLES (BURNS AND ROE, 1982)

Parameter	INFLUENT					
	Number of Samples Analyzed	Number of Times Detected	Percent of Samples Where Detected	Units	Minimum Value Detected	Maximum Value
Zinc	282	282	100	ug/l	22	9250
Cyanide	284	283	100	ug/l	3	7580
Copper	282	281	100	ug/l	7	2300
Toluene	288	276	96	ug/l	1	13000
Chromium	282	268	95	ug/l	8	2380
Tetrachloroethylene	288	273	95	ug/l	1	5700
Methylene chloride	288	266	92	Ug/l	1	49000
bis(2-Chloroethoxy)methane	287	265	92	ug/l	2	670
Chloroform	288	263	91	ug/l	1	430
Trichloroethylene	288	260	90	ug/l	1	1800
1,1,1-Tri chloroethane	288	244	85	ug/l	1	30000
Ethyl benzene	288	231	80	ug/l	1	730
Nickel	282	224	79	ug/l	5	5970
Phenol	288	220	79	ug/l	1	1400
Silver	282	208	71	ug/l	2	320
Mercury	282	196	70	ug/l	200	4000
Di-n-butyl phthalate	287	185	64	ug/l	1	140
Lead	282	176	62	ug/l	16	2540
1,2-trans-Di chloroethyl ene	288	179	62	ug/l	1	200
Benzene	288	175	61	ug/l	1	1560
Butyl benzyl phthalate	287	165	57	ug/l	2	560
Cadmium	282	157	56	ug/l	1	1800
Diethyl phthalate	287	151	53	ug/l	1	42
Napthalene	287	142	49	ug/l	1	150
1,1-Di chloroethane	288	89	31	ug/l	1	24
Pentachlorophenol	287	84	29	ug/l	1	640

TABLE III-39  
(Continued)

Parameter	INFLUENT					
	Number of Samples Analyzed	Number of Times Detected	Percent of Samples Where Detected	Units	Minimum Value Detected	Maximum Value
<b>γ-BHC</b>	288	75	26	ng/l	20	3900
1, 1-Di chloroethyl ene	288	74	26	ug/l	1	243
1, 2-Di chlorobenzene	287	67	23	ug/l	1	440
Phenanthrene	287	57	20	ug/l	1	93
Anthracene	287	52	18	ug/l	1	93
1, 4-Di chlorobenzene	287	49	17	ug/l	2	200
Arsenic	282	43	15	ug/l	2	80
1, 2-Di chloroethane	288	42	15	ug/l	1	76000
Antimony	282	39	14	ug/l	1	192
Chlorobenzene	288	36	13	ug/l	1	1500
Dimethyl phthalate	287	33	11	ug/l	1	110
Methyl chloride	288	33	11	ug/l	1	1900
1, 2, 4-Tri chlorobenzene	287	28	10	ug/l	3	4300
2, 4-Dimethyl phenol	288	28	10	ug/l	1	55
Parameter	EFFLUENT					
	Number of Samples Analyzed	Number of Times Detected	Percent of Samples Where Detected	Units	Minimum Value Detected	Maximum Value
Cyanide	276	268	97	ug/l	2	2140
Zinc	289	272	94	ug/l	18	3150
Copper	289	263	91	ug/l	3	255
Methylene chloride	302	260	86	ug/l	1	62000
Chromium	289	247	85	ug/l	2	759
bis(2-Ethyl hexyl) phthalate	302	254	84	ug/l	1	370

TABLE III-39  
(Continued)

Parameter	EFFLUENT					
	Number of Samples Analyzed	Number of Times Detected	Percent of Samples Where Detected	Units	Minimum Value Detected	Maximum Value
Chloroform	302	247	82	ug/l	1	87
Tetrachloroethylene	302	239	79	ug/l	1	1200
Nickel	289	216	75	ug/l	7	679
Toluene	302	160	53	ug/l	1	1100
Di-n-butyl phthalate	302	158	52	ug/l	1	97
1,1,1-Tri chloroethane	302	157	52	ug/l	1	3500
Tri chloroethylene	302	137	45	ug/l	1	230
<b>Y-BHC</b>	303	99	33	ug/l	10	1400
Mercury	288	86	31	ug/l	200	1200
Phenol	302	87	29	ug/l	1	89
Cadmium	289	81	28	ug/l	2	82
Silver	289	73	25	ug/l	1	30
Ethyl benzene	302	73	24	ug/l	1	49
Benzene	302	69	23	ug/l	1	72
Lead	289	61	21	ug/l	20	217
Pentachlorophenol	301	63	21	ug/l	1	440
Dichlorobromomethane	302	47	16	ug/l	1	6
Diethyl phthalate	301	39	13	ug/l	1	7
1,2-trans-Dichloroethylene	302	39	13	ug/l	1	17
Antimony	289	37	13	ug/l	1	69
Arsenic	289	35	12	ug/l	1	72
Butyl benzyl phthalate	302	34	11	ug/l	1	34
Selenium	289	29	10	ug/l	1	150
1,1-Dichloroethylene	302	29	10	ug/l	1	11

TABLE III-40

MEDIAN PERCENT REMOVALS OF SELECTED POLLUTANTS  
THROUGH POTW TREATMENT PROCESSES (BURNS AND ROE, 1982)

Parameter	Primary	Secondary Activated Sludge *	Secondary Trickling Filter	Secondary O <sub>2</sub> Activated Sludge	Secondary Rotating Biological Contactors	Secondary Aerated Lagoon	Parallel		
							Activated Sludge Side	Filter Plants	
								Activated Sludge Side	Trickling Filter Side
BOD	(12) 19	(22) 90	(5) 77	(3) 91	(1) 92	(1) 80	(4) 92	(4) 82	(8) 93
Total suspended solids	(12) 45	(22) 90	(5) 78	(3) 84	(1) 58	(1) 77	(4) 94	(4) 91	(8) 94
Cadmium	(6) 15	(6) 85	(1) 11	(2) 83	(0) -	(1) 44	(2) 91	(2) 84	(3) 78
Chromium	(12) 27	(22) 84	(3) 48	(3) 76	(0) -	(1) 49	(4) 75	(4) 63	(8) 89
Copper	(12) 22	(22) 84	(5) 49	(3) 92	(1) 97	(1) 21	(4) 89	(4) 75	(8) 90
Cyanide	(12) 27	(22) 62	(5) 57	(3) 80	(1) 96	(1) 7	(4) 66	(4) 68	(3) 57
Lead	(1) 57	(2) 82	(1) 20	(1) 97	(0) -	(1) 0	(0) -	(0) -	(1) 81
Mercury	(8) 10	(8) 76	(2) 56	(3) 83	(0) -	(1) 0	(2) 91	(2) 49	(5) 78
Nickel	(9) 14	(15) 34	(2) 47	(2) 18	(0) -	(1) 14	(4) 34	(4) 0	(5) 39
Silver	(4) 20	(5) 83	(2) 55	(2) 80	(0) -	(1) 0	(2) 79	(2) 83	(1) 75
Zinc	(12) 27	(22) 81	(5) 43	(3) 81	(1) 81	(1) 51	(4) 82	(4) 73	(8) 84
Benzene	(8) 25	(10) 77	(3) 80	(2) 87	(0) -	(0) -	(1) 92	(1) 92	(1) 99
bis(2-Ethylhexyl)phthalate	(12) 0	(8) 62	(5) 24	(3) 64	(1) 86	(1) 23	(4) 87	(4) 72	(8) 65
Butyl benzyl phthalate	(4) 62	(2) 94	(1) 70	(3) 84	(0) -	(1) 93	(1) 80	(1) 93	(3) 86
Chloroform	(11) 14	(20) 62	(5) 75	(3) 50	(0) -	(0) -	(3) 75	(4) 69	(7) 41
Di-n-butyl phthalate	(3) 36	(6) 68	(5) 50	(1) 98	(0) -	(1) 50	(1) 97	(3) 50	(0) -
Diethyl phthalate	(1) 56	(2) 91	(0) -	(0) -	(0) -	(0) -	(0) -	(0) -	(0) -
Ethylbenzene	(12) 13	(10) 90	(5) 90	(3) 86	(0) -	(1) 83	(3) 97	(4) 89	(7) 86



TABLE III-40

(Continued)

Parameter	Primary	Secondary Activated Sludge*	Secondary Trickling Filter	Secondary O <sub>2</sub> Activated Sludge	Secondary Rotating Biological Contactors	Secondary Aerated Lagoon	Parallel Activated Sludge/Trickling Filter Plants		
							Activated Sludge Side	Trickling Filter Side	Tertiary
Methylene chloride	(12) 0 (14) 48 (5) 76 (3) 34 (0) - (1) 96 (4) 52 (4) 32 (8) 78								
Napthalene	(4) 44 (6) 92 (0) - (0) - (0) - (4) 84								
Pheno1	(11) 8 (15) 89 (0) - (3) 99+ (1) 99+ (1) 50 (3) 89 (3) 94 (6) 95								
Tetrachloroethylene	(12) 4 (20) 82 (5) 82 (3) 75 (1) 50 (1) 91 (4) 76 (4) 62 (8) 94								
Toluene	(12) 0 (21) 93 (5) 88 (3) 99+ (1) 99+ (1) 89 (4) 97+ (4) 93 (8) 98								
Trichloroethylene	(12) 20 (20) 90 (5) 96 (2) 67 (1) 67 (1) 97 (4) 97 (4) 95 (7) 97								
1,1,1-Trichloroethane	(10) 40 (17) 88 (5) 92 (3) 80 (0) - (1) 91 (3) 99+ (3) 91 (7) 96								
1,2-trans-Dichloroethylene	(9) 36 (19) 80 (4) 97 (2) 85 (0) - (1) 88 (0) - (0) 88 (3) 88								

\*POTW 8, predominantly (96 percent) activated sludge, was included in the activated sludge plants.

Note: Number in ( ) is number of plants with calculated removals.

Only plants with average influent concentrations greater than three times the most frequent detection limit of each pollutant are included in removal calculations.

TABLE III-41

INDUSTRIAL CATEGORIES AND FREQUENTLY DETECTED  
PRIORITY POLLUTANTS BY CATEGORY

	Soaps & Detergents	Adhesives & Sealants	Leather	Textiles	Gum & Wood	Pulp & Paper	Timber	Printing & Publishing	Paint & Ink	Pesticides	Pharmaceuticals	Organics & Plastics	Rubber	Coal Mining	Ore Mining	Paving & Roofing	Steam & Electric	Petroleum Refining	Iron & Steel	Foundries	Electroplating	Nonferrous Metals	Batteries	Coil Coating	Photographic	Inorganic Chemicals	Electrical	Auto & Other Laundries	Phosphates	Plastics Processing	Explosives	Porcelain/Enameling	Landfill	Mech. Products	Oil & Gas		
Benzene							•	•			•			•					•																		
Carbon tetrachloride											•																										
Chlorobenzene											•																										
1,2 dichloroethane											•																										
1,1,1 trichloroethane											•																									•	
Chloroform								•	•		•			•						•			•														
1,1 dichloroethylene											•																										
1,2 trans-dichloroethylene											•																										
2,4 dimethylphenol											•																										
Ethylbenzene											•																										
Methylene chloride							•	•	•		•			•			•					•					•									•	
Dichlorobromomethane											•																										
Trichlorofluoromethane											•																										
Naphthalene											•									•																	
Pentachlorophenol							•																														
Phenol				•			•				•									•																	•
Bis(2-ethylhexyl) phthalate				•							•			•						•		•		•													
Butyl benzyl phthalate											•									•																	
Di-n-butyl phthalate											•									•																	
Di-n-octyl phthalate											•									•																	
Dimethylphthalate											•									•																	
Chrysene											•									•																	
Anthracene											•									•																	
Flourene											•									•																	
Phenanthrene											•									•																	
Pyrene											•									•																	
Tetrachloroethylene											•									•																	•
Toluene				•			•	•			•			•						•															•	•	
Trichloroethylene											•									•																	
Antimony				•							•									•				•													
Arsenic											•									•				•													
Beryllium											•									•																	
Cadmium								•	•		•									•			•														
Chromium				•	•			•	•		•			•						•						•											
Copper			•	•				•	•		•				•					•		•															
Cyanide				•				•			•									•																	
Lead			•	•				•			•									•																	
Mercury											•									•																	
Nickel				•							•									•																	
Silver				•				•			•									•																	
Thallium											•									•																	
Zinc			•	•							•				•					•						•											

Source: Neptune, 1980

Volume I

- Summary of fate of approximately 200 pollutants in different industries
- Number of times each pollutant detected
- Minimum, maximum, and mean concentration of each pollutant
- Percent removal for different treatment processes
- Effluent concentration ranges

Volume II

- Description of each industrial category
- Pollutants associated with various categories

Volume III

- Technology for control/removal of pollutants (physical-chemical, biological, disposal)
- Removal data

Volume IV

- Cost estimation for treatment.

The treatability manual is typically available at regional EPA headquarters.

## REFERENCES

- Alley, W.M. 1981. Estimation of Impervious-Area Washoff Parameters. *Water Resources Research* 17(4): 1161-1166.
- American Public Works Association. 1974. Nationwide Characterization, Impacts and Critical Evaluation of Stormwater Discharges, Non-sewered Urban Runoff and Combined Sewered Overflows. Monthly Progress Report to the U.S. Environmental Protection Agency.
- Amy, G., R. Pitt, R. Singh, W.L. Bradford, and M.B. LaGraff. 1974. Water Quality Management Planning for Urban Runoff. U.S. Environmental Protection Agency, Washington, D.C., EPA 440/9-75-004. NTIS PB 241 689/AS.
- Aron, G. 1982. Rainfall Abstractions. In: D.F. Kibler (ed.) *Urban Stormwater Hydrology*. Water Resources Monograph 7. American Geophysical Union, Washington, D.C.
- Arthur, R.D., J.D. Cain, and B.F. Barrentine. 1976. Atmospheric Levels of Pesticides in the Mississippi Delta. *Bulletin of Contamination and Toxicology* 15(2): 129-134.
- Bachmat, Y., J. Bredehoeft, B. Andrews, D. Holtz, and S. Sebastian. 1980. *Groundwater Management: The Use of Numerical Models*. Water Resources Monograph 5. American Geophysical Union, Washington, D.C.
- Baes, C.F. III, and R.D. Sharp. 1983. A Proposal for Estimation of Soil Leaching and Leaching Constants for Use in Assessment Models. *J. Environmental Quality* 12(1): 17-28.
- Baker, J.L., 1980. Agricultural Areas as Nonpoint Sources of Pollution. In: M.R. Overcash and J.M. Davidson (cd.) *Environmental Impact of Nonpoint Source Pollution*. Ann Arbor Science. Ann Arbor, Michigan pp. 275-303.
- Barth, E.F. and H.D. Stensel. 1981. International Nutrient Control for Municipal Effluents. *Journal Water Pollution Control Federation*. Vol 53, No. 12. pp. 1691-1701.
- Bave, J.L., P. Danlen, and V.P. Kukreja. 1978. Airborne di-Butyl and di-(2-Ethylhexyl) phthalate at three New York City Air Sampling Stations. *International Journal of Environmental Analytical Chemistry* 5:189-194.
- Brady, N.C.. 1974. *The Nature and Properties of Soil* MacMillan, New York.
- Burns and Roe. 1982. Fate of Priority Pollutants in Publicly Owned Treatment Works. Vol 1 & II. EPA 440/1-82-303.
- Cautreels, W., and K. Van Cauwenberghe. 1978. Experiments on the Distribution of Organic Pollutants Between Airborne Particulate Matter and the Corresponding Gas Phase. *Atmospheric Environment* 12: 1133-1141.
- Donigian, A.S., Jr., and N.H. Crawford. 1976. Modeling Nonpoint Pollution from the Land Surface. U.S. Environmental Protection Agency, Athens, GA. EPA-600/3-76-083.
- Dornbush, J.N., J.R. Anderson, and L.L. Harries. 1974. Quantification of Pollutants in Agricultural Runoff. U.S. Environmental Protection Agency, Washington, D.C. EPA-600/3-76-083.

- Eisenreich, S.J., B.B. Looney, and J.D. Thornton. 1981. Airborne Organic Contaminants in the Great Lakes Ecosystem. *Environmental Science and Technology* 15(1):30-38.
- Freeze, R.A. and J.A. Cherry. 1979. *Groundwater*. Prentice-Hall, Englewood Cliffs, N.J.
- Gakstatter, J.H., M.O. Allure, S.E. Dominguez, M.R. Crouse. 1978. A Survey of Phosphorus and Nitrogen Levels in Treated Municipal Wastewater. *Journal of Water Pollution Control Federation*. Vol. 50, No. 4.
- Giam, C.S., E. Atlas, H.S. Chan, and G.S. Neff. 1980. Phthalate Esters, PCB and DDT Residues in the Gulf of Mexico Atmosphere. *Atmospheric Environment* 14:65-69.
- Gilbertson, C.B., F.A. Norstadt, A.C. Mathers, R.F. Holt, A.P. Barnett, T.M. McCalla, C.A. Onstadt, and R.A. Young. 1979. *Animal Waste Utilization on Cropland and Pasture*. U.S. Environmental Protection Agency. Washington, D.C. EPA-600/2-79-059.
- Gilman, C.S., 1964. Rainfall. In: V.T. Chow (ed). *Handbook of Applied Hydrology*. McGraw-Hill, New York. Chapter 9.
- Hai th, D.A. and L.J. Tubbs. 1981. Watershed Loading Functions for Nonpoint Sources. *J. Environmental Engineering Div., ASCE*. 106(EE1): 121-137.
- Hai th, D.A. 1983. Planning Model for Land Application of Sewage Sludge. *J. Environmental Engineering* 109(1):66-81.
- Hai th, D.A., L.L. Shoemaker, R.L. Doneker, L.D. Delwiche. 1984. Agricultural Nonpoint Source Control of Phosphorus and Sediment - A Watershed Evaluation, Vol. IV. U.S. Environmental Protection Agency, Ada, OK.
- Hamon, W.R. 1961. Estimating Potential Evapotranspiration. *J. Hydraulics Div., ASCE*. 87(HY3):107-120.
- Hartley, G.S. and I.J. Graham-Bryce. 1980. *Physical Principles of Pesticide Behavior*. Academic Press, New York.
- Hawkins, R.H., 1978. Runoff Curve Numbers with Varying Site Moisture. *J. Irrigation and Drainage Div., Proc. of the ASCE* 104(IR4):389-398.
- Heaney, J.P., Huber, W.C., Medina, M.A., Jr., Murphy, M.P., Nix, S.J. and S.M. Hasan. 1977. *Nationwide Evaluation of Combined Sewer Overflows and Urban Stormwater Impacts*. U.S. Environmental Protection Agency, Cincinnati, OH. EPA-600/2-77-064.
- Heaney, J.P. and W.C. Huber, 1979. Nationwide Cost of Wet-Weather Pollution Control. *J. Water Pollution Control Federation*. 51(8):2043-2053.
- Huber, W.C., J.P. Heaney, K.J. Smolenyak, and D.A. Aggidis, 1979. *Urban Rainfall-Runoff-Quality Data Base*. U.S. Environmental Protection Agency, Cincinnati, OH. EPA-600/8-79-004.
- Hydrologic Engineering Center, 1977. *Storage, Treatment, Overflow, Runoff Model "STORM"*. U.S. Army Corps of Engineers, David, CA. 723-S8-L7520.
- Jensen, M.E. (ed.), 1973. *Consumptive Use of Water and Irrigation Water Requirements*. American Society of Civil Engineers, New York.

- E.C. Jordan Company. 1982. Fate of Priority Pollutants in Publicly Owned Treatment Works - 30 Day Study. EPA 440/1-82-302.
- E.C. Jordan Company. 1984. Combined Sewer Overflow Toxic Pollutant Study. EPA-440/1-84-304.
- Kibler, D.F. (ed.) 1982. Urban Stormwater Hydrology. Water Resources Monograph 7. American Geophysical Union. Washington, D.C.
- Knisel, W.B. (ed.) 1980. CREAMS: A Field-Scale Model for Chemicals, Runoff and Erosion from Agricultural Management Systems. Conservation Report No. 26. U.S. Dept. of Agriculture, Washington, D.C.
- Kohler, M.A., T.J. Nordenson, and D.R. Baker, 1959. Evaporation Maps for the United States. U.S. Weather Bureau. Washington, D.C. Tech. Paper 37.
- Langbein, W.B., 1949. Annual Runoff in the United States. U.S. Geological Survey, Washington, D.C. (Circular 52).
- McElroy, A.D., S.Y. Chiu, J.W. Nebgen, A. Aleti, and F.W. Bennett. 1976. Loading Functions for Assessment of Water Pollution from Nonpoint Sources. U.S. Environmental Protection Agency, Washington, D.C. EPA-600/2-76-151.
- Menzel, R.G. 1980. Enrichment Ratios for Water Quality Modeling. Chapter 12. In: CREAMS: A Field Scale Model for Chemicals, Runoff, and Erosion from Agricultural Management Systems, W.G. Knisel, ed. Conservation Research Report No. 26, U.S. Dept. of Agriculture. p. 640.
- Meta Systems, Inc. 1973. Effluent Changes. Prepared for the U.S. Environmental Protection Agency, Contract No. 68-01-0566.
- Metcalf and Eddy, Inc. 1979. Wastewater Engineering: Treatment, Disposal, Reuse. McGraw-Hill, New York.
- Minear, R.A., R.O. Ball, R.L. Church. 1981. Data Base for Influent Heavy Metals in Publicly Owned Treatment Works. EPA-600/2-81-220.
- Mockus, J. 1972. Estimation of Direct Runoff from Storm Rainfall. In: National Engineering Handbook, Sec. 4, Hydrology. U.S. Soil Conservation Service, Washington, D.C.
- Murphy, B.D., W.C. Johnson, and E.C. Schlatter. 1980. Simulated Deposition Rates for SO on a Southeastern U.S. Landscape. Agricultural Meteorology 21: 179-103.
- Nash, R.G. 1980. Dissipation of Pesticides from Soils. In: CREAMS: A Field Scale Model for Chemicals, Runoff, and Erosion from Agricultural Management Systems. U.S. Department of Agriculture. Conservation Research Report No. 26, W.G. Knisel, ed. p. 640.
- Neff, J.M. 1979. Polycyclic Aromatic Hydrocarbons in the Aquatic Environment: Sources, Fates and Biological Effects. Applied Science Publishers, Ltd., London.
- Neptune, D. 1980. Priority Pollutant Frequency Listing Tabulations and Descriptive Statistics. Internal Report to R.B. Schaffer, Director Effluent Guidelines Division, U.S. Environmental Protection Agency, November 4, 1980.

- Novotny, V. and G. Chesters. 1981. Handbook of Nonpoint Pollution. Van Nostrand Reinhold, New York.
- Ogrosky, H.O., and V. Mockus. 1964. Hydrology of Agricultural Lands. In: Handbook of Applied Hydrology, V.T. Chow, ed. McGraw-Hill, New York. Chapter 21.
- Omernik, J.M. 1977. Nonpoint Source-Stream Nutrient Level Relationships: A Nationwide Study. U.S. Environmental Protection Agency, Corvallis, Oregon. EPA-600/3-77-105.
- Parker, C.A., et al. 1946. Fertilizers and Lime in the United States. USDA Misc. Pub. No. 586.
- Pound, C.E., Crites, R.W., and D.A. Griffes. 1976. Land Treatment of Municipal Wastewater Effluents. Design Factors - I. U.S. Environmental Protection Agency, Washington, D.C. EPA-625/4-76-010.
- Powell, G.M. 1976. Land Treatment of Municipal Wastewater Effluents. Design Factors II. U.S. Environmental Protection Agency, Washington, D.C.
- Rae, P.S.C., and J.M. Davidson. 1982. Retention and Transformation of Selected Pesticides and Phosphorus in Soil-Water Systems: A Critical Review. U.S. Environmental Protection Agency, Athens, GA. EPA 600/3-82-060.
- Richardson, C.W., G.R. Foster, and D.A. Wright, 1983. Estimation of Erosion Index from Daily Rainfall Amount. Transactions of the ASAE 206(1): 153-156.
- Startor, J.D. and G.B. Boyd. 1972. Water Pollution Aspects of Street Surface Contaminants. U.S. Environmental Protection Agency. Washington. D.C. EPA-R1-72-081.
- Soil Conservation Service, 1975. Urban Hydrology for Small Watersheds. U.S. Dept. of Agriculture, Washington, D.C.
- Stewart, B.A., D.A. Woolhiser, W.H. Wischmeier, J.H. Care, and M.H. Frere. 1975. Control of Water Pollution from Croplands, Vol. I. U.S. Environmental Protection Agency, Washington, D.C. EPA-600/2-75-026a.
- Tubbs, L.J. and D.A. Hai th, 1981. Simulation Model for Agricultural Nonpoint Source Pollution. J. Water Pollution Control Federation 53(9): 1425-1433.
- U.S. Environmental Protection Agency. 1982. Treatability Data. Vol. 1. EPA-600/2-82-001a.
- U.S. Environmental Protection Agency. 1982. Industrial Descriptions. Vol. 2. EPA-600/2-82-001b .
- U.S. Environmental Protection Agency. 1982. Technology for Control/Removal of Pollutants. Vol. III. EPA-600/2-82-001c.
- U.S. Environmental Protection Agency. 1982. Cost Estimates to Implement Treatment. Vol. IV. EPA-600/2-82-001d.
- Vanoni, V.A. (ed.) 1975. Sedimentation Engineering. American Society of Civil Engineers. New York.

- Weber J. B., 1975. Agricultural Chemicals and Their Importance as a Nonpoint Source of Water Pollution. In: P.M. Ashton and R.C. Underwood (ed.) Nonpoint Sources of Water Pollution. Virginia Water Resources Research Center. Blacksburg, VA.
- Weiner, W.C., H.E. McGuire, and A.F. Gasperinso. 1976. A Review of Land Use Nutrient Loading Rate Relationships. Battelle Northwest Laboratories, Richland, WA.
- Wischmeier, W.H. and D.D. Smith. 1978. Predicting Rainfall Erosion Losses - A Guide to Conservation Planning. Agriculture Handbook No. 537. U.S. Dept. of Agriculture, Washington, DC.
- Yost, K.J., R.F. Wukasch, T.G. Adams, B. Michalczyk. 1981. Heavy Metal Sources and Flows in a Municipal Sewage System: Literature Survey and Field Investigation of the Kokomo, Indiana, Sewage System. EPA-600/2-81-224.



## CHAPTER 4

### RIVERS AND STREAMS

#### 4.1 INTRODUCTION

The purpose of this chapter is to present simplified tools which can be used to predict responses of rivers and streams to the impact of pollutants. The introductory sections to the chapter should be read prior to solving any problems in order to become familiar with the topics that will be covered and the limitations of the formulations presented.

Rivers throughout this country are subject to a wide spectrum of geological, biological, climatological, and anthropogenic impacts which produce a variety of water quality problems. Approaches which provide guidance to the solution of these problems, especially ones restricted to hand calculations, must be limited in scope. The following guidelines have been used in selecting topics to be considered in this chapter: 1. widely occurring problems, 2. those amenable to hand calculations, and 3. those for which planners can obtain sufficient data.

##### 4.1.1 Scope

The major problem areas to be considered are:

- Carbonaceous (CBOD) and nitrogenous (NBOD) biochemical oxygen demand
- Dissolved oxygen
- Temperature (with a discussion of low flow)
- Nutrients and eutrophication potential
- Coliform organisms
- Conservative constituents
- Sedimentation and suspended solids
- Toxic substances.

Beginning in 1974, the U.S. Environmental Protection Agency has for several years published the National Water Quality Inventory which is a compilation of current water quality conditions and recent trends in the nation's rivers and lakes. Several of the tables in that report series are relevant to this document and are included here. Table IV-1 illustrates reference water quality levels used to define acceptable pollutant limits in U.S. waterways. Table IV-2 shows water quality conditions in eight major waterways in the United States, while Table IV-3 summarizes the most widely observed water quality problems in the U.S. These tables will be cited throughout this chapter.

Local water quality standards, when they exist, are preferable to the general guidelines provided in Table IV-1. Table IV-4 shows example standards for dissolved oxygen and water temperature for the states of Virginia and Maryland. Parts of the

TABLE IV-1

REFERENCE LEVEL VALUES OF SELECTED WATER QUALITY  
INDICATORS FOR U.S. WATERWAYS (U.S. EPA, 1976)

Parameter	Reference Level
Ammonia	$\leq 0.02$ mg/l as unionized ammonia (for freshwater aquatic life)
Color	$\leq 75$ platinum-cobalt units (for water supply)
Dissolved Oxygen	$\geq 5.0$ mg/l (to maintain fish populations)
Dissolved Solids	$\leq 250$ mg/l (for water supply)
Fecal Coliforms	log mean $\leq 200$ per ml over 30 days and 90 percent $< 400$ per ml (for bathing waters)
Nitrate-N	$\leq 10$ mg/l (water supply)
pH	between 6.5 and 9.0 (for freshwater aquatic life)
Phenols	$\leq 1$ $\mu\text{g/l}$ (for water supply)
Suspended Solids and Turbidity	shall not reduce the depth of the compensation point by more than 10 percent (aquatic life)
Total Dissolved Gases	$\leq 110$ percent saturation (aquatic life)

standards are significantly different from the reference levels in Table IV-1. For example the daily average dissolved oxygen standard for natural trout water for the state of Virginia is 7.0 mg/l, while 5.0 mg/l is recommended for the protection of aquatic life (Table IV-1). Thus, when local standards exist, they should be used in lieu of general reference levels.

#### 4.1.2 Significance of Problem Areas

Oxygen depletion is often the result of excessive CBOD and NBOD loadings particularly in combination with high temperature and low flow conditions. Increased nutrient loadings to streams which produce elevated ambient concentrations can pose substantial potential for eutrophication. The nutrient problem is currently one of the most widespread areas of concern regarding river water quality. The health

TABLE IV-2  
 CONDITION OF EIGHT MAJOR WATERWAYS (EPA, 1974)

River	Harmful Substances	Physical Modification	Eutrophication Potential
Mississippi		High* turbidity and solids below Missouri River	High*, increasing nutrients but no algae
Missouri	Trace metals present in middle river	High* suspended solids, turbidity in middle and lower river	High*, increasing nutrients but no algae
Ohio	High*, increasing iron and manganese	High* suspended solids in lower river, some improvements	High* nutrients but no algae
Tennessee			Small increase in nutrients but no algae
Detroit area rivers	Cyanide present but diminishing	Suspended solids improving, local temperature effects from discharges	Nutrients discharged to Lake Erie decreasing
Columbia	Severe gas super saturation; some radioactivity in lower river	Occasional high* temperatures	High* nutrients but no algae, except for slime growths in lower river
Snake	Severe gas super-saturation, significant pesticides	Turbidity from natural erosion, agricultural practices, reservoir flushing	Nuisance algal blooms each summer
Willamette	Significant sulfite waste liquor from pulp and paper wastes	High* turbidity at high flow, high temperature in summer	High* level of nutrients but not excessive algae

TABLE IV-2 (continued)

River	Salinity, Acidity, and Alkalinity	Oxygen Depletion	Health Hazards and Aesthetic Degradation
Mississippi	High* salinity, acidity below major tributaries	Oxygen-demanding loads from large cities evident	Commercial fishing eliminated in lower river by phenols, bacteria near cities
Missouri	High* dissolved salts in middle and lower river	High* organic loads from feedlots, improved near cities	High* bacteria and viruses present in wet and dry periods
Ohio	Low* alkalinity especially in upper river	Occasional low* dissolved oxygen near Cincinnati and Pittsburgh	High* bacteria especially in high population areas
Tennessee		Low* BOD and decreasing COD in reservoirs	High* bacteria in small areas near cities, low radionuclides
Detroit area rivers	Acids and chloride low,* improving despite large discharges	Low* dissolved oxygen only at mouths of area tributaries	Phenols decreasing, bacteria unchanged-to-higher
Columbia	Approaches ideal for fresh waters	Dissolved oxygen close to saturation	Very low* bacteria
Snake	High* dissolved solids from irrigation in middle river	Dissolved oxygen close to saturation	High* bacteria below population centers
Willamette	Low* dissolved mineral salts, improved pH	Improved dissolved oxygen, no standards violations	High* bacteria, but improving

\*High (or low) relative to other rivers, or relative to other sections of river, or to national reference levels. Does not necessarily imply standards violations or dangerous condition.

TABLE IV-3  
WATER QUALITY PROBLEM AREAS REPORTED BY STATES\*  
NUMBER REPORTING PROBLEMS/TOTAL (EPA, 1975)

	Middle Atlantic, Northeast	South	Great Lakes	Central	Southwest	West	Islands	Total
Oxygen depletion	11/13	9/9	6/6	6/8	4/4	6/6	4/6	46/52
Eutrophication potential	11/13	6/9	6/6	8/8	2/4	6/6	4/6	43/52
Health hazards	11/13	8/9	5/6	8/8	3/4	5/6	5/6	45/52
Salinity, acidity, alkalinity	3/13	6/9	2/6	6/8	4/4	4/6	2/6	27/52
Physical modification	7/13	3/9	3/6	8/8	3/4	6/6	5/6	35/52
Harmful substances	6/13	6/9	5/6	4/8	4/4	2/6	3/6	30/52

\* Localized or statewide problems discussed by the States in their reports.

hazards category in Table IV-3 lists elevated coliform levels as a problem of particular concern in northeastern and Great Lakes States. Salinity has been identified as a major problem in the central and southwestern states.

Because of their importance, each of the problem areas described will be addressed in this chapter. As shown in Table IV-5, many states routinely measure the parameters associated with these problems. The total number of states responding to the survey was 47. Because of the routine surveys conducted, data are commonly available for performing hand calculations. NBOD, though not directly measured, can be found from measurements of organic and ammonia nitrogen. Chloride concentration measurements can be directly converted to salinity.

#### 4.1.3 Applicability to Other Problems

The tools which are presented in this chapter are designed to address specific water quality problems. However, a number of the tools, which are based on the law of mass conservation, can be directly applied to other problems with little or no modification. In the case of temperature prediction, an energy balance is used (which is analogous to a mass balance).

TABLE IV-4  
EXAMPLE RIVER WATER QUALITY STANDARDS

Class	Description	Dissolved Oxygen		Temperature, °F	
		Minimum	Average	T <sub>N</sub>	T <sub>MAX</sub>
<u>Virginia</u>					
III	Coastal and Piedmont	4.0	5.0	5	90
IV	Mountainous	4.0	5.0	5	87
V	Put and Take Trout Waters	5.0	6.0	5	70
VI	Natural Trout Waters	6.0	7.0	5	68
<u>Maryland</u>					
I	Water Contact, Recreation	4.0*	5.0*		90**
III	Natural Trout Waters	5.0*	6.0*		68**
IV	Recreational Trout Waters	5.0*	5.0*		75**

\*These values apply except where lower values occur naturally.  
 \*\*These apply outside the mixing zone. If natural temperature of receiving water is greater than the standard, then that becomes the standard.

The degree of commonality of source and sinks of a particular pollutant (e.g., a nutrient) or water quality indicator (e.g., dissolved oxygen) is responsible for the similarities and differences among the specific equations. For example, CBOD and NBOD produce a similar general effect (oxygen depletion), generally have similar sources and sinks, and for purposes of this study are assumed to follow first order decay kinetics. Coliforms, also assumed to decay by first order kinetics, are handled by the mass-balance approach. Conservative substances are different from BOD and coliforms in that they do not decay. Finally, there are some instances where a more subjective analysis is indicated and neither a mass nor energy balance is presented.

Once the similarities among water quality parameters are understood, handling two seemingly different problems can often be accomplished in a straightforward and similar fashion. For example, the distribution of toxic substances that are either conservative or follow a first order decay may be evaluated using techniques described for conservative substances and coliforms, respectively.

#### 4.1.4 Sources of Pollutants

Pollutant loadings originate from three general sources: point, nonpoint, and natural. Each of these can constitute a major hurdle in meeting the 1983 goals of

TABLE IV-5  
 WATER QUALITY PARAMETERS  
 COMMONLY MONITORED BY STATES\* (EPA, 1975)

Parameter	Number of States
Flow	47
Dissolved oxygen	47
Coliform bacteria	45
Nitrogen (any form)	39
Phosphorus (any form)	35
pH	35
BOD/COD/TOC	27
Water temperature	29
Turbidity	26
Solids (any type)	27
Metals (any type)	17
Chlorides	19
Alkalinity	15
Conductivity	16
Color	11
Sulfate	14

\*Only parameters listed by at least 10 States and specified as being part of each State's monitoring program are included.

fishable and swimmable waters. Specifically, point sources (30 states), nonpoint sources (37 states), and natural conditions (21 states) are all major contributors to water quality problems (EPA, 1975).

It is imperative that the capacity to assess impacts of nonpoint sources be a part of the hand calculation methodology for rivers. Table IV-6 illustrates the importance of nonpoint source nutrient loading for selected rivers in Iowa. Up to 96 percent of the annual phosphorus load and up to 99 percent of the total nitrogen load are from nonpoint sources. Admittedly, quantification of nonpoint source loads is often difficult. Nevertheless, simplified nonpoint source terms will be included in some of the mass-balance formulations. The methodology supplied in Chapter III can be used to estimate the nonpoint source loading rates.

#### 4.1.5 Assumptions

In deriving the mass-balance equations, a number of assumptions were made. Users should be aware of each assumption so that the tools are not misapplied. The

TABLE IV-6  
ANNUAL PHOSPHORUS AND NITROGEN LOAD FOR SELECTED IOWA RIVER BASINS (EPA, 1975)

River	Total (lbs/year)	Point Sources (lbs/year)	Nonpoint Sources (lbs/year)	Percent of Total from Nonpoint Sources
<u>PHOSPHORUS</u>				
Floyd	720,207	29,807	690,400	95.9
Little Sioux	1,851,632	129,088	1,722,544	93.0
Chariton	879,916	48,203	831,713	94.5
Des Moines	5,621,007	586,015	5,034,992	89.6
Iowa	1,723,975*	103,445*	1,620,530*	94.0
Cedar	5,099,507	1,526,775	3,572,732	70.1
<u>NITROGEN</u>				
Floyd	1,705,984	65,171	1,640,813	96.2
Little Sioux	9,609,556	85,308	9,522,248	99.1
Chariton	1,585,427	24,795	1,560,632	98.4
Des Moines	41,334,897	695,235	40,639,662	98.3
Iowa	2,075,830	91,287	1,984,543	95.6
Cedar	6,804,881	1,552,334	5,252,547	77.2
*Orthophosphate				

most important assumptions are:

- The system is at steady-state.
- Dispersion is small compared to advection (i.e., plug flow is assumed).
- The river system is vertically and laterally mixed.
- When pollutants decay, the rates are first order.

The steady-state assumption means that conditions are not changing with time, but only as a function of distance along the river. The time scale or steady-state generally should be on the order of a week or longer. For example, the summer low flow period generally represents a steady-state situation. However, storm events, and the dynamic responses of a river to them, must be considered a transient phenomenon.

Dispersion effects can usually be neglected when pollutant input into a river is continuous. Under these conditions the plug flow assumption is reasonable because the net dispersive transport is small. However, when a slug of pollutant is discharged instantaneously, dispersive transport is important since high concentration gradients exist around the centroid of the discharged pollutant.

The fully-mixed assumption presupposes that concentration gradients exist only in the direction of flow (longitudinal direction) and not in either the vertical or



lateral direction. The final major assumption is that all decay rates can be approximated by first order kinetics. This means that the decay rate of a substance is proportional to the amount present. First order decay is traditionally used in CBOD computations, and occasionally in nitrogen oxidation. The oxidation of inorganic nitrogen actually proceeds in stages from ammonia-N to nitrite-N to nitrate-N, However, for purposes of this report, the first order decay rate is acceptable for NBOD and coliforms, as well as CBOD. Before applying first order decay to other substances, however, care should be taken to determine the validity of the assumption.

For a few of the analyses which follow, several of the aforementioned assumptions are relaxed. In the discussion of mixing zones, Section 4.1.9, partial mixing is discussed for wide rivers. In the discussion on toxicants, Section 4.9, the spill analysis requires that an unsteady-state situation be analyzed where the effects of dispersion are included.

#### 4.1.6 Data Requirements

Required in the analysis of most water quality problems are one or more types of data. For example, stream velocity (U), volumetric flow rate (Q), and stream temperatures (T) are commonly needed. Decay rates, specific to the Particular problem at hand, are also required.

The U.S. Environmental Protection Agency has published two documents (Bowie et al. , 1985 and Zison et al. , 1978) intended to provide water quality modelers with a comprehensive source of information on rate constants and coefficients. The document provides extensive information on both biological and water quality parameters commonly used in surface water modeling. The contents of the document will be useful to the users of this document who are often faced with limited information on process rates for the water bodies being analyzed.

Stream velocity is the most basic hydraulic parameter needed for the analyses presented in this chapter. Ideally, the appropriate stream velocity is the travel time of neutrally buoyant particles over the reach being investigated divided by the distance traveled. Note that this concept of velocity is different from the velocity determined by:

$$U = \frac{Q}{A} \quad (IV-1)$$

As defined by Equation IV-1, this concept of velocity exists only at the point in the river where the cross-sectional area is A. If the point of measurement is not typical of the reach being investigated, then neither will the velocity be typical. Consequently, should the user predict stream velocity based on cross-sectional area, a location typical of the river reach being investigated should be chosen.

An alternate method of predicting stream velocity, which does not depend on either flowrate Q or cross-sectional area A is Manning's Equation. A complete description of the use of this approach is given in many texts on surface water hydraulics, one of the best being Chow (1959).

According to Manning's Equation stream velocity under uniform flow conditions is expressible as:

$$U = \frac{1.49}{n} S^{1/2} R_H^{2/3} \quad (IV-2)$$

where

$n$  = Manning's  $n$

$S$  = slope, ft/ft

$R_H$  = hydraulic radius, ft.

Manning's  $n$  is the roughness of the stream bed, and can be predicted as outlined in Chow (1959). Barnes (1967) provides roughness data for 90 streams in the United States, and includes cross-sectional areas and photographs of the streams investigated. The slope can be estimated using topographic maps to predict elevation changes between two locations and then overlying a string over the stream path to predict distance. The hydraulic radius (which is the ratio of the cross-sectional area to wetted perimeter) can be estimated in terms of depth when the stream width is much greater than the depth. Specifically:

$$R_H = \begin{cases} \text{depth, if channel cross-section is rectangular} \\ 2/3 \text{ maximum depth, if channel cross-section is parabolic} \end{cases}$$

#### 4.1.7 Selection of Season

It is reasonable to expect that a particular water quality problem may be more severe at one time of the year than another. Table IV-7 shows that pollutant levels can depend on season (summer or winter) and flow rate (high flow or low flow). Dissolved oxygen problems, for example, are clearly associated with summer, low flow conditions. Consequently, for any particular pollution problem, users should strive to perform the analysis under critical conditions. Where planning is performed with consideration of the aggravated situation and where proper abatement action is taken, it is likely that pollution concentrations will be below problem levels during other times of the year. If a problem in fact exists, then it is under these conditions that it will be most pronounced.

In the following sections, hand calculation methods for each problem area are described with illustrative examples. Table IV-8 provides a summary of the material presented.

TABLE IV-7

## MAJOR WATERWAYS: SEASONAL AND FLOW ANALYSIS, 1968-72 (EPA, 1974)

Parameters	Winter,		Summer,		Winter,		Summer,		Dominant Effect
	High Flow	Low Flow	Low Flow	High Flow	Low Flow	High Flow			
(number of reaches exceeding reference levels)**									
Suspended solids	9	3	5	4	0	4			High flow
Turbidity	13	7	4	1	1	7			High flow
Color	11	3	6	4	3	4			High flow
Ammonia	14	3	3	1	7	1			Cold weather
Nitrite	3	7	4	1	5	1			Low flow
Nitrate(as N)	12	4	3	1	8	1			Cold weather
Nitrate(as NO <sub>3</sub> )	8	2	3	1	6	1			Cold weather
Nitrite plus nitrate	2	3	3	1	2	1			Inconclusive
Organic nitrogen	3	6	6	3	0	3			Warm weather
Total Kjeldahl nitrogen	3	5	5	3	0	3			Warm weather
Total phosphorus	10	3	3	2	5	2			Cold weather
Total phosphate	8	3	3	1	5	1			Cold weather
Dissolved phosphate	6	3	3	0	4	0			Cold weather
Dissolved solids(105°C)	4	7	7	3	6	3			Low flow
Dissolved solids(180°C)	3	8	8	2	6	2			Low flow
Chlorides	4	15	15	0	10	0			Low flow
Sulfates	5	13	13	5	5	5			Warm weather, low flow
Alkalinity	6	12	12	0	10	0			Low flow
ph	15	4	4	4	6	4			Cold weather, high flow
Dissolved oxygen	0	19	19	9	0	9			Warm weather
BOD <sub>5</sub>	11	6	6	1	8	1			Cold weather
COD (.025N)	6	5	5	2	3	2			Cold weather
Total coliforms(MFD)*	4	10	10	5	2	5			Warm weather
Total coliforms(MFI)*	8	6	6	4	2	4			High flow, warm weather
Total coliforms(MPN)*	4	2	2	3	3	3			Inconclusive
Fecal coliforms(MF)*	6	6	6	4	3	4			Inconclusive
Fecal coliforms(MPN)*	4	0	0	0	1	0			Cold weather
Phenols	5	0	0	0	1	0			Inconclusive
Odor	4	0	0	0	0	0			Inconclusive

\*Membrane filter delayed, membrane filter immediate, most probable number, membrane filter.

\*\*Reference levels are available in Table IV-1. Thirty reaches were analyzed during each season.

TABLE IV-8  
WATER QUALITY ANALYSES FOR RIVER SCREENING METHODOLOGY

Water Quality Constituent	Computational Procedures	Supporting Information Included
Water temperature	<ul style="list-style-type: none"> <li>- equilibrium temperature</li> <li>- mixing temperature</li> <li>- temperature profile for point sources</li> </ul>	<ul style="list-style-type: none"> <li>- shortwave solar radiation</li> <li>- longwave solar radiation</li> <li>- vapor pressure</li> </ul>
Carbonaceous and nitrogenous biochemical oxygen demand	<ul style="list-style-type: none"> <li>- BOD profiles for point sources</li> <li>- BOD profiles with benthic sources added</li> <li>- BOD profiles with both benthic and nonpoint sources added</li> </ul>	<ul style="list-style-type: none"> <li>- graphs, tables, and equations for decay rates</li> </ul>
Dissolved oxygen	<ul style="list-style-type: none"> <li>- CBOD-NBOD-DO profile for point sources</li> <li>- DO profiles with photosynthetic oxygen production and benthic uptake added</li> <li>- critical dissolved oxygen conditions</li> <li>- waste assimilative capacity</li> </ul>	<ul style="list-style-type: none"> <li>- reaeration rates for shallow and deep streams</li> <li>- saturation dissolved oxygen levels corrected for temperature, altitude, salinity</li> <li>- photosynthetic oxygen production and benthic uptake data</li> <li>- tabulated solutions for critical dissolved oxygen levels</li> </ul>
Nutrients	<ul style="list-style-type: none"> <li>- growth limiting nutrient</li> <li>- nutrient profiles for point sources</li> <li>- nutrient profiles for nonpoint sources</li> </ul>	<ul style="list-style-type: none"> <li>- nitrogen/phosphorus ratios for growth limitation</li> <li>- nonpoint source loading rates by land use type</li> </ul>
Coliform organisms	<ul style="list-style-type: none"> <li>- coliform profiles for point sources</li> <li>- coliform profiles for nonpoint sources</li> </ul>	<ul style="list-style-type: none"> <li>- decay rates</li> </ul>
Sediment	<ul style="list-style-type: none"> <li>- bed load</li> <li>- suspended load</li> <li>- total load</li> </ul>	<ul style="list-style-type: none"> <li>- median bed particle sizes for numerous rivers</li> <li>- critical shear stress</li> <li>- sediment transport propensity factor</li> <li>- approximate bed load/suspended load relationship</li> </ul>
Toxicants	<ul style="list-style-type: none"> <li>- toxicant profiles for point and nonpoint sources</li> <li>- mass flux volatilized, advected, and transformed</li> <li>- spill analysis of low and high density toxicants</li> <li>- time required to desorb toxicant from bedded sediments</li> </ul>	<ul style="list-style-type: none"> <li>- vapor pressure, solubility, octanol - water partition coefficient for priority pollutants</li> <li>- Henry's Law Constant:</li> </ul>

#### 4.1.8 River Segmentation

Although the tools presented in this chapter are of a simplified nature they can be used to analyze complex river systems (i.e., those which have a number of different point and nonpoint sources of pollution, tributaries and withdrawals). Analysis of these systems is accomplished by dividing the river into segments. The basic tenet which must be followed is simply this: Segments are created so that one of the analytical tools presented in this chapter can be used to predict the pollutant

concentration profile within the segment.

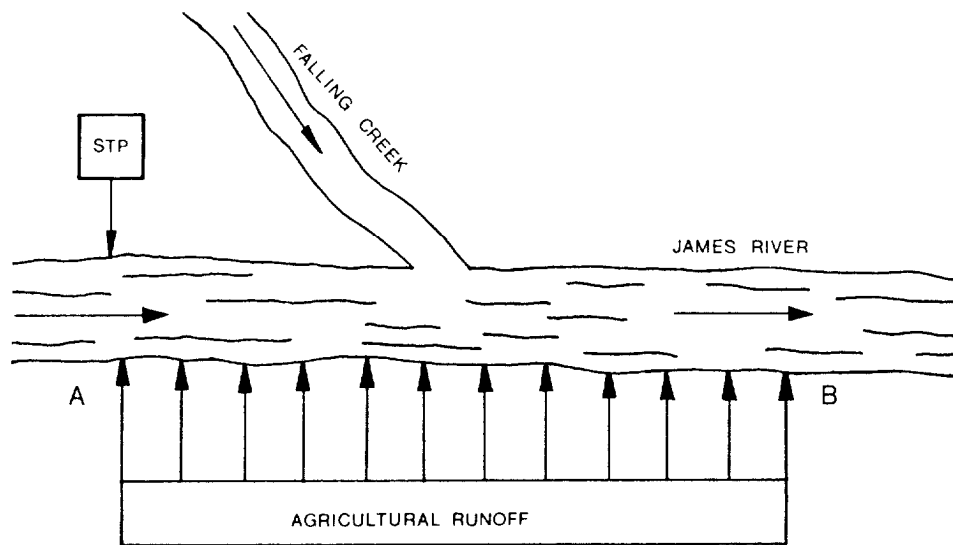
Analyses of river systems normally begin at a segment where the boundary conditions are known, and proceed sequentially downstream. Thus the results found for one segment are used as the upstream boundary condition for the next segment. Based on the tools in this chapter, the following rules should be followed when segmenting:

1. Point sources of pollutants enter the river just above the upstream boundary of a segment. Tributaries are treated as point sources.
2. Nonpoint sources enter a river throughout the length of a segment.
3. Pollutant concentrations at the upstream end of segments are obtained by mixing the pollutant concentration in the river with the contribution of the point source at that location (if one exists). The location where mixing occurs is called a mixing zone.
4. Generally constant hydraulic variables (e.g., depth and velocity) are used throughout a segment. If there is a gradual change in the hydraulic variables over distance, an average value can be used. If there is an abrupt change in the variable, such as a velocity change caused by a significant deepening of the channel, then a new segment can be created at this boundary.
5. Decay rates, reaeration rates, and other rate coefficients remain constant within a segment. If rate coefficients are known to change significantly from one location to another in a river, then different segments should be created. This rule is consistent with rule (4), since rate coefficients are often functions of hydraulic variables.

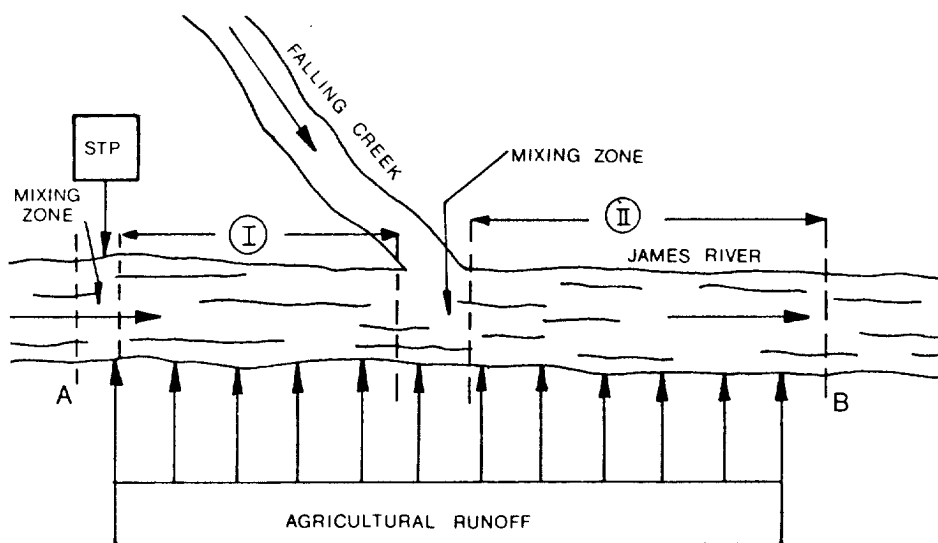
#### EXAMPLE IV-1

Figure IV-1a shows a stretch of the James River, located in Virginia. On the stretch of the river shown, there is a tributary (Falling Creek), a sewage treatment plant (STP), and a nonpoint source of runoff (agricultural). Segment the river between locations A and B in order to determine the profile of a pollutant which is discharged from each of the three sources.

First, it should be noted that often there is more than one way to segment the river to successfully solve the problem. The most obvious method will be illustrated here. Figure IV-1b shows the proposed solution. There are two mixing zones - the first around the treatment plant and the second around the tributary which is treated as a point source. The first segment is located from below the first mixing zone to above the second mixing zone, and has a nonpoint source discharging throughout the length of the segment, consistent with rule (2). The second segment is located below the second mixing zone and continues downstream to



(a) River Segment Being Analyzed



(b) Proposed Segmentation Scheme

FIGURE IV-1 ILLUSTRATION OF RIVER SEGMENTATION  
PROCEDURE ON THE JAMES RIVER

Location B, which is the end of the nonpoint source. If Falling Creek had not been present, a single segment and a single mixing zone would have been sufficient to analyze the problem.

END OF EXAMPLE IV-1

A second, more comprehensive example will illustrate a number of points about segmentation not covered in the previous example. One of these points is that the segmentation scheme used can vary depending on the pollutant being analyzed.

EXAMPLE IV-2

Segment the river shown in Figure IV-2 beginning at location A and continuing to location B in order to determine the instream BOD distribution. How would the segmentation differ when predicting the dissolved oxygen profile?

Both point and nonpoint sources discharge to the river in Figure IV-2. Several flows are diverted, and the river width changes over parts of the reach being investigated. Each of the rules stated earlier will be utilized to segment the river system. Figure IV-3 shows one solution to the problem. Depending on the distances between the various sources of pollutants, which are not given in the

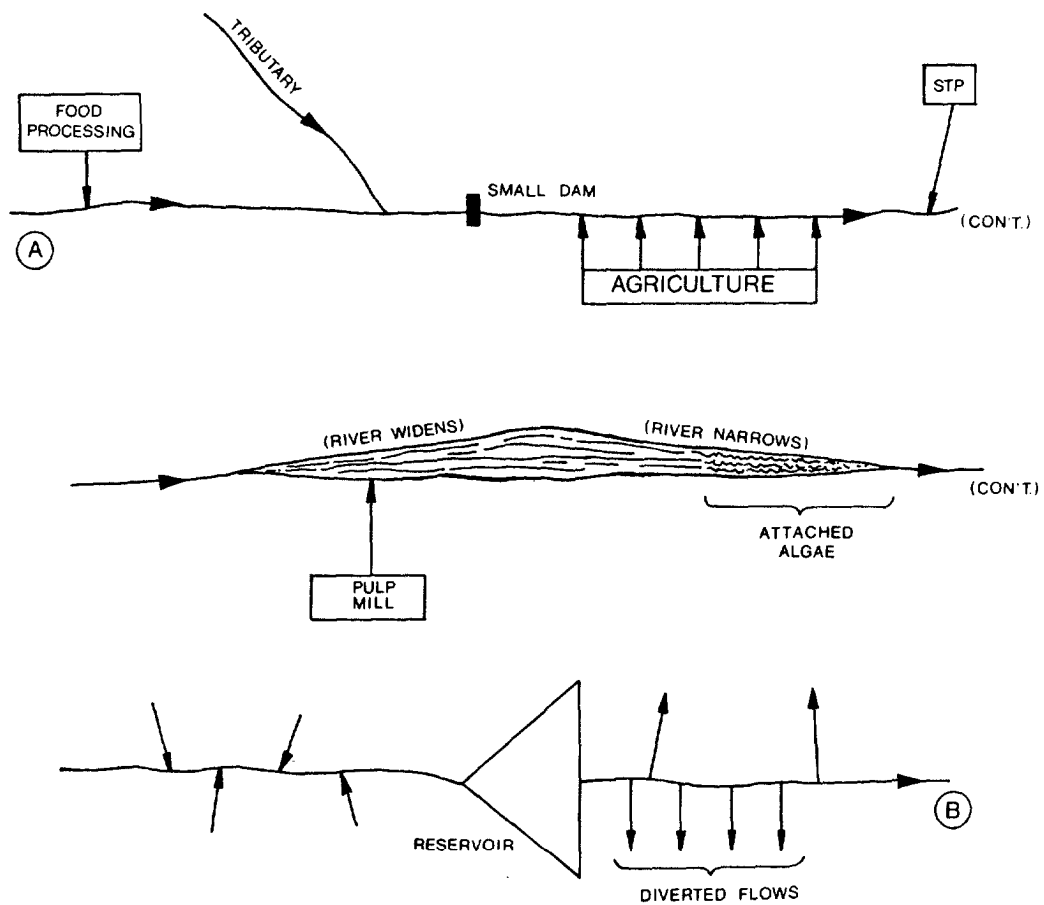


Figure IV-2 HYPOTHETICAL RIVER HAVING A VARIETY OF POLLUTANT SOURCES AND SINKS.

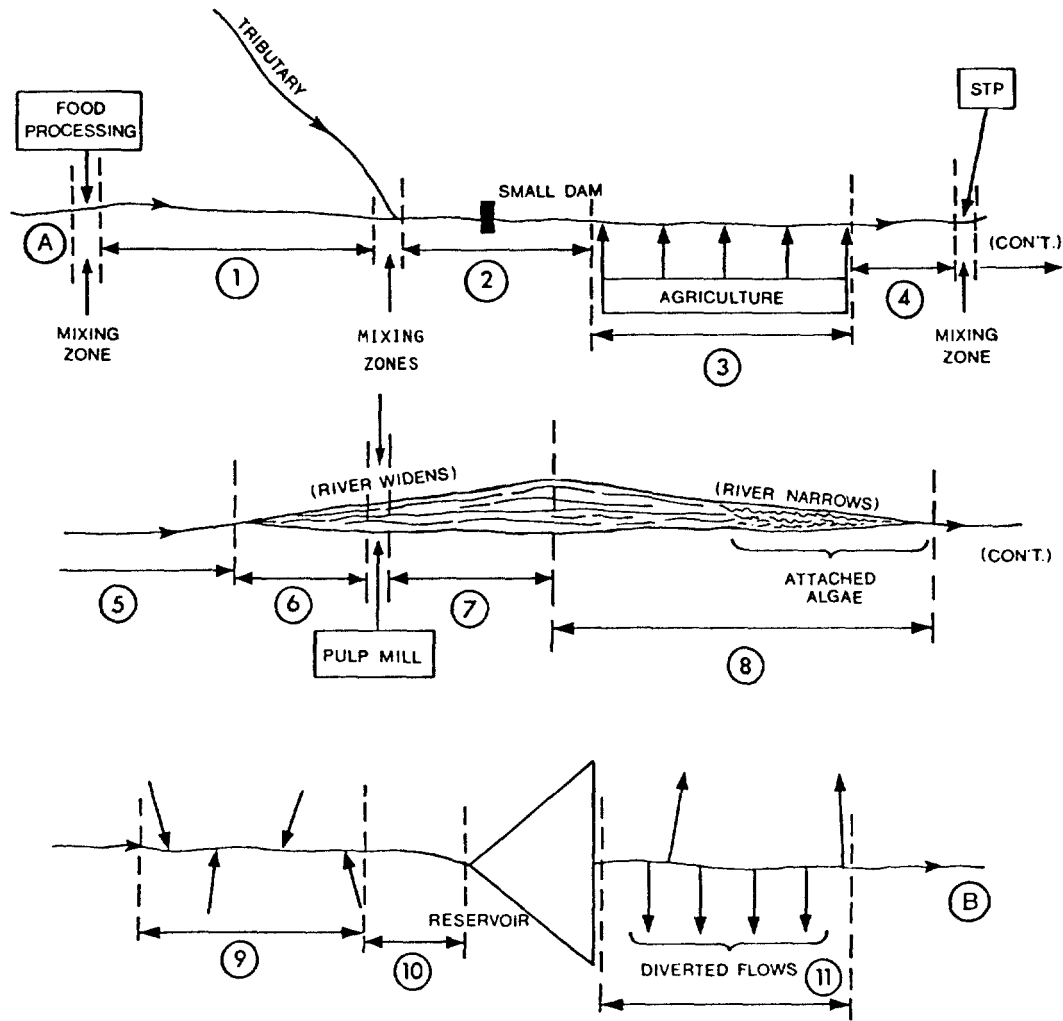


FIGURE IV-3 RIVER SEGMENTATION FOR BOD DISTRIBUTION.

problem, it might be possible to combine some of the segments. The reservoir is assumed to be analyzed using the methods in Chapter 5, and so is not segmented.

Mixing zones are included around the four point sources: the food processing plant, the tributary, the sewage treatment plant, and the pulp mill. In segments 9 and 11 there appear to be a number of point sources and diversions. Strictly speaking, segments 9 and 11 do not follow the rules presented earlier, which require mixing zones around each point source. However, the point sources and sinks within segments 9 and 11 are assumed to represent equivalent nonpoint sources, which act over the length of each segment. This approach can obviously simplify the analysis of complex river systems by decreasing the number of segments analyzed. However, the analysis is more approximate because the nonpoint source is assumed to be uniformly distributed throughout the segment. Example IV-5 presented later shows a specific application of the concept of an equivalent nonpoint source.



In segment 2 the presence of the small dam is assumed not to influence the BOD profile, so that its presence does not require a mixing zone. However if the dissolved oxygen profile were being calculated, segment 2 would be divided into two segments, with a mixing zone around the dam. This division is required because the dissolved oxygen concentration can rapidly change (almost instantaneously) as the water flows over the dam. The dissolved oxygen concentration just below the dam should be used as the upstream boundary conditions for the next segment. The specific information required to accomplish this is discussed later in Section 4.3.

A second difference in segmenting for dissolved oxygen occurs in Segment 8. The presence of the attached algae is assumed not to influence the BOD profile, but the algae are internal sources of oxygen. Thus segment 8 would be subdivided at the upstream location of the attached algal growth.

----- END OF EXAMPLE IV-2 -----

#### 4.1.9 Mixing Zones

A mixing zone, as used in this document, is nothing more than a short reach of a river where a point source and river water mix. It is often assumed, for both simple and more complex approaches (e.g., QUAL-11 computer model), that mixing is instantaneous and complete across the entire width of the channel. With several exceptions, such an approach is used in this document.

Assuming complete mixing, the concentration of a pollutant in a river after mixing is:

$$C = \frac{C_u Q_u + C_w Q_w}{Q_w + Q_u} \quad (IV-3a)$$

$$= \frac{C_u Q_u + W/5.38}{Q_w + Q_u} \quad (IV-3b)$$

where

C = concentration of pollutant in river following mixing, mg/l

C<sub>w</sub> = concentration in point source, mg/l

C<sub>u</sub> = concentration in river above point source, mg/l

Q<sub>w</sub> = discharge rate of point source, ft<sup>3</sup>/sec

Q<sub>u</sub> = flow rate of river above point of discharge, ft<sup>3</sup>/sec

W = pollutant mass emission rate, lbs/day.

The concentration C is the pollutant level in the mixing zones shown in the earlier Figures IV-1 and IV-3. These concentrations become the upstream boundary conditions for the adjacent downstream segment.

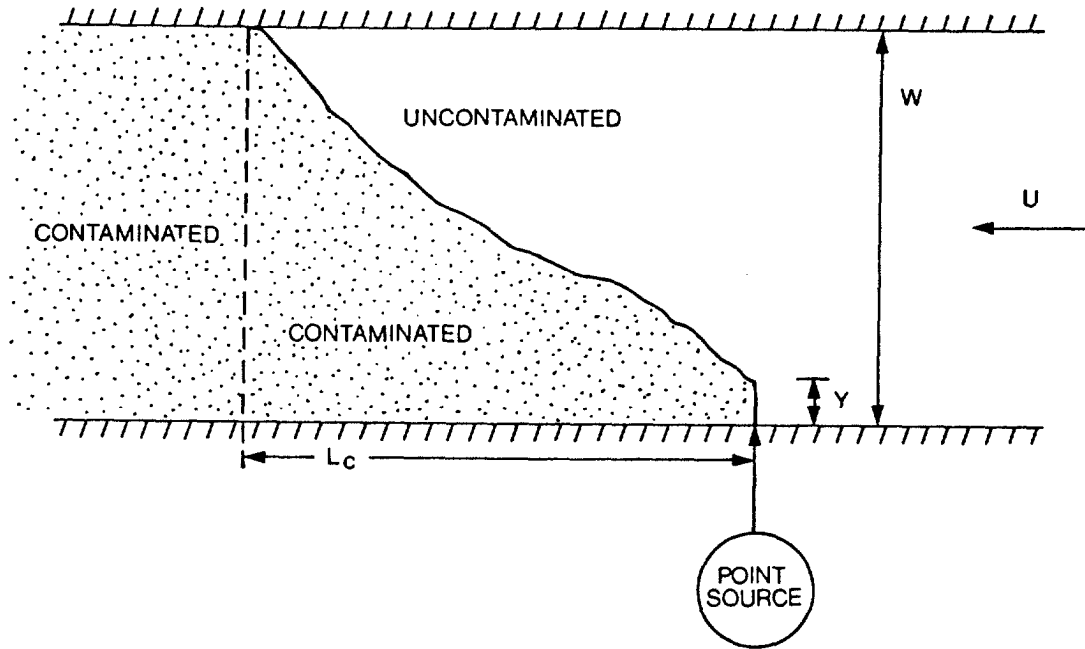


FIGURE IV-4 POLLUTANT DISCHARGE WHERE INITIAL MIXING OCCURS A FRACTIONAL DISTANCE ACROSS THE RIVER.

Although it is convenient to assume that complete mixing occurs, this assumption may be inaccurate for wide rivers, depending on the characteristics of the point source outfall and diffuser. Figure IV-4 illustrates such a case. The river is wide enough so that the wastewater is initially mixed with only a fraction of the total river flow. As the pollutant-riverwater mixture is transported downstream mixing continues until the pollutant is completely mixed across the channel.

The initial pollutant concentration at the point of discharge is:

$$C = \frac{w Q_u C_u + Q_w C_w}{Q_w + \frac{y}{w} Q_u} \quad (IV-4)$$

where

$\frac{y}{w}$  = fractional distance across river where initial mixing occurs.

All other variables have been previously defined.

The significance of incomplete initial mixing is that pollutant concentrations can be initially much higher than if complete mixing occurs. For example, if the upstream contribution of the pollutant is negligible ( $C_u = 0$ ) and if the fraction of river flow which initially mixes is far greater than the wastewater flow ( $\frac{y}{w} Q_u \gg Q_w$ ), then:

$$C = \frac{w}{y} C_{cm} \quad (IV-5)$$

where

$C$  = concentration of pollutant if there is incomplete initial mixing

$C_{cm}$  = concentration of pollutant if there is complete initial mixing.

If  $Y/W = 0.1$ , then the pollutant concentration following incomplete mixing is 10 times higher than if complete mixing were to occur.

The distance  $L_c$  to complete mixing (see Figure IV-4) can be estimated (as an upper limit) by the following expression:

$$L_c = \frac{0.4 W^2 U}{\epsilon_t} \quad (IV-6)$$

where

$L_c$  = distance below point source where complete mixing occurs

$W$  = width of river

$U$  = river velocity

$\epsilon_t$  = lateral diffusion coefficient.

Values of the lateral diffusion coefficient can be estimated from the data given in Table IV-9. Also, the following predictive formula can be used:

$$\frac{\epsilon_t}{Du^*} = \begin{cases} 0.1-0.2, & \text{for a straight rectangular flume} \\ 0.25, & \text{for irrigation channels} \\ 0.4-0.8, & \text{many natural channels} \end{cases} \quad (IV-7)$$

where

$D$  = mean depth of flow

$u^*$  = friction velocity =  $\sqrt{gDS}$

$S$  = slope of channel.

The actual distance  $L_c$  is probably less than that calculated from Equation IV-6 because of secondary mixing, river curvature, and initial momentum of the discharge. It is also sensitive to river width.

#### 4.1.10 Water and Pollutant Balances

Many river systems are hydrologically complex. Flow patterns are influenced by tributaries, nonpoint sources of runoff, flow withdrawals, as well as point sources of pollution. If the planner intends to perform water quality analyses on a basin-wide scale, it is probably prudent that a water budget be first completed. A water budget is a statement that:

$$\frac{dS}{dt} = \sum \text{Inflows} - \sum \text{Outflows} = 0, \text{ for steady-state (IV-8)}$$

TABLE IV-9  
EXPERIMENTAL MEASUREMENTS OF TRANSVERSE MIXING IN  
OPEN CHANNELS WITH CURVES AND IRREGULAR SIDES

Channel	Channel geometry	Channel width, $W$ (m)	Mean depth of flow, $d$ (m)	Mean velocity, $u$ (m/s)	Shear velocity, $u^*$ (m/s)	Transverse mixing coefficient (m <sup>2</sup> /sec)	$\frac{\epsilon_t}{Du^*}$
Missouri River near Blair, Nebraska	Meandering river	200	2.7	1.75	0.074	0.12	0.6
Laboratory	Smooth sides and bottom; 0.15 m long groins on both sides	2.2	0.097	0.11	-	-	0.36-0.49
	Smooth sides and bottom; 0.5 m long groins on both sides	2.2	0.097	0.11	-	-	0.3-0.4
Laboratory model Of the IJssel River	Groins on sides and gentle curvature	1.22	0.9	0.13	0.0078	-	0.45-0.77
IJssel River	Groins on sides and gentle curvature	69.5	4.0	0.96	0.075	-	0.51
Mackenzie River from Fort Simpson to Norman Wells	Generally straight alignment or slight curvature; numerous island and sand bars	1240	6.7	1.77	0.152	0.67	3.4
Missouri River downstream of Cooper Nuclear station, Nebraska	Reach includes one 90° and one 180° bend	210-270	4	5.4	0.08	1.1	3.4
Potomac River: 29 km reach below the Dickerson Power Plant	Gently meandering river with up to 60° bends	350	0.73-1.74	0.29-0.58	0.033-0.051	-	0.52-0.65

from: Fischer, H.B., E.J. List, R.C.Y. Kob, J. Imberger, and N.H. Brooks, 1979. *Mixing in Inland and Coastal Waters*. Academic-Press, New York.

where

$S$  = storage in the river channel.

For the steady-state situations, which are examined here, the water budget simply states that inflows to the system equal outflows from the system. A water budget thus provides a method of determining whether the major flow contributions have been accurately assessed or not. If a large imbalance in the water budget exists, accurate evaluation of the major sources of pollutant might be difficult to achieve. An accurate water balance helps to minimize the possibility of inaccurate assessment of pollutant concentration. It does not eliminate the possibility.

Once a water balance has been completed, then a pollutant balance of a conservative pollutant can be developed based on the following relationship:

$$\sum_{in} \text{Flux} = \sum_{out} \text{Flux} \quad , \text{ at steady-state} \quad (IV-9)$$

where the fluxes are the rates of entry and loss of the pollutant into and out of the system, respectively. One of the following two expressions can be used to predict the mass loading rates:

$$M = 5.38 C Q \quad (IV-10)$$

where

M = mass loading rate, lbs/day

C = concentration, mg/l

Q = flow rate,  $\text{ft}^3/\text{sec}$

and

$$M = 86.4 C Q \quad (IV-11)$$

where

M = mass loading rate, kgs/day

Q = flow rate,  $\text{m}^3/\text{sec}$ .

When nutrient and water balances are developed, the following considerations should be kept in mind:

- In most instances it is probably not possible to develop water or nutrient balances where inflows and outflows balance to within less than 10 percent of each other.
- The system's upstream boundary must be included in the balance as a source and the downstream boundary as a loss.
- All sources and losses should be mutually exclusive of each other.
- Choose system boundaries to coincide with locations of gaging stations when possible.
- Try to use comparable periods of record of data. This will help to minimize the impacts of trends which could be present in one record but not in another.
- It is typically easier to develop water and mass balances on an annual basis, although balances can be developed for each season of the year. However, if the system is not at steady state, inflows and outflows should not balance.

Table IV-10 shows a suggested method of tabulating the results of water and pollutant balances. Total nitrogen (TN) and total phosphorus (TP) are the pollutants. All flow rates and loading rates are tabulated individually. Once total loading rates have been tabulated, the percent contribution from each source can be determined. Percent contributions help to determine the relative importances of each source as a contributor to pollution, and can provide a method to prioritize pollution abatement efforts.

TABLE IV-10

SUGGESTED CONFIGURATION FOR WATER AND NUTRIENT BALANCE TABLE

<u>SOURCES</u>	<u>FLOW RATE</u>	<u>LOADING RATE</u>			
		<u>TN</u>	<u>%</u>	<u>TP</u>	<u>%</u>
- UPSTREAM					
- TRIBUTARIES					
- IRRIGATION RETURNS					
- MUNICIPAL					
- INDUSTRIAL					
• • •					
TOTAL					
<u>LOSSES</u>					
- DOWNSTREAM					
- DIVERSIONS					
• • •					
TOTAL					
$\frac{\text{SOURCES} - \text{LOSSES}}{\text{LOSSES}} \times 100$					

EXAMPLE IV-3

Figure IV-5 shows a hypothetical river which has three tributaries, a nonpoint source of runoff, and two diversions. Develop a water balance for this system. The known flow rates are:

Identification Number	Flow rate (cfs)
1	2000
2	4000
3	1200
4	200
5	800
6	1000
7	2000
8	6000

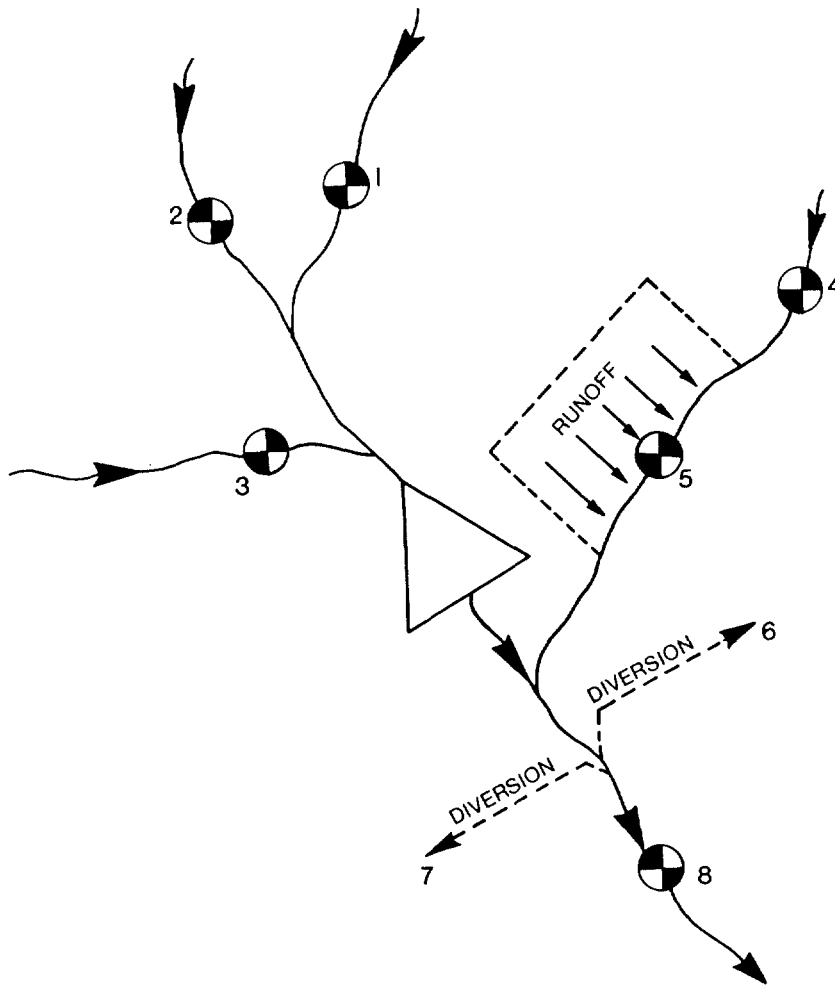


FIGURE IV-5 ILLUSTRATION OF WATER BALANCE

The flowrates at locations 1, 2, 3, and 5 are assumed to comprise the inflow rates to the system. The total inflows are:

<u>Identification Number</u>	<u>Inflows</u>
1	2000 cfs
2	4000 cfs
3	1200 cfs
5	<u>800 cfs</u>
Total	8000 cfs

The inflow from gage 4 is not needed because gage 5 is located further downstream on the same tributary. The outflows consist of diversions 6 and 7 and the downstream outflow past gage 8:

<u>Identification Number</u>	<u>Outflows</u>
6	1000 cfs
7	2000 cfs
8	<u>6000 cfs</u>
	9000 cfs

The inflows and outflows differ by 1000 cfs. There are several reasons for the imbalance. One, the flow rate past each gage is not measured perfectly, but differs by some degree from the actual flow rate. Two, the gage at location 5 does not catch all of the nonpoint source runoff, so there is an additional inflow to the system which has not been quantified. Three, depending on the size of the reservoir, direct precipitation and evaporation might be significant.

----- FND OF EXAMPLE IV-3 -----

The following example illustrates both a water and nutrient balance, and is based on work performed by Tetra Tech on the Snake River in Idaho (Mills 1979).

----- EXAMPLE IV-4 -----

Develop annual water and phosphorus balances for water year 1976 for the Snake River from Heise, Idaho, to below American Falls Reservoir, a distance of 150 miles. A sketch is shown in Figure IV-6. Estimate the phosphorus retention coefficient for American Falls Reservoir. The retention coefficient is defined as:

$$R_p = \frac{\text{Flux Input} - \text{Flux Output}}{\text{Flux Input}}$$



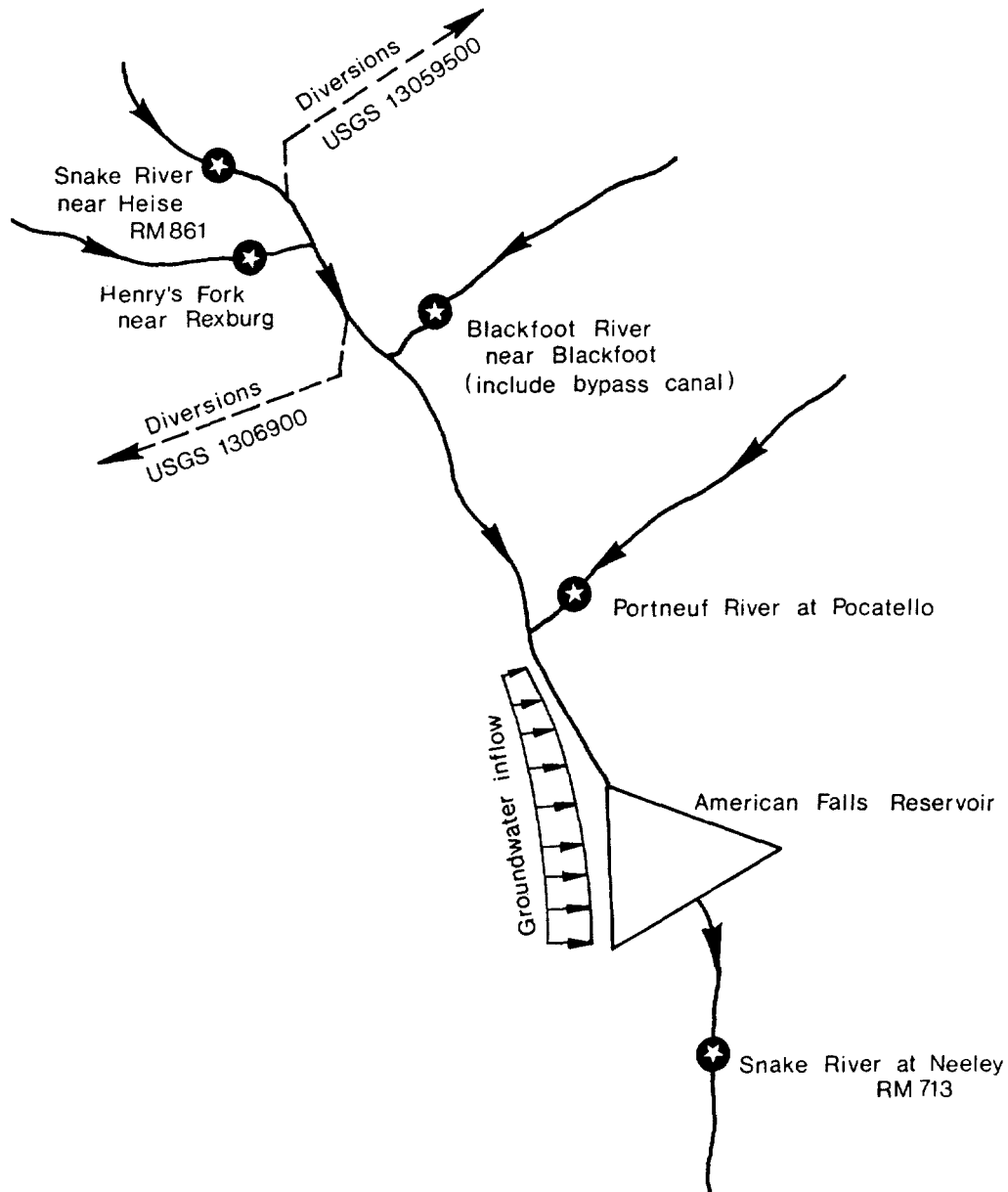


FIGURE IV-6 SKETCH OF SNAKE RIVER FROM HEISE TO NEELEY, IDAHO.

The required data are shown below:

Surface area of American Falls Reservoir = 56,600 acres

Evaporation rate in this part of United States = 33 inches/year

Precipitation = 11 inches/year

Ground water inflow into Snake River: 500 cfs

Ground water inflow into American Falls Reservoir: 2,100 cfs.

The total phosphorus concentrations were generated during the study of Mills (1979) and are provided here:

<u>Source</u>	<u>mg/l</u>
In rainwater	0.03
Snake River near Heise	0.05
Henrys Fork	0.11
Blackfoot River	0.26
Portneuf River	0.68
Groundwater inflow	0.23
Snake River near Neeley	0.08

The surface inflow rates are gaged by the U.S. Geological Survey and are reported in the U.S. Geological Survey Water Data Report for Idaho (1976). An example of how the information is tabulated in these reports is shown in Figure IV-7. From an entry in the Table, the mean flow rate for water year 1976 is 8549 cfs at USGS 30307500; near Heise. Rather than showing the remaining tabulations from the USGS report the flow rates from water year 1976 will simply be tabulated, as contained in the report.

<u>Source</u>	<u>Flow rate</u>
Blackfoot River	453 cfs
Henrys Fork	3,235 cfs
Portneuf River	412 cfs
USGS 13059500 (diversion)	2,333,700 ac-ft/yr
USGS 13069000 (diversion)	800,900 ac-ft/yr

Based on this information the water and total phosphorus balances are calculated and shown in Table IV-11. The flow rates are all converted to units of cfs. This requires converting the precipitation, evaporation, and diversions to these units. A precipitation rate of 11 inches per year is equivalent to 71 cfs:

$$11 \div 12 \times 56600 \times 43560 \div 366 \div 24 \div 3600 = 71 \text{ cfs}$$

The diverted flow in ac-ft/yr is converted to cfs as shown:

$$\text{USGS 13059500: } 2333700 \times 43560 \div 366 \div 24 \div 3600 = 3214$$

The percent difference between inflow rates and outflow rates is 4 percent.

Based on these flow rates, and the concentrations of total phosphorus presented earlier, the sources and losses of total phosphorus can be tabulated. For example, the mass flux of total phosphorus flowing past Heise can be calculated using Equation IV-10:

$$M = 5.38 \times 8549 \times 0.05 = 2300 \text{ lbs/day}$$

Continuing in this manner, the sources and losses are as tabulated in Table IV-11. The large imbalance is caused by retention at American Falls Reservoir.

The phosphorus loading to the reservoir is:

$$9589 - 865 - 415 = 8309 \text{ lbs/day}$$

LOCATION. --Lat 43°36'45", long 111°39'33", in SE/SW¼ sec.5, T.3 N., R.41 E., Bonneville County, Hydrologic Unit 17040104, on left bank, 850 ft (259 m) upstream from Anderson canal headgate, 2.4 mi (3.9 km) upstream from Heise, 6 mi (9.7 km) east of Ririe, 24 mi (38.6 km) upstream from Henry's Fork, and at mile 861.6 (1,386.3 km).  
 DRAINAGE AREA. --5,752 mi<sup>2</sup> (14,898 km<sup>2</sup>). Mean altitude, 7,770 ft (2,368 m).

Discharge, in Cubic Feet per Second, Water Year October 1975 to September 1976  
 Mean Values

Day	Oct	Nov	Dec	Jan	Feb	Mar	Apr	May	Jun	Jul	Aug	Sep
1	7020	3930	3550	3720	4130	4000	10900	18400	19000	9780	13200	5650
2	6920	3910	3580	3730	4140	4800	11100	18400	19100	10000	12600	5960
3	6720	3930	3560	3750	4100	5990	9360	<b>18600</b>	18000	10900	12000	6480
4	6360	3930	3560	3800	4180	6150	9430	18900	14800	10500	10200	6940
6	6120	3930	3730	3800	4540	6300	10400	18200	10800	10200	9880	7140
7	5970	3930	3760	3790	4770	6320	11700	18300	10700	10200	9390	7140
8	5790	3910	3760	3780	4640	6070	12800	18200	10700	10500	8640	7150
9	5430	3830	3760	3440	4710	6120	14000	18100	11000	11500	8410	6990
10	5100	3790	3780	3590	4440	6050	15400	18200	12200	12100	8260	6900
11	4710	3810	3780	3900	4280	7890	16000	18800	12300	11900	8060	6920
12	4440	3810	3780	3910	4270	8800	16100	18400	12100	11700	7670	7000
13	4440	3680	3730	3920	4230	8800	16100	18200	12000	12100	7460	6960
14	4470	3480	3720	3900	3940	8890	<b>16000</b>	18900	11900	12700	7420	6350
15	4240	3320	3710	3900	3740	8550	<b>18000</b>	19500	11800	13500	7450	5800
16	4110	3240	3720	4060	3750	8920	<b>16000</b>	19400	11900	13700	7440	5700
17	4110	3300	3690	4080	3740	9440	16200	19300	11900	13600	7390	5720
18	4110	3290	3680	4090	3670	9780	16300	20400	12000	13700	7450	5500
19	4110	3280	3680	4080	3950	9720	16100	22400	11900	13600	7140	5290
20	4110	3310	3670	4040	3950	9680	16600	23800	11900	13600	6950	5310
21	4090	3120	3680	4040	3960	9820	17200	23800	11900	13600	6750	5290
22	3980	3520	3680	4040	4000	9820	17300	23800	11300	13500	6680	5170
23	3960	3370	3700	4040	4010	9930	17400	23800	10700	13500	6810	4930
24	3930	3370	3700	4060	4010	10100	17400	24200	10100	13500	6250	4840
25	3910	3350	3700	4090	3980	10100	17400	24000	9880	13500	5950	4840
26	3930	3380	3690	4090	3990	10100	17200	24000	9400	13500	5810	4830
27	3960	3390	3700	4090	3980	10000	17100	23900	9370	13500	5710	4820
28	3960	3390	3670	4100	4000	9990	17700	24000	9340	13500	5690	4680
29	3910	3450	3670	4090	4010	10400	18100	22200	9310	13500	5680	4580
30	3930	3520	3700	4100	--	10600	18200	20400	9310	13500	5690	4570
31	3930	--	3700	4100	--	10500	--	19700	--	13500	5640	--
Total	147890	107360	114370	122630	119480	259810	450820	637000	363410	385580	244770	176110
Mean	4770	3573	3689	3955	4120	8380	15027	20548	12113	12438	7895	5870
Max	7020	3930	3780	4100	4770	10600	18200	24200	19100	13700	13200	7150
Min	3910	3120	3550	3720	3740	4000	9330	18100	9310	9780	5640	4570
Ac-Ft†	<b>293300</b>	212900	226900	243200	237000	515300	894200	1283000	720800	764800	485500	349300
Mean	4320	3840	3708	3270	3081	3054	6005	25880	25000	13610	6490	4677
Ac-		228500	228000	201100	177200	187800	357300	1591400	1487300	837100	399100	278300

Cal Yr 1975 Total 2895880 Mean 7933 Max 21700 Min 2940 Ac-Ft 5744000 Mean† 8015 Ac-Ft 5802600  
 Wtr Yr 1976 Total 3129230 Mean 8549 Max 24200 Min 3120 Ac-Ft 6207000 Mean 8595 Ac-Ft 6239600

† Adjusted for storage in Jackson Lake and Palisades Reservoir; no account taken for time of travel between reservoirs and Heise gaging station.

FIGURE IV-7 EXAMPLE OF FLOW RATE INFORMATION TABULATED IN  
 U. S. GEOLOGICAL SURVEY'S WATER DATA REPORT

TABLE IV-11

## SOLUTION TO SNAKE RIVER WATER AND PHOSPHORUS BALANCE PROBLEM

	Flow Rate (cfs)	TP Loading (lbs/day)
<u>Sources</u>		
Snake River at Heise	8,549	2,300.
Blackfoot River	453	1,915.
Henry's Fork	3,235	634.
Portneuf River	412	1,510.
Ground water inflow into Snake River	500	619.
Ground water inflow into American Falls Reservoir	2,100	2,600.
Precipitation on American Falls Reservoir	<u>71</u>	<u>11.</u>
$\Sigma$ Sources	15,320	9,589.
<u>Losses</u>	Flow Rate (cfs)	TP Loading (lbs/day)
USGS 13059500	3,214.	865
USGS 13069000	1,103	415
Snake River at Neelley	11,360.	4,890
Evaporation	<u>215.</u>	<u>-</u>
$\Sigma$ Losses	15,892.	6,170
For flow,	$\left( \frac{\text{Losses} - \text{Sources}}{\text{Losses}} \right)$	100 = 4%

Since the phosphorus leaving the reservoir is 4890 lbs/day, the retention coefficient is:

$$R_p = \frac{8309 - 4890}{8309} = .41$$

American Falls Reservoir retains a significant quantity of the phosphorus which enters the reservoir and consequently tends to keep phosphorus levels in the Snake River below the dam depressed compared with what they would otherwise be.

END OF EXAMPLE IV-4

#### 4.1.11 Hand Held Calculator Programs

It has become apparent that, after applying the river screening techniques contained in the original manual (Zison et al. , 1977) to real systems, a substantial savings of both time and effort could be realized by programming the major computational sequences. To this end, these algorithms have been programmed on the Texas Instrument TI-59 calculator and are available upon request in a document prepared by Tetra Tech (Mills et al. , 1979)\*. To date the algorithms contained in Mills et al. (1979) predict:

- Equilibrium temperature
- Longitudinal instream temperature distribution
- Mixing temperatures
- BOD profiles for point and nonpoint sources
- Reaeration rates
- Dissolved oxygen profiles
- Waste assimilative capacity and critical dissolved oxygen levels
- Coliform profiles for point and nonpoint sources
- Bed material sediment transport.

For each program contained in the document the following information is provided for the user:

- A detailed set of user instructions
- A program listing
- A sample input/output sequence

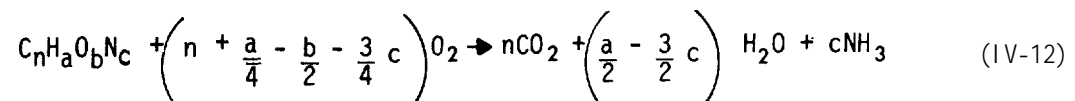
An example set of user instructions is shown in Figure IV-8. The first 6 steps are for data entry and the seventh is for calculation of the required information.

### 4.2 CARBONACEOUS AND NITROGENOUS OXYGEN DEMAND

#### 4.2.1 Introduction

Many wastes discharged into waterways contain biologically oxidizable materials that exert an oxygen demand on waterway resources. This biochemical oxygen demand (BOD) can be subdivided into carbonaceous (CBOD) and nitrogenous (NBOD) components. Table IV-12 illustrates typical concentrations of NBOD and CBOD in untreated municipal waste.

CBOD represents the amount of oxygen required by bacteria to stabilize organic matter under aerobic conditions. The reaction can be approximated by:



---

\* Attention: W.B. Mills, Tetra Tech, Inc.  
3746 Mt. Diablo Blvd., Suite 300 Lafayette, California 94549

PROGRAM DESCRIPTION

Program: Critical Dissolved Oxygen Calculations  
 This program calculates the critical dissolved oxygen deficit downstream from a point source of pollution. It also calculates the travel time to the critical deficit.  
 Note that if the travel time turns out to be negative, then the critical deficit occurs at the point where pollution enters the stream.

USER INSTRUCTIONS

STEP	PROCEDURE	ENTER	PRESS	DISPLAY
1	Enter program - see listing following these instructions	program	D	0
2	Enter re-aeration rate at 20°C, $k_{a20}$ (1/day)	$k_{a20}$	R/S	0
3	Enter deoxygenation rate at 20°C, $k_{d20}$ (1/day)	$k_{d20}$	R/S	0
4	Enter BOD concentration in stream just below source of pollution, $L_0$ (mg/l)	$L_0$	R/S	0
5	Enter dissolved oxygen deficit in stream just below source of pollution, $D_0$ (mg/l)	$D_0$	R/S	0
6	Enter stream temperature, T (°C)	T	R/S	0
7	Calculate and display:			
	- re-aeration rate at stream temperature, $k_a$ (1/day)		R/S	$k_a$
	- deoxygenation rate at stream temperature, $k_d$ (1/day)		R/S	$k_d$
	- travel time to critical deficit, $t_c$ (days)		R/S	$t_c$
	- critical deficit, $D_c$ (mg/l)		R/S	$D_c$

FIGURE IV-8 EXAMPLE SET OF USER'S INSTRUCTIONS FOR HAND HELD CALCULATOR PROGRAMS

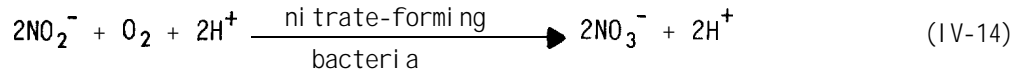
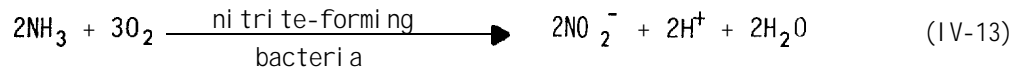
This reaction assumes that the available organic matter is completely oxidized. Bacteria, however, might not be able to completely oxidize all of the available organic matter. Equation IV-13 does illustrate that oxidation of the nitrogen is not included as part of CBOD. The reduced nitrogen is oxidized to nitrate in a two step process as follows:

TABLE IV-12

MUNICIPAL WASTE CHARACTERISTICS  
BEFORE TREATMENT (THOMANN, 1972)

Variable	Unit	Approx. Average	Normal Range
Average Daily Flow	gal /cap/day	125	100-200
Solids			
Total	mg/l	800	450-1200
Total Volatile	mg/l	400	250-800
Total Dissolved	mg/l	500	300-800
Total Suspended	mg/l	300	100-400
Volatile Suspended	mg/l	130	80-200
Settleable	mg/l	150	-
BOD			
Carbonaceous (5 day)	mg/l	180	100-450
Carbonaceous (ultimate)	mg/l	220	120-580
Nitrogenous*	mg/l	220	-
Nitrogen			
Total	mg/l N	50	15-100
Organic	mg/l N	20	5-35
Ammonia	mg/l N	28	10-60
Nitrite + Nitrate	mg/l N	2	0-6
Phosphate			
Total	mg/l PO <sub>4</sub>	20	10-50
Ortho	mg/l PO <sub>4</sub>	10	5-25
Poly	mg/l PO <sub>4</sub>	10	5-25
Coliforms			
Total	million org./100 ml	30	2-50
Fecal	million org./100 ml	4	0.3-17

\*Ultimate, Nitrogenous oxygen demand, exclusive of CBOD.



Based on Equations IV-13 and IV-14 the NBOD is:

$$\text{NBOD} = 4.57 \left( \left[ \text{Org-N} \right] + \left[ \text{NH}_4^+ - \text{N} \right] \right) + 1.14 \left[ \text{NO}_2^- - \text{N} \right] \quad (\text{IV-15})$$

Typically the nitrite concentration is negligible so that:

$$\text{NBOD} = 4.57 (\text{TON}) \quad (\text{IV-16})$$

where TON represents total oxidizable nitrogen, the sum of organic and ammonia nitrogen. Atypical value of TON from Table IV-12 is  $20 + 28 = 48 \text{ mg-N/l}$ , which corresponds to an NBOD of  $220 \text{ mg/l}$ .

Typically in the bottle determination of CBOD and NBOD, the carbonaceous demand precedes the nitrogenous demand by 5 to 10 days, as shown in Figure IV-9. This has led workers to believe that nitrification can be ignored in river environments below a source of pollution up to a distance corresponding to a travel time of five to ten days. Such an assumption might be invalid for several reasons. Given that there are numerous sources of pollution along many rivers a viable population of nitrifying bacteria may already be present within the water column. Second, nitrifiers can grow attached to the bottom substrate. Consequently, significant numbers can exist just below the discharge location and nitrification can proceed immediately. Nitrification by attached bacteria is more likely to be of significance in relatively shallow, wide rivers, which have stable bottom substrate (Mills, 1976).

CBOD is a commonly measured characteristic of waste water. The CBOD used in the formulations presented below is the ultimate CBOD. Often CBOD is expressed as  $\text{CBOD}_5$ , the oxygen utilized in a 5 day test. The relationship between ultimate ( $\text{CBOD}_L$ ) and 5-day CBOD can be approximated by:

$$\text{CBOD}_L = \frac{\text{CBOD}_5}{0.68}$$

This relationship assumes a decay rate of  $0.23/\text{day}$ , and may be different for effluents from advanced wastewater treatment plants.

The mass balance equation used in the CBOD analysis is exactly analogous to the NBOD equation. The first order decay rate assumption for NBOD stabilization is necessary to maintain this analogy, and is sufficient for hand calculations.



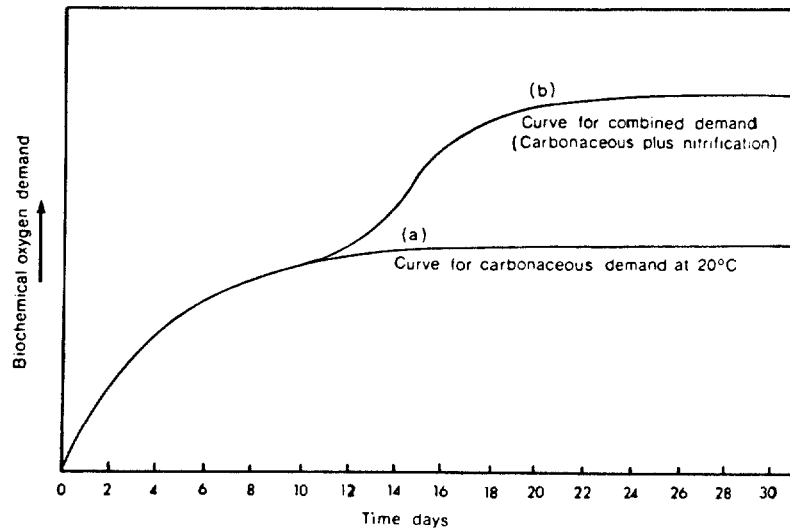


FIGURE IV-9 THE BOD CURVE, (A) CURVE FOR OXIDATION OF CARBONACEOUS MATTER, (B) CURVE SHOWING INFLUENCE OF NITRIFICATION.

Nitrification (the process by which ammonia is oxidized to nitrite, and nitrite to nitrate) is pH dependent with an optimum range of 8.0 to 8.5 (Wild, 1971). If the pH of the river is below 7.0, nitrification is not likely to be important.

#### 4.2.2 BOD Decay Rate

The decay rate for CBOD will be denoted by  $k_L$  and for NBOD by  $k_N$ . Typical values of both  $k_L$  and  $k_N$  lie between 0.1 and 0.6/day, with 0.3/day being typical  $k_L$  values can, however, exceed the range given here. Values of 1 to 3/day have been computed for shallow streams (Thomann, 1972). A figure to be presented shortly will show how  $k_L$  depends on depth. The following discussion will be directed toward  $k_L$ , but in general will also apply to  $k_N$ .

The disappearance of BOD from a river is a reflection of both settling and biochemical oxidation, as shown in Figure IV-10. Biochemical oxidation can consist of instream oxidation ( $k_1L$ ) as well as absorption by attached organisms ( $k_4L$ ). The total oxidation rate then, is  $k_d$ , where:

$$k_d = k_1 + k_4$$

The total loss rate  $k_L$  is:

$$k_L = k_d + k_3$$

where  $k_3$  reflects settling losses.

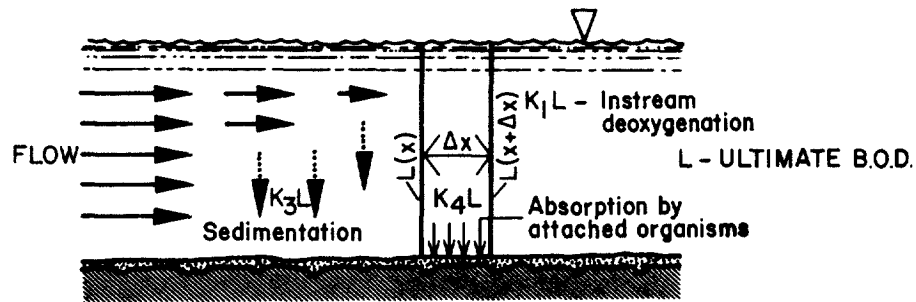


FIGURE IV-10 MECHANISMS OF BOD REMOVAL FROM RIVERS

Settling of BOD is generally more prevalent just below a sewage discharge where the discharged material may contain a large suspended fraction. As this material is transported downstream the settling component becomes less important and the reaction rate  $k_L$  approaches the oxidation rate  $k_d$ . In this chapter, the settling component will not be explicitly considered. Neglecting settling will tend to cause estimated instream BOD levels to be somewhat higher than they actually might be along certain portions of a river. It should be noted that if instream BOD data are used to determine  $k_L$  (one such method will be explained in Figure IV-12) then the effect of settling is automatically included in  $k_L$ .

Figure IV-11 illustrates the dependence of  $k_L$  on river depth. The highest deoxygenation rates occur in shallow streams with stable, rocky beds, reflecting the significance of attached biological organisms. Bowie *et al.* (1985) contains observed and predicted values of  $k_L$  for various natural streams.

The decay coefficients  $k_L$  and  $k_N$  are both temperature dependent and this dependence can be estimated by:

$$k_T = k_{20} 1.047^{(T-20)} \quad (IV-17)$$

where

$$\begin{aligned} k_{20} &= k_L \text{ or } k_N \text{ at } 20^\circ\text{C} \\ k_T &= k_L \text{ or } k_N \text{ at } T^\circ\text{C} \\ T &= \text{water temperature, } ^\circ\text{C.} \end{aligned}$$

Numerous methods for computing  $k_L$  from observed data are available (Nemerow, 1974). One method entails the use of a semi-log plot. The stretch of river containing the data to be plotted must have a constant stream area and flow rate, and the BOD loading must be from a point source located at a position that will be called  $x = 0$ . Plotting the log of BOD concentration versus distance generally produces a

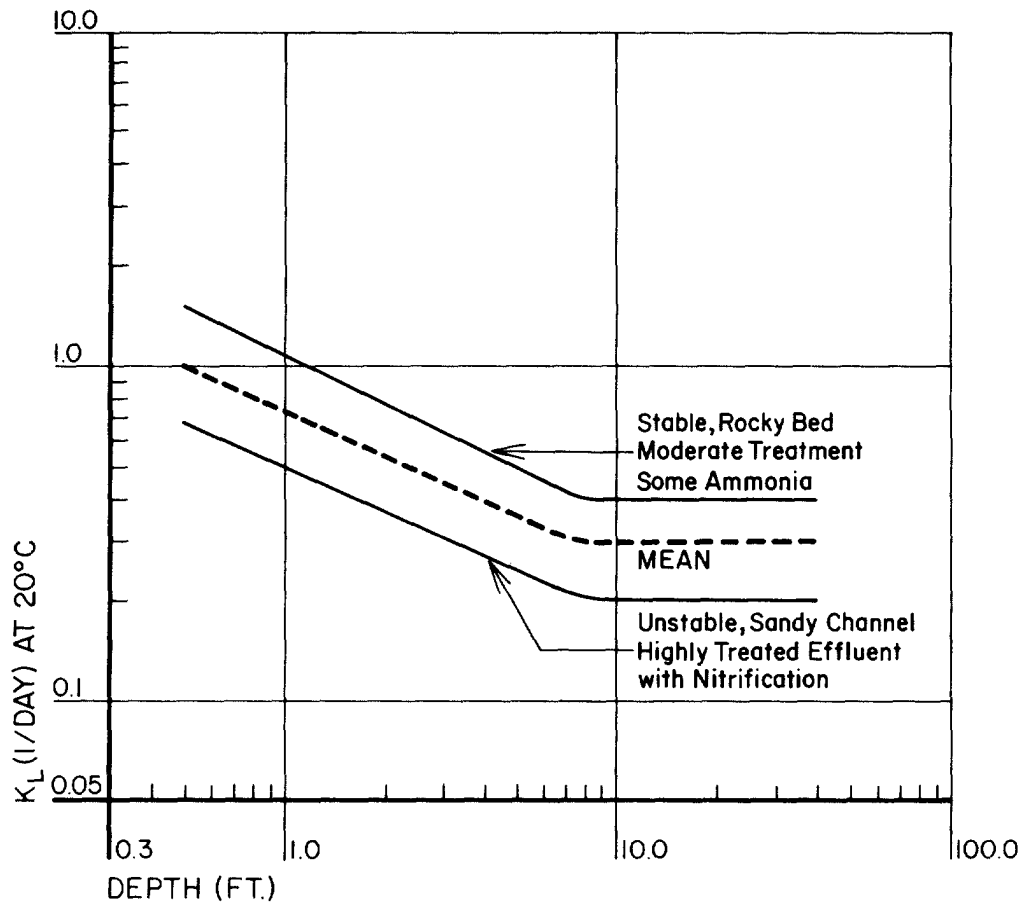


FIGURE IV-11 DEOXYGENATION COEFFICIENT AS A FUNCTION OF DEPTH, (AFTER HYDROSCIENCE, 1971)

straight line with slope of  $-k_L/U$ . An example is shown in Figure IV-12. Either  $CBOD_5$  or  $CBOD_L$  can be plotted as the ordinate. The slope should be converted from base 10 logarithms as given in the semi-log plot to base e logarithms as needed in the formulations used in this chapter. The conversion is made by multiplying the value for log base 10 by 2.303.

Wright and McDonnell (1979) have more recently developed an expression for instream BOD decay rate based on the flow rate of the river. The expression is:

$$k_d \left( \frac{1}{\text{day}} \right) = \begin{cases} k_{1ab} & \text{if } Q > 800 \text{ cfs} \\ \frac{10.3}{\sqrt{Q}} & \text{if } Q < 800 \text{ cfs} \end{cases} \quad \begin{matrix} \text{(IV-18a)} \\ \text{(IV-18b)} \end{matrix}$$

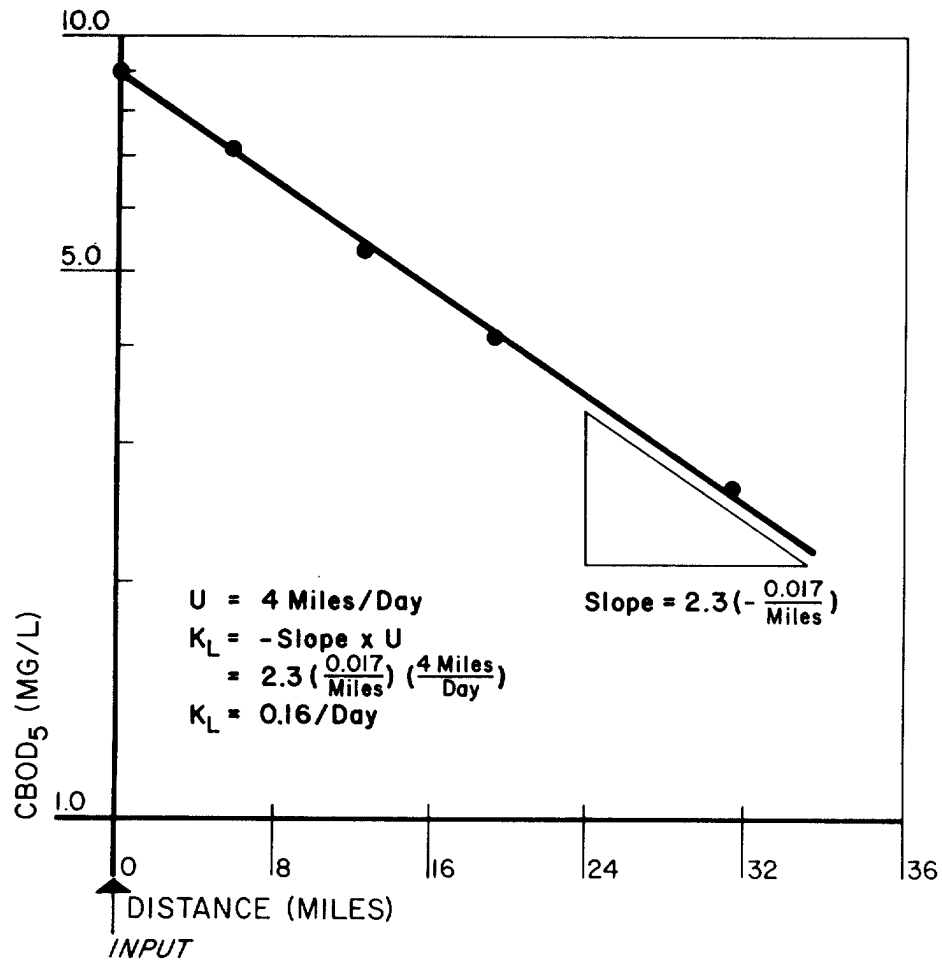


FIGURE IV-12 EXAMPLE OF COMPUTATION OF  $k_L$  FROM STREAM DATA (FROM HYDROSCIENCE, 1971)

This expression is particularly attractive because the only hydraulic variable required is flow rate. Other predictive techniques and rate data from rivers around the country are contained in Zison *et al.* (1978).

#### 4.2.3 Mass Balance of BOD

The general mass-balance equation for BOD in rivers is:

$$\frac{\partial L}{\partial t} = 0 = -\frac{1}{A} \frac{\partial}{\partial x} (QL) - k_L L + L_r \left( \frac{\partial Q}{\partial x} \right) / A + L_{rd} \quad (\text{IV-19})$$

where

- $L$  = CBOD (ultimate) remaining to be oxidized, mg/l
- $Q$  = volumetric flow rate,  $\text{ft}^3/\text{sec}$
- $A$  = cross-sectional area,  $\text{ft}^2$
- $L_r$  = concentration of CBOD entering through an incremental sideflow (distributed source), mg/l
- $L_{rd}$  = mass flux of CBOD entering, with no associated flow, mg/l/sec
- $x$  = stream distance
- $\frac{\partial L}{\partial t} = 0$  indicates that steady-state conditions are being assumed and thus no accumulation of material takes place at any point within the reach.

The NBOD equation is completely analogous in form to Equation IV-19:

$$\frac{\partial N}{\partial t} = 0 = -\frac{1}{A} \frac{\partial}{\partial x} (QN) - k_N N + N_r \left( \frac{\partial Q}{\partial x} \right) / A + N_{rd} \quad (\text{IV-20})$$

where

$N$  = the NBOD.

$N_{rd}$  represents purely a mass flux of nitrogenous material, while  $N_r \left( \frac{\partial Q}{\partial x} \right) / A$  is a source of NBOD entering the river reach through an incremental sideflow. Thus, in cases where a known distributed source of BOD significantly contributes to a river reach under study, and the distributed flow (flow associated with a distributed source) can be neglected,  $N_{rd}$  can be used in lieu of  $N_r \left( \frac{\partial Q}{\partial x} \right) / A$ .  $N_{rd}$  can be estimated by determining the mass  $M$  of BOD entering a volume of river water  $V$  in time  $T$ .  $N_{rd}$  is given by:

$$N_{rd} = \frac{M}{VT}$$

For any particular reach of a river under investigation the stream cross-sectional area can be expressed by:

$$A = A_0 + \left( \frac{A_f - A_0}{x_L} \right) x = A_0 + \Delta_A x \quad (\text{IV-21})$$

where

$$\Delta_A = \frac{A_f - A_0}{x_L}$$

$A_0$  = stream cross-sectional area at upstream end of the reach

$A_f$  = stream cross-sectional area at downstream end of reach

$x$  = distance downstream from beginning of reach

$x_L$  = length of reach.

The cross-sectional area need not be measured directly, but can be computed from:

$$A = \frac{Q}{U}$$

The cross-sectional area change can reflect a change in stream velocity, perhaps due to a bed slope increase or decrease. The length of the reach under investigation,  $X_L$ , is measured in river miles along the river's centerline. If use of a constant stream area is assumed, then  $\Delta_A = 0$  and  $A = A_0$  throughout the reach.

#### 4.2.4 Typical Solutions

Case 1: The only source of CBOD occurs as a point source at  $x = 0$ . The CBOD distribution is then expressed by:

$$L = L_0 \exp \left[ \frac{-j_L}{A_0} \left( A_0 x + \Delta_A \frac{x^2}{2} \right) \right] \quad (IV-22)$$

where

$$j_L = \frac{k_L}{U_0}$$

$U_0$  = stream velocity at  $x = 0$

$L_0$  = ultimate BOD at the upstream end of the reach

$L$  = ultimate BOD at a distance  $x$  downstream

The other terms have previously been defined.

The initial CBOD,  $L_0$ , must reflect both CBOD upstream of the reach as well as that contributed by the point source in question. It is given by:

$$L_0 = \frac{L_u Q_u + W/5.38}{Q_u + Q_w} \quad (IV-23)$$

where

$W$  = mass rate of discharge of CBOD, lb/day

$Q_u$  = upstream river flow, cfs

$Q_w$  = waste flow rate, cfs

$L_u$  = upstream CBOD concentration, mg/l.

Case 2: For a point source of CBOD at  $x = 0$  and a distributed mass influx of CBOD (with no associated flow) entering the river throughout the reach, the solution is:

$$L = \frac{L_{rd}}{k_L} + \left( L_0 - \frac{L_{rd}}{k_L} \right) \exp \left[ \frac{-j_L}{A_0} \left( A_0 x + \Delta_A \frac{x^2}{2} \right) \right] \quad (IV-24)$$

where

$L_{rd}$  = mass rate of CBOD entering the reach per unit volume of river water, mg/l/day.

Case 3: A distributed flow enters the river carrying CBOD and a point source of CBOD exists at  $x = 0$ . The flow rate  $Q$  at a distance  $x$  is:

$$Q = Q_0 + \frac{Q_f - Q_0}{x_L} x = Q_0 + \Delta Q x$$

where

$$\Delta Q = \frac{Q_f - Q_0}{x_L}$$

The BOD distribution is given by (the river cross-sectional area is assumed constant throughout the reach):

$$L = \frac{L_r}{E_1} + \left( L_0 - \frac{L_r}{E_1} \right) \left( \frac{Q_0}{Q} \right)^{E_1} \quad (IV-25)$$

where

$$E_1 = \frac{k_L A_0 + \Delta Q}{\Delta Q}$$

$L_r$  = concentration of CBOD entering the river in the distributed flow, mg/l.

Case 3 can also be used to establish the effect a purely diluting inflow (i.e.  $L_r = 0$ ) would have on the CBOD distribution.

Case 4: For a point source at  $x = 0$ , a distributed source with associated inflow, and a mass flux with no associated flow (constant river cross-sectional area), the solution is:

$$L = L_0 \left( \frac{Q_0}{Q} \right)^{E_1} + \frac{L_r \Delta Q + L_{rd} A_0}{k_L A_0 + \Delta Q} \left( 1 - \left( \frac{Q_0}{Q} \right)^{E_1} \right) \quad (IV-26)$$

where

$$E_1 = \frac{k_L A_0 + \Delta Q}{\Delta Q}, \text{ as in Case 3}$$

#### 4.2.5 Other Simplifying Procedures

The formulations represented by Equations IV-22 through IV-26 offer a range of options for examining BOD distribution in rivers. However, there are additional methods of estimating instream concentrations and determining whether or not significant BOD levels exist. Perhaps the simplest method is assuming that BOD does not decay. An upper limit of the instream concentration at any point can then be determined by incorporating all known sources, and using the methods presented in Section 4.7. If the computed instream concentrations are below a threshold pollution level, then there is no need to apply Equations IV-22 through IV-26 because the inclusion of a decay rate will only lower the concentrations,

It may also be feasible, as a first estimate; to combine the CBOD and NBOD equations into one, and use that equation to estimate the distribution of the total oxygen-demanding material. To do this, all source terms must include both CBOD and NBOD. One decay coefficient is used for both CBOD and NBOD decay. The larger decay coefficient of the two should be used since that will produce the larger oxygen deficit.

In deciding which of Equations IV-22 through IV-26 to use for any analysis, the purpose of the analysis as well as data availability should be considered. If the main purpose is to estimate differences in stream concentrations caused by various levels of abatement at a sewage treatment plant, the diffuse sources of BOD need not be considered. The resulting concentration difference can be expressed as:

$$\Delta L = \begin{cases} \Delta L_0 \exp \left[ \frac{-j_L}{A_0} \left( A_0 x + \Delta A \frac{x^2}{2} \right) \right] & \text{(IV-27a)} \\ \Delta L_0 \left( \frac{Q_0}{Q} \right)^{E_1} & \text{(IV-27b)} \end{cases}$$

where

$\Delta L$  = the change in BOD concentration due to a change,  $\Delta L_0$ , in the initial concentration.

Equation IV-27A should be used for a Case 1 or Case 2 situation, and Equation IV-27B for Case 3 or Case 4. If an estimate of the absolute level of BOD is desired, however, then the appropriate expression including the nonpoint sources should be utilized. It should be noted that if the diffuse sources of BOD are large then the improvement of instream BOD concentrations by point source control will be relatively minor. In that case the planner should focus on nonpoint source control.



EXAMPLE IV-5

Estimating BOD Distribution in a River

Suppose the user wants to calculate the BOD distribution in the river shown below in Figure IV-13. There are nine point sources contributing BOD

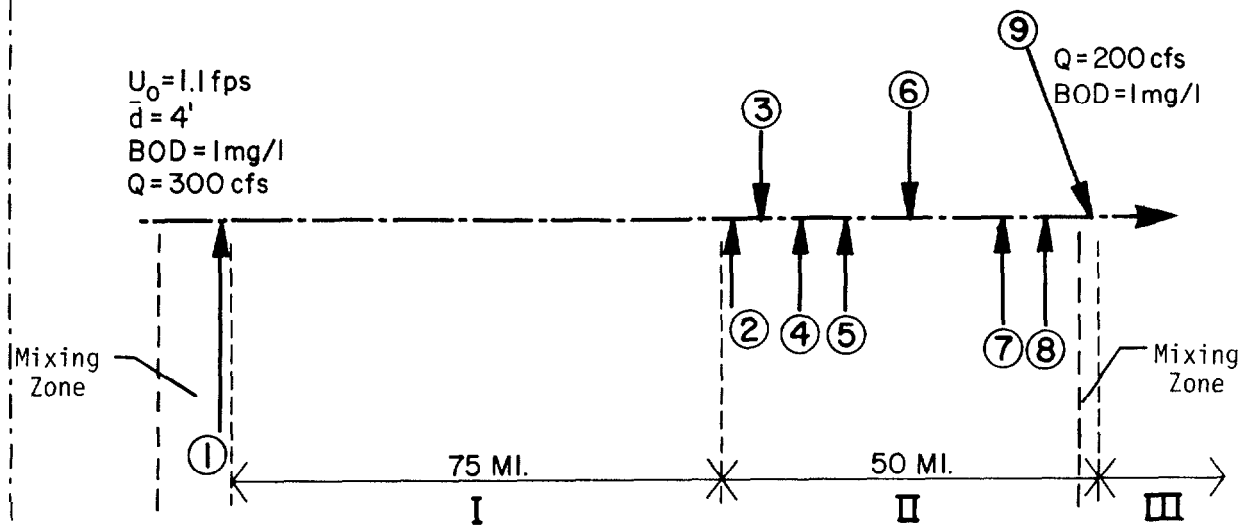


FIGURE IV-13 HYPOTHETICAL BOD WASTE LOADINGS IN A RIVER

in the stretch of river under consideration. The ninth source is assumed to be a tributary, and contributes substantially more flow than the other eight. Begin by dividing the river into reaches. The first reach (I) should include the first 75 miles in which there is one point source of BOD at the upstream end (source (1)). Equation IV-22 is applicable to that reach. Now, there are several choices available regarding the division of the river between sources (2) and (8). One choice is to divide the 50 miles into mini-reaches similar to Reach I, and reapply Equation IV-22 seven more times. A second alternative is to group adjacent point sources into fewer and larger sources, thereby requiring fewer applications of Equation IV-22. A third alternative is to assume that sources (2) through (8) comprise one continuous distributed source, the total pollutant loading of this equivalent source being equal to the sum of the individual loads. For this representation to be valid the sources should be both evenly spread spatially and be discharging comparable loads. The third alternative will be examined here, and reach II will consist of the 50 miles following Reach I. Equation IV-25 will be used to analyze Reach II. Reach III, then, will begin just downstream from the tributary (source (9)).

For Reach I, Equation IV-22 is first solved. Suppose the following characteristics of waste source (1) are known:

$$Q = 20 \text{ MGD} = 1.55 (20) \text{ cfs} \\ = 31 \text{ cfs}$$

$$W = 5000 \text{ lb. BOD}_5/\text{day}$$

Recall that:

$$L_o = \frac{L_u Q_u + W/5.38}{Q_u + Q_w}$$

W must be in lb. BOD ultimate/day:

$$W = \frac{5000}{.68} \\ = 7353 \text{ lb. BOD}_L/\text{day}$$

then

$$L_o = \frac{(1)(300) + 7353/5.38}{300 + 31} \\ = 5.0 \text{ mg/l}$$

The decay coefficient is estimated from Figure IV-11 as 0.4/day. No correction will be made for temperature. Equation IV-22 can now be expressed as (for constant cross-sectional area):

$$L = 5 \exp\left(\frac{-0.4}{(1.1)(24)(3600)} x\right)$$

where x is the downstream distance in feet. Note the correction needed to convert the decay coefficient from units of 1/day to 1/sec.

The results of the above equation for selected distances downstream can be expressed as follows:

x (miles)	L(mg/l)
0	5.0
30	2.6
60	1.3
75	0.9

For Reach II, sources (2) through (8) are assumed to contribute the following loading:

$$\text{BOD} = 8000 \text{ lb/day}$$

$$Q = 120 \text{ MGD}$$

$$= 186 \text{ cfs}$$

The flow distribution, Q, in Reach II, is then:

$$Q = Q_o + \frac{Q_f - Q_o}{x_L} x \\ = 331 + \frac{186}{50} x$$

where  $x$  is in miles (from 0 to 50).  $L_r$ , the average  $BOD_L$  concentration in the incoming flow is:

$$L_r = \frac{8000 \text{ lb/day}}{120 \text{ MGD}} \times \frac{1 \text{ mg/l}}{8.34 \text{ lb/day}} \\ = 8.0 \text{ mg/l}$$

If the average depth in Reach II is assumed to be 5 feet, then:

$$k_L = .3/\text{day}$$

Finally,  $E_1$  is computed:

$$E_1 = \frac{k_L A_o + \Delta Q}{\Delta Q}, \quad A_o = \frac{Q_o}{U_o} = \frac{331}{1.1} = 301 \text{ ft}^2$$

$$E_1 = \frac{\frac{(0.3)(301)}{(24)(3600)}}{\frac{186}{(50)(5280)}} + 1 = 2.5$$

Then, using  $L$  from the 75 mile point of Reach I as  $L_o$ :

$$L = \frac{8.0}{2.5} + \left(0.9 - \frac{8.0}{2.5}\right) \left(\frac{331}{Q}\right)^{2.5} \\ = 3.2 - 2.3 \left(\frac{331}{Q}\right)^{2.5}$$

In tabulated form:

$x$ (mi)	$Q$ (cfs)	$L$ (mg/l)
0	331	0.9
20	405	1.8
40	480	2.3
50	517	2.5

Note that the BOD concentration is increasing within this reach.

For reach III, only enough information is given to compute the initial concentration, utilizing weighted values for the BOD at the end of reach II and that entering through the tributary (source (9)).

$$L_o = \frac{200(1) + 517(2.5)}{200 + 517} = 2.1 \text{ mg/l}$$

END OF EXAMPLE IV-5

#### 4.2.6 Interpretation of Results

The most frequent use of BOD data in river water quality analyses involves their relationship with the dissolved oxygen balance. This relationship will be discussed more fully in Section 4.3. At this point it is sufficient to say that it is necessary to predict the BOD distribution in a river in order to compute dissolved oxygen concentrations.

When a river receives a heavy load of organic matter, the normal processes of self purification result in a series of zones of decreasingly severe conditions succeeding one another downstream. Each zone contains characteristic animals and plants (Nemerow, 1974). A saprobicity system (saprobicity is a measure of biodegradable organic matter) has been developed that relates BOD concentrations in streams to the degree of pollution there. Correlations have been found, for example, among BOD concentrations, coliform bacteria, and dissolved oxygen in rivers (Sladeczek, 1965). Sladeczek (1969) has assigned 5-day BOD values of 5 mg/l to mildly polluted conditions and 10 mg/l to substantial pollution.

Sources of drinking water are subject to restraints on the maximum allowable BOD that can be contained in raw water and still qualify as a drinking water source. Further, the degree of treatment of the raw water is dependent on the concentrations of certain constituents, such as BOD. One reference (HEC, 1975) has stated that water having a 5-day BOD over 4 mg/l, in combination with high levels of other constituents, represents a poor source of domestic water supply.

As discussed above, BOD in a river can come from a number of sources, both point and nonpoint. Although BOD reduction from point source might be easier to accomplish than from nonpoint sources, there is no guarantee that BOD levels will be substantially lowered.

### 4.3 DISSOLVED OXYGEN

#### 4.3.1 Introduction

Historically, dissolved oxygen has been and continues to be the single most frequently used indicator of water quality in streams and rivers. Figure IV-14 shows the seasonal variability of dissolved oxygen in 22 major waterways throughout the country (EPA, 1974) from 1968 to 1972. Invariably the levels observed from June to October are lower than those observed in January to March. This is due primarily to the influence of temperature on the dissolved oxygen levels. Due to the effect of temperature, summer is the most critical season in terms of organic pollutant assimilation in rivers.

The dissolved oxygen calculations presented below range in complexity from a simple CBOD-DO relationship to a more general dissolved oxygen mass balance including CBOD, NBOD, photosynthesis, respiration, and benthic demands. It should be

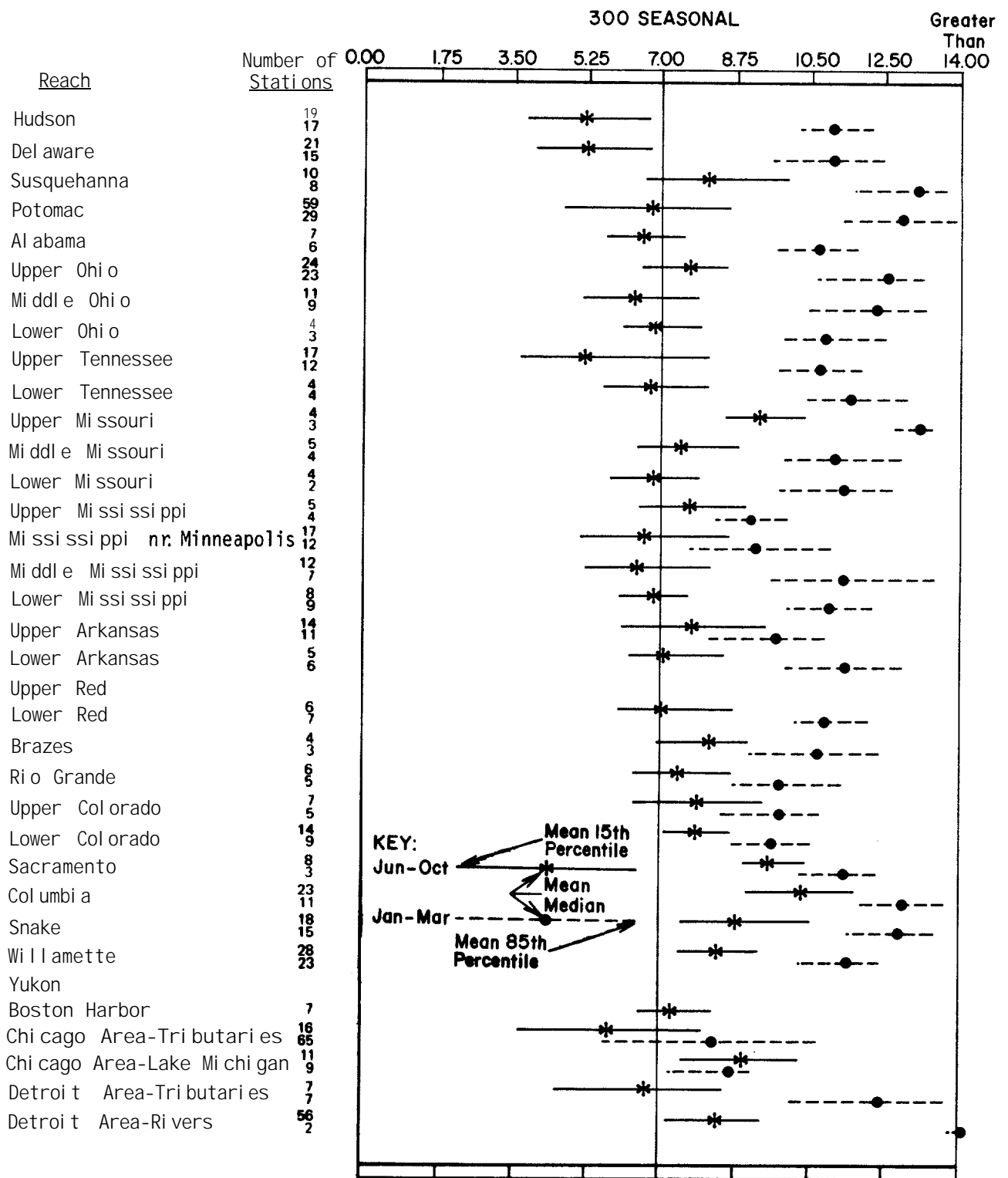


FIGURE IV-14 VARIABILITY OF DISSOLVED OXYGEN BY SEASON FOR 22 MAJOR WATERWAYS, 1968-72 (EPA, 1974)

stressed, however, that the results calculated from any of the relationships provide estimates only since each procedure incorporates various assumptions that might not be fully met. For example, waste loading inflows are assumed to remain constant in quality and quantity over time. In reality loadings probably vary over time. Furthermore the choice of system parameters involves a certain degree of judgement. However, for any given situation, the planner can establish an envelope of possible outcomes by different realistic choices of system parameters.

#### 4.3.2 Dissolved Oxygen Mass-Balance

The general dissolved oxygen mass-balance equation that will be utilized here is given by:

$$\frac{\partial C}{\partial t} = 0 = - \frac{1}{A} \frac{\partial(QC)}{\partial x} - k_L L - k_N N + k_a (C_s - C) - S_b + P - R \quad (IV-28)$$

where the new symbols introduced are:

- C = dissolved oxygen concentration, mg/l
- $k_a$  = reaeration coefficient, 1/day
- $C_s$  = saturation value of dissolved oxygen, mg/l
- $S_b$  = benthic oxygen demand, mg/l/day
- P = rate of oxygen production due to photosynthesis, mg/l/day
- R = rate of oxygen consumption due to algal respiration, mg/l/day.

Stated in words, Equation IV-24 expresses the following relationship:

At steady state, the rate of addition of dissolved oxygen to a river due to reaeration and photosynthesis equals the depletion rate caused by the net advective flow, carbonaceous oxidation, nitrogenous oxidation, benthic demands, and algal respiration.

Commonly, the dissolved oxygen mass-balance equation is expressed in terms of the deficit, D, which is the difference between the saturation and actual concentrations.

#### 4.3.3 Reaeration Rate

The atmosphere acts as the major source for replenishing the dissolved oxygen resources of rivers. Reaeration tends to equilibrate the dissolved oxygen concentration in a river with its saturation value. Most commonly, the dissolved oxygen concentration is below saturation and there is a net influx of oxygen into the river from the atmosphere. On occasion, due to the production of dissolved oxygen by algae, rivers or streams can become supersaturated, in which case there is a net loss of oxygen to the atmosphere.

A number of expressions for the reaeration coefficient,  $k_a$ , have been

developed. Several are presented here. O'Connor's formulation (Thomann, 1972) states that:

$$k_a = \frac{(D_L U)^{1/2}}{H^{3/2}} \text{ at } 20^\circ \text{ C} \quad (\text{IV-29})$$

where

$D_L$  = oxygen diffusivity = 0.000081 ft<sup>2</sup>/hr at 20°C

H = stream depth in ft

U = stream velocity in ft/sec.

Expressed in English units:

$$k_a = \frac{12.9 U^{1/2}}{H^{3/2}} \text{ at } 20^\circ \text{ C} \quad (\text{IV-30})$$

The above formula was verified on streams and rivers ranging in average depth from 1 foot to 30 feet with velocities ranging from 0.5 to 1.6 fps. Its use should be limited to streams where the reaeration coefficient is less than 12/day. Figure IV-15 illustrates how  $k_a$  changes with depth and velocity according to this relationship.

For shallow (0.4 - 2.4 feet), fast moving streams, the following expression developed by Owens (Thomann, 1972) is preferable, as the experimental work to develop this expression was done almost exclusively on shallow streams:

$$k_a = 21.6 \frac{U^{0.67}}{H^{1.85}} \text{ at } 20^\circ \text{ C} \quad (\text{IV-31})$$

where U is in ft/sec and H is in feet. A graphical representation of Equation IV-31 is shown in Figure IV-16.

Covar (1976) showed that there were certain combinations of river depths and velocities where a formula developed by Churchill (Churchill *et al.*, 1962) is more accurate than either the O'Connor or Owens formulations. The Churchill expression is:

$$k_a = 11.6U^{0.969} H^{-1.673} \text{ per day at } 20^\circ \text{ C} \quad (\text{IV-32})$$

The regions of validity, and the predicted values, for the three formulations are shown in Figure IV-17.

Recent studies have suggested that the Owens expression overestimates the reaeration rate for particularly shallow streams (e.g., less than a foot in depth). Under these circumstances the Tsioglou-Wallace method (Tsioglou and Wallace, 1978)

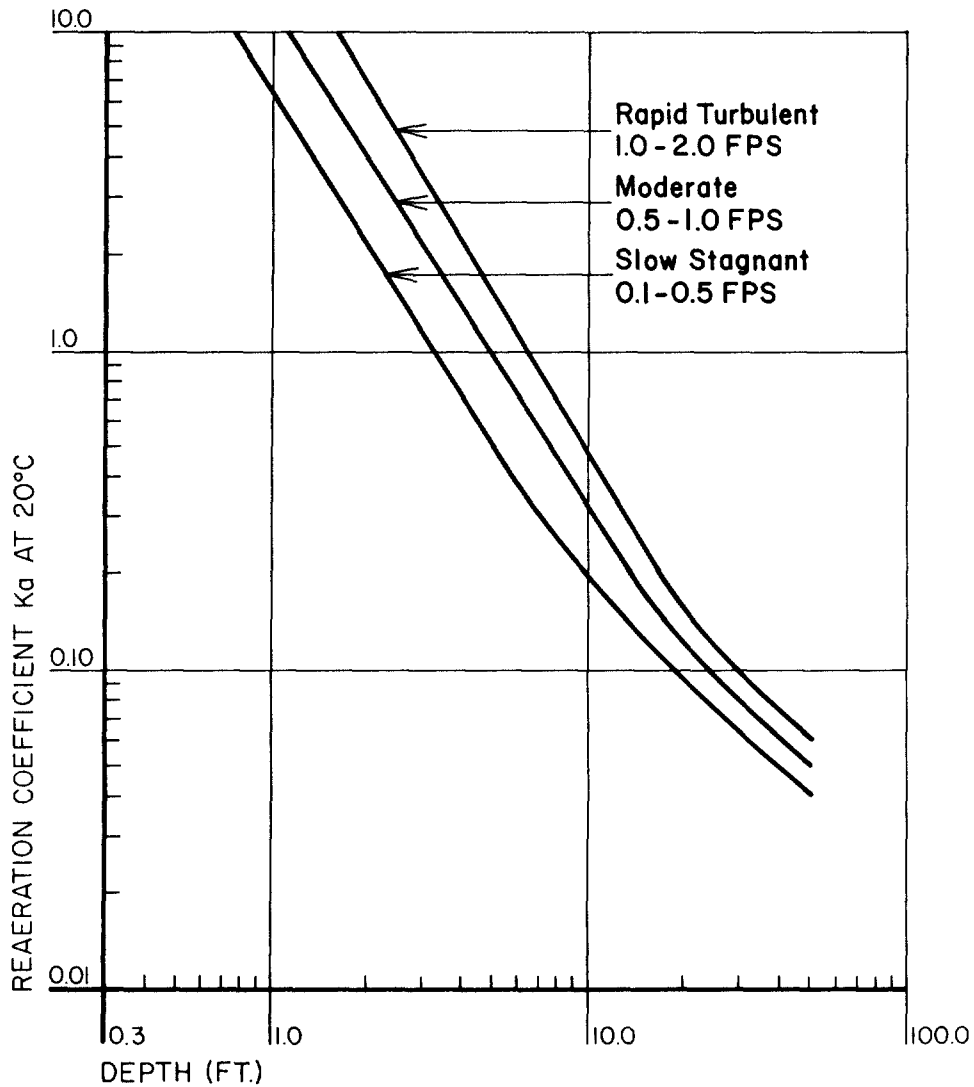


FIGURE IV-15 REAERATION COEFFICIENT AS A FUNCTION OF DEPTH  
(FROM HYDROSCIENCE, 1971)

is more accurate. The expression is:

$$k_a \text{ (1/day)} = \begin{cases} 7776. \text{ US, @ } 25^\circ\text{C, } Q < 10 \text{ cfs} & \text{(IV-33a)} \\ 4665.6 \text{ US, @ } 25^\circ\text{C, } 10 < Q < 3000 \text{ cfs} & \text{(IV-33b)} \\ 2592. \text{ US, @ } 25^\circ\text{C, } Q > 3000 \text{ cfs} & \text{(IV-33c)} \end{cases}$$

where

$s$  = stream slope, ft/ft.

Table IV-13 compares predictions of Tsi voglou-Wallace with observed values for several small streams in Wisconsin. The agreement is good.



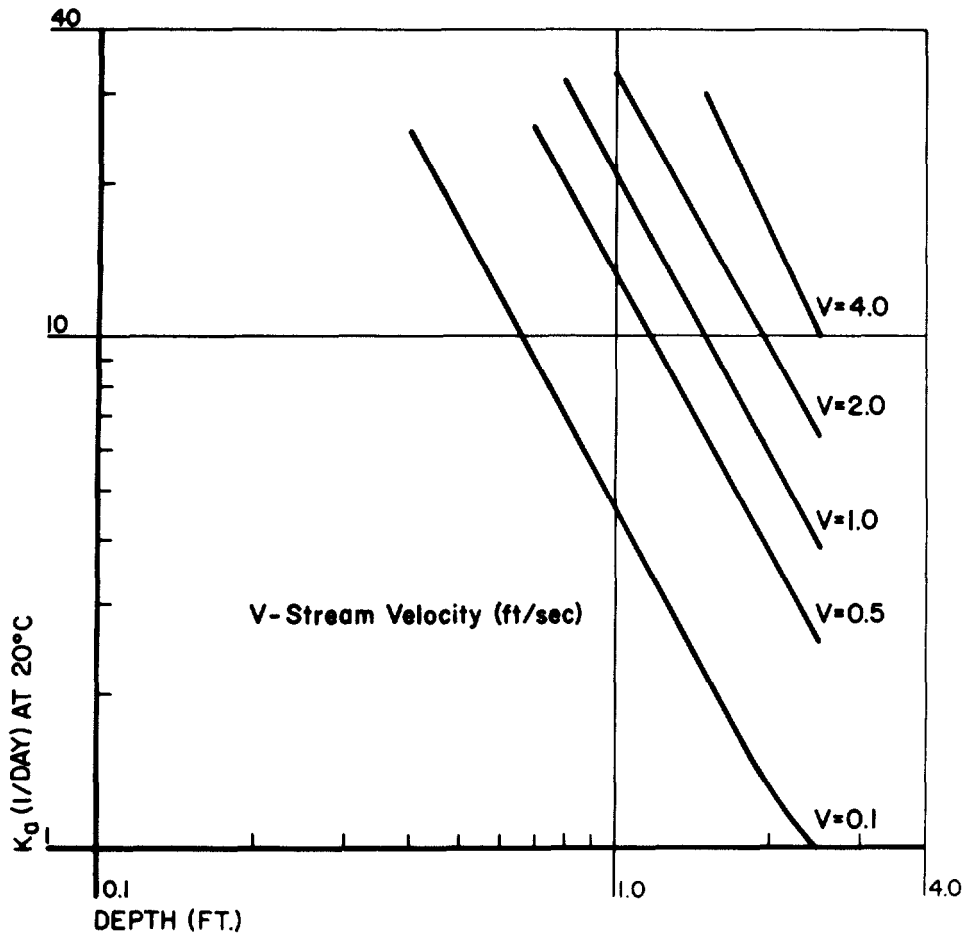


FIGURE IV-16 REAERATION COEFFICIENT FOR SHALLOW STREAMS, OWEN'S FORMULATION

EXAMPLE IV-6

Prediction of Reaeration Rates

In September, 1969, a study was conducted to determine the reaeration rate coefficients on the Patuxent River in Maryland during the low flow period. The study was carried out on a seven mile stretch of the river below Laurel, Maryland. The stream was divided into seven segments, and the reaeration rate determined for each segment. A portion of the results are shown in the Table IV-14. Using the hydraulic data in the table predict the reaeration rates using the methods of Tsioglou-Wallace and of Covar.

Since the method of calculating the reaeration for each reach is the same, an example calculation will be shown for the first reach only. Based on a velocity of 0.39 ft/sec and a slope of 0.0013 ft/ft, the Tsioglou-Wallace method predicts a reaeration rate of:

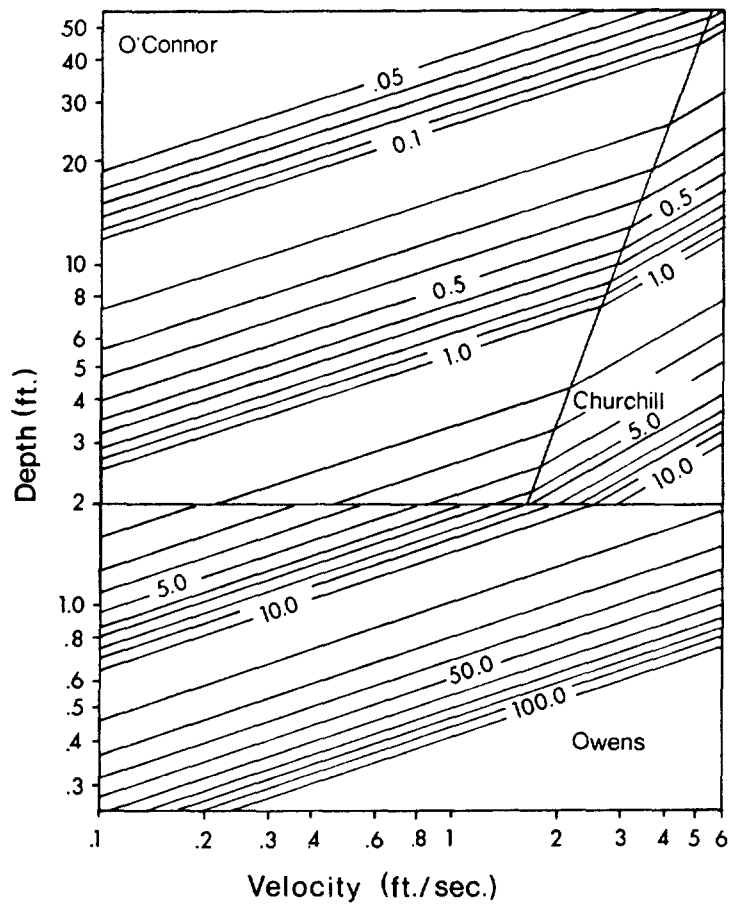


FIGURE IV-17 REAERATION RATE VERSUS DEPTH AND VELOCITY (FROM COVAR, 1976).

$$k_a = 7776 \times 0.39 \times 0.0013$$

$$= 3.9/\text{day at } 25^\circ\text{C}$$

Equation IV-33a is used since  $Q < 10$  cfs.

Using Figure IV-17 and a river depth of 0.8 feet reveals that the Owens formula is applicable. Applying Equation IV-31 shows that:

$$k_a = 21.6 \frac{0.39^{0.67}}{0.8^{1.85}} = 17.4/\text{day at } 20^\circ\text{C}$$

TABLE IV-13

COMPARISON OF PREDICTED AND OBSERVED  
REAERATION RATES ON SMALL STREAMS IN WISCONSIN\*

Stream	Observed $k_a$ (l/day at 25°C)	Predicted $k_a$ Using Tsi vogl ou's Method (l/day at 25°C)
Black Earth Creek	8.46	7.8
Mud Creek tributary	10.7	4.2
Dodge Branch	33.1	34.6
Isabelle Creek	14.	-
Madison effluent channel	2.06	4.1
Mill Creek	3.31	2.2
Honey Creek	18.4	27.4
West Branch Sugar River	42.5	36.4
Koshkonong Creek	6.09	4.8
<u>Badger Mill Creek</u>	7.98	9.1

\*Grant, R. S., 1976. Reaeration-Coefficient Measurements of 10 Small Streams in Wisconsin Using Radioactive Tracers... with a Section on the Energy-Dissipation Model. U. S. Geological Survey. Water Resources Investigations, 76-96.

The results for all the reaches are tabulated below.

Reach	REAERATION RATE (l/day)		
	Observed (25°C)	Tsi vogl ou-Wall ace (25°C)	Owens (20°C)
1-2	3.9	3.9	17.4
2-3	2.7	1.9	7.8
3-4	3.3	3.8	10.7
4-5	3.5	2.9	9.0
5-6	2.4	1.5	7.2
6-7	4.8	2.2	11.0

The predictions using the Tsi vogl ou-wall ace method are good for all reaches, while Owens' method predicts values two to three times too large, and provides evidence that Owens' method probably should not be applied to extremely shallow rivers.

TABLE IV-14

TYPICAL HYDRAULIC PROPERTIES  
PATUXENT RIVER (SEPTEMBER, 1969)

Reach	Flow cfs	Length ft	Velocity ft/sec	Depth ft	Slope ft/ft	Reaeration Rate (1/day)		
						Observed (25°C)	Tsivoglou-Mallace (25°C)	Covar (20°C)
1-2	9.8	5,400	0.39	0.80	.0013	3.9		
2-3	9.8	4,200	0.22	1.00	.0011	2.7		
3-4	9.8	7,200	0.35	1.00	.0014	3.3		
4-5	19.5	8,400	0.35	1.10	.0018	3.5		
5-6	19.5	6,600	0.25	1.10	.0013	2.4		
6-7	19.5	4,800	0.37	1.00	.0013	4.8		

END OF EXAMPLE IV-6

Temperature changes affect the reaeration rate, and the relationship can be approximated by:

$$(k_a)_T = (k_a)_{20} 1.024^{(T-20)} \quad (IV-34)$$

where

$(k_a)_T$  = the reaeration coefficient at T °C.

In addition to temperature, substantial suspended sediment concentrations can appreciably alter the reaeration rate in streams (Alonso *et al.* , 1975). As an approximation,  $k_a$  decreases by 9 percent per 1,000 ppm increase in suspended sediment up to a 4,000 ppm load. Beyond that, concentration data are not available to assess the response of  $k_a$ . It is suggested that a 40 percent decrease be used for higher suspended sediment loads. Rivers with high suspended sediment loads are generally found in the western central states. Measured values of  $k_a$  for various streams and rivers are included in Bowie *et al.* (1985).

#### 4.3.4 Effect of Dams on Reaeration

Many rivers or streams have small to moderate sized dams crossing them in one or more places. Reaeration occurs as the water flows over the dam. Based on experimental data (Gameson *et al.* , 1958), and later verified with field data (Barrett *et al.* , 1960), the following relationship for reaeration over dams has been developed:

$$D_a - D_b = \left[ 1 - \frac{1}{1 + 0.11 ab(1 + 0.046T)H} \right] D_a \quad (IV-35)$$

where

$D_a$  = dissolved oxygen deficit above dam, mg/l

$D_b$  = dissolved oxygen deficit below dam, mg/l

T = temperature, °C

H = height through which the water falls, ft

a = 1.25 in clear to slightly polluted water; 1.00 in polluted water

b = 1.00 for weir with free fall; 1.3 for step weirs or cascades.

An alternate equation developed from data on the Mohawk River and Barge Canal in New York State (Mastropietro, 1968) is as follows:

$$D_a - D_b = 0.037H D_a \quad (IV-36)$$

Equation IV-36 is valid for dams up to fifteen feet high and for temperatures in the range of 20° to 25°C.

In handling the problem of a dam, a new reach can be started just below the dam.

$D_a$  can be calculated as the value that occurs at the end of the upstream reach. The new deficit  $D_b$ , which will become the deficit at the beginning of the next reach, is calculated using either of the above two formulas.

#### 4.3.5 Dissolved Oxygen Saturation

The rate at which atmospheric reaeration occurs depends not only on  $k_a$ , but also on the difference between the saturation concentration  $C_s$  and the actual concentration  $C$ . The saturation value of dissolved oxygen is a function of temperature, salinity, and barometric pressure. The effect of salinity becomes important in estuarine systems, and to a lesser degree in rivers where high irrigation return flow can lead to substantial salinity values. Table IV-15 depicts the relationship between oxygen saturation and chlorinity. The expression relating salinity and chlorinity concentration is:

$$\text{Salinity } (‰) = 0.03 + 0.001805 \text{ chlorinity (mg/l)} \quad (IV-37)$$

where

‰ = parts per thousand.

The temperature dependence (at zero salinity) can be expressed as:

$$C_s = 14.65 - 0.41022T + 0.00791T^2 - 0.00007774T^3 \quad (IV-38)$$

where  $T$  is in °C. This relationship is also found in Table IV-15 for zero chloride concentration.

Barometric pressure affects  $C_s$  as follows:

$$\begin{aligned} C_s' &= C_s \left( \frac{P_b - P_v}{760 - P_v} \right) \\ &\approx C_s \left( 1 - \frac{.027E}{760} \right) \end{aligned} \quad (IV-39)$$

where

$C_s$  = saturation value at sea level, at the temperature of the water, mg/l

$C_s'$  = corrected value at the altitude of the river, mg/l

$P_b$  = barometric pressure at altitude, mm Hg

$P_v$  = saturation vapor pressure of water at the river temperature, mm Hg

$E$  = elevation, feet.

Table IV-16 illustrates the variability of dissolved oxygen saturation with altitude and temperature. The significant effect of altitude is apparent and should not be neglected. For example, at a temperature of 20°C, the saturation value decreases

TABLE IV-15

## SOLUBILITY OF OXYGEN IN WATER (STANDARD METHODS, 1971)

Temp. in °C	Chloride Concentration in Water - mg/l					Di fference per 100 mg Chl ori de
	0	5,000	10,000	15,000	20,000	
	Di ssolved Oxygen - mg/l					
0	14.6	13.8	13.0	12.1	11.3	0.017
1	14.2	13.4	12.6	11.8	11.0	0.016
2	13.8	13.1	12.3	11.5	10.8	0.015
3	13.5	12.7	12.0	11.2	10.5	0.015
4	13.1	12.4	11.7	11.0	10.3	0.014
5	12.8	12.1	11.4	10.7	10.0	0.014
6	12.5	11.8	11.1	10.5	9.8	0.014
7	12.2	11.5	10.9	10.2	9.6	0.013
8	11.9	11.2	10.6	10.0	9.4	0.013
9	11.6	11.0	10.4	9.8	9.2	0.012
10	11.3	10.7	10.1	9.6	9.0	0.012
11	11.1	10.5	9.9	9.4	8.8	0.011
12	10.8	10.3	9.7	9.2	8.6	0.011
13	10.6	10.1	9.5	9.0	8.5	0.011
14	10.4	9.9	9.3	8.8	8.3	0.010
15	10.2	9.7	9.1	8.6	8.1	0.010
16	10.0	9.5	9.0	8.5	8.0	0.010
17	9.7	9.3	8.8	8.3	7.8	0.010
18	9.5	9.1	8.6	8.2	7.7	0.009
19	9.4	8.9	8.5	8.0	7.6	0.009
20	9.2	8.7	8.3	7.9	7.4	0.009
21	9.0	8.6	8.1	7.7	7.3	0.009
22	8.8	8.4	8.0	7.6	7.1	0.008
23	8.7	8.3	7.9	7.4	7.0	0.008
24	8.5	8.1	7.7	7.3	6.9	0.008
25	8.4	8.0	7.6	7.2	6.7	0.008
26	8.2	7.8	7.4	7.0	6.6	0.008
27	8.1	7.7	7.3	6.9	6.5	0.008
28	7.9	7.5	7.1	6.8	6.4	0.008
29	7.8	7.4	7.0	6.6	6.3	0.008
30	7.6	7.3	6.9	6.5	6.1	0.008
31	7.5					
32	7.4					
33	7.3					
34	7.2					
35	7.1					

TABLE IV-16

DISSOLVED OXYGEN SATURATION  
VERSUS TEMPERATURE AND ALTITUDE

Temperature (°C)	ALTITUDE (ft)				
	0	2,000	4,000	6,000	8,000
0	14.6	13.6	12.5	11.5	10.5
5	12.8	11.9	11.0	10.1	9.2
10	11.3	10.5	9.7	8.9	8.1
15	10.2	9.5	8.8	8.0	7.3
20	9.2	8.5	7.9	7.2	6.6
25	8.4	7.8	7.2	6.6	6.0
30	7.6	7.1	6.5	6.0	5.4
35	7.1	6.6	6.1	5.6	5.1

from 9.2 mg/l to 7.2 mg/l as the altitude increases from sea level to 6000 feet, the approximate elevation of Lake Tahoe and the Truckee River in California and Nevada.

4.3.6 DO-BOD Interactions

A widely used dissolved oxygen predictive equation is the Streeter-Phelps relationship which predicts the dissolved oxygen concentration downstream from a point source of BOD. Assuming a constant river cross-sectional area, the dissolved oxygen deficit ( $C_s - C$ ) can be expressed as:

$$D = D_0 \exp\left[\frac{-k_a x}{U}\right] + \frac{L_0 k_L}{k_a - k_L} \left[ \exp\left(\frac{-k_L x}{U}\right) - \exp\left(\frac{-k_a x}{U}\right) \right] \quad (IV-40)$$

where

- $k_a$  = reaeration coefficient, 1/day
- $D_0$  = initial deficit (at  $x = 0$ ), mg/l
- $D$  = deficit at  $x$ , mg/l
- $L_0$  = initial BOD (at  $x = 0$ ), mg/l
- $k_L$  = BOD decay coefficient, 1/day.

$L_0$  and  $D_0$  are found by proportioning BOD and DO deficit concentrations just upstream



of the waste discharge with the influx from the discharge itself. As presented earlier in the BOD section,  $L_o$  is given by:

$$L_o = \frac{W/5.38 + L_u Q_u}{Q_w + Q_u} \quad (IV-41)$$

where

- $W$  = discharge rate of BOD, lb/day
- $L_u$  = concentration of BOD in the river upstream of the waste discharge, mg/l
- $Q_u$  = river flow rate upstream of discharge, cfs
- $Q_w$  = flow rate of waste discharge, cfs
- $Q_w + Q_u$  = flow rate of river in the reach under consideration, cfs.

$W$  in Equation IV-41 should be expressed in terms of ultimate BOD, and not 5-day BOD.

The initial deficit is found from:

$$D_o = C_s - \frac{C_w Q_w + C_u Q_u}{Q_w + Q_u} = \frac{D_w Q_w + D_u Q_u}{Q_w + Q_u} \quad (IV-42)$$

where

- $C_w$  = concentration of dissolved oxygen in the waste, mg/l
- $C_u$  = concentration of dissolved oxygen upstream of the waste discharge, mg/l
- $D_w$  = dissolved oxygen deficit in waste, mg/l
- $D_u$  = dissolved oxygen deficit upstream, mg/l.

In cases where information is lacking,  $D_o$  can normally be assumed to be in the range 1-2 mg/l.

If NBOD is to be considered as well as CBOD, Equation IV-40 can be modified as follows:

$$D = D_o \exp \left[ \frac{-k_a x}{U} \right] + \frac{L_o k_L}{k_a - k_L} \left[ \exp \left( \frac{-k_L x}{U} \right) - \exp \left( \frac{-k_a x}{U} \right) \right] + \frac{N_o k_N}{k_a - k_N} \left[ \exp \left( \frac{-k_N x}{U} \right) - \exp \left( \frac{-k_a x}{U} \right) \right] \quad (IV-43)$$

If the decay coefficient of NBOD is approximately equal to that of CBOD, Equation IV-40 can be utilized instead of the more complicated Equation IV-43. In this case,  $L_o$  in Equation IV-40 is replaced by the sum of  $L_o$  and  $N_o$ .

#### 4.3.7 Dissolved Oxygen Calculations

Calculation of dissolved oxygen in rivers can proceed as shown in Figure IV-19. The planner needs to estimate the waste loading scheme for the prototype, whether it be for a 20 year projection or for current conditions. The river system can then be divided into reaches and by repeated use of Equation IV-40, dissolved oxygen calculations can be performed for each reach, starting from a known boundary condition and proceeding downstream. All data and calculations should be succinctly and clearly recorded to minimize errors.

The dissolved oxygen profile downstream from a waste discharge characteristically has a shape shown in Figure IV-18. If the reach is long enough, the dissolved oxygen deficit will increase to some maximum value,  $D_c$ , at a distance  $x_c$  (termed the critical distance).  $D_c$  is called the critical deficit. Within any reach there will always be a minimum dissolved oxygen value that occurs, but it may not be the critical deficit, which is defined as the minimum point on a dissolved oxygen sag. The difference between the minimum and critical values should be kept in mind. As one example of the difference between the values, a reach may have dissolved oxygen profile where concentrations are monotonically decreasing throughout the reach. The minimum DO will then occur at the downstream end of the reach, but this will NOT be the critical DO value, since DO is still decreasing in the downstream direction.

The travel time to the critical deficit is given by:

$$t_c = \frac{1}{k_a - k_L} \ln \left[ \frac{k_a}{k_L} \left( 1 - \frac{D_o(k_a - k_L)}{k_L L_o} \right) \right] \quad (IV-44)$$

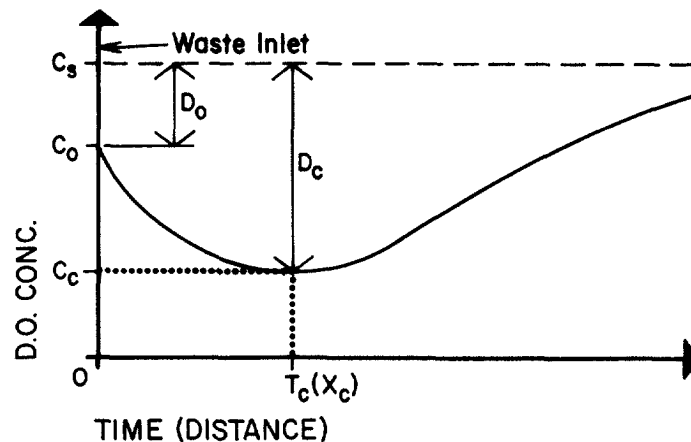


FIGURE IV-18 CHARACTERISTIC DISSOLVED OXYGEN PROFILE DOWNSTREAM FROM A POINT SOURCE OF POLLUTION

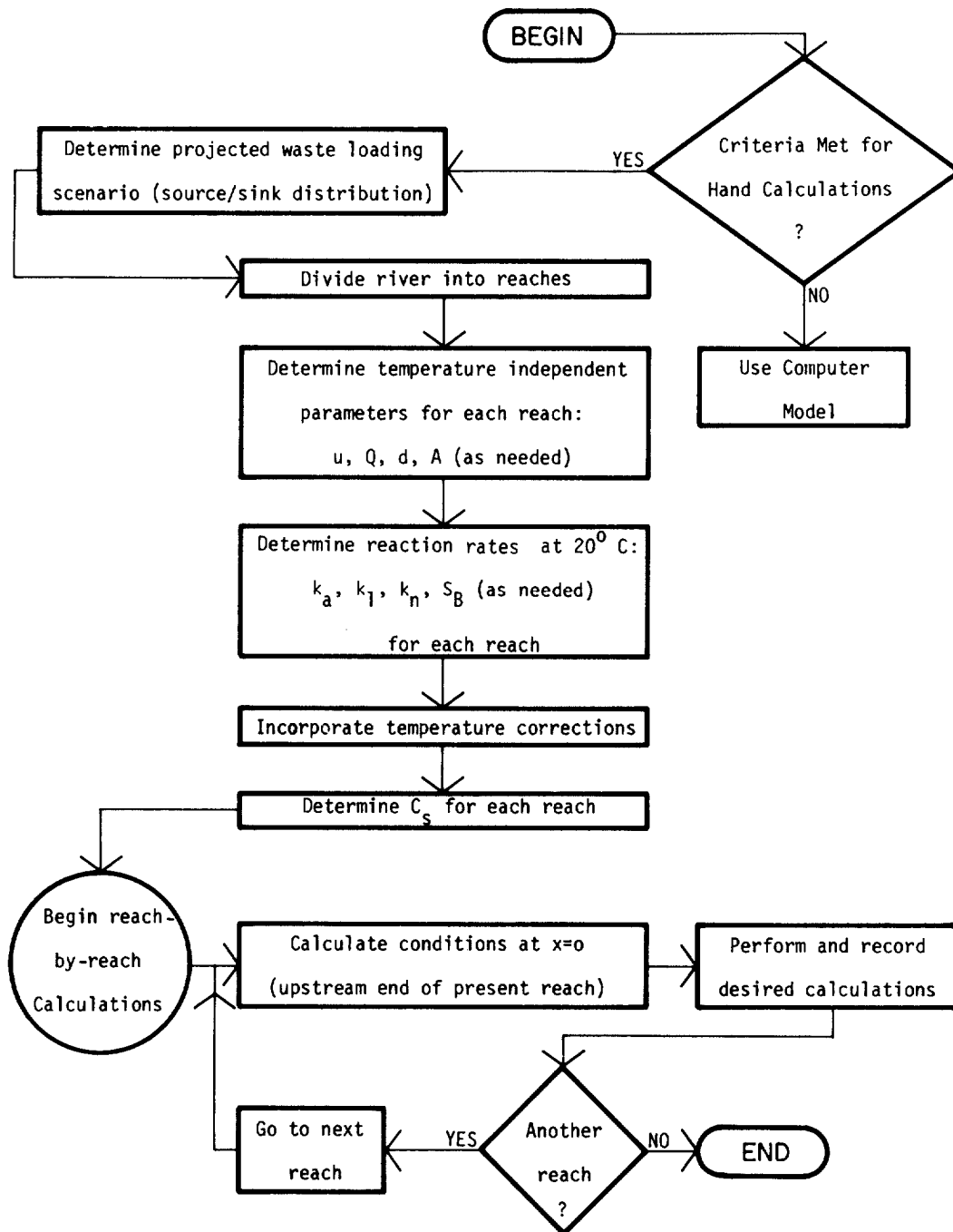


FIGURE IV-19 FLOW PROCESS OF SOLUTION TO DISSOLVED OXYGEN PROBLEM IN RIVERS

The distance downstream can be computed by knowing the travel time and flow velocity:

$$x_c = U \cdot t_c \quad (IV-45)$$

The critical deficit can be found from:

$$D_c = \left( D_o - \frac{L_o k_L}{k_a - k_L} \right) \left( \frac{k_a}{k_L} \left( 1 - \frac{D_o (k_a - k_L)}{k_L L_o} \right) \right)^{\frac{-k_a}{k_a - k_L}} + \frac{L_o k_L}{k_a - k_L} \left[ \frac{k_a}{k_L} \left( 1 - \frac{D_o (k_a - k_L)}{k_L L_o} \right) \right]^{\frac{-k_L}{k_a - k_L}} \quad (IV-46)$$

The formulas for the critical dissolved oxygen deficit are not really applicable in the special case when  $k_a = k_L$ . However, these special cases can readily be handled in one of two ways. First, a small change can be made in either  $k_a$  or  $k_L$  so that  $k_a$  and  $k_L$  are approximately equal. Or second, the following expression can be used to predict critical travel time:

$$t_c = \frac{1}{k_a} \left( 1 - \frac{D_o}{L_o} \right) \quad (IV-47)$$

Then, the critical deficit is given by:

$$D_c = \exp \left[ \ln \left( \frac{k_L}{k_a} L_o \right) - k_L t_c \right] \quad (IV-48)$$

Equation IV-48 is valid for all  $k_a/k_L$  values, and is not limited to cases where  $k_a/k_L = 1$ .

Solutions to both Equations IV-46 and IV-44 are presented in Tables IV-17 and IV-18, respectively. There exist practical limitations to the solutions of both equations, governed by the conditions that the solutions be both positive and real. If in solving Equation IV-44  $t_c$  is negative, the minimum dissolved Oxygen concentration actually occurs at the point of discharge, and concentrations increase immediately below the discharge.

Tables IV-17 and IV-18 are particularly useful for computing the waste assimilative capacity of a river. Waste assimilative capacity (WAC), as defined here, is the





amount of BOD that can be discharged into a river without causing the minimum dissolved oxygen level to fall below a specified value. In constructing Tables IV-17 and IV-18 extra detail was incorporated for  $D_0/L_0$  values between 0.0 and 0.5. This is necessary because most practical problems fall within this range.

The following steps show how to use Table IV-17.

1. Find the reaeration rate ( $k_a$ ) and the BOD decay rate ( $k_L$ ) for the river being investigated.
2. Find the BOD concentration in the river just below the point of mixing ( $L_0$ )
3. Find the dissolved oxygen deficit at this location ( $D_0 = C_s - C$ ).
4. Compute  $k_a/k_L$  and  $D_0/L_0$ .
5. Using the ratios  $k_a/k_L$  and  $D_0/L_0$ , find  $D_c/L_0$  where  $D_c$  is the critical deficit.
6. Finally, calculate  $D_c = (D_c/L_0) L_0$ , and  $C_{min} = C_s - D_c$ .

To use Table IV-18 complete these steps:

- 1.-4. Repeat steps 1 through 3 above.
5. Using the ratios  $k_a/k_L$  and  $D_0/L_0$ , find  $k_a t_c$ .
6. Calculate  $t_c = (k_a t_c)/k_a$ .

#### 4.3.8 General Dissolved Oxygen Deficit Equation

The most general dissolved oxygen mass-balance formulation to be presented in this chapter is as follows:

$$\begin{aligned}
 D = & \left( \frac{k_L}{k_a - k_L} \right) \left( L_0 - \frac{L_{rd}}{k_L} \right) \left[ \exp \left( \frac{-j_L}{A_0} f(x) \right) - \exp \left( \frac{-j_a}{A_0} f(x) \right) \right] \\
 & + \left( \frac{k_N}{k_a - k_N} \right) \left( N_0 - \frac{N_{rd}}{k_N} \right) \left[ \exp \left( \frac{-j_N}{A_0} f(x) \right) - \exp \left( \frac{-j_a}{A_0} f(x) \right) \right] \\
 & + \frac{R + S_B + L_{rd} + N_{rd} - P}{k_a} \left[ 1 - \exp \left( \frac{-j_a}{A_0} f(x) \right) \right] \\
 & + D_0 \exp \left( \frac{-j_a}{A_0} f(x) \right) \tag{IV-49}
 \end{aligned}$$

where

- P = oxygen production rate due to photosynthesis, mg/l/day
- R = oxygen utilization rate due to respiration, mg/l/day
- $S_B$  = benthic demand of oxygen, mg/l/day.

The distance function  $f(x)$  expresses the cross-sectional area relationship throughout

the reach. The area can increase or decrease linearly or remain constant. The general form of the relationship is:

$$f(x) = A_0 x + \Delta_A x^2 / 2, \Delta_A = \frac{A_f - A_0}{x_L}$$

where

$A_f$  = area at  $x = x_L$

$A_0$  = area at  $x = 0$

$x_L$  = length of reach,

For a reach of constant cross-sectional area,  $\Delta_A = 0$ .

In developing Equation IV-49 the following relationship for CBOD was used (as originally presented in the BOD section):

$$L = \left( L_0 - \frac{L_{rd}}{k_L} \right) \exp \left( \frac{-j_L}{A_0} f(x) \right) + \frac{L_{rd}}{k_L} \quad (IV-22)$$

An analogous expression for NBOD was also used.

In Equation IV-49, the distributed sources and sinks ( $P$ ,  $R$ ,  $S_B$ ,  $L_{rd}$ ,  $N_{rd}$ ) are all mass fluxes, and no volumetric flow rate is associated with any of these sources and sinks of dissolved oxygen,

#### 4.3.9 Photosynthesis and Respiration

The difficulty of accurately assessing the impact of photosynthesis and respiration on the dissolved oxygen resources of streams is not readily apparent from the single terms appearing in Equation IV-49. Of concern are both free floating and attached algae, as well as aquatic plants. The extent to which algae impact the dissolved oxygen resources of a river is dependent on many factors, such as turbidity, which can decrease light transmittance through the water column. Additionally, the photosynthetic rate constantly changes in response to variations in sunlight intensity and is not truly constant as implied by Equation IV-49. Hence if algal activity is known to be a significant factor affecting the dissolved oxygen balance, the use of a computer model is recommended in order to accurately assess such influences. For example, in the Truckee River in California and Nevada, the diurnal variation of dissolved oxygen has exhibited a range of from 150 percent saturation during the daylight hours to 50 percent saturation at night due to algal photosynthesis and respiration, respectively. At the most, hand calculations can give estimates of net dissolved oxygen production rates that then can be compared to the other source/sink terms in Equation IV-28. From this comparison the significance of each can be estimated.



TABLE IV-19

SOME AVERAGE VALUES OF GROSS PHOTOSYNTHETIC PRODUCTION OF DISSOLVED OXYGEN (AFTER THOMANN, 1972 AND THOMAS AND O'CONNELL, 1966)

Water Type	Aver. Gross Production (grams/m <sup>2</sup> -day)	Average Respiration (gm/m <sup>2</sup> -day)
Truckee River - Bottom attached algae	9	11.4
Tidal Creek - Diatom Bloom (62-109.10 <sup>6</sup> diatoms/l)	6	
Delaware Estuary - summer	3-7	
Duwamish River estuary - Seattle, Washington	0.5-2.0	
Neuse River System - North Carolina	0.3-2.4	
River level	3.2-17.6	6.7-15.4
North Carolina Streams	9.8	21.5
Laboratory Streams	3.4-4.0	2.4-2.9

Table IV-19 presents some observed values of photosynthetic oxygen production rates. As shown in the table, dissolved oxygen production is expressed in units of rate per unit area (**gm/m<sup>2</sup>-day**). To convert to units of concentration per unit time, the algal production rate must be divided by river depth:

$$P = \frac{\bar{P}}{H} \quad (\text{IV-50})$$

where

$\bar{P}$  = production rate of dissolved oxygen, **gm/m<sup>2</sup>-day**

H = average river depth, meters

P = production rate of dissolved oxygen, mg/l-day.

P can now be directly compared to other terms in Equation IV-28.

By using a regression equation developed by Erdmann (1979a, 1979b), the production rate of dissolved oxygen, P, can be determined directly if the diurnal variation of dissolved oxygen is known. When water temperature is fairly constant throughout the day, the photosynthetic oxygen production rate becomes:

$$P = 2\Delta DO \quad (\text{IV-51})$$

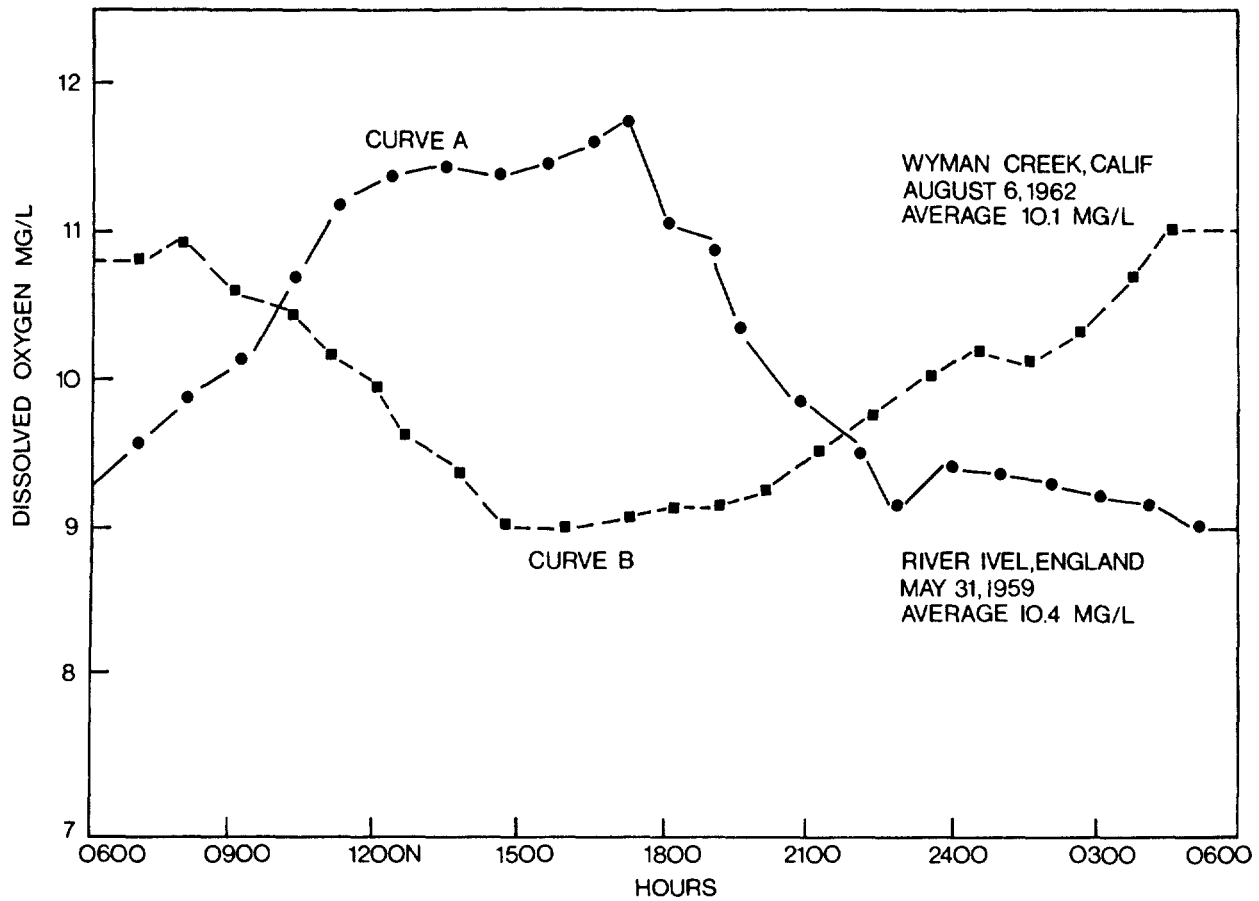


FIGURE IV-20 DAILY DISSOLVED OXYGEN VARIATION IN TWO RIVERS.

where

$\Delta DO$  = difference between the daily maximum dissolved oxygen concentration and the daily minimum dissolved oxygen concentration, mg/l.

Since Equation IV-51 is based on regression analysis, the units are not consistent.

The importance of a constant water temperature is illustrated by Figure IV-20. This figure shows the hourly variation of dissolved oxygen over a 24 hour period for Wyman Creek in California and for the Ivel River in England. Both exhibit large diurnal dissolved oxygen variations, although the reasons differ. In Curve A (Ivel River), the dissolved oxygen level gradually increases from 0600 hr to 1800 hr, and then decreases over the next 12 hours. The cause of the changing dissolved oxygen levels is a net photosynthetic oxygen production during the daylight hours, and a net consumption during evening and night. Curve B is almost a mirror image of curve A since the minimum dissolved oxygen levels occur during daylight hours and the maximum during nighttime. The variations exhibited by curve B are principally caused by a changing water temperature. During the day this creek absorbs considerable solar

radiation causing the water temperature to rise and the dissolved oxygen saturation level to decrease. At night the creek cools off and the dissolved oxygen saturation level increases. Curve B then is free from the influence of photosynthetic effects, so it would be erroneous to apply Equation IV-51. Erdmann (1979a, 1979b) and Kelly et al . (1975) provide more sophisticated methods to predict P when both photosynthetic and temperature effects occur concurrently. Example IV-7 illustrates the utility of Equation IV-51.

EXAMPLE IV-7

Prediction of Photosynthetic Oxygen Production Rate

On Mechums River near Charlottesville, Virginia, Kelly et al . (1975) collected the following data:

<u>Time of Day</u> <u>(hours after midnight)</u>	<u>Stream</u> <u>Temperature, °C</u>	<u>Dissolved</u> <u>Oxygen (mg/l)</u>
0.0	<u>23.3</u>	<u>7.6</u>
0.5	<u>23.3</u>	<u>7.6</u>
1.0	<u>23.4</u>	<u>7.6</u>
1.5	<u>23.4</u>	<u>7.5</u>
2.0	<u>23.5</u>	<u>7.4</u>
2.5	<u>23.5</u>	<u>7.2</u>
3.0	<u>23.5</u>	<u>7.3</u>
3.5	<u>23.5</u>	<u>7.3</u>
4.0	<u>23.4</u>	<u>7.3</u>
4.5	<u>23.4</u>	<u>7.3</u>
5.0	<u>23.3</u>	<u>7.3</u>
5.5	<u>23.2</u>	<u>7.3</u>
6.0	<u>23.1</u>	<u>7.3</u>
6.5	<u>23.0</u>	<u>7.3</u>
7.0	<u>22.9</u>	<b>7.4</b>
7.5	<u>22.8</u>	<b>7.4</b>
8.0	<u>22.7</u>	7.5
8.5	<u>22.7</u>	7.6
9.0	<u>22.7</u>	7.7
9.5	<u>22.7</u>	7.8
10.0	22.8	8.0
10.5	23.0	8.1
11.0	23.2	8.4
11.5	23.5	8.5
12.0	23.6	8.7
12.5	24.3	8.9
13.0	24.8	<b>9.0</b>
13.5	25.3	<b>9.1</b>
14.0	25.5	9.2
14.5	25.5	9.3
15.0	25.9	9.2
15.5	26.1	9.2
16.0	26.1	9.2
16.5	26.1	9.1
17.0	26.1	9.0

<u>Time of Day</u> (hours after midnight)	<u>Stream</u> <u>Temperature, °C</u>	<u>Di ssol ved</u> <u>Oxygen (mg/l)</u>
17.5	25.8	8.9
18.0	25.8	8.8
18.5	25.5	8.6
19.0	25.3	8.5
19.5	25.1	8.3
20.0	24.8	8.2
20.5	24.5	8.0
21.0	24.2	8.0
21.5	24.0	7.9
22.0	23.8	7.6
22.5	23.7	7.7
23.0	23.6	7.7
23.5	23.6	7.6
24.0	23.5	7.5

Using a sophisticated analysis, Kelly et al . found the daily mean photosynthetic oxygen production to be 4.40 mg/l. Using the data shown above and Equation IV-51 estimate the daily photosynthetic oxygen production, P (mg/l/day).

The minimum dissolved oxygen is 7.2 mg/l, which occurs at 0230. The maximum dissolved oxygen is 9.3 mg/l which occurs at 1430. Hence:

$$P = 2\Delta DO = 2(9.3 - 7.2) = 4.2 \text{ mg/l/day}$$

This compares very well with the value found by Kelly et al \_ using a more sophisticated analysis, even though the stream temperature varies by a few degrees during the day. Probably one reason for the good agreement is that the maximum and minimum values occur about 12 hours apart, which the method assumes they do.

END OF EXAMPLE IV-7

Values of photosynthetic respiration vary widely, ranging from 0.5 gm/m<sup>2</sup>/day to greater than 20 gm/m<sup>2</sup>/day. One suggested relationship between respiration and chlorophyll a is given as (Thomann, 1972):

$$R(\text{mg/l/day}) = 0.024 (\text{chl orophyll } \underline{a} ) (\mu\text{g/l}) \quad (\text{IV-52})$$

where

$$1 \mu\text{g/l} = 10^{-3} \text{ mg/l.}$$

Chlorophyll a concentration is most commonly expressed in terms of  $\mu\text{g/l}$ .

#### 4.3.10 Benthic Demand

In addition to oxygen utilization by respiration of attached algae, benthic

deposits of organic material and attached bacterial growth can utilize dissolved oxygen. Table IV-20 illustrates some uptake rates. As with photosynthesis, the uptake rates are expressed in  $\text{gm/m}^2\text{-day}$ . To use these values in Equations IV-28 or IV-49, division by stream depth (in meters) is necessary. Temperature effects can be approximated by:

$$(SB_T) = (SB)_{20} 1.065^{T-20} \quad (IV-53)$$

The areal extent of significant oxygen demanding benthic materials is often limited to the region just below the outfall vicinity. Although the oxygen demand may be great over a short distance, it may be insignificant over larger distances. The response of rivers to areally limited benthic deposits is generally to move the critical deficit upstream, but not to lower its value significantly.

Bowie et al. (1985) contains significantly more data and further discussion of benthic oxygen demand in rivers. Additionally Butts and Evans (1978) conducted extensive studies of sediment oxygen demand on 20 streams in Illinois. They found that benthic oxygen demand could be predicted as:

$$\bar{S}_B = 0.15T + 0.3D_s + 0.11 \log N - 0.56 \quad (IV-54)$$

where

- $\bar{S}_B$  = benthic oxygen demand,  $\text{g/m}^2\text{-day}$
- T = water temperature, °C
- $D_s$  = depth of sediment, inches
- N = number of macroinvertebrates per  $\text{m}^2$ .

They found that N typically ranged from 10,000 to 1,000,000. Within this range the sum of the last two terms is between  $\pm 0.1$ , and is negligible compared to the first two terms. Under these conditions Equation IV-54 simplifies to:

$$\bar{S}_B = 0.15T + 0.3D_s \quad (IV-55)$$

The depths of sediment found during the study of Butts and Evans (1978) ranged from 1 to 17 inches. Consequently Equation IV-55 is applicable to streams which have fairly significant benthic oxygen demands. For cleaner streams Equation IV-55 probably overestimates the benthic oxygen demand.

TABLE IV-20

AVERAGE VALUES OF OXYGEN UPTAKE RATES OF  
RIVER BOTTOMS (AFTER THOMANN, 1972)

Bottom Type and Location	Uptake (gms O <sub>2</sub> /m <sup>2</sup> -day) @ 20°C	
	Range	Approximate Average
<i>Sphaerotilus</i> - (10 gm dry wt/M <sup>2</sup> ) -	-	7
Municipal Sewage Sludge - Outfall Vicinity	2-10.0	4
Municipal Sewage Sludge - "Aged" Downstream of Outfall	1-2	1.5
Cellulosic Fiber Sludge	4-10	7
Estuarine mud	1-2	1.5
Sandy bottom	0.2-1.0	0.5
Mineral soils	0.05-0.1	0.07

#### 4.3.11 Simplifying Procedures in Dissolved Oxygen Calculations

Using Equation IV-49 might be untenable for several reasons, such as lack of available data, or because of the voluminous calculations required to apply it to a large number of reaches. Several suggestions are offered here that should simplify analysis of dissolved oxygen problems.

Since the general scope of this section is to facilitate the determination of existing or potential problem areas, the analysis should proceed from the simple to the more complicated approach. It may be adequate to analyze the dissolved oxygen response to the most severe loadings first, neglecting those of secondary importance. If such an analysis clearly indicates dissolved oxygen problems, then the inclusion of any other pollutant discharges would only reinforce that conclusion. More rigorous procedures (e.g., a computer model) could then be employed to perform a detailed analysis.

Suppose the improvement of dissolved oxygen levels due to decreased loading from a point source is of interest. This is a common situation since it relates to the design of waste loading abatement schemes. Such improvement can be estimated by:

$$\Delta D = \Delta D_0 \exp \left[ \frac{-k_a x}{U} \right] + \left( \frac{k_L}{k_a - k_L} \right) (\Delta L_0) \left[ \exp \left( \frac{-j_L}{A_0} f(x) \right) - \exp \left( \frac{-j_a}{A_0} f(x) \right) \right] \quad (IV-56)$$

where

$\Delta L_0$  = the change in the initial BOD, mg/l

$\Delta D$  = change in deficit in response to  $\Delta L_0$ .

Equation IV-56 was formulated from Equation IV-49 assuming that  $L_0$  and  $D_0$  are the only changes of significance.

Many rivers have a large number of point sources. Although this is not necessarily a complicating factor, a detailed analysis might be too time consuming for hand calculations. There are several possible alternatives to deal with this situation in order to reduce the number of reaches to be analyzed. The first, already mentioned, is to consider only the significant pollutant sources. Second, as was illustrated in Example IV-5, a number of uniformly distributed point sources can be considered as a single distributed source. Third, combining several adjacent point sources is also possible, if the length of the reach under consideration is long relative to the distance of separation between the point sources. Analogously, a distributed source can be approximated as a point source, contributing the same waste loading and located at the center of the distributed source.

It may be that the planner wants only to determine the critical dissolved oxygen concentration in each of a series of reaches. In this case no more than two values of dissolved oxygen per reach need be calculated. Figure IV-21 shows the solution process to be followed.

One final note on dissolved oxygen evaluations should be made here. It may be that if the planner is interested primarily in locating dissolved oxygen problems, he need not perform any computations. This is especially likely where dissolved oxygen data are available at various locations on the river. Plotting dissolved oxygen time trends may reveal when, as well as where, annual dissolved oxygen minima occur.

#### EXAMPLE IV-8

##### Determining River Assimilative Capacity from Tables IV-17 and IV-18

Suppose the user wants to determine waste assimilative capacity (WAC) for a river reach that has the following characteristics:

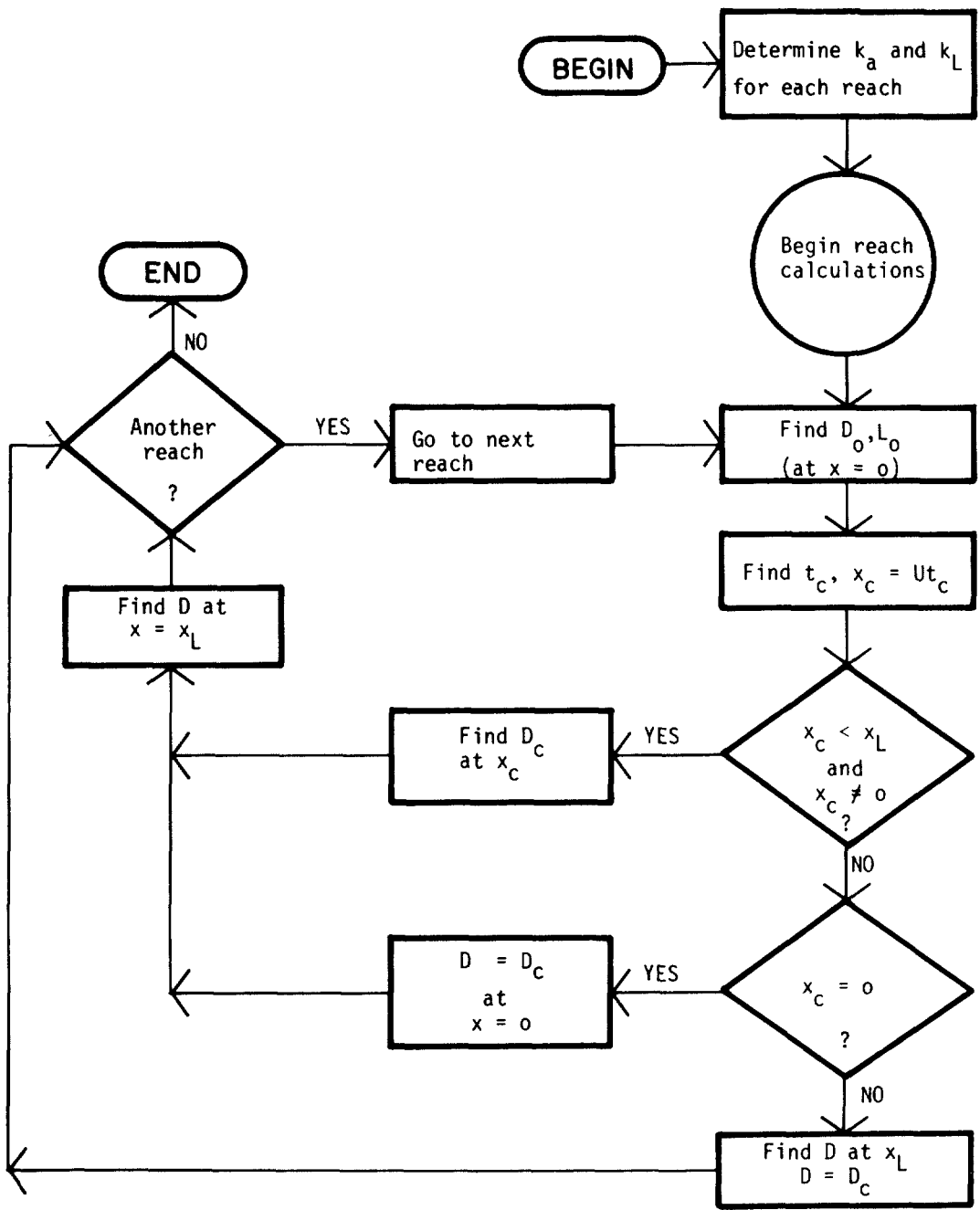


FIGURE IV-21 FLOW PROCESS IN REACH BY REACH SOLUTION TO CRITICAL DISSOLVED OXYGEN VALUES



Critical dissolved oxygen concentration = 5.0 mg/l (user establishes this)  
 Initial deficit = 1.0 mg/l  
 Average velocity = 0.5 fps  
 Average depth = 4 feet  
 Chloride concentration = 0  
 Temperature range = 10°C to 35°C

First,  $k_a$  and  $k_L$  need to be found. From Figure IV-17,  $k_a$  (20°) = 0.8/day, and from Figure IV-11,  $k_L$  = 0.4/day. At any other temperature then,  $k_a$  and  $k_L$  can be found from the temperature relationships previously developed:

$$k_a = (k_a)_{20} 1.024^{T-20} \quad (IV-34)$$

$$k_L = (k_L)_{20} 1.047^{T-20} \quad (IV-17)$$

Using Table IV-15 the dissolved oxygen saturation concentration within the temperature range of interest can be found. This information can then be then compiled into Table IV-21 shown below.

TABLE IV-21  
 COMPILATION OF INFORMATION IN EXAMPLE IV-8

T (°C)	C <sub>s</sub> (mg/l)	C <sub>c</sub> (mg/l)	D <sub>c</sub> (mg/l)	D <sub>o</sub> /D <sub>c</sub>	k <sub>a</sub> /k <sub>L</sub>
10	11.3	5.0	6.3	0.16	2.5
15	10.2	5.0	5.2	0.19	2.2
20	9.2	5.0	4.2	0.24	2.0
25	8.4	5.0	3.4	0.29	1.8
30	7.6	5.0	2.6	0.38	1.6
35	7.1	5.0	2.1	0.48	1.4

Using the values of  $D_o/D_c$  and  $k_a/k_L$ ,  $L_o$  can be found, which in this case is the WAC.

Procedure

1. Table IV-21 is entered at the appropriate  $k_a/k_L$  column. This is 2.5 at 10°C.
2. Next, the entry within the  $k_a/k_L$  column in Table IV-17 is found

such that:

$$\frac{D_o/L_o}{D_c/L_o} = \frac{D_o}{D_c} = 0.16$$

Since the left-most column of Table IV-17 is  $D_o/L_o$  and the entries are  $D_c/L_o$ , the ratio of these values is calculated until that ratio equals 0.16. For example, try  $D_o/L_o = 0.05$ . Then  $D_c/L_o = 0.23$  and  $\frac{0.05}{0.23} = 0.22 > 0.16$ ; too big.

Try  $D_o/L_o = 0.04$ . Then  $D_c/L_o = 0.23$  and  $\frac{0.04}{0.23} = .17$ ; close enough.

$$\text{Then } \frac{D_c}{L_o} = .23, \text{ or } L_o = \frac{6.3}{.23} = \underline{\underline{27.4}} \text{ mg/l}$$

The results are tabulated below for the temperature range 10°C to 35°C.

<u>T(°C)</u>	<u>WAC (mg/l)</u>	<u><math>D_o/L_o</math></u>
10	27.4	0.04
15	20.0	0.05
20	15.0	0.07
25	11.3	0.09
30	7.6	0.13
35	5.4	0.19

$L_o$  is directly related to the loading rate of BOD, as expressed earlier in Equation IV-41:

$$\text{WAC} = (L_o)_{\text{critical}} = \frac{L_u Q_u + W_{\text{critical}}/5.38}{Q_u + Q_w}$$

From equation IV-41 the critical waste loading  $W$  can be found. If desired, this procedure can be repeated for different river flow rates, and WAC and  $W_{\text{critical}}$  found for the various flows. To do this, different average depths and velocities will be needed. Generally this analysis is most applicable to minimum flow conditions, as this is the most critical situation, but higher flows may be of interest to assess the benefits of flow augmentation decisions. Novotny and Krenkel (1975) have used a 20 year, 3-day low flow in analyzing the Holston River in Tennessee. For further discussion of low flow calculations refer to Section 4.4.6.

In interpreting the results of this example the user should be looking more at trends rather than particular results. For example, notice how the WAC decreases with increasing temperature. For every 10° increase the WAC is approximately halved. A similar relationship between WAC and flow rate could also be determined.

Finally, using Table IV-18, the travel time  $t_c$  can be determined to

the point of critical deficit. The appropriate  $D_o/L_o$  and  $k_a/k_L$  values are used to find  $t_c$ . Table IV-22 illustrates these results.

TABLE IV-22  
CRITICAL TRAVEL TIME RESULTS

$T(^{\circ}C)$	$k_a/k_L$	$D_o/L_o$	$t_c k_a$	$k_a$	$t_c$ (days)
10	2.5	0.04	1.4	.63	2.2
15	2.2	.05	1.3	.71	1.8
20	2.0	.07	1.2	.8	1.5
25	1.8	.09	1.13	.9	1.2
30	1.6	.13	1.0	1.0	1.0
35	1.4	.19	0.9	1.1	0.8

END OF EXAMPLE IV-8

EXAMPLE IV-9

Critical Deficit Calculations for Multiple Reaches

Suppose the critical deficit in each of the three reaches of the river illustrated in Figure IV-22 is to be determined. The conditions upstream of the first discharge are:

$$\begin{array}{ll}
 T = 27^{\circ}C & \text{Depth} = 5.0 \text{ feet} \\
 Q = 600 \text{ cfs} & D_u = 1 \text{ mg/l} \\
 U = 0.4 \text{ fps} & L_u = 2 \text{ mg/l}
 \end{array}$$

Using these data, along with the solution process outlined in Figure IV-21, the following procedure can be used:

1. Determine  $k_a$ ,  $k_L$  for each reach. For this example it will be assumed that the average depth, velocity, and temperature remain relatively constant over the three reaches, so that  $k_a$  and  $k_L$  are also the same.

$$\begin{array}{l}
 k_a(20) = 0.5, \text{ (from Figure IV-17)} \\
 k_L(20) = 0.35, \text{ (from Figure IV-11)}
 \end{array}$$

Using the temperature correction:

$$\begin{array}{l}
 k_a(27) = 0.60, \text{ (from Equation IV-34)} \\
 k_L(27) = 0.48, \text{ (from Equation IV-17)}
 \end{array}$$

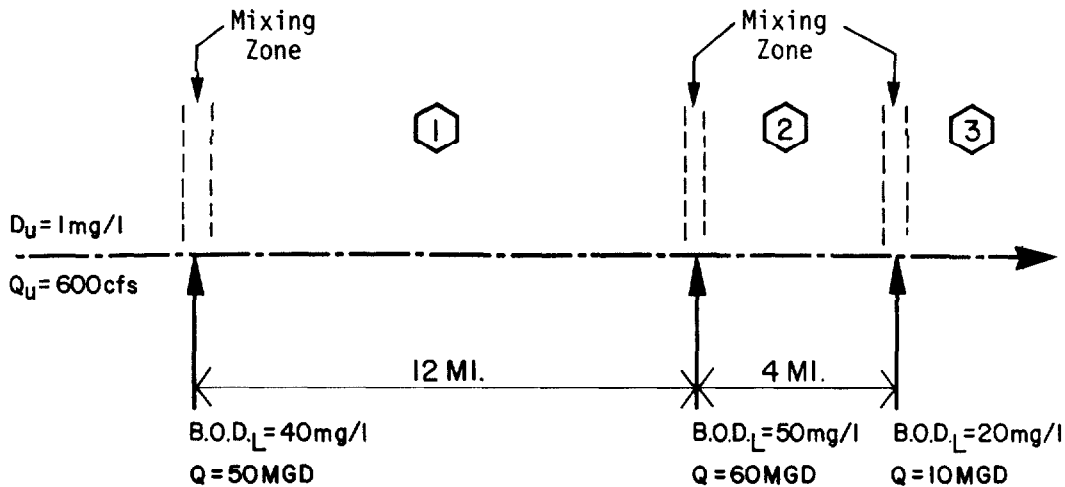


FIGURE IV-22 HYPOTHETICAL RIVER USED IN EXAMPLE IV-9

The saturation dissolved oxygen concentration at 27° C and 0% salinity is (from Table IV-15) 8.1 mg/l.

2. For the first reach, calculate  $L_0$  and  $D_0$ :

$$L_0 = \frac{(2)(600) + (40)(50)(1.55)}{600 + (50)(1.55)}$$

$$= 6.35 \text{ mg/l}$$

For lack of better information about the dissolved oxygen characteristics of the waste, it can be assumed that  $D_o = D_u = 1 \text{ mg/l}$ . The location of the critical deficit can now be calculated using Table IV-18, or Equation IV-45. In this example Table IV-18 will be used. To use that table, the following ratios are needed:

$$D_o/L_0 = 1/6.35 = 0.16$$

and

$$k_a/k_L = 0.60/0.48 = 1.3$$

From Table IV-18,  $k_a t_c = .92$  or

$$t_c = .92/0.6 = 1.53 \text{ days}$$

$$x_c = \frac{(0.4)(1.53)(3600)(24)}{5280} = 10.0 \text{ miles}$$

Since  $x_c < 12$ , the critical deficit actually exists, and is located 10 miles downstream. From Table IV-17  $D_c$  can be found by entering it with the same ratios used in Table IV-18. The result is:

$$\frac{D_c}{L_0} = .38 \rightarrow D_c = 2.4 \text{ mg/l}$$

3. Before the critical conditions in reach 2 can be calculated, the conditions at the upstream end of that reach must be established. The conditions at the downstream end of reach 1 are:

$$D = 2.3 \text{ mg/l, from Equation IV-40}$$

$$L = 2.6 \text{ mg/l from Equation IV-42}$$

The conditions at the upstream end of reach 2 are thus:

$$L_0 = \frac{(2.6)(677) + (60)(1.55)}{677 + 93} = 8.35 \text{ mg/l}$$

$D_0 = 2.3$  can be used for lack of better information on the dissolved oxygen concentration in the effluent to reach 2. For use in Table IV-18, it is found that:

$$D_0/L_0 = .28$$

so

$$k_a t = .76$$

$$t_c = .76/0.6 = 1.3 \text{ days}$$

$$x_c = 8.3 \text{ miles}$$

Since reach 2 is only 4.0 miles long, the critical deficit is not reached. Instead the maximum deficit will occur at the downstream end of reach 2, where

$$D = 3.3 \text{ mg/l (Equation IV-40)}$$

$$L = 6.22 \text{ mg/l (Equation IV-22)}$$

4. For the beginning of reach 3,  $L_0$  and  $D_0$  must be found:

$$L_0 = \frac{(20)(10)(1.55) + (770.5)(6.22)}{770.5 + (10)(1.55)} = 6.5 \text{ mg/l}$$

For  $D_0$ , it can be assumed that  $C_w = 5.0 \text{ mg/l}$ . From Equation IV-41, then:

$$D_0 = 8.1 - \frac{(8.1 - 3.3)(770.5) + (5.0)(10)(1.55)}{770.5 + 15.5} = 3.3 \text{ mg/l}$$

The calculations of critical conditions can now be made for this reach, as for the previous two.

END OF EXAMPLE IV-9

#### 4.4 TEMPERATURE

##### 4.4.1 Introduction

The biota comprising an established aquatic ecosystem generally respond negatively to significant abnormal temperature fluctuations. Anthropogenic modifications of rivers and streams can alter the thermal regime, most often by elevating the maximum and mean water temperatures. Repercussions of elevated temperatures are manifested

through a shift in the ecological balance and in the water quality of rivers. For example, there is a progression in the predominance of algal species from diatoms to green algae to blue-green algae as water temperature increases through a specific range. Thermal discharges can increase the ambient temperature enough to alter the predominant species to the undesirable blue-green algae. Increased metabolic activity of aquatic organisms, such as fish, also accompanies elevated temperature. If the increase is high enough, the results can be lethal. Much data are available today (e.g., Committee on Water Quality Criteria, 1972) which specify lethal threshold temperatures for aquatic organisms.

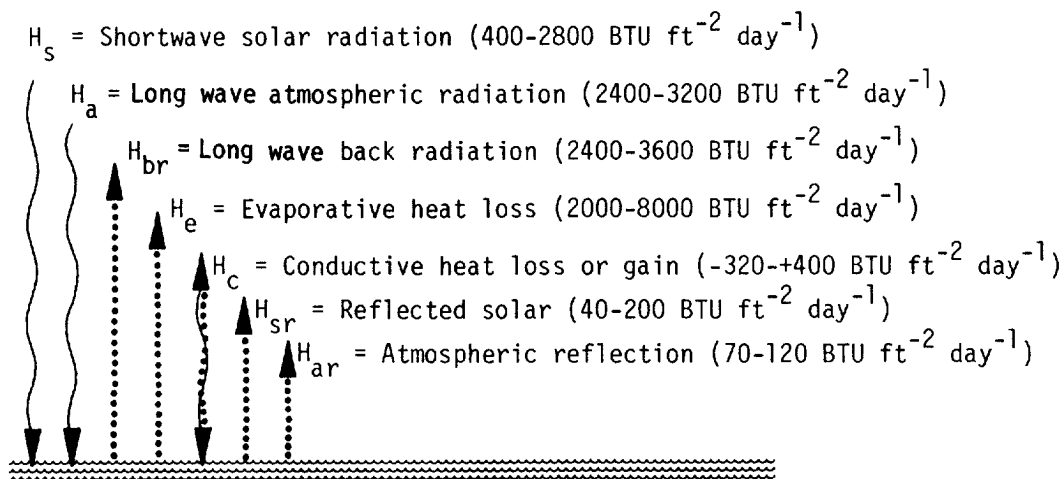
Water quality may be adversely affected through decreased solubility of dissolved oxygen and increased biochemical reaction rates. Adequate dissolved oxygen levels, particularly at elevated temperatures, are critical because of the increased metabolic activity. Yet, as previously discussed the saturation concentration of dissolved oxygen diminishes with rising temperature. Worse still, is the concurrent low flow condition which is associated, in many parts of the country, with the warm summer months. For example, in a study of 30 river reaches in the U.S. (EPA, 1974), 20 had lower flows in the summer months than in the winter. This situation further reduces assimilative capacity and usually results in the most critical dissolved oxygen levels over the year.

Man can alter the thermal regime of rivers by removing trees, changing the flow regime, and by increasing thermal discharges. Diversions of water from a river can reduce the water depth, and increase the mean and diurnal fluctuation of stream temperature.

In Long Island, modification of the natural environment of streams has increased average stream temperatures during the summertime by as much as 9 to 14°F (Pluhowski, 1968). Concurrent temperature differences of as much as 14 to 18°F between sites on the same stream were observed on days of high solar radiation. A principal factor involved in these occurrences was the removal of vegetation along the banks of the streams, permitting significantly greater penetration of solar radiation. Other contributing factors cited by Pluhowski included increased stormwater runoff, a reduction in the amount of groundwater inflow, and the introduction of ponds and lakes.

#### 4.4.2 Equilibrium Temperature

If a body of water at a given initial temperature is exposed to a set of constant meteorological conditions, it will tend to approach some other temperature asymptotically. It may warm by gaining heat or cool by losing heat. Theoretically, after a long period of time the temperature will become constant and the net heat transfer will be zero. This final temperature has been called the equilibrium temperature,  $E$ . At equilibrium, the heat gained by absorbing solar radiation and



NET RATE AT WHICH HEAT CROSSES WATER SURFACE

$$H_n = \left[ \underbrace{(H_s + H_a - H_{sr} - H_{ar})}_{\text{Absorbed Radiation } (H_R)} \quad - \quad \underbrace{(H_{br} \pm H_c + H_e)}_{\text{Temperature Dependent Terms}} \right] \text{BTU ft}^{-2} \text{ day}^{-1}$$

Absorbed Radiation ( $H_R$ )  
Independent of Water Temperature

Temperature Dependent Terms

$$H_{br} \sim (T_s + 460)^4$$

$$H_c \sim (T_s - T_a)$$

$$H_e \sim W(e_s - e_a)$$

FIGURE IV-23 MECHANISMS OF HEAT TRANSFER ACROSS A WATER SURFACE (PARKER AND KRENKEL, 1969)

Long-wave radiation from the atmosphere will exactly balance the heat lost by back radiation, evaporation, and conduction.

These heat fluxes are illustrated in Figure IV-23 which also shows typical ranges for the fluxes. Some of these terms ( $H_s, H_a, H_{sr}, H_{ar}$ ) are independent of water temperature, while the remainder ( $H_{br}, H_c, H_e$ ) are dependent upon water temperature. At equilibrium then,  $H_n$  (net transfer) equals zero, or:

$$H_s - H_{sr} + H_a - H_{ar} - H_{br} - H_c - H_e = 0 \quad \text{(IV-57)}$$

In actuality, the water temperature rarely equals the equilibrium temperature because the equilibrium temperature itself is constantly changing with the local meteorological conditions. The equilibrium temperature will rise during

the day when solar radiation is greatest, and fall to a minimum at night when solar radiation is absent.

A daily average equilibrium temperature may be computed using a number of factors including daily average values of radiation, temperature, wind speed, and vapor pressure. The daily average value will reach a maximum in midsummer and a minimum in midwinter. Since the actual water temperature always tends to approach, but does not reach the equilibrium temperature, it will usually be less than equilibrium in the spring when temperatures are rising, and greater than equilibrium in the fall when temperatures are dropping. During a 24 hour period, the equilibrium temperature usually rises above the actual water temperature during the day and falls below the water temperature at night, forcing the water temperature to follow a diurnal cycle.

The amplitude of the actual diurnal water temperature cycle is generally dampened significantly in comparison to the amplitude of the equilibrium temperature cycle due to the large heat capacity of water. A thermal discharge into a water body will usually increase the actual daily amplitude because of the water temperature dependent terms in Equation IV-57. This situation is illustrated in the following example (Edinger, et al., 1968). Figure IV-24 illustrates a flow through a cooling pond into which a thermal effluent is discharged (at Station B).

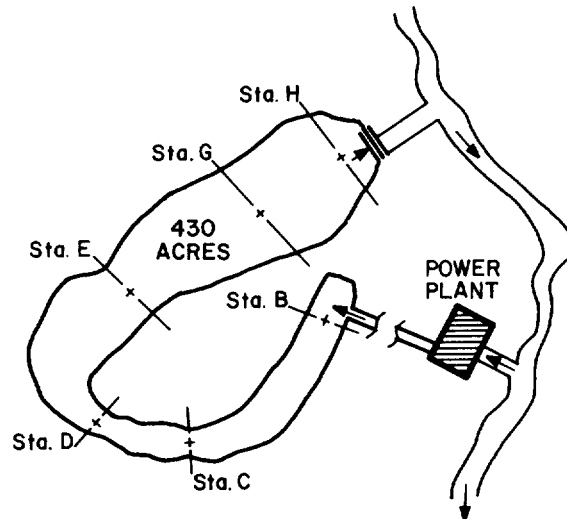


FIGURE IV-24 SCHEMATIC OF SITE No, 3  
COOLING LAKE (FROM EDINGER,  
ET AL, , 1968)

Temperature observations were recorded at Stations B through H at four-hour periods for one week. The findings are depicted in Figure IV-25.



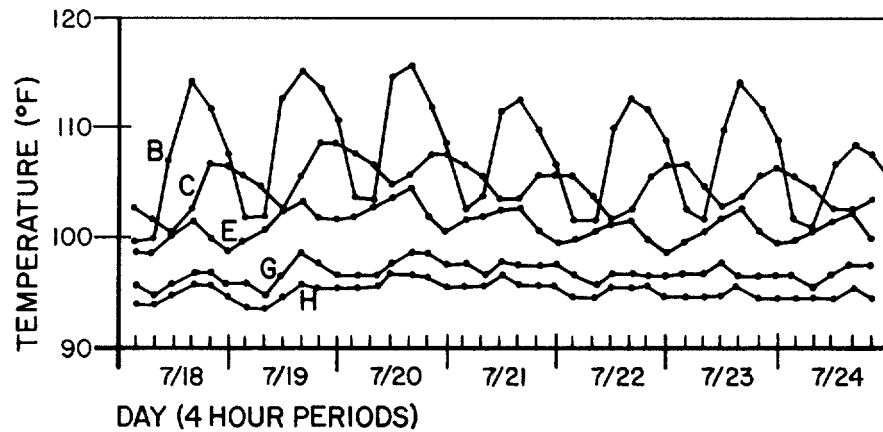


FIGURE IV-25 OBSERVED TEMPERATURES, SITE No 3, JULY 18 - JULY 24, 1965 (EDINGER, ET AL., 1968)

The highest temperatures and largest diurnal temperature variables are recorded at Station B. The peak temperature at Station B occurs just after noon, corresponding to the peak loading from the plant. At Station C the peak temperature is at 1800 hours, indicating the lag in flow time from Stations B to C. The peak temperatures at the remaining stations are more influenced by meteorological conditions, and less by the thermal discharge. The relationship of the observed temperatures to the equilibrium temperature over a 24-hour period is shown in Figure IV-26. Note the amplitude of the equilibrium temperature E (33°F amplitude). The average equilibrium temperature, **E**, is approximately 91°F. A progression from Station B to Station H indicates that the daily water temperature tends to approach the average equilibrium temperature.

Stations G and H, and the ambient temperature  $T_N$ , all reflect the predominating influence of meteorological conditions. When the ambient water temperature is above the instantaneous equilibrium temperature E, it tends to decrease, and when the temperature is below E, it tends to increase. In the early morning and late evening hours, when E is low, the water temperature decreases at these stations. During midday when E is higher, however, the temperatures at these stations increase.

#### 4.4.3 Calculation of Equilibrium Temperature

Studies (Edinger and Geyer, 1965) have shown that the equilibrium temperature of a well mixed body of water can be estimated by:

$$E = \frac{0.05E^2}{K} + \frac{H_R - 1801}{K} + \frac{K - 15.7}{K(.26+B)} \left[ e_a - C(B) + 0.26T_a \right] \quad (IV-58)$$

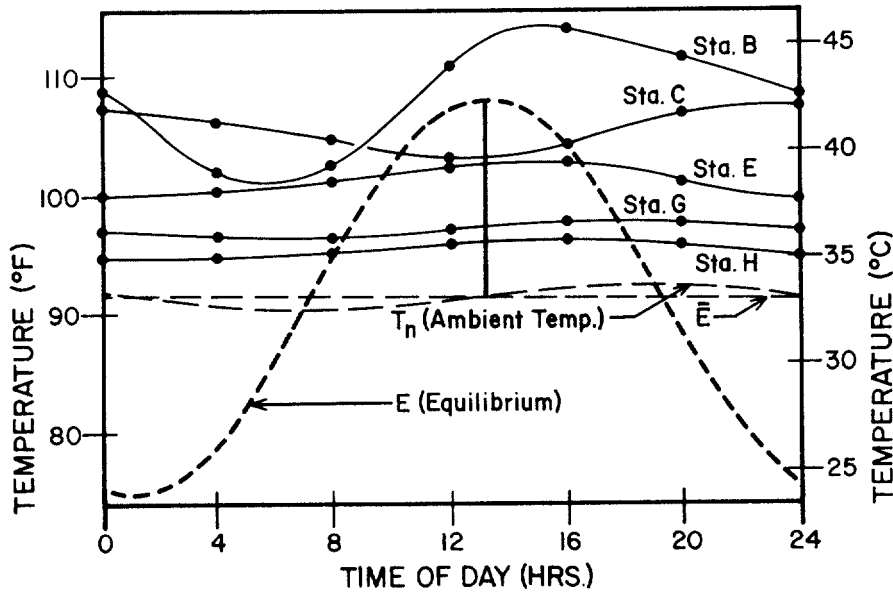


FIGURE IV-26 COMPARISON OF COMPUTED EQUILIBRIUM AND AMBIENT TEMPERATURES WITH OBSERVED MEAN DIURNAL TEMPERATURE VARIATIONS FOR SITE No. 3, JULY 18-JULY 24, 1966 (EDINGER, ET AL., 1968)

where

- E = equilibrium temperature, °F
- K = thermal exchange coefficient, BTU/ft<sup>2</sup>/day/°F
- $H_R$  = net incoming short ( $H_{sn}$ ) and long ( $H_{an}$ ) wave radiation BTU/ft<sup>2</sup>/day
- $T_a$  = air temperature, °F
- $e_a$  = water vapor pressure of ambient air at air temperature, mmHg
- B = proportionality coefficient, mmHg/°F
- C(B) = value dependent on B, mmHg.

The thermal exchange coefficient K is expressible as:

$$K = 15.7 + (0.26 + B) f(u) \quad (IV-59)$$

where

$f(u)$  = a function of wind speed.

Different relationships for  $f(u)$  have been developed. For purposes of hand calculations, the following relationship will be used:

$$f(u) = 11.4u \quad (IV-60)$$

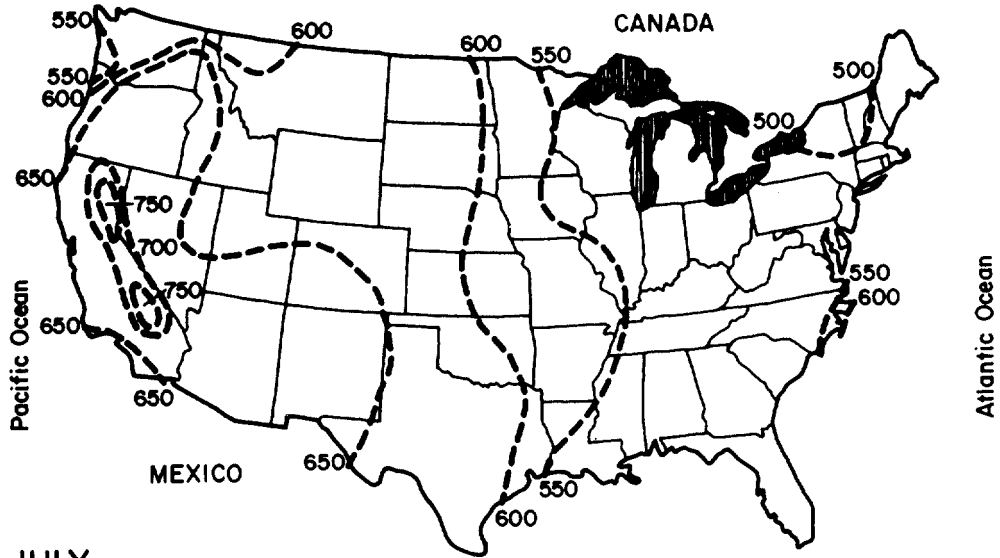
where

$u$  = the daily average wind speed in mph.

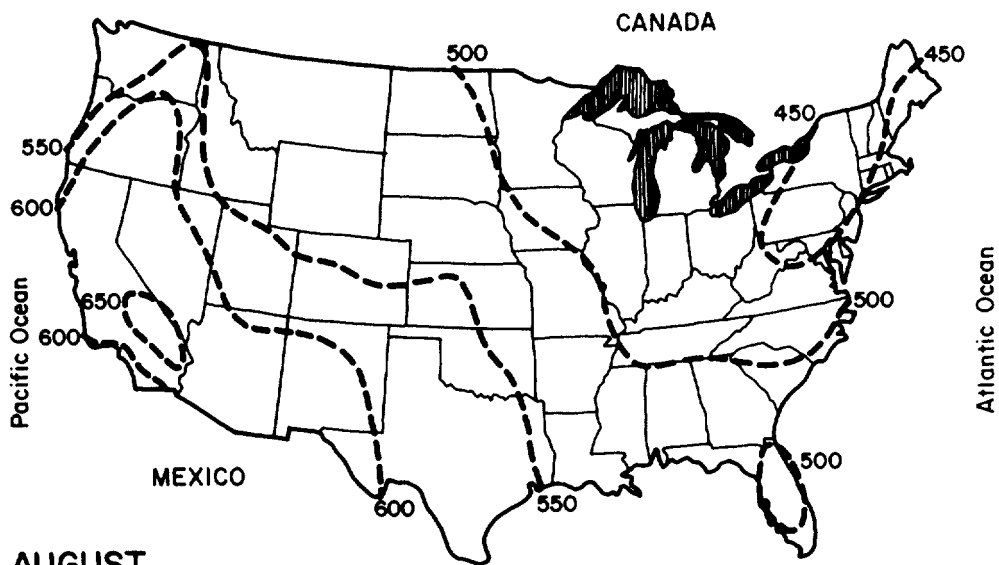
To calculate  $E$  using Equation IV-58 an iterative procedure is needed, since  $K$ ,  $B$ , and  $C(B)$  depend on  $E$ . The following steps outline a solution procedure.

1. Data needed to start the procedure include  $T_a$ , relative humidity, wind speed, and net shortwave solar radiation. Figure IV-27 illustrates daily average solar radiation reaching the continental United States for the months July and August. It is during these months that stream temperatures usually reach their annual maxima. These values do not account for the albedo of water (the percent of incoming solar radiation that is reflected), but since this is small, it can be ignored. Because of the variability caused by topography, vegetative cover, and other factors, local sources of information should be used when possible for solar radiation values.
2. Calculate  $H_R = H_{sn} + H_{an}$  (BTU/ft<sup>2</sup>/day). If Figure IV-27 is utilized for  $H_{sn}$ , convert from Langleys/day to BTU/ft<sup>2</sup>/day by multiplying by 3.7.  $H_{an}$  can be estimated from Table IV-23 by knowing the air temperature and the cloud cover fraction (0.1 to 1.0).
3. Determine  $e_a$  from Table IV-24 by entering with  $T_a$  and relative humidity.
4. Choose an initial value for  $E$ . The air temperature  $T_a$  can be the first guess.
5. Enter Table IV-25 for  $B$  and  $C(B)$  at  $E$  (°F).
6. Knowing  $u$ ,  $f(u)$ , and  $B$ , calculate  $K$  from Equation IV-59.
7. From Equation IV-58 make the next estimate of  $E$  ( $E_{new}$ ) by evaluating the right hand side of that equation (call this result  $F(E)$ ).
8. The next estimate of  $E$  is  $E_{new} = 0.3E + 0.7 F(E)$ .  
(Note: this choice of  $E_{new}$  brings about a more rapid convergence to the answer than would use of  $E$  alone).
9. If  $|E_{new} - E| \leq 1^\circ\text{F}$ , then  $E_{actual} = E_{new}$ .  
If  $|E_{new} - E| > 1^\circ\text{F}$ , return to step 5 with  $E_{new}$  and repeat the procedure until the convergence criterion is met, namely,  $E_{actual} = E_{new}$ .

Instantaneous, daily, weekly, or even longer term average equilibrium temperature,  $\bar{E}$ , can be calculated by using mean meteorological conditions over the period of interest and following the solution procedure just outlined. Calculating the daily average  $\bar{E}$  under the most crucial annual meteorological conditions (usually occurring in July or August) yields the highest temperature about which that water body tends to naturally oscillate. The repercussions of man's activities in terms of altering  $\bar{E}$  can thus be estimated and analyzed for potential impact.



JULY



AUGUST

NOTE: To convert Langleys/day to BTU/ft<sup>2</sup>/day, multiply by 3.7.

FIGURE IV-27 MEAN DAILY SOLAR RADIATION (LANGLEYS) THROUGHOUT THE U. S. FOR JULY AND AUGUST (U. S. DEPARTMENT OF COMMERCE, 1968)

TABLE IV-23  
NET LONG WAVE ATMOSPHERIC RADIATION,  $H_{an}$

Cloud Cover	Temperature (°F)	$H_{an}$ (BTU/Sq. Ft./Day)	Temperature (°F)	$H_{an}$ (BTU/Sq. Ft./Day)	Temperature (°F)	$H_{an}$ (BTU/Sq. Ft./Day)	Temperature (°F)	$H_{an}$ (BTU/Sq. Ft./Day)	Temperature (°F)	$H_{an}$ (BTU/Sq. Ft./Day)	Temperature (°F)	$H_{an}$ (BTU/Sq. Ft./Day)
.1	35	1685	40	1790	45	1900	50	2016	55	2138	60	2266
	65	2400	70	2540	75	2688	80	2842	85	3004	90	3173
.2	35	1694	40	1799	45	1910	50	2026	55	2149	60	2277
	65	2412	70	2553	75	2701	80	2857	85	3019	90	3190
.3	35	1708	40	1814	45	1926	50	2043	55	2167	60	2296
	65	2432	70	2575	75	2724	80	2881	85	3045	90	3216
.4	35	1728	40	1835	45	1949	50	2067	55	2192	60	2323
	65	2461	70	2605	75	2756	80	2914	85	3080	90	3254
.5	35	1754	40	1863	45	1978	50	2098	55	2225	60	2358
	65	2497	70	2644	75	2797	80	2958	85	3126	90	3303
.6	35	1785	40	1896	45	2013	50	2136	55	2265	60	2400
	65	2542	70	2691	75	2847	80	3011	85	3182	90	3362
.7	35	1822	40	1936	45	2055	50	2180	55	2312	60	2450
	65	2595	70	2747	75	2907	80	3074	85	3249	90	3432
.8	35	1865	40	1981	45	2103	50	2232	55	2366	60	2508
	65	2656	70	2812	75	2975	80	3146	85	3325	90	3513
.9	35	1914	40	2033	45	2158	50	2290	55	2428	60	2573
	65	2725	70	2885	75	3053	80	3228	85	3412	90	3604
1.0	35	1968	40	2091	45	2220	50	2355	55	2497	60	2646
	65	2803	70	2967	75	3139	80	3320	85	3509	90	3707

TABLE IV-24  
 SATURATED WATER VAPOR PRESSURE,  $e_s$ , VERSUS AIR TEMPERATURE,  $T_a$ ,  
 AND RELATIVE HUMIDITY

$T_a$	$e_s^*$	R E L A T I V E H U M I D I T Y										
(°F)	(mmHg)	0.1	0.2	0.3	0.4	0.5	0.6	0.7	0.8	0.9	1.0	
35	5.2	0.5	1.0	1.6	2.1	2.6	3.1	3.6	4.2	4.7	5.2	
40	6.3	0.6	1.3	1.9	2.5	3.2	3.8	4.4	5.0	5.7	6.3	
45	7.6	0.8	1.5	2.3	3.0	3.8	4.6	5.3	6.1	6.8	7.6	
50	9.1	0.9	1.8	2.7	3.6	4.6	5.5	6.4	7.3	8.2	9.1	
55	11.0	1.1	2.2	3.3	4.4	5.5	6.6	7.7	8.8	9.9	11.0	
60	13.1	1.3	2.6	3.9	5.2	6.6	7.9	9.2	10.5	11.8	13.1	
65	15.6	1.6	3.1	4.7	6.2	7.8	9.4	10.9	12.5	14.0	15.6	
70	18.6	1.9	3.7	5.6	7.4	9.3	11.2	13.0	14.9	16.7	18.6	
75	22.0	2.2	4.4	6.6	8.8	11.0	13.2	15.4	17.6	19.8	22.0	
80	26.0	2.6	5.2	7.8	10.4	13.0	15.6	18.2	20.8	23.4	26.0	
85	30.5	3.1	6.1	9.2	12.2	15.3	18.3	21.4	24.4	27.5	30.5	
90	35.8	3.6	7.2	10.7	14.3	17.9	21.5	25.1	28.6	32.2	35.8	
95	41.8	4.2	8.4	12.5	16.7	20.9	25.1	29.3	33.4	37.6	41.8	
100	48.7	4.9	9.7	14.6	19.5	24.4	29.2	34.1	39.0	43.8	48.7	

TABLE IV-25

## B AND C(B) AS FUNCTIONS OF TEMPERATURE

Temperature (°F)	B (mmHg/°F)	C(B) (mmHg)	Temperature (°F)	B (mmHg/°F)	C(B) (mmHg)
45	.286	-5.5	70	.660	-22.9
46	.296	-4.5	71	.680	-23.6
47	.306	-4.1	72	.701	-24.4
48	.317	-4.2	73	.722	-25.4
49	.328	-4.6	74	.743	-26.5
50	.340	-5.4	75	.765	-27.8
51	.352	-6.3	76	.787	-29.3
52	.365	-7.5	77	.810	-31.0
53	.378	-8.7	78	.833	-33.0
54	.391	-10.0	79	.857	-35.1
55	.405	-11.2	80	.881	-37.6
56	.419	-12.5	81	.905	-40.3
57	.433	-13.6	82	.930	-43.2
58	.448	-14.7	83	.955	-46.4
59	.464	-15.8	84	.980	-49.7
60	.479	-16.7	85	1.006	-53.3
61	.496	-17.6	86	1.033	-57.1
62	.512	-18.3	87	1.060	-61.0
63	.529	-19.0	88	1.087	-64.9
64	.547	-19.6	89	1.114	-68.9
65	.564	-20.1	90	1.142	-72.9
66	.583	-20.7	91	1.171	-76.7
67	.601	-21.2	92	1.200	-80.4
68	.620	-21.7	93	1.229	-83.8
69	.640	-22.3	94	1.259	-86.8
			95	1.289	-89.3

## EXAMPLE IV-10

Calculation of Equilibrium Temperature

On Long Island, New York, studies done by Pluhowski (1968) have indicated that shading of streams by a natural vegetative canopy can drastically affect the shortwave solar radiation reaching those streams. The results of some of his findings are presented in Table IV-26. In the summer, when leaves are on the trees, the actual solar radiation reaching the Connetquot River can be as low as 29% of that reaching unobstructed sites at nearby Mineola or Brookhaven.

Suppose the user is interested in predicting how the removal of the riparian

TABLE IV-26

SUMMARY OF SOLAR-RADIATION DATA  
FOR MINEOLA, BROOKHAVEN, AND THE CONNETQUOT RIVER SITES

Solar Site	Dates	Mineola	Brookhaven	Mean-Daily Solar Radiation in Langleys: for the Indicated Periods			Ratio=	
				Connetquot River Estimated	Connetquot River Observed	Connetquot River Observed	Connetquot River Unobstructed	
(1)	(2)	(3)	(4)	(5)	(6)	(7)	(7)	
1	Jan. 30, 31, 1967	235	244	240	148	0.62		
2	Jan. 28, 29, 1967	148	130	137	96	.70		
3	Jan. 25, 26, 1967	135	135	135	104	.77		
1	Apr. 21-23, 1967	466	464	465	343	.74		
	Apr. 16-18, 1968	452	502	502	389	.77		
2	Apr. 19, 20, 1967	436	386	429	384	.90		
3	Apr. 24-26, 1967	408	411	410	401	.98		
1	June 9-11, 1967	600	599	599	254	.42		
2	June 7, 8, 1967	664	671	669	531	.79		
3	June 12-14, 1967	527	523	525	443	.84		
1	Aug. 26-28, 1967	275	260	266	78	.29		
2	Aug. 22-24, 1967	277	328	308	162	.53		
3	Aug. 29, 30, 1967	504	484	492	338	.69		
1	Nov. 28, 29, 1967	204	-	204	86	.42		

Notes:

Solar site 1 is typically heavily forested, solar site 2 is moderately to heavily forested, and solar site 3 is moderately forested.

Radiation data in column 5 are estimated unobstructed horizon values for Connetquot River based on data from Mineola and Brookhaven (cols. 3,4).



vegetative cover might effect  $\bar{E}$ . Consider the period 22-24 August, 1967, when the Connetquot River received 162 langleys/day of a possible 308 langleys/day of shortwave solar radiation. Representative meteorological conditions at this time were:

$$T_a = 65^\circ\text{F}$$

$$u = 2 \text{ mph}$$

$$\text{Cloud cover fraction} = 0.5$$

$$\text{Relative humidity} = 80\%$$

The steps in solving for  $\bar{E}$  are as follows:

1. Data have been gathered, as previously listed.
2.  $H_{sn} = 162 (3.7) = 600 \text{ BTU/ft}^2/\text{day}$ . This value assumes that the vegetative canopy blocks 47% of the solar radiation. From Table IV-23,  $H_{an}$  is (.5 cloud cover at  $65^\circ\text{F}$ )  $2497 \text{ BTU/ft}^2/\text{day}$ . Thus,
 
$$H_R = 2497 + 600 = 3097 \text{ BTU/ft}^2/\text{day}.$$
3. At 80% relative humidity and an air temperature of  $65^\circ\text{F}$ ,  $e_a = 12.5 \text{ mmHg}$  from Table IV-24.
4. As an initial guess of  $E$ , assume  $E_1 = 65^\circ\text{F}$ , the air temperature.
5. From Table IV-25,  $B = .56$ ,  $C(B) = -20.1$
6.  $K = 15.7 + (.26 + .56) (11.4) (2) = 34.4$
7. 
$$F(E_1) = \frac{-0.05(65)^c}{34.4} + \frac{3098 - 1801}{34.4} + \frac{34.4 - 15.7}{34.4(.26 + .56)}$$

$$\times [12.5 + 20.1 + .26(65)] = -.6.1 + 37.7 + 33.0 = 64.6$$
8.  $E_2 = .3(65) + .7(64.6) = 64.7$
9. Since  $|E_2 - E_1| < 1^\circ\text{F}$       $\bar{E} = 64.7^\circ\text{F}$

Now suppose the user wants to find  $\bar{E}$  for no reduction in  $H_{sn}$  due to shading. Steps 1 through 9 again are repeated, using  $H_{sn} = 308(3.7) = 1140 \text{ BTU/ft}^2/\text{day}$ , with otherwise the same meteorological conditions. Without detailing the calculations here, it is found that  $\bar{E} = 74.7^\circ$ , a  $10^\circ\text{F}$  increase.

It is evident then that altering the solar radiation penetrating to the stream can significantly change  $\bar{E}$ . Even more severe cases of repression of shortwave radiation (as noted by the 71% reduction on 26-28 August, 1967, Table IV-26) are possible, exemplifying the large differences which may be observed.

-----END OF EXAMPLE IV-10-----

The approach illustrated in Example IV-10 for predicting equilibrium temperature is obviously time consuming, and has been programmed for hand held calculators in Mills et al . (1979) . A simplified approach is also available for predicting equilibrium temperature (Brady et al ., 1969) and is described below. The predictions are usually within  $3^\circ\text{F}$  or less of those found by the more complicated approach.

The data required for the simpler approach are:


$T_d$ , dewpoint temperature ( $^{\circ}\text{F}$ )

$U$ , mean daily wind speed (mph)

$H_{sn}$ , net incoming shortwave radiation ( $\text{Btu}/\text{ft}^2/\text{day}$ ).

Short wave solar radiation data were previously shown in Figure IV-27. The Climatic Atlas (U.S. Department of Commerce, 1968) contains compilations of dewpoint temperature and windspeed. Figures IV-28 and IV-29 show these data for the months of July and August. Figures IV-27 through IV-29 provide the user with all the data needed to predict equilibrium temperature using the approach of Brady *et al.*

To find the equilibrium temperature the following equations are applied sequentially:

COMPUTE ONCE	→	$F(U) = 70 + 0.7 U^2$	(IV-61)
		$T = (E_i + T_d) / 2$	(IV-62)
		$B = 0.255 - 0.0085T + 0.000204T^2$	(IV-63)
ITERATE OVER THESE EQUATIONS		$K = 15.7 + (B + .26) F(U)$	(IV-64)
		$E_{i+1} = T_d + H_s / K$	(IV-65)

The wind speed function  $f(U)$  is found once from Equation IV-61. The dewpoint temperature ( $T_d$ ) is a convenient starting choice as an initial guess of the equilibrium temperature.  $T$  can then be calculated from Equation IV-62;  $B$  from Equation IV-63;  $K$  from Equation IV-64; and finally a new equilibrium temperature ( $E_{i+1}$ ) from Equation IV-65. If  $E_i$  and  $E_{i+1}$  differ by more than  $1^{\circ}\text{F}$ , return to Equation IV-62 with  $E_{i+1}$  and repeat the procedure until convergence is attained (usually within 2 or 3 cycles).

EXAMPLE IV-11

Equilibrium Temperature Using Simplified Approach

Determine the average daily surface water equilibrium temperature for Little Rock, Arkansas during the month of August. Based on Figures IV-27 through IV-29 the following data are found:

$T_d = 68^{\circ}\text{F}$

$u = 7 \text{ mph}$

$H_{sn} = (525)(3.7) = 1943 \text{ Btu}/\text{ft}^2/\text{day}$

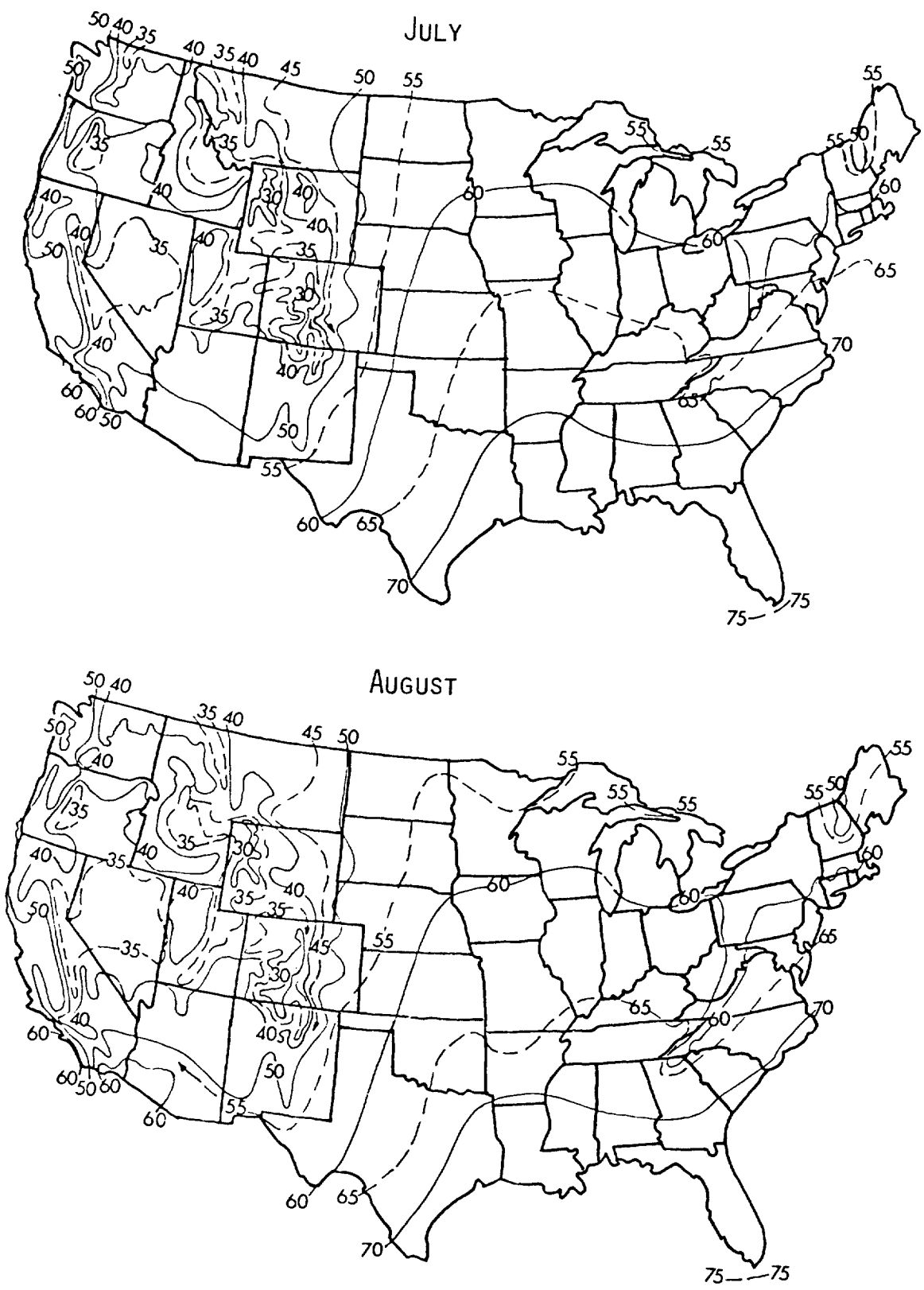


FIGURE IV-28 MEAN DEWPOINT TEMPERATURE (°F) THROUGHOUT THE UNITED STATES FOR JULY AND AUGUST (U. S. DEPARTMENT OF COMMERCE, 1968)

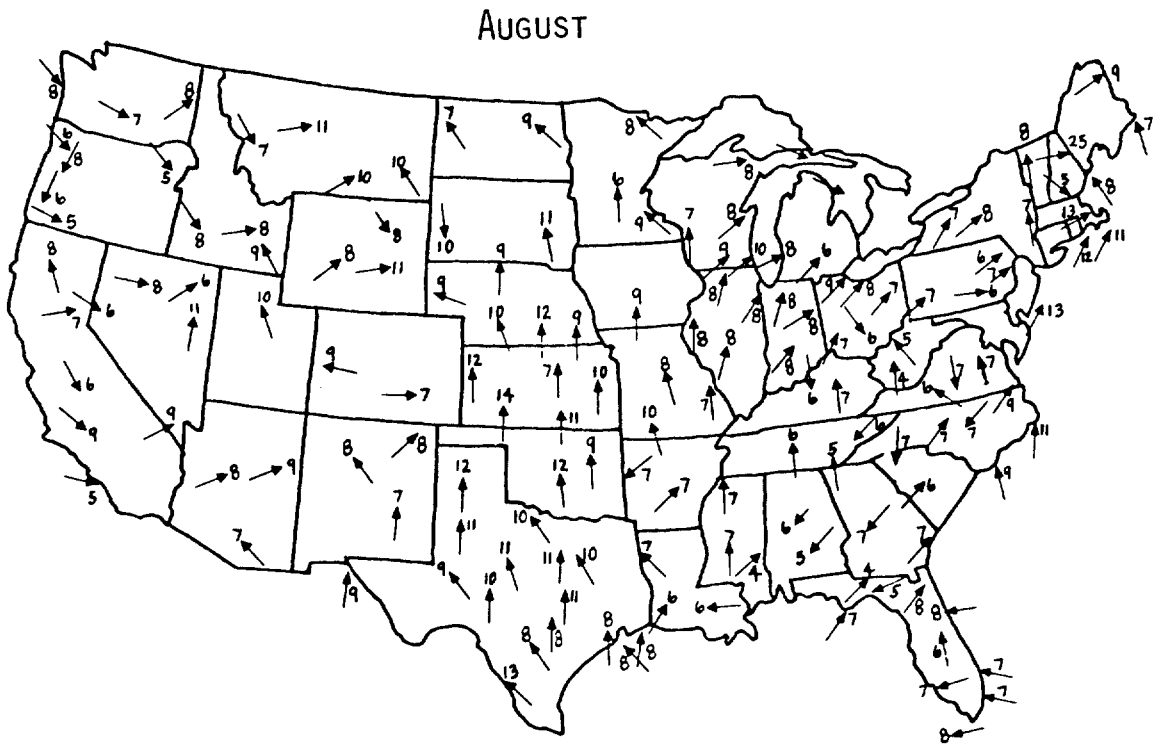
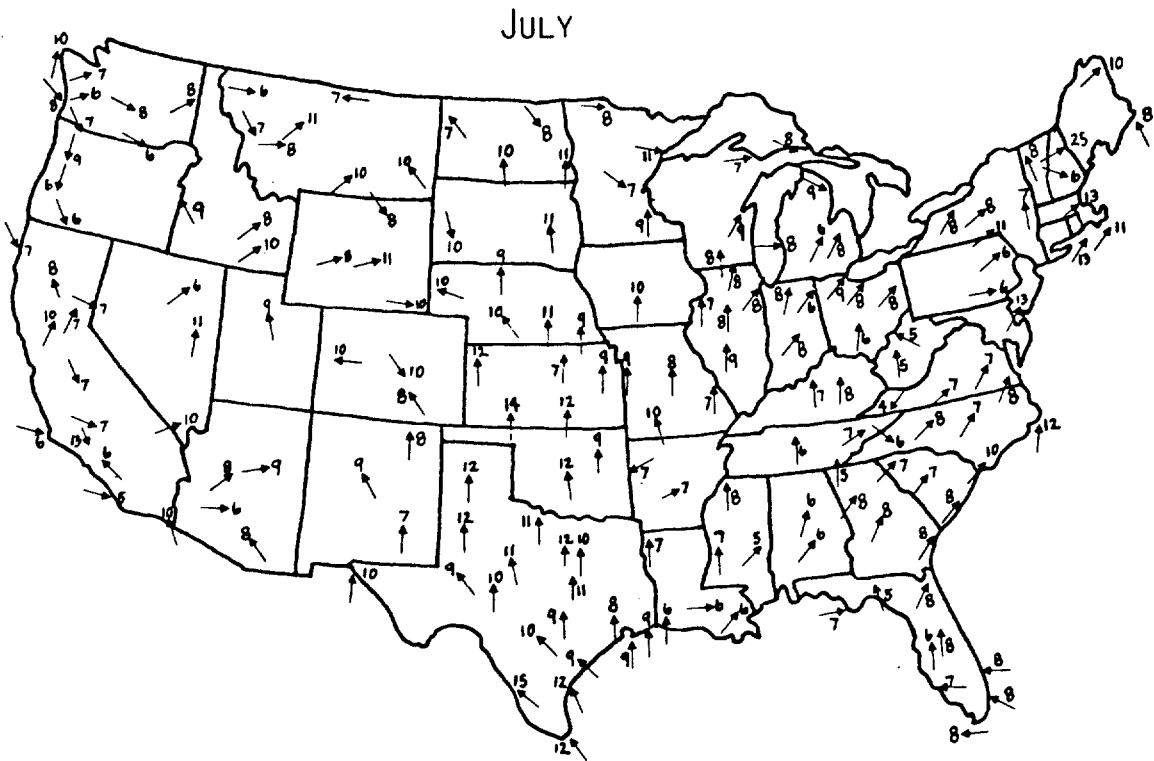


FIGURE IV-29 MEAN DAILY WIND SPEEDS (MPS) THROUGHOUT THE UNITED STATES FOR JULY AND AUGUST (U. S. DEPARTMENT OF COMMERCE, 1968)

Assume as a first guess that  $E = T_d = 68^\circ\text{F}$

then:

$$f(u) = 70 + .7 (7)^2 = 104.$$

$$T = (T_d + T_d)/2 = 68^\circ$$

$$B = .62$$

$$K = 15.7 + (.62 + .26) (104) = 107.$$

$$E = 68 + 1943/107 = 86^\circ\text{F}$$

For the second iteration:

$$T = (86 + 68)/2 = 77$$

$$B = 0.81$$

$$K = 127$$

$$E = 83.3^\circ\text{F}$$

At the end of a third iteration  $E = 83.7^\circ\text{F}$ , so convergence has been attained by three iterations.

As a comparison, the equilibrium temperature will also be calculated using the longer approach. The required data are:

$$T_a = 80^\circ\text{F}$$

$$T_d = 68^\circ\text{F}$$

$$U = 7.$$

$$H_{sn} = 1943$$

sky cover = 0.5 (from climatic atlas)

A summary of the procedure is:

1.  $H_n = 2958$

$$H_R = 1943 + 2958 = 4901$$

2. Since  $T_d = 68^\circ$ ,  $e = 17.4$

3. Choose  $E = T_a = 80^\circ\text{F}$

4.  $B = .881$

$$C(B) = -37.6$$

5.  $f(u) = 70 + 0.7 (7)^2 = 104$

$$K = 15.7 + (0.26 + .881) (104) = 134$$

6.  $F(E) = 79.3$

7.  $E = .3(80) + .7 (79.3) = 80^\circ\text{F}$ , after one pass.

Since the starting guess of  $80^\circ\text{F}$  is virtually identical with the calculated value at step 7, a second iteration is not required. The two procedures predict equilibrium temperatures which differ by about  $4^\circ\text{F}$ .

END OF EXAMPLE IV-11

To estimate the effects of shading, the incoming solar radiation should be calculated first assuming no shading, but otherwise using existing meteorological conditions for the time of the year of interest. The effects of shading should be superimposed upon this result as a percent reduction. The following (Pluhowski, 1968) can serve as guidelines in estimating solar radiation reduction:

- 0-25 percent reduction: shading generally restricted to early morning and late afternoon.
- 25-50 percent reduction: some sunshine penetration in morning and evening. Considerable sunshine between 1000 and 1400 hours.
- 50-75 percent reduction: very little sunshine penetration in morning or late afternoon. Some sunshine between 1000 and 1400 hours.
- Greater than 75 percent reduction: very little penetration even at noon.

#### 4.4.4 Screening of Thermal Discharges

##### 4.4.4.1 Introduction

This section presents a set of procedures which can be used to determine whether the thermal discharge at a proposed power plant site or the discharge from the expansion of an existing site is likely to violate thermal standards. Procedures are presented to test for contravention of the following types of standards:

- The  $\Delta T$  Criterion: The increase in temperature of water passing through the condenser must not exceed a specified maximum.
- The Maximum Discharge Temperature Criterion: The temperature of the heated effluent must not exceed a specified maximum.
- The Thermal Block Criterion: The cross-sectional area of a river occupied by temperatures greater than a specified value must not exceed a specified percentage of the total area.
- The Surface Area Criterion: The surface area covered by isotherms exceeding a specified temperature increment (above ambient) must not exceed a specified maximum.

Actual values associated with the above standards vary by political jurisdiction. Accordingly, regulations must be consulted.

The thermal discharge screening procedures are designed to address the following questions:

- Is the power plant, as proposed, acceptable at the candidate location?
- What is the largest power plant that can be placed at the candidate location? Equivalently, can an existing power plant at the candidate location be expanded?

The methods do not analyze interactions among multiple powerplants on the same river. Such an analysis can be rather more complex. A report by Tetra Tech (1978)

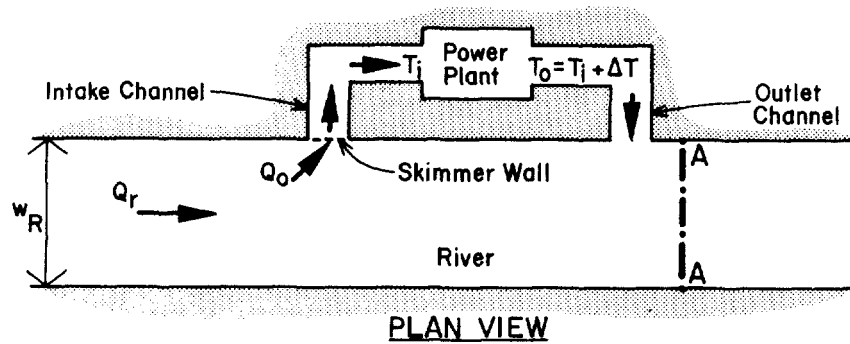


FIGURE IV-30 IDEALIZATION OF A RUN-OF-THE-RIVER POWER PLANT

addresses that question.

The methods developed to evaluate instream thermal criteria use heat balance equations assuming a steady-state, well mixed system at low flow. The power plants are assumed to employ once through cooling, as shown in Figure IV-30.

The selection of well mixed conditions appears to be justified. Studies by Stefan and Gulliver (1978) on the Mississippi and Missouri Rivers have dealt with the lateral mixing of thermal plumes which were released at the shoreline and were not initially well mixed across the river. The investigators found that over a short distance, thermal losses were negligible and that the well-mixed isotherm (the isotherm that would result were the plume initially well-mixed laterally and vertically) eventually extended across nearly the entire width of the river, albeit at some distance downstream. This indicates that if the thermal block criterion is not met for the well mixed case, it is not likely to be met for the shoreline discharge either. A similar conclusion can be reached regarding the surface area constraint. Thus, at this level of analysis, it is not necessary to consider the consequence of incomplete lateral or vertical mixing adjacent to the shoreline discharge.

One simplification which can be used at the option of the user for the surface area calculation should be mentioned. Surface water that is undisturbed by anthropogenic influences (in a thermal sense) approaches the equilibrium temperature. This temperature is dictated by natural meteorological conditions. Surface water temperature in rivers, especially during steady low-flow periods, can be near equilibrium. In calculating the surface area occupied by isotherms exceeding a specified temperature, it is necessary to know the equilibrium temperature. However, since the procedure for calculating equilibrium temperature is fairly complicated, considerable savings in computational effort can be obtained by assuming the ambient water is at its equilibrium temperature.

Some circumstances, in addition to anthropogenic influences, tend to produce ambient temperatures different from equilibrium. For example:

- Locally, large quantities of groundwater may discharge into the river
- Hypolimnetic releases from large reservoirs may occur nearby
- Snow melt may supply a substantial amount of inflow.

As a result of the first two influences, the stream water temperature may be lower than equilibrium since the source of the water comprising the stream flow has been shielded from the heating effect of solar radiation. Snow melt, although not likely to influence the river's thermal regime during the late summer, can be important through spring and into early summer in areas where high-mountain snowpack exists over most, or all, of the year.

The screening procedure that follows assumes the river water, once it has been heated by the thermal plume, is above equilibrium. This means that the water temperature will then decrease in the downstream direction, which is generally, but not always, true.

Table IV-27 shows the data needed to apply the thermal screening methods. The symbols are defined in the table and suggested default values are given for variables where appropriate. The variables are introduced in the table in the order they occur in the screening procedure.

#### 4.4.4.2 Evaluating the Thermal Block Criterion

The initial temperature elevation that results when the thermal plume becomes well mixed with the river water is given as:

$$\Delta T_{wm} = \frac{Q_p}{Q_r} \Delta T \quad (IV-66)$$

$$\frac{1}{Q_r} \frac{e_c}{e_p} MWe \cdot \frac{1}{\rho C_p} \cdot \frac{3.414 \times 10^6}{3600} \quad (IV-67)$$

where

$\Delta T_{wm}$  = temperature elevation of the initially well mixed isotherm (°F)

$Q_p$  = flowrate of cooling water (m<sup>3</sup>/s)

$\Delta T$  =  $T_e - T_r$  (°F)

$T_e$  = temperature of heated effluent (°F)

$T_r$  = temperature of river water upstream of power plant (°F).

All other terms are defined in Table IV-27.

To find  $\Delta T_{wm}$ , Equation IV-67 is solved. If  $\Delta T_{wm}$  is less than the thermal block temperature increment ( $\Delta T_{tb}$ ), the thermal block criterion is not contravened. Otherwise, it is.



TABLE IV-27  
DATA NEEDED FOR THERMAL DISCHARGE SCREENING

Variable	Term Definition	Default Value
$MWe$	Capacity of power plant in megawatts electric (bus bar)	--
$e_p$	Percent of total energy produced that goes to electricity production	new fossil fuel plants: 38 nuclear plants: 32
$e_c$	Percent of total energy produced that is dissipated through the cooling water	new fossil fuel plants: 48 nuclear plants: 68
$Q_r$	River flow rate above power plant ( $m^3/s$ )	$7Q_{10}$
$\rho$	Mass density of water ( $kg/m^3$ )	1000
$C_p$	Specific heat of water ( $Btu/^\circ F \cdot kg$ )	2.2
$\Delta T_{tb}$	Temperature rise in the river cross section that constitutes a thermal block ( $^\circ F$ )	5
$\Delta T_{max1}$	Maximum legal allowable temperature rise across the condenser ( $^\circ F$ )	20
$\Delta T_{max2}$	Maximum allowable temperature rise across the condenser such that $T_e \leq (T_e)_{max}$ ( $^\circ F$ )	--
$T_e$	Temperature of heated effluent ( $^\circ F$ )	--
$(T_e)_{max}$	Maximum legal allowable temperature of heated effluent ( $^\circ F$ )	86
$\Delta T_{maxmin}$	The lesser of $\Delta T_{max1}$ and $\Delta T_{max2}$ ( $^\circ F$ )	--
$(Q_p)_{max}$	The maximum allowable flow rate through the cooling system ( $m^3/s$ )	$.25Q_r$
$\Delta T_{sa}$	The isotherm defining the boundary of the surface area for which legal limits have been established ( $^\circ F$ )	4
$V$	<b>Mean velocity</b> of the river ( $m/s$ )	
$d$	Mean hydraulic depth of river in reach under consideration (m)	--
$E$	Equilibrium temperature ( $^\circ F$ )	--
$K$	Surface thermal transfer coefficient ( $Btu/d \cdot ^\circ F \cdot m^2$ )	--

TABLE IV-27 (continued)

Variable	Term Definition	Default Value
A	Surface area of river down to $\Delta T_{sa}$ isotherm ( $m^2$ )	--
$A_{sa}$	Legal maximum surface area limit which can be covered by the and greater isotherms ( $m^2$ )	- -
w	Average surface width of river down to $\Delta T_{sa}$ isotherm (m)	--
$T_{ra}$	River temperature just above where a tributary joins the mainstream ( $^{\circ}F$ )	--
$T_t$	Temperature of tributary ( $^{\circ}F$ )	--
$Q_t$	Flow rate of tributary ( $m^3/s$ )	--
$T_a$	Air Temperature ( $^{\circ}F$ )	--
Relative humidity	--	--
u	Wind speed at 7 meters above surface (m/s)	--
$H_{sn}$	Net shortwave solar radiation ( $Btu/m^2 \cdot d$ )	--
$H_{an}$	Net long wave solar radiation ( $Btu/m^2 \cdot d$ )	--

4.4.4.3 Acceptability of the Temperature Rise Across the Condenser and of the Temperature of the Heated Effluent

Whether these criteria are met or not depends on a number of factors, such as the cooling water flow rate. Since the cooling water flow rate can be designed to be within a specified range, it is determined here whether a feasible range exists such that the two above mentioned criteria are met.

The minimum acceptable flow rate such that both temperature criteria do not exceed their standards is as follows:

$$(Q_p)_{min} = \frac{e \cdot c}{e_n} \cdot MWe \cdot \frac{1}{\rho C_p \Delta T_{maxmin}} \cdot \frac{3.414 \times 10^6}{3600} \quad (IV-68)$$

where

$(Q_p)_{min}$  = minimum flow rate such that the two temperature criteria are not exceeded ( $m^3/s$ ).

By evaluating Equation IV-68 the minimum cooling water flow can be determined.

As an example of how  $\Delta T_{\text{maxim}}$  is chosen, suppose the following conditions exist:

Maximum legal temperature rise across the condenser = 20°F

Maximum legal temperature of the heated effluent = 86°F

Ambient river temperature = 74°F.

From these conditions,  $\Delta T_{\text{max2}}$  (the allowable temperature increase across the condenser such that the temperature of the effluent does not exceed the legal maximum) = 86°F - 74°F = 12°F. So  $T_{\text{maxmin}} = \text{minimum}(20^\circ\text{F}, 12^\circ\text{F}) = 12^\circ\text{F}$ . 12°F must be chosen, then, as the maximal temperature rise across the condenser.

Once Equation IV-68 has been solved, the ratio of cooling water to river flow should be checked so that the value is within acceptable limits. Equation IV-66 can be rewritten as:

$$\frac{Q_p}{Q_r} = \frac{\Delta T_{\text{wm}}}{\Delta T} \quad (\text{IV-69})$$

Since  $\Delta T_{\text{wm}}$  has been calculated from Equation IV-67 and  $\Delta T$  has been calculated as  $\Delta T_{\text{maxim}}$ , the flow rate fraction can be calculated from Equation IV-69. If this fraction exceeds a certain percent (e.g., 25 percent or some user defined value), then the cooling water flow rate is too large to be acceptable. If the flow rate fraction is not excessive, the actual flow rate can be chosen so that:

$$(Q_p)_{\text{min}} \leq Q_p \leq (Q_p)_{\text{max}} \quad (\text{IV-70})$$

where

$(Q_p)_{\text{max}}$  = maximum allowable cooling water flow rate ( $\text{m}^3/\text{s}$ )

#### 4.4.4.4 Evaluating the Surface Area Constraint

The evaluation of this criterion may require the user to perform considerably more calculations than for any of the other prescreening criteria. The two major complicating factors that are encountered are: 1. determining the river equilibrium temperature, and 2. evaluating the effects of tributaries.

If it is the case that  $\Delta T_{\text{wm}}$  does not exceed  $\Delta T_{\text{sa}}$  the surface area criterion will not be contravened and no calculations have to be performed. If  $\Delta T_{\text{wm}}$  exceeds  $\Delta T_{\text{sa}}$ , the criterion might be exceeded. In this case it is necessary to determine the distance from the location of the thermal discharge to the downstream location of the  $\Delta T_{\text{sa}}$  isotherm. This distance is given by:

$$x_{\text{sa}} = \frac{-\rho C_p V d}{K} \ln \left( \frac{T_{\text{sa}} - E}{T_{\text{wm}} - E} \right) 24 \cdot 3600 \quad (\text{IV-71})$$

where

$$\begin{aligned} T_{sa} &= \Delta T_{sa} + T_r \\ T_{wm} &= \Delta T_{wm} + T_r \end{aligned}$$

Section 4.4.3 discusses procedures for predicting K and E. Once K and E are found,  $x_{sa}$  can be determined from Equation IV-71. If one or more tributaries exist with the distance  $x_{sa}$ , then  $x_{sa}$  should be recalculated as discussed in Section 4.4.4.5.

The surface area included within this reach is:

$$A = x_{sa} \cdot W \quad (IV-72)$$

where

A = surface area of the river from the point of thermal discharge to  $x_{sa}$  ( $m^2$ )

W = average river width in this reach (m).

If  $A < A_{sa}$  then the surface area criterion is not contravened. Otherwise, it is.

#### 4.4.4.5 Evaluating the Effects of a Tributary in Mitigating Temperature Within a Thermal Plume

Tributaries, when they join a river subjected to the influences of a thermal plume, generally act to reduce the elevated river temperature. They may therefore prevent the surface area constraint from being exceeded when it otherwise would.

Equation IV-71 assumes no tributaries exist throughout the reach defined by  $x_{sa}$ . If it is found that  $x_{sa} > x_t$  ( $x_t$  is defined below under Equation IV-73) then it is necessary to examine the impact of the tributary flow on the surface area constraint. This is done by computing the water temperature ("F) just above the location where the tributary joins the mainstream using the following equation:

$$T_{ra} = (T_{wm} - E) \exp\left(\frac{-Kx_t}{\rho C_p V d \cdot 24 \cdot 3600}\right) + E \quad (IV-73)$$

where

$T_{ra}$  = river temperature just upstream of tributary ("F)

$x_t$  = distance from power plant discharge to tributary (m).

After the river has mixed with the tributary the new river temperature ("F) is given by:

$$(T_r)_{new} = \frac{T_{ra}Q_r + T_tQ_t}{Q_r + Q_t} \quad (IV-74)$$

where

$$\begin{aligned} T_t &= \text{temperature of the tributary } (^{\circ}\text{F}) \\ Q_t &= \text{flow rate of tributary } (\text{m}^3/\text{s}). \end{aligned}$$

If:

$$(T_r)_{\text{new}} \leq \Delta T_{\text{sa}} + T_{\text{ra}} \quad (\text{IV-75})$$

then this location marks the downstream location of the  $\Delta T_{\text{sa}}$  isotherm and the surface area  $A$  can be calculated using the distance  $x_{\text{sa}}$  as the distance down to the tributary,  $x_t$ . Otherwise the  $\Delta T_{\text{sa}}$  isotherm is located further downstream. In this case Equation IV-71 is reapplied (first making appropriate adjustments to  $V$  and  $d$ ) where the initial temperature is  $(T_r)_{\text{new}}$  (which was  $T_{\text{wm}}$  in Equation IV-71) and the final temperature is still  $T_{\text{sa}}$ . The distance  $x_{\text{sa}}$  is determined by adding this additional distance to  $x_t$ .

#### 4.4.4.6 Determining Whether the Thermal Block or the Surface Area Constraint Is the More Limiting

One of these two constraints may cause a greater limitation on power plant size than the other. If  $\Delta T_{\text{tb}} < \Delta T_{\text{sa}}$  the thermal block constraint will be more limiting, and there is no need to continue with the analysis in this part. If, however,  $\Delta T_{\text{tb}} > \Delta T_{\text{sa}}$ , the surface area constraint may be more limiting. To determine if it is, find  $\Delta T_{\text{wm}}$  (call it  $\Delta T_{\text{wmsa}}$ ) using the following equation:

$$\Delta T_{\text{wmsa}} = E + (T_{\text{sa}} - E) \exp\left(\frac{-Kx_{\text{sa}}}{\rho C_p V d \cdot 24 \cdot 3600}\right) - T_r \quad (\text{IV-76})$$

where

$$T_{\text{sa}} = \Delta T_{\text{sa}} + T_r \quad (\text{IV-77})$$

$$x_{\text{sa}} = \frac{A_{\text{sa}}}{W} \quad (\text{IV-78})$$

If a tributary exists in the reach delineated by  $x_{\text{sa}}$ , recompute  $x_{\text{sa}}$  as outlined in Section 4.4.4.5.

If  $\Delta T_{\text{wmsa}} < \Delta T_{\text{tb}}$ , the surface area constraint is more restrictive, so set  $\Delta T_{\text{wm}} = \Delta T_{\text{wmsa}}$ . Otherwise set  $\Delta T_{\text{wm}} = \Delta T_{\text{tb}}$ .

4.4.4.7 Determining the Maximum Plant Capacity

The maximum power plant capacity can be determined based upon the maximum well mixed temperature elevation and the river flow rate. It is given by:

$$(MWe)_{\max} = \frac{e_p}{e_c} \cdot \rho C_p \cdot (Q_p \Delta T)_{\max} \frac{3600}{3.414 \times 10^6} \tag{IV-79}$$

$$= \frac{e_p}{e_c} \cdot \rho C_p \cdot \Delta T_{wm} Q_r \cdot \frac{3600}{3.414 \times 10^6} \tag{IV-80}$$

By using Equation IV-80 and the maximum allowable  $\Delta T_{wm}$ , the maximum capacity can be found.

4.4.4.8 Readjusting the Maximum Cooling Water Flow Rate

If the minimum acceptable flow rate is greater than the maximum allowable, the power plant size must be reduced. To do this, set:

$$Q_p = (Q_p)_{\max} \tag{IV-81}$$

where

- $Q_p$  = actual cooling water flow rate ( $m^3/s$ )
- $(Q_p)_{\max}$  = maximum allowable cooling water flow rate ( $m^3/s$ ).

$\Delta T_{wm}$  is recalculated by:

$$\Delta T_{wm} = \Delta T_{\max \min} \frac{(Q_p)_{\max}}{Q_r} \tag{IV-82}$$

where

$$\Delta T_{\max \min} = \Delta T \text{ calculated earlier.}$$

(Note: the surface area and thermal block constraints are still met and need not be recomputed.)

----- EXAMPLE IV-12 -----

Estimating  $\Delta T$  Across a Power Plant Heat Exchange Unit

Suppose the user wants to determine  $\Delta T$  for the Hartford Electric Light Company's South Meadow Steam Electric Power Plant (a fossil fuel plant) located on the Connecticut River. Data available are (Jones et al., 1975):

- Capacity . . . . . 217 MW
- Cooling water flow rate . . . . . 341  $ft^3/sec$

Waste heat discharged to cooling water . . . 422 MW

Since the waste heat being dissipated through the cooling water is known,  $\Delta T$  can be calculated directly using that value in conjunction with the known flow rate. Assume, however, that the waste heat being discharged is not known. It can be estimated from the plant capacity as follows. First, assume the plant efficiency is 33 percent. The rate at which fuel is burned when at capacity is then:

$$\frac{217}{.33} = 658 \text{ MW}$$

If 10 percent of the total energy is lost up the stacks, then approximately 58 percent is dissipated through the cooling water, or:

$$658 (.58) = 382 \text{ MW}$$

Compared with the known 422 MW of heat discharged to the cooling water, the above calculation would underestimate  $\Delta T$ .

$\Delta T$  is calculated by:

$$\Delta T = \frac{\text{thermal loading rate to cooling water in megawatts}}{\gamma C_p Q_o} \times (3.414) \left( \frac{10^6 \text{ BTU/hr}}{\text{MW}} \right) \left( \frac{1 \text{ hr}}{3600 \text{ sec.}} \right) \quad (\text{IV-83})$$

where

$$\begin{aligned} \gamma C &= 62.4 \text{ BTU/ft}^3/\text{°F} \\ Q_o &= \text{flow rate, ft}^3/\text{sec.} \end{aligned}$$

Substituting the appropriate values into the above equation, it is found that (using the known thermal loading to the cooling water):

$$\Delta T = \frac{(422) (3.414) (10^6) / 3600}{(62.4) (341)} = 18.8^\circ\text{F}$$

Equation IV-83 is not feasible to use when the thermal loading rate to the cooling water is unknown. As an alternative approach, the following expression can be employed:

$$\Delta T = \frac{1}{Q_o} \cdot \frac{e_c}{e_p} \text{ MWe} \cdot \frac{1}{\rho C_p} \cdot \frac{3.414 \times 10^6}{3600} \quad (\text{IV-84})$$

where

- $e_p$  = percent of total energy produced that is transmitted as electricity. For new fossil fuel plants: 38 percent; for nuclear plants: 32 percent
- $e_c$  = percent of total energy produced that is dissipated through cooling water. For new fossil fuel plants: 48 percent; for nuclear plants: 68 percent

MWe = capacity of power plant in megawatts electric.  
 Equation IV-84 predicts that  $\Delta T$  is:

$$\frac{1}{341} \cdot \frac{58}{32} \cdot 217 \frac{1}{62.4} \cdot \frac{3.414 \cdot 10^6}{3600} = 17.5^\circ\text{F}$$

It is only about  $1^\circ\text{F}$  less than predicted by Equation IV-83.

----- END OF EXAMPLE IV-12 -----

#### 4.4.5 Longitudinal Temperature Variation

If the temperature at a particular location in a river is known, the steady-state temperature distribution downstream from that point can be estimated by:

$$\frac{T - E}{T_m - E} = \exp\left(\frac{-0.061 \cdot Kx}{\rho C_p U d}\right) \quad (\text{IV-85})$$

where

$T_m$  = temperature at  $x = 0$ ,  $^\circ\text{F}$

$T$  = stream temperature at a distance  $x$ , where  $x$  is measured in miles

$E$  = equilibrium temperature,  $^\circ\text{F}$

$K$  = thermal transfer coefficient,  $\text{BTU}/\text{ft}^2/\text{day}/^\circ\text{F}$

$u$  = stream velocity,  $\text{ft}/\text{sec}$

$d$  = stream depth, feet

$\rho$  = water density,  $\text{lb}/\text{ft}^3$

$C_p$  = heat capacity of water,  $\text{BTU}/\text{lb}/^\circ\text{F}$  ( $\rho C_p = 62.4 \text{ BTU}/\text{ft}^3/^\circ\text{F}$ ).

An important fact is revealed upon inspection of Equation IV-85. Suppose that a thermal discharge heats the ambient water to a temperature  $T_m$ , but  $T_m$  is less than the instantaneous equilibrium temperature  $E$ . In that instance the stream temperature will continue to rise exponentially downstream, approaching  $E$ . The rate at which  $T$  approaches  $E$  is dependent on the thermal transfer coefficient, as well as stream velocity and depth. Equation IV-66 is graphically illustrated in Figure IV-31.

#### ----- EXAMPLE IV-13 -----

##### Use of Figure IV-31

Suppose an average daily thermal transfer coefficient,  $K$ , of  $200 \text{ BTU}/\text{ft}^2/\text{day}$  has been calculated. The river of interest has an initial temperature "excess" (i.e.,  $T_m - E > 0$ ). How far downstream will that excess be 50 percent of the



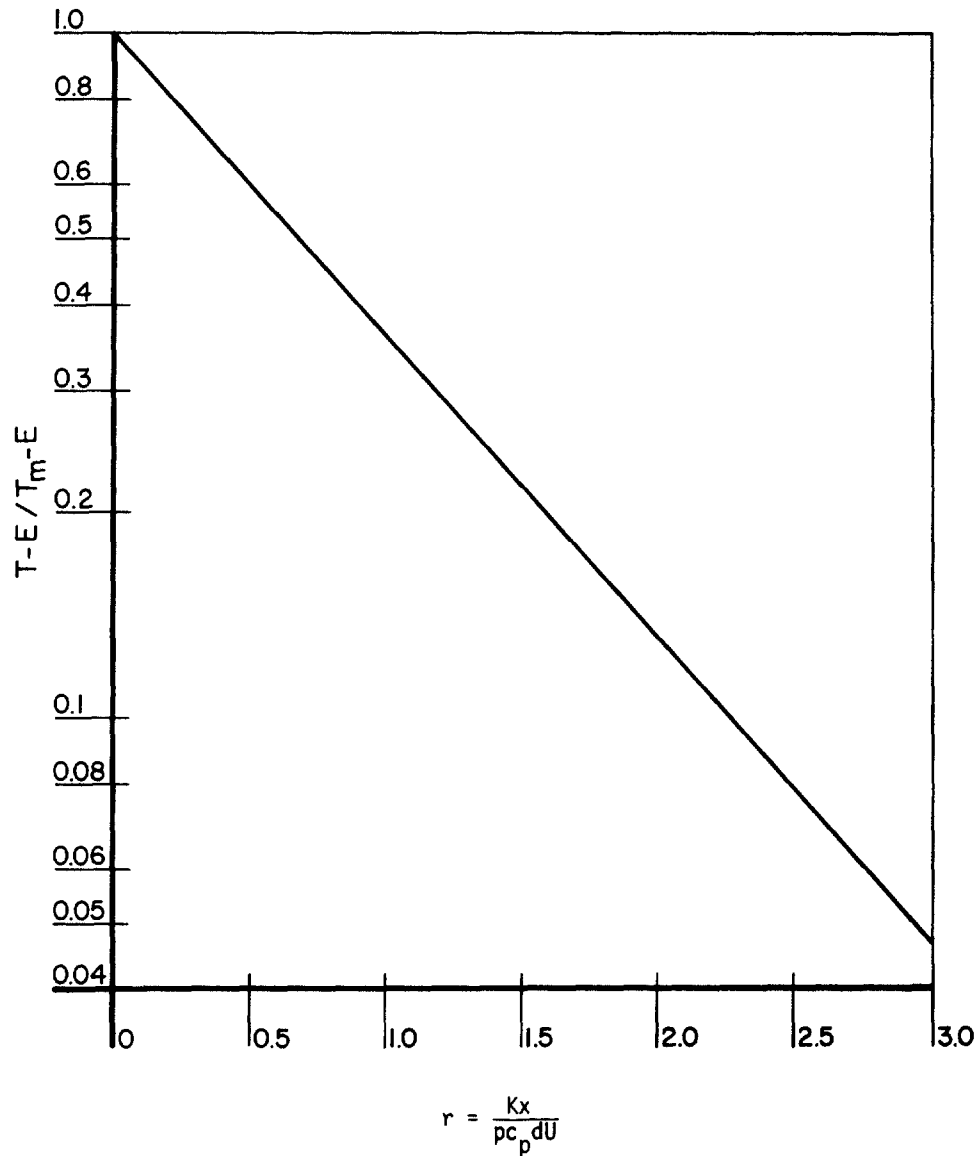


FIGURE IV-31 DOWNSTREAM TEMPERATURE PROFILE FOR COMPLETELY MIXED STREAM,  $T-E/T_m-E$  VS.  $r$  (FROM EDINGER, 1965)

original? Other stream data:

$$U = .5 \text{ fps}$$

$$d = 4 \text{ feet}$$

$$\rho C_p = 62.4 \text{ BTU/ft}^3 \cdot \text{°F}$$

From Figure IV-31,  $r$  is to be found such that:

$$\frac{T - E}{T_m - E} = .5$$

The correct  $r$  equals 0.68. Solving for  $x$  in terms of  $r$  it is found:

$$x = \frac{r_0 C_p dU}{K} = \frac{(0.68) (62.4) (4) (.5) (24) (3600)}{200}$$

$$= 3.6 \times 10^4 \text{ feet} = 6.9 \text{ miles}$$

The associated travel time is  $T = \frac{3.6 \times 10^4}{.5} \times \frac{1}{3600} \text{ hr} = 20.4 \text{ hours}$

----- END OF EXAMPLE IV-13 -----

#### 4.4.6 Diurnal Temperature Variation

Although it is beyond the scope of this report to analyze diurnal stream temperature variations, a few brief statements should be made. Diurnal stream temperature variations on Long Island, New York, were mentioned in Section 4.4.1. Documentation of large diurnal temperature variations is not limited to New York. For example, studies in Oregon (Brown, 1969), Hawaii (Hathaway, 1978) and California have revealed that solar radiation entering shallow streams and rivers produces a significant difference between maximum and minimum daily temperatures. Figure IV-32 shows one such example on the Santa Ana River near Mentone, California. The water temperature varied by **17°F** over a period of 24 hours. One significant effect of the temperature variation is its effect on dissolved oxygen levels. Figure IV-33 shows the measured dissolved oxygen concentrations and predicted saturation levels over the same time period at the same location on the Santa Ana River. The dissolved oxygen concentrations ranged from a high of 9.2mg/l to a low of 8.0mg/l. The variations were caused predominantly by the temperature changes. This illustrates several points:

- Temperature data concomitant with dissolved oxygen data might be needed to properly interpret the cause of dissolved oxygen variations in shallow rivers receiving large amounts of solar radiation
- Removing riparian vegetation around shallow rivers tends to increase the daily maximum temperature and decrease the daily minimum temperature
- Impacts on the dissolved oxygen levels and indigenous biota can be significant.

#### 4.4.7 Low Flow and Temperature

Evidence has previously been cited in this chapter to show that in many parts of the country high temperature conditions are concomitant with low flow. The planner needs to be able to quantify better the nebulous term "low flow" to fruitfully use this concept as a planning tool. For example, suppose a decision is made based on the low flow condition of this year. What are the chances that this low flow will be

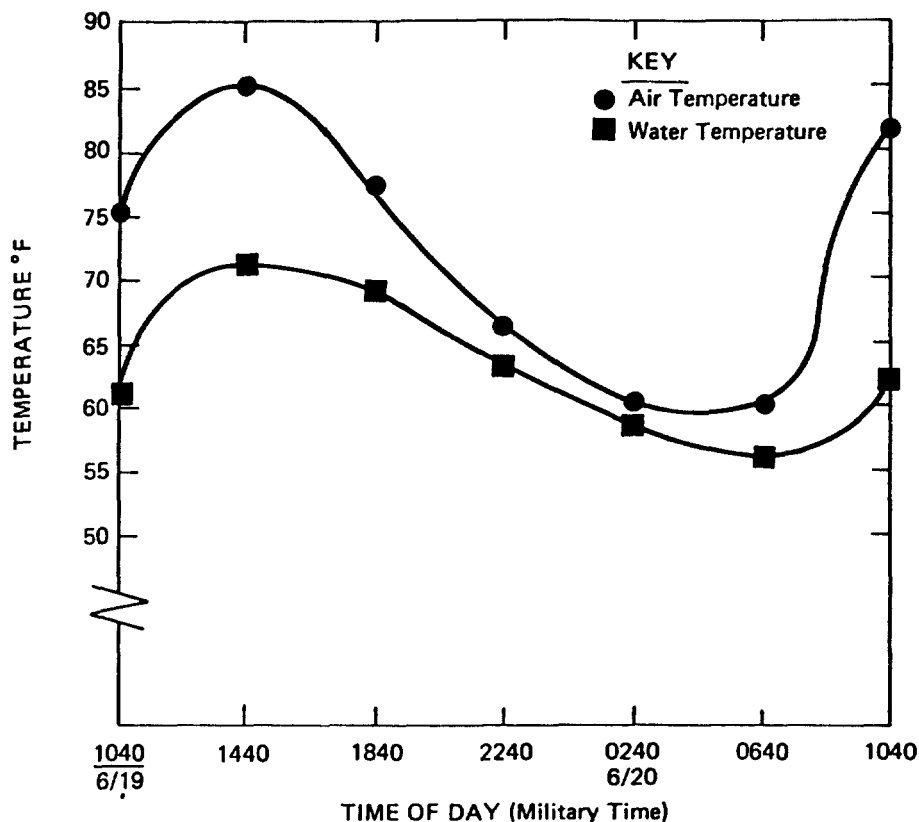


FIGURE IV-32 MEASURED AIR AND WATER TEMPERATURES FOR THE SANTA ANA RIVER NEAR MENTONE, CALIFORNIA, IN JUNE 1979.

exceeded in the future? If they are high, then any decision (e.g. at particular level of waste abatement at a sewage treatment plant) based on the observed conditions could have unexpected deleterious results at a future time. It is paramount then, to predict how often flow will fall below a specified rate.

Two measures or indices of low flow that have been found useful are flow duration and low-flow frequency. Although it is beyond the scope of this report to explain in detail how to develop these measures, examples of each will be presented that explain their utility. The majority of the material in this section is from Cragwall (1966) who provides a discussion on low flow, and cites additional references. Many texts on engineering hydrology (e.g., Linsley et al., 1958) also discuss low flow. Figure IV-34 shows a flow duration curve for the Hatchie River at Bolivar, Tennessee. The vertical axis is the daily discharge and the horizontal is the percent of time a flow is equaled or exceeded. For example, 95 percent of the time from 1930-58 the flow exceeded 177 cfs. It can also be assumed that this flow (177 cfs) will probably be exceeded 95 percent of the time in other years. Thus this concept offers one means by which to quantify "low flow".

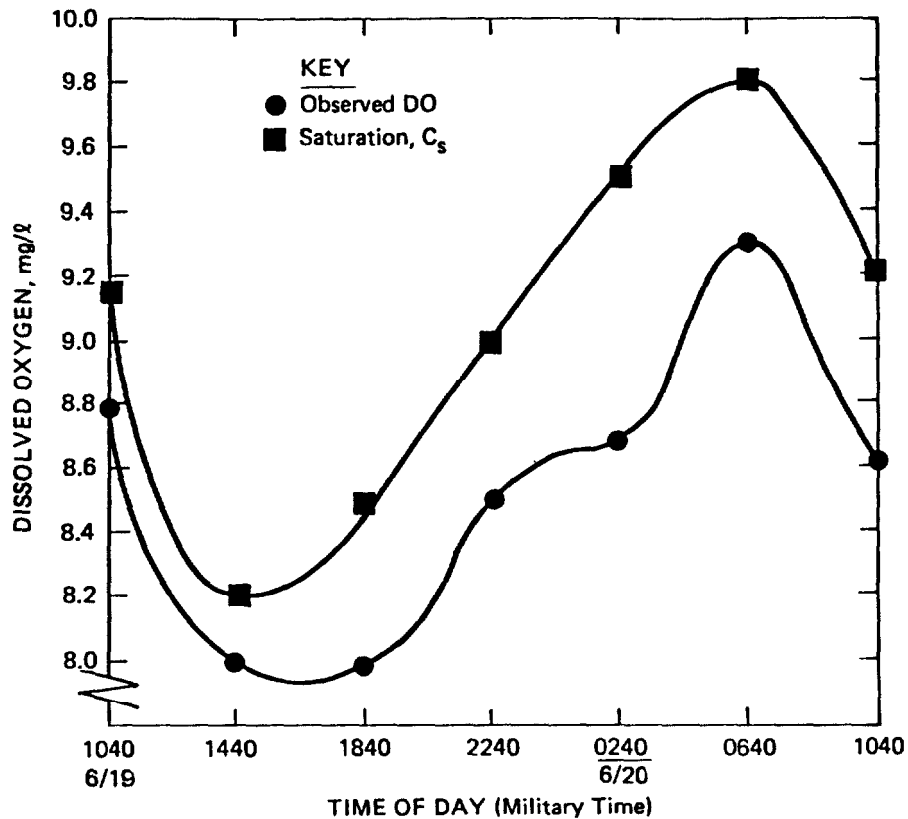


FIGURE IV-33 MEASURED DISSOLVED OXYGEN CONCENTRATION AND PREDICTED SATURATION CONCENTRATION FOR THE SANTA ANA RIVER NEAR MENTONE, CALIFORNIA, IN JUNE 1979.

A second concept is the low flow frequency curve, illustrated in Figure IV-35. This depicts the relationship between discharge and recurrence interval of different duration flows. For example the 7 day mean flow of 100 cfs can be expected to occur once each 19 years. Stated another way, since probability is the reciprocal of recurrence interval, in any one year there is about a 5 percent probability that a seven day mean flow of less than 100 cfs will occur. A commonly used flow for analyses is the 7 day mean flow at a recurrence interval of 10 years, or 7Q10.

#### 4.4.8 Interrelationships Between Temperature Prediction Tools

The three major temperature prediction tools presented in Section 4.4 are:

- Water temperature alterations caused by a power plant
- Equilibrium temperature
- Longitudinal river temperature profile.

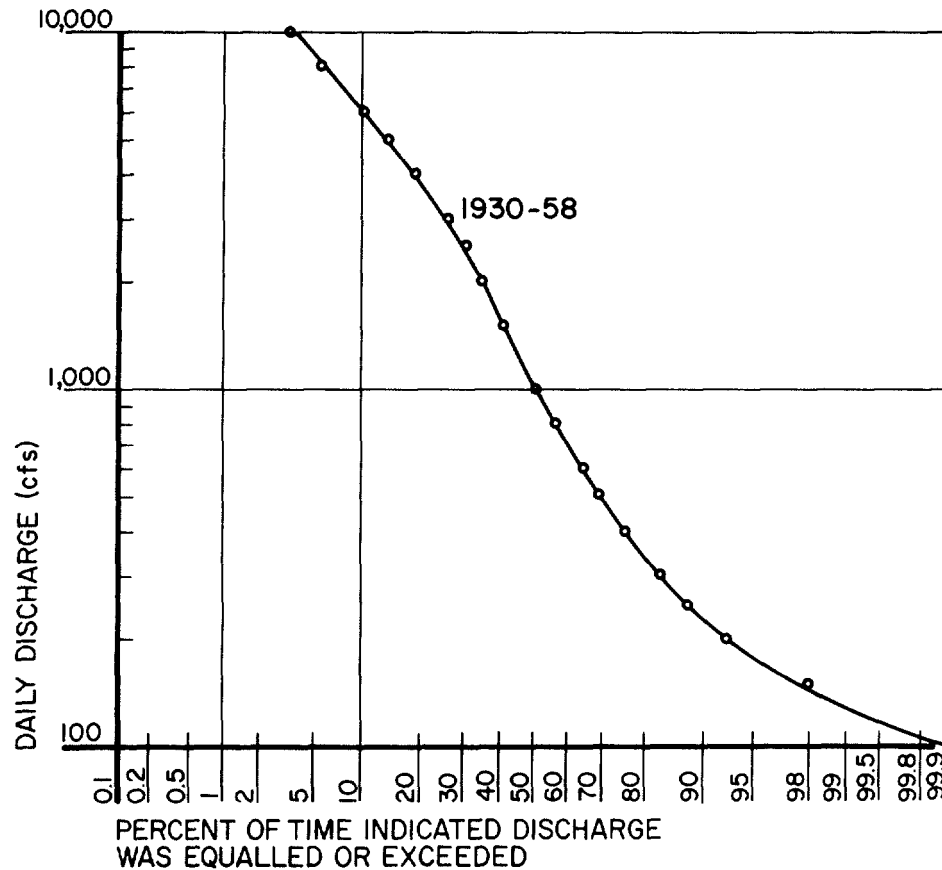


FIGURE IV-34 FLOW DURATION CURVE, HATCHIE RIVER AT BOLIVAR, TENN. (FROM CRAGWALL, 1966)

Figure IV-36 shows three river temperature profiles which illustrate how these tools can be used jointly. Curve A represents a temperature profile of a river where a power plant is located a distance  $D$  below some reference point. The temperature on the river above the power plant is  $T_2$  which is slightly below the equilibrium temperature. Due to the thermal discharge from the power plant, the river's temperature is increased to  $T_4$ , above the equilibrium temperature. Below the mixing zone area, the water temperature gradually decreases toward equilibrium, as the excess heat is dissipated into the atmosphere.

Curve B illustrates the temperature profile of a river whose water comes predominantly from the hypolimnion of a reservoir. While in the reservoir the water is insulated from the solar radiation, so the temperature is below the equilibrium temperature. As the water is withdrawn from the reservoir and begins to flow downstream, its temperature increases due to solar radiation and atmospheric heating. The temperature tends to approach the same equilibrium temperature (the two rivers are assumed to be in the same geographic area).

Curve C shows the temperature profile of river B which now has a power plant,

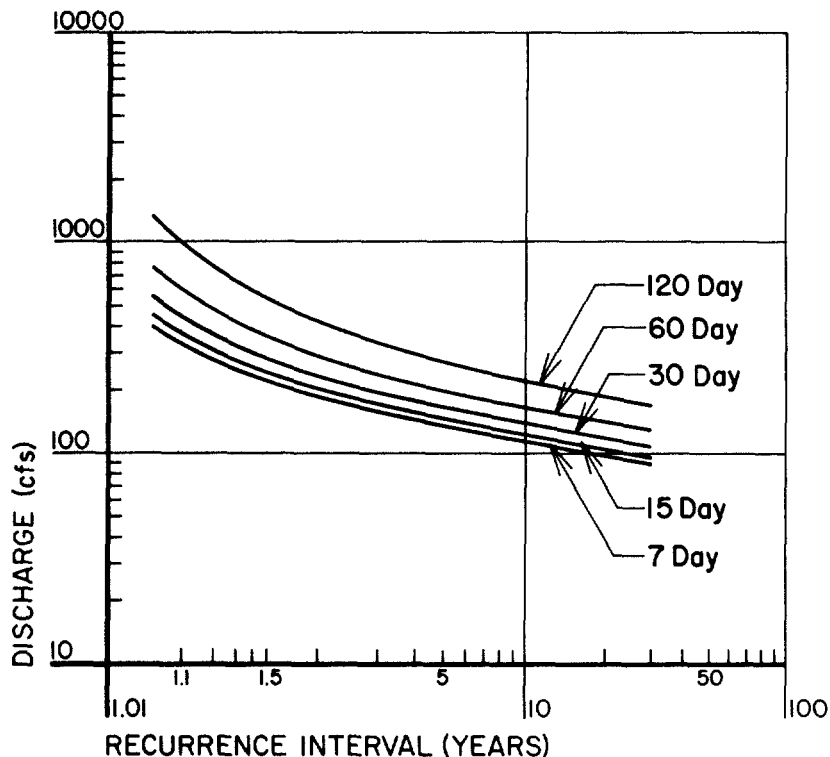


FIGURE IV-35 FREQUENCY OF LOWEST MEAN DISCHARGES OF INDICATED DURATION, HATCHIE RIVER AT BOLIVAR, TENN. (FROM CRAGWALL, 1966)

similar to the one on river A, discharging into it. If the flow rates of the two rivers are the same, so is the initial temperature increase (i.e.,  $T_3 - T_1 = T_4 - T_2$ ). However, the temperature of the river continues to increase, in contrast to profile A, because  $T_3$  is less than E. This illustrates an unusual, but entirely possible, situation where river temperature continues to increase below a thermal discharge.

#### 4.5 NUTRIENTS AND EUTROPHICATION POTENTIAL

##### 4.5.1 Introduction

Within the past decade the elements most often responsible for accelerating eutrophication - nitrogen and phosphorus - have shown generally increasing levels in rivers (EPA, 1974). Median concentrations increased in the period from 1968 to 1972 over the period from 1963 to 1967 in 82 percent of the reaches sampled for total phosphorus, 74 percent for nitrate, and 56 percent for total phosphate.

These increasing concentrations afford more favorable conditions for eutrophication, although many rivers with high nutrient levels do not have algal blooms. Algal

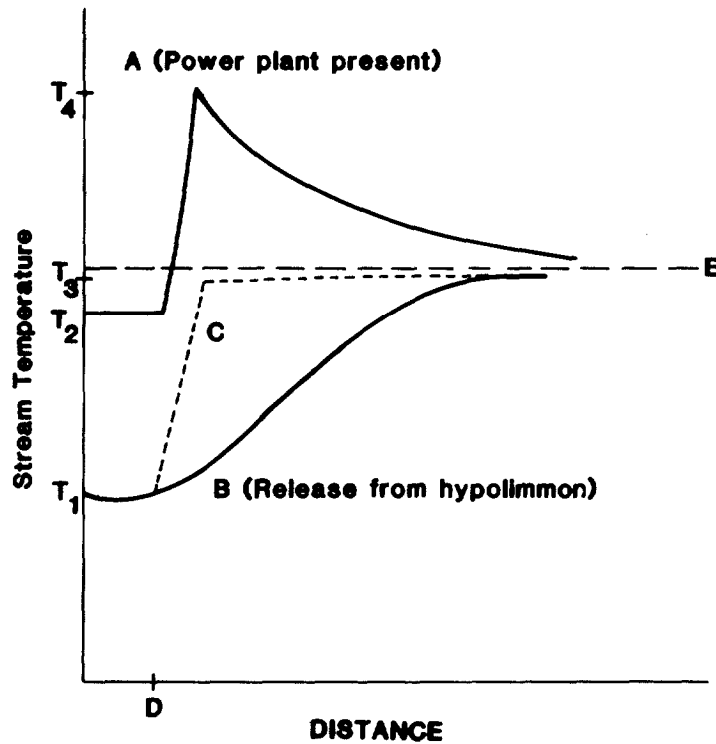
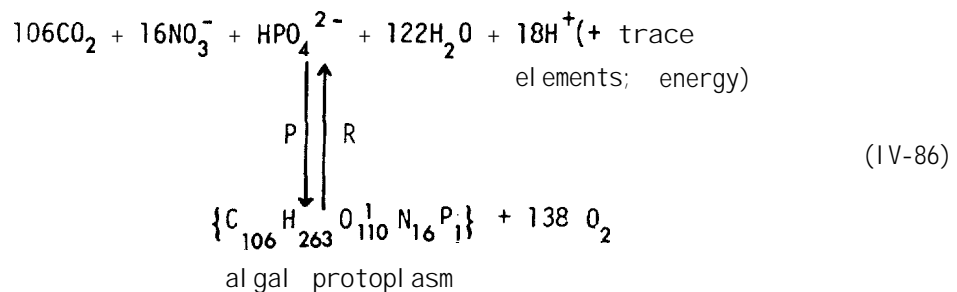


FIGURE IV-36 THREE RIVER TEMPERATURE PROFILES

growth can be inhibited in numerous ways. For example, turbidity can decrease light transmittance through water and effectively stop growth. Decreasing turbidity could, however, have a deleterious side effect of promoting excessive algal growth, unless stream nutrient levels are concurrently decreased. High water velocity can also prevent algae from reaching bloom proportions before they are carried out of the river system. The eutrophication problem, then, is transferred to the water body into which the river empties.

#### 4.5.2 Basic Theory

Stumm and Morgan (1970) have proposed a representation for the stoichiometry of algal growth:



where

P = photosynthesis

R = respiration.

Observe that in the algal protoplasm the ratio of C:N:P is:

$$C:N:P = 106:16:1, \text{ by atomic ratios} \quad (IV-87)$$

$$C:N:P = 41:7:1, \text{ by weight ratios} \quad (IV-88)$$

From the above two equations it can be inferred that only small amounts of phosphorus are needed to support algal growth in relation to the amounts of carbon and nitrogen required. If phosphorus is not present in the amount required for algal growth then algal production will be curtailed, regardless of how much of the other nutrients is available. Phosphorus is then termed growth limiting. It is possible for other elements, particularly nitrogen, and occasionally carbon or trace metals, to be growth limiting as well (Stumm and Stumm-Zollinger, 1972).

Nitrogen uptake by algae is generally in the nitrate form if nitrate is available. However, different types of fresh water algae can utilize either organic nitrogen or inorganic nitrogen in the form of ammonia, depending on which is available (Stumm and Stumm-Zollinger, 1972). Algae typically require phosphorus in an inorganic form, usually as orthophosphate ion (Kormondy, 1969).

Some indication of whether nitrogen or phosphorus is growth limiting may be made by determining the weight ratio of the appropriate forms of nitrogen and phosphorus found in a river, and comparing that with the stoichiometric ratio required for growth. This gives an idea regarding the nutrient on which control efforts should focus. Specifically, let:

$$R = \frac{[TN]}{[OPO_4-P]} \quad (IV-89)$$

where

[TN] = concentration of total nitrogen in river, mg-N/l

[OPO<sub>4</sub>-P] = concentration of orthophosphate, mg-P/l.

If  $R > 10$ , phosphorus is more likely to limit than N.

If  $R < 5$ , nitrogen is more likely limiting than P.

If  $5 < R < 10$ , a determination cannot be made.

Since the N:P ratio in algal biomass can vary from species to species, this makes the determination of the limiting nutrient somewhat uncertain, and leads to the indetermination range of  $5 < R < 10$ . If local data include an inventory of algal species present, then the N:P ratio of the known species should be used in lieu of Equation IV-88.



Both Lehman, et al. (1975) and Lund (1965) provide specific algal data as well as further discussions.

The following table (Table IV-28) shows an approximate relationship between total nitrogen and total phosphorus concentrations and the potential algal biomass that can result. Both nitrogen and phosphorus must be present in the amounts shown for the resultant growth to occur.

TABLE IV-28

EUTROPHICATION POTENTIAL AS A  
FUNCTION OF NUTRIENT CONCENTRATIONS

P (mg-P/l )	N (mg-N/l )	Dry Algal Cells (mg/l )	Significance
0.013	0.092	1.45	Problem threshold
0.13	0.92	14.5	Problem likely to exist
1.3	9.2	745.0	Severe problems possible

4.5.3 Estimating Instream Nutrient Concentrations

Because of the transformations that occur among the different nitrogen and phosphorus compounds it is not possible to conveniently track any particular form of nitrogen or phosphorus through a stretch of river. However, if total nitrogen and total phosphorus can be considered conservative, a mass balance approach can be easily formulated for these constituents. In reality this assumption may not be met for a variety of reasons.

For example, algae utilize nutrients, die, and settle to the bottom. Although there is a recycling of algal cell-bound nutrients, the settling rate may surpass the rate of recycling. Assuming total nitrogen and total phosphorus to be conservative should give an estimate of the upper limit of the instream concentrations of these nutrients.

The instream concentration of total nitrogen (TN) or total phosphorus (TP) resulting from a point discharge is (formulas will be presented for TN only; those for TP are exactly analogous):

$$TN_o = \frac{TN_u Q_u + TN_w Q_w}{Q_u + Q_w} \quad (IV-90a)$$

$$TN_o = \frac{TN_u Q_u + w_p/5.38}{Q_u + Q_w} \quad (IV-90b)$$

where

- $TN_u$  = instream TN upstream of discharge, mg-N/l
- $TN_w$  = concentration of TN in point discharge, mg-N/l
- $Q_u$  = flow in river upstream of point discharge, cfs
- $Q_w$  = flow rate of point discharge, cfs
- $TN_o$  = resulting instream TN concentration, mg-N/l
- $w_p$  = loading rate of point source, lb/day.

The expression for  $TN_o$  is given by either Equation IV-91A or IV-91B. The appropriate form to use will depend on the form of the available data.

To determine the instream concentration of total nitrogen due to a distributed discharge, use:

$$TN = TN_o + \frac{\Delta Q x}{Q} (TN_r - TN_o) \quad (IV-91a)$$

or

$$TN = \frac{TN_o Q_o}{Q} + \frac{wx}{5.38 Q} \quad (IV-91b)$$

where

- $TN_r$  = TN entering with the distributed flow, mg-N/l
- $TN_o$  = instream TN at  $x = 0$ , mg-N/l
- $x$  = distance downstream from the point source discharge
- $Q$  = stream flow rate at  $x$ , cfs
- $Q_o$  = stream flow rate at  $x = 0$ , cfs
- $\Delta Q$  = incremental flow increase per unit distance, cfs/mile
- $w$  = mass flux of TN entering the stream through the distributed source, lb/day/mile.

The choice of whether to use Equation IV-91a or IV-91b depends on the available data. Based on the approach detailed in Chapter III, the mass flux of nutrient entering the stream (in units of lb/day/mile) can be generated. When this approach is used, then Equation IV-91b is applicable.

To use Equation IV-91a the concentration of pollutant from the nonpoint source has to be known. This can be accomplished using the approach of Omernik (1977). Nonpoint source nitrogen and phosphorus concentrations are predicted as fractions of land use type or based on color coded maps if land use categories are not known. The data used to predict nitrogen and phosphorus concentrations were generated in a National Eutrophication Survey (NES) program wherein a nationwide network of 928 nonpoint-source watersheds were monitored. This method accounts for only the nonpoint source contribution. Consequently, if point source exist within the watershed, their contributions must be included as well in order to accurately predict instream concentrations.

Table IV-29 summarizes the predictive formulas developed by Omernik for total phosphorus, orthophosphorus, total nitrogen, and inorganic nitrogen. The formulas are regionalized by eastern, central, and western United States. Agricultural, urban, and forested lands comprise the independent variables in the formulas.

Omernik's analysis of the NES data indicates that:

- Streams draining agricultural watersheds had considerably higher nutrient concentrations than those draining forested watersheds.
- Nutrient concentrations were generally directly proportional to the percent of the land in agriculture and inversely proportional to the percent of land in forest.
- Mean concentrations of total phosphorus and total nitrogen were nearly nine times greater in streams draining agricultural lands than in streams draining forested lands.
- Mean phosphorus concentrations in streams draining forested watersheds in the west were generally twice as high as those in the east.
- Total and inorganic nitrogen in streams draining agricultural watersheds were considerably higher in the heart of the corn belt than elsewhere.

As an alternative to the equations shown in Table IV-29, Omernik provides three colored maps of nonpoint source related concentrations of nutrients in streams. They can be used where detailed information necessary for more accurate prediction is unavailable.

#### 4.5.4 Nutrient Accounting System

It may be desirable to determine the impact of each nutrient source on the total instream concentration in order to distinguish among the major sources. An accounting procedure utilizing Equations IV-90 and IV-91 can be developed to do this. The following steps outline the procedure.

1. Segment River. Divide the river into major segments. These segment divisions may reflect waste loading distributions or another convenient division scheme chosen at the discretion of the planner. The segments are not necessarily the same as the reaches that have previously been discussed (see Section 4.1). The delineation of reaches as described earlier is based upon lengths of river having uniform hydraulic conditions. Segments, as used here, are purely a convenient subdivision of the river.
2. Quantify and Locate Sources of Nutrients. The quantification of point, nonpoint, and natural sources on the mainstem and tributaries should be accomplished using the best available data. Tabulation can be performed for each different season to reflect the discharge pattern characteristic of each season. The quantification should include total nitrogen and total phosphorus. Tabulate data in terms of average daily input (lb/day).

TABLE IV-29  
REGIONAL STREAM NUTRIENT CONCENTRATION PREDICTIVE MODELS

---

<u>Nutrient Form</u> Region	Model , Error	Correlation Coefficient	and Multiplicative Standard
<u>Total phosphorus</u>			
East	$\text{Log}_{10}$ (PCONC) = -1.8364 + 0.00971 (% agric + % urb)	r = 0.74,	f = 1.85
Central	$\text{Log}_{10}$ (PCONC) = -1.5697 + 0.00811 (% agric + % urb) -0.002312 (% for)	r = 0.70,	f = 2.05
West	$\text{Log}_{10}$ (PCONC) = -1.1504 + 0.00460 (%agric + %urb) -0.00632 (% for)	r = 0.70,	f = 1.91
<u>Orthophosphorus</u>			
East	$\text{Log}_{10}$ (OPCONC) = -2.2219 + 0.00934 (% agric + % urb)	r = 0.73,	f = 1.86
Central	$\text{Log}_{10}$ (OPCONC) = -2.0815 + 0.00868 (% agric + % urb)	r = 0.63,	f = 2.05
West	$\text{Log}_{10}$ (OPCONC) = -1.5513 + 0.00510 (% agric + % urb) -0.00476 (% for)	r = 0.64,	f = 1.91
<u>Total nitrogen</u>			
East	$\text{Log}_{10}$ (NCONC) = -0.08557 + 0.00716 (% agric + % urb) -0.00227 (% for)	r = 0.85,	f = 1.51
Central	$\text{Log}_{10}$ (NCONC) = -0.01609 + 0.00399 (% agric + % urb) -0.00306 (% for)	r = 0.77,	f = 1.50
West	$\text{Log}_{10}$ (NCONC) = -0.03665 + 0.00425 (% agric + % urb) -0.00376 (% for)	r = 0.61,	f = 1.75
<u>Inorganic nitrogen</u>			
East	$\text{Log}_{10}$ (INCONC) = -0.3479 + 0.00858 (% agric + % urb) -0.00584 (% for)	r = 0.84,	f = 1.93
Central	$\text{Log}_{10}$ (INCONC) = -0.5219 + 0.00482 (% agric + % urb) -0.00572 (% for)	r = 0.71,	f = 2.06
West	$\text{Log}_{10}$ (INCONC) = -0.6339 + 0.00789 (% agric + % urb) -0.00657 (% for)	r = 0.65,	f = 2.45

---

From: Omernik (1977)

---

Characterize the location of the nutrient sources by river mile. For nonpoint sources characterize by river mile at both the beginning and end of the source.

3. Perform Mass-Balance. Sum the known sources to determine the total nutrient loading to each segment. Then make the following comparisons:
  - a. Compare the total loading with the nutrient input from the mainstem at the upstream end of the segment. This direct comparison permits an assessment of the collective impact of the nutrient sources entering a segment and the upstream contribution of the mainstem.
  - b. Perform an intersource comparison to ascertain the relative impact of each nutrient source. Express the results for each source as a percent of the total loading.

When a tributary has a high percent contribution steps 1 through 3 can be repeated for the tributary itself to track the sources of the nutrients.

Apply Equations IV-90 and IV-91 to each reach within the segment to determine the instream nutrient concentration throughout the segment. Once this is done that step can be repeated for the next reach.

By applying this analysis one can determine the relative impact of any discharge, determined jointly by the flux of the nutrient and the discharge location. Section 4.1.10 provided a detailed example problem which illustrates the procedure. A brief example also follows.

----- **EXAMPLE IV-14** -----

Computing Total Nitrogen Distribution

This example illustrates the use of Equations IV-90b and IV-91b in calculating the total nitrogen distribution in a river. Suppose the user has been able to estimate the point and nonpoint loading of total nitrogen in a river as shown in Table IV-30.

If these loading rates are estimated over a year, then the flow rates used should also be average annual flows. To compute the concentration at mile 0, Equation IV-90b can be used:

$$TN_0 = \frac{(0)(Q_u) + \frac{400}{8.34}}{\frac{300}{1.55}} = 0.25 \text{ mg-N/l}$$

where the following conversions were used:

$$1 \text{ MGD} = 1.55 \text{ cfs}$$

$$1 \text{ mg/l} = 8.34 \text{ lb/MG}$$

To determine the concentration at milepoint 9.99, use Equation IV-91b:

TABLE IV-30

TOTAL NITROGEN DISTRIBUTION IN A RIVER IN  
RESPONSE TO POINT AND NON-POINT SOURCE LOADING

Reach Number	River Mile-Point	TN Added* (lbs/day)	TN Cumulative (lbs/day)	Q Cumulative (cfs)	TN Concentration (mg-N/l)
1	0	400 L	400	300	0.25
	9.99	500 D	900	400	0.42
2	10.0	0	900	400	0.42
	14.99	700 D	1,600	600	0.50
3	15.0	800 L	2,400	700	0.64
	20.99	650 D	3,050	900	0.62
4	21.0	0	3,050	900	0.62
	26.0	900 D	3,950	1,000	0.73

\*"L" indicates a localized or point source. "D" indicates a diffuse or non-point source whose range of input is over the entire reach.

$$TN = (0.25) \frac{300}{400} + \frac{\frac{500}{8.34}}{\frac{400}{1.55}} = 0.42 \text{ mg-N/l}$$

Note that  $w_x$  in Equation IV-91 is the 500 lb/day shown in Table IV-30. By reapplying these two basic equations for each reach the user can work downstream through the four reaches. Also note that the total nitrogen concentration has decreased slightly through reach 3, even though more TN has been added. This is because the incoming flow has served to lower the concentration by dilution.

END OF EXAMPLE IV-14

#### 4.6 TOTAL COLIFORM BACTERIA

##### 4.6.1 Introduction

Total coliform bacteria are considered an indicator of the presence of pathogenic organisms, and as such relate to the potential for public health problems. Allowable levels of total coliform bacteria in rivers vary from state to state and according to the water use description characterizing the particular river segment. For example, in Montana (Montana State Dept. of Health and Environmental Sciences, 1973) the raw

water supply may not have more than an average of 50 MPN/100 ml\* total coliforms if it is to be used as a potable water supply following simple disinfection. In water suitable for bathing, swimming and recreation, as well as growth and marginal propagation of salmonid fishes, an average of 1,000MPN/100 ml is allowable.

Concentrations of total coliforms vary with the season of the year. Often the heaviest loadings occur during the summer months, but this impact is somewhat offset due to the more rapid die-off at higher temperatures and more intense solar radiation. In the Willamette River (Figure IV-37), for example, the highest counts of 1971-72 were actually observed from November through May (EPA, 1974).

Treated municipal sewage comprises a major source of coliform pollution. Urban stormwater runoff can also be significant, especially through combined sewer outflows. Rural storm water runoff transports significant fecal contamination from livestock pastures, poultry and pig feeding pens, and feedlots. Wildlife both within refuges and in the wilds can contribute as well. For guidance in the interpretation of preliminary coliform analyses, Table IV-31 can be used.

#### 4.6.2 Mass Balance for Total Coliforms

The mass balance equations applicable to total coliform organisms are exactly analogous to Equations IV-18, IV-21, and IV-23A and IV-23B, since first order decay is used for both. For purposes of hand computations, the following decay coefficient is acceptable:

$$k_{tc} = 1.0 + 0.02 (T-20) \quad (IV-92)$$

where

$$k_{tc} = \text{decay coefficient for total coliforms, 1/day}$$

$$T = \text{water temperature, } ^\circ\text{C.}$$

Those equations with the widest applicability are listed below. For a point source of coliforms:

$$TC = TC_o \exp \left[ \frac{-j_{tc}}{A_o} \left( A_o x + \Delta_A \frac{x^2}{2} \right) \right] \quad (IV-93)$$

---

\*MPN means "Most Probable Number". Coliform organisms are not counted individually, but their densities are statistically determined and the results stated as MPN/100 ml.

# SEASONAL RIVER PROFILES

WILLAMETTE RIVER

Total Coliforms

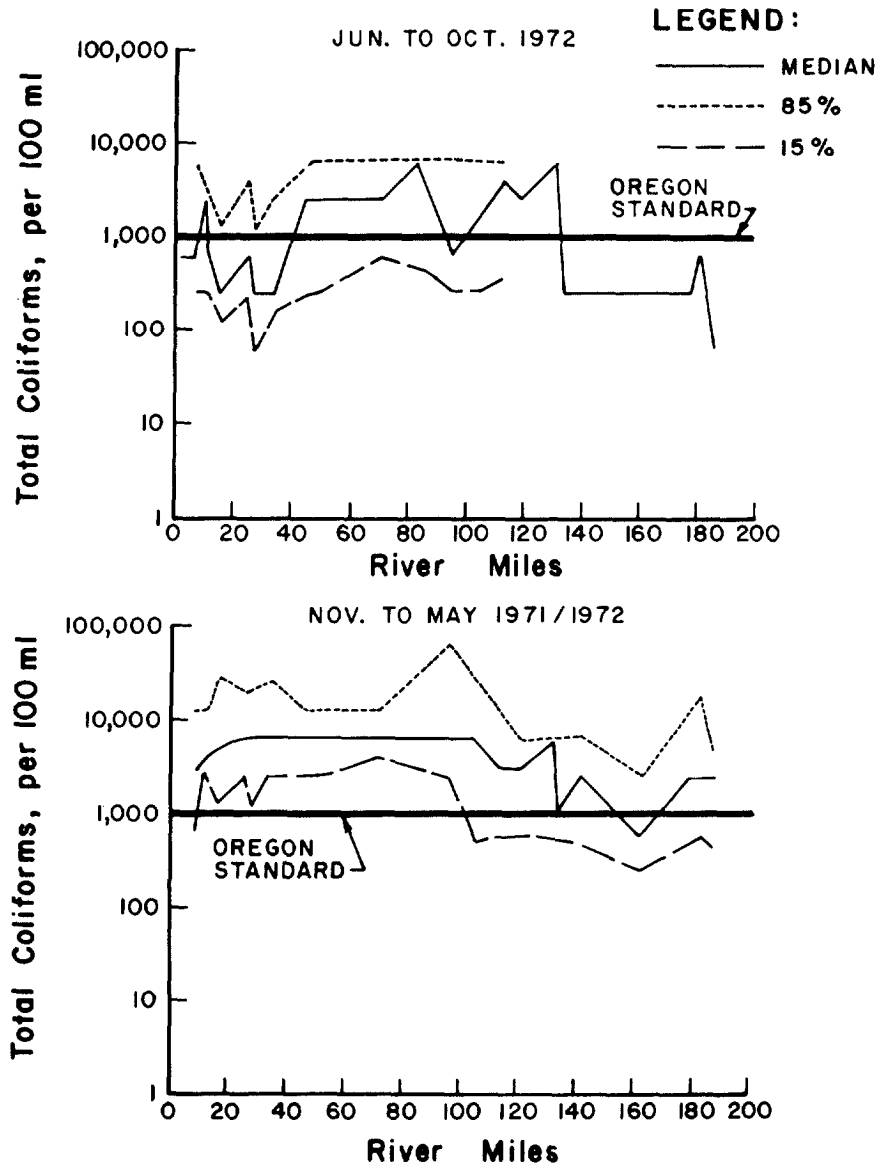


FIGURE IV-37 TOTAL COLIFORM PROFILES FOR THE WILLAMETTE RIVER (EPA, 1974)

TABLE IV-31

TOTAL COLIFORM ANALYSIS (EPA, 1976)

If the Calculated Concentration is:	Probability of a Coliform Problem
Less than 100/100 ml	Improbable
Less than 1,000/100 ml	Possible
More than 1,000/100 ml	Probable
More than 10,000/100 ml	Highly Probable



For both point and distributed sources of coliforms:

$$TC = \frac{TC_r}{E_{tc}} + \left( TC_o - \frac{TC_r}{E_{tc}} \right) \left( \frac{Q_o}{Q} \right)^{E_{tc}} \quad (IV-94)$$

For a change in coliform concentration due to a point source modification:

$$\Delta TC = \begin{cases} \Delta TC_o \exp \left[ \frac{-j_{tc}}{A_o} \left( A_o x + \Delta A \frac{x^2}{2} \right) \right] \\ \Delta TC_o \left( \frac{Q_o}{Q} \right)^{E_{tc}} \end{cases} \quad (IV-95a)$$

(IV-95b)

where

$$\begin{aligned} TC &= \text{total coliform concentration, MPN/100 ml} \\ TC_o &= \text{initial total coliform concentration, MPN/100 ml} \\ j_{tc} &= \frac{k_{tc}}{U_o} \\ TC_r &= \text{total coliform level in distributed flow, MPN/100 ml} \\ E_{tc} &= \frac{k_{tc} A_o + \Delta}{\Delta Q} \end{aligned}$$

Because of the potential variability in coliform loadings, seasonal analyses may be warranted. Typically the summer months are of primary concern because loadings often increase during this time period and water contact recreation is at its maximum. Major storm events may also be of interest, because of the large coliform loading that may be associated with them.

#### EXAMPLE IV-15

##### Estimating the Change in Total Coliform Levels in Response to a Waste Loading Change

Compare the change in total coliform levels,  $\Delta TC$ , produced by a change  $\Delta TC_o$  at a given location in a river. Further, determine how this change is affected by a distributed flow entering the river. Relevant data for the river are as follows:

$$\begin{aligned} U_o &= 1 \text{ fps} \\ T &= 20^\circ\text{C} \\ Q_o &= 500 \text{ cfs} \\ Q_f &= 800 \text{ cfs} \end{aligned}$$

$$x_L = 10 \text{ miles}$$

$$k_{tc} = 1.0/\text{day at } 20^\circ \text{ C}$$

First the computations will be performed assuming no distributed flow. Equation IV-95A is then applicable. Computing the exponent  $j_{tc}x$  (at a flow distance of 10 miles):

$$j_{tc}x = \frac{(1.0)(10)(5280)}{(24)(3600)(1)} = 0.611$$

so

$$\frac{\Delta TC}{\Delta TC_0} = \exp(-.611) = 0.54$$

or

$$\Delta TC = 0.54 \Delta TC_0$$

For example if  $\Delta TC_0 = -1,000$  MPN/100 Oml then  $\Delta TC = -540$  MPN/100 ml (negative  $\Delta TC_0$  indicates that the coliform level has decreased from what it previously was).

Now suppose the distributed flow of 300 cfs is included in the computation. Then:

$$E_{tc} = \frac{k_{tc}A_0 + \Delta Q}{\Delta Q}$$

$$A_0 = Q_0/U_0 = 500/1 = 500 \text{ ft}^2$$

$$\Delta Q = \frac{300}{10(5280)} = 0.0057 \text{ ft}^2/\text{sec}$$

$$E_{tc} = \frac{(1.0)(500)}{(24)(3600)(0.0057)}$$

$$= 2.02$$

Then

$$\frac{\Delta TC}{\Delta TC_0} = \left(\frac{500}{800}\right)^{2.02} = 0.39$$

or

$$\Delta TC = 0.39 \Delta TC_0$$

For  $\Delta TC_0 = 1,000$  MPN/100 nm1,  $\Delta TC = -390$  MPN/100 ml.

Note that this decrease is 150 MPN/100 ml less than if no distributed flow existed.

To determine the absolute total coliform level, simply add to the original level the resulting change caused by the waste loading modification.

----- END OF EXAMPLE IV-15 -----

## 4.7 CONSERVATIVE CONSTITUENTS

### 4.7.1 Introduction

Conservative constituents are those which are not reactive and remain either in solution or in suspension. They are advected through the water column at the velocity of the river with no loss of mass. The analysis of nutrients, already discussed in this report, was performed assuming they acted conservatively. Other substances, such as salinity, can also be considered as conservative. Chapter 3 contains information on salinity in irrigation return flow for many rivers with salinity problems.

### 4.7.2 Mass Balance for Conservative Constituents

Two simple mass balance equations are sufficient for analyzing conservative constituents. The first relates the instream concentration due to a point source loading:

$$S = \frac{S_u Q_u + W/5.38}{Q_u + Q_w} \quad (IV-96)$$

where

- S = resulting pollutant concentration, mg/l
- $S_u$  = upstream concentration, mg/l
- $Q_u$  = upstream flow rate, cfs
- $Q_w$  = point source flow rate, cfs
- w = loading rate of pollutants, lb/day.

When a distributed flow is present along some length of the river, then the distribution of the conservative pollutant is given by:

$$S = \frac{S_0 Q_0}{Q} + \frac{wx}{5.38 Q} \quad (IV-97)$$

where

- w = distributed loading rate, lb/day/mi
- x = distance downstream, miles
- $S_0$  = initial concentration (at  $x = 0$ ), mg/l.

$S_0$  in Equation IV-97 is identical with S in Equation IV-96.

EXAMPLE IV-16

Calculating Salinity Distribution in a River

Salinity problems are receiving increased attention in the western United States, particularly relating to the economic issues in the Colorado River Basin and international compacts with Mexico. In the Colorado River high salinity levels in the lower reaches adversely affect nearly twelve million people and approximately one million acres of fertile irrigated farmland (Bessler and Maletic, 1975). The salinity now averages approximately 865 mg/l at Imperial Dam and is projected to be 1,160 mg/l or more by the year 2000, unless firm control actions are taken.

Consider the river shown in Figure IV-38. Predict the salinity distribution based on the inflows and withdrawals shown. Assume the data are averaged over a period of a year. These data, along with the salinity concentrations at different river mileposts are shown in Table IV-32.

To calculate S (salinity at milepoint 100) use Equation IV-96:

$$S = \frac{0.500 + (2 \times 10^6) (1.55/8.34)}{5000}$$

$$= 186 \text{ mg/l}$$

At milepost 199.9, Equation IV-97 is appropriate and S is given by:

$$S = \frac{(186) (2000)}{5000} + \frac{(4 \times 10^6) (1.55/8.34)}{5000}$$

$$= 223 \text{ mg/l}$$

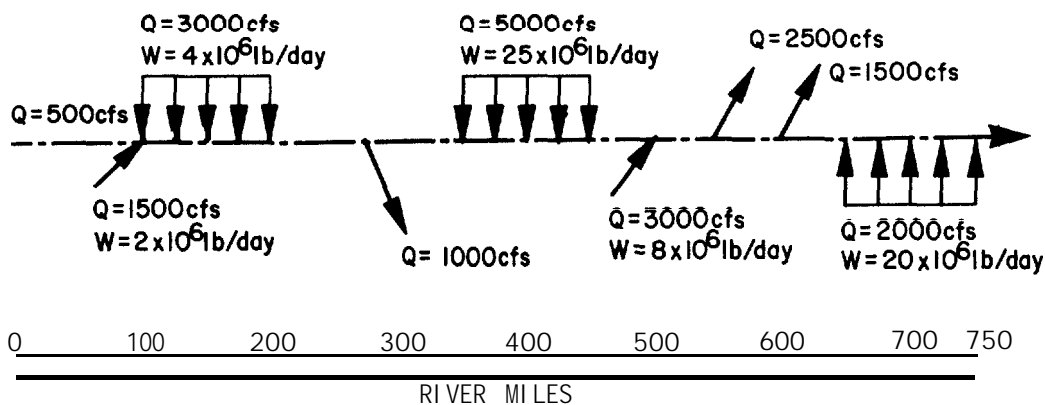


FIGURE IV-38 SALINITY DISTRIBUTION IN A HYPOTHETICAL RIVER

TABLE IV-32

## SALINITY DISTRIBUTION IN A HYPOTHETICAL RIVER

Reach Number	River Mile Point	Salinity Added* (lbs/day)		Salinity Cumulative (lbs/day)	Q Cumulative (cfs)	Salinity Concentration (mg/l)
1	0	0		0	500	0
	99.9	0		0	500	0
2	100	$2 \times 10^6$	L	$2 \times 10^6$	2000	186
	199.9	$4 \times 10^6$	D	$6 \times 10^6$	5000	223
3	200	0		$6 \times 10^6$	5000	223
	279.9	0		$6 \times 10^6$	5000	223
4	280	$-1.2 \times 10^6$	L	$4.8 \times 10^6$	4000	223
	359.9	0		$4.8 \times 10^6$	4000	223
5	360	0		$4.8 \times 10^6$	4000	223
	449.9	$25 \times 10^6$	D	$29.8 \times 10^6$	9000	615
6	450	0		$29.8 \times 10^6$	9000	615
	499.9	0		$29.8 \times 10^6$	9000	615
7	500	$8 \times 10^6$	L	$37.8 \times 10^6$	12000	585
	524.9	0		$37.8 \times 10^6$	12000	585
8	525	$-7.9 \times 10^6$	L	$29.9 \times 10^6$	9500	585
	599.9	0		$29.9 \times 10^6$	9500	585
9	600	$-4.7 \times 10^6$	L	$25.2 \times 10^6$	8000	585
	649.9	0		$25.2 \times 10^6$	8000	585
10	650	0		$25.2 \times 10^6$	8000	585
	750	$20 \times 10^6$	D	$45.2 \times 10^6$	10000	840

\* 'L' indicates a localized or point source at the milepoint shown in the same row.

'D' indicates a diffuse or non-point source ending at the milepoint shown in the same row and beginning at the milepoint in the above row.

At milepoint 280, 1,000 cfs of flow leaves the mainstem (perhaps for irrigation purposes). The concentration of salinity in this flow is the same as that in the mainstem. So the mass rate of withdrawal is:

$$W = \frac{-8.34}{1.55} (223 \times 1000)$$

$$= -1.2 \times 10^6 \text{ lb/day}$$

A negative sign is used to signify a withdrawal. Completing the remainder of the table is solely a matter of reapplying these basic concepts.

END OF EXAMPLE IV-16

#### 4.8 SEDIMENTATION

##### 4.8.1 Introduction

One of the more difficult classes of hydraulic engineering problems associated with rivers involves the erosion, transportation, and deposition of sediment. Sedi-

mentation is important economically, particularly relating to filling of reservoirs and harbors, and to maintaining channel navigability and stability. Table IV-2, located in Section 4.1, documents some suspended solids problems encountered in eight major U.S. waterways.

The sediment load carried in a river can be divided into two components: the bed material load and the wash load. The bed material load is composed of those solid particles represented in the bed. The transport of this material is accomplished both along the bed (bed load) and suspended within the water (suspended load). Although there is no sharp demarcation delineating bed load from suspended load, many researchers have developed individual expressions for each transport component. The total bed material load is the sum of the bed load and the suspended load. Other researchers have developed a unified theory from which the total bed material load can be predicted from a single expression.

The wash load is usually produced through land erosion, rather than channel scour. Wash load is composed of grain sizes finer than found in the bed material. It readily remains in suspension and is washed out of the river without being deposited. A definite relationship between the hydraulic properties of a river and the wash load capacity apparently does not exist, making it difficult to advance an analytical method for washload prediction (Graf, 1971). Not all the erodible material entering a stream is transported as wash load, but a large portion may become part of the bed material and be transported as bed material load.

Figure IV-39 provides a graphical illustration of the difference between wash load and bed material load. For a particular flow condition in a particular river, the river has the capacity to transport a certain quantity of sediment ( $q_s$ ) which generally decreases as particle size increases. At some large particle size the river cannot exert enough force to transport particles of that size or larger. This situation would occur at some point to the right of point D on curve COD. This same river might be supplied with sediment at a rate AOB, which is unrelated to transport capacity.

To the left of point O the river is transporting all the material of that size range being supplied to it. Sediment having diameters less than  $d^*$  are classified as wash load, because the amount being transported is supply limited, and not transport limited. To the right of point O, supply exceeds transport capacity. The amount given by the curve OD is transported, and the difference in OB and OD is deposited in the stream bed. The methods to be presented in the following sections are generally concerned with predicting curve OD (i.e. the bed material load), although Section 4.8.2 does provide a brief description of how to estimate long-term sediment supply rates.

As a guide in evaluating whether a river is carrying a significant quantity of suspended sediment, Table IV-33 can be consulted. 100 mg/l is the delinea-

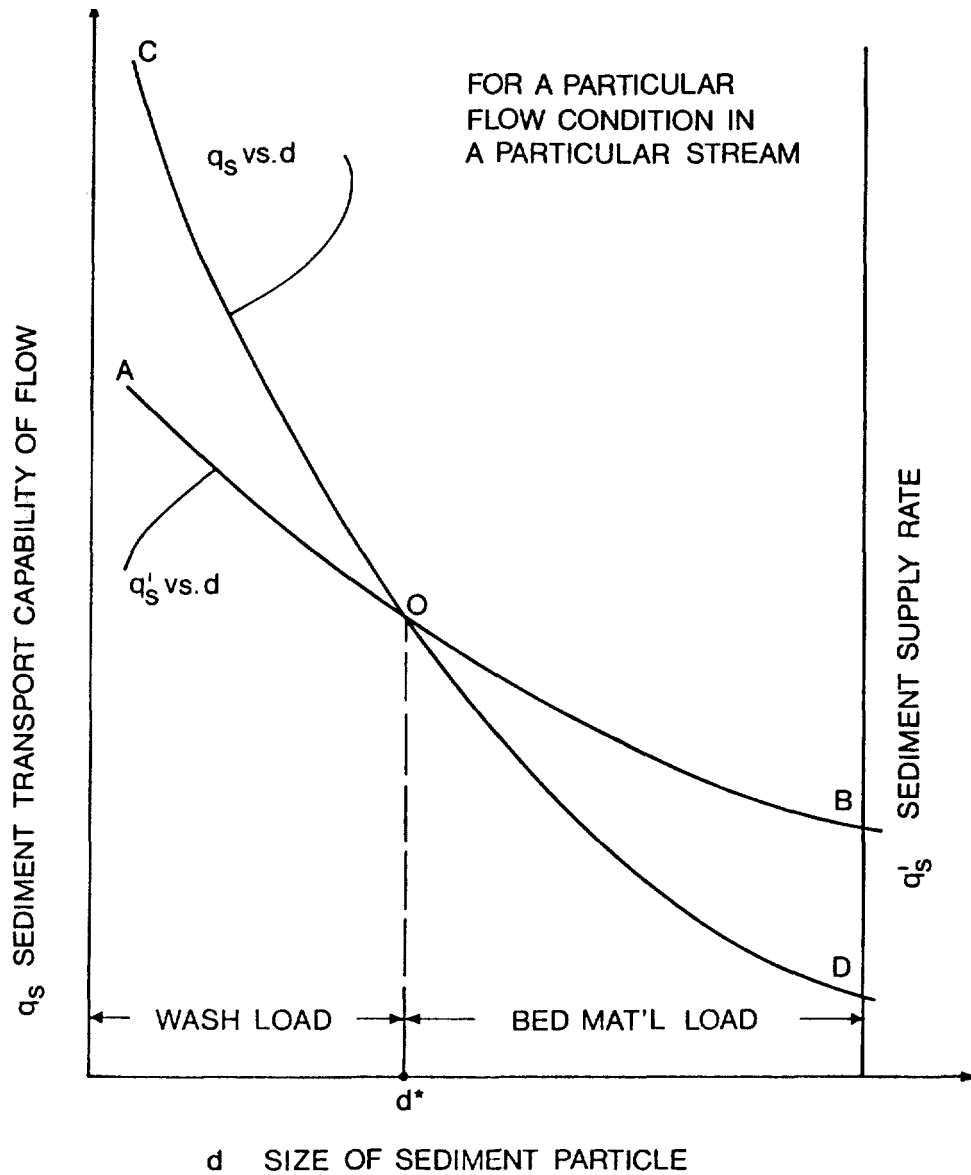


FIGURE IV-39 DIVISION BETWEEN WASH LOAD AND BED MATERIAL LOAD (FROM: COLORADO STATE UNIVERSITY, 1979)

TABLE IV-33  
RELATIONSHIP OF TOTAL SUSPENDED SEDIMENT CONCENTRATION  
TO PROBLEM POTENTIAL (AFTER EPA, 1976)

If Calculated Concentration is:	Probability of a Problem
Less than 10 mg/l	Improbable
Less than 100 mg/l	Potential
More than 100 mg/l	Probable

tion between a potential and probable problem. In a table previously introduced (Table IV-1), a reference level of 80 mg/l was set for protection of aquatic life.

#### 4.8.2 Long-Term Sediment Loading from Runoff

The procedures outlined in Chapter 3 will permit an assessment of the sediment loading to a river on a long-term basis. When using those procedures care should be taken to incorporate the entire drainage area of the watershed. As an estimate, the loading can be assumed conservative (i.e. all sediment that comes into the river will be washed out of the river over an extended time period). Under that assumption the procedure outlined in Section 4.7 can be utilized for an estimate of average yearly suspended solids concentrations at locations throughout the river system. This result should be interpreted as an indicator of the impact of the runoff on sediment loads within a river and not as actual suspended solids concentrations. Not all of the incoming sediment will be transported as suspended load since a large fraction can be transported as bed load. The transport process is generally of an intermittent nature with higher concentrations occurring during periods of high flow.

Care should be taken not to apply the conservative assumption at points on a river where that assumption is clearly violated, such as at reservoirs which can be efficient sediment traps. An example for the computation of sediment loading to rivers has been considered in Chapter 3.

#### 4.8.3 Bed Material Load

As previously mentioned, the estimation of bed material transport poses a difficult problem, and is an area where there is no consensus regarding the best predictive relationship to use. Numerous bed material load relationships (Task Committee on Preparation of Sedimentation Manual, 1971) have been developed over the past century, some requiring considerably more input data than others. In this report the DuBoys relationship (Task Committee on Preparation of Sedimentation Manual, 1971) will be used in part because of its simplicity. The relationship, which is restricted to uniform flow in alluvial channels, is:

$$g_b = \psi \tau_0 (\tau_0 - \tau_c) \quad (IV-98)$$

where

- $g_b$  = bed load, lb/sec/ft of width of river
- $\psi$  = coefficient depending on grain size,  $ft^3/lb/sec$
- $\tau_0 = \gamma R_H S$ , bed shear stress,  $lb/ft^2$
- $\gamma$  = specific weight of water,  $lb/ft^3$
- $R_H$  = river hydraulic radius, ft



$S$  = slope of stream, ft/ft

$\tau_c$  = critical shear stress, lb/ft<sup>2</sup>.

The values of  $\psi$  and  $\tau_c$  can be expressed as functions of the median size (by weight) of the bed sediment ( $d_{50}$ ). These relationships are expressed graphically in Figure IV-40. To aid in determining  $d_{50}$  Table IV-34 is presented to show the size range of sediment and each associated class name. If the class name of the predominant sediment type comprising a stream bed is known, then the sediment size (in mm) can be reestimated.

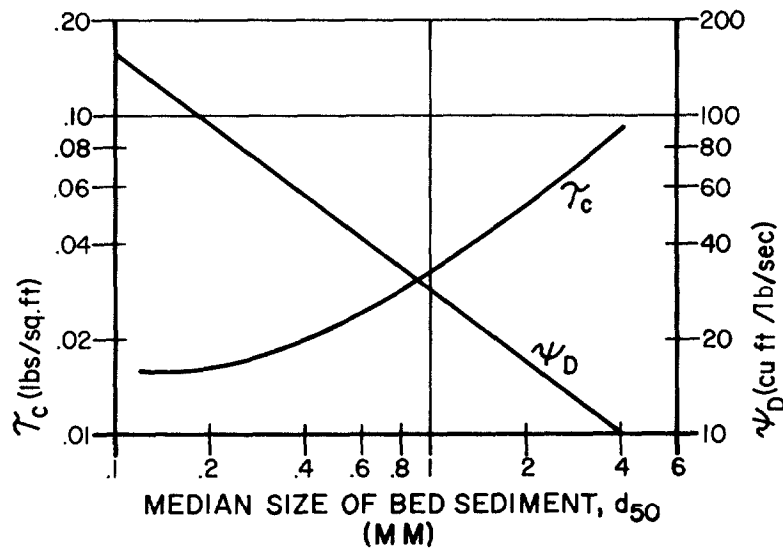


FIGURE IV-40  $\psi$  AND  $\tau_c$  FOR DUBOYS RELATIONSHIP AS FUNCTIONS OF MEDIAN SIZE OF BED SEDIMENT (TASK COMMITTEE ON PREPARATION OF SEDIMENTATION MANUAL, 1971)

Once  $d_{50}$  is estimated, then  $\psi$  and  $\tau_c$  can easily be evaluated, leaving only  $\tau_0$  to compute. A summary of hydraulic radii (the ratio of cross-sectional area to wetted perimeter) for different channel geometries is shown in Figure IV-41. For very wide, shallow channels, the hydraulic radius approximately equals the depth of flow. Many river cross-sections can be approximated by a parabolic section. To calculate "c" in the relationship for hydraulic radius of a parabolic section, refer to Table IV-35.

If the bed slope is unknown it can be estimated by using a topographic map and finding contour lines approximately five hundred feet above and below the point on the river where the measurement is to be made. Dividing this elevation difference by the horizontal distance over which the difference is measured, produces the slope.

TABLE IV-34  
 SEDIMENT GRADE SCALE (TASK COMMITTEE ON PREPARATION  
 OF SEDIMENTATION MANUAL, 1971)

Class Name	Size Range			Approximate Sieve Mesh Openings Per Inch	
	Millimeters	Microns	Inches	Tyler	United States Standard
Very large boulder		4096-2048			
Large boulders		2048-1024			
Medium boulders		1024-512			
Small boulders		512-256			
Large cobbles		246-128			
Small cobbles		128-64			
Very coarse gravel		64-32			
Coarse gravel		32-16			
Medium gravel		16-8		2-1/2	
Fine gravel		8-4		5	5
Very fine gravel		4-2		9	10
Very coarse sand	2-1	2,000-1,000	2000-1000	16	18
Coarse sand	1-1/2	1,000-0.500	1000-500	32	35
Medium sand	1/2-1/4	0.500-0.250	500-250	60	60
Fine sand	1/4-1/8	0.250-0.125	250-125	115	120
Very fine sand	1/8-1/16	0.125-0.062	125-62	250	230
Coarse silt	1/16-1/32	0.062-0.031	62-31		
Medium silt	1/32-1/64	0.031-0.016	31-16		
Fine silt	1/64-1/128	0.016-0.008	16-8		
Very fine silt	1/128-1/256	0.008-0.004	8-4		
Coarse clay	1/256-1/512	0.004-0.0020	4-2		
Medium clay	1/512-1/1024	0.0020-0.0010	2-1		
Fine clay	1/1024-1/2048	0.0010-0.0005	1-0.5		
Very fine clay	1/2048-1/4096	0.0005-0.00024	0.5-0.24		

TABLE IV-35  
COMPUTING D/T FOR DETERMINING THE HYDRAULIC RADIUS OF  
A PARABOLIC SECTION (FROM KING, 1954)

$\frac{D}{T}^*$	.00	.01	.02	.03	.04	.05	.06	.07	.08	.09
.0	.667	.667	.666	.665	.664	.662	.660	.658	.656	.653
.1	.650	.646	.643	.639	.635	.631	.626	.622	.617	.612
.2	.607	.602	.597	.592	.586	.581	.575	.570	.564	.559
.3	.554	.548	.543	.537	.532	.526	.521	.516	.510	.505
.4	.500	.495	.490	.485	.480	.475	.470	.465	.460	.455
.5	.451	.446	.442	.437	.433	.428	.424	.420	.416	.412
.6	.408	.404	.400	.396	.392	.388	.385	.381	.377	.374
.7	.370	.367	.364	.360	.357	.354	.351	.348	.344	.341
.8	.338	.335	.333	.330	.327	.324	.321	.319	.316	.313
.9	.311	.308	.306	.303	.301	.298	.296	.294	.291	.289

$\frac{*D}{T} = c$

Adequate methods that are within the scope of this report and which would provide a straightforward estimation of suspended sediment discharge presently do not exist. Most relationships require a known reference level concentration at some depth within the river to predict the concentration at another depth (Morris and Wiggert, 1972). To determine the suspended sediment load, then, a summation of contributions at each depth must be made. Since these formulas apply to one grain size this procedure should be repeated for all grain sizes present. Einstein (Graf, 1971) has developed a method for computing suspended sediment discharge that does not require knowledge of a reference concentration but it is an advanced approach. For this report the contribution of the suspended load will be estimated from the bed material load by the relationship given in Table IV-36. The relationship in Table IV-36 is valid for graded channels (by graded is meant that the slope is stable over time, being neither steepened nor flattened by flow or other influence). Once the width to depth ratio for the stream in question is determined, the suspended load can then be approximated after first computing the bed material load, and then using Table IV-36.

Once the suspended load discharge is estimated the average concentrations at a section can be computed by:

$$C_{SS} = \frac{G_{SS}}{Q} 1.6 \times 10^4 \quad (IV-99a)$$

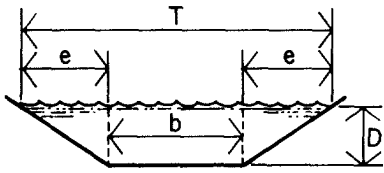
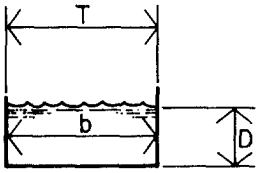
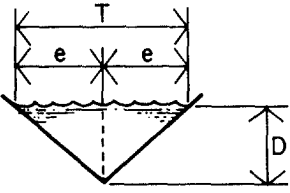
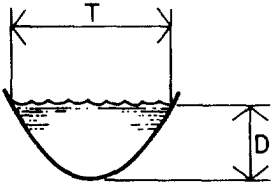
CHANNEL SLOPE	HYDRAULIC RADIUS
 <p>Trapezoidal</p>	$\frac{(1 + zx) D}{1 + 2x \sqrt{1 + x^2}}, x = D/b, z = e/D$
 <p>Rectangular</p>	$\frac{bD}{b + 2D}$
 <p>Triangular</p>	$\frac{zD}{2\sqrt{1 + z^2}} \quad z = e/D$
 <p>Parabolic</p>	$cD \quad (\text{for } c, \text{ see Table IV-35})$

FIGURE IV-41 HYDRAULIC RADIUS FOR DIFFERENT CHANNEL SHAPES (FROM KING, 1954)

TABLE IV-36  
RELATIONSHIP BETWEEN WIDTH TO DEPTH RATIO OF A GRADED STREAM AND  
THE SUSPENDED AND BED LOAD DISCHARGE (AFTER FENWICK, 1969)

Suspended Load % of Total Bed Material	Bed Load % of Total Bed Material Load	Width-Depth Ratio
85-100	0-15	7
65-85	15-35	7-25
30-65	35-70	25

or

$$C_{SS} = \frac{g_{SS}}{q} 1.6 \times 10^4 \quad (IV-99b)$$

where

$C_{SS}$  = average suspended solids concentration, mg/l

$G_{SS}$  = suspended solids discharge, lb/sec

$Q$  = flow rate, cfs

$g_{SS}$  = suspended solids discharge per unit width, lb/sec/ft

$q$  = flow rate per unit width, cfs/ft.

The procedures discussed in this section can be summarized as follows:

1. Determine the bed load discharge  $g_b$  (lb/sec/ft) using Equation IV-98. The required input data are channel slope, hydraulic radius (see Figure IV-41), and the median sediment size,  $d_{50}$ . Once  $d_{50}$  has been estimated the unknown parameters  $\tau_c$  and  $\psi$  can be found from Figure IV-40.
2. Multiply  $g_b$  by the river width to find the total bed load discharge.
3. Determine the width/depth ratio.
4. Use Table IV-36 to determine the suspended load.
5. To determine the suspended sediment concentration use Equation IV-99.
6. Compare the suspended sediment concentration against the data in Table IV-33 to find out if a problem potentially exists.
7. The total bed material load is sum of the total bed load (step 2) and the total suspended load (step 4).

The user may be primarily concerned with the total bed material load rather than either bed load or suspended load individually. Total bed material load can be directly calculated using a number of predictive formulas. The method of Yang (1976) based on unit stream power is presented here. Yang's method has been verified for the following parameter ranges:

Median bed size:	from 0.16 mm to 1.0 mm
Channel depth:	from 0.2 ft to 49.9 ft
Water temperature:	from <b>0°C</b> to <b>29.4°C</b>
Stream velocity:	from 1.23 fps to 7.82 fps
Flow rate:	from 2.7 cfs to 470,000 cfs
Slope:	from 0.0000428 to 0.00188
Total sediment concentration (excluding wash load):	from 2.8 ppm to 2,440 ppm.

The input data are the same as for the DuBoys' method, with the addition of water temperature. The predictive formula, however, is considerably more complicated,

so the method has been programmed on a hand held calculator and the program is included. The predictive expression is:

$$\log C_t = 5.435 - 0.286 \log \frac{wD}{\nu} - 0.457 \log \frac{U_*}{w} + (1.799 - 0.409 \log \frac{wD}{\nu} - 0.314 \log \frac{U_*}{w}) \log \left( \frac{Us}{w} - \frac{U_{cr} S}{w} \right) \quad (IV-100)$$

where

- $C_t$  = total sediment concentration in parts per million by weight
- $D$  = median sieve diameter
- $s$  = water surface slope or energy slope
- $U_*$  = shear velocity
- $u$  = average water velocity
- $U_{cr}$  = critical average water velocity at incipient motion
- $\nu$  = kinematic viscosity
- $w$  = terminal fall velocity.

The term  $\frac{U_{cr}}{w}$  can be calculated as:

$$\frac{U_{cr}}{w} = \frac{2.5}{\log\left(\frac{U_* D}{\nu}\right) - 0.06} + 0.66 \quad \text{when } 1.2 < \frac{U_* D}{\nu} < 70 \quad (IV-101)$$

and

$$\frac{U_{cr}}{w} = 2.05 \quad \text{when } 70 \leq \frac{U_* D}{\nu} \quad (IV-102)$$

Figure IV-42 shows the required user instructions to execute the program on a TI-59. Figure IV-43 contains the program listing and a sample input/output. This program was written by Colorado State University (1979).

#### EXAMPLE IV-17

##### Estimation of Bed Material Load

Table IV-37 shows characteristics of the Colorado River at Taylor's Ferry, California, and of the Niobrara River near Cody, Nebraska. Suppose one desires to calculate the bed load for the Colorado River at this location for flow ranges of 8-35 cfs/ft. The following data will be used:

- $d_{50}$  = 0.33 mm
- $\gamma$  = 62.4 lb/ft<sup>3</sup>, at 60°F
- $S$  = 0.000217 ft/ft

**PROGRAM DESCRIPTION**

**Program:** Yang's Sediment Transport Equation

**USER INSTRUCTIONS**

STEP	PROCEDURE	ENTER	PRESS	DISPLAY
1	Enter kinematic viscosity, $\nu \left( \frac{ft^2}{sec} \right)$	$\nu$	A	$\nu$
2	Enter slope $S_0$ (ft/ft)	$S_0$	B	$S_0$
3	Enter median sediment diameter, $d_s$ (ft)	$d_s$	C	$d_s$
4	Enter flow velocity, $U \left( \frac{ft}{sec} \right)$	U	D	U
5	Enter flow depth, Y (ft)	Y	E	Y
6	Compute sediment concentration (ppm)		2nd A'	$C_t$
7	To input new data, repeat steps 1 through 6.			

FIGURE IV-42 USER INSTRUCTIONS FOR YANG'S SEDIMENT TRANSPORT EQUATION,

Using Figure IV-40 one finds:

$$\psi = 64$$

$$\tau_c = 0.019$$

All that remains is the computation of the hydraulic radius. Since the width is much greater than the depth, assume  $R_H = D$ :

$$R_H = \begin{cases} 4 \text{ ft at } q = 8 \text{ cfs/ft} \\ 12 \text{ ft at } q = 35 \text{ cfs/ft.} \end{cases}$$

Using Equation IV-98 it is found that the bed load is:

$$g_b = \begin{cases} 0.12 \text{ lb/sec/ft at } q = 8 \text{ cfs/ft} \\ 1.5 \text{ lb/sec/ft at } q = 35 \text{ cfs/ft.} \end{cases}$$

The actual bed material load observed at Taylor's Ferry has been compared with the DuBoys prediction for a range of flow rates (Task Committee on Preparation of Sedimentation Manual, 1971). This relationship is shown in Figure IV-44 (The

Program Listing:

```

000 76 LBL
001 77 GE
002 93 .
003 00 0
004 00 0
005 00 0
006 02 2
007 32 X:T
008 43 RCL
009 02 02
010 77 GE
011 88 DMS
012 33 X2
013 65 x
014 02 2
015 93 .
016 09 9
017 05 5
018 01 1
019 07 7
020 55 +
021 43 RCL
022 06 06
023 95 =
024 42 STD
025 00 00
026 92 RTN
027 76 LBL
028 88 DMS
029 53 (
030 53 (
031 53 (
032 43 RCL
033 02 02
034 45 YX
035 03 3
036 65 x
037 03 3
038 06 6
039 93 .
040 00 0
041 06 6
042 04 4
043 85 +
044 03 3
045 06 6
046 65 x
047 43 RCL
048 06 06
049 33 X2
050 54 )
051 34 FX
052 75 -
053 06 6
054 65 x
055 43 RCL
056 06 06
057 54 )
058 55 +
059 43 RCL
060 02 02
061 54 )
062 42 STD
063 00 00
064 92 RTN
065 76 LBL
066 11 A
067 43 STD
068 06 06
069 22 INV
070 52 EE
071 92 RTN
072 76 LBL
073 12 6
074 42 STD
075 01 01
076 92 RTN
077 76 LBL
078 13 C
079 42 STD
080 02 02
081 92 RTN
082 76 LBL
083 14 D
084 42 STD
085 03 03
086 92 RTN
087 76 LBL
088 15 E
089 42 STD
090 04 04
091 92 RTN
092 76 LBL
093 16 A'
094 71 SBR
095 77 GE
096 53 (
097 53 (
098 03 3
099 02 2
100 93 .
101 02 2
102 65 x
103 43 RCL
104 04 04
105 65 x
106 43 RCL
107 01 01
108 54 )
109 34 FX
110 42 STD
111 05 05
112 65 x
113 43 RCL
114 02 02
115 55 +
116 43 RCL
117 06 06
118 54 )
119 42 STD
120 07 07
121 32 X:T
122 07 7
123 00 0
124 32 X:T
125 77 GE
126 89 π
127 53 (
128 53 (
129 02 2
130 93 .
131 05 5
132 55 +
133 53 (
134 43 RCL
135 07 07
136 28 LOG
137 75 -
138 93 .
139 00 0
140 06 6
141 54 )
142 54 )
143 85 +
144 93 .
145 06 6
146 06 6
147 54 )
148 42 STD
149 08 08
150 61 GTD
151 70 RAD
152 76 LBL
153 89 π
154 02 2
155 93 .
156 00 0
157 05 5
158 42 STD
159 08 08
160 76 LBL
161 70 RAD
162 53 (
163 53 (
164 05 5
165 93 .
166 04 4
167 03 3
168 05 5
169 75 -
170 93 .
171 02 2
172 08 8
173 06 6
174 65 x
175 53 (
176 43 RCL
177 00 00
178 65 x
179 43 RCL
180 02 02
181 55 +
182 43 RCL
183 06 06
184 54 )
185 28 LOG
186 42 STD
187 09 09
188 75 -
189 93 .
190 04 4
191 05 5
192 07 7
193 65 x
194 53 (
195 43 RCL
196 05 05
197 55 +
198 43 RCL
199 00 00
200 54 )

```

FIGURE IV-43 PROGRAM LISTING AND SAMPLE INPUT/OUTPUT FOR YANG'S SEDIMENT TRANSPORT EQUATION



Program Listing (continued):

```
201 28 LOG      228 10 10
202 42 STD      229 54 )
203 10 10      230 65 x
204 54 )       231 53 (
205 85 +       232 43 RCL
206 53 (       233 03 03
207 53 (       234 65 x
208 01 1       235 43 RCL
209 93 .       236 01 01
210 07 7       237 55 +
211 09 9       238 43 RCL
212 09 9       239 00 00
213 75 -       240 75 -
214 93 .       241 43 RCL
215 04 4       242 08 08
216 00 0       243 65 x
217 09 9       244 43 RCL
218 65 x       245 01 01
219 43 RCL     246 54 )
220 09 09     247 28 LOG
221 75 -       248 54 )
222 93 .       249 54 )
223 03 3       250 22 INV
224 01 1       251 28 LOG
225 04 4       252 98 ADV
226 65 x       253 99 PRT
227 43 RCL     254 92 RTN
```

Sample Input:

```
v = .0000111
So = .0017
ds = .000623
U = 2.89
Y = 0.51
```

Output:

```
Ct = 2117.066395
```

FIGURE IV-43 (CONTINUED)

DuBoys curve in Figure IV-44 does not quite match the calculations in this example because slightly different data were used). Observe that the DuBoys relationship overpredicts the bed material load for nearly all flow ranges. This pattern is repeated for the Niobrara River (Figure IV-45). This suggests that the bed material load estimated by the DuBoys relationship will in general exceed the actual bed material load. This is further substantiated by other work (Stall et al., 1958). The more accurate predictions of bed material load occur under high flow conditions, which is generally when the prediction of bed material load is most important.

To estimate the suspended load contribution first calculate the width-depth ratio:

$$W/D = \begin{cases} 88 & \text{at } q = 8 \text{ cfs/ft} \\ 29 & \text{at } q = 35 \text{ cfs/ft.} \end{cases}$$

TABLE IV-37

CHARACTERISTICS OF THE COLORADO AND NIobrARA RIVERS  
(TASK COMMITTEE ON PREPARATION OF SEDIMENTATION MANUAL, 1971)

Data	Stream	
	Colorado River (Taylor's Ferry)	Niobrara River (Cody, Neb.)
Depth range, ft	4-12	0.7-1.3
Range in $q$ , in cubic feet per second per foot of width	8-35	1.7-5
Mean width, in feet	350	110
Slope, in feet per foot		
Minimum value	0.000147	0.00116
Maximum value	0.000333	0.00126
Value used in calculations	0.000217	0.00129
Water temperature, in degrees Fahrenheit		
Minimum value	48	33
Maximum value	81	86
Value used in calculations	60	60
Geometric mean*sediment size, in millimeters	0.320	0.283
$d_{35}$ , in millimeters	0.287	0.233
$d_{50}$ , in millimeters	0.330	0.277
$d_{65}$ , in millimeters	0.378	0.335
$d_{90}$ , in millimeters	0.530	0.530
Mean size, $d_m$ , in millimeters	0.396	0.342

\*The geometric mean of a set of values is  $\left(\prod_{i=1}^n x_i\right)^{1/n}$ . Thus the geometric mean of the values 1, 2, 3, and 4 is  $(1 \times 2 \times 3 \times 4)^{1/4} = 2.213$ . Compare with arithmetic mean of 2.5.

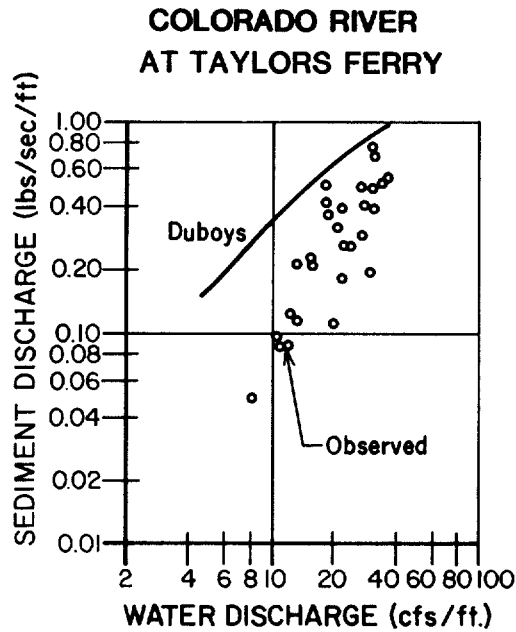


FIGURE IV-44

SEDIMENT DISCHARGE AS A FUNCTION OF WATER DISCHARGE FOR THE COLORADO RIVER AT TAYLOR'S FERRY (TASK COMMITTEE ON PREPARATION OF SEDIMENTATION MANUAL, 1971)

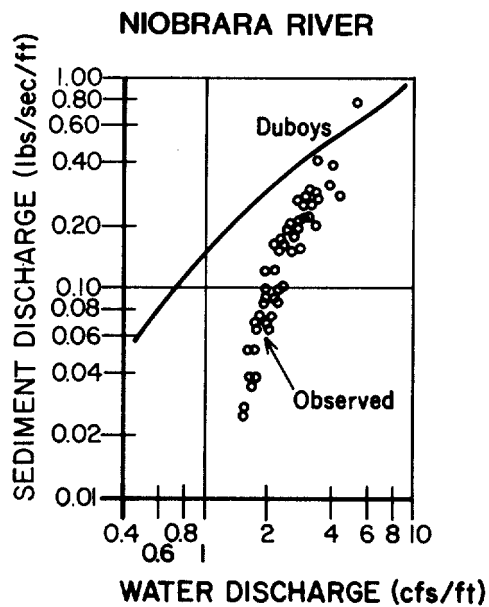


FIGURE IV-45

SEDIMENT DISCHARGE AS A FUNCTION OF WATER DISCHARGE FOR THE NIOBRARA RIVER AT CODY, NEBRASKA (TASK COMMITTEE ON PREPARATION OF SEDIMENTATION MANUAL, 1971)

In both cases  $W/D > 25$ . Referring to Table IV-36, the suspended load should be between 30 and 65 percent of the bed material load. Assume it is on the lower end of the scale, about 40%. Then the suspended load is:

$$g_{ss} = \begin{cases} 0.08 \text{ lb/sec/ft at } q = 8 \text{ cfs/ft} \\ 1.0 \text{ lb/sec/ft at } q = 35 \text{ cfs/ft} \end{cases}$$

or

$$C_{ss} = \begin{cases} 160 \text{ mg/l at } q = 8 \text{ cfs/ft} \\ 440 \text{ mg/l at } q = 35 \text{ cfs/ft} \end{cases}$$

from Equation IV-99. These concentrations indicate that suspended sediment concentrations are excessively high throughout the range of flows normally encountered at Taylor's Ferry. Data on suspended sediment concentrations have been gathered at Taylor's Ferry (U. S. Bureau of Reclamation, 1958). The averages of 30 measurements taken there are as follows:

$$Q = 7350 \text{ cfs (or } q = 21 \text{ cfs/ft)}$$

$$C_{ss} = 132 \text{ mg/l}$$

**Observed** range of suspended sediment concentration: 40-277 mg/l.

The method of Yang predicts total concentrations of 40 to 80 mg/l, which is within but toward the lower end of the observed data. The method of DuBois predicts concentration between 160 and 440 mg/l which is toward, and beyond, the upper end of observation. These results illustrate the possible variability of predictions between different approaches, and are not necessarily atypical.

----- END OF EXAMPLE IV-17 -----

#### 4.9 TOXIC SUBSTANCES

##### 4.9.1 Methods of Entry of Toxic Pollutants into Rivers

Although Chapter 3 discussed both point and nonpoint sources of pollutants, the major pollutant source categories are summarized in Table IV-38 to indicate how these scenarios differentially govern a pollutant's fate. For simplicity, fate is analyzed in terms of volatilization and sorption since these processes are important for a wide number of toxic organic chemicals. These processes govern whether a pollutant remains in the water column and whether the pollutant is transported as solute or sorbate. If the effects of these processes are known, even if only qualitatively, then the influence of processes such as photolysis and biodegradation can be better predicted. For example, if a pollutant is sorbed to suspended and bedded sediments, it is more protected from photolytic reactions than when it is dissolved in the water column.

A common mode of pollutant entry is by a continuous discharge, either from a municipal or industrial source. As mixing of the effluent and river water occurs,

TABLE IV-38

METHODS OF INTRODUCTION OF TOXIC ORGANIC COMPOUNDS INTO RIVERS,  
AND FATE IN TERMS OF VOLATILIZATION AND SORPTION

Pathway	Fate
Continuous input	<ul style="list-style-type: none"> <li>- solute transported and volatilized</li> <li>  sorbate transported with suspended solids and with bed load</li> <li>  sorbed to immobile sediments</li> <li>- buried by sorption and net deposition</li> </ul>
Cessation of continuous input	<ul style="list-style-type: none"> <li>- desorbed from immobile sediments</li> <li>- solute transported and volatilized</li> <li>  resorbed to suspended sediments</li> <li>- contaminated sediments resuspended</li> <li>- portion remains buried</li> </ul>
Washoff from land application	<ul style="list-style-type: none"> <li>- transport of a major portion of pollutant may be governed by first large storm event</li> <li>- transported as solute and sorbate</li> <li>- settles and accumulates on bed</li> <li>- buried</li> <li>  subsequently resuspended</li> </ul>
Accidental releases (e.g. spills)	<ul style="list-style-type: none"> <li>- If s.g. &gt;1, pollutant settles on streambed</li> <li>- Volatilization may be unimportant               <ul style="list-style-type: none"> <li>--reentrained back into stream and sorbed on suspended solids</li> <li>--pollutant can be slowly transported along bottom</li> <li>--diffused into bedded sediments</li> </ul> </li> <li>- If s.g. &lt;1, pollutant tends to remain on surface and be transported at speed of surface current               <ul style="list-style-type: none"> <li>--volatilization can be important</li> <li>--gradually dissolved and sorbed</li> <li>--dispersion attenuates peak concentrations</li> <li>--wind speed and direction influential</li> </ul> </li> </ul>
Leaching	<p>slow movement (years) of solute from dump or disposal site to stream</p> <p>continues for years after cleanup of dump</p>

partitioning begins. The sorbate is transported with the suspended sediments, and can interact with the bed load and immobile bedded sediments. Depending on the rate of exchange of the sorbate with the bedded sediments and on the net sediment deposition rate, some of the sorbate can gradually become buried in the bedded sediments.

If a continuous input ceases, the water column initially tends to clean itself of the pollutant as uncontaminated upstream water replaces contaminated river water downstream from the former source of pollution. However, pollutant from the contaminated bottom sediments can desorb back into the water column at low concentrations and the river bed becomes an internal source of pollutant. The resorption period can last a long period of time, depending on the amount of pollutant contained in the bottom sediments. Section 4.9.3.4 discusses this phenomenon in detail.

Periodic nonpoint sources, such as washoff after an agricultural application, is another pathway of pollutant entry into rivers. The mass of pollutant transported tends to be governed by the timing of the first storm event following application together with the degradation and volatilization processes operative during the interim period.

Accidental releases of pollutants, even through infrequent events, can be important. Exceptionally high concentrations of pollutants can result from spills and the total mass supplied almost instantaneously can be the equivalent of a continuous release lasting for many days. For example, in 1973 a chloroform spill on the Mississippi River resulted in about 800,000 kg (1,750,000 lbs) of chloroform being released over a period of several hours (Thibodeaux, 1977). Based on the background concentration of chloroform in the river (5 ppb), the release was equivalent to a continuous supply of chloroform released at background rates for a period of 300 days.

Many chemicals in their pure or nearly pure form have specific gravities significantly different from unity. Because of this, and their often limited volatility in water, it is a mistake to believe that all spilled pollutants travel with the speed of the river, have infinite dissolution capability, and disperse accordingly. High density pollutants can sink to the river bed and become slowly reentrained back into the water column while simultaneously diffusing and sorbing into the bedded sediments. Depending on the rate of dissolution of the spilled pollutant, as well as the significance of the sorption and diffusion processes, the spilled pollutant may remain in the riverine system for either an extended or brief period of time.

In contrast to high density pollutants, pollutants with specific gravities less than unity tend to at least partially remain on or near the water's surface while undergoing dissolution. For these pollutants, volatilization and photolysis can be extremely important. As the pollutant is dissolved in the water column and moves downstream, dispersion becomes important in attenuating the peak concentration.

Pollutants which leach from a surface or subsurface disposal site may eventually

reach a river. Although the mass input rate may be low, the source can be continuous and last for years, even after cleanup of the site.

The sequence of instream events following the initiation and then the cessation of point sources of toxicants further illustrates the role that sorption plays in governing fate of sorbates. Figure IV-46 illustrates the two situations. Figure IV-46a shows the pollutant distributions below a point source at two distinct times ( $t_1$  and  $t_2$  where  $t_2 > t_1$ ) following initiation of the point source. As the toxicant is discharged the water column concentration (the sum of the dissolved and sorbed phases) abruptly increases at the mixing location. As the pollutant travels downstream, the sorbate tends to partially desorb onto the formerly uncontaminated bottom sediments. Additionally there may be a net exchange between the bedded sediments and water column sediments, even if there is no net deposition. As a result of these processes, the water column concentration tends to decrease in the downstream direction. It may take a period of time greater than  $t_1$  for the effects of the discharge to reach a distance  $D^*$ . Depending on the distance, and on the rate of accumulation of the toxicant in the bottom sediments, as well as on other factors, the time required for the water column concentration to be noticeably elevated at  $D^*$  could greatly exceed the travel time of the river over the distance.

After the discharge of the toxicant has continued for a period of time, the net exchange with the bedded sediment may diminish, so that the toxicant concentration becomes constant over some distance both in the water column and in the sediments. This situation is illustrated by the solid curve in Figure IV-46b. Suppose at this time the input of the pollutant ceases. The water column concentration just below the point source tends to abruptly approach zero. As this happens, resorption of the toxicant from the bedded sediment can occur, tending to replenish pollutant levels in the water column, but to a lower level. Gradually, the pollutant can be desorbed from the bedded sediments at a given location so that the bottom sediments are naturally cleansed, from the upstream to the downstream direction. This process can take many years and low levels of pollutant in the water column can be detected throughout this period. More discussion of this phenomenon is provided later in Section 4.9.3 and Example IV-18. Most of the pathways for river contamination presented in Table IV-38 have been programmed on microcomputers (Mills et al. , 1985).

#### 4.9.2 Vertical Distribution of Sorbate within Rivers

Even though most of the analytical tools presented later in Section 4.9.3 assume that, for simplicity, suspended solids concentrations are uniformly distributed throughout the water column, in reality this is not true. The vertical distribution of solids depends both on particle and river characteristics. Heavier particles (those with the greater settling velocities) are transported closer to the stream bottom while the lighter particles are more uniformly distributed. This observation is significant because pollutants which sorb to the particles also exhibit a non-

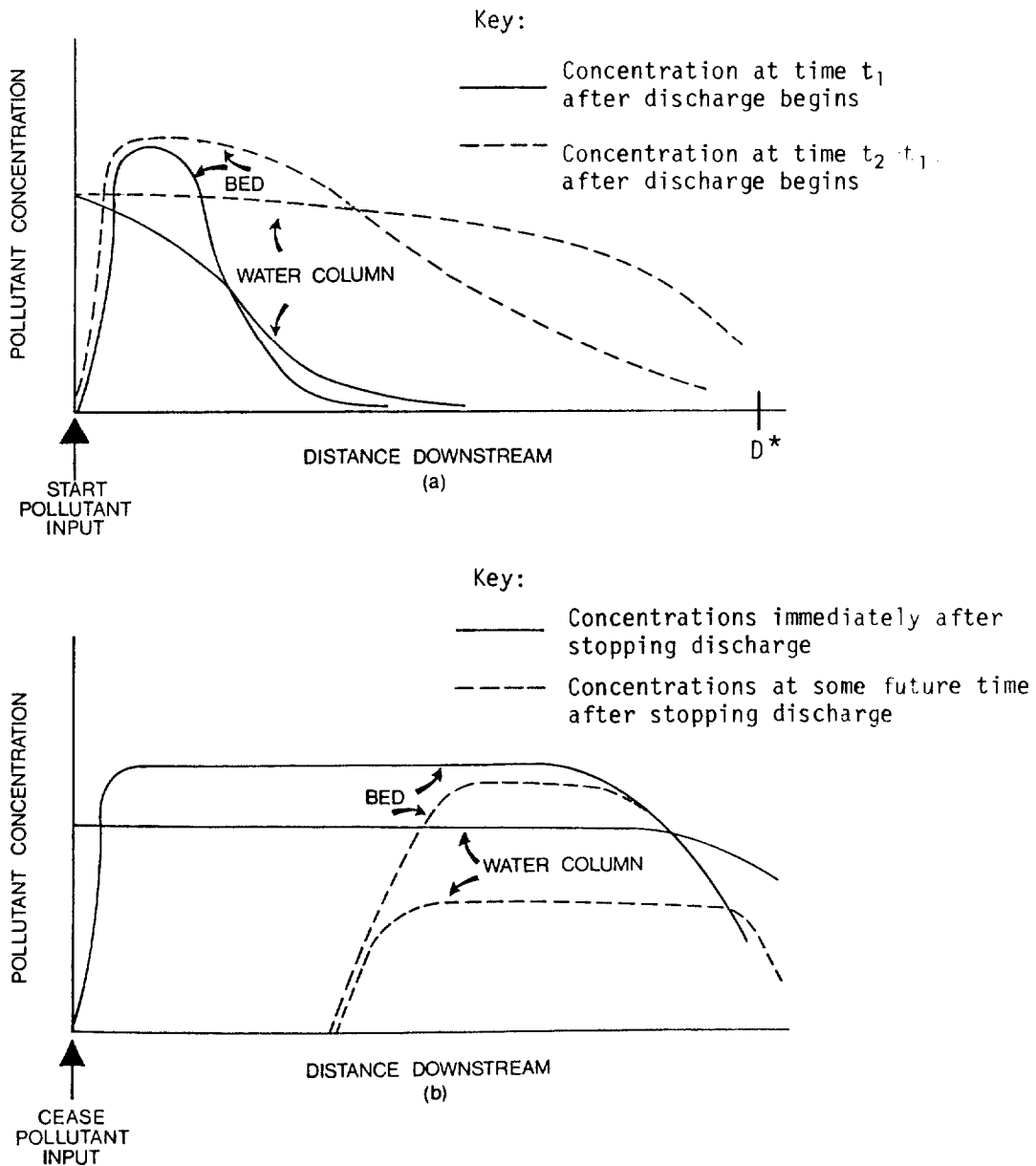


FIGURE IV-46 TOXICANT CONCENTRATIONS FOLLOWING INITIATION AND CESSATION OF POINT SOURCE.

uniform vertical distribution. Pollutants which do not sorb tend to become uniformly distributed vertically, regardless of the sediment distribution. By understanding this, the user can better interpret instream pollutant data, particularly if the pollutant tends to reside as sorbate. It may be that a single pollutant sample is not sufficient to accurately characterize the pollutant distribution, and in fact could be misleading in terms of the total burden of the pollutant carried within the water column. Depth integrated samples might be necessary to gain an accurate knowledge of the pollutant's distribution.



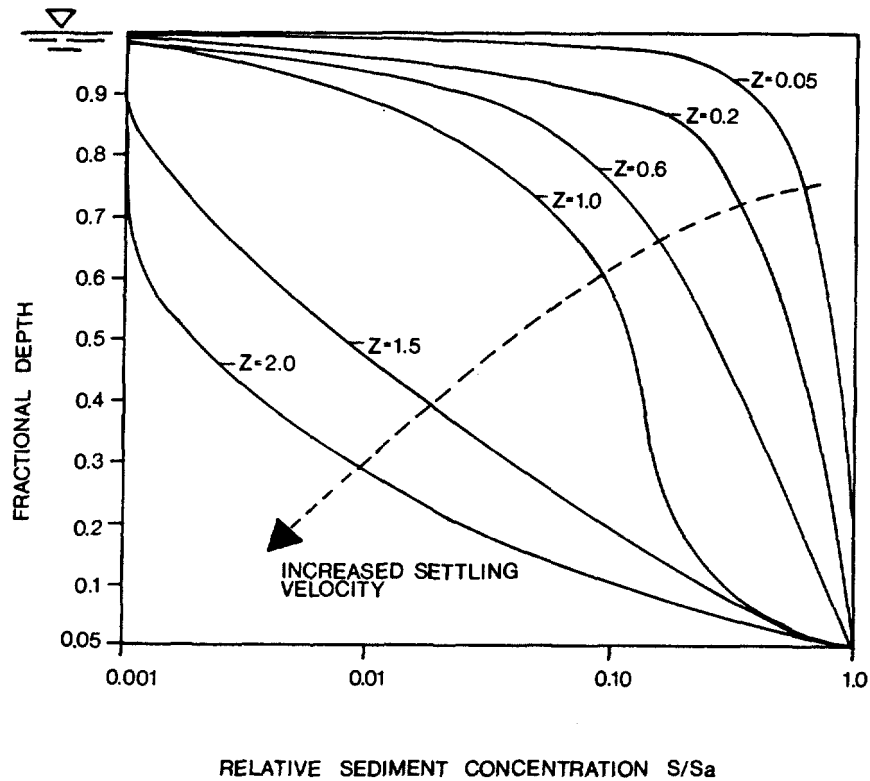


FIGURE IV-47 VERTICAL EQUILIBRIUM DISTRIBUTION OF SUSPENDED SOLIDS IN A RIVER

Figure IV-47 shows the vertical distribution of suspended solids in an equilibrium condition. The parameter shown in the figure is defined:

$$z = \frac{V_s}{\kappa U^*} \quad (IV-103)$$

where

- $V_s$  = settling velocity of suspended solids
- $\kappa$  = von Karman's constant (~0.4)
- $U^*$  = shear velocity =  $(g R_H S)^{0.5}$ , ft/sec
- $g$  = acceleration due to gravity, 32.2 ft/sec<sup>2</sup>
- $R_H$  = hydraulic radius of river, ft
- $S$  = slope, dimensionless.

Very small values of  $z$  represent clay-sized particles, while larger values represent first silt, and then sand. Figure IV-47 illustrates that clay particles tend to be uniformly distributed vertically (50 percent in the top half of the water column). About 75 percent of silt and over 95 percent of the sand particles (typically) reside in the bottom half of the water column. This suggests that in rivers where the suspended sediments are silt and sand, the sorbed pollutant distribution will be

vertically skewed. If the suspended material is predominantly clay the sorbed pollutant distribution will be uniform. Since pollutants tend to sorb to sand to a lesser degree than to silt and clay, the vertical distribution of sorbed pollutant will not be as skewed as the suspended sediment distribution.

Figures IV-48 through IV-49 show the fraction of pollutant present as solute ( $C/C_t$ ) versus relative depth for families of  $z$  values and  $K_p S_a$  values.  $S_a$  is the suspended sediment concentration a small distance above the bottom. For  $K_p S_a$  values less than 0.1, the sorbate concentration is generally negligible compared to the solute concentration regardless of the depth or the nature of the suspended material. For larger  $K_p S_a$  values, the sorbate level can be important, depending of the nature of the suspended material. For extremely large  $K_p S_a$  values, the sorbate concentration will greatly exceed the solute concentration, at least near the river bed.

Based on the hydraulic characteristics of the river, characteristics of the material being transported in suspension, and the partition coefficient of the pollutant, predictions can be made of the pollutant's distribution in the water column. To use Figures IV-48 and IV-49 requires knowledge of  $S_a$ , the suspended solids concentration at a distance  $n = a$  above the bottom (where typically  $a = 0.05$ , or 5 percent of the river's depth). The equilibrium expression for suspended sediments, which is found in numerous sediment transport texts (e.g. Graf, 1971) can be rearranged to express  $S_a$  as:

$$S_a = S(n) \left( \frac{1-n}{n} \frac{a}{1-a} \right)^{-z} \quad (IV-104)$$

where

$n$  = relative depth above bottom.

To use this equation the suspended solids concentration must be known at one depth in the water column. Typically, a depth averaged suspended solids concentration might be readily available. Under these circumstances  $S_a$  can be estimated as:

$$S_a = \frac{S(1-a) \left( \frac{1-a}{n} \right)^z}{\int_a^1 \left( \frac{1-n}{n} \right)^z dn} \quad (IV-105)$$

where

$s$  = depth average suspended sediment concentration.

The denominator of Equation IV-105 can be integrated numerically by one of many available solution techniques (e.g. see Carnahan et al., 1969). For the case

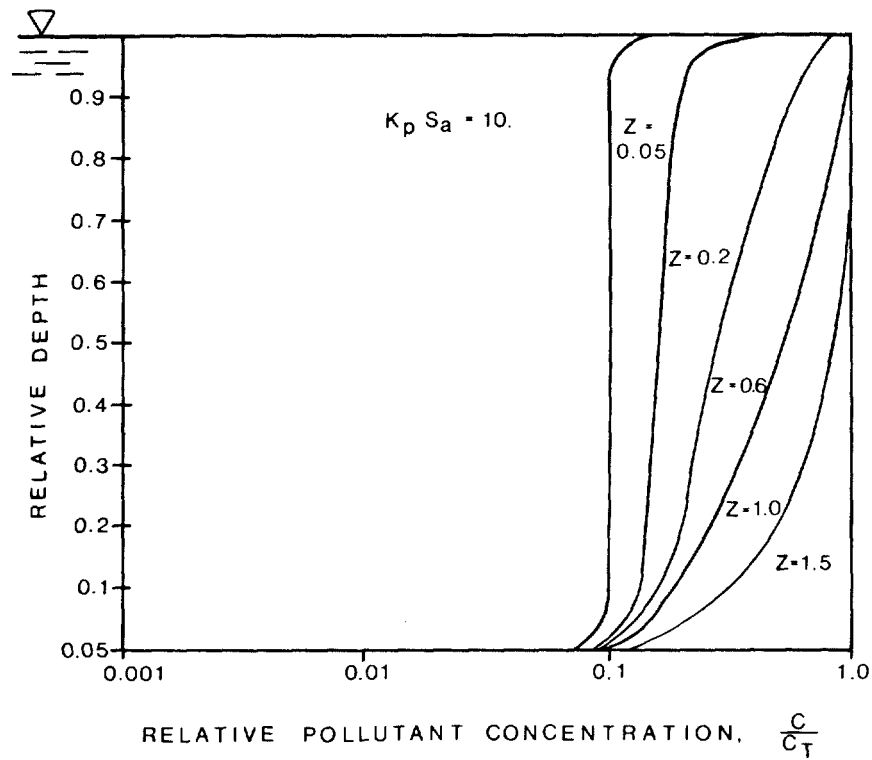


FIGURE IV-48 VERTICAL DISTRIBUTION OF RELATIVE SOLUTE CONCENTRATION,  $K_p S_A = 10$ .

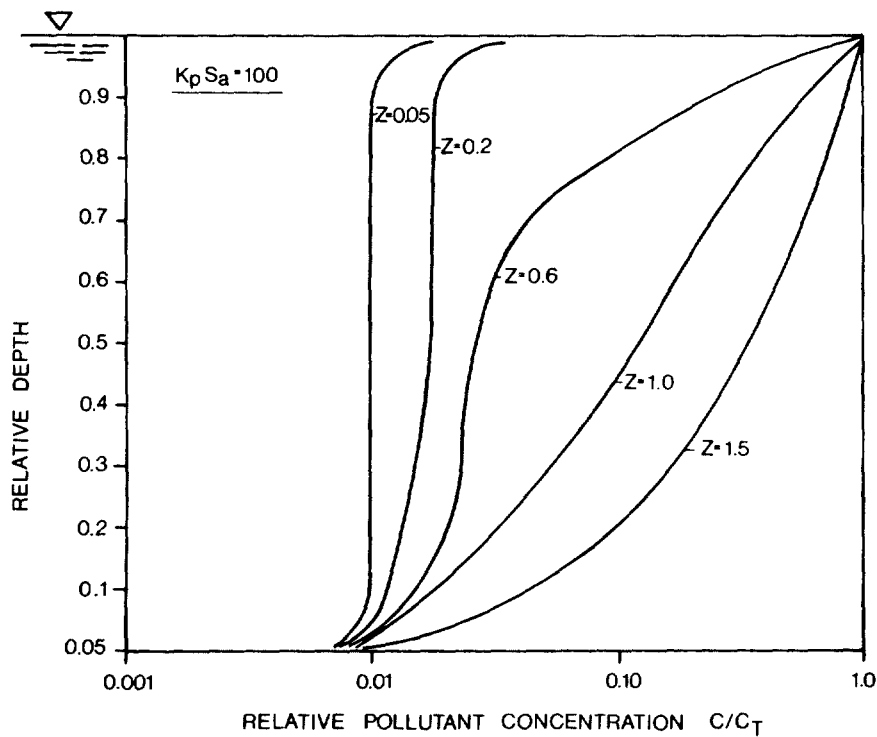


FIGURE IV-49 VERTICAL DISTRIBUTION OF RELATIVE SOLUTE CONCENTRATION,  $K_p S_A = 100$ .

when  $a = 0.05$  the relationship between  $S_a$  and  $S$  is given below:

$$\begin{aligned}
 z = 0 &\longrightarrow S_a = S \\
 z = 0.2 &\longrightarrow S_a = 1.8 S \\
 z = 0.6 &\longrightarrow S_a = 4.4 S \\
 z = 1.0 &\longrightarrow S_a = 8.2 S \\
 z = 2.0 &\longrightarrow S_a = 17 S \\
 z = 5.0 &\longrightarrow S_a = 20 S
 \end{aligned}
 \tag{IV-106}$$

Based on a knowledge of  $S$ ,  $S_a$  can be estimated from Equation IV-106, and in turn can be used in Figures IV-48 and IV-49.

Typically there is a segregation of particle sizes found in suspension compared with these found in the bed load, and in the immobile bed materials. Based on these differences, the following can be hypothesized:

$$X_s > X_{bl} > X_{im}$$

where

$X_s$  = sorbed pollutant concentration on suspended materials, mass pollutant/mass sediment

$X_{bl}$  = sorbed pollutant concentration on bed load, mass pollutant/mass sediment

$X_{im}$  = sorbed pollutant concentration on immovable sediment, mass pollutant/mass sediment.

Investigations carried out by Miles (1976) appear to support this relationship. Miles collected insecticide residues on stream sediments and in the water column. Results of the DOT analysis of Big Creek, Norfolk County, Ontario, 1973 (DDT was banned in 1970) are as follows:

Concentration of DDT on Sediments  
(mass of pollutants/mass of sediments)

Suspended sediments	110 ppb = $X_s$
Bed load	76 ppb = $X_{bl}$
Immovable bed	26 ppb = $X_{im}$

Miles (1976) also found that DDT transported in the dissolved phase ranged from 10 to 92 percent of the total transported in the water column. This finding is consistent with the results in Table 11-14 which shows that the percent of pollutant transported in the dissolved phase can be high even for pollutants such as DDT as long as the suspended solids concentration is not extremely high.

Contaminant data collected in bedded sediments can be very illuminating. Although in a screening approach it is not anticipated the user will go to the field to collect sediment core samples, some data might be available. Depending

on the quantity of data available the following types of information might be determinable:

- The spatial extent of contaminated sediments, and pollutant concentrations in the sediments
- The depth of contaminated sediment
- The quantity of toxicant contained in the sediment
- A time history of pollution levels to determine whether they are increasing or decreasing
- The probable sources of the pollutant, based on the location and quantity of contaminated sediments.

Although extensive sampling is required to accurately determine all of the above items, such programs have been successfully accomplished. For example, an extensive sediment sampling program was conducted in the Hudson River in New York to determine the sources of PCBs in the contaminated sediments, and the degree of contamination (Turk, 1979).

#### 4.9.3 Transport and Transformation Expressions for Toxicants in Rivers

The tools presented in this section can be used to predict instream concentrations of toxicants for a variety of different situations. Specifically, the following scenarios are addressed:

- Mixing zone analysis
- Continuous point source discharges
- Continuous nonpoint source discharges
- Resorption from bedded sediments
- Spills and instantaneous release of soluble chemicals, and
- Spills of high density chemicals which sink to the riverbed.

In contrast to many conventional organic pollutants which degrade into innocuous substances, many toxicants are transformed to other chemicals which can be as harmful or more harmful than the original. Consequently, when toxicants are continuously discharged into a river, in addition to predicting the concentration profile, it is useful to also determine:

- The pollutant's advection rate past a specified location
- The pollutant's volatilization rate over a specified reach
- The pollutant's rate of transformation to other species over a specified reach.

The toxicant's fate is thus segregated into the processes of advection, volatilization, and transformation.

In the following three sections on mixing zones, point sources, and nonpoint sources, the user will find there are different methods of approaching the problems. One way to simplify the analysis is to first assume toxicants act conservatively.

The user can then perform a first level analysis to find out whether criteria are violated. If they are not, then a detailed analysis is really not required if the objective is to determine criteria compliance. If violations are predicted, a more detailed analysis of these "hot spots" can be performed by considering the various processes affecting the toxicant in the river. This approach requires more work, but by judiciously applying the tools available, the analyses can be expedited.

#### 4.9.3.1 Mixing Zone Expressions

Section IV-4.1.9 presented earlier delineated one- and two-dimensional mixing zone expressions for conventional pollutants. The one-dimensional expressions need to be extended in order to differentiate between solute and sorbate. To do this, the following expressions for pollutant concentration and the suspended solids concentrations are needed:

$$S = \frac{S_u Q_u + S_w Q_w}{Q_u + Q_w} \quad (\text{IV-107})$$

$$C_{to} = \frac{C_{ut} Q_u + C_{wt} Q_w}{Q_u + Q_w} \quad (\text{IV-108})$$

where

$S_u, C_{ut}$  = concentration of suspended solids and concentration of sum of solute and sorbate in the river above the location of mixing, respectively

$S_w, C_{wt}$  = concentration of suspended solids and concentration of sum of solute and sorbate in the wastewater, respectively

$S, C_{to}$  = concentration of suspended solids and concentration of sum of solute and sorbate in the river following mixing, respectively

The dissolved phase concentration,  $C$ , of the pollutant at the completion of mixing is given by:

$$C = \frac{C_{to}}{1 + k_p S} \quad (\text{IV-109})$$

where  $C_{to}$  and  $S$  are found from the two previous expressions.

The concentration of the solute following mixing depends on characteristics of the waste source, the river's flow rate, and the suspended solids concentration in the river and waste source. The solute concentration might also change after mixing with a tributary of very high suspended solids concentration (high  $S_w$ ), even if it contains no additional pollutant ( $C_{wt} = 0$ ).

Equation IV-108 is particularly useful because it predicts the total instream

concentration of toxicant following initial mixing. This is often the critical test in establishing whether or not water quality standards are violated by a point source.

In cases where initial mixing is incomplete (that is the waste is initially diluted with a fraction of the total river flow), the two-dimensional mixing equation shown earlier as Equation IV-4 will more accurately predict  $C_{to}$ . Then Equation IV-109 can be used to find the solute concentration.

When there are numerous discharges of the same toxicant, analysis becomes more complicated. The most straightforward method of handling this situation is to sequentially apply Equation IV-108 to the series of discharges to find the concentration as a function of distance downstream. If the solute concentration is needed, then sequential application of Equations IV-108 and IV-109 is required.

The analysis of multiple point sources can be simplified in one of two ways. One, the sources can be transformed to an equivalent nonpoint source by assuming that the toxicant input is uniformly distributed between the series of point sources. This approach is discussed in Section 4.9.3.3. Two, a series of closely grouped point sources can be handled as an equivalent point source. The equivalent point source has a flow rate equal to the sum of the flow rates from the individual plants, or:

$$Q_w = \sum_{i=1}^n Q_{wi} \quad (IV-110)$$

where

$Q_{wi}$  = flow rate from ith treatment plant  
 $n$  = number of treatment plants being grouped.

The total pollutant load can be expressed in one of two ways. If the concentrations in the wastewater are known then the total loading is:

$$C_w Q_w = \sum_{i=1}^n C_{wi} Q_{wi} \quad (IV-111)$$

where

$C_{wi}$  = concentration of toxicant in effluent of ith plant.

If the mass emission rates are known instead then:

$$C_w Q_w = \frac{\sum_{i=1}^n M_i}{5.38} \quad (IV-112)$$

where

$M_i$  = mass emission rate of toxicant from ith plant in lbs/day.

The conversion factor 5.38 converts mass emission rate in lbs/day to flow units in cfs and concentration units in mg/l (ppm).

The grouping procedure described above has been applied by the U. S. Environmental

Protection Agency (1981) to a case study in Indiana to evaluate the economic impact of toxicant standards. Numbers of point sources were grouped together using a procedure called cluster analysis. The cluster analysis added the loadings of major and minor industrial dischargers within a ten-mile radius of each other. Ten clusters were identified and few violations occurred within them once the best available technology was attained.

For certain applications the object of using a mixing zone equation is to directly find the maximum allowable concentration in the discharge so that the receiving water criteria are not violated. Under these circumstances Equation IV-108 can be rewritten as:

$$(C_{wt})_{max} = \frac{C_{tc} (Q_{uc} + Q_w) - C_{ut} Q_{uc}}{Q_w} \quad (IV-113a)$$

$$= C_{TC} \frac{(Q_{uc} + Q_w)}{Q_w}, \text{ when } C_{ut} = 0 \quad (IV-113b)$$

where

$(C_{wt})_{max}$  = maximum allowable concentration of the toxicant in the waste discharge so that the water quality criterion is met under critical conditions

$C_{tc}$  = water quality criterion for the toxicant

$Q_{uc}$  = critical river flow rate (e.g., 7Q10).

Equation IV-113b is applicable when the concentration of the toxicant is zero upstream of the discharge point.

#### 4.9.3.2 Point Source Discharges

For point sources of toxicants, the pollutant interactions depicted in Figure IV-50 are simulated. While transformation of toxicants is generally more complex than this, in many instances these interactions are sufficient to analyze the in-stream processes affecting not only point source discharges but also nonpoint source discharges, and instantaneous releases of soluble pollutants. Figure IV-50 reveals that:

- The solute only is assumed to volatilize.
- First order transformation processes degrade only the solute.
- Adsorption and resorption are assumed to occur at rates much faster than other processes.
- No interactions with the bottom sediments occur (this is analyzed in later sections).



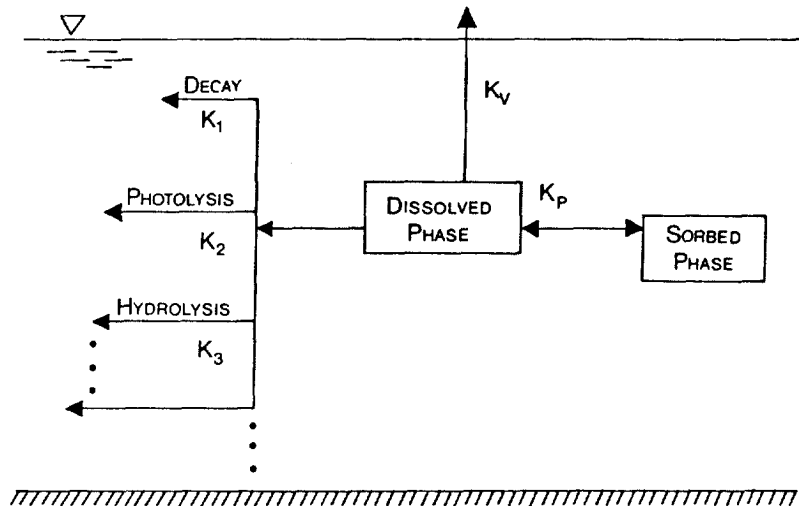


FIGURE IV-50 INSTREAM TRANSFORMATION PROCESSES ANALYZED FOR TOXICANTS.

Based on these interactions, the concentration profile below a point source of toxicant is expressible as:

$$C = \left\{ C_0 - \frac{k'_v}{k'_v + \sum k_i} \frac{P}{K_H} \right\} \exp \left\{ - \frac{k'_v + \sum k_i}{U(1 + K_p S)} x \right\} + \left( \frac{k'_v}{k'_v + \sum k_i} \right) \frac{P}{K_H} \quad (\text{IV-114})$$

where

- $C$  = concentration of dissolved phase of the toxicant at a distance  $x$  below the point source
  - $C_0$  = concentration of the dissolved phase of the toxicant at  $x = 0$  (after the point source discharge has mixed with the river water)
  - $k'_v$  =  $k_v/D$
  - $D$  = water depth
  - $\sum k_i$  = individual first order decay rates which are transforming the toxicant (other than volatilization)
  - $P$  = partial pressure of the toxicant in the atmosphere above the river.
- The remaining variables have previously been defined.

Typically the partial pressure is zero, so that Equation IV-114 simplifies to:

$$C = C_0 \exp \left[ \frac{-(k'_v + \sum k_i)}{1 + K_p S} \cdot \frac{x}{U} \right] \quad (\text{IV-115})$$

The initial dissolved phase concentration is given by:

$$C_0 = \frac{C_{t0}}{1 + K_p S} \quad (IV-116)$$

where

$C_{t0}$  was defined by Equation IV-108.

The total pollutant concentration,  $C_t$ , at any location is:

$$C_t = C (1 + K_p S) \quad (IV-117)$$

The sorbed phase concentration expressed as mass per unit volume of water is:

$$C_s = C_t - C \quad (IV-118)$$

and the sorbed phase concentration expressed as mass per unit mass of sediment is:

$$X = K_p C \quad (IV-119)$$

The most direct application of Equation IV-114 or IV-115, plus Equations IV-117 through IV-119 is to find the instream concentration as a function of distance below the point source. There are, however, other uses of the expressions. Consider Equation IV-115, for example. The ratio  $C/C_0$  can be directly calculated as a function of distance. Thus the fractional dissolved phase concentration can be calculated without ever knowing the initial concentration  $C_0$ . This approach has the advantage of requiring less data. Similarly, the fractional concentration can be calculated for any specified distance, such as the end of a reach. Or, the distance  $x$  can be found so that the fractional concentration is some specified number, which may relate to an acceptable level of toxicant. The length of river subjected to unacceptable levels can then be found.

The user might additionally want to know the distribution of pollutant fluxes in terms of advection ( $\dot{M}_a$ ), volatilization ( $\dot{M}_v$ ), and transformation ( $\dot{M}_t$ ). Expressions for these are presented for the case of  $P = 0$ . These formulae allow the user to predict the fluxes associated with the point source discharge where volatilization is not altered by a background concentration in the atmosphere. Under these conditions:

$$\dot{M} = \dot{M}_a + \dot{M}_v + \dot{M}_t \quad (IV-120)$$

Equation IV-120 states that the rate of entry of the toxicant into the river ( $\dot{M}$ ) equals the rate of advection of that toxicant past some location  $x_s$ , plus the

rate of volatilization across the water surface between the discharge location and some other specified location plus the rate of transformation of the toxicant to other substances within the water column between the same two locations. By knowing expressions for each of  $\dot{M}_a$ ,  $\dot{M}_v$ , and  $\dot{M}_t$  the user knows the major processes controlling the toxicant's fate within any reach of river.

The mass flux advected past a location  $x_s$  is given by:

$$\dot{M}_a = (Q_u + Q_w) C_s \quad (IV-121)$$

where the concentration  $C_s$  is evaluated at  $x = x_s$ . The volatilization mass flux is given by:

$$\dot{M}_v = A_c k'_v C_o \frac{U(1 + K_p S)}{k'_v + \sum k_i} \left[ 1 - \exp \left( - \frac{k'_v + \sum k_i}{U(1 + K_p S)} x_s \right) \right] \quad (IV-122)$$

where

$A_c$  = cross-sectional area of river

All other terms have previously been defined.

In some cases the user might have an estimate of the average dissolved phase concentration,  $C$ , within the reach under consideration. Under these circumstances the volatilization flux is simply:

$$\dot{M}_v = A_s k'_v C \quad (IV-123)$$

where

$A_s$  = surface area of the reach under investigation.

The transformation mass flux is expressible as:

$$\dot{M}_t = A_c \sum k_i C_o \frac{U(1 + K_p S)}{k'_v + \sum k_i} \left[ 1 - \exp \left( - \frac{k'_v + \sum k_i}{U(1 + K_p S)} x_s \right) \right] \quad IV-124$$

Since the sum of Equations IV-121, IV-122, and IV-124 equals the mass emission rate of the toxicant, Equation IV-120 can be used to double check the fluxes calculated.

#### 4.9.3.3 Nonpoint Source Discharge

This section parallels the previous section on point source discharges by presenting expressions for the steady-state concentration profile, and for mass fluxes. In addition to applying this methodology to a nonpoint source, another and possibly more useful application is to express a series of point sources as an

equivalent nonpoint source. The equivalent nonpoint source discharge rate is simply the sum of the discharge rates of the pollutant from all the point sources. This approach is not as accurate as analyzing each point source individually but is much faster depending on the number of point sources. For example, suppose a river segment has ten separate point sources located within 50 miles of each other. The most rigorous analysis would consist of considering each point source individually, where mixing zone and point source equations are applied sequentially ten times each. This obviously is a great deal of work for a hand calculation approach. By considering these point sources as a single equivalent nonpoint source, a single equation application is sufficient to analyze the problem. Example IV-5 shown earlier in the BOD section illustrates this procedure.

The solute concentration in a river resulting from a steady nonpoint source of toxicant is:

$$C = \frac{-k_4}{k_3} + \left( C_0 + \frac{k_4}{k_3} \right) \left( \frac{Q_0 + mx}{Q_0} \right)^{\frac{-k_3}{k_2}} \quad (\text{IV-125})$$

where

$$k_2 = \frac{1 + K_p S}{A_c} m$$

$$k_3 = k_2 + k'_v + \sum k_i$$

$$k_4 = \frac{C_{tn}}{A_c} m - \frac{P}{H} k_v$$

$C_{tn}$  = total concentration of toxicant in nonpoint source

$$m = \frac{Q_f - Q_0}{x_1}$$

$Q_f$  = river flow rate at end of nonpoint source

$Q_0$  = river flow rate at beginning of nonpoint source

$x_1$  = length of nonpoint source.

Equations IV-117 through IV-119 can be used to find  $C_t$ ,  $C_s$ , and  $X$ , respectively.

In a manner similar to point source discharges, Equation IV-120 which expresses the mass balance between toxicant inflow rate to the river and loss rate by advection, and transformation, is valid. The appropriate expressions are (when  $P = 0$ ):

$$\dot{M}_a = \underbrace{(Q_0 + mx)C}_{\text{solute transport}} + \underbrace{(Q_0 + mx) C k_p S}_{\text{sorbate transport}} \text{ at } x = x_s \quad (\text{IV-126})$$

for the advective flux. For the volatilization flux:

$$\dot{M}_V = -k'_V A_C \frac{k_4}{k_3} x_S + k'_V A_S \left( C_0 + \frac{k_4}{k_3} \right) \frac{Q_0}{m} \frac{k_2}{k_2 - k_3} \left\{ \left( \frac{Q_0 + mx_S}{Q_0} \right)^{\frac{-k_3}{k_2} + 1} \right\} \quad (IV-127)$$

For the transformation flux:

$$\dot{M}_t = -\Sigma k_i A_C \frac{k_4}{k_3} x_S + \Sigma k_i A_S \left( C_0 + \frac{k_4}{k_3} \right) \frac{Q_0}{m} \frac{k_4}{k_2 - k_3} \left\{ \left( \frac{Q_0 + mx_S}{Q_0} \right)^{\frac{-k_3}{k_2} + 1} - 1 \right\} \quad (IV-128)$$

As a first cut analysis, the user might want to assume that the toxicants act conservatively. If criteria are not violated under these circumstances, then criteria will not be violated if decay or transformation processes are included.

#### 4.9.3.4 Resorption of Toxicant from a River Bed

Because many toxicants are transported as sorbate rather than as solute, a significant fraction of the pollutant which enters a riverine system can ultimately be deposited in the bedded sediments. If the toxicant is resistant to degradation processes it can remain in the sediments for extended periods of time. During this time, the toxicant can slowly be desorbed back into the water column or scoured into suspension.

Figure IV-46 shown earlier illustrated an idealization of the process of resorption of a toxicant from bedded sediments. The process can be described as follows. Supposed the average concentration of the pollutant in the bedded sediment is  $X_0$  when the analysis begins (called  $t = 0$ ). The concentration  $X$ , at any later time is estimated from mass balance considerations as:

$$X = \begin{cases} X_0, & \text{for } x > \frac{U \delta t}{M_s K_p} \\ 0, & \text{otherwise} \end{cases} \quad (IV-129)$$

where

- $X_0$  = concentration of pollutant in bed at some time  $t = 0$
- $M_s$  = mass of contaminated sediment per unit area of river bed,  $g/cm^2$
- $U$  = stream velocity, cm/sec
- $\delta$  = equivalent depth of water in sediment  $M_s$ , cm
- $K_p$  = partition coefficient.

Equation IV-129 reveals that resorption can be interpreted as a frontal phenomenon where resorption is completed at one location before progressing downstream. Based on this interpretation, an effective removal velocity of the front is:

$$U_e = \frac{U \delta}{M_s K_p} \quad (IV-130)$$

The time  $T_d$  required to desorb the toxicant over any specified distance is:

$$T_d = x_L / U_e \quad (IV-131)$$

where

$x_L$  = length of contaminated river segment.

During the period of resorption the average concentration in the water column is:

$$C = \begin{cases} \frac{X_0 \delta}{K_p D} & \text{for } x > U_e t \\ 0 & \text{, otherwise} \end{cases} \quad (IV-132)$$

$$(IV-133)$$

To use Equations IV-129 through IV-133, estimates for  $X_0$ ,  $M_s$ , and  $\delta$  are required. If both the mass of contaminated sediment per unit area of river bed ( $M_s$ ) and the mass of toxicant in the sediments are known, then  $X_0$  can be determined. Conversely, if both  $X_0$  and the total mass of toxicant in the sediments are known, then  $M_s$  can be calculated.

In lieu of having data on  $M_s$  and  $\delta$ , these quantities can be estimated based on the depth of contaminated sediments by using Table IV-39. In addition to the depth, the percent solids by weight must be estimated. This parameter generally increases with depths and can be chosen as 50 percent, unless better data are available. The data in Table IV-39 were derived from the following two equations:

$$M_s = \frac{D_c}{10 \left( 1/S_s + \frac{100-P}{P} \right)} \quad (IV-134)$$

and

$$\delta = \frac{S_s \times D_c \left( \frac{100-P}{P} \right)}{1 + S_s \left( \frac{100-P}{P} \right)} \quad (IV-135)$$

where

$M_s$  = mass of contaminated sediment,  $g/m^2$

$\delta$  = equivalent water depth, mm

$S_s$  = specific gravity of solids

$D_c$  = depth of contamination, mm,

In cases where the depth of contamination exceeds 100 mm the equations can be used in lieu of Table IV-39.

The Hudson River in New York State provides an illustration of an extreme

TABLE IV-39

MASS OF CONTAMINATED SEDIMENTS AND EQUIVALENT WATER  
DEPTH AS A FUNCTION OF DEPTH OF CONTAMINATION

Depth (mm)	Percent Solids by Weight	$M_s$ (g/cm <sup>2</sup> )	$\delta$ (mm)
1	20	0.02	0.9
	50	0.06	0.6
	80	0.11	0.3
5	20	0.11	4.5
	50	0.30	3.0
	80	0.55	1.4
10	20	0.23	<b>9.1</b>
	50	0.60	<b>6.0</b>
	80	1.1	2.7
20	20	0.45	18.
	50	1.2	12.
	80	2.2	5.5
50	20	1.1	45.
	50	3.0	30.
	80	5.5	14.
100	20	<b>2.3</b>	91.
	50	<b>6.0</b>	60.
	80	11.0	27.

case of PCB contamination (Turk, 1980). Between 1951 and 1977 PCBs were discharged from point sources near Fort Edward and Hudson Falls, about 80 km (50 mi) above Albany, New York. Figure IV-51 shows the general vicinity.

During this time period the mass emission rate of PCBs decreased from 15 kg/day (33 lbs/day) to less than 1 g/day (0.002 lbs/day). PCB concentration in the bottom materials range from about 200  $\mu\text{g/g}$  near Fort Edward to about 4  $\mu\text{g/g}$  near Waterford, about 70 km (43 mi) downstream. In 1975 the New York State Department of Environmental Conservation began a study to determine the source of contamination. At that time they estimated that the total mass of PCBs in the bottom sediments was 225,000 kg (500,000 lbs).

It has been found that PCBs are being naturally desorbed from the river bed under moderate and low flow conditions. The estimated transport rates are:

- At Glen Falls = 0.0 kg/day (above discharge)
- At Schuylersville = 4.0 kg/day
- At Stillwater = 5.0 kg/day
- At Waterford = 4.0 kg/day (70 km downstream).

It is interesting to note that these transport rates are approximately 30 percent as

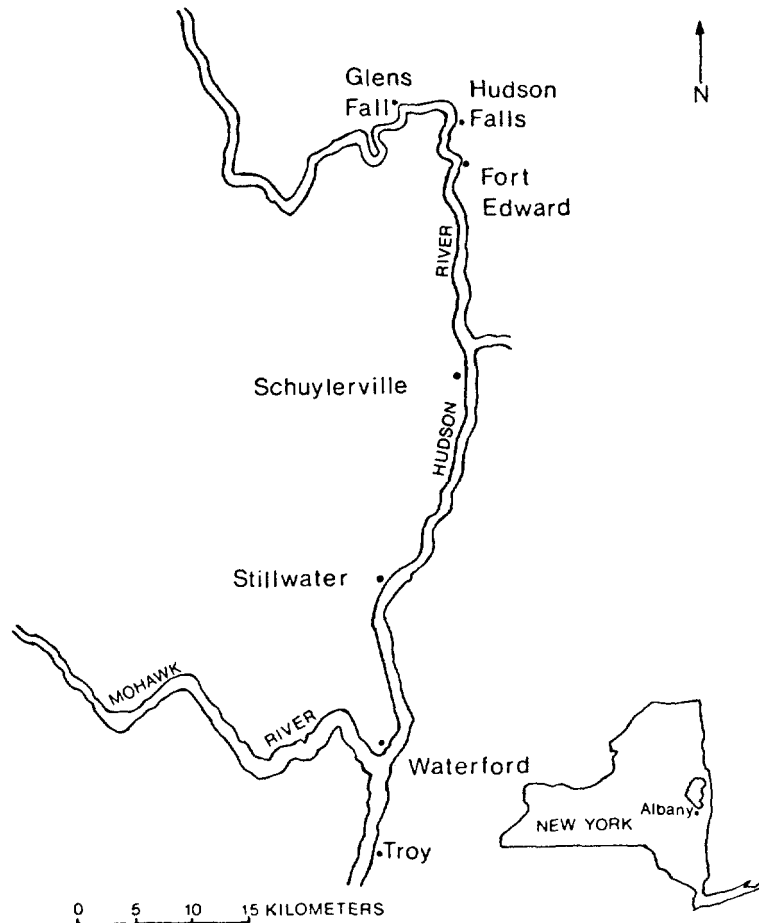


FIGURE IV-51 LOCATION MAP OF HUDSON RIVER, NEW YORK.

high as the original point source mass emission rates. At a resorption rate of about 4 kg/day, the river between Glen Falls and Waterford would be rid of PCBs in about 150 years.

Turk (1980) found that flood events transport large quantities of PCBs, although this transport mechanism is only operative periodically. Turk estimated that due to the combined removal rates of PCBs during high flow periods (by scour) and during low flow periods (by resorption), the residence time of PCBs above Waterford would be about one century.

EXAMPLE IV-18

For discharges of  $600 \text{ m}^3/\text{sec}$  or less, it has been found that the Hudson River bed provides 4 kg/day of PCBs to the water column at locations between Schuylerville and Waterford, New York. Determine the PCB concentration in the water column at the following two flow rates:



- a. 600 m<sup>3</sup>/sec
- b. 50 m<sup>3</sup>/sec.

Compare these concentrations to the freshwater criterion of 0.001 µg/l promulgated in the "Red Book".

Since the mass emission rate and river flow rate are known, Equation IV-11 can be rearranged to yield the total instream concentration:

$$C_t = \frac{M}{86.4Q}$$

where

M = mass loading, kg/day

C<sub>t</sub> = concentration of pollutant, ppm

Q = flow rate, m<sup>3</sup>/sec.

For the problem at hand:

M = 4 kg/day

Q = 50 and 600 m<sup>3</sup>/sec.

For Q = 600 m<sup>3</sup>/sec:

$$C_T = \frac{4}{86.4 \times 600} = 0.08 \times 10^{-3} \text{ ppm}$$

= 0.08 µg/l, or 80 times the Red Book criterion.

For Q = 50 m<sup>3</sup>/sec:

$$C_T = \frac{4}{86.4 \times 50} = 0.9 \times 10^{-3} \text{ ppm}$$

= 0.9 µg/l, or 900 times the criterion.

As a second part to the problem estimate the time required to remove the PCBS in the sediment by resorption (ignoring scour), assuming the resorption rate of 4 kg/day is not known. Base the calculations on Table IV-39 or Equations IV-130 and IV-131. Use the following data:

Depth of contaminated sediment = 600mm

River velocity = 1 fps

Partition coefficient : 10<sup>3</sup> to 10<sup>4</sup>

Because the depth of contamination exceeds the maximum value tabulated in Table IV-39, Equations IV-134 and IV-135 are used instead. Assuming S<sub>s</sub> = 1.5 and p = 80:

$$M_s = \frac{600}{10 \left( \frac{1}{1.5} + \frac{100-80}{80} \right)} = 65 \text{ g/cm}^2$$

$$\delta = \frac{1.5 \times 600 \left( \frac{100-80}{80} \right)}{1 + 1.5 \left( \frac{100-80}{80} \right)} = 160 \text{ mm} = 16 \text{ cm}$$

The effective transport velocity is:

$$U_e = \frac{U \times 16}{65 \times 10^4} = .25 \times 10^{-4} U \quad \text{for } K_p = 10^4$$

and

$$U_e = \frac{U \times 15}{65 \times 10^3} = .25 \times 10^{-3} U \quad \text{for } K_p = 10^3$$

The time required for resorption over the 70 km (43 mi) reach is:

$$T = \frac{43 \times 5280}{.25 \times 10^{-4} \times 1} \text{ Sec} = 290 \text{ year for } K_p = 10^4$$

and

$$T = 29 \text{ years for } K_p = 10^3$$

Probably the biggest unknown in this problem is  $K_p$ . Based on a range of  $K_p$  from  $10^3$  to  $10^4$ , the time of resorption ranges from 29 to 290 years, within the range predicted from observed resorption rates.

----- END OF EXAMPLE IV-18 -----

#### 4.9.3.5 Instantaneous Releases of Low Density Toxicants

Many toxicants have specific gravities less than or equal to unity. Should a toxicant less dense than water be spilled in its pure form, the toxicant can ride atop the water body for a period of time, while (perhaps) being rapidly volatilized and photolyzed as it becomes entrained and dissolved in the river.

Analysis of releases of low density pollutants is complicated and, in many cases, beyond the scope of hand calculation analyses. Often spills of toxicants occur over a part of the river, so the resultant movement is three-dimensional because the toxicant spreads laterally, longitudinally, and vertically due to turbulence and advection. Buoyant spreading and mixing can further complicate the dispersal process.

Toxicant spills can occur in numerous ways. In one instance the toxicant may be discharged directly onto the surface of the river, and depending on the rate of mixing with ambient water a significant portion could volatilize directly from the pure phase. On the other hand submerged spills may result in the chemical becoming mixed with river water before it reaches the water's surface. Under these circumstances volatilization fluxes will not be as great.

When a chemical is spilled in pure form, the time required for the chemical

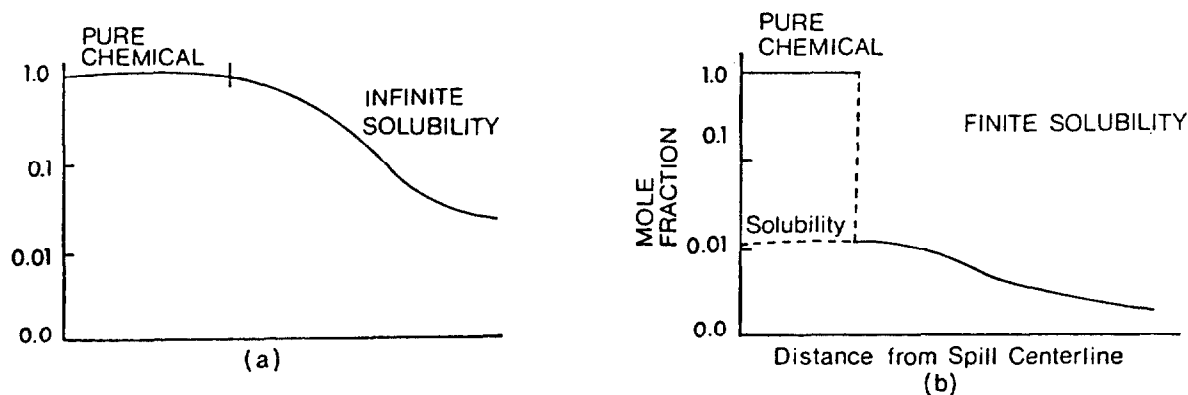


FIGURE IV-52 HYPOTHETICAL CONCENTRATION DISTRIBUTIONS OF FINITELY SOLUBLE AND INFINITELY SOLUBLE TOXICANTS.

to mix with the river water depends, in addition to other factors, on the solubility of the chemicals. Some may be highly soluble in water (essentially infinitely soluble) while others may have a very low solubility. Figure IV-52 illustrates these two different situations.

Figure IV-52a shows the case of a toxicant of infinite solubility. The toxicant maintains its pure state (mole fraction equals unity) for some distance away from the spill site, and then the mole fraction gradually begins to decrease as the chemical mixes with water. Figure IV-52b illustrates the same basic situation, except that the toxicant has a finite solubility. In this case there will be a rapid drop between the mole fraction of the pure toxicant (unity) and the mole fraction at solubility (much less than unity). For the pure phase toxicant shown in Figure IV-52b to become mixed in water at concentrations at or below the solubility limit might require a substantial amount of water.

Based on the discussions in the previous paragraphs, tools for analyses of the following will be presented:

- Volatilization mass flux from a pure toxicant contained within a fixed area
- The fate of a highly soluble toxicant which mixes instantaneously with the river water
- The fate of a low solubility toxicant which mixes with a finite volume of river water.

Toxicants which exist in the gas phase under atmospheric pressure and typical natural temperatures are excluded from analysis here, even though they might be transported as a liquid under high pressure (e.g. liquified chlorine). If a tank transporting such a chemical were to rupture under water, the chemical would boil and

most of the gas would rapidly escape into the atmosphere. Some of the gas would however become dissolved in the river water during ascent of the bubbles.

#### 4.9.3.5.1 Volatilization of Toxicant in Pure State

This section will present a method to predict the volatilization mass flux rate of a pure chemical, and the time required to volatilize a known amount of the chemical which occupies a specific area of river surface. The volatilization flux rate is given by:

$$F = \frac{k_g \cdot P_v \cdot MW}{R_u T} = \frac{k_g \cdot P_v \cdot MW}{82.06 T} \quad (IV-136)$$

where

- F = volatilization mass flux, g/cm<sup>2</sup>/hr
- P<sub>v</sub> = saturation vapor pressure of pure liquid toxicant, atm
- MW = molecular weight of toxicant
- T = temperature of ambient water, °K
- k = gas phase transfer coefficient, cm/hr.

The expression for the gas phase transfer coefficient was shown earlier in Equation II-46. A suggested default value is 3000 cm/hr. The saturation vapor pressure of a number of toxicants were shown earlier in Tables II-5 through II-9. Weast (1969) also contains extensive data.

Based on the amount of pure toxicant (M) contained within a spill area (A), the time required to volatilize the chemical is:

$$t = \frac{M}{10 \times F \times A} \quad (IV-137)$$

where

- t = time, hr
- M = mass, kilograms
- A = area, m<sup>2</sup>

This expression is limited to situations where the spill area A is of constant size over the period of volatilization so it is not applicable to unconfined spills where the area could change rapidly with time.

#### 4.9.3.5.2 Analysis of Chemicals Which Instantaneously Mix

Depending on the mass of spilled toxicant and its volatility, the spilled toxicant may rapidly attain concentrations in the water column below volatility. Under these circumstances, Equation IV-138 presented below can be used. The analysis below assumes that Henry's Law is valid (e.g. the mole fraction of dissolved chemical is much less than 1.0) which is reasonable for many toxicants only moments after a spill.

It is worthwhile to calculate the volume of water required for a mass  $M$  of spilled chemical to be diluted to its volubility limit. This can provide a rough idea as to whether mixing is likely to be "instantaneous" or not. Suppose that a mass  $M$  of spilled chemical has a volubility  $C_s$ . The volume of water needed to be mixed with the pure chemical so that the volubility limit is achieved is:

$$V_o = \frac{M \times 10^8}{C_s} \quad (IV-138)$$

where

$$\begin{aligned} M &= \text{mass of spill, kg} \\ C_s &= \text{volubility, mg/l} \\ V_o &= \text{volume of water, m}^3 \end{aligned}$$

The concentration profile resulting from an instantaneous spill (and assuming concentrations at or below the volubility limit are rapidly attained) is expressed by:

$$C = \frac{M_D}{2A_c \sqrt{\pi D t}} \exp \left[ \frac{(x-ut)^2}{4Dt} - k_e t \right] + \frac{k'_v}{k'_v + \sum k_i} \cdot \frac{P}{K_H} \left[ 1 - \exp(-k_e t) \right] \quad (IV-139)$$

where

$C$  = dissolved phase concentration

$$k_e = \frac{k'_v + \sum k_i}{1 + K_p S}$$

$$M_D = \frac{M}{1 + K_p S}$$

$M$  = total mass released

The remaining variables have been previously defined.

In most instances the user would like to predict the maximum concentrations remaining in the river for different elapsed times following the spill, given by the peaks in Figure IV-53. Under such conditions, and assuming  $P = 0$ , Equation IV-139 simplifies to:

$$C_{\max} = \frac{M_D}{2A_c \sqrt{\pi D t}} \exp(-k_e t) \quad (IV-140)$$

The various components of the mass balance at time  $t_s$  follow (for  $P = 0$ ).

Mass of dissolved pollutants  $M_D (t = t_s)$ :

$$M_D (t = t_s) = M_D \exp(-k_e t_s) \quad (IV-141)$$

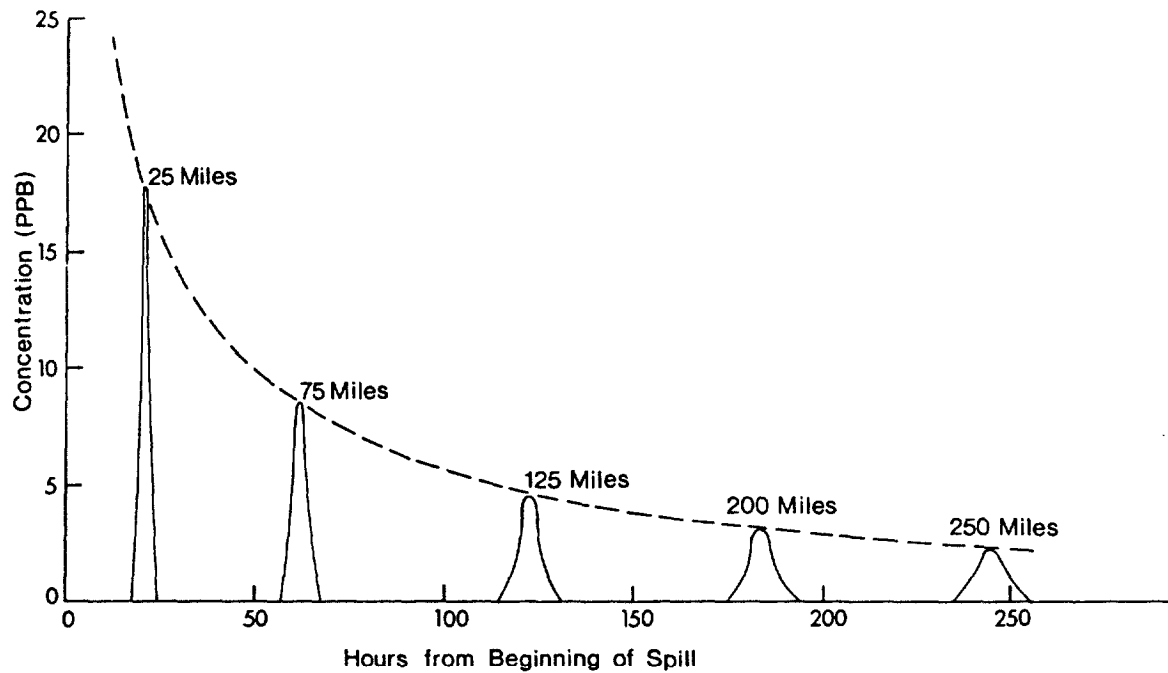


FIGURE IV-53 HYPOTHETICAL DISTRIBUTION OF TOXICANT AT VARIOUS LOCATIONS FOLLOWING A SPILL

Mass of sorbed pollutants  $M_s$  ( $t = t_s$ ):

$$M_s = K_p S M_D \exp(-k_e t_s) \quad (IV-142)$$

Mass of pollutant which was volatilized  $M_v$  ( $t = t_s$ ):

$$M_v(t = t_s) = \frac{M_D k'_v}{k_e} [1 - \exp(-k_e t_s)] \quad (IV-143)$$

Mass of pollutant which has decayed  $M_{Dk}$  ( $t = t_s$ ):

$$M_{Dk}(t = t_s) = \frac{M_D \sum k_i}{k_e} [1 - \exp(-k_e t_s)] \quad (IV-144)$$

Equations IV-140 through IV-144 allow the user to assess the fate of the pollutant for any desired time  $t_s$  following the spill.

A direct extension of the instantaneous pollutant release in a plane is the volumetric release, where the pollutant is effectively released within some initial

volume of water. For this case, the dissolved phase concentration is:

$$C = \frac{M_D}{2V_0} \left[ \operatorname{erf} \left( \frac{X - Ut}{\sqrt{4Dt}} \right) - \operatorname{erf} \left( \frac{X - L - Ut}{\sqrt{4Dt}} \right) \right] \left( \exp(-k_e t) \right) \quad (\text{IV-145})$$

where

L = length of zone of initial contamination

erf = the error function

All other variables have been previously defined.

The location of the maximum concentration for any time  $t_s$  after release is approximately given by:

$$x = Ut_s + L/2 \quad (\text{IV-146})$$

#### 4.9.3.6 Spill Analysis of High Density Toxicants

Spills of hazardous chemicals have been of concern for quite a number of years, and interest will increase as the quantity and variety of toxicants transported increase. In past years the primary emphasis has been on analysis and containment of oil spills. This has probably been for a number of reasons:

- Large quantities of oil are transported, and are therefore subject to more frequent spills.
- The environmental consequences of an oil spill can be severe and visually offensive.
- Oil floats, so oil spills are easy to detect and monitor.

In contrast to oil, many hazardous chemicals have specific gravities greater than one, so that in their pure form, they tend to sink in water. Table IV-40 lists some such chemicals. Chlorine, although it may be transported under pressure as a liquid, is a gas under atmospheric conditions. Even so, if a liquid chlorine barge were involved in an accident on a river some of the chlorine could become dissolved in the water since the volatility of chlorine in water is 50,000 mg/l, although most would probably gasify and form a toxic cloud.

The chemicals shown in Table IV-40 are generally either slightly soluble (10 to 10,000 ppm) or soluble (10,000 to 1,000,000 ppm). In any case the volatility levels generally exceed or greatly exceed proposed water quality criteria. Thus if a mass of chemical were spilled into a river, it is to be expected that concentrations near the chemical's volatility limit could be detected in the immediate vicinity of the spill. As the chemical is dissolved and travels downstream, it could eventually become mixed over the channel cross-section and expose all organisms living within the water column (and perhaps those living in the bedded sediments as well) to its effects. With increasing distance the concentrations of the toxicant will decrease to reflect the additional mixing afforded by the flow of the entire river, plus

TABLE IV-40  
WATER-SOLUBLE, HIGH DENSITY ( $\rho > 1$ ), IMMISCIBLE CHEMICALS

Species	Density in air ( $\text{g}/\text{cm}^3$ )	Solubility in water ( $\text{mg}/\text{l}$ )	Interfacial Tension ( $\text{dynes}/\text{cm}$ ) <sup>a</sup>		
			Air	Water	Vapor
Acetic acid	1.06	50,000	68.0 <sub>30°</sub>	-	27.8 <sub>20°</sub>
Acetic anhydride	1.087	500,000	-	-	32.7 <sub>20°</sub>
Acetophenone	1.03	5,550	-	-	39.8 <sub>20°</sub>
Aniline	1.022	34,000	44.0	-	42.9 <sub>20°</sub>
Benzaldehyde	1.04	1,000	40.04	15.51 <sub>20°</sub>	-
Benzyl alcohol	1.043	46,000	39.0 <sub>20°</sub>	4.75 <sub>22.5°</sub>	39.0 <sub>20°</sub>
Bromine	2.93	41,700	41.5 <sub>20°</sub>	-	41.5 <sub>20°</sub>
Carbon disulfide	1.26	2,200	-	48.36 <sub>20°</sub>	-
Carbon tetrachloride	1.595	500	-	45 <sub>20°</sub>	26.95 <sub>20°</sub>
Chlorine (liquid) <sup>b</sup>	3.2	50,000	-	-	18.4 <sub>20°</sub>
Chloroform	1.5	5,000	27.14 <sub>20°</sub>	32.8 <sub>20°</sub>	-
Chlorophthalene				40.74 <sub>20°</sub>	-
Dichloroethane	1.256	9,000	23.4 <sub>35°</sub>	-	-
Ethyl bromide	1.431	10,600	-	31.2 <sub>20°</sub>	24.15 <sub>20°</sub>
Ethylene bromide	2.18	4,300	-	36.54 <sub>20°</sub>	38.37 <sub>20°</sub>
Furfural	1.159	83,100	43.5 <sub>20°</sub>	-	43.5 <sub>20°</sub>
Glycerol	1.26			63.4 <sub>18°</sub>	-
Hydrogen peroxide	1.46	50,000	-	-	76.1 <sub>18.2°</sub>
<b>Mercury<sup>c</sup></b>	13.54	.0005	470	375 <sub>20°</sub>	-
Naphthalene	1.15	30	28.8 <sub>127°</sub>	-	28.8 <sub>127°</sub>
Nitrobenzene	1.205	1900	43.9 <sub>20°</sub>	-	43.9 <sub>20°</sub>
Phenol	1.071	67,000	40.9 <sub>20°</sub>	-	40.0 <sub>20°</sub>
Phenylhydrazine	1.097			-	46.1 <sub>20°</sub>
Phosphorus trichloride	1.5	50,000	-	-	29.1 <sub>20°</sub>
Trichloroethane	1.325	10	22 <sub>144°</sub>	-	-
N-Propyl bromide	1.353	2,500	-	-	19.65 <sub>20°</sub>
Quinoline	1.095	60,000	45.0 <sub>20°</sub>	-	-
Tetrachloroethane	1.60	3,000	36.3 <sub>22.5°</sub>	-	-
<b>Water<sup>b</sup></b>	1.00	N. A.	73.05 <sub>18°</sub>	N. A.	72

a In air, water, and its own vapor. Temperature is °C.

b Under pressure.

c Mercury and water data included for reference.

From: Thi bodeaux (1979)



dispersion, degradation, and volatilization processes.

A technique is presented here to estimate the concentration which can exist in the water column and the duration of the elevated levels following a spill. In particular tools are presented to predict:

- The concentration of toxicant in the water column at the downstream end of the spill
- The concentration of the toxicant after it has become completely mixed with the entire river
- The time required to dissolve the spilled toxicant
- The amount of toxicant remaining sorbed to the bottom sediments and in the pore water following dissolution.

It is, of course, more accurate but more costly to measure concentrations directly rather than predicting them. However, since the toxicant is "somewhere" on the river bottom, and might not be immobile, detecting the location of the toxicant will take time. By estimating the dissolution time of the spill, it can be determined if it is feasible to even set up and carry out a sampling program.

The tools delineated above are useful not only to analyze spills which have occurred, but also for answering hypothetical questions which relate to the consequence of spills based on river traffic, sizes of containers, kinds of toxicants being transported, and characteristics of the rivers. Based on this information the user can evaluate possible "spill scenarios" to predict impacts before they occur. Such information would be useful to formulate post-spill responses. In situations where a spill of a toxicant would produce extreme consequences, provisions could be made to mitigate the consequences before they occur.

#### 4.9.3.6.1 Description of Spill Process

Spills which contaminate rivers can be the result of a variety of accidents: leaking barges, broken pipelines, highway accidents, and clandestine dumping. The scope here is limited to those situations where the toxicant has been deposited on the bottom of the river. This situation is most likely to result from an accident on or under the water's surface. Figure IV-54 conceptualizes what might happen when a barge carrying a high density pollutant ruptures.

Depending on the volume of contaminant, the size of the hole, among other factors, the toxicant might issue from the barge as a continuous jet. However, because the volumetric flow rate of the jet is probably small, and perhaps even intermittent, the toxicant probably breaks up into drops of various sizes as it falls through the water column. Some of the finest drops might never reach the stream bed, but rather be transported in suspension within the water column, and gradually dissolve. The majority of the toxicant may settle on the river bed and form drops, globs, or pools (using the terminology of Thiobodeaux, 1979). The drop

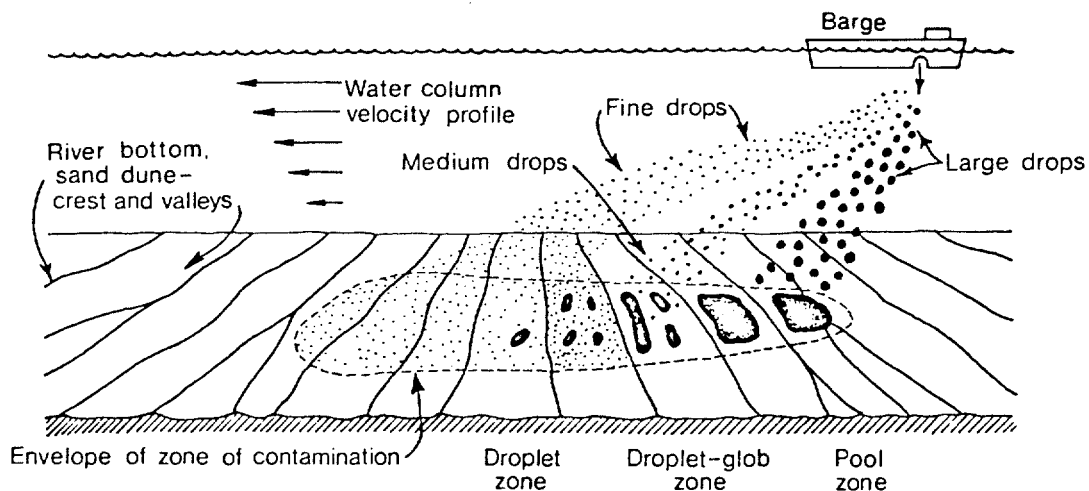


FIGURE IV-54 ILLUSTRATION OF HYPOTHETICAL SPILL INCIDENT  
(FROM THIBODEAUX, 1979),

size depends on the interfacial tension and density differences between the toxicant and the water (Hu and Kintner, 1955). Pools tend to form in the valleys of sand waves, and occur when large drops or globs coalesce. Thibodeaux (1980) provides techniques to estimate the residence time of drops, globs, and pools. For the simplified analyses here the spill is assumed to be in the shape of a continuous pool.

#### 4.9.3.6.2 Fate of Pollutant Following Settling

Once the toxicant has settled on the river bed its fate is governed by numerous processes. Depending on the texture of the bottom materials (e.g. sands, cobbles, boulders), the density of the toxicant, and its interfacial tension, the toxicant could settle in deep depressions, and dissolution would be slowed.

Many pollutants have large partition coefficients so that sorption to bottom sediments is significant. The characteristics of the sediments affect the partition coefficient, but in many cases sorption can compete with dissolution as a major process controlling the pollutant's fate. Although transformation processes other than sorption and dissolution are operative the moment the toxicant enters the water, they are not considered here.

In September 1974 an electrical transformer being loaded onto a barge fell into the Duwamish Waterway in the State of Washington (Thibodeaux, 1980). 260 gallons of Aroclor 1242, a PCB mixture of specific gravity 1.4, were spilled into the river. Divers observed that pools of free PCB on the bottom moved back and forth with the tide. Pools of PCBs were removed from the bottom using suction dredges, and a second stage operation involved a high solids dredge. Probably due to its low volatility (0.2 ppb) and high sorption characteristics, much of the PCB was recovered (from 210 to 240 gallons).

#### 4.9.3.6.3 Predictive Tools

It is hypothesized that a toxicant spill contaminates an area of width  $W_s$  and length  $L_s$ , where the length is measured in the flow direction. The toxicant which reaches the river bed is assumed to be highly concentrated, and its dissolution is controlled by a thin layer immediately above where molecular diffusion limits the vertical flux of the pollutant. Above this layer the toxicant is rapidly entrained into the river. There are several expressions available to determine the thickness of the diffusion layer (e.g. Novotny, 1969 and Mills, 1976). The expression developed by Mills will be used here, because the required information is easier to attain while the two approaches appear to give comparable results. The expression is:

$$\delta_d = \frac{11.6 \cdot 1.49 \nu R_h^{1/6}}{\sqrt{g} U n} \quad (\text{IV-147})$$

where

- $\delta_d$  = thickness of diffusive sublayer
- $\nu$  = dynamic viscosity of water
- $R_h$  = hydraulic radius of the river
- $U$  = river velocity
- $n$  = Manning's coefficient.

Just downstream from the spill zone, but before complete mixing with the river, the concentration of the toxicant in the water column is:

$$C_L = (C_o - C_s) \exp\left(-\frac{D_{cw} L_s}{\delta_d H U}\right) + C_s \quad (\text{IV-148})$$

where

- $C_o$  = background concentration of chemical
- $C_s$  = solubility of chemical in water
- $D_{cw}$  = diffusion coefficient of chemical in water
- $H$  = water depth
- $U$  = river velocity.

The concentration at the location of complete mixing is:

$$C_{WM} = C_L \frac{W_s}{W} + C_o \left(1 - \frac{W_s}{W}\right) \quad (\text{IV-149})$$

where

- $W_s$  = spill width
- $W$  = river width.

The time  $T_d$  required to dissolve the chemical is:

$$T_d = \frac{M_D}{C_L U H W_s} \quad (IV-150)$$

where

$M_D$  = total amount of pollutant which is dissolved (an amount less than or equal to the amount spilled).

As the spilled toxicant dissolves in the flowing river water, it concurrently diffuses into the immobile bedded sediments, where a portion is sorbed onto the sediments. Consequently, some residual toxicant will remain in the bottom sediments following the initial dissolution phase. The residual will then slowly diffuse and desorb back out into the river, although diffusion deeper into the sediments can also occur because of the concentration gradient. The time required for the residual toxicant to naturally desorb and diffuse back into the water column can greatly exceed the original period of dissolution.

The quantity of toxicant which resides in the sediments following the initial dissolution period can be predicted as follows. It is assumed that the dissolution and downward diffusion/sorption proceed independently until all the spilled toxicant has been removed. The time  $t$  can be found such that this statement is true. From a practical standpoint, the user can simply determine the time required for complete dissolution, and then find the total mass which would have diffused/sorbed into the bottom sediments during this period. Since this approach accounts for more toxicant than was originally present, the time period should be decreased by the fractional amount of toxicant created. If the amount of excess toxicant is no more than 15 percent of the total amount spilled, then a time adjustment is not required.

Based on the processes of sorption and diffusion the vertical profile of dissolved chemical in the river bed at time  $t$  following the appearance of the toxicant on the bottom is given by:

$$\frac{C - C_b}{C_s - C_b} = 1 - \operatorname{erf} \left( \frac{z}{\sqrt{4D_p t}} \right) \quad (IV-151)$$

where

$C$  = concentration of dissolved chemical in the pore water, in units of mass of dissolved chemical per unit volume of pore water

$C_b$  = background concentration of chemical in pore water

$C_s$  = solubility of chemical in water

$z$  = vertical distance, measured downward from the sediment-water interface

$$D_p = D_e / \left( 1 + \rho_s K_p \frac{1-n}{n} \right)$$

$D_e$  = effective molecular diffusion coefficient  
 $\rho_s$  = density of sediments  
 $K_p$  = partition coefficient  
 $n$  = porosity of porous medium.

From Equation IV-151, the total mass of pollutant found in the sediments at time  $t$  is:

$$M_T = \int (C + C_s) n dV \quad (IV-152a)$$

$$= A_c n \int (C + C_s) dz \quad (IV-152b)$$

where

$A_c$  = spill area  
 $C_s$  = concentration of pollutant sorbed to sediments, per unit volume of pore water.

$C_s$  can be related to  $C$  by:

$$C_s = C \rho_s K_p \left( \frac{1-n}{n} \right) \quad (IV-153)$$

Combining Equations IV-151, IV-152 and IV-153 the total mass in the sediment is:

$$M_T = 0.563 n C_s \left( 1 + \rho_s K_p \frac{1-n}{n} \right) A_c \sqrt{4D_p t} \quad (IV-154)$$

#### EXAMPLE IV-19

The following is an excerpt from Chemical Engineering Volume 80, September 3, 1973, as reported in Thi bodeaux (1979).

"Approximately  $1.75 \times 10^6$  lbs of chloroform were released from a barge that sank near Baton Rouge, Louisiana, and the chemical began flowing down the Mississippi River toward the Gulf of Mexico. Although state health officials did not push the panic button, noting that they did not anticipate too much trouble from the accident, the U.S. Coast Guard warned downriver communities to keep a close surveillance on their water supply systems, particularly if intakes were close to the river bottom (chloroform is heavier than water)."

Based on the low flow conditions and the time history of the chloroform concentra-

tion much of the chloroform (of specific gravity 1.5) was initially deposited on the river bed. Determine the fate of the chloroform during the first few days following the spill. The following processes are considered:

- Dissolution into the main body of the water
- Diffusion and sorption into the bottom sediments
- Volatilization into the atmosphere
- Sorption to suspended sediments.

Since chloroform is highly volatile and does not have a strong tendency to sorb to solids, volatilization is an important process controlling its fate, while sorption is not. The following analysis substantiates this statement.

The data pertinent to the spill are (Thibodeaux, 1979; Neely et al., 1976):

River flow rate = 7590 m<sup>3</sup>/sec (268,000 cfs)

Width of river = 1220 m = 4000 ft

River velocity = 56.3 cm/sec = 1.85 ft/sec

Water depth = 11 m = 36.3 ft

Diffusion coefficient of chloroform in water =  $1 \times 10^{-5}$  cm<sup>2</sup>/sec

Length of spill zone = 180 m = 590 ft

Background chloroform concentration = 5 ppb.

Using a Manning's n of 0.03, the diffusion layer thickness is:

$$\delta = \frac{11.6 \times 1.49 \times .915 \times 10^{-5}}{\sqrt{32.2 \times 1.85 \times 0.03}} \times (36)^{1/6} = 9 \times 10^{-4} \text{ ft} = 2.8 \times 10^{-2} \text{ cm}$$

The average concentration of chloroform in the water just below the spill zone during the period of dissolution is:

$$C_L = (5 \times 10^{-3} - 8200) \exp\left(\frac{-1. \times 10^{-5} \times 180}{2.8 \times 10^{-2} \times 11. \times 56.3}\right) + 8200$$

$$= 850 \text{ ppb}$$

In order to estimate the time required to dissolve the chloroform the average width of the spill zone is required. The width is estimated to be 256 ft (78 m) (Thibodeaux, 1981).

Based on these data the dissolution time is:

$$T_d = \frac{0.9 \times 1.75 \times 10^6}{5.38 \times .850 \times 1.85 \times 156 \times 36.3} = 20 \text{ days}$$

The factor 0.9 is used in the above expression because about 10 percent of the spill dissolved before ever reaching the bottom (Neely et al. , 1976).

The amount of chloroform which diffused and sorbed into the sediments

during this time period (20 days) will be estimated. The porosity of the sandy bottom is approximately 0.35, and the partition coefficient is assumed to be 1.0. This is a realistic value based on  $K_{ow} = 93$  (see Table II-5). The total mass contained in the sediments after 20 days is:

$$M_{Total} = .35 (180 \times 78) \left(1 + 2.65 \times 1 \times \frac{.65}{.35}\right) 8200 \sqrt{\frac{4.10^{-5} \times 20 \times 86400}{1 \times 2.65 \times 1 \times \frac{.65}{.35}}} \times 10^{-2-3} \times (5-4.437) \approx 6000 \text{ kg}$$

6000 kg is less than 2 percent of the total mass which reaches the bottom (715,000 kg). Based on this result, it is not likely that the dissolution period is markedly affected by diffusion of the chloroform into the bottom sediments. Because of the vertical concentration gradient that has been established in the sediment profile, some of the chloroform will temporarily continue to diffuse downward after the dissolution period. Hence concentrations in the water column due to resorption of the chloroform and upward diffusion back into the water column are not likely to be high compared to those observed during the initial dissolution period.

Following the chloroform spill, chloroform concentrations were measured at several locations in the Mississippi River below the spill. Figure IV-55a shows the time history of the chloroform concentration at a location 16.3 miles below the spill for the first 60 hours following the spill. A more compressed time scale is shown in Figure IV-55b and illustrates how the concentrations varied for 20 days following the spill. The peak concentration passes very rapidly (on the order of 1 day) and the maximum observed concentration is about 365 ppb. At this location, the chloroform is approximately well-mixed with the river at this point (Neely et al., 1976).

Based on Figure IV-55b the total amount of chloroform passing the location can be estimated as follows:

$$\text{Mass} = \int CQdt = Q \int Cdt$$

The right-most integral is simply the area under the concentration-time curve in Figure IV-55b. Without showing the calculations, the total mass of chloroform (above background) which passes the location 16.3 miles below the spill is about 300,000 kg. Since the total amount of chloroform spilled was about 800,000 kg, more than half of the chloroform was unaccounted for. It is unlikely, as earlier calculations showed, that diffusion and sorption into the bottom sediment was significant. Volatilization could be important and will be discussed shortly.

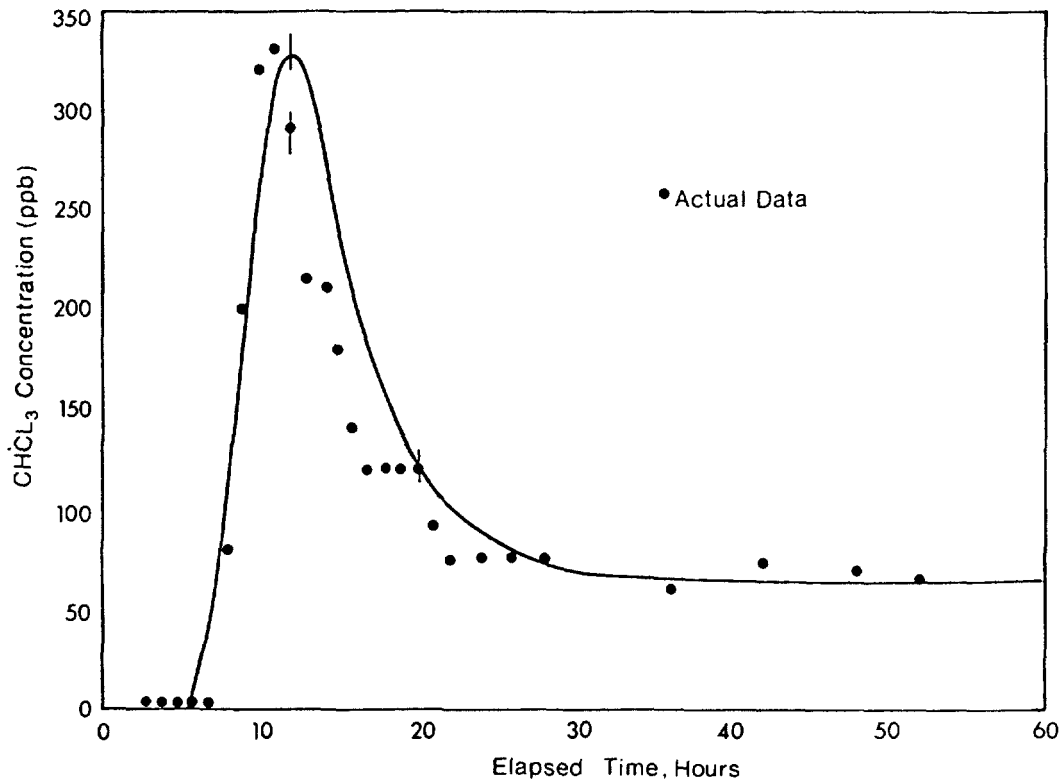


FIGURE IV-55A CHLOROFORM CONCENTRATION IN WATER COLUMN FOR FIRST 60 HOURS FOLLOWING A SPILL 16.3 MILES UPSTREAM.

The observed results shown in Figure IV-55a are compared against those predicted in this example. A concentration of 850 ppb was predicted just below the spill site; the maximum shown in Figure IV-55a is 365 ppb. It is expected, for several reasons, that the concentrations 16.3 miles below the spill site will be less than at the spill site. First it is probable that additional dilution occurred as the chloroform was transported to the sampling site. An estimate of the dilution can be attained by multiplying the river width by the spill width, or:

$$\frac{4000}{260} = 15$$

The well-mixed concentration becomes:

$$\frac{850}{15} = 60 \text{ ppb}$$

Comparing this to Figure IV-55a, it is noted that this value approximates the average concentration following an elapsed time of about 20 hours, but misses the peak during the first 20 hours. There may be a number of factors responsible for



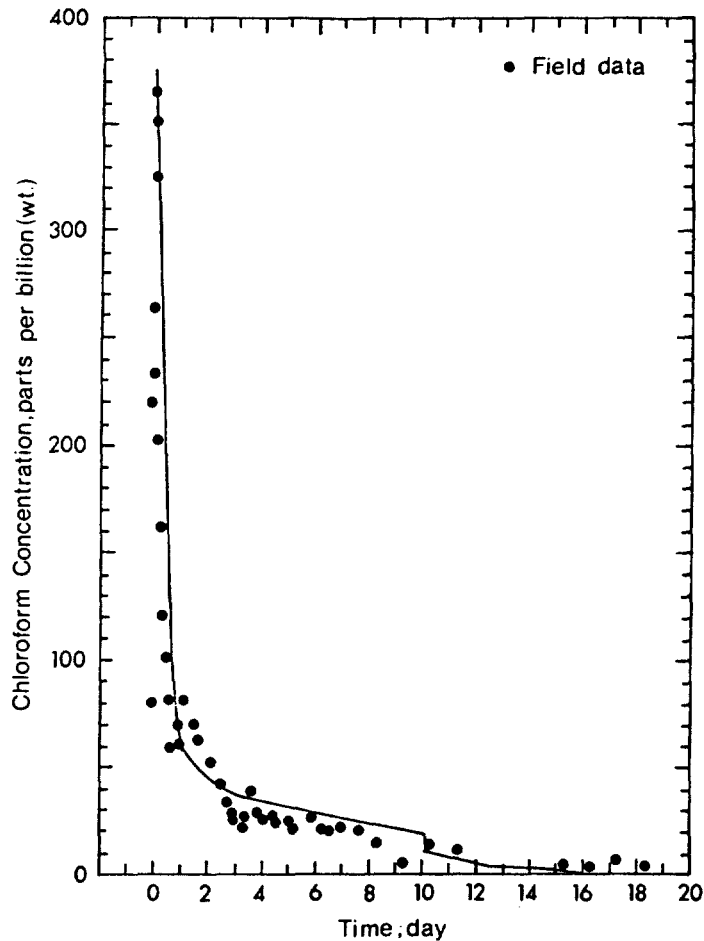


FIGURE IV-55B CHLOROFORM CONCENTRATION IN THE MISSISSIPPI RIVER AT A LOCATION 16.3 MILES BELOW THE AUGUST 19, 1973 SPILL.

this behavior, and one of the most important will be examined here. During the spill of chloroform, it was estimated that about 10 percent, or 80,000 kg were transported downstream directly without ever reaching the river bottom. The travel time to the sampling site is:

$$\frac{16.3 \text{ mi}}{1.26 \text{ mph}} = 13 \text{ hours}$$

Figure IV-55a shows that this coincides with the arrival of the peak at mile 16.3. The peak concentration can be estimated using Equation IV-140 presented earlier. The diffusion coefficient is approximately  $210 \text{ m}^2/\text{sec}$  (Mc Quivey et al., 1976) for the lower Mississippi River. The predicted peak in concentration at mile 16.3 is:

$$C = \frac{80000 \times 10^3}{2 \times 4000 \times 36.3 \times (.3048)^2 \sqrt{\pi \cdot 210 \cdot 3600 \cdot 13}} = 520 \text{ ppb}$$

This concentration is somewhat higher than the maximum 365 ppb observed, but this is to be expected since Equation IV-140 assumes the mass is input instantaneously, while in reality about 8 hours elapsed. Further if the concentration due to the dissolved portion of the spill is calculated at 20 hours, a concentration of 15 ppb is obtained. This illustrates that the mass due to initial dissolution has almost passed the sampling location, and the remaining contribution to the elevated concentrations measured is due largely to dissolution of chloroform which has settled on the river bottom. It appears that there are two basic phenomena which account for the measured concentration-time profile: an initial period of dissolution of chloroform (less than 1 day) before it settles to the bottom, and a subsequent period (10 to 15 days) of dissolution of settled chloroform.

The absence of an adequate mass balance between the amount of chloroform which entered the river as a result of the spill and the amount which passed a location 16.3 mi below the spill has not been addressed. Volatilization losses could be one reason for the imbalance.

Equation IV-123 can be used to estimate the volatilization losses. Since the chloroform was initially deposited on the bottom of the river, during a portion of the travel distance it was not in contact with the atmosphere, and so volatilization could not occur. The approximate travel time for vertical mixing to occur is (Fischer et al., 1979):

$$t = \frac{0.4 H^2}{\epsilon_z}$$

where

H = water depth

$\epsilon_z$  = vertical diffusivity.

Choosing an  $\epsilon_z$  value of 50 cm<sup>2</sup>/sec, based on Fischer et al. (1979) and a depth of 11 m, the travel time required to effect vertical mixing is:

$$t = \frac{0.4 (1100)^2}{50 \cdot 3600} \text{ hr} = 2.7 \text{ hrs}$$

Based on a velocity of 1.85 ft/sec, the travel distance is about 3.3 miles. Hence the pollutant is in contact with the atmosphere for about 13 miles.

Since only the dissolved phase of chloroform volatilizes, the fraction of the total chloroform as solute will be estimated using Equation IV-109:

$$C = \frac{C_t}{1 + K_p S}$$

The partition coefficient  $K_p$  was estimated as 1.0. The sediment concentration is about 400 ppm. Hence:

$$\frac{C}{C_t} = \frac{1}{1 + 1 \times 400 + 10^{-6}} \approx 1.0$$

Thus, essentially all the chloroform is dissolved and is available for volatilization.

Henry's Law constant for chloroform can be found based on the data in Table 11-5:

Vapor pressure = 150 Torr

Volubility in water = 8200 ppm

Molecular weight = 118.

Henry's Law constant is:

$$\frac{150 \times 118}{760 \times 8200} = 3 \times 10^{-3} \frac{\text{atm} \cdot \text{m}^3}{\text{mole}}$$

From Table 11-15 a typical volatilization rate is about 17 cm/hr.

The average chloroform concentrations for the 13 miles above the data collection point are:

200 ppb for 1 day

40 ppb for the next 9 days

10 ppb for the next 9 days.

The total amount of chloroform volatilized is (using Equation 1B-109):

$$\begin{aligned} & \Sigma k_v C_i A_c \Delta t \\ & = 0.17 \times 24 \times 1200 \times 21 \times 10^3 (200 + 40 \times 9 + 10 \times 9 - 5 \times 19) \times 10^3 \\ & = 5.8 \times 10^7 \text{ g} = 58000 \text{ kg} \end{aligned}$$

Hence, all of the unaccounted for chloroform (about 480,000 kg) could not have volatilized within 13 miles.

Over 50 percent of the chloroform still remains unaccounted for. It is possible that other transformation processes were operative. The environmental fate of chloroform in terms of photolysis, hydrolysis, oxidation, and biological degradation was reviewed in Callahan et al., 1979. It was concluded that these processes are of minor importance compared to volatilization and so are probably not significant here.

It is possible that the samples of chloroform shown in Figure IV-55b were not cross-sectional averages. The chloroform concentration could have been weighted toward the stream bottom or toward one side. A dye study performed by Mc Quivey (1976) on the lower Mississippi River showed that 50 miles were required before complete mixing was attained, while the sampling was conducted 16.3 miles below the spill. Even though chloroform does not sorb strongly, there is a possibility that the suspended solids and bed load concentration near the bottom of the river were high enough to cause substantial sorption. Based on the evidence there is a distinct possibility that some of the "missing" chloroform was actually advected past the sampling locations without being detected.

END OF EXAMPLE IV-19

## 4.10 METALS

### 4.10.1 Introduction

#### 4.10.1.1 Background

In addition to organic chemicals, metals comprise a second major category of toxic contaminants which are discharged into rivers. Metals differ from toxic organics in a number of ways, and these differences influence the approach used to predict their fate. One difference is that metals are naturally occurring elements and their fate can be detailed individually since the number of different elements is relatively small. In contrast, an individualized approach is not always feasible for the thousands of organic toxicants. However, basic properties of many organic chemicals have been tabulated or are derivable which can be used to predict their fate.

Two, organic chemicals are occasionally spilled into rivers because many of the chemicals are transported in large volumes. Metals, on the other hand, most often enter rivers from continuous sources. Consequently, methods to handle spills, while being an integral part of the screening procedures presented for organic toxicants in the previous section, are not emphasized here.

Three, metals are naturally occurring and are cycled throughout the environment by biogeochemical processes. Consequently it is not appropriate to arbitrarily ignore background concentrations of metals, an approach reasonable for synthetic organic toxicants. Background sources of metals can produce concentrations which, in certain instances, approach water quality standards.

Four, the fate of many metals is predominantly controlled by transport processes since they generally do not degrade, volatilize, or photolyze as do many organic toxicants (although there are exceptions). However, metals do speciate into many different forms in the aquatic environment, and the species may differ in toxicity and behavior.

#### 4.10.1.2 Organization

Screening methods presented in Section 4.10.3 can be used to predict the fate of metals. These tools assume that metals are distributed between two basic phases: dissolved and adsorbed. Linear partitioning is used to represent equilibrium adsorption and thus to quantitatively relate the two phases.

In Section 4.10.4, a detailed analysis of the speciation of arsenic, cadmium, chromium, copper, lead, mercury, nickel, silver, and zinc (As, Cd, Cr, Cu, Pb, Hg, Ni, Ag, and Zn, respectively) is presented. The major processes affecting speciation are delineated, and the equilibrium model MINEQL is used to predict the speciation of the above solutes for 14 different rivers and an acidified lake in the United States.

Simulated metal concentrations vary from background to well above the 1984 U.S. EPA water quality criteria.

While the tools presented in Section 4.10.3 can be used independently of metal species distribution predicted by MINEQL, the two approaches can be coupled together to estimate species concentrations at different locations throughout a river. The steps required to accomplish this are described at the end of Section 4.10.4.

Because of the potential importance of background contributions of metals, methods are presented in Section 4.10.2 to address this problem. Since background sources can be significant, this contribution should not be arbitrarily dismissed.

Numerous case studies of metals in rivers in the eastern and western United States are also reviewed. The reviews may help the user to understand how metals respond to different aquatic conditions and to establish concentration ranges which have been documented in past studies.

Finally, in Section 4.10.5, guidance is provided for a limited field sampling program and river/stream reconnaissance. A primary reason for suggesting a low-level data collection program is a concession to the difficulty of predicting metal concentrations in rivers. Although users are not required to perform a field study before doing the screening analyses, in some instances they may decide a limited field study is appropriate.

The data requirements for the screening methods are summarized in Table IV-80 of Section 4.10.5. Because degradation or removal rates are not required for the screening analyses, the data requirements are somewhat more modest than for organic toxicants. The more important data are flow rates, loading rates, background levels, and partition coefficients. Section 4.10.5 provides more discussion on the relative importance of the data requirements. A summary of the screening methods for metals is shown in Figure IV-56. An application and summary of the methods has recently been published (Mills and Mok, 1985). Also, many of the algorithms presented in Section 4.10 have been programmed for microcomputers (Mills, et al., 1985).

#### 4.10.2 Water Quality Criteria, Background Concentrations, and Case Studies

##### 4.10.2.1 Water Quality Criteria

Table IV-41 summarizes the most current U.S. EPA criteria (Federal Register July 29, 1985 and November 28, 1980) for the protection of freshwater aquatic life for arsenic, cadmium, chromium, copper, lead, mercury, nickel, silver, and zinc. The 1984 criteria pertain to arsenic, cadmium, chromium, copper, lead, and mercury. The 1980 criteria pertain to nickel, silver, and zinc. Many of the criteria depend on water hardness. Examples are shown in the table for hardnesses of 50, 100, and 200 mg/l as  $\text{CaCO}_3$ . At the bottom of the table, expressions relating hardness to the water quality criteria are shown. Note that the water quality criteria are expressed as total dissolved metal.

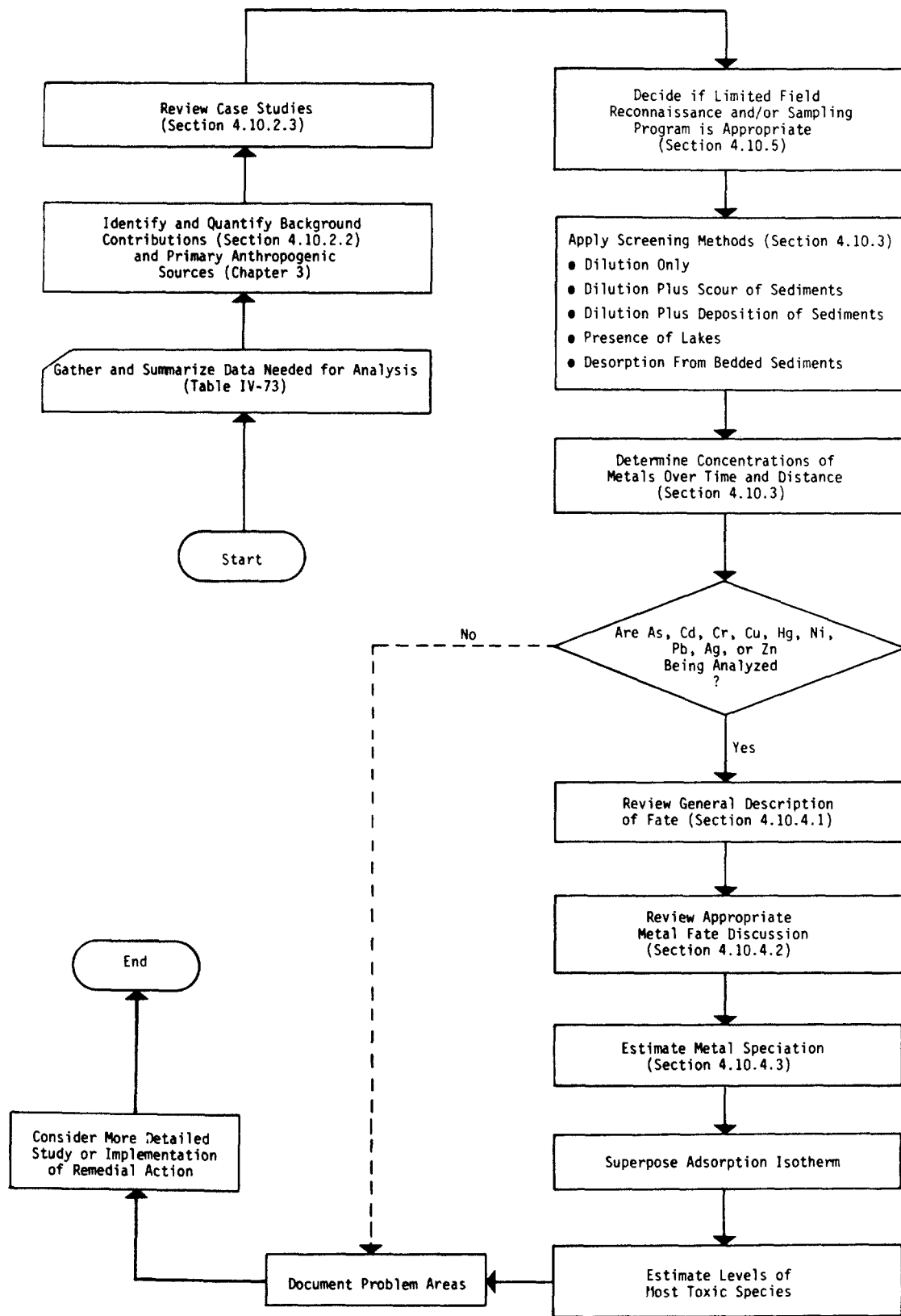


FIGURE IV-56 SUMMARY OF SCREENING PROCEDURES FOR METALS IN RIVERS

TABLE IV-41

WATER QUALITY CRITERIA FOR SELECTED PRIORITY METALS FOR  
PROTECTION OF FRESHWATER AQUATIC LIFE  
(1980 and 1985 U.S. EPA Criteria)

Total Dissolved Metal <sup>a</sup>	4 day Average Concentration Not to Be Exceeded More Than Once Every 3 Years <sup>b,c</sup>	1 hour Average Concentration Not to Be Exceeded More Than Once Every 3 Years <sup>b,c</sup>
Arsenic (trivalent inorganic)	190	360
Cadmium	0.66, 1.1, <b>2c</b>	1.8, 3.9, <b>8.6c</b>
Chromium (hexavalent)	11	16
Chromium (trivalent)	120, 210, <b>370c</b>	980, 1700, <b>3100c</b>
Copper	6.5, 12, <b>21c</b>	9.2, 18, <b>34c</b>
Lead	1.3, 3.2, <b>7.7c</b>	34, 83, <b>200c</b>
Mercury	0.012	2.4
Nickel	56, 96, <b>160c</b> (30 day average)	1100, 1800, <b>3100c</b> (instantaneous maximum)
Silver		1.2, 4.1, <b>13c</b> (instantaneous maximum)
Zinc	<b>47</b> (30 day average)	180, 320, <b>570c</b> (instantaneous maximum)

<sup>a</sup>The total dissolved metal is defined to be "acid soluble". No approved methods are presently available. The total recoverable method is recommended.

<sup>b</sup>The water quality criteria (g/l) are related to water hardness (mg/l as  $\text{CaCO}_3$ ) as:

Arsenic: independent of hardness

Cadmium =  $\exp(0.7852(\ln(\text{hardness})) - 3.49)$ , 4-day average  
 $\exp(1.128(\ln(\text{hardness})) - 3.828)$ , 1-hour average

Chromium (VI): independent of hardness

Chromium (III) =  $\exp(0.819(\ln(\text{hardness})) + 1.56)$ , maximum, 4-day average  
 $\exp(0.819(\ln(\text{hardness})) + 3.688)$ , 1-hour average

Copper =  $\exp(0.8548(\ln(\text{hardness})) - 1.465)$ , 4-day average  
 $\exp(0.9422(\ln(\text{hardness})) - 1.464)$ , 1-hour average

Lead =  $\exp(1.266(\ln(\text{hardness})) - 4.661)$ , 4-day average  
 $\exp(1.266(\ln(\text{hardness})) - 1.416)$ , 1-hour average

Mercury: independent of hardness

Nickel =  $\exp(0.76(\ln(\text{hardness})) + 1.06)$ , 30-day average  
 $\exp(0.76(\ln(\text{hardness})) + 4.02)$ , maximum at any time

Silver =  $\exp(1.72(\ln(\text{hardness})) - 6.52)$ , maximum at any time

Zinc =  $\exp(0.83(\ln(\text{hardness})) + 1.95)$ , maximum at any time

<sup>c</sup>The three water quality criteria are examples for total hardness levels of 50, 100, and 200 mg/l as  $\text{CaCO}_3$ .

#### 4.10.2.2 Background Levels of Metals

##### 4.10.2.2.1 Introduction

In contrast to most organic toxicants which are not initially present in the environment, metals occur naturally and cycle by biogeochemical processes throughout the environment. Consequently, of the metals that may be present in a stream or river, a small fraction, a moderate fraction, or nearly all might be from natural sources.

When trace metal concentrations in streams are analyzed to see whether water quality standards are violated, and whether wasteload allocation schemes are required, a knowledge of background sources should be included as a part of the analysis. Background sources can be defined to include both natural sources and sources produced by man which are transported across watershed boundaries (e.g. dry deposition of metal-enriched ash). Background sources can also be thought of as sources which are not readily controllable, and thus contributions from these sources are likely to be present regardless of the remedial action chosen.

In this section, coverage of background sources is limited to weathering from rocks and riparian soils. Typical values of metal concentrations are provided. However, metals are not uniformly distributed throughout the environment but can be locally enriched in natural deposits. Should a river intersect a mineral deposit, the levels of metals in the stream from this source can be high. Contributions of background sources can be quantified by sampling upstream of the locations of major anthropogenic influence.

##### 4.10.2.2.2 Stream Contributions From Rocks and Soils

Tables IV-42 and IV-43 summarize data which show typical concentrations of metals and inorganic in soils and rocks. The soil samples from New Jersey and New York in Table IV-42 are generally similar to average concentrations in the earth's crust. However, deviations can occur locally, so these numbers should be used with caution. Soil Conservation Service soil surveys might provide data on levels of metals in local soils. Chapter 3 also provides additional data.

Concentrations of metals in streams from the background sources can be estimated from the following formula:

$$C_b = x \cdot S \cdot 10^{-3} \quad (\text{IV-155})$$

where

x = metals concentration in soils,  $\mu\text{g/g}$

S = background instream suspended solids concentration, mg/l

$C_b$  = total metal concentration in the stream due to the soil and rock particles in suspension and may include a dissolved component,  $\mu\text{g/l}$ .

As an example, suppose a stream has a background suspended solids level of 40 mg/l.

Based on a typical zinc concentration of 80  $\mu\text{g/g}$  in soils,



TABLE IV-42  
 TYPICAL CONCENTRATIONS OF METALS IN SEVERAL SOILS  
 AND IN THE EARTH'S CRUST  
 (Values in  $\mu\text{g/g}$ )

Metal	Soils in New Jersey <sup>a</sup>	Soils in Upstate New York <sup>b</sup>	Average in Earth's Crust <sup>c</sup>
Ag	--	--	0.5
As	--	--	5.0
Cd	--	0.2	0.15
Cr	9.3	--	10. -100.
Cu	40.5	21.6	4. -55.
Hg	--	--	0.005. -1.0
Ni	11.9	--	80.
Pb	86.8	7.9	15*
Zn	96.3	79.9	50.

<sup>a</sup>Kubota et al. (1974).

<sup>b</sup>Wilber and Hunter (1979).

<sup>c</sup>Weast (1977).

$$C_b = 40 \cdot 80 \cdot 10^{-3} = 3 \mu\text{g/l of zinc}$$

This is less than 10 percent of the U.S. EPA criteria level of 47  $\mu\text{g/l}$  (Table IV-41). However, for some of the other metals (e.g. copper), typical contributions from background sources can approach the 30-day criteria.

For a number of the metals (Cr, Cu, Ni, Pb, and Zn), background levels of about 1  $\mu\text{g/l}$  are common. For Ag, Cd, and Hg, background levels are probably closer to 0.1  $\mu\text{g/l}$ , or even less.

#### 4.10.2.3 Case Studies of Metals in Rivers

##### 4.10.2.3.1 Introduction

This section provides a sampling of case studies of metals in rivers. Case studies help to reveal important master variables which control the fate of metals.

TABLE IV-43  
 AVERAGE CONCENTRATION OF METALS IN VARIOUS TYPES OF ROCK  
 AND DEEP OCEAN SEDIMENTS  
 (Values in  $\mu\text{g/g}$ )

Plutonic					
	Granitic				
	Ultramafic	Basaltic	Plagioclase	Orthoclase	Syenite
Chromium	$1.6 \times 10^3$	170	22	4.1	30
Manganese	$1.62 \times 10^3$	$1.5 \times 10^3$	540	370	850
Iron	$9.4 \times 10^4$	$8.65 \times 10^4$	$2.64 \times 10^4$	$1.42 \times 10^4$	$3.67 \times 10^4$
Cobalt	150	48	7	1.0	1
Nickel	$2.0 \times 10^3$	130	15	4.5	4
Copper	10	87	30	10	5
Zinc	50	105	60	39	132

	Sedimentary Rock			Deep Ocean Sediments	
	Shale	Sandstone	Carbonate	Carbonate	Clay
Chromium	90	35	11	11	90
Manganese	850	100	$1.1 \times 10^3$	$1.0 \times 10^3$	$6.7 \times 10^3$
Iron	$4.72 \times 10^4$	$9.8 \times 10^3$	$3.8 \times 10^3$	$9.0 \times 10^3$	$6.5 \times 10^4$
Cobalt	19	0.3	0.1	7	74
Nickel	68	2.0	20	30	225
Copper	45	1	4	30	250
Zinc	95	16	20	35	165

From: Rubin, 1976.

Since there are potentially many processes which influence the behavior of metals in aquatic systems (see Section 4.10.4.1), elimination of processes of secondary importance is beneficial in screening analyses.

Some of the questions which users are likely to pose during a fate analysis are:

- Is downstream transport of metals important? That is, do metals move downstream in the water column significant distances below their points of entry or are they rapidly deposited and/or adsorbed in the bedded sediments so that water column concentrations are rapidly depleted?
- Are the metals in the water column present in adsorbed or dissolved form? Dissolved species are likely to be more toxic and can be transported further than the particulate form of the metal.
- What is the relationship between water column concentrations and concentrations in the bedded sediments? Metal concentrations in bedded sediments are often found to far exceed those in the water column.
- What metals are typically present in rivers in the highest concentrations?
- What is the effect of a reservoir (or large backwater region) on the metal concentrations further downstream?
- Is metal resorption from bottom sediments likely to occur as a result of decreased water column concentrations? Resorption is a natural cleansing mechanism, but may also take a significant period of time (e.g. 1 to 5 years for several stream miles). During the period of resorption, a low level of metal is maintained in the water column.

A review of case studies often provides insights into resolving these questions, and others which arise during the course of a study. Methods to address each of these questions are presented in Section 4.10.3, and general qualitative answers to these questions are provided in Section 4.10.3.3.

Before discussing individual case studies, the U.S. Geological Survey's NASQAN network is briefly mentioned. Through the USGS's National Stream Quality Accounting Network (NASQAN), water quality samples are collected at approximately 345 stations throughout the United States (Briggs and Ficke, 1977). Among the quality parameters measured are arsenic, cadmium, chromium, copper, lead, mercury, selenium, and zinc. The data contained in Briggs and Ficke (1977) are summarized in Tables IV-44 and IV-45.

Note that the upper limits of the measured concentrations for cadmium, chromium, copper, lead, and zinc are, at times, close to U.S. EPA criteria for instantaneous maximum levels (see Table IV-41). The upper levels measured for mercury occasionally exceed the suggested criteria of 4.1  $\mu\text{g/l}$  (instantaneous maximum). These results suggest that cadmium, chromium, copper, lead, zinc, and mercury often require careful investigation on a site-by-site basis.

TABLE IV-44

RANGES OF CONCENTRATIONS OF DISSOLVED MINOR ELEMENTS MEASURED AT NASQAN STATIONS DURING THE 1975 WATER YEAR, SUMMARIZED BY WATER RESOURCES REGIONS (Briggs and Ficke, 1977)<sup>a</sup>

Region Number and Name	Range of Concentrations ( $\mu\text{g/l}$ )									
	Arsenic (As)	Cadmium (Cd)	Chromium (Cr)	Copper (Cu)	Lead (Pb)	Mercury (Hg)	Selenium (Se)	Zinc (Zn)		
01 New England	0.0-3 <sup>b</sup>	0.0-10	0.0-20	0.0-20	0.0-45	0.5	0.0-1	0.0-40		
02 Mid-Atlantic	.0-3	.0-5	.0-70	.0-30	.0-42	.0-1.3	.0-2 <sup>b</sup>	.0-130		
03 South Atlantic-Gulf	.0-3	.0-7	.0-11	.0-18	.0-73	.0-2.0	.0-1	.0-100		
04 Great Lakes	.0-5	.0-5	.0-20	.0-24	.0-35	.0-1.1	.0-3	.0-80		
05 Ohio	.0-5	.0-23 <sup>b</sup>	.0-10 <sup>b</sup>	.0-100	.0-34	.0-0.5	.0-2	.0-260		
06 Tennessee	.0-2	.0-2	.0-1	1-8	.0-9	.0-0.3	.0	.0-40		
07 Upper Mississippi	.0-5	.0-5	.0-10	.0-20	.0-38	.0-1.2	.0-3	.0-190		
08 Lower Mississippi	.0-4	.0-190	.0-10	.0-25	.0-10	.0-0.5	.0-2	.0-90		
09 Souris-Red-Rainy	.0-7	.0-2	.0-10	.0-13	.0-6	.0-0.2	.0-2	.0-30		
10 Missouri Basin	.0-65	.0-8	.0-40	.0-320	.0-16	.0-9.0	.0-6 <sup>b</sup>	.0-360		
11 Arkansas-White-Red	.0-10	.0-8	.0-20	.0-80	.0-50	.0-8.2 <sup>b</sup>	.0-25	.0-460		
12 Texas-Gulf	.0-17	.0-1	.0-30	.0-8	.0-34	.0-0.3	.0-7	.0-210		
13 Rio Grande	.0-13	.0-1	.0-20	.0-12	.0-20	.0-1.0	.0-2	.0-60		
14 Upper Colorado	.0-18	.0-2	.0-40	1-46	.0-23	.0-0.6	.0-16	.0-70		
15 Lower Colorado	.0-20	.0-3	.0-20	.0-35	.0-12	.0-0.4	.0-13	.0-70		
16 Great Basin	.0-48	.0-1	.0-20	.0-11	.0-6	.0-1.8	.0-4	.0-40		
17 Pacific Northwest	.0-11	.0-10	.0-40 <sup>b</sup>	.0-30	.0-43	.0-0.3	.0-1	.0-300		
18 California	.0-32	.0-3	.0-40	.0-80	.0-48	.0-1.6	.0-4	.0-150		
19 Alaska	.0-4	.0-1	.0-30	1-10	.0-10	.0-1.8	.0-1	.0-80		
20 Hawaii	.0-8	.0-1	.0-10	.0-5	.0-11	.0-0.2	.0-1 <sup>b</sup>	.0-20		
21 Caribbean	.0-1	.0-5	.0-1	.0-34 <sup>b</sup>	.0-17 <sup>b</sup>	.0-0.3	.0	.0-40		

<sup>a</sup>Figure IV-90 shows the locations of these regions.

<sup>b</sup>The maximum concentration shown exceeds the maximum total metal concentration reported in Table IV-45. No explanation is provided in Briggs and Ficke.

TABLE IV-45  
RANGES OF TOTAL CONCENTRATIONS OF MINOR ELEMENTS MEASURED AT NASQAN STATIONS DURING THE 1975 WATER YEAR,  
SUMMARIZED BY WATER RESOURCES REGIONS (Briggs and Ficke, 1977)<sup>a</sup>

Region Number and Name		Range of Concentrations (µg/l)								
		Arsenic (As)	Cadmium (Cd)	Chromium (Cr)	Copper (Cu)	Lead (Pb)	Mercury (Hg)	Selenium (Se)	Zinc (Zn)	
01	New England	0.0-2 <sup>b</sup>	0.0-18	0.0-70	0.0-30	0.0-100	0.0-1.1	0.0-2	0.0-150	
02	Mid-Atlantic	.0-9	.0-1	.0-70	.0-30	.0-57	.1-1.3	.0-1 <sup>b</sup>	.0-190	
03	South Atlantic-Gulf	.0-50	.0-50	.0-50	.0-40	.0-100	.0-2.2	.0-3	.0-440	
04	Great Lakes	.0-11	.0-20	.0-20	.0-170	.0-100	.0-1.1	.0-3	4-320	
05	Ohio	.0-6	.0-22 <sup>b</sup>	.0-20 <sup>b</sup>	.0-110	.0-250	.0-1.2	.0-3	.0-600	
06	Tennessee	.0-5	.0-13	.0-10	3-40	2-130	.0-0.9	.0-2	10-80	
07	Upper Mississippi	.0-31	.0-20	.0-40	.0-460	1-200	.0-2.1	.0-3	10-380	
08	Lower Mississippi	.0-14	.0-840	.0-160	.0-120	.0-200	.0-0.5	.0-4	.0-230	
09	Souris-Red-Rainy	.0-10	<10-20	.0-20	<10-60	<100-200	.0-0.6	.0-2	6-110	
10	Missouri Basin	.0-2300	.0-40	.0-250	.0-610	1-600	.0-11	.0-5 <sup>b</sup>	.0-1900	
11	Arkansas-White-Red	.0-240	.0-40	.0-290	2-550	.0-400	.0-1 <sup>b</sup>	.0-34	.0-870	
12	Texas-Gulf	.0-200	<10-50	.0-120	<10-180	<100-200	.0-1.2	.0-8	.0-710	
13	Rio Grande	.0-140	.0-30	.0-150	<10-210	<100-500	.0-1.7	.0-7	.0-920	
14	Upper Colorado	.0-56	<10-20	.0-140	<10-1400	<100-200	.0-0.6	.0-21	20-690	
15	Lower Colorado	1-110	<10-20	.0-90	<10-480	<100-300	.0-0.8	.0-14	.0-470	
16	Great Basin	.0-50	.0-40	.0-20	.0-270	<100-300	.0-2.6	.0-4	.0-580	
17	Pacific Northwest	.0-20	.0-20	.0-10 <sup>b</sup>	.0-2300	<100	.0-1.5	.0-4	.0-360	
18	California	.0-220	.0-30	.0-1100	.0-4500	<100-300	.0-1.1	.0-4	.0-1600	
19	Alaska	.0-11	<10	.0-20	10-140	<100	.0-2.2	.0-1	10-90	
20	Hawaii	.0-10	<10	.0-60	.0-1000	<100-200	.0-0.9	.0-2 <sup>b</sup>	10-110	
21	Caribbean	.0-2	.0-20	10	.0-29 <sup>b</sup>	.0-15 <sup>b</sup>	.0-0.3	.0	.0-170	

<sup>a</sup>Figure IV-90 shows the locations of these regions.

<sup>b</sup>The maximum concentration shown is less than the maximum dissolved concentration reported in Table IV-44. No explanation is provided in Briggs and Ficke.

#### 4.10.2.3.2 Case Studies

The following case studies illustrate a range of metal concentrations which are present in rivers and streams in the United States. The case studies are summarized in Table IV-46. A number of different source types are represented.

##### 4.10.2.3.2.1 Flint River, Michigan

The Flint River study in Michigan (Dellos et al., 1983) provides a detailed account of the fate of zinc, cadmium, and copper in the river. Results of the study are used in Section 4.10.3 to compare against predictions made by the analytical screening procedures in this document.

During the Flint River study, zinc, cadmium, and copper were analyzed in a 60 km (37 mile) stretch of the river. Data were collected in August 1981, December 1981, and March 1982. The watershed is both agricultural and urban. Two wastewater treatment plants provide the main sources of metals within the study reach (in addition to the flux of metal across the upstream boundary).

Table IV-47 summarizes the reported average metal concentrations and average suspended solids levels. The metal concentrations shown in the table are the range of averages at the locations sampled (typically 5 to 9 stations in the 60 km reach). Zinc and cadmium levels are generally below the criteria levels of 47  $\mu\text{g/l}$  and 2.0  $\mu\text{g/l}$ , respectively, and copper is near its criterion level.

In most cases, the levels of metals in the water column do not decrease substantially with distance downstream. Figure IV-57 illustrates the total and dissolved copper levels during the August 1981 survey. Wastewater discharges are present at km 41 and km 71. Only minor sources are present between these locations.

##### 4.10.2.3.2.2 Chattanooga Creek, Tennessee

Chattanooga Creek is tributary to the Tennessee River and is 42 km (20 miles) in length. The basin is significantly industrialized and contains 18 permitted industrial sources, as well as agricultural and domestic discharges. Past studies indicate that the creek is degraded by both conventional and toxic pollutants. The September 1980 study of Milligan et al. (1981) report that the creek is contaminated with organic and inorganic toxicants. Their findings related to metals are summarized here.

Figure IV-58 shows the 12 sampling locations selected in the lower 16 km of the creek. The priority metals detected in the water column and in the sediments are summarized in Table IV-48. The metal concentrations are generally indicative of contaminated conditions. Mercury levels in the water column (0.3 to 0.9  $\mu\text{g/l}$ ) are above the 1984 U.S. EPA criteria for the protection of aquatic life (0.2  $\mu\text{g/l}$  for chronic toxicity). Chromium and zinc levels are near their criteria limits. Levels in the water column appear to be fairly constant over distance. As noted by Milligan

Table IV-46

## SUMMARY OF CASE STUDIES

Location	Source of Metal	Metals	Concentrations Measured in Water?	Concentrations in Bed?	EPA Chronic Criteria Exceeded?	Downstream Transport Important?
Flint River, MI	wastewater	Zn, Cd, Cu	Yes	No	No	Yes
Chattanooga Creek, TN	industrial	Cr, Hg, Zn, As,	Yes	Yes	Hg, Zn	Yes
North Fork Holston River, VA	chloralkali plant	Hg	Yes	Yes	Hg	Yes
Slate River, CO	mine drainage	As, Cd, Cr, Cu, Pb, Ni, Ag, Zn	Yes*	No	As, * Cd, * Cu*	Yes
Saddle River, NJ	urban	Pb, Zn, Cu, Ni,	No	Yes	--	not documented
Cayuga Watershed, NY	rural	Pb, Cd, Zn, Cu	Yes	No	No	not documented

\* Acute criteria exceeded.

TABLE IV-47  
SUMMARY OF METAL AND SUSPENDED SOLIDS CONCENTRATIONS IN FLINT RIVER, MICHIGAN

Study Period	Suspended Solids (mg/l)	Zinc (µg/l)			Cadmium (µg/l)			Copper (µg/l)		
		Total	Particulate	Dissolved	Total	Particulate	Dissolved	Total	Particulate	Dissolved
August 1981	4.-13.	8.-24.	6.-20.	4.-12.	0.05-0.16	0.04-0.1	0.02-0.12	2.5-8.	1.-4.	2.-4.
December 1981 (Run 1)	8.-15.	5.-14.	2.-11.	4.-14.	0.05-0.15	0.02-0.08	0.00-0.15	2.-5.	1.-2.	2.-4.
December 1981 (Run 2)	6.-22.	6.-30.	2.-22.	2.-8.	0.02-0.13	0.01-0.08	0.00-0.08	2.-15.	1.-7.	1.-3.
March 1982	16.-24.	7.-17.	4.-8.	4.-6.	0.02-0.06	0.01-0.02	0.00-0.02	2.2-5.2	0.5-1.5	2.-2.5



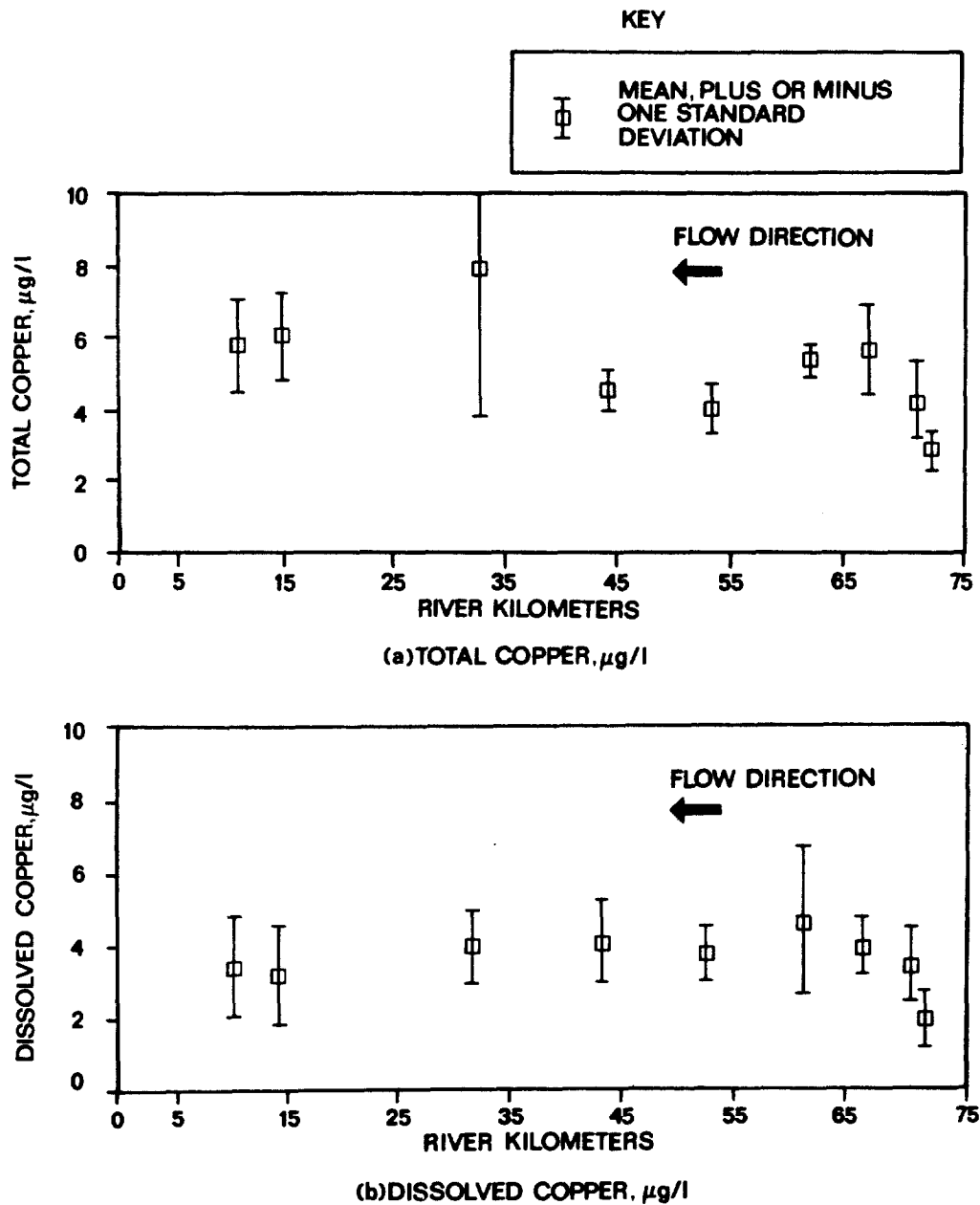


FIGURE IV-57 MEASURED TOTAL AND DISSOLVED COPPER CONCENTRATIONS IN FLINT RIVER, MICHIGAN, DURING AUGUST 1981 SURVEY.

et al. (1981), the levels of metals in the sediments are from 2 to 50 times higher than levels measured in the Tennessee River sediments, which suggest that the source of metal contamination in Chattanooga Creek is local.

#### 4.10.2.3.2.3 North Fork Holston River, Virginia

Wastes from an inactive chloralkali plant closed in 1972 and located on the North Fork Holston River continue to contaminate both the water column and bottom

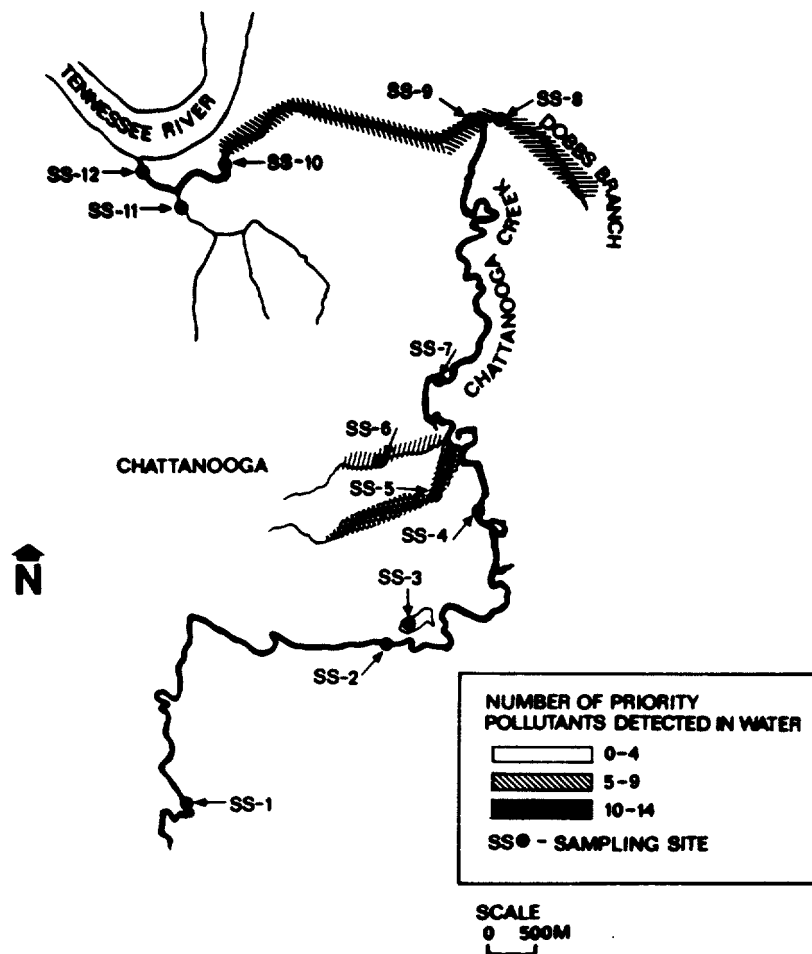


FIGURE IV-58 EXTENT OF PRIORITY POLLUTANT CONTAMINATION IN CHATTANOOGA CREEK WATERS.

sediments of the river (Turner and Lindberg, 1978). The river is a fast-flowing mountain stream with a coarse, rocky substrate in many areas, but with silt and clay substrates in backwater regions.

Two large settling ponds at the plant site drain into the river and provide the source of contamination. Upstream of the ponds the levels of mercury are low. Below the plant, the levels increase significantly, as shown in Table IV-49. Upstream of the plant, the mercury in the water column averages  $0.008 \mu\text{g/l}$ , while downstream, the average is  $0.15 \mu\text{g/l}$ , a 20-fold increase. Approximately a third of the mercury below the discharge is in dissolved form.

Plots of total mercury in the water column versus distance below the waste discharge were developed by Turner and Lindberg for low and high flow rates. They are shown in Figure IV-59. They plotted predicted levels of mercury versus distance, assuming that the mercury behaves conservatively in the water column. At high flow, the mercury appears to be conservative while at low flow rates, some loss of mercury

TABLE IV-48

INORGANIC PRIORITY POLLUTANTS DETECTED IN CHATTANOOGA CREEK, SEPTEMBER 1980

Compound	Station Number and Chattanooga Creek Mile												
	1	2	3	4	5	6	7A	7B	8	9	10	11	12
	9.1	6.6	Pond (6.3)	5.2	(4.5)	(4.5)	(4.15)	(4.15)	(2.2)	2.1	0.6	Unnamed Tributary (0.3)	0.1
Chromium, total	-	-	-	142.	-	-	-	-	-	-	-	-	-
Mercury, total	0.3	0.3	0.3	0.3	0.8	0.9	0.5	0.4	0.9	0.9	0.4	0.5	0.3
Zinc, total	19.	31.	29.	22.	55.	140.	24.	23.	52.	30.	38.	40.	43.
Water Column Samples (µg/l)													
Arsenic, total	0.2	4.1	3.0	13	13.0	8.5	2.0	2.4	2.	4.	1.7	1.2	1.2
Beryllium, total	0.295	0.56	0.48	0.5	0.6	0.7	0.7	0.7	0.5	0.5	0.3	0.4	0.8
Cadmium, total	--	-	-	1.7	1.7	-	-	-	1.2	0.4	1.9	4.0	2.4
Chromium, total	21.	20.	33.	98.	110.	76.	24.0	37.	35.	59.	25.0	12.0	26.0
Copper, total	2.4	8.6	6.7	140.	27.4	11.7	7.4	8.2	32.9	28.6	33.0	48.0	33.0
Lead, total	7.04	26.	21.	66.	37.	38.	10.	16.	232.	106.	140.	250.	150.
Mercury, total	0.85	0.98	0.49	240.	64.4	3.5	0.01	0.9	1.8	2.3	0.24	1.8	0.88
Nickel, total	10.3	23.	12.	18.	7.0	11.0	10.	11.	16.	21.	13.0	20.1	14.5
Selenium, total	-	-	-	-	-	2.5	-	-	-	-	-	-	-
Silver, total	-	-	-	1.0	0.6	-	-	-	0.6	0.4	1.7	1.6	1.7
Zinc, total	25.	45.	29.	230.	83.0	62.	37.	46.	234.	154.	380.	1,100.	340.
Sediment Samples (µg/g)													
Arsenic, total	0.2	4.1	3.0	13	13.0	8.5	2.0	2.4	2.	4.	1.7	1.2	1.2
Beryllium, total	0.295	0.56	0.48	0.5	0.6	0.7	0.7	0.7	0.5	0.5	0.3	0.4	0.8
Cadmium, total	--	-	-	1.7	1.7	-	-	-	1.2	0.4	1.9	4.0	2.4
Chromium, total	21.	20.	33.	98.	110.	76.	24.0	37.	35.	59.	25.0	12.0	26.0
Copper, total	2.4	8.6	6.7	140.	27.4	11.7	7.4	8.2	32.9	28.6	33.0	48.0	33.0
Lead, total	7.04	26.	21.	66.	37.	38.	10.	16.	232.	106.	140.	250.	150.
Mercury, total	0.85	0.98	0.49	240.	64.4	3.5	0.01	0.9	1.8	2.3	0.24	1.8	0.88
Nickel, total	10.3	23.	12.	18.	7.0	11.0	10.	11.	16.	21.	13.0	20.1	14.5
Selenium, total	-	-	-	-	-	2.5	-	-	-	-	-	-	-
Silver, total	-	-	-	1.0	0.6	-	-	-	0.6	0.4	1.7	1.6	1.7
Zinc, total	25.	45.	29.	230.	83.0	62.	37.	46.	234.	154.	380.	1,100.	340.

TABLE IV-49

MERCURY CONCENTRATIONS IN WATER, SUSPENDED MATTER, AND BED SEDIMENTS  
IMMEDIATELY UPSTREAM AND DOWNSTREAM OF FORMER CHLORALKALI PLANT  
ON NORTH FORK HOLSTON RIVER

Statistic	Water Column ( $\mu\text{g/l}$ )		Suspended	Bottom
	Total Hg	Dissolved Hg	Particulate Hg ( $\mu\text{g/g}$ )	Sediment Hg <sup>a</sup> ( $\mu\text{g/g}$ )
<u>Upstream</u>				
Mean	0.008	0.001	0.41	0.13
Standard Deviation	0.004	--	0.17	0.03
Number Samples	10.	9.	7.	7.
<u>Downstream</u>				
Mean	0.15	0.05	7.6	19.3
Standard Deviation	0.05	0.02	3.8	1.2
Number Samples	11.	11.	10.	3.

<sup>a</sup>Silt-clay fraction only.

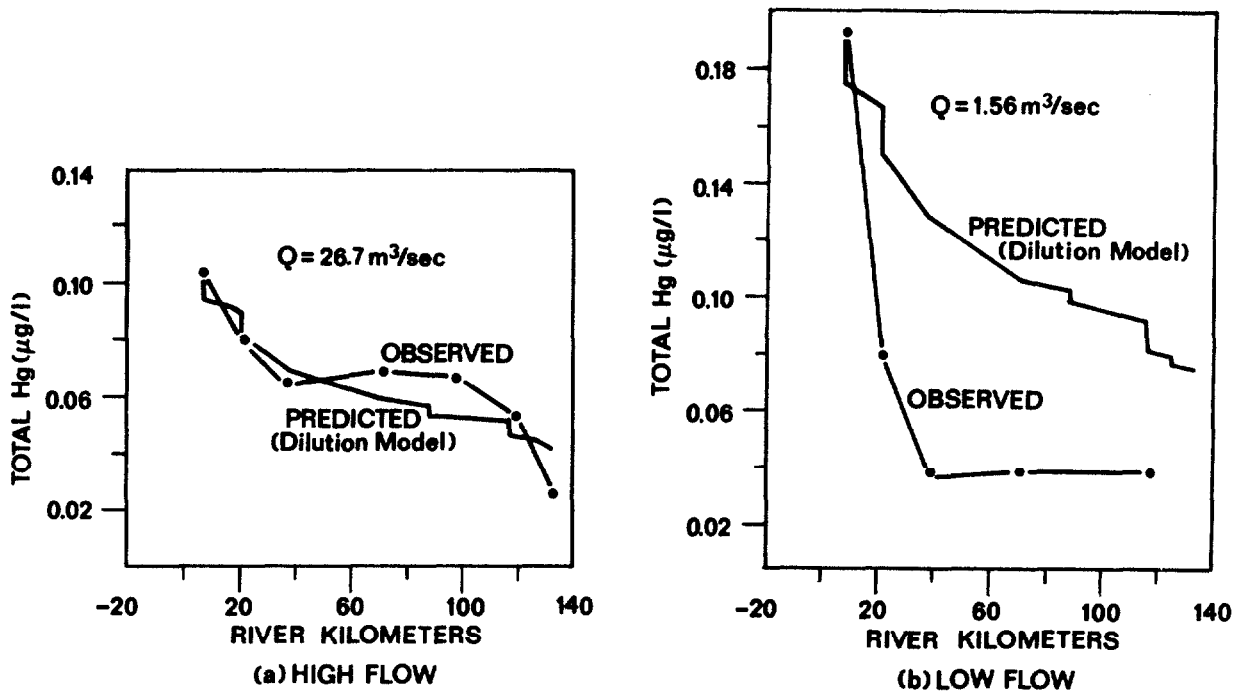
from the water column is evident. In both cases, however, mercury is transported far downstream (120 km) in significant concentrations.

Further down the river, at km 155 (not shown in the figure), is a large impoundment - Cherokee Lake. Much of the suspended sediments settle in this lake and take the adsorbed mercury with them. Mercury in the surficial sediments ranges from about 0.47  $\mu\text{g/g}$  to **2.4  $\mu\text{g/g}$** . These levels are expected based on the levels of mercury found in the suspended matter in the North Fork Holston River (Table IV-49).

#### 4.10.2.3.2.4 Slate River, Colorado

Slate River, Colorado, is one of a number of rivers and creeks (see Table IV-50) investigated in a cooperative effort by U.S. EPA's Environmental Monitoring Systems Laboratory, Las Vegas, Nevada. The purpose of the investigations was to study degradation and recovery of biological communities in streams where the toxic metal concentrations exceed the U.S. EPA's 1980 recommended acute criteria for aquatic life. The Slate River study is summarized here as an example (Janik et al., 1982).

Figure IV-60 shows the station locations on the Slate River and its tributary, Coal Creek, where drainage from the Keystone Mine enters the creek. Locations



REFERENCE: TURNER AND LINDBERG, 1978.

FIGURE IV-59 COMPARISON OF OBSERVED AND PREDICTED MERCURY CONCENTRATION CALCULATED FROM A DILUTION MODEL FOR THE NORTH FORK HOLSTON RIVER.

sampled on the Slate River include a control station (034), two stations in the Impact zone downstream of Coal Creek (035, 036) and two stations in the recovery zone (037, 038) .

Table IV-51 shows average concentrations at each station and the water quality criteria. The criteria are exceeded for arsenic, cadmium, copper, silver, and zinc. There is generally some decrease in the level of total metals from the impact zone to the recovery zone, although statistical tests reported by Janik, *et al.* , indicate that analytical variation or field replicate variation may be an important reason for the difference. Even so, water quality criteria are exceeded in the recovery zone as well as in the impact zone.

Janik *et al.* (1982) also indicate that a large percentage (generally 75 to 100 percent) of the metals are transported in the dissolved fraction. While suspended solid levels are not reported, these results do, in a general sense, appear to be contradictory to the findings of other investigations.

TABLE IV-50

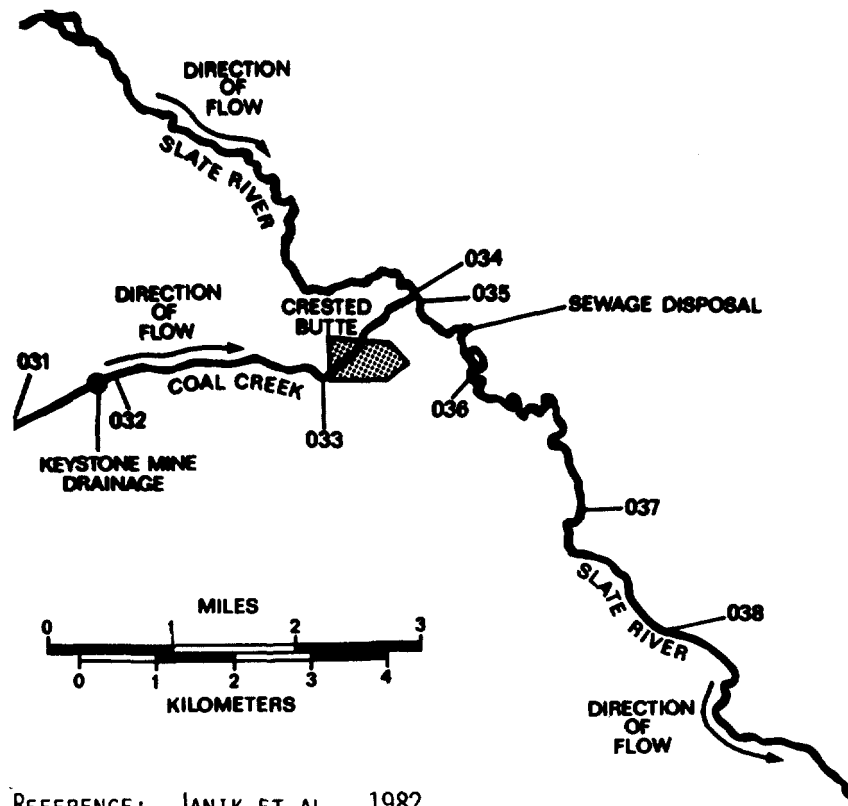
STREAMS SELECTED FOR 1980 U.S. EPA FIELD SURVEYS AND METALS  
ANTICIPATED TO BE PRESENT IN EXCESS OF U.S. EPA RECOMMENDED  
AQUATIC LIFE CRITERIA

Major Pollution Source	
Stream	Metal(s)
<u>Mining</u>	
Prickly Pear Creek, Montana	Copper, Zinc, Cadmium
Silver Bow Creek, Montana	Copper, Cadmium, Zinc
Slate River, Colorado	Copper, Zinc, Silver, Cadmium
Tar Creek, Oklahoma	Zinc, Cadmium, Silver, Lead
Red River, New Mexico	Copper, Cadmium
<u>Industrial</u>	
Leon Creek, Texas	Chromium, Nickel
Little Mississippi River, Indiana	Lead, Chromium
<u>Public-Owned Treatment works (POTW)</u>	
Bird Creek, Oklahoma	Arsenic, Selenium
Cedar Creek, Georgia	Chromium, Silver
Maple Creek, South Carolina	Chromium
Irwin Creek, North Carolina	Chromium, Zinc, Nickel, Lead
Blackstone River, Massachusetts	Cadmium, Lead
Mill River, Ohio	Nickel
Cayadutta Creek, New York	Chromium, Cadmium
White River, Indiana	Copper
References: Janik <u>et al.</u> (1982).	

4.10.2.3.2.5 Saddle River, New Jersey

The Saddle River near Lodi, New Jersey was investigated to determine the impact of urbanization on the levels of heavy metals in the bottom sediments of the river (Wilber and Hunter, 1979). The study area encompasses a distance of about 13 km (8 mi). The lower 8 km (5 mi) are dominated by nonpoint sources of runoff from the city of Lodi. Industries and municipalities do not discharge directly into this section of the river. Further upstream, however, two wastewater treatment plants discharge their effluent.

The average heavy metal concentrations in the sediments of the river are shown in Table IV-52. Ninety-six sediment samples from 18 cores were taken. The priority metals analyzed are lead, zinc, copper, nickel, chromium, and cadmium. The tabulations indicate a general enrichment of each of the priority metals in the lower



REFERENCE: JANIK ET AL., 1982.

FIGURE IV-60 STATION LOCATIONS ON COAL CREEK AND SLATE RIVER, COLORADO.

urbanized Saddle River. Average enrichment factors (concentrations in the lower river divided by concentrations in the upper river) are 6.7 for Pb, 3.5 for Zn, 3.1 for copper, 2.8 for nickel, 5.1 for chromium, and 5.2 for cadmium. The results appear to indicate that the urban nonpoint sources have increased concentrations of metals in the river's sediments.

The heavy metal concentrations were subdivided by bedded sediment particle size. The results are shown in Table IV-53 for sizes ranging from coarse sand to clay. Generally the concentrations increase with decreasing particle size. However; on a total mass basis, most of the metals are associated with the larger particles because the silt-clay fraction comprises only 1 percent of the solids by weight.

#### 4.10.2.3.2.6 Cayuga Lake Basin, New York

The water of 12 streams tributary to Cayuga Lake, New York were sampled for the priority metals lead, cadmium, zinc, and copper (Kubota et al., 1974). A number of the streams flow predominantly through rural countryside and others flow through the City of Ithaca. Sample collection focused on periods of high and low streamflow from March through August 1970.

TABLE IV-51

COMPARISON OF MEAN TOTAL CONCENTRATIONS OF SELECTED METALS ( $\mu\text{g/l}$ )  
IN THE SLATE RIVER VERSUS U. S. EPA CALCULATED ACUTE WATER QUALITY  
CRITERIA FOR AQUATIC LIFE

	Stations				
	Control	Impact		Recovery	
	034	035	036	037	038
Hardness (mg/l)	55.	61.	68.	71.	75.
Total Arsenic (Detection Limit = 110.0)					
Actual ( $\bar{X}$ )	658.9	1069.7	936.5	776.6	617.6
1980 Criterion	440.	440.	440.	440.	440.
Total Cadmium (Detection Limit = 7.5)					
Actual ( $\bar{X}$ )	ND*	13.2	10.2	8.1	9.6
1980 Criterion	2.	2.	2.	2.	2.
Total Chromium (Detection Limit = 5.0)					
Actual (X)	9.2	9.8	7.7	7.6	12.4
1980 Criterion**	21.	21.	21.	21.	21.
Total Copper (Detection Limit = 11.0)					
Actual ( $\bar{X}$ )	11.0	38.8	24.0	16.6	15.6
1980 Criterion	13.	14.	15.	16.	17.
Total Lead (Detection Limit = 120.0)					
Actual ( $\bar{X}$ )	ND	ND	ND	ND	ND
1980 Criterion	83.	95.	107.	113.	122.
Total Nickel (Detection Limit = 9.0)					
Actual (X)	46.5	95.4	72.9	43.8	45.2
1980 Criterion	1174.	1270.	1374.	1418.	1485.
Total Silver (Detection Limit = 12.0)					
Actual ( $\bar{X}$ )	12.4	17.7	ND	ND	ND
1980 Criterion	1.	2.	2.	2.	2.
Total Zinc (Detection Limit = 9.0)					
Actual ( $\bar{X}$ )	55.8	1068.3	1005.2	744.5	430.4
1980 Criterion	196.	214.	233.	241.	254.

\*ND = Nondetectable.

\*\*

Criteria are for hexavalent chromium.



TABLE IV-52  
METAL CONCENTRATIONS IN BOTTOM SEDIMENTS OF SADDLE RIVER,  
NEW JERSEY, AND IN ADJACENT SOILS

River Mile	Metal Concentration ( $\mu\text{g/g}$ )							
	Pb	Zn	Cu	Ni	Cr	Cd	Mn	Fe
	Upper Saddle River							
16.6	38.6	84.2	28.9	6.5	6.5	0.4	197.4	8439
8.2	12.6	66.4	20.5	6.4	3.6	0.4	111.0	5956
	Lower Saddle River							
5.6	163.5	247.6	60.3	17.5	24.6	1.7	200.2	12872
1.3	152.4	275.1	61.5	15.2	17.8	1.6	185.2	11092
0.5	200.0	269.8	104.8	22.3	34.9	2.9	164.0	14565
	Adjacent Soils in Watershed							
N/A	86.8	96.3	40.5	11.9	9.3	not measured	145.0	12300

Data of Wilber and Hunter (1979).

Table IV-54 summarizes the levels of dissolved and particulate lead in the water column. The concentrations of soluble lead in the rural streams do not differ appreciably from concentrations in the streams flowing through urbanized areas. Particulate and dissolved levels of cadmium, zinc, and copper also do not reflect an impact from urbanization (Tables IV-55 and IV-56). The observed levels of trace elements in these streams appear to reflect predominantly natural background sources.

#### 4.10.2.3.2.7 Additional Studies

Numerous other studies of metals in rivers can be found throughout the literature. Of the various priority metals, mercury appears to be the most widely studied. Some of the remaining literature on metals in rivers is briefly summarized here.

Mercury distribution in the Ottawa River, Canada, has been studied and reported by a number of researchers, including Ramamoorthy and Rust, 1976; Kudo *et al.*, 1977;

TABLE IV-53  
 AVERAGE HEAVY METAL CONCENTRATIONS BY PARTICLE SIZE  
 FOR SEDIMENTS OF THE SADDLE RIVER, NEW JERSEY  
 ( $\mu\text{g/g}$ )

Particle Size ( $\mu$ )	River Mile	Pb	Zn	Cu	Ni	Cr	Cd
420-1000 (coarse sand)	16.6	15	22	11	4	5	ND*
	8.2	<b>9</b>	<b>42</b>	<b>7</b>	<b>4</b>	3	0.2
	<b>5.6</b>	<b>310</b>	<b>388</b>	<b>206</b>	<b>20</b>	<b>29</b>	2.0
	<b>0.5</b>	482	413	252	28	<b>46</b>	4.0
250-420 (medium sand)	16.6	23	30	11	4	5	ND
	8.2	13	<b>28</b>		4	3	0.3
	<b>5.6</b>	16	<b>63</b>	<b>10</b>	<b>6</b>	5	0.5
	<b>0.5</b>	90	119	44	<b>12</b>	<b>15</b>	1.0
125-250 (fine sand)	16.6	45	48	14	4	6	0.1
	8.2	18	34	12	5	5	0.5
	<b>5.6</b>	11	35	6	4	<b>4</b>	0.3
	<b>0.5</b>	91	135	29	11	<b>12</b>	0.9
63-125 (very fine sand)	16.6	126	125	81	<b>14</b>	18	1.4
	8.2	349	440	3180	<b>169</b>	34	3.4
	5.6	113	155	31	11	15	1.3
	0.5	173	251	44	21	27	1.3
5.8-63 (silt)	16.6	360	420	735	60	41	5.2
	8.2	1127	3298	1222	202	127	14.5
	<b>5.6</b>	259	389	151	23	<b>33</b>	<b>7.9</b>
	<b>0.5</b>	582	661	258	46	<b>43</b>	<b>6.9</b>
0.15-5.8 (fine to coarse clay)	16.6	860	917	1017	72	201	<b>7.2</b>
	8.2	3073	3365	12221	559	321	27.9
	5.6	816	1320	417	<b>99</b>	126	30.6
	0.5	1940	2348	1042	<b>189</b>	563	26.9
0.01-0.15 (very fine clay)	16.6	1894	2159	2272	ND	530	37.9
	8.2	13372	21279	84302	2907	1337	290.7
	5.6	1476	4715	1145	488	610	120.0
	0.5	2747	4680	1364	444	852	84.0

\* ND = Nondetectable.

Kudo et al., 1975; and in the Proceedings of the International Conference on Transport of Persistent Chemicals in Aquatic Ecosystems, 1974. Much of the research on mercury in rivers deals with adsorption and desorption between the bedded sediments and the water column.

Jenne (1972) summarizes concentrations of mercury in rivers throughout the United States. The U.S. Geological Survey provides a compilation of papers on

TABLE IV-54  
LEAD CONCENTRATIONS IN STREAMS TRIBUTARY TO CAYUGA LAKE, NEW YORK

Sample Source	Soluble $\mu\text{g/l}$			Particulate Fraction, $\mu\text{g/l}$		
	No. Samples With Detectable Amounts <sup>a</sup>	Mean <sup>b</sup>	Maximum	No. Samples With Detectable Amounts	Mean	Maximum
Primarily rural						
Canoga	4/8	1.17	2.67	5/8	1.37	2.06
Great Gully	6/8	0.62	1.33	8/8	1.38	6.17
Little Creek	4/7	0.57	1.00	6/7	0.66	1.85
Shel drake	5/8	0.42	0.67	7/8	1.39	2.62
Taughannock	5/8	0.74	1.00	8/8	1.57	4.01
Salmon	5/9	2.99	16.1	8/9	0.91	2.62
Inlet	8/9	0.66	1.33	8/9	1.89	6.17
Buttermilk	3/8	0.40	0.67	6/8	1.45	3.09
Urbanized						
<b>Trumansburg<sup>c</sup></b>	4/8	1.11	1.67	7/8	3.94	7.41
Six Mile	6/9	0.73	1.33	8/9	3.14	8.23
Cascadilla	5/9	0.50	1.00	9/9	3.88	6.99
Fall Creek	7/9	0.93	2.67	7/9	2.91	8.33

Source: Kubota *et al.*, 1974.

<sup>a</sup>Samples with detectable amounts/total number of samples.

<sup>b</sup>Means are given for detectable amounts.

<sup>c</sup>Sampling site located below sewage treatment plant.

mercury (1970) and lead (1976) in the environment. The U.S. Geological Survey (1970) also has summarized data on selected trace elements (arsenic, cadmium, hexavalent chromium, lead, zinc, and mercury) in surface waters in the United States.

Finally, the U.S. Environmental Protection Agency has published a series of documents that review the environmental effects of pollutants. Among the pollutants reviewed are chromium (Towill *et al.*, 1978), lead (Bell *et al.*, 1978), and cadmium (Hammons *et al.*, 1978).

#### 4.10.3 Analytical Models for Fate Prediction of Metals in Rivers

##### 4.10.3.1 Introduction

Figure IV-61 illustrates a number of important processes which influence the fate of metals in rivers. Consider an example where effluent from the pond in the

TABLE IV-55  
SUMMARY OF CADMIUM, ZINC, AND COPPER IN PARTICULATE CARRIED  
BY TRIBUTARY STREAMS OF CAYUGA LAKE

Stream	Cadmium, $\mu\text{g/l}$		Zinc, $\mu\text{g/l}$		Copper, $\mu\text{g/l}$	
	No. Samples With Detectable Amounts <sup>a</sup>	Mean <sup>b</sup>	No. Samples With Detectable Amounts	Mean	No. Samples with Detectable Amount	Mean
Primarily rural						
Canoga	5/8	0.09	8/8	6.40	8/8	1.69
Great Gully	6/8	0.06	8/8	10.28	8/8	1.35
Little Creek	1/7	$\leq 0.05$	6/7	2.91	7/7	1.72
Shel drake	7/8	0.09	8/8	5.48	8/8	1.11
Taughannock	7/8	0.11	8/8	6.95	8/8	1.46
Salmon	6/9	0.10	9/9	3.94	9/9	1.37
Inlet	4/9	0.13	8/9	10.71	9/9	3.37
Buttermilk	5/8	0.10	7/8	8.96	8/8	1.64
Urbanized						
Trumansburg <sup>c</sup>	5/8	0.09	8/8	9.45	8/8	1.30
Six Mile	4/9	0.21	8/8	10.05	9/9	5.92
Cascadilla	6/9	0.10	8/8	14.67	9/9	2.43
Fall Creek	5/9	0.44	8/9	14.29	9/9	2.89

Source: Kubota et al., 1974.

<sup>a</sup>Samples with detectable amounts/total number of samples.

<sup>b</sup>Means are given for detectable amounts.

<sup>c</sup>Sampling site located below sewage treatment plant.

figure overflows into the river. The main objective of predictive analyses for metals is normally to find their concentration distributions with distance, and possibly with time (i.e., to find  $C_1$ ,  $C_2$ ,  $C_3$ , and  $C_4$  as depicted in the figure). Once metals enter a river, they begin to adsorb to particles suspended in the water column and to particles in the river bed. Eventually, the bed can become contaminated with metals at depths below the sediment-water interface ranging from a few millimeters to many centimeters. If the flow rate in the river were to increase enough, the shear force exerted by the moving water on the bed would be sufficient to scour metal-contaminated solids back into the water column. In zones where velocity is significantly diminished, as in a reservoir, the metal-contaminated sediments can settle out of the water column, and establish a metal-contaminated

TABLE IV-56  
SUMMARY OF SOLUBLE CADMIUM, ZINC, AND COPPER IN  
TRIBUTARY STREAMS OF CAYUGA LAKE

Stream	Cadmium, $\mu\text{g/l}$		Zinc, $\mu\text{g/l}$		Copper, $\mu\text{g/l}$	
	No. Samples with Detectable Amounts <sup>a</sup>	Mean <sup>b</sup>	No. Samples with Detectable Amounts	Mean	No. Samples with Detectable Amounts	Mean
Primarily rural						
Canoga	6/8	0.25	8/8	7.97	8/8	0.79
Great Gully	5/8	0.07	8/8	1.88	8/8	0.40
Little Creek	3/7	0.20	7/7	2.24	7/7	0.32
Shel drake	6/8	0.10	8/8	1.61	8/8	0.53
Taughannock	4/8	0.28	8/8	1.17	8/8	0.53
Sal mon	8/9	0.10	9/9	2.27	9/9	0.51
Inlet	6/9	0.28	9/9	2.71	9/9	0.39
Buttermilk	7/8	1.10	8/8	0.83	8/8	0.54
Urbanized						
<b>Trumansburg<sup>c</sup></b>	6/8	0.07	8/8	3.20	8/8	0.77
Six Mile	6/9	0.25	9/9	1.57	8/9	0.88
<b>Cascadilla</b>	2/9	0.29	9/9	1.40	9/9	1.70
Fall Creek	7/9	0.17	9/9	3.51	8/9	0.75

Source: Kubota *et al.*, 1974.

<sup>a</sup>Samples with detectable amounts/total number of samples.

<sup>b</sup>Means are given for detectable amounts.

<sup>c</sup>Sampling site located below sewage treatment plant.

layer on the bottom. In the thin layer of contaminated sediments along the bottom, metal concentrations can be hundreds to thousands of times higher on a unit-volume basis than in water column.

Tributaries provide dilution water which can rather abruptly decrease metal concentrations. Also partitioning between the dissolved and sorbed phases can be shifted if the suspended solid concentrations or other water quality parameters are altered.

Suppose that the pond overflow in Figure IV-61 is eliminated after a period of discharge of many years. During the period of the discharge the bottom sediment on the river has probably accumulated metals. Once the metal concentrations in the water column are lowered due to elimination of the pond overflow, the metal in the bed tends to desorb back into the water column, a process which may continue (depend-

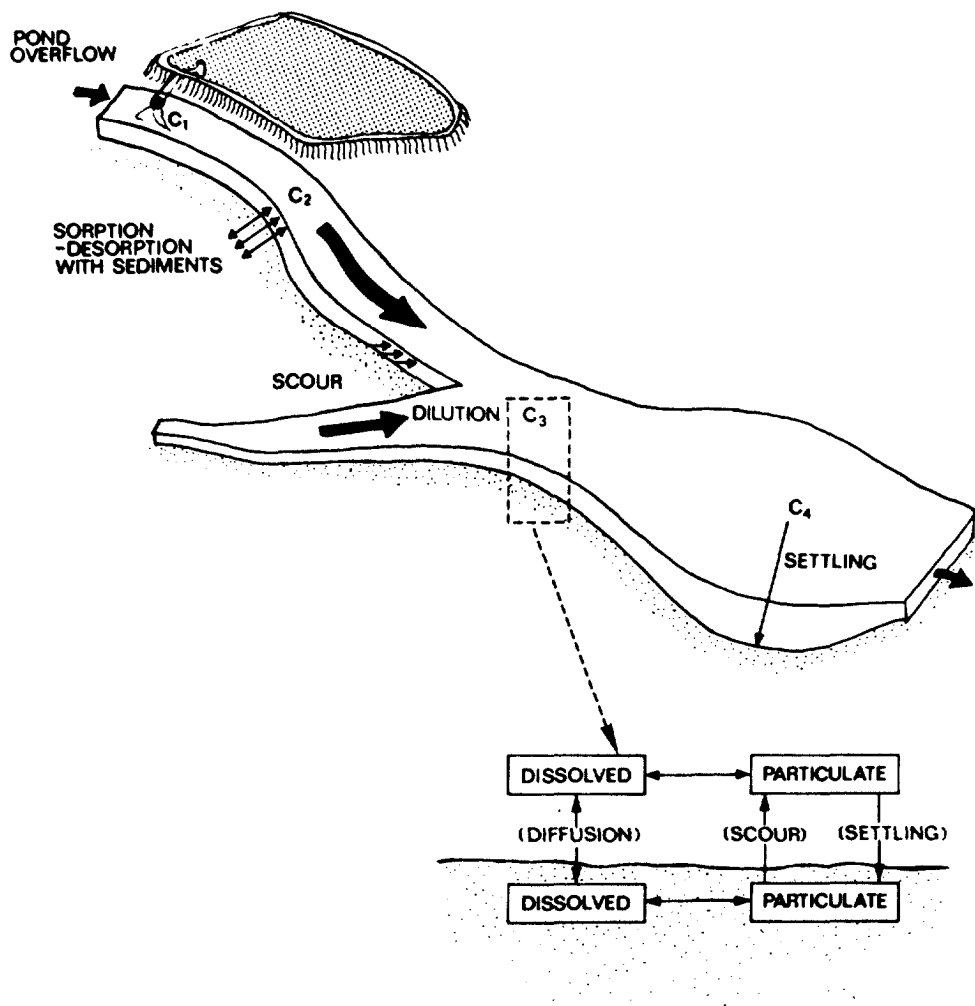


FIGURE IV-61 PHYSICAL PROCESSES INFLUENCING THE FATE OF METALS IN RIVERS

ing on the rate of resorption) for years. Thus, the recovery period of the metal-contaminated river may take considerably longer than anticipated from the point source elimination.

The tools presented in this section can be used to address the cases described above and are limited to steady-state analyses, with the exception of the method which predicts adsorption and resorption of metals on bottom sediments. The methods treat metals as pollutants with two phases: an adsorbed phase and a dissolved phase. Each approach is summarized below.

- Dilution Approach. The change in metal concentration in a river is assumed due to loading from point and nonpoint sources, and dilution with background water.
- Dilution Plus Scour or Deposition of Metal-Contaminated Sediments. Exchange of metal-contaminated sediments between the water column and river bed can alter the concentration in the water column.

- Influence of Small Lakes. Small lakes or backwater regions are often present on river systems, and potentially could be a sink of adsorbed metals which settle along with suspended solids in these quiescent regions.
- Resorption from (or Adsorption to) Bedded Sediments. Dissolved metal in the water column can be adsorbed to bedded sediments if a nonequilibrium condition exists between the bed and the water column. Similarly, resorption of particulate metal from bedded sediments may occur if metal concentrations are reduced in the water column (for example, by waste load allocation).
- Concentration Factors in Bedded Sediments. Concentrations of metals in many bedded sediments are often significantly higher than levels in the water column.

While some of the equations presented in the following sections may appear complicated, the equations are no more sophisticated than the more familiar BOD-DO analyses presented earlier in the chapter. Even the data requirements are generally less comprehensive than for dissolved oxygen analyses. However, since the methods are less familiar, they may require some study before they are fully understood.

#### 4.10.3.2 Dilution Approach

Using the dilution approach, total metal concentration (particulate plus dissolved) is simulated as a conservative pollutant. The dissolved component is estimated from the total concentration using linear partitioning:

$$C = \frac{C_T}{1 + K_p S \cdot 10^{-6}} \quad (IV-156)$$

where

$C$  = dissolved phase metal concentration,  $\mu\text{g/l}$

$C_T$  = total metal concentration,  $\mu\text{g/l}$

$S$  = suspended solids concentration,  $\text{mg/l}$

$K_p$  = partition coefficient,  $\text{cm/gm}$  (or  $\text{l/kg}$ ).

Partition coefficients are summarized later in Section 4.10.4.1.

Under the appropriate conditions the dilution approach appears to be useful for predicting metal concentrations throughout a river. Before the method is discussed, the major assumptions inherent in the procedure are reviewed. Decay or other loss processes (e.g., volatilization) are not considered. For metals this is generally a good assumption for the range of environmental conditions likely to be encountered in rivers. Even though the species distribution can change with distance (in response to a pH change, for example), total metal typically is not degraded. A second important assumption made in the dilution approach is that the metal in the water column does not interact with the river bed, either in the particulate form or in the

dissolved form. This situation is generally true when:

- The suspended solids in the river remain fairly constant with distance. If scour or deposition is significant then a net influx or loss of solids and metals may occur.
- The sources of metals to the river are fairly constant over time. If major changes in the discharge of metals occur, this can create a driving force for adsorption to (or resorption from) the bed, which then acts as an internal source or sink.

Field data of suspended solids can be reviewed to determine whether significant losses or gains of solids occur within the study reach. Alternatively, a predictive method, such as Figure IV-62, can be used. Based on the mean river velocity, the figure shows when deposition, transport, and erosion of solid particles is likely to occur. Note that the velocity when erosion occurs is significantly higher than the sedimentation velocity, except for particle sizes larger than sand (which are not of concern for metals adsorption). This means that as the stream velocity first drops below the velocity required to erode a certain size particle, the particle is not deposited, but continues to be transported unless the velocity further decreases below the sedimentation velocity.

As the figure shows, sedimentation of clays and small silts is not likely to occur in free flowing rivers, but can occur in relatively small reservoirs on the river with detention times exceeding a few days. Under such conditions the net velocity can be on the order of 0.1 cm/see, or less, and the effects of settling of particulate may be important.

While sedimentation of clays and small silts is not likely in most free flowing rivers, scour of these same sized particles is more probable. Clay is likely to be scoured at velocities near 3 fps (100 cm/see), and silts between 1 and 3 fps (30 to 100 cm/see), depending on their size. Consequently, during high flow conditions when the water is moving rapidly, bottom scour of silts and clays, and perhaps of sand is possible. If the scoured sediments are contaminated with metals then the total metal being transported will increase over distance (assuming for the moment that further dilution is negligible). Based on Figure IV-62, a fairly large envelope of stream velocities exists such that the clay and silt fractions of solids (those which adsorb most of the metals) are transported in suspension with the stream water.

Dilution models are useful for both point and nonpoint sources. While dilution models have been presented elsewhere in this document they are summarized here for ease of reference. For point sources, the concentration in a stream following mixing,  $C_{Tf}$  is:

$$C_{Tf} = \frac{C_{Tu} Q_u + C_{Tw} Q_w}{Q_u + Q_w} \quad (IV-157a)$$



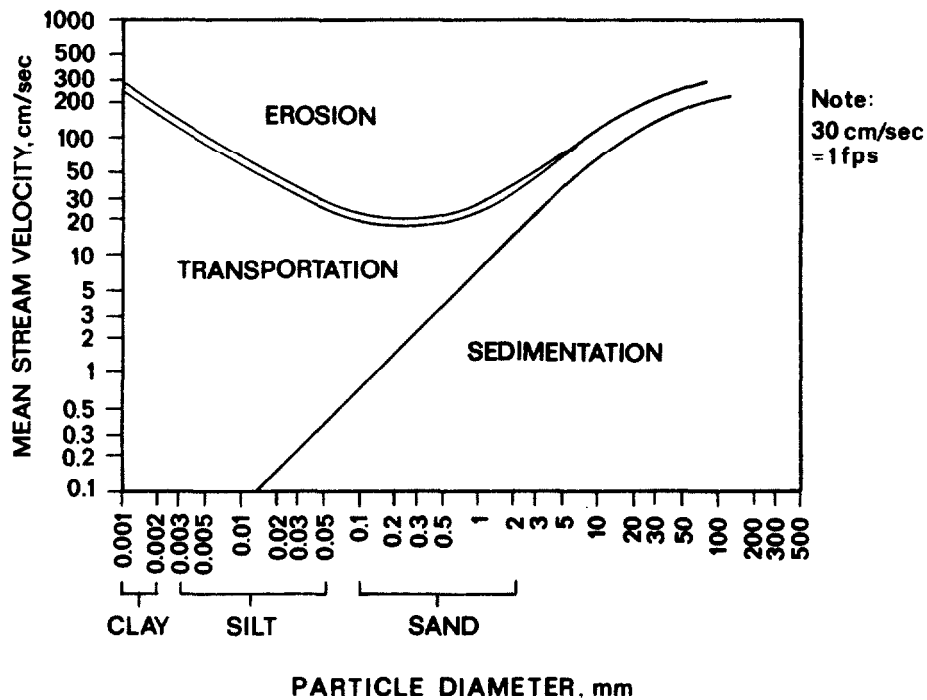


FIGURE IV-62 RELATIONSHIP BETWEEN STREAM VELOCITY, PARTICLE SIZE, AND THE REGIMES OF SEDIMENT EROSION, TRANSPORT, AND DEPOSITION (FROM GRAF, 1971),

where

$C_{Tu}$  = concentration of total metal in the river above the point source,  $\mu\text{g/l}$

$Q_u$  = flow rate in the river above the point source,  $\text{m}^3/\text{s}$  or cfs

$C_{Tw}$  = concentration of total metal in the point source,  $\mu\text{g/l}$

$Q_w$  = flow rate of the point source,  $\text{m}^3/\text{s}$  or cfs.

According to the dilution model, the metal's concentration does not change with distance downstream unless there are additional inflows as loadings of metals.

When  $C_{Tu}$  is negligible, Equation IV-157a can be rewritten as:

$$C_{Tf} = \frac{C_{Tw}}{\frac{Q_u + Q_w}{Q_w}} = \frac{C_{Tw}}{D} \quad (\text{IV-157b})$$

where

$D$  = dilution attained after mixing.

The nonpoint source representation can be written in one of two forms:

$$C_T = \frac{A_0}{A(x)} (C_{T0} - C_{Tb}) + C_{Tb} \quad (IV-158)$$

or

$$C_T = \frac{Q_0}{Q(x)} (C_{T0} - C_{Tb}) + C_{Tb} \quad (IV-159)$$

where

- $A_0$  = drainage basin area at location where  $CT = C_{T0}$ ,  $m^2$
- $A(x)$  = drainage basin area at a distance  $x$  further downstream,  $m^2$
- $C_{Tb}$  = average total metal concentration in nonpoint source (background concentration),  $\mu g/l$
- $Q_0$  = river flow rate at location where  $CT = C_{T0}$ ,  $m^3/s$  or  $cfs$
- $Q(x)$  = flow rate at a distance  $x$  further downstream,  $m^3/s$  or  $cfs$ .

In some instances these equations can be quite useful. One particularly useful feature of these equations (beyond their applicability to nonpoint sources) is that they can be applied to a series of point sources by treating the point sources as one or more equivalent nonpoint sources. For example, if a particular river has 30 small sources entering along a stretch of river, it may be more convenient for screening purposes to treat the series as an equivalent nonpoint source. Using this approach there is no need to apply the point source equation 30 times; rather the nonpoint source equation can be used once. For more details of this procedure, see Example IV-5.

The approach of treating metals as conservative pollutants is one which some investigators have considered before. Turner and Lindberg (1978) investigated the mercury distribution in the North Fork Holston River downstream from an inactive chloralkali plant (mercury cell process). Mercury was still being leached into the river at a steady rate years after the plant had closed. Turner and Lindberg plotted total mercury versus distance during both high flow and low flow conditions, and then compared the observed concentrations against predicted concentrations, assuming the mercury levels are influenced only by dilution processes. Figure IV-59 shown earlier summarizes their results. During high flow mercury acts conservatively, while during low flow mercury levels are overestimated by a factor of two to three. In both cases, however, the importance of downstream transport is apparent: much of the mercury remains in the water column either in adsorbed or dissolved form, and is advected downstream. Thus, even for a metal which adsorbs as strongly as mercury, a dilution model is able, at least under certain conditions, to provide reasonable estimates of instream concentrations of total metal.

EXAMPLE IV-20

The Flint River study described earlier (Section 4.10.2.3.2.1) provides an opportunity to test the dilution approach under a variety of hydrologic conditions. To implement the dilution approach, the data required are river and wastewater flow rates, and associated metal concentrations. The data used are summarized in Table IV-57. Two wastewater treatment plants are the largest sources of metals in the study reach. Together with the upstream contributions from the river, these three sources are assumed to comprise the total metal input to the system (the minor sources shown in Table IV-57 are neglected).

The Flint Wastewater Treatment Plant discharges at km 70.7, which is about 1.2 km below the boundary at Mill Street. After mixing, the levels of total zinc, cadmium, and copper in the river are:

Zinc:

$$Zn_T = \frac{2.66 \times 7.7 + 1.68 \times 55}{2.66 + 1.68} = 26 \mu\text{g/l}$$

Cadmium:

$$Cd_T = \frac{2.66 \times 0.067 + 1.68 \times 0.16}{2.66 + 1.68} = 0.10 \mu\text{g/l}$$

Copper

$$Cu_T = \frac{2.66 \times 2.9 + 1.68 \times 8.3}{2.66 + 1.68} = 5.0 \mu\text{g/l}$$

By ignoring the minor sources, these instream concentrations can be assumed to remain constant down to the Ragnone WWTP at km 41.1. After mixing with the effluent from the Ragnone WWTP, the instream concentrations for the metals become:

Zinc:

$$Zn_T = \frac{26 \times 4.34 + 0.69 \times 84}{4.34 + 0.69} = 34 \mu\text{g/l}$$

Cadmium:

$$Cd_T = \frac{0.10 \times 4.34 + 0.69 \times 0.54}{4.34 + 0.69} = 0.16 \mu\text{g/l}$$

TABLE IV-57  
BOUNDARY CONDITIONS AND POINT SOURCES TO FLINT RIVER  
FOR AUGUST 4-7, 1981

Source	Discharge Flow (m <sup>3</sup> s)	Discharge Concentration				
		Suspended Solids (mg/l)	Solids (kg/d)	Total Zinc (μg/l)	Total Cadmium (μg/l)	Total Copper (μg/l)
Upstream Boundary Mill Road (km 71.9)	2.66	13.5	3100.	7.7	0.067	2.9
Flint WWTP (km 70.7)	1.68	4.1	600.	55.	0.16	8.3
Flint Fly Ash Ponds (km 70.0)	0.04	39.5	150.	63.	1.32	80.
Brent Run (km 41.6)	0.15	5.9	77.	3.8	0.11	3.8
Ragnone WWTP (km 41.1)	0.69	58.7	3500.	84.	0.54	28.5
Pine Run (km 29.7)	0.06	7.0	33.7	5.0	0.04	3.8
Silver Creek (km 25.2)	0.085	6.8	50.0	5.0	0.04	3.8

Modified from: Delos et al. (1983)

Copper:

$$Cu_T = \frac{5.0 \times 4.34 + 0.69 \times 28.5}{4.34 + 0.69} = 8.2 \mu\text{g/l}$$

Neglecting the minor sources below the Ragnone WWTP, the profiles of total zinc, cadmium, and copper are shown in Figure IV-63. Also shown in the figure are observed data (mean and one standard deviation) and predictions from the MICHRI V model as reported by Delos et al. (1983). MICHRI V is a computer model which analyzes metals in greater detail than the screening procedures, and therefore requires more data.

The dilution model generally predicts values within 25 to 50 percent of the means of the observed values, and also within 25 to 50 percent of the MICHRI V

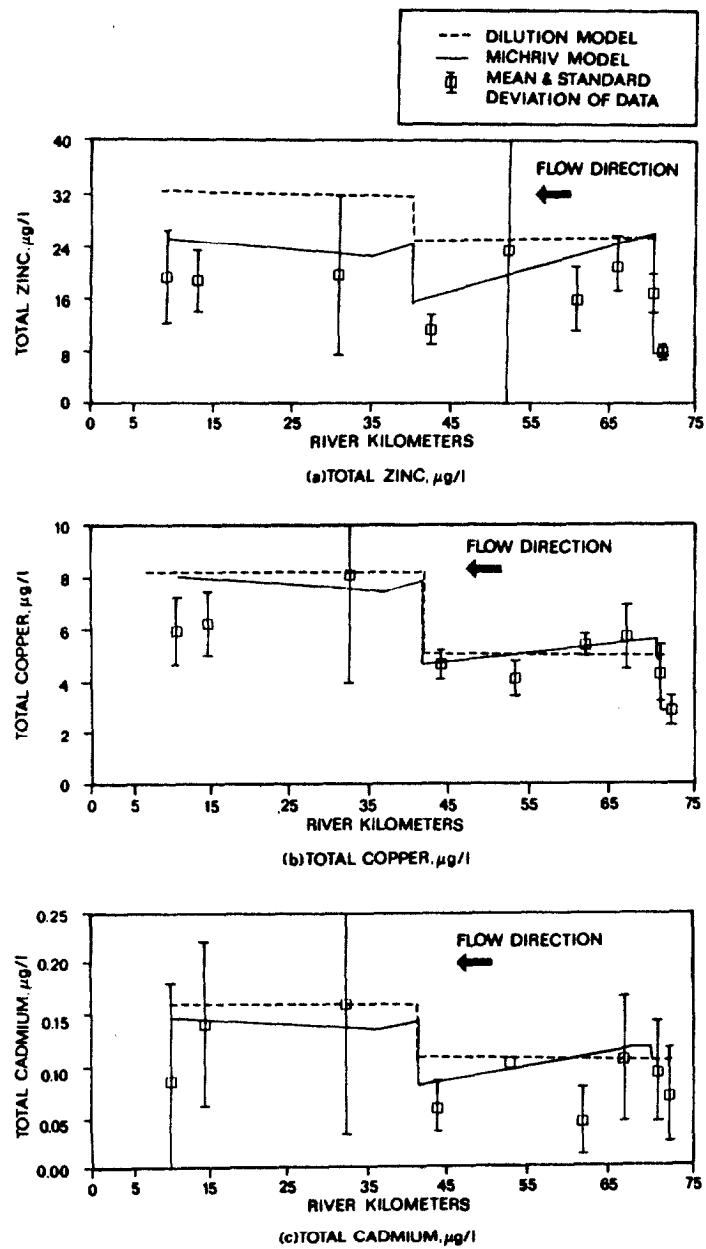
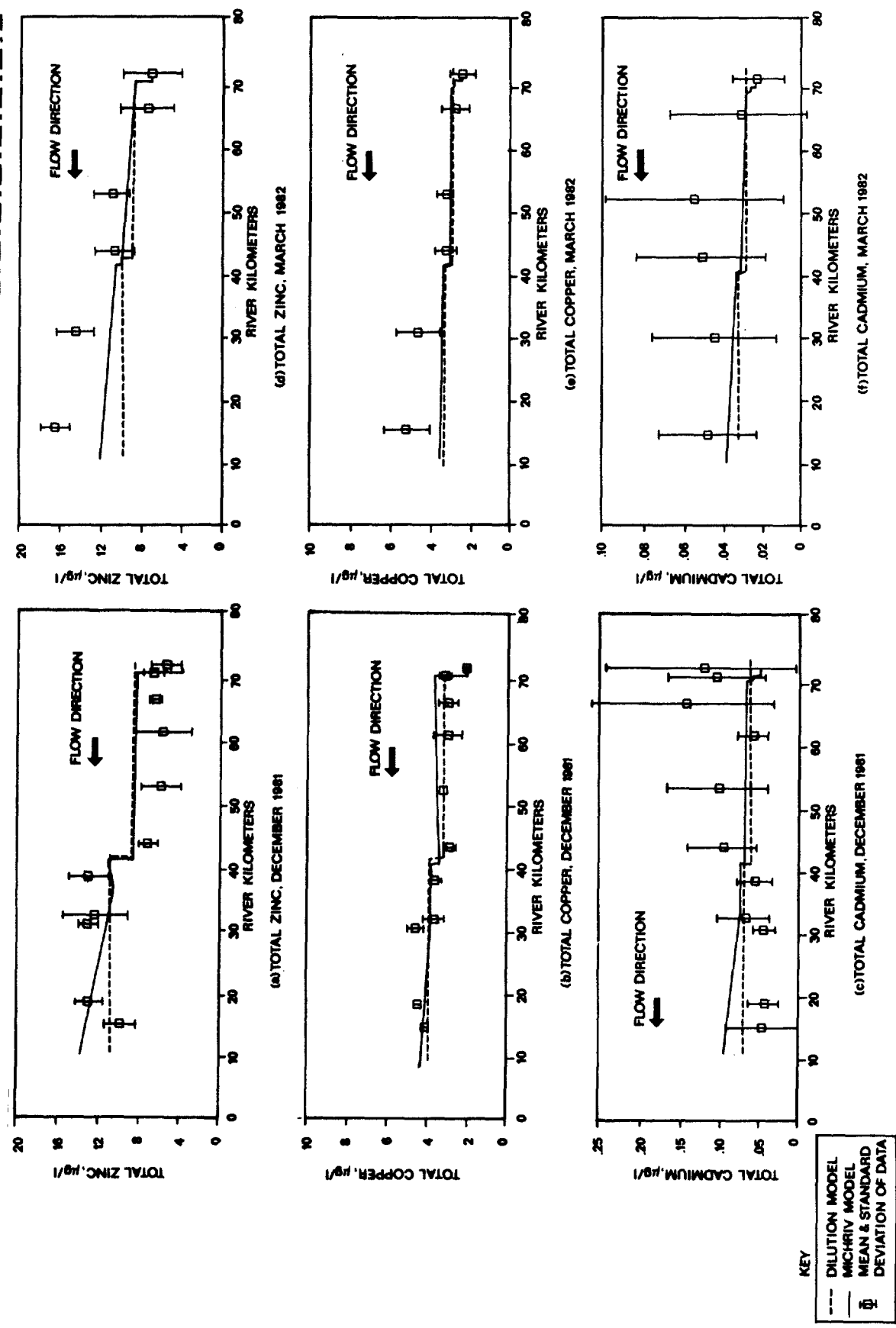


FIGURE IV-63 COMPARISON OF PREDICTED AND OBSERVED TOTAL METAL CONCENTRATIONS IN FLINT RIVER, MICHIGAN (AUGUST 1981), (AVERAGE FLOW =  $2,66 \text{ m}^3/\text{SEC}$  (94 cfs) AT KM 71.9)

model predictions. Figure IV-64 shows that the dilution model also is applicable under other flow regimes in the Flint River: December when the flow rate was about  $26.4 \text{ m}^3/\text{sec}$  (930 cfs), and March when the flow rate was  $93.4 \text{ m}^3/\text{sec}$  (3300cfs). For both the December and March surveys, there do not appear to be significant differences between predictions from the dilution model and from the MICHRIV model.



END OF EXAMPLE IV-20

FIGURE IV-64 TOTAL ZINC, COPPER, AND CADMIUM IN THE FLINT RIVER

While dilution modeling can produce quite acceptable results under a variety of conditions, the user should have access to tools which can be used when processes in addition to dilution are important. The following section addresses some of these situations.

#### 4.10.3.3 Settling and Resuspension of Adsorbed Metals in Rivers

This section begins with a brief discussion of the recently completed MICHRIV model (Delos et al., 1983). This model's framework is shown in Figure IV-65. The most interesting feature of the model is that it attempts to handle the exchange of contaminants between the water column and the bed. Resuspension and deposition of contaminated sediments redistributes adsorbed contaminants to and from the bed. Also, diffusion can be a driving force for dissolved phase interaction between the sediment and water column. For purposes of illustration, the MICHRIV model is simplified here, but the essence of the model (exchange of metal between the water column and bed) is retained.

The model is simplified based on these two assumptions:

- $K_{d1} = K_{d2} = 0$ ; that is, there is no degradation or decay of metals, and
- $K_{p1} = K_{p2}$ ; that is, the partition coefficient in the bedded sediments and in the water column are the same.

The first assumption is quite reasonable since most metals do not decay or otherwise degrade (an exception is elemental mercury which can volatilize).

Regarding the second assumption, there is reason to suspect that the solids partition coefficients for suspended and bedded sediments can differ since the characteristics of solids in the bed can differ from those suspended in the water column. However, because of the range of uncertainty inherent in partition coefficient prediction, there is no reason to consider differences between  $K_{p1}$  and  $K_{p2}$  for these screening analyses.

Using these two assumptions, the model formulations from Delos et al. (1983) are simplified as follows. The simplification procedure is shown in detail so the user can clearly see how the two assumptions are used. The final results of these simplifications are shown later as Equations IV-172 through IV-175, and show how the metal concentrations in the water column and bed are related.

From Delos et al. the relationship between the total concentration of metal in the water column ( $C_{T1}$ ) and in the bed ( $C_{T2}$ ) is:

$$\frac{C_{T2}}{C_{T1}} = \frac{w_s f_{p1} + K_L f_{d1}}{(w_{rs} + w_d) f_{p2} + K_L f_{d2} + K_{d2} f_{d2} H_2} \quad (IV-160)$$

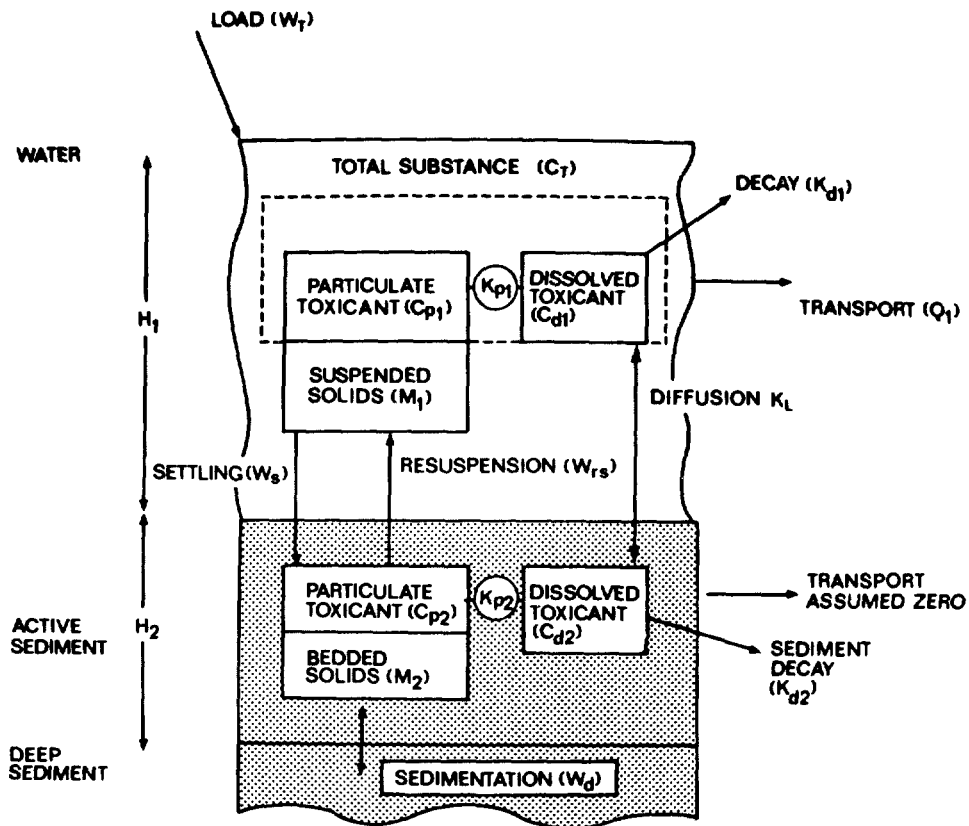


FIGURE IV-65 FRAMEWORK FOR RIVER MODEL MI CHRI V (REDRAWN FROM DELOS ET AL , , 1983)

where

- $f_{p1}, f_{p2}$  = particulate fraction of metal in water column and in bed, respectively
- $f_{d1}, f_{d2}$  = dissolved fraction of metal in water column and in bed, respectively
- $w_s$  = settling velocity, m/day
- $w_{rs}$  = resuspension velocity, m/day
- $K_L$  = diffusion coefficient, m/day
- $K_{d2}$  = decay rate in sediment, 1/day
- $H_2$  = depth of active sediment, m
- $m_1, m_2$  = solids concentration in water column and in bed, respectively, kg/l .

From Equation IV-160:

$$\frac{C_{d2}}{C_{d1}} = \frac{f_{d2} C_{T2}}{f_{d1} C_{T1}} = \frac{[f_{d2} w_s f_{p1} + K_L f_{d1}]}{f_{d1} [(w_{rs} + w_d) f_{p2} + K_L f_{d2} + K_{d2} f_{d2} H_2]}$$



$$= \frac{w_s \frac{f_{p1}}{f_{d1}} + K_L}{w_s \frac{m_1}{m_2} \frac{f_{p2}}{f_{d2}} + K_L + K_{d2} H_2} \quad (\text{IV-161})$$

since

$$\frac{m_1}{m_2} w_s = (w_{rs} + w_d)$$

Now

$$f_{p2} = \frac{m_2 K_{p2}}{1 + m_2 K_{p2}} \quad (\text{IV-162})$$

and

$$f_{d2} = 1/(1 + m_2 K_{p2})$$

so

$$\frac{f_{p2}}{m_2} = \frac{K_{p2}}{1 + m_2 K_{p2}} = K_{p2} f_{d2} \quad (\text{IV-163})$$

or

$$\frac{f_{p2}}{f_{d2} m_2} = K_{p2} \quad (\text{IV-164})$$

Similarly

$$\frac{f_{p1}}{m_1} = K_{p1} f_{d1} \quad (\text{IV-165})$$

or

$$\frac{f_{p1}}{f_{d1}} = K_{p1} m_1 \quad (\text{IV-166})$$

Substituting Equations IV-164 and IV-166 into Equation IV-161 produces:

$$\frac{C_{d2}}{C_{d1}} = \frac{w_s m_1 K_{p1} + K_L}{w_s m_1 K_{p2} + K_L + K_{d2} H_2} \quad (IV-167)$$

Since  $K_{d2}$  is assumed to equal zero for metals:

$$\frac{C_{d2}}{C_{d1}} = \frac{w_s m_1 K_{p1} + K_L}{w_s m_1 K_{p2} + K_L} \quad (IV-168)$$

With the further assumption that  $K_{p1} = K_{p2}$

$$\frac{C_{d2}}{C_{d1}} = \frac{w_s m_1 K_{p1} + K_L}{w_s m_1 K_{p1} + K_L} = 1 \quad (IV-169a)$$

or

$$C_{d2} = C_{d1} \quad (IV-169b)$$

Thus, the dissolved phase concentration of the metal in the bed and in the water column are equal to each other for the conditions specified above. This result is often an implicit assumption made in water quality analyses when the effects of the bed are ignored.

Since  $C_{d1} = C_{d2}$ , the net diffusive flux transfer between the bed and water column is zero, so that there is no need to include the K term in the following analyses.

In Delos et al. (1983) the total water column concentration is given by:

$$C_{T1}(x) = C_{T1}(0) \exp(-k_T x/u) \quad (IV-170)$$

where

$x$  = distance downstream, m

$u$  = stream velocity, m/day

$k_T$  = effective first order decay term, 1/day.

Delos et al. show that the first order decay term is:

$$k_T = K_{d1} f_{d1} + \frac{w_s f_{p1}}{H_1} + \frac{K_L f_{d1}}{H_1} - \frac{m_2 H_2 f_{p1}}{m_1 H_1 f_{p2}} \frac{1}{H_2} \frac{r_2}{r_1} (w_{rs} f_{p2} + K_L f_{d2}) \quad (IV-171a)$$

where

$$\frac{r_2}{r_1} = \frac{(w_{rs} + w_s) f_{p2} + K_L (K_{p2}/K_{p1}) f_{d2}}{(w_{rs} + w_s) f_{p2} + K_L f_{d2} + K_{d2} f_{d2} H_2}$$

Using the assumptions made before ( $K_{p1} = K_{p2}$  and  $K_{d1} = K_{d2} = 0$ ),  $r_2/r_1 = 1$ . Thus  $k_t$  simplifies to:

$$k_T = \frac{w_s f_{p1}}{H_1} - \frac{m_2 f_{p1} w_{rs}}{m_1 H_1} = \frac{f_{p1}}{H_1} \left[ w_s - \frac{m_2}{m_1} w_{rs} \right]. \quad (IV-171b)$$

To summarize, under the simplifications made here, the MICHRIV model equations become:

$$C_{T1}(x) = C_{T1}(0) \exp \left[ - \frac{f_{p1}}{H_1} \left( w_s - \frac{m_2}{m_1} w_{rs} \right) \frac{x}{u} \right] \quad (IV-172)$$

$$C_{d1}(x) = \frac{C_{T1}(x)}{1 + K_{p1} m_1} \quad (IV-173)$$

$$C_{d2} = C_{d1} \quad (IV-169b)$$

$$\frac{C_{p1}}{m_1} = \frac{C_{p2}}{m_2} \quad (IV-174a)$$

or

$$x_1 = x_2 \quad (IV-174b)$$

$$C_{T2} = C_{T1} \frac{f_{d1}}{f_{d2}} = C_{T1} \frac{1 + K_{p2} m_2}{1 + K_{p1} m_1} \quad (IV-175)$$

and

$$m_2 = \rho_s (1-n). \quad (IV-176)$$

where

- $X_1, X_2$  = mass of pollutant adsorbed per mass of sediment in the water column and in the bed, respectively,  $\mu\text{g/g}$
- $\rho_s$  = density of solids in sediment,  $\text{gm/cm}^3$  (e.g. for sand 2.54  $\text{gm/cm}^3$ )
- $n$  = porosity of sediment (volume fraction occupied by water).

The most notable results obtained in the above analyses are that the dissolved metal concentration in the water column and in the bedded sediments are the same (Equation IV-169b), and so are the particulate metal concentrations, expressed per unit weight of sediment (Equation IV-174b). However, on a unit volume basis, the total metal concentration in the sediment far exceeds the concentration in the water column (Equation IV-175).

Typically, first order decay rates are positive numbers, which indicate that pollutants decrease in concentration with distance. However, the  $k_T$  term in Equation IV-171b can either be positive or negative. For example, if significant scour of particulate metal from the bottom is occurring, then  $k_T < 0$  and the total metal concentration can increase downstream.

While it is possible that metal concentrations can increase in the water column due to scour (e.g., see Figure IV-64 which shows total zinc and copper in the Flint River during March 1982), at steady-state conditions this should not happen when the only source of loading is a single source located at  $x = 0$ . Rather than use Equation IV-172 to simulate the effects of scour on water column concentration, one of two other alternatives has been selected. One approach is to retain the unsteady-state nature of the transient scour situation. While this introduces more complexity, it shows that elevated metal concentrations in the water column caused by scour are due to a previous discharge or hydrologic condition when metals had contaminated the bed, and not due to the current steady discharge conditions.

The two unsteady equations relating the total metal concentrations in the bed and in the water column are (using the previous notation):

$$\frac{\partial C_{T2}}{\partial t} - \frac{w_s f_{p1} C_{T1}}{H_2} - \frac{w_{rs} f_{p2} C_{T2}}{H_2} + \frac{K_L f_{d1} C_{T1}}{H_2} - \frac{K_L f_{d2} C_{T2}}{H_2} \quad (\text{IV-177})$$

and

$$\frac{\partial C_{T1}}{\partial t} + u \frac{\partial C_{T1}}{\partial x} = \frac{-w_s f_{p1} C_{T1}}{H_1} + \frac{w_{rs} f_{p2} C_{T2}}{H_1} - \frac{K_L f_{d1} C_{T1}}{H_1} + \frac{K_L f_{d2} C_{T2}}{H_1} \quad (\text{IV-178})$$

While these equations can be solved exactly and used to predict the total instream metal concentration due to a scour condition, they are not practical for screening analyses. The primary emphasis here is to predict longitudinal pollutant distribution when scour is much more important than deposition or diffusion. The approach is to specify (rather than calculate) the concentration in the bed and to assume it remains constant over the period of analysis. Thus the screening tools which are presented on the following pages are fundamentally different from the previous MICHRIV equations, such as Equation IV-172. Table IV-58 summarizes the screening equations and defines the variables used in each equation.

$$C_{T1}(x) = \frac{w_{rs} f_{p2} C_{2i}}{H_1 u} x + C_{T1}(0) \quad (IV-179)$$

where

- $C_{2i}$  = concentration of total metal in the bedded sediments,  $\mu\text{g/l}$  (a direct measurement of this value is preferable)
- $C_{T1}(0)$  = concentration of total metal in the water column at an upstream boundary,  $\mu\text{g/l}$ .

While Equation IV-179 represents steady-state conditions, it is valid only as long as the sediments being scoured have a total metal concentration of  $C_{2i}$ . Once the contaminated sediments have been scoured, then the instream metal concentration is expected to return to  $C_{T1}(0)$ . The period of validity,  $T$ , of the equation can be approximated by:

$$T = \frac{H_2}{w_{rs}} \quad (IV-180)$$

where

- $H_2$  = depth of contaminated sediment, m
- $w_{rs}$  = resuspension velocity, m/day

Typically, Equation IV-179 is expected to be used during high flow conditions, perhaps for a seasonal analysis. For an application of this type, the period of validity of the equation should be on the order of one to two months. Using representative data ( $H_2 = 5 \text{ cm}$  and  $w_{rs} = 2 \times 10^{-4} \text{ m/day}$ ) for an example,

$$T = \frac{5 \times 10^{-2} \text{ m}}{2 \times 10^{-4} \text{ m/day}} = 250 \text{ days.}$$

For the example conditions, Equation IV-179 is applicable for seasonal analysis.

When settling of solids is insignificant, the resuspension velocity,  $w_{rs}$ , can be estimated as:

$$w_{rs} = \frac{uH_1 \Delta SS}{m_2 \Delta x \cdot 10^6} \quad (IV-181)$$

TABLE IV-58  
SUMMARY OF SCREENING PROCEDURES FOR METALS IN RIVERS AND LAKES

Equation	Use	Data Requirements	Comments
<u>Dilution Analysis</u>			
IV-157a	This equation is used to calculate the concentration of total metal in a river after a point source discharge mixes with river water.	<p><math>Q_u</math> = flow rate in river above point source</p> <p><math>Q_w</math> = flow rate of point source</p> <p><math>C_{TW}</math> = concentration of total metal in point source</p> <p><math>C_{TU}</math> = concentration of total metal in river above the point source</p>	This equation is most applicable when exchange of suspended solids and metals with bed is negligible. See Figure IV-62: when mean water velocity is in "transportation" regime, this condition is approximately true. Also, the equation can be used as a first approximation regardless of exchange with bed.
IV-156	Once the total concentration versus distance is found from Equation IV-157a, the amount dissolved can be calculated using this equation.	<p><math>S</math> = suspended solids concentration</p> <p><math>K_p</math> = partition coefficient</p> <p><math>C_T</math> = total metal concentration</p>	This equation is used to find total dissolved metal at locations in a river once total metal concentration at these same locations has been calculated.
<u>Dilution and Scour of Metal-Contaminated Sediments</u>			
IV-179	This equation is used to predict the total metal concentration in a river when metal-contaminated sediments are resuspended into the water column.	<p><math>C_{21}</math> = concentration of total metal in bedded sediments</p> <p><math>C_{T1}(0)</math> = concentration of total metal in the water column at an upstream boundary</p> <p><math>H_1</math> = water depth</p> <p><math>u</math> = stream velocity</p> <p><math>f_{P2}</math> = fraction of metal in bed which is in particulate form (<math>\leq 1</math>)</p> <p><math>w_{rs}</math> = resuspension velocity (see Equation IV-181)</p>	The equation does not keep track of the depth of contaminated sediments. It assumes this depth is not exceeded during the period of scour. Equation IV-180 can be used to estimate the period of validity of the equation. Figure IV-66 illustrates the importance of scour.

TABLE IV-58 (continued)

Equation	Use	Data Requirements	Comments
IV-182	This equation is used to calculate the total metal concentration in a river when metal-contaminated sediments are resuspended into the water column. This is an alternate form of Equation IV-179. See Comments.	<p>Dilution and Scour of Metal-Contaminated Sediments (continued)</p> <p><math>\Delta SS</math> = change in suspended concentration over the distance where the total metal concentration is to be calculated</p> <p><math>K_p</math> = partition coefficient</p> <p><math>S_p</math> = average suspended solids concentration during the previous steady hydrologic period</p> <p><math>C_{T1p}</math> = concentration of total metal in water column during the previous steady hydrologic period</p>	This equation can be used in lieu of Equation IV-179 when the concentration of total metal in the bed, $C_{21}$ , is unknown.
Dilution and Deposition of Metal-Contaminated Sediments			
IV-185d	This equation is used to predict the concentration of total metal in a river when metal-contaminated solids are settling.	<p><math>C_{T0}</math> = concentration of total metal at an upstream boundary</p> <p><math>K_p</math> = partition coefficient</p> <p><math>SS(0)</math> = suspended solids concentration at upstream boundary</p> <p><math>H_1</math> = depth of water</p> <p><math>u</math> = velocity of water</p> <p><math>w_s</math> = settling velocity (see Equation IV-184)</p>	Figure IV-67 illustrates the importance of deposition.
IV-186a	This equation is a simplification of Equation IV-185d. See Comments.	<p><math>C_{T0}</math> - see above</p> <p><math>SS(0)</math> - see above</p> <p><math>SS(x)</math> = suspended solids concentration at a distance <math>x</math> below upstream boundary, where total metal concentration is to be calculated</p>	This equation is used when the metal is highly adsorbed to the suspended solids (i.e., when $K_p \cdot SS \cdot 10^{-6} \gg 1$ ).

TABLE IV-58 (continued)

Equation	Use	Data Requirements	Comments
		Dilution and Deposition of Metal-Contaminated Sediments (continued)	
IV-186b	This equation is also a simplification of Equation IV-185d. See Comments.	$C_{T0}$ - see above $K_p$ - see above $SS(0)$ - see above $w_s$ - see above $H_1$ - see above $u$ - see above	This equation is applicable when the amount of metal which is adsorbed is small. When this is true, settling is relatively unimportant, as Equation IV-186c shows, and the metal tends to act conservatively in the water column.
		Settling of Metals in Lakes	
IV-188c	This equation predicts the concentration of total metal leaving a lake, based on the suspended solids concentrations entering and leaving the lake.	$C_T^i$ = concentration of total metal coming into the lake $S^i, S^o$ = concentration of suspended solids entering and leaving the lake, respectively (See Equation IV-187). $K_p$ = partition coefficient	This equation considers a median-size suspended solid, and does not differentiate by size fraction.
IV-189	This equation shows that the dissolved phase metal concentration is not affected by the settling adsorbed metal.		
IV-195b	This equation predicts the concentration of total metal leaving a lake, based on concentrations of suspended solids by size fraction.	$C_T^i$ - see above $S_{j,j}^i, S_{j,j}^o$ = concentration of suspended solids in class j entering and leaving the lake, respectively (see Equation-190) $K_{pj}$ = partition coefficient of metals associated with sediment size j	Size fractions of sand, silts, and clays entering a lake are required. Settling velocity of solids in each group are predicted using Equation IV-191.



TABLE IV-58 (continued)

Equation	Use	Data Requirements	Comments
<u>Settling of Metals in Lakes (continued)</u>			
IV-197	This equation is the same as Equation IV-195b, except the partition coefficients are related to specific surface area.	Same as Equation IV-195b, except specific surface areas (SA's) are required	Typical values of specific surface areas for this equation are 10 m <sup>2</sup> /g for sand, 60 m <sup>2</sup> /g for silt, and 200 m <sup>2</sup> /g for clay.
<u>Adsorption and Desorption of the Metal Between Water Column and Bed</u>			
IV-199	This equation is used to predict water column concentration of metal due to adsorption or desorption with bed.	<p><math>C_0</math> = initial total metal concentration in water column (at <math>t=0</math>)</p> <p><math>C_b</math> = upstream boundary concentration (at <math>x=0</math>)</p> <p><math>M_s</math> = mass of contaminated sediments per unit area (see Table IV-39)</p> <p><math>H</math> = water depth</p> <p><math>u</math> = stream velocity</p> <p><math>K_p</math> = partition coefficient</p> <p><math>D_M</math> = vertical diffusion coefficient</p> <p><math>\theta</math> = void fraction of underlying sediment</p> <p><math>\rho_b</math> = bulk density</p>	<p>This equation differs from all of the above in that it is an unsteady-state equation (i.e., time variability is considered). This equation is intended to provide only a crude approximation of the importance of adsorption or desorption from the bed, because some of the required data will likely be difficult to estimate. Equation IV-200 is a simplification of Equation IV-199 when the mixed layer is small. Equation IV-201 is also a simplification useful when the boundary concentration is negligible.</p>

The term  $\Delta SS/\Delta x$  is the change in suspended solids concentration over distance  $\Delta x$  [mg/ (l · m)]

If  $C_{2i}$  in Equation IV-179 is not available, Equation IV-179 can be expressed in the alternate form as:

$$C_{T1}(x) = \frac{\Delta SS K \cdot 10^{-6}}{1 + K_p S_p \cdot 10^{-6}} C_{T1p} + C_{T1}(0) \quad (IV-182)$$

where

$C_{T1p}$  = concentration of total metal in the water column during the previous steady period (previous to the period of sustained scour)

$S_p$  = suspended solids concentration during previous steady period, mg/l.

The purpose of using the previous steady-state period (a non-scour period) is that the concentration in the bedded sediments during the scour period is to a large degree dictated by the previous conditions.

Equation IV-182 shows that the product

$$\frac{\Delta SS K \cdot 10^{-6}}{1 + K_p S_p \cdot 10^{-6}}$$

is a helpful indicator of the importance of scour. If

$$\frac{\Delta SS K \cdot 10^{-6}}{1 + K_p S_p \cdot 10^{-6}} > 1,$$

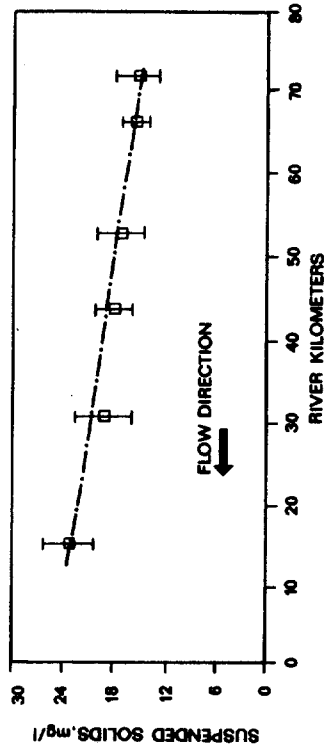
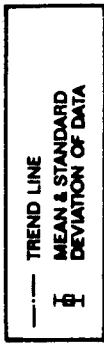
then the total metal concentration during the scour period (at a distance downstream where the suspended solids have increased by ASS) will exceed the total metal concentration during the previous steady-state period. If this fraction is less than unity then the background concentration ( $C_{T1}(0)$ ) is important in determining whether scour produces higher concentrations than the previous period.

#### EXAMPLE IV-21

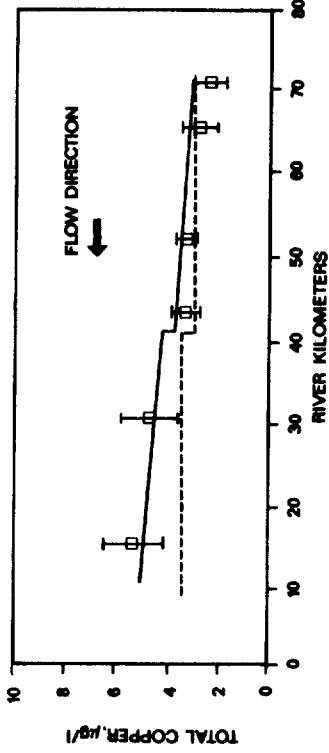
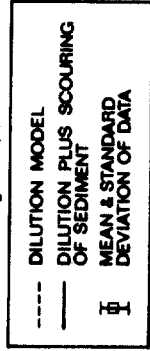
The Flint River study provides a source of data to simulate a scour condition. Figure IV-66a shows the suspended solids concentration in the river during the March 1982 survey and indicates a net scour condition exists. The resuspension velocity is:

$$w_{rs} = \frac{1 \cdot 2 \cdot (25 - 12)}{0.2 \cdot 80 \cdot 10^3 \cdot 10^6} 86400 = 1.4 \cdot 10^{-4} \text{ m/day}$$

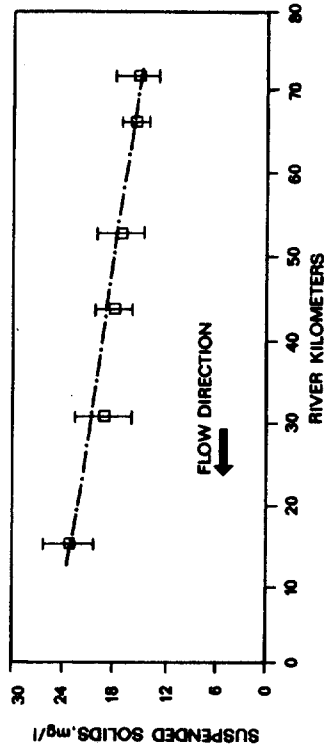
KEY (Figure a)



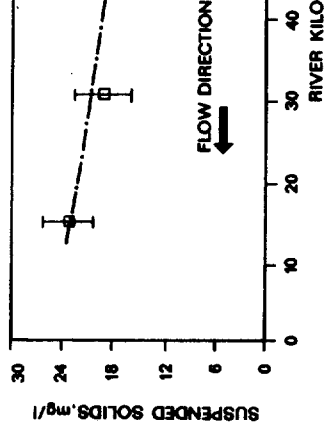
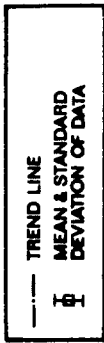
KEY (Figures b,c,d)



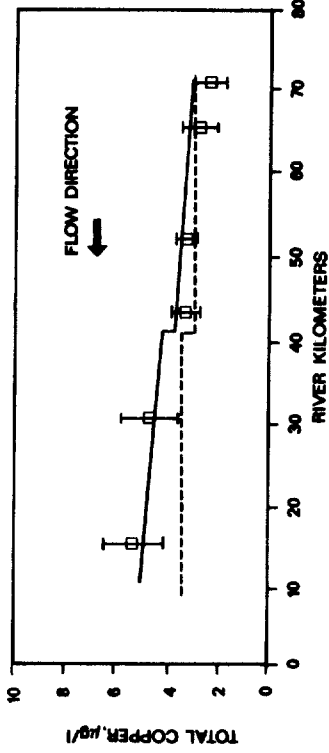
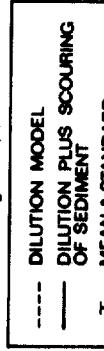
KEY (Figure b)



KEY (Figure d)



KEY (Figure c)



KEY (Figure d)

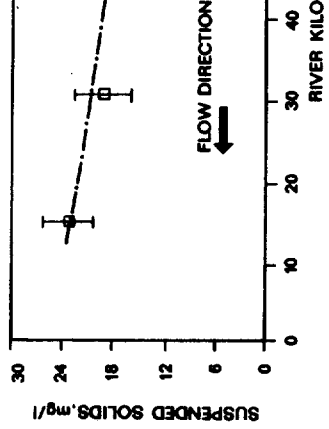
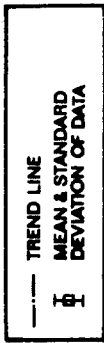


FIGURE IV-66 SUSPENDED SOLIDS AND TOTAL METAL CONCENTRATIONS IN THE FLINT RIVER, MICHIGAN (MARCH 1982).

The data for velocity (1 m/sec), depth (2 m) and bedded sediment concentration (0.2 kg/l) are from Delos et al. (1983). Note that Figure IV-62 shown earlier suggests that scour may be important at a stream velocity of 1 m/sec.

The fraction  $f_{p2}$  is probably very close to unity for each of the three metals zinc, copper, and cadmium. To use Equation IV-179, the concentration in the bed,  $C_{2i}$ , and the upstream concentrations  $C_{T1}(0)$  are needed. The  $C_{T1}(0)$  values are the same as those calculated in preparing the dilution analyses for Figures IV-64(d) through (f).

The  $C_{2i}$  values can be estimated looking at the historical data for the previous steady period (December), and by calculation based on total metal concentration as found by the dilution model (Figure IV-64a, b, and c). For the present analysis,  $C_{2i}$  is based on the particulate levels in the water column (during December 1981);

$$C_{2i} \approx C_{p2} = \frac{m_2}{m_1} C_{p1}$$

The levels are shown below:

	$C_{p1}, \mu\text{g/l}$	$C_{p2}, \mu\text{g/l}$
Zinc	6.	12 x 10
Copper	1.	2 x 10
Cadmium	0.03	0.06 x 10

These numbers are based on  $m_1 = 0.00001$  kg/l (for December 1981) and  $m_2 = 0.2$  kg/l. Substituting the required information into Equation IV-179, the results are shown plotted in Figure IV-66b, c, and d. Equation IV-156 is applied twice, since there are two point sources in the reach.

The increase in concentration due to scour over the 70 km region for each metal is:

	$\Delta C_1, \mu\text{g/l}$ , due to scour over 70 km
Zinc	6.8
Copper	1.1
Cadmium	0.04

For example, the incremental zinc concentration is:

$$\frac{w_{rs} f_{p2} C_{2i}}{H_1 u} x = \frac{1.4 \cdot 10^{-4} \cdot 1 \cdot 12 \cdot 10^{+4}}{2 \cdot 1 \cdot 86400} \cdot 70 \cdot 10^3 = 6.8 \mu\text{g/l}$$

END OF EXAMPLE IV-21

During periods when settling rather than scour is the predominant mechanism affecting suspended solid concentrations in the water column, the suspended solids concentrations,  $SS(x)$ , change over distance:

$$SS(x) = SS(0) \exp\left(\frac{-w_s x}{H_1 u}\right) \quad (IV-183)$$

The effective settling velocity can be found directly from this equation:

$$w_s = \frac{-H_1 u}{x} \ln\left[\frac{SS(x)}{SS(0)}\right] \quad (IV-184)$$

When metal-contaminated solids settle out of the water column, the process can be modeled by the following ordinary differential equation:

$$u \frac{dC_T}{dx} = \frac{-w_s C_s}{H_1} \quad (IV-185a)$$

where  $C_s$  is the particulate metal concentration,  $\mu\text{g/l}$ .  $C_s$  can be related to  $C_T$  by

$$\frac{C_s}{C_T} = \frac{K SS \cdot 10^{-6}}{(1 + K_p SS \cdot 10^{-6})} \quad (IV-185b)$$

Upon substitution of  $C_s$  from Equation IV-185b and  $SS$  from Equation IV-183 into Equation IV-185a, and by specifying the boundary condition for  $C_T$  as:

$$C_T = C_{T0} \text{ at } x = 0 \quad (IV-185c)$$

it is possible to solve Equation IV-185a as a function of distance to get:

$$C_T = C_{T0} \exp\left[ \ln\left( K_p SS(0) \cdot 10^{-6} + 1 \right) + e^{\frac{w_s x}{H_1 u}} \right. \\ \left. - \ln\left( K_p SS(0) \cdot 10^{-6} + 1 \right) - \frac{w_s}{H_1 u} x \right] \quad (IV-185d)$$

When the metal is highly sorbed to the sediment (i.e.,  $K_p SS \cdot 10^{-6} \gg 1$ ), this equation simplifies to:

$$C_T = C_{T0} \exp\left(\frac{-w_s}{H_1 u} x\right) = \frac{C_{T0}}{SS(0)} SS(x) \quad (IV-186a)$$

If settling were to continue indefinitely downstream, then the metal would eventually be depleted from the water column. The above equation also shows that the decrease in metal concentration is directly proportional to decrease in solids concentration. By monitoring solids the decrease in metals can be directly estimated as long as  $K_p SS \cdot 10^{-6} \gg 1$ .

If the fraction of metal which is adsorbed is small, Equation IV-185 simplifies to

$$C_T = C_{T0} \exp \left[ K_p SS(0) \cdot 10^{-6} \left( e^{\frac{-w_s x}{uH_1}} - 1 \right) \right] \quad (IV-186b)$$

Eventually, as the solids are depleted from the water column, the total concentration approaches

$$C_T = \frac{C_{T0}}{\exp(K_p SS(0) \cdot 10^{-6})} \quad (IV-186c)$$

Under these conditions ( $K_p SS(0) \cdot 10^{-6} < 1$ ), the total loss from the water column by settling is not likely to be large. For example, if  $K_p SS(0) \cdot 10^{-6} = 0.1$ , then  $C_T = 0.9 C_{T0}$ .

#### EXAMPLE IV-22

During the August 1981 Flint River survey, the suspended solids profile (Figure IV-67a) indicates that a net deposition of suspended solids was occurring between km 40 and km 70. Based on Equation IV-184, the approximate deposition rate between km 70 and km 40 is:

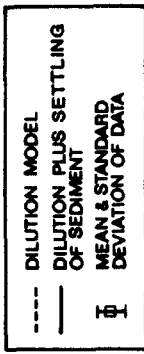
$$w_s = \frac{0.5 \times 0.2}{30 \times 10^3} \ln \left( \frac{10}{4} \right) \times 86400 = 0.26 \text{ m/day}$$

where the depth (0.5 m) and velocity (0.2 m/sec) are taken from Delos et al. (1983).

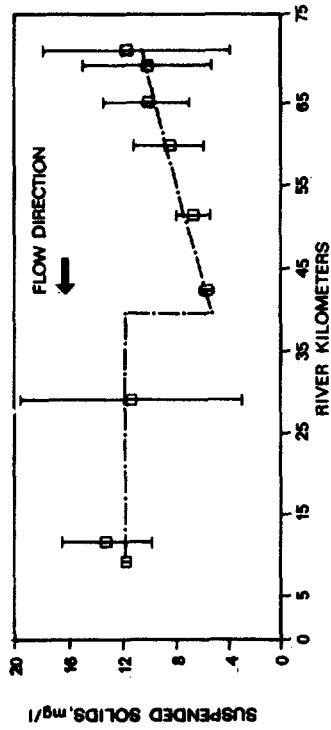
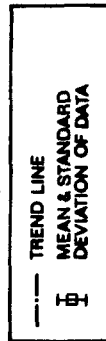
Average partition coefficients are also obtained from estimates in Delos et al. (1983) and are:

<u>Metal</u>	<u>K (cm<sup>3</sup>/gm)</u>
Zinc	$0.2 \times 10^6$
Copper	$0.06 \times 10^6$
Cadmium	$0.1 \times 10^6$

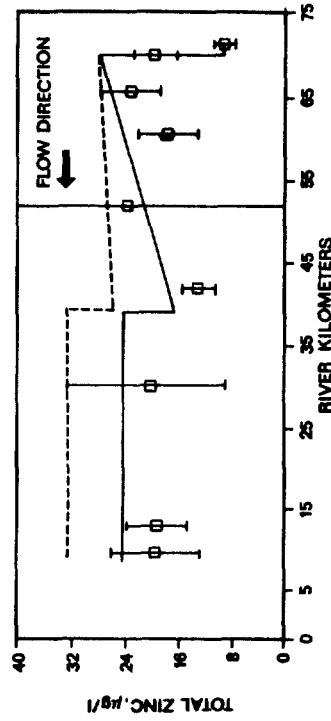
KEY (Figures b,c,d)



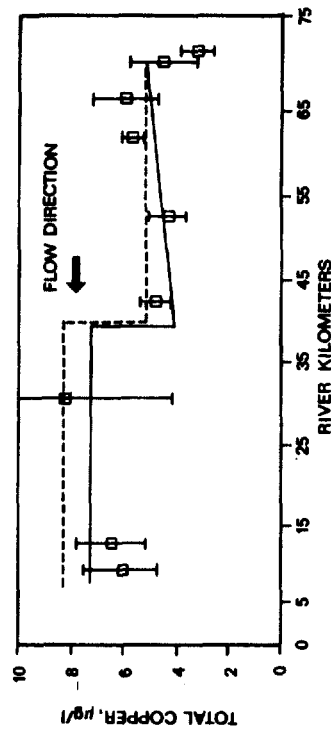
KEY (Figure a)



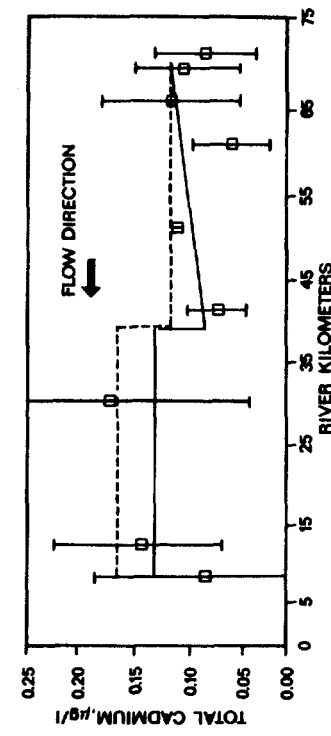
(a) SUSPENDED SOLIDS, mg/l



(b) TOTAL ZINC, µg/l



(c) TOTAL COPPER, µg/l



(d) TOTAL CADMIUM, µg/l

FIGURE IV-67 SUSPENDED SOLIDS AND TOTAL METAL CONCENTRATIONS IN FLINT RIVER, MICHIGAN (AUGUST 1981). (AVERAGE FLOW = 2.66M<sup>3</sup>/SEC (94 CFS) AT KM 71.9.)

Based on these partition coefficients, the product  $K_p S S 10^{-6}$  is between 0.6 to 2.0 for the metals. Hence, Equation IV-185d is probably more applicable than Equations IV-186a, b, or c. The equation is used to predict the concentration at km 40 based on the boundary concentration calculated in the dilution example (Example IV-20) and the remaining data shown earlier. The calculation is shown in detail for zinc:

Zinc:

$$Zn_T = 26 \exp \left[ \ln \left( 0.2 \times 10^6 \times 10 \times 10^{-6} + \exp \left( \frac{.26 \times 30000}{.5 \times .2 \times 86400} \right) \right) - \ln \left( 0.2 \times 10^6 \times 10 \times 10^{-6} + 1 \right) - \frac{.26 \times 30000}{.5 \times .2 \times 86400} \right]$$

$$= 26 (0.6) = 16 \mu\text{g/l}$$

Copper:

$$Cu_T = 5 (.8) = 4 \mu\text{g/l}$$

Cadmium:

$$Cd_T = 0.1 (.7) = 0.07 \mu\text{g/l}$$

The results are plotted in Figure IV-67b, c, and d. The predicted values agree more closely with the observed values than do the predictions from the dilution analyses.

----- END OF EXAMPLE IV-22 -----

#### 4.10.3.4 Settling of Metals in Small Impoundments on Rivers

The preceding section presented models which could be used to predict the effects of either settling or scour of solids on trace metal concentrations in rivers. While settling of metal contaminated solids certainly can occur in rivers during low flow conditions, most settling is likely to occur in reservoirs or lakes located on rivers. Investigations frequently reveal that total metal concentrations in river systems, when averaged over a long period of time, decrease with distance. This indicates there is a net loss of metal from the water column, and that perhaps settling is a primary reason. In an extreme approach, some researchers have ignored downstream transport of metals altogether, outside of a small mixing zone, and have hypothesized that metals are rapidly depleted from the water column either by settling



or adsorption to bedded sediments. However, this approach contradicts the results presented earlier which show that metals, even ones which adsorb strongly such as mercury, can be transported downstream.

Solids that are suspended in the water column do tend to settle because of gravitational forces, but also tend to remain in suspension because of turbulence. Evidence shows that suspended solids levels can remain fairly constant over long distances. In reservoirs which are more quiescent than rivers, the turbulent eddies diminish, and often gravitational settling becomes important. Thus for these screening analyses, reservoirs are modeled as sinks of metals.

Based on the idealized reservoir and nomenclature shown in Figure IV-68, mass balances for solids and metals are developed. The solids mass balance is:

$$S^0 = \frac{S^i}{\left(\frac{Tw_s}{H} + 1\right)} \quad (\text{IV-187})$$

where

- T = hydraulic detention time, days
- $S^i, S^0$  = concentration of suspended solids in inflow and outflow, respectively, mg/l
- H = mean depth of reservoir, m
- $w_s$  = settling velocity, m/day.

The total metal concentration leaving the reservoir at steady state can be approximated as:

$$C_T^0 = \frac{C_T^i}{1 + \frac{Tw_s}{H} \frac{S^0 K \cdot 10^{-6}}{1 + S^0 K_p \cdot 10^{-6}}} \quad (\text{IV-188a})$$

$$\frac{C_T^i}{1 + \frac{(S^i - S^0) K \cdot 10^{-6}}{1 + S^0 K_p \cdot 10^{-6}}} \quad (\text{IV-188b})$$

$$= \frac{C_T^i (1 + S^0 K \cdot 10^{-6})}{1 + S^i K_p \cdot 10^{-6}} \quad (\text{IV-188c})$$

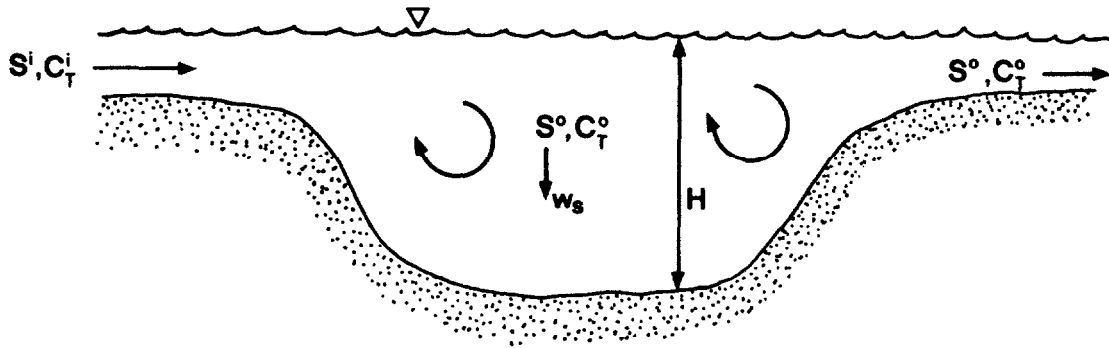


FIGURE IV-68 DEFINITION SKETCH OF IDEALIZED RESERVOIR

The dissolved metal concentration is:

$$C^o = \frac{C^i (1 + K S^i \cdot 10^{-6}) C_T^1}{(1 + K_p S^i \cdot 10^{-6})} = \frac{C^i C_T^1}{1 + K_p S^i \cdot 10^{-6}} = C^i \quad (IV-189)$$

If the particle sizes of suspended sediments in the inflowing and outflowing waters are significantly different, then the partition coefficient can also be quite different in the two waters. This is primarily because the smaller particles have greater surface area available for adsorption. The following analysis shows how to approximately account for these differences.

For the solids balance, each particle size (e.g., fine silt) can be accounted for individually:

$$S_j^o = \frac{S_j^i}{\left(\frac{T w_{sj}}{H} + 1\right)} \quad (IV-190)$$

where the subscript  $j$  denotes particle class.

If the inflowing and outflowing concentrations of particles can be estimated by class size then the settling velocities can be calculated as:

$$w_{sj} = \frac{H}{T} \left( \frac{S_j^i}{S_j^o} - 1 \right) \quad (IV-191)$$

This approach assumes the internally generated solids in class  $j$  are of negligibly small amount.

The linear adsorption isotherm for particle class  $j$  is:

$$X_j = K_{pj} C \quad (IV-192)$$

where

$X_j$  = mass of metal adsorbed per mass of sediment in  $j$ th particle class

$k_{pj}$  = partition coefficient for  $j$ th particle size

then

$$C_{sj}^0 = k_{pj} C^0 S_j^0 \cdot 10^{-6} \quad (\text{IV-193})$$

or

$$C_s^0 = \sum C_{sj}^0 = C^0 \sum k_{pj} S_j^0 \cdot 10^{-6} \quad . \quad (\text{IV-194})$$

The concentration of metal in the outflow becomes:

$$C_T^0 = \frac{C_T^i}{1 + \frac{\sum k_{pj} (S_j^i - S_j^0) 10^{-6}}{(1 + \sum k_{pj} S_j^0 \cdot 10^{-6})}} \quad (\text{IV-195a})$$

$$= \frac{C_T^i (1 + \sum k_{pj} S_j^0 \cdot 10^{-6})}{(1 + \sum k_{pj} S_j^i \cdot 10^{-6})} \quad (\text{IV-195b})$$

$$= C^i (1 + \sum k_{pj} S_j^0 \cdot 10^{-6}) \quad (\text{IV-195c})$$

and

$$C^0 = \frac{C_T^0}{1 + \sum k_{pj} S_j^0 \cdot 10^{-6}} = C^i \quad . \quad (\text{IV-189b})$$

Equation IV-189b shows that the dissolved fraction of the metal is not affected, by the reservoir so that if most of the metal is dissolved, then the reservoir is not an effective sink for the metal.

To handle multiple partition coefficients in a manner amenable to simplified calculation, it is hypothesized that partition coefficients are inversely proportional to specific surface area, or

$$\frac{k_{pr}}{SA_r} = \frac{k_{pj}}{SA_j} \quad (\text{IV-196})$$

where

$r$  denotes a reference particle group (e.g., clay)

$SA_r$  = specific surface,  $m^2/g$ .

The tabulations below show ranges and typical values for specific areas for sands, silts, and clays.

<u>Solid</u>	<u>Range of Specific Areas (<math>m^2/g</math>)</u>	<u>Typical Value (<math>m^2/g</math>)</u>
Sand	1 - 50	10
Silt	50 - 100	60
Clay	100 - 800	200

Rai et al. (1983) provide a good summary of specific surface areas (and other adsorption related parameters) for a variety of solid surfaces, including metal hydroxides. Using the relationship embodied in Equation IV-196,  $C_T^0$  becomes:

$$C_T^0 = C_T^i \frac{1 + \frac{K_{pr} \cdot 10^{-6}}{SA_r} \sum SA_j S_j^0}{1 + \frac{K_{pr} \cdot 10^{-6}}{SA_r} \sum SA_j S_j^i} \quad (IV-197)$$

----- EXAMPLE IV-23 -----

Consider a river with two reservoirs located on it (Figure IV-69). The detention time and depth of each reservoir are:

<u>Reservoir</u>	<u>Detention Time (days)</u>	<u>Depth (m)</u>
Haley	3	3
Dell	20	6

Suppose the suspended solids entering the first reservoir from upstream are:

<u>Category</u>	<u>Percent by Weight</u>	<u>Concentration (mg/l)</u>	<u>Settling Velocity (cm/sec)</u>	<u>Specific Surface Area (<math>m^2/g</math>)</u>
Sand	50	100	0.1	10
Silt	25	50	$5 \times 10^{-2}$	60
Clay	25	50	$3 \times 10^{-4}$	200

The total zinc concentration in the river upstream of Haley Reservoir is assumed to be  $150 \mu g/l$ . Find the total zinc concentration in "the water column below Haley Reservoir and below Dell Reservoir assuming that the loss from the water column is by sedimentation only.

Assume that a typical partition coefficient for zinc on clays is  $10^4 \text{ cm}^3/\text{gm}$ .

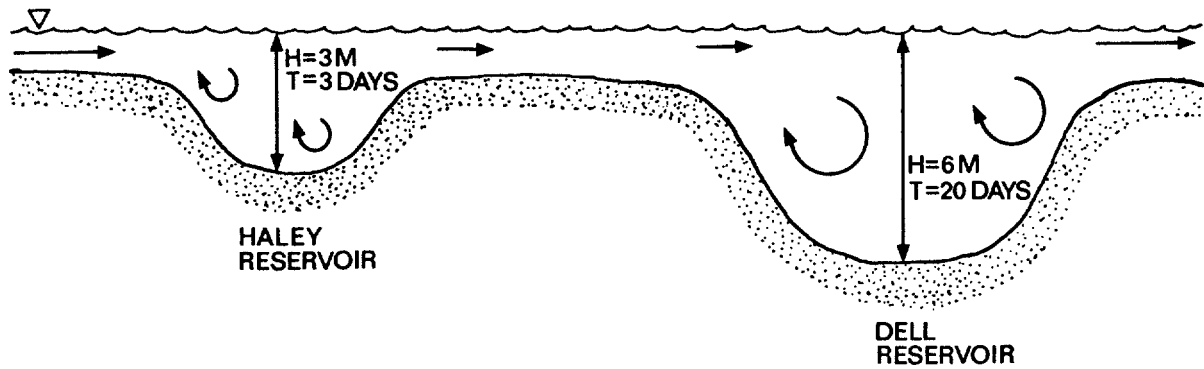


FIGURE IV-69 DEFINITION SKETCH USED IN EXAMPLE IV-23

The specific surface areas of the solids are typical values based on the data presented earlier. The settling velocities are based on Stokes Law, as described in Chapter 5.

From Equation IV-190, the concentrations of the suspended materials leaving Haley Reservoir are:

$$S_{\text{sand}} = \frac{100}{\frac{3 (.001) 86400}{3} + 1} = 1.1 \text{ mg/l}$$

$$S_{\text{silt}} = \frac{50}{\frac{3 \cdot 5 \cdot 10^{-4}}{3} 86400 + 1} = 1.1 \text{ mg/l}$$

$$S_{\text{clay}} = \frac{50}{\frac{3 \cdot 3 \cdot 10^{-6}}{3} 86400 + 1} = 40 \text{ mg/l}$$

Nearly all the silt and sand are deposited in the reservoir, but only 20 percent of the clay. The metal concentration in the outflow from Haley Reservoir is:

$$\begin{aligned} \text{Zn} &= 150 \frac{1 + 10^{4-6}/200 (10 \times 1.1 + 60 \times 1.1 + 200 \times 40)}{1 + 10^{4-6}/200 (10 \times 100 + 60 \times 50 + 200 \times 50)} \\ &= 150 (.83) = 120 \text{ } \mu\text{g/l} . \end{aligned}$$

Considering Dell Reservoir, it is apparent at a glance that the quantity of sand and silt leaving the reservoir is negligible. The concentration of clay leaving the reservoir is:

$$S_{\text{clay}} = \frac{40}{\frac{20 \cdot 3 \cdot 10^{-6}}{3} 86400 + 1} = 15 \text{ mg/l} .$$

The total metal in the outflow of Dell Reservoir is:

$$\begin{aligned} \text{Zn} &= 120 \frac{1 + \frac{10^{4-6}}{200} 200 \cdot 15}{1 + \frac{10^{4-6}}{200} (10 \times 1.1 + 60 \times 1.1 + 200 \times 40)} \\ &= 120 (.82) = 100 \mu\text{g/l} . \end{aligned}$$

It is somewhat surprising that the zinc remains in such high concentrations after passing through two reservoirs. However, consider that the dissolved zinc upstream of the first reservoir is:

$$\begin{aligned} \text{Zn}_{\text{dissolved}} &= \frac{150}{1 + \frac{10^{4-6}}{200} (100 \times 10 + 50 + 60 + 50 + 200)} \\ &= 88 \mu\text{g/l} . \end{aligned}$$

Hence, most of the zinc remaining in the river downstream of Dell Reservoir is dissolved.

----- END OF EXAMPLE IV-23 -----

#### 4.10.3.5 Adsorption and Resorption of Metal Between the Water Column and Bedded Sediments

The analyses presented in the previous sections are steady-state analyses, and ignore diffusive transport between the water column and bed. This is justified if the degradation rate of metal is negligible and the partition coefficients in the water column and the bed are the same. From these assumptions, the dissolved phase concentrations of metal are found to be the same in the water column and in the bed. Consequently, there is no net adsorption or resorption between the bedded and suspended materials.

However, situations do occur when the steady-state assumption is not valid. For example, consider a new discharge which begins operation on a previously uncontaminated river reach. As the contaminated water moves downstream, the metal in the water column is in contact with uncontaminated bedded sediment, and some of the dissolved metal can adsorb onto and diffuse into the bedded sediment. During this

process, the concentration in the water column decreases with distance. Figure IV-46 shown previously in this chapter illustrates the converse situation which occurs when an influx of metal is reduced so that the metal in the bedded sediments is no longer in equilibrium with the metal in the water column. Then, resorption tends to occur.

An approach is shown below that can address these situations, and can be used to answer questions such as:

- How long is required for river sediments to be cleansed of excessive metal concentrations by the process of natural resorption?
- If a new source of metal contamination begins discharge, how long is required before the impact of the elevated metal concentrations is fully felt downstream?

The following approach considers adsorption and resorption as the mechanisms of transporting metal between the water column and bed. The effects of resuspension and deposition are not considered mainly because the time frame of interest here is likely to be months to years. Resuspension and deposition rates fluctuate considerably over extended time periods, and tend to negate each other.

Figure IV-70 illustrates the relationship between the dissolved metal concentration in the water column and in the bedded sediments during a period when conditions are not in equilibrium. Near the sediment-water interface, there is likely to exist a relatively thin layer where the dissolved phase concentration is approximately the same as in the water column. Below this mixed layer, vertical diffusion in the sediment controls movement of the dissolved metal. By developing and simultaneously solving mass balance equations for the metal in the water column, in the mixed layer, and in the diffusion layer, the dissolved phase concentration in the water column is found to be:

$$C = \begin{cases} (C_b - C_0) G(t, x) + C_0, & x < \frac{t}{B} \\ C_0, & x > \frac{t}{B} \end{cases} \quad \begin{matrix} \text{(IV-198a)} \\ \text{(IV-198b)} \end{matrix}$$

where

$C_0$  = initial concentration in the water column (at  $t = 0$ ),  $\mu\text{g/l}$

$C_b$  = constant background concentration (at  $x = 0$ ),  $\mu\text{g/l}$

$t$  = time, days

$x$  = distance below location where  $C = C_b$ , m

$$B = \frac{1}{u} + \frac{M_s K \cdot 10^{-6}}{uH (1 + K_p S \cdot 10^{-6})}, \text{ days/ m}$$

$u$  = stream velocity, m/day

$M_s$  = mass of contaminated sediments, per unit area, in thin mixed layer,  $\text{g/m}^2$

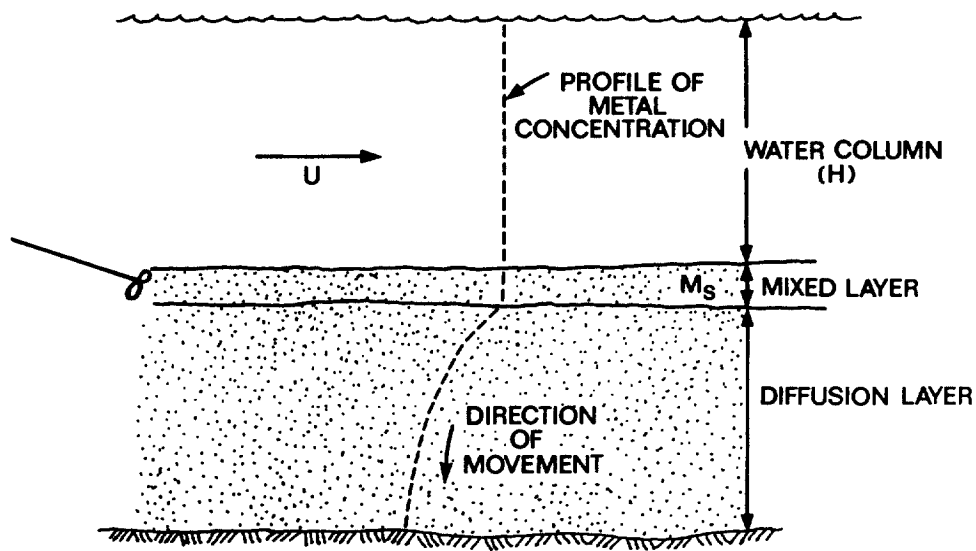


FIGURE IV-70 RELATIONSHIP BETWEEN METAL CONCENTRATION IN WATER COLUMN AND IN BEDDED SEDIMENTS DURING A NONEQUILIBRIUM ADSORPTION PERIOD

$H$  = water depth, m

$K_p$  = partition coefficient, l/kg

$S$  = suspended sediment concentration, mg/L

$G(t, x)$  = an unspecified function of time and distance, unitless.

Equation IV-198b above indicates that the boundary condition ( $C = C_b$ ) propagates downstream at a speed  $1/B$  which, depending on the magnitude of  $M_s K_p$ , can be significantly slower than the stream velocity. The quantity  $1/B$  is a useful parameter because it can be used to estimate the time required for the effects of a change in pollutant loading to be propagated downstream.

Equation IV-198 can be used to estimate the residual concentration in a river when the boundary concentration is set equal to zero after a period when metals have been accumulating in the bed (i.e., when  $C_b = 0$  and  $C_o > 0$ ). Conversely, the same equation can be used to predict the adjustment in stream metal concentration following start-up of a discharge where formerly there was none (i.e., when  $C_b > 0$ ,  $C_o = 0$ ).

To perform these calculations, the function  $G(t, x)$  is required. Using an approximation:

$$C \approx (C_b - C_o) \operatorname{erfc} \left[ \frac{\sqrt{D} x}{2uH (1 + K_p S \cdot 10^{-6}) \sqrt{t - Bx}} \right] + C_o \quad (IV-199)$$



where

$$D = \frac{D_m \theta}{\theta + \rho_b K_p}$$

$D_m$  = vertical diffusion coefficient,  $m^2/\text{day}$

$\theta$  = void fraction

$\rho$  = bulk density,  $g/m^3$

$K_p$  = partition coefficient, l/kg.

This is the equivalent of Equation IV-198a, which is valid for large times following a change in mass loading to a river (e.g., one year or greater). The major difficulty in using Equation IV-199 is finding appropriate input data for two of the important unknowns:  $D$  (or  $D_m$ ) and  $M_s$ . When  $K_p S$  is significantly less than unity and the depth of the mixed layer is small, Equation IV-199 can be further simplified to

$$C = (C_b - C_o) \operatorname{erfc}\left(\frac{\sqrt{D} x}{2uH \sqrt{t}}\right) + C_o \quad (\text{IV-200})$$

Suppose the temporarily changing concentration due to metal resorption from bedded sediments is desired. Set  $C_b = 0$ , so

$$\frac{C}{C_o} = \operatorname{erf}\left(\frac{\sqrt{D} x}{2uH \sqrt{t}}\right) \quad (\text{IV-201})$$

In this case, when the mixed layer is of negligible thickness, substituting typical values of  $D$ ,  $u$ ,  $H$  into Equation IV-201 shows that  $C \ll C_o$ . That is, resorption of metal back into the water column produces metal concentrations which are significantly below  $C_o$ , so the levels are not likely to be significant enough to be of concern. On the other hand, under these conditions the concentrations in the bed are likely to remain elevated for a long period of time, and could adversely impact the benthic community. In summary, it appears that unless there exists a mixed layer of sediments which can exchange metal with the water column at a rate substantially higher than by diffusion processes alone, resorption of metals from the bed back into the water column is likely to produce concentrations in the water column of secondary importance. Scour of the contaminated sediments is probably more responsible for reintroducing the metal back into the water column at rates where noticeably elevated concentrations may occur.

#### 4.10.3.6 Summary

##### 4.10.3.6.1 Overall Approach

The tools presented in the previous sections can be used to evaluate the influ-

ence of three hydrological conditions (all steady-state) on metal concentrations in rivers. The hydrologic conditions can be defined in terms of the suspended solids levels in rivers:

- a period of net settling
- a period of net scour
- a period of equilibrium (scour and sedimentation balance out each other, or each is negligible).

In order to use these concepts within the screening framework presented here, the annual cycle of events in a river is viewed as a series of steady-state conditions (each of which may be of several months' duration) separated by unsteady transition periods. The term "steady-state" is used cautiously here because each of the pseudo-steady periods may have elements of unsteadiness. For example, consider a high flow condition where metal-contaminated solids are continually being scoured from the bottom. Scouring of contaminated sediments will continue only as long as they are present, i.e., until the depth of contamination is exceeded. After that happens, the solids being scoured no longer contribute metal to the water column. This illustrates that a river's steady-state periods may really have some dependency on a previous steady period. To properly use the steady-state approach in the screening manual requires the user to carefully define the pseudo-steady periods, and select the data appropriate for each period.

To begin the analysis, a dilution approach is recommended, in the case of either single or multiple sources. This implies that multiple sources interact with each other, and downstream concentrations depend on both total mass loading and total dilution. A dilution analysis does not require either suspended solids concentrations or partition coefficients, unless the fraction of dissolved metal is required. Large reservoirs in the river system may require that settling of metal contaminated sediments within the reservoir be calculated, especially if most of the metal is being transported in particulate form.

As a next step, the user may wish to perform a scour analysis to see if metal concentrations become elevated in the water column during scour even though the flow rate is probably higher (thus, more dilution water is available). In such a case, the user might want to perform an analysis of each hydrologic condition throughout the annual cycle since each condition is not truly independent of the other.

#### 4.10.3.6.2 Uncertainty

Analysis of uncertainty for these screening methods is limited to a perturbation analysis: perturb (or change) the value of a variable within the range of uncertainty and see how the results change. If significant changes occur, the results are sensitive to that variable. At that time, some data could be collected to remedy the situation (see Section 4.10.5). Typically, for analyses discussed in this document,

the variables which require more accurate quantification are background and point sources, flow rates, and partition coefficients.

A particular use of uncertainty analyses is to address the question: Is there a significant difference in the metal concentration in the water column when the dilution approach is used compared to when settling and/or scour occur? For example, a user may have to decide whether concentration levels predicted to be 25 percent higher during a scour period, compared to an equilibrium period when net scour and settling are zero, are really different. By perturbing important variables within the range of realism, their questions can be addressed.

#### EXAMPLE IV-24

For the river shown in Figure IV-71, three point sources and three background sources contribute copper to the river system. Calculate the total copper concentration at locations P1, P2, P3, P4, and P5 for the following two conditions. Condition 1 is a moderate to low flow period where the solids within the water column appear to be in equilibrium over distance. Perform a dilution analysis during this period. Condition 2 is a high flow period which follows Condition 1. Data collected reveal that solids are being scoured along the mainstem during Condition 2 as follows:

- $\Delta SS = 50\text{mg/l}$ , from point source 1 to P1
- $\Delta SS = 25\text{mg/l}$ , from just below tributary B to P2
- $\Delta SS = 10\text{mg/l}$ , from just below tributary C to P4.

Determine which condition (the steady-state or scour condition) produces higher instream metal concentrations. Table IV-59 summarizes the required source data.

The dilution analysis (Condition 1) proceeds by applying the mixing equation (Equation IV-156) at each location, working from upstream to downstream:

$$C_{p1} = \frac{C_A Q_A + C_1 Q_1}{Q_A + Q_1} = \frac{5 \cdot 50 + 500 \cdot 5}{50 + 5} = 50 \mu\text{g/l}$$

$$C_{p2} = \frac{50 \cdot 55 + 5 \cdot 10}{55 + 10} = 43 \mu\text{g/l}$$

$$C_{p3} = \frac{C_C Q_C + C_2 Q_2}{Q_C + Q_2} = \frac{5 \cdot 20 + 75 \cdot 2}{22} = 11 \mu\text{g/l}$$

$$C_{p4} = \frac{11 \cdot 22 + 43 \cdot 65}{22 + 65} = 35 \mu\text{g/l}$$

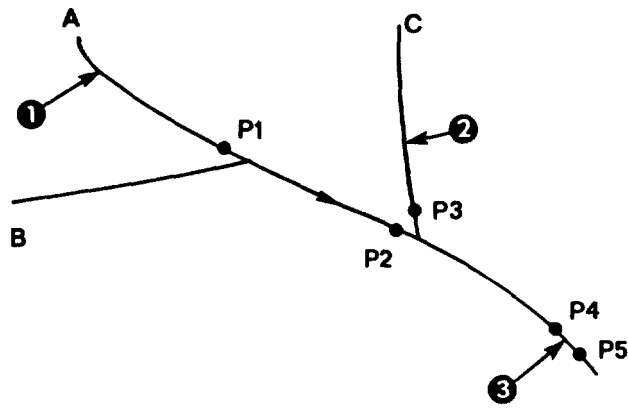


FIGURE IV-71 RIVER SYSTEM FOR EXAMPLE IV-24

TABLE IV-59  
SOURCE DATA REQUIRED FOR EXAMPLE IV-24

Source	Condition 1		Condition 2	
	Q(cfs)	Total-Cu( $\mu\text{g/l}$ )	Q(cfs)	Total-Cu( $\mu\text{g/l}$ )
A	50	5	500	5
B	10	5	100	5
c	20	5	200	5
1	5	500	5	500
2	2	75	2	75
3	10	400	10	400

$$C_{p5} = \frac{35 \cdot 87 + 400 \cdot 10}{87 + 10} = 73 \mu\text{g/l} .$$

The results are summarized in Table IV-60.

For condition 2, the incremental total metal concentration in each of the three reaches of the mainstem is, based on Equation IV-182:

$$\Delta SS \cdot K_p \cdot C_{SS} \cdot 10^{-6}$$

where

$K_p$  = partition coefficient for copper ( $\sim 10^4$  l/kg, assumed for this example)

TABLE IV-60

## SUMMARY OF RESULTS OF EXAMPLE IV-24

Location	Condition 1		Condition 2	
	Q(cfs)	Total-Cu( $\mu\text{g/l}$ )	Q(cfs)	Total-Cu( $\mu\text{g/l}$ )
P1	55	50	505	24
P2	65	43	605	28
P3	22	11	202	6
P4	87	35	807	25
P5	97	73	817	30

$C_{SS}$  = steady-state concentration of dissolved copper in the water column during Condition 1.

For  $C_{SS}$ , use an average value over the river:

$$\frac{50 + 43 + 35}{3} f_d = 43 f_d, \mu\text{g/l}$$

$$f_d = \frac{1}{1 + 10^4 \cdot 50 \cdot 10^{-6}} = 2/3, \text{ assuming SS} = 50\text{mg/l during Condition 1.}$$

The incremental copper concentration in each of the three reaches caused by scour are:

$$\text{Reach 1: } 50 \cdot 10^4 \cdot \frac{2}{3} \cdot 43 \cdot 10^{-6} = 14 \mu\text{g/l}$$

$$\text{Reach 2: } 25 \cdot 10^4 \cdot \frac{2}{3} \cdot 43 \cdot 10^{-6} = 7 \mu\text{g/l}$$

$$\text{Reach 3: } 10 \cdot 10^4 \cdot \frac{2}{3} \cdot 43 \cdot 10^{-6} = 3 \mu\text{g/l}$$

To each of these results, the concentration at the upstream end of each reach is added as shown in Equation IV-182. This is done by dilution analysis. For example, below point source 1:

$$C = \frac{5 \cdot 500 + 500 \cdot 5}{505} = 10 \mu\text{g/l} .$$

At location P1:  $C = 10 + 14 = 24 \mu\text{g/l}$

The results at the remaining locations are shown in Table IV-58.

The total copper levels in the river during the high flow are only 50 percent as high as during the lower flow condition. Apparently, the effects of dilution caused by the higher flow are more important than the scouring effect of the copper contaminated sediments. The fact that the factor  $\Delta SS \cdot K_p \cdot 10^{-6}$  is less than unity further indicates that the importance of scour is mitigated by the moderate size ( $<1$ ) of this product.

- - - - - END OF EXAMPLE IV-24 - - - - -

#### 4.10.3.6.3 Answers to Questions

In Section 4.10.2.3 (Selected Case Studies), a number of questions were posed which pertain to the the fate of metals in rivers. Based on the predictive tools just presented, these questions are answered here in a qualitative sense.

- Is downstream transport of metals important? Metals can be transported far downstream from their place of input. In some cases, dilution models appear adequate to predict the total metal concentration in the water column. Dilution models are appropriate when scouring of metal contaminated solids or settling of adsorbed metals are of secondary concern.
- Are metals which are present in the water column present entirely in adsorbed form or is there a significant dissolved fraction? Depending on the quantity and characteristics of the solids in the water column and the partition coefficient of the metals, the metal can be present in predominantly adsorbed form ( $>90\%$ ) or predominantly in dissolved form ( $>90\%$ ). When most of the metal is dissolved then downstream transport of the metal will be important. However, if most of the metal is adsorbed to suspended solids, downstream transport can still be important unless significant settling of the suspended matter occurs. Note that while solids tend to settle by gravitational forces, they are also kept in suspension by turbulent eddies which are generally present in free flowing rivers. Consequently, solids (and the adsorbed metals) can travel a long distance before settling.
- What is the relationship between the water column concentrations and concentrations in the bedded sediments? At steady-state conditions, the following approximation appears to be valid:

$$\begin{aligned} C_w &= C_b \\ X_w &= X_b \end{aligned}$$

where

$C_w, C_b$  = dissolved phase concentration in water column and bed, respectively  
 $X_w, X_b$  = mass of metal adsorbed per mass of sediment in water column and bed, respectively.

At first glance, these relationships appear to imply that there is no difference in water column and bed metal concentration. However, this is not true. Based on the above, the following can be concluded:

$$C_{Tw} \ll C_{Tb}$$

$$C_{sw} \ll C_{sb}$$

where

$C_{Tw}, C_{Tb}$  = total concentration in water column and in bed, on a unit volume basis, respectively

$C_{sw}, C_{sb}$  = adsorbed phase concentration in water column and in bed, on a unit volume basis, respectively.

On a unit volume basis, then, the metal concentration in the bed (within the contaminated layer, which might be quite thin) is likely to be significantly higher than in the water column. The primary reason for this is that the bed acts as a concentrator for metals that are settling. For example if solids that were suspended in a 1 m deep river settle onto a thin 1 mm layer at the sediment-water interface, then the concentration factor for solids and metals is 1000. Thus, a sorbed phase concentration of 10  $\mu\text{g/l}$  in the water column becomes 10000  $\mu\text{g/l}$  or 10 mg/l in the contaminated bed.

- What is the effect of reservoirs on metal concentrations downstream? If most of the metal that enters the reservoir is adsorbed, then the reservoir can act as a sink for the metal, depending on the hydraulic detention time and depth of the reservoir. If the detention time of the reservoir is relatively short and if the reservoir is shallow, only a small percentage of the total surface area in suspension might settle so that much of the adsorbed metal can still pass through the reservoir. Also, the dissolved fraction of the metal does not settle, so that unless the adsorbed fraction is great and most of it settles, then much of the metal that enters the reservoir can move downstream.
- What is the effect of metal resorption from river beds? Metal resorption from bedded sediments back into the water column appears to occur but at slow rates. If external sources of metals were suddenly cut back, then the equilibrium which may have existed between the bed and water column concentrations is disrupted. Under these conditions there is net resorption of metal into the water column, which tends to provide an internal source until an equilibrium is reestablished again. Complete resorption of metals from bedded sediments may take years, effectively slowing the recovery of the river in response to point source reduction.

These concentrations may be low enough to be of secondary concern to organisms in the water column, but may be high enough to be of primary concern to the benthic community.

#### 4.10.4 Speciation of Metals and Equilibrium Modeling

##### 4.10.4.1 Introduction

While the analyses in the preceding sections have proceeded under the assumption that the fate of metals can be determined based on analysis of a single dissolved species and a single adsorbed species, metals do not obey such a simplified pattern of behavior. Figure IV-72 illustrates a more general picture of behavior. Dissolved metal might be present as the free ion, or as complexes with inorganic or organic ligands. The adsorbed metal can be adsorbed to a variety of surface types and appears to obey different adsorption isotherms. If concentrations of metals become too high, precipitates may form and settle from the solution, or remain suspended in solution if particle size remains small enough. This section introduces the processes affecting the speciation of metals. A generic discussion of processes precedes a metal-by-metal discussion of nine of the priority metals. The generic discussion emphasizes fate in freshwater environments. It does not detail all processes, but rather those which are often of greatest importance. This discussion should be balanced against the screening procedures found earlier in this document. This second point of view can help the user to see more clearly the simplification and assumptions made in the screening procedures and to interpret results of the screening analysis more intelligently.

##### 4.10.4.2 Major Processes Affecting Speciation

This discussion emphasizes the predominant fate processes likely to be of importance for metals discharged to freshwater rivers and streams under oxic conditions. This scenario, while not completely general, does encompass many commonly occurring situations and is consistent with the scope of this section. Figure IV-73 shows the general range of pH-pe values considered here, as well as the range which can be found in different environments. The pH-pe range for each environment are typical but not all inclusive. Higher pe values in ground water systems are possible, for example.

It is not necessary that users actually perform calculations relating to the processes that are discussed here. Rather, the calculations have been performed by a metal speciation model called MINEQL, which is applied to a number of different water bodies (Section 4.10.4.4). The major processes that are discussed in this section include:

- Precipitation-dissolution



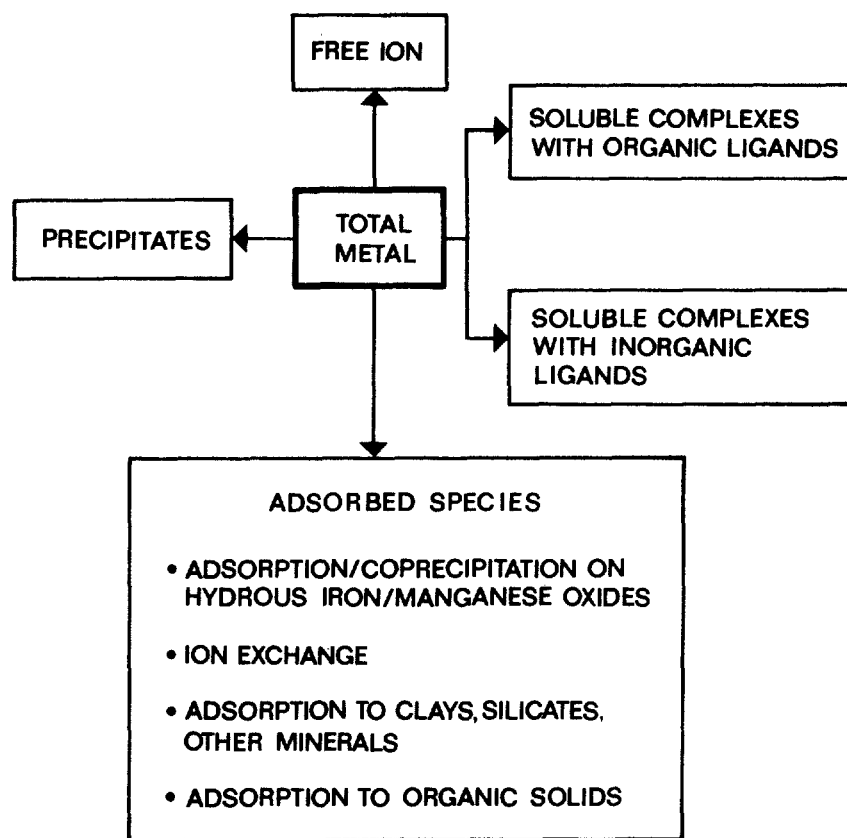


FIGURE IV-72 SPECIATION OF METALS IN THE AQUATIC ENVIRONMENT

- Adsorption
- Oxidation-reduction
- Dilution.

Several other processes of minor importance are also specifically addressed.

Before beginning the process-by-process discussion, some of the important "master variables" (terminology often used by Stumm and Morgan, 1970) that control the fate of the metals are reviewed. These master variables are pH, pe, ionic strength, and water temperature.

The solution pH ( $= -\log \{H^+\}$ , where  $\{H^+\}$  is hydrogen ion activity -hydrogen ion concentration) is a measure of the hydrogen ion concentration. Typically, in fresh water, pH = 7 denotes neutral conditions, while pH values exceeding 7 denote basic conditions, and pH less than 7 denote acidic conditions. Ocean waters have a relatively constant pH of 8.3-8.5, due to their buffering capacity. The pH of rainwater containing only atmospheric carbon dioxide is typically 5.6-5.7. However, when other acidic inputs are significant, rainwater pH can be lowered to 4.2 or so (acid rain). The pH of river water is more variable than that of the ocean, and most often ranges from 6.2 to 8.0. Solution pH can strongly influence the speciation of metals (i.e. their form, such as  $Cu^{2+}$  or  $CuOH^+$ ) and hence their fate and toxicity.

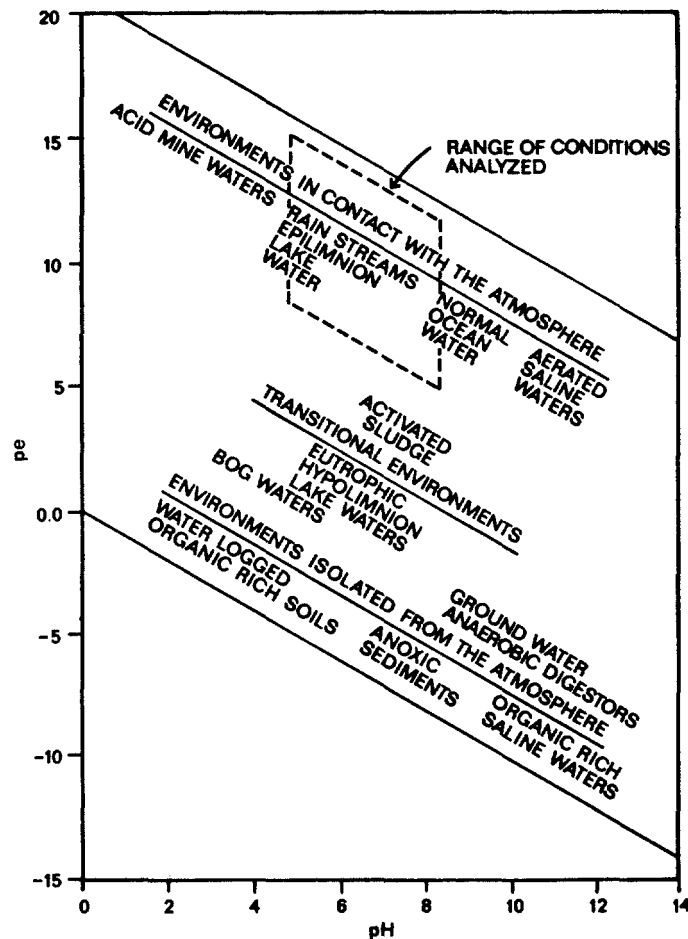


FIGURE IV-73 RELATIVE CHARACTERIZATIONS OF ENVIRONMENTS BY PE AND pH

A related concept is  $pe$  ( $= -\log \{e^-\}$ , where  $\{e^-\}$  is the electron activity). The  $pe$  describes the oxidation-reduction status of a water body, and is influential in dictating species likely to be present in water bodies. Together with  $pH$ ,  $pe$  can be used to create equilibrium phase diagrams.

Another measure of oxidation-reduction often used is the electrochemical redox potential,  $E_H$ .  $E_H$  and  $pe$  are related as follows:

$$E_H \text{ (in volts)} = 0.059 pe, \text{ at } 25^\circ\text{C}$$

The dissolved oxygen level can also be related to  $pe$ . Based on the oxygen-water redox reaction, this relationship is:

$$pe = 1/4 \log P_{O_2} + 20.75 - pH$$

where

$$P_{O_2} = \text{partial pressure of dissolved oxygen, atmospheres.}$$

For dissolved oxygen levels corresponding to saturation ( $P_{O_2} = 0.2$ ),  $pe = 13.6$

at pH = 7. For dissolved oxygen levels of about 0.1 mg/l,  $p_e = 13.1$  at pH = 7. Hence, in most surface water systems, even in the presence of a small amount of dissolved oxygen, the  $p_e$  values are typically in the range of 12 to 13.6. Only in anoxic systems (or under nonequilibrium conditions) are  $p_e$  values negative. While the concept of redox equilibrium is a useful one, the user is cautioned that many natural systems are not likely to be in redox equilibrium.

Ionic strength is a measure of the concentration of ionic species in a solution. In very dilute solutions, with low concentrations of ions, the ions behave independently of each other. However, as the concentrations of ions increase, electrostatic interactions between the ions also increase. Consequently under these conditions, activities rather than concentrations are used in chemical equilibrium equations. Activities are defined as:

$$\{C\} = \gamma [C] \quad (IV-202)$$

where

$\{C\}$  = activity of species C

$[C]$  = concentration of species C

$\gamma$  = activity coefficient.

For ideal or very dilute solutions,  $\gamma = 1$  and activity equals concentration. Figure IV-74 illustrates how activity coefficients change with ionic strength and charge. An ionic strength of 0.5M corresponds to seawater and an ionic strength of 0.0000M corresponds to distilled water. Unless ionic strength is extremely low, activity coefficients are not expected to equal unity, especially for divalent and trivalent ions.

For the analyses here, ionic strength corrections are automatically accounted for in the equilibrium model MINEQL. The user simply has to specify the "typical" water appropriate for the conditions being analyzed (see Section 4.10.4.3).

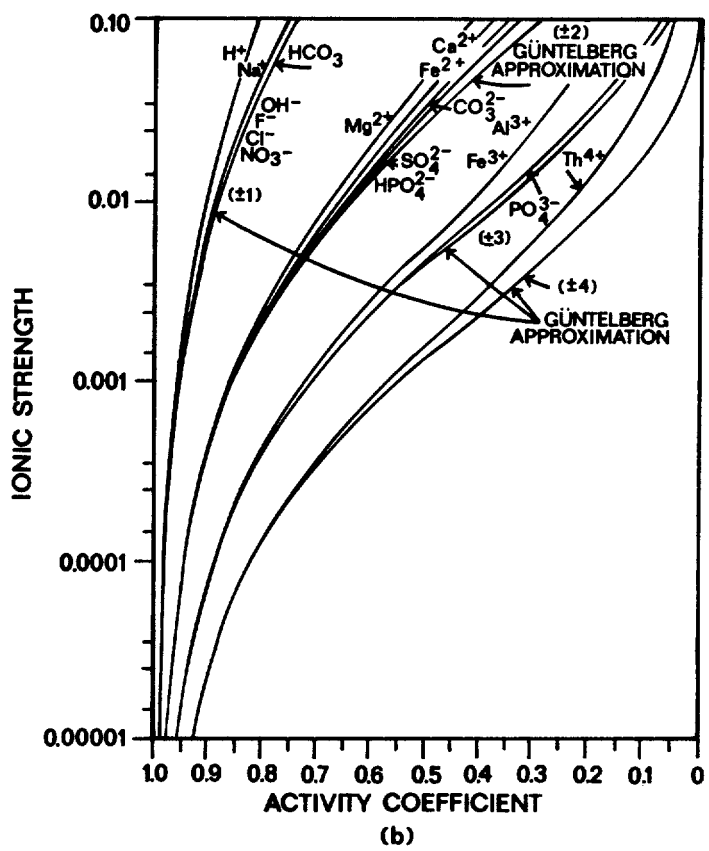
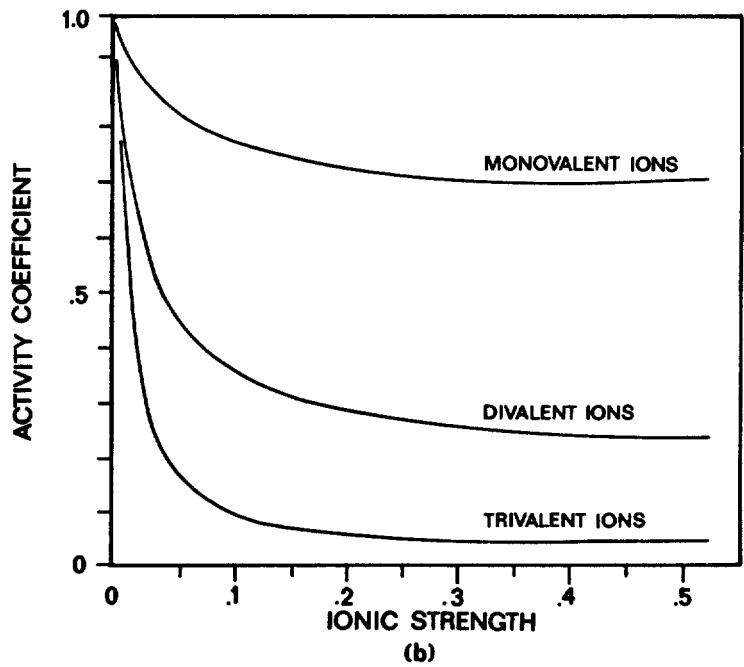
Ionic strength (I) can be estimated from either total dissolved solids (TDS) or specific conductivity, two commonly available parameters. The appropriate relationship between TDS and ionic strength is:

$$I = 2.5 \cdot 10^{-5} \cdot \text{TDS} \quad (IV-203)$$

where

TDS = total dissolved solids, mg/l.

The relationship between specific conductivity ( $\mu\text{mho}$ ) and ionic strength is shown in Figure IV-75. The relationships between ionic strength and TDS and between ionic strength and conductivity are valid for ionic strengths less than 0.1, which is more than adequate for fresh water systems. TDS levels for most fresh water in this country are less than 1200 mg/l. Corresponding to Equation (IV-203) above, the ionic strength is:



REFERENCE: MOREL AND SCHIFF, 1980, AND SNOEYINK AND JENKINS, 1980

FIGURE IV-74 ACTIVITY COEFFICIENT AND IONIC STRENGTH RELATIONSHIPS FOR TYPICAL IONS (A) AND SPECIFIC IONS (B),

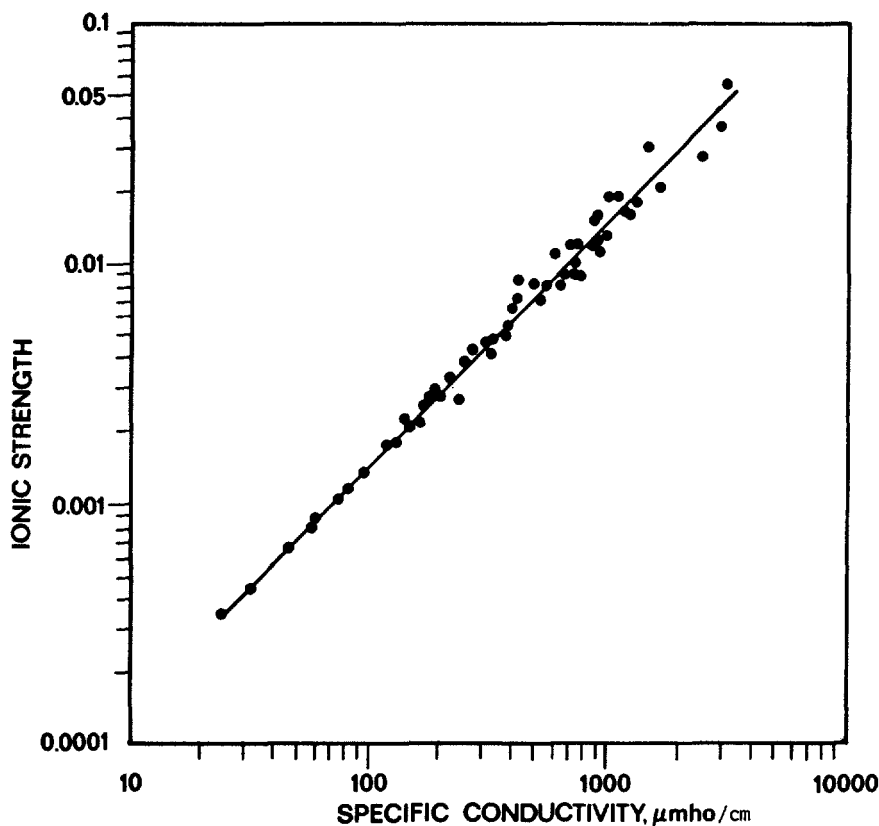


FIGURE IV-75 IONIC STRENGTH VERSUS SPECIFIC CONDUCTIVITY FOR SURFACE MATERS (FROM LIND, 1970)

$$I = 2.5 \times 10^{-5} \times 1200 = 0.03$$

At this ionic strength, activity coefficients are likely to be about 0.8 to 0.9 for monovalent ions, 0.5 to 0.6 for divalent ions, and 0.1 to 0.3 for trivalent ions (see Figure IV-74b).

Water temperature influences virtually every aspect of the chemistry of metals, including solubility and equilibrium constants, and reaction kinetics. Temperature corrections can be used in MINEQL.

#### 4.10.4.2.1 Precipitation and Dissolution

Metals are subject to solubility limitations in natural waters. Should the solubility product (defined below) be exceeded, then that metal tends to precipitate. By precipitating, the metal forms a solid phase (say lead hydroxide,  $\text{Pb}(\text{OH})_2$  (s)) which might remain suspended in the water column if the solid phase particles are small enough and do not grow and if water turbulence is sufficient to keep them in suspension. However, should the solid grow to sufficient size, or be transported to a slowly moving backwater region, then sedimentation of the solid is likely.

The solubility product for a metal cation (a cation is a positively charged ion) with an anion (a negatively charged ion) is represented as:



where

$M_a B_b(s)$  = the solid phase species

$M^{b+}$  = the positively charged metal cation (with charge b+)

$B^{a-}$  = the anion (with charge a-).

The equilibrium constant for this reaction is defined as:

$$K_{sp} = \frac{\{M^{b+}\}^a \{B^{a-}\}^b}{\{M_a B_b(s)\}} \quad (IV-205a)$$

$$= \{M^{b+}\}^a \{B^{a-}\}^b \quad (IV-205b)$$

where

$\{M_a B_b(s)\}$  = activity of solid phase, defined as unity by convention

$\{M^{b+}\}$  = activity of metal cation

$\{B^{a-}\}$  = activity of anion

$K_{sp}$  = the equilibrium constant, called the solubility product.

The relationship between activity and concentration can be invoked so that Equation IV-205b can be expressed in terms of concentrations (and activity coefficients) rather than in terms of activities. This is desirable because concentration prediction, rather than activity prediction, is the objective of the analyses. Invoking the definition of activity coefficient as the ratio of activity to concentration, Equation IV-205b can be rewritten as:

$$K_{sp} = \left( \gamma_M [M^{b+}] \right)^a \left( \gamma_B [B^{a-}] \right)^b \quad (IV-206a)$$

$$= \gamma_M^a \gamma_B^b [M^{b+}]^a [B^{a-}]^b \quad (IV-206b)$$

where

$\gamma_M, \gamma_B$  = activity coefficients for the metal cation and the anion, respectively

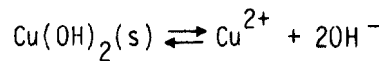
$[M^{b+}]$  = concentration of metal cation

$[B^{a-}]$  = concentration of anion.

When  $\gamma_M \approx 1$ , and  $\gamma_B \approx 1$ , Equation IV-206b can be written in the simpler, more familiar, form:

$$K_{sp} = [M^{b+}]^a [B^{a-}]^b \quad (IV-207)$$

As an example of the above concepts, consider copper solubility and assume solubility is controlled by copper hydroxide:



The solubility relationship is:

$$[Cu^{2+}][OH^-]^2 = K_{sp} = 10^{-19.3}, \text{ at } 25^\circ C$$

The equilibrium constant is contained in standard chemistry texts, such as Snoeyink and Jenkins (1980). This relationship predicts that at high pH (or high  $OH^-$  concentrations), the amount of  $Cu^{2+}$  in the dissolved form is less than at lower pH. For example, suppose the pH were to change from pH 6 to pH 8. If the only species of copper present is the above one, then the maximum amount of  $Cu^{2+}$  which could be dissolved is decreased by:

$$\frac{[Cu^{2+}]_{pH=8}}{[Cu^{2+}]_{pH=6}} = \frac{[10^{-8}]^2}{[10^{-6}]^2} = 10^{-16+12} = 10^{-4} = \frac{1}{10,000}$$

Or,  $Cu^{2+}$  concentration is potentially decreased by a factor of 10,000.

The user is not required to perform calculations of the type given in Equations IV-205 or IV-207. They are performed by the equilibrium model MINEQL.

Determining the solubility of a metal in a natural water body is complicated by the fact that a metal's solubility may be controlled by one of several solid phases. Typically, in oxic environments, carbonates or hydroxides control solubility, while in anoxic environments, sulfide often controls (Forstner and Wittmann, 1979). The size of the solubility product equilibrium constant for each possible controlling phase does not reveal the controlling phase; that is, solubility products cannot be directly compared against each other (one reason is that the units of one equilibrium constant are generally not the same as the units of another). This complication is one reason that equilibrium models such as MINEQL are so valuable: they can sort out the controlling solid phase.

As another complication, supersaturation of constituents in natural waters can, and does, occur. The supersaturation of a water with respect to a given solid should not be unexpected. Aqueous systems are not always at equilibrium.

#### 4.10.4.2.2 Adsorption

Adsorption, or the accumulation of metals at the boundary region of solid-liquid

interfaces, is typically quite important for natural waters. Partition coefficients (assuming linear isotherms) for many priority metals can be expected to be in the neighborhood of  $10^3$  to  $10^6$  l/kg, but for a given metal, appear to be quite variable.

Adsorption of metals is generally influenced by pH, adsorbent concentration (surface available for adsorbing), competing ligands, competing adsorbates, and adsorbate concentrations (Leckie, *et al.*, 1980). Figure IV-76 illustrates how adsorption depends on pH and adsorbent concentration for both cationic and anionic metallic species. Uncompleted, or free metal cations, typically behave according to Figure IV-76(a). At low pH values, very little of the metal ion is adsorbed, while at higher pH levels, most of the cation is adsorbed. The pH range within which this occurs can be quite narrow, as shown by the steep slope (or "edge") of these curves.

Most metallic species in freshwater environments are typically present as cations (e.g.,  $\text{Cu}^{2+}$ ). However, some anionic species do exist (e.g.,  $\text{CrO}_4^{2-}$  and  $\text{AsO}_4^{3-}$ ). Adsorption of anionic species follows curve IV-76b so that most of these species are adsorbed at low pH and dissolved at high pH.

The presence of organic and inorganic ligands can dramatically influence adsorption. The table below illustrates different categories of species that can result from a combination of solid surfaces, metals, and organic and inorganic ligands.

<u>Components</u>	<u>Primary Species</u>	<u>Secondary Species</u>
x: solid surfaces	XY	M-XY
M: metal	MX	Y- MX
Y: organic ligand	MY	None
z: inorganic ligand	MZ	X-MZ

The primary metal species that form can either be dissolved organic or inorganic complexes, or species adsorbed to solid surfaces. Then, a number of secondary adsorbed metal species can form which are combinations of the components and primary species. Note that the addition of organic ligands (Y) results in both soluble metallic species (MY) and adsorbed metal species (M-XY and Y-MX). It is not always possible to state whether the organic ligands result in more or less adsorbed species.

Dissolved organic carbon levels in most rivers typically range between 1 to 10 mg/l, while adsorbed or solid phase organic carbon levels are often between 0.1 to 1.0 mg/l. Thus, since much of the organic carbon is dissolved, it is expected that soluble metal-organic complexes can form and in many cases, might tend to increase the fraction of dissolved metal.

When multiple metal sorbates are present together, they can compete for a limited number of adsorption sites. If concentrations of adsorbates are high and sites limited, then adsorption of some ions may be limited.

As the above discussion makes evident, metal adsorption can be quite complex. The discussion thus far has not addressed either adsorption kinetics, or the various



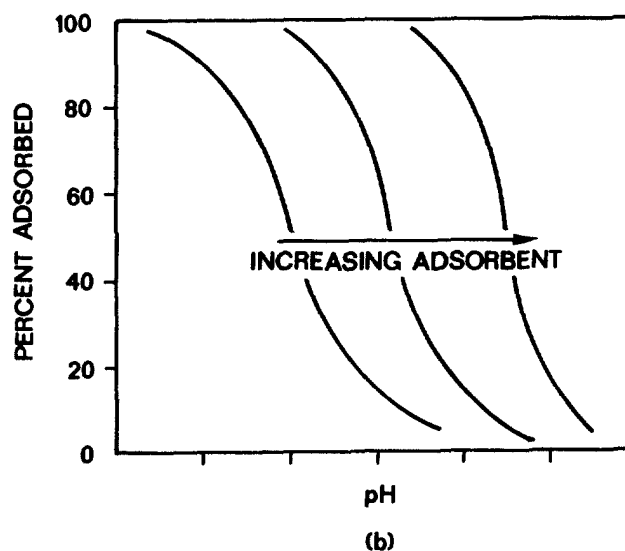
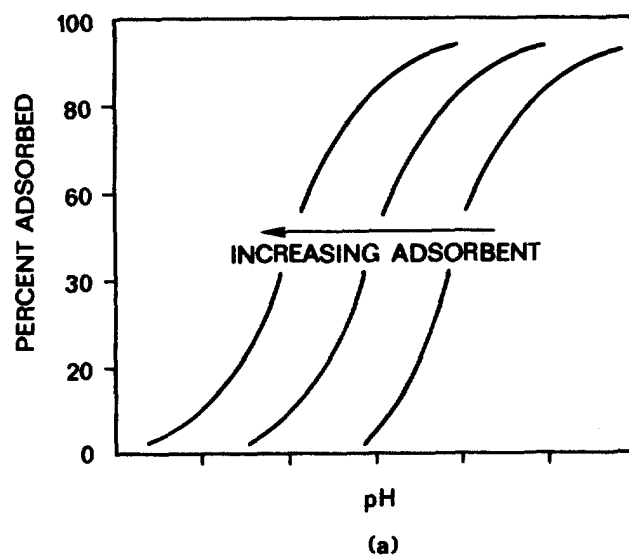


FIGURE IV-76 TYPICAL ADSORPTION CURVES FOR METAL CATIONS (A) AND ANIONS (B) FOR A RANGE OF pH AND ADSORBENT LEVELS,

linear and nonlinear equilibrium isotherms or other mechanistic approaches for predicting adsorption (e.g. electric double-layer theory). For this screening approach, the linear equilibrium adsorption isotherm is used. Linear partition coefficients are presented from the literature.

HydroQual, as documented in Delos et al. (1983), has calculated linear partition coefficients for rivers and lakes for various metals. They analyzed approximately 20,000 records from data bases such as STORET in order to arrive at their predictions.

They found the partition coefficients to be dependent on suspended solids concentrations, but to be independent of pH. Table IV-61 summarizes their results. Under most conditions, the expressions in the table predict that the partition coefficients are likely to exceed  $10^4$  l/kg, and in some cases, exceed  $10^6$  l/kg.

Based on linear partitioning, the fraction of metal dissolved is given by:

$$\frac{C}{C_T} = \frac{1}{1 + K_p \cdot SS \cdot 10^{-6}} \quad (IV-208)$$

where

$\frac{C}{C_T}$  = fraction dissolved

$K_p$  = linear partition coefficient, l/kg

$SS$  = suspended solids, mg/l.

The results of this equation are shown in Table IV-62 for each of the metals in Table IV-61 for a range of suspended solids from 1 mg/l to 1000 mg/l. In most instances, the percent of the metal which is adsorbed exceeds 50 percent. This is in contrast to many toxic organics which often have smaller partition coefficients and, therefore, more of the toxicant is transported in the dissolved state (see, for example, Table 11-14).

While the results in Tables IV-61 and IV-62 provide useful information, the possible error associated with the predicted partition coefficients is quite large. Figure IV-77 illustrates this for copper. The envelope of values encompasses an order of magnitude.

Rai et al. (1983) have summarized adsorption data for numerous priority metals. The summary includes  $K_p$  values for linear partitioning as well as data for other types of isotherms. As a result of reviewing the work of Rai et al. (1983), and other literature sources it appears that there is generally no consistency as to "expected" values of  $K_p$  for a particular metal in the natural environment. Some researchers **report** relatively small partition coefficients for metals while others, such as Delos et al. (1983), report significantly larger values. This uncertainty (or variability) emphasizes that site-specific  $K_p$  values should be used if possible and that better methods for predicting the importance of partitioning are probably warranted. Based on the fact that metals speciate and each species exhibits different adsorption tendencies, it is not difficult to see why a " $K_p$  approach" is limited in predictive ability. However, the alternative **approaches** are not well supported either and site-specific data can be quite beneficial, regardless of the approach.

#### 4.10.4.2.3 Oxidation-Reduction

Oxidation-reduction reactions are conceptually analogous to acid-base reactions, except they are significantly slower. Oxidants and reductants are defined as electron

TABLE IV-61

LINEAR PARTITION COEFFICIENTS FOR PRIORITY METALS IN STREAMS AND LAKES  
(Delos *et al.*, 1983)

Metal	Streams			Lakes		
	# Records	$K_{po}$	$\alpha$	# Records	$K_{po}$	$a$
Arsenic	1635	$0.48 \times 10^6$	-0.73	1	--	--
Cadmium	254	$4.00 \times 10^6$	-1.13	296	$3.52 \times 10^6$	-0.92
Chromium	345	$3.36 \times 10^6$	-0.93	211	$2.17 \times 10^6$	-0.27
Copper	2722	$1.04 \times 10^6$	-0.74	577	$2.85 \times 10^6$	-0.90
Lead	1545	$0.31 \times 10^6$	-0.19	411	$2.04 \times 10^6$	-0.53
Mercury	369	$2.9 \times 10^6$	-1.14	169	$1.97 \times 10^6$	-1.17
Nickel	1394	$0.49 \times 10^6$	-0.57	285	$2.21 \times 10^6$	-0.76
Zinc	2253	$1.25 \times 10^6$	-0.70	914	$3.34 \times 10^6$	-0.68

Partition Coefficient:

$$K_p (1/\text{kg}) = K_{po} \cdot \text{SS}^\alpha$$

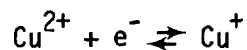
where SS = suspended solids concentration, mg/l, and  $K_{po}$  and  $\alpha$  are found from the table.

Example:

Assume SS = 100 mg/l in a river. Find  $K_p$  for copper.

$$K_p = 1.04 \cdot 10^6 \cdot 100^{-0.74} = 3.4 \cdot 10^4 \text{ 1/kg.}$$

acceptors and electron donors, respectively. An example redox half reaction is:



where  $\text{Cu}^{2+}$  is the oxidant and is reduced to  $\text{Cu}^+$  when it accepts an electron.

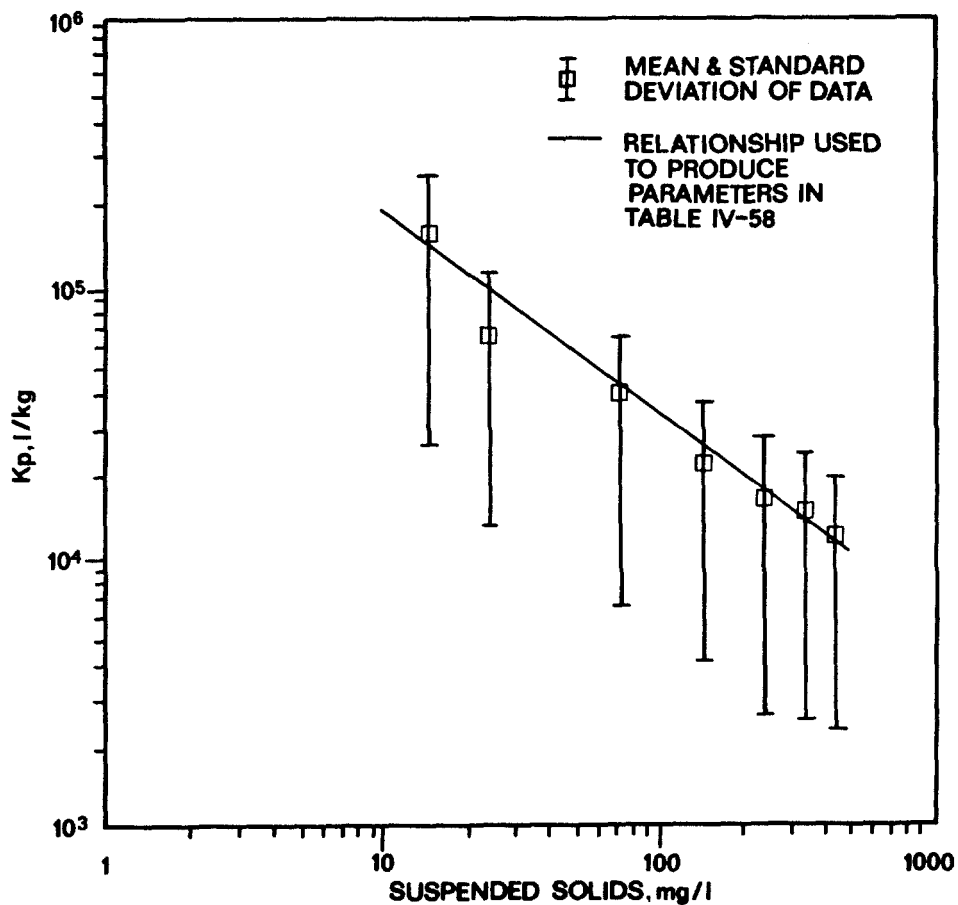
As discussed earlier, the measure of electron activity is commonly expressed as pe (=  $-\log \{e^-\}$ ). The oxidation state is important because it can control the species present in solution (at equilibrium).

For screening purposes, oxidizing conditions are assumed to exist. This assumption is good for rivers and streams as long as even a small amount of dissolved

TABLE IV-62

SPECIATION OF PRIORITY METALS BETWEEN DISSOLVED AND ADSORBED PHASES  
AS A FUNCTION OF SUSPENDED SOLIDS CONCENTRATIONS IN STREAMS

Metal	SS (mg/l)	$K_p$ (l/kg)	% Dissolved	% Adsorbed
Arsenic	1	$5 \cdot 10^5$	70	30
	10	$9 \cdot 10^4$	50	50
	100	$2 \cdot 10^4$	30	70
	1000	$3 \cdot 10^3$	24	76
Cadmium	1	$4 \cdot 10^6$	20	80
	10	$3 \cdot 10^5$	25	75
	100	$2 \cdot 10^4$	30	70
	1000	$2 \cdot 10^3$	40	60
Chromium	1	$3 \cdot 10^6$	25	75
	10	$4 \cdot 10^5$	20	80
	100	$5 \cdot 10^4$	17	83
	1000	$5 \cdot 10^3$	15	85
Copper	1	$1 \cdot 10^6$	50	50
	10	$2 \cdot 10^5$	30	70
	100	$3 \cdot 10^4$	25	75
	1000	$6 \cdot 10^3$	14	86
Lead	1	$3 \cdot 10^5$	75	25
	10	$2 \cdot 10^5$	30	70
	100	$1 \cdot 10^5$	10	90
	1000	$9 \cdot 10^4$	1	99
Mercury	1	$3 \cdot 10^6$	25	75
	10	$2 \cdot 10^5$	30	70
	100	$2 \cdot 10^4$	30	70
	1000	$1 \cdot 10^3$	45	55
Nickel	1	$5 \cdot 10^5$	70	30
	10	$1 \cdot 10^5$	50	50
	100	$4 \cdot 10^4$	20	80
	1000	$9 \cdot 10^3$	10	90
Zinc	1	$1 \cdot 10^6$	40	60
	10	$2 \cdot 10^5$	30	70
	100	$5 \cdot 10^4$	17	83
	1000	$1 \cdot 10^4$	10	90



REFERENCE: DELOS ET AL., 1983

FIGURE IV-77 PARTITION COEFFICIENT FOR COPPER IN STREAMS

oxygen is present. The model MINEQL has been run for conditions corresponding to oxidizing environments.

#### 4.10.4.2.4 Dilution

When wastewater is discharged into a river, the metal speciation of the wastewater-river water mixture can be significantly altered compared with metal speciation in the wastewater. This is because the master variables of pH, pe, ionic strength, and temperature in the wastewater-river mixture can be quite different from those of the wastewater alone.

Examples of processes likely to be important during mixing are:

- Volubility changes due to significant changes in species concentrations and redox conditions (say from anoxic conditions where sulfides can control volubility to oxic conditions and where carbonates or hydroxides can control volubility).

- pH changes can influence the fraction of species adsorbed and the relative distribution of the dissolved species.

#### 4.10.4.2.5 Processes of Secondary Importance

Other processes that can influence the fate of a few of the priority metals are volatilization, photolysis, and biodegradation. Each of these processes is discussed in detail in Chapter II of this document as they relate to organic contaminants. Volatilization is the physical transfer of metal from the water column into the atmosphere. Elemental mercury can volatilize and so possibly can arsenic. Photolysis is the chemical process of degradation through absorption of solar energy and may influence the fate of cyanide and mercury. Biodegradation, or the microbial degradation of metal complexes, can influence a number of priority metals. In this section, the processes of volatilization, photolysis, and biodegradation are given minor attention. While photolysis and biodegradation may influence metal speciation, the metal itself can still be present in the water column, although as a complex which may have different toxicity than before.

#### 4.10.4.3 Metal-by-Metal Discussion

This section summarizes the fate of nine priority metals in oxidizing surface water environments. Figure IV-78 shows a periodic table of the elements and illustrates the placement of each of the priority metals discussed (see the circled elements). The common oxidation states of each metal are shown above and to the left of the symbol for each metal. Table IV-63 summarizes the discussion that is to follow. The table shows the metals affected by oxidation-reduction, the primary species which are likely to be present in each environment, the solids controlling solubility, and pH-pe combinations that are conducive to mobilizing the metals (e.g., increasing solubility).

##### 4.10.4.3.1 Arsenic

A source of arsenic in the natural environment in the United States is coal-fuel power plants, which emit approximately 3000 tons of arsenic per year (Nelson, 1977). Arsenic trioxide,  $\text{As}_2\text{O}_3(\text{s})$ , is formed and is often the compound which first reaches surface waters. Concentrations of arsenic in surface waters of the United States range from 5 to 340 ppb, with a mean value of 64 ppb (Kopp, 1969). In contrast, average arsenic concentrations in ocean waters are about 2 ppb.

Figure IV-79 is a pe-pH diagram for arsenic, without the influence of organic material, showing its behavior for total arsenic ranging from  $10^{-6}$  to  $10^{-3}$  M (0.1 to 100 ppm). In oxidizing environments likely to exist in most surface waters (i.e. pe

PERIODIC TABLE OF THE ELEMENTS

Representative Elements s block		Transition Elements d block										Representative Elements p block					Noble gases	
IA												IIA	IIIA	IVA	VA	VIA	VIIA	0
1	+1 H 1 0079	Transition Elements d block															2 He 4 003	
2	+1 3 Li 6 941	+2 4 Be 9 012											+3 5 B 10 81	+4 6 C 12 011	+5 7 N 14 007	8 O 15 999	9 F 18 998	10 Ne 20 18
3	+1 11 Na 22 99	+2 12 Mg 24 30											+3 13 Al 26 98	+4 14 Si 28 08	+5 15 P 30 97	+6 16 S 32 06	+7 17 Cl 35 45	18 Ar 39 95
4	+1 19 K 39 10	+2 20 Ca 40 08	21 Sc 44 96	22 Ti 47 88	23 V 50 94	+6 24 Cr 52 00	+7 25 Mn 54 94	+8 26 Fe 55 85	+8 27 Co 58 93	+8 28 Ni 58 71	+2 29 Cu 63 55	+2 30 Zn 65 38	+3 31 Ga 69 72	+4 32 Ge 72 59	+5 33 As 74 92	+6 34 Se 78 96	+7 35 Br 79 90	36 Kr 83 80
	+1 37 Rb 85 47	+2 38 Sr 87 62	39 Y 88 91	40 Zr 91 22	41 Nb 92 91	42 Mo 95 94	43 Tc 98 91	44 Ru 101 07	45 Rh 102 91	46 Pd 106 4	+1 47 Ag 107 87	+2 48 Cd 112 40	+3 49 In 114 82	+4 50 Sn 118 69	+5 51 Sb 121 75	+6 52 Te 127 60	+7 53 I 126 90	54 Xe 131 30
5	+1 55 Cs 132 91	+2 56 Ba 137 34	57 La 138 91	72 Hf 178 49	73 Ta 180 95	74 W 183 85	75 Re 186 2	76 Os 190 2	77 Ir 192 22	78 Pt 195 09	79 Au 196 97	+2 80 Hg 200 6	+3 81 Tl 204 4	+4 82 Pb 207 2	+5 83 Bi 209 0	+6 84 Po (210)	85 At (210)	86 Rn (222)
6	+1 87 Fr (223)	+2 88 Ra 226 0	89 Ac (227)	104 Ku*	105 Ha*	Inner Transition Elements f block												
Lanthanum Series			58 Ce 140 12	59 Pr 140 9	60 Nd 144 24	61 Pm (147)	62 Sm 150 4	63 Eu 151 96	64 Gd 157 2	65 Tb 158 93	66 Dy 162 50	67 Ho 164 93	68 Er 167 26	69 Tm 168 93	70 Yb 173 04	71 Lu 174 97		
Actinium Series			90 Th 232 0	91 Pa 231 0	92 U 238 0	93 Np 237 0	94 Pu (242)	95 Am (243)	96 Cm (247)	97 Bk (247)	98 Cf (247)	99 Es (254)	100 Fm (253)	101 Md (256)	102 No (254)	103 Lr (257)		

Mass numbers of the most stable or most abundant isotopes are shown in parentheses. The elements to the right of the bold lines are called the nonmetals and the elements to the left of the bold line are called the metals. Common oxidation numbers are given for the representative elements and some transition elements. \*Kurchatovium and Hahnium are tentative names for these elements.

FIGURE IV-78 PERIODIC TABLE OF THE ELEMENTS (FROM SNOEYINK AND JENKINS, 1980)

values exceeding 8 or so), the pentavalent arsenic and  $\text{HAsO}_4^{2-}$  being the most likely anions. Only at relatively low pe values (around 0 or less) at the pH range likely to exist in natural waters will the trivalent form be stable. As evidenced from the pe-pH diagram, arsenic(V) is a triprotic acid, and its behavior is quite similar to that of phosphoric acid.

Arsenic(V) forms a series of salts with alkaline-earth metals (magnesium, calcium, strontium, and barium) and with a number of the heavy metals (such as nickel, copper, zinc, cadmium, and lead) which are quite insoluble. For example, oversaturation with respect to  $\text{Pb}_3(\text{AsO}_4)_2(\text{s})$  at an As(V) concentration of  $10^{-5}$  M can occur when lead concentrations exceed  $10^{-5}$  M at pH = 7. However,  $10^{-5}$  M of either lead or arsenic is high and far exceeds the 1980 U.S. EPA's water quality criteria, and the simultaneous occurrence of both is unlikely. While thermodynamics favor oxida-

TABLE IV-63

## SUMMARY OF METAL SPECIATION IN OXIDIZING AND REDUCING ENVIRONMENTS, SOLIDS CONTROLLING SOLUBILITY, AND pH-pe COMBINATIONS CONDUCTIVE TO METAL MOBILIZATION

Element	Unaffected by Oxidation-Reduction	Oxidizing Environment	Reducing Environment	Controlling Solids	Mobilizing Conditions
As		$H_2AsO_4^-$ , $HAsO_4^{2-}$	$H_3AsO_3^0$ , $H_2AsO_3^-$	$FeAsO_4$ , $As_2S_3$	high pH, high pe
Cd	$Cd^{2+}$ , $CdSO_4^0$ , $CdCO_3^0$			$CdCO_3$ , $Cd_3(PO_4)_2$ , $(Ca,Cd)CO_3$	low pH
Cr		$HCrO_4^{2-}$	$Cr^{3+}$ , $CrF^{2+}$ , $CrOH^{2+}$ , $Cr(OH)_3^0$ , $Cr(OH)_4^-$	$Cr(OH)_3$ , $FeCr_2O_4$	III: low pH, low pe VI: high p high pe
Cu		$Cu^{2+}$ , $CuSO_4^0$ , $Cu(OH)_2^0$	$Cu^+$ , $CuCl_2^-$ , $Cu(OH)_2^0$	$Cu(OH)_2$ , $Cu_3(PO_4)_2$ , $Cu_2(OH)_2CO_3$	low pH
Pb	$Pb^{2+}$ , $PbCO_3^0$ , $Pb(CO_3)_2^{2-}$			$Pb(OH)_2$ , $PbCO_3$ , $Pb_3(PO_4)_2$	low pH
Hg		$HgCl_2^0$ , $Hg(OH)_2^0$ , $HgClOH^0$	$Hg^0$	HgS	low pH, high Cl <sup>-</sup>
Ni	$Ni^{2+}$ , $NiHCO_3^+$ , $NiSO_4^0$			$NiS$ , $NiFeO_4$	low pH
Se		$SeO_4^{2-}$	$HSeO_3^-$ , $SeO_3^{2-}$ , $HSe^-$	$Fe_2(SeO_3)_3$	high pH
Zn	$Zn^{2+}$ , $ZnSO_4^0$ , $ZnCO_3^0$ , $Zn(CO_3)_2^{2-}$			$Zn(OH)_2$ , $ZnCO_3$ , $ZnSiO_4$ , $ZnFe_2O_4$	low pH



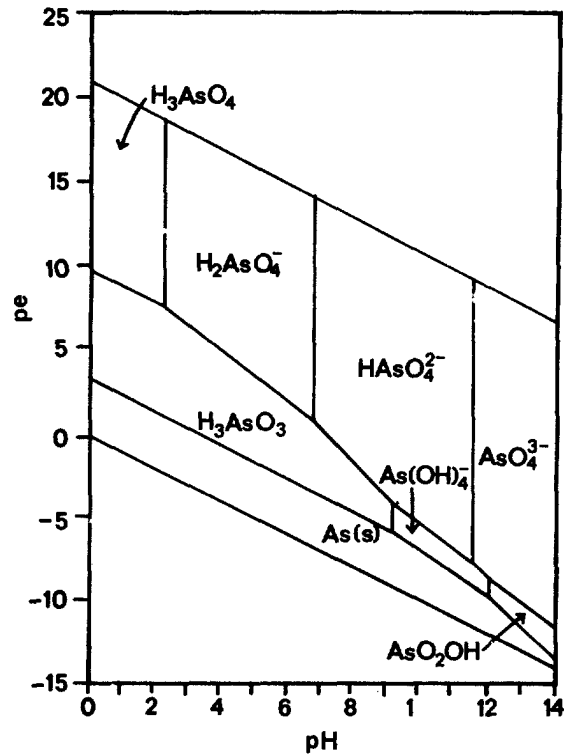


FIGURE IV-79 PE/PH STABILITY FIELD DIAGRAM FOR ARSENIC AT 25<sup>0</sup>C

tion of As(III) to As(V) in oxic surface waters, the kinetics of the oxidation process are thought to be such that As(III) can remain in this reduced form for relatively long periods of time; e.g. order of months (Tallman and Shaikh, 1980). As indicated earlier, arsenic from combustion can enter Surface waters as  $As_2O_3(s)$ . This compound then reacts with water to form arsenious acid,  $H_3AsO_3$  which is in the +3 oxidation state (see Figure IV-79). Depending on the rate of the oxidation reaction, the more toxic trivalent arsenic might remain present in the water.

Both As(III) and As(V) species are expected to adsorb onto surfaces, such as oxide surfaces and clays. The As(V) species have greater adsorptive tendency than do the As(III) species. Adsorption generally decreases with increasing pH, indicating that adsorption is more likely to be important in acidic waters.

#### 4. 10. 4. 3. 2 Cadmium

In natural fresh water, cadmium can be present in extremely low concentrations (e.g. less than 0.01  $\mu g/l$ ). Sources of cadmium include both industrial effluents (pigments, plastics, alloys, and electroplating) and municipal effluents industrial sources may account for up to 90 percent of the cadmium released domestically (Environmental Science and Technology, 1971). Cadmium is extremely toxic to fish, and effects on the growth rate have been observed at concentrations between 5 and 10

$\mu\text{g/l}$  (Gardiner, 1974). The suggested U.S. EPA criteria for protection of aquatic life are quite low also, varying from 0.01 to 0.05  $\mu\text{g/l}$  for waters having hardnesses of 50 and 200  $\text{mg/l}$  as  $\text{CaCO}_3$ , respectively.

Cadmium speciation is similar to that of zinc, as might be expected, since they are located in the same group in the periodic table and in adjacent periods 4 and 5 (see Figure IV-78). In oxic surface waters, cadmium is present in the 2+ oxidation state, so that redox reactions are not important for this element.

Cadmium can form complexes with hydroxide, carbonate, chloride, sulfate, and humic materials. Complexes with humic materials can be important when sufficient organic matter is present.

In fresh water, the concentrations of cadmium are usually far below the maximum permitted by its solubility products. Solubility is probably controlled by the carbonate, which should limit the soluble  $\text{Cd(II)}$  to between 0.1 to 1.0  $\text{mg/l}$ . In the pH range of natural waters, hydroxide solubility is about an order of magnitude greater than this.

Figure IV-80 shows the speciation of cadmium in freshwater as a function of pH in the presence of an adsorbate  $\text{SiO}_2(\text{s})$ . The total cadmium present is  $10^{-6}$  M (0.1  $\text{mg/l}$ ). Even at these high concentrations, cadmium does not begin to precipitate until the pH exceeds about 6.9. The uncomplexed cadmium is the dominant species below this pH.

Adsorption of cadmium appears to follow a linear isotherm at total cadmium concentrations of about 5.0  $\mu\text{g/l}$  or less (Gardiner, 1974). Concentrations of cadmium in natural waters are generally less than this, except in cases of extreme pollution.

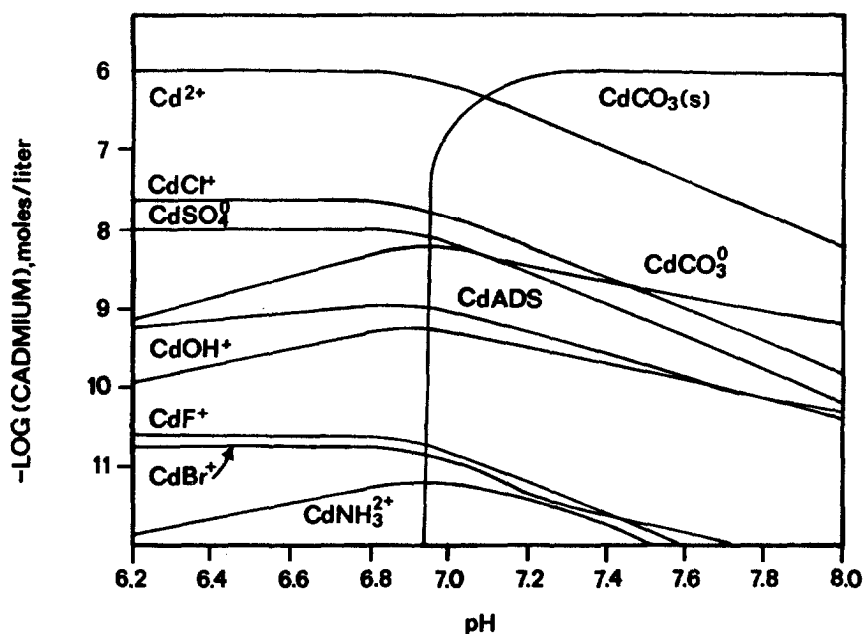
The proportion of cadmium adsorbed in the water column can be significant. Gardiner (1974) found that between 30 and 46 percent of cadmium in the water column was sorbed at total cadmium levels between 2.1 and 5.5  $\mu\text{g/l}$ , and at a suspended solids level of 34  $\text{mg/l}$ .

According to the work of Gardiner, levels of EDTA, a strong organic complexing agent, below about 30  $\mu\text{g/l}$  did not significantly affect cadmium speciation. At higher levels (i.e. 300  $\mu\text{g/l}$ ), the percent adsorbed was decreased by about half.

#### 4.10.4.3.3 Chromium

Background chromium levels in many natural waters are approximately  $10^{-8}$  M (0.5 ppb). Chromium levels in wastewater range up to  $10^{-5}$  M (500 ppb), which is near the solubility for chromium at neutral pH, where  $\text{Cr(OH)}_3(\text{s})$  can control solubility (for anoxic conditions).

Figure IV-81 is a pe-pH diagram showing the stability of chromium species at a total chromium concentration of  $10^{-5}$  M (The effects of organic species are not included but can be important.) At the pe values normally encountered in river waters (above 5), the free  $\text{Cr}^{3+}$  ion is expected to be present only in very acidic water ( $\text{pH} < 4$ ).



<u>CONSTITUENT</u>	<u>-log MOLAR CONCENTRATION</u>
Cl	3.65
NH <sub>3</sub>	5.5
Br	6.62
F	5.5
SO <sub>4</sub>	3.9
P <sub>CO2</sub>	3.5

REFERENCE: VUCETA AND MORGAN, 1978

FIGURE IV-80 CADMIUM SPECIATION AS A FUNCTION OF pH IN THE PRESENCE OF 1.55 M<sup>2</sup>/L SiO<sub>2</sub>(s), C<sub>Dt</sub> = 10<sup>-6</sup>M.

However, as the pH increases, at low pe, important soluble Cr(III) species are likely to be CrOH<sup>2+</sup> and Cr(OH)<sub>2</sub><sup>+</sup>. The most important Cr(VI) species are HCrO<sub>4</sub><sup>-</sup> and CrO<sub>4</sub><sup>2-</sup>, and they are likely to be present at pH values between 6.2 and 8 at high pe values. These anionic forms of chromium are fairly soluble and are relatively mobile in surface waters.

The presence of other metals can control the concentration of Cr(VI). Such metals include barium, calcium, strontium, copper, and lead. Lead concentrations as low as 10<sup>-7</sup> M (10 ppb) can produce chromate precipitation if concentrations of chromium (VI) exceed 10<sup>-7</sup> M at pH = 7.

While Cr(VI), in the presence of Fe(III) and dissolved sulfides, can be readily reduced to Cr(III), these compounds are not likely to be present in oxic surface waters. Cr(III) on the other hand can be oxidized by dissolved oxygen, but rather slowly. The fate of chromium depends on its oxidation state: Cr(III) is likely to

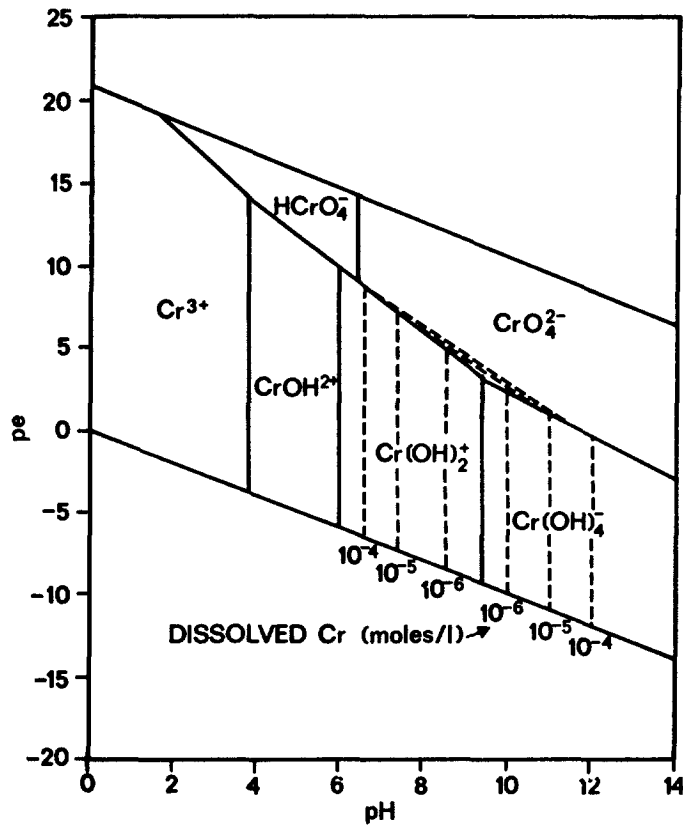


FIGURE IV-81 PE/PH DIAGRAM SHOWING STABILITY OF CHROMIUM SPECIES FOR CRT =  $10^{-5}$  M.

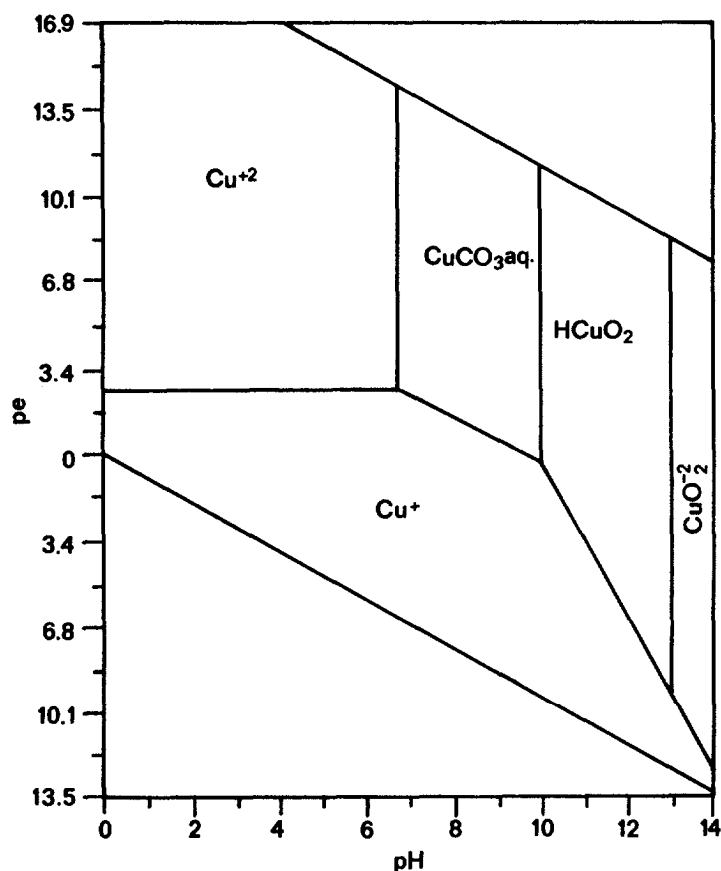
be sorbed and found in bottom sediments, and Cr(VI) is more likely to be carried in the water column.

#### 4.10.4.3.4 Copper

Elemental copper is a soft metal with an atomic weight of 63.5 and a density of  $8.9 \text{ g/cm}^3$ . It is a ubiquitous element in rocks and minerals and usually occurs as sulfides and oxides. Its concentrations in natural rocks typically vary from 4 ppm to 55 ppm, and natural background levels are often between 1 to 10  $\mu\text{g/l}$  in rivers. Industrial sources of copper include smelting and refining industries, copper-wire mills, and iron- and steel-producing industries.

The 2+ valence state is stable in oxic environments, while copper complexes with 1+ valences exist in reducing environments (Figure IV-82). For oxic waters, pe is typically near 10, and the equilibrium valence state is 2+ regardless of pH.

Several different researchers have investigated the equilibrium speciation of copper, both in the presence and in the absence of organic competing agents. Figure IV-83a shows the predictions of Long and Angino (1977) in fresh water in the presence of the ligands  $\text{OH}^-$ ,  $\text{Cl}^-$ ,  $\text{CO}_3^{2-}$ ,  $\text{SO}_4^{2-}$ , and  $\text{HCO}_3^-$ . The results show that either the free



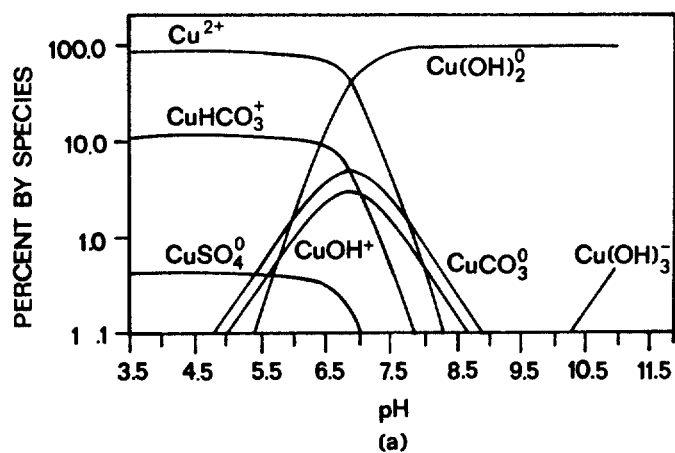
REFERENCE: HEM (1975).

FIGURE IV-82 PE/PH DIAGRAM SHOWING AREAS OF DOMINANCE OF FIVE SPECIES OF COPPER AT EQUILIBRIUM AT 25°C AND 1 ATM.

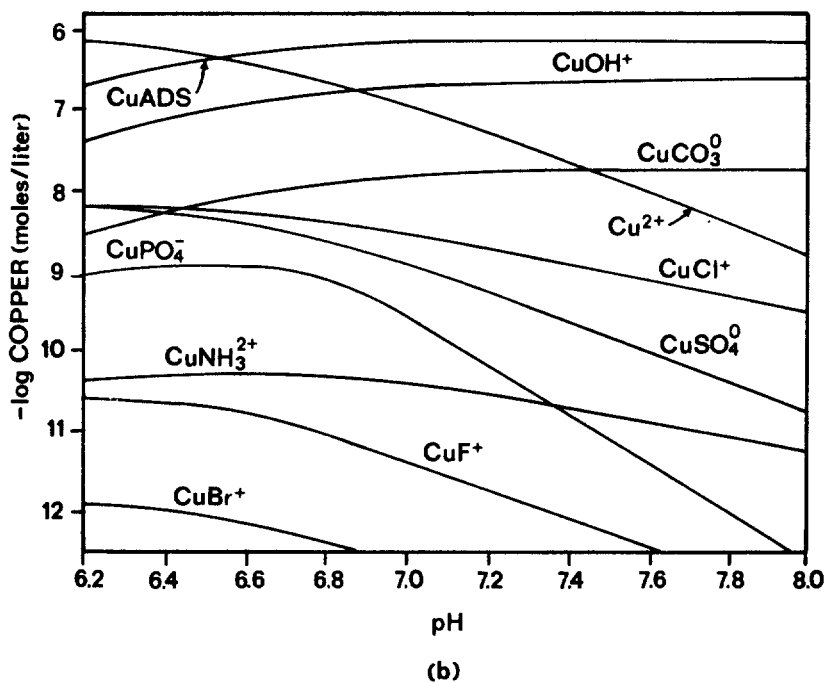
copper predominates (at pH values below about 6.5) or  $\text{Cu}(\text{OH})_2^0$  predominates at higher pH values.

Vuceta and Morgan (1978) investigated the speciation of  $10^{-6}$  M of total copper also in the presence of inorganic ligands, plus an adsorbing surface expressed as  $\text{SiO}_2$  (s). Their results are shown in Figure IV-83b, and indicate that for  $\text{pH} \geq 6.5$ , the adsorbed form of copper predominates. The free ion is probably present in significant quantities below pH 7 and is the predominant species below pH 6.5. Copper solubility in most fresh water appears to be controlled by malachite ( $\text{Cu}_2(\text{OH})_2\text{CO}_3$ ) rather than the hydroxide (Stiff, 1971). However, precipitation of malachite is a slow process.

Organic ligands can complex copper and increase its solubility in water. Vuceta and Morgan (1978) found that when EDTA was added as an organic ligand to their equilibrium model, the adsorbed and organically complexed copper were the predominant species, when at least  $10^{-6.3}$  M EDTA was present. At higher amounts of organic



CONSTITUENT	-log MOLAR CONCENTRATION
Cl	3.66
SO <sub>4</sub>	3.0
Ca	3.4
Mg	3.8



CONSTITUENT	-log MOLAR CONCENTRATION
Cl	3.65
NH <sub>3</sub>	5.5
Br	6.62
F	5.5
SO <sub>4</sub>	3.9
P <sub>CO2</sub>	3.5

REFERENCE: (A) LONG AND ANGINO, 1977  
 (B) VUCETA AND MORGAN, 1978

FIGURE IV-83 COPPER SPECIATION (A) IN THE PRESENCE OF INORGANIC LIGANDS; (B) IN THE PRESENCE OF INORGANIC LIGANDS AND AN ADSORBING SURFACE, 1.55 M<sup>2</sup>/L SiO<sub>2</sub> (S).

completing agents, a greater quantity of adsorbing surface is required for the sorbed phase to be of significance. Gupta and Harrison's (1982) investigations produced similar results. They found that the addition of humic materials reduced the adsorption coefficient,  $K_p$ , in a dilute system of kaolin and copper in water. The influence of the humic acid was evident at concentrations below 1 mg/l (Figure IV-84).

#### 4.10.4.3.5 Lead

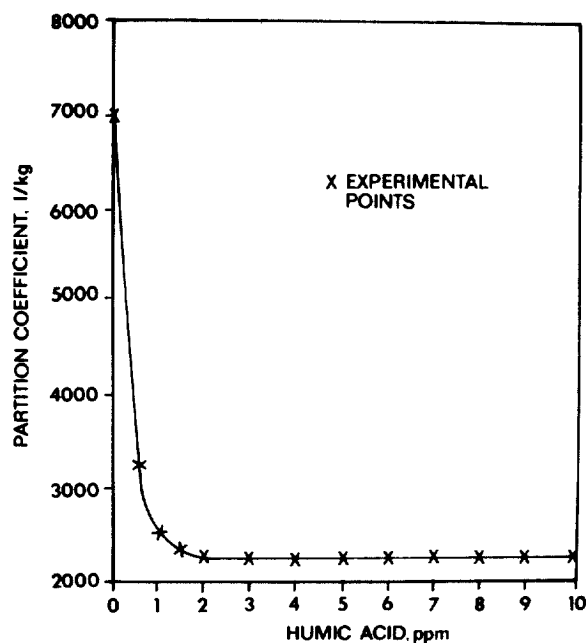
Lead is a constituent of hundreds of natural minerals, and its average abundance in the earth's crust is 15 ppm. Natural background levels of lead in inland waters typically average 1 pg/l or less. However, areas impacted by man, such as from lead mining, can have concentrations on the order of 50  $\mu\text{g/l}$ . Lead is used in metal products (with storage batteries being a primary use), pigments, gasoline antiknock additives, and other miscellaneous uses.

While lead exists in three oxidation states (0,  $2^+$ , and  $4^+$ ), the  $2^+$  oxidation state predominates in natural surface waters. Long and Angino (1977) evaluated the equilibrium speciation of lead in a freshwater environment containing only the inorganic ligands  $\text{OH}^-$ ,  $\text{Cl}^-$ ,  $\text{CO}_3^{2-}$ ,  $\text{SO}_4^{2-}$ , and  $\text{HCO}_3^-$ . Figure IV-85a shows their results. The  $\text{Pb}^{2+}$  ion is the predominant specie at  $\text{pH} \leq 7$ , while at  $7 \leq \text{pH} \leq 9$ ,  $\text{PbCO}_3^0$  is the major specie.

Vuceta and Morgan (1978) also used an equilibrium model approach for lead speciation in fresh water in the presence of inorganic ligands plus an adsorbing surface. Figure IV-85b shows their results. Again,  $\text{Pb}^{2+}$  predominates below  $\text{pH} = 7$ , and  $\text{PbCO}_3^0$  predominates at higher pH. For the amount of adsorbing surface used in the analysis ( $1.55 \text{ m}^2/\text{l SiO}_2(\text{s})$ ), the concentration of adsorbed lead was approximately an order of magnitude below the dissolved phase concentration. Small additions of iron and manganese oxides to the model data base, which provide further adsorption surfaces, did not appreciably change the results.

Lead can precipitate as a number of compounds including  $\text{PbSO}_4(\text{s})$ ,  $\text{PbCO}_3(\text{s})$ ,  $\text{Pb}(\text{OH})_2(\text{s})$ ,  $\text{PbS}(\text{s})$ , and  $\text{Pb}_3(\text{PO}_4)_2$ . The  $\text{PbCO}_3(\text{s})$  can control volatility in natural waters. Near  $\text{pH} = 8$ , the lead volatility is probably between 30 to 100  $\mu\text{g/l}$ , and rapidly increases at lower pH values. In soft waters at low pH values, lead volatility can be quite high so that using such a water type for drinking may be a health hazard if lead pipes comprise the water distribution system.

Lead readily forms complexes with organic ligands, which tend to increase the amount of lead which can be dissolved in water. In Vuceta and Morgan's equilibrium modeling results (1978), they found that when a strong completing agent such as EDTA exceeded about  $10^{-6.3} \text{ M}$ , more of the lead was complexed than was not. The total lead present was  $10^{-7} \text{ M}$  (20  $\mu\text{g/l}$ ).



REFERENCE: GUPTA AND HARRISON, 1982

FIGURE IV-84 EFFECT OF HUMIC ACID ON PARTITIONING OF COPPER,  
 (NOTE. THE HUMIC ACID WAS OBTAINED FROM THE  
 ALDRIDGE CHEMICAL COMPANY; NA-SALT, WATER  
 SOLUBLE.)

Lead is readily adsorbed to numerous solid surfaces, including organic matter, clay, silica, and iron and manganese oxides. Lead adsorption is pH dependent and the adsorption edge occurs at lower pH than that of either copper or zinc.

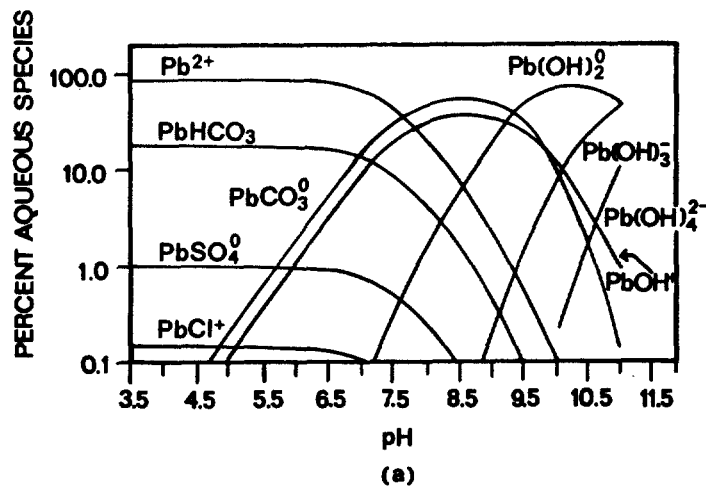
#### 4.10.4.3.6 Mercury

Elemental mercury is a silver-white metal and is a liquid at room temperature. It has a specific gravity of 13.5 and a vapor pressure of 0.0012 torr. It is used in the electrolytic preparation of chlorine and caustic soda, in electrical apparatus such as mercury battery cells, in control instruments such as thermometers, in laboratory applications, and in other industrial applications. Concentrations of mercury in natural rocks range from about 5 to 1000 ppb, with 80 ppb being a typical value. Typical background mercury levels in natural surface waters average 0.01 to 0.1  $\mu\text{g/l}$ .

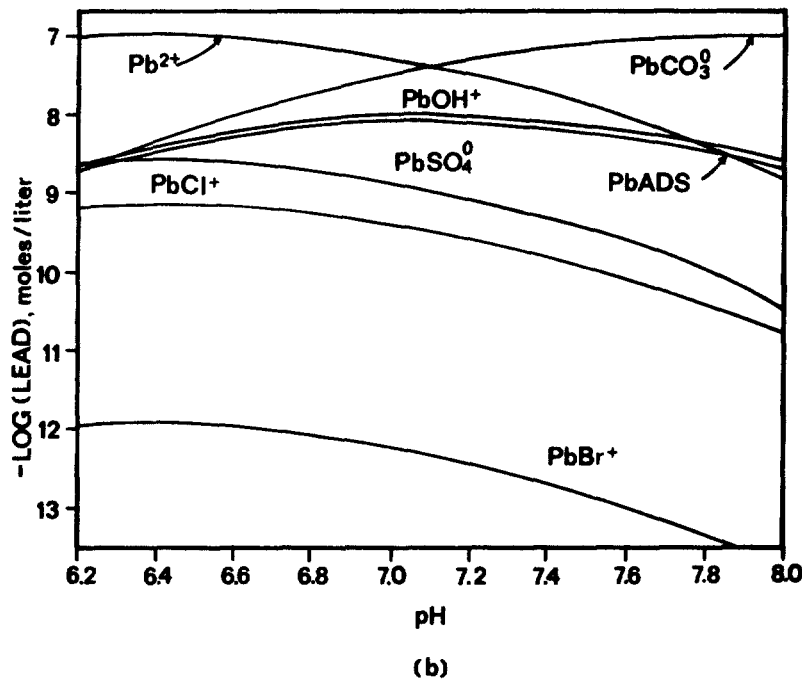
Mercury can exist in the natural environment in one of three oxidation states: 0 (the metallic form), 1+ (mercurous), or 2+ (mercuric). Figure IV-86 illustrates for the predominant inorganic species present in water under equilibrium conditions (Gavis and Ferguson, 1972).

For typical pe-pH values in surface waters, either the chloride or hydroxide





CONSTITUENT	-log MOLAR CONCENTRATION
Cl	3.66
SO <sub>4</sub>	3.0
Ca	3.4
Mg	3.8



CONSTITUENT	-log MOLAR CONCENTRATION
Cl	3.65
NH <sub>3</sub>	5.5
Br	6.62
F	5.5
SO <sub>4</sub>	3.9
P <sub>CO2</sub>	3.5

REFERENCES: (A) LONG AND ANGINO (1977)  
 (B) VUCETA AND MORGAN (1978)

FIGURE IV-85 LEAD SPECIATION (A) IN THE PRESENCE OF INORGANIC LIGANDS; (B) IN THE PRESENCE OF INORGANIC LIGANDS AND A SOLID ADSORBING SURFACE (1.55 M<sup>2</sup>/L SiO<sub>2</sub>(s)).

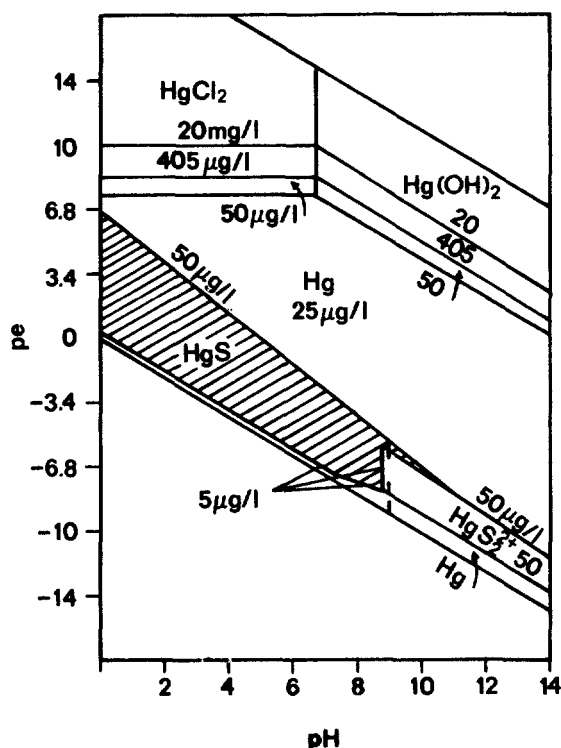


FIGURE IV-86 PE/PH DIAGRAM FOR Hg, SHOWING PREDOMINANT SPECIES IN SOLUTION FOR CONCENTRATIONS OF TOTAL Hg GREATER THAN 5 µg/L.

species predominate for the conditions shown. The solubilities of these compounds are great enough that precipitation of mercury in oxidizing environments is usually not a concern.

Mercury possesses an affinity for sulfhydryl groups (-SH) and can form organic sulfhydryl complexes. Mercury also forms compounds with alkyl groups (e.g. dimethyl mercury). The methyl mercury ion ( $\text{CH}_3\text{Hg}^+$ ) can be discharged from industrial effluents and can be synthesized from inorganic mercury by bacteria which reside in sediments.

Mercury strongly adsorbs to a variety of solids, including organics, clays, metal oxides, and sand. Halide ions (e.g.  $\text{Cl}^-$ ,  $\text{Br}^-$ ,  $\text{I}^-$ ) appear to suppress mercury adsorption.

Based on elemental mercury volatility of 19.2 µg/l at 50°C and 81.3 µg/l at 30°C and a vapor pressure of 0.0012 torr, the calculated Henry's Law constant lies between  $10^{-2}$  to  $10^{-3}$  atm·m<sup>3</sup>/mole. Elemental mercury is relatively volatile. Both organic and inorganic mercury compounds exhibit volatility.

#### 4.10.4.3.7 Nickel

Nickel is present in the earth's crust at an average concentration of approximately 80 ppm. Background levels in surface waters are 1 µg/l or less. Although nickel forms compounds with valences of 0, 1+, 2+, 3+, and 4+, the important valence state is 2+.

Nickel can precipitate as the hydroxide and carbonate, as studied by Patterson et al. (1977). Figure IV-87 shows the solubility limits for nickel carbonate and nickel hydroxide in the presence of  $10^{-1.2}$  M total inorganic carbon (TIC). While this amount of total carbon is significantly greater than found in natural rivers, the figure does illustrate that neither nickel carbonate nor the hydroxide is likely to limit solubility in the natural environment except at high nickel concentrations.

Nickel can be adsorbed by a variety of substances, including iron and manganese oxides and organics. However, nickel is thought to be relatively mobile in the aquatic environment, especially in comparison with other metals. The work of Vuceta and Morgan (1978) appear to substantiate this. They evaluated the chemical speciation and adsorption of  $10^{-6.5}$  M (19  $\mu\text{g/l}$ ) of total nickel in the presence of inorganic ligands which included  $\text{OH}^-$ ,  $\text{CO}_3^{2-}$ , and  $\text{SO}_4^{2-}$  and a solid surface expressed as  $\text{SiO}_2(\text{s})$  (the equivalent of 310mg/l). They found that at pH = 7, practically all of the Ni (18  $\mu\text{g/l}$ ) was present on the free divalent cation and that only a small amount was adsorbed. Adding small amounts of  $\text{Fe}(\text{OH})_3(\text{s})$  and  $\text{MnO}_2(\text{s})$  had little influence on the amount of nickel adsorbed; the free ion again was the predominant species.

Complexation with organic ligands can be very important for nickel, and tends to further increase the mobility of this metal. Vuceta and Morgan (1978) found that  $10^{-6.5}$  M (90  $\mu\text{g/l}$ ) of EDTA added to natural water at pH = 7 complexed about 50 percent of the nickel, with the remainder present as the free ion.

#### 4.10.4.3.8 Silver

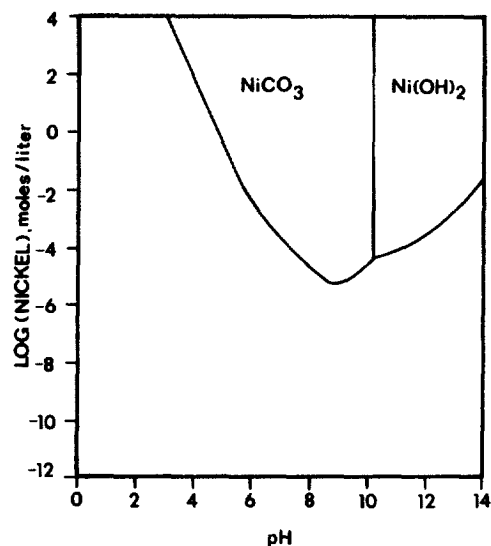
Elemental silver is a white ductile metal having an atomic weight of 107.9. It is primarily used in electroplating, as a conductor, in alloys, paints, jewelry, silverware, and mirror production. Background levels of silver are low in the aquatic environment, ranging from about 0.09  $\mu\text{g/l}$  to 0.6  $\mu\text{g/l}$  (Kharkov et al. , 1968). In the earth's crust, silver typically occurs in concentrations of about 0.1 ppm.

Silver is quite toxic to bacteria, invertebrates, and fish. Chronic toxicity to freshwater aquatic life may occur at concentrations as low as 0.12  $\mu\text{g/l}$ . Of the heavy metals only mercury is considered more toxic.

Silver can have valence states of 0, 1+, 2+, and 3+. The 0 and 1+ valence states are the most prevalent in the aquatic environment.

Solubility controls in the aquatic environment are probably not exerted by either the oxide or carbonates. However, silver halides are quite insoluble and can control solubility. Hem (1970) states that chloride concentrations as low as  $10^{-3}$  M (35mg/l) can limit solubility to below about 10  $\mu\text{g/l}$ .

Silver adsorbs to a variety of surfaces, including ferric hydroxides, clay minerals, and organics. Also, adsorption to manganese dioxide can be significant (Kharkov et al. , 1968).



REFERENCE: PATTERSON ET AL. (1977).

FIGURE IV-87 NICKEL CARBONATE AND NICKEL HYDROXIDE  
VOLUBILITY PHASE DIAGRAM ( $TIC = 10^{-1.2}M$ ).

#### 4. 10. 4. 3. 9 Zinc

The chemistry of zinc is similar to that of cadmium, which is found directly below it in the periodic table. Zinc, however, is more abundant than cadmium; and is an essential element in trace quantities for building tissues. In oxic aqueous systems, zinc exists in the 2+ oxidation state.

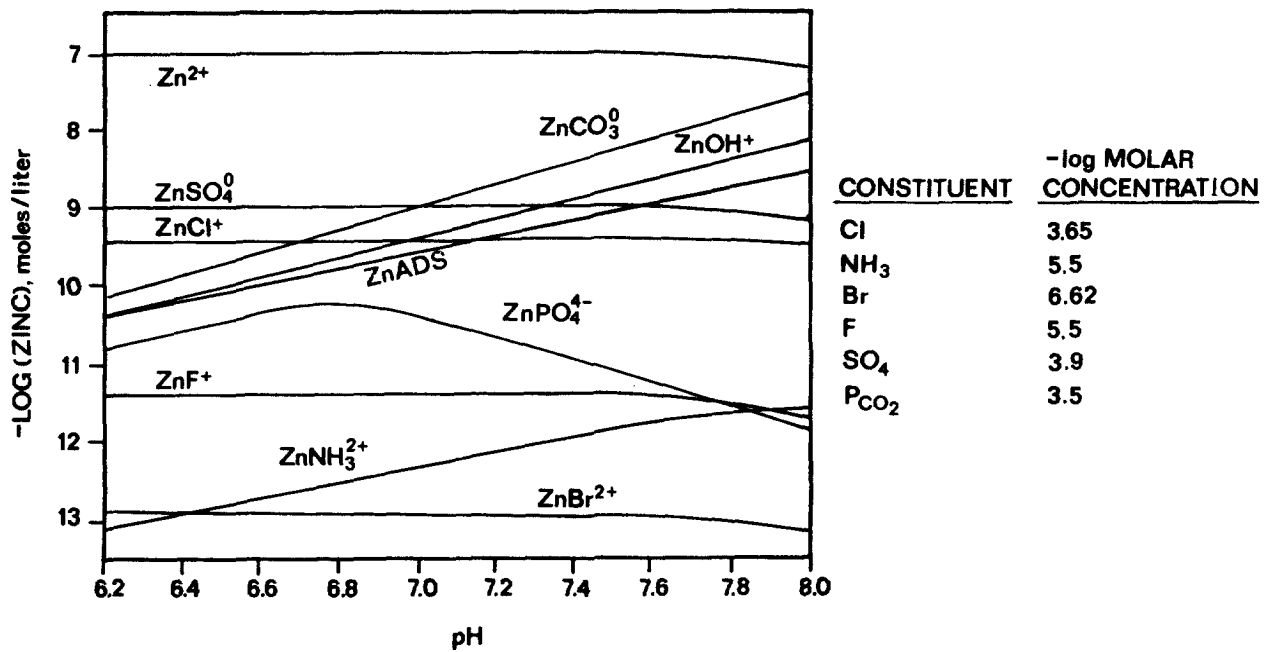
Typical concentrations of zinc in soils range from 10 to 300 ppm, with the average being approximately 50 ppm (Bowen, 1966). The median concentration of Zn in surface waters of the United States is approximately 20  $\mu g/l$  (Durum et al. , , 1971).

Zinc is used as an oxide pigment in rubber and paint, in agricultural fertilizers and sprays, in the textile industry, and battery production. The major metallurgical uses are in the galvanizing of metal and production of brass and other alloys.

Figure IV-88 from Vuceta and Morgan (1978) shows zinc speciation as a function of pH, assuming the total zinc is  $10^{-7} M$  (7  $\mu g/l$ ), and in the presence of an adsorbing surface, expressed as  $SiO_2(s)$ . Throughout the pH range shown (6.2 to 8.0), the free metal ion predominates. The next most predominate species are sulfate and carbonate, even more prevalent than the adsorbed zinc.

Models of zinc speciation based on inorganic ligands are altered in the presence of organic matter, which appear to increase soluble zinc. The results of Vuceta and Morgan (1978) suggest that organic complexation is important at pH values below approximately 6 and at ligand concentrations exceeding 100  $\mu g/l$

Zinc is normally undersaturated in natural waters. Potential volubility controls

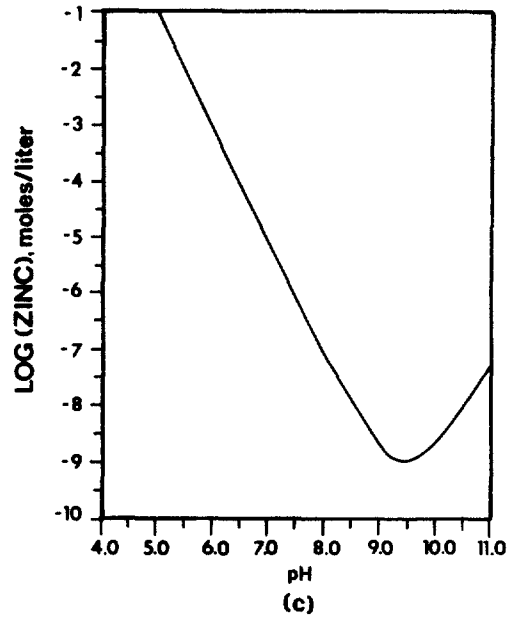
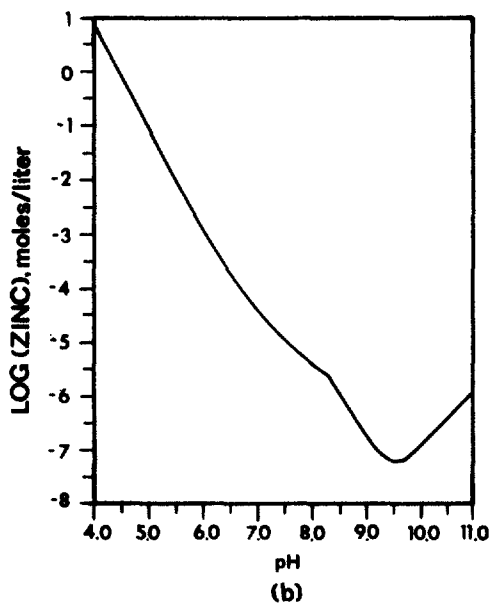
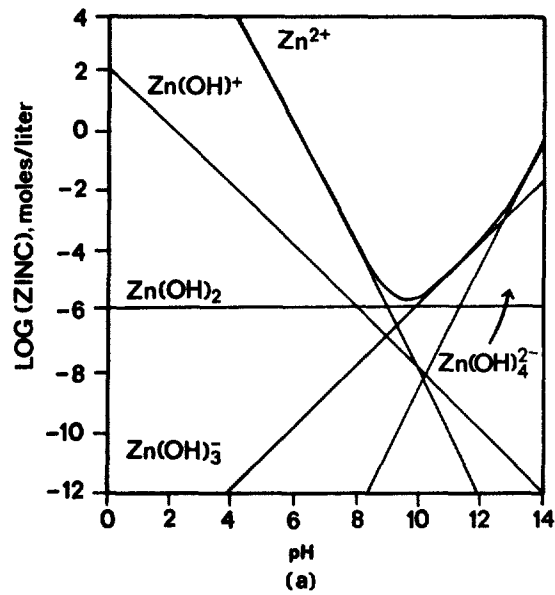


REFERENCE: VUCETA AND MORGAN, 1978

FIGURE IV-88 ZINC SPECIATION IN THE PRESENCE OF INORGANIC LIGANDS AND AN ADSORBING SURFACE ( $1.55 \text{ M}^2/\text{L SiO}_2(\text{s})$ ).

include  $\text{Zn}(\text{OH})_2(\text{s})$ ,  $\text{ZnCO}_3(\text{s})$  and, as suggested by Hem (1970), zinc silicate. Figure IV-89a shows the theoretical zinc hydroxide solubility curve (Patterson et al., 1977). The minimum total zinc occurs at pH 9.5 and is approximately  $130 \mu\text{g}/\text{l}$ . At pH values slightly lower, and in the range of natural water, the solubility can be 1 to 2 orders of magnitude higher. The carbonate species is expected to provide a slightly more severe limitation on zinc solubility. Figure IV-89b shows solubility of zinc in the presence of  $10^{-7} \text{ M}$  of total inorganic carbon, which corresponds to approximately  $60 \text{ mg}/\text{l HCO}_3^-$  in the pH range of natural waters. At pH 8, the total zinc solubility is approximately  $200 \mu\text{g}/\text{l}$ . Figure IV-89c illustrates the solubility of zinc silicate for a total dissolved silica concentration of about  $10^{-4} \text{ M}$  ( $6 \text{ mg}/\text{l}$ ), typical of many rivers. At a pH of about 8, the total zinc is limited to less than  $10 \mu\text{g}/\text{l}$ , which is considerably below solubility for the total hydroxide or carbonate.

Zinc can strongly adsorb to solid, such as hydrous metal oxides, clays, and organic matter. Even though zinc does adsorb to a high degree, Vuceta and Morgan (1978) found that zinc can complex with organic ligands which increases the dissolved fraction found in the water column. For the conditions they investigated, the complexed fraction plus the free ion comprised about 80 percent of the zinc in the water column, while the adsorbed fraction was 20 percent or less.



REFERENCE: (A) PATTERSON ET AL. (1977)

(B) AND (C) HEM (1970).

FIGURE IV-89 ZINC VOLUBILITY, (A) ZINC HYDROXIDE;  
(B) ZINC CARBONATE; (C) ZINC SILICATE,

#### 4.10.4.4 Equilibrium Modeling Analysis

##### 4.10.4.4.1 Introduction

The analysis in Section 4.10.3 treats metals as pollutants which speciate into either adsorbed or dissolved form. Based on this approach, the distribution of metals in the water column or in the bedded sediments can be estimated using a relatively modest amount of data, particularly with respect to the chemical characteristics of the water which transports the metals. In contrast to this simplified picture of metal behavior, the previous section showed that metals can form a large number of compounds, soluble and insoluble, with organic and inorganic ligands and can become adsorbed to organic or inorganic solids.

Although approaches that consider metal speciation require more information to implement, they can also address questions that the analyses in Section 4.10.3 can not. For example:

- How do the chemical properties of the river water affect metal speciation?
- What are likely to be the predominant species of metal present?
- When is precipitation likely to occur?
- Under what conditions are the more toxic species likely to be present?

Equilibrium models provide a key for answering these questions since they can calculate the species' distribution of metals for a specific set of receiving water conditions. The models assume that rate-limited processes are so fast that the species quickly come to a state of equilibrium. While equilibrium models themselves are not transport models, they can be combined with transport models. That equilibrium models rather than rate models have been developed by researchers indicates that knowledge is still quite limited regarding the fate of metals in aquatic systems and that rate models do not appear to be feasible at present.

Based on the foregoing, the approach selected here is to choose an equilibrium model and to apply it to a variety of water types found throughout the United States. The results are tabulated for easy reference.

##### 4.10.4.4.2 Choice of Typical Waters

Typical waters chosen for the purposes of this report are based on the United States Geological Survey's National Water Quality Network (NASQAN; Briggs and Ficke, 1977). That report is based on the 1975 water year and is their most recent report. Figure IV-90 shows the USGS's water resources regions within the United States.

Fifteen stations were selected within these regions based on regional representation, population, and interrelationships of the chemical constituents in the rivers. They are also shown in Figure IV-90.

The characteristics of the waters at the selected stations are shown in Table IV-64. The standard deviation as well as mean values are given for water temperature,

**Region numbers and names**

01 New England	12 Texas-Gulf
02 Mid Atlantic	13 Rio Grande
03 South Atlantic-Gulf	14 Upper Colorado
04 Great Lakes	15 Lower Colorado
05 Ohio	16 Great Basin
06 Tennessee	17 Pacific Northwest
07 Upper Mississippi	18 California
08 Lower Mississippi	19 Alaska
09 Souris-Red-Rainy	20 Hawaii
10 Missouri Basin	21 Coribbean
11 Arkansas-White-Red	

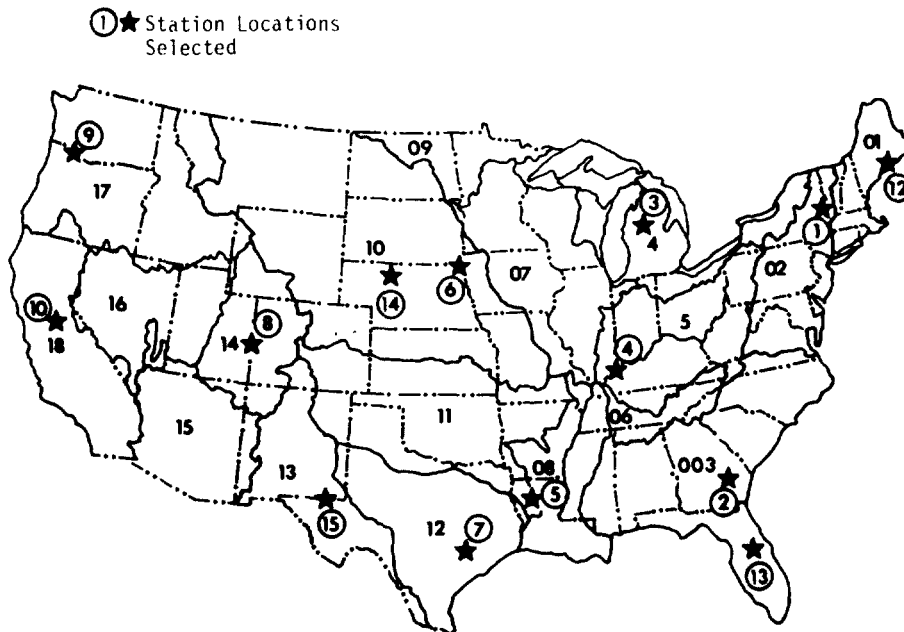


FIGURE IV-90 WATER RESOURCES REGIONS OF THE UNITED STATES

suspended solids, and pH. The range, rather than the mean, is shown for total organic carbon.

For comparison against the standard waters, a low pH water at the outlet of Woods Lake in the Adirondack Mountains in New York State has been added. The pH of the water averages 4.7, the alkalinity is  $-10 \mu\text{eq/l}$ , and the water is very soft (hardness = 6 mg/l as  $\text{CaCO}_3$ ). In such a water, metals might tend to dissolve, and due to the low hardness, criteria levels would be quite low for the metals whose standards relate to hardness.

4.10.4.4.3 Equilibrium Model Chosen

A variety of equilibrium models capable of predicting metal speciation have been developed in the past decade. Summaries of the performance and capabilities of the



TABLE IV-64

CHARACTERISTICS OF RIVER WATERS CHOSEN FOR ANALYSIS

Station No.	Region No.	River	USGS Station No.	Temperature °C	Suspended Solids <sup>a</sup> mg/l	Percent Silt-Clay	Total Dissolved Solids mg/l	Specific Conductance $\mu$ mhos	Total Organic Carbon <sup>b</sup> mg/l	pH <sup>a</sup>	Dissolved Calcium mg/l	Dissolved Magnesium mg/l	Dissolved Sodium mg/l	Dissolved Potassium mg/l	Dissolved Iron mg/l	Total Hardness mg/l as CaCO <sub>3</sub>	Total NO <sub>2</sub> +NO <sub>3</sub> mg/l-N	Total Phosphorus mg/l-P	Bicarbonate mg/l	Dissolved Sulfate mg/l	Dissolved Chloride mg/l
1	2	Hudson	01372043	15.±8.	13±7.	89.	82.	178.	2.-14.	7.740.2	19.	3.	6.	1.	0.06	60.	0.7	0.07	66.	18.	10.
2	3	Ogeechee	02202500	16.±7.	14±13.	-	45.	54.	6.-12.	6.941.2	7.	1.	4.	1.	0.7	21.	0.07	0.04	23.	5.	5.
3	4	Mustegon	04122030	10.±8.	21±9.	95.	203.	357.	5.-12.	8.140.2	43.	13.	10.	1.	0.07	163.	0.2	0.03	186.	19.	19.
4	5	Ohio	03612500	17.±9.	78±44.	87.	160.	292.	4.-5.	7.240.6	33.	8.	10.	2.	0.02	117.	0.9	0.23	88.	45.	13.
5	8	Mississippi	09267000	12.±11.	17±17.	-	152.	276.	7.-12.	7.940.3	36.	12.	4.	2.	0.12	140.	0.1	0.06	161.	7.	2.
6	10	Missouri	06818000	12.±11.	1130±1100.	50.	440.	720.	4.-12.	8.040.2	61.	21.	59.	6.	0.5	240.	0.8	0.3	213.	164.	16.
7	12	Brazos	08116450	21.±7.	770±680.	91.	380.	700.	5.-32.	7.040.5	57.	11.	63.	4.	0.1	190.	0.4	0.4	170.	62.	91.
8	14	Colorado	09163530	13.±8.	2450±1440.	-	690.	1000.	5.	8.140.2	96.	33.	86.	4.	0.03	374.	0.7	0.18	172.	300.	68.
9	17	Columbia	14128910	10.±5.	23±16.	84.	95.	188.	2.-11.	7.640.4	18.	6.	6.	1.	0.06	69.	0.4	0.05	77.	13.	3.
10	18	Sacramento	11447650	16.±5	100±100.	84.	82.	119.	3.-8.	7.040.4	10.	5.	8.	1.	0.03	47.	0.06	0.12	60.	7.	4.
11	4	Woods Lake, NY	---	11.±7.	1.	-	10.	25.	5.	4.740.2	2.	0.2	0.6	0.2	0.3	6.	2.0	0.01	0	6.0	0.3
12	1	Penobscot	01034500	9.±9.	5±2.	90	34.	59.	3.-9.5	6.640.2	6.6	1.4	3.1	0.6	0.1	22.	.045	0.02	14.	8.6	3.0
13	3	St. Marys	02231000	20.±5.	5±3.	-	30.	47.	10.-32.	5.141.0	3.3	1.2	3.4	0.4	0.5	13.	0.06	0.05	7.5	5.9	6.6
14	10	Grand	06357800	14.±10.	5222±1860.	-	1376.	1805.	9.-25.	8.740.5	42.	29.	376.	10.	0.01	226.	0.10	0.30	408.	566.	134.
15	13	Pecos	08407500	19.±7.	32±19.	73.	8058.	11520.	6.-14.	8.340.3	467.	213.	2073.	73.	0.15	2040.	0.4	0.07	129.	1725.	3425.

Source: Briggs and Ficke, 1977.

<sup>a</sup>Mean ± one standard deviation.

<sup>b</sup>Range.

models can be found in Nordstrom et al. , 1979. The model selected for this project is MINEQL.

MINEQL (Westall et al. , 1976) has evolved over the years and is based on an earlier equilibrium model called REDEQL. The version of MINEQL used in this chapter is called MINEQL+STANFORD, in recognition of modifications done at Stanford University.

MINEQL uses the equilibrium constant approach (in contrast to the direct minimization of the Gibbs free energy function) to attain equilibrium composition of species. The model is quite versatile and allows the user numerous options. For example, redox reactions can be considered or not at the discretion of the user. Adsorption can be modeled using the electrical double layer theory, which considers the interaction of charged ions in solution and at a solid surface. Precipitation can be considered at the discretion of the user, or suppressed as desired.

#### 4.10.4.4 Results

Tables IV-65 through IV-79 summarize the predictions of MINEQL for the 15 natural waters selected. For each metal, a range of concentrations is analyzed beginning at typical background levels and continuing for concentrations well above the water quality criteria. Concentrations are expressed as  $-\log$  molar and  $\mu\text{g/l}$ .

Organic ligands have not been included in this analyses. Organics are not included because major uncertainties exist as to the effects of organics on metals (particularly how to quantify the effects) and not because they are unimportant.

In selecting surface waters for analysis, the primary variables that should be considered by the user include pH, hardness, bicarbonate (an approximate measure of alkalinity), and specific conductivity. By cross-comparing results from several similar rivers, sensitivity to parameters can be estimated.

While Tables IV-65 through IV-79 are straightforward in their use, a number of features of the tables may not be readily apparent, and are listed here.

1. The concentrations of numerous metals are elevated enough in model simulations so that they precipitate in some rivers. For example, in the Hudson River, 81 percent of the lead is predicted to precipitate as  $\text{Pb}(\text{OH})_2(\text{s})$  when the total lead is  $1000 \mu\text{g/l}$  (see Table IV-65). The solubility of lead as limited by this process would be  $0.19 (1000) = 190 \mu\text{g/l}$ .
2. If the metals are present in low enough concentrations so that precipitation does not occur, the percent metal speciation is largely independent of total metal concentration. For example, Table IV-65 shows that speciation of zinc in the Hudson River at concentrations below  $1000 \mu\text{g/l}$  can be predicted by knowing that approximately 72 percent is  $\text{Zn}^{2+}$ , 15 percent is  $\text{ZnCO}_3^0$ , 8 percent is  $\text{ZnHCO}_3^+$ , and 2 percent is  $\text{ZnOH}^+$ . Thus, the user has the flexibility of ignoring precipitates

TABLE IV-65  
METAL SPECIATION IN THE HUDSON RIVER

Metal	Tested Range of Total Metal Concentrations as $\mu\text{M}$ and $\mu\text{g/l}$	Species
Arsenic	8.9-5.4 (0.1-540 $\mu\text{g/l}$ )	74% $\text{HAsO}_4^{2-}$
		26% $\text{H}_2\text{AsO}_4^-$
Cadmium	9.5-6.2 (0.1-70 $\mu\text{g/l}$ )	95% $\text{Cd}^{2+}$
		2% $\text{CdSO}_4^0$
		2% $\text{CdCl}^+$
Chromium(III) (without redox)	5.0 (520 $\mu\text{g/l}$ )	96% $\text{Cr(OH)}_3(\text{s})^*$
		3% $\text{Cr(OH)}_2^+$
		2% $\text{Cr(OH)}_4^-$
	5.6 (130 $\mu\text{g/l}$ )	81% $\text{Cr(OH)}_3(\text{s})^*$
		11% $\text{Cr(OH)}_2^+$
		7% $\text{Cr(OH)}_4^-$
	6.0 (40 $\mu\text{g/l}$ )	23% $\text{Cr(OH)}_3(\text{s})^*$
		47% $\text{Cr(OH)}_2^+$
		30% $\text{Cr(OH)}_4^-$
	8.7-6.6 (0.1-4 $\mu\text{g/l}$ )	61% $\text{Cr(OH)}_2^+$
	38% $\text{Cr(OH)}_4^-$	
Chromium(VI)	8.7-5.0 (0.1-520 $\mu\text{g/l}$ )	93% $\text{Cr}_2^{2-}$
		7% $\text{HCrO}_4^-$
Copper	4.8 (1000 $\mu\text{g/l}$ )	95% $\text{Cu}_2(\text{OH})_2\text{CO}_3(\text{s})^*$
		3% $\text{Cu(OH)}_2^0$
		1% $\text{CuCO}_3^0$
	5.4 (250 $\mu\text{g/l}$ )	81% $\text{Cu}_2(\text{OH})_2\text{CO}_3(\text{s})^*$
		12% $\text{Cu(OH)}_2^0$
		6% $\text{CuCO}_3^0$
	1% $\text{Cu}^{2+}$	

TABLE IV-65 (Continued)

Metal	Tested Range of Total Metal Concentrations as $\mu\text{M}$ and $\mu\text{g/l}$	Species
Copper (Continued)	6.0 (60 $\mu\text{g/l}$ )	49% $\text{Cu}(\text{OH})_2^0$ 24% $\text{CuCO}_3^0$ 21% $\text{Cu}_2(\text{OH})_2\text{CO}_3(\text{s})^*$ 4% $\text{Cu}^{2+}$
	8.5-6.6 (0.2-16 $\mu\text{g/l}$ )	62% $\text{Cu}(\text{OH})_2^0$ 31% $\text{CuCO}_3^0$ 6% $\text{Cu}^{2+}$ 1% $\text{Cu}(\text{OH})^+$
Lead	5.3 (1000 $\mu\text{g/l}$ )	81% $\text{Pb}(\text{OH})_2(\text{s})^*$ 16% $\text{PbCO}_3^0$ 1% $\text{Pb}(\text{OH})^+$
	5.8 (316 $\mu\text{g/l}$ )	52% $\text{PbCO}_3^0$ 41% $\text{Pb}(\text{OH})_2(\text{s})^*$ 4% $\text{Pb}(\text{OH})^+$ 3% $\text{Pb}^{2+}$
	8.3-6.3 (0.4-100 $\mu\text{g/l}$ )	88% $\text{PbCO}_3^0$ 7% $\text{Pb}(\text{OH})^+$ 4% $\text{Pb}^{2+}$
Mercury	12-9 (0.0002-0.2 $\mu\text{g/l}$ )	84% $\text{Hg}(\text{OH})_2^0$ 15% $\text{HgClOH}^0$
Nickel	7.8-4.8 (1-1000 $\mu\text{g/l}$ )	94% $\text{Ni}^{2+}$ 4% $\text{NiOH}^+$ 2% $\text{NiSO}_4^0$
Silver	8.8-6.2 (0.1-70 $\mu\text{g/l}$ )	65% $\text{Ag}^+$ 33% $\text{AgCl}^0$
Zinc	7.3-4.8 (2-1000 $\mu\text{g/l}$ )	72% $\text{Zn}^{2+}$ 15% $\text{ZnCO}_3^0$ 8% $\text{ZnHCO}_3^+$ 2% $\text{ZnOH}^+$

\*Predicted solubility limitations.

TABLE IV-66  
METAL SPECIATION IN THE OGEECHEE RIVER

Metal	Tested Range of Total Metal Concentrations as $\mu\text{M}$ and $\mu\text{g/l}$	Species
Arsenic	8.9-5.4 (0.1-540 $\mu\text{g/l}$ )	54% $\text{H}_2\text{AsO}_4^-$ 46% $\text{HAsO}_4^{2-}$
Cadmium	9.5-6.2 (0.1-70 $\mu\text{g/l}$ )	98% $\text{Cd}^{2+}$ 1% $\text{CdCl}^+$
Chromium(III) (without redox)	5.0 (520 $\mu\text{g/l}$ )	91% $\text{Cr}(\text{OH})_3(\text{s})^*$ 9% $\text{Cr}(\text{OH})_2^+$
	5.5 (160 $\mu\text{g/l}$ )	61% $\text{Cr}(\text{OH})_3(\text{s})^*$ 35% $\text{Cr}(\text{OH})_2^+$ 2% $\text{Cr}(\text{OH})_4^-$ 1% $\text{Cr}(\text{OH})_2^{2+}$
	8.7-6.0 (0.1-50 $\mu\text{g/l}$ )	90% $\text{Cr}(\text{OH})_2^+$ 6% $\text{Cr}(\text{OH})_4^-$ 4% $\text{CrOH}_2^{2+}$
Chromium(VI)		77% $\text{CrO}_4^{2-}$ 23% $\text{HCrO}_4^-$
Copper	4.8 (1000 $\mu\text{g/l}$ )	93% $\text{Cu}_2(\text{OH})_2\text{CO}_3(\text{s})^*$ 3% $\text{Cu}(\text{OH})_2^0$ 2% $\text{Cu}^{2+}$ 1% $\text{CuCO}_3^0$
	5.4 (250 $\mu\text{g/l}$ )	72% $\text{Cu}_2(\text{OH})_2\text{CO}_3(\text{s})^*$ 11% $\text{Cu}(\text{OH})_2^0$ 10% $\text{Cu}^{2+}$ 6% $\text{CuCO}_3^0$
	8.5-6.5 (0.2-60 $\mu\text{g/l}$ )	40% $\text{Cu}(\text{OH})_2^0$ 36% $\text{Cu}^{2+}$ 22% $\text{CuCO}_3^0$ 3% $\text{CuOH}^+$

TABLE IV-66 (Continued)

Metal	Tested Range of Total Metal Concentrations as $pM_T$ and $\mu g/l$	Species
Lead	5.3 (1000 $\mu g/l$ )	72% $PbCO_3(s)^*$
		16% $PbCO_3^0$
	5.8 (316 $\mu g/l$ )	8% $Pb^{2+}$
		4% $PbOH^+$
8.3-6.3 (0.4-100 $\mu g/l$ )	52% $PbCO_3^0$	
	23% $Pb^{2+}$	
	13% $PbOH^+$	
	11% $PbCO_3(s)^*$	
Mercury	12-9 (0.0002-0.2 $\mu g/l$ )	58% $PbCO_3^0$
		26% $Pb^{2+}$
		15% $PbOH^+$
Nickel	7.8-4.8 (1-1000 $\mu g/l$ )	77% $Hg(OH)_2^0$
		23% $HgClOH^0$
Silver	8.8-6.2 (0.1-70 $\mu g/l$ )	98% $Ni^{2+}$
		1% $NiOH^+$
Zinc	7.3-4.8 (2-1000 $\mu g/l$ )	79% $Ag^+$
		21% $AgCl^0$
		92% $Zn^{2+}$
		4% $ZnHCO_3^+$
		2% $ZnCO_3^0$

\*Predicted solubility limitations.

TABLE IV-67  
METAL SPECIATION IN THE MUSKEGON RIVER

Metal	Tested Range of Total Metal Concentrations as $pM_T$ and $\mu g/l$	Species
Arsenic	8.9-5.4 (0.1-540 $\mu g/l$ )	94% $HAsO_4^{2-}$
		6% $H_2AsO_4^-$
Cadmium	6.2 (70 $\mu g/l$ )	50% $Cd^{2+}$
		46% $CdCO_3(s)^*$
		2% $CdCl^+$
		1% $CdSO_4^0$
Cadmium	9.5-6.8 (0.1-20 $\mu g/l$ )	1% $CdCO_3^0$
		91% $Cd^{2+}$
		4% $CdCl^+$
		2% $CdSO_4^0$
Chromium(III) (without redox)	5.0 (520 $\mu g/l$ )	2% $CdCO_3^0$
		91% $Cr(OH)_3(s)^*$
	5.6 (130 $\mu g/l$ )	7% $Cr(OH)_4^-$
		62% $Cr(OH)_3(s)^*$
Chromium(III) (without redox)	8.7-6.3 (0.1-20 $\mu g/l$ )	36% $Cr(OH)_4^-$
		2% $Cr(OH)_2^+$
		94% $Cr(OH)_4^-$
		6% $Cr(OH)_2^+$
Chromium(VI)	8.7-5.0 (0.1-520 $\mu g/l$ )	99% $CrO_4^{2-}$
		1% $HCrO_4^-$
Copper	4.8 (1000 $\mu g/l$ )	95% $Cu_2(OH)_2CO_3(s)^*$
		4% $Cu(OH)_2^0$
Copper	5.4 (250 $\mu g/l$ )	1% $CuCO_3^0$
		80% $Cu_2(OH)_2CO_3(s)^*$
		16% $Cu(OH)_2^0$
		4% $CuCO_3^0$

TABLE IV-67 (Continued)

Metal	Tested Range of Total Metal Concentrations as $\mu\text{M}$ and $\mu\text{g/l}$	Species
Copper (Continued)	6.0 (60 $\mu\text{g/l}$ )	65% $\text{Cu}(\text{OH})_2^0$ 18% $\text{CuCO}_3$ 16% $\text{Cu}_2(\text{OH})_2\text{CO}_3(\text{s})^*$
	8.5-6.6 (0.2 -16 $\mu\text{g/l}$ )	77% $\text{Cu}(\text{OH})_2^0$ 21% $\text{CuCO}_3$
Lead	5.3 (1000 $\mu\text{g/l}$ )	92% $\text{Pb}(\text{OH})_2(\text{s})^*$ 7% $\text{PbCO}_3$
	5.8 (316 $\mu\text{g/l}$ )	75% $\text{Pb}(\text{OH})_2(\text{s})^*$ 23% $\text{PbCO}_3$
	6.3 (100 $\mu\text{g/l}$ )	72% $\text{PbCO}_3$ 22% $\text{Pb}(\text{OH})_2(\text{s})^*$ 3% $\text{PbOH}^+$ 3% $\text{Pb}(\text{CO}_3)_2^{2-}$
	8.3-6.9 (0.4-15 $\mu\text{g/l}$ )	93% $\text{PbCO}_3$ 4% $\text{Pb}(\text{OH})^+$ 3% $\text{Pb}(\text{CO}_3)_2^{2-}$
Mercury	12-9 (0.0002-0.2 $\mu\text{g/l}$ )	94% $\text{Hg}(\text{OH})_2^0$ 6% $\text{HgClOH}^0$
Nickel	4.8 (1-1000 $\mu\text{g/l}$ )	93% $\text{Ni}(\text{OH})_2(\text{s})^*$ 6% $\text{Ni}^{2+}$ 1% $\text{NiOH}^+$
	5.3 (300 $\mu\text{g/l}$ )	77% $\text{Ni}(\text{OH})_2(\text{s})^*$ 18% $\text{Ni}^{2+}$ 4% $\text{NiOH}^+$
	5.8 (90 $\mu\text{g/l}$ )	58% $\text{Ni}^{2+}$ 28% $\text{Ni}(\text{OH})_2(\text{s})^*$ 12% $\text{NiOH}^+$ 1% $\text{NiSO}_4$
	7.8-6.3 (1-15 $\mu\text{g/l}$ )	80% $\text{Ni}^{2+}$ 17% $\text{NiOH}^+$ 2% $\text{NiSO}_4$



TABLE IV-67 (Continued)

Metal	Tested Range of Total Metal concentrations as <b>pM<sub>T</sub></b> and <b>μg/l</b>	Species
Silver	6.2 (70 μg/l)	41% <b>Ag<sup>+</sup></b> 40% <b>AgCl<sup>0</sup></b> 17% <b>AgCl(s)*</b> 2% <b>AgCl<sup>-</sup><sub>2</sub></b>
	8.8-6.7 (0.1-15 μg/l)	50% <b>Ag<sup>+</sup></b> 48% <b>AgCl<sup>0</sup></b> 3% <b>AgCl<sup>-</sup><sub>2</sub></b>
Zinc	4.8 (1000 μg/l)	58% <b>ZnCO<sub>3</sub>(s)*</b> 21% <b>ZnCO<sup>0</sup><sub>3</sub></b> 10% <b>Zn(CO<sub>3</sub>)<sup>2-</sup><sub>2</sub></b> 7% <b>Zn<sup>2+</sup></b> 2% <b>ZnHCO<sup>+</sup><sub>3</sub></b>
	7.3-5.3 (2-320 μg/l)	49% <b>ZnCO<sup>0</sup><sub>3</sub></b> 23% <b>Zn(CO<sub>3</sub>)<sup>2-</sup><sub>3</sub></b> 17% <b>Zn<sup>2+</sup></b> 6% <b>ZnHCO<sup>+</sup><sub>3</sub></b> 3% <b>Zn(OH)<sup>0</sup><sub>2</sub></b> 2% <b>ZnOH<sup>+</sup></b>

\*Predicted solubility limitations.

TABLE IV-68  
METAL SPECIATION IN THE OHIO RIVER

Metal	Tested Range of Total Metal Concentrations as $\mu\text{M}_T$ and $\mu\text{g/l}$	Species
Arsenic	8.9-5.4 (0.1-540 $\mu\text{g/l}$ )	66% $\text{HAsO}_4^{2-}$
		34% $\text{H}_2\text{AsO}_4^-$
Cadmium	9.5-6.2 (0.1-70 $\mu\text{g/l}$ )	93% $\text{Cd}^{2+}$
		5% $\text{CdSO}_4$
		3% $\text{CdCl}^+$
Chromium(III) (without redox)	5.0 (520 $\mu\text{g/l}$ )	94% $\text{Cr}(\text{OH})_3(\text{s})^*$
		4% $\text{Cr}(\text{OH})_2^+$
		1% $\text{Cr}(\text{OH})_4^-$
	5.5 (160 $\mu\text{g/l}$ )	76% $\text{Cr}(\text{OH})_3(\text{s})^*$
		18% $\text{Cr}(\text{OH})_2^+$
		5% $\text{Cr}(\text{OH})_4^-$
	6.0 (50 $\mu\text{g/l}$ )	75% $\text{Cr}(\text{OH})_2^+$
		19% $\text{Cr}(\text{OH})_4^-$
		4% $\text{Cr}(\text{OH})_3(\text{s})^*$
		2% $\text{CrOH}^+$
6.5-8.7 (0.1-8 $\mu\text{g/l}$ )	79% $\text{Cr}(\text{OH})_2^0$	
	20% $\text{Cr}(\text{OH})_4^-$	
	2% $\text{CrOH}^+$	
Chromium(VI)	8.7-5.0 (0.1-520 $\mu\text{g/l}$ )	90% $\text{CrO}_4^{2-}$
		10% $\text{HCrO}_4^-$
Copper	4.8 (1000 $\mu\text{g/l}$ )	95% $\text{Cu}_2(\text{OH})_2\text{CO}_3(\text{s})^*$
		2% $\text{CuCO}_3$
		2% $\text{Cu}(\text{OH})_2^0$

TABLE IV-68 (Continued)

Metal	Tested Range of Total Metal Concentrations as $pM_T$ and $\mu g/l$	Species
Copper (Continued)	5.3 (300 $\mu g/l$ )	81% $Cu_2(OH)_2CO_3(s)^*$
		8% $CuCO_3^0$
		8% $Cu(OH)_2^0$
	5.8 (100 $\mu g/l$ )	2% $Cu^{2+}$
		35% $CuCO_3^0$
		34% $Cu(OH)_2^0$
		21% $Cu_2(OH)_2CO_3(s)^*$
	8.5-6.5 (0.2-15 $\mu g/l$ )	9% $Cu^{2+}$
		44% $CuCO_3^0$
43% $Cu(OH)_2^0$		
Lead	5.3 (1000 $\mu g/l$ )	11% $Cu^{2+}$
		81% $PbCO_3(s)^*$
		16% $PbCO_3^0$
	5.8 (316 $\mu g/l$ )	1% $Pb^{2+}$
		52% $PbCO_3^0$
		41% $PbCO_3(s)^*$
		3% $Pb^{2+}$
	6.3-8.3 (0.4-100 $\mu g/l$ )	3% $PbOH^+$
		88% $PbCO_3^0$
6% $Pb^{2+}$		
Mercury	12-9 (0.0002-0.2 $\mu g/l$ )	6% $PbOH^+$
		72% $Hg(OH)_2^0$
		27% $HgClOH^0$
		1% $HgCl_2^0$
Nickel	7.8-4.8 (1-1000 $\mu g/l$ )	93% $Ni^{2+}$
		5% $NiSO_4^0$
		2% $NiOH^+$
Silver	8.8-6.2 (0.1-70 $\mu g/l$ )	93% $Ag^+$
		38% $AgCl^0$
		1% $AgCl_2^0$

TABLE IV-68 (Continued)

Metal	Tested Range of Total Metal Concentrations as $pM_T$ and $\mu g/l$	Species
Zinc	7.3-4.8 (2-1000 $\mu g/l$ )	72% $Zn^{2+}$ 11% $ZnCO_3^0$ 10% $ZnHCO_3^+$ 4% $ZnSO_4^0$

\*Predicted solubility limitations.

TABLE IV-69  
METAL SPECIATION IN THE MISSISSIPPI RIVER

Metal	Tested Range of Total Metal Concentrations as $pM_T$ and $\mu g/l$	Species
Arsenic	8.9-5.4 (0.1-540 $\mu g/l$ )	90% $HAsO_4^{2-}$ 10% $H_2AsO_4^-$
Cadmium	6.2 (70 $\mu g/l$ )	91% $Cd^{2+}$ 6% $CdCO_3(s)^*$ 1% $CdCO_3^0$
	9.5-6.7 (0.1-20 $\mu g/l$ )	97% $Cd^{2+}$ 1% $CdCO_3^0$
Chromium(III) (without redox)	5.0 (520 $\mu g/l$ )	94% $Cr(OH)_3(s)^*$ 6% $Cr(OH)_4^-$
	5.5 (160 $\mu g/l$ )	74% $Cr(OH)_3(s)^*$ 23% $Cr(OH)_4^-$ 4% $Cr(OH)_2^+$
	6.3-8.7 (0.1-20 $\mu g/l$ )	86% $Cr(OH)_4^-$ 14% $Cr(OH)_2^+$ 1% $HgClOH^0$

TABLE IV-69 (Continued)

Metal	Tested Range of Total Metal concentrations as $\mu\text{M}$ and $\mu\text{g/l}$	Species
Chromium(VI)	8.7-5.0 (0.1-520 $\mu\text{g/l}$ )	98% $\text{CrO}_4^{2-}$ 2% $\text{HCrO}_4^-$
Copper	4.8 (1000 $\mu\text{g/l}$ )	95% $\text{Cu}_2(\text{OH})_2\text{CO}_3(\text{s})^*$ 3% $\text{Cu}(\text{OH})_2^0$ 1% $\text{CuCO}_3^0$
	5.4 (250 $\mu\text{g/l}$ )	81% $\text{Cu}_2(\text{OH})_2\text{CO}_3(\text{s})^*$ 14% $\text{Cu}(\text{OH})_2^0$ 5% $\text{CuCO}_3^0$
	6.0 (60 $\mu\text{g/l}$ )	56% $\text{Cu}(\text{OH})_2^0$ 22% $\text{Cu}_2(\text{OH})_2\text{CO}_3(\text{s})^*$ 21% $\text{CuCO}_3^0$
	8.5-6.6 (0.2-16 $\mu\text{g/l}$ )	71% $\text{Cu}(\text{OH})_2^0$ 27% $\text{CuCO}_3^0$
Lead	5.3 (1000 $\mu\text{g/l}$ )	87% $\text{Pb}(\text{OH})_2(\text{s})^*$ 12% $\text{PbCO}_3^0$
	5.8 (316 $\mu\text{g/l}$ )	60% $\text{Pb}(\text{OH})_2(\text{s})^*$ 37% $\text{PbCO}_3^0$
	8.3-6.4 (0.4-100 $\mu\text{g/l}$ )	94% $\text{PbCO}_3^0$ 4% $\text{PbOH}^+$ 2% $\text{PbCO}_3^{2-}$
Mercury	12-9 (0.0002-0.2 $\mu\text{g/l}$ )	99% $\text{Hg}(\text{OH})_2^0$

TABLE IV-69 (Continued)

Metal	Tested Range of Total Metal Concentrations as pMT and $\mu\text{g/l}$	Species
Nickel	4.8 (1000 $\mu\text{g/l}$ )	83% $\text{Ni}(\text{OH})_2(\text{s})^*$ 15% $\text{Ni}^{2+}$ 2% $\text{NiOH}^+$
	5.3 (320 $\mu\text{g/l}$ )	47% $\text{Ni}(\text{OH})_2(\text{s})^*$ 46% $\text{Ni}^{2+}$ 6% $\text{NiOH}^+$
	7.8-5.8 (1-40 $\mu\text{g/l}$ )	87% $\text{Ni}^{2+}$ 12% $\text{NiOH}^+$
Silver	8.8-6.2 (0.1-70 $\mu\text{g/l}$ )	91% $\text{Ag}^+$ 9% $\text{AgCl}^0$
Zinc	4.8 (1000 $\mu\text{g/l}$ )	55% $\text{ZnCO}_3(\text{s})^*$ 21% $\text{ZnCO}_3^0$ 14% $\text{Zn}^{2+}$ 5% $\text{Zn}(\text{CO}_3)_2^{2-}$ 4% $\text{ZnHCO}_3^+$
	7.3-5.3 (2-320 $\mu\text{g/l}$ )	46% $\text{ZnCO}_3^0$ 30% $\text{Zn}^{2+}$ 12% $\text{Zn}(\text{CO}_3)_2^{2-}$ 2% $\text{ZnOH}^+$

\*Predicted solubility limitations.

TABLE IV-70  
METAL SPECIATION IN THE MISSOURI RIVER

Metal	Tested Range of Total Metal Concentrations as $\mu\text{M}$ and $\mu\text{g/l}$	Species
Arsenic	8.9-5.4 (0.1-540 $\mu\text{g/l}$ )	93% $\text{HAsO}_4^{2-}$
		7% $\text{H}_2\text{AsO}_4^-$
Cadmium	6.2 (70 $\mu\text{g/l}$ )	66% $\text{Cd}^{2+}$
		21% $\text{CdCO}_3(\text{s})^*$
		10% $\text{CdSO}_4$
	9.5-6.8 (0.1-20 $\mu\text{g/l}$ )	2% $\text{CdCl}^+$
		83% $\text{Cd}^{2+}$
		12% $\text{CdSO}_4$
Chromium(III) (without oxidation-reduction)	5.0 (520 $\mu\text{g/l}$ )	92% $\text{Cr}(\text{OH})_3(\text{s})^*$
		7% $\text{Cr}(\text{OH})_4^-$
	5.6 (100 $\mu\text{g/l}$ )	67% $\text{Cr}(\text{OH})_3(\text{s})^*$
		30% $\text{Cr}(\text{OH})_4^-$
	8.7-6.3 (0.1-20 $\mu\text{g/l}$ )	3% $\text{Cr}(\text{OH})_2^+$
		91% $\text{Cr}(\text{OH})_4^-$
9% $\text{Cr}(\text{OH})_2^+$		
	Chromium(VI)	8.7-5.0 (0.1-520 $\mu\text{g/l}$ )
1% $\text{HCrO}_4^-$		
Copper	4.8 (1000 $\mu\text{g/l}$ )	95% $\text{Cu}_2(\text{OH})_2\text{CO}_3(\text{s})^*$
		3% $\text{Cu}(\text{OH})_2^0$
		1% $\text{CuCO}_3$
	5.4 (250 $\mu\text{g/l}$ )	81% $\text{Cu}_2(\text{OH})_2\text{CO}_3(\text{s})^*$
		13% $\text{Cu}(\text{OH})_2^0$
	5% $\text{CuCO}_3$	
6.0 (60 $\mu\text{g/l}$ )		55% $\text{Cu}(\text{OH})_2^0$
	22% $\text{Cu}_2(\text{OH})_2\text{CO}_3(\text{s})^*$	
21% $\text{CuCO}_3$		

TABLE IV-70 (Continued)

Metal	Tested Range of Total Metal Concentrations as $\mu\text{M}$ and $\mu\text{g/l}$	Species
Copper (Continued)	8.5-6.6 (0.2-16 $\mu\text{g/l}$ )	72% $\text{Cu}(\text{OH})_2^0$ 30% $\text{CuCO}_3^0$ 1% $\text{Cu}(\text{CO}_3)_2^{2-}$
Lead	5.3 (1000 $\mu\text{g/l}$ )	89% $\text{Pb}(\text{OH})_2(\text{s})^*$ 10% $\text{PbCO}_3^0$
	5.8 (316 $\mu\text{g/l}$ )	66% $\text{Pb}(\text{OH})_2(\text{s})^*$ 31% $\text{PbCO}_3^0$ 1% $\text{Pb}(\text{CO}_3)_2^{2-}$ 1% $\text{Pb}(\text{OH})^+$
	8.3-6.3 (0.4-100 $\mu\text{g/l}$ )	93% $\text{PbCO}_3^0$ 3% $\text{Pb}(\text{CO})_2^{2-}$ 3% $\text{Pb}(\text{OH})^+$
Mercury	12-9 (0.0002-0.2 $\mu\text{g/l}$ )	93% $\text{Hg}(\text{OH})_2^0$ 7% $\text{HgClOH}^0$
Nickel	4.8 (1-1000 $\mu\text{g/l}$ )	86% $\text{Ni}(\text{OH})_2(\text{s})^*$ 10% $\text{Ni}^{2+}$ 2% $\text{NiSO}_4^0$ 2% $\text{NiOH}^+$
	5.3 (300 $\mu\text{g/l}$ )	56% $\text{Ni}(\text{OH})_2(\text{s})^*$ 33% $\text{Ni}^{2+}$ 5% $\text{NiSO}_4^0$ 5% $\text{NiOH}^+$
	7.8-5.8 (1-90 $\mu\text{g/l}$ )	77% $\text{Ni}^{2+}$ 12% $\text{NiOH}^+$ 11% $\text{NiSO}_4^0$
Silver	6.2 (70 $\mu\text{g/l}$ )	53% $\text{Ag}^{2+}$ 40% $\text{AgCl}^0$ 5% $\text{AgCl}(\text{s})^*$
	8.8-6.8 (0.1-20 $\mu\text{g/l}$ )	55% $\text{Ag}^{2+}$ 42% $\text{AgCl}^0$ 1% $\text{AgSO}_4^0$



TABLE IV-70 (Continued)

Metal	Tested Range of Total Metal Concentrations as $pM_T$ and $\mu g/l$	Species
Zinc	4.8 (1000 $\mu g/l$ )	53% $ZnCO_3(s)^*$ 21% $ZnCO_3^0$ 10% $Zn^{2+}$ 10% $Zn(CO_3)_2^{2-}$ 2% $ZnSO_4^0$ 3% $ZnHCO_3^+$
	7.3-5.3 (2-320 $\mu g/l$ )	44% $ZnCO_3^0$ 21% $Zn^{2+}$ 21% $Zn(CO_3)_2^{2-}$ 7% $ZnHCO_3^+$ 4% $ZnSO_4^0$ 2% $ZnOH^+$ 2% $Zn(OH)_2^0$

\*Predicted solubility limitations.

TABLE IV-71  
METAL SPECIATION IN THE BRAZOS RIVER

Metal	Tested Range of Total Metal Concentrations as $\rho M_T$ and $\mu g/l$	Species
Arsenic	8.9-5.4 (0.1-540 $\mu g/l$ )	57% $HAso_4^{2-}$
		43% $H_2AsO_4^-$
Cadmium	9.5-6.2 (0.1-70 $\mu g/l$ )	81% $Cd^{2+}$
		15% $CdCl^+$
		4% $CdSO_4^0$
Chromium(III) (no redox)	5.0 (520 $\mu g/l$ )	92% $Cr(OH)_3(s)^*$
		7% $Cr(OH)_2^+$
	5.6 (130 $\mu g/l$ )	66% $Cr(OH)_3(s)^*$
		30% $Cr(OH)_2^+$
		3% $Cr(OH)_4^-$
	8.7-6.3 (0.1-20 $\mu g/l$ )	88% $Cr(OH)_2^+$
	9% $Cr(OH)_4^-$	
	4% $CrOH^{2+}$	
Chromium(VI)	8.7-5.0 (0.1-520 $\mu g/l$ )	88% $CrO_4^{2-}$
		12% $HCrO_4^-$
Copper	4.8 (1000 $\mu g/l$ )	95% $Cu_2(OH)_2CO_3(s)^*$
		4% $CuCO_3^0$
		1% $Cu(OH)_2^0$
	5.3 (300 $\mu g/l$ )	77% $Cu_2(OH)_2CO_3(s)^*$
		15% $CuCO_3^0$
		5% $Cu(OH)_2^0$
		3% $Cu^{2+}$
	6.0 (60 $\mu g/l$ )	60% $CuCO_3^0$
		29% $Cu(OH)_2^0$
	14% $Cu^{2+}$	
	4% $Cu_2(OH)_2CO_3(s)^*$	

TABLE IV-71  
(Continued)

Metal	Tested Range of Total Metal Concentrations as $\rho M_T$ and $\mu g/l$	Species
Copper (Continued)	8.5-6.6 (0.2-16 $\mu g/l$ )	63% $CuCO_3^0$
		21% $Cu(OH)_2^0$
		15% $Cu^{2+}$
Lead	5.3 (1000 $\mu g/l$ )	82% $PbCO_3(s)^*$
		16% $PbCO_3^0$
	5.8 (316 $\mu g/l$ )	52% $PbCO_3^0$
		42% $PbCO_3(s)^*$
Mercury	12-9 (0.0002-0.2 $\mu g/l$ )	3% $Pb^{2+}$
		2% $PbOH^+$
		90% $PbCO_3^0$
		5% $Pb^{2+}$
Nickel	7.8-4.8 (1-1000 $\mu g/l$ )	3% $PbOH^+$
		60% $HgClOH^0$
		25% $HgCl_2^0$
Silver	6.2 (70 $\mu g/l$ )	15% $Hg(OH)_2^0$
		93% $Ni^{2+}$
		5% $NiSO_4^0$
Zinc	8.8-6.8 (0.1-15 $\mu g/l$ )	1% $NiOH^+$
		41% $AgCl(s)^*$
		40% $AgCl^0$
		10% $AgCl_2^-$
Zinc	7.3-4.8 (2-1000 $\mu g/l$ )	9% $Ag^+$
		67% $AgCl^0$
		17% $AgCl_2^-$
		16% $Ag^+$
Zinc	7.3-4.8 (2-1000 $\mu g/l$ )	66% $Zn^{2+}$
		17% $ZnHCO_3^+$
		11% $ZnCO_3^0$
		4% $ZnSO_4^0$

\* Predicted solubility limitations.

TABLE IV-72  
METAL SPECIATION IN THE COLUMBIA RIVER

Metal	Tested Range of Total Metal Concentrations as $\mu\text{M}_T$ and $\mu\text{g/l}$	Species
Arsenic	8.9-5.4 (0.1-540 $\mu\text{g/l}$ )	82% $\text{HAsO}_4^{2-}$
		18% $\text{H}_2\text{AsO}_4^-$
Cadmium	9.5-6.2 (0.1-70 $\mu\text{g/l}$ )	97% $\text{Cd}^{2+}$
		2% $\text{CdSO}_4^0$
Chromium(III) (no redox)	5.0 (520 $\mu\text{g/l}$ )	96% $\text{Cr}(\text{OH})_3(\text{s})^*$
		3% $\text{Cr}(\text{OH})_4^-$
		2% $\text{Cr}(\text{OH})_2^+$
	5.6 (130 $\mu\text{g/l}$ )	82% $\text{Cr}(\text{OH})_3(\text{s})^*$
		11% $\text{Cr}(\text{OH})_4^-$
		7% $\text{Cr}(\text{OH})_2^+$
	6.3 (20 $\mu\text{g/l}$ )	47% $\text{Cr}(\text{OH})_4^-$
		30% $\text{Cr}(\text{OH})_2^+$
		24% $\text{Cr}(\text{OH})_3(\text{s})^*$
	8.7-6.8 (0.1-5 $\mu\text{g/l}$ )	61% $\text{Cr}(\text{OH})_4^-$
	39% $\text{Cr}(\text{OH})_2^+$	
Chromium(VI)	8.7-5.0 (0.1-520 $\mu\text{g/l}$ )	95% $\text{CrO}_4^{2-}$
		4% $\text{HCrO}_4^-$
Copper	4.8 (1000 $\mu\text{g/l}$ )	95% $\text{Cu}_2(\text{OH})_2\text{CO}_3(\text{s})^*$
		3% $\text{Cu}(\text{OH})_2^0$
		1% $\text{CuCO}_3^0$
	5.4 (250 $\mu\text{g/l}$ )	81% $\text{Cu}_2(\text{OH})_2\text{CO}_3(\text{s})^*$
	14% $\text{Cu}(\text{OH})_2^0$	
	5% $\text{CuCO}_3^0$	

TABLE IV-72 (Continued)

Metal	Tested Range of Total Metal Concentrations as $\mu\text{M}$ and $\mu\text{g/l}$	Species
Copper (Continued)	6.0 (60 $\mu\text{g/l}$ )	57% $\text{Cu}(\text{OH})_2^0$ 21% $\text{CuCO}_3^0$ 20% $\text{Cu}(\text{OH})_2\text{CO}_3(\text{s})^*$ 2% $\text{Cu}^{2+}$
	8.5-6.6 (0.2-16 $\mu\text{g/l}$ )	71% $\text{Cu}(\text{OH})_2^0$ 20% $\text{CuCO}_3^0$ 3% $\text{Cu}^{2+}$
Lead	5.3 (1000 $\mu\text{g/l}$ )	88% $\text{Pb}(\text{OH})_2(\text{s})^*$ 11% $\text{PbCO}_3^0$
	5.8 (316 $\mu\text{g/l}$ )	61% $\text{Pb}(\text{OH})_2(\text{s})^*$ 35% $\text{PbCO}_3^0$ 3% $\text{PbOH}^+$ 1% $\text{Pb}^{2+}$
	8.3-6.3 (0.4-100 $\mu\text{g/l}$ )	90% $\text{PbCO}_3^0$ 7% $\text{PbOH}^+$ 3% $\text{Pb}^{2+}$
Mercury	12-9 (0.0002-0.2 $\mu\text{g/l}$ )	97% $\text{Hg}(\text{OH})_2^0$ 3% $\text{HgClOH}^0$
Nickel	4.8 (1000 $\mu\text{g/l}$ )	57% $\text{Ni}^{2+}$ 39% $\text{Ni}(\text{OH})_2(\text{s})^*$ 4% $\text{NiOH}^+$
	7.8-5.3 (1-250 $\mu\text{g/l}$ )	92% $\text{Ni}^{2+}$ 6% $\text{NiOH}^+$ 2% $\text{NiSO}_4^4$
Silver	8.8-6.2 (0.1-70 $\mu\text{g/l}$ )	86% $\text{Ag}^{2+}$ 13% $\text{AgCl}^0$
Zinc	4.8 (1000 $\mu\text{g/l}$ )	55% $\text{Zn}^{2+}$ 21% $\text{ZnCO}_3^0$ 12% $\text{ZnCO}_3(\text{s})^*$ 7% $\text{ZnHCO}_3^+$ 2% $\text{ZnOH}^+$

TABLE IV-72 (Continued)

Metal	Tested Range of Total Metal Concentrations as $\mu\text{M}$ and $\mu\text{g/l}$	Species
Zinc (Continued)	7.3-5.3 (2-200 $\mu\text{g/l}$ )	62% $\text{Zn}^{2+}$ 24% $\text{ZnCO}_3^0$ 8% $\text{ZnHCO}_3^+$ 2% $\text{ZnOH}^+$ 1% $\text{ZnCO}_3^0$ 1% $\text{ZnSO}_4^0$ 1% $\text{Zn(OH)}_2^0$

\*Predicted solubility limitations.

TABLE IV-73  
METAL SPECIATION IN THE SACRAMENTO RIVER

Metal	Tested Range of Total Metal Concentrations as $\mu\text{M}$ and $\mu\text{g/l}$	Species
Arsenic	8.9-5.4 (0.1-540 $\mu\text{g/l}$ )	53% $\text{HAsO}_4^{2-}$ 47% $\text{H}_2\text{AsO}_4^-$
Cadmium	9.5-6.2 (0.1-70 $\mu\text{g/l}$ )	98% $\text{Cd}^{2+}$
Chromium (III) (no redox)	5.0 (520 $\mu\text{g/l}$ )	92% $\text{Cr(OH)}_3(\text{s})^*$ 7% $\text{Cr(OH)}_2^+$
	5.6 (130 $\mu\text{g/l}$ )	68% $\text{Cr(OH)}_3(\text{s})^*$ 28% $\text{Cr(OH)}_4^+$ 3% $\text{Cr(OH)}_4^-$
	8.7-6.3 (0.1-20 $\mu\text{g/l}$ )	88% $\text{Cr(OH)}_2^+$ 9% $\text{Cr(OH)}_4^-$ 3% $\text{CrOH}^{2+}$

TABLE IV-73 (Continued)

Metal	Tested Range of Total Metal Concentrations as $\rho_{MT}$ and $\mu\text{g/l}$	Species
Chromium(VI)	8.7-5.0 (0.1-520 $\mu\text{g/l}$ )	82% $\text{CrO}_4^{2-}$ 18% $\text{HCrO}_4^-$
Copper	4.8 (1000 $\mu\text{g/l}$ )	95% $\text{Cu}_2(\text{OH})_2\text{CO}_3(\text{s})^*$ 2% $\text{CuCO}_3^0$ 2% $\text{Cu}(\text{OH})_2^0$ 1% $\text{Cu}^{2+}$
	5.4 (250 $\mu\text{g/l}$ )	78% $\text{Cu}_2(\text{OH})_2\text{CO}_3(\text{s})^*$ 9% $\text{CuCO}_3^0$ 8% $\text{Cu}(\text{OH})_2^0$ 5% $\text{Cu}^{2+}$
	6.0 (60 $\mu\text{g/l}$ )	37% $\text{CuCO}_3^0$ 32% $\text{Cu}(\text{OH})_2^0$ 19% $\text{Cu}^{2+}$ 10% $\text{Cu}_2(\text{OH})_2\text{CO}_3(\text{s})^*$
	8.5-6.6 (0.2-16 $\mu\text{g/l}$ )	41% $\text{CuCO}_3^0$ 36% $\text{Cu}(\text{OH})_2^0$ 21% $\text{Cu}^{2+}$ 2% $\text{CuOH}^+$
Lead	5.3 (1000 $\mu\text{g/l}$ )	79% $\text{PbCO}_3(\text{s})^*$ 16% $\text{PbCO}_3^0$ 2% $\text{Pb}^{2+}$ 2% $\text{PbOH}^+$
	5.8 (316 $\mu\text{g/l}$ )	52% $\text{PbCO}_3^0$ 35% $\text{PbCO}_3(\text{s})^*$ 8% $\text{Pb}^{2+}$ 5% $\text{PbOH}^+$
	8.3-6.4 (0.4-100 $\mu\text{g/l}$ )	80% $\text{PbCO}_3^0$ 12% $\text{Pb}^{2+}$ 8% $\text{PbOH}^+$

TABLE IV-73 (Continued)

Metal	Tested Range of Total Metal Concentrations as $\mu\text{M}$ and $\mu\text{g/l}$	Species
Mercury	12-9 (0.0002-0.2 $\mu\text{g/l}$ )	84% $\text{Hg}(\text{OH})_2^0$ 10% $\text{HgClOH}^0$
Nickel	7.8-4.8 (1-1000 $\mu\text{g/l}$ )	97% $\text{Ni}^{2+}$ 2% $\text{NiOH}^+$
Silver	8.8-6.2 (0.1-70 $\mu\text{g/l}$ )	83% $\text{Ag}^{2+}$ 17% $\text{AgCl}^0$
Zinc	7.3-4.8 (2-1000 $\mu\text{g/l}$ )	83% $\text{Zn}^{2+}$ 9% $\text{ZnHCO}_3^+$ 6% $\text{ZnCO}_3^0$

\* Predicted solubility limitations.

TABLE IV-74  
METAL SPECIATION IN THE COLORADO RIVER

Metal	Tested Range of Total Metal Concentrations as $\mu\text{M}$ and $\mu\text{g/l}$	Species
Arsenic	8.9-5.4 (0.1-540 $\mu\text{g/l}$ )	95% $\text{HAsO}_4^{2-}$ 5% $\text{H}_2\text{AsO}_4^-$
Cadmium	6.2 (70 $\mu\text{g/l}$ )	69% $\text{Cd}^{2+}$ 18% $\text{CdSO}_4^0$ 9% $\text{CdCl}^+$ 3% $\text{CdCO}_3(\text{s})^*$
	8.7-6.8 (0.1-20 $\mu\text{g/l}$ )	71% $\text{Cd}^{2+}$ 18% $\text{CdSO}_4^0$ 9% $\text{CdCl}^0$



TABLE IV-74 (Continued)

Metal	Tested Range of Total Metal concentrations as $\mu\text{M}$ and $\mu\text{g/l}$	Species
Chromium(III) (no redox)	5.0 (520 $\mu\text{g/l}$ )	90% $\text{Cr}(\text{OH})_3(\text{s})^*$ 9% $\text{Cr}(\text{OH})_4^-$
	5.6 (130 $\mu\text{g/l}$ )	60% $\text{Cr}(\text{OH})_3(\text{s})^*$ 38% $\text{Cr}(\text{OH})_4^-$ 2% $\text{Cr}(\text{OH})_2^0$
	8.7-6.3 (0.1 -20 $\mu\text{g/l}$ )	94% $\text{Cr}(\text{OH})_4^-$ 6% $\text{Cr}(\text{OH})_2^0$
Chromium(VI)		99% $\text{CrO}_4^{2-}$
Copper	4.8 (1000 $\mu\text{g/l}$ )	95% $\text{Cu}_2(\text{OH})_2\text{CO}_3(\text{s})^*$ 4% $\text{Cu}^{2+}$
	5.4 (250 $\mu\text{g/l}$ )	79% $\text{Cu}_2(\text{OH})_2\text{CO}_3(\text{s})^*$ 17% $\text{Cu}(\text{OH})_2^0$ 4% $\text{CuCO}_3^0$
	6.0 (60 $\mu\text{g/l}$ )	70% $\text{Cu}(\text{OH})_2^0$ 17% $\text{CuCO}_3^0$
	8.5-6.6 (0.2-16 $\mu\text{g/l}$ )	12% $\text{Cu}_2(\text{OH})_2\text{CO}_3(\text{s})^*$ 79% $\text{Cu}(\text{OH})_2^0$ 19% $\text{CuCO}_3^0$ 3% $\text{Cu}^{2+}$
Lead	5.3 (1000 $\mu\text{g/l}$ )	95% $\text{Pb}(\text{OH})_2(\text{s})^*$ 4% $\text{PbCO}_3^0$
	5.8 (316 $\mu\text{g/l}$ )	85% $\text{Pb}(\text{OH})_2(\text{s})^*$ 14% $\text{PbCO}_3^0$
	6.3 (100 $\mu\text{g/l}$ )	51% $\text{Pb}(\text{OH})_2(\text{s})^*$ 44% $\text{PbCO}_3^0$ 3% $\text{PbOH}^+$
	8.3-6.8 (0.4-60 $\mu\text{g/l}$ )	91% $\text{PbCO}_3^0$ 6% $\text{PbOH}^+$

TABLE IV-74 (Continued)

Metal	Tested Range of Total Metal Concentrations as <b>pMT</b> and <b>g/l</b>	Species
Mercury	12-9 ( <b>0.0002-0.2 <math>\mu\text{g/l}</math></b> )	81% $\text{Hg}(\text{OH})_2^0$ 19% $\text{HgClOH}^0$
Nickel	4.8 ( <b>1000 <math>\mu\text{g/l}</math></b> )	90% $\text{Ni}(\text{OH})_2(\text{s})^*$ 7% $\text{Ni}^{2+}$ 2% $\text{NiSO}_4$
	5.3 ( <b>300 <math>\mu\text{g/l}</math></b> )	68% $\text{Ni}(\text{OH})_2(\text{s})^*$ 22% $\text{Ni}^{2+}$ 6% $\text{NiSO}_4$
	7.8-5.8 ( <b>1-40 <math>\mu\text{g/l}</math></b> )	4% $\text{NiOH}^+$ 69% $\text{Ni}^{2+}$ 18% $\text{NiSO}_4$
		13% $\text{NiOH}^+$
Silver	6.2 ( <b>70 <math>\mu\text{g/l}</math></b> )	40% $\text{AgCl}(\text{s})^+$ 40% $\text{AgCl}^0$ 13% $\text{Ag}^{2+}$ 8% $\text{AgCl}^-$
	8.8-6.8 ( <b>0.2-15 <math>\mu\text{g/l}</math></b> )	66% $\text{AgCl}^0$ 21% $\text{Ag}^{2+}$ 13% $\text{AgCl}_2^-$
Zinc	4.8 ( <b>1000 <math>\mu\text{g/l}</math></b> )	50% $\text{ZnCO}_3(\text{s})^*$ 21% $\text{ZnCO}_3^0$ 10% $\text{Zn}(\text{CO}_3)_2^{2-}$ 10% $\text{Zn}^{2+}$ 3% $\text{ZnSO}_4$ 2% $\text{ZnHCO}_3^+$

TABLE IV-74 (Continued)

Metal	Tested Range of Total Metal Concentrations as $\mu\text{M}$ and $\mu\text{g/l}$	Species
Zinc (Continued)	7.3-5.3 (2-250 $\mu\text{g/l}$ )	42% $\text{ZnCO}_3^0$ 21% $\text{Zn}^{2+}$ 21% $\text{Zn}(\text{CO}_3)_2^{2-}$ 6% $\text{ZnSO}_4^0$ 5% $\text{ZnHCO}_3^+$ 3% $\text{Zn}(\text{OH})_2^+$ 2% $\text{ZnOH}^+$

\*Predicted solubility limitations.

TABLE IV-75  
METAL SPECIATION IN WOODS LAKE OUTLET

Metal	Tested Range of Total Metal concentrations as $\mu\text{M}$ and $\mu\text{g/l}$	Species
Arsenic	8.9-5.4 (0.1-540 $\mu\text{g/l}$ )	99% $\text{H}_2\text{AsO}_4^-$
Cadmium	9.5-6.2 (0.1-70 $\mu\text{g/l}$ )	99% $\text{Cd}^{2+}$ 1% $\text{CdSO}_4^0$
Chromium(III) (without redox)	8.7-5.0 (520 $\mu\text{g/l}$ )	73% $\text{CrOH}_2^+$ 12% $\text{CrSO}_4^+$ 11% $\text{Cr}(\text{OH})_2^+$ 3% $\text{Cr}^{3+}$
Chromium(VI)	8.7-5.0 (0.1-520 $\mu\text{g/l}$ )	66% $\text{CrOH}_2^+$ 11% $\text{CrSO}_4^+$ 11% $\text{HCrO}_4^-$ 10% $\text{Cr}(\text{OH})_2^+$ 3% $\text{Cr}^{3+}$
Copper	8.5-4.8 (0.2-1000 $\mu\text{g/l}$ )	99% $\text{Cu}^{2+}$ 1% $\text{CuSO}_4^0$

TABLE IV-75 (Continued)

Metal	Tested Range of Total Metal Concentrations as $\mu\text{M}$ and $\mu\text{g/l}$	Species
Lead	8.3-5.3 (1-1000 $\mu\text{g/l}$ )	97% $\text{Pb}^{2+}$ 1% $\text{PbSO}_4$
Mercury	12-9 (0.0002-0.2 $\mu\text{g/l}$ )	60% $\text{HgClOH}^0$ 22% $\text{Hg}(\text{OH})_2^0$ 18% $\text{HgCl}_2^0$
Nickel	7.8-4.8 (1-1000 $\mu\text{g/l}$ )	99% $\text{Ni}^{2+}$ 1% $\text{NiSO}_4$
Silver	8.8-6.2 (0.1-70 $\mu\text{g/l}$ )	98% $\text{Ag}^+$ 2% $\text{AgCl}^0$
Zinc	7,3-4.8 (2-1000 $\mu\text{g/l}$ )	99% $\text{Zn}^{2+}$ 1% $\text{ZnSO}_4$

TABLE IV-76  
METAL SPECIATION IN PENOBSCOT RIVER, MAINE

Metal	Concentration Range	Species
Arsenic	0.3 - 1000 $\mu\text{g/l}$	70% $\text{H}_2\text{AsO}_4^-$ 30% $\text{HAsO}_4^{2-}$
Cadmium	0.008 - 80 $\mu\text{g/l}$	98.1% $\text{Cd}^{2+}$ 1.3% $\text{CdSO}_4$
Chromium III (without redox)	solubility = 95 $\mu\text{g/l}$ <95 $\mu\text{g/l}$	$\text{Cr}(\text{OH})_3(\text{s})$ is solubility control 91% $\text{Cr}(\text{OH})_2^+$ 8% $\text{Cr}(\text{OH})_2^{2+}$ 1% $\text{Cr}(\text{OH})_4^-$
Chromium VI	0.1 - 500 $\mu\text{g/l}$	63% $\text{CrO}_4^{2-}$ 37% $\text{HCrO}_4^-$

TABLE IV-76 (Continued)

Metal	Concentration Range	Species
Copper	solubility = <b>130 µg/l</b> <130 µg/l	<b>Cu<sub>2</sub>(OH)<sub>2</sub>CO<sub>3</sub>(s)</b> is solubility control 66% <b>Cu<sup>2+</sup></b> 18% <b>Cu(OH)<sub>2</sub><sup>0</sup></b> 13% <b>CuCO<sub>2</sub><sup>0</sup></b> 2% <b>CuOH<sup>+</sup></b>
Lead	solubility = <b>510 µg/l</b> <510 µg/l	<b>Pb(OH)<sub>2</sub>(s)</b> is solubility control 44% <b>Pb<sup>2+</sup></b> 42% <b>PbCO<sub>3</sub><sup>0</sup></b> 1% <b>PbOH<sup>+</sup></b> 2% <b>PbSO<sub>4</sub><sup>0</sup></b>
Mercury	0.0002 - <b>0.2 µg/l</b>	73% <b>Hg(OH)<sub>2</sub><sup>0</sup></b> 26% <b>HgClOH<sup>0</sup></b>
Nickel	1. - <b>1000 µg/l</b>	98% <b>Ni<sup>2+</sup></b> 1% <b>NiSO<sub>4</sub><sup>0</sup></b>
Silver	0.03- 100 µg/l	86% <b>Ag<sup>+</sup></b> 14% <b>AgCl<sup>0</sup></b>
Zinc	1. - 1000 µg/l	9% <b>Zn<sup>2+</sup></b> 3% <b>ZnHCO<sub>3</sub><sup>+</sup></b> 2% <b>ZnSO<sub>4</sub><sup>0</sup></b>

TABLE IV-77  
METAL SPECIATION IN ST. MARYS RIVER, FLORIDA

Metal	Concentration range	Species
Arsenic	<b>0.3-1000 <math>\mu\text{g/l}</math></b>	99% $\text{H}_2\text{AsO}_4^-$ 1% $\text{HAsO}_4^{2-}$
Cadmium	0.008-80 $\mu\text{g/l}$	97% $\text{Cd}^{2+}$ 2% $\text{CdCl}^+$
Chromium III (without redox)	<b>0.1-500 <math>\mu\text{g/l}</math></b>	69% $\text{CrOH}^{2+}$ 25% $\text{Cr}(\text{OH})_2^+$ 4% $\text{CrSO}_4^+$ 1% $\text{Cr}^{3+}$
Chromium VI	0.1-500 $\mu\text{g/l}$	92% $\text{HCrO}_4^-$ 5% $\text{CrO}_4^{2-}$ 2% $\text{CrOH}^{2+}$
Copper	<b>0.1-1000 <math>\mu\text{g/l}</math></b>	99% $\text{Cu}^{2+}$
Lead	0.1-1000 $\mu\text{g/l}$	96% $\text{Pb}^{2+}$ 2% $\text{PbSO}_4^0$
Mercury	0.0002-0.2 $\mu\text{g/l}$	71% $\text{HgCl}_2$ 28% $\text{HgClOH}^0$ 1% $\text{Hg}(\text{OH})_2^0$
Nickel	0.1-1000 $\mu\text{g/l}$	99% $\text{Ni}^{2+}$
Silver	<b>0.1-70 <math>\mu\text{g/l}</math></b>	74% $\text{Ag}^+$ 26% $\text{AgCl}^0$
Zinc	0.1-1000 $\mu\text{g/l}$	97% $\text{Zn}^{2+}$ 1% $\text{ZnHCO}_3^+$

TABLE IV-78  
METAL SPECIATION IN GRAND RIVER, SOUTH DAKOTA

Metal	Concentration Range	Species
Arsenic	1-1000 $\mu\text{g/l}$	99% $\text{HAsO}_4^{2-}$ 1% $\text{H}_2\text{AsO}_4^-$
Cadmium	solubility = 10 $\mu\text{g/l}$ <10 $\mu\text{g/l}$	$\text{CdCO}_3(\text{s})$ is solubility control 57% $\text{Cd}^{2+}$ 20% $\text{CdSO}_4^0$ 12% $\text{CdCl}^+$ 9% $\text{CdCO}_3^0$ 2% $\text{Cd}(\text{OH})^+$
Chromium III	solubility = 240 $\mu\text{g/l}$ <240 $\mu\text{g/l}$	$\text{Cr}(\text{OH})_3(\text{s})$ 99% $\text{Cr}(\text{OH})_4^-$
Chromium VI	1-500 $\mu\text{g/l}$	100% $\text{CrO}_4^{2-}$
Copper	solubility = 70 $\mu\text{g/l}$ <70 $\mu\text{g/l}$	$\text{Cu}_2(\text{OH})_2\text{CO}_3(\text{s})$ is solubility control 86% $\text{Cu}(\text{OH})_2^0$ 10% $\text{CuCO}_3^0$ 5% $\text{Cu}(\text{CO}_3)_2^{2-}$
Lead	solubility = 35 $\mu\text{g/l}$ <35 $\mu\text{g/l}$	$\text{Pb}(\text{OH})_2(\text{s})$ is solubility control 56% $\text{PbCO}_3^0$ 44% $\text{Pb}(\text{CO}_3)_2^{2-}$
Mercury	0.002-0.2 $\mu\text{g/l}$	92% $\text{Hg}(\text{OH})_2^0$ 8% $\text{HgClOH}^0$
Nickel	solubility = 30 $\mu\text{g/l}$ <30 $\mu\text{g/l}$	$\text{Ni}(\text{OH})_2(\text{s})$ is solubility control 43% $\text{Ni}^{2+}$ 35% $\text{NiOH}^+$ 15% $\text{NiSO}_4^0$ 6% $\text{Ni}(\text{OH})_2^0$

TABLE IV-78 (Continued)

Metal	Concentration Range	Species
Silver	solubility = 60 $\mu\text{g/l}$ <60 $\mu\text{g/l}$	$\text{AgCl(s)}$ is solubility control 64% $\text{AgCl}^0$ 24% $\text{AgCl}_2^-$ 11% $\text{Ag}^+$
Zinc	1-1000 $\mu\text{g/l}$	84% $\text{Zn(CO}_3)_2^{2-}$ 13% $\text{ZnCO}_3^0$ 2% $\text{Zn(OH)}_2^0$

TABLE IV-79  
METAL SPECIATION IN PECOS RIVER, NEW MEXICO

Metal	Concentration Range	Species
Arsenic	1-1000 $\mu\text{g/l}$	98% $\text{HAsO}_4^{2-}$ 2% $\text{H}_2\text{HsO}_4^-$
Cadmium	0.1-80 $\mu\text{g/l}$	59% $\text{CdCl}^+$ 17% $\text{Cd}^{2+}$ 17% $\text{CdCl}_2^0$ 6% $\text{CdSO}_4^0$
Chromium III	solubility = 85 $\mu\text{g/l}$ <85 $\mu\text{g/l}$	$\text{Cr(OH)}_3(\text{s})$ is solubility control 98% $\text{Cr(OH)}_4^-$ 2% $\text{Cr(OH)}_2^+$
Chromium VI	1-500 $\mu\text{g/l}$	99% $\text{CrO}_4^{2-}$
Copper	solubility = 70 $\mu\text{g/l}$ <70 $\mu\text{g/l}$	$\text{Cu}_2(\text{OH})_2\text{CO}_3(\text{s})$ is solubility control 90% $\text{Cu(OH)}_2^0$ 9% $\text{CuCO}_3^0$



TABLE IV-79 (Continued)

Metal	Concentration Range	Species
Lead	solubility = 8 $\mu\text{g/l}$ <8 $\mu\text{g/l}$	$\text{Pb(OH)}_2(\text{s})$ is solubility control 83% $\text{PbCO}_3^0$ 9% $\text{Pb(CO}_3)_2^{2-}$ 4% $\text{PbOH}^+$
Mercury	0.002-0.2 $\mu\text{g/l}$	37% $\text{HgClOH}^0$ 24% $\text{HgCl}_2^0$ 18% $\text{HgCl}_3^-$ 15% $\text{HgCl}_4^{2-}$ 6% $\text{Hg(OH)}_2^0$
Nickel	solubility = 90 $\mu\text{g/l}$ <90 $\mu\text{g/l}$	$\text{Ni(OH)}_2(\text{s})$ is solubility control 60% $\text{Ni}^{2+}$ 23% $\text{NiSO}_4^0$ 11% $\text{NiOH}^+$ 6% $\text{NiCl}^+$
Silver	0.1-70 $\mu\text{g/l}$	65% $\text{AgCl}_2^-$ 18% $\text{AgCl}_4^{3-}$ 11% $\text{AgCl}_3^{2-}$
Zinc	solubility = 800 $\mu\text{g/l}$ <800 $\mu\text{g/l}$	$\text{ZnCO}_3(\text{s})$ is solubility control 26% $\text{ZnCO}_3^0$ 24% $\text{Zn(CO}_3)_2^{2-}$ 23% $\text{Zn}^{2+}$ 10% $\text{ZnSO}_4^0$ 4% $\text{Zn(OH)}_2^0$ 4% $\text{ZnClOH}^0$ 2% $\text{ZnOH}^+$

and being able to estimate metal speciation at these higher concentrations exactly the same way as for lower concentrations.

- The tables do not consider the influence of adsorption. While MINEQL can simulate adsorption using electric double-layer theory, this option was not utilized. However, adsorption can be superimposed on the results in the table as follows. First consider the case without precipitation, the case most likely to be of concern for these screening analyses. The information required to account for adsorption is the partition coefficient,  $K_p$ , and suspended solids concentration,  $S$ , so that the dissolved fraction can be calculated:

$$\frac{C}{C_T} = \frac{1}{1 + K_p S \cdot 10^{-6}}$$

where

$C_T$  = total metal in water column

$C$  = total dissolved phase concentration.

The dissolved species can be approximated using the same percent distributions present when no adsorption occurs, except the percents in the tables become the percent of total dissolved metal, not total metal.

As an example, consider the results from MINEQL shown below for a river when pH = 8.

Species	Without Adsorption	With Adsorption (Area=6.9 m <sup>2</sup> /l)
Cu-Adsorbed	0.0%	98.1%
$Cu(OH)_2^0$	95.6%	1.8% (95.6)
$CuCO_3^0$	2.1%	<< 1% (2.1)
$Cu^{2+}$	1.1%	<< 1% (1.1)
$CuOH^+$	0.6%	<< 1% (0.6)
$CuSO_4^0$	0.5%	<< 1% (0.5)

Without adsorption, 95.6% of the total copper is present as  $Cu(OH)_2^0$ . When 6.9 m<sup>2</sup>/l of adsorbing surface is added for the conditions simulated, about 98% of the copper adsorbs, leaving only 2% dissolved. However, the percentage distributions of the dissolved species (the percents are shown in parentheses) are the same percent distributions without adsorption (e.g. 95.6 percent of the dissolved copper is  $Cu(OH)_2^0$ ). Figure IV-91 provides a mathematical justification for the procedure suggested above.

- Now consider adsorption at metal concentrations where precipitation is predicted to occur. The sketch below will help to explain the species shift when adsorption occurs.

- Consider a system with 3 dissolved metal species

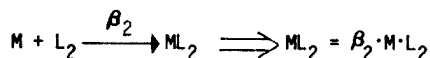
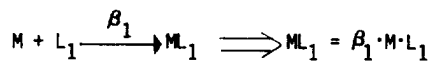
M (free ion)

ML<sub>1</sub> (1st metal-ligand complex)

ML<sub>2</sub> (2nd metal-ligand complex)

where  $M + ML_1 + ML_2 = \text{total dissolved metal} = M_{To}$

- The equilibrium reactions are:



- The equilibrium speciation fraction for free metal ion is:

$$\frac{M}{M_{To}} = \frac{1}{1 + \frac{\beta_1 \cdot L_{1T}}{1 + \beta_1 M} + \frac{\beta_2 L_{2T}}{1 + \beta_2 M}}$$

If  $1 \gg \beta_1 M$ ,  $1 \gg \beta_2 M$  (typically true in many natural systems)

Then:

$$\frac{M}{M_{To}} = \frac{M}{M_{Total}} \cdot \frac{M_{Total}}{M_{To}} = \frac{M}{M_{Total}} \cdot \frac{1}{\alpha} = \frac{1}{1 + \beta_1 L_{1T} + \beta_2 L_{2T}} = \text{constant for each river analyzed}$$

↑  
α = fraction dissolved (e.g.,  $\frac{1}{1 + K_p \cdot S \cdot 10^{-6}}$ )

So

$$M = (M_{Total}) \cdot (\alpha) \cdot \left( \frac{1}{1 + \beta_1 L_{1T} + \beta_2 L_{2T}} \right)$$

Concentration of total metal in river, based on procedures summarized in Table IV-58

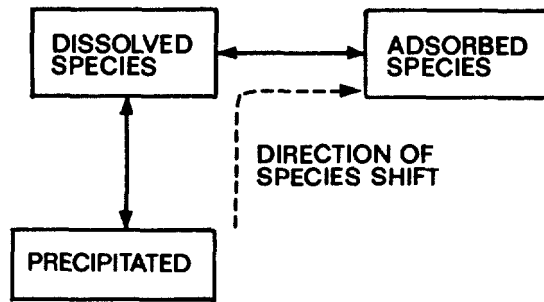
Determine from local data or use Table IV-62

These are the fractional species in Tables IV-65 through IV-79

- Summary:

To account for adsorption, use Tables IV-65 through IV-79 directly but consider the percent species to be dissolved metal rather than total metal.

FIGURE IV-91 EXAMPLE PROCEDURE FOR SUPERPOSITION OF ADSORPTION



As an adsorbing species is added to a water where dissolved and precipitated species are in equilibrium, some of the dissolved species become adsorbed. In turn, precipitates begin to re-dissolve to satisfy solubility conditions. As long as an excess of precipitates are present, the concentrations of total dissolved species will not change with or without adsorption. However, when all of the precipitated solids re-dissolve, then the concentration of dissolved species will decrease compared to the case with no adsorption. The tabulations below illustrate an example from MINEQL for a total copper concentration of  $5 \cdot 10^{-6}$  M (318  $\mu\text{g/l}$ ).

Species	No Adsorption	Adsorption (Area=0.69 m <sup>2</sup> /l)	Adsorption (Area=69 m <sup>2</sup> /l)
Cu-Adsorbed	0.0%	15.4%	98.7%
Cu(OH) <sub>2</sub> (s)	58.3%	42.9%	0.0%
Cu(OH) <sub>2</sub> <sup>o</sup>	39.9%	39.9%	1.2%

When a relatively small amount of adsorbing species is added (0.69 m<sup>2</sup>/l), 15.4% of the copper adsorbs, and the total precipitated copper decreases from 58.3% to 42.9%. However, the total dissolved copper remains constant at 39.9%. When significantly more surface area is added, more copper adsorbs until eventually the dissolved copper in the water column is below solubility, and all of the precipitated copper redissolves. Based on the above illustration, the following procedure is suggested to account for the possibility of simultaneous precipitation and adsorption. Using the total concentration CT of interest from the appropriate table, find

$$C = \frac{C_T}{1 + K_p S \cdot 10^{-6}}$$

If C is less than  $C_{sol}$ , the solubility of the metal which can be found as described previously in step (I), then all of the precipitate is re-dissolved and only the adsorbed and dissolved species exist. Thus,

both  $C$  and  $C_s (= C_T - C)$  are known, and the species of  $C$  can be found as described in step (3).

If  $C > C_{s01}$ , the dissolved metal concentration becomes  $C_{s01}$ , and the total dissolved plus adsorbed concentration,  $C_T$ , is:

$$C_T = C_{s01} (1 + K_p S \cdot 10^{-6})$$

where  $C_T$  is less than  $C_T$ . The precipitated metal is  $C_T - C_{s01} \cdot (1 + K_p S \cdot 10^{-6})$ . Again, the species distribution of  $C_{s01}$  can be found using step (3).

The following tabulations summarize the two cases:

	$C > C_{s01}$	$C < C_{s01}$
Amount dissolved	$C_{s01}$	$C$
Amount adsorbed	$K_p S C_{s01} \cdot 10^{-6}$	$K_p S C \cdot 10^{-6}$
Amount precipitated	$C_T - C_{s01} - K_p S C_{s01} \cdot 10^{-6}$	0

As mentioned previously, the results in the tables are valid for oxidizing conditions, with one exception. Chromium (III), which is thermodynamically stable under reducing conditions, was allowed to exist by not involving redox reactions. The oxidation of chromium (III) to chromium (VI) is thought to be very slow, so if chromium enters a river as the III+ ion, it may persist. However, chromium(III) relatively insoluble in most waters (from 30 to 50  $\mu\text{g/l}$ ) and is also less toxic than chromium so that chromium(III) is likely to be of secondary importance.

Throughout the range of metal concentrations examined, some of the metals did not precipitate at all. Those metals are: arsenic, chromium, and mercury. The remaining metals precipitate under at least some of the conditions, and the precipitates are:

- Cd:  $\text{CdCO}_3(\text{s})$
- Cr(III):  $\text{Cr}(\text{OH})_3(\text{s})$
- Cu:  $\text{Cu}_2(\text{OH})_2\text{CO}_3(\text{s})$
- Pb:  $\text{Pb}(\text{OH})_2(\text{s})$  or  $\text{PbCO}_3(\text{s})$
- Ni:  $\text{Ni}(\text{OH})_2(\text{s})$
- Ag:  $\text{AgCl}(\text{s})^2$
- Zn:  $\text{ZnCO}_3(\text{s})$

The only natural water where no metal precipitation occurred was at Woods Lake outlet, where the pH is 4.7. Also, in Woods Lake, most of the chromium is likely to be present as Cr(III) regardless of pe because of the low pH.

The fact that MINEQL (or any other equilibrium model) predicts certain metals will precipitate under certain conditions must be interpreted with a certain amount

of judgment because of the supersaturation possibility and because of uncertainty in solubility products. For example, the solubility products used by MINEQL for  $\text{Pb(OH)}_2(\text{s})$  and  $\text{Ni(OH)}_2(\text{s})$  appear to be on the lower end of an acceptable scale which spans 3 to 4 orders of magnitude for the solubility product (Sillen, 1966), i.e. the solubilities are taken to be lower rather than higher. Hence, predicted hydroxide solubility limitations for lead and nickel, which occur in a number of the surface waters chosen, should be interpreted with this in mind.

While the mathematical tools presented in Section 4.10.3 can be used independently of metal species distribution, the results from MINEQL can also be used in conjunction with the mathematical tools. The approach is as follows:

1. Using the transport-fate expressions in Section 4.10.3, find the temporal and spatial distributions of the metal(s) of interest. Record  $C_T$  (total concentration),  $C$  (the dissolved concentration), and  $C/C_T$  (the fraction dissolved) at each location of interest.
2. Select an appropriate natural water from Tables IV-65 through IV-79, and enter the table using the total metal concentration found from step (1) at each location of interest in the water body (if three locations are of interest, for example, the procedure outlined here is repeated three times).
3. Since the effects of adsorption are not directly included in the tables, the procedure outlined earlier should be used to account for adsorption and to find the percent distribution and amount of each dissolved species. Note that  $C/C_T$  values (see step (1)) do not have to be recalculated for the earlier procedure.
4. In all likelihood, the percent distribution of the dissolved species will not change significantly within a given river, although the total dissolved concentration can change. (An exception is an acid-mine-drainage situation, where pH can change significantly over distance.) When this is the case, the first three steps have to be completed only one time. The percentages found are then multiplied by  $C$  at each location to find the species distribution at each location.

#### EXAMPLE IV-25

This example illustrates some differences in lead speciation likely to exist between two of the river waters shown earlier in Table IV-64: the Ogeechee River in Georgia and the Colorado River in Colorado. Some of the water quality characteristics of the rivers are summarized below.

<u>Ri ver</u>	<u>pH</u>	<u>Suspended Solids, mg/l</u>	<u>Total Hardness</u>
Ogeechee	6.9	14	21.
Colorado	8.1	2450	374.

The water in the Colorado is quite hard while the Ogeechee River water is very soft. Consequently, hardness-related water quality criteria are different for the two rivers. For example, the 24-hour average criteria levels for cadmium and lead are 20 and 870 times higher in the Colorado than in the Ogeechee, respectively.

Lead solubility in the Ogeechee is controlled by the carbonate (see Table IV-66) while in the Colorado, the hydroxide controls (see Table IV-74). The lead solubility in the Ogeechee appears to be about 220 µg/l. This is found from the prediction by MINEQL that 11 percent of the total lead of 250 µg/l is present as  $PbCO_3(s)$ . The remaining 89%, or 220 µg/l, is dissolved.

In the Colorado River, the  $Pb(OH)_2(s)$  limits the total soluble lead to approximately 50 µg/l (49 percent of 100 µg/l is soluble). Note that in the absence of precipitation, the percent distribution of lead is independent of the total lead in the water column. As shown in Tables IV-66 and IV-74, the predominant species of dissolved lead are:

<u>Ri ver</u>	<u>Speci es</u>
Ogeechee	58% $PbCO_3^0$
	26% $Pb^{2+}$
	15% $PbOH^+$
Colorado	91% $PbCO_3^0$
	6% $PbOH^+$

Now, consider adsorption of lead to the suspended matter in the rivers. Based on the suspended solids levels and typical partition coefficients, it is assumed that 70 percent of the lead is adsorbed in the Ogeechee River and 99 percent in the Colorado River (see Table IV-62). Because such high fractions of the metals adsorb, it is unlikely that precipitates form even at high concentrations of metal, based on the procedure described earlier in this section. As an example, consider a total lead concentration of 60 µg/l in the Colorado River. In the absence of adsorption, precipitation of  $Pb(OH)_2(s)$  is predicted. However, if 99 percent of the 60 µg/l is adsorbed, then only 1 percent or 0.6 µg/l of the lead is dissolved in the water column. This is considerably below the 50 µg/l solubility of lead, so that precipitation does not occur. According to Table IV-74, nearly all (91 percent) of the 0.6 µg/l dissolved lead is present as  $PbCO_3^0$

----- END OF EXAMPLE IV-25 -----

#### 4.10.5 Execution of Limited Field Reconnaissance and Sampling Program

##### 4.10.5.1 Introduction

Since a screening level analysis is intended to make use of a minimal amount of existing data to estimate where severe water quality problems are likely to occur and where problems are unlikely to occur, the suggestion that a limited field reconnaissance and sampling program be conducted appears incongruous with the intent of the approach. However, a limited field reconnaissance and sampling program may be useful on a screening level for a number of reasons.

Perhaps the most important is the complexity of the problem of predicting fate of metals. Researchers are still far from developing a well accepted unified theory which can be used to predict the fate of metals in the natural aquatic environment. A review of the literature quickly reveals the divergency of views that now exist, particularly in the area of quantification. A good example is the partitioning of metals onto solids. Ignoring the fact that a variety of approaches exist related to adsorption, and considering only the linear isotherm adsorption approach used in this chapter, documented results show that the adsorption coefficient,  $K_p$ , is quite variable for a given metal under the conditions encountered in natural rivers. While in groundwater systems this variability may not be as important because of the large amount of solids surface area for the metal to adsorb (i.e., well over 99 percent of the metal is likely to be adsorbed for  $K_p > 10^3$  l/kg), in surface water the available solid surface area is typically only about 0.01 to 0.02 percent as great as in groundwater systems. With these much smaller surface areas, the percent metal that is dissolved can vary considerably.

For example, at a suspended solids level of 100 mg/l, a metal is 91 percent dissolved when  $K_p = 10^3$  l/kg and 9 percent dissolved when  $K_p = 10^5$  l/kg. In the first instance, **much** of the metal is transported **downstream** and is influenced to a small degree by solids settling or scour. Under these conditions, multiple waste sources on a river interact with each other to produce gradually elevating levels of metals over distance (unless dilution is important).

On the other hand, when only 9 percent of the metal is dissolved, then settling zones in the river tend to remove the metal from the water column, and downstream sources can act independently of each other. Thus, the partition coefficient becomes an important parameter to quantify.

The best way of interpreting  $K_p$  for metals is to consider the coefficient as a parameter (not necessarily of solid scientific validity) that relates concentrations of solid and particulate metals and is likely to be highly variable from one set of conditions to another. Because of its importance, local determination of  $K_p$  is recommended.

A second reason for local sampling is the importance and variability of natural metal sources. In some cases, natural sources of metals may be largely or entirely



responsible for exceeding standards. Thus, removing a large percentage of point source contributions may have a negligible impact on levels of metals.

Before undertaking a field reconnaissance and sampling program, the following questions should be answered:

1. Have all potential sources of information been accessed? Delos et al. (1983) summarize likely sources.
2. Have the available data been summarized, categorized, and compared against the information needs required to conduct a screening analysis? Table IV-80 shows the kinds of information required to carry out the screening analyses presented in this document. While supporting information may be useful for other purposes envisioned by the user, they are not likely to be critical for the purposes of these screening procedures.
3. Have preliminary screening analyses been carried out to see whether the missing, or poorly quantified data are important? The proposed screening analyses should be performed first with "best judgment" data to verify that the missing information do make a significant difference. If not, there is no reason, within the scope of the objectives of this chapter, to collect that kind of data.
4. Have the objectives of the field reconnaissance/sampling program been defined and have these activities been planned thoroughly? Before setting foot into the field, all the reasons for doing so should have been carefully thought out. Pre-planning will save time and money, and more likely produce the intended results. Particularly, personnel requirements and assignments and equipment needs (including backup equipment) should be carefully addressed.

#### 4.10.5.2 Field Reconnaissance

A field reconnaissance is a firsthand survey of the system under investigation. A reconnaissance can be used to verify, if only in a qualitative sense, some of the data which are being used for the screening analysis. In particular, this kind of data can consist of:

- Identification and locations of point sources
- Locations of appropriate upstream and downstream boundaries
- Estimation of water depths in different reaches of the river
- Estimation of surface widths in different reaches of the river
- Identification of free-flowing reaches, backwater areas, and locations and sizes of lakes or reservoirs
- Visual (photographic) documentation of the system.

TABLE IV-80

SUMMARY OF DATA REQUIREMENTS FOR SCREENING OF METALS IN RIVERS

Data	Methodology Where Data Are Used*	Remarks	
<u>Hydraulic Data</u>			
1. Rivers:			
● River flow rate, Q	D, R, S, L	An accurate estimation of flow rate is very important because of its dilution capability.	
● Cross-sectional area, A	D, R, S	The average water depth is volume divided by surface area. Watershed subareas can be used to estimate flow rates.	
● Water depth, H	D, R, S, L, AD		
● Reach lengths, x	R, S, AD		
● Watershed areas by tributary drainage, $A_w$	D		
● Stream velocity, U	R, S, AD	The required velocity is distance divided by travel time. It can be approximated by Q/A only when A is representative of the reach being studied.	
2. Lakes:			
● Hydraulic residence time, T		Hydraulic residence times of lakes can vary seasonally as the flow rate through the lakes' changes.	
● Mean depth, H			
<u>Source data</u>			
Source data include both natural and anthropogenic sources.			
1. Background			
● Metal concentrations, C <sub>U</sub>	D, R, S, L	Background concentrations should generally not be set to zero without justification.	
● Boundary flow rates, Q <sub>u</sub>	D, R, S, L	One important reason for determining suspended solids concentrations is to determine the dissolved concentration, C, of metals, based on CT, S, and K <sub>p</sub> . However, if C is known along with C and S, use this information to find K <sub>p</sub> rather than using literature values.	
● Boundary suspended solids, S <sub>u</sub>	D, R, S, L, AD		
● Silt, clay fraction of suspended solids	L		
● Locations	D, R, S, L		
2. Point Sources			
● Locations	D, R, S, L		
● Flow rate, Q <sub>w</sub>	D, R, S, L		
● Metal concentration, C <sub>TW</sub>	D, R, S, L		
● Suspended solids, S <sub>w</sub>	D, R, S, L, AD		
<u>Bed Data</u>			
● Depth of contamination		For the screening analysis, the depth of contamination is most useful during a period of prolonged scour when metal is being input into the water column from the bed.	
● Porosity of sediments, n			
● Density of solids in sediments (e.g., 2.7 for sand), ρ <sub>s</sub>			
● Metal concentration in bed during prolonged scour period, C <sub>T2</sub>			
<u>Derived Parameters</u>			
● partition coefficient, K <sub>p</sub>	All	The partition coefficient is a very important parameter. Local determination is preferable.	
● Settling velocity, w <sub>s</sub>	S, L	This parameter is derived based on Equation IV-184.	
● Resuspension velocity, w <sub>rs</sub>	R	This parameter is derived based on Equation IV-181.	
<u>Equilibrium Modeling</u>			
Water quality characterization of river:	E	Table IV-64 summarizes the chemical characteristics chosen to characterize 14 rivers and 1 lake throughout the United States.	
● pH		Water quality criteria for many metals are keyed to hardness, and increase with increasing hardness (see Table IV-41).	
● Suspended solids			
● Conductivity			
● Temperature			
● Hardness			
● Total organic carbon			
● Other major cations and anions			
*D - dilution			
*R - dilution and resuspension			
*S - dilution and settling			
*L - lake on river			
*AD - adsorption/desorption rates			
*E - equilibrium modeling			

One of the primary purposes of the reconnaissance, in addition to verifying data used in the screening analyses, is to gain a feel for the importance of settling and scour of solids, as a function of reach, throughout the study area. If there are extensive settling zones where a high percentage of the solids settle, and if the partition coefficients of the metals under investigation are high, then much of the metals are likely to settle also. On the other hand, if the suspended solids are transported downstream with relatively little settling or if  $K_p S \cdot 10^{-6}$  is small (e.g., <1) then downstream transport of metals is likely to be significant. Comparison of the behavior of the surface water with predicted metal distributions go hand in hand, and provide an opportunity for the user to obtain a consistency between prediction and observation.

As part of characterizing settling zones, samples of bottom sediments (the top 1 to 3 inches) can be collected for visual observation. A qualitative comparison of grain size and texture might confirm whether fine, as well as coarse, particles settle in quiescent zones in rivers.

The very limited field reconnaissance described above requires little data collection, with the exception of water depths and widths. The appropriate water depth is the average depth across a section. If the section is approximately parabolic, then the average depth approximately equals 2/3 of the maximum depth. An added benefit of knowing average depths and surface widths is that the cross-sectional area can be estimated which can directly be used to find stream velocity. Choosing "typical" sections for characterizing width and depths means that the calculated velocity is likely to be typical as well.

The next question to be addressed in a field reconnaissance is when to go into the field. A variety of possibilities exist, with the major candidate situations being:

- Steady, low to moderate flow conditions
- Pseudo-steady high flow conditions, such as snow runoff periods during spring melt or during a long, low intensity storm
- Highly unsteady conditions when stream flow is rapidly changing due to a transient high intensity storm event.

Without question, the steady, low to moderate flow condition is most appropriate for a first, low effort reconnaissance, even if this is not the most critical water quality condition. Generally the results obtained during a steady-state period are more readily and accurately interpretable because time variability is not a consideration. Additionally, results from a field reconnaissance conducted at steady-state can help to determine critical conditions.

#### 4.10.5.3 Sampling Guidelines

Table IV-80 shown earlier summarizes the data required for the screening procedures contained in this document. Based on a comparison between the data available and the data required to perform a screening analyses, sampling priorities can be

generated. While it is not possible to always decide beforehand what are the most important parameters for a particular situation, some preliminary calculations with the screening tools will be useful to reveal what appears most important. In many cases, the magnitude of the partition coefficient is likely to play an important role. The partition coefficient is not measured directly, but is calculated from measured values of adsorbed metal per unit suspended solids (X) and dissolved metal (C); i.e.,  $K_p = X/C$ .

If resources permit, a comprehensive survey where samples are collected at the system boundaries and at important sources at a single point in time is generally very useful for predictive purposes. If the survey is performed during steady-state conditions, all samples do not have to be collected in a truly simultaneous fashion. The principal advantage of a comprehensive survey over repeated sampling at one or two stations is that the information collected can be used to more accurately reconstruct overall cause and effect mechanisms, understand better system responses and thus more reliably predict concentrations throughout the system.

## REFERENCES

- Alonso, C.V., Jr. McHenry, and J.-C.S. Hong. 1975. The Influence of Suspended Sediment on the Reaeration of Uniform Streams. *Water Research* 9:695-700.
- American Public Health Association. 1973. *Standard Methods for the Examination of Water and Waste Water*, 13th ed. American Public Health Assn., Washington, D.C.
- Bansal, M.K. 1975. Deoxygenation in Natural Streams, *Water Resources Bulletin* 11(3):491-504.
- Barnes, H.H. 1967. Roughness Characteristics of Natural Channels. *Geological Survey Water-Supply Paper* 1849.
- Barrett, M.J., A.L. Gameson, and C.G. Ogden. 1960. *Aeration Studies of Four Wier systems*. Water and Water Engineering, London.
- Bell, M.A., R.A. Ewing, G.A. Lutz, V.L. Holoman, B. Paris, H.H. Krause. 1978. *Reviews of the Environmental Effects of Pollutants: VII. Lead*. Battelle-Columbus Laboratories for U.S. Environmental Protection Agency. EPA-600/1-78-029.
- Bessler, M.B., and J.T. Maletic. 1975. Salinity Control and Federal Water Quality Act. *American Society of Civil Engineers, Journal of the Hydraulics Division*. 101(HY5):581-594.
- Bowie, G.L., W.B. Mills, D.B. Porcella, C.L. Campbell, J.R. Pogenkopf, G.L. Rupp, K.M. Johnson, P.W.H. Chan, and S.A. Gherini. 1985. *Rates, Constants and Kinetic Formulations in Surface Water Quality Modeling (Ed. 2)*. For U.S. Environmental Protection Agency.
- Brady, D.K., W.L. Graves, and J.C. Geyer. 1969. *Surface Heat Exchange at Power Plant Cooling Lakes*. Edison Electric Institute.
- Briggs, J.C. and J.F. Ficke. 1977. *Quality of Rivers of the United States, 1975 Water Year - Based on the National Stream Quality Accounting Network (NASQAN)*. USGS Open-File Report 78-200.
- Brown, G.W. 1969. Predicting Temperature of Small Streams. *Water Resources Research*. 5(1).
- Butts, T.A., and R.L. Evans. 1978. *Sediment Oxygen Research Studies of Selected Northeastern Illinois Streams*. Office of Water Research and Technology.
- Callahan, M.A. et al. 1979. *Water Related Environmental Fate of 129 Priority Pollutants*, EPAW4-79-029.
- Carnahan, B., H.A. Luther, and J.O. Wilkes. 1969. *Applied Numerical Methods*. John Wiley & Sons, New York.
- Chadderton, R.A. et al. 1981. *Analysis of Waste Load Allocation Procedures*. *Water Resources Bulletin*. 17: 760.
- Chow, V.T. 1959. *Open Channel Hydraulics*. McGraw-Hill, New York.
- Committee on Water Quality Criteria, National Academy of Sciences and National Academy of Engineering. 1973. *Water Quality Criteria 1972*. U.S. Environmental Protection Agency, Washington, D.C. EPA-R3-73-033.

- Covar, A.P. 1976. Selecting the Proper Reaeration Coefficient for Use in Water Quality Models. Presented at the U.S. Environmental Protection Agency Conference on Environmental Simulation and Modeling, April 19-22.
- Cragwall, J.S. 1966. Low-Flow Analysis of Streamflow Data. 5th Annual Sanitary and Water Resources Engineering Conference. Nashville, TN.
- Delos, C.G., W.L. Richardson, J.V. DePinto, D.W. Rogers, K. Rygwelski, R. Wethington, R.B. Ambiose, J. P. St. John. 1983. Technical Guidance Manual for Performing Waste Load Allocations. Book II: Streams and Rivers. Chapter 3: Toxic Substances, For the U.S. Environmental Protection Agency. Draft.
- Driscoll, E.D., J.L. Mancini, and P.A. Mangarella. 1981. Technical Guidance Manual for Performing Waste Load Allocations. Book II: Streams and Rivers. Chapter 1: BOD/DO and Ammonia Toxicity. For U.S. Environmental Protection Agency.
- Durum, W.H., J.D. Hem, and S.G. Heidel. 1971. Reconnaissance of Selected Minor Elements in Surface Waters of the United States. Geological Survey Circular 643.
- Edinger, J.E. 1965. Heat Exchange in the Environment. Johns Hopkins University, Baltimore, MD. p. 43.
- Edinger, J.E., D.K. Brady, and J.C. Graves. 1968. The Variations of Water Temperature Due to Electric Cooling Operations. Journal of Water Pollution Control Federation. 40(9): 1637-1639.
- Edinger, J.E., and J.C. Geyer. 1965. Heat Exchange in the Environment. Edison Electric Institute. Publication 65-902.
- Environmental Science and Technology. 1971. Metals Focus Shift to Cadmium. 5(9).
- Erdmann, J.B. 1979a. Systematic Diurnal Curve Analysis. Journal Water Pollution Control Federation. 51(1).
- Erdmann, J.B. 1979b. Simplified Diurnal Curve Analysis. Journal Environmental Engineering Division, ASCE, 105(EE6).
- Fenwick, G.B. 1969. State of Knowledge of Channel Stabilization in Major Alluvial Rivers. U.S. Army Corps of Engineers, Technical Report No. 7.
- Fischer, H.B., E.J. List, R.C.Y. Koh, J. Imberger, N.H. Brooks. 1979. Mixing in Inland and Coastal Waters. Academic Press. p. 483.
- Forstner, U. and G.T.W. Wittmann. 1979. Metal Pollution in the Aquatic Environment. Springer-Verlag.
- Gameson, A.L., K.G. Vandyke, and C.G. Oger. 1958. The Effect of Temperature on Aeration at Wiers. Water and Water Engineering. London.
- Gardiner, J. 1974. The Chemistry of Cadmium in Natural Water-II. The Adsorption of Cadmium on River Muds and Naturally Occurring Solids. Water Research, Vol. 8, pp. 157-164.
- Gavis, J. and J.F. Ferguson. 1972. The Cycling of Mercury Through the Environment. Water Research. Vol. 6.
- Graf, W.H. 1971. Hydraulics of Sediment Transport. McGraw-Hill, New York.
- Gupta, G.C. and F.L. Harrison. 1982. Effect of Humic Acid on Copper Adsorption By Kaolin. Water, Air, and Soil Pollution. Vol. 17.

- Hammons, A. S., J.E. Huff, H.M. Braunstein, J.S. Drury, C.R. Shriner, E.B. Lewis, B.L. Whitfield, L.E. Towill. 1978. Reviews of the Environmental Effects of Pollutants: IV. Cadmium. Oak Ridge National Laboratory for U.S. Environmental Protection Agency. EPA-600/1-78-026.
- Hem, J.D. 1970. Study and Interpretation of the Chemical Characteristics of Natural Waters. U.S. Geological Survey Water Supply Paper 1473.
- Hem, J.D. 1975. Discussion of "Role of Hydrous Metal Oxide in the Transport of Heavy Metals in the Environment" by G.F. Lee. In Heavy Metals in the Aquatic Environment. P.A. Krenkel (ed.).
- Hu, S., and R.C. Kintner. 1955. The Fall of Single Liquid Drops Through Water. Amer. Inst. Chem. Eng. J. 1(1):42.
- Hydrologic Engineering Center, Corps of Engineers. 1975. Water Quality Modeling of Rivers and Reservoirs. U.S. Army Corps of Engineers
- Hydroscience Inc. 1971. Simplified Mathematical Modeling of Water Quality. U.S. Environmental Protection Agency, Washington, D.C.
- Janik, J.J., S.M.S. Melancon, L.S. Blakey. 1982. Site Specific Water Quality Assessment: State River, Colorado. For U.S. Environmental Protection Agency, Las Vegas. EPA-600/X-82-027.
- Jenne, E.A. 1972. Mercury in Water of the United States. U.S. Geological Survey Open File Report.
- Jones, H.G.M., H. Bronheim, and P.F. Palmedo. 1975. Electricity Generation and Oil Refining. Mesa New York Bight Atlas. Monograph No. 25. New York Sea Grant Institute, Albany, NY.
- Karmondy, E.J. 1969. Concepts of Ecology. Prentice-Hall, Englewood Cliffs, NJ.
- Kelly, M.G., G.M. Hornberger, B.J. Cosby. 1975. A Method for Monitoring Eutrophication in Rivers. University of Virginia.
- Kharkor, D.P., K.K. Turekian, and K.K. Bertine. 1968. Stream Supply of Dissolved Silver, Molybdenum, Antimony, Selenium, Chromium, Cobalt, Rubidium, and Cesium to the Oceans. Geochem. Cosmochim. Acts. Vol. 32.
- King, H.W. 1954. Handbook of Hydraulics. McGraw-Hill, New York.
- Kopp, J.F. 1969. The Occurrence of Trace Elements in Water. In D.D. Hemphill (ed.), Proc. 3rd Annual Conference on Trace Substances in Environmental Health.
- Krenkel, P.A., and F.L. Parker. 1969. Biological Aspects of Thermal Pollution. Vanderbilt University Press.
- Kubota, J., E.L. Mills, and R.T. Oglesby. 1974. Lead, Cd, Zn, Cu, and Co in streams and Lake Waters of Cayuga Lake Basin, New York. Environmental Science and Technology. 8(3), March.
- Kudo, A., D.C. Mortimer, J.S. Hart. 1975. Factors Influencing Resorption of Mercury from Bed Sediments. Canadian Journal of Earth Sciences, Vol. 112.
- Kudo, A., R.D. Townsend, and D.R. Miller. 1977. Prediction of Mercury Distribution in River Sediments. Journal of the Environmental Engineering Division, ASCE. Vol. 103, No. EE4. Altmann. 1980.

- Leckie, J.O., M.M. Benjamin, K. Hayes, G. Kaufman, S. Altman. 1980. Adsorption/Coprecipitation of Trace Elements from Water with Iron Oxyhydroxide. Prepared for Electric Power Research Institute. CS-1513.
- Lehman, J.T., D.B. Butkin, and G.E. Likens. 1975. The Assumptions and Rationales of a Computer Model of Phytoplankton Population Dynamics. *Limnology and Oceanography*, 20(3): 343-362.
- Lind, C.J. 1970. U.S. Geological Survey Professional Paper 700D, pp. D272-280.
- Linsley, R.K., M.A. Kohler, and J.H. Paulhus. 1958. *Hydrology for Engineers*. McGraw-Hill, New York.
- Long, D.T. and E.E. Angino. 1977. Chemical Speciation of Cd, Cu, Pb, and Zn in Mixed Freshwater, Seawater, and Brine Solutions. *Geochemica et Cosmochimica Acta*, vol. 41.
- Lovering, T.G. Lead in the Environment. 1976. Geological Survey Professional Paper 951.
- Lund, J.W.G. 1965. The Ecology of Freshwater Phytoplankton. *Biol. Rev.* 40: 231-293.
- Mastropietro, M.A. 1968. Effects of Dam Reaeration on Waste Assimilation Capacities of the Mohawk River. Proceedings of the 23rd Industrial Waste Conference. Purdue University.
- McElroy, A.D., S.Y. Chi u, J.W. Nebjen, A. Aleti, and F.W. Bennett. 1976. Loading Functions for Assessment of Water Pollution from Nonpoint Sources. U.S. Environmental Protection Agency. Washington. D.C. EPA-600/3-76-151.
- McQuivey, P.S., and T.N. Keefer. 1976. Dispersion-Mississippi River Below Baton Rouge, LA. *Journal of Hydraulics Division, ASCE* 102(HY10).
- Miles, J.R.W. 1976., Insecticide Residues on Stream Sediments in Ontario, Canada. *Pesticide Monitoring Journal* 10(3).
- Milligan, J.D., K.F. Nelson, and I.E. Wallace. 1981. Chattanooga Creek: The Occurrence and Distribution of Toxic Pollutants - September 1980. Tennessee Valley Authority. PB81-241119.
- Mills, W.B. 1976. A Computational Model That Simulates Biofilm Vitriification in Streams. Engineer's Thesis. Stanford University.
- Mills, W.B. 1979. A Nutrient Analysis of the Snake River and Its Tributaries within the State of Idaho. Tetra Tech Report TC-3923. Prepared for Idaho Department of Health and Welfare.
- Mills, W.B., V.H. Colber, and J.D. Dean. 1979. Hand-Held Calculator Programs for Analysis of River Quality Interactions. Supplemental Volume to: Water Quality Assessment, a Screening method for Nondesignated 208 Areas.
- Mills, W.B. 1981. Workshop on Screening Methods for Conventional and Toxic Pollutants in Rivers, unpublished notes.
- Mills, W.B., V. Kwong, L. Mok, M.J. Ungs. 1985. Microcomputer Methods for Toxicants in Ground Waters and Rivers. Proceedings of 1985 Conference on Environmental Engineering, ASCE. Boston, MA.
- Mills, W.B. and L. Mok. 1985. Simplified Methods to Predict the Fate of Metals in Rivers. Proceedings of 1985 Conference on Environmental Engineering, ASCE. Boston, MA.



- Montana State Dept. of Health and Environmental Sciences. 1973. Water Quality Standards. MAC 16-2.14(10)-S14480.
- Morel, F.M.M. and S.L. Schiff. 1980. Geochemistry of Municipal Waste in Coastal Waters. Ralph Parsons Laboratory, Massachusetts Institute of Technology.
- Neely, W.B., G.E. Blau, and T. Alfrey, Jr. 1976. Mathematical Models Predict Concentration-Time Profiles Resulting from Chemical Spill in a River. Environmental Science and Technology 10(1):72-76.
- Nemerow, N.L. 1974. Scientific Stream Pollution Analysis. Scripts Book Co., Washington, D.C.
- Nordstrom, D.K., L.N. Plummer, T.M.L. Wigley, T.J. Wolery, J.W. Ball, E.A. Jenne, R.L. Bassett, D.A. Crerar, T.M. Florence, B. Fritz, M. Hoffman, G.R. Holdren, Jr., G.M. Lafon, S.V. Mattigod, R.E. McDuff, F. Morel, M.M. Reddy, G. Sposito, J. Thraill. 1979. Comparison of Computerized Chemical Models for Equilibrium Calculations in Aqueous Systems. In Chemical Modeling in Aqueous Systems. ACS Symposium Series 93.
- Novotny, V. 1969. Boundary Layer Effects on the Course of the Self-Purification of Small Streams. In: Adv. Water Pollution Res. ed. S. H. Jenkins, Pergamon. pp. 39-50.
- Novotny, V., and P.A. Krenkel. 1975. A Waste Assimilative Capacity Model for a Shallow, Turbulent Stream. Water Research 9:233-241.
- Odum, H.T., W. McConnel, and W. Abbott. 1958. The Chlorophylls of Communities. Institute of Marine Science. V:65-69.
- Omernik, J.M. 1977. Nonpoint Source--Streams Nutrient Level Relationships: A Nationwide Study. Corvallis Environmental Research Laboratory. EPA-600/3-77-105.
- Parker, F.L., and P.A. Krenkel. 1969. Engineering Aspects of Thermal Pollution. Vanderbilt University Press.
- Patterson, J.W., H.E. Allen, J.J. Scala. 1977. Carbonate Precipitation for Heavy Metal Pollutants. J. Water Pollution Control Federation. 49(12).
- Pluhowski, E.J. 1970. Urbanization and Its Effect on Stream Temperature. U.S. Geological Survey Professional Paper 627-D. pp. 1-109.
- Proceedings of the International Conference on Transport of Persistent Chemicals on Aquatic Ecosystems. 1974.
- Rai, D., J.M. Zachara, A.P. Schwab, R.L. Schmidt, D.C. Girvin, and J.E. Rogers. 1983. Attenuation Rates, Coefficients, and Constants in Leachate Migration: A Critical Review. Battelle Pacific Northwest Laboratories. Electric Power Research Institute RP-2485-3.
- Ramamoorthy, S., and B.R. Rust. 1976. Mercury Sorption and Resorption Characteristics of Some Ottawa River Sediments. Canadian Journal of Earth Sciences. Vol. 13.
- Schumm, S.A. 1960. The Shape of Alluvial Channels in Relation to Sediment Type. Professional paper 352-B. U.S. Geological Survey, Washington, D.C.
- Sillen, L.G. 1964. Stability Constants of Metal-Ion Complexes. Special Publication No. 17.
- Sladeczek, V. 1965. The Future of the Saprobity System. Hydrobiologia 25:518-537.

- Sladeczek, V. 1969. The Measures of Saprobity. Verb. Int. Ver. Limnol. 17: 546-559.
- Snoeyink, V.L. and D. Jenkins. 1980. Water Chemistry. John Wiley & Sons.
- Stall, J.B., N.L. Rupani, and P.K. Kandaswamy. 1958. Sediment Transport in Money Creek. American Society of Civil Engineers, Journal of the Hydraulics Division 84(HY1): 1531-1 to 1531-27.
- Stefan, H., and J.S. Gulliver. 1978. Effluent Mixing in a Shallow River. Journal Environmental Engineering Division, ASCE. 104(2): 199-213.
- Sterney, D.H., and M.S. Stern. 1982. The Distribution of Heavy Metals in the Bottom Sediments of Three Streams in the Kansas City, Missouri, Metropolitan Area. Missouri Water Resources Research Center.
- Stiff, M.J. 1971. The Chemical States of Copper in Polluted Fresh Water and a Scheme of Analysis to Differentiate Them. Water Research, Vol. 5.
- Stumm, W., and J.J. Morgan. 1970. Aquatic Chemistry. Wiley-Interscience, New York.
- Stumm, W. and J.J. Morgan. 1981. Aquatic Chemistry: An Introduction Emphasizing Chemical Equilibrium in Natural Waters, Second Edition, Wiley Interscience, New York.
- Stumm, W., and Stumm-E. Zollinger. 1972. The Role of Phosphorus in Eutrophication. Water Pollution Microbiology, Wiley-Interscience, New York.
- Tallman, D.E. and A.U. Shaikh. 1980. Redox Stability of Inorganic Arsenic (III) and Arsenic (V) in Aqueous Solution. Anal. Chem., Vol. 52.
- Task Committee on Preparation of Sedimentation Manual. 1971. Sediment Discharge Formulas. Journal of the Hydraulic Division. 97(HY4). Proc. Paper No. 7786.
- Tetra Tech, Inc. 1978. Methodology for Evaluation of Multiple Power Plant Cooling System Effects, Volumes 1 and 3. Tetra Tech Report TC-3810.
- Thibodeaux. 1979. Chemodynamics: Environmental Movement of Chemicals in Air, Water, and Soil. John Wiley & Sons, New York. p. 501.
- Thibodeaux, L.J. 1980. Spill of Soluble, High Density Immiscible Chemicals on Water. U.S. Department of Transportation Report No. CG-UOA-80-011. p. 131.
- Thibodeaux, L.G. 1981. Personal Communication of August 18.
- Thomann, R.V. 1972. Systems Analysis and Water Quality Management. Environmental Research and Applications, New York.
- Thomas, N.A., and R.L. O'Connell. 1966. A Method for Measuring Primary Production by Stream Benthos, Limnology and Oceanography 2(3): 386-392.
- Towill, L.E., C.R. Shriner, J.S. Drury, A.S. Hammons, J.W. Holleman. 1978. Reviews of the Environmental Effects of Pollutants: III. Chromium.
- Tsioglou, E.C., and J.R. Wallace. 1972. Characterization of Stream Reaeration Capacity. EPA-R3-72-012.
- Turk, J.T. 1980. Applications of Hudson River Basin PCB-Transport Studies. In: Contaminants and Sediments, Vol. 1. Ann Arbor Science, Ann Arbor, MI.

- Turner, R.R. and S.E. Lindberg. 1978. Behavior and Transport of Mercury in River-Reservoir System Downstream of Inactive Chloralkali Plant. Environmental Science and Technology. 12(8).
- U.S. Bureau of Reclamation, Interim Report. 1958. Total Sediment Transport Program, Lower Colorado River Basin. USBR. Denver, CO.
- U.S. Department of Commerce. 1968. Climatic Atlas of the United States. U.S. Dept. of Commerce, Environmental Sciences Services Administration, Environmental Data Service, Washington, D.C.
- U.S. Environmental Protection Agency. 1975. National Water Quality Inventory. Report to Congress. EPA-440/9-75-014.
- U.S. Environmental Protection Agency. 1976. The Influence of Land Use on Stream Nutrient Levels. Ecological Research Series. EPA-600/13-76-014.
- U.S. Environmental Protection Agency. 1976. Quality Criteria for Water.
- U.S. Environmental Protection Agency. 1980. Ambient Water Quality Criteria for Nickel.
- U.S. Environmental Protection Agency. 1980. Ambient Water Quality Criteria for Silver.
- U.S. Environmental Protection Agency. 1980. Ambient Water Quality Criteria for Zinc.
- U.S. Environmental Protection Agency. 1981. The Economic Impact of Promulgating Toxic Standards for Indiana--A Case Study.
- U.S. Environmental Protection Agency. 1985. Federal Register. No. 145, July 29, p 30784.
- U.S. Geological Survey. 1970. Mercury in the Environment. Professional Paper 713.
- U.S. Geological Survey. 1976. Lead in the Environment. Professional Paper 957.
- Vuceta, J. and J.J. Morgan. 1978. Chemical Modeling of Trace Metals in Fresh Waters: Role of Complexation and Adsorption. Environmental Science and Technology. 12(12).
- Weast, R.C. (ed.) 1977. Handbook of Chemistry and Physics, 58th Edition. CRC Press, Cleveland, Ohio. 2398 pp.
- Westall, J.C., J.L. Zachary, and F. Morel. 1976. MINEQL: A Computer Program for the Calculation of Chemical Equilibrium Composition of Aqueous Systems. Technical Note No. 18, Massachusetts Institute of Technology.
- Wilber, W.G., and J.V. Hunter. 1979. The Impact of Urbanization on the Distribution of Heavy Metals in Bottom Sediments of the Saddle River. Water Resources Bulletin. 15(3), June.
- Wild, H.E., C.N. Sawyer, and T.C. McMahon. 1971. Factors Affecting Vitriification Kinetics. Journal of the Water Pollution Control Federation 43:1845.
- Wright, R.M., and A.J. McDonnell. 1979. In-Stream Deoxygenation Rate Prediction. Journal Environmental Engineering Division, ASCE. 105(EE2).
- Yang, C.T. 1976. Minimum Unit Stream Power and Fluvial Hydraulics. Journal of the Hydraulics Division, ASCE 102(HY7).

Zison, S. W., K.F. Haven, and W.B. Mills. 1977. Water Quality Assessment: A Screening Method for Nondesignated 208 Areas. EPA-600/19-77-023.

Zison, S.W., W.B. Mills, D. Deimer, and C.W. Chen. 1978. Rates, Constants, and Kinetics Formulations in Surface Water Quality Modeling. EPA-600/3-78-105.

United States  
Environmental Protection  
Agency

Center for Environmental Research  
Information  
Cincinnati OH 45268

Official Business  
Penalty for Private Use, \$300

J. Russell Boulding  
4664 N. Rob's Lane  
Bloomington IN 47401

**FOURTH CLASS MAIL**

Please make all necessary changes on the above label,  
detach or copy, and return to the address in the upper  
left-hand corner.

If you do not wish to receive these reports CHECK HERE   
detach, or copy this cover, and return to the address in the  
upper left-hand corner.

EPA/600/6-85/002a

Research and Development



# Water Quality Assessment:

A Screening  
Procedure for Toxic and  
Conventional Pollutants in  
Surface and Ground  
Water—Part II  
(Revised 1985)



EPA/600/6-85/002b  
September 1985

WATER QUALITY ASSESSMENT:  
A Screening Procedure for Toxic  
and Conventional Pollutants  
(Revised 1985)

Part II

by

W. B. Mills, D. B. Porcella, M. J. Unga, S. A. Gherini, K. V. Summers,  
Lingfung Mok, G. L. Rupp, and G. L. Bowie  
Tetra Tech, Incorporated  
Lafayette, California 94549

and

D. A. Hai th  
Cornell University  
Ithaca, New York 14853

Produced by:

JACA Corporation  
Fort Washington, Pennsylvania 19034

Contract No. 68-03-3131

Prepared in Cooperation with U. S. EPA's

Center for Water Quality Modeling  
Environmental Research Laboratory  
Athens, Georgia

Monitoring and Data Support Division  
Office of Water Regulations and Standards  
Office of Water  
Washington, D. C.

Technology Transfer  
Center for Environmental Research Information  
Cincinnati, Ohio

ENVIRONMENTAL RESEARCH LABORATORY  
OFFICE OF RESEARCH AND DEVELOPMENT  
U. S. ENVIRONMENTAL PROTECTION AGENCY  
ATHENS, GEORGIA 30613

DISCLAIMER

Mention of trade names or commercial products does not constitute endorsement or recommendation for use by the U.S. Environmental Protection Agency.



## ABSTRACT

New technical developments in the field of water quality assessment and a reordering of water quality priorities prompted a revision of the first two editions of this manual. The utility of the revised manual is enhanced by the inclusion of methods to predict the transport and fate of toxic chemicals in ground water, and by methods to predict the fate of metals in rivers. In addition, major revisions were completed on Chapter 2 (organic toxicants), Chapter 3 (waste loadings), and Chapter 5 (impoundments) that reflect recent advancements in these fields.

Applying the manual's simple techniques, the user is now capable of assessing the loading and fate of conventional pollutants (temperature, biochemical oxygen demand-dissolved oxygen, nutrients, and sediments) and toxic pollutants (from the U.S. EPA list of priority pollutants) in streams, impoundments, estuaries, and ground waters. The techniques are readily programmed on hand-held calculators or microcomputers. Most of the data required for using these procedures are contained in the manual.

Because of its size, the manual has been divided into two parts. Part I contains the introduction and chapters on the aquatic fate of toxic organic substances, waste loading calculations, and the assessment of water quality parameters in rivers and streams. Part II continues with chapters on the assessment of impoundments, estuaries, and ground water and appendices E, H, I, and J. Appendices D, F, and G are provided on microfiche in the EPA-printed manual. Appendices A, B, and C, which appeared in the first two editions, are now out of date and have been deleted.

This report is submitted in fulfillment of Contract No. 68-03-3131 by JACA Corp. and Tetra Tech, Inc. under the sponsorship of the U.S. Environmental Protection Agency. Work was completed as of May 1985.

TABLE OF CONTENTS

<u>Chapter</u>		<u>Page</u>
PART II		
	DISCLAIMER . . . . .	ii
	ABSTRACT. . . . .	iii
	LIST OF FIGURES (Part II).....	ix
	LIST OF TABLES (Part II)....	xv
5	IMPOUNDMENTS. . . . .	1
	5.1 INTRODUCTION. . . . .	1
	5.2 IMPOUNDMENT STRATIFICATION. . . . .	2
	5.2.1 Discussion. . . . .	2
	5.2.2 Prediction of Thermal Stratification. . . . .	6
	5.3 SEDIMENT ACCUMULATION . . . . .	19
	5.3.1 Introduction. . . . .	19
	5.3.2 Annual Sediment Accumulation. . . . .	20
	5.3.3 Short-Term Sedimentation Rates. . . . .	23
	5.3.4 Impoundment Hydraulic Residence Time. . . . .	29
	5.3.5 Estimation of Sediment Accumulation . . . . .	43
	5.4 EUTROPHICATION AND CONTROL. . . . .	49
	5.4.1 Introduction. . . . .	49
	5.4.2 Nutrients, Eutrophy, and Algal Growth . . . . .	50
	5.4.3 Predicting Algal Concentrations . . . . .	<b>51</b>
	5.4.4 Mass Balance of Phosphorus. . . . .	<b>52</b>
	5.4.5 Predicting Algal Productivity, Secchi Depth, and Biomass. . . . .	60
	5.4.6 Restoration Measures . . . . .	64
	5.4.7 Water Column Phosphorus Concentrations. . . . .	64
	5.5 IMPOUNDMENT DISSOLVED OXYGEN. . . . .	71
	5.5.1 Simulating Impoundment Dissolved Oxygen . . . . .	73
	5.5.2 A Simplified Impoundment Dissolved Oxygen Model . . . . .	74
	5.5.3 Temperature Corrections . . . . .	85
	5.6 TOXIC CHEMICAL SUBSTANCES . . . . .	97
	5.6.1 Overall Processes. . . . .	99
	5.6.2 Guidelines for Toxics Screening . . . . .	104
	5.7 APPLICATION OF METHODS AND EXAMPLE PROBLEM. . . . .	109
	5.7.1 The Occoquan Reservoir. . . . .	110
	5.7.2 Stratification. . . . .	111
	5.7.3 Sedimentation. . . . .	115
	5.7.4 Eutrophication. . . . .	123
	5.7.5 Hypolimnetic DO Depletion . . . . .	128
	5.7.6 Toxicants . . . . .	133

<u>Chapter</u>		<u>Page</u>
	REFERENCES . . . . .	136
	GLOSSARY OF TERMS . . . . .	139
6	ESTUARIES . . . . .	142
6.1	INTRODUCTION. . . . .	142
6.1.1	General . . . . .	142
6.1.2	Estuarine Definition . . . . .	143
6.1.3	Types of Estuaries. . . . .	143
6.1.4	Pollutant Flow in an Estuary. . . . .	145
6.1.5	Estuarine Complexity and Major Forces . . . . .	149
6.1.6	Methodology Summary. . . . .	151
6.1.7	Present Water-Quality Assessment. . . . .	153
6.2	ESTUARINE CLASSIFICATION. . . . .	155
6.2.1	General . . . . .	155
6.2.2	Classification Methodology. . . . .	155
6.2.3	Calculation Procedure . . . . .	155
6.2.4	Stratification-Circulation Diagram Interpretation . . . . .	157
6.2.5	Flow Ratio Calculation. . . . .	163
6.3	FLUSHING TIME CALCULATIONS. . . . .	165
6.3.1	General . . . . .	165
6.3.2	Procedure. . . . .	165
6.3.3	Fraction of Fresh Water Method. . . . .	170
6.3.4	Calculation of Flushing Time by Fraction of Freshwater Method. . . . .	171
6.3.5	Branched Estuaries and the Fraction of Freshwater Method. . . . .	176
6.3.6	Modified Tidal Prism Method . . . . .	176
6.4	FAR FIELD APPROACH TO POLLUTANT DISTRIBUTION IN ESTUARIES. . . . .	184
6.4.1	Introduction. . . . .	184
6.4.2	Continuous Flow of Conservative Pollutants. . . . .	185
6.4.3	Continuous Flow Non-Conservative Pollutants . . . . .	197
6.4.4	Multiple Waste Load Parameter Analysis. . . . .	204
6.4.5	Dispersion-Advection Equations for Predicting Pollutant Distributions . . . . .	207
6.4.6	Pritchard's Two-Dimensional Box Model for Stratified Estuaries. . . . .	216
6.5	POLLUTANT DISTRIBUTION FOLLOWING DISCHARGE FROM A MARINE OUTFALL. . . . .	226
6.5.1	Introduction. . . . .	226
6.5.2	Prediction of Initial Dilution. . . . .	227
6.5.3	Pollutant Concentration Following Initial Dilution. . . . .	248
6.5.4	pH Following Initial Dilution . . . . .	250
6.5.5	Dissolved Oxygen Concentration Following Initial Dilution. . . . .	255
6.5.6	Far Field Dilution and Pollutant Distribution . . . . .	257
6.5.7	Farfield Dissolved Oxygen Depletion . . . . .	263
6.6	THERMAL POLLUTION. . . . .	266
6.6.1	General . . . . .	266

<u>Chapter</u>		<u>Page</u>
6.6.2	Approach . . . . .	267
6.6.3	Appl i cati on . . . . .	269
6.7	TURBI DI TY . . . . .	274
6.7.1	Introduction, . . . . .	274
6.7.2	Procedure to Assess Impacts of Wastewater Discharges on Turbidity or Related Parameters. . . . .	276
6.8	SEDI MENTATI ON. . . . .	282
6.8.1	Introduction. . . . .	282
6.8.2	Qual i tati ve Descripti on of Sedi mentati on. . . . .	282
6.8.3	Estuarine Sedi ment' Forces and Movement. . . . .	283
6.8.4	Settling Velociti es . . . . .	287
6.8.5	Null Zone Cal culati ons. . . . .	291
	REFERENCES. . . . .	295
7	GROUND WATER. . . . .	300
7.1	OVERVI EW. . . . .	300
7.1.1	Purpose of Screening Methods. . . . .	300
7.1.2	Ground Water vs. Surface Water. . . . .	301
7.1.3	Types of Ground" Water Systems Sui table for Screening Method. . . . .	302
7.1.4	Pathways for Contami nation. . . . .	303
7.1.5	Approach to Ground Water Contami nation Problems . . . . .	305
7.1.6	Organi zati on of Thi s Chapter. . . . .	309
<b>7.2</b>	<b>AQUI FER CHARACTERIZATI ON. . . . .</b>	<b>310</b>
<b>7.2.1</b>	<b>Physical Properties of Water. . . . .</b>	<b>310</b>
7.2.2	Physical Properties of Porous Media . . . . .	310
7.2.3	Flow Properties of Saturated Porous Media . . . . .	319
7.2.4	Flow Properties of Unsaturated Porous Media . . . . .	323
7.2.5	Data Acqui si ti on or Esti mati on. . . . .	329
7.3	GROUND WATER FLOW REGIME. . . . .	345
7.3.1	Approach to Analysis of Ground Water Contami nation Sites. . . . .	345
7.3.2	Water Levels and Flow Directi ons. . . . .	346
7.3.3	Flow Velociti es and Travel Times. . . . .	353
<b>7.4</b>	<b>POLLUTANT TRANSPORT PROCESSES . . . . .</b>	<b>363</b>
<b>7.4.1</b>	<b>Di spersi on and Di ffi usi on. . . . .</b>	<b>363</b>
7.4.2	Chemical and Bi ologi cal Processes Affecti ng Poll utant Transport. . . . .	374
7.5	METHODS FOR PREDICTING THE FATE AND TRANSPORT OF CONVENTIONAL AND TOXIC POLLUTANTS . . . . .	382
7.5.1	Introduction to Analytical Methods. . . . .	382
7.5.2	Contami nant Transport to Deep Wells . . . . .	390
7.5.3	Solute Injecti on Wells: Radial Flow. . . . .	396
7.5.4	Contami nant Release on the Surface wi th 1-D Vertical Downward Transport. . . . .	403
7.5.5	Two-Dimensi onal Hori zontal Flow wi th a Slug Source. . . . .	410
7.5.6	Two-Dimensi onal Hori zontal Flow wi th Conti nuous Solute Li ne Sources . . . . .	417

<u>Chapter</u>	<u>Page</u>
7.6	INTERPRETATION OF RESULTS . . . . . 423
7.6.1	Appropriate Reference Criteria. . . . . 423
7.6.2	Quantifying Uncertainty . . . . . 424
7.6.3	Guidelines for Proceeding to More Detailed Analysis . . . . .
	REFERENCES. . . . . 435
	References Cited. . . . . 435
	Additional References on Ground Water Sampling . . . . . 444
APPENDIX A . . . . .	<b>A-1</b>
APPENDIX B . . . . .	<b>B-1</b>
APPENDIX C . . . . .	<b>C-1</b>
APPENDIX D	IMPOUNDMENT THERMAL PROFILES. . . . . D-1
APPENDIX E	MODELING THERMAL STRATIFICATION IN IMPOUNDMENTS . . . . . E-1
APPENDIX F	RESERVOIR SEDIMENT DEPOSITION SURVEYS . . . . . F-1
APPENDIX G	INITIAL DILUTION TABLES . . . . . G-1
APPENDIX H	EQUIVALENTS BY COMMONLY USED UNITS OF MEASUREMENTS. . . . . H-1
APPENDIX I	ADDITIONAL AQUIFER PARAMETERS . . . . . I-1
APPENDIX J	MATHEMATICAL FUNCTIONS. . . . . J-1

LIST OF FIGURES

PART II

<u>Figure</u>		<u>Page</u>
V-1	Water Density as a Function of Temperature and Dissolved Solids Concentration . . . . .	3
V-2	Water Flowing into an Impoundment Tends to Migrate toward a Region of Similar Density. . . . .	3
V-3	Annual Cycle of Thermal Stratification and Overturn in an Impoundment . . . . .	5
V-4	Thermal Profile Plots Used in Example V-1. . . . .	15
V-5	Thermal Profile Plots Appropriate for Use in Example V-2 . . . . .	18
V-6	Sediment Rating Curve Showing Suspended Sediment Discharge as a Function of Flow. . . . .	21
V-7	Relationship between the Percentage of Inflow-Transported Sediment Retained within an Impoundment and Ratio of Capacity to Inflow. . . . .	22
V-8	Plot of $C/R$ and $CR^2$ Versus $R$ . . . . .	25
V-9	Drag Coefficient ( $C$ ) as Function of Reynold's Number ( $R$ ) and Particle Shape. . . . .	26
v-10	Schematic Representation of Hindered Settling of Particles in Fluid Column. . . . .	27
V-n	Velocity Correction Factor for Hindered Settling . . . . .	27
V-12	Upper and Lower Lakes and Environs, Long Island, New York. . . . .	32
V-13	Impoundment Configurations Affecting Sedimentation . . . . .	34
V-14	Kellis Pond and Surrounding Region, Long Island, New York. . . . .	37
V-15	Hypothetical Depth Profiles for Kellis Pond. . . . .	38
V-16	Hypothetical Flow Pattern in Kellis Pond . . . . .	38
V-17	Hypothetical Depth Profiles for Kellis Pond Not Showing Significant Shoaling . . . . .	39
V-18	Lake Owyhee and Environs . . . . .	41
V-19	New Millpond and Environs. . . . .	42
V-20	Significance of Depth Measures $D$ , $D'$ and $D''$ and the Assumed Sedimentation Pattern. . . . .	44
V-21	Settling Velocity for Spherical Particles. . . . .	45
V-22	Nomograph for Estimating Sediment Trap Efficiency. . . . .	46

<u>Figure</u>	<u>Page</u>
V-23 Formulations for Evaluating Management Options for Pollutants in Lakes and Reservoirs. . . . .	53
V-24 US OECD Data Applied to Vollenweider (1976) Phosphorus Loading and Mean Depth/Hydraulic Residence Time Relationship . . . . .	55
V-25 Relationship between Summer Chlorophyll and Spring Phosphorus.	61
V-26 Maximal Primary Productivity as a Function of Phosphate Concentration . . . . .	63
V-27 Conceptualization of Phosphorus Budget Modeling. . . . .	66
V-28 Typical Patterns of Dissolved Oxygen (DO) in Hyrum Reservoir . . . . .	72
V-29 Geometric Representation of a Stratified Impoundment . . . . .	74
V-30 Quality and Ecologic Relationships . . . . .	75
V-31 Rate of BOD Exertion at Different Temperatures Showing the First and Second Deoxygenation Stages. . . . .	78
V-32 Quiet Lake and Environs . . . . .	86
V-33 Thermal Profile Plots for Use in Quiet Lake Example. . . . .	93
V-34 Nomograph for Estimating Sediment Trap Efficiency. . . . .	106
V-35 Generalized Schematic of Lake Computations . . . . .	110
V-36 The Occoquan River Basin. . . . .	111
V-37 Thermal Profile Plots for Occoquan Reservoir . . . . .	114
V-38 Summary of Reservoir Sedimentation Surveys Made in the United States through 1970. . . . .	116
V-39 Dissolved Oxygen Depletion Versus Time in the Occoquan Reservoir. . . . .	132
VI-1 Typical Main Channel Salinity and Velocity for Stratified Estuaries. . . . .	146
VI-2 Typical Main Channel Salinity and Velocity Profiles for Well Mixed Estuaries. . . . .	147
VI-3 Typical Main Channel Salinity and Velocity Profiles for Partially Mixed Estuaries. . . . .	148
VI-4 Estuarine Dimensional Definition . . . . .	150
VI-5 Suggested Procedure to Predict Estuarine Water Quality . . . . .	154
VI-6 Estuarine Circulation-Stratification Diagram . . . . .	156
VI-7 Examples of Estuarine Classification Plots . . . . .	156

<u>Figure</u>	<u>Page</u>
VI-8	Circulation and Stratification Parameter Diagram . . . . . 158
VI-9	The Stuart Estuary . . . . . 160
VI-10	Stuart Estuary Data for Classification Calculations. . . . . 161
VI-11	Estuarine Circulation-Stratification Diagram . . . . . 162
VI-12	Alsea Estuary Seasonal Salinity Variations . . . . . 163
VI-13	Estuary Cross-Section for Tidal Prism Calculations . . . . . 165
VI-14	Patuxent Estuary Salinity Profile and Segmentation Scheme Used in Flushing Time Calculations . . . . . 175
VI-15	Hypothetical Two-Branched Estuary. . . . . 178
VI-16	Cumulative Upstream Water Volume, Fox Mill Run Estuary . . . . . 182
VI-17	River Borne Pollutant Concentration for One Tidal Cycle. . . . . 190
VI-18	Alsea Estuary Riverborne Conservative Pollutant Concentration. . . 192
VI-19	Pollutant Concentration from an Estuarine Outfall. . . . . 193
VI-20	Hypothetical Concentration of Total Nitrogen in Patuxent Estuary. . . . . 196
VI-21	Relative Depletions of Three Pollutants Entering the Fox Mill Run Estuary, Virginia . . . . . 203
VI-22	Additive Effect of Multiple Waste Load Additions . . . . . 204
VI-23	Dissolved Oxygen Saturation as a Function of Temperature and Salinity. . . . . 213
VI-24	Predicted Dissolved Oxygen Profile in James River. . . . . 215
VI-25	Definition Sketch for Pritchard's Two-Dimensional Box Model. . . . 218
VI-26	Patuxent Estuary Model Segmentation. . . . . 225
VI-27	Waste Field Generated by Marine Outfall. . . . . 228
VI-28	Example Output of MERGE -Case 1 . . . . . 240
VI-29	Example Output of MERGE -Case 2 . . . . . 241
VI-30	Schematic of Plume Behavior Predicted by MERGE in the Present Usage. . . . . 244
VI-31	Cross Diffuser Merging . . . . . 247
VI-32	Plan View of Spreading Sewage Field. . . . . 259
VI-33	Outfall Location, Shellfish Harvesting Area, and Environs. . . . . 262



<u>Figure</u>	<u>Page</u>	
VI -34	Dissolved Oxygen Depletions Versus Travel Time . . . . .	265
VI -35	Centerline Dilution of Round Buoyant Jet in Stagnant Uniform Environment. . . . .	274
VI -36	Mean Suspended Solids in San Francisco Bay . . . . .	276
VI -37	Water Quality Profile of Selected Parameters Near a Municipal Outfall in Puget Sound, Washington . . . . .	279
VI -38	Sediment Movement in San Francisco Bay System. . . . .	287
VI -39	Idealized Estuarine Sedimentation. . . . .	288
VI -40	Particle Diameter vs Settling Fall per Tidal Cycle Under Quiescent Conditions . . . . .	291
VI -41	Estuarine Null Zone Identification . . . . .	293
VII -1	Major Aquifers of the United States. . . . .	304
VII -2	Geologic Section in Western Suffolk County, Long Island, Showing Both Confined and Unconfined Aquifers. . . . .	305
VII -3	Detailed Quaternary Geologic Map of Morris County. . . . .	306
VII -4	Generalized Cross-sections Showing Features Common in Arid Western Regions of the United States . . . . .	307
VII -5	Number of Waste Impoundments by State. . . . .	308
VII -6	Schematic Showing the Solid, Liquid and Gaseous Phases in a Unit Volume of Soil. . . . .	312
VII -7	Soil Texture Trilinear Diagram Showing Basic Soil Textural Classes. . . . .	315
VII -8	Typical Particle-Size Distribution Curves for Various Soil Classifications . . . . .	315
VII -9	Schematic Cross-section Showing Both a Confined and an Unconfined Aquifer. . . . .	320
VII -10	Schematic of Matric and Osmotic Soil-Water Potential . . . . .	326
VII -11	Characteristic Curves of Moisture Content as a Function of Matric Potential for Three Different Soils . . . . .	328
VII -12	Characteristic Curves of Moisture Content and Hydraulic Conductivity as a Hysteretic Function of Matric Potential for a Naturally Occurring Sandy Soil . . . . .	330
VII -13	Hydraulic Conductivity as a Function of Moisture Content for Three Different Soils. . . . .	331
VII -14	Cross-Sectional Diagram Showing the Water Level as Measured by Piezometers Located at Various Depths . . . . .	348

<u>Figure</u>	<u>Page</u>
VII-15 An Example of a Contour Plot of Water Level Data With Inferred Flow Directions. . . . .	351
VII-16 Schematic Showing the Construction of Flow Direction Lines from Equipotential Lines for Isotropic Aquifers and Anisotropic Aquifers . . . . .	352
VII-17 Schematic Diagrams Showing Permeameters to Demonstrate Darcy's Law. . . . .	354
VII-18 Schematic Showing How Travel Time Can Be Calculated for Solute Transport When the Flow Velocity Varies: a) Original Problem, b) Discretized Representation of the Flow Line. . . . .	360
VII-19 Example Problem: Calculation of Travel Time for Sulfate from Holding Basin to River. . . . .	362
VI 1-20 Schematic Showing the Effect of Scale on Hydrodynamic Dispersion Processes . . . . .	365
VII-21 Field Measured Values of Longitudinal Dispersivity as a Function of Scale Length for Saturated Porous Media. . . . .	367
VII-22 A Plot of Longitudinal Dispersivity, vs. Scale Length for Saturated Porous Media . . . . .	368
VII-23 A Plot of Longitudinal Dispersivity vs. Scale Length for Unsaturated Porous Media. . . . .	369
VII-24 Schematic Showing the Solution of Equation VII-50 and the Effect of Dispersion. . . . .	371
VII-25 Schematic Showing Hypothetical Vertical Variation in the Ground Water Flow Velocity. . . . .	375
VII-26 Major Equilibrium and Rate Processes in Natural Waters . . . . .	376
VII-27 Hypothetical Adsorption Curves for Cations and Anions Showing Effect of pH and Organic Matter. . . . .	379
VII-28 Dehydrochlorination Rate of Tetrachloroethylene and the Production Rate of its Dechlorination Products . . . . .	383
VII-29 Summary of Model Describing Contaminant Transfer to Deep Wells. . . . .	385
VII-30 Summary of Model Describing Radial Flow from an Injection Well . . . . .	386
VI 1-31 Summary of Model Describing One-Dimensional, Vertically Downward Transport of a Contaminant Released on the Surface. . . . .	387
VII-32 Summary of Model Describing Two-Dimensional Horizontal Flow With a Slug Source. . . . .	388
VII-33 Summary of Model Describing Two-Dimensional Horizontal Flow With Continuous Solute Line Sources. . . . .	389

<u>Figure</u>	<u>Page</u>
VII-34 Schematic of Flow to a Well Beneath a Contaminated Zone. . . . .	392
VII-35 Normalized Solute Concentration vs. Dimensionless Time . . . . .	393
VII-36 Schematic of Example Problem for Flow to Well from a Shallow Contaminated Zone. . . . .	395
VII-37 Schematic View of a Well Injection Solute into a Confined Aquifer. . . . .	397
VII-38 Schematic of the Example Problem Showing Radial Flow of Plating Waste from an Injection Well . . . . .	401
VII-39 Schematic Showing Equation for 1-D Vertical Transport from a Surface Waste Source . . . . .	404
VII-40 Schematic of Example 1-D Problem . . . . .	407
VII-41 Schematic Showing a Slug Discharge of Waste Into a Regional Flow Field. . . . .	412
VII-42 Schematic Showing a Continuous Discharge of Waste Into a Regional Flow Field. . . . .	419
VII-43 General Sequence to Determine If a Modeling Effort is Needed . .	433
VII-44 Steps Involved in Model Application. . . . .	434

LIST OF TABLES

PART II

<u>Table</u>	<u>Page</u>
V-1	Parameter Values Used in Generation of Thermal Gradient Plots. . . . . 8
V-2	Temperature, Cloud Cover, and Dew Point Data for the Ten Geographic Locales Used to Develop Thermal Stratification Plots. . . . . 9
V-3	Limpid Lake Characteristics. . . . . 14
V-4	Physical Characteristics of Lake Smith . . . . . 16
V-5	Comparison of Monthly Climatologic Data for Shreveport, Louisiana and Atlanta, Georgia . . . . . 17
V-6	Hypothetical Physical Characteristics and Computations for Upper Lake, Brookhaven, Suffolk County, New York . . . . . 31
V-7	Hypothetical Physical Characteristics and Computations for Lower Lake, Brookhaven, Suffolk County, New York . . . . . 33
V-8	Hypothetical Physical Characteristics and Computations for Lower Lake, Brookhaven, Suffolk County, New York . . . . . 36
V-9	Preliminary Classification of Trophic State Based on Investigator Opinion . . . . . 56
V-10	Classification of Lake Restoration Techniques. . . . . 65
V-11	Oxygen Demand of Bottom Deposits . . . . . 79
V-12	Volubility of Oxygen in Water. . . . . 81
V-13	Characteristics of Quiet Lake. . . . . 87
V-14	Water Quality and Flow Data for Tributaries to Quiet Lake. . . . . 87
V-15	Precipitation and Runoff Data for Quiet Lake Watershed . . . . . 90
V-16	DO Sag Curve for Quiet Lake Hypolimnion. . . . . 97
V-17	Significant Processes Affecting Toxic Substances in Aquatic Ecosystems. . . . . 98
V-18	Comparison of Modeled Thermal Profiles to Observed Temperatures in Occoquan Reservoir. . . . . 115
V-19	Annual Sediment and Pollutant Loads in Occoquan Watershed in Metric Tons per Year. . . . . 118
V-20	Sediment Loaded into Lake Jackson. . . . . 118
V-21	Calculation Format for Determining Sediment Accumulation in Reservoirs. . . . . 119

<u>Table</u>	<u>Page</u>
V-22 Particle Sizes in Penn Silt Loam . . . . .	120
V-23 Calculation Format for Determining Sediment Accumulation in Reservoirs . . . . .	121
V-24 Sewage Treatment Plant Pollutant Loads in Bull Run Sub-Basin in Metric Tons per Year. . . . .	125
V-25 Calculated Annual Pollutant Loads to Occoquan Reservoir. . . . .	125
V-26 Observed Annual Pollutant Loads to Occoquan Reservoir. . . . .	126
V-27 Calculated and Observed Mean Annual Pollutant Concentrations in Occoquan Reservoir. . . . .	127
VI-1 Summary of Methodology for Estuarine Water Quality Assessment. . . . .	152
VI-2 Tidal Prisms for Some U.S. Estuaries . . . . .	166
VI-3 Sample Calculation Table for Calculation of Flushing Time by Segmented Fraction of Freshwater Method. . . . .	173
VI-4 Patuxent Estuary Segment Characteristics for Flushing Time Calculations . . . . .	175
VI-5 Flushing Time for Patuxent Estuary . . . . .	177
VI-6 Sample Calculation Table for Estuarine Flushing Time by the Modified Tidal Prism Method. . . . .	180
VI-7 Data and Flushing Time Calculations for Fox Mill Run Estuary . . . . .	184
VI-8 Pollutant Distribution in the Patuxent River . . . . .	188
VI-9 Incremental Total Nitrogen in Patuxent River, Expressed as Kilograms. . . . .	188
VI-10 Sample Calculation Table for Distribution of a Locally Discharged Conservative Pollutant by the Fraction of Freshwater Method. . . . .	194
VI-11 Nitrogen Concentration in Patuxent Estuary Based on Local Discharge. . . . .	195
VI-12 Typical Values for Decay Reaction Rates 'k'. . . . .	198
VI-13 Sample Calculation Table for Distribution of a Locally Discharged Non-conservative Pollutant by the Modified Tidal Prism Method. . . . .	200
VI-14 Salinity and CBOD Calculations for Fox Mill Run Estuary. . . . .	202
VI-15 Distribution of Total Nitrogen in the Patuxent Estuary Due to Two Sources of Nitrogen . . . . .	207
VI-16 Tidally Averaged Dispersion Coefficients for Selected Estuaries. . . . .	209

<u>Table</u>	<u>Page</u>	
VI-17	Tidally Averaged Dispersion Coefficients . . . . .	210
VI-18	Salinity and Pollutant Distribution in Patuxent Estuary Under Low Flow Conditions. . . . .	224
VI-19a	Water Densities (Expressed as Sigma-T) Calculated Using the Density Subroutine Found in Merge. . . . .	231
VI-19b	Water Densities (Expressed as Sigma-T) Calculated Using the Density Subroutine Found in Merge. . . . .	233
VI-19C	Water Densities (Expressed as Sigma-T) Calculated Using the Density Subroutine Found in Merge. . . . .	235
VI-20	Plume Variables, Units, and Similarity Conditions. . . . .	238
VI-21	Values of Equilibrium Constants and Ion Product of Water as a Function of Temperature for Freshwater and Salt Water. . . . .	251
VI-22	Estimated pH Values After Initial Dilution . . . . .	253
VI-23	Dissolved Oxygen Profile in Commencement Bay, Washington . . . . .	256
VI-24	Subsequent Dilutions for Various Initial Field Widths and Travel Times . . . . .	260
VI-25	Data Needed for Estuary Thermal Screening. . . . .	268
VI-26	Allowable Channel Velocity to Avoid Bed Scour. . . . .	284
VI-27	Sediment Particle Size Ranges. . . . .	289
VI-28	Rate of Fall in Water of Spheres of Varying Radii and Constant Density of 2 as Calculated by Stokes' Law . . . . .	290
VII-1	Aquifer Parameters and Their Relative Importance as Screening Parameters. . . . .	311
VII-2	Range and Mean Values of Dry Bulk Density. . . . .	314
VII-3	Effective Grain Size and the Range of Soil Particle Sizes for Various Materials. . . . .	316
VII-4	Range and Mean Values of Porosity. . . . .	318
VII-5	Typical Values of Saturated Hydraulic Conductivity and Intrinsic Permeability. . . . .	321
VII-6	Summary of Methods for Measuring Soil Moisture . . . . .	333
VII-7	Techniques for Measuring Saturated Hydraulic Conductivity. . . . .	336
VII-8	Sample Size for Various Confidence Levels Using the Student's t-Distribution. . . . .	342
VII-9	Standard Normal Distribution Function. . . . .	343

<u>Table</u>	<u>Page</u>
VII-10 Percentage Points of the Student's t-Distribution. . . . .	343
VII-11 Methods for Measuring Ground Water Flow Velocity . . . . .	358
VII-12 Summary of Solution Methods. . . . .	384
VII-13 Primary Drinking Water Standards . . . . .	425
VII-14 Interim Secondary Drinking Water Standards . . . . .	426
VII-15 Data Needs for Numerical Models. . . . .	432

CHAPTER 5  
IMPOUNDMENTS

5.1 INTRODUCTION

This chapter contains several methods for assessing water quality and physical conditions in impoundments. The general topics covered are sediment accumulation, thermal stratification, DO-BOD, eutrophication, and toxicant concentrations. These topics cover the major water problems likely to occur in impoundments. The methods developed are easy to use and require readily obtainable data. Because the methods depend upon a number of simplifying assumptions, estimates should be taken only as a guide pending further analysis. Also, since pollutant inputs are dependent on previous calculations, familiarity with the methods in previous chapters will be very helpful and expand understanding of the various processes.

Some of the techniques are more mechanistic and reliable than others. For example, the thermal stratification technique is based upon output of a calibrated and validated hydrothermal model. The model has been shown to be a good one, and to the extent that physical conditions in the studied impoundments resemble those of the model, results should be very reliable. On the other hand, the methods for predicting eutrophication are empirical and based upon correlations between historical water quality conditions and algal productivity in a number of lakes and reservoirs. Because algal blooms are sensitive to environmental factors and the presence of toxicants and factors other than those involved in the estimation methods, the methods for predicting eutrophication will occasionally be inapplicable. Additional approaches have been developed to broaden the applicability of these empirical models.

In using the techniques to be presented, it is important to apply good "engineering judgment" particularly where sequential application of methods is likely to result in cumulative errors. Such would be the case, for example, in evaluating impoundment hypolimnion DO problems resulting from algal blooms. If methods presented below are used to evaluate hypolimnion DO, the planner should determine when stratification occurs, the magnitude of point and nonpoint source BOD loads, and algal productivity and settling rates. From all of this, he may then predict BOD and DO levels in the hypolimnion. Since each of these techniques has an error associated with it, the end result of the computation will have a significant error envelope and results must be interpreted accordingly. The best way to use any of the techniques is to assume a range of values for important coefficients in order to obtain a range of results within which the studied impoundment is likely to fall.

Although scientists and engineers are familiar with the metric system of units, planners, local interest groups, and the general public are more accustomed to the English system. Most morphometric data on lakes and impoundments are in English



units. The conversion tables in Appendix H should be thoroughly familiar before using these techniques and users should be able to perform calculations in either system even though metric units are simpler to use. Also, dimensional analysis techniques using unit conversions are very helpful in performing the calculations.

The methods presented below are arranged in an order such that the planner should be able to use each if he has read preceding materials. The order of presentation is:

- Impoundment stratification (5.2)
- Sediment accumulation (5.3)
- Eutrophication (5.4)
- Impoundment dissolved oxygen (5.5)
- Fate of Priority Pollutants (Toxics) (5.6).

It is strongly recommended that all materials presented be read and examples worked prior to applying any of the methods. In this way a better perspective can be obtained on the kinds of problems covered and what can be done using hand calculations. A glossary of terms has been placed after the reference section so that equation terms can easily be checked.

The final section (5.7) is an example application to a selected site. This example allows the user to have an integrated view of an actual problem and application. Also "the goodness of fit" to measured results can be evaluated.

## 5.2 IMPOUNDMENT STRATIFICATION

### 5.2.1 Discussion

The density of water is strongly influenced by temperature and by the concentration of dissolved and suspended matter. Figure V-1 shows densities for water as a function of temperature and dissolved solids concentration (from Chen and Orlob, 1973).

Regardless of the reason for density differences, water of lowest density tends to move upward and reside on the surface of an impoundment while water of greatest density tends to sink. Inflowing water seeks an impoundment level containing water of the same density. Figure V-2 shows this effect schematically.

Where density gradients are very steep, mixing is inhibited. Thus, where the bottom water of an impoundment is significantly more dense than surface water, vertical mixing is likely to be unimportant. The fact that low density water tends to reside atop higher density water and that mixing is inhibited by steep gradients often results in impoundment stratification. Stratification, which is the establishment of distinct layers of different densities, tends to be enhanced by quiescent conditions. Conversely, any phenomenon encouraging mixing, such as wind stress, turbulence due to large inflows, or destabilizing changes in water temperature will tend to reduce or eliminate strata.

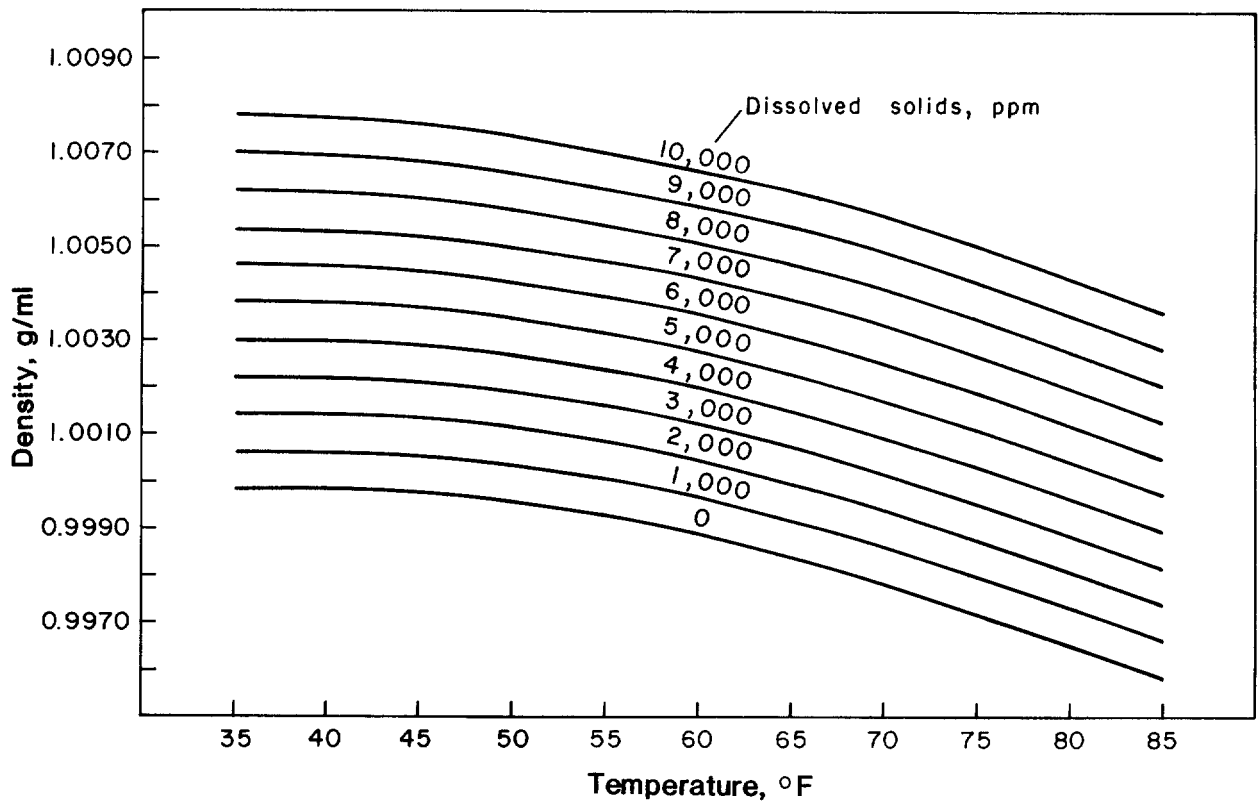


FIGURE V-1 WATER DENSITY AS A FUNCTION OF TEMPERATURE AND DISSOLVED SOLIDS CONCENTRATION (FROM CHEN AND ORLOB, 1973)

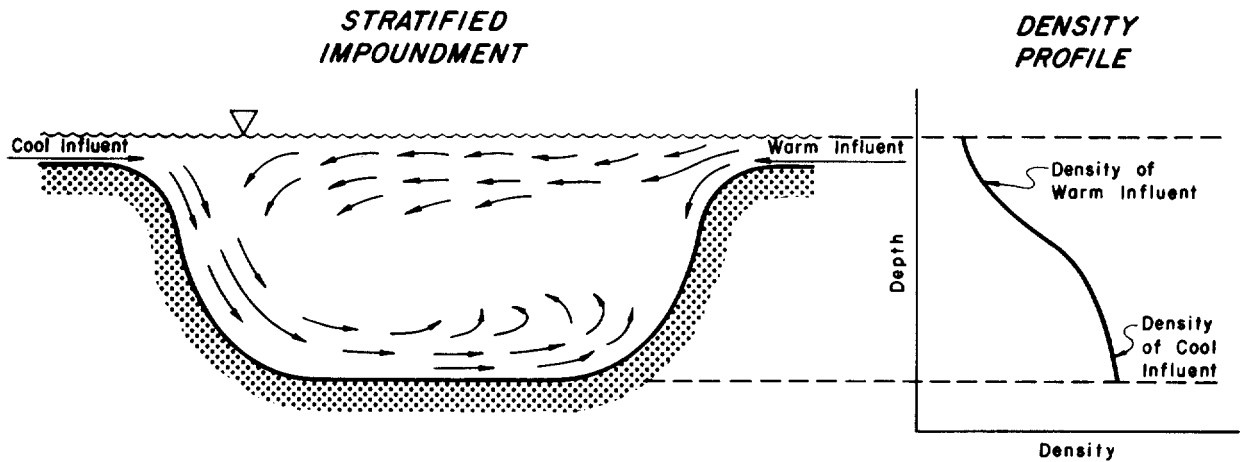


FIGURE V-2 WATER FLOWING INTO AN IMPOUNDMENT TENDS TO MIGRATE TOWARD A REGION OF SIMILAR DENSITY

### 5.2.1.1 Annual Cycle in a Thermally Stratified Impoundment

Figure V-3 shows schematically the processes of thermal stratification and overturn which occur in many impoundments. Beginning at "a" in the figure (winter), cold water (at about 4°C) flows into the impoundment which may at this point be considered as fully mixed. There is no thermal gradient over depth and the impoundment temperature is about 6°C. During spring ("b"), inflowing water is slightly warmer than that of the impoundment because of the exposure of the tributary stream to warmer air and increasingly intense sunlight. This trend continues during the summer ("c"), with tributary water being much warmer and less dense than the deep waters of the impoundment. At the same time, the surface water of the impoundment is directly heated by insolation. Since the warm water tends to stay on top of the impoundment, thermal strata form.

As fall approaches ("d"), day length decreases, air temperatures drop, and solar intensity decreases. The result is cooler inflows and a cooling trend in the surface of the impoundment. The bottom waters lag behind the surface in the rate of temperature change, and ultimately the surface may cool to the temperature of the bottom. Since continued increases in surface water density result in instability, the impoundment water mixes (overturns).

### 5.2.1.2 Monomictic and Dimictic Impoundments

The stratification and overturn processes described in Figure V-3 represent what occurs in a monomictic or single-overturn water body. Some impoundments, especially those north of 40°N latitude and those at high elevation, may undergo two periods of stratification and two overturns. Such impoundments are termed "dimictic." In addition to the summer stratification and resulting fall overturn, such impoundments stratify in late winter. This occurs because water is most dense near 4°C, and bottom waters may be close to this temperature, while inflowing water is colder and less dense. As the surface goes below 4°C, strata are established. With spring warming of the surface to 4°C, wind induced mixing occurs.

### 5.2.1.3 Importance of Stratification

Stratification is likely to be the single most important phenomenon affecting water quality in many impoundments. Where stratification is absent, water mixes vertically, and net horizontal flow is significant to considerable depths. Since the water is mixed vertically, DO replenishment usually occurs even to the bottom and anoxic. (literally "no oxygen") conditions are unlikely. Generally speaking, fully mixed impoundments do not have DO deficiency problems.

When stratification occurs, the situation is vastly different. Flow within the impoundment is especially limited to the epilimnion (surface layer). Thus surface velocities are somewhat higher in an impoundment when stratified than when unstrati-

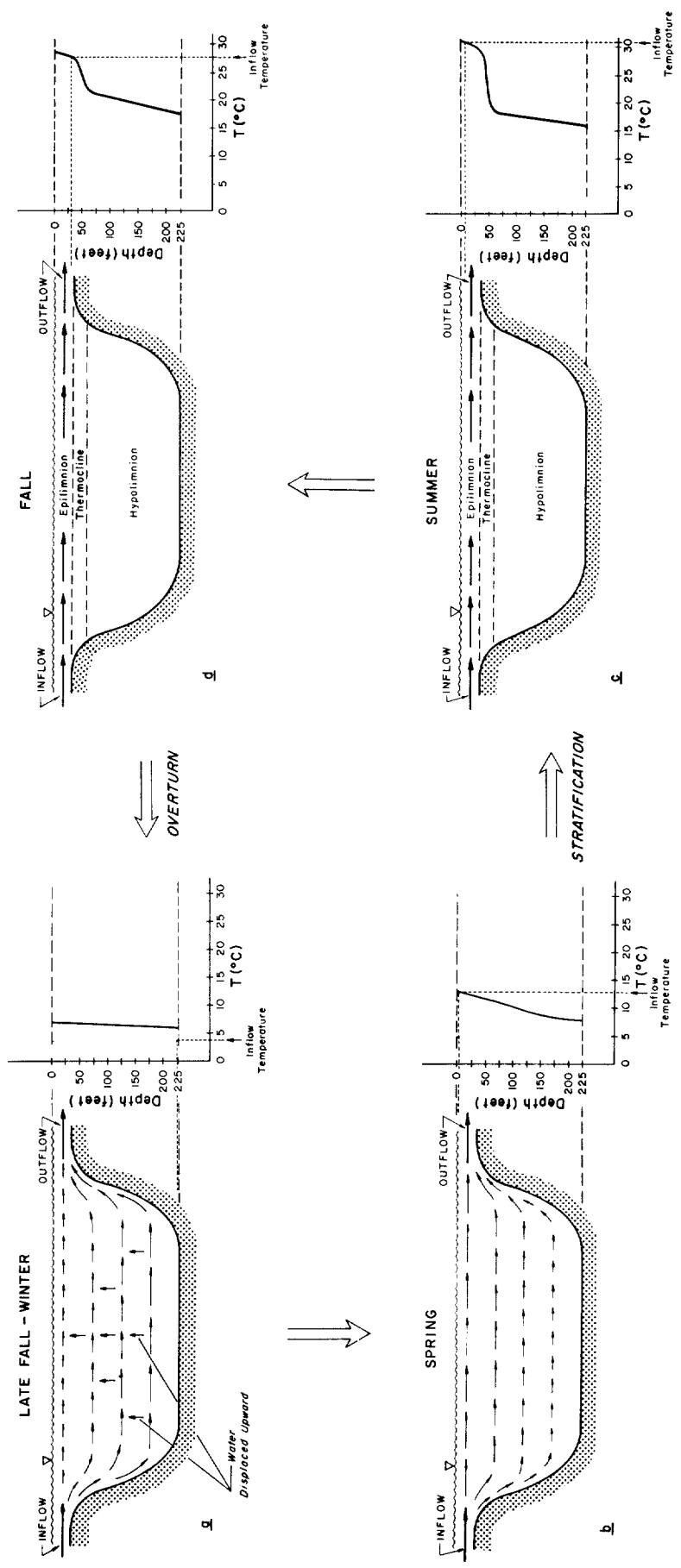


FIGURE V-3 ANNUAL CYCLE OF THERMAL STRATIFICATION AND OVERTURN IN AN IMPOUNDMENT

fied. Since vertical mixing is inhibited by stratification, reaeration of the hypolimnion (bottom layer) is virtually nonexistent. The thermocline (layer of steep thermal gradient between epilimnion and hypolimnion) is often at considerable depth. Accordingly, the euphotic (literally "good light") zone is likely to be limited to the epilimnion. Thus photosynthetic activity does not serve to reoxygenate the hypolimnion. The water that becomes the hypolimnion has some oxygen demand prior to the establishment of strata. Because bottom (benthic) matter exerts a further demand, and because some settling of particulate matter into the hypolimnion may occur, the DO level in the hypolimnion will gradually decrease over the period of stratification.

Anoxic conditions in the hypolimnion result in serious chemical and biological changes. Microbial activity leads to hydrogen sulfide ( $H_2S$ ) evolution as well as to formation of other highly toxic substances, and these may be harmful to indigenous biota.

It should be noted that the winter and spring strata and overturn are relatively unimportant here since the major concern is anoxic conditions in the hypolimnion in summer. Thus all impoundments will be considered as monomictic.

Strong stratification is also important in prediction of sedimentation rates and trap efficiency estimates. These topics are to be covered later.

### 5.2.2 Prediction of Thermal Stratification

Computation of impoundment heat influx is relatively straightforward, but prediction of thermal gradients is complicated by prevailing physical conditions, physical mixing phenomena, and impoundment geometry. Such factors as depth and shape of impoundment bottom, magnitude and configuration of inflows, and degree of shielding from the wind are much more difficult to quantify than insolation, back radiation, and still air evaporation rates. Since the parameters which are difficult to quantify are critical to predicting stratification characteristics, no attempt has been made to develop a simple calculation procedure. Instead, a tested model (Chen and Orlob, 1973; Lorenzen and Fast, 1976) has been subjected to a sensitivity analysis and the results plotted to show thermal profiles over depth and over time for some representative geometries and climatological conditions. The plots are presented in Appendix D.

The plots show the variation in temperature ( $^{\circ}C$ ) with depth (meters). Temperature is used as an index of density. Engineering judgment about defining layers is based on the pattern of temperature with depth. If stratification takes place, the plot will show an upper layer of uniform or slightly declining temperature (epilimnion), an intermediate layer of sharply declining temperature (thermocline), and a bottom layer (hypolimnion). A rule of thumb requires a temperature change of at least  $1^{\circ}C/meter$  to define the thermocline. However, this can be tempered by the observation of a well defined mixed layer.

To assess thermal stratification in an impoundment, it is necessary only to determine which of the sets of plots most closely approximates climatic and hydrologic conditions in the impoundment studied. Parameters which were varied to generate the plots and values used are shown in Table V-1.

Table V-2 shows the climatological conditions used to represent the geographic locales listed in Table V-1. For details of the simulation technique, see Appendix E.

#### 5.2.2.1 Using the Thermal Plots

Application of the plots to assess stratification characteristics begins with determining reasonable values for the various parameters listed in Table V-1. For geographic locale, the user should determine whether the impoundment of interest is near one of the ten areas for which thermal plots have been generated. If so, then the set of plots for that area should be used. If the impoundment is not near one of the ten areas, then the user may obtain data for the parameters listed in Table V-2 (climatologic data) and then select the modeled locale which best matches the region of interest.

Next, the user must obtain geometric data for the impoundment. Again, if the impoundment of interest is like one for which plots have been generated, then that set should be used. If not, the user should bracket the studied impoundment. As an example, if the studied impoundment is 55 feet deep (maximum), with a surface area of about  $4 \times 10^7$  feet<sup>2</sup>, then the 40 and 75 foot deep impoundment plots should be used.

Mean hydraulic residence time ( $\tau_w$ , years) may be estimated using the mean total inflow rate ( $Q$ , m<sup>3</sup>/year) and the impoundment volume ( $V$ , m<sup>3</sup>):

$$\tau_w = V/Q \quad (v-1)$$

Again, the sets of plots bracketing the value of  $\tau_w$  should be examined. Where residence times are greater than 200 days, the residence time has little influence on stratification (as may be verified in Appendix D) and either the 200 day or infinite time plots may be used.

Finally, the wind mixing coefficient was used to generate plots for windy areas (high wind) and for very well protected areas (low wind). The user must judge where his studied impoundment falls and interpolate in the plots accordingly (See Appendix D).

TABLE V-1

PARAMETER VALUES USED IN GENERATION OF  
THERMAL GRADIENT PLOTS (APPENDIX D)

Parameter	Value		
Geographic Locale	Atlanta, Georgia Billings, Montana Burlington, Vermont Flagstaff, Arizona Fresno, California Minneapolis, Minnesota Salt Lake City, Utah San Antonio, Texas Washington, D.C. Wichita, Kansas		
Geometry	Depth (maximum, feet)	Surface Area (feet <sup>2</sup> )	Volume (feet <sup>3</sup> )
	20	$8.28 \times 10^6$	$7.66 \times 10^7$
	40	$3.31 \times 10^7$	$6.13 \times 10^8$
	75	$1.16 \times 10^8$	$4.04 \times 10^9$
	100	$2.07 \times 10^8$	$9.58 \times 10^9$
	200	$8.28 \times 10^8$	$7.66 \times 10^{10}$
Mean Hydraulic Residence Time	<u>Days</u>		
	10		
	30		
	75		
	250		
	$\infty$		
Wind Mixing*	High		
	Low		

\*See Appendix E.

TABLE V-2

TEMPERATURE, CLOUD COVER, AND DEW POINT DATA  
FOR THE TEN GEOGRAPHIC LOCALES USED TO DEVELOP THERMAL  
STRATIFICATION PLOTS (APPENDIX D). SEE FOOT OF TABLE FOR NOTES.

	Temperature (°F)			Dew Point (°F)	Cloud Cover Fraction	Wind (MPH)
	Max.	Mean	Min.			
Atlanta (Lat: 33.8°N, Long: 84.4°W)						
January	54	45	36	34	.63	11
February	57	47	37	34	.62	12
March	63	52	41	39	.61	12
April	72	61	50	48	.55	11
May	81	70	57	57	.55	9
June	87	77	66	65	.58	8
July	88	79	69	68	.63	8
August	88	78	68	67	.57	8
September	83	73	63	62	.53	8
October	74	63	52	51	.45	9
November	62	51	40	40	.51	10
December	53	44	35	34	.62	10
*Billings (Lat: 45.8°N, Long: 108.5°W)						
January	27	18	9	11	.68	13
February	32	22	12	16	.68	12
March	38	27	16	20	.71	12
April	51	38	26	28	.70	12
May	60	47	34	38	.64	11
June	68	54	40	46	.60	11
July	79	63	46	48	.40	10
August	78	61	45	46	.42	10
September	67	52	37	38	.54	10
October	55	42	30	31	.56	11
November	38	29	20	22	.66	13
December	32	22	14	15	.66	13



TABLE V-2 - CONT.

	Temperature (°F)			Dew Point (°F)	Cloud Cover Fraction	Wind (MPH)
	Max.	Mean	Min.			
Burlington (Lat: 44.5°N, Lat: 73.2°W)						
January	27	18	9	12	.72	10
February	29	19	10	12	.69	10
March	38	29	20	20	.66	10
April	53	43	33	32	.67	10
May	67	56	44	43	.67	9
June	54	66	77	54	.61	9
July	82	71	59	59	.58	8
August	80	68	57	58	.57	8
September	71	60	49	51	.60	8
October	59	49	39	40	.65	9
November	44	38	29	30	.79	10
	31	23	15	17	.78	10
Flagstaff (Lat: 35.2°N, Long: 111.3°W)						
January	40	27	14	14	.59	8
February	43	30	17	16	.49	9
March	50	36	22	17	.50	11
April	59	43	28	20	.49	12
May	68	51	34	22	.41	11
June	77	60	42	25	.24	11
July	81	66	50	43	.54	9
August	79	64	49	43	.53	9
September	75	59	42	35	.29	8
October	63	47	31	25	.31	8
November	51	36	21	20	.34	8
December	44	30	17	15	.44	7

TABLE V-2 CONT.

	Temperature (°F)			Dew Point (°F)	Cloud Cover Fraction	Wind (MPH)
	Max.	Mean	Min.			
Fresno (Lat: 36.7°N, Long: 119.8°W)						
January	55	46	37	38	.67	6
February	61	51	40	41	.61	6
March	68	55	42	41	.53	7
April	76	61	46	44	.44	7
May	85	68	52	45	.34	8
June	92	75	57	48	.19	8
July	100	81	63	51	.11	7
August	98	79	61	52	.11	6
September	92	74	56	51	.15	6
October	81	65	49	46	.28	5
November	68	54	40	42	.44	5
December	57	47	38	40	.70	5
Minneapolis (Lat: 45.0°N, Long: 93.3°W)						
January	22	12	3	6	.65	11
February	26	16	5	10	.62	11
March	37	28	18	20	.67	12
April	56	45	33	32	.65	13
May	70	58	46	43	.64	12
June	79	67	56	55	.60	11
July	85	76	61	60	.49	9
August	82	71	59	59	.51	9
September	72	61	49	50	.51	10
October	60	48	37	40	.54	11
November	40	31	21	25	.69	12
December	27	18	9	13	.69	11

TABLE V-2 CONT.

	Temperature ( $^{\circ}\text{F}$ )			Dew Point ( $^{\circ}\text{F}$ )	Cloud Cover Fraction.	Wind (MPH)
	Max.	Mean	Min.			
Salt Lake City (Lat: 40.8 $^{\circ}$ N, Long: 111.9 $^{\circ}$ W)						
January	37	27	18	20	.69	7
February	42	33	23	23	.70	8
March	51	40	30	26	.65	9
April	62	50	37	31	.61	9
May	72	58	45	36	.54	10
June	82	67	52	40	.42	9
July	92	76	61	44	.35	9
August	90	75	59	45	.34	10
September	80	65	50	38	.34	9
October	66	53	39	34	.43	9
November	49	38	28	28	.56	8
December	40	23	32	24	.69	7
San Antonio (Lat: 29.4 $^{\circ}$ N, Long: 98.5 $^{\circ}$ W)						
January	62	52	42	39	.64	9
February	66	55	45	42	.65	10
March	72	61	50	45	.63	10
April	79	68	58	55	.64	11
May	85	75	65	64	.62	10
June	92	82	72	68	.54	10
July	94	84	74	68	.50	10
August	94	84	73	67	.46	8
September	89	79	69	65	.49	8
October	82	71	60	56	.46	8
November	70	59	49	46	.54	9
December	65	42	54	41	.57	9

TABLE V-2 CONT.

	Temperature (°F)			Dew Point (°F)	Cloud Cover Fraction	Wind (MPH)
	Max.	Mean	Min.			
Washington, D. C. (Lat: 38.9°N, Long: 77.0°W)						
January	44	37	30	25	.61	11
February	46	38	29	25	.56	11
March	54	45	36	29	.56	12
April	60	56	46	40	.54	11
May	76	66	56	52	.54	10
June	83	74	65	61	.51	10
July	87	78	69	65	.51	9
August	85	77	68	64	.51	8
September	79	70	61	59	.48	9
October	68	59	50	48	.47	9
November	57	48	39	36	.54	10
December	46	43	31	26	.58	10
Wichita (Lat: 37.7°N, Long: 97.3°W)						
January	42	32	22	21	.50	12
February	47	36	26	25	.51	13
March	56	45	33	30	.52	15
April	68	57	45	41	.53	15
May	77	66	55	53	.53	13
June	88	77	65	62	.46	13
July	92	81	69	65	.39	12
August	93	81	69	53	.38	11
September	84	71	59	55	.39	12
October	72	60	48	43	.40	12
November	34	55	44	33	.44	13
December	45	36	27	25	.50	12

TABLE V-2 CONT.

Notes: Mean:	Normal daily average temperature,	$^{\circ}\text{F}$ .
Max.:	Normal daily maximum temperature,	$^{\circ}\text{F}$ .
Min.:	Normal daily minimum temperature,	$^{\circ}\text{F}$ .
Wind:	Mean wind speed,	MPH
Dew Point:	Mean dew point temperature,	$^{\circ}\text{F}$ .

\*Complete data were not available for Billings. Tabulated data are actually a synthesis of available data for Billings, Montana and Yellowstone, Wyoming.

All data taken from Climatic Atlas of the U.S., 1974.

EXAMPLE V-1

Thermal Stratification

Suppose one wants to know the likelihood that hypothetical Limpid Lake is stratified during June. The first step is to compile the physical conditions for the lake in terms of the variables listed in Table V-1. Table V-3 shows how this might be done. Next, refer to the indexes provided in Appendix D to locate the plot set for conditions most similar to those of the studied impoundment. In this case, the Wichita plots for a 200-foot deep impoundment with no inflow and high mixing rate would be chosen (see Table V-3). Figure V-4 is a reproduction of the appropriate page from Appendix D.

TABLE V-3

LIMPID LAKE CHARACTERISTICS

Item	Limpid Lake	Available Plot
Location	Manhattan, Kansas	Wichita, Kansas
Depth, ft (maximum)	180	200
volume, $\text{ft}^3$	$6 \times 10^{10}$	$7.66 \times 10^{10}$
Mean residence time ( $\tau_w$ )	500 days	$\infty$ (no inflow)
Mixing	high (windy)	high coefficient

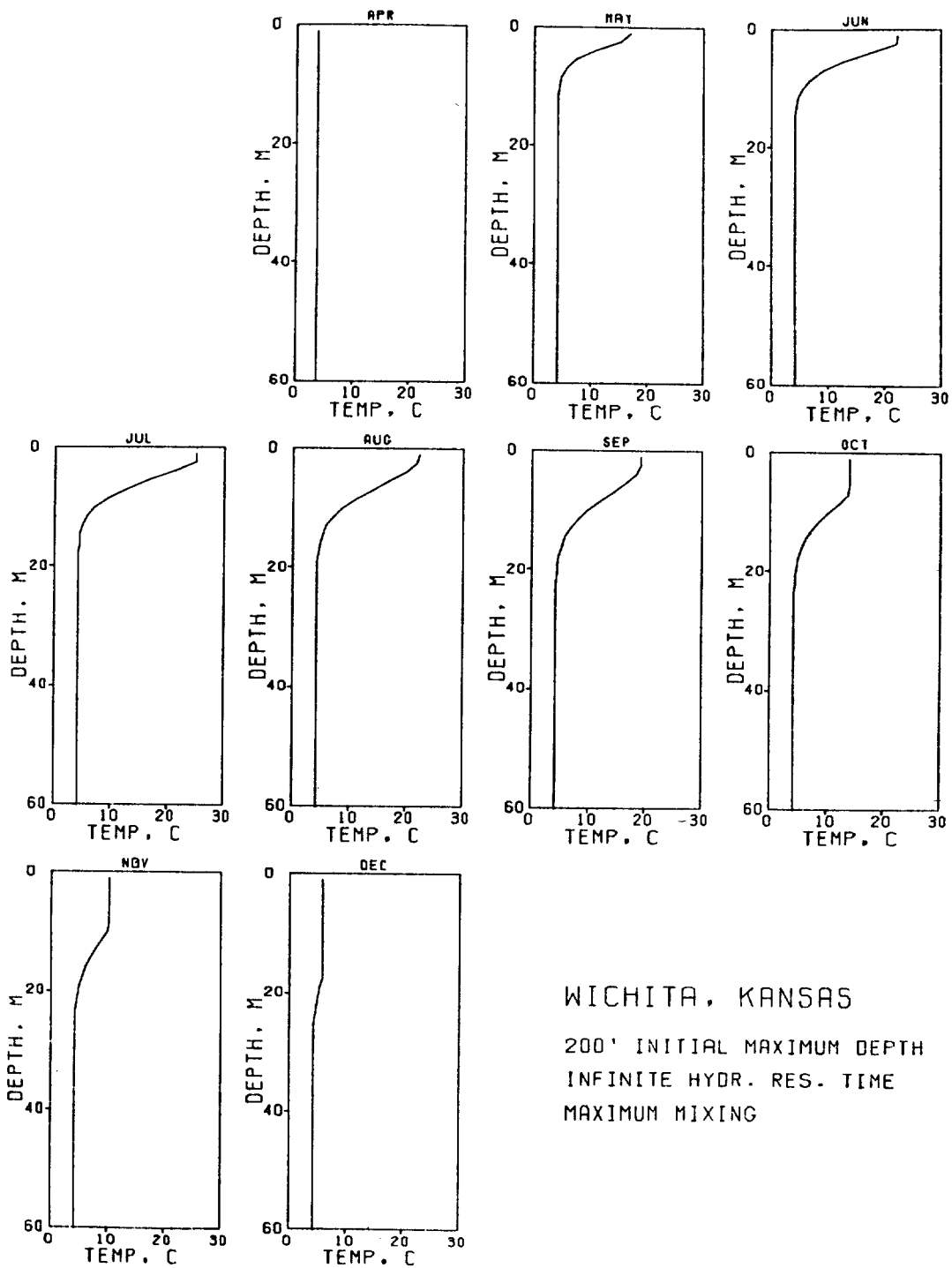


FIGURE V-4 THERMAL PROFILE PLOTS USED IN EXAMPLE V-1

According to the plots, Limpid Lake is likely to be strongly stratified. Distinct strata form in May and overturn probably occurs in December. During June, the epilimnion should extend down to a depth of about eight or ten feet, and the thermocline should extend down to about 30 feet. The gradient in the thermocline should be about 1° C per meter.

END OF EXAMPLE V-1

EXAMPLE V-2

Thermal Stratification

What are the stratification characteristics of Lake Smith?

The hypothetical lake is located east of Carthage, Texas, and Table V-4 shows its characteristics along with appropriate values for the thermal plots.

TABLE V-4

PHYSICAL CHARACTERISTICS OF LAKE SMITH

Item	Lake Smith	Plot Values
Location	15 miles east of Carthage Texas	
Depth, ft (maximum)	23	20
Volume, ft <sup>3</sup>	$3 \times 10^8$	$1.66 \times 10^8$
Mean residence time	250 days	$\infty$
Mixing	low (low wind)	low mixing coefficient

From the available data for Lake Smith, it appears that plots for a 20-foot deep impoundment with no inflow and low mixing coefficient should give a good indication of the degree of summertime stratification. The one remaining problem is climate. Data for nearby Shreveport, Louisiana compare well with those of Atlanta (Table V-5), for which plots are provided in Appendix D, and latitudes are similar. Shreveport is somewhat warmer and insolation is higher, but this is a relatively uniform difference over the year. The net effect should be to shift the thermal plots to a slightly higher temperature but to influence the shape of the plots and the timing of stratification little. As a result, the plots for

TABLE V-5

COMPARISON OF MONTHLY CLIMATOLOGIC DATA  
FOR SHREVEPORT, LOUISIANA AND ATLANTA, GEORGIA  
DATA ARE PRESENTED AS SHREVEPORT/ATLANTA  
(CLIMATIC ATLAS OF THE U. S. , 1974)

	Temperature, °F			Dew Point, °F	Cloud Cover, Fraction	Wind, MPH
	Max.	Mean	Min.			
January	57/54	48/45	38/36	38/34	.60/.63	9/11
February	60/57	50/47	41/37	40/34	.58/.62	9/12
March	67/63	57/52	47/41	44/39	.54/.61	10/12
April	75/72	65/61	55/50	54/48	.50/.55	9/11
May	83/81	73/70	63/57	62/57	.48/.55	9/9
June	91/87	81/77	71/66	69/65	.44/.58	8/8
July	92/88	82/79	72/69	71/68	.46/.63	7/8
August	94/88	83/78	73/68	70/67	.40/.57	7/8
September	88/83	78/73	67/63	65/62	.40/.53	7/8
October	79/74	67/63	55/52	55/51	.38/.45	7/9
November	66/62	55/51	45/40	45/40	.46/.51	8/10
	59/53	50/44	40/35	39/34	.58/.62	9/10

Shreveport Lat: 32.5°N, Long: 94°W

Atlanta Lat: 33.8°N, Long: 84.4°W,

Atlanta may be used, bearing in mind that the temperatures are likely to be biased uniformly low. Figure V-5 (reproduced from Appendix D) shows thermal plots for a 20-foot deep Atlanta area impoundment having no significant inflow and low wind stress. From the figure, it is clear that the lake is likely to stratify from April or May through September, the epilimnion will be very shallow, and the thermocline will extend down to a depth of about 7 feet. The thermal gradient is in the range of about 7°C per meter, as an upper limit, during June. Bottom water warms slowly during the summer until the impoundment becomes fully mixed in October.



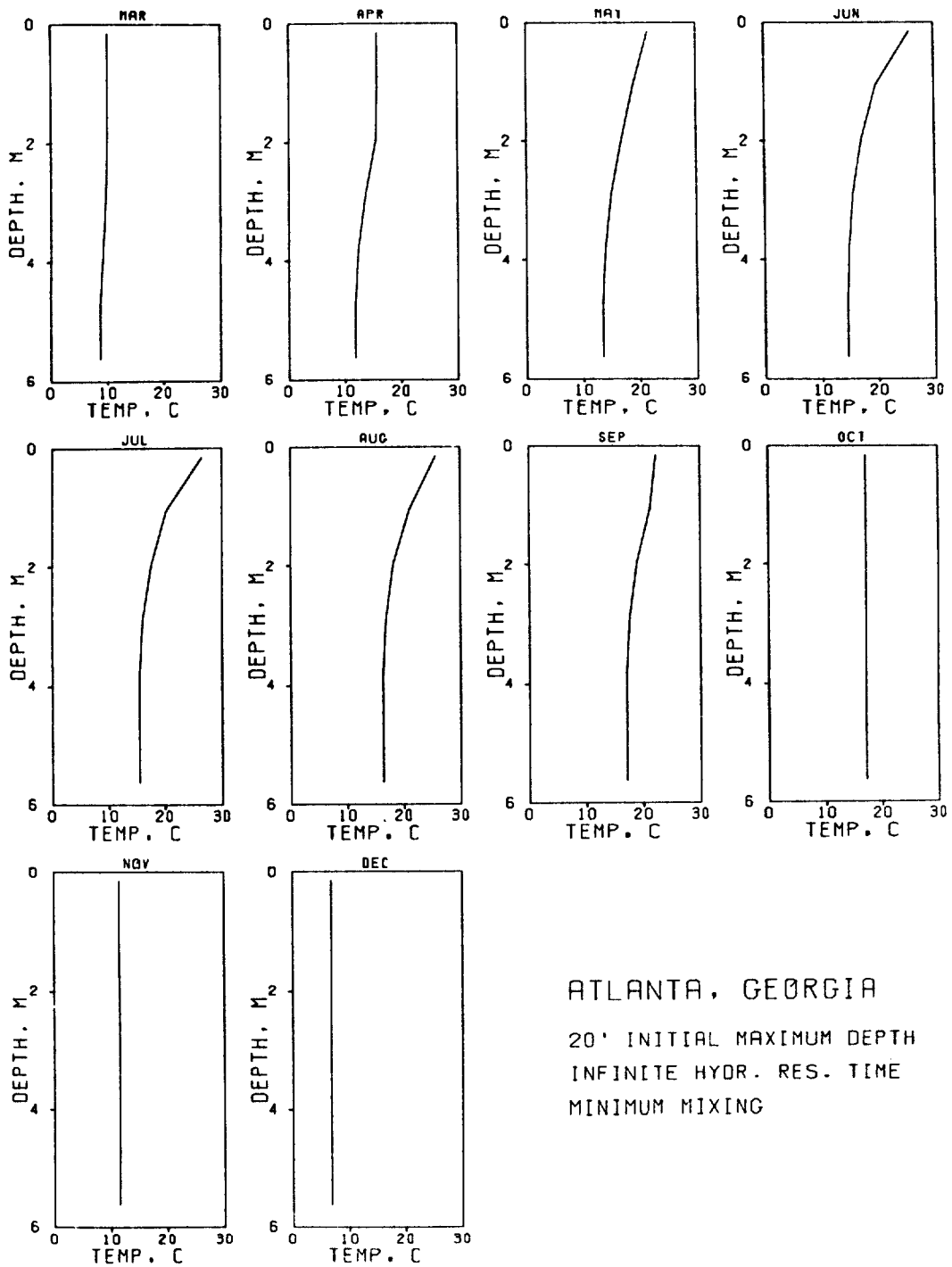


FIGURE V-5 THERMAL PROFILE PLOTS APPROPRIATE FOR USE IN EXAMPLE V-2

END OF EXAMPLE V-2

## 5.3 SEDIMENT ACCUMULATION

### 5.3.1 Introduction

Reservoirs, lakes, and other impoundments are usually more quiescent than tributary streams, and thus act as large settling basins for suspended particulate matter. Sediment deposition in impoundments gradually diminishes water storage capacity to the point where lakes fill in and reservoirs become useless. In some cases, sediment accumulation may reduce the useful life of a reservoir to as little as ten to twenty years (Marshet al.,1975).

Just how much suspended matter settles out as water passes through an impoundment, as well as the grain size distribution of matter which remains suspended, is of interest to the planner for several reasons. Suspended sediment within an impoundment may significantly reduce light penetration thus limiting algal and bottom-rooted plant (macrophyte) growth. This, in turn, can adversely affect food availability for indigenous fauna, or may slow plant succession, as part of the natural aging process of lakes.

Settling of suspended matter may eliminate harborage on impoundment bottoms thus reducing populations of desirable animal species. More directly, suspended particulate impinging on the gills of fish may cause disease or death.

Some minerals, particularly clays, are excellent absorbents. As a result, farm chemicals and pesticides applied to the land find their way to an impoundment bottom and into its food chain. The sediment which settles is likely to have a substantial component of organic matter which can exert an oxygen demand, and under conditions of thermal stratification, anoxic conditions on the impoundment bottom (in the hypolimnion) can result in generation of toxic gases. Indigenous biota may be harmed or even killed as a result.

Knowing the rate of sediment transport and the deposition within an impoundment allows for effective planning to be initiated. If sedimentation rates are unacceptable, then the planner can begin to determine where sediments originate, and how to alleviate the problem. For example, densely planted belts may be established between highly erodible fields and transporting waterways, farming and crop management practices may be changed, or zoning may be modified to prevent a worsening of conditions.

These considerations, along with others relating to sediment carriage and deposition in downstream waterways, make estimates of sedimentation rates of interest here. Impoundment sediment computation methods discussed in this section will permit the planner to estimate annual impoundment sediment accumulation as well as short term accumulation (assuming constant hydraulic conditions). Application of the methods will permit the planner to estimate the amount of sediment removed from transport in a river system due to water passage through any number of impoundments.

### 5.3.2 Annual Sediment Accumulation

Three different techniques are used to estimate annual sediment accumulation: available data, sediment rating curves, and a three step procedure to determine short-term sedimentation rates. As discussed under each technique, caution should be used in selecting one method or another. If data are not available, it may not be feasible to use one or more techniques. When drawing conclusions, the uncertainty in the results should be considered in drawing conclusions based on whichever analysis that is selected. In addition, each technique has its own degree of uncertainty, which should be considered when drawing conclusions.

#### 5.3.2.1 Use of Available Data

Data provided in Appendix F permit estimation of annual sediment accumulation in acre-feet for a large number of impoundments in the U.S. The data and other materials presented provide some basic impoundment statistics useful to the planner in addition to annual sediment accumulation rates.

To use Appendix F, first determine which impoundments within the study area are of interest in terms of annual sediment accumulation. Refer to the U.S. map included in the appendix and find the index numbers of the region within which the impoundment is located. The data tabulation in the appendix, total annual sediment accumulation in acre feet, is given by multiplying average annual sediment accumulation in acre feet per square mile of net drainage area ("Annual Sediment Accum.") by the net drainage area ("Area") in square miles:

$$\text{Total Accumulation} = \text{Annual Sediment Accum.} \times \text{Area} \quad (V-2)$$

To convert to average annual loss of capacity expressed as a percent, divide total annual accumulation by storage capacity (from Appendix F), and multiply by 100. Note that this approach and those presented later do not account for packing of the sediment under its own weight. This results in an overestimate in loss of capacity. Note also that other data in Appendix F may be of interest in terms of drainage area estimates for determining river sediment loading and assessment of storm water sediment transport on an annual basis.

#### 5.3.2.2 Trap Efficiency and the Ratio of Capacity to Inflow

Where data are not available in Appendix F for a specific impoundment, the following method will permit estimation of annual or short-term sediment accumulation rates. The method is only useful, however, for normal ponded reservoirs.

To use this approach, a suspended sediment rating curve should be obtained for tributaries to the impoundment. An example of a sediment rating curve is provided in Figure V-6.

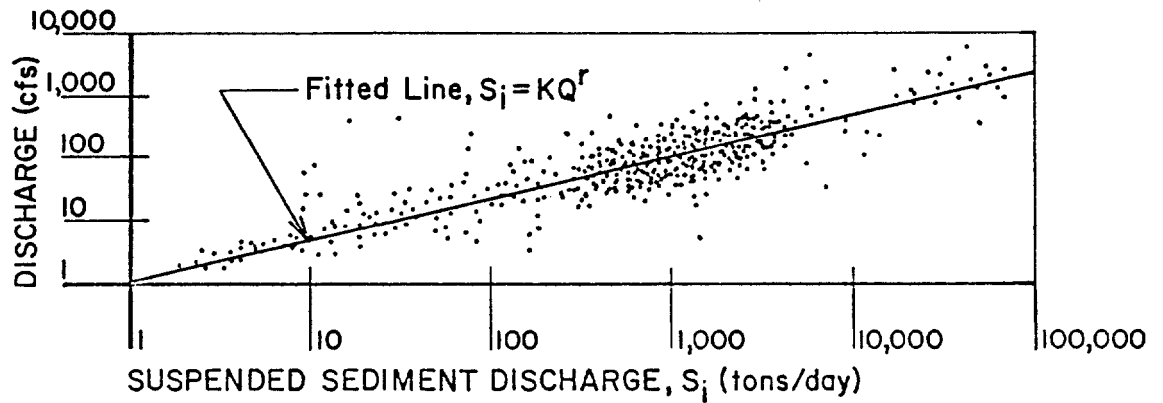


FIGURE V-6 SEDIMENT RATING CURVE SHOWING SUSPENDED SEDIMENT DISCHARGE AS A FUNCTION OF FLOW (AFTER LINSLEY, KOHLER, AND PAULHUS, 1958)

On the basis of such a curve, one can estimate the mean sediment mass transport rate ( $S_i$ ) in mass per unit time for tributaries. If neither rating curve nor data are available, one may estimate sediment transport rates on a basis of data from nearby channels, compensating for differences by using mean velocities. To a first approximation, it would be expected that:

$$S_i \approx S_j \left( \frac{V_i}{V_j} \right)^2 \quad (V-3)$$

where

$S_i$  = sediment transport rate to be determined in tributary "i" in mass per unit time

$S_j$  = known transport rate for comparable tributary (j) in same units as  $S_i$

$V_i$  = mean velocity for tributary i over the time period

$V_j$  = mean velocity in tributary j over the same time period as  $V_i$ .

Once average transport rates over the time period of interest have been determined, the proportion, and accordingly the weight of sediment settling out in the impoundment may be estimated. Figure V-7 is a graph showing the relationship between percent of sediment trapped in an impoundment versus the ratio of capacity to inflow rate. The implicit relationship is:

$$P = f(V/Q_i) \quad (v-4)$$

where

P = percent of inflowing sediment trapped

v = capacity of the impoundment in acre-feet

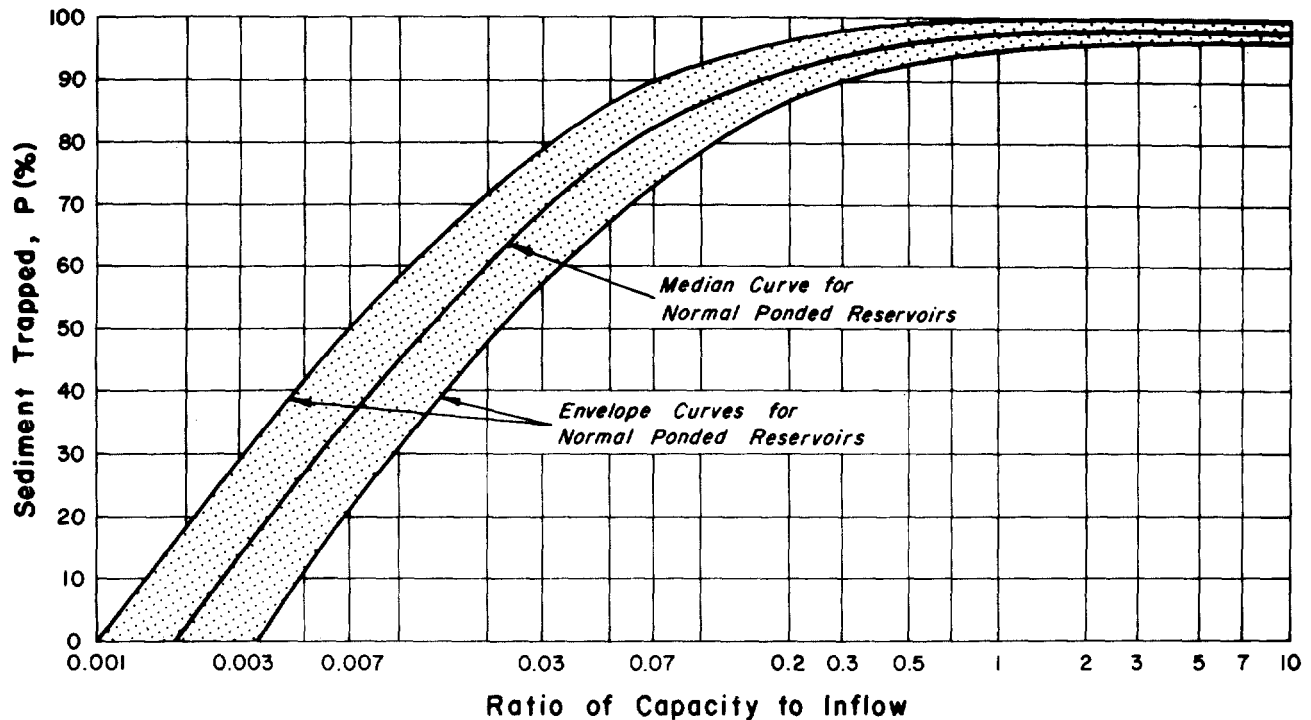


FIGURE V-7 RELATIONSHIP BETWEEN THE PERCENTAGE OF INFLOW-TRANSPORTED SEDIMENT RETAINED WITHIN AN IMPOUNDMENT AND RATIO OF CAPACITY TO INFLOW (LINSLEY, KOHLER, AND PAULHUS, 1958)

$Q_i$  = water inflow rate in acre-feet per year.

Data used for development of the curves in Figure V-7 included 41 impoundments of various sizes throughout the U.S. (Linsley, Kohler, and Paulhus, 1958).

To estimate the amount of suspended sediment trapped within an impoundment using this method, the capacity of the impoundment in acre-feet must first be determined. Next, average annual inflow, or better, average flow for the time period of interest is estimated.

Then:

$$S_t = S_j P \quad (V-5)$$

where

$S_t$  = weight of sediment trapped per time period  $t$

$P$  = trap efficiency (expressed as a decimal) from Figure V-7.

A word of caution is in order here. The above described techniques for evaluating sediment deposition in impoundments are capable of providing reasonable estimates, but only where substantial periods of time are involved - perhaps six months or longer. The methods may be used for shorter study periods, but results must then be taken only as very rough estimates, perhaps order-of-magnitude.

### 5.3.3 Short-Term Sedimentation Rates

The three-step procedure presented below provides a means to make short-term sediment accumulation rate estimates for storm-event analysis and to estimate amounts of different grain-size fractions passing through an impoundment. The steps are:

- Determine terminal fall velocities for the grain size distribution
- Estimate hydraulic residence time
- Compute trap (sedimentation) rate.

#### 5.3.3.1 Fall Velocity Computation

When a particle is released in standing water, it will remain roughly stationary if its density equals that of the water. If the two densities differ, however, the particle will begin to rise or fall relative to the water. It will then tend to accelerate until the drag force imposed by the water exactly counterbalances the force accelerating the particle. Beyond this point, velocity is essentially constant, and the particle has reached terminal velocity. For spheres of specific gravity greater than 1, Stokes' law expresses the relationship between fall velocity (terminal velocity) and several other physical parameters of water and the particles:

$$V_{\max} = \frac{g}{18\mu}(\rho_p - \rho_w)d^2 = \frac{1}{18\mu}(D_p - D_w)d^2 \quad (V-6)$$

where

- $V_{\max}$  = terminal velocity of the spherical particle (ft sec<sup>-1</sup>)
- $g$  = acceleration due to gravity (32.2 ft sec<sup>-2</sup>)
- $\rho_p$  = mass density of the particle (slugs ft<sup>-3</sup>)
- $\rho_w$  = mass density of water (slugs ft<sup>-3</sup>)
- $d$  = particle diameter (ft)
- $\mu$  = absolute viscosity of the water (lb sec ft<sup>-2</sup>)
- $D_p$  = weight density of particle (lb ft<sup>-3</sup>)
- $D_w$  = weight density of water (lb ft<sup>-3</sup>).

Stokes' law is satisfactory for Reynolds numbers between  $1 \times 10^{-4}$  and 0.5 (Camp, 1968). Reynolds number is given by:

$$R = \frac{vd}{\nu} \quad (V-7)$$

where

- $R$  = Reynolds number
- $v$  = particle velocity
- $\nu$  = kinematic viscosity of water.

Generally, for particles of diameter less than  $3 \times 10^{-2}$  inches (0.7 mm) this

criterion is met. For large particles, how far conditions deviate from this may be observed using the following approach (Camp, 1968). According to Newton's law for drag, drag force on a particle is given by:

$$F_d = CA\rho_w v^2/2 \quad (V-8)$$

where

$F_d$  = the drag force

$c$  = unitless drag coefficient

$A$  = projected area of the particle in the direction of motion.

Equating the drag force to the gravitational (driving) force for the special case of a spherical particle, velocity is given by:

$$v_{\max} = \sqrt{\frac{4g(\rho_p - \rho_w)d}{3C\rho_w}} \quad (V-9)$$

All variables in the expression for  $v_{\max}$  (Equation V-9) may be easily estimated except  $C$ , since  $C$  is dependent upon Reynolds number. According to Equation V-7, Reynolds number is a function of  $v$ . Thus a "trial and error" or iterative procedure would ordinarily be necessary to estimate  $C$ . However, a somewhat simpler approach is available to evaluate the drag coefficient and Reynolds number. First, estimate  $CR^2$  using the expression (Camp, 1968):

$$CR^2 = 4\rho_w(\rho_p - \rho_w)gd^3/3\mu^2 \quad (V-10)$$

Then, using the plot in Figure V-8, estimate  $R$  and then  $C$ . For  $R > 0.1$  use of Equation V-9 will give better estimates of  $v_{\max}$  than will Equation V-6.

Generally, one of the two approaches for spherical particles will give good estimates of particle fall velocity in an effectively laminar flow field (in impoundments). Occasionally, however, it may prove desirable to compensate for nonsphericity of particles. Figure V-9, which shows the effect of particle shape on the drag coefficient  $C$ , may be used to do this. Note that for  $R < 1$ , shape of particle does not materially affect  $C$ , and no correction is necessary.

A second problem in application of the Newton/Stokes approach described above is that it does not account for what is called hindrance. Hindrance occurs when the region of fluid surrounding a falling particle is disrupted (by the particle motion) and the velocity of other nearby particles is thereby decreased. Figure V-10 shows this effect schematically.

A very limited amount of research has been done to determine the effect of particle concentration on fall velocity (Camp, 1968). Some data have been collected

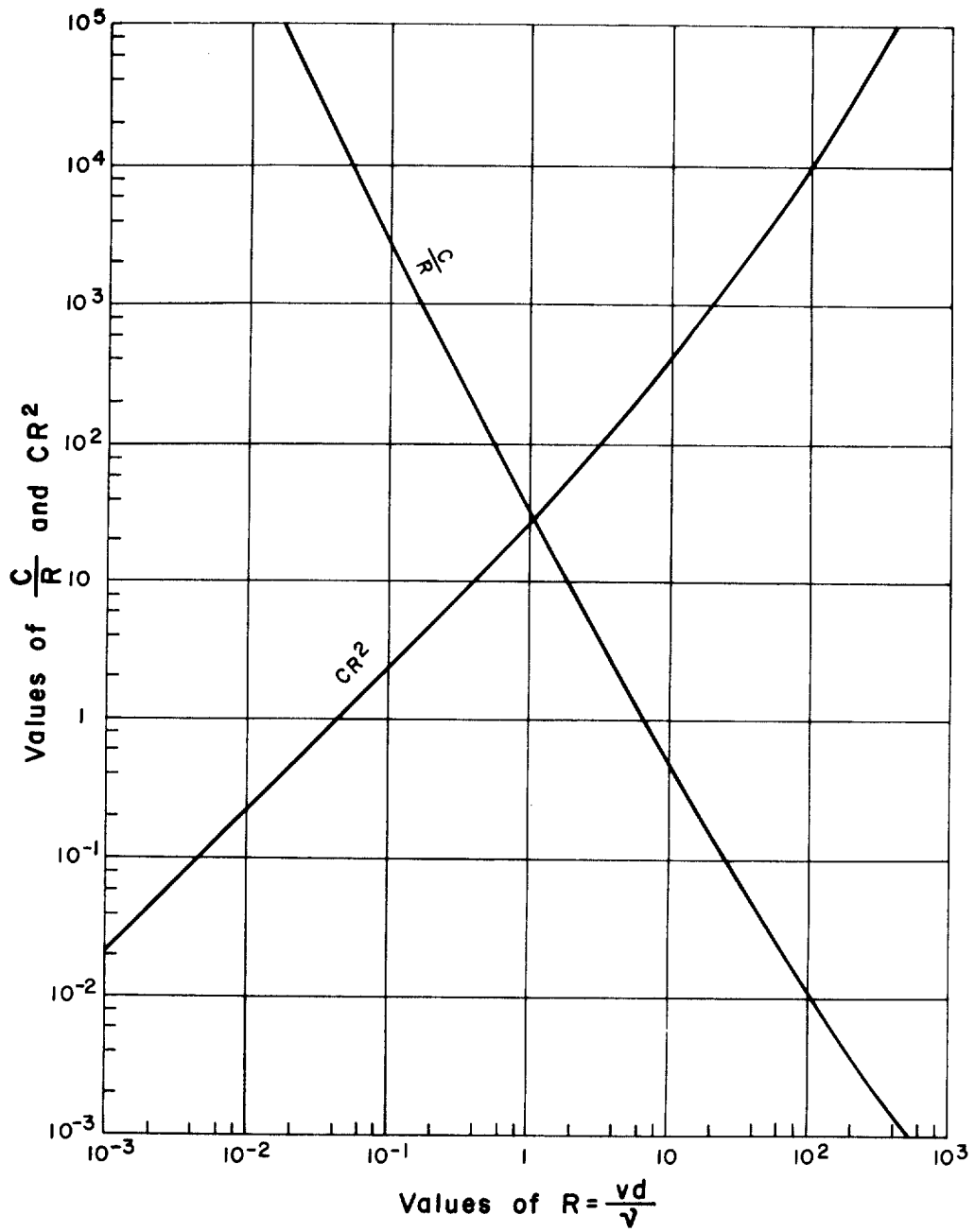


FIGURE V-8 PLOT OF  $C/R$  AND  $CR^2$  VERSUS  $R$  (CAMP, 1968)



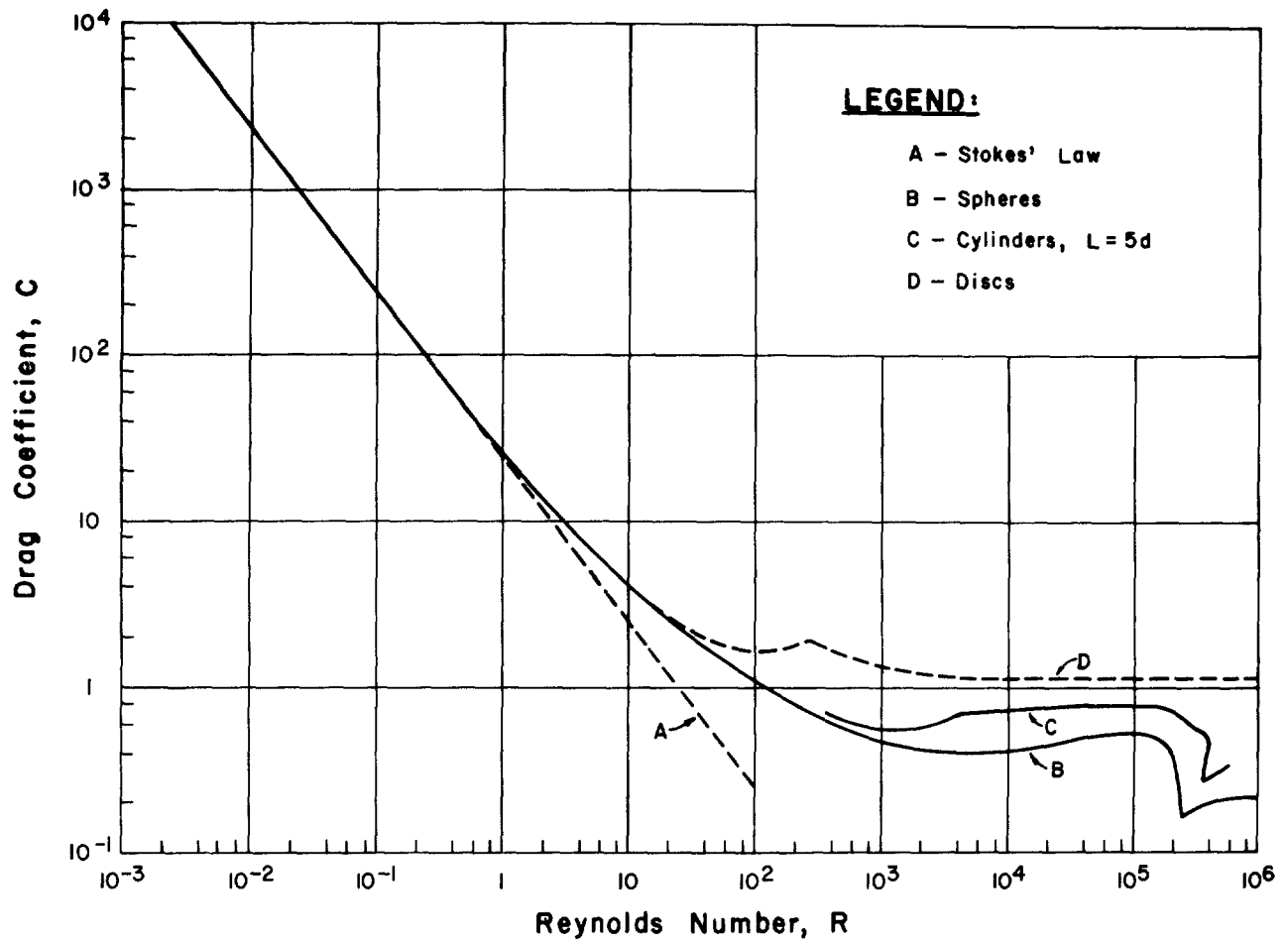


FIGURE V-9 DRAG COEFFICIENT (C) AS FUNCTION OF REYNOLD'S NUMBER (R) AND PARTICLE SHAPE (CAMP, 1968)

however, and Figure V-n is a plot of a velocity correction factor,  $v'/v$ , as a function of volumetric concentration. Volumetric concentration is given by:

$$C_{vol} = \frac{C_{wt} \rho_w}{\rho_p} \quad (V-11)$$

where

$C_{vol}$  = volumetric concentration

$C_{wt}$  = weight concentration.

As an approximation, the curve for sand may be used to correct  $v$  as a function of  $C_{vol}$ .

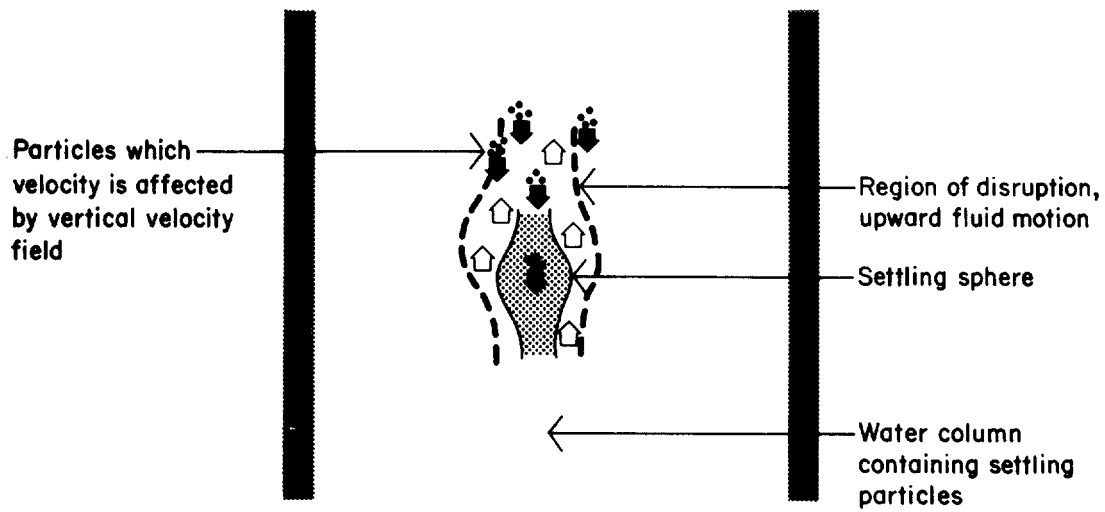


FIGURE V-10 SCHEMATIC REPRESENTATION OF HINDERED SETTLING OF PARTICLES IN FLUID COLUMN

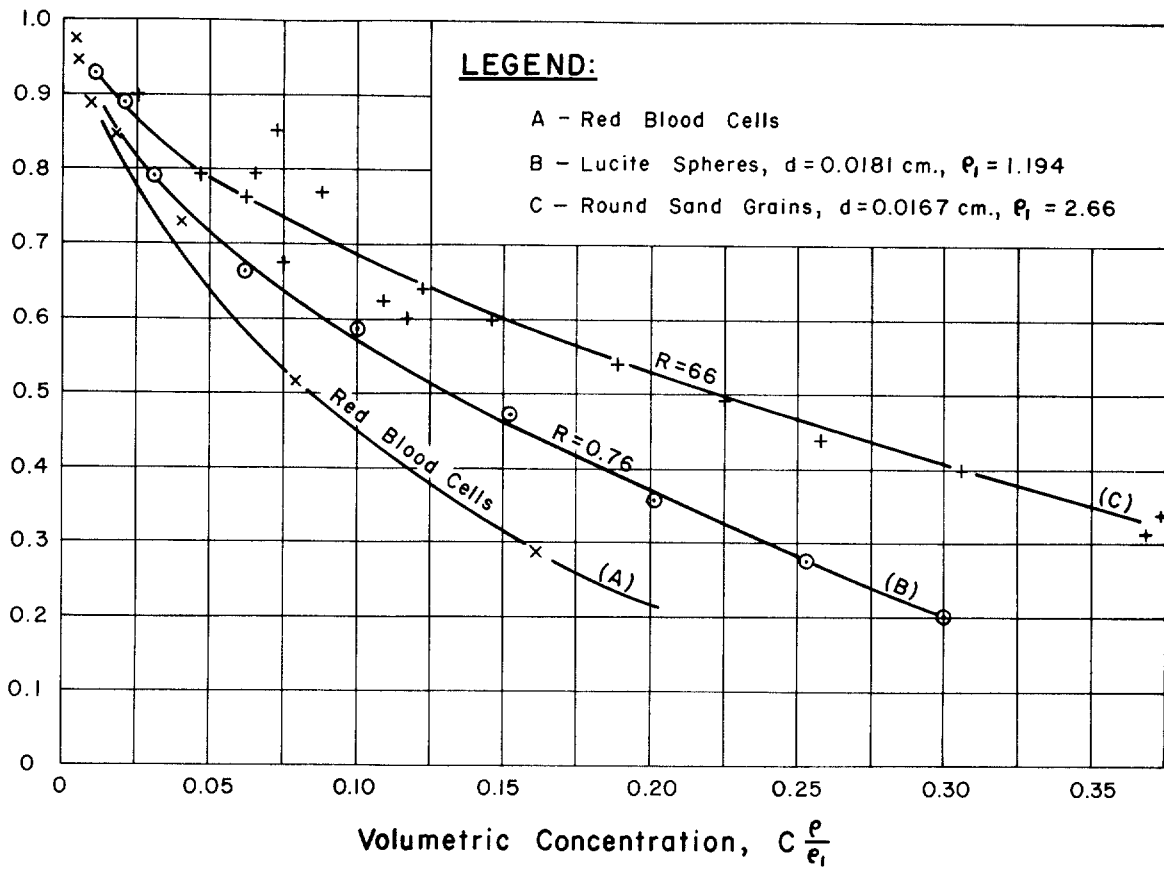


FIGURE V-11 VELOCITY CORRECTION FACTOR FOR HINDERED SETTLING (FROM CAMP, 1968)

EXAMPLE V-3

Settling Velocity

Assume that a swiftly moving tributary to a large reservoir receives a heavy loading of sediment which is mostly clay particles. The particles tend to clump somewhat and average diameters are on the order of 2 microns. The clumps have a specific gravity of 2.2. Applying Stokes' Law for 20°C water:

$$V_{\max} = \frac{g}{18\mu} (\rho_p - \rho_w) d^2$$
$$V_{\max} = \frac{32.2}{(18 \times 2.1 \times 10^{-5})} \times [(2.2 \times 62.4/32.2) - (62.4/32.2)] \times (6.56 \times 10^{-6})^2$$
$$= 8.53 \times 10^{-6} \text{ ft sec}^{-1} = .03 \text{ ft hr}^{-1}$$

Thus the particles of clay might be expected to fall about nine inches per day in the reservoir. It should be noted that for such a low settling rate, turbulence in the water can cause very significant errors. In fact, the estimate is useful only in still waters having a very uniform flow lacking substantial vertical components.

END OF EXAMPLE V-3

EXAMPLE V-4

Settling Velocity for a Sand and Clay

Suppose a river is transporting a substantial sediment load which is mainly sand and clay. The clay tends to clump to form particles of 10 micron diameter while the sand is of 0.2 mm diameter. The sand particles are very irregular in shape tending toward a somewhat flattened plate form. The specific gravity of the clay is about 1.8 while that of the sand is near 2.8. Given that the water temperature is about 5°C, the terminal velocity of the clay may be estimated as in Example V-3:

$$V_{\max} = \frac{g}{18\mu} (\rho_p - \rho_w) d^2$$
$$V_{\max} = \frac{32.2}{(18 \times 3.17 \times 10^{-5})} \times (0.8 \times 62.4 / 32.2) \times (3.28 \times 10^{-5})^2$$
$$= 9.4 \times 10^{-5} \text{ ft sec}^{-1}$$
$$= 8 \text{ ft day}^{-1}$$

For the sand, apply Equation V-10:

$$\begin{aligned}
 CR^2 &= 4\rho_w (\rho_p - \rho_w) gd^3/3u^2 \\
 &= 4 \times \frac{62.4}{32.2} \times \frac{1.8 \times 62.4}{32.2} \times \frac{32.2 \times (6.56 \times 10^{-4})^3}{3 \times (3.17 \times 10^{-5})^2} \\
 CR^2 &= 82
 \end{aligned}$$

Referring to Figure V-8, a value of  $CR^2$  equal to 82 represents  $R \cong 2.8$  and  $C \cong 10.3$ . From Figure V-9, the corrected drag coefficient for discs is close to 10.3 (no correction really necessary). Then, using Equation V-9 as an approximation:

$$v_{\max} = \sqrt{\frac{49 (\rho_p - \rho_w) d}{3C\rho_w}}$$

$$v_{\max} = \sqrt{\frac{4 \times 32.2 \times (1.8 \times 62.4 / 32.2) \times 6.56 \times 10^{-4}}{10.3 \times 62.4 / 32.2}}$$

$$v_{\max} = 0.07 \text{ ft sec}^{-1} = 252 \text{ ft hr}^{-1}$$

Thus the clay will settle about 8 feet per day while the sand will settle about 6,048 feet per day (252 feet per hour).

----- END OF EXAMPLE V-4 -----

#### 5.3.4 Impoundment Hydraulic Residence Time

Once settling velocities have been estimated for selected grain sizes, the final preparatory step in estimating sediment deposition rates is to compute hydraulic residence time.

Hydraulic residence time represents the mean time a particle of water resides within an impoundment. It is not, as is sometimes thought, the time required to displace all water in the impoundment with new. In some impoundments, inflowing water may be conceptualized as moving in a vertical plane from inflow to discharge. This is called plug flow. In long, narrow, shallow impoundments with high inflow velocities, this is often a good assumption. As discussed later, however, adoption of this model leads to another problem, namely, is water within the plug uniform or does sediment concentration vary over depth within the plug?

A second model assumes that water flowing into an impoundment instantaneously mixes laterally with the entire receiving layer. The layer may or may not represent the entire impoundment depth. This simplification is often a good one in large surfaced, exposed impoundments having many small inflows.

Regardless of the model assumed for the process by which water traverses an impoundment from inflow to discharge, hydraulic residence time is computed

as in Equation V-1. That is:

$$\tau_w = V/Q$$

The only important qualification is that to be meaningful,  $V$  must be computed taking account of stagnant areas, whether these are regions of the impoundment isolated from the main flow by a sand spit or promontory, or whether they are isolated by a density gradient, as in the thermocline and hypolimnion. Ignoring stagnant areas may result in a very substantial overestimate of  $\tau_w$ , and in sediment trap computations, an overestimate in trap efficiency. Actually  $\tau_w$  computed in this way is an adjusted hydraulic residence time. All references to hydraulic residence time in the remainder of Section 5.3 refer to **adjusted  $\tau_w$** .

Hydraulic residence time is directly influenced by such physical variables as impoundment depth, shape, side slope, and shoaling, as well as hydraulic characteristics such as degree of mixing, stratification, and flow velocity distributions. The concepts involved in evaluating many of these factors are elementary. The evaluation itself is complicated, however, by irregularities in impoundment shape and data inadequacies. Commonly, an impoundment cannot be represented well by a simple 3-dimensional figure, and shoaling and other factors may restrict flow to a laterally narrow swath through the water body.

In most cases, hydraulic residence time may be estimated, although it is clear that certain circumstances tend to make the computation error-prone. The first step in the estimation process is to obtain impoundment inflow, discharge, and thermal regime data as well as topographic/bathymetric maps of the system. Since a number of configuration types are possible, the methods are perhaps best explained using examples.

#### EXAMPLE V-5

##### Hydraulic Residence Time in Unstratified Impoundments

The first step in estimating hydraulic residence time for purposes of sedimentation analysis is to determine whether there are significant stagnant areas. These would include not only regions cut off from the main flow through the body, but also layers isolated by dense strata. Consequently, it must be determined whether or not the impoundment stratifies. Consider Upper Lake located on the Carmans River, Long Island, New York. The lake and surrounding region are shown in Figure V-12, and hypothetical geometry data are presented in Table V-6. Based upon Upper Lake's shallowness, its long, narrow geometry, and high tributary inflows, it is safe to assume that Upper Lake is normally unstratified. Also, because of turbulence likely at the high flows, one can assume that the small sac northeast of the discharge is not stagnant and that Upper Lake represents a slow

TABLE V-6  
 HYPOTHETICAL PHYSICAL CHARACTERISTICS AND  
 COMPUTATIONS FOR UPPER LAKE, BROOKHAVEN, SUFFOLK COUNTY, NEW YORK

Distance Downstream from Inflow Miles (feet)	D Average Depth ft.	w Average Width ft.	CSA Cross-sectional Area, D x W ft <sup>2</sup>
0.05 (264)	3	63	189
0.10 (528)	4	110	440
0.15 (792)	6	236	1,416
0.20 (1,056)	7	315	2,205
0.25 (1,320)	7	340	2,380
0.30 (1,584)	8	315	2,520
0.35 (1,848)	7	550	3,850
0.40 (2,112)	8	550	4,400
0.45 (2,376)	7	354	2,478
0.50 (2,640)	10	350	3,500
			mean 2,338

Total length = 0.5mi. (2,640 ft.)

Inflow from upstream = 380 cfs  
 Outflow to downstream = 380 cfs } (steady-state)

Computation

Volume (Vol) = Total length x mean cross-sectional area  
 = 2,640 ft. X 2,338 ft<sup>2</sup> = 6.17 X 10<sup>6</sup> ft<sup>3</sup>

Residence time ( $\tau_w$ ) = Vol / flow  
 = 6.17 x 10<sup>6</sup> ft<sup>3</sup> / (380 ft<sup>3</sup>/sec) = 1.62 x 10<sup>4</sup> sec (4.5 hr)

Velocity (Vel) = length/ $\tau_w$   
 = 2,640 ft / 1.62 x 10<sup>4</sup> sec = .163 ft/sec

moving river reach. With these assumption-s, the computation of hydraulic residence time is as shown in Table V-6.

Also shown in Figure V-12 is Lower Lake. According to the hypothetical data presented in Table V-7, Lower Lake is much deeper than Upper Lake. Its volume is significantly greater also, but the inflow rate is similar. In this case, particularly during the summer, it should be determined if the lake stratifies. For this example, however, we will assume that the time of the year makes stratifica-

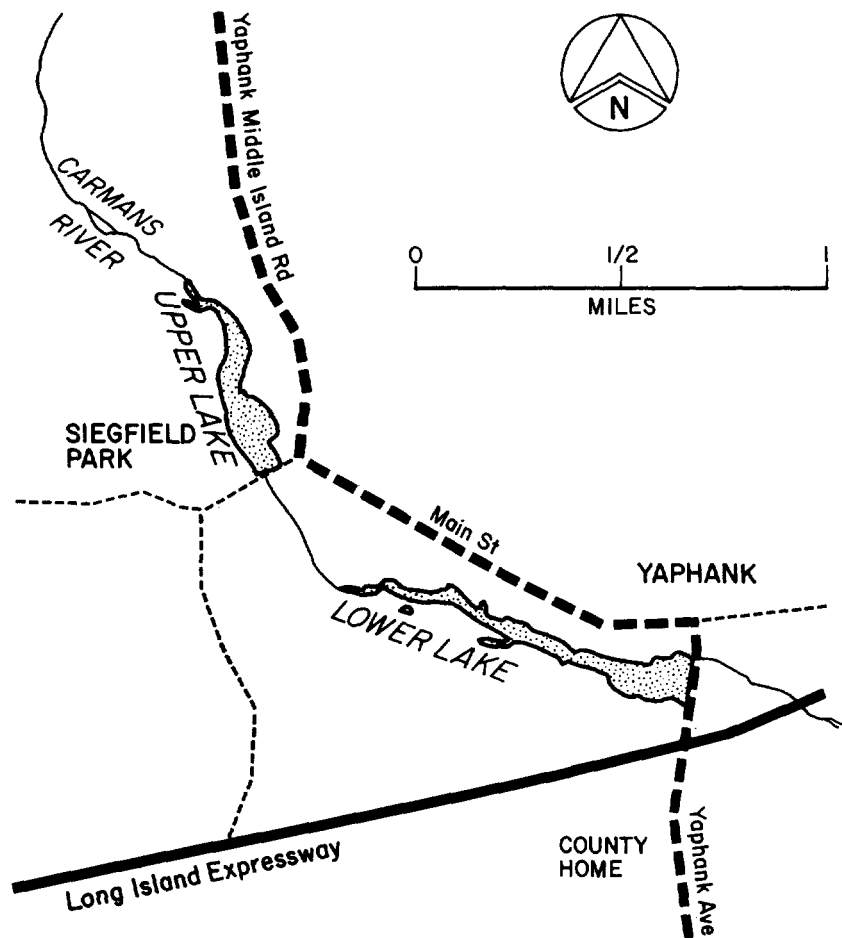


FIGURE V-12 UPPER AND LOWER LAKES AND ENVIRONS,  
LONG ISLAND, NEW YORK

tion very unlikely, and that Lower Lake is a slow moving river reach. We then compute hydraulic residence time as shown in Table V-7. Figure V-13, in particular diagram 1, shows what these assumptions mean in terms of a flow pattern for both lakes.

TABLE V-7  
 HYPOTHETICAL PHYSICAL CHARACTERISTICS AND  
 COMPUTATIONS FOR LOWER LAKE, BROOKHAVEN, SUFFOLK COUNTY, NEW YORK

Distance Downstream from Inflow Miles (feet)	D Average Depth ft.	w Average Width ft.	CSA Cross-sectional Area, D x W ft <sup>2</sup>
0.075 ( 396)	15	157	2,355
0.150 ( 792)	20	165	3,300
0.225 (1,188)	20	173	3,460
0.300 (1,584)	25	197	4,925
0.375 (1,980)	35	197	6,895
0.450 (2,376)	30	228	6,840
0.525 (2,772)	35	232	8,120
0.600 (3,168)	35	197	6,895
0.675 (3,564)	<b>40</b>	220	8,800
0.750 (3,960)	<b>42</b>	315	13,230
0.825 (4,356)	41	433	17,753
0.900 (4,752)	51	591	30,141
0.975 (5,148)	42	551	23,142
1.050 (5,544)	40	433	17,320
1.125 (5,940)	37	323	11,951
			mean 11,008

Total length = 1.125 mi (5,940 ft.)

Inflow from upstream 400 cfs }  
 Outflow to downstream 390 cfs } (surface rising)  
 Average flow = 395 cfs

Computation

Volume (Vol) = Total length x mean cross-sectional area  
 = 5,940 ft. X 11,008 ft<sup>2</sup> = 6.54 X 10<sup>7</sup> ft<sup>3</sup>

Residence Time ( $\tau_w$ ) = vol / flow  
 = 6.54 x 10<sup>7</sup> / (395 ft<sup>3</sup>/sec) = 1.65 x 10<sup>5</sup> sec (46 hr)

Velocity (Vel) = length /  $\tau_w$   
 = 5,940 ft / 1.65 x 10<sup>5</sup> sec = .036 ft/sec



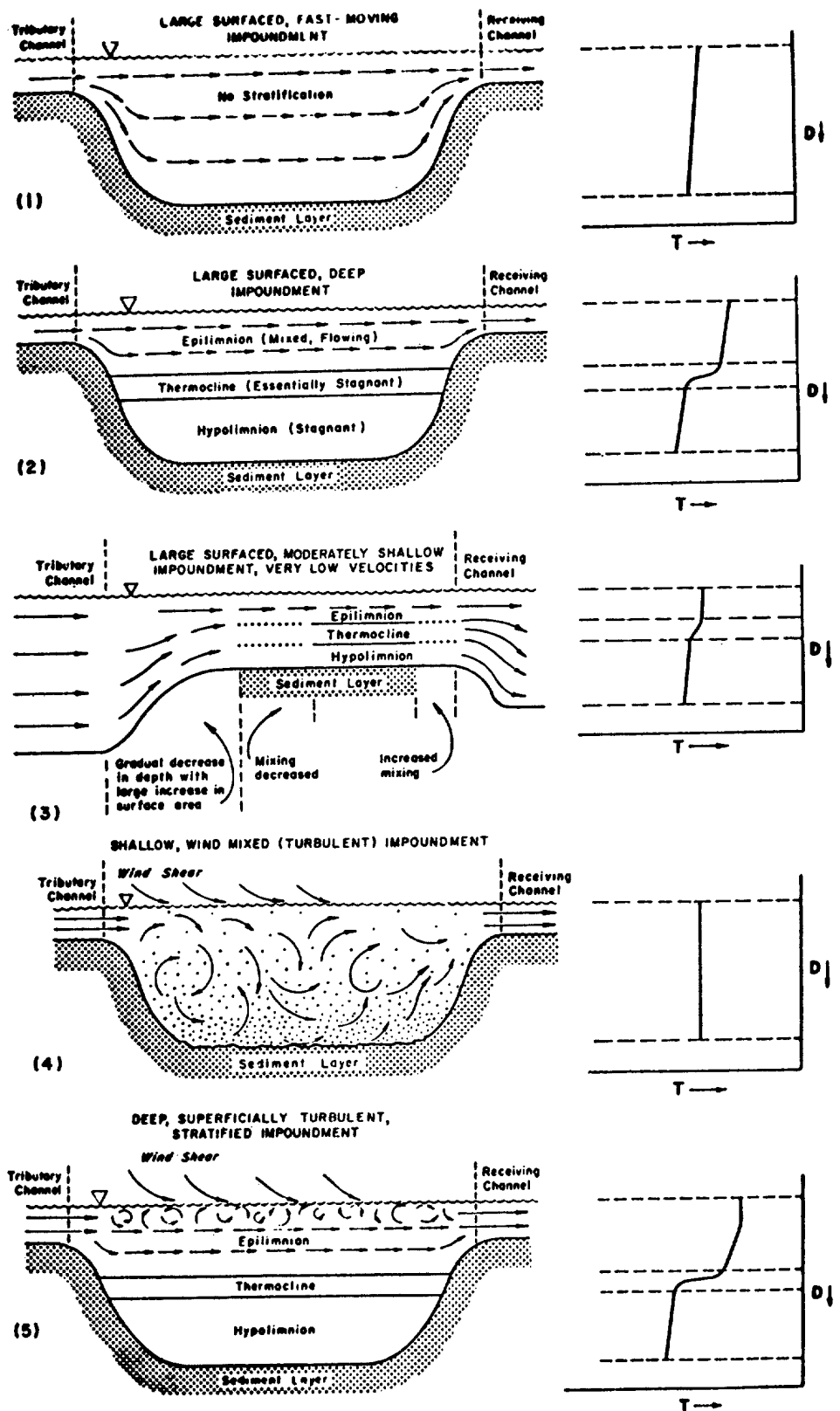


FIGURE V-13 IMPOUNDMENT CONFIGURATIONS AFFECTING SEDIMENTATION

END OF EXAMPLE V-5

#### EXAMPLE V-6

Assume for this example that Lower Lake is stratified during the period of interest. This significantly changes the computation of residence time. To a first approximation, one can merely revise the effective depth of the impoundment to be from the surface to the upper limit of the thermocline rather than to the bottom. Figure V-13 shows schematically what this simple model suggests for Lower Lake as a stratified impoundment (diagram 2 or possibly 3). The figure also shows wind-driven shallow, and deep impoundments. To the right of each diagram is a plot of the temperature profile over depth. Actually, the profile could represent a salinity gradient as well as a thermal gradient.

Table V-8 shows the procedure to estimate travel time for stratified Lower Lake. The upper boundary of the thermocline is assumed to be at a depth of 10 feet. For all later computations of sediment accumulation, this same 10 foot depth would be adopted. Such an assumption is valid presuming that the thermocline and hypolimnion are relatively quiescent. Thus once a particle enters the thermocline it can only settle, and cannot leave the impoundment.

END OF EXAMPLE V-6

#### EXAMPLE V-7

##### Large, Irregular Surface Impoundment

Figure V-14 shows Kellis Pond and surrounding topography. This small pond is located near Bridgehampton, New York and has a surface area of about 36 acres. From the surface shape of the pond, it is clear that it cannot be considered as a stream reach.

Figure V-15 shows a set of hypothetical depth profiles for the pond. From the profiles, it is evident that considerable shoaling has resulted in the formation of a relatively well defined flow channel through the pond. Peripheral stagnant areas have also formed. Hypothetical velocity vectors for the pond are presented in Figure V-16. Based upon them, it is reasonable to consider the pond as being essentially the hatched area in Figure V-15. To estimate travel times, the hatched area may be handled in the same way as for the Upper Lake example presented above. It should be noted, however, that this approach will almost certainly result in underestimation of sediment deposition in later computations. This is true for two reasons. First, estimated travel time will be smaller than the true value since impoundment volume is underestimated. Second, since the approach ignores the low flow velocities to

TABLE V-8

HYPOTHETICAL PHYSICAL CHARACTERISTICS AND  
COMPUTATIONS FOR LOWER LAKE, BROOKHAVEN, SUFFOLK COUNTY, NEW YORK  
(ASSUMING AN EPI LIMNION DEPTH OF 10 FEET)

Distance Downstream from Inflow Miles (feet)	D Average Depth ft.	W Average Width ft.	CSA Cross-sectional Area ft <sup>2</sup> D x W
0.075	10	160	1,600
0.150	10	170	1,700
0.225	10	175	1,750
0.300	10	200	2,000
0.375	10	198	1,980
0.450	10	230	2,300
0.525	10	233	2,330
0.600	10	200	2,000
0.675	10	222	2,220
0.750	10	316	3,160
0.825	10	435	4,350
0.900	10	590	5,900
0.975	10	552	5,520
1.050	10	435	4,350
1.125	10	325	3,250

Total length = 1.125 mi (5,940 ft.)

mean CSA = 2,961 ft<sup>2</sup>

Inflow from upstream 397cfs  
Outflow to downstream 393cfs

(steady-state surface, difference  
due to loss to water table)

Average flow = 395 cfs

Computation

Volume (Vol) = Total length x mean cross-sectional area  
= 5,940 ft. X 2,961 ft<sup>2</sup> = 1.76 X 10<sup>7</sup>

Residence Time ( $\tau_w$ ) = Vol / flow  
= 1.76 x 10<sup>7</sup> / (395 ft<sup>3</sup>/sec) = 4.46 x 10<sup>4</sup> sec (12.3hr)

Velocity (Vel) = length/ $\tau_w$   
= 5,940 ft / 4.46 x 10<sup>4</sup> sec = 0.133 ft/sec

# SOUTHAMPTON

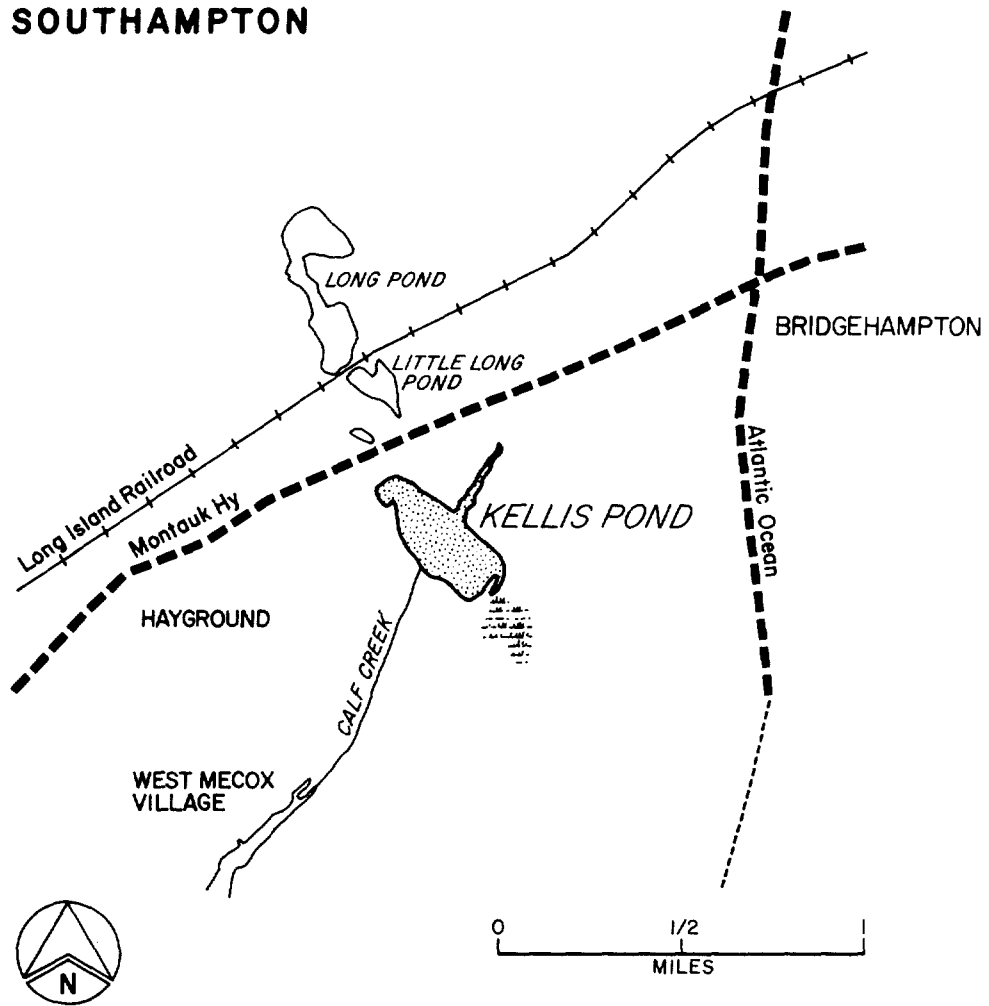


FIGURE V-14 KELLIS POND AND SURROUNDING REGION, LONG ISLAND, NEW YORK

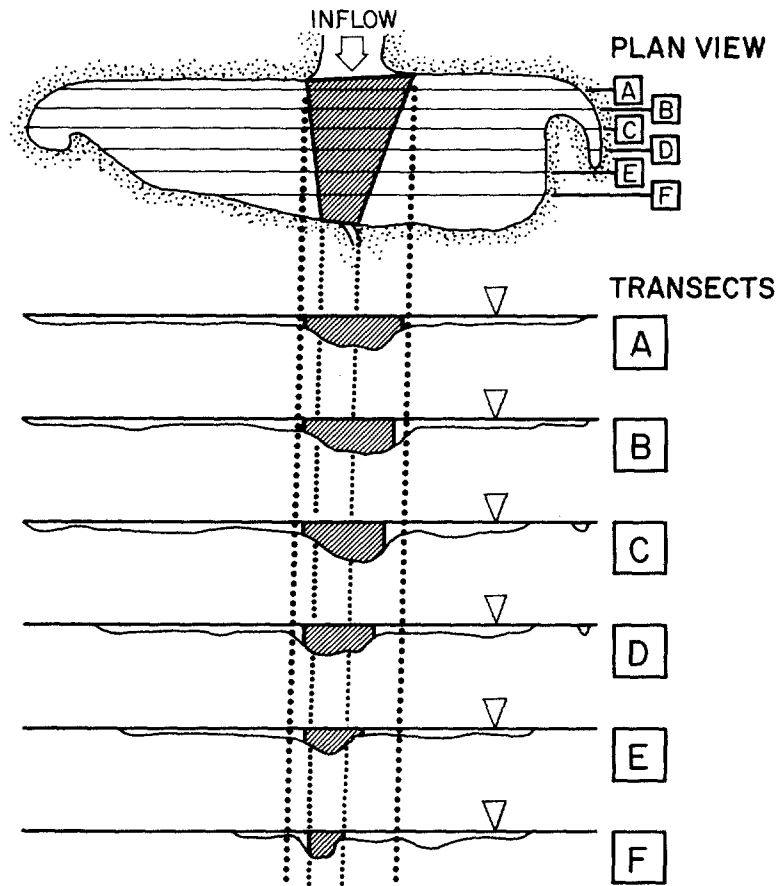


FIGURE V-15 HYPOTHETICAL DEPTH PROFILES FOR KELLIS POND

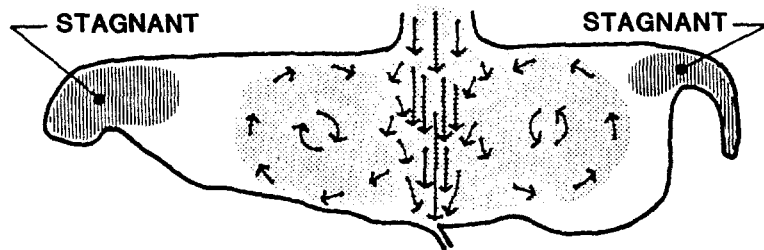


FIGURE V-16 HYPOTHETICAL FLOW PATTERN IN KELLIS POND

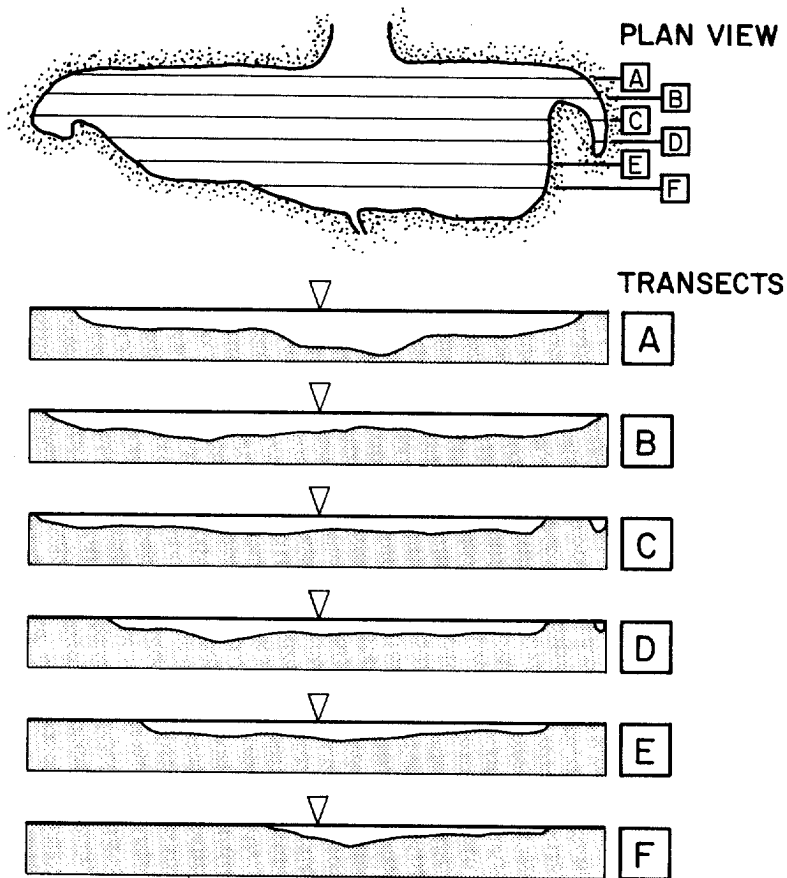


FIGURE V-17 HYPOTHETICAL DEPTH PROFILES FOR KELLIS POND  
NOT SHOWING SIGNIFICANT SHOALING

either side of the central channel and nonuniform velocities within it, heavier sedimentation than computed is likely.

Still more difficult to evaluate is the situation where shoaling and scour have not resulted in formation of a distinct central channel. Figure V-17 shows hypothetical depth profiles for Kellis Pond for such a case.

Here, velocity distribution data should be obtained, particularly if the impoundment is of much importance. If such data are not available but it is deemed worthwhile to do field studies, methods available for evaluating flow patterns include dye tracing and drogue floats. A simple but adequate method (at least to evaluate the surface velocity distribution) is to pour a large number of citrus fruits (oranges, grapefruit) which float just below the surface, into the impoundment, and to monitor both their paths and velocities. Although it is true that surface velocities may be greater than the velocity averaged over depth, this

will permit estimation of hydraulic residence time directly or generation of data to use in the prescribed method. In the latter case, the data might be used to define the major flow path through an impoundment of a form like Kellis Pond.

----- END OF EXAMPLE V-7 -----

----- EXAMPLE V-8 -----

Complex Geometries

The final hydraulic residence time example shows the degree of complexity that sediment deposition problems may entail. Although it is possible to make rough estimates of sediment accumulation, it is recommended that for such impoundments more rigorous methods be used - mathematical modeling and/or detailed field investigations.

Figure V-18 shows Lake Owyhee in eastern Oregon. This impoundment is well outside the range of complexity of water bodies which can be evaluated using these calculation methods. Because of geometry, the number of tributaries, and size, it is not feasible to conceptually reduce the impoundment in such a way as to estimate travel times. Flow patterns are likely to be very complex, and sediment deposition is difficult to predict both in terms of quantity and location.

In contrast, Figure V-19 shows New Millpond near Islip, New York and surrounding features. Although this water body does not have a simple surface geometry, it can be reduced to three relatively simple components as shown in the figure. Bearing in mind the limitations imposed by wind mixing, stratification, and the presence of stagnant regions described in earlier examples, deposition might nevertheless be estimated in arms A, B, and C. Because of the difficulty of predicting velocities and turbulence in section D, estimates of sedimentation cannot be reliably made there. However, it is likely that much of inflowing sediments will have settled out by the time water flows through the arms and into section D.

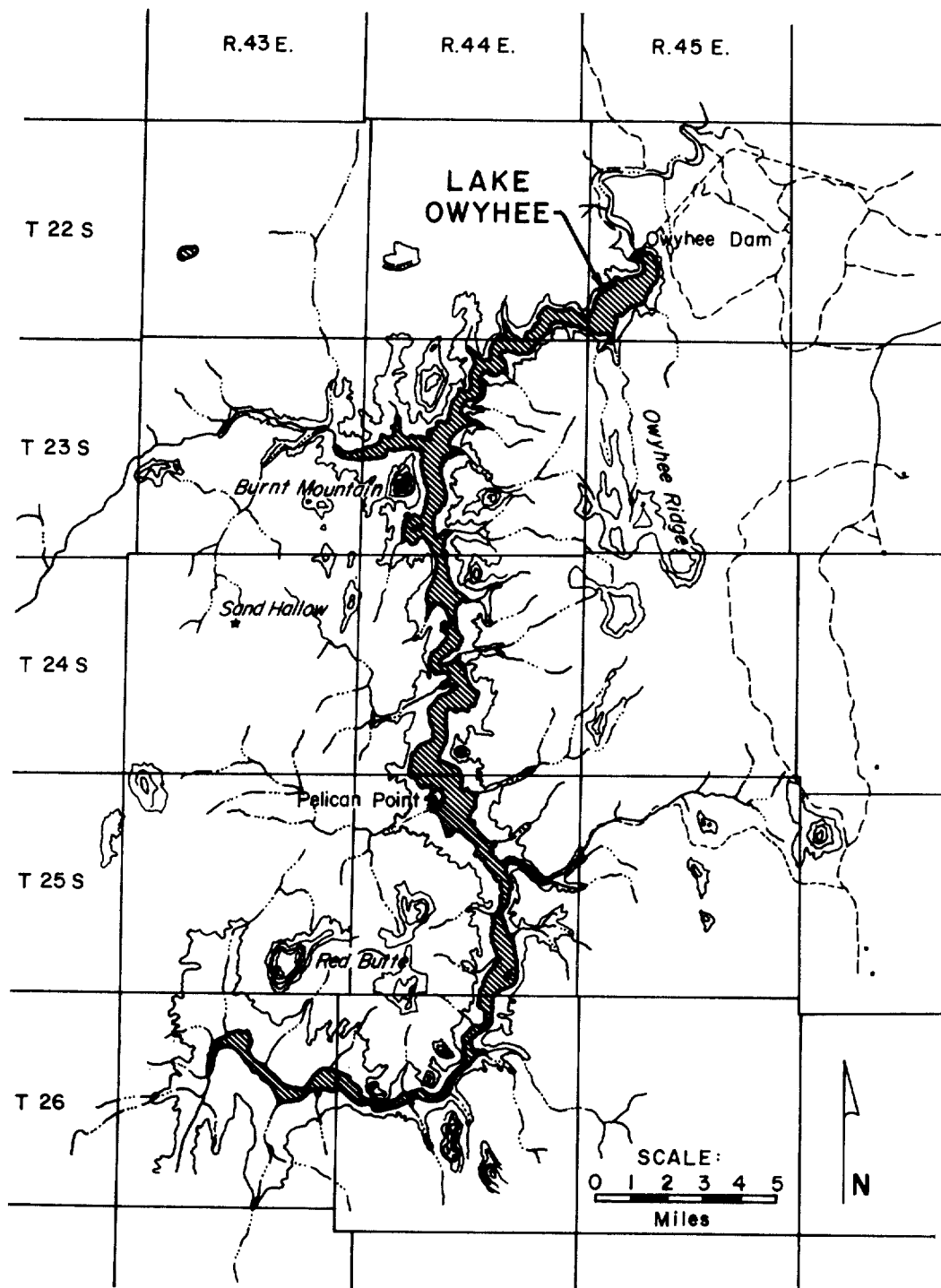


FIGURE V-18 LAKE OWYHEE AND ENVIRONS



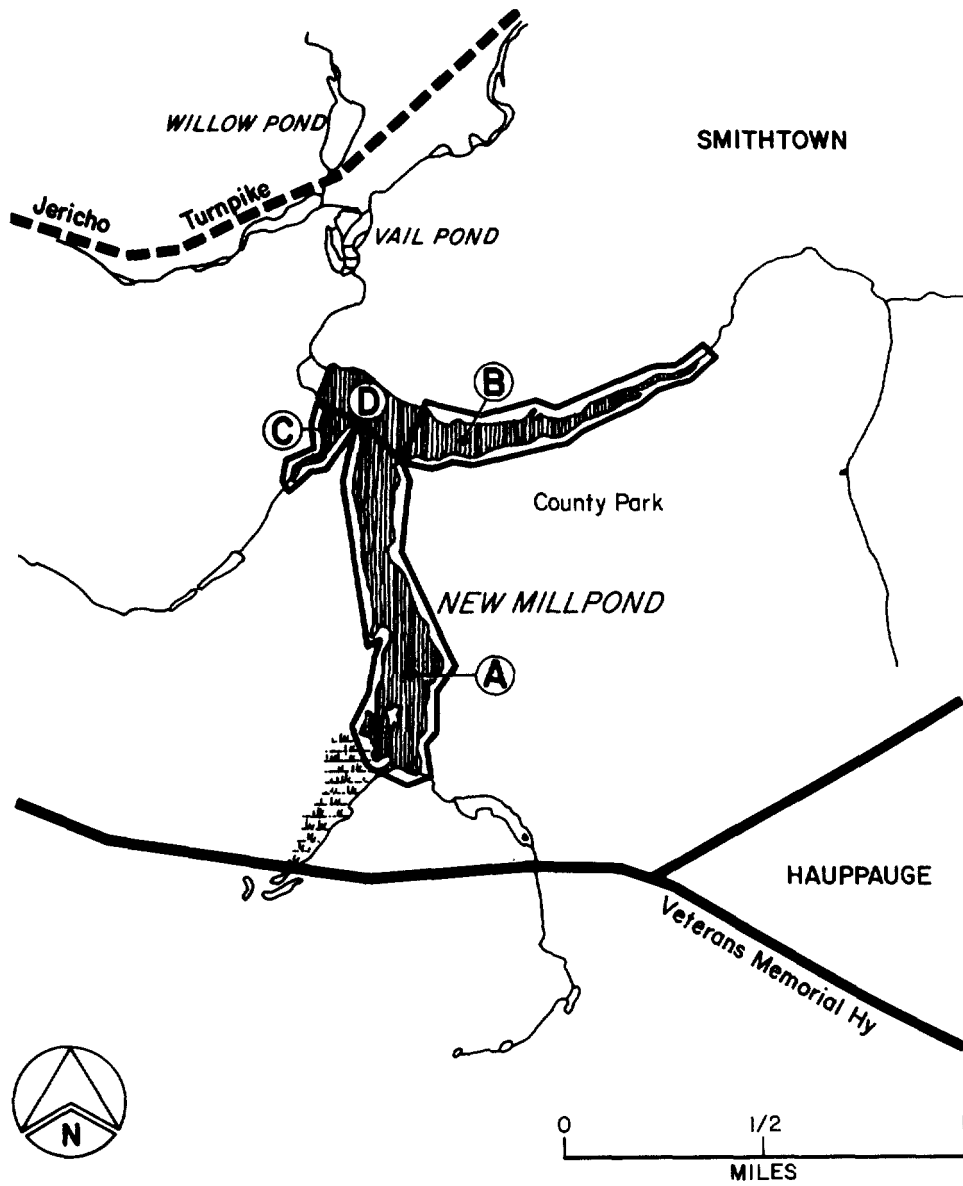


FIGURE V-19 NEW MILLPOND AND ENVIRONS. NEW MILLPOND IS SUBDIVIDED FOR PURPOSES OF ESTIMATING SEDIMENTATION IN REGIONS A, B, AND C.

END OF EXAMPLE V-8

### 5.3.5 Estimation of Sediment Accumulation

Estimation of quantities of sediment retained in an impoundment follows directly from the computations of settling velocity and travel time, although the computation depends upon whether the adopted model is plug flow, or a fully mixed layer or impoundment.

In the case of plug flow, one of two subordinate assumptions is made: that the plug is fully mixed as in turbulent flow, or that it moves in a "laminar" flow through the impoundment. In terms of sediment accumulation estimates, the fully mixed plug assumption is handled in the same way as the fully mixed impoundment model. Thus we have two kinds of computations:

- Case A ● Plug flow with the plug not mixed vertically.
- Case B { ● Plug flow assuming a vertically mixed plug  
● A fully mixed impoundment or stratum.

Equation V-12 is pertinent to both cases A and B. It defines the mass of sediment trapped as a function of trap efficiency and inflowing sediment mass. Equation V-13 should be used for case A, and Equation V-14 for case B:

$$S_t = S_i P \quad (V-12)$$

$$P = \left( \frac{\tau_w v}{D'} + D'' - D \right) / D'' \quad (V-13)$$

$$P = \frac{v \tau_w}{D'} \quad (V-14)$$

where

- P = mean proportion of  $S_i$  trapped ( $1 \geq P \geq 0$ )  
 $S_t$  = mass of sediment trapped per unit time  
 $S_i$  = mass of sediment in inflows per unit time  
v = particle settling velocity  
D = discharge channel depth  
D' = flowing layer depth  
D'' = inflow channel depth.

Figure V-20 shows the significance of the various depth measures D, D', D'', and the assumed sedimentation pattern. In case B, in the absence of substantial erratic turbulence and unpredicted vertical velocity components, and within the constraints of available data, it is clear that this approach can give reasonable estimates of trap efficiencies. In case A, however, small changes in D or D'' can strongly affect trap efficiencies. It is important to remember in applying case A that P is a mean, preferably used over a period of time. It is also important to recognize that conditions within an impoundment leading to selection of case A or B are subject to change, thus affecting estimates.

For convenience, Figure V-21 is included to provide estimates of  $V_{max}$

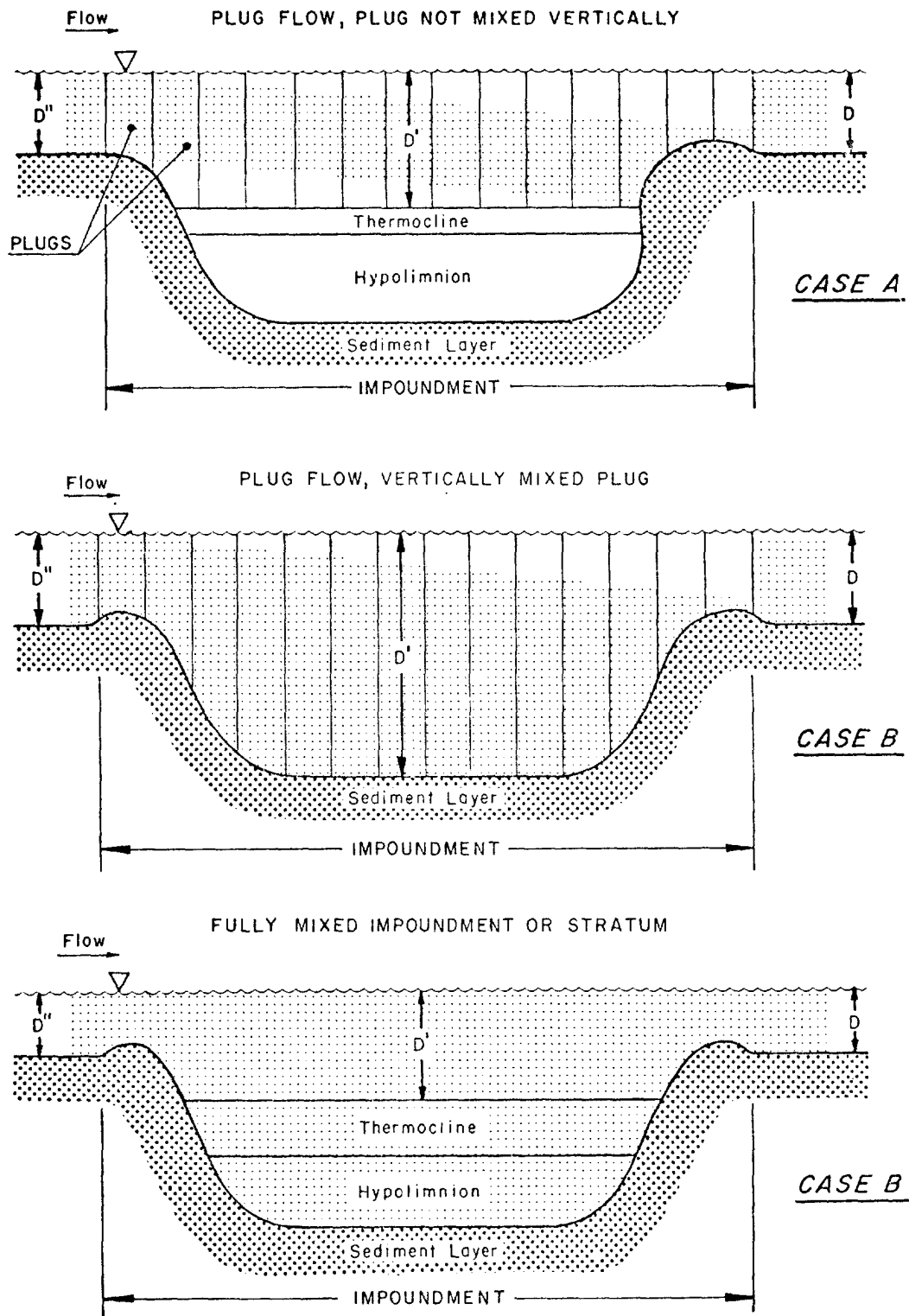


FIGURE V-20 SIGNIFICANCE OF DEPTH MEASURES  $D$ ,  $D'$ , AND  $D''$ , AND THE ASSUMED SEDIMENTATION PATTERN

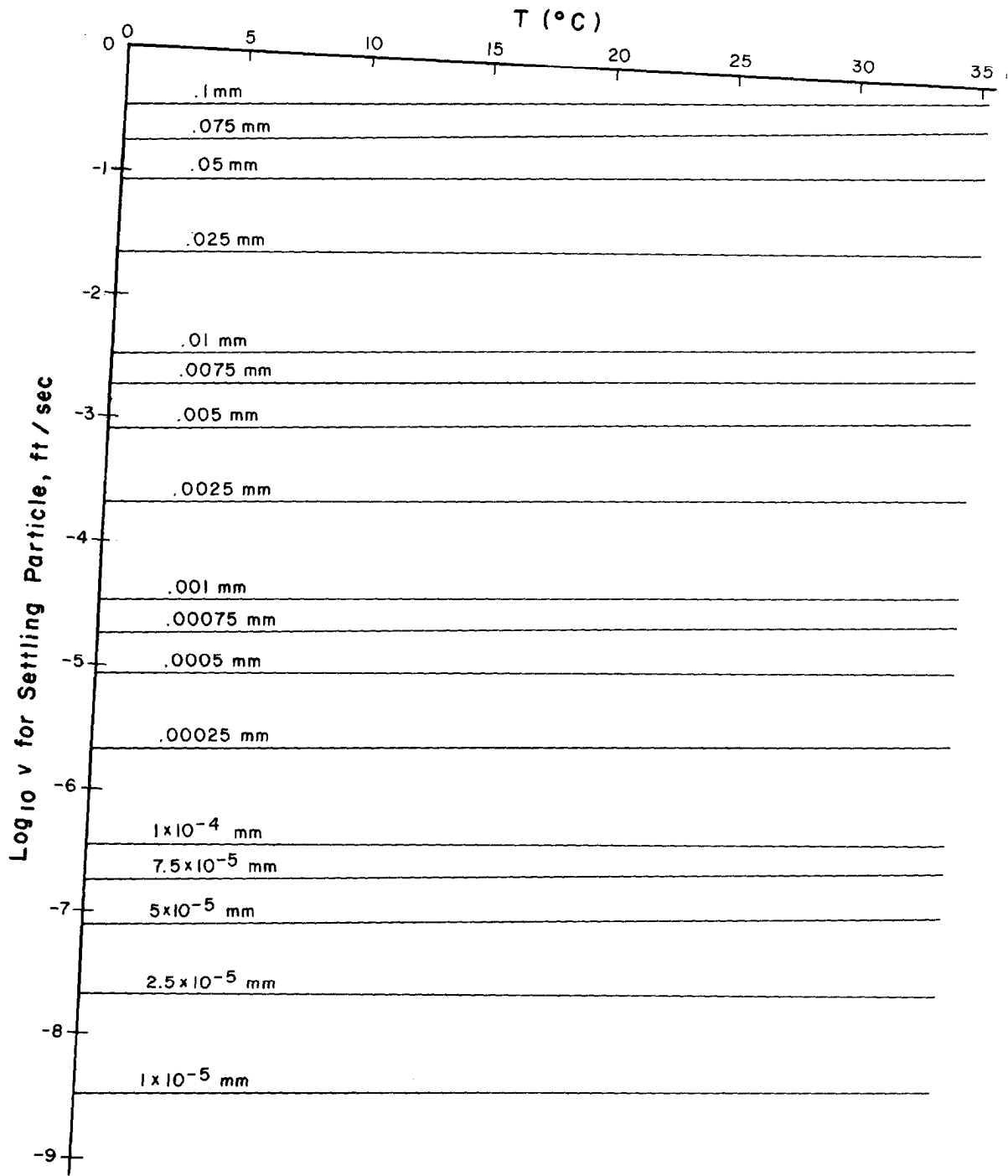


FIGURE V-21 SETTLING VELOCITY FOR SPHERICAL PARTICLES

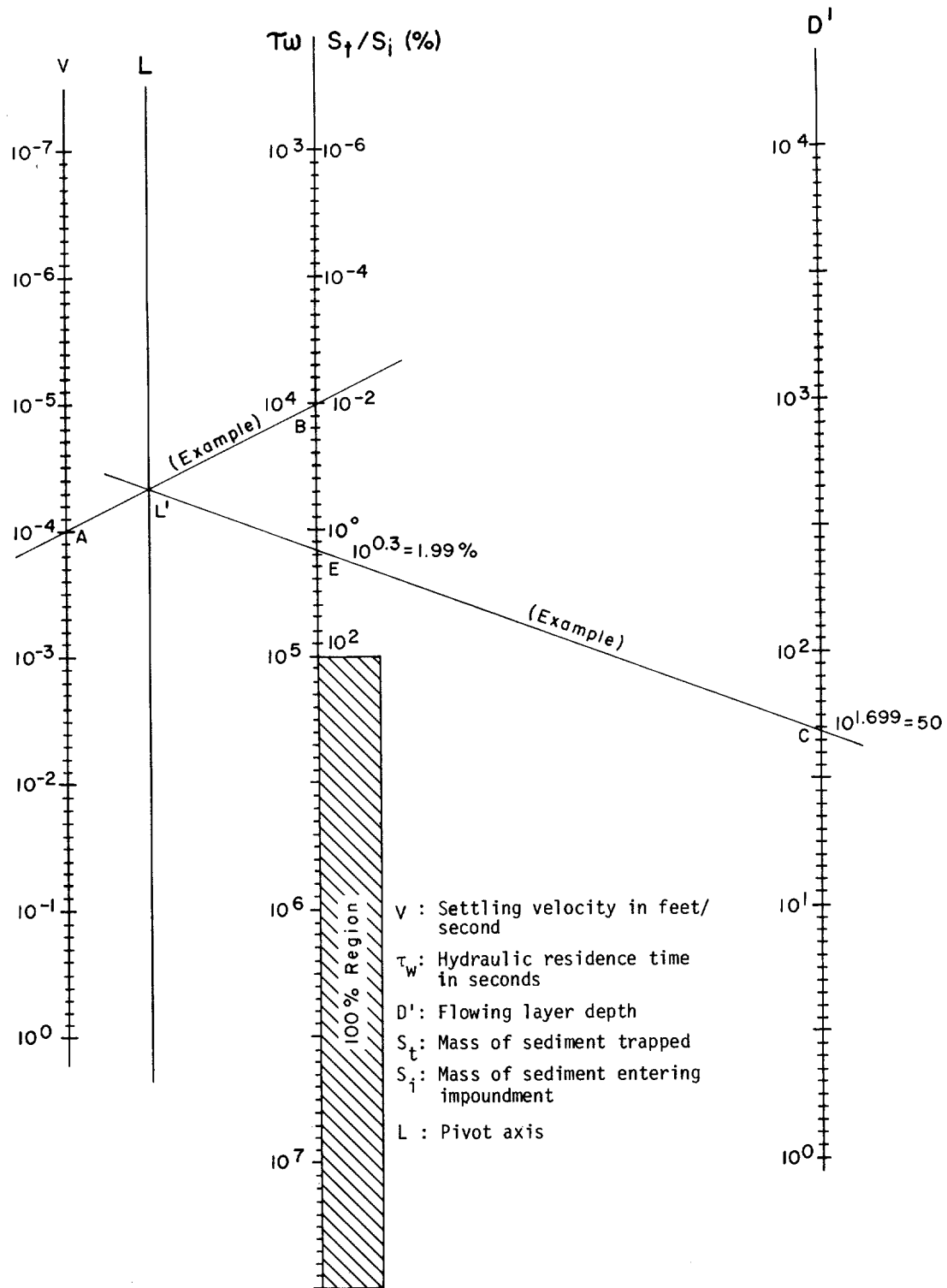


FIGURE V-22 NOMOGRAPH FOR ESTIMATING SEDIMENT TRAP EFFICIENCY

for spherical particles of 2.7 specific gravity. The data are presented as a function of particle diameter and temperature. Figure V-22 is a nomograph relating trap efficiency,  $P$  (in percent) to depth  $D'$ ,  $V_{\max}$ , and  $\tau_w$ . The nomograph is useful only for case B assumptions.

EXAMPLE V-9

Sedimentation in Upper and Lower Lakes

Using the data from Table V-6 and settling velocities for the clay and sand of Example V-4, for case A:

$$\tau_w = 1.6 \times 10^4 \text{ sec}$$

$$V_{\max} \text{ for clay} = 8 \text{ ft day}^{-1}$$

$$V_{\max} \text{ for sand} = 252 \text{ ft hour}^{-1}$$

Although it is not specified in Table V-6, the inflow channel depth at the entrance to Upper Lake is 3 feet. The discharge channel depth is 10 feet. Assuming "laminar" flow with minimal vertical components (Case A), for clay:

$$p = \frac{[(\tau_w \times v) + D'' - D]}{D''}$$

$$p = \frac{[(1.6 \times 10^4 \times 9.3 \times 10^{-5}) + 3 - 10]}{3}$$

$$= -5.5$$

The negative value implies that the proportion settling out is virtually zero. Thus the clay will to a large extent pass through Upper Lake. However,  $\tau_w$  for this example is very small (4.5 hours). Many impoundments will have substantially larger values.

For the sand:

$$p = \frac{[(1.6 \times 10^4 \times 7 \times 10^{-2}) + 3 - 10]}{3}$$

$$= 371$$

All of the sand will clearly be retained. Note that a clay or very fine silt of  $V_{\max} = 5 \times 10^{-4} \text{ ft sec}^{-1}$  would be only partially trapped:

$$p = \frac{[(1.6 \times 10^4 \times 5 \times 10^{-4}) + 3 - 10]}{3}$$

$$= 0.33$$

Thus about one-third of this sediment loading would be retained. Note that if D is large, trap efficiency drops using this algorithm. For the silt, a discharge channel depth (at the outflow from Upper Lake) of 11 feet rather than 10 would give:

$$p = \frac{[(1.6 \times 10^4 \times 5 \times 10^{-4}) + 3 - 11]}{3}$$

$$= 0$$

Thus with  $D = 11$ , all silt exits the impoundment. If  $D$  is only 9 feet, then:

$$P = \frac{[(1.6 \times 10^4 \times 5 \times 10^{-4}) + 3 - 9]}{3}$$

$$= .66$$

Two-thirds of the silt is retained. Remember that  $P$  represents a mean value. Clearly during some periods none of the silt will be retained (due to turbulence, higher velocities) while during other periods, all of the silt will be trapped. The key here is the word "mean."

If the impoundment is assumed to be vertically mixed (case B), compute the mean depth  $\bar{D}$ :

$$\bar{D} = \frac{\sum_{i=1}^n D_i}{n}$$

where

$n$  = the number of cross-sections

$D_i$  = depth at the  $i$ th cross-section.

For Upper Lake:

$$\bar{D} = 6.7 = D'$$

Then:

$$P = \frac{v \tau_w}{D'}$$

For the clay:

$$P = \frac{9.3 \times 10^{-5} \times 1.6 \times 10^4}{6.7}$$

$$= 0.22$$

About one-fourth of the clay is retained:

For the sand:

$$P = \frac{7 \times 10^{-2} \times 1.6 \times 10^4}{6.7}$$

$$= 167$$

All of the sand will be trapped within about 1/167 times the length of the lake. If the daily influent loading of sand is one ton, while the loading of clay is fifteen tons, then the daily accumulation will be one ton of sand and  $0.22 \times 15 = 3.3$  tons of clay.

Finally, as an example of use of Figures V-21 and V-22, assume that the sediment loading consists primarily of silt particles in the size range of .002mm diameter, and that the water temperature is 5°C. Further, assume  $\tau_w$  has been estimated as 2.77 days (104 seconds), and that  $D' = 50$  feet. From Figure V-21, the settling velocity is about  $1 \times 10^{-4}$  feet per second.

In Figure V-22, draw a line from 10<sup>-4</sup> on the V axis to 10<sup>4</sup> on the T<sub>w</sub> axis. The point of intersection with axis L is L'. Next, compute  $\log_{10} 50 = 1.699$ . Draw a line from this point on the D' axis to L'. Where this line crosses the S<sub>t</sub>/S<sub>i</sub> (%) axis gives the log of the percent of the sediment trapped. This is  $10^{0.3} = 1.99 \cong 2\%$ .

----- END OF EXAMPLE V-9 -----

## 5.4 EUTROPHICATION AND CONTROL

### 5.4.1 Introduction

Eutrophication is the process of increasing nutrients in surface waters. The presence of nutrients in an impoundment generally favors plant growth. Depending upon antecedent conditions, the relative abundance of nitrogen, phosphorus, light, and heat, and the status of a number of other physical and chemical variables, the predominant forms may be diatoms, other microscopic or macroscopic algae, or bottom-rooted or free-floating macrophytes. The quantity of plant matter present in an impoundment is important for several reasons. First, plant cells produce oxygen during photosynthesis, thereby providing an important source of dissolved oxygen to the water column during daylight hours. Plant cells also consume oxygen through the process of respiration. Respiration occurs along with photosynthesis during the day, but occurs at night when photosynthesis does not. Oxygen consumed at night may be considerable, not only because it serves to sustain the plant cells, but because the cells actively perform various vital metabolic functions in the dark. Also, cells that fall below the photic zone will consume additional oxygen irrespective of the time of day.

Plant growth within an impoundment is also important because plant biomass is a major source of nutrition for indigenous fauna, and the growth of plants constitutes what is called "primary production." The stored energy and nutrients provide food for various grazers higher in the food chain, either through direct consumption of living plant tissue by fishes and zooplankton or through consumption of detritus by fishes, microorganisms, and zooplankton. The grazers, in turn, provide food for predatory fishes, mammals, insects, and other higher forms. The kinds and amounts of primary producers affect the other members of the food chain resulting in a good sport fishery or "trash fish," depending on nutrient conditions.

Finally, plant development in impoundments is important because it tends to accelerate impoundment aging. As plants grow, organic matter and sediment accumulate. As the impoundment fills with rock fragments, soil, and plant detritus, an excellent substrate forms upon which more suspended matter may be trapped and which may ultimately support the growth of higher plants and trees. The gradual filling in of an



impoundment in this way reduces its usefulness, and may finally eliminate the impoundment completely.

#### 5.4.2 Nutrients, Eutrophy, and Algal Growth

Eutrophy means literally a state of good nutrition. Plants require a number of nutrients, but to vastly different degrees. Some nutrients, such as carbon, nitrogen, potassium, and phosphorus, are needed in large quantity. These are termed macronutrients. The micronutrients, e.g. iron, cobalt, manganese, zinc, and copper, are needed in very small amounts. In nature, the micronutrients, carbon, and potassium are usually in adequate supply (although not always), while nitrogen and phosphorus are commonly growth limiting.

Nitrogen, particularly as nitrate and ammonium ions, is available to water-borne plant cells to be used in synthesis of proteins, chlorophyll a and plant hormones. Each of these substances is vital for plant survival.

Phosphorus, an element found in a number of metabolic cofactors, is also necessary for plant nutrition. The biosynthesis and functioning of various biochemical cofactors rely on the availability of phosphorus, and these cofactors lie at the very foundation of plant cell metabolism. Without adequate phosphorus, plant cells cannot grow.

Since nitrogen and phosphorus are commonly in limited supply, many impoundments tend inherently to be clear and essentially free of clogging algae and vascular plants. Over long periods of time and depending on geological conditions, natural sources of nutrients may lead to eutrophication in lakes. Because of society's ever-increasing size and need for food, chemical sources of nitrogen and phosphorus are synthesized and spread over vast tracts of farmland. Stormwater washes off these nutrients, which then flow through streams and into natural and artificial impoundments. Also, excessive nutrients occur in wastewaters from municipalities and industry. Due to the fact that many impoundments have very low flow velocities, impoundments represent excellent biological culturing vessels, and often become choked with plant life when nutrients increase.

Since a plant cell has at any point in time a specific need for nitrogen and for phosphorus, one or the other or both may limit cell growth or replication. Where nitrogen is the nutrient that restricts the rate of plant growth, that is, where all other nutrients and factors are present in excess, we say that nitrogen is growth limiting. In general, N:P mass ratios in the range of 5 to 10 are usually associated with plant growth being both nitrogen and phosphorus limited. Where the ratio is greater than 10, phosphorus tends to be limiting, and for ratios below 5, nitrogen tends to be limiting (Chiudani, et al 1974). In most lakes, phosphorus is the limiting nutrient. In many nitrogen-limited lakes, phosphorus is still controlling because of the process of nitrogen fixation. Thus, the focus in this manual is on phosphorus.

In addition to nitrogen and phosphorus, any necessary nutrient or physical condition may limit plant growth. For example, in high nutrient (eutrophic) waters, algal biomass may increase until light cannot penetrate, and light is then limiting. At such a point, a dynamic equilibrium exists in which algal cells are consumed, settle or lyse (break) at the same rate as new cells are produced. In other cases, light may be limiting due to non-algal particulate material.

To summarize, the process of eutrophication (or fertilization) is enrichment of a lake with nutrients, particularly nitrogen and phosphorus. However, the problems of eutrophication are caused by increased plant biomass as a result of enrichment. Therefore, the objective is to predict plant biomass as related to nutrient concentrations. The method for predicting plant biomass is based on the rate of phosphorus supply (loading), the concentration of phosphorus in the lake, and the amount of plant biomass that is predicted based on the phosphorus concentration. The plant biomass is exemplified by the phytoplankton (algae) concentration but macrophytes (aquatic weeds) are also of concern. The plant biomass and related variables define the scalar relationships of eutrophication.

#### 5.4.3 Predicting Algal Concentrations

Predicting algal blooms or predominance of macrophytes using a mechanistic approach can be a very complex problem, and most methods are not suited to a simple hand calculation technique. However, relationships regarding algal productivity have been derived that permit an evaluation of the eutrophic state of an impoundment. Because the methods permit algal biomass to be estimated with relatively little, easily obtained data, and because algae are very important in assessing impoundment water quality, these techniques are useful here. The methods presented below are based upon the fact that in most cases (perhaps 60 percent) phosphorus is the biomass limiting nutrient (EPA, 1975). One such approach has been developed by Vollenweider (Vollenweider, 1976; Vollenweider and Kerkes, 1981; Lorenzen, 1976). It may be used to predict the degree of impoundment eutrophication as a function of phosphorus loading.

##### 5.4.3.1 Nutrient Limitation

Before considering application of any of the methods to assess eutrophication, it is important to examine the nitrogen to phosphorus ratio. This indicates whether any of the methods presented below is likely to give realistic results. Generally, an average algal cell has an elemental composition for the macronutrients of  $C_{106}N_{16}P_1$ . With 16 atoms of nitrogen for each atom of phosphorus, the average composition by weight is 6.3 percent nitrogen and 0.87 percent phosphorus or an N/P ratio of 7.2/1. Although all nutrient requirements must be met, the relative rate of supply is significant and must be determined to know which is limiting. For N/P

ratios greater than 7.2, phosphorus would be less available for growth ("limiting") and when less than 7.2, nitrogen would be limiting. In practice, values of less than 5 are considered nitrogen limiting, greater than 10 are phosphorus limiting, and between 5 and 10, both are limiting.

In many cases of eutrophic lakes, nitrogen is not limiting because of the process of nitrogen fixation. Some blue-green algae, a particularly noxious type of algae, have enzymatic processes for the biochemical conversion of dissolved elemental nitrogen into reduced nitrogen (amine groups) suitable for growth and metabolism. Special cells called heterocysts perform this process and only appear when nitrogen is limiting. It can be argued that in general nitrogen is not limiting (Schindler, 1977) and a "worst case" analysis can be made for a screening approach using phosphorus. This is the basis for the eutrophication screening method. However, it should be remembered that the chlorophyll produced is affected by the N/P ratio as are the algal species (Smith, 1979).

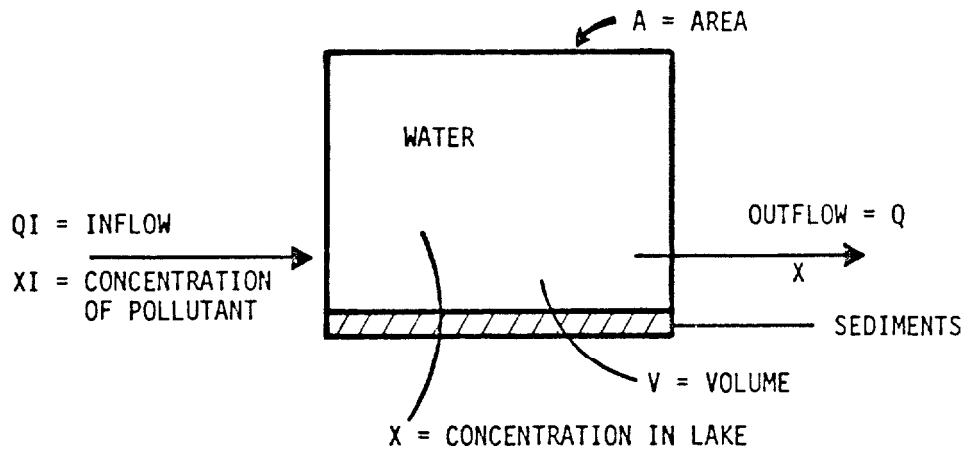
#### 5.4.3.2 Nutrient Availability

Availability of nutrients is also important. Particulate nitrogen and phosphorus in the inflowing tributaries generally settle and can therefore be considered unavailable. Few estimates of bioavailable nutrients have been made. The estimates have been made primarily for phosphorus using algal assay techniques. Cowen and Lee (1976) indicated that 30 percent or less of urban runoff phosphorus was available to algae while Dorich et al. (1980) found a value of 20 to 30 percent for sediment bound phosphorus (as would occur in rural runoff). It appears that a fraction of 0.3 would provide a conservative estimate of bioavailable phosphorus in the absence of actual measurements.

#### 5.4.4 Mass Balance of Phosphorus

A material entering a lake or impoundment will partition between the aqueous and solid phases. The solid phase can settle and become bottom sediment or outflow can remove suspended and aqueous phase material. A diagrammatic presentation of the concept of inflow, partitioning and settling, and outflow is shown in Figure V-23. The concentration of the material can be calculated very simply after making several assumptions: the lake is completely mixed, the lake is at steady state and inflowing water equals outflow, and the annual average rates are constant. Although these assumptions are not met entirely for phosphorus, they are satisfied well enough to meet requirements for a screening analysis of eutrophication. Based on its historical development the eutrophication screening method is termed the "Vollenweider Relationship".

As shown in Figure V-23, any of three different forms of the steady state equation can be used to predict phosphorus concentrations in lakes. Each form may be



For Example - Phosphorus,  $P = X$

LOADING

$$L_p = QI \cdot PI / A, \text{ mg/m}^2 \text{ year}$$

MASS BALANCE

Assumptions: completely mixed, steady state,  $Q \cong QI$ , annual average rates are constant

Definitions: Mean depth,  $\bar{Z} = V/A$ ; hydraulic flushing or dilution rate,  $D = Q/V$ ; hydraulic loading,  $q = Q/A$ ;  $M = QI \cdot PI$ ;  $K =$  net rate of solid phase removal and release (proportional to  $P$ ), typically negative when averaged over the annual cycle.

$$\frac{dP}{dt} = \frac{Q \cdot PI}{V} - \frac{Q \cdot P}{V} - KP = 0$$

Solving for  $P$ ,

$$P = \frac{D \cdot PI}{D + K} \quad (\text{Mass Balance Form}) \quad (1)$$

$$P = \frac{M}{Q} \left( \frac{D}{D + K} \right) \quad (\text{Mass Inflow Form}) \quad (2)$$

$$P = \frac{L_p}{\bar{Z} (D + K)} \quad (\text{Loading Form}) \quad (3)$$

FIGURE V-23 FORMULATIONS FOR EVALUATING MANAGEMENT OPTIONS FOR POLLUTANTS IN LAKES AND RESERVOIRS

more or less suitable for a specific data set. The important variables are the hydraulic flushing or dilution rate ( $Q/V$ , inverse of residence time), lake volume to area ratio ( $V/A$ , equals mean depth), phosphorus in the influent ( $PI$ ), and the net rate of removal ( $K$ ).

The variables  $Q$ ,  $V$ ,  $A$  must be determined from other data. The influent phosphorus can be based on measurements or estimated from calculations performed as in Chapter 3 and including any municipal and industrial effluents. Generally, effluents are considered totally available for growth. Nonpoint sources should be assessed as 100 percent available and as 30 percent available to provide limits for screening purposes.

Estimation of the net rate of removal ( $K$ ) is not as clear. Vollenweider (1976) and Larsen and Mercier (1976) independently estimated the net rate of removal as a function of dilution rate:

$$K = \sqrt{D}$$

This is the most accepted approach for screening. Jones & Bachmann (1976) estimated that  $K = 0.65$  by least squares fitting of data for 143 lakes.

Equivalently, Vollenweider and Kerekes (1981) provide a derivation of the mass balance equation (Equation 1, Figure V-23) in terms of phosphorus residence time and based on regression analysis:

$$P = \frac{1}{1 + \sqrt{D}} (PI) = \frac{PI}{1 + \sqrt{D}}$$

Regression of predicted phosphorus and actual phosphorus for 87 lakes showed a reasonable correlation ( $r = 0.93$ ) but indicated that there was a predicted slight underestimate at low concentrations ( $<8 \mu\text{g/l}$ ) and a slight overestimate at higher concentrations ( $<20 \mu\text{g/l}$ ) (Vollenweider and Kerekes, 1981).

Also the value of  $K$  can be estimated from the ratio ( $R$ ) of the measured mass phosphorus retained (in minus out) and the mass inflow:

$$R = \frac{QI \cdot PI - Q \cdot P}{QI \cdot PI} \approx \frac{PI - P}{PI}$$

$$K = \frac{Lp}{P \cdot \bar{Z}} (R)$$

To assess the placement of a specific lake relative to a set of lakes, phosphorus loading ( $Lp$ ) is graphed as a function of hydraulic loading ( $q_s$ ) (Figure V-24). The data for 49 measurements of U.S. lakes are shown. (Some lakes occur more than once because of multi-year studies.)

More recently, Vollenweider and Kerekes (1981) have presented the OECD Eutrophication Program results showing that lakes can be classified into discrete groups according to their eutrophication characteristics (Table V-9). However, as they note, there is overlap between the different categories showing that these characteristics are not complete descriptors of trophic state but are relative indicators.

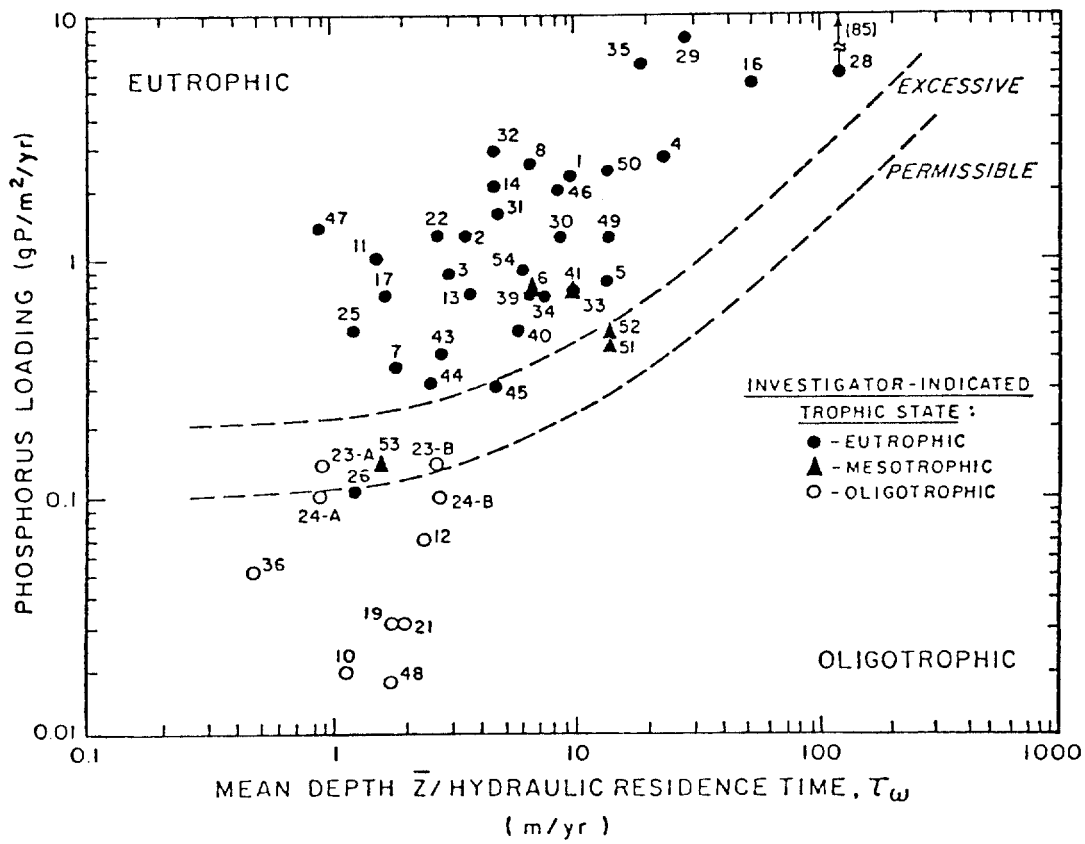


FIGURE V-24 US OECD DATA APPLIED TO VOLLENWEIDER (1976)  
 PHOSPHORUS LOADING AND MEAN DEPTH/HYDRAULIC  
 RESIDENCE TIME RELATIONSHIP (TAKEN FROM RAST  
 AND LEE, 1973)

TABLE V-9

PRELIMINARY CLASSIFICATION OF TROPHIC STATE BASED ON INVESTIGATOR OPINION  
(ADAPTED FROM VOLLENWEIDER AND KEREKES, 1981)

Variable*	Oligotrophic	Mesotrophic	Eutrophic
Total Phosphorus			
mean	<b>8</b>	<b>27</b>	<b>84</b>
range (n)	3-18(21)	11-6(19)	16-390(71)
Total Nitrogen			
mean	660	750	1900
range (n)	310-1600(11)	360-1400(8)	390-6100(37)
Chlorophyll <u>a</u>			
mean	<b>1.7</b>	4.7	<b>14</b>
range (n)	0.3-4.5(22)	3-11(16)	2.7-78(70)
Peak Chlorophyll <u>a</u>			
mean	<b>4.2</b>	<b>16</b>	<b>43</b>
range (n)	1.3-11(16)	5-50(12)	10-280(46)
Secchi Depth, m			
mean	<b>9.9</b>	<b>4.2</b>	<b>2.4</b>
range (n)	5.4-28(13)	1.5-8.1(20)	0.8-7.0(70)

\*  $\mu\text{g/l}$  (or  $\text{mg/m}^3$ ) except Secchi depth; means are geometric annual means  
(except peak chlorophyll a).

EXAMPLE V-10

Big Reservoir and  
The Vollenweider Relationship

To use the Vollenweider relationship for phosphorus loading, data on long-term phosphorus loading rates must be available. It is also important that the rates represent average loading conditions over time because transient phosphorus loading pulses will give misleading results. Big Reservoir is a squarish reservoir and has the following characteristics:

Big Reservoir

Available Data (all values are means):

Length	2.0 mi = 3.22 km
Width	5. mi = .805 km
Depth (Z)	200 ft = 20 m
Inflow (Q)	50 cfs = 1.42 cms

Total phosphorus concentration in water column	0.482 ppm
Total nitrogen concentration in water column	2.2 ppm
Total phosphorus concentration in the inflow	1.0 ppm

In order to apply the plot in Figure V-24, the first step is to make as certain as possible that algal growth is phosphorus limited. In this case, the weight to weight N:P ratio is  $2.2/.48 = 4.6$ . Presumably, algal growth in Big Reservoir is not phosphorus limited, and the Vollenweider relationship for phosphorus is not a good one to use. In this case a rigorous model should be used. If nitrogen fixation is observed to occur (heterocystous blue-green algae), an estimate of the potential problem can be obtained by assuming phosphorus to be limiting:

$$\begin{aligned}
 V &= \text{length} \cdot \text{depth} \cdot \text{width} \\
 &= 3220\text{m} \cdot 805\text{m} \cdot 20\text{m} = 51.8 \text{ million m}^3 \\
 D &= \frac{1.42 \text{ m}^3}{\text{sec } 51.8\text{Mm}^3} \cdot \frac{86400 \text{ sec}}{\text{day}} \cdot \frac{365 \text{ day}}{\text{yr}} = \frac{0.865}{\text{yr}} \\
 \tau_w &= 1.16 \text{ years} \\
 K &= \sqrt{D} = 0.93/\text{yr} \\
 P &= \frac{D \cdot PI}{D + K} = 0.482 \text{ mg/l} \\
 L_p &= Q \cdot PI/A = 17.3 \text{ g/m}^2 \text{ yr} \\
 q_s &= Q/A = \bar{Z}/\tau_w = 20/1.16 = 17.2 \text{ m/yr}
 \end{aligned}$$

Plotting  $L_p$  and  $q_s$  on Figure V-24 shows that the reservoir could be extremely eutrophic.

----- END OF EXAMPLE V-10 -----

#### EXAMPLE V-11

##### Bigger Reservoir and The Vollenweider Relationship

The physical characteristics of Bigger Reservoir are:

##### Bigger Reservoir

Available Data (all values are means):

Length	20 mi = 32.2 km
Width	10 mi = 16.1 km
Depth ( $\bar{Z}$ )	200 ft = 61 m
Inflow (Q)	500 cfs
Total phosphorus concentration in inflow	0.8 ppm
Total nitrogen concentration in inflow	10.6 ppm

As in the preceding example, first determine whether phosphorus is likely to be growth limiting. Since data are available only for influent water, and since



no additional data are available on impoundment water quality, N:P for influent water will be used.

$$N:P = 10.6/0.8 = 13.25$$

Thus algal growth in Bigger Reservoir is probably phosphorus limited. Compute the approximate surface area, volume and the hydraulic residence time.

$$\text{Volume (V)} = 20 \text{ mi} \times 10 \text{ mi} \times 200 \text{ ft} \times 5280^2 = 1.12 \times 10^{12} \text{ ft}^3 = 3.16 \times 10^{10} \text{ m}^3$$

$$\text{Hydraulic residence time } (\tau_w) = V/Q = 1.12 \times 10^{12} \text{ ft}^3 / 500 \text{ ft}^3 \text{ sec}^{-1} = 2.24 \times 10^9 \text{ sec} = 71 \text{ yr}$$

$$\text{Surface area (A)} = 20 \text{ mi} \times 10 \text{ mi} \times 5280^2 = 5.57 \times 10^9 \text{ ft}^2 = 5.18 \times 10^8 \text{ m}^2$$

Next, compute  $q_s$

$$q_s = \bar{Z} / \tau_w$$

$$q_s = 61 \text{ m} / 71 \text{ yr} = 0.86 \text{ m yr}^{-1}$$

Compute annual inflow,  $Q_y$

$$Q_y = Q \times 3.15 \times 10^7 \text{ sec yr}^{-1}$$

$$Q_y = 1.58 \times 10^{10} \text{ ft}^3 \text{ yr}^{-1}$$

Phosphorus concentration in the inflow is 0.8 ppm or 0.8 mg/l. Loading ( $L_p$ ) in grams per square meter per year is computed from the phosphorus concentration, in mg/l:

$$L_p = \frac{28.31 \text{ g}}{\text{ft}^3} \times \frac{1 \text{ g}}{1000 \text{ mg}} \times \frac{0.8 \text{ mg}}{\text{L}} \times \frac{1}{5.18 \times 10^8 \text{ m}^2} \times 1.58 \times 10^{10} \frac{\text{ft}^3}{\text{yr}}$$

$$L_p = 0.70 \text{ gm}^{-2} \text{ yr}^{-1}$$

Now, referring to the plot in Figure V-24, we would expect that Bigger Reservoir possibly with severe summer algal blooms.

----- END OF EXAMPLE V-11 -----

----- EXAMPLE V-12 -----

The Vollenweider Relationship  
Using Monthly Inflow Quality Data

Is Frog Lake eutrophic? Frog Lake's physical characteristics are as shown below:

Frog Lake

Available Data:

Mean length	2 mi
Mean width	1/2 mi
Mean depth	25 ft

Available Inflow Water Quality Data:

<u>Month</u>	<u>Q (monthly mean, cfs)</u>		<u>Total P (mg/l)</u>		<u>Inorganic N (mg/l)</u>	
	1972	1974	1972	1974	1972	1974
October	50	65	0.1	0.08	7.2	6.0
November	80	90	0.02	0.02	6.3	2.4
December	40	40	0.03	0.04	3.1	1.5
January	-	-	-	-	-	-
February	-	-	-	-	-	-
March	60	58	0.01	0.02	2.0	1.9
April	80	80	0.01	0.01	2.3	0.50
May	75	76	0.04	0.05	0.55	0.52
June	40	70	0.03	0.08	1.20	1.35
July	-	25	-	0.11	-	2.01
August	38	20	0.09	0.04	3.50	1.29
September	38	25	0.06	0.05	2.80	1.00

First, estimate the mean annual flow and the hydraulic residence time. To compute mean annual flow,

$$Q = \frac{\sum_{i=1}^y \sum_{j=1}^{n_i} Q_{i,j}}{\sum_{i=1}^y n_i}$$

where

$Q_{i,j}$  = the individual flow measurements

$y$  = the number of years of data

$n_i$  = the number of observations per year

$Q$  =  $1050/19 = 55.3$  cfs =  $1.75 \times 10^9$  ft<sup>3</sup>/yr

Now estimate the volume, surface area, hydraulic residence time, and  $q_s$

$$V = 2 \text{ mi} \times 1/2 \text{ mi} \times 25 \text{ ft} \times \frac{(5280 \text{ ft})^2}{5280 \text{ ft}} = 6.97 \times 10^8 \text{ ft}^3 =$$

$$1.98 \times 10^7 \text{ m}^3$$

$$A = 2 \text{ mi} \times 1/2 \text{ mi} \times \frac{(5280 \text{ ft})^2}{5280 \text{ ft}} = 2.79 \times 10^7 \text{ ft}^2 = 2.59 \times 10^6 \text{ m}^2$$

$$\tau_w = V/Q = 6.97 \times 10^8 \text{ ft}^3 / 55.3 \text{ cfs} = 1.26 \times 10^7 \text{ sec} = 0.4 \text{ yr}$$

$$q_s = \bar{Z} / \tau_w$$

$$q_s = 25 \text{ ft.} \cdot \frac{0.3048 \text{ m}}{\text{ft}} / 0.4 \text{ yr} = 19.05 \text{ m/yr}$$

Next, calculate the weight mean inflow phosphorus and nitrogen concentrations  $\bar{P}$  and  $\bar{N}$  as follows:

$$\bar{P} \text{ (or } \bar{N}) = \left( \sum_{i=1}^y \sum_{j=1}^{n_i} Q_{i,j} \times C_{i,j} \right) / \left( \sum_{i=1}^y \sum_{j=1}^{n_i} Q_{i,j} \right)$$

$$\bar{P} = 43.86 / 1050 = 0.042 \text{ mg/l}$$

$$\bar{N} = 2671.902 / 1050 = 2.54 \text{ mg/l}$$

The N:P ratio in the inflows is 60. Therefore if one of the two is growth limiting, it is probably phosphorus. Compute the phosphorus loading,  $L_p$ .

$$L_p = \frac{28.31 \ell}{\text{ft}^3} \times \frac{1 \text{ g}}{1000 \text{ mg}} \times \frac{0.042 \text{ mg}}{\ell} \times \frac{1}{2.59 \times 10^6 \text{ m}^2} \times \frac{1.75 \times 10^9 \text{ ft}^3}{\text{yr}}$$

$$L_p = 0.80 \text{ g/m}^2 \text{ yr}$$

Now, referring to the plot in Figure V-24 with  $L_p = 0.80 \text{ g/m}^2 \text{ yr}$  and  $q_s = 19 \text{ m/yr}$ , the impoundment is well into the mesotrophic region.

--- END OF EXAMPLE V-12 ---

#### 5.4.5 Predicting Algal Productivity, Secchi Depth, and Biomass

The prediction of eutrophication effects is based primarily on prediction of chlorophyll a concentrations from phosphorus concentrations rather than on general impoundment trophic status. The method has been advanced by several researchers including Sakamoto (1966), Lund (1971), Dillon (1974), and Dillon and Rigler (1975). Originally, the method related mean summer chlorophyll a concentrations to spring mean total phosphorus. As shown in Figure V-25, the relationship is highly correlated, and a regression of the log of summer mean chlorophyll a on the log of spring mean phosphorus is linear (units are  $\mu\text{g/l}$ ). Using a least squares method gives the equation of the line as (Lorenzen, 1978):

$$\log(\text{chl } \underline{a}) = 1.5 \log(P) - 1.1$$

or

$$\text{chl } \underline{a} = 0.08(P)^{1.5} \text{ for } P < 250 \text{ mg/m}^3 = 0.25 \text{ ppm}$$

More recently (Vollenweider and Kerekes, 1981), additional data have been compiled and equations have been derived for predicting annual average chlorophyll a from annual average total phosphorus ( $r = 0.88$ ,  $n=78$ ):

$$\text{chl } \underline{a} = 0.27(P)^{0.99} \quad (\text{V-15})$$

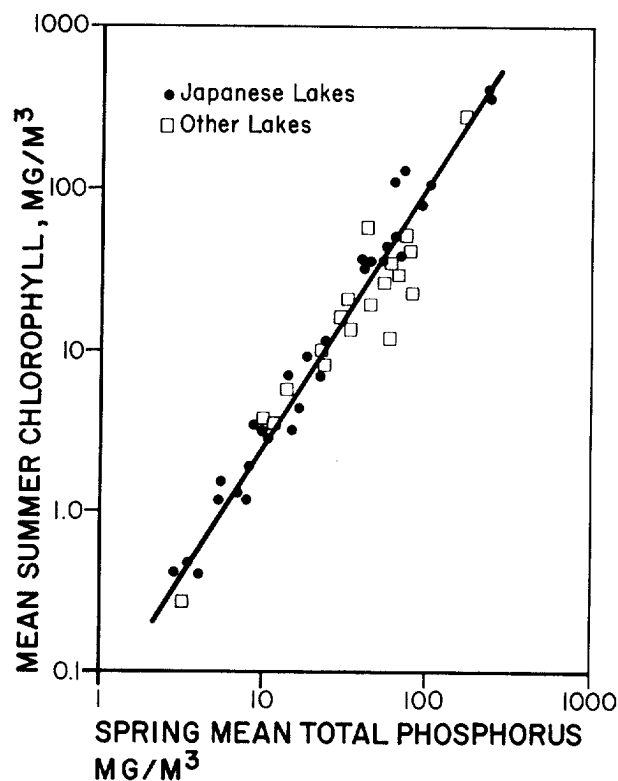


FIGURE V-25 RELATIONSHIP BETWEEN SUMMER CHLOROPHYLL AND SPRING PHOSPHORUS (FROM LORENZEN, UNPUBLISHED)

Perhaps more important from a water quality point of view, peak chlorophyll  $\underline{a}$  can be computed from annual average total phosphorus ( $r = 0.89$ ,  $n=51$ ):

$$\text{peak chl } \underline{a} = 0.58(P)^{1.07} \quad (\text{V-16})$$

The peak is approximately 2-3 times as much as the average chlorophyll  $\underline{a}$ . If the relationships are computed from phosphorus loading equations, the equations change:

$$\text{chl } \underline{a} = 0.37(P_L)^{0.79}$$

and

$$\text{peak chl } \underline{a} = 0.74(P_L)^{0.8}$$

One of the major diagnostic tools in analysis of eutrophication is measurement of water transparency. Algal blooms decrease light penetration by light absorption and scattering that can be approximated by the Beer-Lambert law.

A simple method of estimating light penetration in the vertical direction is with a Secchi disk, where the disappearance depth is defined as the Secchi depth (SD) (Hutchinson, 1957):

$$\ln(I_{SD}/I_0) = -k * SD$$

where

$I_0$  = initial light intensity, light units

$I_{SD}$  = intensity at Secchi depth, light units

SD = Secchi depth, m

k = extinction coefficient, 1/m.

Algal blooms reduce transparency. Algal blooms are measured using the average summertime (July-August) chlorophyll a concentration (CA,  $\mu\text{g/l}$ ) in the mixed layer epilimnion) since non-plant materials do not contain chlorophyll. Lorenzen (1973, 1980) showed that the extinction coefficient (k) could be considered in two parts; that is, light attenuation would be the result of absorption and scattering by algal cells and by the water and non-algal materials in the water column:

$$k = a + b * CA$$

Hutchinson (1957) and others have shown that the Secchi depth occurs over a relatively narrow range of light intensity ratios ( $I/I_0$ ). If it is assumed that this ratio is a constant ( $\ln(I/I_0) = R$ ), we can substitute ( $A = a/R$ ;  $B = b/R$ ), and solve for Secchi depth as a function of chlorophyll a:

$$I/SD = A + B * CA$$

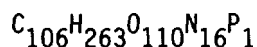
In the equation, A represents non-algal attenuation while  $B*CA$  represents attenuation by chlorophyll a. Larsen and Malueg (1981) used data from several lakes to compute this relationship. Similarly, data from 226 lakes were used to obtain the following equation:

$$I/SD = 0.02 CA + 0.6$$

However, B is considered a constant ( $B = 0.02$ , Megard et al., 1980), while A will vary with the background light attenuation in the water due to dissolved and particulate matter (Lorenzen, 1980). It should be noted that as the particulate matter increases, the relationship will be less likely to hold.

Figure V-26 shows a plot of maximal primary production in terms of milligrams carbon incorporated in algae per square meter per day as a function of phosphate phosphorus levels. As was the case with predicting chlorophyll a concentrations, the relationship appears to be reasonably robust and therefore useful.

Because dried algae contain very roughly 3 percent chlorophyll a (J.A. Elder, pers. comm., 1977), dry algal biomass may be estimated from chlorophyll a concentration by multiplying by thirty-three. Similarly, carbon productivity, as in the plot in Figure V-26, may be converted to total algal biomass. Since approximate analysis of dried algae has been determined as (Stumm and Morgan, 1970):



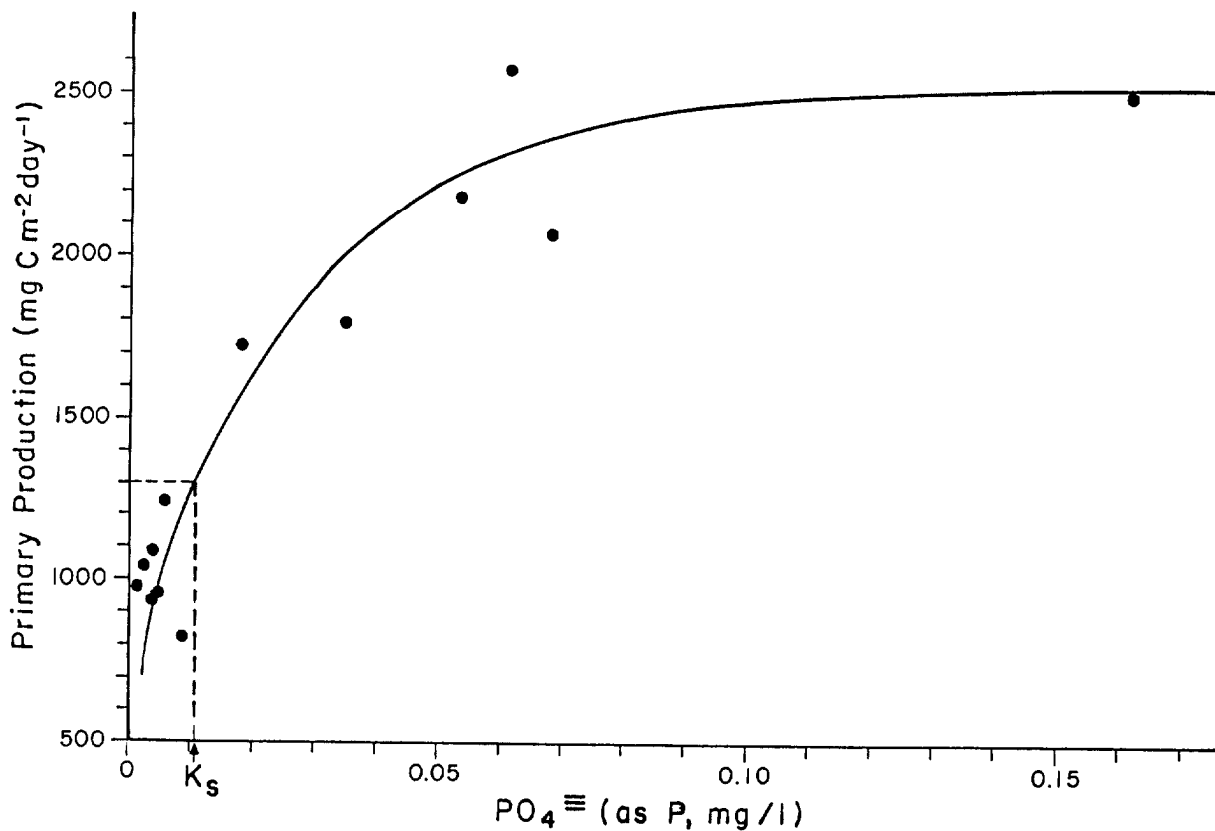


FIGURE V-26 MAXIMAL PRIMARY PRODUCTIVITY AS A FUNCTION OF PHOSPHATE CONCENTRATION (AFTER CHIAUDAN ET AL., 1974)

the gravimetric factor is  $\frac{3550}{1271} \approx 2.8$ . Thus, maximal carbon productivity may be multiplied by 2.8 to give a rough estimate of maximal algal biomass productivity.

The user should bear in mind that applying this technique can only lead to rough estimates. If it is desired to predict biomass or productivity with accuracy, more sophisticated approaches may be necessary.

EXAMPLE V-13

Phosphorus and Summer Chlorophyll a

Lake Sara mean annual total phosphorus concentration,  $P = .03 \text{ mg/l} = 30 \text{ mg/m}^3$

$$\text{chl } \underline{a} = 0.27(P)^{0.99}$$

$$\text{chl } \underline{a} = 7.8 \text{ mg/m}^3$$

$$\text{algal dry biomass} \cong 7.8 \times 33 = 258 \text{ mg/m}^3$$

Peak chlorophyll a would be  $22 \text{ mg/m}^3$ . If calculated from loading rates, the

numbers would differ. Secchi depth would be approximately 1.3 meters assuming that the average background light extinction was 0.6.

----- END OF EXAMPLE V-13 -----

In the absence of measured data, the in-lake concentration (P) can be computed based on the various point and nonpoint loadings (n):

$$L_p = \sum_{i=1}^n Q_i P I_i$$

$$P = \left( \frac{PI}{1 + \sqrt{D}} \right)$$

Then chlorophyll a can be estimated as shown in the previous paragraphs.

#### 5.4.6 Restoration Measures

Control of eutrophication in lakes can be evaluated by a variety of approaches (Table V-10). Some methods are directed at external sources (PI) and others at recycling from in-lake sources (K). Changes in volume (V) and inflow (Q) obviously will affect predicted results. For example, on a long term basis dredging will decrease the return of phosphorus for the sediments (i.e. increase K) and increase the volume (and therefore decrease the dilution rate, D). If the input concentration (PI) is the critical variable, then source controls should be investigated. If internal sources are involved, then in-lake controls should be evaluated. In many lakes, both source and in-lake controls will be needed.

Problem treatment is directed at the productivity directly. These controls are often the only alternative for many lake situations. These methods are evaluated only in a qualitative way. Indexes for evaluating lake restoration have been developed (Carlson, 1977; Porcella et al., 1980). These are useful for prioritizing lake restoration projects and for evaluating progress.

#### 5.4.7 Water Column Phosphorus Concentrations

The relationships described in 5.4.5 for predicting algal biomass are predicated on phosphorus levels within the impoundment. A more precise mechanism for estimating phosphorus lake concentrations based on interactions between bottom sediments and overlying water has been developed.

Lorenzen, et al. (1976) developed a phosphorus budget model (Figure V-27 which may be used to estimate water column and sediment bound phosphorus in a fully mixed system. A mass balance on both sediment and water column phosphorus concentrations

TABLE V-10

CLASSIFICATION OF LAKE RESTORATION TECHNIQUES

- 
- I. Source Controls
    - A. Treatment of inflows
    - B. Diversion of inflows
    - c. Watershed management (land uses, practices, nonpoint source control, regulations and/or treatments).
    - D. Lake riparian regulation or modification
    - E. Product modification or regulation
  
  - II. In-Lake Controls
    - A. Dredging
    - B. Volume changes other than by dredging or compaction of sediments
    - c. Nutrient inactivation
    - D. Dilution/Flushing
    - E. Flow adjustment
    - F. Sediment exposure and dessication
    - G. Lake bottom sealing
    - H. In-lake sediment leaching
    - I. Shoreline modification
    - J. Riparian treatment of lake water
    - K. Selective discharge
  
  - III. Problem Treatment (directed at biological consequences of lake condition)
    - A. Physical techniques (harvesting, water level fluctuations, habitat manipulations)
    - B. Chemical (algicides, herbicides, pesticides)
    - c. Biological (predator-prey manipulations, pathological reactions).
    - D. Mixing (aeration, mechanical pumps, lake bottom modification)
    - E. Aeration (add DO; e.g. hypolimnetic aeration)
-



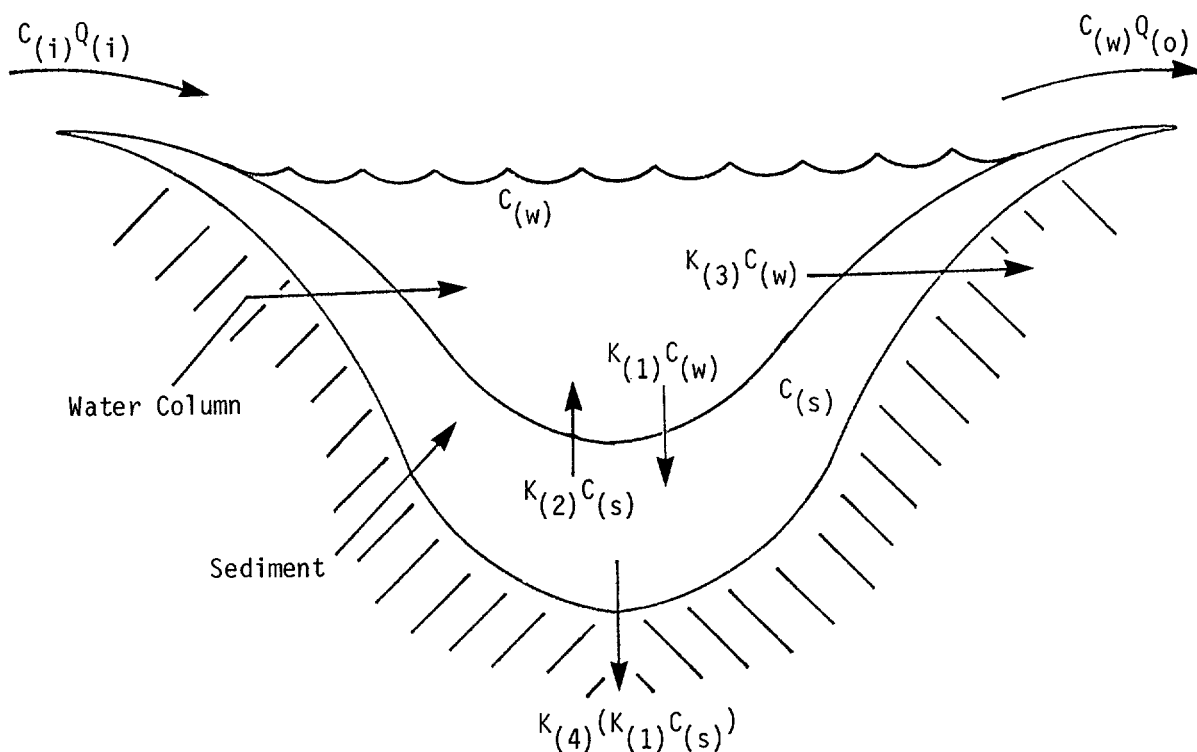


FIGURE V-27 CONCEPTUALIZATION OF PHOSPHORUS BUDGET MODELING (LORENZEN ET AL, . 1976)

yields the coupled differential equations:

$$\frac{dC_w}{dt} = \frac{M}{V} + \frac{K_2 A C_s}{V} - \frac{K_1 A C_w}{V} - \frac{C_w Q}{V} \quad (V-17)$$

$$\frac{dC_s}{dt} = \frac{K_1 A C_w}{V_s} - \frac{K_2 A C_s}{V_s} - \frac{K_1 K_3 A C_w}{V_s} \quad (V-18)$$

- $C_w$  = average annual total phosphorus concentration in water column ( $g/m^3$ )
- $C_s$  = total exchangeable phosphorus concentration in the sediments ( $g/m^3$ )
- $M$  = total annual phosphorus loading ( $g/yr$ )
- $V$  = lake volume ( $m^3$ )
- $V_s$  = sediment volume ( $m^3$ )
- $A$  = lake surface area ( $m^2$ ) - sediment area ( $m^2$ )
- $Q$  = annual outflow ( $m^3/yr$ )
- $K_1$  = specific rate of phosphorus transfer to the sediments ( $m/yr$ )
- $K_2$  = specific rate of phosphorus transfer from the sediments ( $m/yr$ )
- $K_3$  = fraction of total phosphorus input to sediment that is unavailable for the exchange process

When the differential equations relating water column phosphorus to the various controlling phenomena are solved analytically, the following equation results for steady-state water column phosphorus concentration:

$$C_w = \frac{C_{in}}{1 + \frac{K_1 K_3 A}{Q}} \quad (V-19)$$

or

$$C_w = \frac{M}{Q + K_1 K_3 A} \quad (V-20)$$

where

$C_w$  = steady-state water column phosphorus concentration in ppm

$C_{in}$  = steady-state influent phosphorus concentration in ppm

The steady-state sediment phosphorus concentration is then given by:

$$C_s = \frac{C_{in} K_1 (1 - K_3)}{K_2 (1 + (K_1 K_3 A / Q))} \quad (V-21)$$

It is important to observe that these relationships are valid only for steady-state conditions. Where phosphorus loading is changing with time, where sediment deposition or physical characteristics are changing, or where there are long-term changes in physical conditions, the steady-state solutions are not applicable. Lorenzen applied the model to Lake Washington data and obtained very good results. With their data set, the most satisfactory coefficients had the following values:

$$K_1 = 43 \text{ m/yr}$$

$$K_2 = 0.0014 \text{ m/yr}$$

$$K_3 = 0.5$$

It should be recognized, however, that this model is relatively untested and that coefficient values for other impoundments will vary from those cited here.

----- EXAMPLE V-14 -----

A Comprehensive Example  
Impoundment Water Column Phosphorus

What will be the steady-state concentration of phosphorus in the water column of Lake Jones following diversion of flow? How will this affect algal abundance?

Lake Jones:

$$\begin{aligned} \text{Area, } A &= 20 \text{ miles}^2 = 5.6 \times 10^8 \text{ ft}^2 = 5.2 \times 10^7 \text{ m}^2 \\ \text{Volume, } V &= 3.08 \times 10^{11} \text{ ft}^3 = 8.73 \times 10^9 \text{ m}^3 \end{aligned}$$

Available Data (prior to diversion):

Inflows:

	Mean Annual Flow, cfs	Mean P, mg/1
1. Janes River	75	.15
2. Jennies River	22	.07
3. Johns Creek	5	.21
4. Direct stormwater influx (nominal, may be disregarded)		

The diversion, which is for irrigation purposes, has decreased the mean annual inflow from Jennies River to 1 cfs with an average annual phosphorus concentration of 0.01 mg/1. Additionally, there is a reduction of flow in Janes River to 55 cfs. but the mean P concentration stays the same.

To apply the Vollenweider relationship, first to the prediversion status of Lake Jones, compute  $q_s$ :

$$q_s = \frac{\bar{z}}{\tau_w}$$

$$\bar{z} = \frac{8.73 \times 10^9 \text{ m}^3}{5.2 \times 10^7 \text{ m}^2} = 168 \text{ m}$$

Based upon the conceptualization (see Figure V-27), it is reasonable that the coefficients interact. For example,  $K_1$ , the rate of phosphorus uptake by the sediment must be related to the rate of phosphorus release by the sediment. The model requires however, that the product  $K_1 K_3$  be constant. The value used by Lorenzen, *et al.* was 21.6. As they point out, the coefficients must satisfy certain conditions, specifically those established by the derived equations. The equations are:

$$C_w = \frac{M}{Q + K_1 K_3 A} \quad (\text{V-22})$$

and

$$\frac{C_w}{C_s} = \frac{K_2}{K_1 (1 - K_3)} \quad (\text{V-23})$$

From (V-22)

$$K_1 K_3 = \frac{M - Q C_w}{C_w A} \quad (\text{V-24})$$

Computation of  $K_1$ , therefore, requires a value for  $K_3$ . This coefficient, ( $K_3$ ) unfortunately, is usually unavailable. It represents the fraction of phosphorus entering the sediment which is not returned to the water column. Processes contributing to this phenomenon are burial caused by steady-state sediment accumulation, and steady-state chemical precipitation of phosphorus, such as with iron to form  $\text{Fe}_3(\text{PO}_4) \cdot 8\text{H}_2\text{O}$  (vivianite). Lorenzen's value for Lake Washington was 50 percent. Because the fraction is likely to vary significantly from system to system and because the coefficient is difficult to evaluate, the planner is advised to use 30 percent as the lower limit, 50 percent as a probable value, and 70 percent as an upper limit for estimating sediment phosphorus content. The water column concentration is independent of changes in  $K_3$  because the product of  $K_1$  and  $K_3$  is a constant.

Using Equation (V-24),  $K_3$  uniquely defines  $K_1$ . Then, from Equation (V-23) :

$$K_2 = \frac{C_w K_1 (1 - K_3)}{C_s}$$

$K_2$  is therefore also defined by fixing  $K_3$ , providing  $C_w$  and  $C_s$  are known.

$$M = \left[ \left( \frac{75 \text{ ft}^3}{\text{Sec}} \times \frac{0.15 \text{ mg}}{\ell} \right) + \left( \frac{22 \text{ ft}^3}{\text{Sec}} \times \frac{.07}{\ell} \right) \text{mg} \left( \frac{5 \text{ ft}^3}{\text{Sec}} \times \frac{.21 \text{ mg}}{\ell} \right) \right] \\ \times \frac{28.31 \ell}{\text{ft}} \times \frac{1 \text{ g}}{1000 \text{ mg}} \times \frac{3.16 \times 10^7 \text{ sec}}{\text{yr}}$$

$$M = 1.24 \times 10^7 \text{ gP/yr}$$

$$Q = \frac{(75+22+5) \text{ ft}^3}{\text{sec}} \times \frac{3.16 \times 10^7 \text{ sec}}{\text{yr}} = \frac{3.22 \times 10^9 \text{ ft}^3}{\text{yr}} = \frac{9.13 \times 10^7 \text{ m}^3}{\text{yr}}$$

$$\tau_w = 8.73 \times 10^9 \text{ m}^3 / 9.13 \times 10^7 \text{ m}^3 \text{ yr}^{-1} = 95.6 \text{ yr}$$

$$q_s = 168 / 95.6 = 1.76 \text{ m yr}^{-1}$$

Compute phosphorus loading:

$$L_p = \frac{M}{A}$$

$$L_p = \frac{1.24 \times 10^7 \text{ g yr}^{-1}}{5.2 \times 10^7 \text{ m}^2} = 0.24 \text{ gm}^{-2} \text{ yr}^{-1}$$

Referring to Figure V-24 with  $q_s = 1.76$  and  $L_p = 0.24$ , one can see that this lake may have eutrophication problems under pre-diversion conditions. After the diversion,

$$\tau_w = \frac{8.73 \times 10^9 \text{ m}^3}{6.98 \times 10^7 \text{ m}^3/\text{yr}} = 125 \text{ yr}$$

Assuming the lake depth is not materially changed over the short term,

$$q_s = 168/125 = 1.34 \frac{\text{m}}{\text{yr}}$$

For the new conditions,

$$M = 8.33 \times 10^6 \text{ gP yr}^{-1}$$

$$L_p = \frac{8.33 \times 10^6 \text{ g yr}^{-1}}{5.2 \times 10^7 \text{ m}^2} = .16 \text{ gP/m}^2\text{yr}$$

Now, according to the Vollenweider plot (Figure V-24), this is in the region between "dangerous" and "permissible" - the mesotrophic region. Under the new circumstances, algal blooms are less likely than before the flow diversions were established, but blooms are by no means to be ruled out.

Turning now to an estimate of algal biomass under pre-diversion conditions, we must calculate the inlake concentration (P).

$$\text{First, } D = 1/\tau_w = 1/125 = 0.008; K = \sqrt{D} = 0.09$$

Since our data are already in the loading form:

$$P = \frac{PL}{Z} \frac{1}{D+K} \\ = \frac{0.24}{168} \frac{1}{0.008+0.09} = 15 \text{ mg/m}^3$$

Based on annual average chlorophyll  $a$ ,

$$\text{chl } a = 0.37(P)^{0.79} \\ \text{chl } a = 3.1 \text{ mg/m}^3$$

Under post-diversion conditions,

$$P = \frac{0.16}{168} \frac{1}{0.008+0.09} = 10 \text{ mg/m}^3 \\ \text{chl } a = 2.3 \text{ mg/m}^3$$

Note that these low levels of chlorophyll  $a$  almost certainly mean that the lake is oligotrophic to mesotrophic, and that the Vollenweider method suggests worse conditions than may actually exist in this case (Table V-9).

Consequently, one might choose to use the Lorenzen model to evaluate  $K_1$  and  $K_3$  and determine whether the impoundment is at steady state with respect to phosphorus levels in the water column and sediment. Generally, this is the case where  $K_1K_3$  lies in the range of 20 to 40. If  $K_1K_3$  is outside of

this range, field data should be obtained for current water column phosphorus.

Sediment volume, $V_s$	Irrelevant for steady-state solution
Phosphorus (water column)	.15 mg/l

$$K_3 = 0.5$$

$$K_1 = \frac{M - QC_w}{K_3 C_w A}$$

$$C_w = 0.15 \text{ mg/l} = .015 \text{ g/m}^3$$

$$K_1 = \frac{\left( \frac{1.24 \times 10^7 \text{ gP}}{\text{yr}} - \frac{9.13 \times 10^7 \text{ m}^3}{\text{yr}} \times \frac{.015 \text{ g}}{\text{m}^3} \right)}{\left( .5 \times \frac{.015 \text{ g}}{\text{m}^3} \times 5.2 \times 10^7 \text{ m}^2 \right)} = 28.3 \frac{\text{m}}{\text{yr}}$$

$$K_1 K_3 = 44 \times 0.5 = 14$$

This result, therefore, gives reason to suspect non steady-state conditions for water column phosphorus. If more definitive answers are needed, additional field data should be collected.

END OF EXAMPLE V-14

## 5.5 IMPOUNDMENT DISSOLVED OXYGEN

Organic substances introduced into an impoundment with inflowing water, falling onto its surface, or generated in the water column itself through photosynthesis, may be oxidized by indigenous biota. The process consumes oxygen which may, in turn, be replenished through surface reaeration, photosynthetic activity, or dissolved oxygen in inflowing water. The dynamic balance between DO consumption and replenishment determines the net DO concentration at any point in time and at any location within the water column.

These processes result in characteristic dissolved oxygen (DO) concentrations in the water columns of stratified lakes and reservoirs (Figure V-28). During stratification, typically during summer months, the DO is highest on the surface due to photosynthesis and reaeration. It decreases through the thermocline and then, in the hypolimnion, the DO decreases to zero in those lakes that have high organic matter concentrations.

During spring, after turnover, when lakes are not stratified, the DO is essentially uniform. However, in highly organic lakes benthic processes can already begin to deplete oxygen from lower depths, as shown in Figure V-28.

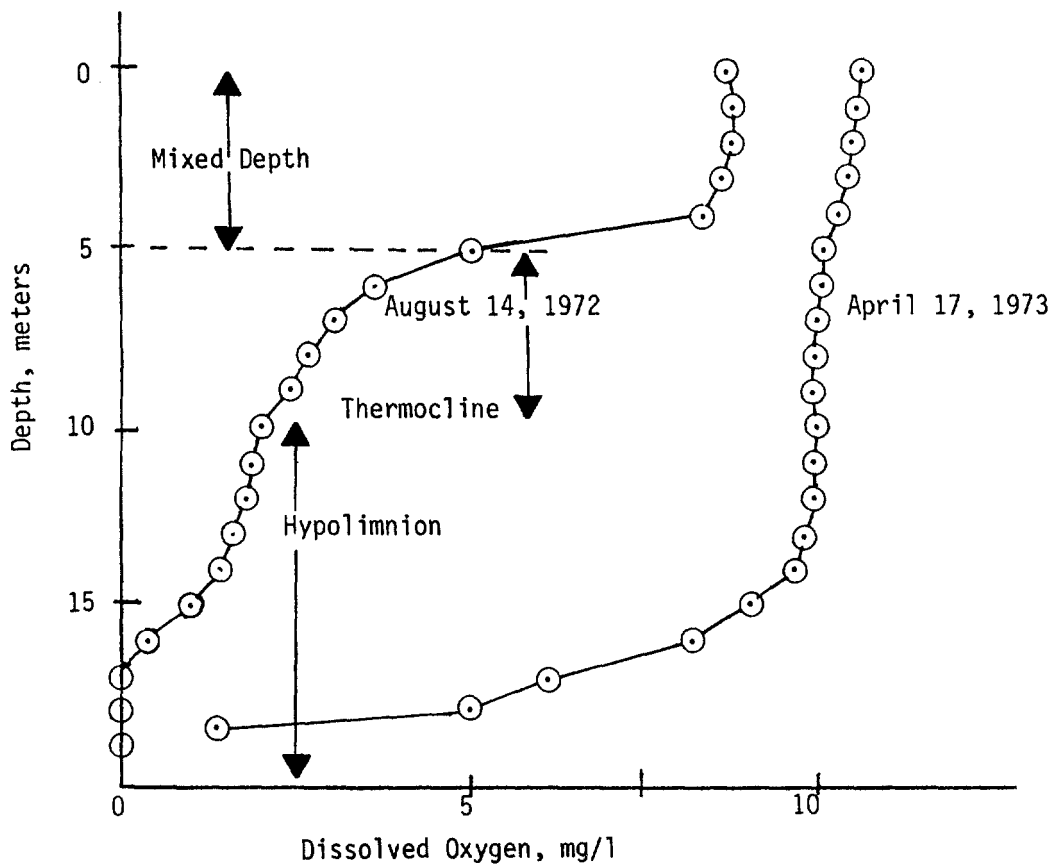


FIGURE V-28 TYPICAL PATTERNS OF DISSOLVED OXYGEN (DO) IN HYRUM RESERVOIR (DRURY, ET AL., 1975)

Essentially, the patterns result from processes that are restricted due to incomplete mixing. The overall effects of such patterns as shown in Figure V-28, are to restrict fishery habitat and create water quality problems for downstream users, especially for deep water discharge.

BOD exertion is not the only sink for DO. Some important sources and sinks of impoundment dissolved oxygen are listed below:

<u>Sources</u>	<u>Sinks</u>
Photosynthesis	Water Column BOD
Atmospheric reaeration	Benthic BOD
Inflowing water	Chemical oxidation
Rainwater	Deoxygenation at surface
	Plant and animal respiration

Many of the processes listed above have a complex nature. For example, the atmospheric reaeration rate is dependent in part upon the near-surface velocity gradient over depth. The gradient, in turn, is influenced by the magnitude, direc-

tion, and duration of wind, as well as the depth and geometry of the impoundment.

Photosynthetic rates are affected by climatological conditions, types of cells photosynthesizing, temperature, and a number of biochemical and biological factors. Exertion of BOD is dependent upon the kind of substrate, temperature, dissolved oxygen concentration, presence of toxicants, and dosing rate.

Despite this degree of complexity, a number of excellent models of varying degrees of sophistication have been developed which include simulation of impoundment dissolved oxygen.

#### 5.5.1 Simulating Impoundment Dissolved Oxygen

Because an unstratified impoundment generally may be considered as a slow-moving stream reach, only stratified impoundments are of interest here. For estimating DO in unstratified impoundments, one should refer to the methods described in Chapter 4.

To understand the phenomena affecting dissolved oxygen in a stratified impoundment and to gain an appreciation of both the utility and limitations of the approach presented later, it is useful to briefly examine a typical dissolved oxygen model. Figure V-29 shows a geometric representation of a stratified impoundment. As indicated in the diagram, the model segments the impoundment into horizontal layers. Each horizontal layer is considered fully mixed at any point in time, and the model advects and diffuses mass vertically into and out of each layer. The constituents and interrelationships modeled are shown schematically in Figure V-30.

The phenomena usually taken into account in an impoundment DO model include:

- Vertical advection
- Vertical diffusion
- Correction for element volume change
- Surface replenishment (reaeration)
- BOD exertion utilizing oxygen
- Oxidation of ammonia
- Oxidation of nitrite
- Oxidation of detritus
- Zooplankton respiration
- Algal growth (photosynthesis) and respiration
- DO contribution from inflowing water
- DO removal due to withdrawals.

Many of the processes are complex and calculations in detailed models involve simultaneous solution of many cumbersome equations. Among the processes simulated are zooplankton-phytoplankton interactions, the nitrogen cycle, and advection-diffusion. Thus it is clear that a model which is comprehensive and potentially capable of simulating DO in impoundments with good accuracy is not appropriate for hand calculations. A large amount of data (coefficients, concentrations) are needed



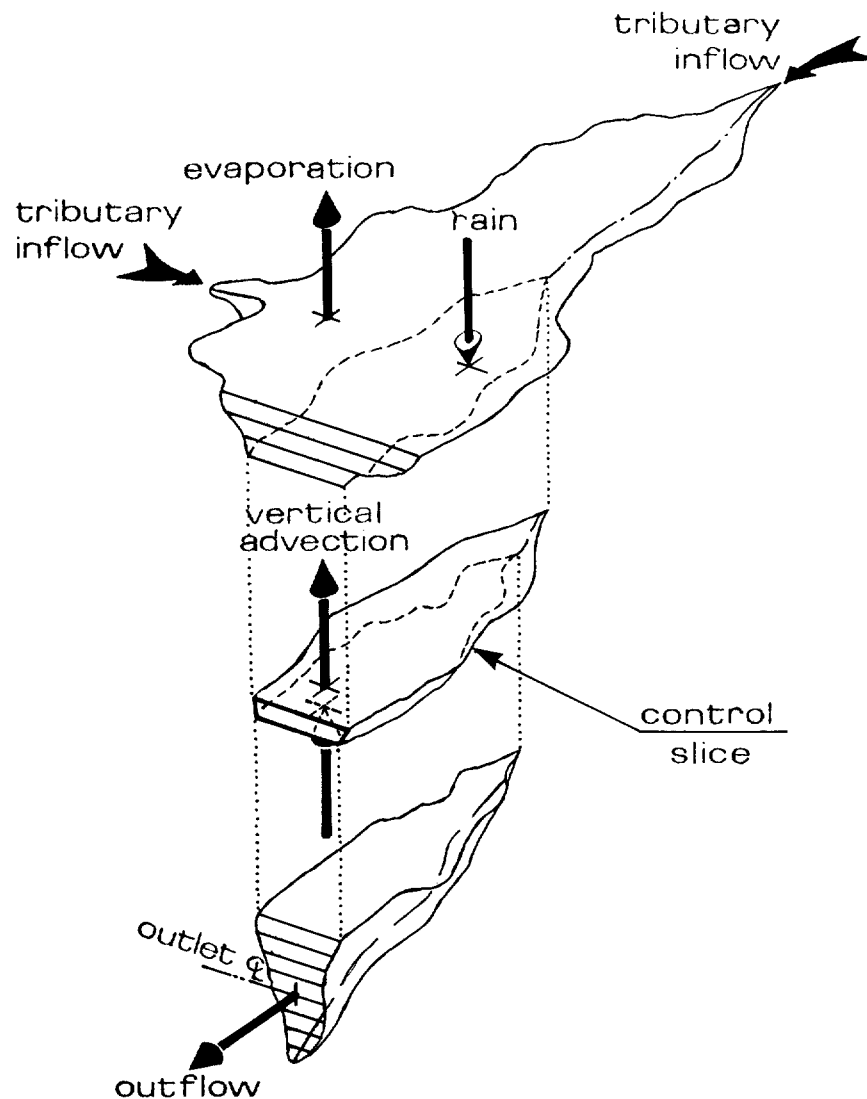


FIGURE V-29 GEOMETRIC REPRESENTATION OF A STRATIFIED IMPOUNDMENT (FROM HEC, 1974)

to apply such a model, and solution is most easily done by computer. Furthermore, some of the terms in the model equation of state do not improve prediction under some circumstances. This is true, for example, where there are no withdrawals or in an oligotrophic impoundment where chlorophyll *a* concentrations are very low.

Hand calculations must be based upon a greatly simplified model to be practical. Since some DO-determining phenomena are more important than others, it is feasible to develop such a model if some assumptions are made about the impoundment itself.

#### 5.5.2 A Simplified Impoundment Dissolved Oxygen Model

For purposes of developing a model for hand calculations, the following assump-

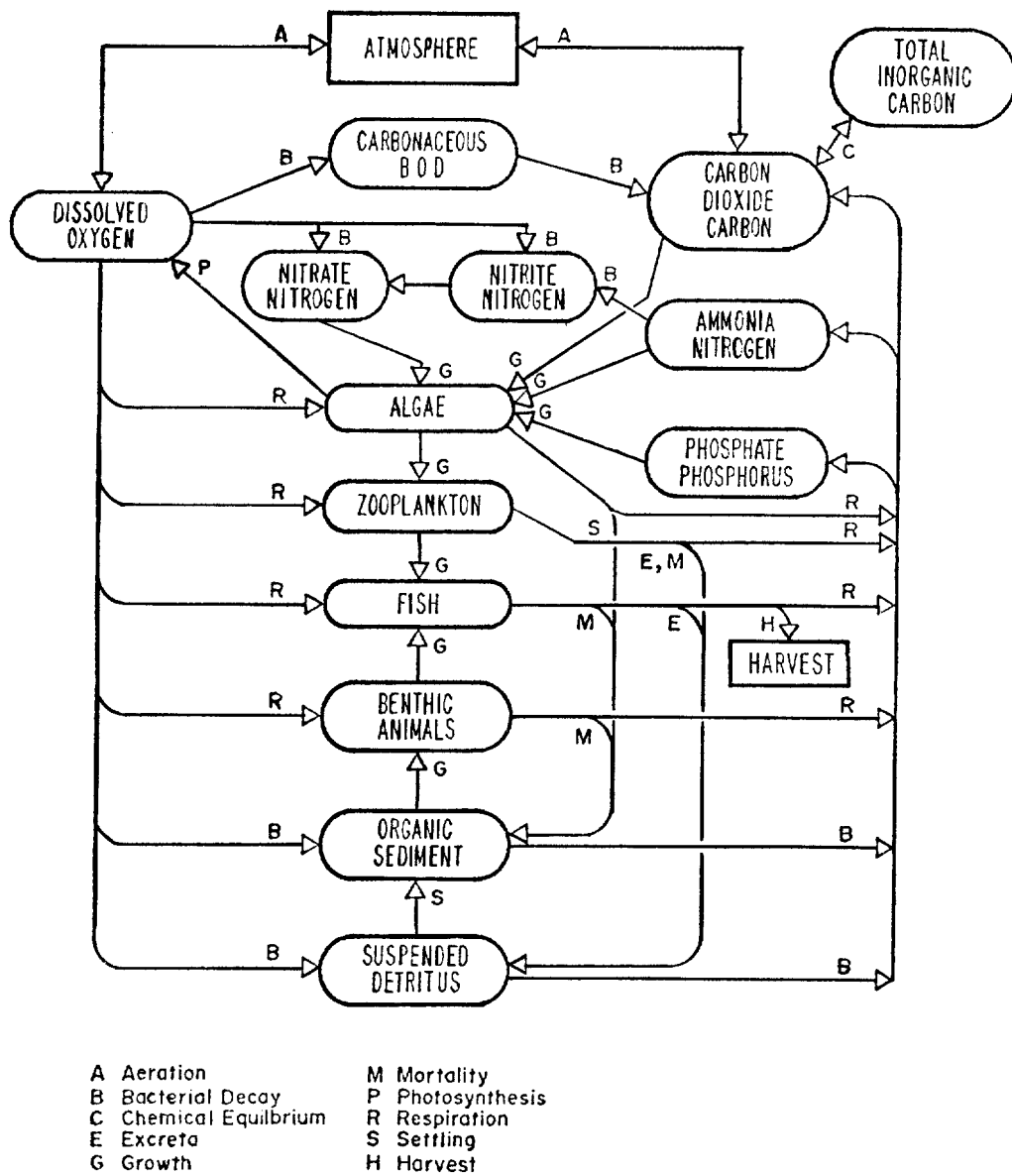


FIGURE V-30 QUALITY AND ECOLOGIC RELATIONSHIPS  
 (FROM HEC, 1974)

tions are made:

- The only condition where DO levels may become dangerously low is in an impoundment hypolimnion and during warm weather.
- Prior to stratification, the impoundment is mixed. After strata form, the epilimnion and hypolimnion are each fully mixed.
- Dissolved oxygen in the hypolimnion is depleted essentially through BOD exertion. Significant BOD sources and sinks to the water column prior to stratification are algal mortality, BOD settling, and outflows. A

minor source is in fluent BOD. Following formation of strata, sources and sinks of BOD are BOD settling out onto the bottom, water column BOD at the time of stratification, and benthic BOD.

- Photosynthesis is unimportant in the hypolimnion as a source of DO.
- Once stratification occurs (a thermocline gradient of 1°C or greater per meter of depth) no mixing of thermocline and hypolimnion waters occurs.
- BOD loading to the unstratified impoundment and to the hypolimnion are in steady-state for the computation period.

#### 5.5.2.1 Estimating a Steady-State BOD Load to the Impoundment

Equation V-25 is an expression to describe the rate of change of BOD concentration as a function of time:

$$\frac{dC}{dt} = k_a - k_s C - k_1 C - \frac{QC}{V} \quad (V-25)$$

where

- $c$  = the concentration of BOD in the water column in  $\text{mg l}^{-1}$
- $k_a$  = the mean rate of BOD loading from all sources in  $\text{mg l}^{-1} \text{ day}^{-1}$
- $k_s$  = the mean rate of BOD settling out onto the impoundment bottom in  $\text{day}^{-1}$
- $k_1$  = the mean rate of decay of water column BOD in  $\text{day}^{-1}$
- $Q$  = mean export flow rate in liters  $\text{day}^{-1}$
- $V$  = impoundment volume in liters.

Integrating Equation V-25 gives:

$$C_t = \frac{(k_a + k_b C_0) e^{(k_b t)} - k_a}{k_b} \quad (V-26)$$

where

- $C_t$  = concentration of BOD at time  $t$
- $C_0$  = initial concentration of BOD
- $k_b = -k_s - k_1 - \frac{Q}{V}$

To estimate the steady-state loading of BOD, we set  $dc/dt = 0$  and obtain:

$$C_{ss} = -\frac{k_a}{k_b} \quad (V-27)$$

where

- $C_{ss}$  = steady-state water column BOD.

Thus Equation V-27 may be used to estimate a steady-state water column BOD concentration and Equation V-26 may be used to compute BOD as a function of time, initial concentration of BOD, and the various rates.

### 5.5.2.2 Rates of Carbonaceous and Nitrogenous Demands

The rate of exertion of BOD and therefore the value of  $k_1$  is dependent upon a number of physical, chemical, and biological factors. Among these are temperature, numbers and kinds of microorganisms, dissolved oxygen concentration, and the kind of organic substance involved. Nearly all of the biochemical oxygen demand in impoundments is related to decaying plant and animal matter. All such material consists essentially of carbohydrates, fats, and proteins along with a vast number of minor constituents. Some of these are rapidly utilized by bacteria, for example, the simple sugars, while some, such as the cellulose, are metabolized slowly.

Much of the decaying matter in impoundments is carbonaceous. Carbohydrates (cellulose, sugars, starches) and fats are essentially devoid of nitrogen. Proteins, on the other hand, are high in nitrogen (weight of carbon/ weight of nitrogen  $\approx 6$ ) and proteins therefore represent both carbonaceous and nitrogenous demands.

The rate of exertion of carbonaceous and nitrogenous demands differ. Figure V-31, which shows the difference graphically and as a function of time and temperature, may be considered to represent the system response to a slug dose of mixed carbonaceous and nitrogenous demands. In each two-section curve, especially where concentrated carbonaceous wastes are present, the carbonaceous demand is exerted first, and this represents the first stage of deoxygenation. Then nitrifiers increase in numbers and ammonia is oxidized through nitrite and ultimately to nitrate. This later phase is called the second phase of deoxygenation.

BOD decay (either nitrogenous or carbonaceous alone) may be represented by first order kinetics. That is, the rate of oxidation is directly proportional to the amount of material remaining at time  $t$ :

$$\frac{dC}{dt} = -kC \quad (V-28)$$

The rate constant,  $k$ , is a function of temperature, bacterial types and numbers, composition and structure of the substrate, presence of nutrients and toxicants, and a number of other factors. The value of the first stage constant  $k_1$  was first determined by Phelps in 1909 for sewage filter samples. The value was 0.1 (Camp, 1968). More recent data show that at 20°C, the value can range from 0.01 for slowly metabolized industrial waste organics to 0.3 for relatively fresh sewage (Camp, 1968).

The typical effect of temperature on organic reactions is to double reaction rates for each temperature rise of 15°C. The relationship for correcting  $k_1$  for temperature is:

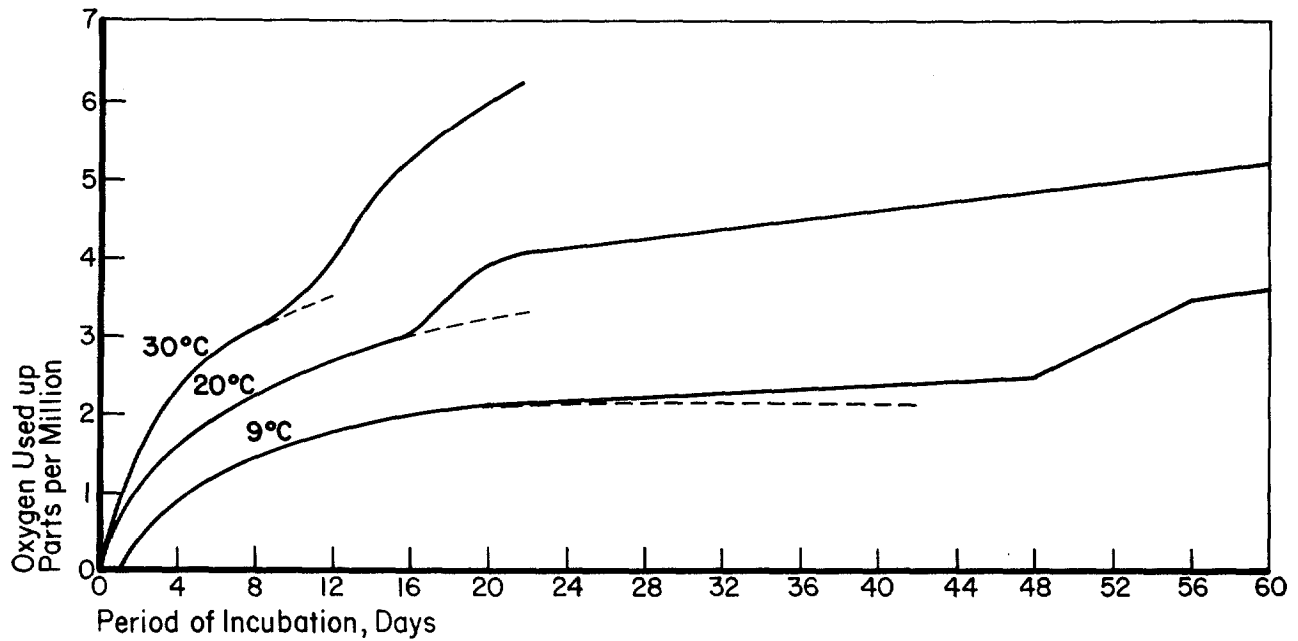


FIGURE V-31 RATE OF BOD EXERTION AT DIFFERENT TEMPERATURES SHOWING THE FIRST AND SECOND DEOXYGENATION STAGES

$$k_{1,(T)} = k_{1,(20^{\circ}\text{C})} \theta^{(T-20)} \quad (\text{V-29})$$

where

T = the temperature of reaction

$\theta$  = correction constant = 1.047.

However, Thereault has used a value for  $\theta$  of 1.02, while Moore calculated values of 1.045 and 1.065 for two sewages and 1.025 for river water (Camp, 1968).

Streeter has determined the rate of the vitrification or second deoxygenation stage in polluted streams. At 20°C,  $k_1$  for vitrification is about 0.03 (Camp, 1968). Moore found the value to be .06 at 20°C and .035 at 10°C (Camp, 1968). For purposes of this analysis, BOD exertion will be characterized as simple first order decay using a single rate constant.

Benthic demand, which is important in later computations, may vary over a wide range because in addition to the variability due to the chemical nature of the benthic matter, rates of oxidation are limited by upward diffusion rates of oxidizable substances through pores in the benthos. Since the nature of the sediment is highly variable, benthic oxygen demand rates vary more than values for  $k_1$  in the water column. In a study using sludges through which oxygenated water was passed, initial rates of demand ranged from 1.02 g/m<sup>2</sup> day (see Table V-n) for a sludge depth of 1.42 cm to 4.6 g/m<sup>2</sup> day for a sludge depth of 10.2 cm (Camp, 1968).

TABLE V-11  
OXYGEN DEMAND OF BOTTOM DEPOSITS  
(AFTER CAMP, 1968)

Benthic Depth (mean) cm	Initial Volume of Solids, kgm <sup>-2</sup>	Initial Area Demand		day <sup>-1</sup> k <sub>4</sub> (20° C)
		L (gm <sup>-2</sup> )	initial Demand gm <sup>-2</sup> day <sup>-1</sup>	
10.2	3.77	739	4.65	.0027
4.75	1.38	426	3.09	.0031
2.55	0.513	227	1.70	.0032
1.42	0.188	142	1.08	.0033
1.42	0.188	134	1.02	.0033

In that study, the values found were for initial demand since the sludge was not replenished. The rate per centimeter of sludge depth, then, can vary from a low of 0.46 g/m<sup>2</sup> day for 10.2 centimeter depth sludge up to 0.76 g/m<sup>2</sup> day for 1.42 centimeter depth sludge.

The constant loading rate ( $k_a$ ) used in Equation V-25 is best estimated from historical data. Alternatively, inflow loading (see Chapter IV) and algal productivity estimates (this chapter) may be used. In the latter case, a value must be adopted for the proportion of algal biomass ultimately exerted as BOD. To a first approximation,  $k_a$  may be estimated using this value and adopting some percentage of maximal primary productivity (see Figure V-25). Thus:

$$k_a(\text{algae}) = \text{SMP} \times 10^{-3}/D \quad (\text{V-30})$$

where

- $k_a(\text{algae})$  = algal contribution to BOD loading rate
- s = stoichiometric conversion from algal biomass as carbon to BOD = 2.67
- M = proportion of algal biomass expressed as an oxygen demand (unitless)
- P = Primary production in mgCm<sup>-2</sup>day<sup>-1</sup>.

The difference between algal biomass and the parameter M representing the proportion of algal biomass exerted as BOD may be conceptualized as accounting for such phenomena as incorporation of algal biomass into fish tissue which either leaves the impoundment or is harvested, loss of carbon to the atmosphere as CH<sub>4</sub>, and loss

due to outflows.

The settling rate coefficient,  $k_s$  in Equation V-25 must be estimated for the individual case. It represents the rate at which dead plant and animal matter (detritus) settles out of the water column prior to oxidation. Clearly, this coefficient is sensitive to the composition and physical characteristics of suspended matter and the turbulence of the system. Quiescence and large particle sizes in the organic fraction will tend to give high values for  $k_s$  while turbulence and small organic fraction particle sizes will give small values for  $k_s$ .

#### 5.5.2.3 Estimating a Pre-Stratification Steady-State Dissolved Oxygen Level

Prior to stratification, the impoundment is assumed to be fully mixed. One of the important factors leading to this condition is wind stress, which also serves to reaerate the water. As a rule, unless an impoundment acts as a receiving body for large amounts of nutrients and/or organic loading, dissolved oxygen levels are likely to be near saturation during this period (D.J. Smith, pers. comm., November, 1976). Table V-12 shows saturation dissolved oxygen levels for fresh and saline waters as a function of temperature and chloride concentrations, and DO levels may be estimated accordingly.

The hypolimnetic saturation dissolved oxygen concentration is determined by using the average (or median) temperature for the hypolimnion as determined during the period of interest throughout the depth of the hypolimnion. Information on the hypolimnion is obtained using the procedures described in Section 5.2. For example, hypolimnetic water at the onset of stratification might be 4-5°C and during the critical summer months be 10°C. The value 10°C should be used having a saturation DO of 11.3 mg/l.

Most lakes are near sea level (<2000 ft elevation) and are relatively fresh (<2000mg TDS/l). For lakes that do not meet these criteria, corrections for atmospheric pressure differences and salting out due to salinity might be needed. Pressure effects can be approximated by using a ratio of barometric pressure (B) for the elevation of interest and sea level (BSTP) as follows:

e.g. B at 4600 ft elevation,

$$\frac{B}{BSTP} = \frac{640}{760}, \text{ in mm Hg,} \\ = 0.84$$

$$DO_{\text{sat at } 10^\circ\text{C}} = 0.84 \times 11.3 \\ = 9.5 \text{ mg/l.}$$

Chloride is an estimator of dilutions of sea water in fresh water where 20000 mg Chloride/l is equivalent to 35000 mg salt (TDS/l), that is, typical ocean water.

TABLE V-12

## VOLUBILITY OF OXYGEN IN WATER (STANDARD METHODS, 1971)

Temp. in °C	Chloride Concentration in Water - mg/l					Di fference per 100 mg Chl ori de
	0	5,000	10,000	15,000	Sea Water	
	Di ssol ved Oxygen - mg/l					
0	14.6	13.8	13.0	12.1	11.3	0.017
1	14.2	13.4	12.6	11.8	11.0	0.016
2	13.8	13.1	12.3	11.5	10.8	0.015
3	13.5	12.7	12.0	11.2	10.5	0.015
4	13.1	12.4	11.7	11.0	10.3	0.014
5	12.8	12.1	11.4	10.7	10.0	0.014
6	12.5	11.8	11.1	10.5	9.8	0.014
7	12.2	11.5	10.9	10.2	9.6	0.013
8	11.9	11.2	10.6	10.0	9.4	0.013
9	11.6	11.0	10.4	9.8	9.2	0.012
10	11.3	10.7	10.1	9.6	9.0	0.012
11	11.1	10.5	9.9	9.4	8.8	0.011
12	10.8	10.3	9.7	9.2	8.6	0.011
13	10.6	10.1	9.5	9.0	8.5	0.011
14	10.4	9.9	9.3	8.8	8.3	0.010
15	10.2	9.7	9.1	8.6	8.1	0.010
16	10.0	9.5	9.0	8.5	8.0	0.010
17	9.7	9.3	8.8	8.3	7.8	0.010
18	9.5	9.1	8.6	8.2	7.7	0.009
19	9.4	8.9	8.5	8.0	7.6	0.009
20	9.2	8.7	8.3	7.9	7.4	0.009
21	9.0	8.6	8.1	7.7	7.3	0.009
22	8.8	8.4	8.0	7.6	7.1	0.008
23	8.7	8.3	7.9	7.4	7.0	0.008
24	8.5	8.1	7.7	7.3	6.9	0.008
25	8.4	8.0	7.6	7.2	6.7	0.008
26	8.2	7.8	7.4	7.0	6.6	0.008
27	8.1	7.7	7.3	6.9	6.5	0.008
28	7.9	7.5	7.1	6.8	6.4	0.008
29	7.8	7.4	7.0	6.6	6.3	0.008
30	7.6	7.3	6.9	6.5	6.1	0.008
31	7.5					
32	7.4					
33	7.3					
34	7.2					
35	7.1					



#### 5.5.2.4 Estimating Hypolimnion DO Levels

The final step in use of this model is preparation of a DO-versus-time plot for the hypolimnion (or at least estimation of DO at incipient overturn) and estimation of BOD and phosphorus loadings which result in acceptable hypolimnion DO levels. An equation to compute DO at any point in time during the period of stratification is:

$$\frac{dO}{dt} = -k_1C - k_4L/D \quad (V-31)$$

where

- O = dissolved oxygen in ppm
- k<sub>4</sub> = benthic decay rate in day<sup>-1</sup>
- L = areal BOD load in gm<sup>-2</sup>
- D = depth in m.

The second term in the equation requires that an estimate be made of the magnitude of BOD loading in benthic deposits. To do this within the present framework, it is assumed that BOD settles out throughout the period of stratification. Although many different assumptions have been made concerning benthic BOD decay, it was assumed that benthic demand was a function of BOD settling and the rate of benthic BOD decay. This BOD includes that generated in the system by algal growth and that which enters in tributaries and waste discharges. Based upon the rate of settling used earlier in estimating a steady-state BOD concentration (Equation V-25) and rate of decay for conditions prior to stratification, the rate of benthic matter accumulation is:

$$\frac{dL}{dt} = k_s C_{SS} D - k_4 L \quad (V-32)$$

where

C<sub>SS</sub> = concentration of BOD in the water column in gm<sup>-3</sup> at steady-state. The assumption of steady-state BOD concentration reduces Equation V.32 to the same form as Equation V-25 and integration gives:

$$L_t = \frac{(k_s D C_{SS} - k_4 L_0) e^{-k_4 t} - k_s D C_{SS}}{-k_4} \quad (V-33)$$

For steady-state deposition (dL/dt = 0, Dk<sub>s</sub>C<sub>SS</sub> = constant):

$$L_{SS} = \frac{k_s C_{SS} D}{k_4} \quad (V-34)$$

where

$L_{SS}$  = steady-state benthic BOD load in  $gm^{-2}$ .

Application of Equation V-34 with  $k_5$  and  $k_4$  appropriately chosen for the month or two preceding stratification will give an estimate of the benthic BOD load upon stratification. Application of Equation V-33 gives the response of L to different water column BOD (steady-state) loading rates and changes in rate coefficients.

After strata form, benthic matter decays while hypolimnion water column BOD decays and settles. The change in L over the period of stratification is:

$$\frac{dL}{dt} = -k_4L + Dk_5C \quad (V-35)$$

Since

$$\frac{dC}{dt} = -k_5C - k_1C = -(k_1+k_5)C \quad (V-36)$$

and

$$C_t = C_0 e^{-(k_1 + k_5)t} \quad (V-37)$$

$$\frac{dL}{dt} = -k_4L + Dk_5C_0e^{-(k_1 + k_5)t} \quad (V-38)$$

then

$$L_t = \left( L_0 + \frac{Dk_5C_0}{k_5+k_1-k_4} \right) e^{-k_4t} - \left( \frac{Dk_5C_0}{k_5+k_1-k_4} \right) e^{-(k_5+k_1)t} \quad (V-39)$$

Water column BOD in the hypolimnion is given by Equation V-36 and the integrated form is Equation V-37.

Note that  $k_5$ , the settling coefficient is equal to  $v_s/D$  where  $v_s$  is the settling velocity of the BOD, and D is the depth of the hypolimnion (or when the impoundment is unstratified, D is the depth of the entire impoundment). Also note that we usually assume that the D0 is at saturation at the onset of stratification. Thus we can ignore the assumptions and calculations (Equation V-32 to V-34) done for periods prior to onset.

The equation presented earlier (Equation V-31) for hypolimnion D0 was:

$$\frac{dD_0}{dt} = -k_1C - k_4L/D$$

Equation V-31 is not integrable in its present form, but since L and C are defined as functions of t (Equations V-39 and V-37 respectively), it is possible to determine dissolved oxygen in the water column. The equation for oxygen at time t is:

$$O_t = O_0 - \Delta O_L - \Delta O_C \quad (V-40)$$

where

$O_t$  = dissolved oxygen at time t

$O_0$  = dissolved oxygen at time t = 0

$\Delta O_L$  = dissolved oxygen decrease due to benthic demand

$\Delta O_C$  = dissolved oxygen decrease due to hypolimnion BOD.

From Equation V-39, and using  $L_{SS}$  as  $L_0$  and  $C_{SS}$  as  $C_0$ :

$$\Delta O_L = \left( \frac{L_{SS}}{D} + \frac{k_s C_{SS}}{k_s + k_1 - k_4} \right) \left( 1 - e^{-k_4 t} \right) - \left( \frac{k_s C_{SS}}{k_s + k_1 - k_4} \right) \left( \frac{k_4}{k_s + k_1} \right) \left( 1 - e^{-(k_s + k_1)t} \right) \quad (V-41)$$

and from Equation V-37:

$$\Delta O_C = \frac{k_1 C_{SS}}{k_1 + k_s} \left( 1 - e^{-(k_1 + k_s)t} \right) \quad (V-42)$$

Solution of Equation V-40 gives an estimated DO concentration in the hypolimnion as a function of time.

To compute equation V-40, a simpler form of equation V-41 can be derived by substituting as follows:

$$\text{since } L_{SS} = \frac{k_{SS} C_{SS} D}{k_4},$$

$$\Delta O_L = \left( \frac{k_s C_{SS}}{k_s + k_1 - k_4} \right) \left( \frac{k_s + k_1}{k_4} \right) \left( 1 - e^{-k_4 t} \right) - \left( \frac{k_4}{k_s + k_1} \right) \left( 1 - e^{-(k_s + k_1)t} \right) \quad (V-43)$$

To simplify computations, the following stepwise solutions can be made:

$$A = \frac{k_s C_{SS}}{k_s + k_1 - k_4}$$

$$B = \frac{k_s + k_1}{k_4}$$

$$C = 1 - e^{-k_4 t}$$

$$E = 1 - e^{-(k_s + k_1)t}$$

$$F = \frac{k_1 C_{SS}}{k_1 + k_s}$$

then

$$\Delta O_L = A \left( B \cdot C - \frac{E}{B} \right)$$

$$\Delta O_C = E \cdot F$$

### 5.5.3 Temperature Corrections

All reactions are computed on the basis of the optimum temperature, but the environment is often at different temperatures. Some rate coefficients for chemical and biological reactions vary with temperature. A simple correction for such rate coefficients to 20°C is as follows:

$$K_T = K_{T20} \times 1.047^{(T - 20^\circ\text{C})}$$

For example, if a rate at 20°C = 0.01 and the lake is at 10°C, then:

$$K_T = 0.01 \times 1.047^{(10 - 20)}$$

$$K_T = 0.00632.$$

Generally the following optima are used:

$k_1$  - first order decay rate for water column BOD,  
use 20°C

$k_4$  - benthic BOD decay, use 20°C

P - productivity rate, use 30°C.

In the screening methods we do not have to correct for temperature except in the oxygen calculation for the rate coefficients,  $K_1$ ,  $K_4$ , P and in the toxics section (5.6) for the biodegradation rate coefficients.

#### EXAMPLE V-15

##### Quiet Lake (Comprehensive Example)

Quiet Lake is located a few miles south of Colton, New York. The lake is roughly circular in plan view (Figure V-32) and receives inflows from three tributaries. There is one natural outlet from the lake and one withdrawal used for quarrying purposes.

The first step in evaluation of lake hypolimnion DO levels is physical and water quality data collection. Table V-13 shows characteristics of Quiet Lake, Table V-14 shows tributary discharge data along with withdrawal and outflow levels, and Table V-15 provides precipitation and runoff information.

In order to evaluate hypolimnion DO as a function of time, the very first question to be answered is, does the impoundment stratify? If so, what are the beginning and ending dates of the stratified period, how deep is the upper surface

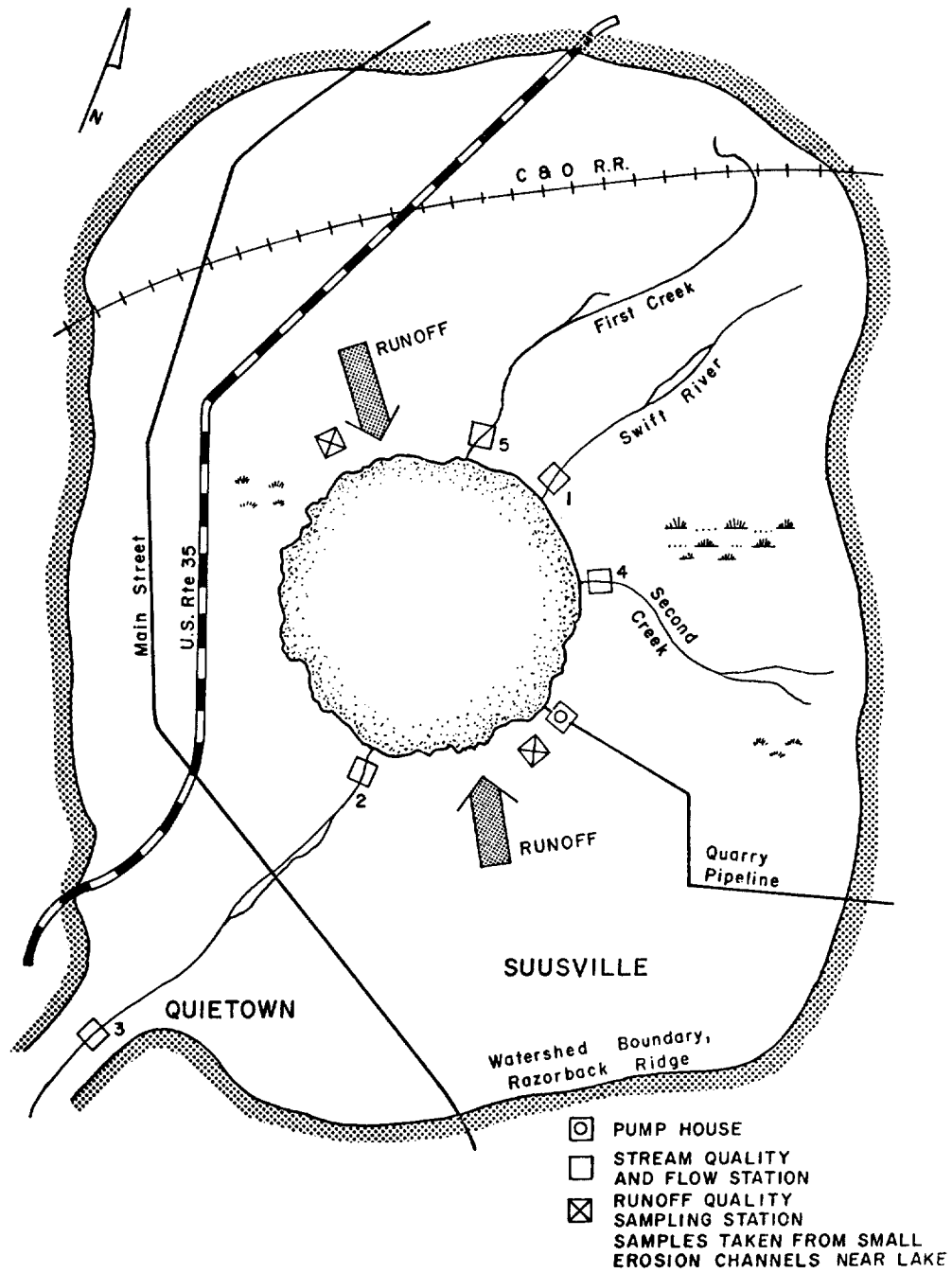


FIGURE V-32 QUIET LAKE AND ENVI RONS

TABLE V-13

## CHARACTERISTICS OF QUIET LAKE

Length (in direction of flow)	3.5 miles = 18,480 ft.
Width	4.0 miles = 21,120 ft.
Mean Depth	22 ft.
Maximum Depth	27 ft.
Water Column P	0.014 <math>\leq P \leq</math> 0.032

TABLE V-14

WATER QUALITY AND FLOW DATA FOR TRIBUTARIES TO QUIET LAKE.  
DATA REPRESENT MEAN FIGURES FOR 1970-1975.

Swift River (Station 1, above Quiet Lake)				
Month	Mean Flow, cfs	Total N	Total P ppm	BOD
October	54	2.2	0.2	3
November	38	4.?	0.08	4
December	10	5.3	0.10	6
January	5	6.1	0.20	12
February	2	5.0	0.15	10
March	8	4.3	0.08	12
April	40	3.3	0.04	10
May	55	2.1	0.02	8
June	85	2.8	0.02	4
July	150	2.9	0.02	2
August	70	1.0	0.02	1
September	85	2.4	0.03	1

TABLE V-14 (Continued)

<u>First Creek (Station 5)</u>				
<u>Month</u>	<u>Mean Flow, cfs</u>	<u>Total N</u>	<u>Total P</u>	<u>BOD</u>
			ppm	
October	5	1.0	.01	0.5
November	3	2.0	.01	1.0
December	2	0.5	.02	1.5
January	2	1.2	.01	1.0
February	3	1.3	.02	0.8
March	4	2.3	.01	0.6
April	6	2.0	.01	0.5
May	8	1.8	.02	0.6
June	10	1.6	.01	0.8
July	8	1.4	.01	0.8
August	6	1.5	.00	1.0
September	4	0.8	.00	1.2

<u>Second Creek (Station 4)</u>				
<u>Month</u>	<u>Mean Flow, cfs</u>	<u>Total N</u>	<u>Total P</u>	<u>BOD</u>
			ppm	
October	14.0	15	.15	7
November	13.0	16	.08	8
December	12.5	10	.20	10
January	5.0	9	.15	7
February	1.2	12	.12	7
March	2.0	13	.10	6
April	2.5	8	.11	7
May	4.0	6	.07	9
June	8.0	5	.08	12
July	12.0	7	.20	3
August	8.0	6	.22	4
September	5.5	8	.25	8

TABLE V-14 (Continued)

Swift River (Stations 2 and 3) and Pumped Withdrawal			
Month	Pumped Withdrawal, cfs	Mean Monthly Flow, cfs	
		Station 2	Station 3
October	22.6	69.5	77.0
November	22.0	50.0	55.0
December	3.5	20.0	22.0
January	1.2	7.5	9.0
February	0.8	1.2	1.4
March	0.4	9.1	10.1
April	12.0	44.5	48.75
May	24.0	63.2	69.5
June	30.7	100.0	110.0
July	89.5	168.5	184.8
August	29.8	80.6	88.5
September	43.9	91.3	100.25

Notes: All three tributaries have their headwaters within the shed. The net inflow-outflow to the groundwater is known to be close to zero in the two creeks. Swift River is usually about 10% effluent over its entire length (10% of flow comes into the river from the groundwater table).

of the hypolimnion, and what is its volume, and what is the distribution of hypolimnion mean temperatures during the period? To answer these questions, either use field observation data, or apply some computation technique such as that presented earlier in this section. Assuming that methods presented earlier are used, the selection of appropriate thermal profile curves hinges around three factors. These are:

- Climate and location
- Hydraulic residence time
- Impoundment geometry.



TABLE V-15

PRECIPITATION AND RUNOFF DATA FOR QUIET LAKE WATERSHED.  
 VALUES ARE MEANS OF DATA COLLECTED FROM BOTH STATIONS  
 (SEE FIGURE V- 31). THE WATERSHED HAS AN AREA OF 55  
 SQUARE MILES INCLUDING THAT OF THE LAKE

	Mean Total Monthly Precipitation, inches	Runoff Quality		
		Total N	Total P	BOD ppm
October	3.0	6.0	0.1	27
November	2.4	6.5	0.2	37
December	1.0	4.0	0.1	46
January	0.5	3.0	0.008	34
February	0.3	1.0	0.07	33
March	0.6	1.5	0.1	30
April	2.0	2.5	0.15	40
May	2.8	3.2	0.25	50
June	4.2	3.6	0.20	40
July	7.6	7.0	0.40	37
August	3.5	7.8	0.60	45
September	4.2	9.2	0.80	50
<u>Total</u>	32.1			

Note: Infiltration to the water table on a monthly basis accounts for roughly 30% of precipitation volume.

In terms of climate and location, the Quiet Lake area is similar to Burlington, Vermont. Examination of the Burlington plots from Appendix D reveals that a 20-foot maximum depth impoundment can stratify in an area shielded from the wind. The area surrounding Quiet Lake does provide good shielding, so the next task is to estimate the hydraulic residence time to select a specific set of plots.

Inspection of all Burlington plots indicates that stratification is likely to occur at most from May to August. Accordingly, for purposes of plot selection, we are most interested in a mean hydraulic residence time based on flows in the period from about March to August. Since hydraulic residence time ( $\tau_w$ ) is given by  $t_w = V/Q$ , we compute mean  $Q$  ( $\bar{Q}$ ).  $\bar{Q}$  represents the



have their headwaters within the watershed. If one were concerned about a subshed with tributary headwaters above the subshed boundary, the difference in Q between each of stations 1, 4, and 5 and the respective flows at the upstream subshed boundary would be used.

To estimate hydraulic residence time add the mean stormwater contribution over the months of interest to that of the tributaries, as computed earlier. The individual stormwater computations are not shown. The method is as just described.

$$\bar{Q}_{\text{total}} = 81.1 + \frac{6.6 + 20.7 + 29.4 + 41.4 + 92.5 + 36.6}{6} = 119 \text{ cfs}$$

Then the hydraulic residence time is given by:

$$\tau_w = V/Q \approx \pi r^2 D/Q$$

$$r = \left[ \frac{L+W}{4} \times 5280 \right]$$

where

L = length of the lake in mi

W = width of the lake in mi

D = mean depth in ft

r = radius in ft.

$$\tau_w = 3.14 \times \left[ \frac{3.5+4}{4} \times 5280 \right]^2 \times 22/119$$

$$= 5.69 \times 10^7 \text{ sec} = 658 \text{ days}$$

Accordingly, the infinite hydraulic residence time plots for a 20-foot deep, wind-protected, Burlington, Vermont, impoundment should suffice. Note that the entire impoundment volume was used in the above computation. Strictly, one should use the epilimnion volume during stratification. In this case, such a change would not alter selection of the plots because  $\tau_w$  would still be greater than 200 days. A reproduction of the appropriate plot from Appendix D is presented in Figure V-33. As indicated, Quiet Lake is likely to be weakly stratified from May to August inclusive, with a thermocline temperature gradient of about  $1^\circ \text{ft}^{-1}$ . The hypolimnion should extend downward to the bottom from a depth of about 3-1/2 meters, giving a mean hypolimnion depth of:

$$D_H = \frac{22 \text{ ft}}{3.29 \text{ ft m}^{-1}} - 3.5 \text{ m} = 3.2 \text{ meters}$$

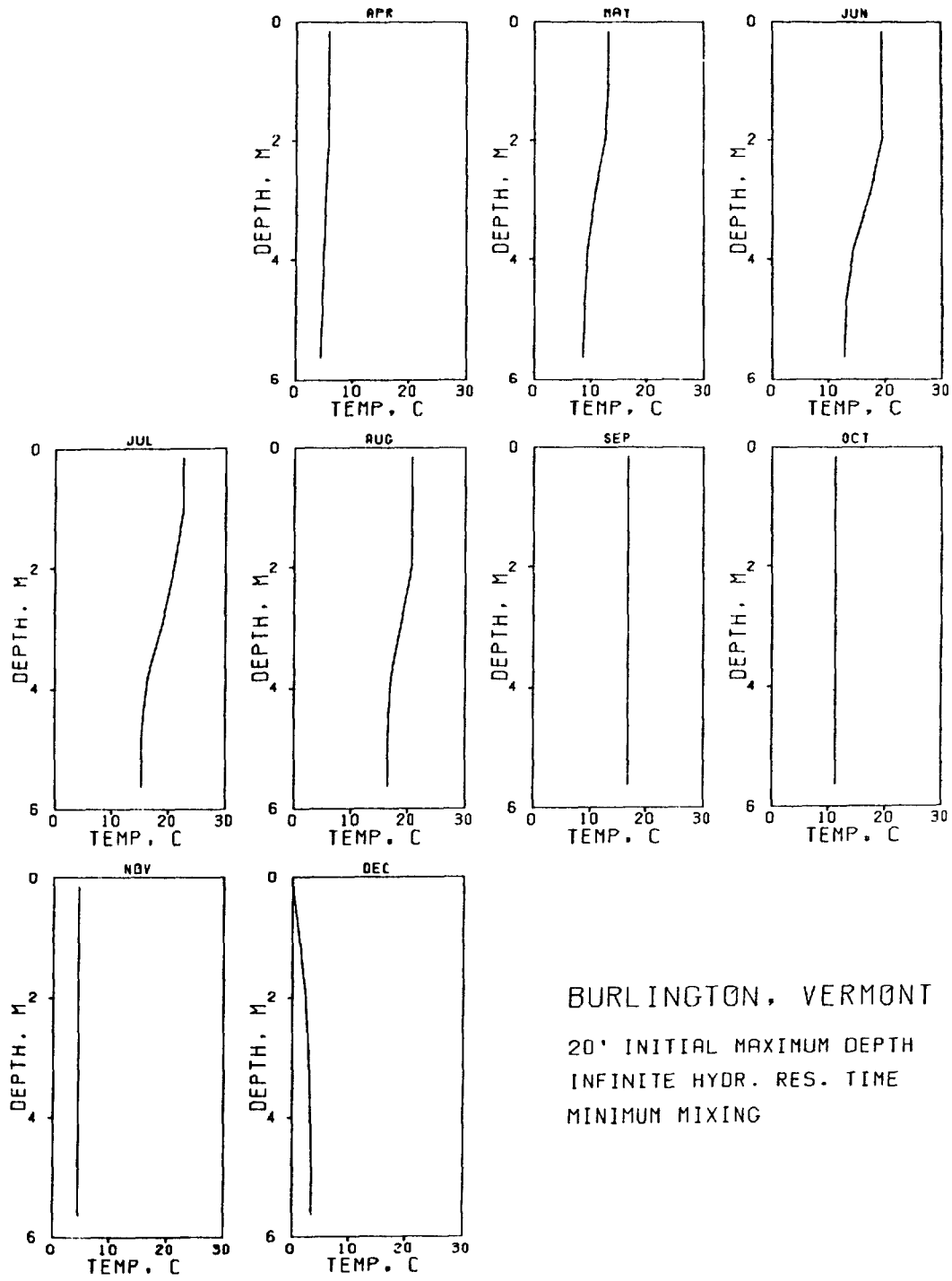


FIGURE V-33 THERMAL PROFILE PLOTS FOR USE IN QUIET LAKE EXAMPLE

The approximate hypolimnion volume, then, is:

$$V_H = \frac{D_H}{D_{Total}} \times V_{Total}$$

$$V_H = \frac{3.2\text{m}}{6.7\text{m}} \times 1.9 \times 10^{11} \text{L} = 9.2 \times 10^{10} \text{L}$$

Over the period of interest, the hypolimnion mean temperature distribution is:

Month	Mean Temperature, °C
March	2.0
April	5.5
May	9.5
June	12.5
July	14.0
August	15.5

The next step in use of the DO model is to determine a steady-state or mean water column BOD loading ( $k_a$ ) and DO level prior to stratification. This is a multi-step process because of the several BOD sources. The sources are tributaries, runoff, and primary productivity. First, we estimate algal productivity using methods of this chapter (or better, field data).

Using the curve in Figure V-26 and phosphorus data from Table V-14, the maximal primary productivity should be in the range  $1,400 \text{ mg Cm}^{-2}\text{day}^{-1}$  to  $1,900 \text{ mg Cm}^{-2}\text{day}^{-1}$ . To convert to loading in  $\text{mg l}^{-1}\text{day}^{-1}$ , divide by  $(1000 \text{ l m}^{-3} \times 6.7\text{m})$ . This gives the loading as 0.21 to  $0.28 \text{ mg l}^{-1}\text{day}^{-1}$ .

Now assuming that maximal productivity occurs at about  $30^\circ\text{C}$  and that productivity rates obey the same temperature rule as BOD decay, temperature-adjusted estimates of productivity rates can be made. Using the maximal rate range of 0.21 to  $0.28 \text{ mg l}^{-1}\text{day}^{-1}$ , the adjusted rates are:

$$\begin{aligned} \text{Productivity} &= (0.21, 0.28) \times 1.047^{(3.75-30)} \\ &= (.06, .08) \text{ mg l}^{-1} \text{ day}^{-1} \end{aligned}$$

Then, according to Equation V-30 and assuming  $M = 1$ ,  $k_a$  due to algae is estimated by:

$$k_a(\text{algae}) = 2.67 \times (.06, .08) = (.16, .21) \text{ mg l}^{-1}\text{day}^{-1}$$

The next contributor to water column BOD is BOD loading of inflowing waters. The value to be computed is the loading in milligrams per liter of impoundment water per day:

$$\text{Daily BOD Loading rate} = \left( \sum_{i=1}^n \sum_{j=1}^{L_i} d_i Q_{i,j} C_{i,j} \right) / \sum_{k=1}^n d_k$$

where

$n$  = the number of time periods of measurement

$V$  = volume of impoundment in liters

$d$  = the number of days per time period

$L$  = the number of inflows.

For all inflows, the value is therefore approximately:

$$k_a(\text{Trib}) = (2185 + 48.3 + 643.9 + 14240) \times 2.45 \times 10^6 \times \frac{1}{1.9 \times 10^{11}}$$

(Swift River)
(First Creek)
(Second Creek)
(Storm water Runoff)
(Units Conversion)
(Impoundment Volume)

$$= 0.22 \text{ mg l}^{-1} \text{ day}^{-1}$$

Now, summing the two contributions:

$$k_a = k_a(\text{algae}) + k_a(\text{Trib})$$

$$k_a = (.16, .21) + .22 = (.38, .43) \text{ mg l}^{-1} \text{ day}^{-1}$$

The value of  $k_1$  will be assumed as 0.1 at 20°C with  $\theta$  in Equation (V-29) equal to 1.047. Then at 3.75°C:

$$k_1(3.75^\circ\text{C}) = k_1(20^\circ\text{C}) \times 1.047^{(3.75-20)}$$

$$= .1 \times 1.047^{(-16.25)} = 0.047$$

Now  $Q(\text{discharge})$  (mean for March and April) and  $V$  are known, with:

$$Q(\text{discharge}) = 26.8 \text{ (Swift River, Station 2)}$$

$$+ 6.2 \text{ (pumped withdrawal)} \times \frac{28.32 \text{ ft}^3}{\text{sec}} = 935 \text{ ft}^3 \text{ sec}^{-1}$$

$$V = 1.9 \times 10^{11} \text{ ft}^3$$

then

$$C_{ss} = \frac{.38, .43}{(0.3 + .047 + (935/1.9 \times 10^{11}))} = 4.94, 5.58$$

For further computations,  $C_{ss} = 5.25$  will be assumed.

Since  $k_s$  has been defined as .03, a steady-state areal concentration of benthic BOD prior to stratification can be estimated. If  $k_4(20^\circ\text{C}) = .003$  and  $C_{ss} = 5.25$ , using Equation (V-34):

$$L_{ss} = \frac{k_s C_{ss} D}{k_4(3.75^\circ\text{C})}$$

$$k_4(3.75^\circ\text{C}) = .003 \times 1.047^{(3.75-20)}$$

$$= .0014$$

$$L_{ss} = \frac{.03 \times 5.25 \times 6.7}{.0014}$$

$$= 754 \text{ gm}^{-2}$$

The next step in evaluating hypolimnion DO depression is to estimate pre-stratification DO levels. If we assume saturation at the mean temperature in April (5.5°C), the dissolved oxygen concentration at onset of strata should be about 12.7 (from Table V-12).

Now we have all values needed to plot hypolimnion DO versus time using Equations V-40 through V-42.

Using

$$L_o = L_{ss}$$

$$C_o = C_{ss}$$

$$k_1 = 0.1 \times 1.047^{(9.5-20)} = .062, (T = 9.5^\circ\text{C for May})$$

$$k_s = 0.03$$

$$k_4 = .003 \times 1.047^{(9.5-20)} = .002$$

$$t = 5 \text{ days}$$

and applying Equation V-42:

$$\Delta O_c = \frac{k_1 C_{ss}}{k_1 + k_s} \left( 1 - e^{-(k_1 + k_s)t} \right)$$

$$\Delta O_c = \frac{0.062 \times 5.25}{0.062 + 0.03} \left( 1 - e^{-(0.062 + 0.03)5} \right) = 1.30$$

then, according to Equation V-41:

$$\Delta O_L = \left( \frac{L_{ss}}{D} + \frac{k_s C_{ss}}{k_s + k_1 - k_4} \right) \left( 1 - e^{-k_4 t} \right) - \left( \frac{k_s C_{ss}}{k_s + k_1 - k_4} \right) \left( \frac{k_4}{k_s + k_1} \right) \left( 1 - e^{-(k_s + k_1)t} \right)$$

$$\Delta O_L = \left( \frac{754}{3.2} + \frac{0.03 \times 5.25}{0.03 + 0.062 - 0.002} \right) \left( 1 - e^{-0.002 \times 5} \right) - \left( \frac{0.03 \times 5.25}{0.03 + 0.062 - 0.002} \right)$$

$$\left( \frac{0.002}{0.062 + 0.03} \right) \left( 1 - e^{-(0.062 + 0.03)5} \right) = 2.35$$

then from Equation V-40:

$$O_t = O_o - \Delta O_c - \Delta O_L$$

$$O_5 = 12.7 - 1.30 - 2.35 = 9.05$$

Solving the same equations with increasing  $t$  gives the data in Table V-16.

If it has been necessary to develop more data for the remainder of the stratified period, appropriately updated coefficients might be used starting at the beginning of each month.

TABLE V-16  
DO SAG CURVE FOR QUIET LAKE HYPOLIMNION

Date	$\Delta O_L$	$\Delta O_c$	$O_t$
$t = 0$	0	0	12.70
5/5	2.35	1.30	9.05
5/10	4.68	2.13	5.89
5/15	6.99	2.65	3.06
5/20	9.22	2.98	0.50
5/25	11.54	3.18	0.00

Finally, if it is desired to evaluate the impact of altered BOD or phosphorus loadings, the user must go back to the appropriate step in the evaluation process and properly modify the loadings.

END OF EXAMPLE V-15

## 5.6 TOXIC CHEMICAL SUBSTANCES

Although reasonably accurate and precise methods have been prepared for screening only a few of the many priority pollutants (Hudson and Porcella, 1981), a reasonable approach for assessing priority pollutants in lakes based on the methods presented in Chapter 2 can be made if certain assumptions are made:

- The major processes affecting the fate and transport of toxicants in aquatic ecosystems are known
- That reasonable safety factors are incorporated by making reasonable most case analyses
- Because it is a screening approach, prioritization can be done to identify significant constituents, lakes where human health or ecological problems can realistically be expected, and processes which might require detailed study.

The major processes affecting toxicants are listed in Table V-17. The primary measure of the impact of a toxic chemical in a lake depends on its concentration in the water column. Thus, these screening methods are primarily directed at fate and



TABLE V-17

SIGNIFICANT PROCESSES AFFECTING  
TOXIC SUBSTANCES IN AQUATIC ECOSYSTEMS

Processes	Rate Coefficient Symbol, $\text{time}^{-1}$
<u>Physical-Chemical Processes</u>	
Sorption and sedimentation	SED
Volatilization	$k_v$
Hydrolysis	$k_h$
Photolysis	$k_p$
Oxidation	not assessed
Precipitation	not assessed
<u>Biological Processes</u>	
Biodegradation	B
Bioconcentration	BCF (unitless)

transport of toxic chemicals. A secondary target is the concentration in aquatic biota, principally fish. Because of the complexity of various routes of exposure and bioaccumulation processes, the approach of bioconcentration is used to identify compounds likely to accumulate in fish. These can be applied to lakes using the following method:

- A fate model is used that incorporates sediment transport, sorption, partitioning, and sedimentation
- Significant processes include the kinetic effects of sedimentation, volatilization and biodegradation
- Significant biochemical processes can affect the fate of a toxic chemical as well as affect biota, such as, bioaccumulation, biodegradation, and toxicity
- In keeping with the conservative approach of the toxics screening methodology, some important processes are neglected for simplicity; for example, lake stratification, photolysis, oxidation, hydrolysis, coagulation-flocculation, and precipitation are neglected. Also, it is assumed that the organic matter is associated with inorganic particles and therefore organic matter settles with the inorganic particles.

Generally the toxic chemical concentrations are calculated conservatively, that is, higher concentrations are calculated than would occur in nature because of the assumptions that are made. The water column concentrations are calculated as the

primary focus of the screening method. Then bioconcentration is estimated, based on water concentration. To determine concentration and bioaccumulation, point and nonpoint source loadings of the chemicals being studied are needed. Other data (hydrology, sediments, morphology) are obtained from the problems previously done in earlier chapters or sections of this chapter. The person doing the screening would have to compile or calculate such data.

Occasionally, such information must be estimated based on production, use, and discharge data. Information on chemical and physical properties is important to determine the significance of these estimates.

### 5.6.1 Overall Processes

Several processes affecting distribution of toxic chemicals are more significant than others. Equilibrium aquatic processes include suspended sediment sorption of chemicals. Organics in sediments can have a significant effect on chemical sorption. Hydrolysis and acid-base equilibria can alter sorption equilibria. Volatilization is an equilibrium process that tends to remove toxic chemicals from aquatic ecosystems. Removal processes include settling of toxics sorbed on sediments, volatilization, and biodegradation. Chemical reactions for hydrolysis and photolysis are included and precipitation and redox reactions could be included if refinement of the method were desired. Generally, bioaccumulation will be neglected as a removal process.

These removal processes are treated as first-order reactions that are simply combined for a toxicant (C, mg/l) to give:

$$dC/dt = -K \times C \tag{V-44}$$

where

- K = SED + B + k<sub>v</sub> + k<sub>p</sub> + k<sub>h</sub>
- SED = sedimentation rate, toxicant at equilibrium with sediments
- k<sub>v</sub> = volatilization rate
- B = biodegradation rate
- k<sub>p</sub> = photolysis rate
- k<sub>h</sub> = hydrolysis rate.

This equation is analogous to the BOD decay rate equation used in the hypolimnetic DO screening method.

The input of toxic chemical substances is computed simply (refer to Figure V-23):

$$\frac{dC}{dt} = \frac{Q}{V} \times C_{in} - \frac{C}{\tau_w} \tag{v-45}$$

where

- C<sub>in</sub> = the concentration in the inflow (tributary or discharge);
- flow (Q), volume of reservoir (V) and time (t) are as defined previously.

At steady state, accounting for inflow ( $Q \cdot C_{in}$ ) and outflow ( $Q \cdot C$ ), and using  $Q/V = 1/\tau_w$ :

$$\frac{dC}{dt} = \frac{1}{\tau_w} (C_{in} - C) - K \times C = 0 \quad (V-46)$$

and solving:

$$C = C_{in} / (1 + \tau_w \times K) \quad (V-47)$$

To determine the concentration at any time during a non-steady state condition (assuming  $C_{in}$  is a constant):

$$C = \frac{C_{in}}{f} (1 - e^{-ft/\tau_w}) + C_0 e^{-ft/\tau_w} \quad (V-48)$$

where

$$f = 1 + \tau_w \times K$$

$C_0$  = reservoir concentration at  $t = 0$ .

#### 5.6.1.1 Sorption and Sedimentation

Suspended sediment sorption is treated as an equilibrium reaction which includes partitioning between water ( $C_w$ ) and the sediment organic phases ( $C_s$ ). The concentration sorbed on sediment can be computed as follows:

$$\frac{C_s}{C} = a \times K_p \times S \quad (V-49)$$

where

$C$  = the total concentration ( $C_w + C_s$ ), mg/l

$S$  = input suspended organic sediment =  $OC \times S_o$ , mg/l

$OC$  = fraction of organic carbon.

$S_o$  = input of suspended sediment, mg/l

$K_p$  = distribution coefficient between organic sediment and water

$a$  = fraction of pollutant in solution  
 $= 1 / (1 + (K_p \times S))$ .

If  $K_p$  is large, essentially all of the compound will be sorbed onto the sediments. Note that  $S$  and  $C$  must be estimated or otherwise obtained.

The organic matter content of suspended sediment and the lipid volatility of the compound are important factors for certain organic chemicals. Other sorption can be ignored for screening. A simple linear expression can be used to calculate the sediment partition coefficient ( $K_p$ ) based on the organic sediment carbon concentration ( $OC$ ) and the octanol-water coefficient ( $k_{ow}$ ) for the chemical:

$$k_p = 0.63 (k_{ow}) (OC)$$

The sedimentation rate (SED) of a toxic chemical is computed as follows:

$$SED = a \times D \times K_p \quad (V-50)$$

where

D = P x S x Q/V, sedimentation rate constant

P = sediment trapping efficiency

$$Q/V = 1/\tau_w$$

#### 5.6.1.2 Biodegradation

The biodegradation rate (B) is obtained from the literature or is computed as follows:

$$B = - \frac{\Delta C}{\Delta t} \quad (V-51)$$

Modification to the rate can be made for nutrient limitation using phosphorus ( $C_p$ ) as the limiting nutrient:

$$B_{\text{limited}} = \frac{B (0.0277) C_p}{1 + 0.177 \times C_p} \quad (V-52)$$

Temperature correction can be performed using the following equation:

$$B(T) = B(20^\circ C) \times 1.072^{(T-20)} \quad (V-53)$$

Previous exposure to the pollutant is important for most toxic organic compounds. Higher rates of degradation occur in environments with frequent or longterm loading (discharges, nonpoint sources, frequent spills) than infrequent loadings (one-time spills). In pristine areas, rates of one to two orders of magnitude less should be used.

It is assumed that the suspended sediment decay rate is the same as aqueous phase decay. Also benthic decay is disregarded because bottom sediment release may be negligible.

#### 5.6.1.3 Volatilization

Many organics are not volatile so this process is applied only to those which are. It is assumed that the mass flux of volatile organics is directly proportional to the concentration difference between the actual concentration and the concentration at equilibrium with the atmosphere. The latter can be neglected in lakes.

Also, only the most volatile are assessed.

Thus:

$$\frac{dC}{dt} = -k_v \times C \quad (V-54)$$

where

$k_v$  = volatilization rate constant,  $hr^{-1}$

The rate coefficient is derived from the 2 resistance model for the liquid-gas interface, but it can be estimated using correlation with the oxygen reaeration coefficient (based on Zison et al., 1978):

$$k = K_a (D_w/D_o) \quad (V-55)$$

and estimate  $(D_w/D_o) = (32/mw)^{1/2}$

and the surface film thickness, SFT =  $(200-60 \cdot \sqrt{w}) \times 10^{-6}$

and  $K_a = D_o/SFT$

$K_a = K_a/ZB$

where

$K_a$  = reaeration rate,  $hr^{-1}$

$D_w$  = pollutant diffusivity in water

$D_o$  = diffusivity of oxygen in water ( $2.1 \times 10^{-9} m^2/sec, 20^\circ C$ )

$mw$  = pollutant molecular weight

$w$  = wind speed, m/sec

$Z$  = mean depth, m.

The volatilization rate coefficient ( $k_v, hr^{-1}$ ) is determined by  $k_v = K_a \times k$  where  $k$  is obtained from literature values or computed as above ( $\sqrt{D_w/D_o}$ ). The rate should be corrected for temperature ( $k_{vt}$ ) even though temperature has only a relatively small effect:

$$k_{vt} = k_v \times 1.024^{(T-20)} \quad (V-56)$$

#### 5.6.1.4 Hydrolysis

Not all compounds hydrolyze and those that do can be divided into three groups: acid catalyzed, neutral, and base catalyzed reactants. A pseudo first-order hydrolysis constant ( $k_h$ ) is estimated for the hydrolysis of the compound:

$$\frac{dC}{dt} = -k_h \cdot C \quad (V-57)$$

The rate constant ( $k_h$ ) is pH dependent and varies as discussed in Chapter 2.

The typical pH of the lake for the appropriate season should be obtained for the

necessary calculations. Generally, the pH is a common measurement and is available for most lakes. If not, pH values for most open lakes lie between 6-9 and can be estimated based on the following empirical values based on Hutchinson, (1957):

	Hardness (or Alkalinity)	pH
acid lakes	<25	6 - 6.5
neutral lakes	25 - 75	6.5 - 7.5
hard water lakes	75 - 200	7.5 - 8.5
eutrophic and alkaline lakes	0 - 300	8.0 - 10.0

Median values on a range of values can be used to evaluate the significance of hydrolysis as a factor affecting the fate of compounds.

#### 5.6.1.5 Photolysis

Generally, photolysis is a reaction between ultraviolet light (UV, 260 to 380 nm is most important) and photosensitive chemicals. Not all compounds are subject to photolysis nor does UV light penetrate significantly in turbid lakes. In the absence of turbidity data, light transmission can be estimated by seasonally averaged Secchi disk readings according to the following equation:

$$\ln(I_{SD}/I_0) = -k_e(SD) - \ln 0.1 = -2.3$$

$$k_e = 2.3/SD$$

where

$k_e$  = the extinction coefficient

$SD$  = the Secchi depth in meters

$(I_{SD}/I_0 = 0.1)$  = relative intensity based on Hutchinson (1957).

Photolysis for appropriate chemicals (discussed in detail in Chapter 2) depends on a first order rate constant ( $k_p$ ) incorporating environmental variables (solar irradiance,  $I_0$ ) and chemical variables (quantum yield,  $\phi$ , and absorbance,  $E$ ). Turbidity effects are included as estimated as above since turbidity data are generally not available. These values are incorporated into the rate constant and the concentration reduced as described in Chapter 2:

$$\frac{dC}{dt} = -k_p C \quad (V-58)$$

where

$$k_r = f(I_0, \phi, E, k_e, \bar{Z})$$

and

$$k_p = \frac{k_r}{k_e \cdot \bar{Z}}$$

where

$k_r$  = photolysis rate constant uncorrected for depth and turbidity of the lake.

Depth (Z) is generally applied only to the photic zone; mean depth (Z) is an appropriate measure since it approximates the mixed depth and the photic zone.

#### 5.6.1.6 Bioconcentration

Bioconcentration is a complex subject that depends on many variables. The simplest approach has been developed for organic compounds using the octanol-water coefficient ( $k_{ow}$ ) to calculate tissue concentrations (Y):

$$Y = BCF \times C, \text{ g/kg fresh weight of fish flesh} \quad (V-59)$$

where

BCF = Bioconcentration factor

$$\log BCF = 0.75 \log k_{ow} - 0.23$$

(The coefficients for the equation (0.75, - 0.23) are median estimates obtained from correlation equations and are default values for occasions where no other data are available.)

#### 5.6.2 Guidelines for Toxics Screening

Generally metals do not biodegrade nor volatilize. However, pH, hardness, alkalinity and other ions are very important and can cause their removal by precipitation. The conservative approach is taken here and metals are calculated without removal ( $K = 0$ ).

Organics may have variable sorption, volatilization, and biodegradation rates. If data are available in the literature, these should be used. Otherwise, a conservative approach should be used and calculations made without removal ( $K = 0$ ). For chlorinated (and other halogens) compounds or refractory compounds, biodegradation should be assumed to be zero.

#### EXAMPLE V-16

##### Estimating Trichloroethylene and Pyrene Concentrations in an Impoundment

An impoundment with a single tributary is located in a windy valley. The following conditions are known for E.G. Lake:

Mean tributary flow rate =  $3.6 \times 10^4 \text{ m}^3/\text{hour}$

Total volume =  $1.1 \times 10^8 \text{ m}^3$

Mean depth = 11 m  
 Tributary average sediment load = 200 mg/l  
 Sediment average organic carbon content = .05  
 Inlet average pyrene concentration = 50  $\mu\text{g/l}$   
 Inlet average trichloroethylene concentration = 100  $\mu\text{g/l}$   
 Lake average phosphorus concentration = 50  $\mu\text{g/l}$   
 Mean water temperature = 15°C  
 Mean wind speed = 6 m/sec (35 mph)  
 Secchi depth = 1 m

Determine the steady state concentration of pyrene and trichloroethylene in the lake, assuming  $V_{\text{max}}$  for the sediment (mostly clay) is  $3.2 \times 10^{-5}$  feet/second. The trapping efficiency is obtained from Figure V-34.

<u>Other data</u>	<u>Pyrene</u>	<u>Tri chloroethylene</u>
$k_{ow}$	148000	190
$B$	$1 \times 10^{-4}$	
$k_v$		0.45xKa

The processes of photolysis and hydrolysis can be neglected because turbidity prevents photolysis ( $SD = 1$  meter) and these compounds have negligible hydrolysis (see Chapter 2).

We use the summary equation V-47 for the analysis:

$$C = C_{in} / (1 + \tau \cdot K)$$

The hydraulic residence time of E.G. Lake is:

$$\begin{aligned}
 \tau_w &= 1.1 \times 10^8 \text{ m}^3 / (3.6 \times 10^4 \text{ m}^3/\text{hr}) \\
 &= 3048 \text{ hours} \\
 &= 127 \text{ days} \\
 &= .349 \text{ year} \\
 &= 1.1 \times 10^6 \text{ seconds}
 \end{aligned}$$

### Sedimentation

First, the suspended sediment concentration in E.G. Lake must be estimated. The trapping efficiency of the impoundment is estimated from Figure V-34.

Data:	<u>log 10</u>
$V_{\text{max}} = 5 \times 10^{-6}$ fps	-5.30
$\tau_w = 1.1 \times 10^6$ sec	6.04
$D^1 = 11$ m = 36.1 ft	1.56

A value of  $10^{1.95}$  is obtained which yields:

$$P \cong 90 = 0.9$$



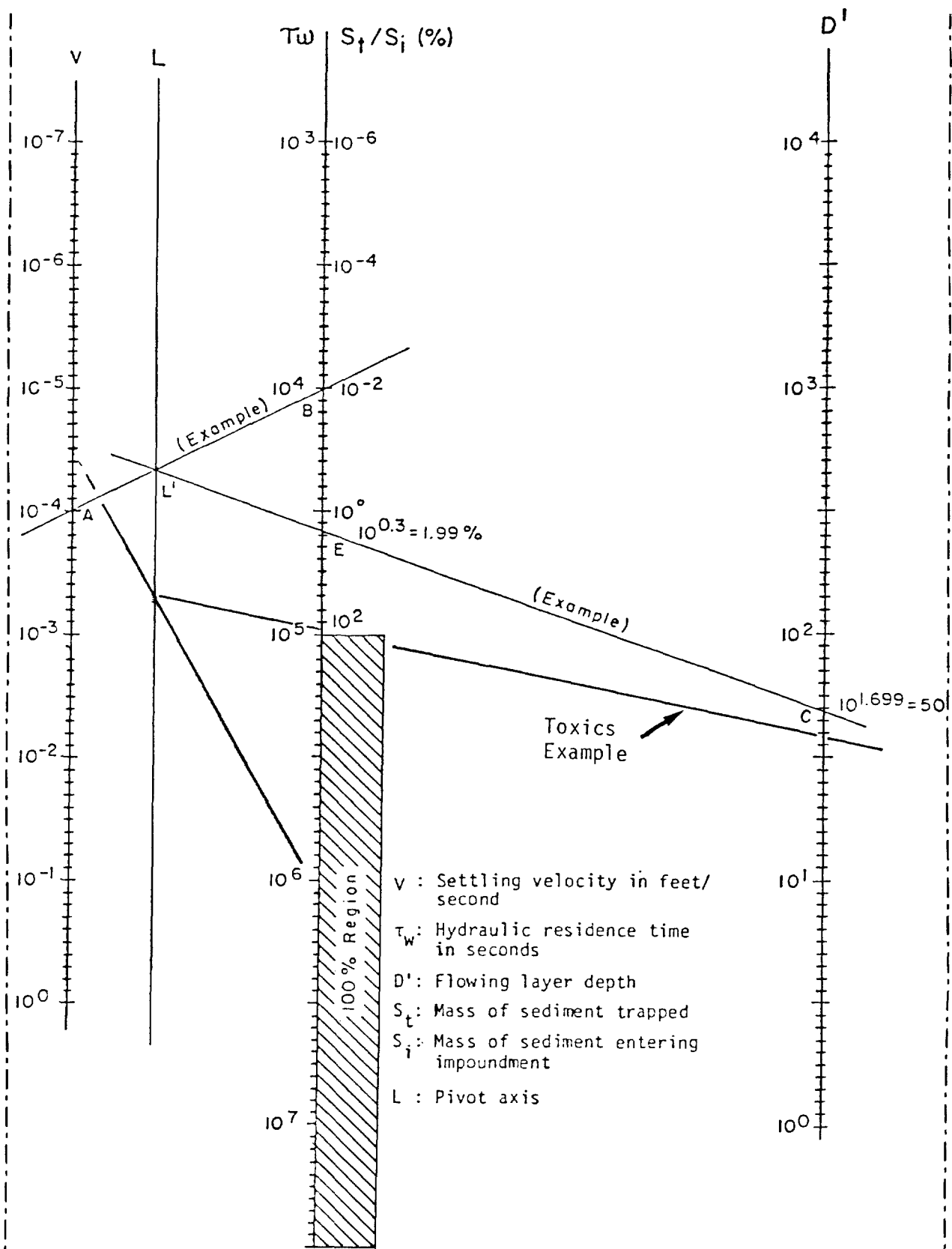


FIGURE V-34 NOMOGRAPH FOR ESTIMATING SEDIMENT TRAP EFFICIENCY

In the inflowing stream, the toxicants are assumed to be at equilibrium with the organic matter. Thus:

$$S = OC \times S_o = .05 \times 200 \times 10^{-6} = 1 \times 10^{-5} \text{ kg/l}$$

Therefore, for pyrene:

$$K_p = 0.63 \times 148000 \times 0.05 = 4660$$

$$a = 1/(1 + 4660 \times 1 \times 10^{-5}) = 0.955$$

$$\frac{C_s}{C} = 0.955 \times 4660 \times 1 \times 10^{-5} = 0.044$$

and

$$SED = a \times D \times K_p$$

$$D = P \times S \times Q/V$$

$$D = 0.9 \times 200 \times 10^{-6} \times \frac{1}{3048} \text{ hours}$$

$$D = 5.91 \times 10^{-8} \text{ hour}$$

$$SED = .955 \times 5.91 \times 10^{-8} \times 4660$$

$$SED = 2.63 \times 10^{-4} \text{ hr}^{-1}$$

For trichloroethylene:

$$K_p = .63 \times 190 \times 1 \times .05 = 6$$

$$a = 1/(1 + 6 \times 1 \times 10^{-5}) = 1$$

$$\frac{C_s}{C} = 1 \times 6 \times 1 \times 10^{-5} = 6 \times 10^{-5} \cong 0$$

and

$$SED = 1 \times 5.91 \times 10^{-8} \times 6$$

$$SED = 3.54 \times 10^{-7} \text{ hr}^{-1}$$

#### Biodegradation

Assume that the presence of trichloroethylene does not affect the biodegradation of pyrene. Trichloroethylene does not biodegrade. The temperature corrected and nutrient limited rate constant for microbial decay of pyrene are:

$$B_o = 1. \times 10^{-4} \text{ hr}^{-1}$$

$$B = .0277 \times 50 / (1 + .0277 \times 50)$$

$$= .58$$

$$B(15) = .58 \times 1. \times 10^{-4} \times 1.072^{(15-20)}$$

$$\times 10^{-5} \text{ hr}^{-1}$$

;

The reaeration coefficient for E.G. Lake will be estimated for trichloroethylene only, because pyrene does not volatilize:

$$K_a = 2.1 \times 10^{-9} / (200 - 60 \times 6^{1/2}) 10^{-6}$$

$$= 3.96 \times 10^{-5} \text{ m/sec m/sec}$$

$$= .143 \text{ m/hr}$$

$$K_a = (.143 \text{ m/hr}) / 11 \text{ m} = .013 \text{ hr}^{-1}$$

For trichloroethylene (TCE):

$$k_v = [MW(\text{TCE})/MW(\text{O}_2)]^{1/2} \cdot K_a = .45 \times .013 = .0058 \text{ hr}^{-1}$$

When adjusted for temperature:

$$k_v = .0058 \times 1.024^{(15-20)} \\ = .0052 \text{ hr}^{-1}$$

Volatilization for pyrene may be neglected.

#### Pollutant Mass Balance

The overall decay rate constants are:  $K = \text{SED} + B + k_v$

Pyrene:  $K = 2.63 \times 10^{-4} + 4.1 \times 10^{-5}$   
 $= .000304 \text{ hr}^{-1}$

Trichloroethylene:  $K = 3.54 \times 10^{-7} + 0 + 0.0051$   
 $= .0052 \text{ hr}^{-1}$

Using the steady state equation:

$$C = C_{in} / (1 + \tau_w K)$$

For Pyrene:

$$C = 50 \mu\text{g/l} / (1 + 3048 \text{ hr} \times .000304 \text{ hr}^{-1})$$

$$C = 27 \mu\text{g/l}$$

Note: WQC for human health is  $0.0028 \mu\text{g/l}$  at  $10^{-6}$  Risk (FR: 11/28/80 p. 79339).

For Trichloroethylene:

$$c = 100 \mu\text{g/l} / (1 + 3048 \text{ hr} \times .0052 \text{ hr}^{-1}) \\ = 5.9 \mu\text{g/l}$$

Note: WQC for human health is  $2.7 \mu\text{g/l}$  at  $10^{-6}$  Risk (FR: 11/28/80 p. 79341)

Tissue burdens (Y) can be calculated:

$$Y = \text{BCF} \times C$$

where

$$\log \text{BCF} = .75 \log \text{kow} - 0.23$$

For Pyrene:

$$= 120000 \mu\text{g/kg fish flesh}$$

For Trichloroethylene:

$$= 30 \times 6 = 180 \mu\text{g/kg fish flesh}$$

Comments

Several conclusions are apparent from this analysis:

- Certain processes dominate the overall fate for a specific toxic

chemical so that, practically speaking, errors in estimating coefficients are negligible except for the important processes. After identifying the important processes, the coefficients can be varied to determine the range of concentrations. For example, sedimentation of trichloroethylene can be ignored; however, volatilization should be studied.

- The more stringent Water Quality Criteria are for toxicants that have significant bioconcentration; e.g. compare pyrene to trichloroethylene
- Volatilization of trichloroethylene would be investigated in detail since this process might not be significant in this lake because of its depth. Also, the physical properties are important; e.g. trichloroethylene has a specific gravity of about 1.5. Thus, it may accumulate on the bottom of the reservoir and remain there unless it is completely dispersed.
- Based on this analysis, sources of pyrene would be assessed first, then trichloroethylene.
- What other observations can you draw from this analysis?

--- END OF EXAMPLE V-16 ---

## 5.7 APPLICATION OF METHODS AND EXAMPLE PROBLEM

This chapter has presented several approaches to evaluation of five impoundment problem areas. These are thermal stratification, sediment accumulation, eutrophication, hypolimnion DO/BOD, and toxic chemicals. Figure V-35 shows how the different approaches are linked together with their data needs. In studying any or all of the potential problem areas in an impoundment, the user should first define the potential problems as clearly as he can. Often the nature of a problem will change entirely when its various facets are carefully described and examined en masse.

Once the decision is made that an aspect of impoundment water quality should be evaluated and the problem is clearly stated, the user should examine available solution techniques presented both in this document and elsewhere. The examination should address the questions of applicability, degree of accuracy, and need for data. The user will generally know what funds are available for data collection as well as the likelihood of procuring the needed data from previously developed bases. Also, the decision concerning needed accuracy rests with the user, and he should make decisions based upon the way in which his results will be used.

Once appropriate methods have been selected, the next task is to set down the data and to manipulate it according to computational requirements. Data are best displayed first in tabular form and then plotted in some meaningful way. Careful tabulation of data and graphing can themselves sometimes provide a solution to a

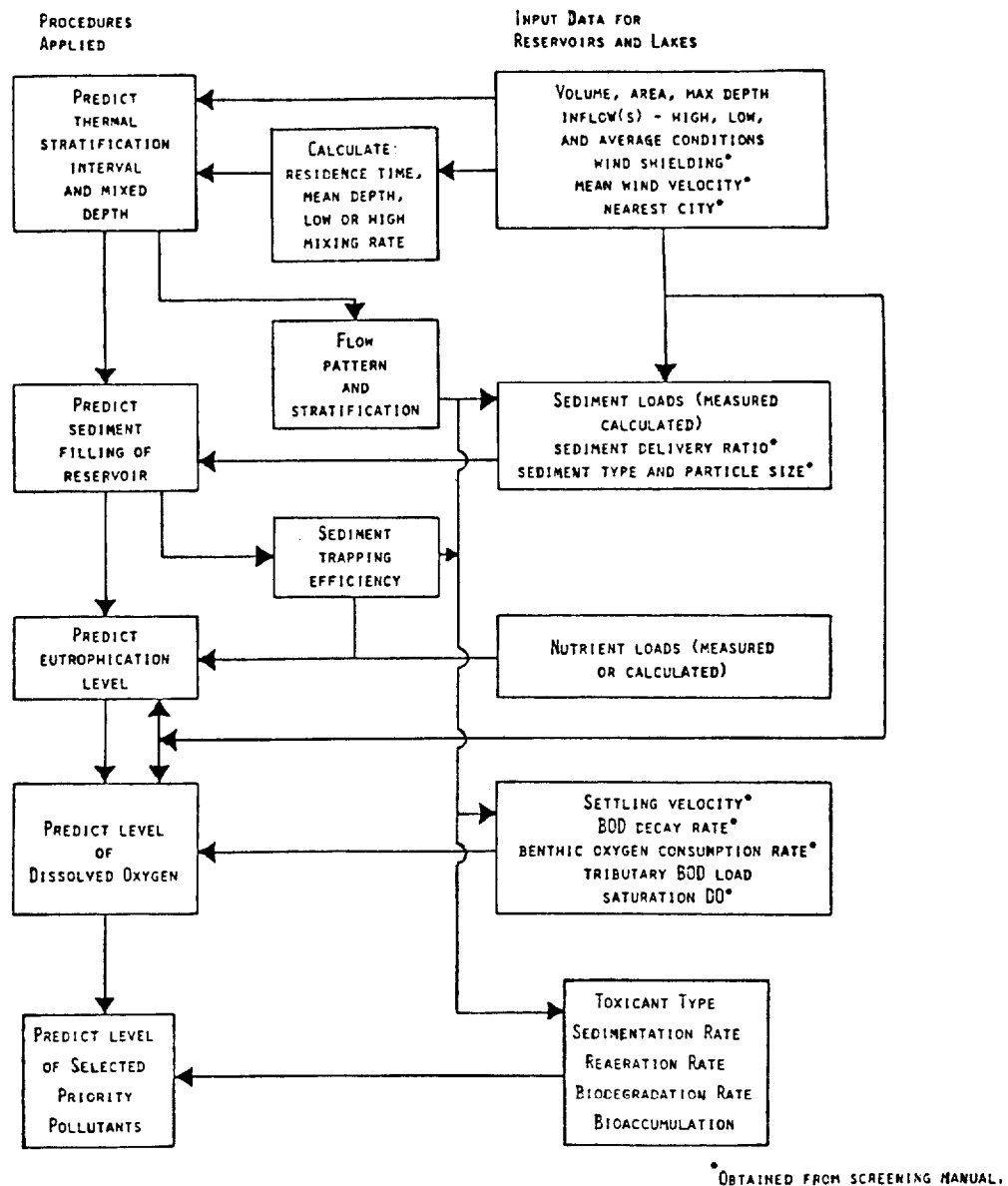


FIGURE V-35 GENERALIZED SCHEMATIC OF LAKE COMPUTATIONS

problem, negating need for further analysis. To illustrate these steps, a comprehensive application to a river basin system was performed in this section.

### 5.7.1 The Occoquan Reservoir

The Occoquan River basin in Virginia was used to demonstrate the screening approach. A basin map is shown in Figure V-36. Because the Occoquan Reservoir is a public drinking water supply downstream from metropolitan areas, water quality data were available to compare to the screening method's outputs.

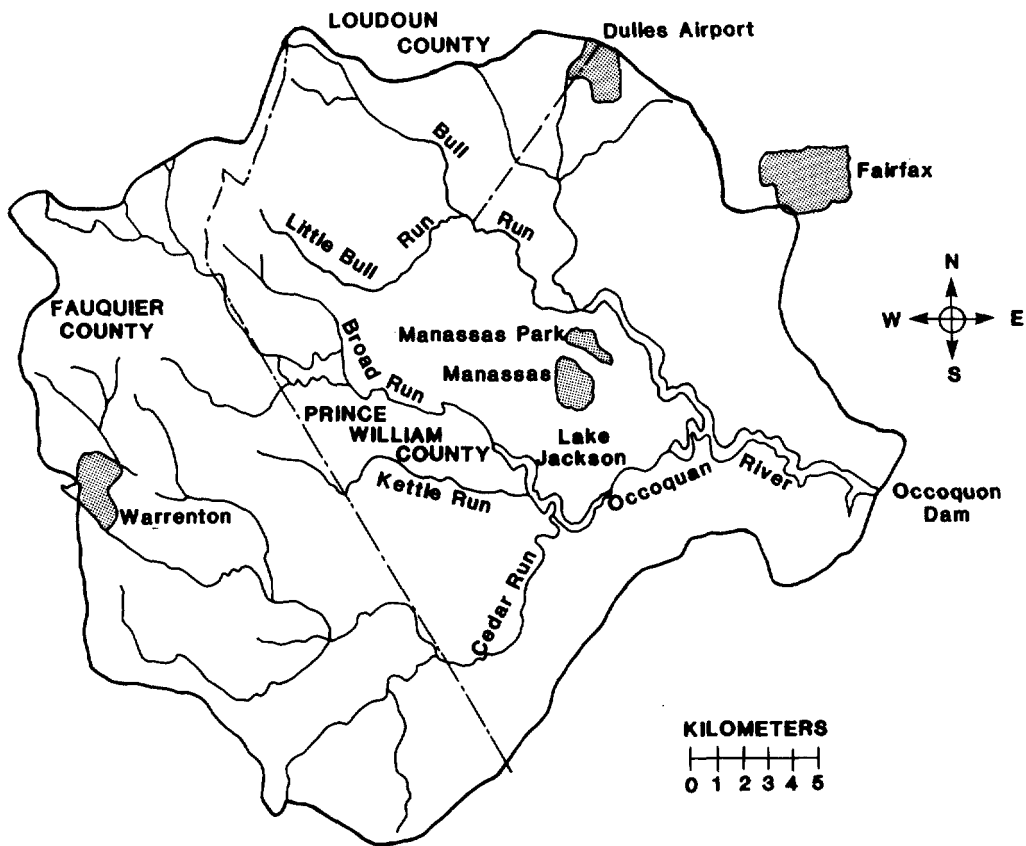


FIGURE V-36 THE OCCOQUAN RIVER BASIN

5.7.2 Stratification

Occoquan Reservoir is about 32 km southwest of Washington, D.C. and has the following morphometric characteristics:

- Volume,  $m^3 = 3.71 \times 10^7$
- Surface area,  $m^2 = 7.01 \times 10^6$
- Maximum depth,  $m = 7.1$  (Occoquan Dam)
- Mean depth,  $m = 5.29$

Based upon the above geometry and the thermal plots, determine whether the lake will stratify, the thickness of the epilimnion and the hypolimnion, the depth to the thermocline, and the interval and starting and ending date of stratification. Also note the temperature of the hypolimnion at the onset of stratification.

Predicting the extent of shielding from the wind requires use of topographic maps. The reservoir is situated among hills that rise 25 meters or more above the lake surface within 200 meters of the shore. The relief provides little access for wind to the lake surface. Average annual wind speeds are 15.6 km/hr in Washington, D.C. and 12.6 km/hr in Richmond, VA. Inflow comes essentially from two creeks, the

Occoquan River and Bull Run River (Figure V-35).

First, determine needed information and then do metric/English conversions as necessary.

The first step in assessing impoundment water quality is to determine whether the impoundment thermally stratifies. This requires knowledge of local climate, impoundment geometry, and inflow rates. Using this information, thermal plots likely to reflect conditions in the prototype are selected from Appendix D.

For the thermal plots to realistically describe the thermal behavior of the prototype, the plots must be selected for a locale climatically similar to that of the area under study. Because the Occoquan Reservoir is within 32 kilometers of Washington, D.C., the Washington thermal plots (Appendix D) should best reflect the climatic conditions of the Occoquan watershed.

The second criterion for selecting a set of thermal plots is the degree of wind stress on the reservoir. This is determined by evaluating the amount of protection from wind afforded the reservoir and estimating the intensity of the local winds. Table V-2 shows annual wind speed frequency distribution for Washington, D.C. and Richmond, Virginia. The data suggest that winds in the Occoquan area are of moderate intensity.

Predicting the extent of shielding from the wind requires use of topographic maps. The reservoir is situated among hills that rise 25 meters or more above the lake surface within 200 meters of the shore. The relief provides little access for wind to the lake surface. The combination of shielding and moderate winds implies that low wind stress plots are appropriate.

The geometry of the reservoir is the third criterion used in the selection of thermal plots. Geometric data for the Occoquan Reservoir are summarized in the problem. The volume, surface area, and maximum depth are all nearly midway between the parameter values used in the 40-foot and 75-foot maximum-depth plots. However, the mean depth is much closer to the mean depth of the 40-foot plot.

The mean depth represents the ratio of the volume of the impoundment to its surface area. Because the volume and surface area are proportional to the thermal capacity and heat transfer rates respectively, the mean depth should be useful in characterizing the thermal response of the impoundment. It follows that the 40-foot thermal profiles should match the temperatures in the Occoquan Reservoir more closely than the 75-foot profiles. However, it is desirable to use both plots in order to bracket the actual temperature.

Flow data provide the final information needed to determine which thermal plots should be used. The inflow from the two tributaries adds up to be 20.09  $\text{m}^3/\text{sec}$ .

The hydraulic residence time can be estimated by using the expression:

$$\tau_w = \frac{V}{Q} = \frac{3.71 \times 10^7 \text{ m}^3}{20.09 \frac{\text{m}^3}{\text{sec}} \times 86400 \frac{\text{sec}}{\text{day}}} = 21.4 \text{ days}$$

Since the residence time is midway between the thermal plot parameter values of 10 and 30 days, both should be used to bracket the mean hydraulic residence time in the prototype. It should be noted that these flow estimates do not include runoff from the area immediately around the lake. However, the upstream Occoquan watershed is large enough relative to the immediate runoff and direct precipitation to justify the assumption that the contribution of the immediate area is not significant.

The likelihood that the Occoquan Reservoir thermally stratifies can now be evaluated. For a hydraulic residence time of ten days, the thermal plots show that stratification is not likely for maximum depths of 40 to 75 feet. In the case of a 30-day hydraulic residence time, the profiles suggest that the reservoir develops a thermal gradient between  $1^\circ\text{C m}^{-1}$  and  $3^\circ\text{C m}^{-1}$  for either value of maximum impound depth. The 40-foot plots (Figure V-37) indicate stratification occurs from May to August at 5-7 meters depth. However, the 75-foot plots predict that the impoundment will have a thermal gradient greater than  $1^\circ\text{C m}^{-1}$  only at depths greater than 17 meters. Since the Occoquan Reservoir is 17.1 meters deep at the deepest station, this suggests that the impoundment does not stratify.

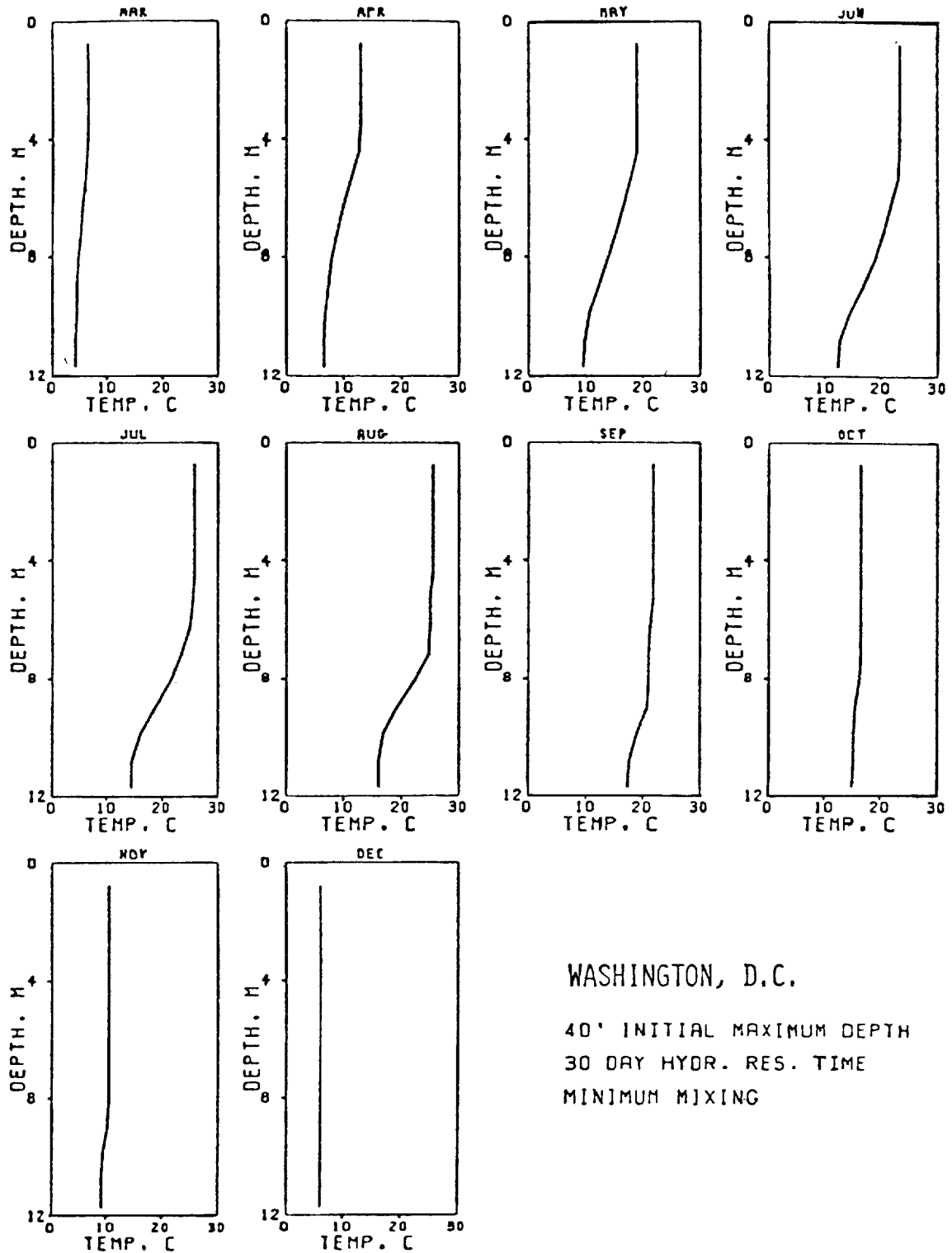
The mean hydraulic residence time can be computed using either the average annual flow rate or the flow rate just prior to stratification. In order to use the latter method, the flow rate during the months of March and April should be computed. The flow rate for this period,  $25.4 \text{ m}^3 \text{ sec}^{-1}$ , reduces the hydraulic retention time to 17 days. Since the model predicts no stratification for a ten-day residence time, the judgment as to whether stratification occurs becomes difficult.

Because lower flows occur during the summer, the 30-day residence time, 40 foot depth and minimum mixing should be used. In borderline cases such as this, the reservoir will almost certainly stratify during some part of the summer.

The temperatures predicted by the thermal plots match those actually measured in the reservoir quite closely. A comparison of predicted and observed monthly mean temperatures (1974-1976) in both the epilimnion and hypolimnion can be made using observed data (Table V-18) and the plot of the 40 foot, 30 day residence time, maximum mixing (Figure V-37). The difference between the two epilimnion temperatures averages  $1.0^\circ\text{C}$  and varies between  $0.2$  and  $1.8^\circ\text{C}$ . The difference in the hypolimnion temperatures averages  $1.0^\circ\text{C}$  and ranges from  $0.2$  to  $2.7^\circ\text{C}$ .

The close agreement of the predicted and observed impoundment temperatures probably results from the relatively long hydraulic residence times observed in two of the three years on which the averages are based. In 1974, 1975, and 1976, the mean hydraulic residence times were 31, 18, and 25 days, respectively. The 30-day





WASHINGTON, D.C.

40' INITIAL MAXIMUM DEPTH  
 30 DAY HYDR. RES. TIME  
 MINIMUM MIXING

FIGURE V-37 THERMAL PROFILE PLOTS FOR OCCOQUAN RESERVOIR

TABLE V-18

COMPARISON OF MODELED THERMAL PROFILES TO  
OBSERVED TEMPERATURES IN OCCOQUAN RESERVOIR

Month	Mean Epilimnion Temp., °C		Mean Hypolimnion Temp., °C,		Epilimnion Depth (m) 40-foot Plot <sup>b</sup>
	40-foot Plot <sup>a</sup>	Observed <sup>c</sup>	40-foot Plot <sup>b</sup>	Observed <sup>c</sup>	
March	7	8.4	6	6.3	--
April	13.5	12.6	10	9.2	--
May	19	20.5	15	14.4	4.5
June	24	24.8	18	17.2	5.0
July	26	26.6	20	21.2	6.5
August	26	26.5	21	23.7	7
September	22	23.8	20	20.2	--
October	17	17.2	16	15.8	--
November	11	12.2	10	11.6	--
December	7	6.2	7	5.8	--

Source: Northern Virginia Planning District Commission. January, 1979.

<sup>a</sup>Mean temperatures in epilimnion from thermal plots with  $\tau_w = 30$  days and a maximum depth of 40 feet.

<sup>b</sup>Mean temperatures in thermocline and hypolimnion from thermal plots with  $\tau_w = 30$  days and a maximum depth of 40 feet.

<sup>c</sup>Means of observed temperatures in "upper" and "lower" layers of Occoquan Reservoir for 1974-1976, at Sandy Run.

thermal plots should predict results relatively close to the two low-flow years. The differences expected for 1975 would be less pronounced when averaged with the other two.

In conclusion, Occoquan Reservoir does apparently stratify, the depth to the thermocline or the epilimnion approximates the mean depth (5.29), the hypolimnion has a depth of 11.8 m (17.1-5.3), and the interval of stratification approximates May 1 to mid September or 138 days. The hypolimnetic temperature is about 11 degrees C, typically.

### 5.7.3 Sedimentation

To evaluate potential sedimentation problems, Appendix F is examined to see if any data exist on the upstream reservoir (Jackson) or Occoquan Reservoir (Figure V-36). Some data exist for Jackson but not for Occoquan Reservoir (Figure V-38 taken

DATA SHEET NUMBER	RESERVOIR	STREAM	NEAREST TOWN	DRAINAGE AREA (SQUARE MILES)		DATE OF SURVEY	PERIOD BETWEEN SURVEYS (YEARS)	STORAGE CAPACITY (ACRE-FT.)	CAPACITY ANNUAL INFLOW (ACRE-FT. PER ACRE-FT.)	SPECIFIC WEIGHT (DRY) (LB. PER CU. FT.)	AVG. ANN. SEDIMENT ACCUMULATION PER SQ. MI. AREA FOR PERIOD SHOWN	AGENCY SUPPLYING DATA
				TOTAL	NET							
POTOMAC, RAPPANNOCK, YORK, AND JAMES RIVER BASINS												
5-1a	Lake Barcroft	Trib. of Potomac River	Falls Church, Va.	14.5	14.3	Jan. 1915	--	9/1,647	.142	--	--	SCS
5-2	Padlar	Padlar River	Oronoco, Va.	--	33.07	Aug. 1957	23.1	2/2,092	.134	*60	.257	SCS
5-3	Burnt Mill	M. & Br. Anacostia River	Silver Spring, Md.	27.0	26.97	Mar. 1938	31	1,723	--	--	.134	SCS
5-4b	Greenball Lake	Trib. of Indian Creek	Greenbelt, Md.	10/82	.79	July 1938	7.8	186	*.312	*60	.408	SCS
5-5a	Stanton	North River	Stanton, Va.	25	25	Aug. 1957	19.5	151	*.296	*60	7.91	10,337
5-6	Jacks	Oceanic Creek	Manassas, Va.	337	336.4	June 1957	17.5	385	*.240	*60	2.27	2,970
5-7a	Tridale L. (Brighton D.)	Patuxent River	Brighton, Md.	81.4	80.0	Oct. 1940	7.2	4,100	--	*60	.034	--
5-8	Gordon Lake	Evitts Creek	Cumberland, Md.	64	33/4	Sept. 1913	5.9	3,129	.327	--	.114	184
5-9	Thomas W. Noon Lake	Thomas W. Noon Lake	Bloomington, Md.	105.0	104.44	Apr. 1940	8.1	7,424	.172	--	.036	--
5-10	Rocky Gorge	Patuxent River	Laurel, Md.	132.8	50.14	Mar. 1956	4.0	20,800	.169	*60	.643	840
5-11	South River, Site 26	Inch Branch	Waynesboro, Va.	2.7	2.7	May 1956	10.4	20,789	--	67	1.15	1,678
5-12	Wide Lake	Trib. Little Patuxent	Columbia, Md.	1.88	1.85	Sept. 1965	14.5	186.97	.28	*60	.087	110
5-13	--	--	--	--	--	Aug. 1968	1.9	170.99	.112	*60	15/7,3915/11,278	SCS
5-14	--	--	--	--	--	Aug. 1969	1.0	163.72	.117	*60	1.93	5,133
CHOMAN, ROANAKE, TAB, NEUSE, AND CAPE FEAR RIVER BASINS												
6-1	Lake Apex	Swift Creek	Apex, N. C.	4.0	4.0	June 1925	--	106	--	--	--	SCS
6-2	Franklin	Kallis Keany Creek	Franklin, N. C.	1.13	1.12	Jan. 1925	16	24.7	--	--	.19	--
6-3	Greenboro (I. Brant)	Reidy Fork	Greenboro, N. C.	74.1	73.4	May 1938	13.3	27.3	--	67	.509	743
6-4	High Point	Deep River	High Point, N. C.	62.8	62.3	Aug. 1934	11.5	2,610	--	*60	.308	402
6-5	--	--	--	--	--	Jan. 1928	6.5	4,134	--	50.6	.541	596
6-6	--	--	--	--	--	Apr. 1938	3.75	4,038	--	--	.418	458

1/ Includes estimated 112 acre-feet passing through Shandaken Tunnel.  
2/ Includes 103 acre-feet of sediment dredged in 1937-1939.  
3/ Partial survey covering segments 1-14 in Stony Brook Arm Only.  
4/ Net sediment contributing area was 299.4 sq. mi. until 1933 when Prettyboy Dam was completed.  
5/ This area was used in the 1943 calculations.  
6/ Revised after 1961 survey.  
7/ No operation or sediment pool only.  
8/ Based on original spillway crest elevation 205 feet m. s. l.  
9/ Based on original spillway crest elevation 210 feet m. s. l. and estimated capacity of 2,380 acre-feet resulting from 1942 addition to top of dam.  
10/ Revised 1968.  
11/ 9 acre-feet washed by dredging.  
12/ Revised due to movable control gate.  
13/ Koon Lake, upstream, was built in 1932.  
14/ Based on total sediment in both Gordon Lake and Koon Lake.  
15/ Does not include 4.34 acre-feet dredged.  
16/ Includes 4.34 acre-feet dredged in early spring 1968.  
17/ Estimated or assumed.

FIGURE V-38 SUMMARY OF RESERVOIR SEDIMENTATION SURVEYS MADE IN THE UNITED STATES THROUGH 1970

from Appendix F). Thus, we can determine the trapping of sediment in Jackson Reservoir but trapping must be calculated for the Occoquan. To refine the analysis, calculations on Jackson Reservoir will also be made and the results calibrated.

To apply the Stokes' law approach to a reservoir, we need to know the loading first. The necessary sediment loading estimates for the tributaries were provided by the methods in Chapter 3 and are listed in Table V-19 (Dean *et al.*, 1980) Before they are used in further computations, a delivery factor must be applied to these values. This factor (the sediment delivery ratio or SDR) accounts for the fact that not all the sediment removed from the land surface actually reaches the watershed outlet. Nonpoint loads from urban sources are presumed to enter the reservoir through Bull Run River since most of the urbanized portion of the watershed lies in this sub-basin.

Computing the annual sediment load into Occoquan Reservoir is complicated by the presence of Lake Jackson immediately upstream from the reservoir. The trap efficiency must be computed for Lake Jackson as well in order to determine the amount of sediment entering the Occoquan Reservoir from Lake Jackson. The steps involved are to compute the sediment delivered (Table V-20), the size range, the fraction trapped for each size range and the total amount trapped. A table has been devised to simplify these steps (Table V-21).

Soil types provide an indication of the particle sizes in the basin under study. Soils in the Occoquan basin are predominately silt loams. Particle size data on the principal variety, Penn silt loam, are given in Table V-22. These data and all calculations are transcribed into Table V-23.

Some effort can be conserved by first calculating the smallest particle size that will be completely trapped in the impoundment. To do so, P, the trap efficiency, must first be computed. Because both reservoirs are long and narrow and have relatively small residence times, the flow will be assumed to approximate vertically mixed plug flow (Case B1). In this case, P is found from the expression:

$$P = \frac{V_{\max} \tau_w}{D'}$$

where

D' = mean flowing layer depth, m.

To calculate the smallest particle that is trapped in the impoundment, P is set equal to unity and the above equation is solved for  $V_{\max}$ :

$$V_{\max} = \frac{D' \cdot 1.0}{\tau_w}$$

This expression for  $V_{\max}$  is then substituted into the fall velocity equation (Stokes' law), which in turn is solved for d:

TABLE V-19  
ANNUAL SEDIMENT AND POLLUTANT LOADS IN OCCOQUAN  
WATERSHED IN METRIC TONS PER YEAR<sup>a</sup>

Type of Load	Kettle Run	Cedar Run	Broad Run	Bull Run	Occoquan River	Urban Runoff
→ Sediment	46,898	396,312	142,241	232,103	139,685	12,699
Total Nitrogen	164.46	1,457.42	518.91	789.24	469.46	12.88
Available Nitrogen	16.45	145.74	51.89	78.92	46.05	5.38
Total Phosphorus	39.01	341.95	114.22	202.71	119.42	2.59
Available Phosphorus	2.18	14.95	5.57	12.50	8.43	1.27
BOD <sub>5</sub>	328.92	2,925.63	1,042.45	1,578.47	925.85	77.47
Rainfall Nitrogen	0.72	5.50	2.00	3.92	2.48	-

<sup>a</sup> Estimates provided by Midwest Research Institutes Nonpoint Source Calculator. These values have not yet had a sediment delivery ratio (SDR) applied to them. We will use 0.1 and 0.2 as lower and upper bounds. The SDR does not apply to rainfall nitrogen.

Note: A large number of significant figures have been retained in these values to ensure the accuracy of later calculations.

TABLE V-20  
SEDIMENT LOADED INTO LAKE JACKSON,  
1,000 Kg/Year

Tributaries to Lake Jackson	Total Available Sediment	Sediment Delivered to Lake Jackson	
		Case I (SDR=0.1)	Case II (SDR=0.2)
Kettle Run	46,898	4,690	9,380
Cedar Run	396,312	39,630	79,260
Broad Run	142,241	<u>14,220</u>	<u>28,440</u>
Total		58,540	117,080

TABLE V-21  
 CALCULATION FORMAT FOR DETERMINING SEDIMENT ACCUMULATION IN RESERVOIRS (NOTE UNITS)

Size Fraction	Percent Composition	Density		Mean Particle Diameter	V <sub>max</sub>	Fraction Trapped (P)		Test Case	Incoming Sediment	Trapped Sediment
		Absolute	Bulk			A	B			

TABLE V-22

## PARTICLE SIZES IN PENN SILT LOAM

Particle Size (mm)	% of Particles Smaller Than (By Weight)
4.76	100
2.00	99
0.42	93
0.074	84
0.05	78
0.02	50
0.005	26
0.002	16

$$V_{max} = \frac{4.8 \times 10^6 (D_p - D_w) d^2}{\mu} = \frac{D'}{\tau_w}$$

The resulting expression is:

$$d = \sqrt{\frac{D' \mu}{4.8 \times 10^6 (D_p - D_w) \cdot \tau_w}}$$

The trap efficiency of Lake Jackson is calculated first. The data required for these calculations are:

$$V = 1.893 \times 10^6 \text{ m}^3$$

$$Q = 12.47 \text{ m}^3 \text{ sec}^{-1}$$

$$\bar{D} = 3.34 \text{ m}$$

$$\mu = 1.11 \quad (\text{Assuming } T = 16^\circ\text{C as in Occoquan Reservoir})$$

$$\text{and } \tau_w = \frac{V}{Q} = \frac{1.893 \times 10^6 \text{ m}^3}{12.47 \text{ m}^3 \cdot \text{sec}^{-1} \cdot 86400 \text{ sec} \cdot \text{day}^{-1}} = 1.76 \text{ days}$$

The minimum particle size for 100 percent trapping is computed as:

$$d = \sqrt{\frac{3.34 \text{ m} \times 1.11}{4.8 \times 10^6 (2.66 - 1.0) \cdot 1.76}} = 5.14 \times 10^{-4} \text{ cm}$$

TABLE V-23

CALCULATION FORMAT FOR DETERMINING SEDIMENT ACCUMULATION IN RESERVOIRS (NOTE UNITS)

Size Fraction	Percent Composition	Density		Mean Particle Diameter	V <sub>max</sub>	Fraction Trapped (P)		Test Case	m <sup>3</sup> /yr	
		Absolute	Bulk			A	B		Incoming Sediment	Trapped Sediment
cin					m/day					
.000514	0.3	2.66	2.24	N/A	1.90	N/A	1.00	I II	176 352	176 352
.00050	5	2.66	2.24	N/A	1.79	N/A	0.94	I II	2927 5854	2751 5502
.00035	5	2.66	2.24	N/A	0.88	N/A	0.46	I II	2927 5854	601 1209
.00020	16	2.66	1.28	N/A	0.29	N/A	0.15	I II	9366 18732	1405 2810
>.000518	73.7	2.66	2.33 (average)	N/A	-	N/A	1.00	I II	43144 86288	43144 86288
Totals Trapped									I mtons/yr II mtons/yr	48822 97644
Example Calculation									I m <sup>3</sup> /yr II m <sup>3</sup> /yr	21523 43046
SDR = 0.115										
Vol = 24750 m <sup>3</sup> /yr										
Vol of Jackson Reservoir last per year =									24750m <sup>3</sup> /yr	= 1.3%/year
(75 yrs lifetime)									$\frac{24750 \times 75}{1893000}$	



The amount trapped of each size fraction is computed separately for Case B-1 from the equation:

$$P = \frac{V_{\max} \tau_w}{D'}$$

For example, for size fraction 0.00035 cm:

$$P = \frac{(0.88)(1.76)}{(3.34)} = 0.46$$

A composite trapping efficiency can be obtained by determining the total percent trapped ( $48822/58540 = 0.83$ ).

The sediment accumulated in Lake Jackson for each size range is determined from the expression:

$$S_t = P \cdot S_i$$

where

P = trap efficiency

$S_i$  = sediment load from tributary i

$S_t$  = sediment trapped.

For the two cases (I, II):

$$\begin{aligned} S_t &= (0.1, 0.1) \times 0.83 [46898 + 132241] \text{ metric tons/year} \\ &= (48822, 97644) \text{ metric tons/year.} \end{aligned}$$

Data obtained from Appendix F of the screening manual show that the estimated rate of sedimentation in Lake Jackson is 56,153 metric tons/year. This indicates that an SDR of 0.115 would be appropriate.

Bulk density (g/cc) includes the water that fills pore spaces in sediment that has settled to the bottom and this must be accounted for when determining volume lost due to sedimentation. Bulk density varies with particle size and some approximate values for the size ranges for sand (0.005-0.2 cm), silt (0.0002-0.005 cm), and clay (<0.0002 cm) are as follows: 2.56 for sand, 2.24 for silt and 1.28 for clay. Thus, using an SDR of .115, 24,750 m<sup>3</sup> (or 1.3%) of reservoir volume would be lost per year. In comparing to Appendix F data, we find that this value is conservative. The loss of volume was estimated by the SCS to be 47.5 acre feet/year while these calculations show only 20 acre feet/year being lost. The estimated bulk density used by the SCS was 0.93 g/cc and we used a more conservative value. If the SCS figure is used, the volume lost is determined to be 46.4 acre feet/year.

Now we compute the sedimentation in Occoquan Reservoir. The minimum particle size that is completely trapped is computed using the following values:

$$D' = 5.29$$

$$\mu = 1.11 \text{ (T= } 16^\circ\text{C = mean of Table V-18)}$$

$$D_w = 2.66 \text{ g cm}^{-3}$$

$$D_w = 1.0 \text{ g cm}^{-3}$$

$$T_w = 21.4 \text{ days.}$$

Under stratified conditions, the epilimnion thickness should be used for  $D'$ . Since stratification is uncertain in this case and the predicted average hypolimnion thickness, 5.75 m, is greater than the mean depth, the latter value will be used. All particles with diameter,  $d$ , such that:

$$d = \sqrt{\frac{5.29 \times 1.11}{4.8 \times 10^6 (2.66 - 1.0) \cdot 21.4}} = 1.86 \times 10^{-4} \text{ cm}$$

will be completely trapped in the Occoquan Reservoir. Because this value is smaller than the smallest size calculated for Lake Jackson ( $2 \times 10^{-4}$  cm), our computations are simple. We assumed that 84 percent of the sediment is totally trapped and the remainder is trapped at an efficiency calculated for particle sizes of 0.0001 cm:

$$V_{\max} = \frac{4.8 \times 10^6 (2.66 - 1.) (1 \times 10^{-4})^2}{1.11}$$

$$= 0.072 \text{ m/day}$$

$$p = \frac{V_{\max} \tau_w}{D'} = \frac{0.072 \cdot 21.4}{5.29} = 0.29$$

The annual sediment trapped is:

$$S_t = P \cdot S_i$$

but corrections for sources and SDR must be made:

$$S_i = \text{SDR} \times \text{sediment from each source.}$$

$$S_i = 13390 \text{ (Lake Jackson, already corrected for SDR)} + 0.115 \text{ (232103)} \\ \text{(Bull Run)} + 0.115 \text{ (139685)} \text{ (Occoquan River)} + 12699 \text{ (Urban Runoff)}$$

$$S_i = 68845 \text{ metric tons/year}$$

Assuming the distribution of particle sizes for all sources are essentially the same and accounting for the fractions ( $f$ ) of material that are in the two different size ranges:

$$S_i = f_1 P_1 S_i + f_2 P_2 S_i$$

$$S_t = (0.84) (1.0)(68845) + (0.16) (0.29) (68845)$$

$$S_t = 57830 ; 3194 = 61024 \text{ metric tons}$$

The volume lost is  $\frac{61024}{0.93} = 65620 \text{ m}^3/\text{year}$  or 0.2 percent per year of the reservoir volume.

#### 5.7.4 Eutrophication

What would be the consequences to eutrophication in Occoquan Reservoir of instituting 90 percent phosphorus removal at the treatment plant? If, in addition to

phosphorus removal, nonpoint source (NPS) phosphorus was reduced by 90 percent by instituting urban runoff and erosion control, green belts, and other NPS controls, would an improvement in lake quality occur?

Several assumptions concerning pollutants in the Occoquan watershed-reservoir system are necessary in order to calculate the desired annual loads:

- The unavailable phosphorus is adsorbed on sediment particles. Therefore, of the unavailable forms coming into Lake Jackson, only the fraction  $(1 - P_c [\text{Jackson}])$  is delivered to the Occoquan Reservoir; available P gets through Jackson.
- All of the phosphorus and nitrogen from the sewage treatment plants (STPs) is in available form.
- The output of STPs outside the Bull Run sub-basin is negligible compared to that of the STPs in Bull Run. This is justified by the fact that during the period under study, the plants in Bull Run had a combined capacity several times larger than the few plants outside the sub-basin.
- The problems of eutrophication depend on loading of phosphorus.

By applying these assumptions to the nonpoint source data in Tables V-19 and V-24 the total load of each pollutant type may be calculated (Table V-25). The computation for the total annual phosphorus load in Occoquan Reservoir is computed in the following paragraphs. First the quantity of total phosphorus coming into the Occoquan Reservoir through Lake Jackson is calculated by:

$$TP_{\text{Jackson}} = (1 - P_{c\text{Jackson}}) \times [\text{Total P} - \text{Available P}] + \text{Available P}$$

The total phosphorus from Broad run, Cedar Run, and Kettle Run are summed and the available phosphorus loads are subtracted to give the unavailable load. This load is multiplied by the trap efficiency of the lake,  $P_c = 0.83$ , which yields the unavailable load passing through. This value, plus the available load, is an estimate of the total phosphorus entering Occoquan Reservoir from Lake Jackson. This quantity is 103.24 metric tons  $\text{yr}^{-1}$  (Table V-25). This value is added to the non-urban, nonpoint source loads from Bull Run and areas adjacent to the Occoquan Reservoir (Table V-18):

$$\begin{aligned} T_{\text{NPNU}} &= 202.71 + 119.42 + 103.24 \\ &= 425.37 \text{ metric tons } \text{yr}^{-1} \end{aligned}$$

This quantity is modified by the sediment delivery ratio. The urban nonpoint loads and STP (Table V-24) loads are added to complete the calculation:

$$\begin{aligned} TP &= (0.115) (425) + 2.59 + 11.92 \\ &= 63.3 \text{ metric tons } \text{yr}^{-1} \end{aligned}$$

Similarly the SDR was applied to nonpoint sources of nitrogen and BOD. The results of load calculations are summarized in Table V-25.

The calculated annual total phosphorus and nitrogen loads (Table V-25) may

TABLE V-24

SEWAGE TREATMENT PLANT POLLUTANT LOADS  
IN BULL RUN SUB-BASIN IN METRIC TONS PER YEAR<sup>a</sup>

Total Nitrogen	Total Phosphorus	BOD <sub>5</sub>
108.0	11.92	54.80

Source: Northern Virginia Planning District  
Commission, March 1979.

<sup>a</sup>Averages for July 1974 - December 1977

TABLE V-25

CALCULATED ANNUAL POLLUTANT LOADS TO OCCOQUAN RESERVOIR

Load Source	Metric Tons/Year				BOD <sub>5</sub>
	Total N	Avail. N	Total P	Avail. P	
Urban runoff	12.88	5.38	2.59	1.27	77.47
Sewage treatment	108.00	108.00	11.92	11.92	54.80
Rainfall	14.62	14.62	-	-	-
Other Nonpoint Source*	391.00	39.10	48.83	2.65	802.00
TOTAL	526.50	167.10	63.34	15.84	934.27
Nonpoint Source %	80	35	81	25	94
Point Source %	20	65	19	75	6

\* Used SDR of 0.115.

be compared with the observed loads listed in Table V-26. The loads observed are 1.5 to 6 times higher than highest calculated loads for nitrogen. Comparison of loadings (kg/ha year) with literature values suggest that Grizzard is most accurate (Likens *et al.*, 1977).

The first method of predicting algal growth is known as the Vollenweider Relationship. In the graph of total phosphorus load ( $\text{g m}^{-2} \text{yr}^{-1}$ ) versus mean

TABLE V-26

## OBSERVED ANNUAL POLLUTANT LOADS TO OCCOQUAN RESERVOIR

Period	Mean Flow <sup>a</sup> Rate (m <sup>3</sup> sec <sup>-1</sup> )	Total Nitrogen Load (metric tons year <sup>-1</sup> )	Total Phosphorus Load (metric tons year <sup>-1</sup> )
10/74 - 9/75	24.7	805 <sup>b</sup>	110 <sup>b</sup>
7/75 - 6/76	24.0	1905 <sup>c</sup>	188 <sup>c</sup>
7/76 - 6/77	10.4	4763 <sup>c</sup>	454 <sup>c</sup>

<sup>a</sup> Source: USGS Regional Office, Richmond, Virginia.

<sup>b</sup> Grizzard et al., 1977

<sup>c</sup> Northern Virginia Planning District Commission, March, 1979.  
Data gathered by Occoquan Watershed Monitoring Laboratory.

depth (m) divided by hydraulic retention time (yrs) (see Figure V-24), areas can be defined that roughly correspond to the nutritional state of the impoundment. For the Occoquan Reservoir, the values of the parameters are:

$$L_p = \frac{(63.34) \times 10^6 \text{ g/yr}}{7.01 \times 10^6 \text{ m}^2} = 9.04 \text{ g m}^{-2} \text{ yr}^{-1}$$

$$\frac{\bar{z}}{\tau_w} = \frac{5.29 \text{ m}}{0.0586 \text{ yr}} = 90 \text{ m yr}^{-1}$$

According to the Vollenweider Relationship, Occoquan Reservoir is well into the eutrophic region for loading of total phosphorus. Based on these predictions a more in-depth study of the algal productivity seems to be in order.

Solving for the phosphorus concentration in this reservoir:

$$P = \frac{L_p}{\bar{z}} \frac{1}{D + \sqrt{D}} = \frac{9.04 \text{ g m}^{-2} \text{ yr}^{-1}}{5.29 \text{ m} [(17.1 + \sqrt{17.1}) \text{ yr}^{-1}]}$$

$$P = 0.0805 \text{ g/m}^3 = 80.5 \text{ } \mu\text{g/l.}$$

Calculated and observed pollutant concentrations are listed in Table V-27. The mean summer concentrations of phosphorus and nitrogen are closer to the concentrations calculated than would be expected on the basis of the comparison of annual loads.

TABLE V-27

CALCULATED AND OBSERVED MEAN ANNUAL POLLUTANT  
CONCENTRATIONS IN OCCOQUAN RESERVOIR

	Total Nitrogen <sup>b</sup> (g m <sup>-3</sup> )	Available Nitrogen <sup>a</sup> (g m <sup>-3</sup> )	Total Phosphorus (g m <sup>-3</sup> )
Calculated (SDR = 0.115)	0.831	0.264	0.08
Observed Values <sup>a</sup>			
Mean	0.88	0.16	0.08
Max.	1.50	0.24	0.12
Min.	0.35	0.10	0.04

a Assuming no removal processes for nitrogen.

b Averages for April-October between 1973 and 1977.

Source: Northern Virginia Planning District Commission,  
March, 1979.

The ratio of nitrogen to phosphorus concentration in the reservoir can be used to estimate which nutrient will limit the rate of plant growth. For the Occoquan Reservoir, the N:P ratios are 10 to 1 for total N to total P. The calculated nutrient ratios and the N:P ratio of the observed data (11.0) indicates that phosphorus is probably growth limiting.

The available data also permits the estimation of the maximal primary production of algae from the Chaudani and Vighi Curve (Figure V-26). The theoretical phosphorus concentration should be about 0.08 g m according to calculations. The maximal primary production of algae is found from Figure V-26 to be about 2500 mgC m<sup>-2</sup> day<sup>-1</sup>. This level of algal production is roughly the maximum production shown on the curve. Both this result and the Vollenweider Relationship suggest algal growth will contribute significantly to the BOD load in the impoundment.

Effects of 90 percent P removal at treatment plant on TP loading:

$$M = 52.61 \text{ m ton/yr}$$

$$L = \frac{52.61 \times 10^6 \text{ g/yr}}{7.01 \times 10^9 \text{ m}^2} = 7.50 \text{ g m}^{-2} \text{ y}^{-1}$$

$$q_s = 90 \text{ m yr}^{-1}$$

Although improved, we conclude that loading is still too great according to figure V-24.

Effects of 90 percent STP removal of TP plus 90 percent NPS removal of TP:

$$M = 6.334 \text{ m ton/yr}$$

$$L_p = \frac{6.334 \times 10^6}{7.01 \times 10^6} = 0.90 \text{ g m}^{-2} \text{ y}^{-1}$$

This would move Occoquan Reservoir into the bottom of the mesotrophic range.

Lake concentrations of total P would be:

$$P = \frac{(7.5)}{(5.29) \cdot (21.2)} = 66.9 \text{ } \mu\text{g/l}$$

$$P = \frac{0.90}{(5.19) \cdot (21.2)} = 8 \text{ } \mu\text{g/l}$$

Although the screening method shows marked improvement in Occoquan eutrophication, 90 percent control of phosphorus NPS would be very expensive. Careful analysis of assumptions made in the screening method and of control alternatives would be necessary before proceeding to map such a control strategy. Moreover, careful study of reservoir TP sources and sinks and of algal productivity would be necessary. The screening method has served to illustrate the feasibility and potential value of such further analysis.

#### 5.7.5 Hypolimnetic DO Depletion

Excessive nutrient loading plus inputs of BODs suggest that DO problems in the hypolimnion could result. We will use the data obtained in the first three problems to determine the hypolimnetic DO. These data are summarized below. All rate coefficients listed have already been corrected for temperature.

#### Physical/Biological

$$\text{Area} = 7.01 \times 10^6 \text{ m}^2$$

$$\text{Volume} = 3.71 \times 10^7 \text{ m}^3$$

$$Q = 20.09 \text{ m}^3 \text{ sec}^{-1} = 1.74 \times 10^6 \text{ m}^3 \text{ day}^{-1}$$

$$\text{Depth to thermocline} = 5.29 \text{ m (average depth)}$$

$$\text{Interval of stratification (May to mid-September)} = 138 \text{ days}$$

$$\text{BOD loading} = 934.27 \text{ } 10^6 \text{ g} \cdot \text{yr}^{-1}$$

$$\text{Algal loading} = 1800 \text{ mgCm}^{-2} \text{ day}^{-1}$$

$$\text{BOD concentration} = \frac{934.27 \times 10^6 \text{ g/yr}}{3.71 \times 10^7 \text{ m}^3 \times 365 \text{ days/yr}} = 0.069 \text{ mg/l}$$

$$\text{Temperature} = 10^\circ\text{C}$$

#### Rates and Input Values

M	= 0.8	$k_1$	= 0.063 $\text{day}^{-1}$
S	= 2.67	k	= 0.0378 $\text{day}^{-1}$
P	= 0.824 $\text{gC m}^{-2} \cdot \text{day}^{-1}$	$k_4$	= 0.0019 $\text{day}^{-1}$
$\bar{D}$	= 5.29 m	$\text{DO}_{\text{sat}}$	= 11.3 mg/l
$\tau_w$	= 21.4 day	t	= 138

The simplified model used to predict hypolimnion dissolved oxygen levels assumes that the only substantial dissolved oxygen sinks are water column and benthic deposit BOD (Section 5.5). Additionally, all sources of oxygen, photosynthesis, etc., are neglected in the hypolimnion after the onset of stratification. Thus, the procedure requires that pre-stratification levels of BOD and dissolved oxygen be estimated in order to compute the post-stratification rates of oxygen disappearance. The pre-stratification concentration of water column BOD is determined first. A simple mass balance leads to the following relationship, if steady state conditions are assumed:

$$C_{SS} = -\frac{k_a}{k_b}$$

where

$$C_{SS} = \text{steady state concentration of BOD in water column, mg/l}^{-1}$$

$$k_a = \text{mean rate of BOD loading from all sources g m}^{-3} \text{ day}^{-1}$$

$$k_b = -k_s - k_1 - \frac{1}{\tau_w}$$

where

$$k_s = \frac{V_s}{\bar{Z}} = \text{mean rate of BOD settling out onto impoundment bottom, day}^{-1}$$

$$k_1 = \text{mean rate of decay of water column BOD, day}^{-1}$$

$$Q = \text{mean export flow rate, m}^3 \text{ day}^{-1}$$

$$V = \text{impoundment volume, m}^3$$

$$V_s = \text{settling velocity, m day}^{-1}$$

$$\bar{Z} = \text{impoundment mean depth, m.}$$

The BOD load to the impoundment originates in two principal sources: algal growth and tributary loads. The algal BOD loading rate is computed from the expression:

$$k_a(\text{algae}) = \text{SMP}/\bar{Z}$$

where

$$S = \text{stoichiometric conversion from algal biomass as carbon to BOD} = 2.67$$

$$M = \text{proportion of algal biomass expressed as oxygen demand}$$

$$P = \text{algal primary production, g m}^{-2} \text{ day.}$$

Since the Chiudani and Vighi curve (Figure V-26) gives the maximal algal production, a correction should be made for the actual epilimnion temperature. If the maximal rate occurs at 30°C and the productivity decreases by half for each 15°C decrease in temperature, the algal production can be corrected for temperature using the expression:

$$P_{(T)} = P_{(30)} \times 1.047^{(T-30^\circ\text{C})}$$

According to the data in Table 1, the epilimnion temperature during the month prior to stratification is approximately 13°C. Thus:

$$P_{(13^\circ)} = (1.8) \text{ gC m}^{-2} \text{ day}^{-1} \times 1.047^{(13^\circ\text{C}-30^\circ\text{C})}$$

$$= 0.824 \text{ gC m}^{-2} \text{ day}^{-1}$$



If M is assumed to be 0.8, then:

$$k_a(\text{algae}) = \frac{2.67 \times 0.8 \times 0.824 \text{ gC m}^{-2} \text{ day}^{-1}}{5.293 \text{ m}}$$

$$= 0.333 \text{ g m}^{-3} \text{ day}^{-1}$$

The BOD load borne by tributaries is found by the expression:

$$k_a(\text{trib}) = \frac{\text{Mean Daily BOD from Tributaries (Table V-18)}}{\text{Impoundment Volume}}$$

$$= \frac{034.27 \times 10^6 \text{ g yr}^{-1}}{3.71 \times 10^7 \text{ m}^3} \times \frac{1 \text{ yr}}{365 \text{ days}}$$

$$= 0.069 \text{ g m}^{-3} \text{ day}$$

The total BOD load to Occoquan Reservoir is then:

$$k_a = k_a(\text{algae}) + k_a(\text{trib})$$

$$= 0.33 \text{ g m}^{-3} \text{ day}^{-1} + 0.069 \text{ g m}^{-3} \text{ day}^{-1}$$

$$= 0.402 \text{ g m}^{-3} \text{ day}^{-1}$$

Before the water column BOD concentration can be computed, the constants comprising  $k_b$  must be evaluated. The first of these,  $k_s$ , requires knowledge of the settling velocities of BOD particles. Ideally these would be determined by using values of the physical properties of the particles and the water in the settling velocity equation, V-6. Because such data are lacking, a settling velocity of  $0.2 \text{ m day}^{-1}$  reported for detritus will be substituted. The reported values lie between 0 and 2 meters  $\text{day}^{-1}$ , with most values close to  $0.2 \text{ m day}^{-1}$  (Zison et al., 1978). Then:

$$k_s = 0.2 \text{ m m day}^{-1} / 5.29 \text{ m m} = 0.0378 \text{ day}^{-1}$$

The second constant comprising  $k_b$  is the first-order decay rate constant for water column BOD. Reported values of  $k_1$  vary widely depending on the degree of waste treatment. Zison et al. (1978)<sup>1</sup> presents data for rivers, but contains only two values for  $k_1$  in lakes and estuaries. Both are  $k_1 = 0.2 \text{ day}^{-1}$ . Camp (1968) reports values from 0.01 for slowly metabolized industrial wastes to 0.3 for raw sewage. Because there is considerable sewage discharge into the Occoquan Reservoir,  $k_1$  may be assumed to be in the upper range of these values, between 0.1 and 0.3 or  $0.15 \text{ day}^{-1}$ . Like the algal production rate,  $k_1$  must be corrected for the water temperature. In April, the mean water temperature is about  $11^\circ\text{C}$ .

Then:

$$k = 0.095 \text{ day}^{-1} \times 1.047 (11^\circ\text{C}-20^\circ\text{C})$$

$$= 0.063 \text{ day}^{-1}$$

Finally,  $k_b$  is evaluated as follows:

$$k_b = -0.0378 \text{ day}^{-1} - 0.063 \text{ day}^{-1} - \frac{1}{21.4 \text{ days}}$$

$$= -0.148 \text{ day}^{-1}$$

Next,  $k_a$  and  $k_b$  may be substituted into the following equation to obtain  $C_{ss}$ .

$$C_{SS} = \frac{k_a}{k_b}$$

$$= \frac{0.402}{0.148} = 2.72 \text{ g m}^{-3}$$

Once the water column BOD concentration is known, the benthic BOD is computed from the expression:

$$L_{SS} = \frac{k_s C_{SS} \bar{D}}{k_4}$$

where

$$k_4 = \text{mean rate of benthic BOD decay, day}^{-1}$$

Values for the benthic BOD decay rate constant span a greater range than those for water column BOD. Camp (1968), however, reports values of  $k_4$  very near  $0.003 \text{ day}^{-1}$  for a range of benthic depth from 1.42 to 10.2 cm (Table V-10). Assuming this to be a good value, a temperature-corrected value of  $k_4$  may be computed at an April hypolimnion temperature of  $10^\circ\text{C}$  (Table V-18):

$$k_4 = 0.003 \text{ day}^{-1} \times 1.047^{(10-20)} = 0.0019 \text{ day}^{-1}$$

Then:

$$L_{SS} = \frac{0.0378 \text{ day}^{-1} \times 2.72 \text{ g m}^{-3} \times 5.29 \text{ m}}{0.0019 \text{ day}^{-1}}$$

$$= 286 \text{ g m}^{-2}$$

Prior to stratification the impoundment is assumed to be fully mixed and saturated with oxygen. During April, the hypolimnion temperature is  $10^\circ\text{C}$ . Saturated water at this temperature contains 11.3 ppm oxygen (Table V-12).

Finally, the dissolved oxygen level in the hypolimnion may be predicted during the period of stratification. The applicable expressions are:

$$\Delta O_L = (1.04) [(53.1) (0.231) - (1/53.1)]$$

$$\Delta O_L = 12.74$$

$$\Delta O_C = (1.7) (1) = 1.7$$

$$O_t = 11.3 - 12.74 - 1.7$$

Therefore the hypolimnion is depleted of oxygen at the end of the stratification period (138 days). By selecting different conditions for decay rates and for time of stratification a family of curves was generated that can be compared with actual observations (Figure V-39). As can be seen situations 3 and 4 (BOD decay of  $0.3 \text{ day}^{-1}$  later corrected for temperature and a total BOD loading of  $0.36$  or  $0.57 \text{ g l m}^{-3} \text{ day}^{-1}$ ) gave a reasonable fit of observed data at the deepest station (Occoquan Dam, 1973).

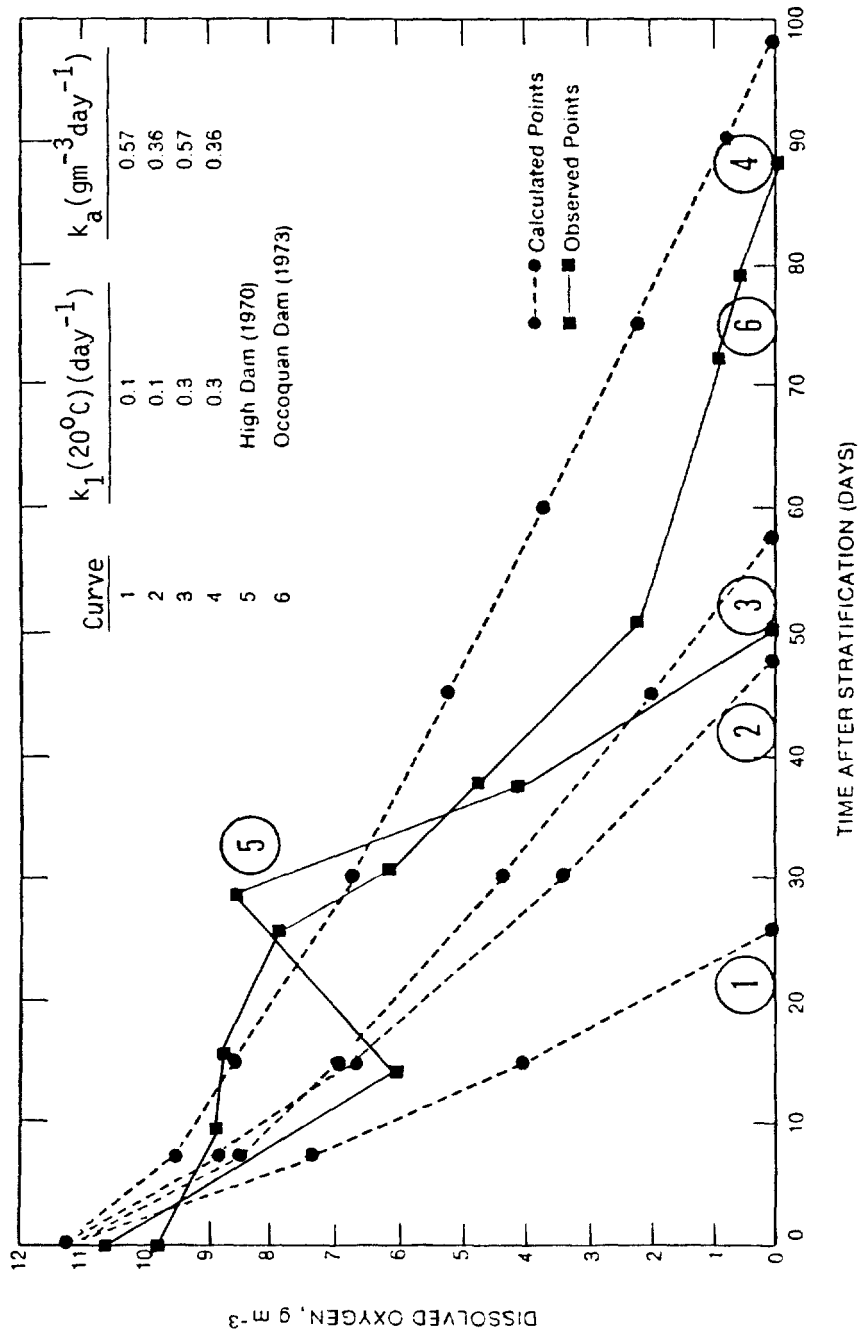


FIGURE V-39 DISSOLVED OXYGEN DEPLETION VERSUS TIME IN THE OCCOQUAN RESERVOIR

Interpretation of the dissolved oxygen-time data at High Dam in 1970 presented in Figure V-39 is complicated by the introduction of fresh oxygen after the onset of stratification. Although a direct comparison of oxygen depletion times is not possible, the rates of oxygen level follows curve 2 of Figure V-39 very closely, while during the second period of oxygen consumption the oxygen concentrations closely match those of curve 1. Since the reservoir is shallowest at High Dam and the substantially lower than average flow rate in 1970 resulted in strongly stratified conditions, the oxygen depletion rates in this case should be among the highest likely to be observed in the impoundment. Curve 1 represents the fastest decay rates predicted by the model. Thus, the observed oxygen consumption times should be greater than the lower limit predicted by the model in nearly all cases.

The above agreement of the observed with the predicted limits for the range of oxygen depletion times in Occoquan Reservoir implies that the typical or average time must also fall within the predicted range. Since it was for "average" conditions that the impoundment was modeled, it may be concluded that the model does accurately describe the behavior of the Occoquan Reservoir.

#### 5.7.6 Toxicants

It was not possible to obtain data on toxicants in Occoquan Reservoir. In order to provide a problem with some realism, published data on a priority pollutant in another reservoir were obtained. In Coralvine Reservoir, Iowa, commercial fishing was banned in 1976 because of excessive accumulation of dieldrin residues in flesh of commercially important bottom feeding fish (Schnoor, 1981). The dieldrin arose from biodegraded aldrin, an insecticide in wide use along with dieldrin before cancellation of registration of both pesticides by USEPA in 1975.

After 1976 there was steady diminution of dieldrin in the waters, fish, and bottom sediments of Coralville Reservoir, until the late 1970's when dieldrin levels in fish flesh declined to less than 0.3 mg/kg (Food & Drug Administration guideline). In 1979, the fishing ban was rescinded.

Using the screening methods and data abstracted from Schnoor's paper, the potential dieldrin problem can be evaluated in Coralville Reservoir. Available and back-calculated data include the following values:

	<u>Reservoir</u>	<u>Dieldrin</u>
$T_w$	= 14 days = 336 hrs	$k_{ow}$ = 305000
$Z$	= 8 feet = 2.4 m	$k_{oc}$ = 35600
$C$	= 0.05 $\mu\text{g/l}$ dieldrin	volubility in fresh water $\approx$ 200 $\mu\text{g/l}$
$OC$	= 0.05 (estimate)	
$S_o$	= 200 $\mu\text{g/l}$ (estimate)	
	= 200 $\times 10^{-6}$ kg/kg	
$P$	= 0.9 (estimate)	

Assuming that conditions remained constant, the steady state concentration of dieldrin can be computed using the approach described in Section 5.6 as follows:

$$C = C_{in} / (1 + \tau_w \cdot k)$$

where

$$K = SED + B + k_v + k_p + k_h$$

Evaluation of K depends on estimation of the separate rate constants. Information in Chapter 2 and in Callahan, et al. (1977) indicate that the biodegradation rate (B) in aquatic systems is extremely small. Similarly volatilization ( $k_v$ ) and hydrolysis ( $k_h$ ) are negligible processes affecting the fate of dieldrin. Photolysis ( $k_p$ ) can be significant in some circumstances but the high turbidity in Coralville Reservoir indicates that minimal photolysis takes place. Consequently,  $K \cong SED$ . These assumptions are supported by Schnoor (1981).

Calculation of the sedimentation rate constant (SED) is as follows:

$$SED = a \times D \times K_p$$

$$\begin{aligned} k_p &= 0.63 \times k_{ow} \times OC \\ &= 0.63 \times 305000 \times 0.05 \\ &= 9610 \end{aligned}$$

$$\begin{aligned} D &= P \times 50 \times \frac{1}{\tau_w} \\ D &= 0.9 \times 200 \times 10^{-6} \times \frac{1}{336} = 5.36 \times 10^{-6} m^{-1} \end{aligned}$$

$$\begin{aligned} a &= 1 / (1 + k_p S) \\ s &= OC \times 50 = .05 \times 200 \times 10^{-6} = 1 \times 10^{-5} \\ a &= 0.912 \times 5.36 \times 10^{-5} \times 9610 \\ &= 0.0047 m^{-1} \end{aligned}$$

The steady state concentration of dieldrin in Coralville Reservoir is estimated to be:

$$\begin{aligned} C &= 0.05 \mu g/l (1 + (0.0047 hr^{-1} \times 336 hr)) \\ C &= 0.019 \mu g/l \end{aligned}$$

This value is much greater than the present fresh water quality criteria of 0.0023 dieldrin  $\mu g/l$  (Federal Register: 79318-79379. Nov. 28, 1980) and would indicate a serious potential problem in the reservoir that would require significant action and study.

Evaluation of bioconcentration supports this conclusion:

$$Y = BCF \times C$$

If the default estimate is used (Section 5.6.1.6):

$$\begin{aligned} \log BCF &= 0.75 \log KOW - 0.23 \\ &= 3.88 \end{aligned}$$

$$BCF = 7642$$

$$Y = 7642 \times 0.019 = 145 \mu g/kg \text{ fish flesh}$$

This value would be less than the FDA guideline. However, two published BCF values are available: 35600 from Chapter 2; 70000 from Schnoor (1981). These values produce much higher tissue burdens, both of which violate the FDA guideline:

$$Y = 35600 \times 0.019 = 676 \mu\text{g/kg}$$

$$Y = 70000 \times 0.019 = 1330 \mu\text{g/kg}$$

In 1979, it is estimated that  $C_{in} = 0.01$  (calculated from Schnoor, 1981). Therefore, assuming other conditions are constant:

$$C = 0.01 / (1 + (.0047 \times 336)) \\ = 0.0039 \mu\text{g/l}$$

A value about double the water quality criterion. Flesh concentration would be (using BCF = 70000):

$$Y = 70000 \times 0.0039 = 270 \mu\text{g/kg}$$

This value (**0.27  $\mu\text{g/kg}$** ) would be less than the FDA guidelines of **0.3  $\mu\text{g/kg}$**  and support the conclusion to lift the fishing ban. Schnoor (1981) shows the following measured data that can be compared to the screening results:

	1970		1979	
	<u>Water</u>	<u>Fish</u>	<u>Water</u>	<u>Fish</u>
Screening	0.019	1300	0.04	270
Measured	0.015	1100	0.005	250

## REFERENCES

- Callahan, M., M. Slimak, N. Gabel, I. May, C. Fowler, R. Freed, P. Jennings, R. Durfee, F. Whitmore, B. Maestri, W. Mabey, B. Holt, C. Gould. 1979. Water-Related Environmental Fate of 129 Priority Pollutants, Volumes 1 and 2. U.S. Environmental Protection Agency Report. EPA 440/4-79-029a, b. NTIS Reports: PB80 204373, PB80 204381.
- Camp, T.R. 1968. Water and Its Impurities. Reinhold Book Corporation, New York.
- Carlson, R.E. 1977. A Trophic State Index for Lakes. *Limnol. Oceanogr.* 22:361-369.
- Chen, C.W., and G.T. Orlob. 1973. Ecologic Study of Lake Koochanusa Libby Dam. U.S. Army Corps of Engineers, Seattle District.
- Chiudani, G., and M. Vighi. 1974. The N:P Ratio and Tests with *Selenastrum* to Predict Eutrophication in Lakes. *Water Research* 8:1063-1069.
- Cowen, W.F., and G.F. Lee. 1976. Phosphorus Availability in Particulate Materials Transported by Urban Runoff. *JWPCF* 48:580-591.
- Dean, J.D., R.J.M. Hudson, and W.B. Mills. 1979. Chesapeake-Sandusky: Non-designated 208 Screening Methodology Demonstration. Midwest Research Institute, Kansas City, MO. U.S. Environmental Protection Agency Rept. for Env. Res. Lab, Athens, GA. In Press.
- Dillon, P. 1974. A Manual for Calculating the Capacity of a Lake for Development. Ontario Ministry of the Environment.
- Dillon, P., and F. Rigler. 1975. *Journal Fisheries Research Board of Canada* 32(9).
- Dorich, R.A., D.W. Nelson, and L.E. Sommers. 1980. Algal Availability of Sediment Phosphorus in Drainage Water of the Black Creek Watershed. *J. Environ. Qual.* 9:557-563.
- Drury, D.D., D.B. Porcella, and R.A. Gearheart. 1975. The Effects of Artificial Destratification on the Water Quality and Microbial Populations of Hyrum Reservoir. PRJEW011-1. Utah State University, Logan, UT.
- Grizzard, T.J., J.P. Hartigan, C.W. Randall, J.I. Kim, A.S. Librach, and M. Derewianka. 1977. Characterizing Runoff Pollution-Land Use. Presented at MSDGC-AMSA Workshop, Chicago. VPI SU, Blacksburg, VA. 66 pp.
- Hudson, R.J.M., and D.B. Porcella, 1980. Selected Organic Consent Decree Chemicals: Addendum to Water Quality Assessment, A Screening Method for Non-designated 208 areas. U.S. Environmental Protection Agency Rept. for Env. Res. Lab, Athens, GA. In Press.
- Hutchinson, G.E. 1957. A Treatise on Limnology, Volume I. John Wiley & Sons, New York. 1015 pp.
- Hydrologic Engineering Center (HEC), Corps of Engineers. 1974. Water Quality for River-Reservoir Systems. U.S. Army Corp of Engineers.
- Jones, J.R., and R.W. Bachmann. 1976. Prediction of Phosphorus and Chlorophyll Levels in Lakes. *JWPCF* 48:2176-2182.

- Larsen, D. P., and K.W. Malueg. 1981. Whatever Became of Shagawa Lake? In: International Symposium on Inland Waters and Lake Restoration. U.S. Environmental Protection Agency. Washington, D.C. p. 67-72. EPA 440/5-81-010.
- Larsen, D.P., and H.T. Mercier. 1976. Phosphorus Retention Capacity of Lakes. J. Fish. Res. Board Can. 33:1731-1750.
- Likens, G.E. et al. 1977. Biogeochemistry of a Forested Ecosystem. Springer-Verlog, New York. 146 pp.
- Linsley, R.K., M.A. Kohler, and J.H. Paulhus. 1958. Hydrology for Engineers. McGraw-Hill, New York.
- Lorenzen, M.W. 1978. Phosphorus Models and Eutrophication. In press.
- Lorenzen, M.W. 1980. Use of Chlorophyll-Secchi Disk Relationships. Limnol. Oceanogr. 25:371-3727.
- Lorenzen, M.W., and A. Fast. 1976. A guide to Aeration/Circulation Techniques for Lake Management. For U.S. Environmental Protection Agency, Corvallis, OR.
- Lorenzen, M.W. et al. 1976. Long-Term Phosphorus Model for Lakes: Application to Lake Washington. In: Modeling Biochemical Processes in Aquatic Ecosystems. Ann Arbor Science, Ann Arbor, MI. pp. 75-91.
- Lund, J. 1971. Water Treatment and Examination 19:332-358.
- Marsh, P.S. 1975. Siltation Rates and Life Expectancies of Small Headwater Reservoirs in Montana. Report No. 65, Montana University Joint Water Resources Research Center.
- Megard, R.O., J.C. Settles, H.A. Boyer, and W.S. Combs, Jr. 1980. Light, Secchi Disks, and Trophic States. Limnol. Oceanogr. 25:373-377.
- Porcella, D.B., S.A. Peterson, and D.P. Larson. 1980. An Index to Evaluate Lake Restoration. Journal Environmental Engineering Division ASCE 106:1151-1169.
- Rast, W., and G.F. Lee. 1978. Summary Analysis of the North American (US Portion) OECD Eutrophication Project. U.S. Environmental Protection Agency, Corvallis, OR. 454 pp. EPA-600/3-78-008.
- Sakamoto, M. 1966. Archives of Hydrobiology 62:1-28
- Schnoor, J.L. 1981. Fate and Transport of Dieldrin in Coralville Reservoir: Residues in Fish and Water Following a Pesticide Ban. Science 211:804-842.
- Smith, V.H., and J. Shapiro. 1981. Chlorophyll-Phosphorus Relations in Individual Lakes: Their Importance to Lake Restoration Strategies. Env. Sci. and Tech. 15:444-451.
- Stumm, W., and J.J. Morgan. 1970. Aquatic Chemistry. Wiley-Interscience, New York.
- Vollenweider, R.A. 1976. Advances in Defining Critical Loading Levels for Phosphorus in Lake Eutrophication. Mem. Ist. Ital. Idrobiol. 33:53-83.
- Vollenweider, R.A., and J.J. Kerekes. 1981. Background and Summary Results of the OECD Cooperative Program on Eutrophication. In: International Symposium on Inland Waters and Lake Restoration. U.S. Environmental Protection Agency, Washington, D.C. p. 25-36. EPA 440/5-81-010.



- U.S. Department of Commerce. 1974. Climatic Atlas of the United States. U.S. Department of Commerce, Environmental Sciences Services Administration, Environmental Data Service, Washington, D.C.
- U.S. Environmental Protection Agency. 1975. National Water Quality Inventory, Report to Congress. EPA-440/9-75-014.
- Zison, S.W., W.B. Mills, D. Deimer, and C.W. Chen. 1978. Rates, Constants, and Kinetics Formulations in Surface Water Quality Modeling. U.S. Environmental Protection Agency, Athens, GA. 316 pp. EPA-600/3-78-105.

## GLOSSARY OF TERMS

Significant variables are shown with typical units. Units must be compatible or use conversion factors (Chapter 1). Note that some symbols are used for more than one term.

A	Lake surface area, $m^2$ - sediment area, $m^2$
a	Fraction of pollutant in solution = $1/(1+K_p \times S)$ , unitless
B	Biodegradation rate, $hr^{-1}$
B(T)	Biodegradation rate, corrected for temperature T, $hr^{-1}$
BCF	Bioconcentration factor, unitless
Bo	Initial microbial biodegradation rate, uncorrected for temperature or nutrient concentration, $hr^{-1}$
C	Reservoir concentration at time, t, $mg\ l^{-1}$
$C_0$	Initial concentration, $mg\ l^{-1}$
$C_p$	Concentration of phosphorus, $\mu g\ P\ l^{-1}$
$C_s$	Total exchangeable phosphorus concentration in the sediments, $g\ m^{-3}$
$C_s$	Toxicant concentration sorbed on sediment, $mg\ l^{-1}$
$C_t$	Concentration of BOD at time t, $mg\ l^{-1}$
$C_w$	Concentration in water phase, $mg\ l^{-1}$
$C_w$	Steady-state water column phosphorus concentration, $mg\ l^{-1}$ , $g\ m^{-3}$
$C_{in}$	Steady state influent concentration, mg/l
$C_{ss}$	Steady-state water column BOD, $g\ m^{-3}$
$C_{wt}$	Weight concentration
$C_{vol}$	Volumetric concentration
D	Depth, m
D	Discharge channel depth, ft
D	Sedimentation rate constant = $P \times S \times Q/V$ , $mg\ l^{-1}\ day^{-1}$
D	Dilution rate, $day^{-1}$
D'	Flowing layer depth, ft
D"	Inflow channel depth, ft
$\bar{D}$	Mean depth, m
$\bar{D}$	Depth to thermocline, m
$D_h$	Mean hypolimnion depth, m
$D_i$	Depth at the i <sup>th</sup> cross-section, m
Do	Diffusivity of oxygen in water ( $2.1 \times 10^{-9}\ m^2\ sec^{-1}$ , 20°C)
$D_p$	Weight density of a particle, $lb\ ft^{-3}$
$D_w$	Weight density of water, $lb\ ft^{-3}$ , $g\ cm^{-3}$
$D_w$	Pollutant diffusivity in water, $m^2\ sec^{-1}$
d	Number of days per time period, days
d	Particle diameter, cm

f	$1 + (\tau_w \times K)$ , unitless
g	Acceleration due to gravity, 32.2 ft $\text{sec}^{-2}$
$I_{SD}$	Intensity of light at Secchi depth, relative units
$I_0$	Initial intensity of light at surface, relative units
K	Pollutant removal rate, = $SED + B + k_v + k_p + k_h$ , $\text{hr}^{-1}$
K	Net rate of phosphorus removal, $\text{hr}^{-1}$
$K_1$	Specific rate of phosphorus transfer to the sediments, $\text{m yr}^{-1}$
$K_2$	Specific rate of phosphorus transfer from the sediments, $\text{m yr}^{-1}$
$K_3$	Fraction of total phosphorus input to sediment that is available for the exchange process, unitless
$K_a$	Reaeration rate, $\text{hr}^{-1}$
$Ka_1$	Reaeration coefficient, $\text{m hr}^{-1}$
$K_p$	Distribution coefficient between organic sediment and water, unitless
$K_1$	First order decay rate for water column BOD at 20°C, $\text{day}^{-1}$
$K_4$	Benthic BOD decay rate at 20°C, $\text{day}^{-1}$
$K_a$	Mean rate of BOD loading from all sources, $\text{g m}^{-3}\text{day}^{-1}$
$K_a(\text{algae})$	Algal contribution to BOD loading rate, $\text{g m}^{-3}\text{day}^{-1}$
$K_a(\text{trib})$	Tributary or point source contribution to BOD loading rate, $\text{g m}^{-3}\text{day}^{-1}$
$K_b$	$= -K_s - K_1 - (1/\tau_w)$ , $\text{day}^{-1}$
$k_e$	Extinction coefficient, $\text{m}^{-1}$
$k_h$	Hydrolysis rate, $\text{hr}^{-1}$
$k_p$	Photolysis rate, $\text{hr}^{-1}$
$k_r$	Photolysis rate constant uncorrected for depth and turbidity of the lake, $\text{m}^{-1}$
$k_s$	Mean rate of BOD settling out onto the impoundment bottom, $\text{day}^{-1}$
$k_v$	Volatilization rate, $\text{hr}^{-1}$
koc	Organic carbon based partition coefficient, unitless
kow	Octanol-water coefficient, unitless
L	Areal BOD load, $\text{gm}^{-2}$
$L_p$	Phosphorus loading, $\text{g m}^{-2}\text{yr}^{-1}$
$L_{ss}$	Steady-state benthic BOD load, $\text{g m}^{-2}$
M	Total annual phosphorus loading, $\text{g yr}^{-1}$
M	Proportion of algal biomass expressed as an oxygen demand (unitless)
MW	Molecular weight, $\text{g mole}^{-1}$
OC	Sediment organic carbon fraction, unitless
$\Delta O_c$	Dissolved oxygen decrease due to hypolimnion BOD, $\text{mg l}^{-1}$
$\Delta O_L$	Dissolved oxygen decrease due to benthic demand, $\text{mg l}^{-1}$

$O_0$	Dissolved oxygen at time $t = 0$ , $\text{mg l}^{-1}$
$O_t$	Dissolved oxygen at time $t$ , $\text{mg l}^{-1}$
$P$	Sediment trapping efficiency, unitless $1 > P > 0$
$P$	primary productivity rate, $\text{g Carbon m}^{-2} \text{ day}^{-1}$
$P$	Total phosphorus in the water column, $\text{mg m}^{-3}$
$PI$	Influent phosphorus, $\text{mg l}^{-1}$
$QI$	Mean annual inflow, $\text{m}^3 \text{ yr}^{-1}$
$Q$	Mean annual outflow, $\text{m}^3 \text{ yr}^{-1}$
$q_s$	Hydraulic loading $(\bar{Z}/\tau_w)$ , $\text{m yr}^{-1}$
$R$	Reynolds number, unitless
$r$	Radius, ft
$S$	Stoichiometric conversion from algal biomass as carbon to BOD, 2.67, unitless
$S$	Input suspended organic sediment = $OC \times S_o$ , $\text{mg l}^{-1}$
$S_i$	Mass of sediment in inflow per unit time, $\text{mg l}^{-1}$
$S_o$	Input of suspended sediment, $\text{mg l}^{-1}$
$S_t$	Sediment trapped, metric tons $\text{yr}^{-1}$
$SD$	Secchi depth, m
$SDR$	Sediment delivery ratio, unitless
$SED$	Sorption and sedimentation rate (toxicant at equilibrium with sediments), $\text{hr}^{-1}$
$T$	Temperature, degrees centigrade
$V$	Lake or impoundment volume, $\text{m}^3$
$V_H$	Hypolimnion volume, l
$V_s$	Sediment volume, $\text{m}^3$
$V_{\text{max}}$	Terminal velocity of a spherical particle, $\text{ft sec}^{-1}$
$W$	Wind speed, $\text{m sec}^{-1}$
$Y$	Tissue concentration of pollutant, $\text{g kg}^{-1}$ fish flesh
$y$	Number of years
$Z$	Depth, m
$Z$	Mean depth, m
$\mu$	Absolute viscosity of water, $\text{lb sec ft}^{-2}$ , $\text{g sec cm}^{-2}$
$\rho_p$	Mass density of a particle, slugs $\text{ft}^{-3}$
$\rho_w$	Mass density of water, slugs $\text{ft}^{-3}$
$\tau_w$	Mean hydraulic residence time ( $V/Q$ ), days

## 6.1 INTRODUCTION

### 6.1.1 General

Estuaries are of primary social, economic, and ecological importance to America. Forty-three of 110 of the Department of Commerce's Standard Metropolitan Statistical Areas are on estuaries (DeFalco, 1967). Estuaries are the terminal or transfer point for essentially all waterborne national and international commerce in this country, and biologically are more productive on a mass per unit area basis than any other type of water body. Essentially all conservative wastes and much of the nonconservative wastes discharged into any inland stream in America eventually pass into an estuary. Yet these coastal formations on which there is such a demand for services are less stable geologically than any other formation found on the continent (Schubel, 1971). Sedimentation processes, for example, are filling, destroying, or at least altering all estuaries. While this process is always rapid in a geological sense, the actual length of time required for complete estuarine sedimentation is a function primarily of the stability of the sea level, the rate of sediment influx, and the intra-estuarine circulation pattern (Schubel, 1971). The instability, variation, and complexity of estuaries make water quality assessment and prediction especially difficult, yet the demands placed on estuaries require a most active water quality management program.

This chapter will describe a systematic approach which may be used to provide estuarine water quality assessment and prediction. Its purpose is two-fold. First, the planner will be provided the capability of making elementary assessments of current estuarine water quality. Second, methodologies are presented by which the planner can evaluate changes in water quality which might result from future changes in waste loading.

Chapter 3 provided methodologies for assessing the waste load directly entering an estuary. Chapter 4 provided methodologies which can be used to assess the water quality of a river or stream as it enters an estuary. The output of these chapters will provide information about present and projected estuarine water quality which can be used to identify regions having greatest water quality problems, water quality parameters of special concern, and areas for which subsequent computer study is necessary. Methods presented below comprise a screening tool which may be used by the planner to focus attention on critical spatial regions and water quality parameters. These can then be fully assessed using computer models or other techniques, as desired.

### 6.1.2 Estuarine Definition

It is difficult to provide a concise, comprehensive definition of an estuary. The basic elements included in most current definitions are that an estuary is:

- o A semi-enclosed coastal body of water
- o Freely connected to the open sea
- o Influenced by tidal action
- o A water body in which sea water is measurably diluted with fresh water derived from land drainage (Pritchard, 1967; Pritchard and Schubel, 1971).

The seaward end of an estuary is established by the requirement that an estuary be semi-enclosed. Because this boundary is normally defined by physical land features, it can be specifically identified. The landward boundary is not as easily defined, however. Generally tidal influence in a river system extends further inland than does salt intrusion. Thus the estuary is limited by the requirement that both salt and fresh water be measurably present. Accordingly, the landward boundary may be defined as the furthest measurable inland penetration of sea salts. The location of this inland boundary will vary substantially from season to season as a function of stream flows and stream velocities and may be many miles upstream from the estuarine mouth (e.g., approximately 40 miles upstream on the Potomac River, 27 miles on the James River, and approximately 16 miles upstream for the small Alsea Estuary in Oregon) (Pritchard, 1971). This definition also separates estuaries from coastal bays (embayments) by the requirement for a fresh water inflow and measurable sea water dilution.

### 6.1.3 Types of Estuaries

While the above definition provides adequate criteria for segregating estuaries from other major types of water bodies, it does not provide a means to separate the various types of estuaries from one another. The variations in estuarine circulation patterns and resulting variations in pollution dispersion from estuary to estuary make classification a necessary part of any water quality assessment. Two basic estuarine classification systems have been used in recent years to accomplish estuarine subclass separation: a topographical system and a physical processes system (Dyer, 1973, Chapter 2 or Ippen, 1966, Chapter 10).

#### 6.1.3.1 Topographical Classification

Under a topographical system, estuaries are divided into four subclasses. These are briefly described below.

- Drowned River Valley (Coastal Plain Estuary). These estuaries are the result of a recent (within the last 10,000 years) sea level rise

which has kept ahead of sedimentation processes at a river's mouth. Such estuaries are, quite literally, rivers whose lower basins have been drowned by the rising oceans. Coastal plain estuaries are characteristically broad, relatively shallow estuaries (rarely over 30 m deep) with extensive layers of recent sediment.

- Fjord-like Estuaries. These estuaries are usually glacially formed and are extremely deep (up to 800 m) with shallow sills at the estuarine mouth. Fjord-like estuaries are restricted to high latitude mountainous regions and are not found in the United States outside of Alaska and Puget Sound in the state of Washington.
- Bar-built Estuaries. When offshore barrier sand islands build above sea level and form a chain between headlands broken by one or more inlets, a bar-built estuary is formed. These estuaries are characteristically very shallow, elongated, parallel to the coast, and frequently are fed by more than one river system. As a result bar-built estuaries are usually very complex hydrodynamically. A number of examples of bar-built estuaries can be found along the southeast coast of the United States.
- Tectonic Process Estuaries. Tectonic estuaries exist as the result of major tectonic events (movement of tectonic plates with associated faulting or subsidence and coastal volcanic activity). San Francisco Bay is a good example of an American estuary of this type.

Based on this topographic classification system, the vast majority of American estuaries fall into the drowned river class. As a result, this system is not functional for categorization of American estuaries. The classification system described below is based on physical processes and is more useful. Further, the parameters used in physical classification are directly applicable to estuarine pollution analysis. Consequently, a physical parameter classification system will be used for the water quality assessment approach to be presented.

#### 6.1.3.2 Physical Process Classification

Physical process classification systems are generally based on the velocity and salinity patterns in an estuary. Using these two parameters, estuaries can be divided into three classes, each of which is of potential importance to planners concerned with American coastal plain estuaries. The classes are: stratified, partially mixed, and well mixed.

The general behavior of salinity and velocity regimes in the three types of estuaries has been described by a number of researchers (Glennie, 1967, Duxbury, 1970, Pritchard, 1960, and Dyer, 1973, among others) and is summarized below:

- Stratified (Salt Wedge) Estuary. In this type of estuary, large fresh water inflows ride over a salt water layer which intrudes landward

along the estuary bottom. Generally there is a continuous inland flow in the salt water layer as some of this salt water is entrained into the upper seaward-moving fresh water flow. Tidal action is not sufficient to mix the separate layers. Salinity (S) and Velocity (U) profiles and a longitudinal schematic of this flow pattern are shown in Figure VI-1. The Mississippi River Estuary is usually a salt wedge estuary.

- Well Mixed. In well mixed estuary, the tidal flow (or the tidal prism\*) is much greater than the river outflow. Tidal mixing forces create a vertically well mixed water column with flow reversing from ebb to flood at all depths. Typical salinity and velocity profiles and a longitudinal flow schematic for a well mixed estuary are shown in Figure VI-2. As examples, the Delaware and Raritan River estuaries are both normally well mixed.
- Partially mixed. Partially mixed estuaries lie between stratified and well mixed in terms of flow and stratification characteristics. Tide-related flows in such estuaries are substantially greater than river flows. Significant salinity gradients exist as in fully stratified estuaries, but are much less steep. While velocity at all depths normally reverses with ebb and flood tide stages, it is possible for net inland flow to be maintained in the lowest layers. Typical salinity and velocity profiles and a longitudinal schematic flow diagram are shown in Figure VI-3. There are many partially mixed coastal plain estuaries in the United States; the lower James River Estuary is typical.

Classification primarily depends on the river discharge at the time of classification. Large river flows result in more stratified estuaries while low flow conditions in the same estuaries can lead to full mixing. Thus the classification of any single estuary is likely to vary from season to season as river flows vary. As examples, many West Coast estuaries are partially mixed in winter when river flows are high and are well mixed in summer when river flows are very low.

#### 6.1.4 Pollutant Flow in an Estuary

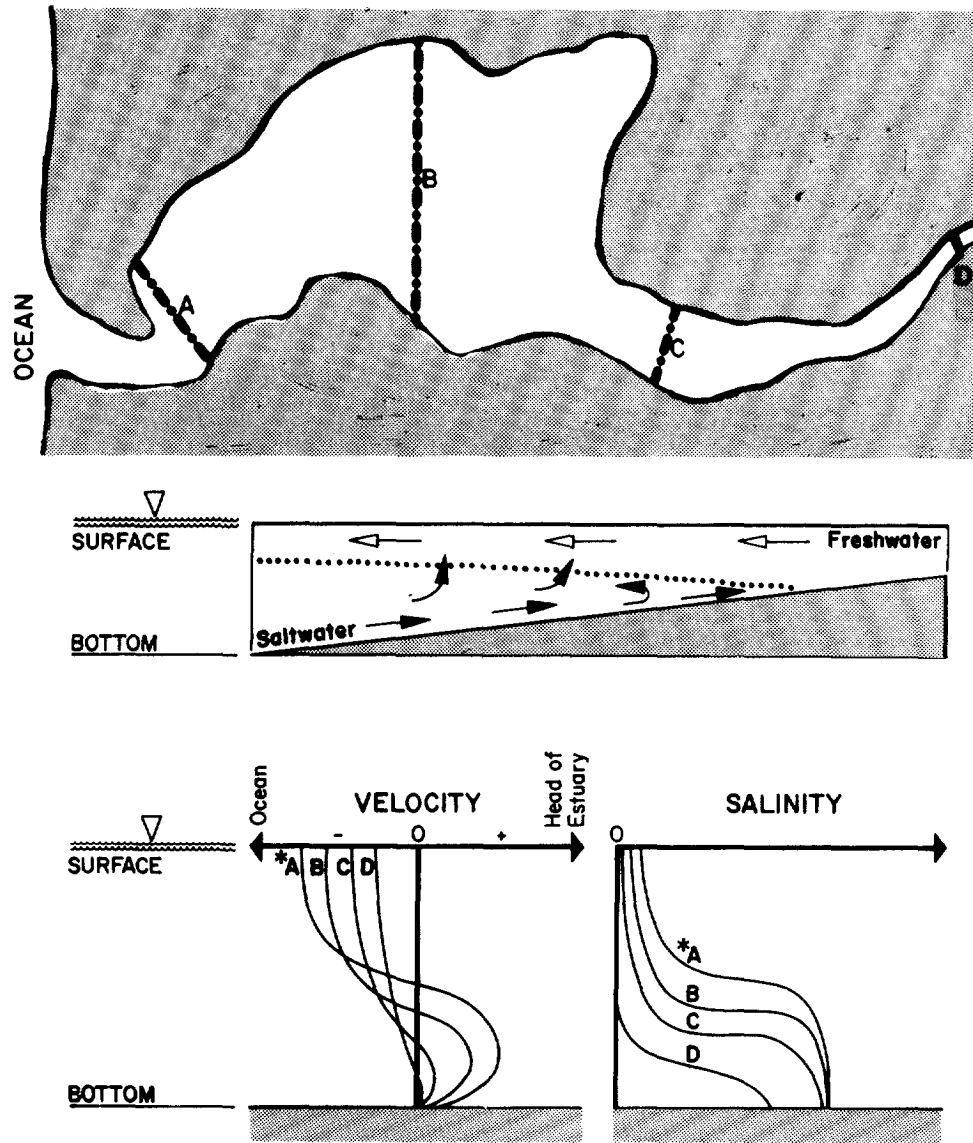
The importance of understanding the basic types of estuarine systems may be appreciated by briefly reviewing the general advective movements of a pollutant released into each of the three types of estuaries (summarized from Pritchard, 1960). The associated spatial and temporal variability of pollutant levels have water system management as well as water quality implications.

If a pollutant flow of density greater than the receiving water column is introduced into a salt wedge type estuary, the pollutant tends to sink into the

---

\*The tidal prism is that volume of water which enters an estuary during an incoming (flood) tide and equals high tide estuarine volume minus low tide volume.



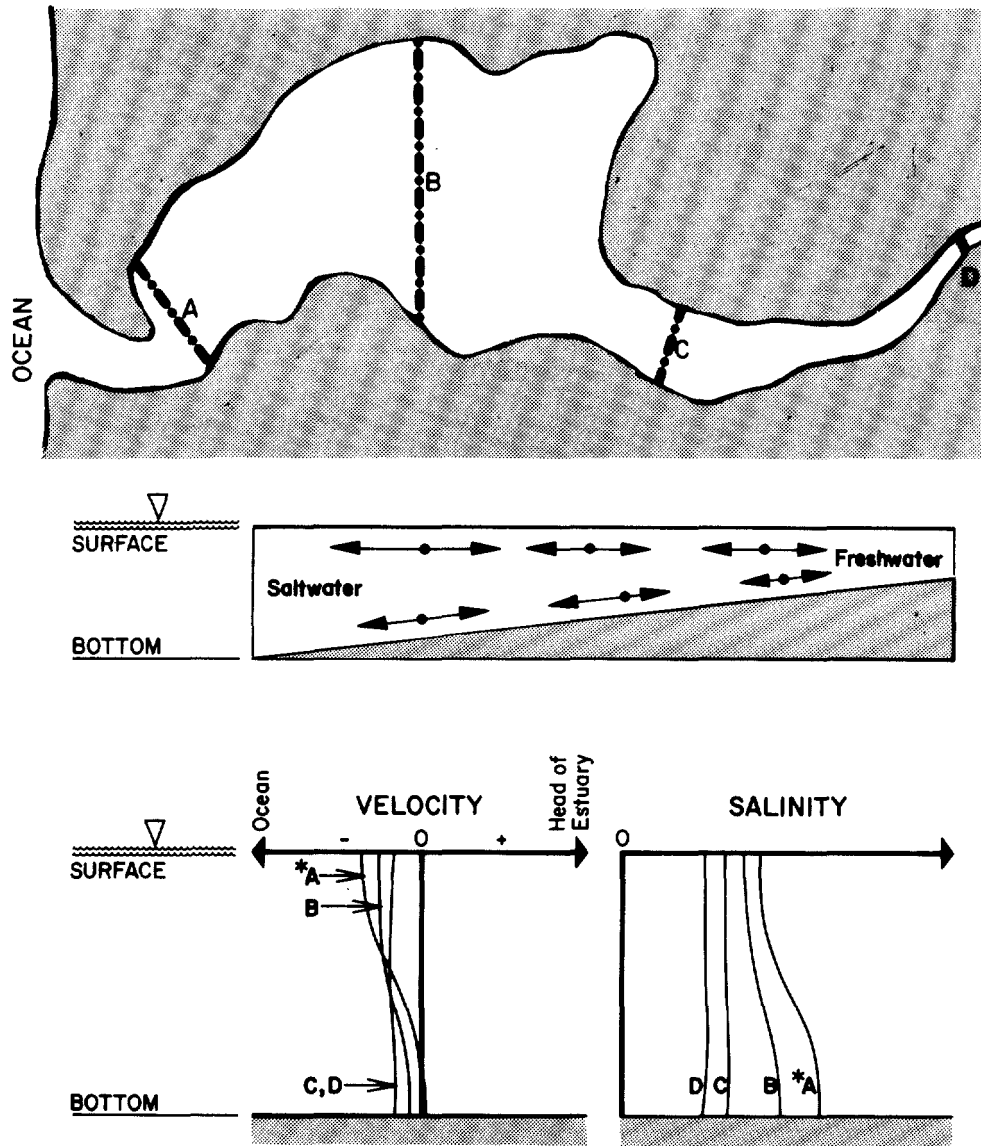


\*Letters correspond to cross sections

FIGURE VI -1 TYPICAL MAIN CHANNEL SALINITY AND VELOCITY FOR STRATIFIED ESTUARIES

bottom salt water layer and a portion can be advectively carried inland toward the head of the estuary. Frictionally induced vertical entrainment of the pollutant into the surface water flow is slow, residence time of the pollutant is high, and the time required to flush the pollutant from the estuary is also high. Some pollutants which are sufficiently dense and stable remain in or settle to the bottom layer of water, and are not transported out of a salt wedge estuary. Such constituents build up in the estuarine sediment layer.

Conversely, if a pollutant of lower density than the receiving water column is introduced into a salt wedge estuary, it remains in the surface layer is readily



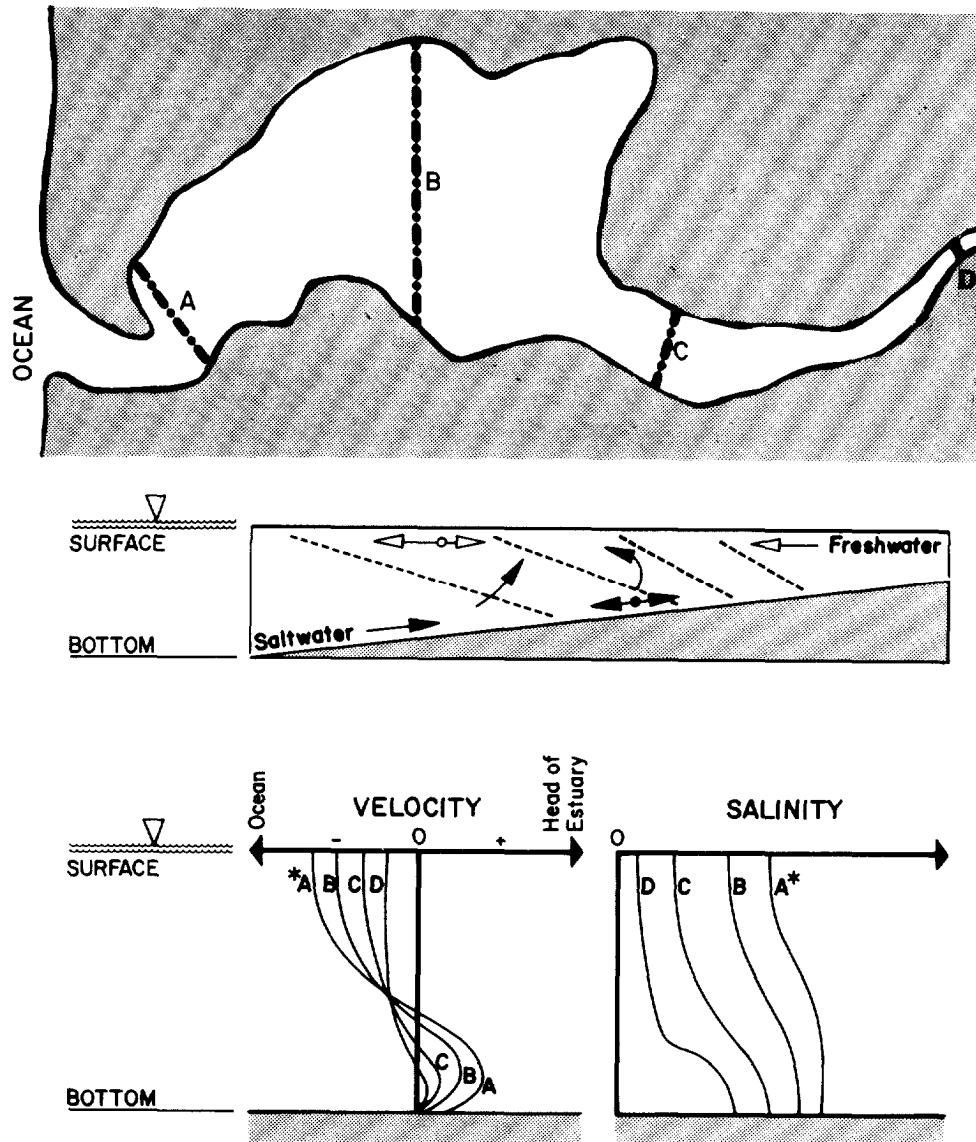
\*Letters correspond to channel cross-sections.

FIGURE VI -2 TYPICAL MAIN CHANNEL SALINITY AND VELOCITY PROFILES FOR WELL MIXED ESTUARIES

flushed from the system. This is the case because seaward flows strongly predominate in this layer.

At the opposite end of the estuary classification scale, a pollutant introduced into a well mixed estuary is advectively transported in a manner independent of the pollutant's density. Tidal forces cause turbulent vertical and lateral mixing. The pollutant is carried back and forth with the oscillatory motion of the tides and is slowly carried seaward with the net flow.

Pollutants introduced into partially mixed estuaries are dispersed in a manner



\*Letters denote channel cross-sections

FIGURE VI - 3 TYPICAL MAIN CHANNEL SALINITY AND VELOCITY PROFILES FOR PARTIALLY MIXED ESTUARIES

intermediate between the transport patterns exhibited in well mixed and stratified estuaries. Pollutant transport is density dependent but nevertheless involves considerable vertical mixing. Eventual flushing of the pollutant from an estuary in this case depends on the relative magnitudes of the net river outflow and the tidal seawater inflow.

### 6.1.5 Estuarine Complexity and Major Forces

Before outlining the complexities of estuarine systems, a brief review of the nomenclature used in this chapter will be helpful. This information is shown in Figure VI-4. This figure shows top, side, and cross sectional views of an estuary and indicates the basic estuarine dimensions. Additionally, the relationship between tidal elevation (or tidal stage) and surface water velocity is shown in the upper right quadrant of Figure VI-4.

The complexities of estuarine hydrodynamics are evident from even the brief qualitative descriptions presented above. Many variations in flow pattern and many of the forces acting on an estuarine water column have been omitted in order to permit a verbal description of the normally predominant phenomena, and it should be understood that the descriptions do not fully account for the complexities of estuarine motion. Estuarine circulation may be conceived as a three-dimensional flow field with variations possible in salinity and velocity along the longitudinal, the vertical, and the lateral axes. As a result of this complexity, and because an estuary is a transitional zone between fresh water and marine systems, great variations in a number of major water quality and physical parameters are possible. For example:

- pH. Typical concern pH is 7.8 to 8.4. Typically, rivers are slightly acidic ( $\text{pH} < 7$ ). Thus the pH can change from slightly acidic to basic across an estuary with resulting major changes in chemical characteristics of dissolved and suspended constituents. pH variations from 6.8 to 9.25 across an estuary have been recorded (Perkins, 1974, p. 29).
- Salinity. Over the length of an estuary, salinity varies from fresh water levels (typically less than 1 ppt) to oceanic salinity levels (usually 32 ppt to 34 ppt)\*. Moreover, salinity at any given location in an estuary may vary substantially over one tidal cycle and over the depth of the water column at any single point in time. Salinity variations are especially significant in estuarine calculations for a variety of reasons. First, salinity distribution can be used to predict the distribution of pollutants; second, salinity is a prime determinant of water density; and third, variations in salinity affect other major water quality parameters. For example, the saturated dissolved oxygen concentration normally diminishes by 2 mg/l as salinity increases from 0 to 35 ppt.
- River Flow. River flow is a major determinant of estuarine circulation and flushing characteristics. Instantaneous flow rates for some western rivers vary by orders of magnitude from winter high flow to summer low flow periods (Goodwin, et al. , 1970). These differences in river flow result in major variations in estuarine water quality characteristics.

---

\*ppt represents parts per thousand by mass. Sometimes the symbol ‰ is used.

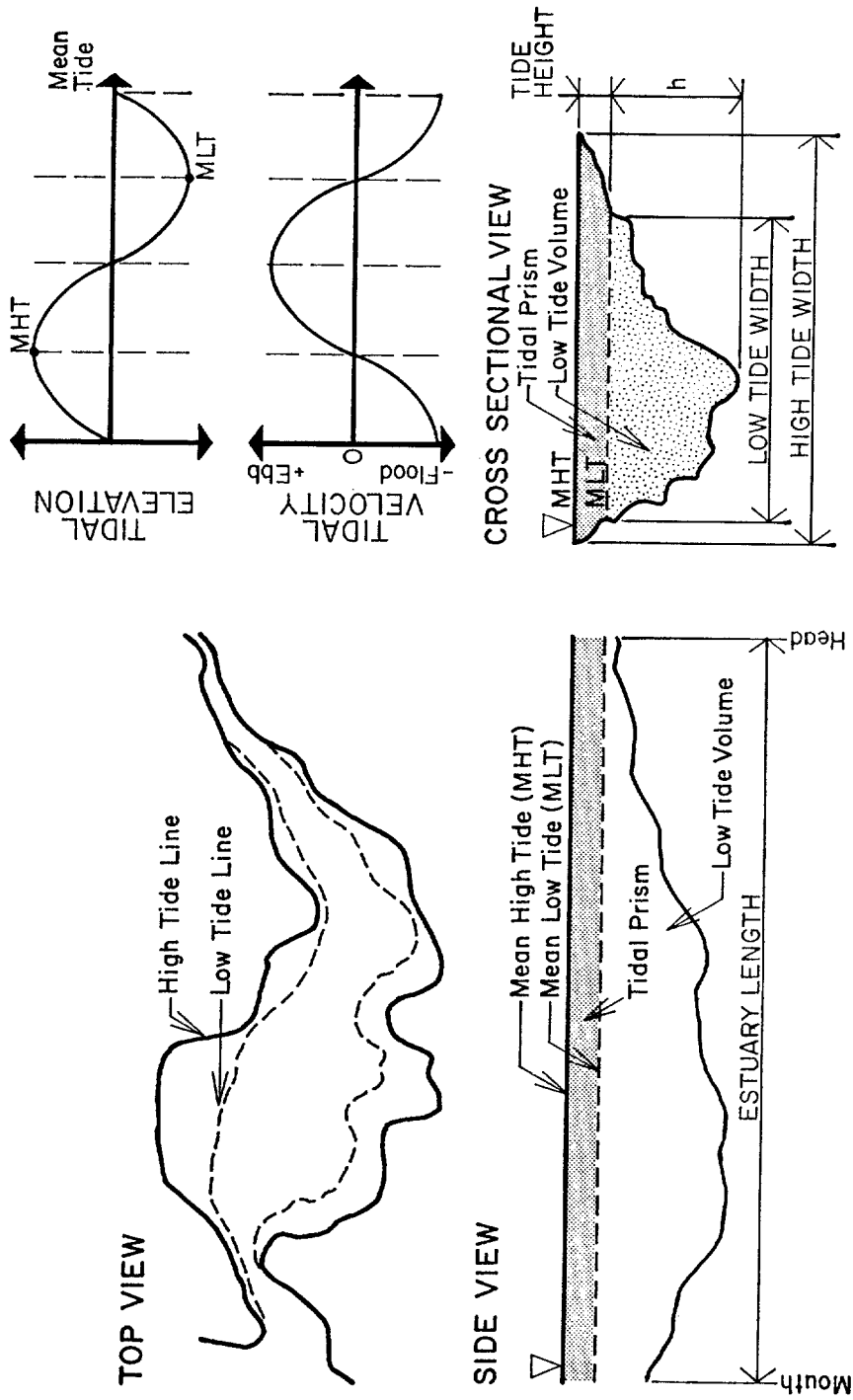


FIGURE VI-4 ESTUARINE DIMENSIONAL DEFINITION

- Time. Estuarine water quality parameters vary over several separate time scales. First, variations occur with each tidal cycle over a period of hours. Second, tidal cycles vary in mean amplitude from spring (maximum amplitude) to neap tides (minimum amplitude) every two weeks. This affects water quality since flushing characteristics are in part dependent on the tidal prism which is, in turn, dependent on tide stage. Third, there are seasonal variations in river flow, temperature and waste loadings.

The four factors just listed affecting the range and rate of variation of estuarine parameters pose part of the difficulty in analyzing estuarine water quality. In order to avoid large errors, both small time increments and small spatial increments must be used. This, in turn, necessitates a large number of individual calculations to fully analyze the variation of even a single parameter over the estuary and sometimes requires the use of a computer model.

Further complicating the analytical process is the large number of independent forces acting on the estuarine water column which should be considered. This group includes (from Harleman and Lee, 1969):

- Ocean tides
- Local wind stresses
- Bottom roughness and bottom sediment types
- Channel geometry
- Coriolis forces\*
- Nearby coastal features and coastal processes.

#### 6.1.6 Methodology Summary

A variety of techniques are presented in this chapter to assess water quality in estuaries. Table VI-1 summarizes the techniques and indicates if they are applicable to one-dimensional (well-mixed) or two-dimensional (vertically stratified) estuaries. Many of the techniques can be applied to conventional or toxic pollutants. If decay rates for toxic pollutants are needed, Chapter 2 can be used.

It is redundant to describe in detail each method at this point in the chapter, because the procedures are presented later. As a general statement, however, most of the methods for prediction of water quality apply to continuous, steady-state discharges of pollutants. The discharges can be located anywhere within the estuary,

---

\*Coriolis forces reflect the effect of a rotating reference plane (the earth) on particle motion. The net effect is to cause a water flow to drift to one side as it moves down a channel. The same effect tends to laterally segregate fresh water flows (moving from head to mouth) and salt water inflows (moving from mouth to head) in an estuary and in the northern hemisphere to create a counterclockwise flow pattern with fresh water to the right (looking from the head of the estuary toward the mouth) flowing toward the sea and salt water on the left flowing toward the head of the estuary.

TABLE VI -1

## SUMMARY OF METHODOLOGY FOR ESTUARINE WATER QUALITY ASSESSMENT

Calculations	Methods	Type of Estuary Applicable*
Estuarine Classification	• Hansen and Rattray	one- or two-dimensional
	• Flow ratio	one- or two-dimensional
Flushing Time	• Fraction of freshwater	one-dimensional
	• Modified tidal prism	one-dimensional
Pollutant Distribution	• Fraction of freshwater (conservative pollutants)†	one-dimensional
	• Modified tidal prism (conservative or first-order decay pollutants)†	one-dimensional
	• Dispersion-advective equations (conservative, first-order decay pollutants, † and dissolved oxygen)	one-dimensional
	• Pritchard's Box Model (conservative pollutants)†	two-dimensional
	• Initial dilution	one- or two-dimensional
	• Pollutant concentration at completion of initial dilution (conservative Pollutants, † pH, dissolved oxygen)	one- or two-dimensional
	• Farfield distribution (conservative and first-order pollutants, and dissolved oxygen)	two-dimensional
Thermal Pollution	• AT of water passing through condenser	not applicable
	• Maximum discharge temperature	not applicable
	• Thermal block criterion	one- or two-dimensional
	• Surface area criterion	one- or two-dimensional
	• Surface temperature criterion	one- or two-dimensional
Turbidity	• Turbidity at completion of initial dilution	one- or two-dimensional
	• Suspended solids at the completion of initial dilution	one- or two-dimensional
	• Light attenuation and turbidity relationship	one- or two-dimensional
	• Secchi disk and turbidity relationship	one- or two-dimensional
Sedimentation	• Description of sediment movement	one- or two-dimensional
	• Settling velocity determination	one- or two-dimensional
	• Null zone calculations	two-dimensional

\*One dimensional means a vertically well mixed system. A two dimensional estuary is vertically stratified.

†These methods apply to either conventional or toxic pollutants.

from head to mouth. Multiple sources of pollutants can be analyzed by applying the method of superposition, which is illustrated subsequently.

Although no single sequence of calculations must be followed to use the methodology, Figure VI-5 shows a suggested procedure. It is often useful to begin by classifying the estuary by season to find out when it is well mixed and when it is stratified. If the estuary is never well mixed, then the tools listed in Table VI-1 pertaining to one-dimensional estuaries should not be used.

Users are cautioned that the methods in this chapter are of a simplified nature, and consequently there are errors inherent in the calculations. Additionally, inappropriate data can produce further systematic errors. Data used should be appropriate for the period being studied. For example, when salinity profiles are needed, they should correspond to steady flow periods close to the critical period being analyzed.

Even though the methods presented in this chapter are amenable to hand calculations, some methods are more difficult to apply than others. The fraction of freshwater and modified tidal prism methods are relatively easy to apply, while the advective-dispersion equations offer greater computational challenge. Since the advective-dispersion equations require numerous calculations, the user might find it advantageous to program the methods on a hand calculator (e.g. TI-59 or HP-41C).

#### 6.1.7 Present Water-Quality Assessment

The first step in the estuarine water quality assessment should be the evaluation of existing water quality. Before an analysis of the impact of future waste load changes is made, the planner should know whether or not current estuarine water quality is acceptable, marginal, or substandard.

By far the best way to assess existing water quality is to measure it. The planner should attempt to locate other agencies which might have already collected acceptable samples and/or data. Candidate organizations include the United States Geologic Survey, the U.S. Army Corps of Engineers, state water quality control and monitoring agencies, and engineering and oceanographic departments of local colleges and universities. If such data cannot be located, a data collection program could be undertaken. If at all possible, high tide, and especially low tide in-situ measurements and samples should be collected along the full length of the estuary's main channel and in all significant side embayments. Analyses should then be made in an appropriate laboratory facility. If funds for such data collection efforts are not available, the use of a mathematical estimation of existing water quality is an alternative. The methods presented in subsequent sections and applied to the existing discharges can be used. However, it should be remembered that actual data are preferable to a mathematical estimate of existing water quality.



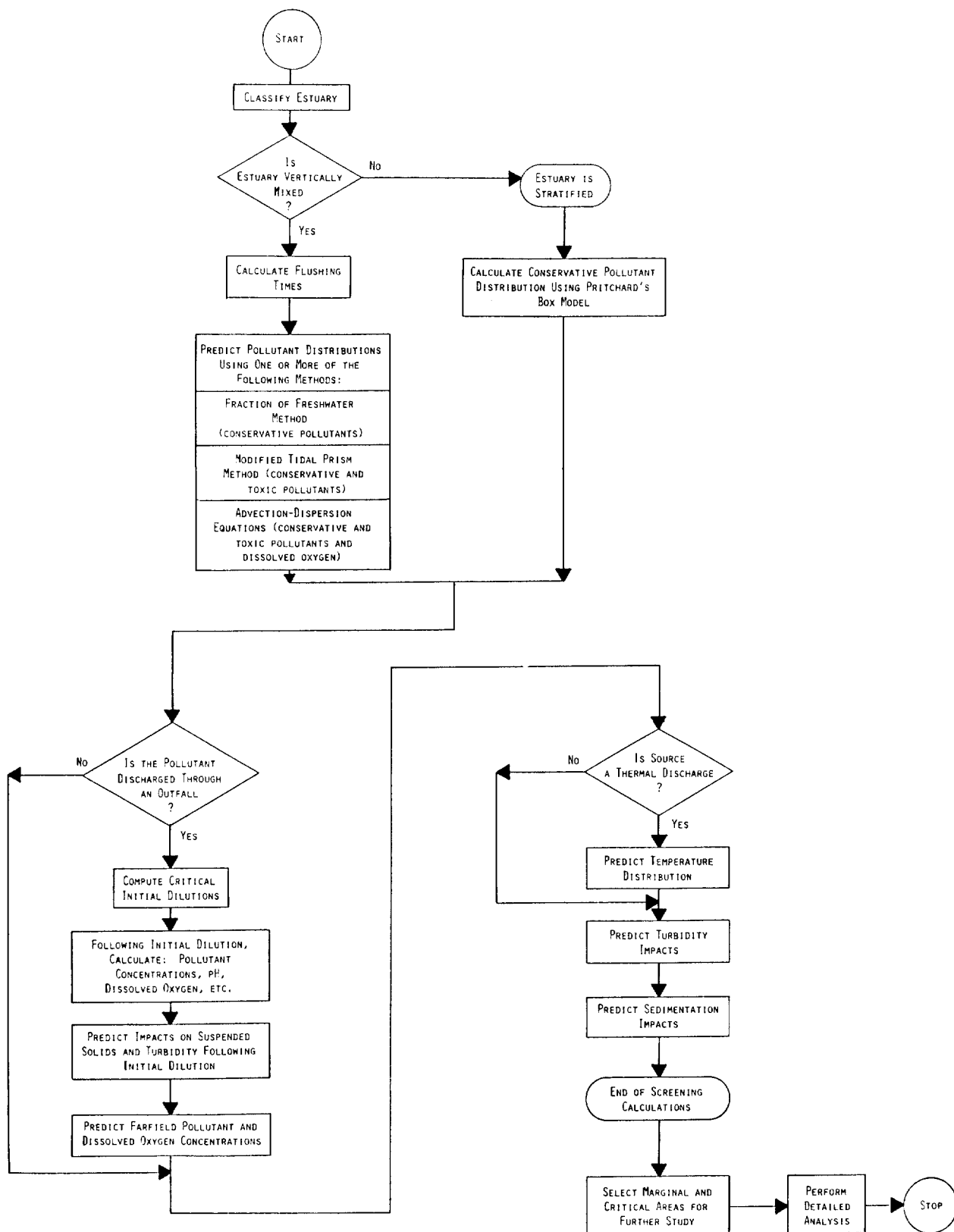


FIGURE VI -5 SUGGESTED PROCEDURE TO PREDICT ESTUARINE WATER QUALITY

## 6.2 ESTUARINE CLASSIFICATION

### 6.2.1 General

Section 6.1.7 discussed making a first estimate of current estuarine water quality. This section begins a calculation methodology designed to look at the effect of future changes in waste loading patterns.

The goal of the classifications process presented below is to predict the applicability of the hand calculations to be presented. The classification process is normally the first step to be taken in the calculation procedure since it reveals which techniques can be applied.

### 6.2.2 Classification Methodology

The classification system recommended for purposes of hand calculations is based on salinity and velocity profiles within the estuary. As both of these parameters vary seasonally and spatially for each estuary, their use will result in a range of values rather than in one single classification number. The following section will describe in detail the procedure for use of this system, and show examples of the procedure.

### 6.2.3 Calculation Procedure

Hansen and Rattray (1966) developed an estuarine classification system using both salinity stratification and water circulation patterns (based on water column velocities). This procedure involves the calculation of values for two parameters at various points along the main estuarine channel and the plotting of these intersections on the graph shown in Figure VI-6. Figure VI-7 shows plots made by Hansen and Rattray for various estuaries at a single point in time. It should be noted that each estuary is not represented by a point but by a line connecting the points calculated for the mouth and head areas.

The area designations (e.g. 1a, 1b, 2b) on Figure VI-6 were related by Hansen and Rattray to previously used classification titles (e.g. stratified, well mixed). In general, area 1a corresponds to well mixed estuaries. Area 1b has the water circulation pattern of a well mixed estuary yet shows increased stratification. Areas 2 and 3 correspond to the "partially mixed" class of estuaries with area 3 showing more significant vertical circulation within the estuary. Designations 2a/b and 3a/b, as was true of 1a and 1b, indicate increasing degrees of vertical stratification. Type 3b includes fjord-type estuaries. Area 4 represents highly stratified salt wedge estuaries.

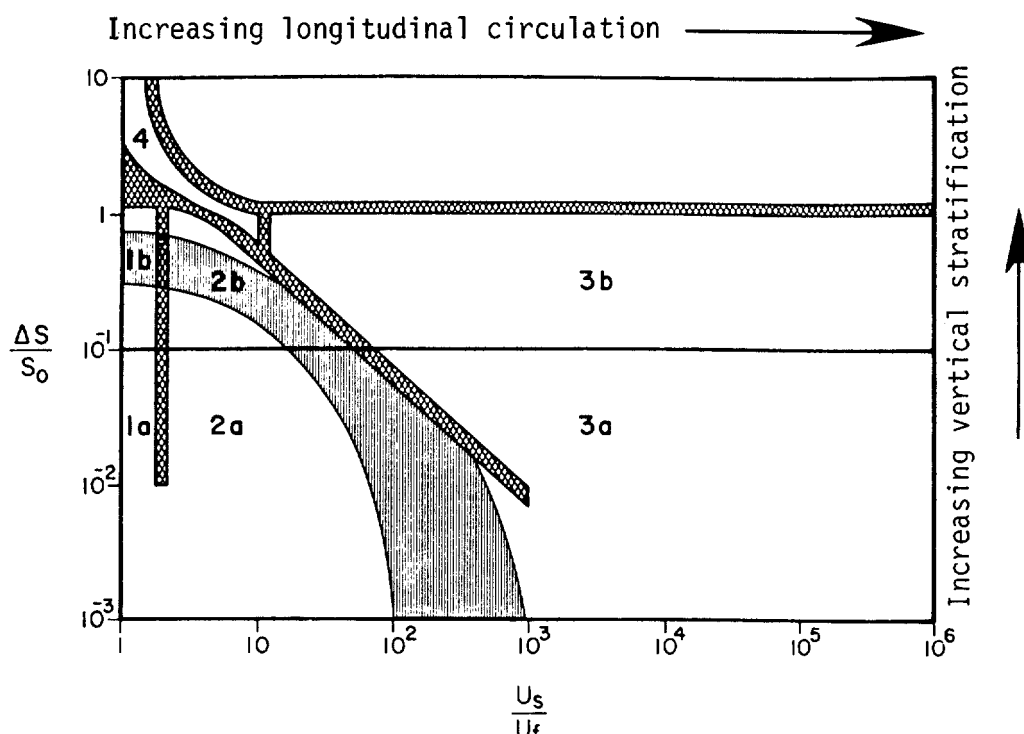
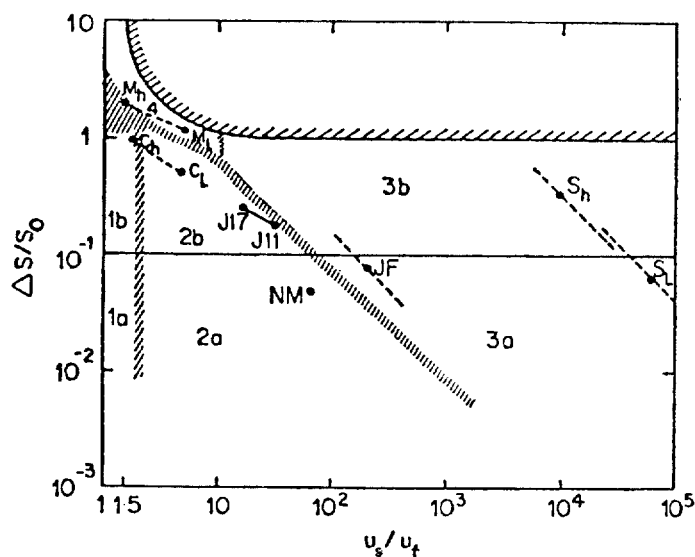


FIGURE VI -6 ESTUARINE CIRCULATION-STRATIFICATION DIAGRAM



(Station code: M, Mississippi River mouth; C, Columbia River estuary; J, James River estuary; NM, Narrows of the Mersey estuary; JF, Strait of Juan de Fuca; S, Silver Bay. Subscripts h and l refer to high and low river discharge; numbers indicate distance (in miles) from mouth of the James River estuary.

FIGURE VI -7 EXAMPLES OF ESTUARINE CLASSIFICATION PLOTS  
(FROM HANSEN AND RATTRAY, 1966)

#### 6.2.4 Stratification-Circulation Diagram Interpretation

The closer an estuary falls to the lower left hand corner of a stratification-circulation diagram, the more vertically and laterally homogeneous it is. On the stratification-circulation diagram (Figure VI-6), two types of zonal demarcation can be seen. First are the diagonally striped divisions between adjacent estuarine classifications used by Hansen and Rattray to indicate a transitional zone between separate classifications. The second is a wide solid band arching around the lower left corner of the diagram. Estuaries falling primarily inside of this band (to the lower left of the band) are those for which the one dimensional calculation methods may be applied to obtain reasonably accurate results. If an estuary falls outside of this band, the planner should use only the methods presented which pertain to stratified estuaries, or use computer analyses. Within the band is a borderline of marginal zone. Calculations for one-dimensional estuaries can be used for estuaries falling principally within this zone, however the accuracy of the calculations will be uncertain.

The two parameters used with the stratification-circulation diagram are described below:

- a. Stratification Parameter: The stratification parameter is defined as:

$$\text{Stratification Parameter} = \frac{\Delta S}{S_0} \quad (\text{VI-1})$$

where

$$\begin{aligned} \Delta S &= \text{time averaged difference in salinity between surface and bottom} \\ &\quad \text{water } (S_{\text{bottom}} - S_{\text{surface}}), \text{ ppt} \\ S_0 &= \text{cross-section mean salinity, ppt.} \end{aligned}$$

The diagrammatic relationship of these values is shown in Figure VI-8.

- b. Circulation Parameter: The circulation parameter is defined as:

$$\text{Circulation Parameter} = \frac{U_s}{U_f} \quad (\text{VI-2})$$

where

$$U_s = \text{net non-tidal sectional surface velocity (surface velocity through the section averaged over a tidal cycle) measured in ft/sec. See Figure VI-8 for a diagrammatic representation of } U_s.$$

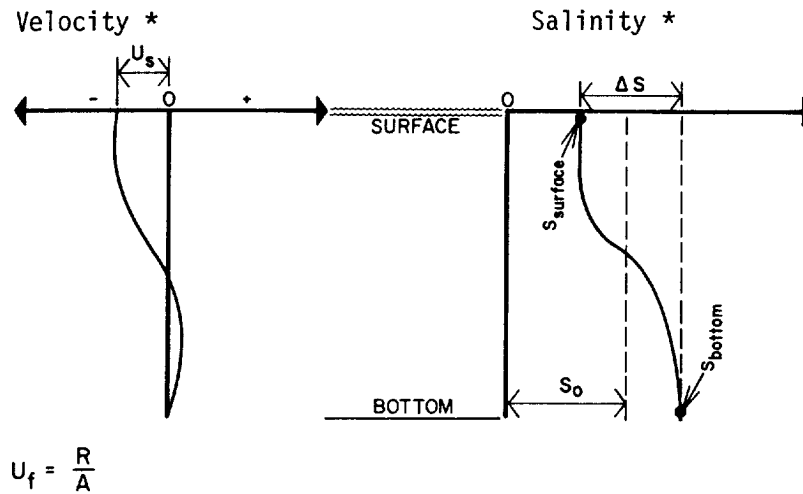
$$U_f = \text{mean fresh water velocity through the section, ft/sec.}$$

In equation form:

$$U_f = \frac{R}{A} \quad (\text{VI-3})$$

CIRCULATION PARAMETER

STRATIFICATION PARAMETER



$$U_f = \frac{R}{A}$$

\*Both velocity and salinity values for these profiles are averaged over a tidal cycle (net velocity and salinity) rather than being instantaneous values. Of the two the stratification parameter is much less sensitive to variations over a tidal cycle and can be approximated by mean tide values for salinity. Surface velocity ( $U_s$ ) must be averaged over a tidal cycle.

FIGURE VI -8 CIRCULATION AND STRATIFICATION PARAMETER DIAGRAM

where

R = fresh water (river) inflow rate,  $ft^3/sec$

A = cross-sectional area of the estuary through the point being used to calculate the circulation pattern and stratification parameters based on a mean tide surface elevation,  $ft^2$ .

If good cross-sectional area data are not available, cross-sectional profiles can be approximated from the U.S. Geological Survey (USGS) coastal series topographical maps, or, more recently, from NOAA National Ocean Survey charts. The circulation and stratification parameters should be plotted for high and low river flow periods and for stations near the mouth and head of the estuary. The area enclosed by these four points should then include the full range of possible instantaneous estuary hydrodynamic characteristics. In interpreting the significance of this plotted area, by far the greater weight should be given to the low river flow periods as these periods are associated with the poorest pollutant flushing characteristics and the lowest estuarine water quality. The interpretation of the circulation-stratification diagrams will be explained more fully after an example of parameter computation.

EXAMPLE VI-1

Calculation of Stratification and Circulation Parameters

The estuary for this example is the Stuart Estuary which is shown in Figure VI-9. The estuary is 64,000 feet long, is located on the U.S. west coast, and is fed by the Scott River. Two stations were selected for parameter calculation (A and B) with station A located on the southern edge of the main channel 6,500 feet from the estuary's mouth and station B in center channel 47,500 feet from the mouth (16,500 feet from the head of the estuary).

Necessary salinity data were obtained from the coastal engineering department of a nearby university. USGS gage data were available for river flow, and, as a result of its own dredging program, the local district office of the U.S. Corps of Engineers could provide cross-sectional profiles in the approximate areas of both stations. The cross-sections are labeled (1) and (2) on Figure VI-9. The mean low tide depth reading on NOAA Coastal charts was used to verify Corps data. Current meters were tied to buoy channel markers at A and B to provide velocity data. The information obtained from these various sources is shown in graphical form in Figure VI-10.

The calculations proceed as follows:

Stratification Parameter:

		STATION		
		A	B	
$\frac{\Delta S}{S_0} = \frac{S_{\text{bottom}} - S_{\text{surface}}}{S_0}$	→	$\frac{33 - 30}{31.5} = .095$	$\frac{14.5 - 10.5}{12.5} = .32$	SUMMER
		$\frac{31.5 - 24.2}{27.8} = .26$	$\frac{4 - 2.1}{3.25} = .58$	WINTER

b. Circulation Parameter:

1. Calculate  $A_i$ 's using cross sectional information on Figure VI-10:

$$A_a = (630 \text{ ft}) (20 \text{ ft}) (1/2) + (630 \text{ ft}) (20 \text{ ft}) + (1590 \text{ ft}) (20 \text{ ft}) (1/2)$$

$$= 34,800 \text{ ft}^2$$

$$A_b = (2580 \text{ ft}) (16 \text{ ft}) (1/2) + (1720 \text{ ft}) (16 \text{ ft}) (1/2)$$

$$= 34,400 \text{ ft}^2$$

For most cross-sections it is advisable to use more finely divided segments than in the simple example above in order to reduce the error associated with this approximation. The method for this calculation,

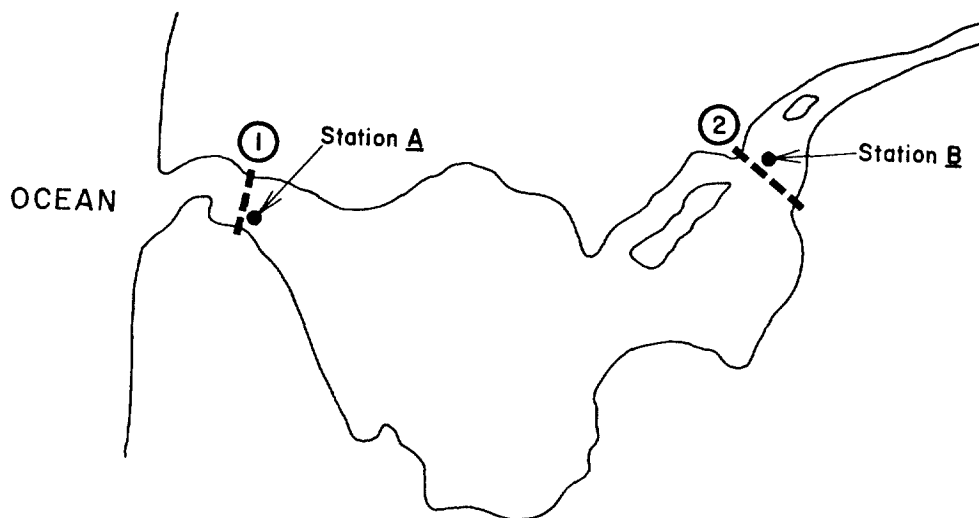


FIGURE VI -9 THE STUART ESTUARY

however, is identical regardless of the number of regular segments used.

- Calculate  $U_f$ 's (with R and  $A_i$  values obtained from Figure VI-10):

		STATION		
		A	B	
$U_f = \frac{R}{A_i}$	→	$\frac{550 \text{ ft}^3/\text{sec}}{3.48 \times 10^4 \text{ ft}^2} = 1.58 \times 10^{-2} \text{ ft/sec}$	$\frac{550 \text{ ft}^3/\text{sec}}{3.44 \times 10^4 \text{ ft}^2} = 1.60 \times 10^{-3} \text{ ft/sec}$	SUMMER
		$\frac{1800 \text{ ft}^3/\text{sec}}{3.48 \times 10^4 \text{ ft}^2} = 5.17 \times 10^{-2} \text{ ft/sec}$	$\frac{1800 \text{ ft}^3/\text{sec}}{3.44 \times 10^4 \text{ ft}^2} = 5.23 \times 10^{-2} \text{ ft/sec}$	WINTER

- Calculate  $U_s$ 's:

$$U_f$$

$U_s$  values are read from Figure VI-10. The precise value for  $U_s$  is the integral of the velocity curve (area under "ebb" velocity curve minus the area under the "flood" velocity curve) divided by the elapsed time period (length of one tidal cycle). If the elapsed time for flood flow at a station is only slightly below the elapsed time for ebb flow  $U_s$  may be approximated as

$$(U_{\text{ebb(max)}} - U_{\text{flood(max)}}) / 2.$$

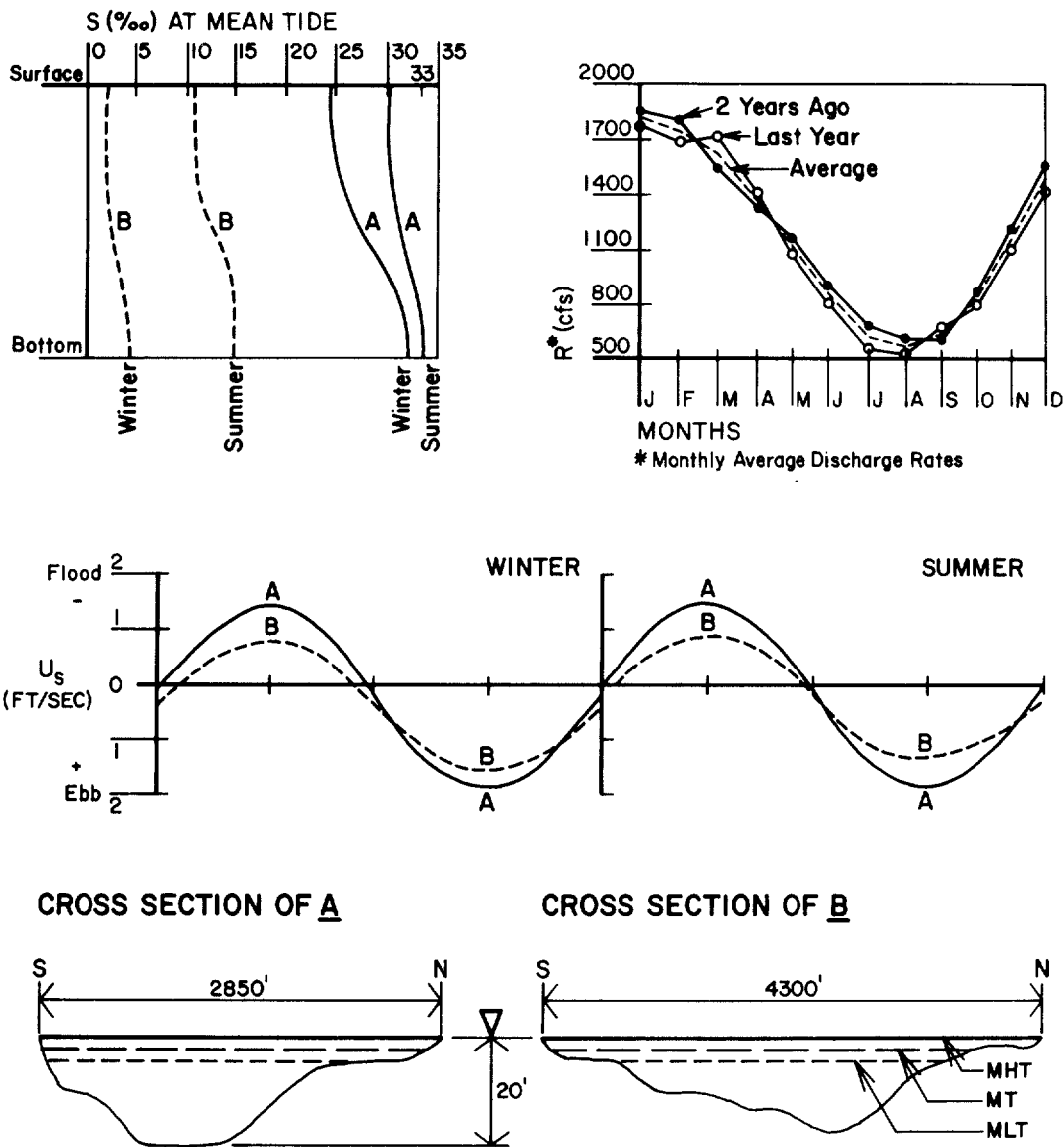


FIGURE VI -10 STUART ESTUARY DATA FOR CLASSIFICATION CALCULATIONS

		STATION		
		A	B	
$\frac{U_s}{U_f} \rightarrow$		$\frac{0.15 \text{ ft/sec}}{1.58 \times 10^{-2} \text{ ft/sec}} = 9.5$	$\frac{0.3 \text{ ft/sec}}{1.60 \times 10^{-2} \text{ ft/sec}} = 18.8$	SUMMER
		$\frac{0.2 \text{ ft/sec}}{5.17 \times 10^{-2} \text{ ft/sec}} = 3.9$	$\frac{0.4 \text{ ft/sec}}{5.23 \times 10^{-2} \text{ ft/sec}} = 7.65$	WINTER



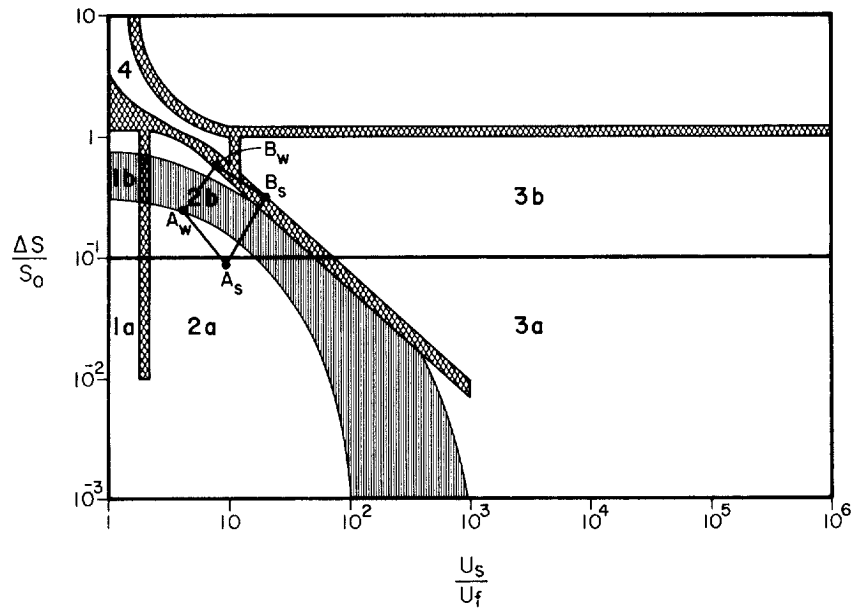


FIGURE VI - 11 ESTUARINE CIRCULATION - STRATIFICATION DIAGRAM

The circulation-stratification plots for the Stuart Estuary are shown in Figure VI-11 with points  $A_s$  (station A, summer value),  $A_w$  (station A, winter value),  $B_s$  (station B, summer value), and  $B_w$  (station B, winter value).

As indicated, this estuary shows a significant amount of vertical stratification (especially at station A) but little evidence of major vertical variations in net circulation.

END OF EXAMPLE VI-1

Turning to Figure VI-11, the Stratification-Circulation diagram for the Stuart Estuary, it is apparent that this estuary lies principally within the marginal area. Moreover, the low flow classification (line  $A_s-B_s$ ) also lies primarily within the marginal area. Thus, the planner for the Stuart Estuary should calculate an additional criterion (see below) to help determine the suitability of using the calculation procedures for well mixed estuaries. If the Stuart Estuary plotted more predominately below the marginal zone, the planner could proceed with flushing time calculations since the estuary would then meet the well mixed classification criteria.

It should be noted that the data for the Stuart Estuary produced a fairly tight cluster of data points. As can be seen in Figure VI-12, the salinity profiles for one west coast estuary (the Alsea River and Estuary along the central Oregon coast) vary considerably more from season to season than those of the Stuart Estuary.

## ALSEA RIVER

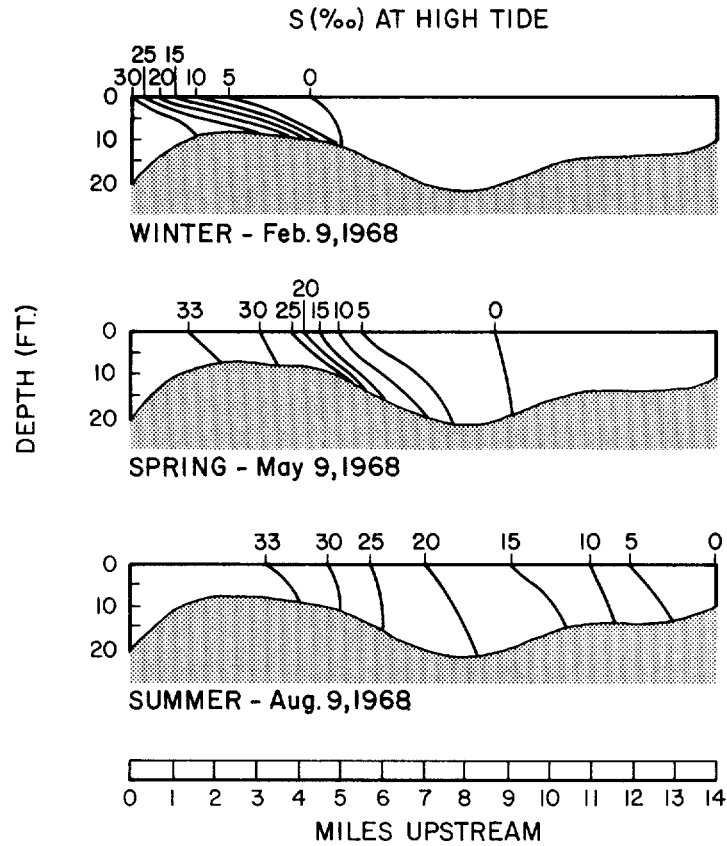


FIGURE V1-12 ALSEA ESTUARY SEASONAL SALINITY VARIATIONS (FROM GIGER, 1972)

This increased variation would produce a far greater spread in the summer and winter  $\Delta S/S_0$  parameter values.

### 6.2.5 Flow Ratio Calculation

If application of the above classification procedure results in an ambiguous outcome regarding estuary classification, another criterion should be applied. This is the flow ratio calculation. Schultz and Simmons (1957) first observed the correlation between the flow ratio and estuary type. They defined the flow ratio for an estuary as:

$$F = \frac{R}{P} \tag{VI-4}$$

where

F = the flow ratio,

R = the river flow measured over one tidal cycle (measured in  $m^3$  or  $ft^3$ )

P = the estuary tidal prism (in  $m^3$  or  $ft^3$ ).

Thus the flow ratio compares the tidally induced flow in an estuary with the river induced flow. Schultz and Simmons observed that when this ratio was on the order of 1.0 or greater, the associated estuary was normally highly stratified. Conversely, ratios of about 0.1 or less were usually associated with very well-mixed estuaries and ratios in the range of 0.25 were associated with partially mixed estuaries. A flow ratio of 0.2 or less warrants inclusion of the estuary in the hand calculation process for one dimensional estuaries. Flow ratios in the range 0.2 to 0.3 should be considered marginal. Estuaries with flow ratios greater than 0.3 should not be included in the one-dimensional category.

----- EXAMPLE VI-2 -----

Calculation of the Flow Ratio for an Estuary

The following data apply to the Patuxent Estuary, Maryland:

R, total river discharge over one tidal cycle =  $1.42 \times 10^5 m^3$  (low flow)  
 $3.58 \times 10^6 m^3$  (high flow)

P, estuary tidal prism volume =  $3.51 \times 10^7 m^3$

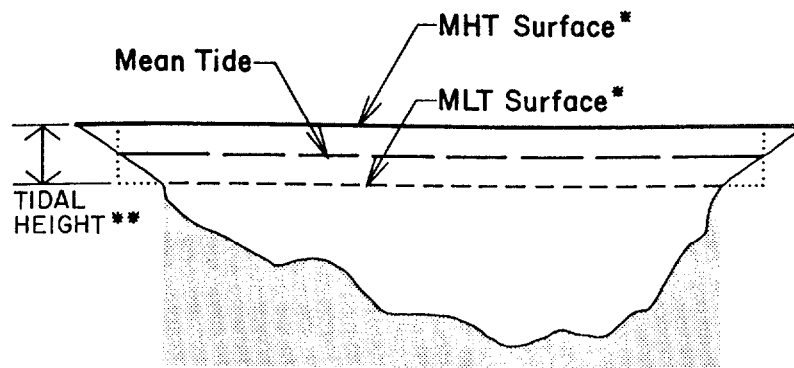
The flow ratios for the Patuxent Estuary at low and high river flows are thus:

$$F = \frac{R}{P}$$
$$F_{\text{low flow}} = \frac{1.42 \times 10^5 m^3}{3.51 \times 10^7 m^3}$$
$$= 0.004$$
$$F_{\text{high flow}} = \frac{3.58 \times 10^6 m^3}{3.51 \times 10^7 m^3}$$
$$= 0.10$$

Values of  $F < 0.1$  are usually associated with well mixed estuaries. The F values calculated above indicate a well mixed estuary. However, historical data indicate the Patuxent River Estuary is partially stratified at moderate and high river flows.

----- END OF EXAMPLE VI-2 -----

When tidal data are not available, NOAA coastal charts may be used to estimate the difference between mean high tide and mean low tide estuary surface areas. As



$$P_i \text{ (section } i) = \text{section Length} \times \text{tidal height} \times \left( \frac{\text{MHT width} + \text{MLT width}}{2} \right)$$

$$P_{\text{estuary}} = \sum_i P_i \text{ for all sections}$$

\* Widths obtained from NOAA tide table for the area

\*\*Available from Local Coast Guard Stations

FIGURE VI -13 ESTUARY CROSS-SECTION FOR TIDAL PRISM CALCULATIONS

can be seen in the cross-section diagram in Figure VI-13 the estuarine tidal prism can be approximated by averaging the MLT and MHT surface areas and multiplying this averaged area by the local tidal height. Mean tidal heights (approximately 1 week before or after spring tides) should be used for this calculation. As indicated in Figure VI-13, the estuary can be conveniently subdivided into longitudinal sections for this averaging process, to reduce the resulting error. Table VI-2 lists tidal prisms estimated for many U.S. estuaries. These values may be used as an alternate to tidal prism calculations.

### 6.3 FLUSHING TIME CALCULATIONS

#### 6.3.1 General

Flushing time is a measure of the time required to transport a conservative pollutant from some specified location within the estuary (usually, but not always, the head) to the mouth of the estuary. Processes such as pollutant decay or sedimentation which can alter the pollutant's distribution within the estuary are not considered in the concept of flushing time.

It was mentioned earlier in this chapter that the net non-tidal flow in an

TABLE VI-2  
TIDAL PRISMS FOR SOME U. S. ESTUARIES  
(FROM O' BRIEN, 1969 AND JOHNSON, 1973)

Estuary	Coast	Tidal Prism (ft <sup>3</sup> )
Plum Island Sound, Mass.	Atlantic	1.32 x 10 <sup>9</sup>
Fire Island Inlet, N. Y.	Atlantic	2.18 x 10 <sup>9</sup>
Jones Inlet, N. Y.	Atlantic	1.50 x 10 <sup>9</sup>
Beach Haven Inlet (Little Egg Bay), N. J.	Atlantic	1.51 x 10 <sup>9</sup>
Little Egg Inlet (Great Bay), N. J.	Atlantic	1.72 x 10 <sup>9</sup>
Brigantine Inlet, N. J.	Atlantic	5.23 x 10 <sup>8</sup>
Absecon Inlet (before jetties), N. J.	Atlantic	1.65 x 10 <sup>9</sup>
Great Egg Harbor Entr, N. J.	Atlantic	2.00 x 10 <sup>9</sup>
Townsend Inlet, N. J.	Atlantic	5.56 x 10 <sup>8</sup>
Hereford Inlet, N. J.	Atlantic	1.19 x 10 <sup>9</sup>
Chincoteague Inlet, Va.	Atlantic	1.56 x 10 <sup>9</sup>
Oregon Inlet, N. C.	Atlantic	3.98 x 10 <sup>9</sup>
Ocracoke Inlet, N. C.	Atlantic	5.22 x 10 <sup>9</sup>
Drum Inlet, N. C.	Atlantic	5.82 x 10 <sup>8</sup>
Beaufort Inlet, N. C.	Atlantic	5.0 x 10 <sup>9</sup>
Carolina Beach Inlet, N. C.	Atlantic	5.25 x 10 <sup>8</sup>
Steno Inlet, S. C.	Atlantic	2.86 x 10 <sup>9</sup>
North Edisto River, S. C.	Atlantic	4.58 x 10 <sup>9</sup>
St. Helena Sound, S. C.	Atlantic	1.53 x 10 <sup>10</sup>
Port Royal Sound, S. C.	Atlantic	1.46 x 10 <sup>10</sup>
Calibogue Sound, S. C.	Atlantic	3.61 x 10 <sup>9</sup>
Wassaw Sound, Ga.	Atlantic	8.2 x 10 <sup>9</sup>
Ossabaw Sound, Ga.	Atlantic	6.81 x 10 <sup>9</sup>
Sapelo Sound, Ga.	Atlantic	7.36 x 10 <sup>9</sup>
St. Catherine Sound, Ga.	Atlantic	6.94 x 10 <sup>9</sup>
Doboy Sound, Ga.	Atlantic	4.04 x 10 <sup>9</sup>
Altamaha Sound, Ga.	Atlantic	2.91 x 10 <sup>9</sup>
Hampton River, Ga.	Atlantic	1.01 x 10 <sup>9</sup>
St. Simon Sound, Ga.	Atlantic	6.54 x 10 <sup>9</sup>
St. Andrew Sound, Ga.	Atlantic	9.86 x 10 <sup>9</sup>
Ft. George Inlet, Fla.	Atlantic	3.11 x 10 <sup>8</sup>
Old St. Augustine Inlet, Fla.	Atlantic	1.31 x 10 <sup>9</sup>

TABLE VI -2 (Cont.)

Estuary	Coast	Tidal Prism (ft <sup>3</sup> )
Ponce de Leon, Fla. (before jetties)	Atlantic	5.74 x 10 <sup>8</sup>
Delaware Bay Entrance	Atlantic	1.25 x 10 <sup>11</sup>
Fire Island Inlet, N.Y.	Atlantic	1.86 x 10 <sup>9</sup>
East Rockaway Inlet, N.Y.	Atlantic	7.6 x 10 <sup>8</sup>
Rockaway Inlet, N.Y.	Atlantic	3.7 x 10 <sup>9</sup>
Masonboro Inlet, N.C.	Atlantic	8.55 x 10 <sup>8</sup>
St. Lucie Inlet, Fla.	Atlantic	5.94 x 10 <sup>8</sup>
Nantucket Inlet, Mass.	Atlantic	4.32 x 10 <sup>8</sup>
Shinnecock Inlet, N.Y.	Atlantic	2.19 x 10 <sup>8</sup>
Moriches Inlet, N.Y.	Atlantic	1.57 x 10 <sup>9</sup>
		8.46 x 10 <sup>8</sup>
Shark River Inlet, N.J.	Atlantic	1.48 x 10 <sup>8</sup>
Manasquan Inlet, N.J.	Atlantic	1.75 x 10 <sup>8</sup>
Barneгат Inlet, N.J.	Atlantic	6.25 x 10 <sup>8</sup>
Absecon Inlet, N.J.	Atlantic	1.48 x 10 <sup>9</sup>
Cold Springs Harbor (Cape May), N.J.	Atlantic	6.50 x 10 <sup>8</sup>
Indian River Inlet, Del.	Atlantic	5.25 x 10 <sup>8</sup>
Winyah Bay, S.C.	Atlantic	3.02 x 10 <sup>9</sup>
Charleston, S.C.	Atlantic	5.75 x 10 <sup>9</sup>
Savannah River (Tybee Roads), Ga.	Atlantic	3.1 x 10 <sup>9</sup>
St. Marys (Fernandina Harbor), Fla.	Atlantic	4.77 x 10 <sup>9</sup>
St. Johns River, Fla.	Atlantic	1.73 x 10 <sup>9</sup>
Fort Pierce Inlet, Fla.	Atlantic	5.81 x 10 <sup>8</sup>
Lake Worth Inlet, Fla.	Atlantic	9.0 x 10 <sup>8</sup>
Port Everglades, Fla.	Atlantic	3.0 x 10 <sup>8</sup>
Bakers Haulover, Fla.	Atlantic	3.6 x 10 <sup>8</sup>
Captiva Pass, Fla.	Gulf of Mexico	1.90 x 10 <sup>9</sup>
Boca Grande Pass, Fla.	Gulf of Mexico	1.26 x 10 <sup>10</sup>
Gasparilla Pass, Fla.	Gulf of Mexico	4.7 x 10 <sup>8</sup>
Stump Pass, Fla.	Gulf of Mexico	3.61 x 10 <sup>8</sup>
Midnight Pass, Fla.	Gulf of Mexico	2.61 x 10 <sup>8</sup>
Big Sarasota Pass, Fla.	Gulf of Mexico	7.6 x 10 <sup>8</sup>
New Pass, Fla.	Gulf of Mexico	4.00 x 10 <sup>8</sup>
Longboat Pass, Fla.	Gulf of Mexico	4.90 x 10 <sup>8</sup>

TABLE VI -2 (Cont.)

Estuary	Coast	Tidal Prism (ft <sup>3</sup> )
Sarasota Pass, Fla.	Gulf of Mexico	$8.10 \times 10^8$
Pass-a-Grille	Gulf of Mexico	$1.42 \times 10^9$
Johns Pass, Fla.	Gulf of Mexico	$5.03 \times 10^8$
Little (Clearwater) Pass, Fla.	Gulf of Mexico	$6.8 \times 10^8$
Big (Dunedin) Pass, Fla.	Gulf of Mexico	$3.76 \times 10^8$
East (Destin) Pass, Fla.	Gulf of Mexico	$1.62 \times 10^9$
Pensacola Bay Entr., Fla.	Gulf of Mexico	$9.45 \times 10^9$
Perdido Pass, Ala.	Gulf of Mexico	$5.84 \times 10^8$
Mobile Bay Entr., Ala.	Gulf of Mexico	$2.0 \times 10^{10}$
Barataria Pass, La.	Gulf of Mexico	$2.55 \times 10^9$
Caminada Pass, La.	Gulf of Mexico	$6.34 \times 10^8$
Calcasieu Pass, La.	Gulf of Mexico	$2.97 \times 10^9$
San Luis Pass, Tex.	Gulf of Mexico	$5.84 \times 10^8$
Venice Inlet, Fla.	Gulf of Mexico	$8.5 \times 10^7$
Galveston Entr., Tex.	Gulf of Mexico	$1.59 \times 10^{10}$
Aransas Pass, Tex.	Gulf of Mexico	$1.76 \times 10^9$
Grays Harbor, Wash.	Pacific	$1.3 \times 10^{10}$
Willapa, Wash.	Pacific	$1.3 \times 10^{10}$
Columbia River, Wash.-Ore.	Pacific	$2.9 \times 10^{10}$
Necanicum River, Ore.	Pacific	$4.4 \times 10^7$
Nehalem Bay, Ore.	Pacific	$4.3 \times 10^8$
Tillamook Bay, Ore.	Pacific	$2.5 \times 10^9$
Netarts Bay, Ore.	Pacific	$5.4 \times 10^8$
Sand Lake, Ore.	Pacific	$1.1 \times 10^8$
Nestucca River, Ore.	Pacific	$2.6 \times 10^8$
Salmon River, Ore.	Pacific	$4.3 \times 10^7$
Devils Lake, Ore.	Pacific	$1.1 \times 10^8$
Siletz Bay, Ore.	Pacific	$3.5 \times 10^8$
Yaquina Bay, Ore.	Pacific	$8.4 \times 10^8$
Alsea Estuary, Ore.	Pacific	$5.1 \times 10^8$
Siusslaw River, Ore.	Pacific	$2.8 \times 10^8$
Umpqua, Ore.	Pacific	$1.2 \times 10^9$
Coos Bay, Ore.	Pacific	$1.9 \times 10^9$
Caquille River, Ore.	Pacific	$1.3 \times 10^8$
Floras Lake, Ore.	Pacific	$6.8 \times 10^7$

TABLE VI -2 (Cont.)

Estuary	Coast	Tidal Prism (ft <sup>3</sup> )
Rogue River, Ore.	Pacific	1.2 x 10 <sup>8</sup>
Chetco River, Ore.	Pacific	2.9 x 10 <sup>7</sup>
Smith River, Ca.	Pacific	9.5 x 10 <sup>7</sup>
Lake Earl, Ca.	Pacific	5.1 x 10 <sup>8</sup>
Freshwater Lagoon, Ca.	Pacific	4.7 x 10 <sup>7</sup>
Stove Lagoon, Ca.	Pacific	1.2 x 10 <sup>8</sup>
Big Lagoon, Ca.	Pacific	3.1 x 10 <sup>8</sup>
Mad River, Calif.	Pacific	2.4 x 10 <sup>7</sup>
Humbolt Bay, Calif.	Pacific	2.4 x 10 <sup>9</sup>
Eel River, Calif.	Pacific	3.1 x 10 <sup>8</sup>
Russian River, Calif.	Pacific	6.3 x 10 <sup>7</sup>
Bodega Bay, Calif.	Pacific	1.0 x 10 <sup>8</sup>
Tomales Bay, Calif.	Pacific	1.0 x 10 <sup>9</sup>
Abbotts Lagoon, Calif.	Pacific	3.5 x 10 <sup>7</sup>
Drakes Bay, Calif.	Pacific	2.7 x 10 <sup>8</sup>
Bolinas Lagoon, Calif.	Pacific	1.0 x 10 <sup>8</sup>
San Francisco Bay, Calif.	Pacific	5.2 x 10 <sup>10</sup>
Santa Cruz Harbor, Calif.	Pacific	4.3 x 10 <sup>6</sup>
Moss Landing, Calif.	Pacific	9.4 x 10 <sup>7</sup>
Morro Bay, Calif.	Pacific	8.7 x 10 <sup>7</sup>
Marina Del Rey, Calif.	Pacific	6.9 x 10 <sup>7</sup>
Alamitos Bay, Calif.	Pacific	6.9 x 10 <sup>7</sup>
Newport Bay, Calif.	Pacific	2.1 x 10 <sup>8</sup>
Camp Pendleton, Calif.	Pacific	1.1 x 10 <sup>7</sup>
Aqua Hedionda, Calif.	Pacific	4.9 x 10 <sup>7</sup>
Mission Bay, Calif.	Pacific	3.3 x 10 <sup>8</sup>
San Diego Bay, Calif.	Pacific	1.8 x 10 <sup>9</sup>

estuary is usually seaward\* and is dependent on the river discharge. The non tidal flow is one of the driving forces behind estuarine flushing. In the absence of this advective displacement, tidal oscillation and wind stresses still operate to

\*While net flow is always seaward for the estuaries being considered here, it is possible to have a net upstream flow in individual embayments of an estuary. While this occurrence is rare in the United States, an example of such a situation is the South Bay of San Francisco Bay where freshwater inflows are so small that surface evaporation exceeds freshwater inflow. Thus, net flow is upstream during most of the year.



disperse and flush pollutants. However, the advective component of flushing can be extremely important. Consider Tomales Bay, California as an example. This small, elongated bay has essentially no fresh water inflow. As a result there is no advective seaward motion and Pollutant removal is dependent upon dispersion and diffusion processes. The flushing time for the bay is approximately 140 days (Johnson, et al. , 1961). This can be compared with the Alsea Estuary in Oregon having a flushing time of approximately 8 days, with the much larger St. Croix Estuary in Nova Scotia having a flushing time of approximately 8 days (Ketchum and Keen, 1951), or with the very large Hudson River Estuary with a short flow flushing time of approximately 10.5 days (Ketchum, 1950).

### 6.3.2 Procedure

Flushing times for a given estuary vary over the course of a year as river discharge varies. The critical time is the low river flow period since this period corresponds with the minimum flushing rates. The planner might also want to calculate the best flushing characteristics (high river flow) for an estuary. In addition to providing a more complete picture of the estuarine system, knowledge of the full range of annual flushing variations can be useful in evaluating the impact of seasonal discharges (e.g., fall and winter cannery operation in an estuary with a characteristic summer fresh water low flow). Further, storm sewer runoff normally coincides with these best flushing conditions (high flow) and not with the low flow, or poorest flushing conditions. Thus analysis of storm runoff is often better suited for high flow flushing conditions, However, the low flow calculation should be considered for use in primary planning purposes.

There are several ways of calculating flushing time. Two methods are presented here: the fraction of freshwater method and the modified tidal prism method.

### 6.3.3 Fraction of Fresh Water Method

The flushing time of a pollutant, as determined by the fraction of freshwater method is:

$$T_f = \frac{V_f}{R} \quad (VI-5)$$

where

- $V_f$  = volume of freshwater in the estuary
- $T_f$  = flushing time of a pollutant which enters the head of the estuary with the river flow.

Equation VI-5 is equivalent to the following concept of flushing time which is

more intuitively meaningful:

$$T_f = \frac{M}{R} \quad (\text{VI-6})$$

where

M = total mass of conservative pollutant contained in the estuary

R = rate of pollutant entry into the head of the estuary with the river water.

Since the volume of freshwater in the estuary is the product of the fraction of freshwater (f) and the total volume of water (V), Equation VI-5 becomes:

$$T_f = \frac{fV}{R} \quad (\text{VI-7})$$

If the estuary is divided into segments the flushing time becomes:

$$T_f = \sum \frac{f_i V_i}{R_i} \quad (\text{VI-8})$$

Equation VI-8 is more general and accurate than the three previous expressions because both  $f_i$  (the fraction of freshwater in the ith segment) and  $R_i$  (the freshwater discharge through the ith segment) can vary over distance within the estuary. Note that the flushing time of a pollutant discharged from some location other than the head of the estuary can be computed by summing contributions over the segments seaward of the discharge.

A limitation of the fraction of freshwater method is that it assumes uniform salinity throughout each segment. A second limitation is that it assumes during each tidal cycle a volume of water equal to the river discharge moves into a given estuarine segment from the adjacent upstream segment, and that an equal volume of the water originally in the segment moves on to the adjacent one downstream. Once this exchange has taken place, the water within each segment is assumed to be instantaneously and completely mixed and to again become a homogeneous water mass. Proper selection of estuarine segments can reduce these errors.

#### 6.3.4 Calculation of Flushing Time by Fraction of Freshwater Method

This is a six step procedure:

1. Graph the estuarine salinity profiles.
2. Divide the estuary into segments. There is no minimum or maximum number of segments required, nor must all segments be of the same length. The divisions should be selected so that mean segment salinity is relatively constant over

the full length of the segment. Thus, stretches of steep salinity gradient will have short segments and stretches where salinity remains constant may have very long segments. Example VI-3 provides an illustration.

3. Calculate each segment's fraction of fresh water by:

$$f_i = \frac{S_s - S_i}{S_s} \quad (\text{VI-9})$$

where

$f_i$  = fraction of fresh water for segment "i"

$S_s$  = salinity of local sea water\*, 0/00

$S_i$  = mean salinity for segment "i", 0/00.

4. Calculate the quantity of fresh water in each segment by:

$$W_i = f_i \times V_i \quad (\text{VI-10})$$

where

$W_i$  = quantity of fresh water in segment "i"

$V_i$  = total volume of segment "i" at MTL.

5. Calculate the exchange time (flushing time) for each segment by:

$$T_i = W_i/R \quad (\text{VI-11})$$

where

$T_i$  = segment flushing time, in tidal cycles

$R$  = river discharge over one tidal cycle.

6. Calculate the entire estuary flushing time by summing the exchange times for the individual segments:

$$T_f = \sum_{i=1}^n T_i \quad (\text{VI-12})$$

where

$T_f$  = estuary flushing time, in tidal cycles

$n$  = number of segments.

Table VI-3 shows a suggested method for calculating flushing time by the fraction of freshwater method.

\*Sea surface salinity along U.S. shores vary spatially. Neuman and Pierson (1966) mapped Pacific mean coastal surface salinities as varying from 32.4 0/00 at Puget Sound to 33.9 0/00 at the U.S.-Mexico border; Atlantic mean coastal surface salinities as varying from 32.5 0/00 in Maine to 36.2 0/00 at the southern extreme of Florida; and Gulf coast salinities as varying between 36.2 0/00 and 36.4 0/00. Surface coastal salinities in Long Island Sound (Hardy, 1972) and off Long Island south coast (Hydroscience, 1974) vary between 26.5 and 28.5 0/00.

TABLE VI-3

SAMPLE CALCULATION TABLE FOR CALCULATION OF FLUSHING TIME  
BY SEGMENTED FRACTION OF FRESHWATER METHOD

Segment Number	Mean Segment Salinity $S_i$ (ppt)	Mean Segment Length (m)	Mean Segment Cross-sectional Area ( $m^2$ )	Segment Mean Tide Volume $V_i$ ( $m^3$ )	Fraction of River Water $f_i = \frac{S_s - S_i}{S_s}$	River Water Volume $W_i = f_i \times V_i$ ( $m^3$ )	Segment Flushing Time $T_i = W_i / R$ (tidal cycles)	
							$\sum_{i=1}^n T_i =$	

↑ Up Estuary

EXAMPLE VI-3

Flushing Time Calculation by Fraction of Fresh Water Method

This example pertains to the Patuxent Estuary. This estuary has no major side embayments, and the Patuxent River is by far its largest source of fresh water. This estuary therefore lends itself well to analysis by the segmented fraction of fresh water method.

Salinity profiles for July 19, 1978 are used to find segment salinity values. Chesapeake Bay water at the mouth of the Patuxent Estuary had a salinity of 10.7 ppt ( $S_s$ ). The Patuxent River discharge over the duration of one tidal cycle is:

$$\begin{aligned} R &= (12 \text{ m}^3/\text{sec}) (12.4 \text{ hr/tidal cycle}) (3600 \text{ sec/hr}) \\ &= 5.36 \times 10^3 \text{ m}^3 / \text{tidal cycle} \end{aligned}$$

A segmentation scheme based on the principles laid out above is used to divide the estuary into eight segments; their measured characteristics are shown Table VI-4. The segmentation is shown graphically on the estuary salinity profile (Figure VI-14).

The next step is to find the fraction of fresh water for each segment. For segment 1:

$$f_1 = \frac{S_s - S_1}{S_s}$$

where

$f_1$  = fraction of fresh water, segment 1

$S_s$  = salinity of local seawater

$S_1$  = measured mean salinity for segment 1

$$f_1 = \frac{10.7 \text{ ppt} - 0.8 \text{ ppt}}{10.7 \text{ ppt}} = 0.93$$

The calculation is reported in Table IV-4 for segments 2 through 8.

The volume of fresh water (river water) in each segment is next found using the formula:

$$W_i = f_i \times V_i$$

For segment 1:

$$\begin{aligned} W_1 &= f_1 \times V_1 = 0.93 (0.79 \times 10^7 \text{ m}^3) \\ &= 7.35 \times 10^6 \text{ m}^3 \end{aligned}$$

The flushing time for each segment is next calculated by:

$$T_i = W_i / R$$

TABLE VI -4

PATUXENT ESTUARY SEGMENT CHARACTERISTICS FOR  
FLUSHING TIME CALCULATIONS

Segment Number	Mean Segment Salinity $S_i$ , ppt	Segment Length meters	Mean Segment Cross-Sectional Area meter <sup>2</sup>	Mean Tide Segment Volume $V_i$ meters <sup>3</sup>
8	10.3	10,400	16,000	$16.6 \times 10^7$
7	9.5	10,400	12,500	$13.0 \times 10^7$
6	8.7	6,100	11,400	$6.95 \times 10^7$
5	7.6	6,100	7,500	$4.58 \times 10^7$
4	5.8	5,800	4,300	$2.49 \times 10^7$
3	3.3	5,000	3,100	$1.55 \times 10^7$
2	1.8	4,650	2,200	$1.02 \times 10^7$
1	0.8	4,650	1,700	$0.79 \times 10^7$

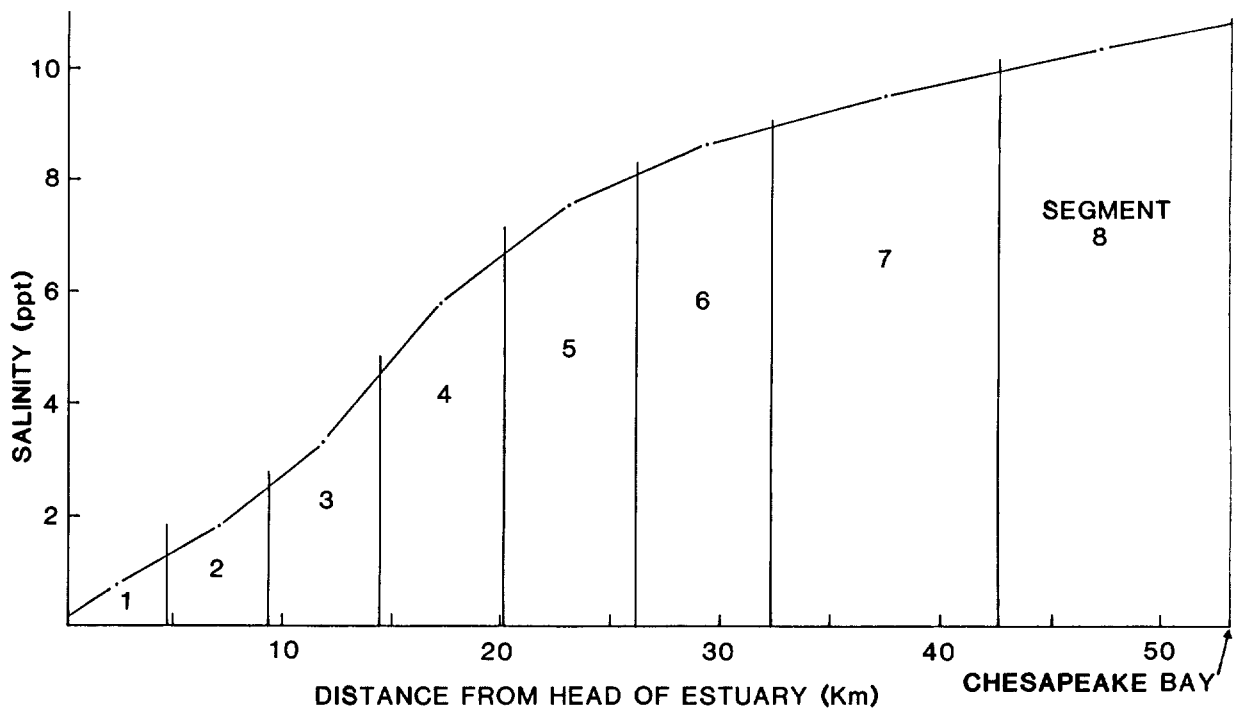


FIGURE VI -14 PATUXENT ESTUARY SALINITY PROFILE AND SEGMENTATION SCHEME  
USED IN FLUSHING TIME CALCULATIONS,

For segment 1:

$$T_1 = W_1/R = 7.35 \times 10^6 \text{ m}^3 / (5.36 \times 10^5 \text{ m}^3 / \text{tidal cycle})$$

$$= 13.7 \text{ tidal cycles}$$

Fraction of freshwater, river water volume and flushing time values for the eight segments are compiled in Table VI-5.

The final step is to determine the flushing time for the estuary. In this case:

$$T_f = \sum_{i=1}^8 T_i =$$

$$11.4 + 27.2 + 24.6 + 24.8 + 21.5 + 20.0 + 15.8 + 13.7$$

$$= 159 \text{ tidal cycles, or 2.74 months}$$

### 6.3.5 Branched Estuaries and the Fraction of Freshwater Method

Branched estuaries, where more than one source of freshwater contributes to the salinity distribution pattern, are common. The fraction of freshwater method can be directly applied to estuaries of this description. Consider the estuary shown in Figure VI-15, having two major sources of freshwater (River 1,  $R_1$ ; and River 2,  $R_2$ ). The flushing time for pollutants entering the estuary with river flow  $R_2$  is:

$$T_f (R_2) = T_1 + T_2 + T_3 + T_4 + T_5 + T_6 =$$

$$\frac{f_1 V_1}{R_2} + \frac{f_2 V_2}{R_2} + \frac{f_3 V_3}{R_2} + \frac{f_4 V_4}{R_2} + \frac{f_5 V_5}{R_1 + R_2} + \frac{f_6 V_6}{R_1 + R_2}$$

For the pollutants entering with  $R_1$ , the flushing time is:

$$T_f (R_1) = \frac{f_a V_a}{R_1} + \frac{f_b V_b}{R_1} + \frac{f_c V_c}{R_1} + \frac{f_5 V_5}{R_1 + R_2} + \frac{f_6 V_6}{R_1 + R_2}$$

The flushing time computations are similar in concept for the case of a single freshwater source, modified to account for a flow rate of  $R_1 + R_2$  in segments 5 and 6.

### 6.3.6 Modified Tidal Prism Method

This method divides an estuary into segments whose lengths are defined by the maximum excursion path of a water particle during a tidal cycle. Within each segment the tidal prism is compared to the total segment volume as a measure of the

TABLE VI-5  
FLUSHING TIME FOR PATUXENT ESTUARY

Segment Number	Mean Segment Salinity $S_i$ , ppt	Segment Length meters	Mean Segment Cross-Sectional Area meter <sup>2</sup>	Segment Mean Tide Volume $V_i$ meter <sup>3</sup>	Fraction of River Water $f_i = \frac{S_s - S_i}{S_s}$ ( $S_s = 10.7$ )	River Water Volume $W_i = f_i \times V_i$ (meters <sup>3</sup> )	Segment Flush Time $T_i = W_i/R$ tidal cycles
8	10.3	10,400	16,000	$16.6 \times 10^7$	0.037	$6.14 \times 10^6$	11.4
7	9.5	10,400	12,500	$13.0 \times 10^7$	0.112	$14.6 \times 10^6$	27.2
6	8.7	6,100	11,400	$6.95 \times 10^7$	0.19	$13.2 \times 10^6$	24.6
5	7.6	6,100	7,500	$4.58 \times 10^7$	0.29	$13.3 \times 10^6$	24.8
4	5.8	5,800	4,300	$2.49 \times 10^7$	0.46	$11.5 \times 10^6$	21.5
3	3.3	5,000	3,100	$1.55 \times 10^7$	0.69	$10.7 \times 10^6$	20.0
2	1.8	4,650	2,200	$1.02 \times 10^7$	0.83	$8.47 \times 10^6$	15.8
1*	0.8	4,650	1,700	$0.79 \times 10^7$	0.93	$7.35 \times 10^6$	13.7

Sum = 159 tidal cycles  
or 2.74 months

\*In this numbering scheme segment 1 is the most upstream segment.

END OF EXAMPLE VI-3



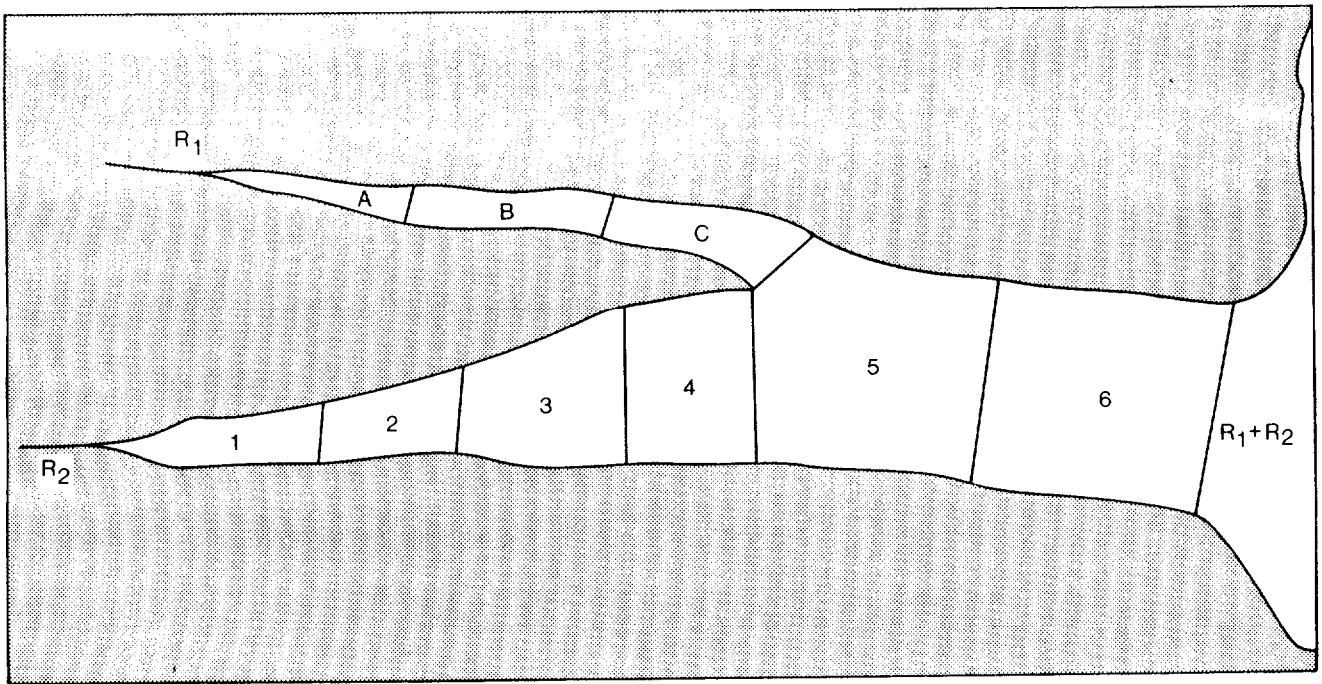


FIGURE VI -15 HYPOTHETICAL TWO-BRANCHED ESTUARY

flushing potential of that segment per tidal cycle (Dyer, 1973). The method assumes complete mixing of the incoming tidal prism waters with the low tide volumes within each segment. Best results have been obtained in estuaries when the number of segments is large (i.e. when river flow is very low) and when estuarine cross-sectional area increases fairly quickly downstream (Dyer, 1973).

The modified tidal prism method does not require knowledge of the salinity distribution. It provides some concept of mean segment velocities since each segment length is tied to particle excursion length over one tidal cycle. A disadvantage of the method is that in order to predict the flushing time of a pollutant discharged midway down the estuary, the method still has to be applied to the entire estuary.

The modified tidal prism method is a four-step methodology. The steps are:

1. Segment the estuary. For this method an estuary must be segmented so that each segment length reflects the excursion distance a particle can travel during one tidal cycle. The innermost section must then have a tidal prism volume completely supplied by river flow. Thus:

$$P_0 = R$$

where

$$P_0 = \text{tidal prism (intertidal volume) of segment "0"}$$

$$R = \text{river discharge over one tidal cycle.}$$

The low tide volume in this section ( $V_0$ ) is that water volume occupying the space under the intertidal volume  $P_0$  (which has just been defined as being equal to  $R$ ). The seaward limit of the next seaward segment is placed such that its low tide volume ( $V_1$ ) is defined by:

$$V_1 = P_0 + V_0 \quad (\text{VI-13})$$

$P_1$  is then that intertidal volume which, at high tide, resides above  $V$ . Successive segments are defined in an identical manner to this segment so that:

$$V_i = P_{i-1} + V_{i-1} \quad (\text{VI-14})$$

Thus each segment contains, at high tide, the volume of water contained in the next seaward section at low tide.

2. Calculate the exchange ratio ( $r$ ) by:

$$r_i = \frac{P_i}{P_i + V_i} \quad (\text{VI-15})$$

Thus the exchange ratio for a segment is a measure of a portion of water associated with that segment which is exchanged with adjacent segments during each tidal cycle.

3. Calculate segment flushing time by:

$$T_i = \frac{1}{r_i} \quad (\text{VI-16})$$

where

$T_i$  = flushing time for segment "i", measured in tidal cycles.

4. Calculate total estuarine flushing time by summing the individual segment flushing times:

$$T_f = \sum_{i=1}^n T_i \quad (\text{VI-17})$$

where

$T_f$  = total estuary flushing time

$n$  = number of segments.

Table VI-6 shows a suggested method for calculating flushing time by the modified tidal prism method.

TABLE VI-6  
SAMPLE CALCULATION TABLE FOR ESTUARINE FLUSHING TIME BY  
THE MODIFIED TIDAL PRISM METHOD

Down Estuary

Segment Number	Segment Dimensions				Subtidal Water Volume, $V_i$ ( $m^3$ )	Intertidal Water Volume $P_i$ ( $m^3$ )	Segment Exchange Ratio $r_i$	Segment Flushing Time, $T_i$ (Tidal Cycles)	
	Starting Distance Above Mouth (m)	Ending Distance Above Mouth (m)	Distance of Center Above Mouth (m)	Segment Length (m)					
	$\sum_{i=1}^n T_i =$								

EXAMPLE VI-4

Estuary Flushing Time Calculation by the  
Modified Tidal Prism Method

The Fox Mill Run Estuary, Virginia, was selected for this example. During low flow conditions, the discharge of Fox Mill Run has been measured at 0.031 m<sup>3</sup>/sec.

$$\begin{aligned} R &= \text{river discharge over one tidal cycle} \\ &= 0.031 \text{ m}^3/\text{sec} \times 12.4 \text{ hrs/tidal cycle} \times 3600 \text{ sec/hr} \\ &= 1384 \text{ m}^3/\text{tidal cycle} \end{aligned}$$

The estuary flushing time is found in four steps:

1. Segmentation

From bathymetric maps and tide gage data, cumulative upstream volume was plotted for several positions along the estuary (see Figure VI-16).

Since:

$$\begin{aligned} P_0 &= R \\ P_0 &= 1384 \text{ m}^3 \end{aligned}$$

Reading across the graph from "a" to the intertidal volume curve, then down the subtidal volume curve and across to "b":

$$V_0 = 490 \text{ m}^3$$

The known cumulative upstream water volume also establishes the downstream segment boundary. Reading downward from the subtidal volume curve to "c", a  $V_0$  of 490 m<sup>3</sup> corresponds to an upstream distance of 2.700 meters for the segment 0 lower boundary.

The low tide water volume for the next segment can be found by the equation:

$$V_1 = P_0 + V_0$$

or

$$V_1 = 1384 + 490 = 1874 \text{ m}^3$$

Since the graphs of Figure VI-16 are cumulative curves, it is necessary, when entering a  $V_i$  value in order to determine a  $P_i$  value, to sum the upstream  $V_i$ 's. For  $V_1$  the cumulative upstream low-tide volume is:

$$V_0 + V_1 = 490 + 1874 = 2364 \text{ m}^3$$

Entering the graph where the subtidal volume is equal to 2,364 m<sup>3</sup> (across from "d"), we can move upward to read the corresponding cumulative intertidal volume "e" on the vertical scale, and downward to read the

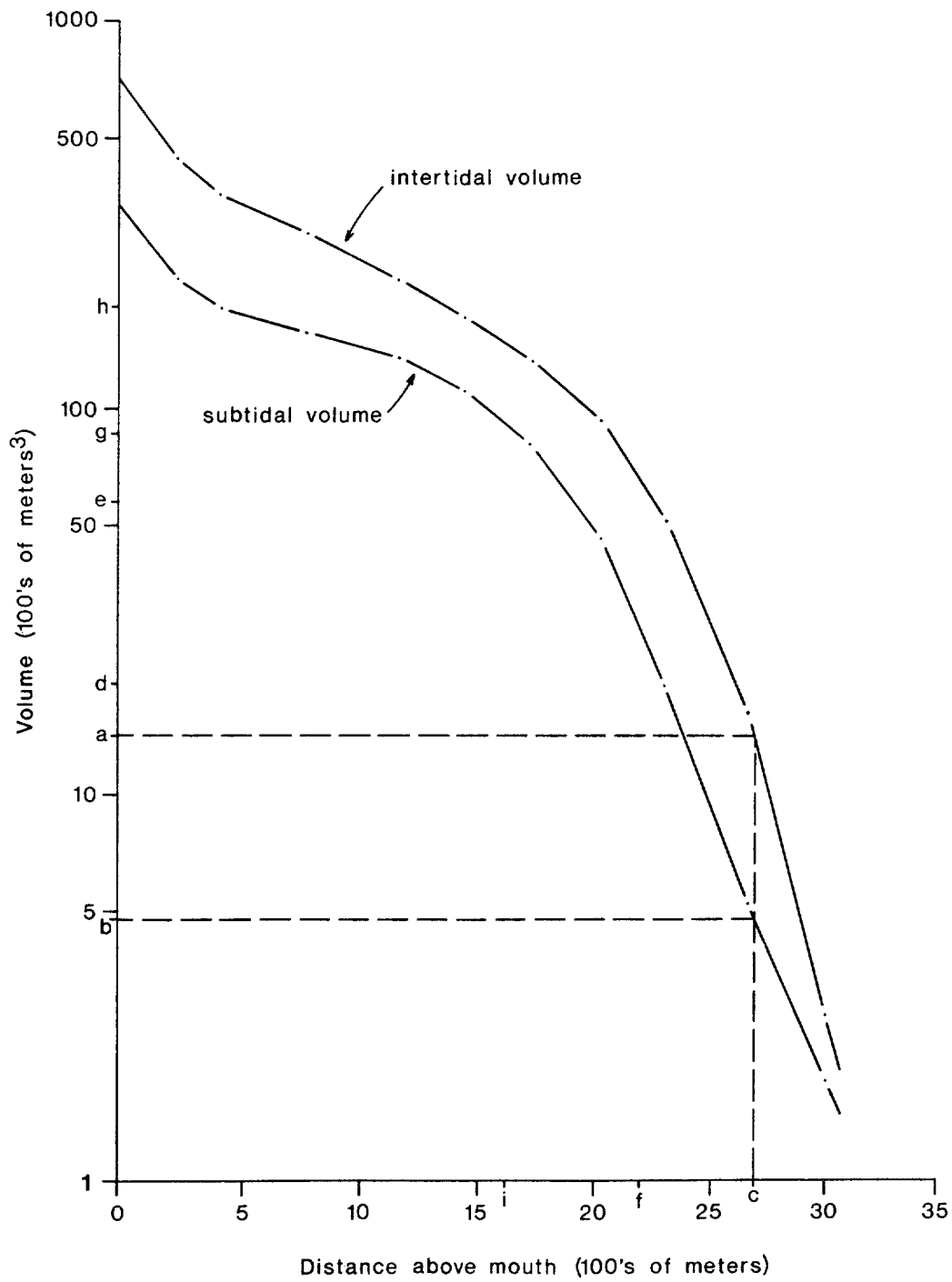


FIGURE VI -16 CUMULATIVE UPSTREAM WATER VOLUME,  
FOX MILL RUN ESTUARY

downstream boundary of segment 1 at "f" on the horizontal scale. The cumulative upstream intertidal volume is  $5900 \text{ m}^3$ .

Since:

$$5900 \text{ m}^3 = P_0 + P_1$$

$$P_1 = 5900 - 1384 = 4516 \text{ m}^3$$

For segment 2:

$$V_2 = P_1 + V_1 = 1874 + 4516 = 6390 \text{ m}^3$$

To find  $P_2$ , it is necessary to enter the graph at a cumulative subtidal volume of:

$$V_0 + V_1 + V_2 = 490 + 1874 + 6390 = 8759 \text{ m}^3 \text{ (across from "g")}$$

This yields a cumulative intertidal volume of  $14,000 \text{ m}^3$  (across from "h") and a downstream segment boundary of  $1,650 \text{ m}^3$ .

The tidal prism of Segment 2 is found by:

$$14000 = P_0 + P_1 + P_2$$

or

$$P_2 = 14000 - 1384 - 4516 = 8100 \text{ m}^3$$

The procedure is identical for Segment 3. For this final segment:

$$V_3 = 14,490 \text{ m}^3$$

$$P_3 = 36,000 \text{ m}^3$$

Dimensions and volumes of the four segments established by this procedure are compiled in Table VI-7.

- The exchange ratio for segment 0 is found by:

$$r_0 = \frac{P_0}{P_0 + V_0} = \frac{1384 \text{ m}^3}{1384 \text{ m}^3 + 490 \text{ m}^3}$$

Exchange ratios are calculated similarly for the other three segments.

- Flushing time for each segment "i" is given by:

$$T_i = \frac{1}{r_i}$$

so

$$T_0 = \frac{1}{r_0} = \frac{1}{0.74} = 1.35$$

Exchange ratios and flushing times for the four segments are shown in Table IV-7.

- Flushing time for the whole estuary is found by:

$$T_f = \sum_{i=0}^3 T_i$$

TABLE VI -7  
DATA AND FLUSHING TIME CALCULATIONS FOR FOX MILL RUN ESTUARY

Segment Number	Segment Dimensions				Water Volume at Low Tide $V_i$ meters <sup>3</sup>	Intertidal Volume $P_i$ meters <sup>3</sup>	Exchange Ratio For Segment $i$ $r_i$	Flushing Time for Segment $i$ $T_i$
	Starts at this Distance Above Mouth-meters	Stops at this Distance Above Mouth-meters	Center Point Distance Above Mouth-meters	Segment Length meters				
0	3,200	2,700	2,950	500	490	1,384	0.74	1.35
1	2,700	2,240	2,470	460	1,874	4,516	0.71	1.41
2	2,240	1,650	1,945	590	6,390	8,100	0.56	1.79
3	1,650	180	915	1,470	14,490	36,000	0.71	1.41

$$\Sigma T_i = 5.96 \text{ tidal cycles}$$

or

$$\begin{aligned} T &= 1.35 + 1.41 + 1.79 + 1.41 \\ &= 5.96 \text{ tidal cycles} \\ &= 73.9 \text{ hours} \\ &= 3.1 \text{ days} \end{aligned}$$

END OF EXAMPLE VI-4

## 6.4 FAR FIELD APPROACH TO POLLUTANT DISTRIBUTION IN ESTUARIES

### 6.4.1 Introduction

Analysis of pollutant distribution in estuaries can be accomplished in a number of ways. In particular, two approaches, called the far field and near field approaches, are presented here (Sections 6.4 and 6.5, respectively). As operationally defined in this document, the far field approach ignores buoyancy and momentum effects of the wastewater as it is discharged into the estuary. The pollutant is assumed to be instantaneously distributed over the entire cross-section of the estuary (in the case of a well-mixed estuary) or to be distributed over a lesser portion of the estuary in the case of a two-dimensional analysis. Whether or not these assumptions are realistic depends on a variety of factors, including the rapidity of mixing compared to the kinetics of the process being analyzed (e.g. compared to dissolved oxygen depletion rates). It should be noted that far field analysis (either one- or two-dimensional) can be used even if actual mixing is less than assumed by the method. However, the predicted pollutant concentrations will be lower than the actual concentrations.

Near field analysis considers the buoyancy and momentum of the wastewater as it is discharged into the receiving water. Pollutant distribution can be calculated on a smaller spatial scale, and assumptions such as "complete mixing" or "partial mixing" do not have to be made. The actual amount of mixing which occurs is predicted as an integral part of the method itself. This is a great advantage in analyzing compliance with water quality standards which are frequently specified in terms of a maximum allowable pollutant concentration in the receiving water at the completion of initial dilution. (Initial dilution will be defined later in Section 6.5.2.)

The following far field approaches for predicting pollutant distribution are presented in this chapter:

- Fraction of freshwater method
- Modified tidal prism method
- Dispersion-advective equations
- Pritchard's Box Model.

The near field analysis uses tabulated results from an initial dilution model called MERGE. At the completion of initial dilution predictions can be made for the following:

- Pollutant concentrations
- pH levels
- Dissolved oxygen concentrations.

The near field pollutant distribution results are then used as input to an analytical technique for predicting pollutant decay or dissolved oxygen levels subsequent to initial dilution. The remainder of Section 6.4 will discuss those methods applicable to the far field approach.

#### 6.4.2 Continuous Flow of Conservative Pollutants

The concentration of a conservative pollutant entering an estuary in a continuous flow varies as a function of the entry point location. It is convenient to separate pollutants entering an estuary at the head of the estuary (with the river discharge) from those entering along the estuary's sides. The two impacts will then be addressed separately.

##### 6.4.2.1 River Discharges of Pollutants

The length of time required to flush a pollutant from an estuary after it is introduced with the river discharge has already been calculated, and is the estuarine flushing time. Now consider a conservative pollutant continuously discharged into a river upstream of the estuary. As pollutant flows into the estuary, it begins to disperse and move toward the mouth of the estuary with the net flow. If, for example, the estuary flushing time is 10 tidal cycles, then 10 tidal cycles following its initial flow into the estuary, some of the pollutant is flushed out to



the ocean. Eventually, a steady-state condition is reached in which a certain amount of pollutant enters the estuary, and the same amount is flushed out of the estuary during each tidal cycle. The amount of this pollutant which resides in the estuary at steady-state is a function of the flushing time. From the definition of flushing time, the amount of fresh water (river water) in the estuary may be calculated by:

$$W_E = T_f R \quad (VI-18)$$

where

$W_E$  = quantity of freshwater in the estuary

$T_f$  = estuary flushing time

$R$  = river discharge over one tidal cycle.

Using the same approach, the quantity of freshwater in any segment of the estuary is given by:

$$W_i = T_i R \quad (VI-19)$$

where

$W_i$  = quantity of freshwater in the  $i^{th}$  segment of the estuary

$T_i$  = flushing time for the  $i^{th}$  segment calculated by the fraction of freshwater method.

If a conservative pollutant enters an estuary with the river flow, it can be assumed that its steady-state distribution will be identical to that of the river water itself. Thus:

$$M_i = W_i C_r = T_i R C_r \quad (VI-20)$$

and

$$C_i = W_i/V_i \quad (VI-21)$$

where

$M_i$  = quantity of pollutant in estuary segment "i"

$C_r$  = concentration of pollutant in the river inflow

$C_i$  = concentration of pollutant in estuary segment "i" assuming all of pollutant "i" enters the estuary with the river discharge.

Thus direct discharges into the estuary are excluded.

$V_i$  = water volume segment "i".

The same values for  $C_i$  and  $M_i$  may also be obtained by using the fraction of

freshwater,  $f_i$ , for each segment by:

$$C_i = f_i C_r \quad (VI-22)$$

and

$$M_i = C_i V_i \quad (VI-23)$$

Thus both the quantity of a pollutant in each segment and its concentration within each segment are readily obtainable by either of the above methods. The use of one of these methods will be demonstrated in Example VI-5 below for calculation of both  $C_i$  and  $M_i$ .

#### EXAMPLE VI-5

##### Calculation of Concentration of Conservative River Borne Pollutant in an Estuary

The Patuxent Estuary is the subject of this example. The problem is to predict the incremental concentration increase of total nitrogen (excluding  $N_2$  gas) in the estuary, given that the concentration in river water at the estuary head is 1.88 mgN/l.

Assume that total nitrogen is conservative and that the nitrogen concentration in local seawater is negligible. The segmentation scheme used in Example VI-2 (fraction of freshwater calculation) will be retained here. For each segment, the total nitrogen concentration is directly proportional to the fraction of freshwater in the segment:

$$C_i = f_i C_r$$

The total nitrogen concentration for the uppermost segment is therefore given by:

$$\begin{aligned} C_1 &= 0.93 (1.88 \text{ mgN/l}) \\ &= 1.75 \text{ mgN/l} \end{aligned}$$

For the next segment it is:

$$C_2 = 0.83 (1.88 \text{ mgN/l}) = 1.56 \text{ mgN/l}$$

and so on. Nitrogen concentrations for all the segments are compiled in Table VI-8. Note that these are not necessarily total concentrations, but only nitrogen inputs from the Patuxent River.

The incremental mass of nitrogen in each segment is found by:

$$M_i = W_i C_r$$

TABLE VI -8  
 POLLUTANT DISTRIBUTION IN THE PATUXENT RIVER

Segment Number*	Fraction of Freshwater* in Segment $f_i$	Resultant Pollutants** Concentration $=f_i \times 1.88 \text{ mgN/l}$
8	0.037	0.07
7	0.112	0.21
6	0.19	0.36
5	0.29	0.55
4	0.46	0.86
3	0.69	1.30
2	0.83	1.56
1	0.93	1.88
River	1.00	1.88

\*From Example VI -2  
 \*\*These are the increment concentrations of total nitrogen in the estuary due to the river-borne input.

TABLE VI -9  
 INCREMENTAL TOTAL NITROGEN IN PATUXENT RIVER,  
 EXPRESSED AS KILOGRAMS  
 (See Problem VI -5)

Segment Number	River Water Volume $W_i = f_i \times V$ meters	Incremental Total N $M_i = W_i (1.88)$ kilograms
8	$6.14 \times 10^6$	11,500
7	$14.6 \times 10^6$	27,400
6	$13.2 \times 10^6$	24,800
5	$13.3 \times 10^6$	25,000
4	$11.5 \times 10^6$	21,600
3	$10.7 \times 10^6$	20,100
2	$8.47 \times 10^6$	15,900
1	$7.35 \times 10^6$	13,800

The  $W_i$  values for the eight segments were determined in Example VI-2. For segment 1, the incremental nitrogen is given by:

$$\begin{aligned} M_1 - W_1 C_r &= (7.35 \times 10^6 \text{ m}^3)(1.88 \text{ mgN/l})(10^3 \text{ l/m}^3) \\ &= 1.38 \times 10^{10} \text{ mg or } 13,800 \text{ kg} \end{aligned}$$

Increased total nitrogen (in kilograms) for the entire estuary is shown in Table VI-9.

----- END OF EXAMPLE VI-5 -----

In this example, low tide volumes were used to calculate  $M_i$  since low tide volumes had been used to calculate  $f_i$ 's. The approach assumes that  $C_i$ 's are constant over the tidal cycle and that  $M_i$ 's are constant over the tidal cycle. This leads to the assumption that calculation of a low tide  $C_i$  and  $M_i$  will fully characterize a pollutant in an estuary. This, however, is not strictly true. Figure VI-17 depicts one tidal cycle in an estuary and shows the periods of the cycle during which a pollutant is flushed out of the estuary and during which river discharge brings pollutants into the estuary. During periods of high tide, rising tidal elevation blocks river discharge and backs up river flow in the lower stretches of the river. Figure VI-17 also shows the resulting quantity of a pollutant in residence in the estuary ( $W_{pe}$ ) over the tidal cycle. This variation over the tidal cycle as a percentage of  $M_E$  is dependent on the flushing time but is usually small. The change in the total volume of water in an estuary over a tidal cycle is equal to the tidal prism which is often of the same magnitude as the low tide volume. As an example, the Alsea Estuary in Oregon has  $P_t = 5.1 \times 10^8 \text{ ft}^3$  while  $V_t = 2.1 \times 10^8$  (Goodwin, Emmet, and Glenne, 1970). Thus the variation in estuarine volume is 2.5 times the low tide volume. As a result, estuarine volume variations over a tidal cycle have a much greater impact on variations in pollutant concentrations in the estuary than do changes in the quantity of pollutant present in the estuary over a tidal cycle. It is important to note, however, that low tidal volume and low  $M_E$  nearly coincide, so that variations in mean pollutant concentrations are less severe than are estuarine water mass changes.

This qualitative description of pollutant flow into and out of an estuary is somewhat simplistic since it assumes that high tide and low tide at the mouth of an estuary coincide with those at the head of the estuary. This is usually not the case. There is normally a lag time between tidal events at an estuarine mouth and those at its head. Thus river discharge into the estuary which depends on tidal conditions at the head, and tidal discharge which depends on tidal conditions at the mouth, are not as directly tied to each other as indicated in Figure VI-17.

While  $W_E$  does not vary substantially over a tidal cycle under steady-state

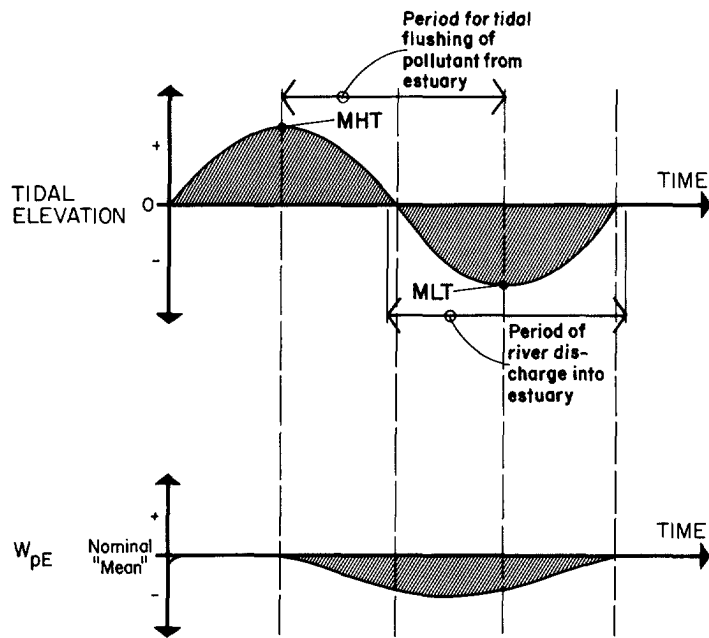


FIGURE VI -17 RIVER BORNE POLLUTANT CONCENTRATION FOR ONE TIDAL CYCLE

conditions, the mean concentration of a pollutant in an estuary ( $C_E$ ) does. At sea Estuary data can be used to show this  $C_E$  variation over a tidal cycle. Using data for the estuary as a whole (mean concentration), the equations for this comparison are:

$$M_E = W_r T_f \quad (VI-24)$$

and

$$C_E = M_E / (V_t + P_t) \quad (VI-25)$$

with

$$W_r = (566.4 \mu\text{g}/\text{ft}^3) (4.64 \times 10^6 \text{ft}^3/\text{tidal cycle})$$

or

$$W_r = 2.628 \times 10^9 \mu\text{g}/\text{tidal cycle}.$$

Then:

$$M_E = (2.628 \times 10^9 \mu\text{g}/\text{tidal cycle}) (20.8 \text{ tidal cycle})$$

$$M_E = 5.466 \times 10^{10} \mu\text{g}$$

and

$$C_{E(\text{low})} = 5.466 \times 10^{10} \mu\text{g} / 2.1 \times 10^8 \text{ft}^3$$

or

$$C_{E(\text{low})} = 260.31 \mu\text{g}/\text{ft}^3, \text{ or } 46 \text{ percent of river concentration.}$$

However:

$$C_{E(\text{high})} = 5.466 \times 10^{10} \mu\text{g}/(2.1 \times 10^8 \text{ft}^3 + 5.1 \times 10^8 \text{ft}^3)$$

$$C_{E(\text{high})} = 75.92 \mu\text{g}/\text{ft}^3 \text{ or } 13 \text{ percent of river concentration.}$$

In an actual estuary, the concentration of a pollutant is not a stepwise function as indicated by segment  $C_i$  values, but is more realistically a continuous spectrum of values. By assigning the longitudinal midpoint of each segment a concentration value equal to that segment's  $C_i$ , a resulting continuous curve can be constructed as shown in Figure VI-18. This type of plot is useful in estimating pollutant concentrations within the estuary. It can also be used, however, to estimate maximum allowable  $C_r$  to maintain a given level of water quality at any point within the estuary. This latter use of Figure VI-18 is based on determining the desired concentration level ( $C_x$ ) and then using the ratio of  $C_x$  to  $C_r$  to calculate an allowable  $C_r$ .

#### 6.4.2.2 Other Continuous Conservative Pollutant Inflows

In the previous section, an analysis was made of the steady-state distribution of a continuous flow pollutant entering at the head of an estuary. The result was a graph of the longitudinal pollutant concentration within the estuary (Figure VI-18). This section addresses a continuous, conservative pollutant flow entering along the side of an estuary. Such a pollutant flow (e.g. the conservative elements of a municipal sewer discharge, industrial discharge, or minor tributary) is carried both upstream and downstream by tidal mixing, with the highest concentration occurring in the vicinity of the outfall. Once a steady state has been achieved, the distribution of this pollutant is directly related to the distribution of fresh river water (Dyer, 1973).

The average cross-sectional concentration at the outfall under steady-state conditions is:

$$C_o = \frac{Q_p}{R} f_o \quad (\text{VI-26})$$

where

$C_o$  = mean cross-sectional concentration of a pollutant at the point of discharge, mass/volume

$Q_p$  = discharge rate of pollutant, mass/tidal cycle

$f_o$  = segment fraction of freshwater

$R$  = river discharge rate, volume/tidal cycle.

Downstream of the outfall, the pollutant must pass through any cross section at

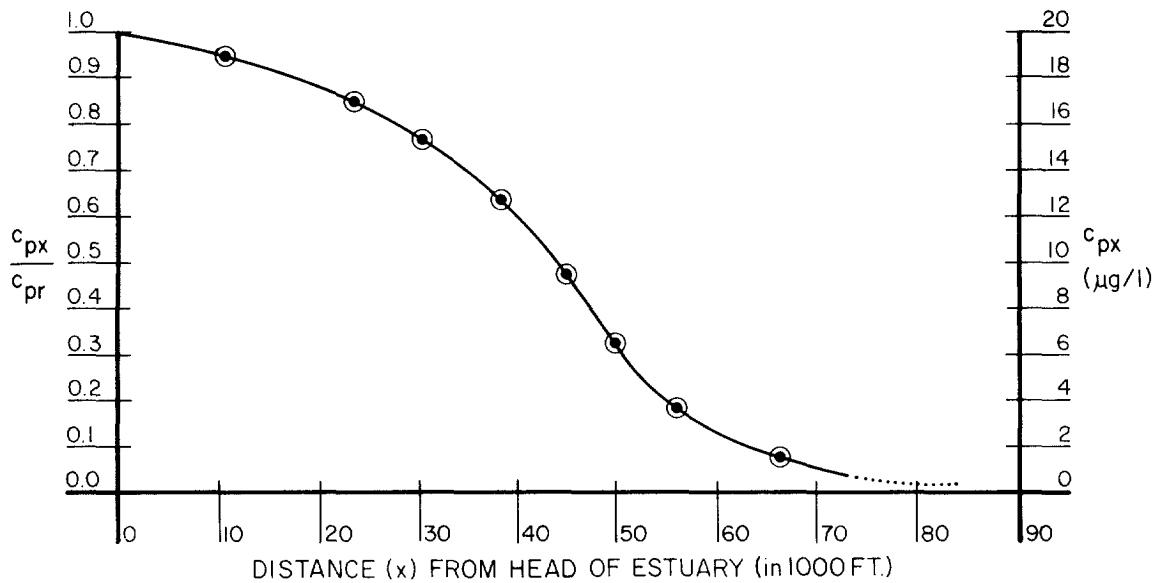


FIGURE VI -18 ALSEA ESTUARY RIVERBORNE CONSERVATIVE POLLUTANT CONCENTRATION

a rate equal to the rate of discharge. Thus:

$$C_x = C_0 \frac{f_x}{f_0} = C_0 \left( \frac{\frac{S_s - S_x}{S_s}}{\frac{S_s - S_0}{S_s}} \right) = C_0 \left( \frac{S_s - S_x}{S_s - S_0} \right) = f_x \frac{Q_p}{R} \quad (\text{VI -27})$$

where

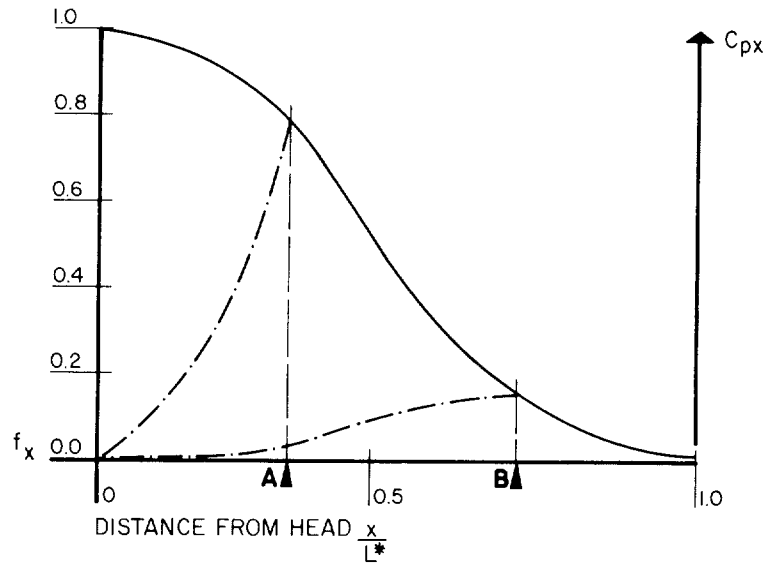
$S_x, C_x$  and  $f_x$  denote downstream cross-sectional values

$S_0, C_0$  and  $f_0$  denote the cross-sectional values at the discharge point (or segment into which discharge is made).

Upstream of the outfall, the quantity of pollutant diffused and advectively carried upstream is balanced by that carried downstream by the nontidal flow so that the net pollutant transport through any cross section is zero. Thus, the pollutant distribution is directly proportional to salinity distribution and (Dyer, 1973) :

$$C_x = C_0 \frac{S_x}{S_0} \quad (\text{VI -28})$$

Downstream of the outfall, the pollutant concentration resulting from a point discharge is directly proportional to river-borne pollutant concentration. Upstream from the discharge point, it is inversely proportional to river-borne pollutant concentrations. Figure VI-19 is a graph of  $f_x$  versus distance from the estuary



\*L = Total Estuarine Length

FIGURE VI -19 POLLUTANT CONCENTRATION FROM AN ESTUARINE OUTFALL (AFTER KETCHUM, 1950)

head for a typical estuary. The solid  $f_x$  line is also a measure of pollutant concentration for all points downstream of a pollutant outfall (either discharge location A or B). The actual concentration ( $C_x$ ) for any point is equal to this  $f_x$  value multiplied by  $Q_p/R$  which is a constant over all  $x$ , Upstream concentrations decrease from  $C_0$  in a manner proportional to upstream salinity reduction (see dotted lines). It is important to note how even a small downstream shift in discharge location creates a very significant reduction in upstream steady-state pollutant concentration. Table VI-10 shows a suggested format for tabulating pollutant concentrations by the fraction of freshwater method,

EXAMPLE VI-6

Calculation of Conservative Pollutant Concentration  
for a Local Discharge

This example will again utilize the eight-segment scheme devised for the Patuxent Estuary in Example VI-2. The objective is to predict the concentration distribution of total nitrogen in the estuary resulting from a discharge of 80,000 mgN/sec into segment 4.

The first step is to determine the nitrogen concentration in segment 4.



TABLE VI -10

SAMPLE CALCULATION TABLE FOR DISTRIBUTION OF A LOCALLY DISCHARGED CONSERVATIVE POLLUTANT BY THE FRACTION OF FRESHWATER METHOD

From Table VI-3			$\frac{f_i}{f_0}$	$\frac{S_i}{S_0}$	Pollutant Concentrations* (mg/l)
Segment Number	Fraction of Freshwater $f_i$	Mean Segment Salinity (ppt)			
Segment Containing Discharge			1	1	

Up Estuary  
↓

$$*Pollutant\ concentration = \begin{cases} C_0 \frac{f_i}{f_0}, & \text{down estuary of the discharge} \\ C_0 \frac{S_i}{S_0}, & \text{up estuary of the discharge} \end{cases}$$

$$\text{where } C_0 = \frac{W}{R} f_0$$

From Equation VI -26:

$$C_0 = \frac{Q_p f_0}{R} = \frac{(8 \times 10^4 \text{ mgN/sec} \times 12.4 \text{ hrs/tidal cycle} \times 3600 \text{ sec/hr})(0.46)}{5.36 \times 10^5 \text{ m}^3/\text{tidal cycle}}$$

$$= \frac{3065 \text{ mgN}}{\text{m}^3} = 3.065 \text{ mgN/l}$$

For segments 1-3, upstream from the discharge, nitrogen concentration is found by Equation VI -28:

$$C_i = C_0 \frac{S_i}{S_0}$$

For segment 1:

$$S_1 = 0.8 \text{ ‰}$$

$$S_0 = S_4 = 5.8 \text{ ‰}$$

$$C_4 = 3.065 \text{ mgN/l}$$

so

$$C_1 = 3.065 \text{ mgN/l} \left( \frac{0.8 \text{ ‰}}{5.8 \text{ ‰}} \right) = 0.42 \text{ mgN/l}$$

Nitrogen concentrations in segments 2 and 3 are found in an identical way. Table VI-11 summarizes the information used in the calculation.

For the segments downstream of the discharge, total nitrogen concentration is found using Equation VI-27:

$$C_i = C_0 \frac{f_i}{f_0}$$

In segment 5:

$$f_5 = 0.29$$

$$f_0 = f_4 = 0.46$$

TABLE VI-11

NITROGEN CONCENTRATION IN PATUXENT ESTUARY  
BASED ON LOCAL DISCHARGE

Segment Number	Fraction of Freshwater $f_i$	Mean Segment Salinity	$\frac{S_i}{S_0}$	$\frac{f_i}{f_0}$	Concentration mgN/l
8	0.037	10.3		0.08	0.25
7	0.112	9.5		0.24	0.74
6	0.19	8.7		0.41	1.26
5	0.29	7.6		0.63	1.93
<b>Discharge</b> → 4	0.46	5.8	1	1	3.06
3	0.69	3.3	0.57	-	1.75
2	0.83	1.8	0.31	-	0.95
1	0.93	0.8	0.14	-	0.43

and

$$C_4 = 3.065 \text{ mgN/l}$$

so

$$C_5 = 3.065 \text{ mgN/l} \left( \frac{0.29}{0.46} \right) = 1.93 \text{ mgN/l}$$

The same procedure yields nitrogen concentrations in segments 6-8, also downstream of the discharge.

Figure VI-20 below shows the nitrogen concentration distribution over the entire estuary. Note that the nearer a discharge is to the estuary's mouth, the greater the protection rendered the upstream reaches of the estuary.

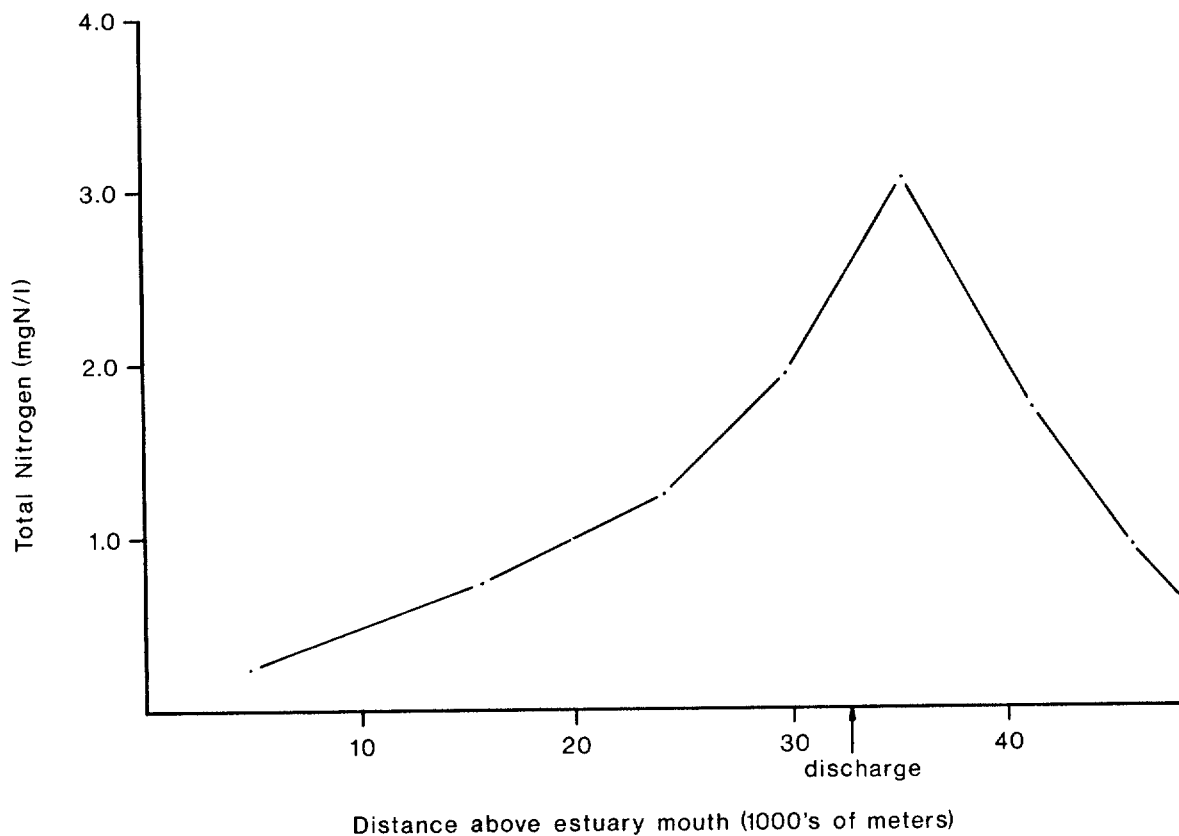


FIGURE VI-20 HYPOTHETICAL CONCENTRATION OF TOTAL NITROGEN IN PATUXENT ESTUARY

END OF EXAMPLE VI-6

### 6.4.3 Continuous Flow Non-Conservative Pollutants

Most pollutant discharges into estuaries have some components which behave non-conservatively. A number of processes mediate the removal of compounds from natural waters, among these:

- Sorption by benthic sediments on suspended matter
- Partitioning
- Decay (by photolysis or biologically mediated reactions)
- Biological uptake
- Precipitation
- Coagulation.

The latter two processes are particularly significant in estuaries. Thus, in addition to dispersion and tidal mixing, a time-dependent component is incorporated when calculating the removal of non-conservative pollutants from estuarine waters. The concentrations of non-conservative pollutants are always lower than those of conservative pollutants (which have a decay rate of zero) for equal discharge concentrations. The results of the previous section for conservative constituents serve to set upper limits for the concentration of non-conservative continuous flow pollutants. Thus, if plots similar to Figure VI-17 for river discharges and to Figure VI-19 for other direct discharges have been prepared for flow rates equal to that of the non-conservative pollutant under study, some reasonable approximations can be made for steady-state non-conservative pollutant concentrations without requiring additional data. Assuming a first order decay rate for the non-conservative constituent, its concentration is given by:

$$C_t = C_0 e^{-kt} \quad (\text{VI-29})$$

where

- $C_t$  = pollutant concentration at time "t"
- $C_0$  = initial pollutant concentration
- $k$  = decay rate constant.

For conservative pollutants  $k = 0$  and  $C = C_0$  under steady-state conditions. Decay rates are determined empirically and depend on a large number of variables. Typical decay rates for BOD and coliform bacteria are shown in Table VI-12. If data are not available for a particular estuary, the use of these average values will provide estimates.

It should be noted that decay rates are dependent upon temperature. The values given assume a temperature of  $20^\circ\text{C}$ . Variations in  $k$  values for differing temperatures are given by Equation VI-30:

$$k_T = k_{20^\circ} \theta^{T-20^\circ} \quad (\text{VI-30})$$

TABLE VI -12

TYPICAL VALUES FOR DECAY REACTION RATES 'k' \*

Source	BOD	Coliform
Dyer, 1973		.578
Ketchum, 1955		.767
Chen and Orlob, 1975	.1	.5
Hydroscience, 1971	.05-.125	1-2
McGaughhey, 1968	.09	
Harleman, 1971	.069	

\*k values for all reactions given on a per tidal cycle basis, 20° C.

where

- $k_T$  = decay rate at temperature T  
 $k_{20}$  = decay rate at 20°C (as given in Table VI-12)  
 $\theta$  = a constant (normally between 1.03 and 1.05).

Thus an ambient temperature of 10°C would reduce a k value of 0.1 per tidal cycle to 0.074 for a  $\theta = 1.03$ .

Decay effects can be compared to flushing effects by setting time equal to the flushing time and comparing the resulting decay to the known pollutant removal rate as a result of flushing. If  $kt$  in Equation VI-29 is less than 0.5 for  $t = t_f$ , decay processes reduce concentration by only about one-third over the flushing time. Here mixing and advective effects dominate and non-conservative decay plays a minor role. When  $kt_f > 12$  decay effects reduce a batch pollutant to 5 percent of its original concentration in less than one-fourth of the flushing time. In this case, decay processes are of paramount importance in determining steady-state concentrations. Between these extremes, both processes are active in removing a pollutant from the estuary with  $3 < kt_f < 4$  being the range for approximately equal contributions to removal. Dyer (1973) analyzed the situation for which decay and tidal exchange are of equal magnitude for each estuarine segment. Knowing the conservative concentration, the non-conservative steady-state concentration in a segment is given by:

$$C_i = C_0 \frac{f_i}{f_0} \prod_{i=1, \dots, n} \left( \frac{r_i}{1 - (1-r_i)e^{-kt}} \right) \quad \begin{array}{l} \text{for segments downstream} \\ \text{of the outfall} \end{array} \quad \text{(VI-31)}$$

and

$$C_i = C_o \frac{S_i}{S_o} \prod_{i=1, \dots, n} \left( \frac{r_i}{1 - (1 - r_i)e^{-kt}} \right) \quad \text{for segments upstream of the outfall} \quad (\text{VI-32})$$

where

- $C_i$  = non-conservative constituent mean concentration in segment "i"
- $C_o$  = conservative constituent mean concentration in segment of discharge
- $r_i$  = the exchange ratio for segment "i" as defined by the modified tidal prism method
- $n$  = number of segments away from the outfall (i.e.  $n = 1$  for segments adjacent to the outfall;  $n = 2$  for segments next to these segments, etc. )

Other parameters are as previously defined.

In the case of a non-conservative pollutant entering from the river,  $n = 1$ , and the only concentration expression necessary is:

$$C_i = C_{i-1} \frac{f_i}{f_{i-1}} B_i \quad (\text{VI-33})$$

where

$$B_i = \frac{r_i}{1 - (1 - r_i)e^{-kt}} \quad (\text{VI-34})$$

Table VI-13 shows a suggested format for tabulating pollution concentrations by the modified tidal prism method.

EXAMPLE VI-7

Continuous Discharge of a Non-Conservative Pollutant  
into the Head of an Estuary

The Fox Mill Run Estuary (see Example VI-3) is downstream of the Gloucester, Virginia, sewage treatment plant. Knowing the discharge rate of CBOD in the plant effluent, the purpose of this example is to determine the concentration of CBOD throughout the estuary.

It is first necessary to determine the concentration of CBOD in Fox Mill Run as it enters the estuary (assume no CBOD decay within the river). The following information has been collected:

$$C_r, \text{ Background CBOD in river} = 3 \text{ mg/l}$$

TABLE VI-13  
 SAMPLE CALCULATION TABLE FOR DISTRIBUTION OF A LOCALLY DISCHARGED  
 NON-CONSERVATIVE POLLUTANT BY THE MODIFIED TIDAL PRISM METHOD

From Table VI-6		Mean Salinity (from salinity plot) $S_i$ ppt	Fraction of River Water $f_i = \frac{S - S_i}{S_s}$	$B_i$	Pollutant Concentration $C = C_{i-1} f_{i-1} + B_i$ (mg/l)
Segment Number	Distance of Center Above Mouth (m)				

Down Estuary →

$$\begin{aligned}
Q_r, \text{ River flow below treatment plant discharge} &= 0.031 \text{ m}^3/\text{sec} \\
Q_d, \text{ Treatment plant discharge rate} &= 0.006 \text{ m}^3/\text{sec} \\
C_d, \text{ Treatment plant effluent CBOD} &= 45 \text{ mg/l}
\end{aligned}$$

The CBOD concentration in the river downstream of the treatment plant is found using the equation:

$$C = \frac{C_r(Q_r - Q_d) + C_d Q_d}{Q_r}$$

or

$$\begin{aligned}
C &= \frac{3 \text{ mg/l} (.031 - .006 \text{ m}^3/\text{sec}) + 45 \text{ mg/l} (0.006 \text{ m}^3/\text{sec})}{0.031 \text{ m}^3/\text{sec}} \\
&= 11.1 \text{ mg/l}
\end{aligned}$$

To find the CBOD concentration distribution in the estuary, the following additional data are used:

$$\begin{aligned}
S_s, \text{ Chesapeake Bay salinity} &= 19.0 \text{ ‰ (at the mouth of} \\
&\hspace{15em} \text{Fox Mill Run Estuary)} \\
k, \text{ CBOD decay constant} &= 0.3/\text{day} \\
T, \text{ Tidal cycle} &= 12.4 \text{ hours}
\end{aligned}$$

so

$$\begin{aligned}
kt &= 0.3/\text{day} \times 12.4 \text{ hr} \times 1 \text{ day}/24 \text{ hours} \\
&= 0.155
\end{aligned}$$

Also necessary are mean salinity values for each estuary segment. Values for the Fox Mill Run Estuary are summarized in Table VI-14. Fraction of freshwater values for each segment are found using the formula:

$$f_i = \frac{S_s - S_i}{S_s}$$

The variables are as previously defined.

Next, values of the coefficient  $B_i$  must be calculated for each segment

"1." For segment 0:

$$r_0, \text{ the segment exchange ratio,} = 0.74$$

and

$$\begin{aligned}
B_0 &= \frac{r_0}{1 - (1 - r_0)e^{-kt}} = \frac{0.74}{1 - (1 - 0.74)e^{-0.155}} \\
&= 0.95
\end{aligned}$$

Coefficient values for all segments are compiled in Table VI-14.

Finally, CBOD concentrations for the individual segment are calculated, beginning with the uppermost segment and working downstream. The concentration in segment "i" is found by:

$$C_i = C_{i-1} \frac{f_i}{f_{i-1}} B_i$$



TABLE VI-14  
SALINITY AND CBOD CALCULATIONS FOR FOX MILL RUN ESTUARY

From Problem VI-3						
Segment Number	Center Point Distance Above Est. Mouth, Meters	Exchange Ratio For Segment $r_i$	Mean Segment Salinity $S_i$ , ppt (From Sal. Plot)	Fraction of Fresh (River) $f_i = \frac{S - S_i}{S_s}$ ( $S_s = 19.0$ )	$B_i$	Concentration of CBOD <sub>u</sub> $C_i = C_{i-1} \frac{f_i}{f_{i-1}} \cdot B_i$ (mg/l)
River	(>3200)	-	~0	1.00	-	11.1
0	2950	0.74	4.7	0.75	0.95	8.1
1	2470	0.71	8.6	0.55	0.94	5.5
2	1945	0.56	11.6	0.39	0.90	3.6
3	915	0.71	15.3	0.19	0.94	1.6

For segment 0, the river is taken as segment "i-1", and the calculation is as follows:

$$C_0 = 11.13 \text{ mg/l} \left( \frac{.75}{1.0} \right) 0.95 = 8.1 \text{ mg/l}$$

For segment 1:

$$C_1 = 8.1 \text{ mg/l} \left( \frac{.55}{.75} \right) 0.94 = 5.6 \text{ mg/l}$$

and so on.

Figure VI-21 depicts this estimate of the distribution of CBOD in the estuary. In addition, hypothetical concentrations of a conservative pollutant ( $k = 0$ ) and coliform bacteria ( $k = 1.0$ ) are plotted. Downstream concentration diminishes faster for substances having larger decay constants, as might be expected.

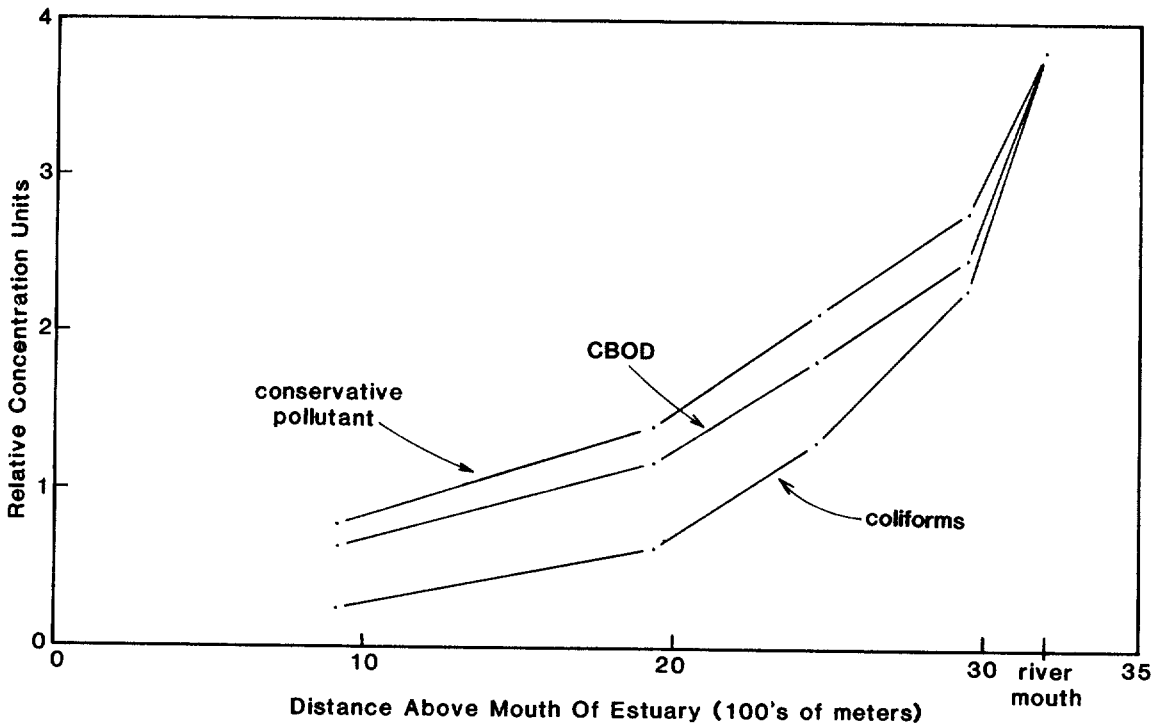


FIGURE VI -21 RELATIVE DEPLETIONS OF THREE POLLUTANTS ENTERING THE FOX MILL RUN ESTUARY, VIRGINIA

END OF EXAMPLE VI-7

#### 6.4.4 Multiple Waste Load Parameter Analysis

The preceding analysis allowed calculation of the longitudinal distribution of a pollutant, either conservative or non-conservative, resulting from a single waste discharge. However, the planner will probably want to simultaneously assess both conservative and non-conservative elements from several separate discharges. This can be accomplished by graphing all desired single element distributions on one graph showing concentration versus length of the estuary. Once graphed, the resulting concentration may be linearly added to obtain a total waste load.

The pollutant concentration increment from each source is calculated by assuming the source is the sole contribution of pollution (i.e. other waste loadings are temporarily set equal to zero). This method, called superposition, is valid as long as volumetric discharge from any of the sources does not significantly influence the salinity distribution within the estuary. This assumption is typically true, unless the estuary is extremely small and poorly flushed, and the volumetric discharge is large relative to tidal and advective flushing components.

An example of the superposition procedure is shown in Figure VI-22. Three local

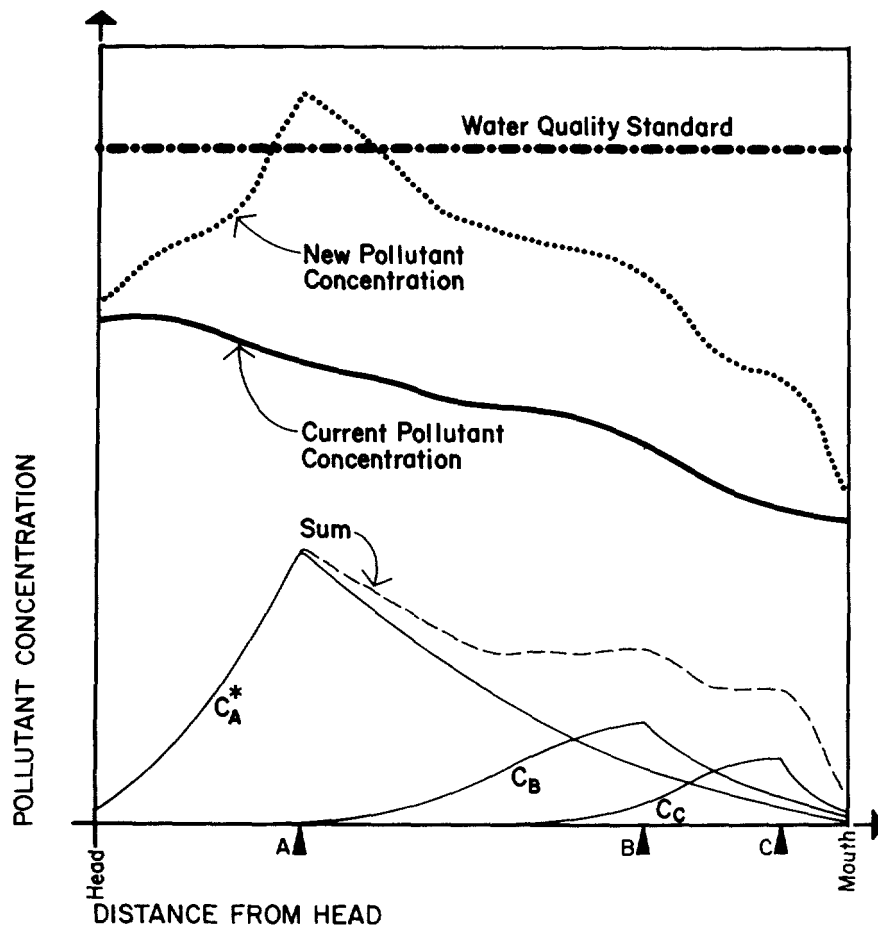


FIGURE VI -22 ADDITIVE EFFECT OF MULTIPLE WASTE LOAD ADDITIONS

point sources of pollutants discharge at locations A, B, and C. A background source enters the estuary with the river discharge. The contribution due to each source can be found from the fraction of freshwater method (assuming the pollutants act conservatively) as follows:

$$C_b = \frac{W_R}{R} f_x, \quad x > 0, \text{ where } x \text{ is measured from the head of the estuary}$$

$$C_A = \begin{cases} \frac{W_A}{R} f_x, & x > A \\ \frac{W_A}{R} f_A \frac{S_x}{S_A}, & x < A \end{cases}$$

$$C_B = \begin{cases} \frac{W_B}{R} f_x, & x > B \\ \frac{W_B}{R} f_B \frac{S_x}{S_B}, & x < B \end{cases}$$

$$C_C = \begin{cases} \frac{W_C}{R} f_x, & x > C \\ \frac{W_C}{R} f_C \frac{S_x}{S_C}, & x < C \end{cases}$$

where

- $C_b$  = concentration due to river discharge
- $C_A, C_B, C_C$  = concentrations due to sources A, B, and C, respectively
- $R$  = river flow rate
- $f_A, f_B, f_C$  = fraction of freshwater at locations A, B, C, respectively
- $S_A, S_B, S_C$  = salinity at locations A, B, C, respectively.

The pollutant concentration (above background) at any location in the estuary is:

$$\text{Sum} = C_A + C_B + C_C$$

and is shown in Figure VI-22. When this is added to the background level, the total pollutant concentration becomes:

$$C_T = (C_A + C_B + C_C) + C_b$$

The dotted line in Figure VI-22 depicts  $C_T$ .

The technique of graphing outfall location and characteristics with resulting estuarine pollutant concentration can be done for all anticipated discharges. This will provide the planner with a good perspective on the source of potential water quality problems.

Where the same segmentation scheme has been used to define incremental pollutant distributions resulting from several sources, the results need not even be plotted to determine the total resultant concentrations. In this case, the estuary is evaluated on a segment-by-segment basis. The total pollutant concentration in each segment is calculated as the arithmetic sum of the concentration increments resulting from the various sources.

#### EXAMPLE VI-8

The previous two example problems involved calculations of nitrogen concentration in the Patuxent Estuary resulting from individual nitrogen sources. The objective of this example is to find the total nitrogen concentration in the estuary resulting from both nitrogen sources.

The eight-segment scheme of Examples VI-6 and VI-7 is retained for this problem. For each segment, the incremental nitrogen increases are summed to give the total concentration:

$$C = C_b + C_A$$

where

$C_b$  - concentration resulting from the N source discharging into the estuary at point A.

For segment 1, the calculation is:

$$\begin{aligned} C &= 1.75 \text{ mg/l (from river)} + 0.43 \text{ mg/l (from local source)} \\ &= 2.18 \text{ mg/l total nitrogen} \end{aligned}$$

Necessary data and final concentrations for each segment are shown in Table VI-15.

TABLE VI -15

## DISTRIBUTION OF TOTAL NITROGEN IN THE PATUXENT ESTUARY DUE TO TWO SOURCES OF NITROGEN

Segment Number	Results From Problem VI -4 Total Nitrogen From River mgN/l, $C$	Results From Problem VI -5 Total Nitrogen From Point A Source (Segment 4) mgN/l, $C_A$	Resultant Concentration $C=C_b + C_A$ mgN/l
8	0.07	0.25	0.32
7	0.21	0.74	0.95
6	0.36	1.26	1.62
5	0.55	1.93	2.48
4	0.80	3.06	3.92
3	1.30	1.74	3.04
2	1.56	0.95	2.51
1	1.75	0.43	2.18
River	1.88	0.00	1.88

- - - - - END OF EXAMPLE VI-8 - - - - -

6.4.5 Dispersion-Advection Equations for Predicting Pollutant Distributions

Dispersion-advection equations offer an attractive method, at least theoretically, of predicting pollutant and dissolved oxygen concentrations in estuaries. However, from the point of view of hand calculation, the advection-dispersion equations are usually tedious to solve, and therefore mistakes can unknowingly be incorporated into the calculations.

Dispersion-advection equations have been developed in a variety of forms, including one-, two-, and three-dimensional representations. The equations in this section are limited to one-dimensional representations in order to reduce the amount of data and calculations required.

One-dimensional dispersion-advection equations can be expressed in quite divergent forms, depending on boundary conditions, cross-sectional area variation over distance, and source-sink terms. O'Connor (1965), for example, developed a variety of one-dimensional advection-dispersion equations for pollutant and dissolved oxygen analyses in estuaries, some of which are infeasible for use on the hand-calculation level.

The advection-dispersion equations to be presented subsequently in this chapter can be used to predict:

- Distributions of conservative or non-conservative pollutants
- Pollutant distributions in embayments
- Dissolved oxygen concentrations.

Solutions from advection-dispersion can be superposed to account for multiple discharges. Example VI-9, to be presented subsequently, will illustrate this process.

As the name of the equations implies, dispersion coefficients are needed in order to solve advection-dispersion equations. Tidally averaged dispersion coefficients are required for the steady-state formulations used here. The tidally averaged dispersion coefficient ( $E_L$ ) can be estimated from the following expression:

$$E_L = \frac{RS}{A \, dS/dx} \quad (\text{VI-35})$$

$$\approx \frac{2RS\Delta x}{A(S_{x+\Delta x} - S_{x-\Delta x})} \quad (\text{VI-36})$$

where

$S$  = tidally and cross sectionally averaged salinity in vicinity of discharge

$2\Delta x$  = distance between the salinity measurements  $S_{x+\Delta x}$  (at a distance  $\Delta x$  down estuary) and  $S_{x-\Delta x}$  (at a distance of  $\Delta x$  up estuary)

$R$  = freshwater flow rate in vicinity of discharge.

The distance interval  $2\Delta x$  should be chosen so that no tributaries are contained within the interval.

In the absence of site specific data, the dispersion coefficients shown in Tables VI-16 and VI-17 can provide estimates of dispersion coefficients.

For pollutants which decay according to first order decay kinetics, the steady state mass balance equation describing their distribution is:

$$E_L \frac{d^2C}{dx^2} - \frac{U \, dC}{dx} - kC = 0 \quad (\text{VI-37})$$

The solution to Equation VI-37 is:

$$C = \begin{cases} C_0 e^{j_2 x} & x > 0 \text{ (down estuary)} \\ C_0 e^{j_1 x} & x < 0 \text{ (up estuary)} \end{cases} \quad (\text{VI-38a})$$

$$(\text{VI-38b})$$

TABLE VI -16

TIDALLY AVERAGED DISPERSION COEFFICIENTS FOR SELECTED ESTUARIES (FROM HYDROSCIENCE, 1971)

Estuary	Freshwater Inflow (cfs)	Low Flow Net Nontidal Velocity (Fps) Head - Mouth	DISPERSION Coefficient (mi <sup>2</sup> /day*)
Delaware River	2,500	0.12-0.009	5
Hudson River (N. Y.)	5,000	0.037	20
East River (N. Y.)	0	0.0	10
Cooper River (S. C.)	10,000	0.25	30
Savannah R. (Ga., S. C.)	7,000	0.7-0.17	10-20
Lower Raritan R. (N. J.)	150	0.047-0.029	5
South River (N. J.)	23	0.01	5
Houston Ship Channel (Texas)	900	0.05	27
Cape Fear River (N. C.)	1,000	0.48-0.03	2-10
Potomac River (Va.)	550	0.006-0.0003	1-10
Compton Creek (N. J.)	10	0.01-0.013	1
Wappinger and Fishkill Creek (N. Y.)	2	0.004-0.001	0.5-1

$$*1 \text{ mi}^2/\text{day} = 322,67 \text{ ft}^2/\text{sec}$$

where

$$j_2 = \frac{R}{2AE_L} \left( 1 - \sqrt{1 + \frac{4kE_L A^2}{R^2}} \right)$$

$$j_1 = \frac{R}{2AE_L} \left( 1 + \sqrt{1 + \frac{4kE_L A^2}{R^2}} \right)$$

$$C_0 = \frac{W}{R} \frac{1}{\sqrt{1 + (4kE_L/U^2)}}$$

U = net velocity

k = decay rate

W = discharge rate of pollutant (at x = 0).

For Equations VI -38a and VI -38b to accurately estimate the pollutant distribution in an estuary, the cross-sectional area of the estuary should be fairly constant over



TABLE VI -17  
TIDALLY AVERAGED DISPERSION COEFFICIENTS  
(FROM OFFICER, 1976)

Estuary	Dispersion Coefficient Range ( $\text{ft}^2/\text{sec}$ )	Comments
San Francisco Bay Southern Arm Northern Arm	200-2,000 500-20,000	Measurements were made at slack water over a period of one to a few days. The fraction of freshwater method was used. Measurements were taken over three tidal cycles at 25 locations.
Hudson River	4,800-16,000	The dispersion coefficient was derived by assuming $E_L$ to be constant for the reach studied, and that it varied only with flow. A good relationship resulted between $E_L$ and flow, substantiating the assumption.
Narrows of Mercey	1,430-4,000	The fraction of freshwater method was used by taking mean values of salinity over a tidal cycle at different cross sections.
potomac River	65-650	The dispersion coefficient was found to be a function of distance below the Chain Bridge. Both salinity distribution studies (using the fraction of freshwater method) and dye release studies were used to determine $E_L$ .
Severn Estuary	75-750 (by Stommel) 580-1,870 (Bowden)	Bowden recalculated $E_L$ values originally determined by Stommel, who had used the fraction of freshwater method. Bowden included the freshwater inflows from tributaries, which produced the larger estimates of $E_L$ .
Tay Estuary	530-1,600 (up estuary) 1,600-7,500 (down estuary)	The fraction of freshwater method was used. At a given location, $E_L$ was found to vary with freshwater inflow rate.
Thames Estuary	600-1,000 (low flow) <b>3,600</b> (high flow)	Calculations were performed using the fraction of freshwater method, between 10 and 30 miles below London Bridge.
Yaquina Estuary	650-9,200 (high flow) <b>140-1,060</b> (low-flow)	The dispersion coefficients for high flow conditions were substantially higher than for low flow conditions, at the same locations. The fraction of freshwater method was used.

distance, and the estuary should be relatively long. For screening purposes the first constraint can be met by choosing a cross-sectional area representative of the length of estuary being investigated. If the estuary is very short, however, pollutants might be washed out of the estuary fast enough to prevent attainment of a steady-state distribution assumed by Equations VI-38a and VI-38b. For shorter estuaries the fraction of freshwater method, modified tidal prism method, or near field approach are more appropriate.

At times when the freshwater flow rate in an estuary is essentially zero pollutant concentrations might increase to substantial levels, if tidal flushing is small. Under these conditions the mass-balance expression for a pollutant obeying first order kinetics is:

$$E_L \frac{d^2C}{dx^2} - kC = 0 \quad (VI-39)$$

The solution to this equation is:

$$C = \begin{cases} C_0 \exp\left(-\sqrt{\frac{k}{E_L}} x\right) & \text{for } x > 0 \text{ (down estuary)} \\ C_0 \exp\left(\sqrt{\frac{k}{E_L}} x\right) & \text{for } x < 0 \text{ (up estuary)} \end{cases} \quad (VI-40a)$$

$$(VI-40b)$$

where

$$C_0 = \frac{W}{A \sqrt{4kE_L}} \quad (VI-41)$$

When the pollutant is conservative (i.e.,  $k = 0$ ), Equation VI-39 reduces to:

$$E_L \frac{d^2C}{dx^2} = 0 \quad (VI-42)$$

The solution is:

$$C = \begin{cases} C_0, & x < 0 \text{ (up estuary)} \\ \frac{W}{E_L A} (L-x) + C_L, & x > 0 \text{ (down estuary)} \end{cases} \quad (VI-43a)$$

$$(VI-43b)$$

where

$$C_0 = C_L + \frac{WL}{E_L A}$$

$C_L$  = background concentration of the pollutant at the mouth of the estuary

$L$  = distance from the discharge location to the mouth of the estuary.

Equation VI-43 illustrates the important concept that the concentrations of conservative pollutants are constant up estuary from the discharge location (when the river discharge is negligible) and decrease linearly from the discharge point to the mouth of the estuary. Equations VI-40 and VI-43 apply to estuaries of constant, or approximately constant, cross-sectional area (e.g. sloughs). If the cross-sectional area increases rapidly with distance toward the mouth, the methods presented in Section 6.5 are more appropriate.

The dissolved oxygen deficit equation (where deficit is defined as the difference between the saturation concentration and the actual dissolved oxygen concentration) for one-dimensional estuaries at steady-state conditions is:

$$U \frac{dD}{dx} = \left[ \frac{d^2D}{dx^2} - k_2D + kL \right] \quad (\text{VI-44})$$

where

- D = dissolved oxygen deficit
- L = BOD concentration
- $k_2$  = reaeration rate
- k = BOD decay rate.

Using Equation IV-38 to represent the BOD distribution, the expression for the deficit D is:

$$D = \frac{kW}{A(k_2 - k)} \left[ \frac{1}{\sqrt{a_1}} \exp\left(\frac{U \pm \sqrt{a_1}}{2 E_L} x\right) - \frac{1}{\sqrt{a_2}} \exp\left(\frac{U \pm \sqrt{a_2}}{2 E_L} x\right) \right] + \frac{M}{A\sqrt{a_2}} \exp\left(\frac{U \pm \sqrt{a_2}}{2 E_L} x\right) \quad (\text{VI-45})$$

where

- The plus sign (+) is used to predict concentrations up estuary ( $x < 0$ )
- The minus sign (-) is used to predict concentrations down estuary ( $x > 0$ )

$$a_1 = U^2 + 4kE_L$$

$$a_2 = U^2 + 4k_2E_L$$

M = mass flux of dissolved oxygen deficit contained in the discharge.

W = mass flux of ultimate BOD contained in the discharge,  $(C_s - C_e)\psi_e$ .

$C_s$  = saturation concentration of dissolved oxygen.

$C_e$  = effluent concentration of dissolved oxygen.

$\psi_e$  = effluent flowrate.

The advantage of expressing the dissolved oxygen concentration in terms of the deficit is that the principle of superposition can be invoked for multiple discharges within a single estuary. Specifically:

$$D = \sum D_i \quad (\text{VI-46})$$

and

$$C = C_s - \sum D_i \tag{VI-47}$$

where

$D_i$  = dissolved oxygen deficit resulting from the  $i^{\text{th}}$  discharge

$C$  = final dissolved oxygen concentration

$C_s$  = dissolved oxygen saturation level.

Figure VI-23 shows the relationship between dissolved oxygen saturation and temperature and salinity.

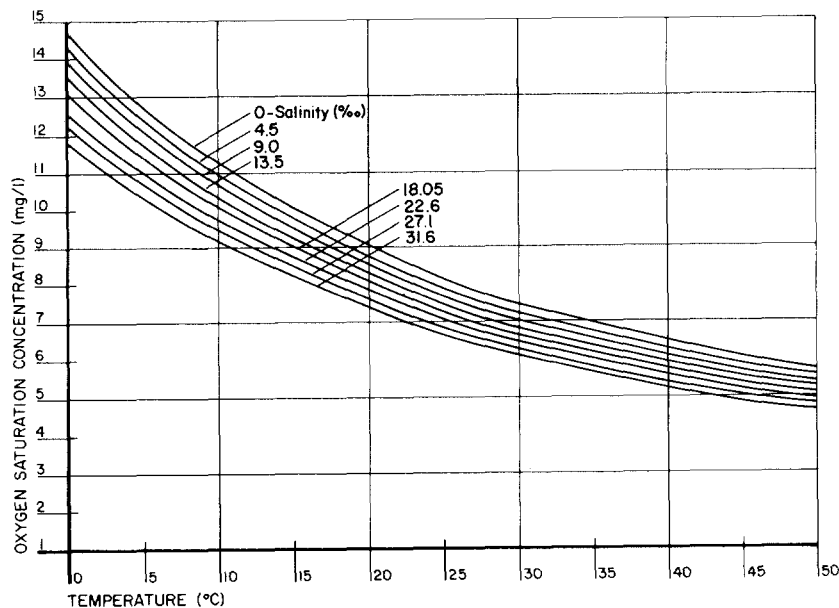


FIGURE VI -23 DISSOLVED OXYGEN SATURATION AS A FUNCTION OF TEMPERATURE AND SALINITY

EXAMPLE VI-9

Dissolved Oxygen Concentration Resulting from Two Sources of BOD

Two municipal wastewater treatment plants discharge significant quantities of BOD into the James River in Virginia. One discharges near Hopewell, and the second 10 miles further down estuary, near West Point. Calculate the dissolved oxygen concentration in the estuary as a function of distance. Pertinent data are:

BOD<sub>5</sub> in Hopewell plant effluent = 69,000 lbs/day

BOD<sub>5</sub> in West Point plant effluent, located 10 miles downstream from Hopewell = 175,000 lbs/day

Freshwater flow rate = 2,900 cfs

Dissolved oxygen saturation = 8.2 mg/l

Cross sectional area = 20,000 ft<sup>2</sup>

Reaeration rate = 0.2/day

Deoxygenation rate = 0.3/day

Dispersion coefficient = 12.5 mi<sup>2</sup>/day

Effluent dissolved oxygen = 0.0 mg/l.

The dissolved oxygen deficit due to each of the two contributions can be determined independently of the other using Equation IV-45. The results are plotted in Figure VI-24. The deficits are added to produce the total deficit (D(x)) due to both discharges (Figure VI-24a). The distance scale in Figure VI-24a is referenced to the Hopewell plant. The West Point plant is placed at mile 10. When the deficit at this location due to the West Point plant is calculated, set x= 0 in Equation VI-45. The dissolved oxygen concentration then becomes C(x) = 8.2-D(x), and is shown in Figure VI-24b.

One example calculation of dissolved oxygen deficit will be shown to illustrate the process. Consider the deficit produced at mile 0.0, due to the Hopewell plant. The waste loading from the Hopewell plant is:

$$\begin{aligned} 69,000 \times 1.46 &= 100,000 \text{ lbs/day, BOD-ultimate} \\ &= 1.16 \text{ lbs/sec} \end{aligned}$$

When x = 0, Equation VI-45 simplifies to:

$$D = \frac{kW}{A(k_2 - k)} \left( \frac{1}{\sqrt{a_1}} - \frac{1}{\sqrt{a_2}} \right)$$

$$a_1 = U^2 + 4k_1 E_L \left( \frac{2900}{20000} \right)^2 + \frac{4(.3)(12.5)(5280)(5280)}{81400 \cdot 86400} = .077 \frac{\text{ft}^2}{\text{sec}^2}$$

so

$$\sqrt{a_1} = .278 \text{ ft/sec}$$

$$a_2 = U^2 + 4k_2 E_L = 0.058 \text{ ft}^2/\text{sec}^2$$

50

$$\sqrt{a_2} = .242 \text{ ft/sec}$$

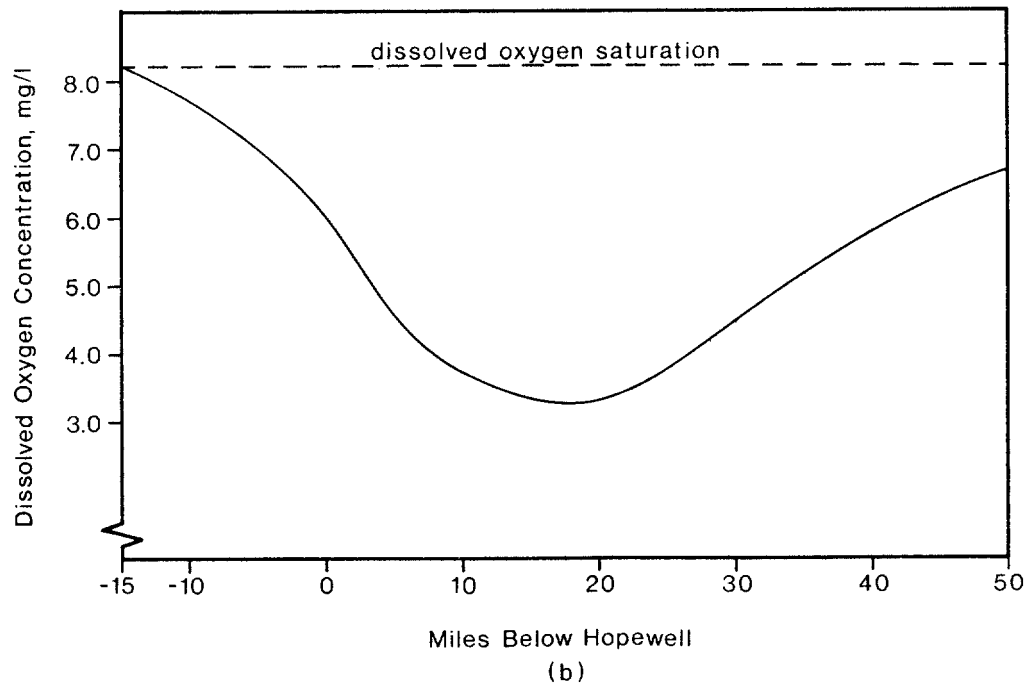
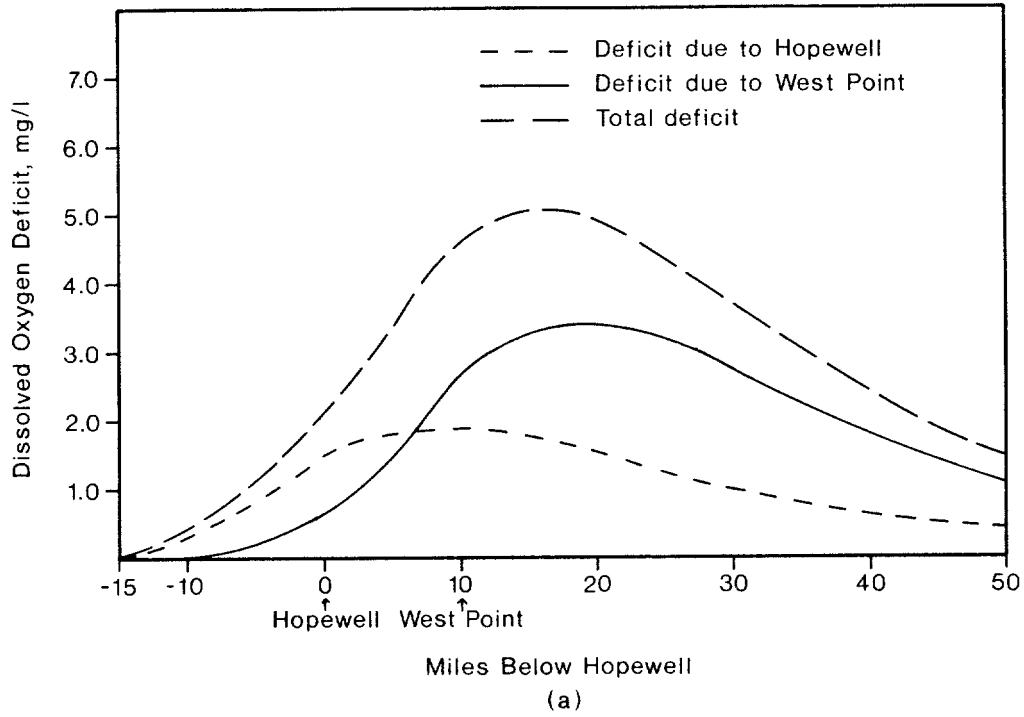


FIGURE VI -24 PREDICTED DISSOLVED OXYGEN PROFILE  
IN JAMES RIVER

The deficit is:

$$D = \frac{(.3)(1.16)}{20000(.2-.3)} \left[ \frac{1}{.278} - \frac{1}{.242} \right] = 9.3 \times 10^{-5} \text{ lb/ft}^3 = 1.5 \text{ mg/l}$$

This value is then plotted in Figure VI-24 at mile point 0.0. The deficit at this location due to West Point is evaluated at  $x = -10$  miles in Equation VI-45, since West Point is located 10 miles down estuary of Hopewell. A deficit of 0.6 mg/l is found, and is plotted in Figure VI-24 at mile point 0.0. The total deficit at Hopewell is  $1.5 + 0.6 = 2.1$  mg/l, as shown in the figure.

----- END OF EXAMPLE VI-9 -----

#### 6.4.6 Pritchard's Two-Dimensional Box Model for Stratified Estuaries

Many estuaries in the United States are either stratified or partially mixed. Because the circulation of stratified systems is fairly complex, few hand calculation methods are available for their analysis. Instead computerized solutions are generally used.

One method developed by Pritchard (1969) which predicts the distribution of pollutants in partially mixed or stratified estuaries is suitable for hand calculations provided the user does not require too much spatial resolution. This method, called the "two-dimensional box model," divides the estuary horizontally from head to mouth into a series of longitudinal segments. Each segment is divided into a surface layer and a bottom layer. The analysis results in a system of  $n$  simultaneous linear equations with  $n$  unknowns, where  $n$  equals twice the number of horizontal segments. The unknowns are the pollutant concentrations in each layer.

Division of the estuary into only two horizontal segments results in four simultaneous equations, which is probably the most one would like to solve entirely by hand. However, many programmable hand calculators contain library routines for solving systems of 10 or more simultaneous equations, which would allow the estuary to be divided into 5 or more horizontal segments. If many more segments are desired, the solution could be easily implemented on a computer using a numerical technique such as Gaussian elimination to solve the resulting system of simultaneous linear equations.

The following information is required for the two-dimensional box analysis: 1) the freshwater flow rate due to the river; 2) the pollutant mass loading rates; and 3) the longitudinal salinity profiles along the length of the estuary in the upper and lower layers, and the salinity at the boundary between these two layers. The upper layer represents the portion of the water column having a net nontidal flow directed seaward, and the lower layer represents the portion of the water column having net nontidal flow directed up to the estuary. If no velocity data are avail-

able, these layers can generally be estimated based on the vertical salinity profiles.

Figure VI-25 shows the parameters used in the analysis, which are defined as follows:

$n$	= segment number, increasing from head toward mouth
$(S_u)_n$	= salinity in upper layer of segment $n$
$(S_l)_n$	= salinity in lower layer of segment $n$
$(S_v)_n$	= salinity at the boundary between the upper and lower layers of segment $n$
$(S_u)_{n-1, n}$	= salinity in the upper layer at the boundary between segments $n-1$ and $n$
$(S_l)_{n-1, n}$	= salinity in the lower layer at the boundary between segments $n-1$ and $n$
$(Q_u)_{n-1, n}$	= net nontidal flow rate in the upper layer from segment $n-1$ to $n$
$(Q_l)_{n-1, n}$	= net nontidal flow rate in the lower layer from segment $n$ to $n-1$
$(Q_v)_n$	= net upward vertical flow from the lower to the upper layer of segment $n$
$E_n$	= vertical exchange coefficient between the lower and upper layers of segment $n$
$R$	= freshwater flow rate due to river
$(q_u)_n$	= pollutant mass loading rate to upper layer of segment $n$ (from external sources)
$(q_l)_n$	= pollutant mass loading rate to lower layer of segment $n$ (from external sources)
$(C_u)_n$	= pollutant concentration in the upper layer of segment $n$
$(C_l)_n$	= pollutant concentration in the lower layer of segment $n$ .

Pritchard's two-dimensional box analysis as presented here requires the following assumptions:

- Steady-state salinity distribution
- The pollutant is conservative
- The concentration of the pollutant is uniform within each layer of each segment and
- The pollutant concentration at the boundary between segments or layers is equal to the average of the concentrations in the two adjacent segments or layers.

Application of the two-dimensional box model involves six steps. These are:

1. Plot the longitudinal salinity profiles in the upper and lower



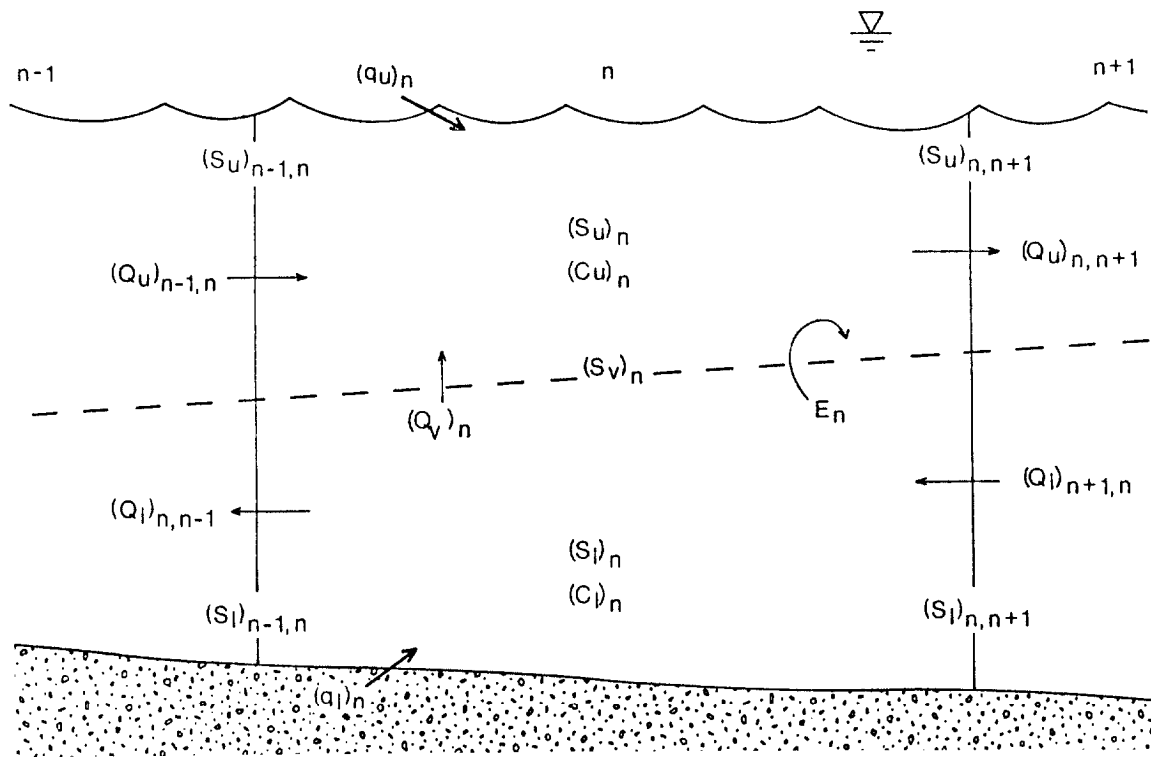


FIGURE VI -2J DEFINITION SKETCH FOR PRITCHARD'S TWO-DIMENSIONAL BOX MODEL

layers, and at the interface between the two layers. If information on the net nontidal velocity distribution is not available to define the layers, the boundary may be estimated for a given section of the estuary as the depth at which the vertical salinity gradient is maximum. The resulting plots will be used to determine the average salinities in each segment and layer, and the salinities at the boundaries between each segment and layer.

2. Segment the estuary. The number of segments will depend on the degree of spatial resolution desired, and the limitations of the hand calculators used to solve the system of simultaneous equations. The accuracy of the results will generally increase with the number of segments used, since the assumptions of the analysis are better satisfied. A minimum of three horizontal segments should probably be used to obtain even a rough estimate of the pollutant distribution in the estuary. This will require the solution of six equations and six unknowns.
3. Compute the net nontidal flows in the upper layer and lower layer at the boundary between each horizontal segment using Knudson's

Hydrographical Theorem (Dyer, 1973):

$$(Q_u)_{n-1, n} = R \frac{(S_1)_{n-1, n}}{(S_1)_{n-1, n} - (S_u)_{n-1, n}} \quad (\text{VI-48})$$

$$(Q_l)_{n, n-1} = R \frac{(S_u)_{n-1, n}}{(S_1)_{n-1, n} - (S_u)_{n-1, n}} \quad (\text{VI-49})$$

At the upstream freshwater boundary of the estuary:

$$(Q_l)_{n, n-1} = 0.$$

4. Compute the net upward vertical flows between layers for each segment using the continuity equation for the upper layer of the segment:

$$(Q_v)_n - (Q_u)_{n, n+1} - (Q_u)_{n-1, n} \quad (\text{VI-50})$$

5. Compute the vertical exchange coefficients between layers for each segment using the salinity balance equation for the upper layer of the segment, which can be arranged in the following form:

$$E_n = \frac{(Q_u)_{n, n+1} (S_u)_{n, n+1} - (Q_u)_{n-1, n} (S_u)_{n-1, n} - (Q_v)_n (S_v)_n}{(S_1)_n - (S_u)_n} \quad (\text{VI-51})$$

6. Set up and solve a system of simultaneous linear equations with one equation for each segment and layer where the pollutant concentrations are the unknowns. These equations are based on a pollutant mass balance for each segment and layer. The mass balance equations are:

$$(Q_u)_{n-1, n} \left[ \frac{(C_u)_{n-1} + (C_u)_n}{2} \right] + (Q_v)_n \left[ \frac{(C_u)_n + (C_1)_n}{2} \right] + E_n \left[ (C_1)_n - (C_u)_n \right] - (Q_u)_{n, n+1} \left[ \frac{(C_u)_n + (C_u)_{n+1}}{2} \right] + (q_u)_n = 0 \quad (\text{VI-52})$$

for the upper layer of segment n and

$$\begin{aligned}
(Q_1)_{n+1, n} \left[ \frac{(C_1)_{n+1} + (C_1)_n}{2} \right] - (Q_1)_{n, n-1} \left[ \frac{(C_1)_n + (C_1)_{n-1}}{2} \right] \\
- (Q_v)_n \left[ \frac{(C_1)_n + (C_u)_n}{2} \right] - E_n \left[ (C_1)_n - (C_u)_n \right] + (q_1)_n = 0
\end{aligned} \tag{VI-53}$$

for the lower layer of segment n.

Since most pollutant discharges are buoyant, they should be considered as loadings to the upper layer, even though they may be physically introduced at the bottom. Pollutants which are denser than the upper waters and which would sink to the bottom should be considered as loadings to the lower layer. However, the analysis is not applicable to pollutants which tend to remain near the bottom and accumulate in or react with the bottom sediments.

The above mass balance equations can be simplified and rearranged into the following form:

$$\begin{aligned}
\left[ (Q_u)_{n-1, n} \right] (C_u)_{n-1} + \left[ -2E_n \right] (C_u)_n + \left[ 2E_n + (Q_v)_n \right] (C_1)_n \\
+ \left[ -(Q_u)_{n, n+1} \right] (C_u)_{n+1} = -2(q_u)_n
\end{aligned} \tag{VI-54}$$

for the upper layer of segment n and

$$\begin{aligned}
\left[ -(Q_1)_{n, n-1} \right] (C_1)_{n-1} + \left[ 2E_n - (Q_v)_n \right] (C_u)_n + \left[ -2E_n \right] (C_1)_n \\
+ \left[ (Q_1)_{n+1, n} \right] (C_1)_{n+1} = -2(q_1)_n
\end{aligned} \tag{VI-55}$$

for the lower layer of segment n. This pair of equations is written for each segment, resulting in a system of simultaneous equations where the concentrations,  $(C_u)_n$  and  $(C_1)_n$ , are the unknowns, the terms enclosed in square brackets are the coefficients, and the terms on the right hand side of the equations are the constants.

However, since each equation involves both the upstream and downstream segments

for a given layer, the boundary conditions at both the upstream and downstream end of the estuary must be applied so that there will not be more unknowns than equations. At the upstream end of the estuary, the following boundary conditions apply:

$$\begin{aligned} (Q_u)_{n-1, n} &= R = \text{river flow rate} \\ (C_u)_{n-1} &= C_R = \text{pollutant in river} \\ (Q_1)_{n, n-1} &= 0 = \text{(no salt water movement upstream into the river)}. \end{aligned}$$

These conditions simplify the previous equations to:

$$\left[ -2E_1 \right] (C_u)_1 + \left[ 2E_1 + (Q_v)_1 \right] (C_1)_1 + \left[ -(Q_u)_{1,2} \right] (C_u)_2 - (C_u)_1 R = -2(q_u)_1 - 2RC_R \quad (\text{VI-56})$$

for the upper layer of the first upstream segment and

$$\left[ 2E_1 - (Q_v)_1 \right] (C_u)_1 + \left[ -2E_1 \right] (C_1)_1 + \left[ (Q_1)_{2,1} \right] (C_1)_2 = -2(q_1)_1 \quad (\text{VI-57})$$

for the lower layer of the first upstream segment.

For the lower layer of the last downstream segment at the ocean end of the estuary, the following boundary condition is used to simplify the equation:

$$(C_1)_{n+1} = 0 \text{ (no pollutant entering the lower layer from the ocean waters outside the mouth of estuary)}$$

which simplifies the corresponding equation to:

$$\left[ -(Q_1)_{n, n-1} \right] (C_1)_{n-1} + \left[ 2E_n - (Q_v)_n \right] (C_u)_n + \left[ -2E_n \right] (C_1)_n = -2(q_1)_n \quad (\text{VI-58})$$

For the upper layer of the last segment at the mouth of the estuary, some assumption must be made about the pollutant concentration in the upper layer just outside the mouth to eliminate the  $(n + 1)$  term from the equation. If actual data are available based on field measurements, a measured value of  $(C_u)_{n+1}$  can be used. This simplifies the corresponding equation to:

$$\left[ (Q_u)_{n-1, n} \right] (C_u)_{n-1} + \left[ -2E_n \right] (C_u)_n + \left[ 2E_n + (Q_v)_n \right] (C_1)_n = -2(q_u)_n + (Q_u)_{n, n+1} C_o \quad (\text{VI-59})$$

where  $C_o$  is the measured pollutant concentration in the surface waters outside the mouth of the estuary. If no data are available, the simplest assumption that can be made is that the concentration outside the mouth equals the concentration in the surface layer of the last segment inside the mouth, or  $(C_u)_{n+1} = (C_u)_n$ . Alternatively, the concentration outside the mouth may be assumed to equal some fraction of the concentration inside the mouth, or:

$$(C_u)_{n+1} = f_c (C_u)_n$$

where  $f_c$  is the selected fraction. The previous assumption  $(C_u)_{n+1} = (C_u)_n$  is one case of this second assumption where the fraction equals one ( $f_c = 1$ ).

Using the second more general assumption, the equation of the upper layer of the last downstream segment simplifies to:

$$\left[ (Q_u)_{n-1, n} \right] (C_u)_{n-1} + \left[ -2E_n - f_c (Q_u)_{n, n+1} \right] (C_u)_n + \left[ 2E_n + (Q_v)_n \right] (C_1)_n = -2(q_u)_n$$

VI -60)

Step (6) of the two-dimensional box analysis involves computing all of the coefficients and constants in the system of equations defining each segment and layer (Equations VI-54 and VI-55) and applying the boundary conditions to produce equations for the first upstream and last downstream segments in the estuary (Equations VI-56 through VI-60). The coefficients and constants are functions of the variables previously computed in steps (3) through (5). The resulting equations are then solved using library routines in programmable hand calculators, or by programming an appropriate numerical technique such as Gaussian elimination on either a programmable hand calculator or a computer.

Since the analysis requires application of the boundary conditions at the freshwater head of the estuary and the coastal mouth of the estuary to obtain the same number of equations as unknowns, the entire estuary must be included in the first cut analysis. The initial analysis will yield the overall pollutant distribution throughout the entire estuary. Once this is determined, the analysis could be repeated to obtain more detail for smaller portions of the estuary by using the first cut results to estimate the pollutant boundary conditions at each end of the region of concern, and then rearranging equations (7) and (8) so the terms involving the concentrations outside the specified regions are treated as constants and moved to the right hand side of the equations.

The Pritchard Model theoretically allows external pollutant loading to be introduced directly into any segment along the estuary. By moving external loadings from the head to near the mouth of the estuary, the planner can predict how pollutant levels are affected. However, experience with the model has shown that when external side loadings are considerably larger than those which enter at the head of the estuary, model instabilities can arise. When this occurs, the pollutant profile oscillates from segment to segment, and negative concentrations can result. It is recommended that the user first run the Pritchard Model by putting all pollutant loading into the head of the estuary. This situation appears to be always stable, and, as the following example shows, reasonable pollutant profiles are predicted.

EXAMPLE VI-10

Pollutant Distribution in a Stratified Estuary

The Patuxent River in Maryland is a partially stratified estuary, where the degree of stratification depends on the freshwater flow rate discharged at the head of the estuary. Table VI-18 shows the salinity distribution within the estuary under low flow conditions for each segment and layer. The location of each layer is shown in Figure VI-26. Also shown in the table is the pollutant distribution by layer and segment for a mass flux of 125 lbs/day (57 kg/day) of conservative pollutant input at the head of the estuary.

The pollutant distribution was predicted by solving on a computer the 12-segment, 2-layer system (24 simultaneous equations). The salinity distribution shown in Table VI-18 was used as input data. As a point of interest, the same network was solved using the model WASP (courtesy of Robert Ambrose, ERL, U.S. Environmental Protection Agency, Athens, Georgia), which is a dynamic two-dimensional estuary model. Instead of using salinity directly, WASP predicts the salinity distribution based on dispersive and advective exchange rates. The salinity distribution predicted by WASP is the same as shown in Table VI-18, which was used as input to Pritchard's Model. After running WASP to steady-state conditions, the pollutant distribution throughout the estuary was virtually the same as predicted by Pritchard's Model.

The pollutant distribution in the Patuxent estuary will be solved in detail using 4 segments instead of 12. The resulting system of 8 simultaneous equations can be solved on a variety of hand-held calculators. The tabulations below show salinities at each segment boundary, and the horizontal flow rates in the upper and lower layers.

Boundary n-1, n	$(S_u)_{n-1, n}$ mg/l -Cl	$(S_l)_{n-1, n}$ mg/l -Cl	$(Q_u)_{n-1, n}$ m <sup>3</sup> /sec	$(Q_l)_{n-1, n}$ m <sup>3</sup> /sec
0, 1	0.0	0.0	3.3*	0.0
1, 2	4960.	5080.	116.7	113.4
2, 3	9420.	9640.	139.5	136.2
3, 4	11445.	11860.	94.3	91.0
4, 5	13500.	13500.	156.8	153.5

\*This is the specified river inflow rate, R.

The flow rates were calculated from Equations VI-48 and VI-49, while the salinities were found directly from Table VI-18.

TABLE VI -18

SALINITY AND POLLUTANT DISTRIBUTION IN PATUXENT  
ESTUARY UNDER LOW FLOW CONDITIONS

Segment Number	Salinity (as Chloride, mg/l)		Pollutant Concentration (mg/l)	
	Upper Layer	Lower Layer	Upper Layer	Lower Layer
1	496.	524.	0.193	0.192
2	1831.	1940.	0.173	0.171
3	3771.	3970.	0.144	0.141
4	6050.	6280.	0.100	0.108
5	8040.	8220.	0.081	0.078
6	9310	9910.	0.062	0.053
7	10010.	10660.	0.051	0.042
8	10790.	11070.	0.040	0.036
9	11240.	11760.	0.033	0.025
10	11830.	12120.	0.025.	0.020
11	12100.	12650.	0.021	0.013
12	12750.	12850.	0.011	0.009
boundary	13500.	13500.	0.0	0.0

The salinities within each layer, the salinity and flow rate between the interface of each layer, and the exchange coefficients are tabulated below.

Segment $n$	$(S_u)_n$ mg/l-Cl	$(S_v)_n$ mg/l-Cl	$(s_1)_n$ mg/l-Cl	$(Q_v)_n$ $m^3/sec$	$E_n$ $m^3/sec$
1	1830	1890	1940	113.	3260.
2	8040	8130	8220	23.	3140.
3	10790	10930	11070	-45.	930.
4	12100	12380	12650	63.	280.

The flow rates were found from Equation VI -50, and the exchange coefficients from Equation VI -51.

Substituting these data into the pollutant mass balance expressions (Equations

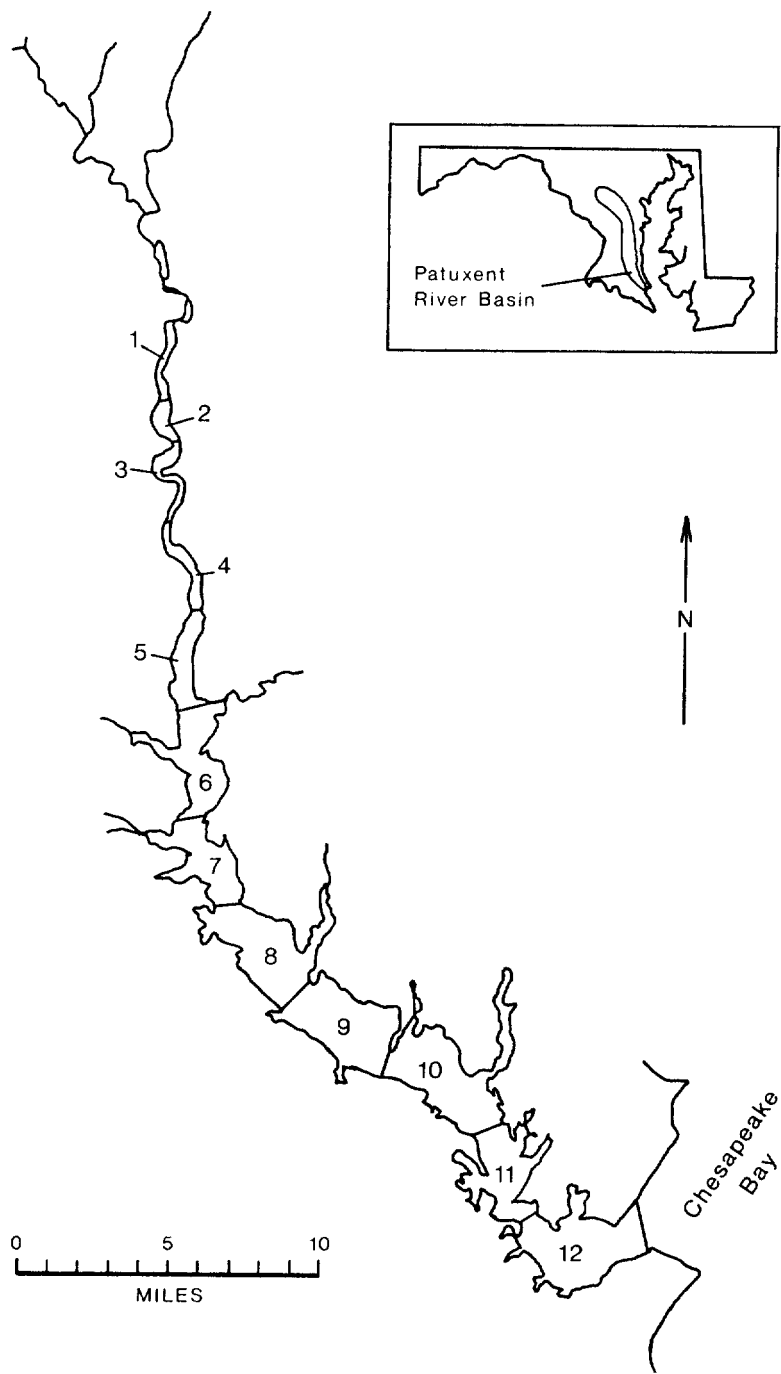


FIGURE VI -26 PATUXENT ESTUARY MODEL SEGMENTATION



VI-54 through VI-59), the following system of equations result:

$$\begin{bmatrix}
 -6528. & 6638. & -117. & 0. & 0. & 0. & 0. & 0. \\
 6411. & -6525. & 0.0 & 113. & 0. & 0. & 0. & 0. \\
 117. & 0.0 & -6275. & 6297. & -139. & 0. & 0. & 0. \\
 0. & -113. & 6252. & -6275. & 0.0 & 136 & 0. & 0. \\
 0. & 0. & 139. & 0.0 & -1856. & 1811. & -94. & 0. \\
 0. & 0. & 0. & -136. & 1901 & -1856. & 0.0 & 91. \\
 0. & 0. & 0. & 0. & 94. & 0.0 & -561 & 624. \\
 0. & 0. & 0. & 0. & 0. & -91. & 499. & -561
 \end{bmatrix}
 \begin{Bmatrix}
 (C_u)_1 \\
 (C_1)_1 \\
 (C_u)_2 \\
 (C_1)_2 \\
 (C_u)_3 \\
 (C_1)_3 \\
 (C_u)_4 \\
 (C_1)_4
 \end{Bmatrix}
 =
 \begin{Bmatrix}
 -1.32 \\
 0. \\
 0. \\
 0. \\
 0. \\
 0. \\
 0. \\
 0.
 \end{Bmatrix}$$

The value -1.32 in the first row of the right-hand side column vector is twice the loading of pollutant which comes into the upper layer of the first segment, as required in Equation VI-56. The units are in gm/sec to be compatible with the units of the remaining terms in the equations:

$$\begin{aligned}
 \dot{M} &= 125 \text{ lbs/day} = 0.66 \text{ gm/sec} \\
 \text{so } 2\dot{M} &= 250 \text{ lbs/day} = 1.32 \text{ gm/sec}
 \end{aligned}$$

The pollutant distribution which results from solving the eight linear equations is:

$$\begin{aligned}
 (C_u)_1 &= (0.17) \\
 (C_1)_1 &= (0.17) \\
 (C_u)_2 &= (0.08) \\
 (C_1)_2 &= (0.08) \\
 (C_u)_3 &= (0.04) \\
 (C_1)_3 &= (0.04) \\
 (C_u)_4 &= (0.02) \\
 (C_1)_4 &= (0.01)
 \end{aligned}$$

These values are nearly the same as found when 12 segments were used, which indicates 4 segments are sufficient to accurately predict pollutant distribution for this problem.

END OF EXAMPLE VI-10

## 6.5 POLLUTANT DISTRIBUTION FOLLOWING DISCHARGE FROM A MARINE OUTFALL

### 6.5.1 Introduction

Numerous coastal states have enacted water quality standards which limit the maximum allowable concentration of pollutants, particularly metals and organic

toxics, which can be discharged into estuarine and coastal waters. The standards normally permit that an exempt area, called a mixing zone, be defined around the outfall where water quality standards are not applicable. For example, the Water Quality Control Plan for Ocean Waters of California (State Water Resources Control Board, 1978) sets forth the following statement directed at toxic substance limitations:

"Effluent limitations shall be imposed in a manner prescribed by the State Board such that the concentrations set forth . . . as water quality objectives, shall not be exceeded in the receiving water upon the completion of initial dilution."

The mixing zone, or zone of initial dilution (ZID), is non-rigorously defined as the volume of water where the wastewater and ambient saline water mix during the first few minutes following discharge, when the plume still has momentum and buoyancy. As the wastewater is discharged, it normally begins to rise because of its buoyancy and momentum, as illustrated in Figure VI-27.

If the ambient water column is stratified and the water depth is great enough, the rising plume will not reach the surface of the water, but rather will stop at the level where the densities of the plume and receiving water become equal. This level is called the plume's trapping level. (See Figure VI-27.) Due to residual momentum, the plume might continue to rise beyond the trapping level, but will tend to fall back after the momentum is completely dissipated. Once the plume stops rising, the waste field begins to drift away from the ZID with the ambient currents. At this time, initial dilution is considered complete. Section 6.5.2, which follows, shows how initial dilution is calculated, and then Sections 6.5.3 and 6.5.4 illustrate how pollutant concentrations at the completion of initial dilution can be predicted. Sections 6.5.5 and 6.5.6 explain methods of predicting pollutant and dissolved oxygen concentrations, respectively, as the waste field migrates away from the ZID.

The methods presented in Sections 6.5.2 through 6.5.6 are applicable to stratified or non-stratified estuaries, embayments, and coastal waters. The methods assume that reentrainment of previously discharged effluent back into the ZID is negligible. Reentrainment can occur if the wastewater is discharged into a confined area where free circulation is impaired or because of tidal reversals in narrow estuaries.

## 6.5.2 Prediction of Initial Dilution

### 6.5.2.1 General

Discharge to bodies of water through submerged diffusers is a common waste water management technique. A diffuser is typically a pipe with discharge ports spaced at regular intervals. Such discharges are often buoyant with high exit velocity relative to the ambient velocity. The resulting waste streams act as plumes or buoyant jets. The velocity shear between ambient and plume fluids results in the

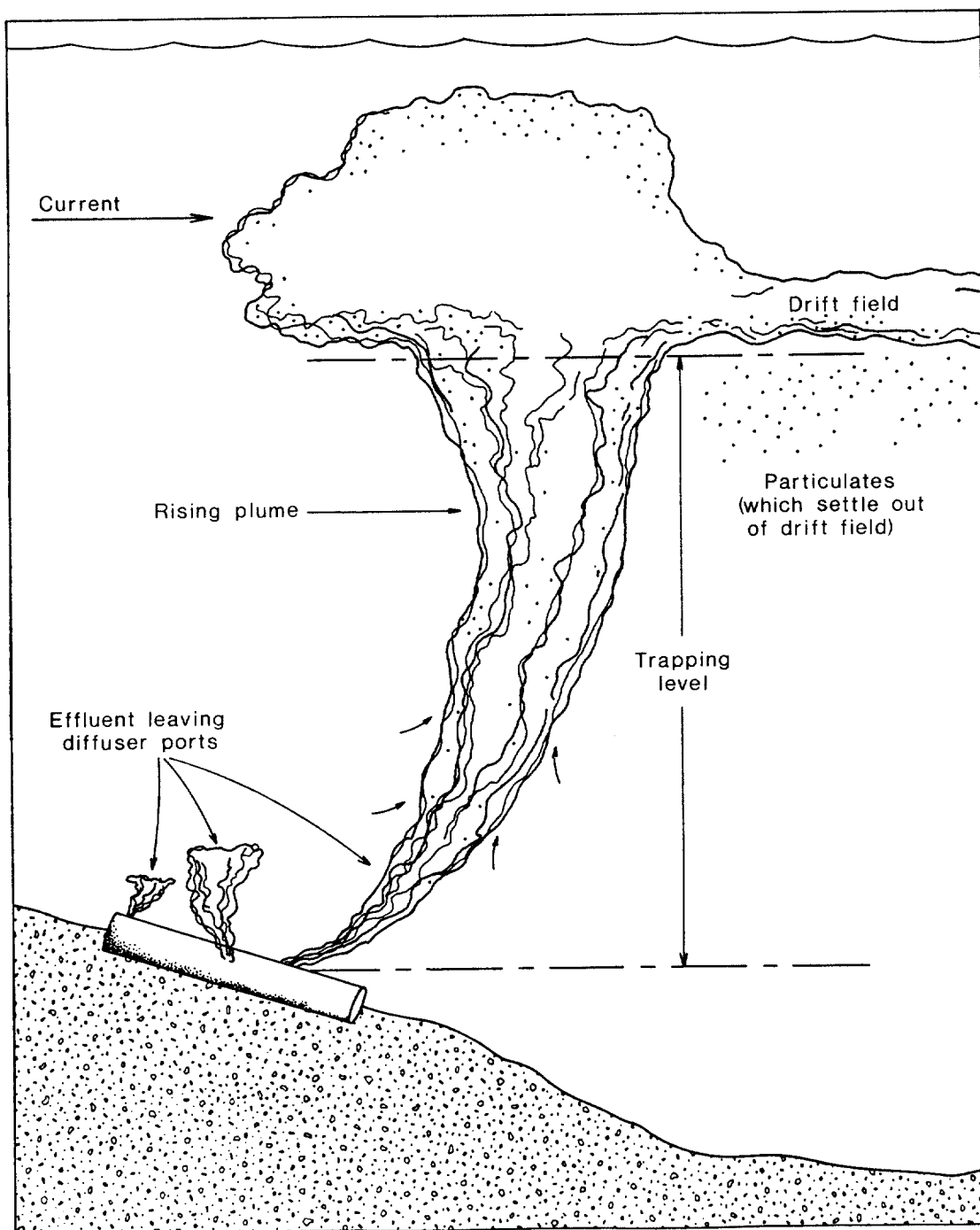


FIGURE VI -27 WASTE FIELD GENERATED BY MARINE OUTFALL

incorporation of ambient fluid into the plume, a process called entrainment. Initial dilution results from the entrainment of ambient fluid into the plume as the plume rises to its trapping level.

The magnitude of initial dilution depends on a number of factors including, but not limited to, the depth of water, ambient density stratification, discharge

rate, buoyancy, port spacing (i.e. plume merging), and current velocity. These factors may be referred to collectively as the diffuser flow configuration or simply the flow configuration. Depending on the flow configuration, the initial dilution may be less than 10 or greater than 500. As attaining water quality criteria may often require relatively high initial dilution, the need to be able to estimate initial dilution for various flow configurations becomes apparent.

Other than actually sampling the water after a facility is in operation, there are various ways to estimate pollutant concentrations achieved in the vicinity of a particular diffuser. A scale model faithful to all similarity criteria could yield the necessary dilution information. Dimensional analysis and empirical formulae may also be very useful. Alternatively, a numerical model based on the laws of physics may be developed. This method is chosen to provide initial dilution estimates here because it is more cost-effective than field sampling and more accurate than a scale model.

Any numerical model used to provide dilution estimates should faithfully replicate the relevant plume relationships and should be verified for accuracy. The plume model MERGE (Frick, 1981c) accounts for the effects of current ambient density stratification and port spacing on plume behavior. In addition, it has been extensively verified (Frick, 1981a, 1981b; Tesche *et al.*, 1980; Policastro *et al.*, 1980; Carhart *et al.*, 1981).

There are several ways of presenting the initial dilution estimates. MERGE may be run for specific cases or run for many cases spanning a range of conditions and presented in nomogram or tabular form. The latter method is the most compact. The resulting initial dilution tables display values of dilution achieved at the indicated depths and densimetric Froude numbers. One hundred tables are presented in Appendix G for various combinations of port spacing, density stratification, and effluent-to-current velocity ratio.

Before describing the tables in more detail and discussing examples, it may be helpful for some users to read the following, occasionally technical, discussions of the plume model MERGE (Section 6.5.2.2) and of basic principles of similarity (Section 6.5.2.3). Others may want to advance directly to Section 6.5.2.4 describing table usage.

#### 6.5.2.2 The Plume Model MERGE

MERGE is the latest in a series of models whose development began in 1973. Various stages of model development have been recorded (Winiarski and Frick, 1976 and 1978; Frick, 1981c). In the realm of plume modeling, MERGE belongs to the Lagrangian minority since more models are Eulerian. The model can be demonstrated to be basically equivalent to its Eulerian counterparts (Frick and Winiarski, 1975; Frick, 1981c). Time is the independent variable which is incremented in every program iteration based on the rate of entrainment.

To simplify the problem, many assumptions and approximations are made in plume modeling. In MERGE, steady-state is assumed and the plume is assumed to have a round cross section everywhere.

The MERGE user may input arbitrary current and ambient density profiles. The model includes a compressible equation of continuity so that the predictions are also valid for highly buoyant plumes. It accounts for merging of adjacent plumes but only when the ambient current dilution is normal to the diffuser pipe. In many cases, this is not a significant restriction as many diffusers are oriented to be normal to the prevailing current direction.

The model contains an option for using either constant or variable coefficients of bulk expansion in the equation of state. The water densities in Table VI-19 are generated using the model's density subroutine based on actual temperatures and salinities (i.e. effectively using variable coefficients). If temperature and salinity data are unavailable then the model can be run based on density data alone. The latter method is satisfactory for relatively high temperatures and salinities because the equation of state is relatively linear with these variables in that range. However, for low densities and temperatures gross inaccuracies may result. Unfortunately, the initial dilution tables are based on the latter method. A more accurate representation would greatly increase the number of tables necessary to cover all the cases. Users with applications involving cold, low salinity water are urged to run the more accurate form of the model.

The success of MERGE in predicting plume behavior is primarily attributable to two unique model features. The first of these relates to the expression of forced entrainment. Entrainment may be attributed to the velocity shear present even in the absence of currents, i.e. aspiration, and to current-induced entrainment, sometimes called forced entrainment.

The forced entrainment algorithm in MERGE is based on the assumption that all fluid flowing through the upstream projected area of the plume is entrained. This hypothesis is based on well-established principles and observations (Rawn *et al.*, 1960; Jirka and Harlman 1973). Paradoxically, the hypothesis has never been implemented in numerical models before. The projected area normally contains linear and quadratic terms in plume diameter, whereas in conventional modeling, forced entrainment is generally expressed as a linear function of diameter. It is necessary to include additional sources of entrainment to make up the difference when so expressed.

The second feature is the use of a constant aspiration coefficient. This coefficient is often considered to be variable (e.g. Fan, 1967). The need for a variable coefficient is attributable to the fact that many models predict centerline plume values. For plumes discharged vertically upward into density stratified ambient water, such models are expected to predict the maximum penetration of the plume. To achieve agreement requires a relatively small aspiration coefficient.

TABLE VI-19a

WATER DENSITIES (EXPRESSED AS SIGMA-T)\* CALCULATED  
USING THE DENSITY SUBROUTINE FOUND IN MERGE

Salinity ( $\sigma_{\infty}$ )	TEMPERATURE ( $^{\circ}\text{C}$ )														
	0	2	4	5	8	10	12	14	15	16	17	18	19	20	
0	-0.093	-0.034	.007	.031	.039	.030	.006	-0.032	-0.086	-0.154	-0.235	-0.330	-0.438	-0.558	-0.691
5	.721	.776	.814	.835	.839	.827	.800	.758	.702	.632	.548	.450	.340	.217	.082
10	1.535	1.586	1.620	1.637	1.638	1.623	1.593	1.548	1.489	1.416	1.329	1.230	1.117	.992	.854
15	2.348	2.395	2.425	2.439	2.437	2.419	2.385	2.338	2.276	2.200	2.111	2.008	1.893	1.766	1.626
20	3.159	3.203	3.230	3.240	3.234	3.213	3.177	3.126	3.061	2.983	2.891	2.786	2.669	2.539	2.397
25	3.970	4.010	4.033	4.040	4.031	4.007	3.968	3.914	3.847	3.765	3.671	3.564	3.444	3.312	3.168
30	4.781	4.817	4.836	4.840	4.818	4.800	4.758	4.701	4.631	4.547	4.450	4.341	4.218	4.084	3.938
35	5.590	5.623	5.639	5.639	5.623	5.593	5.548	5.488	5.415	5.329	5.229	5.117	4.992	4.856	4.708
40	6.399	6.428	6.441	6.437	6.418	6.385	6.337	6.274	6.199	6.109	6.007	5.893	5.766	5.627	5.477
45	7.207	7.233	7.242	7.235	7.213	7.176	7.125	7.060	6.982	6.890	6.785	6.668	6.539	6.398	6.245
50	8.015	8.037	8.042	8.032	8.007	7.967	7.913	7.845	7.764	7.670	7.563	7.443	7.312	7.168	7.014
55	8.822	8.840	8.842	8.829	8.801	8.758	8.701	8.630	8.546	8.449	8.340	8.218	8.084	7.939	7.782
60	9.628	9.643	9.642	9.625	9.594	9.548	9.488	9.415	9.328	9.228	9.116	8.992	8.856	8.708	8.549
65	10.434	10.446	10.441	10.421	10.387	10.338	10.275	10.199	10.109	10.007	9.893	9.766	9.628	9.478	9.317
70	11.240	11.248	11.240	11.217	11.179	11.127	11.062	10.983	10.890	10.786	10.669	10.540	10.399	10.247	10.084
75	12.045	12.049	12.038	12.012	11.971	11.916	11.848	11.766	11.671	11.564	11.445	11.313	11.170	11.016	10.851
80	12.850	12.851	12.836	12.807	12.763	12.705	12.634	12.549	12.452	12.342	12.220	12.087	11.941	11.785	11.618
85	13.654	13.652	13.634	13.602	13.555	13.494	13.420	13.332	13.232	13.120	12.996	12.860	12.712	12.554	12.384
90	14.459	14.453	14.432	14.396	14.346	14.282	14.205	14.115	14.013	13.898	13.771	13.633	13.483	13.322	13.151
95	15.263	15.254	15.229	15.190	15.137	15.071	14.991	14.898	14.793	14.676	14.547	14.406	14.254	14.091	13.917
100	16.067	16.054	16.027	15.985	15.929	15.859	15.777	15.681	15.573	15.453	15.322	15.179	15.025	14.860	14.684
105	16.870	16.855	16.824	16.779	16.720	16.647	16.562	16.464	16.354	16.231	16.097	15.952	15.796	15.628	15.451
110	17.674	17.655	17.621	17.573	17.511	17.436	17.347	17.247	17.134	17.009	16.873	16.725	16.566	16.397	16.217
115	18.478	18.455	18.418	18.367	18.302	18.224	18.133	18.030	17.914	17.787	17.648	17.498	17.337	17.166	16.984
120	19.281	19.225	19.255	19.161	19.093	19.012	18.919	18.813	18.694	18.565	18.424	18.271	18.108	17.935	17.751

TABLE VI-19a  
(Continued)

Salinity ( $\sigma_{\theta}$ )	TEMPERATURE ( $^{\circ}\text{C}$ )														
	0	2	4	5	8	10	12	14	16	18	20	22	24	26	
25	20.085	20.056	20.012	19.955	19.884	19.801	19.704	19.596	19.475	19.343	19.199	19.045	18.880	18.704	18.518
	20.888	20.856	20.810	20.749	20.676	20.589	20.490	20.379	20.256	20.121	19.975	19.819	19.651	19.473	19.285
	21.692	21.657	21.607	21.544	21.467	21.378	21.276	21.162	21.037	20.900	20.751	20.592	20.423	20.243	20.053
	22.496	22.457	22.405	22.338	22.259	22.167	22.063	21.946	21.818	21.678	21.528	21.367	21.195	21.013	20.821
	23.300	23.258	23.202	23.133	23.051	22.956	22.849	22.730	22.599	22.458	22.305	22.141	21.967	21.783	21.589
30	24.104	24.059	24.001	23.929	23.843	23.746	23.636	23.514	23.381	23.237	23.082	22.916	22.740	22.554	22.358
	24.908	24.861	24.799	24.724	24.636	24.536	24.423	24.299	24.164	24.017	23.859	23.691	23.513	23.325	23.127
	25.713	25.662	25.598	25.520	25.429	25.326	25.211	25.084	24.946	24.797	24.637	24.467	24.287	24.097	23.897
	26.518	26.464	26.397	26.316	26.223	26.117	25.999	25.870	25.729	25.578	25.416	25.243	25.061	24.869	24.667
	27.324	27.267	27.196	27.113	27.016	26.908	26.788	26.656	26.513	26.359	26.195	26.020	25.836	25.641	25.437
35	28.130	28.070	27.996	27.910	27.811	27.700	27.577	27.442	27.297	27.141	26.974	26.798	26.611	26.414	26.208
	28.936	28.873	28.797	28.708	28.606	28.492	28.366	28.230	28.082	27.923	27.754	27.575	27.387	27.188	26.980
	29.743	29.677	29.598	29.506	29.401	29.285	29.157	19.017	28.867	28.706	28.535	28.354	28.163	27.963	27.753
	30.550	30.482	30.399	30.305	30.197	30.078	29.948	29.806	29.653	29.490	29.317	29.133	28.940	28.738	28.526
	31.358	31.287	31.202	31.104	30.994	30.872	30.739	30.595	30.440	30.275	20.099	29.913	29.718	29.514	29.300
40	32.167	32.092	32.005	31.904	31.792	31.667	31.532	31.385	31.227	31.060	30.882	30.694	30.497	30.290	30.075

\*Sigma-t ( $\sigma_t$ ) is defined as: (density-1)  $\times 10^3$ . For example, for seawater with a density of 1.02500 g/cm<sup>3</sup>,  $\sigma_t = 25$ .

TABLE VI-19b

WATER DENSITIES (EXPRESSED AS SIGMA-T)\* CALCULATED  
USING THE DENSITY SUBROUTINE FOUND IN MERGE

Salinity (‰)	TEMPERATURE (°C)												
	16	18	20	22	24	26	28	30	32	34			
0	-0.836	-1.161	-1.532	-1.733	-1.945	-2.167	-2.399	-2.641	-2.893	-3.154	-3.425	-3.704	-3.993
	-0.065	-0.394	-0.768	-0.971	-1.185	-1.409	-1.642	-1.886	-2.139	-2.402	-2.674	-2.956	-3.246
	.705	.372	-0.006	-0.211	-0.426	-0.651	-0.887	-1.132	-1.387	-1.651	-1.925	-2.208	-2.499
	1.475	1.312	.756	.550	.333	.106	-0.131	-0.378	-0.635	-0.901	-1.176	-1.460	-1.753
	2.244	2.079	1.903	1.716	1.518	1.309	1.091	.862	.623	.375	.117	-0.150	-0.427
5	3.012	2.845	2.667	2.478	2.279	2.068	1.848	1.618	1.377	1.127	.868	.599	.321
	3.780	3.611	3.431	3.240	2.039	2.827	2.605	2.373	2.131	1.880	1.619	1.348	1.069
	4.548	4.377	4.195	4.002	3.799	3.585	3.362	3.128	2.884	2.631	2.369	2.097	1.816
	5.315	5.142	4.958	4.763	4.558	4.343	4.118	3.882	3.637	3.383	3.119	2.846	2.563
	6.082	5.907	5.721	5.524	5.317	5.100	4.873	4.636	4.390	4.134	3.868	3.594	3.310
10	6.848	6.671	6.483	6.285	6.076	5.857	5.629	5.390	5.142	4.885	4.618	4.342	4.057
	7.614	7.435	7.245	7.045	6.835	6.614	6.384	6.144	5.894	5.635	5.367	5.089	4.803
	8.379	8.198	8.007	7.805	7.593	7.371	7.139	6.897	6.646	6.385	6.116	5.837	5.549
	9.145	8.962	8.768	8.565	8.351	8.127	7.893	7.650	7.397	7.135	6.864	6.584	6.295
	9.910	9.725	9.530	9.324	9.108	8.883	8.648	8.403	8.149	7.885	7.613	7.331	7.041
15	10.675	10.488	10.291	10.083	9.866	9.639	9.402	9.156	8.900	8.635	8.361	8.078	7.786
	11.439	11.251	11.052	10.843	10.623	10.395	10.156	9.908	9.651	9.385	9.109	8.825	8.532
	12.204	12.013	11.813	11.602	11.381	11.150	10.910	10.661	10.402	10.134	9.858	9.572	9.278
	12.969	12.776	12.573	12.361	12.138	11.906	11.664	11.413	11.153	10.884	10.606	10.319	10.023
	13.733	13.539	13.334	13.120	12.895	12.662	12.418	12.166	11.904	11.634	11.354	11.066	10.769
20	14.498	14.301	14.095	13.879	13.653	13.417	13.173	12.919	12.656	12.384	12.103	11.813	11.515
	15.262	15.064	14.856	14.638	14.410	14.173	13.927	13.671	13.407	13.134	12.851	12.560	12.261
	16.027	15.827	15.617	15.397	15.168	14.929	14.681	14.424	14.158	13.884	13.600	13.308	13.007
	16.792	16.590	16.378	16.156	15.925	15.685	15.436	15.177	14.910	14.634	14.349	14.056	13.754
	17.557	17.353	17.139	16.916	16.683	16.441	16.190	15.931	15.662	15.384	15.098	14.803	14.500
													14.189
													13.869



TABLE VI-19b  
(Continued)

Salinity ( $\sigma_{\text{t}}$ )	TEMPERATURE ( $^{\circ}\text{C}$ )														
	16	18	20	22	24	26	28	30	35	40					
25	18.322	18.116	17.901	17.676	17.441	17.198	16.945	16.684	16.414	16.135	15.848	15.552	15.247	14.935	14.614
	19.087	18.880	18.662	18.436	18.200	17.955	17.701	17.438	17.166	16.886	16.597	16.300	15.995	15.681	15.359
	19.853	19.643	19.424	19.196	18.958	18.712	18.456	18.192	17.919	17.637	17.347	17.049	16.742	16.428	16.105
	20.619	20.408	20.187	19.957	19.717	19.469	19.212	18.946	18.672	18.389	18.098	17.798	17.490	17.175	16.851
	21.385	21.172	20.949	20.718	20.477	20.227	19.968	19.701	19.425	19.141	18.849	18.548	18.239	17.922	17.597
30	22.152	21.937	21.713	21.479	21.236	20.985	20.725	20.456	20.179	19.894	19.600	19.298	18.988	18.670	18.344
	22.919	22.702	22.476	22.241	21.997	21.744	21.482	21.212	20.934	20.647	20.352	20.049	19.738	19.419	19.091
	23.687	23.468	23.240	23.003	22.757	22.503	22.240	21.968	21.689	21.401	21.104	20.800	20.488	20.168	19.840
	24.455	24.235	24.005	23.766	23.519	23.263	22.998	22.725	22.444	22.155	21.857	21.552	21.239	20.917	20.588
	25.224	25.001	24.770	24.530	24.281	24.023	23.757	23.483	23.200	22.910	22.611	22.304	21.990	21.668	21.338
35	25.993	25.769	25.536	25.294	25.043	24.784	24.516	24.241	23.957	23.665	23.365	23.058	22.742	22.419	22.088
	26.763	26.537	26.302	26.058	25.806	25.545	25.277	24.999	24.714	24.421	24.120	23.811	23.495	23.171	22.839
	27.534	27.306	27.069	26.824	26.570	26.308	26.037	25.759	25.472	25.178	24.876	24.566	24.248	23.923	23.590
	28.305	28.075	27.837	27.590	27.334	27.071	26.799	26.519	26.231	25.936	25.632	25.321	25.003	24.677	24.343
	29.077	28.846	28.605	28.357	28.100	27.834	27.561	27.280	26.991	26.694	26.390	26.078	25.758	25.431	25.096
40	29.850	29.617	29.375	29.124	28.866	28.599	28.324	28.042	27.751	27.453	27.148	26.835	26.514	26.186	25.851

\*Sigma-t ( $\sigma_{\text{t}}$ ) is defined as: (density-1)  $\times 10^3$ . For example, for seawater with a density of 1.02500 g/cm<sup>3</sup>,  $\sigma_{\text{t}} = 25$ .

TABLE VI-19C

WATER DENSITIES (EXPRESSED AS SIGMA-T)\* CALCULATED  
USING THE DENSITY SUBROUTINE FOUND IN MERGE

Salinity (°/oo)	TEMPERATURE (°C)														
	30	32	34	36	38	40	42	44	46	48					
0	-4.291	-4.597	-4.912	-5.235	-5.567	-5.906	-6.254	-6.610	-6.973	-7.345	-7.723	-8.110	-8.503	-8.904	-9.313
	-3.545	-3.853	-4.169	-4.494	-4.827	-5.168	-5.518	-5.875	-6.240	-6.613	-6.993	-7.381	-7.777	-8.180	-8.590
	-2.800	-3.109	-3.427	-3.753	-4.088	-4.430	-4.781	-5.140	-5.507	-5.881	-6.263	-6.653	-7.050	-7.455	-7.867
	-2.055	-2.366	-2.685	-3.013	-3.349	-3.693	-4.045	-4.405	-4.774	-5.150	-5.534	-5.925	-6.324	-6.730	-7.144
	-1.311	-1.623	-1.943	-2.273	-2.610	-2.956	-3.309	-3.671	-4.041	-4.418	-4.804	-5.197	-5.597	-6.006	-6.421
5	-0.567	-0.880	-1.202	-1.533	-1.872	-2.219	-2.574	-2.937	-3.308	-3.687	-4.074	-4.469	-4.871	-5.281	-5.698
	.177	-0.138	-0.461	-0.793	-1.134	-1.482	-1.839	-2.203	-2.576	-2.956	-3.345	-3.741	-4.145	-4.556	-4.975
	.920	.604	.279	-0.054	-0.396	-0.745	-1.103	-1.469	-1.843	-2.225	-2.615	-3.013	-3.418	-3.831	-4.252
	1.663	1.345	1.019	.685	.342	-0.009	-0.368	-0.736	-1.111	-1.494	-1.886	-2.285	-2.691	-3.106	-3.528
	2.406	2.087	1.759	1.424	1.079	.727	.367	-0.002	-0.379	-0.763	-1.156	-1.556	-1.965	-2.380	-2.804
10	3.148	2.828	2.499	2.162	1.817	1.463	1.101	.731	.354	-0.032	-0.426	-0.828	-1.238	-1.655	-2.080
	3.890	3.569	3.239	2.901	2.554	2.199	1.836	1.465	1.086	.699	.304	-0.099	-0.510	-0.929	-1.355
	4.633	4.310	3.979	3.639	3.291	2.935	2.571	2.199	1.818	1.430	1.034	.629	.217	-0.203	-0.630
	5.375	5.051	4.718	4.378	4.029	3.671	3.306	2.932	2.551	2.161	1.764	1.358	.945	.524	.095
	6.117	5.792	5.458	5.116	4.766	4.408	4.041	3.666	3.284	2.893	2.494	2.088	1.673	1.251	.820
15	6.859	6.532	6.198	5.855	5.503	5.144	4.776	4.400	4.016	3.625	3.225	2.817	2.401	1.978	1.547
	7.601	7.273	6.937	6.593	6.241	5.880	5.511	5.134	4.750	4.357	3.956	3.547	3.130	2.706	2.273
	8.343	8.014	7.677	7.332	6.978	6.617	6.247	5.869	5.483	5.089	4.687	4.277	3.860	3.434	3.001
	9.085	8.755	8.417	8.070	7.716	7.353	6.982	6.604	6.217	5.822	5.419	5.008	4.589	4.163	3.728
	9.827	9.496	9.157	8.809	8.454	8.090	7.718	7.338	6.951	6.555	6.151	5.739	5.320	4.892	4.457
20	10.569	10.237	9.897	9.549	9.192	8.827	8.455	8.074	7.685	7.288	6.884	6.471	6.050	5.622	5.186
	11.312	10.979	10.638	10.288	9.931	9.565	9.191	8.809	8.420	8.022	7.617	7.203	6.782	6.353	5.915
	12.055	11.721	11.378	11.028	10.669	10.303	9.928	9.546	9.155	8.757	8.350	7.936	7.514	7.084	6.646
	12.798	12.463	12.119	11.768	11.408	11.041	10.666	10.282	9.891	9.491	9.084	8.669	8.246	7.816	7.377
	13.541	13.205	12.861	12.508	12.148	11.780	11.403	11.015	10.627	10.227	9.819	9.403	8.980	8.548	8.109

TABLE VI-19c  
(Continued)

Salinity ( $\sigma_{\text{t}}$ )	TEMPERATURE ( $^{\circ}\text{C}$ )														
	30	32	34	36	38	40	42	44							
25	14.285	13.948	13.602	13.249	12.888	12.519	12.142	11.757	11.364	10.963	10.554	10.138	9.714	9.282	8.842
	15.029	14.691	14.345	13.990	13.628	13.258	12.881	12.495	12.101	11.700	11.291	10.874	10.449	10.016	9.576
	15.773	15.434	15.087	14.732	14.369	13.999	13.620	13.233	12.839	12.437	12.027	11.610	11.184	10.751	10.310
	16.518	16.178	15.830	15.475	15.111	14.739	14.360	13.973	13.578	13.175	12.765	12.347	11.921	11.487	11.046
	17.264	16.923	16.574	16.217	15.853	15.481	15.101	14.713	14.317	13.914	13.503	13.084	12.658	12.224	11.782
30	18.010	17.668	17.318	16.961	16.596	16.223	15.842	15.454	15.057	14.654	14.242	13.823	13.396	12.962	12.520
	18.757	18.414	18.063	17.705	17.339	16.965	16.584	16.195	15.798	15.394	14.982	14.563	14.136	13.701	13.258
	19.504	19.160	18.809	18.450	18.083	17.709	17.327	16.937	16.540	16.135	15.723	15.303	14.876	14.441	13.998
	20.252	19.907	19.555	19.195	18.828	18.453	18.070	17.680	17.283	16.878	16.465	16.045	15.617	15.182	14.739
	21.000	20.655	20.302	19.941	19.573	19.198	18.815	18.424	18.026	17.621	17.208	16.787	16.359	15.924	15.481
35	21.749	21.403	21.050	20.688	20.320	19.944	19.560	19.169	18.771	18.365	17.952	17.531	17.103	16.667	16.224
	22.499	22.153	21.798	21.436	21.067	20.690	20.306	19.915	19.516	19.110	18.696	18.276	17.847	17.412	16.969
	23.250	22.903	22.547	22.185	21.815	21.438	21.054	20.662	20.263	19.856	19.442	19.021	18.593	18.157	17.714
	24.002	23.653	23.298	22.935	22.564	22.187	21.802	21.409	21.010	20.603	20.190	19.768	19.340	18.904	18.461
	24.754	24.405	24.049	23.685	23.314	22.936	22.551	22.158	21.759	21.352	20.938	20.517	20.088	19.653	19.210
40	25.508	25.158	24.801	24.437	24.065	23.687	23.301	22.808	22.508	22.101	21.687	21.266	20.838	20.402	19.960

\*Sigma-t ( $\sigma_{\text{t}}$ ) is defined as: (density-1) x  $10^3$ . For example, for seawater with a density of 1.02500 g/cm<sup>3</sup>,  $\sigma_{\text{t}}$  = 25.

However, when the same models are used to predict the trajectories of horizontally discharged buoyant plumes, a larger coefficient is required. Consequently the aspiration coefficient must be variable.

Although relatively advanced, MERGE does have its limitations. Some of these are a result of the assumptions already discussed. For example, the plumes are assumed to be round, whereas some evidence indicates substantial deviation from this idealization (Abramovich, 1963). Other important limitations are listed below:

- Diffuser parallel current: The model does not predict plume dilution for cases of current flowing parallel to the diffuser pipe. This is a severe limitation especially in some ocean applications because this case may be expected to result in the lowest initial dilutions.
- Surface entrainment interference: The model does not properly account for interracial boundary conditions. Dilutions near the surface or bottom may be overestimated because entrainment will be assumed where water is unavailable for entrainment.
- Horizontal homogeneity: The model assumes homogeneous horizontal current although bottom topography, internal waves, or other factors may cause considerable spatial flow variations. This is in addition to temporal variations which are excluded by virtue of assumed steady-state.
- Uniform discharge: It is assumed that an infinitely long diffuser exists for which there is no port-to-port variation in effluent characteristics.

#### 6.5.2.3 Similarity

The success of a set of tables in describing an infinite number of possible diffuser, effluent, and ambient flow configurations depends on the principles of similarity. Basically, similarity theory states that model and prototype will display equivalent behavior if a limited number of similarity conditions or parameters are preserved. Equivalent behavior means that relative to appropriate measures the behavior will be equal. For example, if all similarity parameters are preserved, then the height of rise predicted by the model and observed in the prototype will be equal when measured in terms of the initial diameters of the corresponding plumes.

The number of similarity conditions is determined by the difference between the number of independent variables and primary variables involved in the problem (Streeter, 1961). Primary variables must include mass, time, and distance. The present problem involves eleven independent variables implying eight similarity conditions. The independent variables, corresponding symbols, units, similarity parameters, and their names are listed in Table VI-20. As the dilution tables are based on a linear equation of state, the effluent and ambient densities  $\rho_e$  and  $\rho_a$ , respectively, replace four independent variables: the effluent and ambient salinities and temperatures. This effectively reduces the number of similarity conditions by two to six.

Table VI-20

## PLUME VARIABLES, UNITS, AND SIMILARITY CONDITIONS

Variable	Symbol	Units	Dimensionless Sim. Parm	Name
Effluent density	$P_e$	$ML^{-3}$	none--primary variable	none
Effluent velocity	$v$	$LT^{-1}$	none--primary variable	none
Effective diameter	$d_o$	$L$	none--primary variable	none
Ambient density	$P_a$	$ML^{-3}$	$P_e/P_a$	density ratio
Reduced gravity	$g'$	$LT^{-2}$	$v/\sqrt{g'd_o}$	densimetric Froude number: Fr
Density stratification	$dp_a/dz$	$ML^{-4}$	$p_e/(d_o dp_a/dz)$	stratification parm.
Current velocity	$u_a$	$LT^{-1}$	$u_a/v$	current to effluent velocity ratio: k
Kinematic viscosity	$\nu$	$L^2T^{-1}$	$d_o/\nu$	Reynolds number: Re
Port spacing	$S_1$	$L$	$S_1/d_o$	Port spacing parm.: $PS$

Notes: 1.  $g' = ((P_a - P_e)/P_e)g$  where  $g$  is the acceleration of gravity ( $9.807 \text{ msec}^{-2}$ ).

2. In the present application a composite stratification parameter,  $SP$ , is used in lieu of the density ratio and the stratification parameter.  $SP = (P_a - P_e)/(d_o dp_a/dz)$ .

3. The diameter,  $d_o$  is taken to be the vena contracta diameter.

It is advantageous to further reduce the number of similarity conditions to minimize the number of tables necessary to represent the flow configurations of interest. From experimental observations, it is found that plume behavior is basically invariant for large Reynolds numbers reducing the number of similarity conditions to five. Finally, the ratio  $p_e/p_a$  and the stratification parameter can be combined in a composite stratification parameter, SP, where:

$$SP = (p_a - p_e) / (d_o dp_a / dz)$$

This is a satisfactory similarity parameter providing that differences in model and prototype densities are not too great. The assumption is valid for discharge of municipal waste water into estuarine or coastal waters. Figures VI-28 and VI-29 demonstrate the effectiveness of this parameter. The same similarity conditions are shared for both cases. The two figures show rise and dilution to be within about a percent of each other even though the stratification and initial buoyancies are much different. With only four similarity conditions to be satisfied, the problem can be represented by considerably fewer model runs than if six similarity conditions were required.

#### 6.5.2.4 Table Usage

To use the dilution tables to estimate dilutions, it is necessary to calculate the appropriate similarity parameters and know the depth of the outfall. Calculation of the four similarity parameters Fr, SP, k, and PS, given in Table VI-20 requires knowledge of all the variables except v. The dilution tables are shown in Appendix G.

The depth used in the dilution tables is expressed in terms of the diameter of the ports; that is, the vena contracta diameter. For bell-mouthed ports, this diameter is approximately equal to the physical diameter of the port. Thus, if the actual depth of water is 10 m and the port diameter is 10 cm, then the depth of water is 100-port diameters.

The dilution tables are numbered from 1 through 100 and are grouped by port spacing as listed below:

<u>Tables</u>	<u>Port Spacing (PS) (Diameters)</u>
1-20	2
21-40	5
41-60	10
61-80	25
81-100	1000 (effluent from each port acts as a single plume)

CASE NUMBER 1

\*\*\*\*\* TEST OF COMPOSITE STRATIFICATION PARAMETER

INPUT DATA PSEUDO=ECHO

U 7.0200 0.0000 0.1160 0.0000 0.0000 0.0000 0.0500 100.0000 0.0000

NDP ITER IFRO NAA NAB NAC IDENSW 2 1000 25 0 0 0 1

(IF IDENSW=1 THEN DENSITY VERSION USED--USE 2ND SIGMAT COL)

AMBIENT STRATIFICATION (AND CALCULATED SIGMAT)

DEPTH(M) TEMP(C) SAL(O/00) CUR(M/S) SIGMAT SIGMAT(DEN VER) 0.000 0.000 0.000 0.000 -0.093 0.000 10.000 0.000 0.000 -0.093 27.000

EFFLUX TO CURRENT RATIO(K) . . . = 99999.0
DENSIMETRIC FROUDE NO. . . . = 43.1
VOLUME FLUX(M\*\*3/S) . . . . = 0.055
DEPTH AVE STRATIFICATION PARH. = 3703.7
DEPTH(M) . . . . . = 10.0
DISCHARGE VELOCITY(M/S) . . . = 7.02
CURRENT SPEED(M/S) . . . . = 0.000
PORT RADIUS(M) . . . . . = 0.0500
PORT SPACING(M) . . . . . = 100.00

MODEL OUTPUT AFTER -J- ITERATIONS (MKS UNITS)

Table with columns: O, HOR, COR(X), DEPTH(Z), DIAMETER, VOL OIL, HOR VEL(U), VFR VEL(V), TOTAL VEL, DEN DIFF, TIME, CURRENT. Rows 1-450 showing model output data.

NOMINAL TRAPPING LEVEL REACHED

Table with columns: NOMINAL TRAPPING LEVEL REACHED, O, HOR, COR(X), DEPTH(Z), DIAMETER, VOL OIL, HOR VEL(U), VFR VEL(V), TOTAL VEL, DEN DIFF, TIME, CURRENT. Rows 469-519 showing nominal trapping level data.

FIGURE VI-28 EXAMPLE OUTPUT OF MERGE - CASE 1

CASE NUMBER 2

\*\*\*\* TEST OF COMPOSITE STRATIFICATION PARAMETER

INPUT DATA PSEUDO-ECHO

U	V	A	T	S	B	SPC	ALT DEN
2.3400	0.0000	0.1160	0.0000	0.0000	0.0500	100.0000	0.0000

NDP ITER	IFRO	NAA	NAB	MAC	IDENSW
2	1000	25	0	0	0

(IF IDENSW=1 THEN DENSITY VERSION USED--USE 2ND SIGMAT COL)

AMBIENT STRATIFICATION (AND CALCULATED SIGMAT)

DEPTH(M)	TEMP(C)	SAL(O/00)	CUR(M/S)	SIGMAT	SIGMAT(DEN VER)
0.000	0.000	0.000	0.000	-0.093	0.000
10.000	0.000	0.000	0.000	-0.093	3.000

EFFLUX TO CURRENT RATIO(K)	99999.0
DENSIMETRIC FROUDE NO.	43.1
VOLUME FLUX(M**3/S)	0.018
DEPTH AVE STRATIFICATION PARAM.	33333.3
DEPTH(M)	10.0
DISCHARGE VELOCITY(M/S)	2.34
CURRENT SPEED(M/S)	0.000
PORT RADIUS(M)	0.0500
PORT SPACING(M)	100.00

MODEL OUTPUT AFTER -J- ITERATIONS (MKS UNITS)

J	HOR	COR(X)	DEPTH(Z)	DIAMETER	VOL OIL	HOR VEL(U)	VER VEL(V)	TOTAL VEL	DEN DIFF	TIME	CURRENT
1	0.001	0.100	10.000	0.100	1.007	2.324	0.000	2.324	2.979	0.001	0.000
25	0.041	0.118	10.000	0.118	1.189	1.968	0.000	1.968	2.523	0.019	0.000
50	0.089	0.141	10.000	0.141	1.413	1.655	0.001	1.655	2.121	0.046	0.000
75	0.146	0.167	10.000	0.167	1.680	1.391	0.001	1.391	1.784	0.084	0.000
100	0.214	0.199	10.000	0.199	1.997	1.170	0.002	1.170	1.500	0.138	0.000
125	0.292	0.237	10.000	0.237	2.374	0.984	0.003	0.984	1.261	0.214	0.000
150	0.392	0.282	9.999	0.282	2.823	0.827	0.003	0.827	1.061	0.322	0.000
175	0.506	0.335	9.999	0.335	3.356	0.696	0.004	0.696	0.892	0.474	0.000
200	0.643	0.398	9.996	0.398	3.991	0.585	0.005	0.585	0.749	0.689	0.000
225	0.805	0.473	9.996	0.473	4.746	0.492	0.006	0.492	0.630	0.994	0.000
250	0.998	0.563	9.993	0.563	5.643	0.414	0.007	0.414	0.529	1.425	0.000
275	1.227	0.669	9.988	0.669	6.710	0.348	0.009	0.348	0.443	2.034	0.000
300	1.500	0.796	9.980	0.796	7.979	0.293	0.011	0.293	0.370	2.895	0.000
325	1.824	0.946	9.966	0.946	9.488	0.246	0.013	0.246	0.308	4.112	0.000
350	2.209	1.124	9.942	1.124	11.283	0.207	0.015	0.207	0.252	5.830	0.000
375	2.666	1.336	9.902	1.336	13.417	0.174	0.017	0.174	0.201	8.254	0.000
400	3.206	1.585	9.838	1.585	15.955	0.146	0.020	0.146	0.152	11.666	0.000
425	3.843	1.879	9.736	1.879	18.973	0.123	0.022	0.123	0.100	16.450	0.000
450	4.592	2.225	9.585	2.225	22.563	0.103	0.023	0.106	0.043	23.140	0.000

NOMINAL TRAPPING LEVEL REACHED

468	5.213	9.443	2.518	25.561	0.091	0.021	0.094	-0.002	29.563	0.000
475	5.476	9.382	2.644	26.832	0.087	0.020	0.089	-0.019	32.525	0.000
500	6.537	9.177	3.167	31.909	0.073	0.010	0.074	-0.073	45.931	0.000
517	7.390	9.117	3.583	35.900	0.065	0.000	0.065	-0.083	58.378	0.000

FIGURE VI-29 EXAMPLE OUTPUT OF MERGE - CASE 2



Each group of 20 is further subdivided by current velocity to effluent velocity ratio (k), i.e. :

<u>Tables</u>	<u>Current Velocity to Effluent Velocity Ratio (k)</u>
1-5	0.1
6-10	0.05
11-15	0.02
16-20	0.00 (no current)

Each subgroup of five tables is comprised of tables of varying composite density stratification (SP):

<u>Tables</u>	<u>Composite Stratification Parameter (SP)</u>
1	200 (high stratification)
2	500
3	2000
4	10000
5	infinity (no stratification)

Finally, each table includes densimetric Froude number,  $Fr = 1, 3, 10, 30, 100,$  and 1000 to represent cases ranging from highly buoyant plumes to almost pure jets. The dilutions are tabulated with plume rise. The following examples demonstrate how the tables may be applied.

----- EXAMPLE VI-11 -----

Calculation of Initial Dilution

Example A. This example demonstrates many of the basic features of the dilution tables and their Usage. It also includes a method for estimating the plume diameter indirectly using information derived from the tables. The method is used in cases of unmerged or slightly merged plumes and is necessary to better estimate plume dilution when the plume is shown to interact with the water surface.

waste water is discharged horizontally at a depth of 66 m from a simple pipe opening and that:

- $u_a$  = the current velocity = 0.15 m/s
- $v$  = the effluent velocity = 1.5 m/s
- $p_e$  = the effluent density = 1000 kg/m<sup>3</sup>
- $p_a$  = the ambient density at discharge depth = 1015 kg/m<sup>3</sup>
- $L$  = the port spacing = infinite

$d_0$  = the port discharge vena contracta diameter = 1.7 m

$dp_a/dz$  = the ambient density stratification = 0.0441 kg/m<sup>4</sup>

The four similarity parameters necessary to use the tables are:

Fr = the densimetric Froude number = 3.0

k = the current to effluent velocity ratio = 0.1

SP = the composite stratification parameter = 200

PS = the port spacing parameter = infinity.

The infinite port spacing indicates that the dilutions will be found in the last 20 tables of the dilution tables in Appendix G, i.e., Tables 81-100. These tables are appropriate because merging does not occur with PS = infinity. The current to effluent velocity ratio of 0.1 indicates that the appropriate dilutions are among the first five of these 20 tables. The stratification parameter 200 identifies the first of these five tables as the correct reference location. Finally, the densimetric Froude number of 3.0 isolates the second column as the one containing the information of interest.

The column of dilutions contains a wealth of information about the plume whose overall behavior is described in Figure VI-30. After rising one diameter (1.7 m), the average plume dilution (expressed in terms of volume dilution) is 2.8. In other words, a given amount of plume volume has been diluted with 1.8 times as much ambient fluid. After rising 2 diameters (3.4 m), the average dilution is 3.7, and so on. At 15 diameters rise, the dilution is 21.4. The next entry follows in a line headed by "T", indicating that the initial trapping level has been reached. This means that the plume and ambient densities are equal at this level and momentary equilibrium has been attained. The "trapping" level dilution is 26.2 and the corresponding plume rise, set off in parentheses to the right of the dilution, is 17.0 diameters. The parentheses are a mnemonic for indicating trapping while values set off in square brackets are merging level plume rises.

When a plume intercepts the water surface, it is deprived of some of its entraining surface and consequently the dilution is less than that indicated in the tables. For well-diluted, unmerged or slightly merged plumes, with k not equal to zero, the plume diameter, d, may be estimated:

$$d = d_0 \sqrt{D/k} \quad (\text{VI-61})$$

In dimensionless units, or diameters:

$$d/d_0 = \sqrt{D/k} \quad (\text{VI-62})$$

In the present case, the diameter at maximum rise calculated in this way is

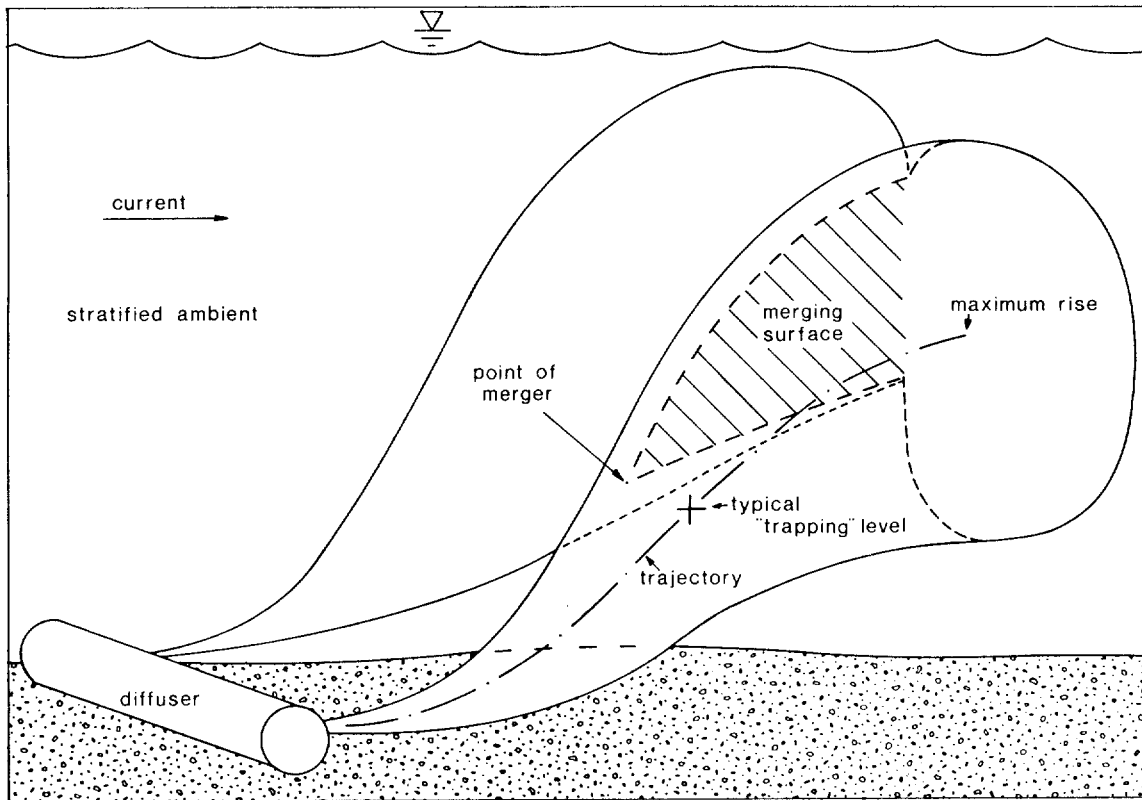


FIGURE VI -30 SCHEMATIC OF PLUME BEHAVIOR PREDICTED BY MERGE IN THE PRESENT USAGE

25.2 diameters (42.8M). Thus the top of the plume is 34.8 diameters (22.2 + 12.6) above the level of the outfall, i.e. 12.6 diameters above the plume centerline, and 4.0 diameters below the surface. Therefore, surface interaction does not occur.

For the sake of comparison, the plume diameter calculated by the program at maximum rise is 23.5 diameters which compares favorably with the simplified estimate made above.

Example B. Suppose that all the conditions given in Example A apply here except that the depth of water is only 29.7 diameters (50.5 m). Table 81 is again used to provide dilution estimates; however, surface interaction does occur. A conservative estimate of initial dilution is obtained by assuming that entrainment stops as soon as the top boundary of the plume intersects the surface. In reality, some additional ambient water could be expected to enter through the sides of the plume.

When the centerline depth of the plume is 20 diameters, its dilution is 37.3 and its approximate diameter is 19.4 diameters (33m). Consequently, the top boundary of the plume is 29.7 diameters above the level of the outfall and is equal to the depth of water. Thus the dilution of 37.3 provides a conservative

estimate of initial dilution in this case.

Example C. Suppose the following data apply:

$$\begin{aligned}u_a &= 0.15 \text{ m/s} \\v &= 1.5 \text{ m/s} \\p_e &= 1000 \text{ kg/m} \\p_a &= 1015 \text{ kg/m} \\S_l &= 0.34 \text{ m} \\d_o &= 0.17 \text{ m} \\dp_a/dz &= 0.0441 \text{ kg/m}^4\end{aligned}$$

Then,  $Fr = 9.5$ ,  $k = 0.1$ ,  $SP = 2000$ , and  $PS = 2$ , and Table 3 in Appendix G is the appropriate source of dilution information. As the Froude number is almost equal to 10, column 3 information can be used without modification although interpolation may be appropriate in some applications. The plumes merge almost immediately at a dilution of 2.1. The initial trapping level is encountered after the plume rises 89.4 diameters (15.2 m). The maximum dilution is 76.2 after rising 125 diameters (21.3).

For closely spaced plumes, the diameter may be estimated from the relationship:

$$d/d_o = (\pi D) (4 k PS) \quad (VI-63)$$

The maximum diameter estimated in this way is 299 diameters (50.9 m). In contrast, the program gives a value of 268 diameters (45.5 m). No surface interaction occurs in deep water. In very shallow water, a conservative estimate of dilution may be made by dividing the total flow across the length of the diffuser by the flow through the diffuser. It is conservative because no aspiration entrainment is included in the estimate.

Table 3 contains a blank entry in the second column of the 90-diameter rise line. The previous entry in the column indicates trapping. This means that trapping and the 90-diameter rise level occurred in the same iteration. Therefore, the dilution of 41.3 is the appropriate value for this blank.

Example D. The methods given in Examples A and C for estimating the plume diameter are not accurate when intermediate degrees of merging exist. If surface interaction is important, it may be necessary to run the model to obtain accurate Plume diameter predictions.

Example E. Sometimes outfalls or diffusers are located in water only a few port diameters deep and, as a result, initial dilutions may be expected to be quite small. However, after the plumes reach the surface, they still have substantial horizontal velocity and continue to entrain ambient water more vigorously than a plume whose trajectory is unhindered by surface constraints. The workbook by Shirazi and Davis (1976) may be consulted to estimate additional dilution.

Example F. Strong stratification inhibits plume rise. As stratification weakens, plume rise and dilution tend to increase. Predicting large dilutions and plume rises can require more program iterations than used to develop the tables in Appendix G. On the other hand, very large dilutions are usually of lesser interest. Consequently, the number of iterations is arbitrarily limited to 1000 and rise to 300 diameters. Table 94 provides examples in which the runs for each densimetric Froude number are limited by the permitted number of iterations. The final dilutions listed are underlined to remind the user that larger dilutions and plume rises occur. When the rise limitation criterion has been reached, a rise of 300 diameters or slightly more will be indicated.

Example G. Many diffusers have horizontally discharging paired ports on each side of the diffuser. In cross current, the resulting plume behavior appears somewhat like that shown in Figure VI-31. The upstream plume is bent over the counterflowing current and ultimately may be entrained by the downstream plume. The entrainment of pollutant laden fluid will reduce the overall dilution in the merged plumes. Estimates of the magnitude of this effect may be made if it may be assumed that:

- o The interaction occurs
- o There is merging of adjacent plumes to assure cross diffuser merging and not interweaving of plumes
- o The opposite plumes have similar rise and overall entrainment
- o There are no surface constraints

$$D_f = (D^2)/(2D - D_e) \quad (VI-64)$$

where D is the dilution at maximum rise of the downstream plume as given in the tables and  $D_e$  is the dilution of the downstream plume upon entry into the bottom of the bent over upstream plume (see Figure VI-31).  $D_e$  is estimated by finding the distance in diameters,  $Z_e$ , between the depth at entry and the port depth. The dilution at this depth is read from the appropriate line in the dilution tables or interpolated. The maximum radius of the plume is added to the depth at which maximum rise occurs. The difference between the port depth and the depth so calculated is  $Z_e$ .

Given that  $Fr = 3$ ,  $PS = 25$ ,  $SP = 2000$ , and  $k = 0.1$ , and that identical plumes are injected into the ambient water from both sides of the diffuser. From Table 63, it is found that the dilution is 270 and the rise is 55.1 diameters. The width of the plumes may be estimated:

$$d/d_o = (\pi 270)/[4(0.1)(25)] = 85$$

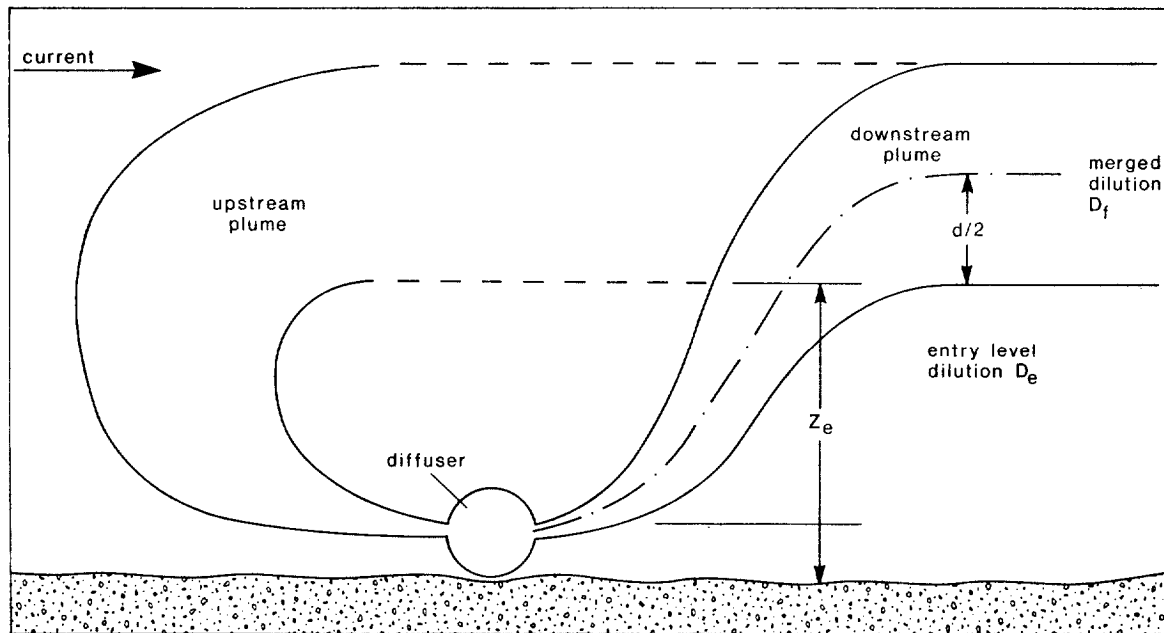


FIGURE VI-31 CROSS DIFFUSER MERGING

(cf. the computer calculated width of 83 diameters). Therefore, the vertical distance between the ports and the plume entry level is  $55.1 - 85/2 = 12.6$  diameters, and  $D_e = 15.5$  as estimated from the table at rise equal to 12 diameters.

$D_f$  may now be calculated:

$$D_f = 270 / [ 2(270) - 15.5 ] = 139$$

This result may have been anticipated: the dilution is effectively halved. This is the outcome whenever the entry level,  $Z_e$ , is small. In many cases, halving the dilution provided in the tables gives an adequate estimate of the overall dilution achieved by the cross diffuser merging plumes.

Example H. Given that  $PS = 25$ ,  $SP = 200$ ,  $k = 0.0$ ,  $Fr = 10$ , and that an estimate of the centerline dilution at maximum rise is required. By consulting Table 77, it is found that the average dilution at maximum rise is 26.0. Since there is no current and virtually no merging, this value can be divided by 1.77 to obtain the centerline dilution (based on a gaussian profile, see Teeter and Baumgartner, 1979). The centerline dilution is 14.7.

With identical conditions except for port spacing of 2 instead of 25, Table 16 shows that the dilution at maximum rise is 11.6. The centerline dilution is again smaller but not by the same percentage amount. For the  $3/2$  power profile, similar to the gaussian, the peak-to-mean ratio in stagnant ambient and complete merging is 1.43 (Teeter and Baumgartner, 1979). Thus the centerline dilution may be found to be 8.1.

The peak-to-mean ratios given above are flow-weighted and are obtained through a straightforward integration. Unfortunately the problem is not as simple when current is present because the gaussian or other arbitrary profiles of velocity are superimposed onto a non-zero average velocity. Hence, in high current, the peak-to-mean ratio for single plumes assuming the 3/2 power profile is 3.89. For merged plumes, the ratio is lower. For intermediate currents, the ratio is between the corresponding extremes depending on the degree of merging and the actual current velocity.

Fortunately, many standards and regulations - for example, the Federal 301(h) regulations - are written in terms of average dilutions. Also, repeated measurements in the field are likely to provide estimates of average concentrations before estimates of maximum concentrations are possible. Thus, the user of MERGE is normally not concerned with centerline dilutions. It is useful to remember that estimating average dilutions using centerline models involves not only the use of variable peak-to-mean ratios but also variable aspiration coefficients.

----- END OF EXAMPLE VI-11 -----

### 6.5.3 Pollutant Concentration Following Initial Dilution

The concentration of a conservative pollutant at the completion of initial dilution is expressible as:

$$C_f = C_a + \frac{C_e - C_a}{S_a} \quad (\text{VI-65})$$

where

$C_a$  = background concentration, mg/l

$C_e$  = effluent concentration, mg/l

$S_a$  = initial dilution (flux-averaged)

$C_f$  = concentration at the completion of initial dilution, mg/l.

When the background level,  $C_a$ , is negligible Equation VI-65 simplifies to:

$$C_f = \frac{C_e}{S_a} \quad (\text{VI-66})$$

This expression can be used to predict the increased pollutant concentration above ambient, as long as the effluent concentration greatly exceeds the ambient concentration. It is interesting to note that when the effluent concentration is below ambient, the final pollutant concentration is also below ambient.

Since water quality criteria are often prescribed as maximum values not to be exceeded following initial dilution, it is useful to rearrange Equation VI-65 to

express the maximum allowable effluent concentration as follows:

$$(C_e)_{\max} = C_a + (Sa)_{\min} (C_c - C_a) \quad (VI-67)$$

where

- $(C_e)_{\max}$  = maximum allowable effluent concentration such that water quality criteria are not exceeded
- $C_c$  = applicable water quality criterion
- $(Sa)_{\min}$  = minimum expected initial dilution.

Since initial dilution is a function of discharge and receiving water characteristics, as discussed in detail in Section 6.5.2, finding an appropriate "minimum" initial dilution is not a trivial problem. Most often, initial dilutions are lowest when density stratification is greatest. For a given stratification profile, dilutions generally decrease at lower ambient current speeds and higher effluent flow rates. Based on expected critical conditions in the vicinity of the discharge, the tables in Appendix G can be used to predict  $(Sa)_{\min}$ .

----- EXAMPLE VI-12 -----

Analysis of the effluent wastewater from a treatment plant discharging into a large west coast estuary revealed that the effluent contained a number of priority pollutants. A few of the pollutants and their measured concentrations are shown below.

Priority Pollutant	Concentrations ( $\mu\text{g/l}$ )		Criterion Level ( $\mu\text{g/l}$ )
	Dry Weather	Wet Weather	
copper	32.3	61.9	4.0
zinc	33.0	180.0	58.0
mercury	not detected	3.5	0.025
lindane	8.6	not detected	0.16

The critical initial dilution has been determined to be 30. If the criterion levels are designed to be complied with at the completion of initial dilution, determine if the criteria for the four priority pollutants are contravened.

A cursory review of the tabulations above shows that all detected effluent pollutant concentrations (i.e., undiluted concentrations) exceed the criteria levels, other than zinc during dry weather flow conditions. Hence if initial dilutions were to become low enough, each of the four priority pollutants could violate water quality criterion for either dry or wet weather conditions.

Using the minimum initial dilution of 30, the final pollutant levels can be predicted using Equation VI-66, by assuming background levels are negligible. The final pollutant levels compared with the criterion levels are shown below.



Priority Pollutant	Final Concentrations ( $\mu\text{g/l}$ )		Criterion Level ( $\mu\text{g/l}$ )
	Dry Weather	Wet Weather	
copper	1.1	2.1	4.0
zinc	1.1	6.0	58.0
mercury		0.1	0.025
lindane	0.3		0.16

Both mercury and lindane violate the criteria while copper and zinc do not. However, copper levels are sufficiently close to the criterion of 4.0  $\mu\text{g/l}$  to warrant further attention.

--- END OF EXAMPLE VI-12 ---

#### 6.5.4 pH Following Initial Dilution

The pH standard governing wastewater discharges into estuarine or coastal waters is usually quite strict. Typically, state standards require that the pH following initial dilution not deviate by more than 0.2 units from background. A step by step approach is presented here that can be used to determine whether a discharge will comply with a standard of this type.

Step 1. The following input data are required:

- $S_a$  = initial dilution
- $Alk_a$  = alkalinity of receiving water, eq/l
- $Alk_e$  = alkalinity of effluent wastewater, eq/l
- $pH_a$  = pH of receiving water
- $pH_e$  = pH of effluent wastewater
- $K_{a,1}, K_{a,1}^c$  = equilibrium constant for dissociation of carbonic acid in wastewater and receiving water, respectively (first acidity constants)
- $K_{a,2}, K_{a,2}^c$  = equilibrium constant for dissociation of bicarbonate in wastewater and receiving water, respectively (second acidity constants)
- $K_w, K_w^c$  = ion product for wastewater and receiving water, respectively.

Table VI-21 shows values of the equilibrium constants and ion product of water. For seawater, typical values of pH and alkalinity are 8.3 units and 2.3meq/l, respectively.

Step 2. Calculate the total inorganic carbon concentrations in the effluent wastewater ( $C_{te}$ ) and receiving water ( $C_{ta}$ ):

$$C_{te} = \frac{Alk_e - \frac{K_w}{[H^+]_e} + [H^+]_e}{(\alpha_1 + 2\alpha_2)_e} \quad (VI-68)$$

TABLE VI -21

VALUES OF EQUILIBRIUM CONSTANTS AND ION PRODUCT OF WATER AS A FUNCTION OF TEMPERATURE FOR FRESHWATER AND SALT WATER

Temp.	$- \log K_{a1}$		$- \log K_{a2}$		$- \log K_w$	
	Freshwater	Seawater	Freshwater	Seawater	Freshwater	Seawater
5	6.52	6.00	10.56	9.23	14.63	14.03
10	6.46	5.97	10.49	9.17		
15	6.42	5.94	10.43	9.12	14.35	13.60
20	6.38	5.91	10.38	9.06	14.17	13.40
25	6.35	5.84	10.33	8.99	14.00	13.20

and

$$C_{ta} = \frac{Alk_a - \frac{C_{K_w}}{[H^+]_a} + [H^+]_a}{(\alpha_1 + 2\alpha_2)_a} \quad (VI-69)$$

where

$$\alpha_1 = \frac{[H^+] K_{a,1}}{[H^+]^2 + [H^+] K_{a,1} + K_{a,1} K_{a,2}} \quad (VI-70)$$

$$\alpha_2 = \frac{K_{a,1} k_{a,2}}{[H^+]^2 + [H^+] K_{a,1} + K_{a,1} K_{a,2}} \quad (VI-71)$$

Note:  $C_{K_{a,1}}$  and  $C_{K_{a,2}}$  are used in  $\alpha_1$  and  $\alpha_2$  to calculate  $C_{ta}$ .

Step 3. Calculate the alkalinity ( $Alk_f$ ) and total inorganic carbon ( $C_{tf}$ ) at the completion of initial dilution:

$$Alk_f = Alk_a + \frac{Alk - Alk}{S_a} \quad (VI-72)$$

$$C_{tf} = C_{ta} + \frac{C_{te} - C_{ta}}{S_a} \quad (VI-73)$$

Step 4. Express the final alkalinity as:

$$Alk_f = C_{tf} (\alpha_1 + 2\alpha_2)_f + \frac{C_{K_w}}{[H^+]_f} - [H^+]_f \quad (VI-74)$$

Rather than solving for  $[H^+]_f$  directly in Equation VI-74, it is easier to calculate  $Alk_f$  in equation VI-72 for a range of  $[H^+]$  values, until the alkalinities computed from equations VI-72 and VI-74 match.

In most cases  $pH_f$  will not differ from the ambient pH by more than 0.1 to 0.3 units. Consequently it is usually most expeditious to begin by assuming  $pH_f = pH_a$ . If  $pH_e > pH_a$ , then each subsequent calculation should be at 0.1 pH units higher than  $pH_a$ . If  $pH_e < pH_a$ , each subsequent calculation should be 0.1 pH units lower than  $pH_a$ .

For typical values of wastewater alkalinity (2.0 meq/l) and receiving water alkalinity (2.3 meq/l), the pH at the completion of initial dilution can be tabulated for selected values of effluent pH, initial dilution, and water temperature. Table VI-22 shows the results, which can be used to provide a quick indication of whether the water quality criterion for pH is violated.

#### EXAMPLE VI-13

A wastewater treatment plant receives alkaline waste process water, and because of the low level of treatment received in the plant, effluent pH values as high as 11.1 units have been observed. The effluent wastewater is discharged into a water body where the pH standard permits a 0.2 unit deviation from ambient at the completion of initial dilution. Determine if the standard is violated by the discharge. The required pertinent data are:

$$\begin{aligned}
 pH_a &= 8.3 \\
 Alk_a &= 2.3 \text{ meq/l} \\
 Alk_e &= 2.0 \text{ meq/l} \\
 c_{K_w} &= 6.3 \times 10^{-14}, \text{ for the ambient water} \\
 K_w &= 10^{-14}, \text{ for the wastewater} \\
 c_{K_{a,1}} &= 8 \times 10^{-7}, \text{ for the ambient water} \\
 K_{a,1} &= 5 \times 10^{-7}, \text{ for the wastewater} \\
 c_{K_{a,2}} &= 4.68 \times 10^{-10}, \text{ for the ambient water} \\
 K_{a,2} &= 0.5 \times 10^{-10}, \text{ for the wastewater} \\
 Sa &= 20
 \end{aligned}$$

The dissociation constants for the wastewater  $\alpha_1$ , and  $\alpha_2$ , are:

$$\alpha_1 = \frac{10^{-11.1} \times 5 \times 10^{-7}}{(10^{-11.1})^2 + 10^{-11.1} \times 5 \times 10^{-7} + 5 \times 10^{-7} \times 0.5 \times 10^{-10}} = .137$$

$$\alpha_2 = \frac{5 \times 10^{-7} \times 0.5 \times 10^{-10}}{(10^{-11.1})^2 + 10^{-11.1} \times 5 + 10^{-7} + 5 \times 10^{-7} \times 0.5 \times 10^{-10}} = .863$$

TABLE VI -22  
ESTIMATED pH VALUES AFTER INITIAL DILUTION

Seawater Temp. °C	5°C					15°C					25°C					
	Seawater pH	10	Initial Dilution		75	100	10	Initial Dilution		75	100	10	Initial Dilution		75	100
Effluent pH = 6.0 Alk = 0.1																
7.0	6.94	6.97	6.98	6.98	6.99	6.95	6.97	6.98	6.99	6.99	6.95	6.98	6.99	6.99	6.99	6.99
7.5	7.37	7.44	7.47	7.47	7.48	7.40	7.45	7.47	7.48	7.48	7.42	7.45	7.48	7.48	7.48	7.49
7.7	7.56	7.64	7.67	7.67	7.68	7.59	7.65	7.67	7.68	7.68	7.62	7.66	7.68	7.68	7.68	7.69
8.0	7.88	7.95	7.97	7.97	7.98	7.91	7.96	7.98	7.98	7.99	7.94	7.97	7.98	7.99	7.99	7.99
8.3	8.21	8.26	8.28	8.28	8.29	8.24	8.27	8.28	8.29	8.29	8.25	8.25	8.29	8.29	8.29	8.29
8.5	8.43	8.47	8.48	8.48	8.49	8.45	8.48	8.49	8.49	8.49	8.46	8.48	8.49	8.49	8.49	8.49
Effluent pH = 6.0 Alk = 0.6																
7.0	6.74	6.87	6.93	6.95	6.96	6.77	6.89	6.94	6.96	6.97	6.77	6.89	6.94	6.96	6.97	6.97
7.5	6.98	7.23	7.35	7.40	7.42	7.03	7.27	7.38	7.42	7.44	7.08	7.31	7.40	7.43	7.45	7.45
7.7	7.07	7.39	7.53	7.59	7.61	7.16	7.45	7.57	7.61	7.63	7.24	7.51	7.60	7.64	7.65	7.65
8.0	7.27	7.70	7.85	7.90	7.93	7.44	7.79	7.90	7.93	7.95	7.60	7.85	7.93	7.95	7.96	7.96
8.3	7.66	8.08	8.20	8.23	8.25	7.89	8.15	8.23	8.25	8.26	8.02	8.19	8.24	8.26	8.27	8.27
8.5	8.01	8.33	8.42	8.44	8.46	8.18	8.38	8.44	8.46	8.47	8.27	8.41	8.45	8.47	8.47	8.47
Effluent pH = 6.0 Alk = 1.0																
7.0	6.63	6.81	6.89	6.92	6.94	6.66	6.83	6.90	6.93	6.95	6.67	6.84	6.91	6.93	6.95	6.95
7.5	6.80	7.10	7.27	7.34	7.37	6.86	7.15	7.31	7.36	7.39	6.90	7.20	7.33	7.38	7.41	7.41
7.7	6.86	7.23	7.43	7.52	7.56	6.94	7.30	7.49	7.56	7.59	7.01	7.38	7.53	7.58	7.61	7.61
8.0	6.98	7.48	7.75	7.83	7.87	7.12	7.63	7.82	7.88	7.91	7.29	7.73	7.86	7.90	7.92	7.92
8.3	7.21	7.91	8.12	8.18	8.21	7.51	8.04	8.17	8.21	8.23	7.76	8.10	8.19	8.22	8.23	8.23
8.5	7.51	8.20	8.35	8.40	8.42	7.89	8.28	8.39	8.42	8.44	8.06	8.32	8.40	8.42	8.43	8.43
Effluent pH = 6.0 Alk = 2.0																
7.0	6.45	6.68	6.81	6.86	6.89	6.48	6.71	6.83	6.88	6.90	6.50	6.72	6.84	6.88	6.91	6.91
7.5	6.55	6.88	7.11	7.21	7.27	6.60	6.94	7.16	7.25	7.31	6.64	6.99	7.20	7.29	7.34	7.34
7.7	6.58	6.96	7.23	7.36	7.43	7.64	7.04	7.31	7.43	7.50	6.70	7.12	7.39	7.49	7.54	7.54
8.0	6.64	7.11	7.49	7.66	7.75	6.73	7.28	7.65	7.77	7.83	6.93	7.45	7.75	7.84	7.88	7.88
8.3	6.73	7.41	7.91	8.06	8.12	6.89	7.73	8.06	8.14	8.18	7.11	7.91	8.12	8.18	8.21	8.21
8.5	6.83	7.78	8.20	8.31	8.36	7.10	8.07	8.30	8.37	8.40	7.48	8.18	8.35	8.40	8.42	8.42
Effluent pH = 6.5 Alk = 0.5																
7.0	6.92	6.96	6.98	6.98	6.99	6.93	6.97	6.98	6.98	6.99	6.93	6.97	6.98	6.98	6.99	6.99
7.5	7.32	7.42	7.45	7.47	7.47	7.34	7.43	7.46	7.47	7.48	7.37	7.44	7.46	7.47	7.48	7.48
7.7	7.49	7.61	7.65	7.66	7.67	7.53	7.63	7.66	7.67	7.67	7.56	7.64	7.66	7.67	7.67	7.67
8.0	7.80	7.92	7.96	7.97	7.97	7.85	7.94	7.96	7.97	7.98	7.88	7.94	7.96	7.97	7.97	7.97
8.3	8.15	8.24	8.26	8.27	8.28	8.19	8.25	8.27	8.27	8.28	8.20	8.25	8.26	8.27	8.27	8.27
8.5	8.38	8.45	8.47	8.48	8.48	8.40	8.45	8.47	8.47	8.48	8.40	8.44	8.46	8.46	8.46	8.46
Effluent pH = 6.5 Alk = 1.0																
7.0	6.85	6.93	6.96	6.97	6.98	6.87	6.94	6.97	6.98	6.98	6.88	6.94	6.97	6.98	6.98	6.98
7.5	7.18	7.35	7.42	7.44	7.46	7.22	7.37	7.43	7.45	7.46	7.26	7.40	7.45	7.46	7.47	7.47
7.7	7.31	7.53	7.61	7.64	7.65	7.39	7.57	7.63	7.65	7.66	7.45	7.60	7.65	7.66	7.67	7.67
8.0	7.60	7.84	7.92	7.95	7.96	7.72	7.89	7.94	7.96	7.97	7.80	7.92	7.96	7.97	7.97	7.97
8.3	8.00	8.19	8.24	8.26	8.27	8.09	8.22	8.26	8.27	8.28	8.14	8.24	8.27	8.28	8.28	8.28
8.5	8.26	8.41	8.45	8.47	8.47	8.33	8.43	8.46	8.47	8.48	8.36	8.44	8.47	8.48	8.48	8.48
Effluent pH = 6.5 Alk = 2.0																
7.0	6.75	6.88	6.93	6.95	6.96	6.78	6.89	6.94	6.96	6.97	6.79	6.90	6.94	6.96	6.97	6.97
7.5	6.99	7.23	7.35	7.39	7.42	7.04	7.27	7.37	7.41	7.43	7.08	7.30	7.39	7.42	7.44	7.44
7.7	7.07	7.38	7.53	7.58	7.61	7.15	7.44	7.56	7.61	7.63	7.23	7.49	7.59	7.62	7.64	7.64
8.0	7.25	7.67	7.84	7.89	7.92	7.41	7.77	7.88	7.92	7.94	7.55	7.82	7.90	7.93	7.94	7.94
8.3	7.61	8.06	8.18	8.22	8.24	7.84	8.13	8.21	8.23	8.25	7.96	8.16	8.22	8.24	8.25	8.25
8.5	7.95	8.30	8.40	8.43	8.45	8.12	8.35	8.42	8.44	8.45	8.20	8.36	8.42	8.43	8.44	8.44
Effluent pH = 9.0 Alk = 2.0																
7.0	7.03	7.01	7.00	7.00	7.00	7.04	7.01	7.00	7.00	7.00	7.04	7.01	7.00	7.00	7.00	7.00
7.5	7.52	7.51	7.50	7.50	7.50	7.51	7.50	7.50	7.50	7.50	7.51	7.50	7.50	7.50	7.50	7.50
7.7	7.71	7.70	7.70	7.70	7.70	7.70	7.70	7.70	7.70	7.70	7.70	7.70	7.70	7.70	7.70	7.70
8.0	8.00	8.00	8.00	8.00	8.00	8.00	8.00	8.00	8.00	8.00	8.00	8.00	8.00	8.00	8.00	8.00
8.3	8.30	8.30	8.30	8.30	8.30	8.30	8.30	8.30	8.30	8.30	8.30	8.30	8.30	8.30	8.30	8.30
8.5	8.50	8.50	8.50	8.50	8.50	8.50	8.50	8.50	8.50	8.50	8.50	8.50	8.50	8.50	8.50	8.50
Effluent pH = 9.0 Alk = 4.0																
7.0	7.07	7.03	7.01	7.01	7.00	7.08	7.03	7.01	7.01	7.00	7.08	7.03	7.01	7.01	7.00	7.00
7.5	7.54	7.51	7.50	7.50	7.50	7.54	7.51	7.50	7.50	7.50	7.53	7.51	7.50	7.50	7.50	7.50
7.7	7.71	7.70	7.70	7.70	7.70	7.71	7.70	7.70	7.70	7.70	7.70	7.70	7.70	7.70	7.70	7.70
8.0	8.00	8.00	8.00	8.00	8.00	8.00	8.00	8.00	8.00	8.00	8.00	8.00	8.00	8.00	8.00	8.00
8.3	8.30	8.30	8.30	8.30	8.30	8.30	8.30	8.30	8.30	8.30	8.30	8.30	8.30	8.30	8.30	8.30
8.5	8.50	8.50	8.50	8.50	8.50	8.50	8.50	8.50	8.50	8.50	8.50	8.50	8.50	8.50	8.50	8.50
Effluent pH = 9.0 Alk = 6.0																
7.0	7.10	7.04	7.02	7.01	7.01	7.11	7.04	7.02	7.01	7.01	7.11	7.05	7.02	7.01	7.01	7.01
7.5	7.56	7.52	7.51	7.50	7.50	7.56	7.52	7.51	7.50	7.50	7.54	7.51	7.50	7.50	7.50	7.50
7.7	7.72	7.71	7.70	7.70	7.70	7.71	7.70	7.70	7.70	7.70	7.70	7.70	7.70	7.70	7.70	7.70
8.0	8.00	8.00	8.00	8.00	8.00	8.00	8.00	8.00	8.00	8.00	8.00	8.00	8.00	8.00	8.00	8.00
8.3	8.30	8.30	8.30	8.30	8.30	8.30	8.30	8.30	8.30	8.30	8.30	8.30	8.30	8.30	8.30	8.30
8.5	8.50	8.50	8.50	8.50	8.50	8.50	8.50	8.50	8.50	8.50	8.50	8.50	8.50	8.50	8.50	8.50

Note: Values are shown to 2 decimal places to allow interpolation but should be rounded to 1 decimal place for comparison to standards.

The total inorganic carbon of the wastewater is:

$$C_{te} = \frac{.002 - \frac{10^{-14}}{10^{-11.1}} + 10^{-11.1}}{0.137 + 2 \times .863} = 0.000398 \text{ mole/l}$$

The dissociation constants for the ambient water are:

$$\alpha_1 = \frac{10^{-8.3} \times 8 + 10^{-7}}{(10^{-8.3})^2 + 10^{-8.3} \times 8 \times 10^{-7} + 8 \times 10^{-7} \times 4.68 \times 10^{-10}} = 0.909$$

and

$$\alpha_2 = 0.085$$

The total inorganic carbon content is:

$$C_{ta} = \frac{0.0023 - \frac{6.3 \times 10^{-14}}{10^{-8.3}} + 10^{-8.3}}{.909 + 2 \times 0.085} = .00212 \text{ mole/l}$$

The final alkalinity and inorganic carbon are:

$$Alk_f = 0.0023 + \frac{0.002 - 0.0023}{20} = .00229 \text{ eq/l}$$

$$C_{tf} = 0.00212 + \frac{0.000398 - 0.00212}{20} = 0.0020 \text{ mole/l}$$

Using Equation VI-74, the alkalinity is calculated for the range of pH values tabulated below, beginning at 8.3 and incrementing by 0.1 units.

pH	Alkalinity, eq/l
8.3	0.00217
8.4	0.00222
8.5	0.00228
8.6	not needed
8.7	not needed
8.8	not needed

The actual and calculated alkalinities match at a pH barely exceeding 8.5. Since this slightly is more than 0.2 units above ambient, the pH standard is violated.

The pH problem that results from this discharge could be mitigated in a number of ways, such as increasing initial dilution, or by treating the wastewater in order to lower the effluent pH.

END OF EXAMPLE VI-13

### 6.5.5 Dissolved Oxygen Concentration Following Initial Dilution

Dissolved oxygen standards in estuarine and coastal waters can be quite stringent. For example, the California Ocean Plan (State Water Resources Control Board, 1978) specifies that:

"The dissolved oxygen concentration shall not at any time be depressed more than 10 percent from that which occurs naturally, as the result of the discharge of oxygen demanding waste materials."

Since dissolved oxygen concentrations can naturally range as low as 4.0 to 5.0 mg/l at certain times of the year in estuarine or coastal waters, allowable depletions under these conditions are only 0.4 to 0.5 mg/l.

The dissolved oxygen concentration following initial dilution can be predicted using the following expression:

$$DO_f = \overline{DO}_a + \left[ \frac{DO_e - IDOD - \overline{DO}_a}{S_a} \right] \quad (VI-75)$$

where

- $DO_f$  = final dissolved oxygen concentration of receiving water at the plume's trapping level, mg/l
- $\overline{DO}_a$  = ambient dissolved oxygen concentration averaged from the diffuser to the trapping level, mg/l
- $DO_e$  = dissolved oxygen of effluent, mg/l
- $IDOD$  = immediate dissolved oxygen demand, mg/l
- $S_a$  = initial dilution.

The immediate dissolved oxygen demand represents the oxygen demand of reduced substances which are rapidly oxidized during initial dilution (e.g. sulfides to sulfates). The procedure for determining IDOD is found in standard methods (APHA, 1976). IDOD values are often between 1 and 5 mg/l, but can be considerably higher. When the effluent dissolved oxygen concentration is 0.0 mg/l and IDOD is negligible (which is a common situation), Equation VI-75 simplifies to:

$$DO_f = \overline{DO}_a \left( 1 - \frac{1}{S_a} \right) \quad (VI-76)$$

The ambient dissolved oxygen concentration which appears in Equations VI-75 and VI-76 is the concentration in the water column averaged between the location of the diffuser and the trapping level, while the final dissolved oxygen concentration is referenced to the plume's trapping level.

The dissolved oxygen concentration can change significantly over depth, depending on the estuary or coastal system as well as on seasonal influences (e.g. upwelling). As the plume rises during initial dilution, water from deeper parts of the water column is entrained into the plume and advected to the plume's trapping level. If

the dissolved oxygen concentration is much lower in the bottom of the water column than in the top, the low dissolved oxygen water is advected to a region formerly occupied by water containing higher concentrations of dissolved oxygen, and then a "pseudo" dissolved oxygen depletion results, solely caused by entrainment and advection and not consumption of oxygen-demanding material. The following example illustrates this process.

----- EXAMPLE VI-14 -----

Puget Sound, located in the northwest corner of the state of Washington, is a glacially carved, fjord-type estuary. The average depth of water is about 100 m (330 ft). During periods of upwelling, low dissolved oxygen water enters the estuary at depth and produces a vertical dissolved oxygen gradient throughout much of the estuary. In Commencement Bay, near Tacoma, dissolved oxygen profiles similar to the one shown in Table VI-23 have been observed. Suppose the trapping level is 43 ft (13 m) above the bottom and the minimum initial dilution is 28. Find the final dissolved oxygen concentration and calculate the percent depletion.

TABLE VI-23  
DISSOLVED OXYGEN PROFILE IN COMMENCEMENT BAY, WASHINGTON

Depth ft(m)	Temperature, °C	Dissolved Oxygen, mg/l
0 (0)	14.0	7.8
3 (1)	12.0	7.7
7 (2)	12.0	7.6
10 (3)	11.7	7.4
16 (5)	11.7	7.2
23 (7)	11.7	7.0
33 (10)	12.5	6.8
49 (15)	13.5	6.5
66 (20)	11.5	6.1
98 (30)	11.5	5.3
108 (33)	11.5	5.0

The dissolved oxygen concentration varies significantly over depth, from 5.0 mg/l at the bottom to 7.8 mg/l at the water's surface. The average concentration over the plume's trapping level is:

$$\frac{5.0 + 6.1}{2} = 5.6 \text{ mg/l}$$

Using Equation VI-76, the final dissolved oxygen concentration at the trapping level is:

$$DO_f = 5.6 \left( 1 - \frac{1}{28} \right) = 5.4 \text{ mg/l}$$

Compared to the ambient concentration at the trapping level (6.1 mg/l), the percent depletion is:

$$\frac{6.1 - 5.4}{6.1} \times 100 = 11 \text{ percent}$$

Compared to the average over the height of rise, the percent depletion is only:

$$\frac{5.6 - 5.4}{5.6} \times 100 = 4 \text{ percent}$$

----- END OF EXAMPLE VI-14 -----

In contrast to the deep estuaries on the west coast of the United States, those on the east coast are quite shallow. In the Chesapeake Bay, the largest east coast estuary, water depths are often in the 20- to 30-ft (6 to 9 m) range, with channels as deep as 60 to 90ft (18 to 27 m) in places. Because of the shallow water depths, initial dilution is often limited by the depth of the water and can be 10 or less at times of low ambient current velocity.

#### 6.5.6 Far Field Dilution and Pollutant Distribution

After the initial dilution process has been completed, the wastewater becomes further diluted as it migrates away from the ZID. Since concentrations of coliform organisms are often required not to exceed certain specified values at sensitive locations (e.g. public bathing beaches), a tool is needed to predict coliform (or other pollutant) levels as a function of distance from the ZID. This can be accomplished by solving the following expression:

$$u \frac{\partial C}{\partial x} = \epsilon_y \frac{\partial^2 C}{\partial y^2} - kC \quad (\text{VI-77})$$

where

- C = pollutant concentration
- u = current speed



$\epsilon_y$  = lateral turbulent diffusion coefficient  
 $k$  = pollutant decay rate.

Figure VI-32 shows how the sewage field spreads laterally as a function of distance from the ZID. The concentration within the wastefield,  $C(x, y)$ , depends on both  $x$  and  $y$ , with the maximum concentrations occurring at  $y = 0$ , for any  $x$  value.

It is the maximum concentration  $C(x, y = 0)$  which is of interest here. Solving Equation VI-77, the maximum concentration as a function of distance  $x$  is:

$$C = C_a + \frac{C_f - C_a}{D_s} \exp\left(-\frac{kx}{u}\right) \quad (\text{VI-78})$$

where

$D_s$  = dilution attained subsequent to the initial dilution and is a function of travel time

All other symbols have been previously defined.

The subsequent dilution is unity when  $x = 0$  (i.e., at the completion of initial dilution), so  $C = C$  at  $x = 0$ , as required. In many instances, the background concentration is negligible, so that Equation VI-78 simplifies to:

$$C = \frac{C_f}{D_s} \exp(-kt) \quad (\text{VI-79})$$

Subsequent dilution gradually increases as the wastefield travels away from the ZID and depends on mixing caused by turbulence, shear flows, and wind stresses. Often, dilution caused by lateral entrainment of ambient water greatly exceeds that caused by vertical entrainment. This is assumed to be the case here.

In open coastal areas, the lateral dispersion coefficient is often predicted using the so-called 4/3 law (Brooks, 1960), where the diffusion coefficient increases as the 4/3 power of the wastefield width. In mathematical form:

$$\epsilon = \epsilon_0 \left(\frac{L}{b}\right)^{4/3} \quad (\text{VI-80})$$

where

$\epsilon_0$  = diffusion coefficient when  $L = b$   
 $L$  = width of sewage field at any distance from the ZID  
 $b$  = initial width of sewage field.

The initial diffusion coefficient can be predicted from:

$$\epsilon_0 = 0.001b^{4/3} \quad (\text{VI-81})$$

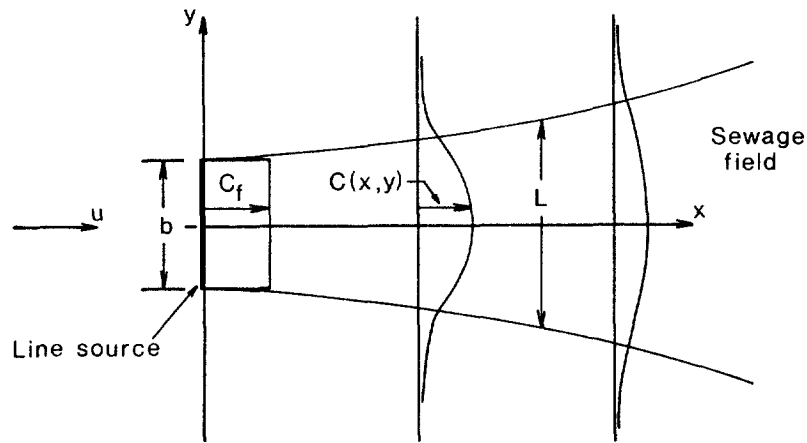


FIGURE VI -32 PLAN VIEW OF SPREADING SEWAGE FIELD

where

$\epsilon_0$  = initial diffusion coefficient,  $ft^2/sec$   
 $b$  = initial width of sewage field, ft.

Based on Equation VI-80, the centerline dilution,  $D_s$ , is given by:

$$D_s = \left[ \operatorname{erf} \left( \frac{1.5}{\left( 1 + \frac{8 \epsilon_0 t}{b^2} \right)^3 - 1} \right)^{1/2} \right]^{-1} \quad \text{(VI-82)}$$

where

$t$  = travel time  
 $\operatorname{erf}$  = error function.

The 4/3 law is not always applicable and in confined estuaries might overestimate the diffusion coefficient. Under these circumstances, it is more conservative to assume the diffusion coefficient is a constant. Equation VI-81 can be used to estimate the constant diffusion coefficient, unless the user has better data. Under these circumstances, the subsequent dilution is expressible as:

$$D_s = \left[ \operatorname{erf} \left( \frac{b^2}{16 \epsilon_0 t} \right)^{1/2} \right]^{-1} \quad \text{(VI-83)}$$

Equations VI-82 and VI-83 are cumbersome to use, especially if repeated applications are needed. To facilitate predicting subsequent dilutions, values of  $D_s$  are tabulated in Table VI-24 for different initial widths ( $b$ ) and travel times ( $t$ ).

TABLE VI-24  
 SUBSEQUENT DILUTIONS\* FOR VARIOUS INITIAL  
 FIELD WIDTHS AND TRAVEL TIMES

Travel Time(hr)	Initial Field Width (ft)													
	10	50	100	500	1000	5000	10	50	100	500				
0.5	2.3/	5.5	1.5/	2.0	1.3/	1.6	1.0/	1.1	1.0/	1.0	1.0/	1.0	1.0/	1.0
1.0	3.1/	13.	2.0/	3.9	1.6/	2.6	1.2/	1.3	1.1/	1.1	1.0/	1.0	1.0/	1.0
2.0	4.3/	32.	2.7/	8.5	2.2/	5.1	1.4/	1.9	1.2/	1.5	1.0/	1.0	1.0/	1.0
4.0	6.1/	85.	3.7/	21.	3.0/	11.	1.9/	3.5	1.5/	2.3	1.1/	1.2	1.1/	1.2
8.0	8.5/>100.		5.2/	53.	4.1/	29.	2.5/	7.3	2.0/	4.4	1.4/	1.7	1.4/	1.7
12.	10. />100.		6.3/	95.	5.1/	50.	3.0/	12.	2.4/	6.8	1.6/	2.3	1.6/	2.3
24.	15. />100.		8.9/>100.		7.1/	100.	4.2/	30.	3.4/	16.	2.1/	4.4	2.1/	4.4
48.	21. />100.		13. />100.		10. />100.		5.9/	80.	4.7/	41.	2.8/	10.	2.8/	10.
72.	26. />100.		15. />100.		12. />100.		7.3/>100.		5.8/	73	3.4/	17.	3.4/	17.
96.	29. />100.		18. />100.		14. />100.		8.4/>100.		6.6/	100.	3.9/	24.	3.9/	24.

\*The dilutions are entered in the table as  $N_1/N_2$ , where  $N_1$  is the dilution assuming a constant diffusion coefficient, and  $N_2$  is the dilution assuming the  $4/3$  law.

The initial sewage field widths range from 10 to 5,000 feet and travel times range from 0.5 to 96 hours.

The dilutions presented in the table reveal that as the initial field width increases, the subsequent dilution decreases for a given travel time. For a wider wastefield, a larger time is required to entrain ambient water into the center of the wastefield, so dilutions are lower. This illustrates that a tradeoff exists between large diffusers where initial dilution is high but subsequent dilution low, and small diffusers where initial dilution is low and subsequent dilution high.

The table also reveals that the predicted dilutions are significantly different, depending on whether Equation VI-82 or VI-83 is used. In many cases likely to be evaluated by users of this document, the 4/3 law might overestimate subsequent dilution, even if the outfall is in coastal waters. To attain the subsequent dilutions predicted by the 4/3 law at large travel times, a significant amount of dilution water must be available. Since many outfalls, particularly small ones, are often not too far from shore, the entrainment rate of dilution water can be restricted by the presence of the shoreline and the depth of the water. The wastefield from diffusers located further offshore might entrain water at a rate corresponding to the 4/2 law for an initial period of time. As the wastefield widens significantly, the rate of entrainment could decrease, and the 4/3 law no longer be obeyed.

When travel times are small (e.g., 12 hours or less), there is less discrepancy between the two methods of calculating subsequent dilution, except for the very small initial wastefield widths.

----- EXAMPLE VI-15 -----

Figure VI-33 shows an outfall which extends about one mile offshore. At the end of the outfall is a multiport diffuser, 800 feet in length. Occasionally, fecal coliform bacteria counts as high as 10,000 MPN/100 ml have been detected in the effluent of the treatment plant.

The allowable fecal coliform level at the shellfish harvesting area inshore of the diffuser is 70 MPN/100 ml. Typically, the ambient current is parallel to shore so that effluent is not carried onshore. However, when wind conditions are right, onshore transport has been observed, and the sustained transport velocity is 4 cm/s-cc (0.13 ft/sec). Determine whether the coliform standard is likely to be violated or not. Other information needed is:

Coliform decay rate = 1.0/day

Minimum initial dilution = 35

The width of the diffuser is 800 feet and will be used as the initial field width. Note, however, that the diffuser is not exactly perpendicular to shore, so that the initial field width is probably less than 800 feet in the travel direction. Using 800 feet is conservative because subsequent dilution

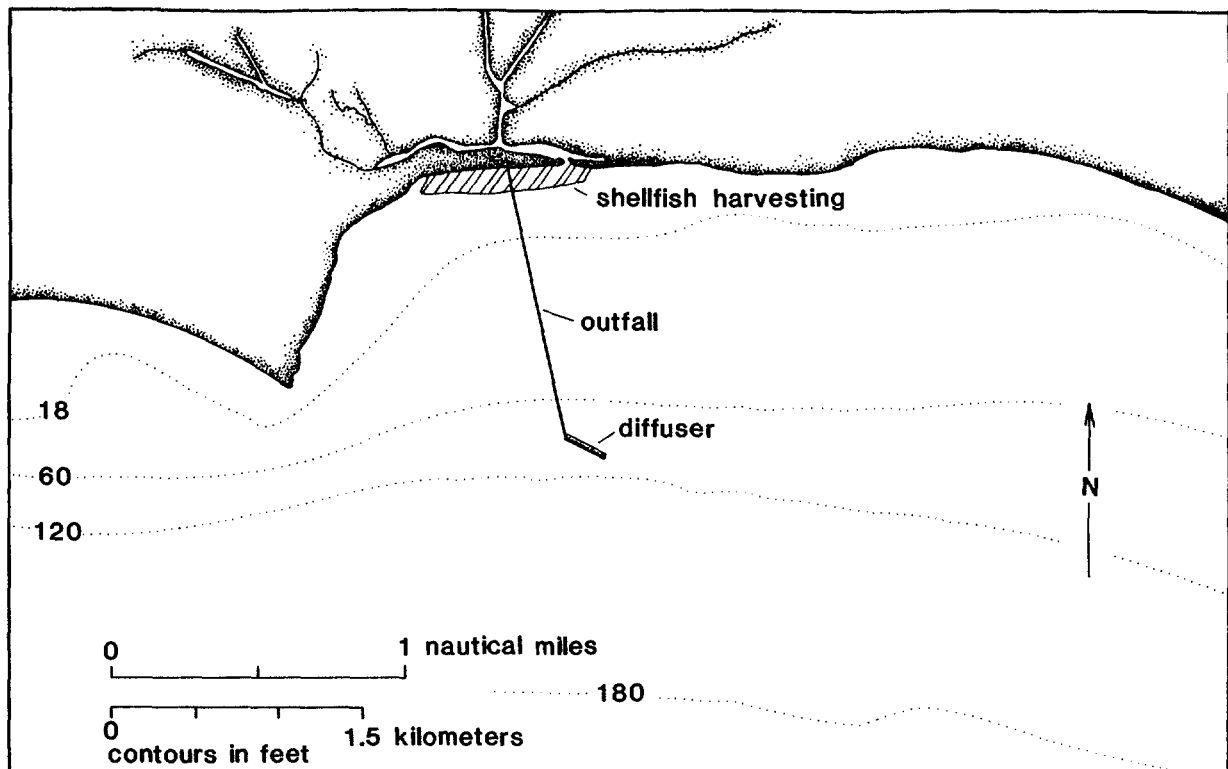


FIGURE VI-33 OUTFALL LOCATION, SHELLFISH HARVESTING AREA, AND ENVIRONS IS

will be somewhat lower under this assumption.

The coliform count following initial dilution is, using Equation VI-66:

$$C_f = \frac{10000}{35}$$

$$= 290 \text{ MPN/100 ml}$$

The travel time to the shore is:

$$\frac{5280}{0.13 \times 06} = 11 \text{ hours}$$

Interpolating from Table VI-24, the subsequent dilution is about 2.6.

Using Equation VI-79, the coliform concentration at the shoreline is:

$$C = \frac{290}{2.6} \exp \left[ -1 \times \frac{11}{24} \right]$$

$$= 70 \text{ MPN/100 ml}$$

The predicted coliform count is equal to the water quality standard. Since the subsequent dilution was conservatively estimated, it is possible that actual coliform counts will be less than 70 MPN/100 ml. However, the prediction does indicate that careful monitoring of coliform levels at the shoreline is needed to

see that the standard is not violated. Since shoreward transport of effluent is infrequent, sampling has to be conducted at times when the transport is shoreward; otherwise detected coliform levels might not represent worst-case conditions.

END OF EXAMPLE VI-15

### 6.5.7 Farfield Dissolved Oxygen Depletion

Oxygen demanding materials contained in the effluent of wastewater treatment plants can produce dissolved oxygen deficits following discharge of the effluent into receiving waters. A method will be presented here to predict the depletion following discharge from a marine outfall. The most critical cases occur when the plume and wastefield remain submerged, so that reaeration does not occur. The analysis presented here is applicable to submerged plumes only. When the wastefield is mixed uniformly across the estuary, the methods presented earlier in Section 6.4.5 are applicable.

The oxygen-demanding materials in the wastewater are the sum of the carbonaceous and nitrogenous materials (CBOD and NBOD, respectively). It is possible that the nitrogenous demand might not be exerted if a viable background population of nitrifiers is absent from the receiving water. Under these circumstances, the wastefield is likely to be dispersed before the nitrifying population can increase to numbers capable of oxidizing the NBOD. The user can perform analyses with and without NBOD exertion and then determine whether NBOD is significant or not. If it is, it is suggested that some sampling be conducted to find out whether nitrification is occurring.

The dissolved oxygen concentration in the receiving waters can be expressed as a function of travel time as follows:

$$DO(t) = DO_a + \frac{DO_f - DO_a}{D_s} - \left[ \frac{L_f}{D_s} [1 - \exp(-Kt)] \right] \quad (VI-84)$$

where

$DO(t)$  = dissolved oxygen concentration in a submerged wastefield as a function of travel time  $t$ , mg/l

$DO_a$  = ambient dissolved oxygen concentration, mg/l

$DO_f$  = dissolved oxygen concentration following initial dilution  
(see Equation VI-75)

$k$  = BOD decay rate

$L_f$  = ultimate BOD concentration above ambient at the completion of initial dilution

$D_s$  = subsequent centerline dilution.

Equation VI-84 expresses the dissolved oxygen deficit which arises due to an initial deficit at the completion of initial dilution ( $DO_f - DO_a$ ) plus that caused by

elevated BOD levels in the water column ( $L_f$ ). The elevated BOD level is either the CBOD or sum of CBOD and NBOD. The initial dissolved oxygen deficit tends to decrease at longer and longer travel times because subsequent dilution increases. However, BOD is being exerted simultaneously and tends to cause the dissolved oxygen level to drop. Depending on the particular case being analyzed, one influence can dominate the other over a range of travel times so that a minimum dissolved oxygen level can occur either immediately following initial dilution, or at a subsequent travel time. The following example illustrates both cases.

----- EXAMPLE VI-16 -----

A municipal wastewater treatment plant discharges its effluent through an outfall and diffuser system. The maximum daily CBOD value is 270mg/l, and the critical initial dilution is 114. Limited analyses have been performed on IDOD and the results vary widely, from 0 to 66 mg/l. The length of the diffuser is 500 m (1,640 ft) and can be used as the initial sewage field width. Determine the dissolved oxygen deficit produced by the discharge, assuming the wastefield remains submerged and the ambient dissolved oxygen concentration is 7.0 mg/l.

The BOD concentration at the completion of initial dilution is:

$$\begin{aligned} \frac{270}{114} &= 2.4 \text{ mg/l, BOD}_5 \\ &= 3.5 \text{ mg/l, BOD-ultimate} \end{aligned}$$

The dissolved oxygen concentration at the completion of initial dilution is (from Equation VI-75):

$$\begin{aligned} DO_f &= 7.0 + \left[ \frac{0.0 - 66. - 7.0}{114} \right] \\ &= 6.4 \text{ mg/l, when IDOD} = 66 \end{aligned}$$

$$\begin{aligned} DO_f &= 7.0 + \left[ \frac{0.0 - 0.0 - 7.0}{114} \right] \\ &= 6.9 \text{ mg/l, when IDOD} = 0 \end{aligned}$$

Note that the IDOD of 66 mg/l produces a deficit of 0.6 mg/l.

Since values of IDOD vary widely due to the limited analyses, the far field oxygen depletion curves will be calculated for the following three IDOD'S: 0, and 66 mg/l. A BOD decay rate of 0.2/day is used. When IDOD = 66mg/l, the

following oxygen depletions are predicted:

Travel Time(hr)	$D_s$ (Table VI-24)	$DO_a - DO_t$ (Equation VI-84)
1	1.	0.6
4	1.4	0.5
8	1.9	0.4
12	2.3	0.4
24	3.2	0.4
48	4.6	0.4
72	5.5	0.4
96	6.3	0.4

These results are plotted in Figure VI-34 (Curve A), along with the cases for  $IDOD_i = 40 \text{ mg/l}$  (Curve B), and  $IDOD_i = 0.0 \text{ mg/l}$  (Curve C).

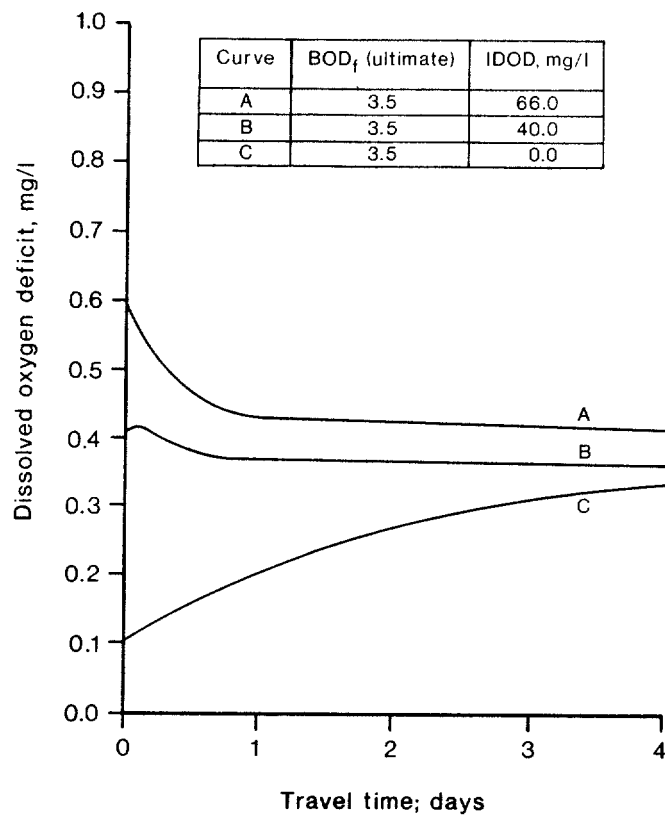


FIGURE VI -34 DISSOLVED OXYGEN DEPLETIONS  
VERSUS TRAVEL TIME



When the IDOD is 66 mg/l, the maximum dissolved oxygen deficit is 0.6 mg/l and occurs at the completion of initial dilution (a travel time of 0.0 hr). Thus, the processes which occur during initial dilution are more significant than the subsequent BOD exertion. Curve C (IDOD = 0.0 mg/l) shows the opposite situation: farfield BOD exertion is primarily responsible for the maximum oxygen depletion of 0.3mg/l. The middle curve (Curve B) shows the case when the oxygen depletion remains relatively constant over time and both the near field and farfield processes are important.

In summary, when the IDOD is above 40 mg/l, in this example the maximum oxygen depletion is controlled by the processes occurring during initial dilution. When IDOD is below 40 mg/l, BOD exertion in the far field is primarily responsible for the oxygen depletion. For primary treatment plants, IDOD values of 66 mg/l are atypical; values from 1 to 10 mg/l are much more common. Depending on whether the state dissolved oxygen standard is violated by Curve A, the user might need to make further IDOD determinations to firmly establish the true range of IDOD values.

----- END OF EXAMPLE VI-16 -----

## 6.6 THERMAL POLLUTION

### 6.6.1 General

The presence of one or more major heat sources can have a significant impact on both the local biotic community and local water quality. As a result, consideration of significant thermal discharges by the planner is essential in any comprehensive water quality analysis. Thermal power plants account for the vast majority of both the number of thermal discharges and the total thermal load. However, some industrial processes generate significant amounts of excess heat.

The most important of the impacts of heat discharge are:

- Ecological Effects: Water temperature increases change the productivity of planktonic and many benthic species. As a result local community structures are altered. Many of the species benefited by warmer conditions (e.g., blue green algae) may be considered to be undesirable. In addition, many species can perform certain life cycle functions only within a limited temperature range. Elevated temperatures may prevent some species from completing one or more life stages, thus disrupting the reproductive cycle and destroying the stability of the population.
- Water Quality Effects: Figure VI-23 showed the relative effect of salinity and ambient temperature on oxygen saturation. From this

figure, note that a 10°C\* rise in temperature decreases the oxygen saturation concentration by 1.5 to 2.0 mg/l.

- Sediment Effects: Estuarine sedimentation rates are increased by increasing local water column temperature. The significance of this increase was discussed by Parker and Krenkel (1970). They concluded that not only are sedimentation rates increased, but vertical particle size distribution, particle fall velocity, and thus bottom composition are also affected.
- Beneficial Effects: The effects of thermal discharges are not all negative. It has been shown for example, that marine biofouling is substantially reduced in warmed waters (Parker and Krenkel, 1970). In fact, the recirculation of heated discharge through the condenser has proven to be a less expensive and equally effective method of biofouling control than chlorination for several California coastal power plants. Estuarine contact recreation potentials are increased by increasing local water temperatures, and extreme northern estuaries have reduced winter ice coverage as a result of thermal discharges.

#### 6.6.2 Approach

A number of the algorithms which appear in this section were originally prepared by Tetra Tech, (1979) for the Electric Power Research Institute. The thermal screening approach for estuaries is composed of procedures that can be used to evaluate the following standards:

- The AT Criterion: The increase in temperature of water passing through the condenser must not exceed a specified maximum.
- The Maximum Discharge Temperature Criterion: The temperature of the heated effluent must not exceed a specified maximum.
- The Thermal Block Criterion: The cross-sectional area of an estuary occupied by temperatures greater than a specified value must not exceed a specified percentage of the total area .
- The Surface Area Criterion: The surface area covered by isotherms exceeding a specified temperature increment (above ambient) must not exceed a specified maximum .
- The Surface Temperature Criterion: No discharge shall cause a surface water temperature rise greater than a specified maximum above the natural temperature of the receiving waters at any time or place.

Table VI-25 presents a summary of the information needed to apply the thermal screening procedure. Data needed for the T criterion and the maximum discharge temperature criterion were included earlier in the thermal screening section for

---

\*Such a rise is common near power plant thermal Plumes.

TABLE VI -25  
DATA NEEDED FOR ESTUARY THERMAL SCREENING

Variable	Criteria Where Variable Used	Definition	Default Value
$\Delta T_c$	All	Temperature rise across the condenser ( $^{\circ}\text{F}$ )	20
$D_p$	All	Diameter of discharge pipe or equivalent diameter of discharge canal (m)	--
$U_p$	Thermal block, surface area	Exit velocity of thermal discharge (m/s)	--
$Q_p$	All	Flow rate of discharge ( $\text{m}^3/\text{s}$ )	--
$\Delta T_{tb}$	Thermal block	Temperature rise in estuary cross section that constitutes a thermal block ( $^{\circ}\text{F}$ )	5
$A_{tb}$	Thermal block	Portion of estuarine cross-sectional area that constitutes a thermal block ( $\text{m}^2$ )	25% of the estuarine cross-sectional area
$d_{tb}$	Thermal block	Average depth of estuary from discharge location to $\Delta T_{tb}$ isotherm at slack tide (m)	--
R	Thermal block, surface area	Average freshwater flow rate flowing in the estuary past the power plant site ( $\text{m}^3/\text{s}$ )	$7Q_{10}$
W	Thermal block, surface area	Width of estuary at power plant site (m)	--
$A_t$	Thermal block	Cross-sectional area at power plant site ( $\text{m}^2$ )	--
$D_l$	Thermal block, surface area	Longitudinal dispersion coefficient ( $\text{m}^2/\text{s}$ )	see text discussion
K	Thermal block, surface area	Surface thermal transfer coefficient ( $\text{Btu}/\text{m}^2 \cdot \text{d} \cdot ^{\circ}\text{F}$ )	--
$\rho$	Thermal block, surface area, surface temperature	Average mass density of ambient water at power plant site ( $\text{kg}/\text{m}^3$ )	1000 (zero salinity)
$C_p$	Thermal block, surface area	Specific heat of water ( $\text{Btu}/\text{kg} \cdot ^{\circ}\text{F}$ )	22
S	Thermal block, surface area	Tidally and cross-sectionally averaged salinity (ppt. $^{\circ}/\text{oo}$ )	--
n	Thermal block,	Manning's n ( $\text{m}^{1/6}$ )	0.016 - 0.06
$U_{\max}$	Thermal block, surface area	Maximum tidal velocity over a tidal cycle (m/s)	--
$R_h$	Thermal block, surface area	Hydraulic radius (cross-sectional area divided by wetted perimeter) (m)	--
$\Delta T_{sa}$	Surface area	Isotherm associated with legal surface area constraint ( $^{\circ}\text{F}$ )	4
$\bar{d}_s$	Surface area	Average depth under the surface area calculated for the surface area constraint (m)	--
$A_{sa}$	Surface area	Legally allowable surface area surrounded by isotherms equaling and exceeding $\Delta T_{sa}$ ( $\text{m}^2$ )	--
g	Surface temperature	Gravitational constant ( $\text{m}/\text{s}^2$ )	9.8
$\rho_p$	Surface temperature	Mass density of thermal effluent ( $\text{kg}/\text{m}^3$ )	--
h	Surface temperature	Depth to centerline of discharge jet (m)	--
$\Delta T_{st}$	Surface temperature	Maximum legally allowable surface temperature produced by a submerged discharge ( $^{\circ}\text{F}$ )	4
$\rho_s$	Surface temperature	Mass density of water at depth of submerged discharge ( $\text{kg}/\text{m}^3$ )	1000
$\frac{-d\rho}{dz}$	Surface temperature	Linear density gradient over water column depth ( $\text{kg}/\text{m}^3 \cdot \text{m}$ )	--

rivers and are not repeated here. That the maximum discharge temperature criterion for rivers can be applied to estuaries assumes the intake temperature is near ambient, and that tidal action does not cause significantly elevated temperatures near the intake.

### 6.6.3 Application

The  $\Delta T$  criterion and the effluent temperature criterion can be evaluated first following the procedures outlined in the river thermal screening section. The maximum allowable flow rate through the plant, which needs to be identified for use in evaluating those criteria, may not always have a readily determinable upper limit, unlike plants sited on rivers. For estuaries that are essentially tidal rivers, a fraction (say 20%) of the net freshwater flow rate might be used as an upper limit.

The remainder of the estuary physical screening procedure consists of evaluating the following three criteria: the thermal block, the isotherm surface area, and the surface water temperature criteria. Because of the complexity of the flow field in estuaries, slack tide conditions have been chosen as a basis for computations when possible. It is during these conditions that the effects of plume momentum and buoyancy are propagated the greatest distance across the estuary from the discharge site. It is also during slack tide that the thermal block is most likely to occur because of the absence of an ambient current that normally enhances plume entrainment of ambient water.

As the plume spreads across the estuary, the methodology assumes it to be vertically mixed. Although most plumes do not generally exhibit this behavior due to such effects as buoyancy and stratification, this approach will roughly estimate the capacity of the estuary at the power plant location to assimilate the excess heat.

In some instances, when the estuary is relatively narrow, the plume may extend across the estuary's entire width. In these cases (guidelines are given later to determine when this occurs) the near field momentum approach can be used. By using the well mixed assumption (even if the actual estuary is stratified) a lower limit on the expected temperature elevation across the estuary is obtained.

Slack tide conditions will also be used to evaluate the maximum surface temperature produced by a submerged discharge. Both vertically homogeneous and linearly stratified conditions can be evaluated.

#### 6.6.3.1 Evaluating the Thermal Block Constraint

Based upon momentum considerations, the relationship between the  $\Delta T_y$

isotherm and the distance (y) it extends from the discharge point is given by (Weigel, 1964):

$$y = \frac{y_0}{2} \left( \frac{\Delta T_c}{\Delta T_y} \right)^2, \text{ for } y \geq y_0 \quad (\text{VI-85})$$

where

$\Delta T_c$  = temperature rise across the condenser (°F)

$\Delta T_y$  = temperature excess at a distance y from the discharge outlet (°F)

y = distance measured along the jet axis originating at the discharge point (m)

$y_0$  = virtual source position (m)

The virtual source position is usually about two to ten times the diameter of the discharge orifice. The equivalent diameter of a discharge canal is the diameter of a circle whose cross-sectional area is the same as that of the discharge canal.

Brooks (1972) has shown that for round orifices, the virtual source position is approximately six times the orifice diameter. At the virtual discharge position (y =  $y_0$ ) the average excess temperature is approximately 70 percent that at the discharge location.

Since one of the assumptions used in developing Equation VI-85 is that momentum is conserved along the jet axis, an upper limit on y must be established to prevent the user from seriously violating this assumption. The upper limit can be chosen to be where the plume velocity has decreased to 1 ft/sec or 0.31 meters per second. This implies that the minimum  $\Delta T_y$  that can be evaluated using the equation is:

$$(\Delta T_y)_{\min} = 0.3 \frac{\Delta T_c}{U_p} \quad (\text{VI-86})$$

where

$U_p$  = exit velocity of thermal discharge (m/s)

$(\Delta T_y)_{\min}$  = minimum excess temperature that can be evaluated using Equation VI-86 (°F).

This constraint generally does not restrict practical application of Equation VI-85.

Using the value estimated by Brooks (1972) for the virtual source position, Equation VI-85 can be rewritten as:

$$y = 3D_p \left( \frac{\Delta T_c}{\Delta T_y} \right)^2, \text{ for } y \geq 6D_p \quad (\text{VI-87})$$

The distance, then, to the  $\Delta T_{tb}$  isotherm (the isotherm establishing the thermal block) is given as:

$$y_{tb} = 3D_p \left( \frac{\Delta T_c}{\Delta T_{tb}} \right)^2, \text{ for } \Delta T_{tb} \geq (\Delta T_y)_{\min} \quad (\text{VI-88})$$

The cross sectional area to the  $\Delta T_{tb}$  isotherm is (assuming the plume remains vertically mixed):

$$A_c = y_{tb} \bar{d}_{tb} \quad (\text{VI-89})$$

where

$A_c$  = cross sectional area measured out to the distance  $y_{tb}$  ( $\text{m}^2$ )  
 $\bar{d}_{tb}$  = average water depth over the distance  $y_{tb}$  (m).

If  $A_c < A_{tb}$  (where  $A_{tb}$  is the cross sectional area that legally defines a thermal block, e.g., 25% of the total estuary cross sectional area) then a thermal block does not develop.

If the estuary is sufficiently narrow so that  $y_{tb}$  as found by Equation VI-88 equals or exceeds the width of the estuary, the approach given above should not be used. Instead, a steady-state well mixed  $\Delta T_{ss}$  can be found as follows:

$$\Delta T_{ss} = \frac{\Delta T_c Q_p}{\sqrt{R^2 + W A_t E_L K / (\rho C_p \cdot 24 \cdot 3600)}} \quad (\text{VI-90})$$

where

$\Delta T_{ss}$  = steady state well mixed excess temperature ( $^{\circ}\text{F}$ ).

In this steady state approach,  $\Delta T_{ss}$  can no longer be estimated independently of the estuarine flow field characteristics. The surface transfer coefficient K can be determined by reference to the equilibrium temperature discussion in the river thermal screening section. Although the equilibrium temperature does not appear explicitly in Equation VI-90, its effect is indirectly included since K can not be determined independently of E. In the process of finding K, the ambient surface water temperature of the estuary generally should not be assumed to be at equilibrium because of the combined influence of ocean and river water (TRACOR, 1971), each of which may be at different temperatures.

The dispersion coefficient,  $E_L$ , is dependent on estuary characteristics. A value obtained from past studies in the vicinity of the power plant site should be used if possible. Alternatively, the methods and data provided earlier in Section 6.4.5 can be used.

### 6.6.3.2 Surface Area Constraint

The surface area constraint can be evaluated employing the same approach used to evaluate the thermal block constraint. Before beginning, Equation VI-86 should be evaluated to ensure that  $\Delta T_{sa}$  exceeds  $(\Delta T_y)_{min}$ , since  $(\Delta T_y)_{min}$  establishes the minimum excess isotherm that can be evaluated using these methods.

The distance offshore to the  $\Delta T_{sa}$  isotherm (the isotherm associated with the legal surface area constraint) can be found as:

$$y_{sa} = 3D_p \left( \frac{\Delta T_c}{\Delta T_{sa}} \right)^2 \quad \text{for } y \geq 6D_p \quad (\text{VI-91})$$

$y_{sa}$  = distance offshore at  $\Delta T_{sa}$  isotherm (m).

The **surface** area enclosed by that  $\Delta T_{sa}$  isotherm can be estimated as:

$$A_s = 6D_p \left( \frac{W_o + D_p}{2} \right) + (y_{sa} - 6D_p) \frac{W_o}{2} \left( 1 + \frac{y_{sa}}{6D_p} \right) \quad (\text{VI-92})$$

where

$$W_o = \frac{2Q_p}{U_o d_s}$$

When the estuary depth drops off rapidly from the outfall location, an appropriate average depth would be the depth to the bottom of the discharge orifice. If  $A_s < A_{sa}$ , then the surface area constraint is not violated.

When  $y_{sa}$  exceeds the width of the estuary, Equation VI-92 should not be used to find  $A_s$ . Instead, a surface area based on steady state, well mixed conditions is more appropriate and can be found from the following expression:

$$A_s = W \left[ \frac{1}{C_1} + \frac{1}{C_2} \right] \ln \left( \frac{\Delta T_{sa}}{\Delta T_{ss}} \right) \quad (\text{VI-93})$$

where

$w$  = width of estuary (m)

$$C_1 = 1/2 \left[ R/(A_t D_1) + \sqrt{(R/A_t D_1)^2 + (4WL/(\rho C_p A_t D \cdot 24 \cdot 3600))} \right]$$

$$C_2 = 1/2 \left[ R/(A_t D_1) + \sqrt{(R/A_t D_1)^2 + (WK/(\rho C_p A_t D_1 \cdot 24 \cdot 3600))} \right]$$

$\Delta T_{ss}$  was given by Equation VI-90.

When  $A_s \leq A_{sa}$  the surface area constraint is not exceeded.

### 6.6.3.3 Surface Temperature Constraint

This section provides a method for estimating the surface temperature of a buoyant plume resulting from a subsurface discharge. Slack tide conditions and a horizontal discharge configuration are considered. A horizontal configuration

should approximate conditions under which the lowest maximum surface water temperature excess is attained.

When the ambient water density is constant over depth the following two dimensionless parameter groups are needed:

$$G = \frac{h}{D_p} \quad (IV-94)$$

and

$$F \text{ (Froude Number)} = \frac{1.07 U_p}{\sqrt{\frac{\rho_s - \rho_p}{\rho_s} D_p g}} \quad (VI-95)$$

After calculating G and F, Figure VI-35 can be used to find  $S_0$ , the centerline dilution relative to the virtual source position. From this information, the maximum surface temperature elevation can be estimated as:

$$\Delta T_{\text{surface}} = \frac{\Delta T_c}{1.15 S_0} \quad (VI-96)$$

If  $\Delta T_{\text{surface}} < \Delta T_{\text{st}}$  (the legal allowable surface temperature excess), the surface temperature constraint is not violated.

In cases where the estuary is stratified more often than not at the power plant site, the maximum surface temperature calculation would more appropriately be performed under stratified conditions. If the stratification is substantial, it is possible the discharge may be prevented from reaching the surface entirely. A procedure is given here for a linearly stratified environment. Under stratified conditions the maximum height of rise of the thermal plume can be estimated by (Brooks, 1972):

$$\frac{z_{\text{max}}}{D_p} = 3.86 F^{1/4} T^{3/8} \quad (VI-97)$$

where

$$F = \frac{1.07 U}{\frac{\rho_s - \rho_p}{\rho_s} D_p g}$$

$$T = \frac{0.87 (\rho_s - \rho)}{D_p \left( \frac{-d\rho}{dz} \right)}$$

$z_{\text{max}}$  = maximum height of rise of thermal plume (m)

$\frac{d\rho}{dz}$  = linear density gradient ( $\text{kg/m}^3/\text{m}$ ).



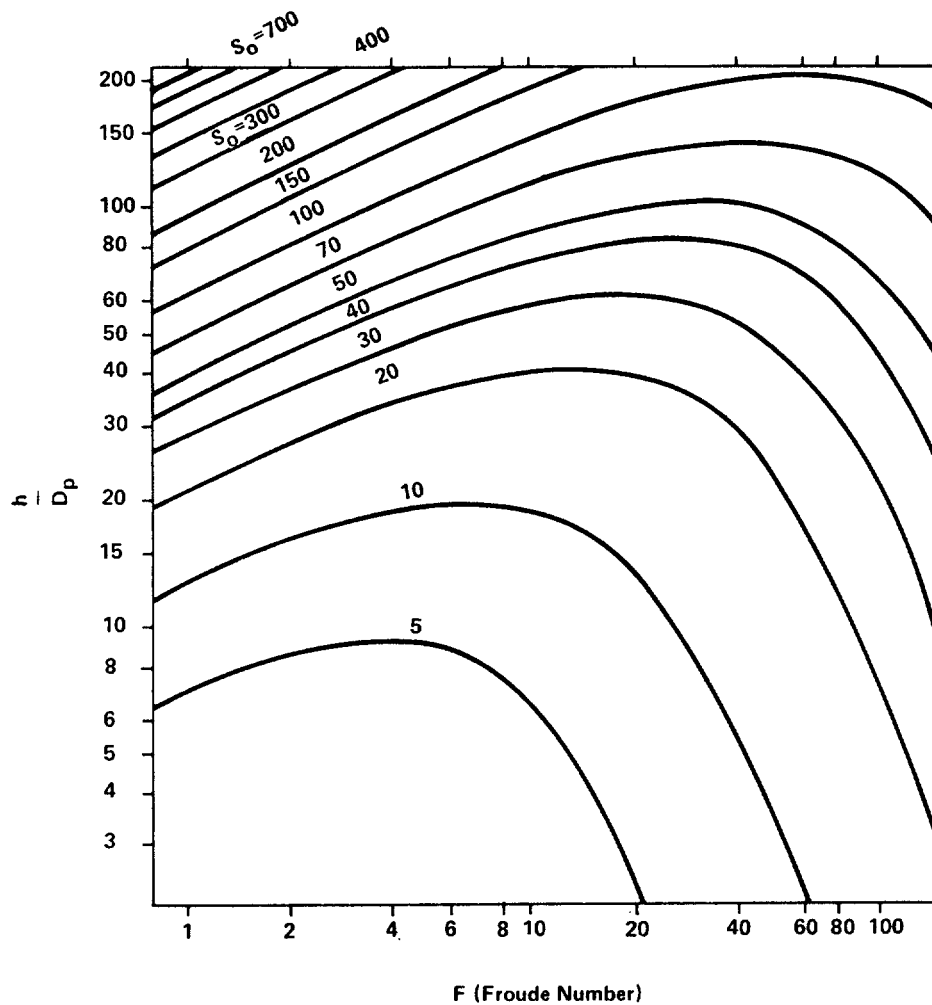


FIGURE VI -35 CENTERLINE DILUTION OF ROUND BUOYANT JET IN STAGNANT UNIFORM ENVIRONMENT (AFTER FAN, 1967)

Using Equation VI-97, the maximum rise of the thermal plume can be estimated. If it is less than the depth of water, the plume remains submerged. If, however,  $z_{max}$  exceeds the water depth, the plume will surface. In this case the methods given previously for the nonstratified case can be used to estimate the maximum surface temperature where the ambient water density should be chosen to be the depth-averaged mean.

## 6.7 TURBIDITY

### 6.7.1 Introduction

Turbidity is a measure of the optical clarity of water and is dependent upon the light scattering and absorption characteristics of both suspended and dissolved

material in the water column (Austin, 1974). The physical definition of turbidity is not yet fully agreed upon, and varies from equivalence with the scattering coefficient (Beyer, 1969), to the product of an extinction coefficient and measured pathlength (Hodkinson, 1968), and to the sum of scattering and absorption coefficients (Vandehulst, 1957). Turbidity affects water clarity and apparent water odor, and hence is of aesthetic significance. It also affects light penetration, so that increased turbidity results in a decreased photic zone depth and a decrease in primary productivity.

Turbidity levels in an estuary are likely to vary substantially in both temporal and spatial dimensions. Temporal variations occur as a function of seasonal river discharge, seasonal water temperature changes, instantaneous tidal current, and wind speed and direction. Spatially, turbidity varies as a function of water depth, distance from the head of the estuary, water column biomass content, and salinity level. Much of the complexity in the analysis of turbidity results from different sources of turbidity responding differently to the controlling variables mentioned above. As an example, increased river discharge tends to increase turbidity because of increased inorganic suspended sediment load. However, such an increase curtails light penetration, thus reducing water column photosynthesis. This, in turn, reduces the biologically induced turbidity.

Methods employed to monitor turbidity include use of a "turbidimeter". Light extinction measurements are commonly given in Jackson Turbidity Units (JTU) which are based on the turbidity of a standard clay suspension. Once standardized, this arbitrary scale\* can be used as a basis to measure changes in turbidity. The turbidity calibration scale is given in APHA (1980). From a measured change in turbidity a relative change in water quality may be inferred. Estuarine water is almost always extremely turbid, especially when compared to ocean or lake waters.

The JTU scale is not the only available turbidity scale. In 1926 Kingsbury and Clark devised a scale based on a Formazin suspension medium which resulted in Formazin Turbidity Units (FTU'S). More recently volume scattering functions (VSF) and volume attenuation coefficients have been proposed (Austin, 1974). However, JTU'S are still most commonly used as an indicator of estuarine turbidity levels.

As a rough indication of the wide variations possible in turbidity, Figure VI-36 shows suspended solid concentrations for the various sub-bays of San Francisco Bay for one year (Pearson, et al 1967). The solid line shows annual mean concentrations while the dashed lines indicate concentrations exceeded by 20% and 80% of the samples taken at each station over the one year time period. These variations at stations located near bay heads (left and right extremities of Figure VI-36) typically exceed 300% of the annual 20th percentile values. Use of extreme high/low values would produce correspondingly larger annual variations.

---

\*The JTU scale is an arbitrary scale since it cannot be directly related to physical units when used as a calibration basis for turbidimeter measurement.

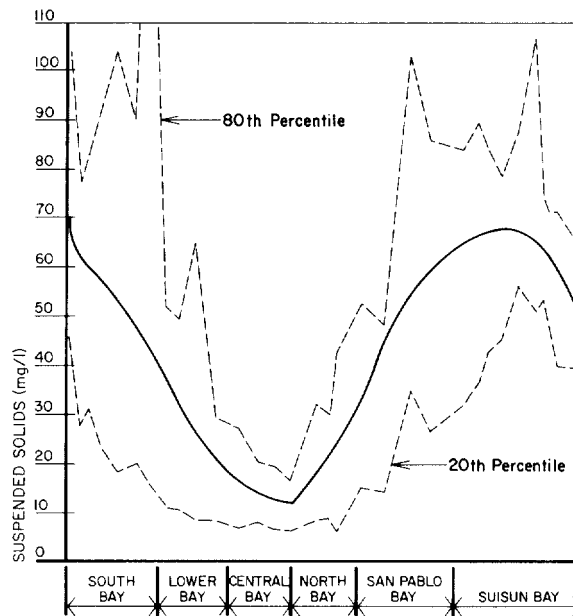


FIGURE VI -36 MEAN SUSPENDED SOLIDS IN SAN FRANCISCO BAY  
FROM: PEARSON ET AL . , 1967, PG V-15

#### 6.7.2 Procedure to Assess Impacts of Wastewater Discharges on Turbidity or Related Parameters

Numerous states have enacted water quality standards which limit the allowable turbidity increase due to a wastewater discharge in an estuary or coastal water body. The standards, however, are not always written in terms of turbidity, but are sometimes expressed as surrogate parameters such as light transmittance or Secchi disk. The following three standards provide illustrations:

##### For class AA water in Puget Sound, State of Washington:

Turbidity shall not exceed 5 NTU over background turbidity when the background turbidity is 50 NTU or less, or have more than a 10 percent increase in turbidity when the background turbidity is more than 50 NTU.

##### For class A water in the State of Hawaii:

Secchi disk or Secchi disk equivalent as "extinction coefficient" determinations shall not be altered more than 10 percent.

##### For coastal waters off the State of California:

The transmittance of natural light shall not be significantly reduced at any point outside of the initial dilution zone. A significant difference is defined as a statistically significant difference in the means of two distributions of sampling results at the 95 percent confidence level.

These standards illustrate the need for developing interrelationships between turbidity related parameters, since data might be available for one parameter while the state standard is expressed in terms of another. Based on these considerations methods will be presented to:

- Predict the turbidity in the receiving water at the completion of initial dilution
- Predict the suspended solids concentrations in the receiving water at the completion of initial dilution
- Relate turbidity and light transmittance data
- Relate Secchi disk and turbidity data.

By treating turbidity as a conservative parameter the turbidity in the receiving water at the completion of initial dilution can be predicted as:

$$T_f = T_a + \frac{T_e - T_a}{S_a} \quad (\text{VI-98})$$

where

$T_f$  = turbidity in receiving water at the completion of initial dilution  
(typical units: JTU)

$T_a$  = ambient or background turbidity

$T_e$  = effluent turbidity

$S_a$  = initial dilution.

Initial dilution can be predicted based on the methods presented earlier in Section 6.5.2. Equation VI-98 can be used, then, to directly evaluate those standards written in terms of maximum allowable turbidity or turbidity increase.

An expression similar to Equation VI-98 can be used to evaluate the suspended solids concentration in an estuary following completion of initial dilution.

Specifically:

$$SS_f = SS_a + \frac{SS_e - SS_a}{S_a} \quad (\text{VI-99})$$

where

$SS_f$  = suspended solids concentration at completion of initial dilution,  
mg/l

$SS_a$  = ambient suspended solids concentration, mg/l

$SS_e$  = effluent suspended solids concentration, mg/l

$S_a$  = initial dilution.

Consider now a situation where light transmittance data have been collected but the state standard is expressed in terms of turbidity. A relationship between the two parameters would be useful. Such a relationship can be developed by first

considering the Beer-Lambert law for light attenuation:

$$T_d = \exp(-\alpha d) \quad (\text{VI-100})$$

where

- $T_d$  = fraction of light transmitted over a depth  $d$ , dimensionless
- $\alpha$  = light attenuation, or extinction coefficient, per meter
- $d$  = vertical distance between two locations where light is measured, meters.

Austin (1974) has shown that the attenuation coefficient is expressible in terms of turbidity as:

$$\alpha = k \cdot \text{JTU} \quad (\text{VI-101})$$

where

- $\text{JTU}$  = turbidity, in Jackson turbidity units
- $k$  = coefficient ranging from 0.5 to 1.0.

Combining Equations VI-100 and VI-101 the turbidity is expressible as:

$$\text{JTU} = -\frac{1}{kd} \ln T_d \quad (\text{VI-102})$$

The increased turbidity ( $\Delta\text{JTU}$ ) is expressible as:

$$\Delta\text{JTU} = \frac{-1}{kd} \ln\left(\frac{T_{d2}}{T_{d1}}\right) \quad (\text{VI-103})$$

where

- $T_{d2}$  = light transmittance at the final turbidity
- $T_{d1}$  = light transmittance at the initial turbidity.

Vertical profiles of several water quality parameters, including percent light transmittance, have been collected in the vicinity of a municipal wastewater discharge in Puget Sound. Figure VI-37 shows each of the three profiles. If the maximum allowable turbidity increase is 5 NTU, does the discharge, based on the light transmittance profile shown in Figure VI-37 violate this requirement?

It is known that the wastefield is submerged between about 10 to 20 m below the water's surface. Light transmittances at these depths are about 18 to 20 percent. Deeper within the water column light transmittances are at background values of about 55 percent. Note that in the top few meters the

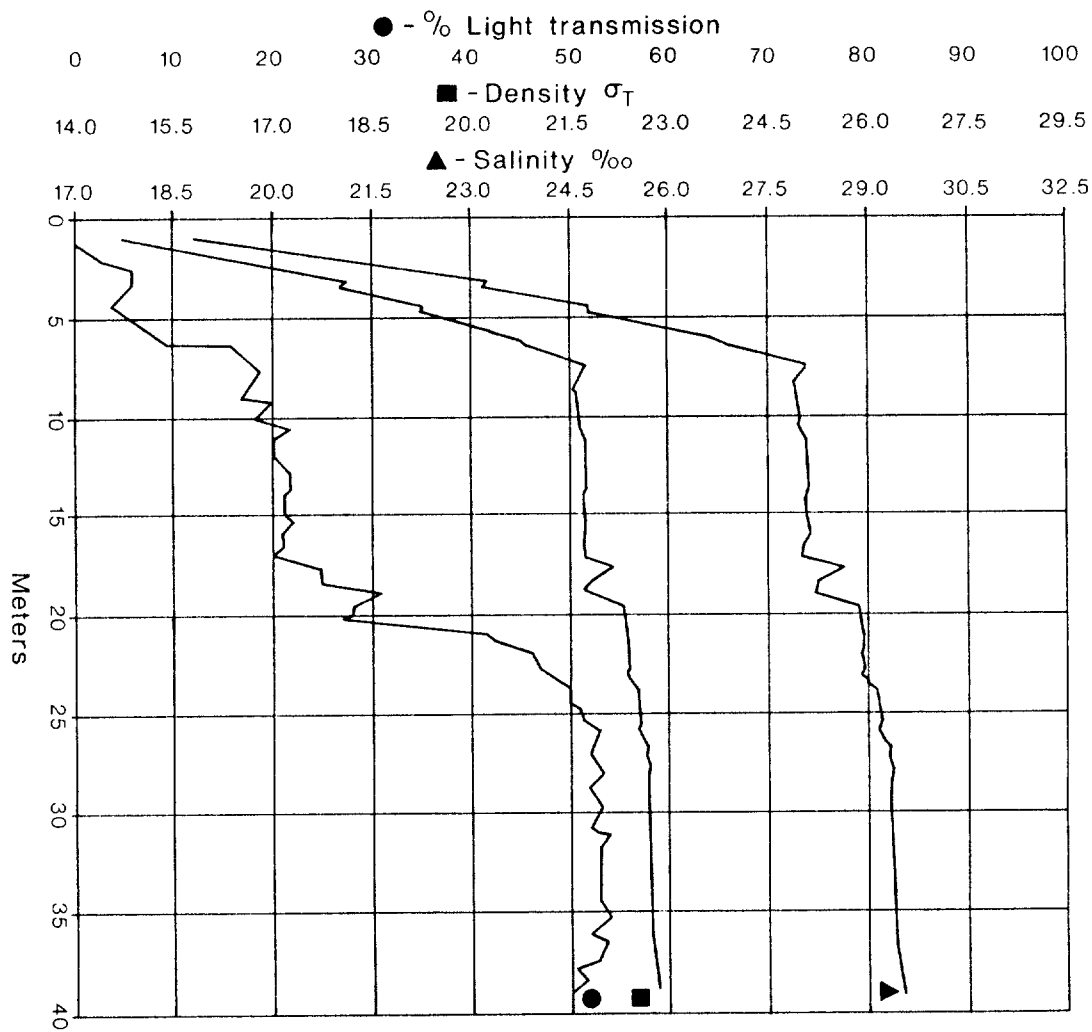


FIGURE VI -37 WATER QUALITY PROFILE OF SELECTED PARAMETERS  
NEAR A MUNICIPAL OUTFALL IN PUGET SOUND.  
WASHINGTON

Light transmittances are between 0 and 10 percent. These low transmittances are not due to the wastefield, but rather are caused by a lens of turbid freshwater. Consequently, the following data will be used here:

- k = 0.5
- d = 1 m (i.e., percent transmittance measured over 1 m)
- $T_{d2}$  = 18 percent
- $T_{d*}$  = 55 percent.

The turbidity increase is:

$$\Delta J_{TU} = \frac{-1}{(0.5)(1)} \ln \left( \frac{0.18}{0.55} \right) = 2.2 \text{ JTU}$$

Assuming JTU and NTU units are equivalent (EPA, 1979), then the increased turbidity is less than the 5.0 NTU allowable.

It is of interest to calculate the percent light transmittance within the plume that would cause a 5 NTU increase in turbidity. Using a typical background light transmittance of 50 percent found in central Puget Sound, the minimum light transmittance ( $T_{d_2}$ ) is computed to be:

$$T_{d_2} = \begin{cases} 4 \text{ percent for } k = 0.5 \\ 0.5 \text{ percent for } k = 1.0 \end{cases}$$

Light transmittances as low as 0.5 to 4 percent have been found due to causes other than the plume (e.g. plankton blooms and fresh water runoff), but the lowest light transmittances associated with the plume have been about 18 percent per meter.

----- END OF EXAMPLE VI-17 -----

Secchi disk and turbidity can be related to each other in the following manner. Assume that the extinction coefficient of visible light ( $\alpha$ ) is directly proportional to turbidity (T) and inversely proportional to Secchi disk (SD), or:

$$\alpha = k_1 T \quad (VI-104)$$

and

$$\alpha = \frac{k_2}{SD} \quad (VI-105)$$

where  $k_1$  and  $k_2$  are constants which have not yet been specified. These two relationships have theoretical bases, as discussed in Austin (1974) and Graham (1968). Combining those two expressions, the relationship between Secchi disk and turbidity becomes:

$$T = \frac{k_2}{k_1} \frac{1}{SD} \quad (VI-106)$$

Typical values of  $k_1$  and  $k_2$  are:

$k_1 = 0.5$  to  $1.0$ , where T is expressed in JTU'S

$k_2 = 1.7$  where Secchi disk is expressed in meters.

Thus Equation VI-106 provides a method of correlating turbidity and Secchi disk data.

When state standards are written in terms of Secchi disk, it is convenient

to combine Equations VI-98 and VI-106 to yield:

$$\frac{1}{SD_f} = \frac{1}{SD_a} + \frac{\frac{1}{SD_e} - \frac{1}{SD_a}}{S_a} \quad (VI-107)$$

or

$$SD_e = \left[ \left( \frac{1}{SD_f} - \frac{1}{SD_a} \right) S_a + \frac{1}{SD_a} \right]^{-1} \quad (VI-108)$$

where

$SD_f$  = minimum allowable Secchi disk reading in receiving water such that the water quality standard is not violated

$SD_a$  = ambient Secchi disk reading

$S_a$  = minimum initial dilution which occurs when the plume surfaces

$SD_e$  = Secchi disk of effluent.

Since Secchi disk measurements are made from the water's surface downward, critical conditions (in terms of the Secchi disk standard) will occur when the initial dilution is just sufficient to allow the plume to surface. It is notable that maximum turbidity or light transmittance impacts of a wastewater plume will occur when the water column is stratified, the plume remains submerged, and initial dilution is a minimum. Under these same conditions, however, Secchi disk readings might not be altered at all, if the plume is trapped below the water's surface at a depth exceeding the ambient Secchi disk depth.

#### EXAMPLE VI-18

A municipality discharges its wastewater through an outfall and diffuser system into an embayment. The state standard specifies that the minimum allowable Secchi disk is 3m. Determine whether the discharge is likely to violate the standard. Use these data:

$SD_a$  = 5 to 10m, observed range

$S_a$  = 75, minimum initial dilution when the plume surfaces

One method of approaching the problem is to assume that violation of the water quality standard is incipient (i.e.  $SD_f = 3m$ ). Under these conditions the effluent Secchi disk would have to be:

$$SD_e = \left[ \left( \frac{1}{3} - \frac{1}{5} \right) 75 + \frac{1}{5} \right]^{-1} = 0.1 \text{ m} \\ = 4 \text{ inches}$$



Thus, if the Secchi disk of the effluent exceeds 4 inches, the standards will not be violated even under these critical conditions. It would be a simple matter to measure the Secchi disk of the treated effluent to see whether the standard could be violated or not.

----- END OF EXAMPLE VI-18 -----

## 6.8 SEDIMENTATION

### 6.8.1 Introduction

Like turbidity, sedimentation is a multifaceted phenomenon in estuaries. As in rivers, estuaries transport bed load and suspended sediment. However with the time varying currents in estuaries, no equilibrium or steady state conditions can be achieved (Ippen, 1966). Additionally, while any given reach of a river has reasonably constant water quality conditions, an estuary can vary from fresh water (1 ppt. salinity) to sea water (30 ppt. salinity), and from a normally slightly acidic condition near the head to a slightly basic condition at the mouth. The behavior of many dissolved and suspended sediments varies substantially across these pH and salinity gradients. Many colloidal particles\* agglomerate and settle to the bottom. In general, all estuaries undergo active sedimentation which tends to fill them in. It is also true for essentially all U.S. estuaries that the rate of accumulation of sediment is limited not by the available sources of sediment but by the estuary's ability to scour unconsolidated sediments from the channel floor and banks.

### 6.8.2 Qualitative Description of Sedimentation

Before presenting what quantitative information is available concerning sediment distribution in an estuary, a qualitative description of sediment sources, types and distribution will be helpful. Sediment sources may be divided into two general classes: sources external to the estuary and sources internal to the estuary (Schultz and Simmons, 1957). The major sources of sediment within each category are shown below. By far the largest external contributor is the upstream watershed.

#### 1. External:

- Upstream watershed
- Banks and stream bed of tributaries
- Ocean areas adjacent to the mouth of the estuary
- Surface runoff from land adjacent to the estuary

---

\*Colloidal particles are particles small enough to remain suspended by the random thermal motion of the water.

- Wind borne sediments
- Point sources (municipal and industrial).

2. Internal :

- Estuarine marsh areas
- Wave and current resuspension of unconsolidated bed materials
- Estuarine biological activity
- Dredging.

General characterizations of U.S. estuarine sediments have been made by Ippen (1966) and by Schultz and Simmons (1957). Many individual case study reports are available for sediment characterization of most of the larger U.S. estuaries (i.e. Columbia River, San Francisco Bay, Charles Harbor, Galveston Bay, Savannah Harbor, New York Harbor, Delaware River and Bay, etc.). In general, estuarine sediments range from fine granular sand (0.01 in. to 0.002 in. in diameter) through silts and clays to fine colloidal clay (0.003 in. or less in diameter) (Ippen, 1966). Very little, if any, larger material (coarse sand, gravel, etc.) is found in estuarine sediments. Sand plays a relatively minor role in East Coast, Gulf Coast and Southern Pacific Coast estuaries. Usually it constitutes less than 5% by volume (25% by weight) of total sediments for these estuaries with most of this sand concentrated near the estuarine mouth (Schultz & Simmons, 1957.). By contrast, sand is a major element in estuarine shoaling for the north Pacific estuaries (i.e., Washington and Oregon coasts). These estuaries are characterized by extensive oceanic sand intrusion into the lower estuarine segments and by extensive bar formations near the estuarine mouth. The relative distribution of silts and clays, of organic and inorganic material within different estuaries, and, in fact, the distribution of shoaling and scour areas within estuaries, varies widely.

### 6.8.3 Estuarine Sediment Forces and Movement

As sediments enter the lower reaches of a river and come under tidal influence they are subjected to a wide variety of forces which control their movement and deposition. First, net velocities in the upper reaches of estuaries are normally lower than river velocities. Additionally, the water column comes under the influence of tidal action and thus is subject to periods of slack water. During these periods coarse sand and larger materials settle. The scour velocity required to resuspend a particle is higher than that required to carry it in suspension. Thus, once the coarser particles settle out in the lower river and upper estuarine areas, they tend not to be resuspended and carried farther into the estuary (U.S. Engineering District, San Francisco, 1975). Exceptions to this principle can come during periods of extremely high river discharge when water velocities can hold many of these particles in suspension well into or even through an estuary. Table VI-26 lists approximate maximum allowable velocities to avoid scour for various sizes of exposed particles.

TABLE VI -26  
 MAXIMUM ALLOWABLE CHANNEL VELOCITY TO AVOID BED SCOUR (FPS) (KING, 1954)

Original material excavated	Clear water, no detritus	Water transporting colloidal silts	Water transporting non-colloidal silts, sands, gravels or rock fragments
Fine sand	1.50	2.50	1.50
Sandy loam	1.75	2.50	2.00
Silt loam	2.00	3.00	2.00
Alluvial silts	2.00	3.50	2.00
Ordinary firm loam	2.50	3.50	2.25
Volcanic ash	2.50	3.50	2.00
Fine gravel	2.50	5.00	3.75
Stiff clay	3.75	5.00	3.00
Graded, loam to cobbles	3.75	5.00	5.00
Alluvial silt	3.75	5.00	3.00
Graded, silt to cobbles	4.00	5.50	5.00
Coarse gravel	4.00	6.00	6.50
Cobbles and shingles	5.00	5.50	6.50
Shales and hardpans	6.00	6.00	5.00

Values are approximate and are for unarmored sediment (sediment not protected by a covering of larger material).

Sediments are subject to gravitational forces and have size-dependent settling velocities. In highly turbulent water the particle fall velocities can be small compared to background fluid motion. Thus gravitational settling occurs chiefly in the relatively quiescent, shallow areas of estuaries or during periods of slack water. As mentioned earlier, particle settling attains a maximum in each tidal cycle during high water slack and low water slack tides. During periods of peak tidal velocity (approximately half way between high and low water) resuspension of unconsolidated sediment may occur. Thus during a tidal cycle large volumes of sediment are resuspended, carried upstream with flood flow, deposited, resuspended, and carried downstream on the ebb tide. Only those particles deposited in relatively quiescent areas have the potential for long term residence. Compounding this cyclic movement of sediments are seasonal river discharge variations which alter estuarine hydrodynamics. Thus, sediment masses tend to shift from one part of an estuary to another (Schultz and Simmons, 1975).

As fresh waters encounter areas of significant salinity gradients extremely fine particles (primarily colloidal clay minerals) often destabilize (coagulate) and agglomerate to form larger particles (floculate). The resulting floc (larger agglomerated masses) then settles to the bottom. Coagulation occurs when electrolytes, such as magnesium sulfate and sodium chloride, "neutralize" the repulsive forces between clay particles. This allows the particles to adhere upon collision (flocculation), thus producing larger masses of material. Flocculation rates are dependent on the size distribution and relative composition of the clays and electrolytes and upon local boundary shear forces (Ippen, 1966, and Schultz and Simmons, 1957). Flocculation occurs primarily in the upper central segments of an estuary in the areas of rapid salinity increase.

Movement of sediments along the bottom of an estuary does not continue in a net downstream direction as it does in the upper layers and in stream reaches. In all but a very few extremely well mixed estuaries upstream bottom currents predominate at the mouth of an estuary. Thus, upstream flow is greater than downstream flow at the bottom. This is counterbalanced by increased surface downstream flow. However, net upstream flow along the bottom results in a net upstream transport of sediment along the bottom of an estuary near the mouth. Thus, sediments and flocs settling into the bottom layers of an estuary near the mouth are often carried back into the estuary rather than being carried out into the open sea. Consequently, estuaries tend to trap, or to conserve sediments while allowing fresh water flows to continue on out to sea. At some point along the bottom, the upstream transport is counter-balanced by the downstream transport from the fresh water inflow. At this point, termed the "null zone," there is essentially no net bottom transport. Here sediment deposition is extensive. In a stratified estuary this point is at the head of the saline intrusion wedge. In a partially mixed estuary it is harder to pinpoint. Nonetheless, sedimentation is a useful parameter to analyze and will be handled in a quantitative manner beginning with Section 6.8.4.

To this point, flow in a fairly regular channel has been assumed. However, in many estuaries geomorphic irregularities exist. Such irregularities (e.g., narrow headlands) create eddy currents on their lee sides. These eddy currents, or gyres, slow the sediment movement and allow local shoaling. Additionally, large shallow subtidal or tidal flatlands exist in many estuaries. Such areas are usually well out of the influence of primary currents. As a result local water velocities are usually low and increased shoaling is possible.

Wind and waves also have a major influence on estuarine sediment distribution. Seasonal wind driven currents can significantly alter water circulation patterns and associated velocities. This in turn determines, to a large extent, the areas of net shoaling and scour throughout an estuary. Local wind driven and oceanic waves can create significant scour forces. Such scour, or particle resuspension, is particularly

evident in shallow areas where significant wave energy is present at the sediment/water interface. Local wind driven waves are a major counterbalancing force to low velocity deposition in many shallow estuarine areas (U.S. Engineering District, San Francisco, 1975).

Finally, oceanic littoral currents (long shore currents) interact with flood and ebb flows in the area of an estuary mouth. Particularly in the Pacific Northwest, sandy sediment fed from such littoral drift is a major source of estuarine sediment, and the interference of littoral drift with normal flood and ebb flows is the major factor creating estuarine bars.

Figure VI-38 shows the schematic flow of annual sediment movement through San Francisco Bay. With the exception of the magnitude of annual dredging, this is typical for most U.S. estuaries. The most important thing to observe is the dominance of resuspension and redeposition over all other elements of sediment movement including net inflow and outflow. Also note that there is a net annual accumulation of deposited sediment in the bay. This figure is also helpful in conceptualizing the sediment trap or sediment concentration characteristic of estuaries. In any year, 8-10 million cubic yards flow into the estuary and 5 to 9 million cubic yards flow out. However, over 180 million cubic yards are actively involved in annual sediment transport within the estuary.

Figure VI-39 is an idealized conceptualization of the various sediment-related processes in an estuary. It must be remembered that these processes actually overlap spatially much more than is shown and that the processes active at any given location vary considerably over time.

From this qualitative analysis, there are some general statements which can be made. Ippen (1966) drew the following conclusions on the distribution of estuarine sediments:

- The major portion of sediments introduced into suspension in an estuary from any source (including resuspension) during normal conditions is retained therein, and if transportable by the existing currents is deposited near the ends of the salinity intrusion, or at locations of zero net bottom velocity.
- Any measure contributing to a shift of the regime towards stratification causes increased shoaling. Such measures may be: structures to reduce the tidal flow and prism, diversion of additional fresh water into the estuary, deepening and narrowing of the channel.
- Sediments settling to the bottom of an estuary are generally transported upstream and not downstream. Such sediments may at some upstream point be resuspended into the upper layers and carried back downstream.
- Sediments accumulate near the ends of the intrusion zone and form shoals. Shoals also form where the net bottom velocity is zero (in the null zone).

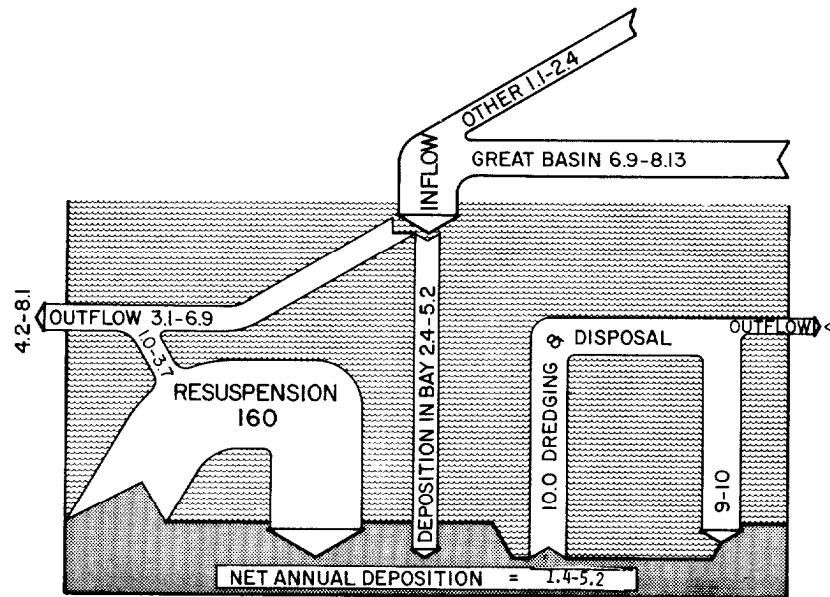


FIGURE VI -38 SEDIMENT MOVEMENT IN SAN FRANCISCO BAY SYSTEM (MILLION CUBIC YARDS), FROM: U. S. ENGINEERING DISTRICT, SAN FRANCISCO, 1975)

- o The intensity of shoaling is most extreme near the end of the intrusion for stratified estuaries and is lessened in the well mixed estuary.
- o Shoals occur along the banks of the main estuarine channel where water is deep enough to prevent wave induced scour and where velocities are reduced from main channel velocities sufficiently to allow settling.

Schultz and Simmons (1957) made similar conclusions but added the presence of shoaling at the mouth where flood and ebb currents intercept littoral drift.

#### 6.8.4 Settling Velocities

As was stated in the previous section, settling velocities do not play a great role in controlling sedimentation patterns in estuaries as they do in lakes. However, it is informative to assess settling rates for various size particles. The possible size classifications of particles and their general inclusive diameter sizes are shown in Table VI-27. Table VI-28 lists terminal settling velocities for each particle size assuming spherical particles and density of 2.0\* in quiescent water. From this table it can be inferred that particles of the medium sand class and coarser probably settle to the bottom within a very short time after entering an estuary.

\*The density of many inorganic suspended particles is approximately equal to that of sand (2.7 gm/cm<sup>3</sup>) while that of biomass and organic detritus is usually much closer to that of water and can be assumed to be about 1.1 gm/cm<sup>3</sup>.

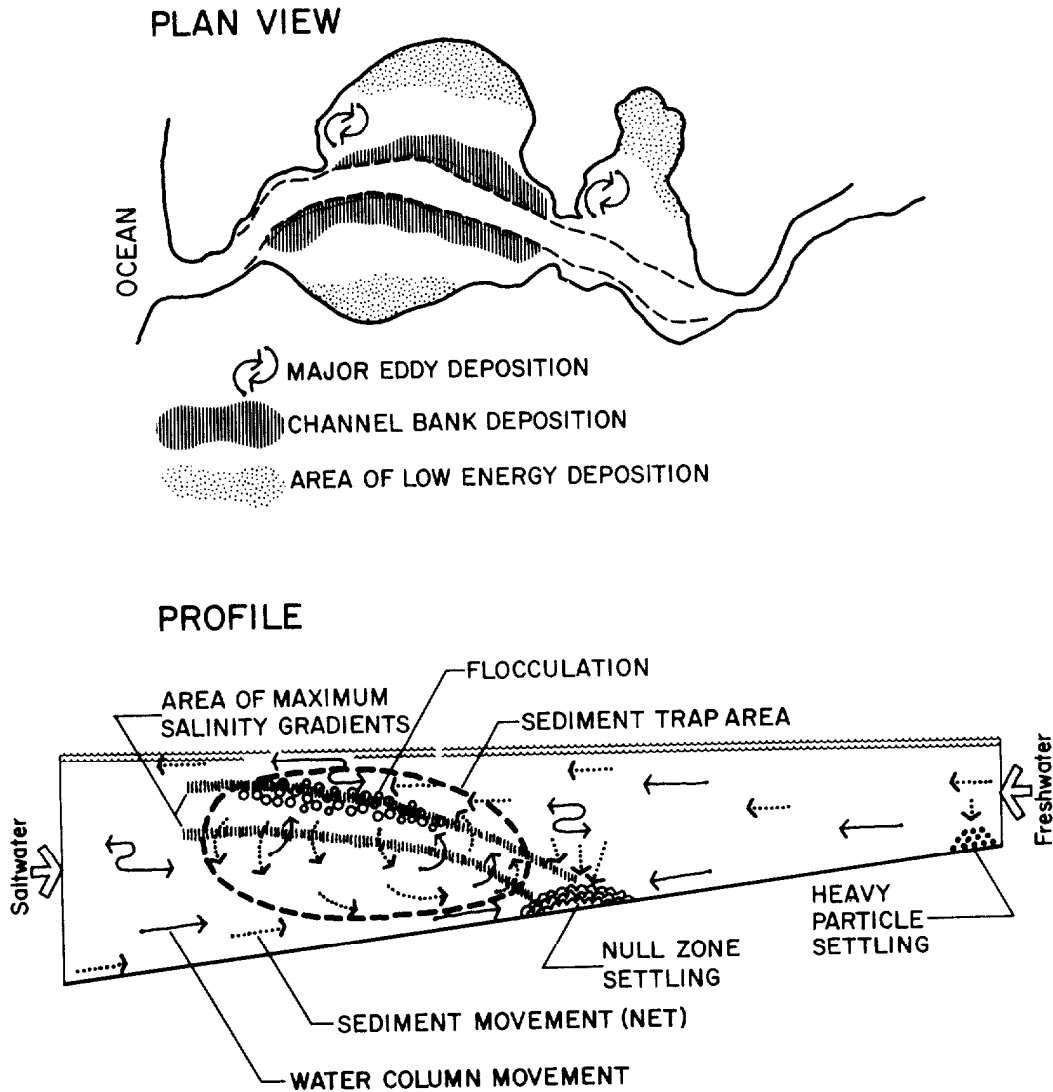


FIGURE VI -39 IDEALIZED ESTUARINE SEDIMENTATION

Turning to the other end of the particle size scale of Table VI-28, particles with a diameter of  $10^{-6}$  mm fall only  $3.1 \times 10^{-7}$  inches per hour in the most favorable environment (calm waters). Such a settling rate is not significant in the estuarine environment. Figure VI-40 shows the quiescent settling rates for particle sizes in between these two extremes since this intermediate size group is of real significance in estuarine management (primarily silts). For particles smaller than those shown in Figure VI-40, gravitational settling is not a significant factor in controlling particle motion. Particles substantially larger than the range shown in Figure VI-40 tend to settle above, or at, the head of an estuary.

Combining Figure VI-40 (fall per tidal cycle)\* with known segment flushing

\* Based on a 12.4 hour tidal cycle.

TABLE VI -27

## SEDIMENT PARTICLE SIZE RANGES (AFTER HOUGH, 1957)

	PARTICLE SIZE RANGE			
	Inches		Millimeters	
	D <sub>max.</sub>	D <sub>min.</sub>	D <sub>max.</sub>	D <sub>min.</sub>
Derrick STONE	120	36	--	--
One-man STONE	12	4	--	--
Clean, fine to coarse GRAVEL	3	1/4	80	10
Fine, uniform GRAVEL	3/8	1/16	8	1.5
Very coarse, clean uniform SAND	1/8	1/32	3	0.8
Uniform, coarse SAND	1/8	1/64	2	0.5
Uniform, medium SAND	--	-	0.5	0.25
Clean, well-graded SAND AND GRAVEL	--	--	10	0.05
Uniform, fine SAND	--	--	0.25	0.05
Well-graded, silty SAND AND GRAVEL	--	--	5	0.01
Silty SAND	--	--	2	0.005
Uniform SILT	--	--	0.05	0.005
Sandy CLAY	--	--	1.0	0.001
Silty CLAY	--	--	0.05	0.001
CLAY (30 to 50% clay sizes)	--	--	0.05	0.0005
Colloidal CLAY ( $-2\mu > 50\%$ )	--	--	0.01	$10^{-6}$ - $6$

times (in tidal cycles) the size of particles tending to settle out in each segment can be estimated. If such predictions reasonably match actual mean segment sediment particle size, then this method can be useful in predicting changes in sediment pattern. Anticipated changes in river-borne suspended sediment load by particle size can be compared to areas where each size of particle would tend to settle. This would then identify areas which would either be subject to increased shoaling or reduced shoaling and increased scour. This type of analysis has been more successful when applied to organic detritus material than for inorganic suspended loads.

A number of simplifying assumptions have gone into this settling velocity analysis. The most significant of these are:

- Water column density changes have been ignored. Inclusion of this



TABLE VI -28  
 RATE OF FALL IN WATER OF SPHERES OF  
 VARYING RADI I AND CONSTANT DENSITY OF 2<sup>a</sup>  
 AS CALCULATED BY STOKES' LAW<sup>b,c</sup> (MYSELS,1959)

Radi us mm.	Termi nal vel oci ty	
	cm. /sec.	cm. /mi n.
10	(>1)	
1	(>1)	
0.1	(>1)	
0.01	2.2x10 <sup>-2</sup>	1.3
10 <sup>-3</sup>	2.2x10 <sup>-4</sup>	0.013
10 <sup>-4</sup>	2.2x10 <sup>-6</sup>	1.3x10 <sup>-4</sup>
10 <sup>-5</sup>	2.2x10 <sup>-8</sup>	1.3x10 <sup>-6</sup>
10 <sup>-6</sup>	2.2x10 <sup>-10</sup>	1.3x10 <sup>-8</sup>
10 <sup>-7</sup>	(2.2 x1 0 <sup>-12</sup> )	

<sup>a</sup> To apply to other conditions, multiply the u value by the pertinent density difference and divide it by the pertinent viscosity in centipoises.

<sup>b</sup> Values in parentheses are calculated by Stokes' law under conditions where this law is not applicable.

<sup>c</sup> Stokes law states that the terminal velocity is proportional to the particle radius squared, the difference in density and inversely proportional to the liquid viscosity.

factor would slightly reduce the settling velocity with increased depth. This effect will be more significant for organic matter because of its lower density.

- Dispersive phenomena and advective velocities have not been considered.
- Table VI -27 and Figure VI -40 are based on the fall of perfectly spherical particles. Non-spherical particles have lower settling velocities.
- Interference between particles has not been considered. However, in a turbulent, sediment-laden estuary such interference is possible (hindered settling). The analysis of the effect of interference on settling velocities was covered in Chapter V for lakes. This analysis is also basically valid for estuaries. The effects introduced there can be applied to Figure VI -40 velocities to adjust for particle interference.

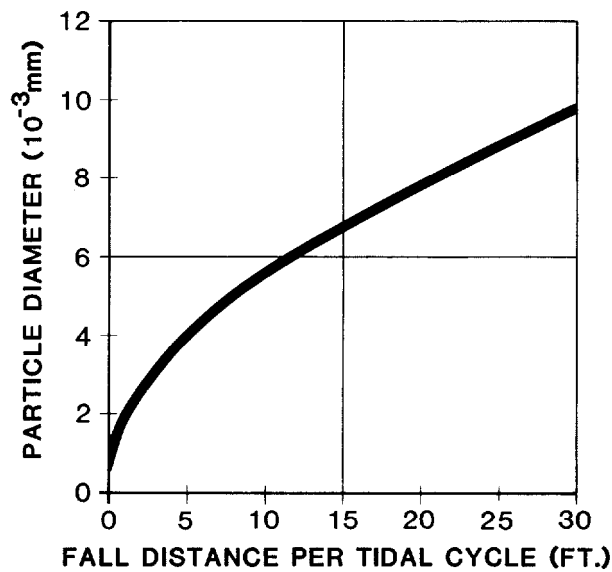


FIGURE VI -40 PARTICLE DIAMETER VS SETTLING FALL PER TIDAL CYCLE (12.3 HRS) UNDER QUIESCENT CONDITIONS (SPHERES WITH DENSITY 2.0 GM/CM<sup>3</sup>)

#### 6.8.5 Null Zone Calculations

It was previously mentioned that substantial shoaling occurs in the area of the null zone. It is possible to estimate the location of this zone, and hence the associated shoaling areas, as a function of water depth and river discharge. In addition to the importance of the null zone to shoaling, Peterson and Conomos (Peterson, et al., 1975) established the biological and ecological importance of this area in terms of planktonic production. The null zone, therefore, is both an area of potential navigational hazard and an area of major ecological importance to the planner.

Silvester (1974) summarized the analysis for estimating the location of the null zone with respect to the mouth of an estuary. The basic equation used in this analysis is:

$$\frac{\bar{S}_n}{S_o} = \frac{1000}{0.7S_o F_n^2} \frac{u_r^2}{gd} \quad (VI-109)$$

where

$\bar{S}_n$  = mean salinity (averaged vertically and over a tidal cycle) at the null point (n), (ppt)

- $S_0$  = ocean surface salinity adjacent to the estuary in parts per thousand (ppt),  
 $U_r$  = fresh water flow velocity (ft/sec)  
 $g$  = gravitational acceleration = 32.2 ft/sec<sup>2</sup>,  
 $d$  = estuarine depth, (ft)  
 $F_n$  = densimetric Froude number at the null zone where  $F_n$  is defined by:

$$F_n = U_r / \sqrt{(\Delta\rho/\rho_n)gd} \quad (\text{VI-110})$$

where

$\Delta\rho/\rho_n$  = difference between fresh water density and that at the the null zone (averaged over the depth of the water column) divided by the density at the null zone. This value may be approximated for estuarine waters by:

Combining Equations VI-109 and VI-110 and solving for  $\frac{\Delta\rho}{\rho_n}$  yields

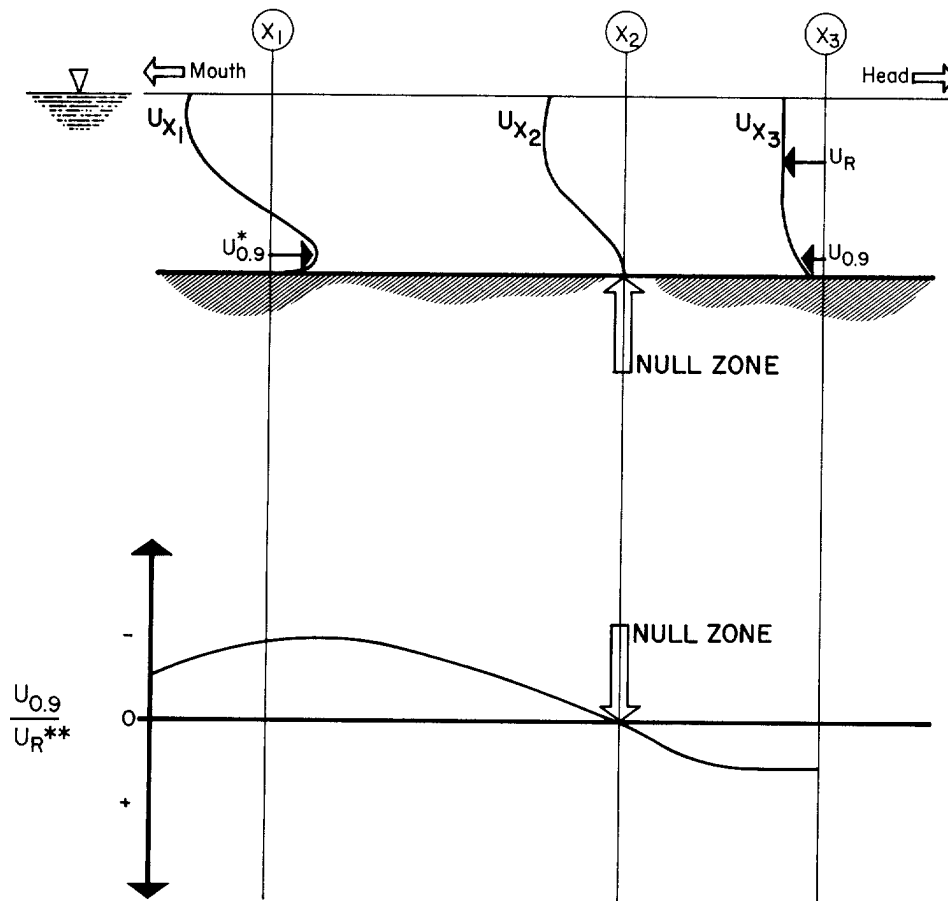
$$\frac{\Delta\rho}{\rho_n} = \frac{0.7}{1000} \xi_n \quad (\text{VI-111})$$

This formulation is particularly good for channels which are either maintained at a given depth (dredged for navigation) or are naturally regular, as "d" represents mean cross section channel depth at the null zone.

The use of these equations first requires location of the present null zone. This can most easily be done by measuring and averaging bottom currents over one tidal cycle to locate the point where upstream bottom currents and downstream river velocities are exactly equal, resulting in no net flow. This situation is schematically shown in Figure VI-41.

When this point has been established for one set of river discharge conditions, Equation VI-111 can be substituted into Equation VI-110 to calculate  $F_n$ . This  $F_n$  value is an inherent characteristic of an estuary and can be considered to be constant regardless of the variations in flow conditions or null zone location (Silvester, 1974).

With this information and a salinity profile for the estuary ( $S_x$  plotted against x from x = 0 at the mouth of the estuary to x = L at the head) the location of future null zones may be calculated. Given the new conditions of  $U_r$  (changes in river discharge) or of d (changes in channel depth, as by dredging activity), Equation VI-109 will allow calculation of a new  $\xi_n$ . This may be plotted on the salinity profile to calculate the location of a new null zone position. Even though these changes will produce a new estuarine salinity profile, the use of



\*  $U_{0.9}$  = tidally averaged velocity at a depth equal to 0.9 of the water column depth.

\*\*  $U_R$  = river flow velocity

FIGURE VI -41 ESTUARINE NULL ZONE IDENTIFICATION

Equation VI-109 and the old (known) salinity profile will produce reasonably good estimates of longitudinal shifts in the location of the null zone. Salinity profiles for appropriate seasonal conditions should be used for each calculation (e.g., low flow profiles for a new low flow null zone calculation).

EXAMPLE VI-19

Estimation of Null Zone Location

An estuary has the tidally averaged salinity profile shown in the Salinity Table below. Mean channel depth in the area of the existing null zone is 18 feet

and the salinity at that point is 10 parts per thousand (ppt). Current (low flow) river discharge velocity is 0.5 ft/sec. Normal winter (high flow) velocity is 1.8 ft/sec. It is desired to know where the null zone will be located in summer and winter if a 30 ft deep channel is dredged up to 70,000 feet from the mouth.

SALINITY DATA FOR EXAMPLE VI-19

Distance from mouth (1000ft)	5	15	25	35	45	55	65	75	85
Salinity (ppt)	30	28	25	20	13	8	6	4	1

From Equation VI-110 and Equation VI-111:

$$F_n = U_r / \sqrt{(.7/1000) (\bar{S}_n) (g) (d)}$$

$$= 0.5 \text{ ft/sec} / \sqrt{(7 \times 10^{-4}) (10 \text{ ppt}) (32.2 \text{ ft/sec}^2) (18 \text{ ft})}$$

or  $F_n = 0.248$

From equation VI-109 the null zone salinity with a deeper channel will be:

$$\bar{S}_n = \frac{S_o 1000 U_r^2}{S_o 0.7 F_n^2 g d}$$

$$= (1000) (0.5 \text{ ft/sec})^2 / 0.7 (0.248)^2 (32.2 \text{ ft/sec}^2) (30 \text{ ft})$$

$$\bar{S}_n = 6.0 \text{ ppt}$$

From the previous tabulation this will occur approximately 65,000 ft from the mouth of the estuary.

Under winter flow conditions:

$$\bar{S}_n = \frac{S_o 1000 U_r^2}{0.7 F_n^2 g d}$$

$$= (1000) (1.8 \text{ ft/sec}) / 0.7 (0.248)^2 (32.2 \text{ ft/sec}^2) (30 \text{ ft})$$

$$\bar{S}_n = 77.9 \text{ ppt}$$

This  $\bar{S}_n$  is greater than ocean salinity and will not actually be encountered. Thus, null zone shoaling will occur at the mouth if it occurs at all. This condition is common for rivers with seasonally variable flow rates.

----- END OF EXAMPLE VI-19 -----

## REFERENCES

- Abramovich, G. 1963. The Theory of Turbulent Jets. MIT Press.
- American Public Health Association. 1976. Standard Methods for the Examination of Water and Wastewater. 14th edition.
- APHA, AWWA, WPCF. 1980. Standard Methods For the Examination of Water and Wastewater. 15th edition. APHA, Washington, D.C. 1134 pp.
- Austin, R.W. 1974. Problems in Measuring Turbidity as a Water Quality Parameter. Proceedings of Seminar on Methodology for Monitoring the Marine Environment. EPA Environmental Monitoring Series. EPA-600/4-74-004.
- Beyer, G.L. 1969. Turbidity and Nephelometry. Encyclopedia of Chemical Technology. New York. pp. 738-798.
- Brooks, N.H. 1972. Dispersion in Hydrologic and Coastal Environments. Report No. KH-R-29, California Institute of Technology, Division of Engineering and Applied Science.
- California State Water Resources Control Board. 1978. Water Quality Control Plan for Ocean Waters of California. State Water Resources Control Board Resolution No. 78-2. 15 pp.
- Carhart, R.A., A.J. Policastro, S. Ziemer, K. Haake, and W. Dunn. 1981. Studies of Mathematical Models for Characterizing Plume and Drift Behavior from Cooling Towers, Volume 2. Mathematical Model for Single-Source (Single-Tower) Cooling Tower Plume Dispersion. Electric Power Research Institute, CS-1683, Volume 2, Research Project 906-1.
- Chen, C.W., and G.T. Orlob. 1975. Ecologic Simulation for Aquatic Environments. Systems Analysis and Simulation in Ecology, Volume 3. Academic Press. New York. pp. 475-558.
- DeFalco, Paul, Jr. 1967. The Estuary-Septic Tank of the Megalopolis. In: Estuaries, Ed. G.H. Lauff. American Association for the Advancement of Science. (83): 701-707.
- Duxbury, A.C. 1970. Estuaries Found in the Pacific Northwest. Proceedings, Northwest Estuarine and Coastal Zone Symposium. Bureau of Sport Fisheries and Wildlife.
- Dyer, K.R. 1973. Estuaries: A Physical Introduction. John Wiley and Sons, New York.
- Edinger, J.E. 1971. Estuarine Temperature Distributions. Estuarine Modeling: An Assessment. Chapter 4, Environmental Protection Agency Water Pollution Control Research Series, No. 16070DZV 02/71.
- Edinger, J.E., and E.M. Polk. 1969. Initial Mixing of Thermal Discharges into a Uniform Current. Water Center Report #1, Vanderbilt University.
- Fan, L.N. 1967. Turbulent Buoyant Jets into Stratified or Flowing Ambient Fluids. KH-4-15. California Institute of Technology. W.M. Keck Laboratory, Pasadena, CA.

- Fisher, H.B. 1968. Methods for Predicting Dispersion Coefficients in Natural Streams, with Applications to Lower Reaches of the Green and Duwamish Rivers, Washington. U.S. Geological Survey Professional Paper 582-A. U.S. Government Printing Office, Washington, D.C.
- Frick, W.E. 1981a. Projected Area in Plume Modeling. Submitted for publication September 1981. Corvallis, OR.
- Frick, W.E. 1981b. Comparison of PLUME and OUTPLM Predictions with Observed Plumes. Tetra Tech, Inc., Corvallis, OR.
- Frick, W.E. 1981c. A Theory and Users's Guide for the Plume Model MERGE. Tetra Tech, Inc., Corvallis, OR.
- Frick, W.E. 1980. Findings and Recommendations on the Use and Modification of the EPA Computer Model DKHPLM. Tetra Tech, Inc., Corvallis, OR.
- Frick, W.E., and L.D. Winiarski. 1980. Why Froude Number Replication Does Not Necessarily Ensure Modeling Similarity. In: Proceedings of the Second Conference on Waste Heat Management and Utilization. Miami Beach, FL.
- Frick, W.E., and L.D. Winiarski. 1975. Comments on: The Rise of Moist Buoyant Plumes. Journal of Applied Meteorology, 14(3):421.
- Giger, R.D. 1972. Some Estuarine Factors Influencing Ascent of Anadromous Cutthroat Trout in Oregon. Proceedings of the Second Annual Technical Conference on Estuaries of the Pacific Northwest. Oregon State University. pp. 18-30.
- Glennie, B. 1967. A Classification System for Estuaries. Journal of the Waterways and Harbors Division. February, 1967. pp. 55-61.
- Goodwin, C.R., W.D. Emmett, and B. Glennie. 1970. Tidal Studies of Three Oregon Estuaries. Oregon State University Engineering Experiment Station Bulletin No. 45.
- Graham, J.J. 1968. Secchi Disc Observations and Extinction Coefficients in the Central and Eastern North Pacific Ocean. Limnology and Oceanography. pp. 184-190.
- Green, J. 1968. The Biology of Estuarine Animals. University of Washington Press, Seattle, WA.
- Hansen, D.V., and M. Rattray. 1966. New Dimensions in Estuarine Classification. Limnology and Oceanography 11(3):319-316.
- Hardy, C.D. 1972. Movement and Quality of Long Island Sound Waters, 1971. Technical Report #17, State University of New York, Marine Sciences Research Center.
- Harleman, D.R.F. 1964. The Significance of Longitudinal Dispersion in the Analysis of Pollution in Estuaries. Proceedings 2nd International Conference on Water Pollution Research. Tokyo. Pergamon Press, New York.
- Harleman, D.R.F. 1971. Hydrodynamic Model - One Dimensional Models. Estuarine Modeling: An Assessment. EPA Water Pollution Control Research Series, No. 16070 DZV 02/71. pp. 34-90.

- Harleman, D., and C.H. Lee. 1969. The Computation of Tides and Current in Estuaries and Canals. U.S. Corps of Engineers Committee on Tidal Hydraulics. Technical Bulletin No. 16.
- Hodkinson, J.R. 1968. The Optical Measurement of Aerosols. In: Aerosol Science, Ed. C.N. Davies. Academic Press, New York. pp. 287-357.
- Hough, B.K. 1957. Basic Soils Engineering. Ronald Press, New York. p. 69.
- Hydroscience, Inc. 1971. Simplified Mathematical Modeling of Water Quality. U.S. Environmental Protection Agency, Water Quality Management Planning Series, Washington, D.C.
- Hydroscience, Inc. 1974. Water Quality Evaluation for Ocean Disposal System - Suffolk County, New York. Bowe, Walsh and Associates Engineers, New York.
- Ippen, A.T. 1966. Estuary and Coastline Hydrodynamics. McGraw-Hill, New York.
- Jirka, G., and D.R.F. Harleman. 1973. The Mechanics of Submerged Multiport Diffusers for Buoyant Discharges in Shallow Water. Report No. 169, MIT. Ralph M. Parsons Laboratory, Department of Civil Engineering. p. 236.
- Johnson, J. 1973. Characteristics and Behavior of Pacific Coast Tidal Inlets. Journal of the Waterways Harbors and Coastal Engineering Division. August, 197. pp. 325-339.
- Johnson, R.G., W.R. Bryant, and J.W. Hedgpeth. 1961. Ecological Survey of Tomales Bay: Preliminary Report of the 1960 Hydrological Survey. University of the Pacific, Pacific Marine Station.
- Ketchum, B.H. 1950. Hydrographic Factors Involved in the Dispersion of Pollutants Introduced Into Tidal Waters. Journal of the Boston Society of Civil Engineers 37:296-314.
- Ketchum, B.H. 1955. Distribution of Coliform Bacteria and Other Pollutants in Tidal Estuaries. Sewage and Industrial Wastes 27:1288-1296.
- Ketchum, B.H., and D.J. Keen. 1951. The Exchanges of Fresh and Salt Waters in the Bay of Fundy and in Passamaquoddy Bay. Woods Hole Oceanographic Institution. Contribution No. 593, Reference Number 51-98.
- King, H.W. 1954. Handbook of Hydraulics. McGraw-Hill, New York. pp. 7-33.
- McGauhey, P.H. 1968. Engineering Management of Water Quality, McGraw-Hill, San Francisco, CA.
- McKinsey, D. 1974. Seasonal Variations in Tidal Dynamics, Water Quality, and Sediment in Alsea Estuary. Oregon State University, Dept. of Civil Engineering, Corvallis, OR.
- Mysels, K.J. 1959. Introduction to Colloid Chemistry. Interscience New York. p.61.
- Neumann, G., and W. Pierson. 1966. Principles of Physical Oceanography. Prentice-Hall, Englewood Cliffs, NJ.



- O'Brien, M.P. 1969. Equilibrium Flow Areas of Inlets on Sandy Coasts. Journal of the Waterways and Harbors Division, Proceedings of the American Society of Civil Engineers. pp. 43-51.
- O'Connor, D.J. 1965. Estuarine Distribution of Nonconservative Substances. Journal of Sanitary Engineering Division, ASCE. SA1:23-42.
- O'Connor, D.J., and R. V. Thomann. 1971. Water Quality Models: Chemical, Physical, and Biological Constituents. Estuarine Modeling: An Assessment, Chapter III. U.S. Environmental Protection Agency Water Pollution Control Research Series No. 16070 DZV 02/71. pp. 102-169.
- Parker, F.L., and P.A. Krenkel. 1970. CRC Physical and Engineering Aspects of Thermal Pollution. Chemical Rubber Company Press, Cleveland, OH.
- Pearson, E. et al. 1967. Final Report: A Comprehensive Study of San Francisco Bay, Volume: Summary of Physical, Chemical and Biological Water and Sediment Data. Report No. 67-2, U.C. Berkeley Sanitary Engineering Research Laboratory.
- Perkins, E.J. 1974. The Biology of Estuaries and Coastal Waters. Academic Press, London.
- Peterson, O.H. et al. 1975. Location of the Non-tidal Current Null Zone in Northern San Francisco Bay. Estuarine and Coastal Marine Science (1975) 3, pp. 1-11.
- Policastro, A.J., R.A. Carhart, S.E. Ziemer, and K. Haake. 1980. Evaluation of Mathematical Models for Characterizing Plume Behavior from Cooling Towers. Dispersion from Single and Multiple Source Natural Draft Cooling Towers, NUREG/CR-1581, Volume 1. Argonne National Laboratory, Argonne, IL.
- Pritchard, D.W. 1960. The Movement and Mixing of Contaminants in Tidal Estuaries, Proceedings of the First International Conference on Waste Disposal in the Marine Environment. University of California, Berkeley.
- Pritchard, D.W. 1967. What is an Estuary: Physical Viewpoint. In: Estuaries, ed, G.H. Lauff. American Association for the Advancement of Science, Publication No. 83. pp. 2-6.
- Pritchard, D.W. 1969. Dispersion and Flushing of Pollutants in Estuaries. Journal of Hydraulics Division, ASCE, HY1. pp. 115-124.
- Pritchard, D.W., and J.R. Schubel. 1971. What is an Estuary, The Estuarine Environment-Estuaries and Estuarine Sedimentation. American Geological Institute.
- Rawn, A.M., F.R. Bowerman, and N.H. Brooks. 1960. Diffusers for Disposal of Sewage in Seawater. Journal of the Sanitary Engineering Division, ASCE, SAR. p. 80.
- Schubel, J.R. 1971. The Origin and Development of Estuaries, The Estuarine Environment-Estuaries and Estuarine Sedimentation. American Geological Institute.
- Schultz, E.A., and H.B. Simmons. 1957. Freshwater-Salt Water Density Current, a Major Cause of Siltation in Estuaries. Commission on Tidal Hydraulics, U.S. Army Corps of Engineers. Technical Bulletin No. 2.

- Serne, R. J., and B.W. Mercer. 1975. Characterization of San Francisco Bay Delta Sediments - Crystalline Matrix Study. Dredge Disposal Study of San Francisco Bay and Estuary, Appendix F. U.S. Army Corps of Engineers, San Francisco District.
- Shiraza, M.A., and L.R. Davis. 1976. Workbook of Thermal Plume Predictions: Surface Discharge. U.S. Environmental Protection Agency, Corvallis Environmental Research Laboratory, OR.
- Silvester, R. 1974. Coastal Engineering, II: Sedimentation, Estuaries, Tides, Effluents and Modeling, Elsevier Scientific Publishing, New York.
- Stommel, H. 1953. Computation of Pollution in a Vertically Mixed Estuary. Sewage and Industrial Wastes, 25(9):1065-1071.
- Streeter, V.L. 1961. Handbook of Fluid Dynamics, McGraw-Hill, New York.
- Stumm, W., and J.J. Morgan. 1970. Aquatic Chemistry: An Introduction Emphasizing Chemical Equilibria in Natural Waters. Wiley-Interscience, New York. pp. 507-513.
- Teeter, A.M., and D.J. Baumgartner. 1979. Prediction of Initial Mixing for Municipal Ocean Discharges, CERL-043. U.S. Environmental Protection Agency, Corvallis Environmental Research Laboratory, OR.
- Tesche, T.W., W.D. Jensen, and J.L. Haney. 1980. Modeling Study of the Proposed SMUD Geothermal Power Plant: Model Application Protocol. SAI No. 118-E780-11, Systems Applications, Inc., San Rafael, CA.
- Tetra Tech, Inc. 1979. Methodology for Evaluation of Multiple Power Plant Cooling System Effects. General Description and Screening. Electric Power Research Institute Report EA-1111. Pal Alto, CA.
- Tracer. 1971. Estuarine Modeling: An Assessment For: Water Quality Office, U.S. Environmental Protection Agency.
- U.S. Engineer District - San Francisco. 1975. Draft Composite Environmental Statement for Maintenance Dredging of Federal Navigation Projects in San Francisco Bay Region, California. U.S. Army Corps of Engineers.
- U.S. Environmental Protection Agency. 1979. Methods for Chemical Analysis of Water and Wastes. EPA-600/4-79-020.
- Van de Hulst, H.C. 1957. Light Scattering by Small Particles. John Wiley and Sons, New York.
- Winiarski, L.D., and W.E. Frick. 1978. Methods of Improving Plume Models. Presented at the Cooling Tower Environment 1978 Conference May 2-4, 1978, at University of Maryland, College Park, MD.
- Winiarski, L.D., and W.E. Frick. 1976. Cooling Tower Plume Model. U.S. Environmental Protection Agency Corvallis Environmental Research Laboratory, Corvallis, OR. EPA-600/3-76-100.

CHAPTER 7  
GROUND WATER

7.1 OVERVIEW

Ground water now serves as a source of drinking water for over 100 million people in the United States, including an estimated 95 percent of the rural population. Ground water is also used for irrigation, industrial process water, and cooling water. Along with its increased usage has come an awareness of the need for protecting its quality. Recent legislation and policy decisions, including the Resource Conservation and Recovery Act, its amendments, and the U.S. EPA's Ground Water Protection Strategy, attempt to minimize the impacts of waste disposal on ground water quality. Predictive methods are needed to determine the hazards associated with existing sites and proposed waste disposal activities.

7.1.1 Purpose of Screening Methods

The purpose of this chapter is to discuss approaches and hand calculation methods which can be used to predict ground water contamination for common waste disposal techniques and hydrogeologic settings. The screening methods can answer questions such as how long it will take contaminants to reach a downgradient location. For example, are the contaminants likely to reach a water supply well in 1 to 2 days or 10 to 20 years? In addition, an initial assessment of the hazard involved can be made. For example, are the predicted concentrations below detectable levels or several times greater than the drinking water standards? Based on such results, decisions can be made to improve the estimates by collecting additional data, to proceed to more detailed analyses including numerical simulation models, or to proceed to other more critical problems. Guidance is included at the end of this chapter suggesting when numerical simulation models should be used.

The hand calculation methods presented in this chapter have been selected based on a series of criteria similar to those used for the surface water methods presented in earlier chapters. The two primary criteria are 1) that, although the method can be simplified, it must be technically defensible and 2) that it require limited data which can be easily estimated or obtained. One simplification in all the methods presented is the use of spatially and temporally averaged data. To do otherwise requires a grid system, a computer, and most importantly--extensive data. Through careful selection of parameter values and the use of sensitivity analyses, results for both worst case and typical conditions can be obtained. The other criteria are 3) that the method be applicable to a range of waste sources and 4) that the method be applicable to a variety of hydrogeologic settings.

The emphasis of this chapter is on prediction of contaminant migration in porous media. Specific methods for handling solute migration in fractured formations have not

been included in this chapter. While fractured formations are important in some parts of the country, predictions of contaminant behavior in such systems are typically not amenable to screening methods. For porous media, the hand calculation methods presented can predict the time for specific concentrations to occur at downgradient locations, the time for contaminants to reach a specified distance, the concentration at a given time and location, or the maximum likely concentration at any location.

### 7.1.2 Ground Water vs. Surface Water

To orient readers who are more familiar with surface water than ground water, the major differences in both physical and chemical processes are presented before proceeding to the remainder of the chapter. Most of the differences stem from the fact that surface waters occur in surface depressions exposed to the atmosphere, while most ground water occurs in porous media typically isolated from the atmosphere. Flow velocities in ground water are much slower, on the order of meters per month rather than meters per second. A consequence of the low velocities is that flow in porous media is generally laminar, with the exception of flow in cavernous limestone formations or volcanic formations with lava tubes. The presence of laminar flow simplifies the flow calculations as will be discussed in more detail in Section 7.3. The low velocities also mean that travel times must be carefully considered in selecting sampling well locations and in interpreting previously collected data. The lower velocities of ground water have several important implications with respect to chemical processes. At low velocities, very slow chemical reactions can become important and faster reactions often can be treated as equilibrium processes.

Mixing or dispersion in ground water is more difficult to quantify than in surface water. Estimation of the extent of a mixing zone when contaminants enter an aquifer is hard to determine and depends on local heterogeneities, particularly with respect to hydraulic conductivity. The extent of vertical dispersion can be critical when interpreting data obtained from wells screened over different intervals.

Another factor which is different is that there is far less temperature fluctuation in most ground waters so that rate coefficients do not have to be continuously adjusted for short-term temperature changes. Except in geothermal waters or where a waste discharge has increased the temperature in its immediate vicinity, ground water temperatures are likely to be between 5 and 15°C.

In addition to the above differences, there are differences in the solution characteristics which influence the behavior of contaminants in subsurface waters. The important solution characteristics are total dissolved solids, dissolved oxygen, pH, redox potential, partial pressure of carbon dioxide, and solid/liquid ratio. Total dissolved solids (TDS) concentrations in ground water typically range from 100-1000 mg/l, ionic strengths are generally close to 0, and activity coefficient corrections are usually not necessary for screening calculations. If the TDS concentrations are

greater than 1000 mg/l and the contaminants are metals, the need for activity corrections should be considered. Dissolved oxygen (DO) had traditionally been considered to be absent in ground waters. However, measurements in the last 10 to 15 years have shown levels up to 4 mg/l in some systems (Wilson and McNabb, 1981). The presence or absence of DO can determine whether certain reactions will occur. For example, dehydrochlorination of trichloroethylene into the dichloro isomers and vinyl chloride can occur under anaerobic conditions but not aerobic conditions.

The presence or absence of dissolved oxygen along with other redox species also determines the redox potential. Reducing conditions (no DO, presence of dissolved iron) are common in ground water. Speciation of metals partly depends on redox conditions. The pH of the ground water influences the degree to which metals adsorb onto the permeable media. The occurrence of reducing conditions complicates sampling and can cause metals to precipitate when the ground water is brought to the surface and is exposed to the atmosphere. Another factor which causes problems in sampling, particularly for metals, is that the ground water is typically supersaturated with respect to atmospheric levels of carbon dioxide. When samples are brought to the surface, the weak acid  $\text{CO}_2$  may be lost. This causes the sample pH to rise and may thereby change the speciation of metals and allow some to precipitate.

The high solid to liquid ratio in ground water is a major difference from surface water. Interfacial phenomena such as adsorption can be important chemical attenuation processes. Example problems presented in later sections clearly show that solutes with strong affinities for the solid phase do not travel far in porous media. Unlike in surface waters, the particles to which the contaminants adsorb are usually immobile. Because the particles are in continual contact with the flowing water the sorbed contaminants can act as secondary sources and may desorb when the concentrations in the ground water decrease. Resorption can occur in rivers but is less important since most of the sorbed contaminants become part of the bottom sediment.

A final difference between surface and ground waters is in the screening methods themselves. As will be discussed in more detail, considerably more analysis is required prior to the use of a particular screening method to determine the flow paths of the contaminants in ground water. Flow paths for rivers are easily determined by visual observation, whereas in ground water they are based on limited data and calculations.

### 7.1.3 Types of Ground Water Systems Suitable for Screening Methods

The screening methods presented in this chapter are applicable to porous media where the capacity to transmit water is due to primary permeability (connected pores) rather than due to secondary permeability (e.g., fractures, lava tubes). If fractures in a formation are relatively uniform in size and spatially distributed over the area of interest, these formations could be analyzed using the screening methods by

substituting an equivalent permeability from pump tests. More complex fractured formations (e.g., when the fractures are predominantly in one direction) are not amenable to screening methods.

Major types of aquifers in the United States are shown in Figure VII-1. The divisions shown are unconsolidated and consolidated formations, alluvial aquifers along major rivers, and areas where aquifer yields are less than  $0.2 \text{ m}^3/\text{min}$  (50 gpm) to individual wells. The stratigraphy in an area can range from a layered system such as on Long Island (Figure VII-2) to a complex system of unconsolidated glacial formations overlying several different types of consolidated rock formations such as occur in New Jersey (Figure VII-3). In such complex hydrogeologic systems, some aquifers may be confined (i.e., not open to the atmosphere). In the arid western part of the country, additional complications can occur. Examples include closed basins where evapotranspiration is the only outflow and highly faulted basins which can have large changes in permeability over short distances (Figure VII-4). Infiltration in such basins typically occurs along the basin boundaries, primarily from runoff in the mountains, instead of directly through the valley floor. There are also more likely to be thick unsaturated zones. Screening methods are presented in this chapter which predict the migration of contaminants in both the unsaturated and saturated zones.

#### 7.1.4 Pathways for Contamination

The usual division of waste sources into point and nonpoint sources can be used for ground water but this kind of division does not indicate the variety of ways in which contaminants can enter ground water systems. Waste can enter the ground water directly, through recharge of contaminated surface water, or through leakage from one aquifer to another. In some cases, recharge of contaminated water may not be considered because of the inferred presence of an impermeable layer or confining bed, when in reality the impermeable layer or bed is discontinuous and contamination of an underlying or overlying aquifer has occurred.

Examples of point sources of importance to ground water include surface impoundments, landfills, spills and leaks, and injection wells. The largest number of impoundments are associated with the oil and gas industry, although larger volumes of waste are disposed by the paper, chemical, and metals processing industries (U.S. EPA, 1979). The relative number of impoundments by state is shown in Figure VII-5. Landfills are used to dispose of sludge from municipal waste treatment plants, ash and flue-gas desulfurization sludge from coal-fired utilities, and wastes from other types of industries. The wastes can contain high concentrations of metals, organic chemicals, and acids. Spills and leaks, particularly from underground storage tanks, have recently been recognized as a major source of contamination, especially with respect to organic chemicals (e.g., trichloroethylene and gasoline). Injection wells have been used primarily for oil field brines and the associated "produced waters", but

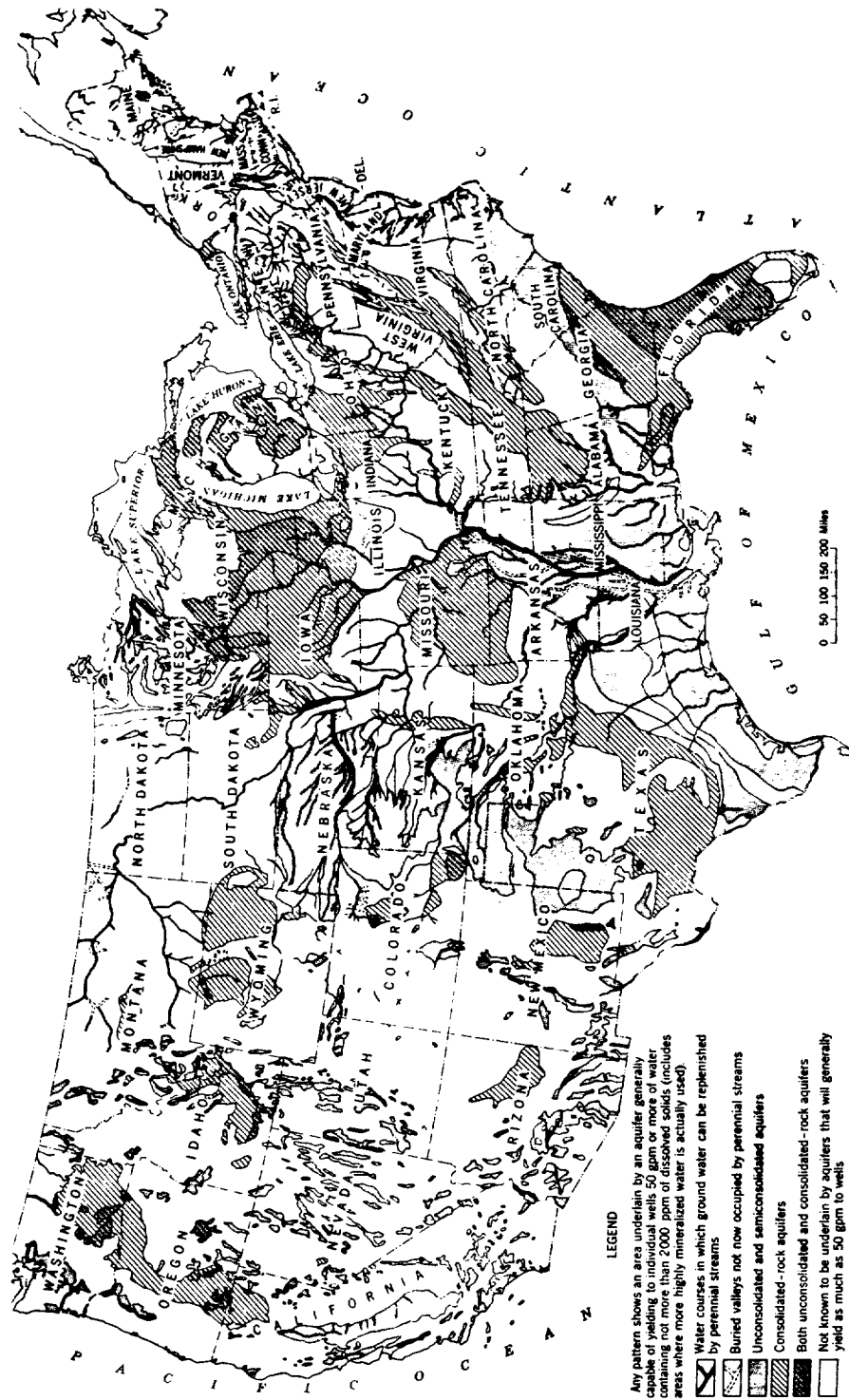


FIGURE VII-1 MAJOR AQUIFERS OF THE UNITED STATES. REFERENCE: THOMAS (1951)

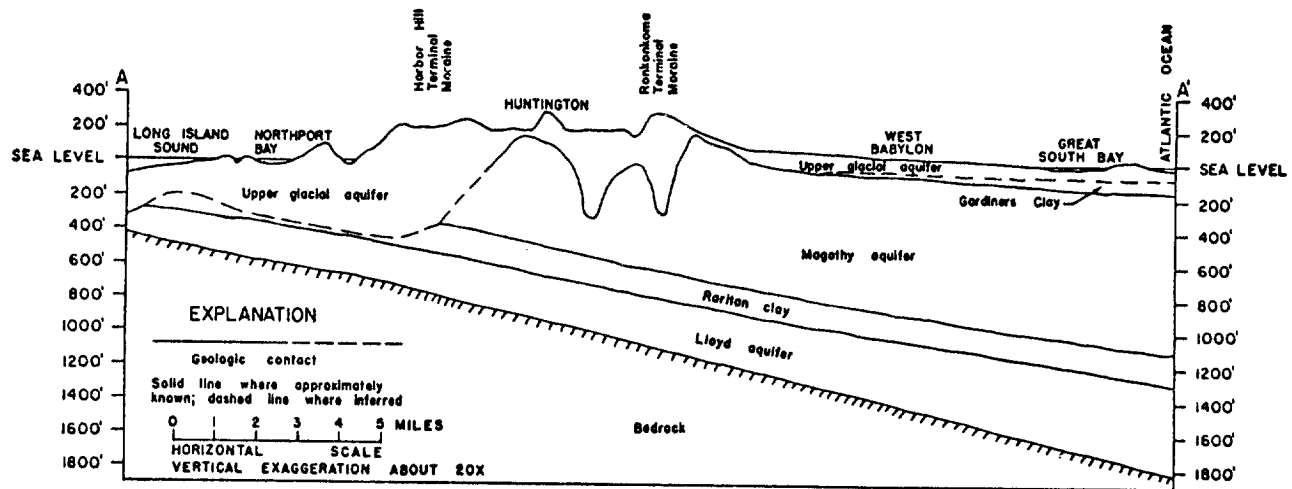


FIGURE VII -2 GEOLOGIC SECTION IN WESTERN SUFFOLK COUNTY, LONG ISLAND, SHOWING BOTH CONFINED AND UNCONFINED AQUIFERS, REFERENCE: TETRA TECH (1977)

some manufacturing process wastes and mining wastes have also been injected into deep aquifers or into dry wells in areas with deep unsaturated zones. Contamination from wells can also occur from migration from one zone or aquifer to another along abandoned or improperly plugged casings.

Nonpoint sources, which result in contaminants being spread over large areas, include seepage from residential areas with septic tank systems, infiltration of runoff, and application of pesticides and fertilizer to agricultural and residential land. The methods presented in this chapter are oriented more towards point sources but can be used to estimate the overall effect on an aquifer of a wide-spread contaminant.

#### 7.1.5 Approach to Ground Water Contamination Problems

The initial step in analyzing a ground water problem is the selection of the spatial and temporal framework for the problem. The spatial representation is determined from the disposal system configuration (i.e., a large pond or landfill versus a leak or an injection well) and the type of question being asked. For example, if the need is to predict the concentration at the water table of a contaminant spilled at the surface, a one-dimensional vertical transport method may be most appropriate. If the need is to predict the areal extent of a ground water plume, a two-dimensional method for flow in the saturated zone would be preferred. The temporal representation of a problem must consider whether a waste source should be considered as a one-time



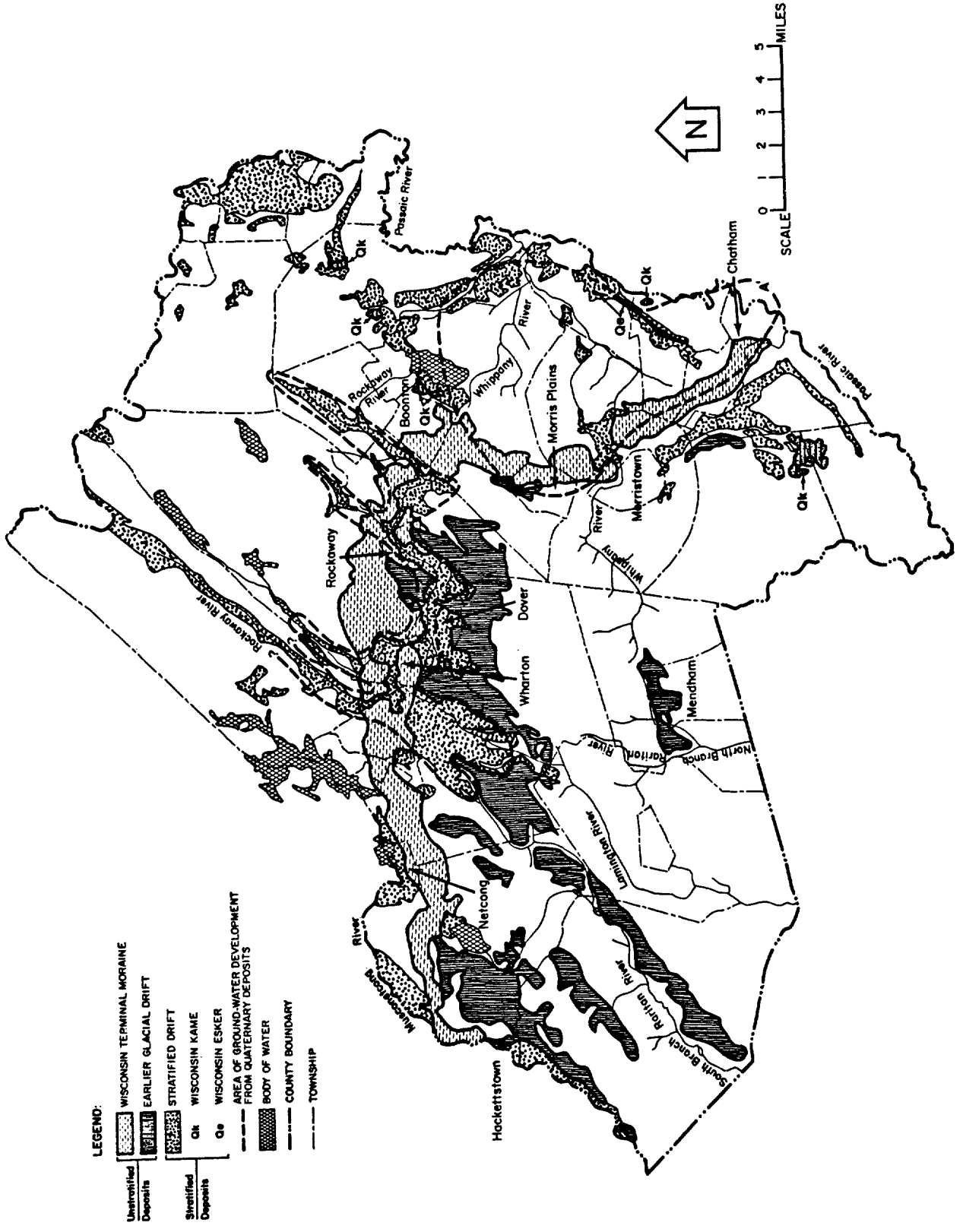
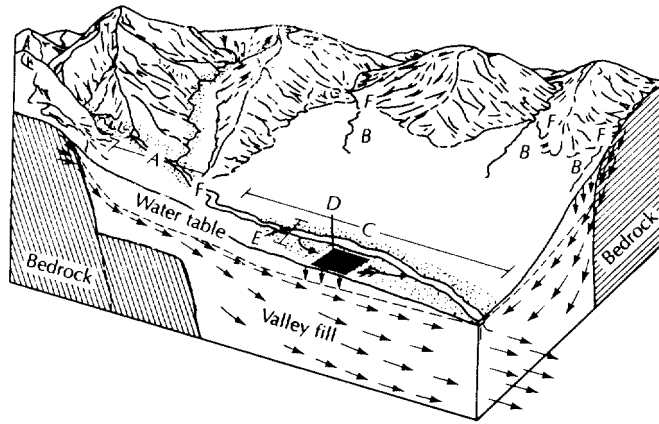
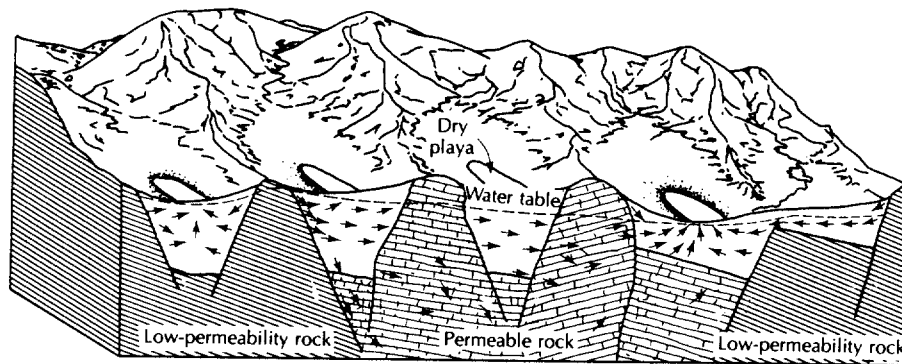


FIGURE VII-3 DETAILED QUATERNARY GEOLOGIC MAP OF MORRIS COUNTY (AFTER GILL AND VECCHIOLI, 1965)



A) VALLEY IN BASIN AND RANGE AREA SHOWING THICK UNSATURATED ZONE OF COARSE SAND AND GRAVEL



B) FAULTED BASINS WHICH CAN BE CLOSED. RECHARGE IS MOSTLY FROM RUNOFF IN MOUNTAINS NOT RAINFALL DIRECTLY ON VALLEY FLOOR

FIGURE VII -4 GENERALIZED CROSS-SECTIONS SHOWING FEATURES COMMON IN ARID WESTERN REGIONS OF THE UNITED STATES. REFERENCE: EAKIN, PRICE, HARRILL (1976)

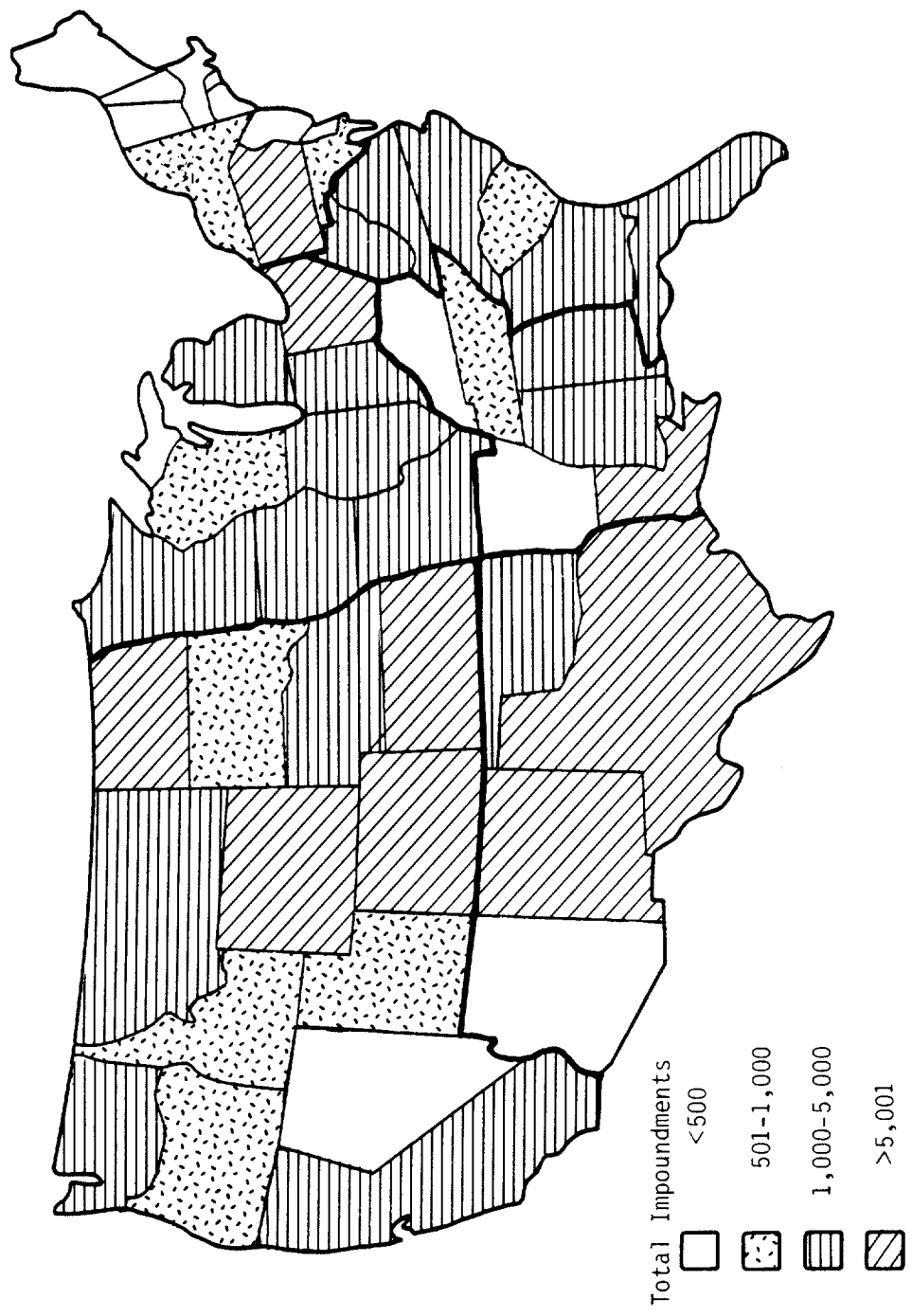


Figure VII-5 Number of Waste Impoundments by State (after U.S. EPA, 1979a)

discharge (slug), as a continuous discharge, or otherwise. This distinction does not have to be made in absolute terms but instead can be made relative to the time scale of the problem. For example, if waste had been discharged to a pond for a one-month period and the objective was to predict concentrations at a downgradient well five years later, the waste source could be considered to act as a slug discharge. Examples of how problems should be proposed (set-up) are given in Section 7.5.

#### 7.1.6 Organization of This Chapter

The remaining sections describe the specific screening methods, how to estimate or obtain the necessary data, and how to interpret the results. Section 7.2, Aquifer Characterization, is intended as a reference section for those readers who may not be familiar with ground water terminology. Parameter nomenclature which may be encountered in the literature is explained, and typical values are provided. Information is also included on methods for estimating the parameters and for quantifying them either in the laboratory or in the field. Section 7.3, Ground Water Flow Regimes, describes detailed procedures for estimating seepage velocities and travel times for conservative constituents and includes example problems. Section 7.4, Pollutant Transport Processes, discusses the major physical and chemical transport processes. A practical approach is provided for estimating dispersion and diffusion. This section also discusses pollutant-soil interactions and the chemical and biological processes which are pertinent to subsurface problems. Methods are described for estimating the necessary rate coefficients and for incorporating them into the screening methods. Section 7.5, Methods for Predicting the Fate and Transport of Conventional and Toxic Pollutants, presents five different calculation methods. The methods predict migration of solutes from a contaminated aquifer to a well, from an injection well out into an aquifer, from the surface down to the water table, and from a one-time or continuous discharge downgradient in the saturated zone. For each method selected the following information is provided:

- Uses of the method
- Brief description of method and its theoretical basis
- Assumptions and simplifications required
- Types of input data needed
- Worked-out example problems
- Limitations of the method.

Finally, Section 7.6, Interpretation of Results, discusses reference criteria which may be of interest, and methods for estimating the uncertainty associated with the results. Guidelines are discussed for suggesting when more detailed analyses, including use of numerical simulation models, are warranted given the relative hazard, the uncertainty associated with the screening results, data availability, and time and budget constraints. Section 7.7, References, includes the references cited in the chapter and a list of additional material which may be helpful, particularly with respect to field sampling.

## 7.2 AQUIFER CHARACTERIZATION

This section is intended as a reference section for those users of the manual who may not be familiar with the parameters used in ground water investigations. It is anticipated that most readers will use this section only as needed to obtain a typical value for a given parameter or to review methods for measuring the parameters.

Before the transport of contaminants in ground water can be predicted, estimates of key properties of the porous media are needed. Section 7.2 discusses the definition and use of these parameters in the screening methods. The key parameters have been grouped into those characteristic of the porous media (Section 7.2.2), those used to estimate flow in the saturated zone (Section 7.2.3), and those used to estimate flow in the unsaturated zone (Section 7.2.4). Tables of average and typical values for a wide range of geologic formations have been included. The specific parameters are listed in Table VII-1. Additional parameters, also shown in this table, are discussed in Appendix I. The parameters given in Appendix I are not generally needed for the screening methods presented later in this chapter but may be encountered in the ground water literature. Methods for measuring the parameters in the field or laboratory or estimating them from other parameters are presented in Section 7.2.5. A discussion has also been included in this section on sample size and confidence levels.

### 7.2.1 Physical Properties of Water

For the vast majority of problems of interest, the concentration of dissolved solids in the ground water is so low that it does not affect the physics of fluid flow. Hence, the physical properties of the transport fluid such as density, viscosity, compressibility, etc. are assumed to be independent of the solute concentrations and to be equal to those of pure water. Situations where this assumption may not be true are when the solute concentrations are very high, (e.g., brackish aquifers or where large quantities of pure solute with a density different than water have been mixed with ground water (e.g., oil, gasoline)). The principal physical properties of water that are of interest in ground water flow are density, viscosity, and compressibility. In most situations these properties can be considered constant as shown below:

Compressibility of water at 1 atm and 4°C:  $4.96 \times 10^{-11}$  cm sec<sup>2</sup>/g

Density of water at 1 atm and 4°C: 1.000 g/cm<sup>3</sup>

Viscosity of water at 1 atm and 4°C: 0.01567 g/cm sec

Values for these properties as a function of temperature are included in Appendix I.

### 7.2.2 Physical Properties of Porous Media

The physical properties of porous media can be described by the relative state of its three phases or primary components. These are the solid, liquid, and gaseous phases. A schematic representation of a soil's three phases is given in Figure VII-6.

TABLE VII-1

## AQUIFER PARAMETERS AND THEIR RELATIVE IMPORTANCE AS SCREENING PARAMETERS

Symbol	Parameter	Section Where Discussed	Relative Importance As A Screening Parameter	
			Low <sup>a</sup>	High <sup>b</sup>
$\rho_w$	density of water	I-1	X	
$\mu$	viscosity of water	I-1	X	
$\beta_w$	compressibility of water	I-1	X	
$\rho_s$	particle density	I-1	X	
$\rho_b$	bulk density	7.2.2.1		
$d_e$	particle-size distribution	7.2.2.2	X	
$p$	porosity	7.2.2.3		
$\theta$	water content	7.2, 2.4		
$S_r$	specific retention	I-1	X	
$S_y$	specific yield	I-1	X	
$\alpha_s$	compressibility of soil	I-1	X	
$S_s$	specific storage	I-1	X	
$S$	storativity	I-1	X	
$b, h$	aquifer thickness	7.2.3.2		X
$K, T$	hydraulic conductivity and transmissivity:			
	saturated media	7.2.3.2		X
	unsaturated media	7.2.4.3		X
$x, y, z$	anisotropy	7.2.3.2	X	
$\theta(\psi)$	soil-moisture characteristic curve	I-1	X	
$\theta-\psi$	hysteresis	I-1	X	
$h$	water level elevation	7.3.2		X
$\phi_g, \psi_g, H_g$	gravitational potential	I-1	X	
$\phi_p, \psi_p, H_p$	pressure potential	I-1	X	
$\phi_o, \psi_o, H_o$	osmotic potential	I-1	X	
$I$	hydraulic gradient	7.3.1		X

<sup>a</sup>Parameter is not essential and/or its value can be easily obtained from tables given in Section 7.2 and Appendix 1.

<sup>b</sup>Parameter is essential. Estimates or measurements of its value are used in the methods included in this chapter.

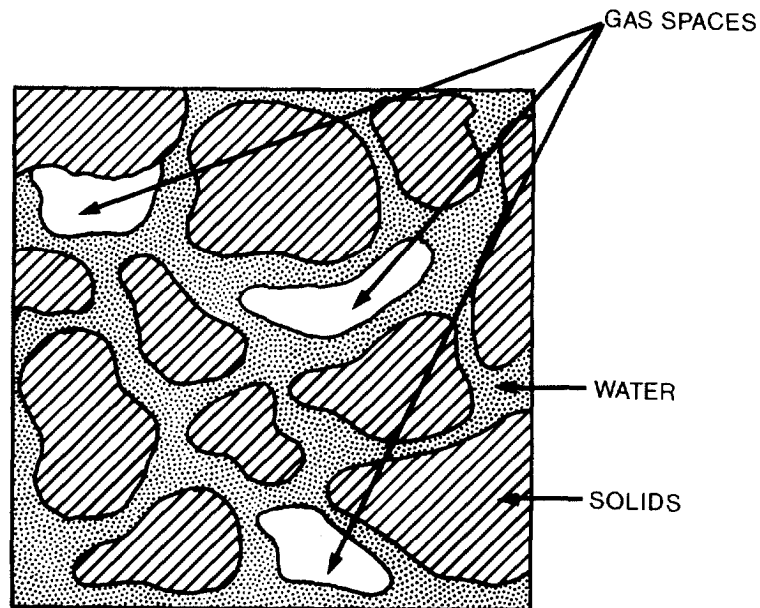


Figure VII-6 Schematic Showing the Solid, Liquid and Gaseous Phases in a Unit Volume of Soil

The solid phase is made up of soil particles that represent the granular skeleton of the aquifer.

A volume of soil  $V$  is equal to the sum of the volume of solids  $V_s$ , the volume of water  $V_w$ , and the volume of gas (vapor phase),  $V_g$ :

$$V = V_s + V_w + V_g \quad (\text{VII-1})$$

The volume of voids or pores  $V_v$  in a soil is defined as the sum of the water and gas volumes:

$$V_v = V_w + V_g \quad (\text{VII-2})$$

hence

$$V = V_s + V_v \quad (\text{VII-3})$$

The total mass  $M$  of these three phases in a volume of soil is the sum of the mass of solids  $M_s$ , the mass of water  $M_w$ , and the mass of gas  $M_g$  (which is negligible):

$$M = M_s + M_w + M_g \quad (\text{VII-4})$$

The quantitative relationship between the three phases can be characterized by such variables as the bulk density of the soil, the particle-size distribution and the porosity or water content.

#### 7.2.2.1 Bulk Density

Bulk density is used in describing the phenomenon of sorption and retardation in contaminant transport equations (see Section 7.4.2.1.1). The dry bulk density of a soil  $\rho_b$  ( $\text{g}/\text{cm}^3$ ) is defined as the mass of a dry soil  $M_s$  (g) divided by its bulk or total volume  $V$  ( $\text{cm}^3$ ):

$$\rho_b = M_s / V \quad (\text{VII-5})$$

The bulk density is affected by the structure of the soil (e.g., its looseness or degree of compaction) as well as its swelling and shrinkage characteristics which are dependent upon its wetness. Loose, porous soils will have low values of bulk density and more compact soils will have higher values. Bulk density values normally range from 1 to 2  $\text{g}/\text{cm}^3$ . Soils with high organic matter content will generally have lower bulk density values. Very compact subsoils, regardless of texture, may have bulk densities higher than 2  $\text{g}/\text{cm}^3$ . Moreover, there is a general tendency for the bulk density to increase with depth. The range and mean value of bulk density for various geologic materials are given in Table VII-2.

#### 7.2.2.2 Particle-Size Distribution

Soil type can be used to estimate porosity, hydraulic conductivity, and specific surface area available for sorption. The texture of a soil is usually determined by the relative proportions (by dry weight) of sand, silt and clay present in the soil. A soil-texture trilinear diagram is then used to determine the soil class (Figure VII-7). Alternatively, soil classification can be characterized on the basis of particle or grain-size distribution. Particle-size distribution curves (Figure VII-8) are obtained by plotting the cumulative percentage (by dry weight) of soil particles in a soil as a function of their particle size. Table VII-3 lists the range of particle sizes for various soil classifications.

An effective particle size,  $d_e$ , is defined as the grain diameter for which "e" percent of the particles (by dry weight) is equal or smaller in diameter. Normally "e" is set to 10 percent for Hazen's effective grain size  $d_{10}$  but  $d_{20}$  will often be used to characterize coarse materials. Hence, if  $d_{10} = 0.6\text{mm}$  (uniform, coarse sand), then 10% of the soil particles of this material (by dry weight) will have a grain diameter less than or equal to 0.6mm. A list of  $d_{10}$  effective grain sizes is given for



TABLE VII-2  
RANGE AND MEAN VALUES OF DRY BULK DENSITY

Material	Range $\rho/cm^3$	Mean <sub>3</sub> ( $g/cm^3$ )
clay	1.18 - 1.72	1.49
silt	1.01 - 1.79	1.38
sand, fine	1.13 - 1.99	1.55
sand, medium	1.27 - 1.93	1.69
sand, coarse	1.42 - 1.94	1.73
gravel, fine	1.60 - 1.99	1.76
gravel, medium	1.47 - 2.09	1.85
gravel, coarse	1.69 - 2.08	1.93
loess	1.25 - 1.62	1.45
eolian sand	1.33 - 1.70	1.58
till, predominantly silt	1.61 - 1.91	1.78
till, predominantly sand	1.69 - 2.12	1.88
till, predominantly gravel	1.72 - 2.12	1.91
glacial drift, predominantly silt	1.11 - 1.66	1.38
glacial drift, predominantly sand	1.36 - 1.83	1.55
glacial drift, predominantly gravel	1.47 - 1.78	1.60
sandstone, fine grained	1.34 - 2.32	1.76
sandstone, medium grained	1.50 - 1.86	1.68
siltstone	1.35 - 2.12	1.61
claystone	1.37 - 1.60	1.51
shale	2.20 - 2.72	2.53
limestone	1.21 - 2.69	1.94
dolomite	1.83 - 2.20	2.02
granite, weathered	1.21 - 1.78	1.50
gabbro, weathered	1.67 - 1.77	1.73
basalt	1.99 - 2.89	2.53
schist	1.42 - 2.69	1.76

Reference: Morris and Johnson (1967).

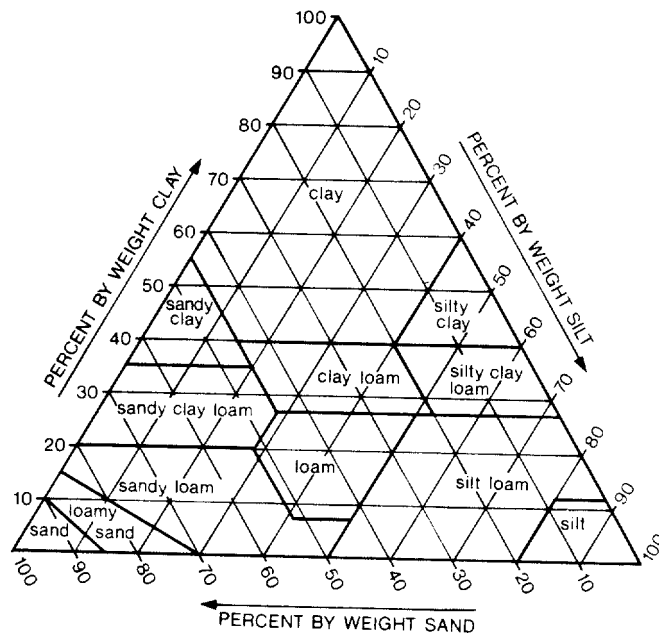


Figure VII-7 Soil Texture Triangular Diagram Showing Basic Soil Textural Classes. Reference: Hillel (1971)

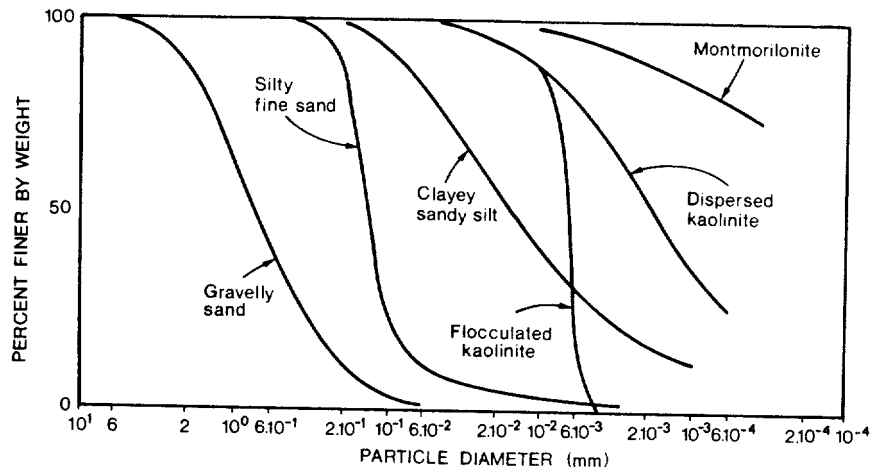


Figure VII-8 Typical Particle-size Distribution Curves for Various Soil Classifications. Reference: Bear (1972)

TABLE VII -3  
EFFECTIVE GRAIN SIZE AND THE RANGE OF SOIL  
PARTICLE SIZES FOR VARIOUS MATERIALS

Material	Effective Grain Size		Particle Size (mm)
	d <sub>20</sub> (mm)	d <sub>10</sub> (mm)	
colloidal clay	--	40Å*	10Å-.01
clay (30 to 50% clay sizes)	--	.0003	.0005-.05
silty clay	--	.0015	.001-.05
sandy clay	--	.002	.001-1
uniform silt	--	.006	.005-.05
silty sand	--	.01	.005-2
well-graded, silty sand and gravel	--	.02	.01-5
uniform, fine sand	--	.06	.05-.25
clean, well-graded sand and gravel	--	.1	.05-10
uniform, medium sand	--	.3	.25-.5
uniform, coarse sand	--	.6	.5-2
very coarse, clean, uniform sand	1.5	--	.8-3
fine, uniform gravel	3	--	1.5-8
clean, fine to coarse gravel	13	--	10-80
one-man stone	150	--	100-300
derrick stone	1200	--	900-3000

\*Å = angstrom = 1 x 10<sup>-8</sup> cm.

Reference: Hough (1957).

various materials in Table VII-3. The d<sub>10</sub> value can be used to predict intrinsic permeability, as shown in Section 7.2.5.2.1.

### 7.2.2.3 Porosity

Porosity is an important screening parameter in saturated aquifers used in computing the velocity of contaminants in the ground water (seepage velocity, Section 7.3.3.1.2) and the sorption and retardation of contaminants (see Section 7.4.2.1.1). Soil porosity "p" (unitless) is defined as the void or pore volume V<sub>v</sub>(cm<sup>3</sup>) of the soil divided by the bulk volume V(cm<sup>3</sup>) of the soil:

$$p = V_v / V \quad \text{(VII-6)}$$

The porosity is expressed as either a decimal fraction or as a percent. The void volume of a soil is defined in Equation VII-2 as the sum of the gas and water filled voids or interstices. Typical values of porosity for various geologic materials are given in Table VII-4.

The term effective porosity  $p_e$  (unitless) is sometimes used but its meaning depends upon its usage. It can equal the specific yield of a water-table aquifer which is defined as the volume of water obtained under a unit drop in head from a unit area of the aquifer. Alternatively, it can refer to that portion of the porous medium through which flow actually takes place. The last definition is important when the porous matrix includes a large number of dead-end pores and hence part of the fluid in the pore space is immobile (or practically so). In either definition, the effective porosity is always less than or equal to the total porosity ( $p_e \leq p$ ). The porosity of consolidated materials depends mainly on the degree of cementation of the grains. The porosity of unconsolidated materials depends on the packing of the grains, their shape, arrangement and size distribution.

#### 7.2.2.4 Water Content

Water content in the unsaturated zone is in some ways analagous to porosity in the saturated zone of an aquifer. The water content is used in the computation of seepage velocity and the sorption and retardation of contaminants. The water or moisture content of a soil is the amount of water in a given amount of soil. It is a dimensionless quantity and can be expressed on either a gravimetric (mass) or a volumetric (volume) basis. The gravimetric water content  $\theta_g$  (unitless) is defined as the mass of water  $M_w$  (g) divided by the dry mass of the soil  $M_s$  (g) (oven dried at 105-110°C) :

$$\theta_g = M_w / M_s \quad (\text{VII-7})$$

The volumetric water content (unitless) is defined as the volume of water  $V_w$  (cm<sup>3</sup>) divided by the volume of the soil  $V$  (cm<sup>3</sup>):

$$\theta = V_w / V \quad (\text{VII-8})$$

These two expressions for water content are related as follows:

$$\theta = \theta_g \rho_b / \rho_w \quad (\text{VII-9})$$

where  $\rho_b$  (g/cm<sup>3</sup>) is the dry bulk density of the soil and  $\rho_w$  (g/cm<sup>3</sup>) is the density of water. The ratio  $\rho_b / \rho_w$  is often called the apparent specific gravity of the soil (unitless). Values for  $\rho_b$  can be found in Table VII-2 for different geologic materials.

TABLE VII-4  
RANGE AND MEAN VALUES OF POROSITY

Material	Range (percent)	Mean (percent)
clay	34.2 - 56.9	42
silt	33.9 - 61.1	46
sand, fine	26.0 - 53.3	43
sand, medium	28.5 - 48.9	39
sand, coarse	30.9 - 46.4	39
gravel, fine	25.1 - 38.5	34
gravel, medium	23.7 - 44.1	32
gravel, coarse	23.8 - 36.5	28
loess	44.0 - 57.2	49
eolian sand (dune sand)	39.9 - 50.7	45
till, predominantly silt	29.5 - 40.6	34
till, predominantly sand	22.1 - 36.7	31
till, predominantly gravel	22.1 - 30.3	26
glacial drift, predominantly silt	38.4 - 59.3	49
glacial drift, predominantly sand	36.2 - 47.6	44
glacial drift, predominantly gravel	34.6 - 41.5	39
sandstone, fine grained	13.7 - 49.3	33
sandstone, medium grained	29.7 - 43.6	37
siltstone	21.2 - 41.0	35
claystone	41.2 - 45.2	43
shale	1.4 - 9.7	6
limestone	6.6 - 55.7	30
dolomite	19.1 - 32.7	26
granite, weathered	34.3 - 56.6	45
gabbro, weathered	41.7 - 45.0	43
basalt	3.0 - 35.0	17
schist	4.4 - 49.3	38

Reference: Morris and Johnson (1967).

In general, at saturation the volumetric water content  $\theta_{\text{sat}}$  equals the porosity (i.e.,  $\theta_{\text{sat}} = \rho$ ). For unsaturated conditions,  $\theta$  is always less than the porosity. However, for swelling, clayey soils, the volume of water at saturation can exceed the porosity of the dry soil.

The volumetric water content is the most used and probably the most convenient method of expressing water content. It is more directly adaptable to the computation of fluxes and water quantities added or subtracted by seepage through ponds and landfills, irrigation or evaporation.

### 7.2.3 Flow Properties of Saturated Porous Media

Saturation of a porous medium means that all of the soil voids or pores are filled with water. Complete saturation, however, is not always possible since some gas may be trapped between soil particles.

In an unconfined aquifer the upper surface of the saturated zone is open to the soil atmosphere. This surface is called the water table or phreatic surface. In a well penetrating an unconfined aquifer, the water will rise only to the level of the water table (i.e., when the ground water flow is predominately horizontal). A schematic of an unconfined aquifer is shown in Figure VII-9. Changes in the level of water in such a well result primarily from changes in the volume of water in storage.

In a confined aquifer, the saturated zone is underlain and overlain by relatively impermeable strata. The ground water in a confined aquifer is under a pressure greater than atmospheric. In a well penetrating a confined aquifer, the water may rise above the bottom of the overlying confining stratum. The water level is called the piezometric or potentiometric surface. A schematic of a confined aquifer is also shown in Figure VII-9. Changes in the level of water in such a well result primarily from changes in pressure rather than from changes in storage volumes. If the piezometric surface lies above the ground, a flowing well will result. In a leaky or semi confined aquifer, the saturated zone is underlain or overlain by a semipervious stratum.

In order to describe flow through saturated porous media, the hydraulic conductivity (or transmissivity) and storativity of the medium must be characterized.

#### 7.2.3.1 Saturated Hydraulic Conductivity

Hydraulic conductivity  $K$  (cm/sec) expresses the ease with which a fluid can be transported through a porous medium. Hydraulic conductivity is an important parameter used in computing seepage velocity. It is also one of the most difficult parameters to measure accurately and is relatively expensive to obtain. Usually "point" values are measured but large variations can occur within short distances, even in apparently uniform geologic formations. It is a function of properties of both the porous medium and the fluid. The range of values for saturated hydraulic conductivity and intrinsic permeability are given in Table VII-5 for various geologic materials.

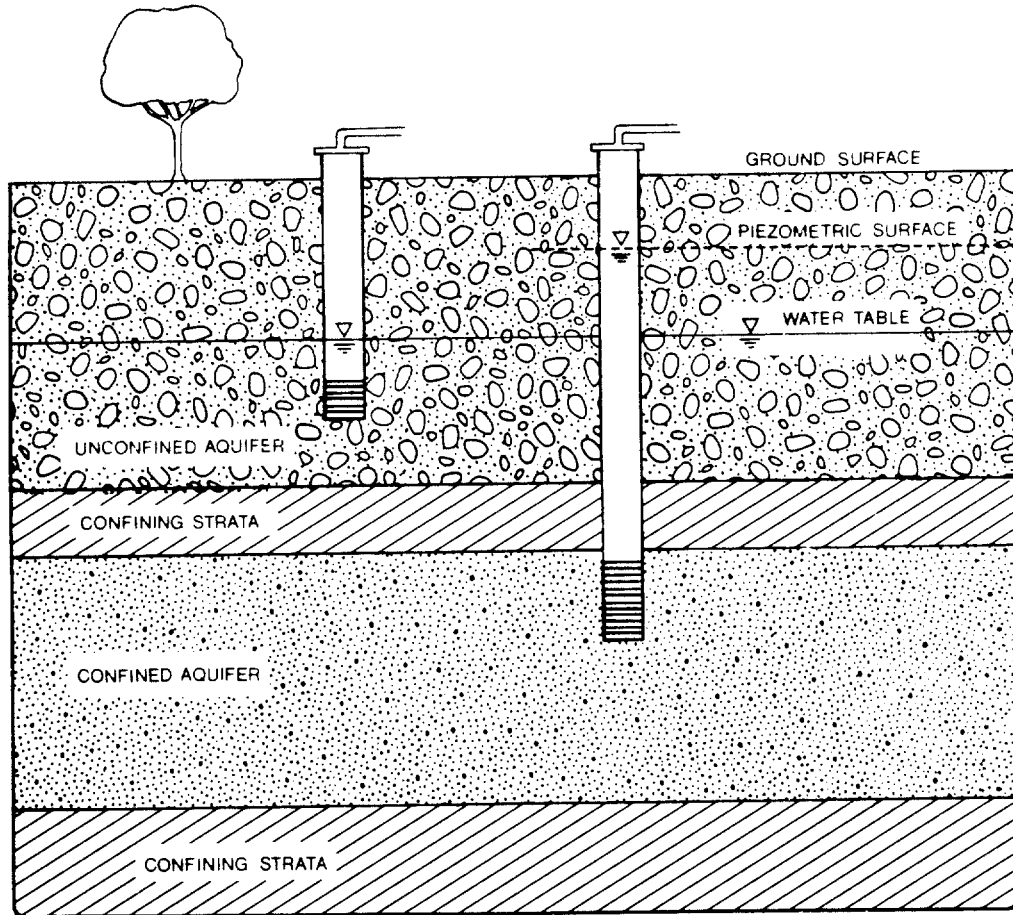


FIGURE VII -9 SCHEMATIC CROSS SECTION SHOWING BOTH A CONFINED AND AN UNCONFINED AQUIFER

These properties can ideally be separated by expressing hydraulic conductivity as follows:

$$K = K_i g \rho_w / \mu \quad (\text{VII-10})$$

where  $K_i$  is the intrinsic permeability ( $\text{cm}^2$ ),  $g$  is the gravitational acceleration ( $980.7 \text{ cm/sec}^2$ ),  $\rho_w$  is the density of water ( $\text{g/cm}^3$ ) and  $\mu$  is the viscosity of water ( $\text{g/cm sec}$ ). Values of  $\rho_w$  and  $\mu$  are given in Table I-1 in Appendix I. The intrinsic permeability is only a function of porous medium properties such as the particle-size distribution, grain or pore shape, and tortuosity. However, the expression in Equation VII-10 for saturated hydraulic conductivity assumes that the water and solid matrix of the soil do not interact in such a way as to change the properties of either. In most soils there is no matrix-water interaction. In addition, the intrinsic permeability may vary with time as a result of chemical, physical and biological processes. These may include structural and textural changes

TABLE VII-5  
TYPICAL VALUES OF SATURATED HYDRAULIC CONDUCTIVITY  
AND INTRINSIC PERMEABILITY

Material	Hydraulic Conductivity <sup>a</sup> K(cm/sec)	Intrinsic <sup>a</sup> Permeability K <sub>i</sub> (cm <sup>2</sup> )
clean gravel	.1 - 100	10 <sup>-6</sup> - 10 <sup>-3</sup>
clean sand	10 <sup>-4</sup> - 1	10 <sup>-9</sup> - 10 <sup>-5</sup>
silty sand	10 <sup>-5</sup> - .1	10 <sup>-10</sup> - 10 <sup>-6</sup>
silt, loess	10 <sup>-7</sup> - 10 <sup>-3</sup>	10 <sup>-12</sup> - 10 <sup>-8</sup>
stratified clay <sup>b</sup>	10 <sup>-7</sup> - 10 <sup>-4</sup>	10 <sup>-12</sup> - 10 <sup>-9</sup>
glacial till	10 <sup>-10</sup> - 10 <sup>-4</sup>	10 <sup>-15</sup> - 10 <sup>-9</sup>
unweathered, marine clay	10 <sup>-11</sup> - 10 <sup>-7</sup>	10 <sup>-16</sup> - 10 <sup>-12</sup>
karst limestone	10 <sup>-4</sup> - 1	10 <sup>-9</sup> - 10 <sup>-5</sup>
permeable basalt	10 <sup>-5</sup> - 1	10 <sup>-10</sup> - 10 <sup>-5</sup>
fractured igneous and metamorphic rocks	10 <sup>-6</sup> - 10 <sup>-2</sup>	10 <sup>-11</sup> - 10 <sup>-7</sup>
limestone and dolomite	10 <sup>-7</sup> - 10 <sup>-4</sup>	10 <sup>-12</sup> - 10 <sup>-9</sup>
sandstone	10 <sup>-8</sup> - 10 <sup>-4</sup>	10 <sup>-13</sup> - 10 <sup>-9</sup>
shale	10 <sup>-11</sup> - 10 <sup>-7</sup>	10 <sup>-16</sup> - 10 <sup>-12</sup>
breccia, granite <sup>b</sup>	10 <sup>-11</sup> - 10 <sup>-9</sup>	10 <sup>-16</sup> - 10 <sup>-14</sup>
unfractured metamorphic and igneous rocks	10 <sup>-12</sup> - 10 <sup>-8</sup>	10 <sup>-17</sup> - 10 <sup>-13</sup>

a Reference: Freeze and Cherry (1979).  
b Reference: Bear (1972).

due to subsidence and consolidation, the development of solution channels, clay swelling, and clogging due to biological growth and by precipitates carried by the water.

If the aquifer properties (e.g., hydraulic conductivity) are independent of position within a geologic formation, the formation is called homogeneous. If the properties are dependent on position within a geologic formation, the formation is called heterogeneous. Heterogeneity is caused by the presence of interlayered deposits, faults, or other large-scale stratigraphic features (such as overburden-bedrock contacts), large scale changes in the sedimentary formations (particularly those which are part of deltas, alluvial fans, and glacial outwash plains) and small-scale layering in an otherwise homogeneous formation.



If hydraulic conductivity is independent of the direction of measurement in a geologic formation, the formation is called isotropic. If the hydraulic conductivity varies with the direction of measurement, the formation is called anisotropic. The primary cause of anisotropy on a small scale is the orientation of clay minerals in sedimentary rocks and unconsolidated sediments. Anisotropy of consolidated geologic materials is governed by the orientation of layers, fractures, solution openings or other structural conditions which may not have a horizontal alignment. Fractured rocks can also be anisotropic because of directional variation in joint aperture and spacing.

The horizontal saturated hydraulic conductivity  $K_h$  (cm/sec) in some materials (e.g., alluvium) is normally greater than the vertical conductivity  $K_v$  (cm/sec); hence  $K_h/K_v \geq 1$ . Ratios of  $K_h/K_v$  usually fall in the range of 2 to 10 for alluvium and glacial outwash (Weeks, 1969) and 1.5 to 3 for sandstone (Piersol *et al.*, 1940) but it is not uncommon to have values of 100 or more occur where clay layers are present (Morris and Johnson, 1967).

#### 7.2.3.2 Transmissivity

The transmissivity or coefficient of transmissibility  $T$  ( $\text{cm}^2/\text{sec}$ ) is defined as:

$$T = Kb \quad (\text{VII-11})$$

where  $K$  is the saturated hydraulic conductivity (cm/sec) and  $b$  is the aquifer thickness (cm). Transmissivity has traditionally been expressed in units of gal/(ft day) but this can be converted to the cgs units of  $\text{cm}^2/\text{sec}$  by multiplying the gal/(ft day) by  $1.438 \times 10^{-3}$ . Thus:

$$1 \text{ gal}/(\text{ft day}) = 1.438 \times 10^{-3} \text{ cm}^2/\text{sec} \quad (\text{VII-12})$$

Transmissivity can be estimated by multiplying the saturated hydraulic conductivity  $K$  (cm/sec) given for various geologic materials in Table VII-5 by the aquifer thickness  $b$  (cm). Because pumping tests can provide values for transmissivity, this type of data may be more available than saturated hydraulic conductivity.

#### 7.2.3.3 Storativity

Storativity or storage coefficient,  $S$ , is defined as the volume of water that is released from storage per unit horizontal area of aquifer per unit decline of hydraulic head. It is a dimensionless quantity. This parameter is obtained in addition to transmissivity from pumping tests. It is used to compute aquifer yields and to compute drawdowns of individual wells.

For confined aquifers, storativity is due to water being released from the compression of the granular skeleton and expansion of the pore water.  $S$  is

mathematically defined as the product of the specific storage,  $S_s$  ( $\text{cm}^{-1}$ ) and the aquifer thickness,  $b$ (cm):  $S = S_s b$ .

The value of the storativity for confined aquifers is generally small, falling between the range of .00005 to .005 (Todd, 1980). Hence, large pressure changes over an extensive area of aquifer are required before substantial water is released.

#### 7.2.4 Flow Properties of Unsaturated Porous Media

The term unsaturated means that the voids or pores of a porous medium are only partially filled with water. Under these conditions, the pressure within a soil pore becomes less than atmospheric because water is under surface-tension forces. These surface-tension forces increase as the water content decreases. Hence, the flow properties of a porous medium (such as hydraulic conductivity) are functionally dependent on the water content. These functional relationships are a characteristic of the particular porous medium.

##### 7.2.4.1 Soil-Water Energy

To describe the movement and behavior of ground water, the relative energy state of the soil water must be known. This is necessary because flow will occur in the direction of decreasing energy and the soil water tends to equilibrate with its surroundings. As stated above, the relative amount of energy contained in the soil water is important and not the absolute amount of energy (i.e., relative to a standard reference state). Generally, the standard state is defined as a hypothetical reservoir of free water, at atmospheric pressure, at the same temperature as that of the soil water, and at a given and constant elevation.

The total energy  $E$  of the soil water is equal to the sum of its kinetic  $E_k$  and potential  $E_{\text{pot}}$  energies:

$$E = E_k + E_{\text{pot}} \quad (\text{VII-13})$$

Kinetic energy  $E_k$  is that energy which the soil water has by virtue of its motion. However, under most typical ground water situations, the kinetic energy will be negligible compared to potential energy by virtue of the low velocities generally encountered in subsurface flow.

Potential energy is that energy which soil water has by virtue of its position. Technically the potential energy of soil water is the amount of work that must be done per unit quantity of pure water in order to transport reversibly and isothermally an infinitesimal quantity of water from a pool of pure water at a specified elevation at atmospheric pressure to the soil water at the point under consideration.

The potential energy,  $E_{\text{pot}}$ , of soil water can be separated into at least three components: gravitational,  $E_g$ ; pressure,  $E_p$ ; and osmotic,  $E_o$ . The total potential energy is the sum of these three:

$$E_{\text{pot}} = E_g + E_p + E_o \quad (\text{VII-14})$$

The three components of the potential energy are considered below.

#### 7.2.4.1.1 Gravitational Potential

Gravitational potential energy is the potential for work resulting from the force of gravity acting on a quantity of pure water located at some point in space that is vertically different from a reference point. The strength of this potential energy  $E_g$  (erg) depends on the strength of the gravitational force  $g$  ( $\text{cm}/\text{sec}^2$ ), the density of water  $\rho_w$  ( $\text{g}/\text{cm}^3$ ) and the vertical elevation of the water from a reference point  $z$  (cm). Hence, the gravitational potential energy acting on a volume  $V_w$  ( $\text{cm}^3$ ) of water is mathematically defined as:

$$E_g = \rho_w g V_w z \quad (\text{VII-15})$$

This potential energy is a positive quantity if the unit volume of soil water is located above the reference level and negative if located below.

#### 7.2.4.1.2 Pressure Potential

Pressure potential energy  $E_p$  (erg) is that potential energy due to the pressure of the surrounding fluid acting on it. Mathematically, this can be represented as follows for the case of constant density  $\rho_w$  ( $\text{g}/\text{cm}^3$ ):

$$E_p = PM_w / \rho_w = PV_w \quad (\text{VII-16})$$

where  $P$  is the relative or gage pressure ( $\text{dyne}/\text{cm}^2$ ) acting on a unit volume  $V_w$  ( $\text{cm}^3$ ) or unit mass  $M_w$  (g) of soil water.

Note that  $P$  is the relative or gage pressure and not the absolute pressure. Hence:

$$P = p_w - p_o \quad (\text{VII-17})$$

where  $p_w$  is the absolute pressure at the point under consideration and  $p_o$  is the absolute pressure at the reference elevation (usually taken to be atmospheric pressure). Thus, pressure potential is a positive quantity under a free-water surface

(saturated zone), a zero potential at the water surface and a negative pressure potential in the unsaturated zone.

In the saturated zone, the pressure potential is a direct result of the weight of overlying water. Hence, the pressure potential at any point in the system is determined by the depth that the point lies below the water table. The relative pressure  $P$  ( $\text{dyne/cm}^2$ ) can thus be expressed as:

$$P = \rho_w gh \tag{VII-18}$$

where  $h$  (cm) is the depth below the water table. The pressure potential is measured in the field with a piezometer. In a confined aquifer, the piezometer head  $h$  is measured as the distance between the point under consideration and the free water level in the piezometer.

In the unsaturated zone, the pressure potential is a negative quantity and is often given a special symbol such as  $\psi$  and a special name such as the matric potential, capillary potential, matric suction or tension. By convention, suction and tension are considered positive quantities, hence:

$$\psi = \text{matric potential} = - \text{matric suction}$$

Under unsaturated conditions, the pressure potential of soil water results from forces attributable to the soil matrix, such as absorption and capillarity (see Figure VII-10). These forces attract and bind water to the soil by the processes of surface tension, molecular attraction and ion exchange. The net effect of these processes is to reduce the free energy of the soil water in comparison to that of pure, bulk water.

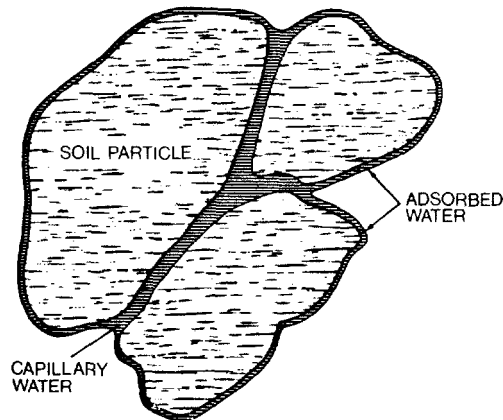
Typical values of pressure potential are given below.

<u>Moisture Level</u>	<u>Pressure Potential* Per Unit Volume (bars)</u>
saturated: confined	greater than 0
saturated: unconfined (at free water surface)	<b>0</b>
field capacity	-.1 to -.2
wilting coefficient	-15
hygroscopic coefficient	-31
molecular bound water to soil solids	-10,000

\*1 bar = 0.987 atmosphere

Reference: Brady (1974).

• MATRIC POTENTIAL (unsaturated soil)



• OSMOTIC POTENTIAL

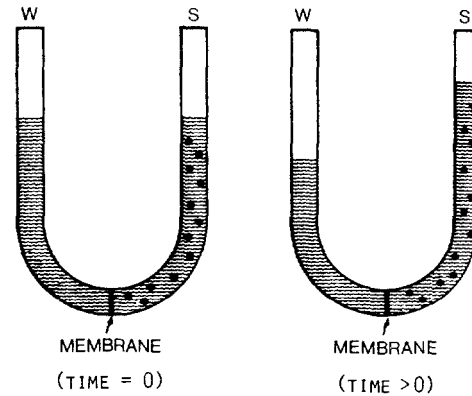


FIGURE VII -10 SCHEMATIC OF MATRIC AND OSMOTIC SOIL-WATER POTENTIAL. REFERENCE: BRADY (1974)

Note that plants cannot obtain water from soil at pressure potentials less than the wilting coefficient and water will not move in liquid form below the hygroscopic coefficient level.

7.2.4.1.3 Osmotic Potential

Osmotic potential energy is that potential energy attributed to the attraction of solutes for water. Attractive forces arising from the polar nature of water tend to orient water around ions. Hence, osmotic potential refers to the work required to pull water away from these attracted ions.

In the absence of a semi permeable membrane, soluble ions will diffuse into a soil solution until the ions are uniformly distributed. With the presence of a semi permeable membrane between two solutions, water molecules will move through the membrane to the side with the higher solute concentration (see Figure VII-10) Water will continue to pass through such a membrane until the hydrostatic pressure difference between the two sides balances the effect of the ion-water attraction forces. Hence, one can measure the osmotic potential of the solute solution by measuring the hydrostatic pressure difference across the membrane. The osmotic potential is a negative quantity because the presence of solutes lowers the vapor pressure and free energy of the soil water and hence lowers the potential energy.

Clays can act as a leaky semi permeable membrane, allowing water to pass more easily than salts. This is sometimes referred to as salt sieving (Nye and Tinker 1977). Thus in sedimentary basins, osmosis can cause significant pressure differentials across clayey strata (Freeze and Cherry, 1979). The osmotic potential

can also be important In saline soils of arid and semiarid regions (Brady, 1974). In addition, the osmotic potential is important to the uptake of water by plant roots and the movement of water vapor. Both the soil-root and water-gas interfaces act as semipermeable membranes. Except for the above cases, however, the contribution of osmotic potential to the mass movement of water is negligible in most soil systems.

#### 7.2.4.2 Soil-Moisture Characteristic Curves

Consider a sample of soil that is maintained at saturation and is exposed to atmospheric pressure. By definition, the pressure potential of the soil water in this soil sample would be zero. Now consider the case of applying a slight suction or subatmospheric pressure across the soil sample. No water will flow out until a certain critical suction (called the air-entry suction) is reached. At this point, the largest soil pores start to empty. As the suction is further increased, additional water flows as progressively smaller pores empty. Finally, at very high suctions, only the micropores remain filled. As the soil becomes increasingly dry, a nearly exponential increase in suction is required to remove additional water.

The functional relationship between the moisture content and matric or suction potential is a characteristic of a particular soil. This relationship is called the soil-moisture characteristic curve, the soil-moisture retention curve or simply the characteristic curve. The soil-moisture characteristic curves for three different textured soils are shown in Figure VII-11. As previously stated, the absolute value of the matric or suction potential increases as the moisture content decreases. In addition, for a given matric potential, a coarse soil (e.g., sand) generally has less water remaining in the soil and has a steeper slope to the curve than a fine soil (e.g., clay). The slope of the soil-moisture characteristic curve (i.e., the change of water content per unit change of matric potential) is called the specific water capacity.

In a coarse, saturated soil, the pores are predominately large and drain quickly under a slight suction. A high suction is required to remove the last water from the remaining, small pores. In a clayey soil, the pore-size distribution is more uniform, so that a more gradual decrease in water content occurs with an increase in suction. In addition, at low suctions (for example, between 0 and 1000 cm  $H_2O$ ) the amount of water remaining in a soil depends primarily on soil structure (i.e., pore-size distribution and particle aggregation). At higher suctions, however, water retention is due increasingly to adsorption and thus is influenced more by the particle-size distribution and specific surface of a soil.

Unfortunately, the water content and matric potential are not always uniquely related to each other because of hysteresis. Hysteresis means that the characteristic curves are different, depending on whether the soil is being wetted or dried. The characteristic curve during a drying cycle is called the drying, resorption or drainage

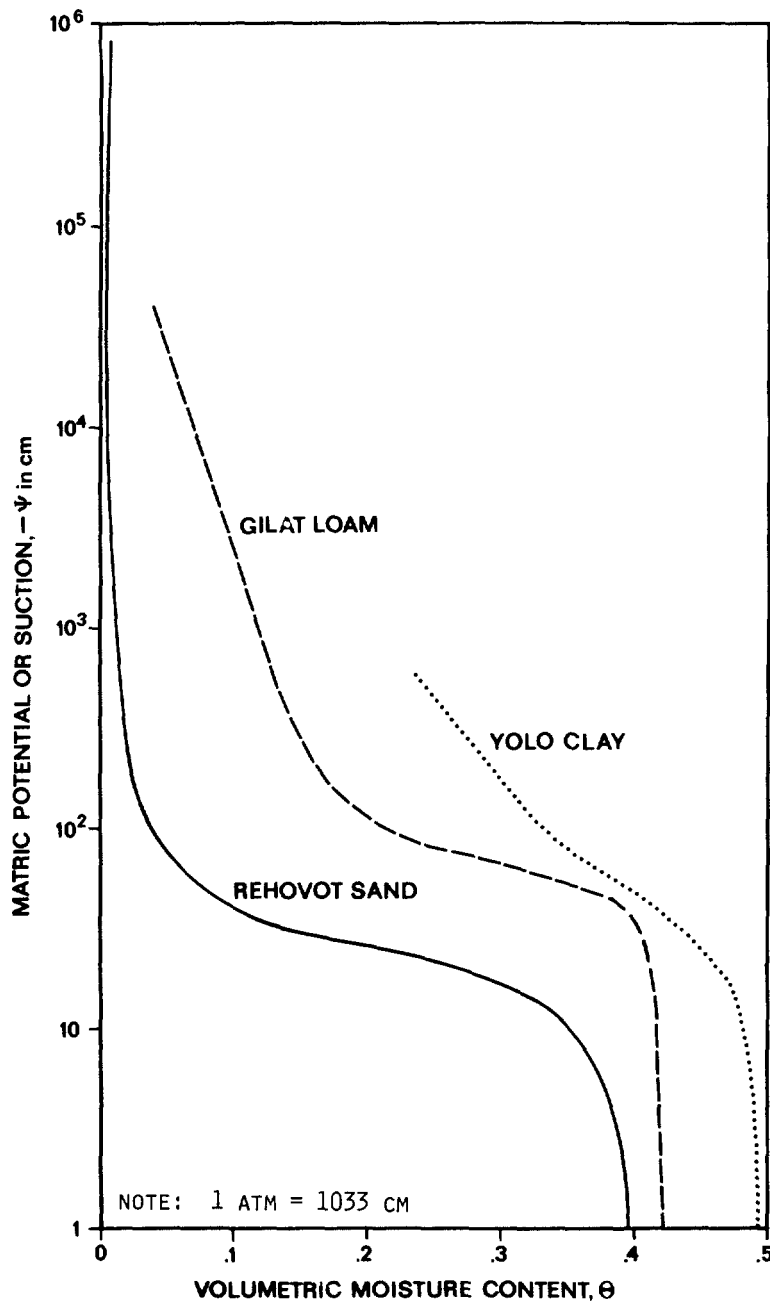


FIGURE VII -11 CHARACTERISTIC CURVES OF MOISTURE CONTENT AS A FUNCTION OF MATRIC POTENTIAL FOR THREE DIFFERENT SOILS. REFERENCE: BRAESTER (1972)

curve; during wetting it is called the wetting, sorption or imbibition curve. A soil which is partially wetted, then dried or vice versa will follow an intermediate characteristic curve called a scanning curve, which lies between the envelope formed by the wetting and drying curves.

Figure VII-12 shows an example of hysteresis in a sandy soil. The hysteresis effect may be attributed to the inkbottle effect (geometric nonuniformity of individual pores), the contact-angle or rain drop effect (differences in the contact angle for advancing and receding fluids), entrapped air, and changes in soil structure (e.g., swelling, shrinking or aging phenomena) caused during the wetting or drying of a soil.

#### 7.2.4.3 Unsaturated Hydraulic Conductivity

In Section 7.2.3.1, the saturated hydraulic conductivity was stated to be affected by an intrinsic property of the solid matrix of a soil and by fluid properties. For unsaturated porous media, the hydraulic conductivity is also a function of the energy state of the soil water (i.e., the water content or pressure potential).

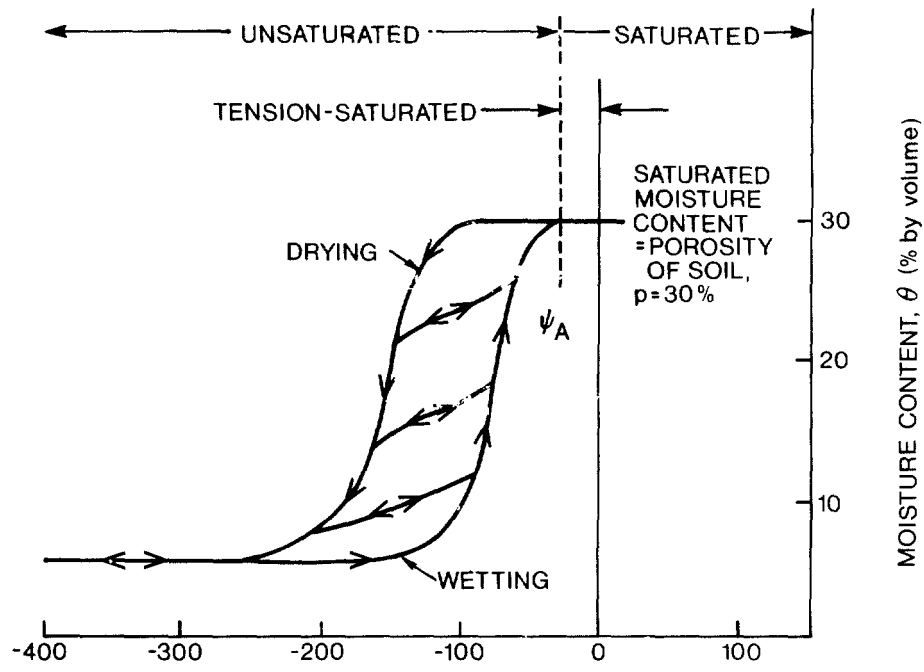
The hydraulic conductivity of three different soils is shown in Figure VII-13 as a function of moisture content. The hydraulic conductivity decreases exponentially as the moisture content decreases. The large pores of a porous media are the most conductive, their relative conductivity being proportional to the square of the pore diameter and their volumetric discharge rate being proportional to the fourth power of the pore diameter. As a soil dries out, the large pores empty first, forcing flow to be conducted through a diminishing cross-sectional area.

Since the moisture content is related to the matric or suction potential, through the soil-moisture characteristic curve (see Section 7.2.4.2), the hydraulic conductivity can be expressed as a function of either the moisture content,  $K(\theta)$ , or of the matric potential,  $K(\psi)$ . Just as with moisture and pressure, hydraulic conductivity is also not a single valued function. Figure VII-12 showed hysteresis in the hydraulic conductivity of a sandy soil. At a given suction, the hydraulic conductivity is generally lower in a wetting soil than in a drying soil. This is because the wetting soil contains less water than the drying one (for a given suction).

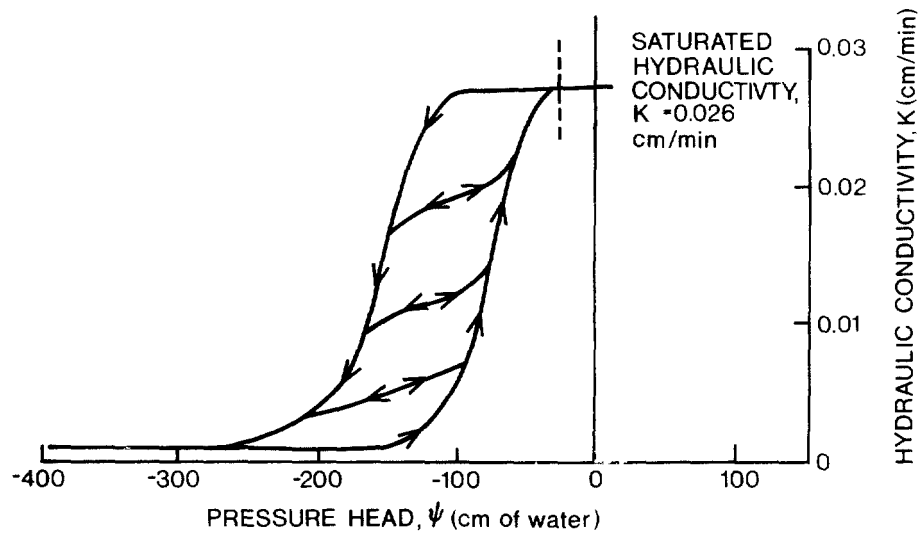
#### 7.2.5 Data Acquisition or Estimation

In Sections 7.2.2 to 7.2.4, the physical and flow properties of porous media were discussed in detail. Tables were included to show what values are typically found in aquifers of various geologic materials. In this section, laboratory and field methods are briefly discussed to show how the properties of a particular aquifer or porous medium can be estimated or measured. Finally, in Section 7.2.5.4 the effect of sample size on measurement precision is discussed from a statistical point of view.





(a)



(b)

FIGURE VII-12 CHARACTERISTIC CURVES OF (A) MOISTURE CONTENT AND (B) HYDRAULIC CONDUCTIVITY AS A HYSTERETIC FUNCTION OF MATRIC POTENTIAL FOR A NATURALLY OCCURRING SANDY SOIL. REFERENCE: FREEZE AND CHERRY (1979)

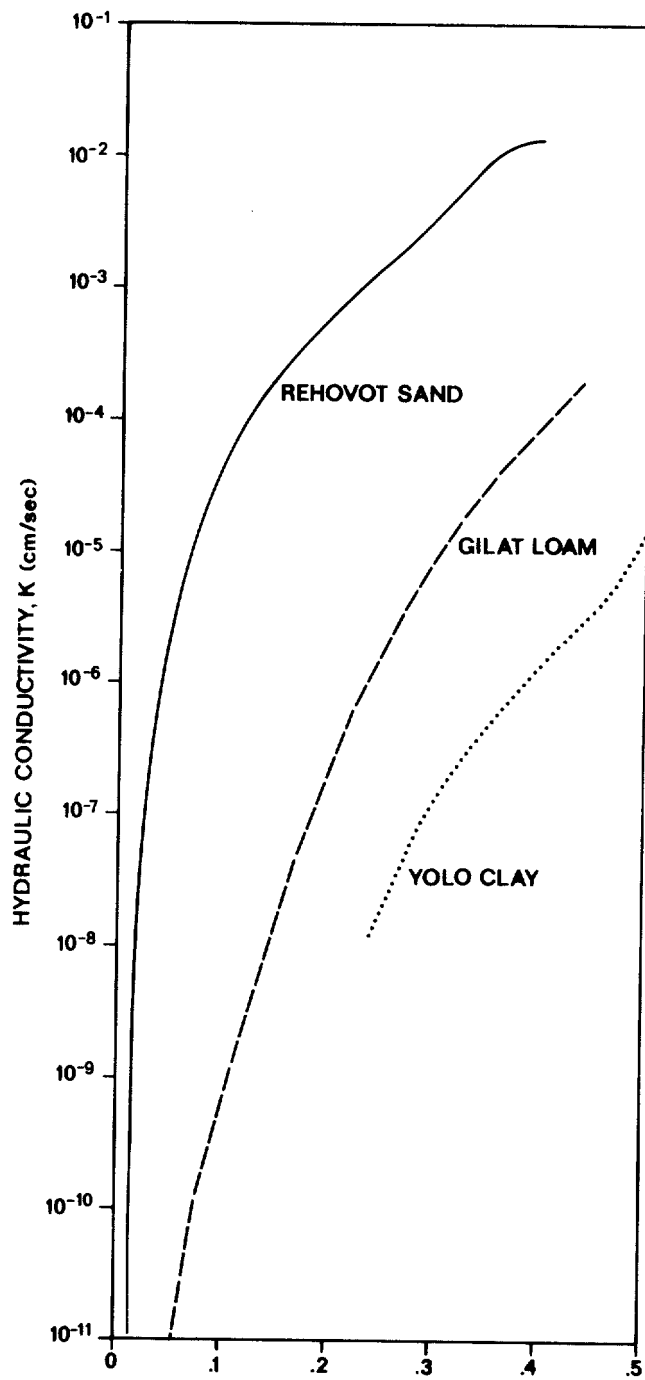


FIGURE VII-13 HYDRAULIC CONDUCTIVITY AS A FUNCTION OF MOISTURE CONTENT FOR THREE DIFFERENT SOILS. REFERENCE: BRAESTER (1972)

#### 7.2.5.1 Methods to Measure the Physical Properties of Porous Media

In Section 7.2.2, the physical properties of bulk density, particle-size distribution, porosity and water content were discussed. Methods to measure and estimate these properties are reviewed below.

Bulk density  $\rho_b$  ( $\text{g}/\text{cm}^3$ ) of a material is measured by taking an undisturbed sample of the material in the field, using a sampler of known volume. The sample is then dried to a constant weight in an oven at 105-110°C. The bulk density of a sample is thus calculated as its oven dry weight divided by the sample volume (see Equation VII-5). Other methods of measuring bulk density include in-situ measurement by gamma radiation and microscopic methods using paraffin fixation. These methods are discussed in detail by Fox and Page-Hanify (1959), Baver *et al.* (1972) and Taylor and Ashcroft (1972).

The determination of particle-size distribution is carried out by mechanical or sieve analysis for particles larger than approximately 0.0625 mm, and hydrometer or sedimentation analysis for smaller particles. In the mechanical analysis, the soil sample is shaken on a sieve with square openings of specified size. Successively smaller and smaller screens are used. For particles less than 0.0625 mm, a sedimentation analysis is done. In this method, the size of a particle is defined as the diameter of a sphere that settles in water at the same velocity as the particle (Morris and Johnson, 1967; Taylor and Ashcroft, 1972).

Soil porosity can be measured directly in the laboratory by either an air-pycnometer technique, a porosimeter, mercury displacement or a gas expansion method (Klock *et al.*, 1969; Bear, 1972; Baver *et al.*, 1972). Porosity,  $p$  (unitless), can also be estimated based on typical values for a given soil or rock type (see Table VII-4).

Soil water content in the laboratory is usually measured by the gravimetric method of determining the soil's moist and dry (oven dried at 105-110°C) weights and then using Equation VII-7 to get the gravimetric water content  $\theta_g$  (unitless). The volumetric water content  $\theta$  (unitless) can be found from  $\theta_g$  through Equation VII-9. Other methods of measuring water content are neutron scattering, gamma ray attenuation, electromagnetic techniques, tensiometric techniques and hydrometric techniques. A summary of the relative advantages and disadvantages of these methods, is given in Table VII-6. For screening calculations, an estimated average water content based on grain-size is usually adequate. If necessary, this estimate could be checked by collecting a few samples and measuring the water content gravimetrically.

#### 7.2.5.2 Methods to Measure the Flow Properties of Saturated Porous Media

The flow properties of saturated porous media are discussed in Section 7.2.3. These properties include specific yield, specific storage, storativity, saturated hydraulic conductivity and transmissivity. The measurement of those properties related to the quantity of water that an aquifer can release or take up (i.e., specific yield,

TABLE VII-6  
SUMMARY OF METHODS FOR MEASURING  
SOIL MOISTURE ( $\theta$ )

Method	Advantages	Disadvantages	References
gravimetric	easy to take samples most accurate of available methods	destructive sampling provides a point value	Black (1965) Reynolds (1970a, b) Taylor and Ashcroft (1972)
neutron scattering	measures moisture in-situ regardless of its physical state can determine $\theta$ versus depth nondestructive can detect rapid changes in $\theta$	depth resolution <u>+0.5</u> ft below a depth of 6 in. below land surface expensive and requires a radioactive source	Gardner and Kirkham (1952) van Bavel (1961, 1962) Rawls and Asmussen (1973) Vachaud <u>et al.</u> (1977)
gamma ray attenuation	can determine $\theta$ versus depth in-situ easy to obtain temporal changes very good depth resolution (2-3 cm) nondestructive automatic recording is possible	assumes bulk density of soil is known and a constant expensive, complicated instrumentation and requires a radioactive source	Gurr (1962) Ferguson and Gardner (1962) Nofziger (1978)
resistivity and capacitance (i.e., gypsum blocks, geophysical methods)	can determine absolute values of $\theta$ versus depth high precision can measure high suction pressures (greater than 800 cm $H_2O$ )	time lag in response some devices can deteriorate sensitive to soil salinity	Thomas (1963) Selig <u>et al.</u> (1975)
tensiometric techniques	easy to design, construct, and install measurement range is between 0 and 800 cm $H_2O$ of tension operable for long time periods rapid response time (with transducers) adaptable to freezing and thawing conditions	gives a direct measure of soil water pressure but an indirect measure of $\theta$ instruments can be broken during installation some electronic drift in pressure transducers sensitive to temperature changes	Kirkham (1964) S.J. Richards (1965) Rice (1969) Taylor and Ashcroft (1972) Williams (1978)
Reference: after Schmugge <u>et al.</u> (1980) and Wilson (1981)			

specific storage and storativity) are discussed in Appendix I. Those properties that describe the rate at which water can move in the aquifer (i.e., hydraulic conductivity and transmissivity) are discussed below.

#### 7.2.5.2.1 Laboratory Methods of Measuring Hydraulic Conductivity

There are two major ways of assessing saturated hydraulic conductivity  $K$  in the laboratory: particle-size analysis and permeameter tests.

In particle-size analysis, soil samples are characterized by their particle-size distribution, and then empirical formulae are used to estimate  $K$ . For example, consider the following empirical formula developed by Hazen for intrinsic permeability  $K_i$  ( $\text{cm}^2$ ):

$$K_i = C d_{10}^2 \quad (\text{VII-19})$$

where  $C$  is a dimensionless coefficient and  $d_{10}$  (mm) is the effective particle diameter obtained from the particle-size gradation curve (see Section 7.2.2.2). The intrinsic permeability is related to hydraulic conductivity through the relation of Equation VII-10. Harleman et al. (1963) found good agreement with experimental values of  $K_i$  using  $C = 6.54 \times 10^{-6}$  (where  $d_{10}$  is in mm and  $K_i$  is in  $\text{cm}^2$ ). Krumbein and Monk (1943) found  $C$  to equal  $6.17 \times 10^{-6}$ . Hazen's approximation for intrinsic permeability in Equation VII-19 was originally determined for uniformly graded sand, but it can give a rough estimate for soils in the fine sand to gravel range (Freeze and Cherry, 1979).

Hydraulic conductivity can also be determined in the laboratory by a permeameter, in which flow is maintained through a soil core that is held in a metal or plastic cylinder while measurements of flow rate and head loss are made. Either a constant head or a variable head permeameter method can be used (Todd, 1980; Morris and Johnson, 1967). The constant head permeameter is generally used for samples of medium to high permeability and the variable head permeameter for samples of low permeability.

However, permeability results from the laboratory may bear only limited relation to values obtained by in-situ methods in the field. Supposedly uniform deposits, for example clays, more often than not contain thin seams or lenses of silt or fine sand. These thin layers may occur as continuous laminations or be randomly dispersed and discontinuous. As a consequence of this stratification, hydraulic conductivity values calculated in-situ in the field for clay or clay/silt deposits are generally several orders of magnitude larger than those derived from laboratory tests (Milligan, 1976). An order of magnitude difference generally occurs for sand and silt deposits. The greater the heterogeneity in a formation, the greater the discrepancy between laboratory and field measured values of saturated hydraulic conductivity. Hence, the most reliable methods are the in-situ or field methods.

#### 7.2.5.2.2 Field Methods of Measuring Hydraulic Conductivity

Field or in-situ determination of saturated hydraulic conductivity can be made by a wide variety of methods. These methods include the auger-hole method, piezometer method, pumping tests, tracer tests, packer tests and the point dilution method. Milligan (1976) reviewed these various in-situ methods as summarized in Table VII-7. Many authors, including Todd (1980) and Milligan (1976), feel that the most reliable in-situ method for estimating hydraulic conductivity is the well pumping test. When such a test is not practical, borehole slug tests can be used to provide adequate estimates for screening calculations. Values of transmissivity  $T$  are obtained from pumping tests by superimposing a plot of nonsteady-state drawdown on a family of type curves. Transmissivity is converted to hydraulic conductivity by dividing  $T$  by the aquifer thickness. Worked out examples using the various pumping and slug tests are given by Lehman (1972) and Fetter (1980). A detailed discussion on designing the geometry or layout of pumping tests can also be found in Kruseman and deRidder (1970) and Stallman (1971).

#### 7.2.5.3 Methods to Measure the Flow Properties of Unsaturated Porous Media

The methods of measuring soil-water potential, such as the gravitational, pressure and osmotic potentials will be discussed in Section 7.2.5.3.1. Measuring the characteristic curves of soil-water retention and unsaturated hydraulic conductivity will be discussed in Section 7.2.5.3.2.

##### 7.2.5.3.1 Measuring Soil-Water Potential

Gravitational potential is easy to measure since only the vertical distance  $z$ (cm) between the reference point and the point under consideration has to be measured. If the point under consideration is above the reference point, the gravitational potential is positive and negative if it lies below the reference point.

Pressure potential is that potential in the soil water due to the pressure of the surrounding fluid acting on the soil water. It is the relative or gauge pressure that is measured (i.e., relative to atmospheric pressure). Hence, the pressure potential is zero at a water surface (e.g., water table) exposed to atmospheric pressure. Pressure potential is positive at any saturated point below a water surface and is generally measured with a piezometer. A piezometer consists of a small diameter casing which has a short section of slotted pipe or well screen at the bottom and is open to the atmosphere at the top. The pressure potential or hydraulic head in a water table aquifer or a confined aquifer is calculated as the distance between the well point and the free water level in the piezometer. Under unsaturated conditions, the pressure potential or matric potential is negative and is measured with a tensiometer. A tensiometer generally consists of a ceramic porous cup attached through an airtight, water filled tube to a manometer. The vacuum created in the tube is a measure of the matric potential of the soil water surrounding the porous cup and is measured by a

TABLE VII-7

## TECHNIQUES FOR MEASURING SATURATED HYDRAULIC CONDUCTIVITY

Method	Technique	Remarks on Application	Method Rating	Reference
a. Direct testing of in-situ permeability in soils				
(A) Open Augerhole Test Pit	Shallow uncased hole in unsaturated material above water level  Square or rectangular test pit (equivalent to circular hole above)	Difficult to maintain water levels in coarse gravels	Poor  Poor	USBR (1968)  Lacroix (1960)
(B) Borehole Slug	i) Falling/rising head, $\Delta h$ in casing measured vs time  ii) Constant head maintained in casing, outflow measured, Q vs time	Borehole must be flushed Possible fines clog base (falling $\Delta h$ )  Pumping (rising $\Delta h$ ) where WL lowered excessively	  Fair to Good	Hvorslev (1951)  USBR (1968)
(C) Piezometers/Permeameters (with or without casing)	Piezometer tip pushed into soft deposits/placed in boring, sealed casing withdrawn/pushed ahead of boring. Constant head, outflow measured vs time. Variable heads also possible.	Possible tip 'smear' when pushed. $\Delta h$ set up in pumping tip  Danger of hydraulic fracture		Gibson (1966) Wilkes (1974) Hvorslev (1951) Bjerrum <u>et al.</u> (1972)
(D) Well pumping test	Drawdown in central well monitored in observation wells on at least two 90° radial directions	Screened portion should cover complete stratum tested	Excellent	Todd (1980)

TABLE VII-7 (continued)

Method	Technique	Remarks on Application	Method Rating	Reference
b. Direct testing of in-situ permeability in rock				
(A) Borehole (simple tests)	i) Water gain/loss in drilling	i) Gives possible indication of previous zones. Must be supplemented by detailed examination of core.	Poor	USBR (1968)
	ii) Simple variable/constant head tests in open boreholes			
(B) Borehole packer tests	i) Single packer tests (during advance of boring)	Expanding leather/rubber packers may provide inadequate seal	i) Fair	USBR (1968) Sherard, et al. (1963)
	ii) Double packer tests (in completed boreholes)	Pneumatic packers superior to other types, but limited to pressures <200 lb/sq. in.	ii) Poor to Fair	Sharp (1970)
(C) Permeameters/inserts	Variable head tests in:			
	i) Sealed individual piezometers (local zone)	i) Similar to Piezometers - local zones tested. Limited application	i) Fair to good (local zone)	i) USBR (1968)
	ii) Continuous borehole piezometers	ii) Possible to monitor water pressure variation over complete boring to 200m depth. Needs interpretation to assess K	ii) Fair (Potential good)	ii) Londe (1973)
(D) Well pumping test	Normally carried out in open central well. Observation wells at radii, 90	Screen/perforated casing often not required	Excellent	Todd (1980)



TABLE VII-7 (continued)

c. Indirect assessment of in-situ permeability in soils and rocks				
Method	Technique	Remarks on Application	Method Rating	Reference
(A) Tests on samples	i) Particle-size distribution	i) D <sub>10</sub> applicable to uniform sands	Fair	Loudon (1952) Golder, Gass (1963) Rowe (1972)
	ii) Laboratory K	ii) Often inapplicable to field conditions	Poor	
(B) Geophysical Logging	i) Multi-electrode resistivity	Continuous profiling of borings can be carried out at low cost (Requires further correlation with in-situ direct testing)	Fair	Guyod (1966) Robinson (1974)
	ii) Single point resistance potential		Future development	
	iii) Fluid conductivity, temperature		good	
(C) Observations of natural or induced seepage	Measurement and analysis of data from:			
	i) Observation wells	Provides method of assessing permeabilities, in-situ	Excellent	Walker (1955) Terzaghi (1960, 1964) Golder, Gass (1963) Sharp (1970)
	ii) Piezometers			
	iii) Dyes, tracers, radioactive isotopes			

Reference: Milligan (1976).

manometer, a vacuum gauge or a transducer. A detailed description of the design and use of tensiometers can be found in Kirkham (1964) and S. J. Richards (1965). Additional discussion is included in Table VII-6.

Osmotic potential is that potential of the soil water due to the physical separation of free water from soil water solutes by a semi permeable membrane. Separate measurement of osmotic potential is not necessary for screening calculations. It is difficult to measure but can be measured with a psychrometer (Richards and Ogata, 1961; Campbell et al. ., 1966; Taylor and Ashcroft, 1972) or a ceramic conductivity cell (Kemper, 1959).

#### 7.2.5.3.2 Measuring the Characteristic Curves of Soil-Water Retention and Hydraulic Conductivity

The soil-moisture characteristic curve can be obtained in the laboratory by a combination of measurement techniques. The hanging water column or tension plate method is generally used to measure the wet range (0 to 100 cm  $H_2O$  suction) of the characteristic curve and a pressure plate or membrane apparatus is generally used for the dry range (100 to 5000 cm  $H_2O$  suction). For suctions greater than 5000 cm  $H_2O$ , the soil-moisture characteristic curve can be determined by a psychrometer or vapor pressure technique using saturated salt solutions (Taylor and Ashcroft, 1972).

There are several methods of obtaining the characteristic curve of unsaturated hydraulic conductivity. These include direct laboratory methods and quasi-empirical methods, such as the instantaneous profile and capillary model techniques. The usual laboratory method of measuring unsaturated hydraulic conductivity is to apply a constant hydraulic head or pressure difference across a soil sample and then measuring the resulting steady flux of water. This pressure difference can be created by applying a vacuum in a tension plate or pressure chamber device or by creating a fixed evaporation rate (Taylor and Ashcroft, 1972). Measurements are made at successive levels of suction, so as to obtain the characteristic function  $K(\theta)$  or  $K(\psi)$ . Additional laboratory methods are described in detail by L. A. Richards (1965), Klute (1965) and Bouwer and Jackson (1974).

Various empirical equations have been proposed to relate hydraulic conductivity with matric potential or with percent saturation. The most commonly employed empirical equation is of the following form:

$$K = a / (b + \psi^m) \quad (VII-20)$$

where a, b and m are empirical constants,  $\psi$  is the absolute value of the matric or suction potential and K is the unsaturated conductivity. The empirical constants a, b and m are found experimentally for each soil by best fit.

The instantaneous profile method can be applied to either laboratory flow columns or to field situations (Klute, 1972). In this method, the unsaturated hydraulic

conductivity is calculated from the measured moisture content profile of a draining soil by averaging the value of the time derivative of the moisture content between successive depths. However, the instantaneous profile method can only determine hydraulic conductivity in the relatively wet range (suctions less than 1000 cm H<sub>2</sub>O). In addition, it is experimentally difficult to carry out this method and generally many duplicate measurements are necessary to make the conductivity-water content relationship reliable.

Another method of calculating the unsaturated hydraulic conductivity is to combine the water retention characteristic with the capillary pore-size distribution. This approach, called the capillary model, is based on the Kelvin equation which relates the surface tension and soil water energy to pore radius. A capillary model with a closed form solution for hydraulic conductivity is given by van Genuchten (1980). A review of previous theoretical capillary models is given by Mualem (1976) and a comparison between six recent models is given by Simmons and Gee (1981).

#### 7.2.5.4 Measurement Precision and Sample Size

Many of the methods given in Section 7.2.5 will give an accurate measurement of an aquifer property but this information usually consists of one or two values that are taken at one point in the aquifer. Because of heterogeneity within an aquifer, one or two measurements may not be representative. In this section, a brief discussion is given on how to achieve a specified level of precision and confidence level when estimating aquifer properties.

The number of measurements necessary to reasonably characterize the mean value of an aquifer property or parameter can be determined after some initial data collection. For the methods discussed below, several assumptions must be made. First, the sample mean of an aquifer parameter is assumed to be normally distributed. This means that if random measurements are made of an aquifer parameter, the deviation of the sample mean from the "true population" mean will be normally distributed. Secondly, the variance or standard deviation of the aquifer property will be assumed to be known or measurable. Based on these assumptions, the number of measurements needed to obtain a specified precision and confidence level of an aquifer parameter can be prescribed. However, the number of measurements and tests which can be made is often dictated by time and budget constraints. Comparison to the sample sizes given below indicates the level of confidence which should be placed in the data obtained. For screening calculations, the number of measurements collected will most likely be small.

The precision or margin of error that can be tolerated in measuring the mean value of a variable X with n samples and with confidence level  $\gamma$  is:

$$P_x = (t_{\gamma, n-1}) S_x / \sqrt{n} \quad (\text{VII-21})$$

where  $P_x$  is the precision of measuring variable  $X$ ,  $t_{\gamma, n-1}$  is the student's  $t$ -distribution percentile with confidence  $\gamma$  and  $n-1$  degrees of freedom,  $S_x$  is the standard deviation of the sample:

$$S_x = \left( \sum_{i=1}^{n^*} \frac{(X_i - \bar{X})^2}{n^* - 1} \right)^{1/2} = \left( \frac{\left( \sum_{i=1}^{n^*} X_i^2 \right) - n^* \bar{X}^2}{n^* - 1} \right)^{1/2} \quad (\text{VII-22})$$

$X_i$  is the  $i$ -th observed value of variable  $X$ ,  $n^*$  is the number of data measurements or observations used to find an estimate of the sample standard deviation,  $\bar{X}$  is the sample mean of variable  $X$ :

$$\bar{X} = \sum_{i=1}^{n^*} X_i / n^* \quad (\text{VII-23})$$

The precision  $P_x$  can also be written as a percent of the sample mean:

$$P_x = \bar{X} d / 100 \quad (\text{VII-24})$$

where  $d$  is the allowed deviation of the sample mean from the true mean, expressed as a percent of the true mean (i.e.,  $d$  can range between 0 and 100).

Upon rearranging Equation VII-21, it is possible to determine the number of measurements necessary to obtain a specified precision and confidence level:

$$n \geq (t_{\gamma, n-1} / e)^2 \quad (\text{VII-25})$$

where the variable "e" is defined as:

$$e = P_x / S_x = \left[ \bar{X} d / (100 S_x) \right] \quad (\text{VII-26})$$

The variable "e" is related to the inverse of the coefficient of variation and is dimensionless.

Equation VII-25 has been solved for various confidence levels and tabulated in Table VII-8 as a function of "e". It is quite clear from this table that the sample size "n" grows dramatically as the numerical value of precision decreases and as the desired confidence level increases.

If some value of "e" is desired other than that given in Table VII-8, then an iterative solution is necessary to solve Equation VII-25. This is because the student's  $t$ -distribution percentile  $t_{\gamma, n-1}$  is also a function of the number of measurements minus one,  $n-1$ . As an initial guess to the size of  $n$ , the standard normal deviate  $Z_\gamma$  can be used in place of the student's  $t$ -distribution in Equation VII-25.

TABLE VII-8  
 SAMPLE SIZE FOR VARIOUS CONFIDENCE LEVELS USING  
 THE STUDENT'S t-DISTRIBUTION

e	Confidence Level $\gamma(\%)$				
	50	80	90	95	99
.01	4549	16424	27055	38414	66349
.05	182	657	1082	1537	2654
.10	46	164	271	384	663
.15	21	74	120	173	295
.20	12	42	70	99	171
.25	8	28	45	64	110
.30	6	20	32	45	78
.40	4	12	19	26	45
.50	3	8	13	18	30
.60	2	6	10	13	22
.70	2	5	8	10	17
.80	2	4	7	9	14
.90	2	4	5	7	12
1.00	2	3	5	6	10
1.25	2	3	4	5	8
1.50	2	3	3	4	7
1.75	2	2	3	4	6
2	2	2	3	4	5
3	2	2	3	3	4
4	2	2	2	3	4
5	2	2	2	3	3
6	2	2	2	2	3
7	2	2	2	2	3
29	2	2	2	2	2

Values of  $Z_\gamma$  are given in Table VII-9 as a function of confidence level. Thus, as a first guess to determining the sample size (called  $n'$ ), solve:

$$n' = (Z_\gamma/e)^2 \tag{VII-26a}$$

With  $n'$  from Equation VII-26a, calculate the student's t-distribution  $t_{\gamma, n'-1}$  and substitute into Equation VII-25. Values of  $t_{\gamma, n'-1}$  are given in Table VII-10 as a function of confidence level and degrees of freedom  $df$ , where  $df = n'-1$ . The correct

TABLE VII-9

## STANDARD NORMAL DISTRIBUTION FUNCTION

Confidence Level $\gamma(\%)$	Deviate $Z_\gamma$
50	0.67449
80	1.28155
90	1.64485
95	1.95996
99	2.57583

$$\text{where } \gamma = 100 \int_{-Z_\gamma}^{Z_\gamma} \frac{e^{-y^2/2}}{\sqrt{2\pi}} dy$$

Reference: after Abramowitz and Stegun (1964).

Table VII-10

PERCENTAGE POINTS OF THE STUDENT'S t-DISTRIBUTION  
 $t_\gamma, df$ 

Degrees of Freedom  df= n-1	Confidence Level (%)				
	50	80	90	95	99
1	1.000	3.078	6.314	12.706	63.657
2	0.816	1.886	2.920	4.303	9.925
3	0.765	1.638	2.353	3.182	5.841
4	0.741	1.533	2.132	2.776	4.604
5	0.727	1.476	2.015	2.571	4.032
10	0.700	1.372	1.812	2.228	3.169
15	0.691	1.341	1.753	2.131	2.947
20	0.687	1.325	1.725	2.086	2.845
25	0.684	1.316	1.708	2.060	2.787
30	0.683	1.310	1.697	2.042	2.750
40	0.681	1.303	1.684	2.021	2.704
60	0.679	1.296	1.671	2.000	2.660
120	0.677	1.289	1.658	1.980	2.617
infinite	0.674	1.282	1.645	1.960	2.576

n = number of measurements.

Reference: after Abramowitz and Stegun (1964).

sample size "n" can be determined after one or two iterations (i.e., iterate until  $n'=n$ ).

Hence, in order to determine the correct sample size, the precision and confidence level have to be specified and an estimate made of the standard deviation. The latter can be made from historical data or by making a rough estimate from previous sampling or from a pilot survey. If no data are available, then a two step sampling procedure would be needed. First, a sample of size  $n^*$  from the initial data set (where  $n^*$  is at least 2 or more) is made from which the standard deviation is estimated using Equation VII-22. Then, Equation VII-26 and Table VII-8 can be used to find a total sample size "n". This and other sampling strategies are discussed in detail by Cochran (1977) and Nelson and Ward (1981).

An example of a two step sampling problem is shown below. In this example, the proper sample size for measuring hydraulic conductivity will be determined. The aquifer consists of alluvial sand. The drawdown versus elapsed time method of Theis is used to evaluate the horizontal hydraulic conductivity at various observation wells.

----- EXAMPLE VII-1 -----

Initially, six tests were conducted. The results are shown below:

<u>Field Data</u>	<u>Data Summary</u>
Saturated, Horizontal	existing data size: $n^* = 6$
Hydraulic Conductivity	confidence level: $\gamma = 95\%$
(cm/sec)	allowed deviation: $d = 10\%$
0.13    0.12    0.18	
0.13    0.13    0.15	

Based on these six initial measurements, a 95 percent confidence level, and a 10 percent deviation or precision in estimating the true mean, the following parameters were calculated. The sample mean  $\bar{X}$  was calculated using Equation VII-23 to give  $\bar{X} = 0.14$  cm/sec, the sample standard deviation  $S_x$  from Equation VII-22 gives  $S_x = 0.022$  cm/sec, precision  $P_x$  from Equation VII-24 gives  $P_x = 0.014$  cm/sec and variable e was calculated from Equation VII-26 to give  $e = 0.64$ . Finally, by using either Equation VII-25 or Table VII-8, it was determined that a total of 12 tests would have to be done (i.e., sample size  $n = 12$ ). Since six tests had already been done, six additional drawdown tests would have to be performed to obtain the desired degree of precision and confidence level.

Note that this precision and confidence refer to the uncertainty or variability of a single site if all 12 drawdown tests are done using the same observation well. Using 12 different observation wells will show the variability of the aquifer over the region measured.

-----END OF EXAMPLE VII-1-----

Before leaving this section on sampling size, one additional consideration needs to be considered: cost. Virtually all of the field tests used to measure the flow properties of aquifers, such as transmissivity or hydraulic conductivity are costly to perform. Typically, most ground water studies use only a few pumping tests per site or per study area. It is clear from Table VII-8 that two tests can only give results with a low confidence level and/or poor precision and one test provides no information about precision. But a few tests can give an "order of magnitude" value to an aquifer characteristic, such as hydraulic conductivity. An order of magnitude value is adequate for most screening calculations. For detailed investigations more data are needed to provide a greater level of confidence and precision.

### 7.3 GROUND WATER FLOW REGIME

#### 7.3.1 Approach To Analysis of Ground Water Contamination Sites

The recommended approach to analysis of ground water contamination problems is to first use existing data and screening methods such as presented in this chapter to gain a basic understanding of the site hydrogeologic characteristics and the relative hazard associated with the particular problem. The steps involved are to first characterize the waste sources in terms of type of waste, quantities disposed, disposal method, and dimensions of the disposal area. Next, hydrogeologic data for water levels, hydraulic conductivity, and porosity or moisture content are obtained. The water level data are plotted as ground water elevation contour maps from which flow directions are then determined. The remaining hydrogeologic data are used to estimate vertical and horizontal seepage velocities. Next, these velocities are used to estimate travel times for conservative solutes to nearby wells or surface water bodies. These estimates are compared to observed solute concentration data which can also be plotted as contour maps. The effects of additional processes including dispersion and chemical attenuation are then considered using the methods discussed in Section 7.5. Finally, estimates of uncertainty associated with the predictions should be made. At this point information is available to determine whether additional field sampling or detailed investigations are warranted.

The procedures for conducting the hydrogeologic portion of the analyses are discussed in detail in the following sections. Section 7.3.2 discusses measurement of water levels and determination of flow directions. Section 7.3.3 presents methods for calculating seepage velocities and travel times.



### 7.3.2 Water Levels and Flow Directions

#### 7.3.2.1 Introduction

Water level data can be found in ground water investigation reports or well logs, by talking to the owners of nearby wells, or by making water level measurements at existing wells. Also, water surface elevations of nearby streams, ponds, lakes, springs, marshes, gravel pits, etc. can be used to estimate water level elevations since these are areas where the ground water table intersects the land surface. (Care should be taken, however, to be sure that these water bodies are not perched.)

In the field, the presence or absence of vegetation common to wet soils and salt tolerant plants (e.g., willow, cottonwood, mesquite, saltgrass, greasewood) may be indicative of discharge areas and hence can be used to locate areas where the ground water table is near the surface. In arid regions, a thicker than normal cover of vegetation or salt outcrop (e.g., saline soils, playas, or salt precipitates) may indicate a discharge area. Field mapping of such occurrences can be valuable in obtaining an initial idea of the depth to water. However, relatively impermeable layers of even small areal extent may result in perched waters, which in turn yield wetlands or ponds. The unforeseen presence of a perched water table may lead to misinterpretations of surface observations.

The following general observations for unconfined water table aquifers in humid areas can be made:

- Ground water discharge zones are in topographic low spots
- Ground water generally flows away from topographic high spots and toward topographic low spots
- The water table may have the same general shape as the land surface.

From the above, it might seem reasonable that the hydraulic gradient (i.e., the change in ground water surface elevation per unit distance) of water table aquifers should vary in a direct relationship with the slope of the land (i.e., the hydraulic gradient is steepest where the land slope is steepest). However, the presence of formations with low hydraulic conductivity, subsurface geologic inhomogeneities and man-made influences (e.g., pumping wells, landfills) can have a profound effect on both the direction and magnitude of ground water flow. Care should be taken in assuming that the direction of the local ground water flow is the same as that of either the surface topography or regional ground water flow directions. For example, the presence of an unknown buried stream channel can cause the local flow to be in the opposite direction of the regional flow. Obtaining reliable water level data from observation wells is indispensable, even in the screening stage of a ground water study.

#### 7.3.2.2 Water Level Measurement

One of the most important measurements in ground water investigations is the determination of water level elevation. Mean sea level is generally taken as the

reference or datum from which water level elevations are measured. Water level elevation is best measured as the height of water in a piezometer or observation well. Such a well has a short, screened interval in the aquifer (confined or unconfined) and is open to the atmosphere at the top. Water level elevation represents the average hydraulic head  $H$  at the location of the well screen.

Most measurement techniques involve measuring depth to water (i.e., depth to water from land surface or from the top of the well casing). Depth to water is converted to water elevation by subtracting depth to water from the elevation of the ground surface. Serious errors in data interpretation can occur if the reference point from which the depth to water was measured (i.e., land surface or well casing top) was not noted.

To convert depth to water table to water level elevations, the land surface elevation (or well casing elevation) needs to be known. The required accuracy in measuring or knowing surface elevation depends in part on the ultimate use of the data and on the scale of the problem. Individually surveying each well is the best method. However, for screening purposes, an estimate based on topographic maps and the height of the casing above the land surface may be adequate in some cases.

Water level elevations are usually measured by means of a chalked steel tape or an electric water-level probe, but air lines, pressure transducers and sound reflection methods may also be used.

Great care should be taken when measuring water level elevations, particularly when the hydraulic gradient or aquifer slope is small. In general though, an accuracy of  $\pm 3$  centimeters in measuring water level elevation should be sufficient for most ground water applications and is easily obtained.

#### 7.3.2.3 Sources of Error in Water Level Data

There are many possible sources of error and misinterpretation when taking water level data. Some of the most serious errors are those caused by vertical flow in the aquifer, water level fluctuation, unknown screen locations and unknown or excessively long screened intervals. These sources are described in more detail in this section.

##### 7.3.2.3.1 Vertical Flow

Under most conditions, flow in a homogeneous formation is predominately horizontal. Under this assumption, the equipotential (equal energy) lines are vertical. Hence, water will rise to the same level in piezometers that are located side-by-side but which penetrate the aquifer to different depths. However, if flow is not horizontal, such as near a discharge or recharge area, the water will rise to different levels. This is schematically shown in Figure VII-14. The observed water level in a piezometer will decrease as the well tip of the piezometer is located at lower and lower depths in a recharge area (compare wells "a" and "b" in Figure VII-14). The water level will increase in a discharge area (compare wells "d" and "e" in Figure VII-14). This same phenomenon can occur near large pumping wells. Hence, a

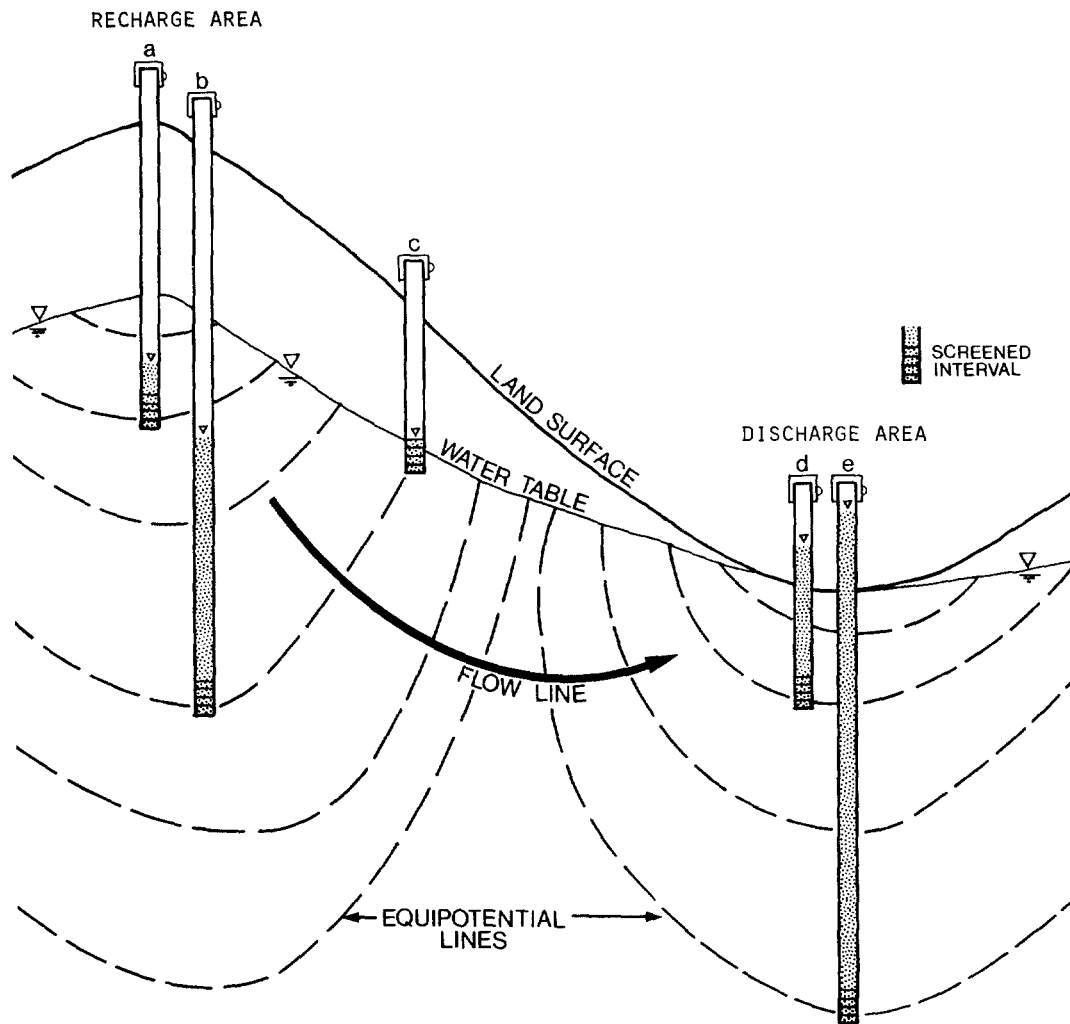


FIGURE VII -14 CROSS-SECTIONAL DIAGRAM SHOWING THE WATER LEVEL AS MEASURED BY PIEZOMETERS LOCATED AT VARIOUS DEPTHS, THE WATER LEVEL IN PIEZOMETER C IS THE SAME AS WELL B SINCE IT LIES ALONG THE SAME EQUIPOTENTIAL LINE

piezometer will only indicate the approximate water table in an unconfined aquifer with vertical flow. What the piezometer does indicate (assuming a short screen length is used) is the exact hydraulic or piezometric head at the point of the well screen. In fact, the vertical flow component of ground water velocity can be determined by placing several piezometers at various depths so that the vertical hydraulic gradient can be measured. This vertical gradient is then multiplied by the vertical hydraulic conductivity to obtain the vertical flow velocity (see Section 7.3.3.1).

Fortunately, the vertical hydraulic gradient in most aquifers is small enough that the component of vertical flow can be ignored. Care must be taken, however, to properly interpret water level data near recharge/discharge areas of the aquifer and near pumping wells. During pumping tests, only short well screens should be used in observation wells to avoid integrating or averaging ground water heads in the vertical direction.

#### 7.3.2.3.2 Water Level Fluctuations

Water levels in wells are usually not static but are constantly fluctuating. The water levels in wells that monitor confined aquifers generally fluctuate more than those in unconfined or water table aquifers. Short term fluctuations in confined aquifers can be caused by many factors, including earthquakes, ocean tides, changes in atmospheric or barometric pressure, changes in surface-water levels and in surface loadings (e.g., a passing train), recharge from precipitation and from drawdown of nearby pumping wells. Water levels in unconfined or water table aquifers are affected by recharge from precipitation (including air entrapment in the unsaturated zone), evapotranspiration, nearby pumping wells and atmospheric pressure changes.

These fluctuations can be observed by maintaining a continuous record of measured water levels over a period of time and then plotting water level as a function of time. The best way to reduce the effect of such fluctuation is to take water level measurements from all observation wells within a 1 to 2 day period. Generally, it is the relative spatial difference in the water level that is the most important information desired (see Section 7.3.3), rather than the absolute water level value.

#### 7.3.2.3.3 Screen Length and Location

Additional interpretation errors may occur when either screen length or screen location of the observation wells are unknown. In addition, excessively long screens (such as used in large production wells and open boreholes) can give conflicting information on water level. Long screens allow flow between different formations within an aquifer and may even penetrate more than one aquifer. Invalid conclusions can also be reached if wells tapping different aquifers are compared. It is important that accurate information be obtained as to screen length and depth. If such information is not obtainable, the water level data should be interpreted most cautiously.

#### 7.3.2.4 Determination of Flow Directions

After water level information has been collected, the data should be plotted as water level elevation contours and used to determine the ground water flow directions.

#### 7.3.2.4.1 Water Level Elevation Contours

A contour map of the water level elevations is prepared from wells screened in the same aquifer. Water level elevation data from the observation wells must all be measured during the same time period (best if measured within a few days) and in the same portion or zone of the aquifer (e.g., upper, middle, lower). A contour map of the water levels can be constructed using the following five steps: 1) plot the spatial location of each well on a map and label each point; 2) write the water level elevation value on the map for every well measured during the same specified time period and in the same aquifer; 3) decide which contour values are desired (e.g., every meter or decimeter change in elevation); 4) locate points on the map corresponding to the contour values chosen in step 3 by interpolating between all of the measured values; 5) draw a line connecting all points of equal value. These lines are drawn so that no two lines ever cross. This process is repeated for each time period and for each aquifer. An example of these steps is shown in Figure VII-15 for a water table aquifer underlying a series of waste ponds.

There are, of course, more sophisticated methods of constructing contour plots, such as contained in several computer programs. SURFACE II is a recent FORTRAN computer program developed by the Kansas Geological Survey (Olea, 1975; Sampson, 1978). This program uses regionalized variable theory or Kriging to perform automatic contouring of point observations. This and many other programs (Davis, 1973) are available but usually hand contouring is more than adequate for screening purposes.

#### 7.3.2.4.2 Water Flow Directions

It was stated in Section 7.2.4.1 that water flows in the direction of decreasing potential energy. In the case of saturated ground water, the potential energy is equal to the water level elevation, as measured by piezometers or wells screened in either confined or unconfined aquifers.

It can be shown that ground water in an isotropic aquifer not only moves in the direction of decreasing water level elevation but also perpendicular to the equipotential lines. Isotropy means that the hydraulic properties (e.g., hydraulic conductivity) of the aquifer are equal in all directions. Hence, if a contour plot of the water level elevation is available and if the horizontal and vertical scales that are used in constructing the contour plot are the same, then the ground water flow direction can easily be found as follows: 1) pick any point along a water level elevation contour or equipotential line; 2) draw a line (called a flow line) from this initial contour line to the next smaller valued contour line, going initially in a direction perpendicular to the first contour line; 3) extend the flow line until it reaches the next contour, making sure that it crosses this new contour line perpendicularly; 4) extend this flow line to as many contour lines as desired, always crossing the contour lines at right angles. Any number of flow lines can be

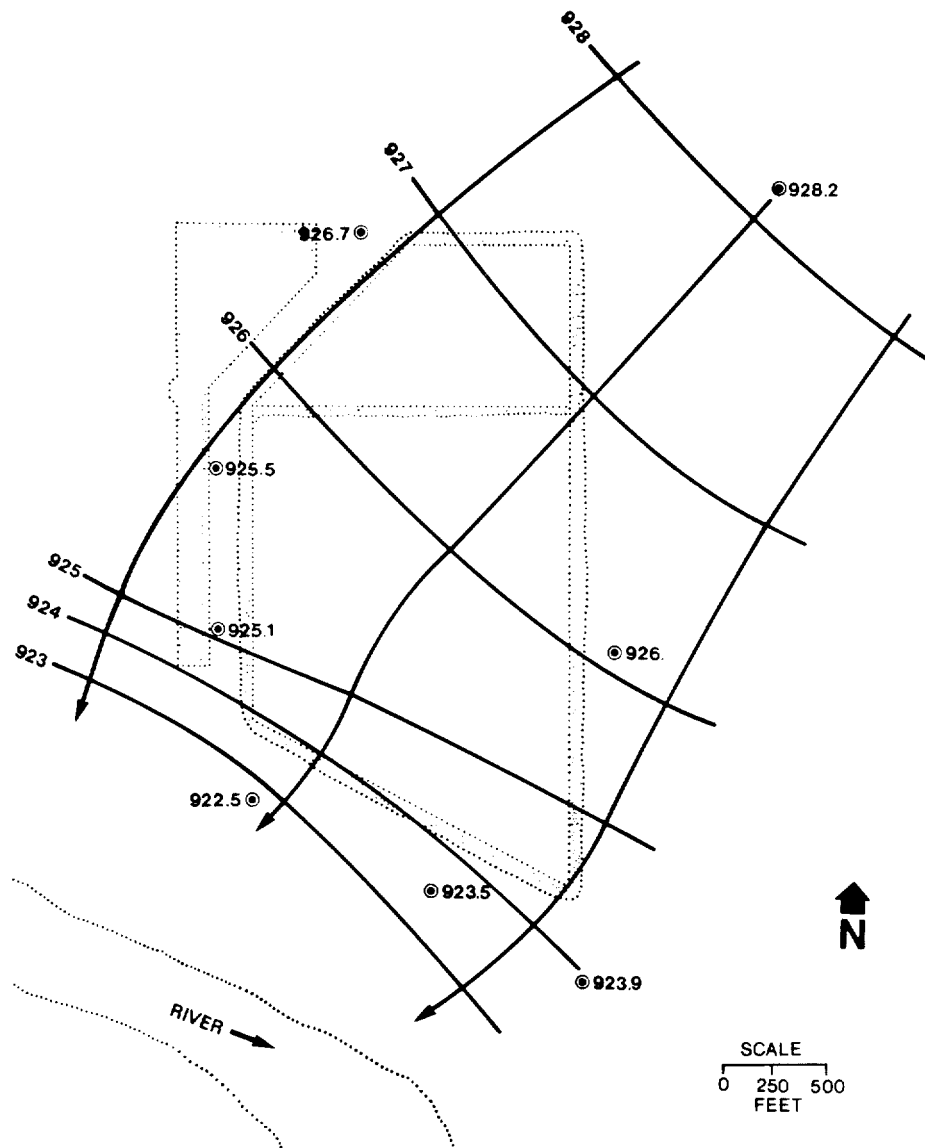


FIGURE VII -15 AN EXAMPLE OF A CONTOUR PLOT OF WATER LEVEL DATA WITH INFERRED FLOW DIRECTIONS.  
 REFERENCE: TETRA TECH, 1985

constructed in this manner. The direction of ground water flow is along these flow lines. An example of constructing flow directions is shown in Figure VII-15, using the water level data shown in the figure. An extensive discussion of graphical methods for constructing flow lines and flow nets can be found in DeWi est (1965).

As shown in Figure VII-16, the graphical construction of flow lines are made by crossing the equipotential lines at right angles. This is always true for isotropic, homogeneous aquifers when the plotted contours are constructed using equal horizontal and vertical scales. However, additional complications or modifications arise if these

conditions are not met. Van Everdingen (1963) discusses the problem of drawing flow lines when the horizontal and vertical scales are not equal as in cross-section diagrams. Liakopoulos (1965) provides theoretical principles for constructing flow lines in homogeneous, anisotropic media (when the hydraulic conductivity varies according to the direction of flow). Fetter (1981) gives a simple graphical method (using a permeability tensor ellipse) to account for anisotropy. Comparison of flow directions in an isotropic aquifer and anisotropic aquifer is shown in Figure VII-16.

The effects of anisotropy and heterogeneity are important but they are difficult to take into account with data generally available during the screening phase of a project. The construction of equipotential and flow lines should be done first assuming a homogeneous and isotropic aquifer. The flow directions could then be adjusted if additional detailed data show this to be necessary.

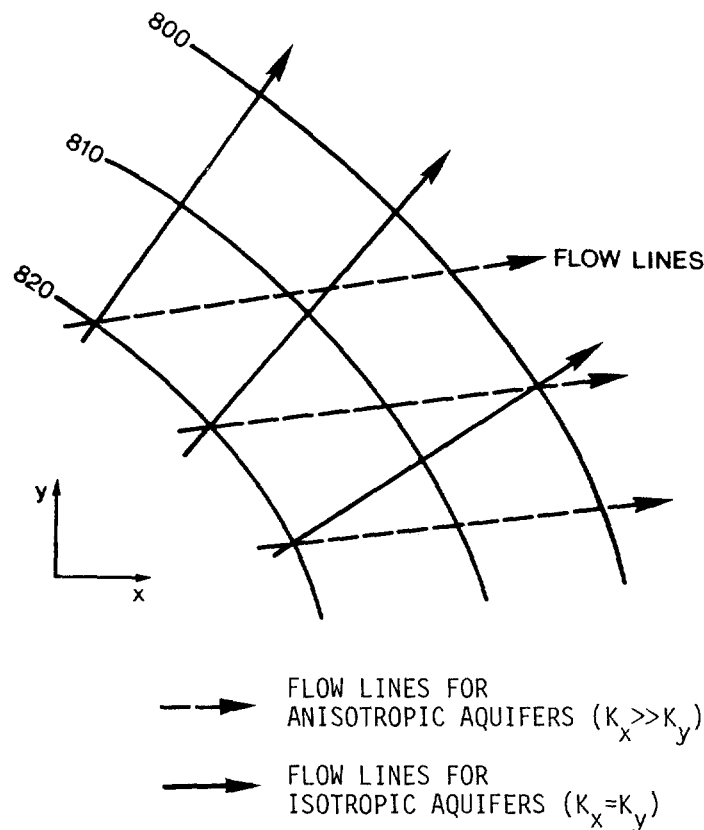


FIGURE VII-16 SCHEMATIC SHOWING THE CONSTRUCTION OF FLOW DIRECTION LINES FROM EQUIPOTENTIAL LINES FOR ISOTROPIC AQUIFERS AND ANISOTROPIC AQUIFERS

### 7.3.3 Flow Velocities and Travel Times

#### 7.3.3.1 Ground Water Flow Velocities

The direction of ground water flow is discussed in Section 7.3.2.4.2 in terms of water level elevations and hydraulic gradient. To determine the magnitude of ground water flow, Darcy's law is used. Section 7.3.3.1.1 presents Darcy's law for both saturated and unsaturated flow situations. The various forms of representing flow velocity are discussed in Section 7.3.3.1.2 and the applicability or range of validity of Darcy's law is reviewed in Section 7.3.3.1.3. Finally, methods of measuring or estimating ground water flow velocities are discussed in Section 7.3.3.1.4.

##### 7.3.3.1.1 Darcy's Law

In 1856, Henri Darcy discovered by experiment that the flow rate through a saturated porous medium was proportional to the change in head across the medium and inversely proportional to the length of the flow path. Darcy's law can be expressed as:

$$Q = -KA \Delta H/\Delta L = -KAI \quad (\text{VII-27})$$

where K is a proportionality constant (the hydraulic conductivity, cm/sec), A is the flow cross-sectional area ( $\text{cm}^2$ ) of the soil (measured at a right angle to the direction of flow),  $\Delta H$  is the change in hydraulic head (cm  $\text{H}_2\text{O}$ ) across the soil,  $\Delta L$  is the distance or length (cm) across the soil (measured parallel to the flow), I is the hydraulic gradient (cm/cm) and Q is the volumetric discharge rate ( $\text{cm}^3/\text{sec}$ ). The negative sign in Equation VII-27 indicates that water flows in the direction of decreasing head or potential energy.

Schematics of the experimental set-ups to demonstrate Darcy's law can be seen in Figure VII-17. In Figure VII-17a, flow occurs along an inclined, saturated soil column. The flow is from left to right, going from the upper to the lower reservoir of water. The change in hydraulic head  $\Delta H$  across the soil column is simply:

$$\Delta H = H_{\text{out}} - H_{\text{in}} \quad (\text{VII-28})$$

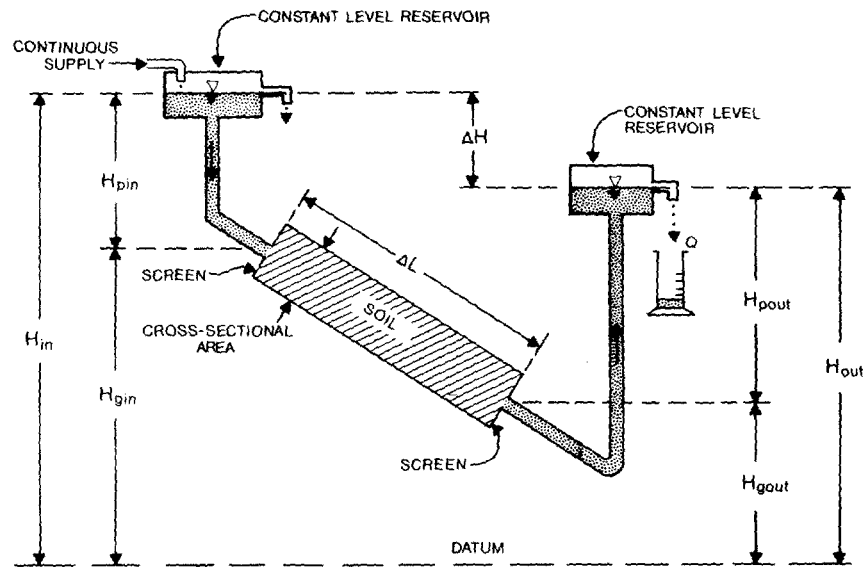
where  $H_{\text{in}}$  is the hydraulic head (cm) at the inlet and  $H_{\text{out}}$  is the hydraulic head (cm) at the outlet.

Darcy's law is also valid for unsaturated flow, the only difference being that the hydraulic conductivity is now a function of pressure potential  $H_p$  or  $\psi$

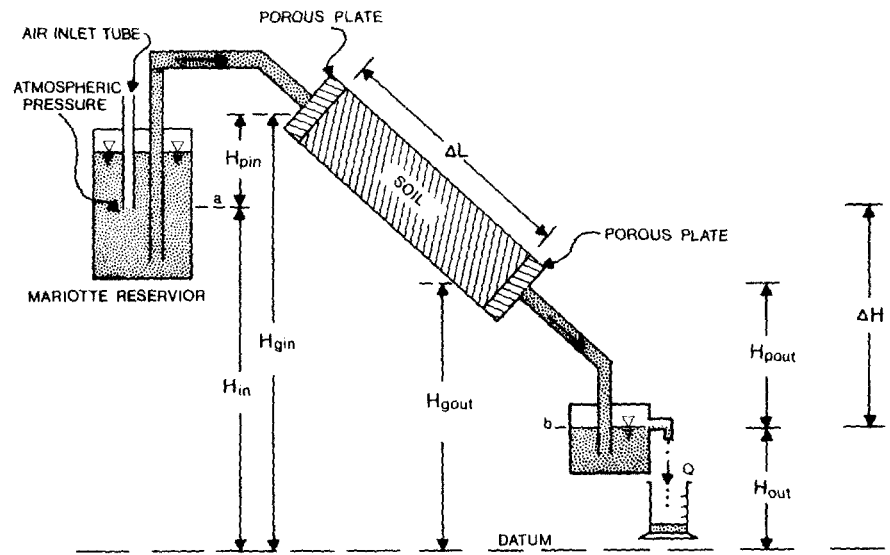
$$Q = -K(\psi) A \Delta H/\Delta L \quad (\text{VII-29})$$

An example of a demonstration of Darcy's law for unsaturated flow can be seen in Figure VII-17b. This example is the same as shown in Figure VII-17a but now the soil





a. Flow in an inclined saturated column of soil.



b. Flow in an inclined, unsaturated column of soil. Note that the Mariotte reservoir maintains a constant reference level at atmospheric pressure, even when the inlet water column is under negative pressure.

FIGURE VII - 17 SCHEMATIC DIAGRAMS SHOWING PERMEAMETERS TO DEMONSTRATE DARCY'S LAW

is subject to a negative pressure (or a positive suction) potential at both ends of the soil sample by hanging water columns. The hanging water columns will exert a negative pressure potential as long as points "a" and "b" are located below the inlet and outlet, respectively. In general, both the pressure potential and hydraulic conductivity will vary along the soil column. As the absolute value of the pressure potential increases, the hydraulic conductivity will decrease. However, a constant hydraulic conductivity can be made by making the pressure potential  $H_{pin}$  equal to  $H_{pout}$ .

The total head or potential at any given point is due to the sum of the gravitational and pressure potentials:

$$H = H_g - |H_p| \quad (VII-30)$$

The minus sign was put in front of the absolute value of the pressure potential to avoid any confusion as to the contribution of the pressure potential to the total head in unsaturated soil. Upon substitution of Equation VII-30 into Equation VII-28 and VII-29, Darcy's law for the unsaturated flow case illustrated in Figure VII-17b can be described by:

$$Q = -K^*A(H_{gout} - |H_{pout}| - H_{gin} + |H_{pin}|)/\Delta L \quad (VII-31)$$

where all of the H terms are expressed in units of length (cm). Since unsaturated hydraulic conductivity is a nonlinear function of pressure potential (see Section 7.2.4.3), the  $K^*$  (cm/sec) used in Equation VII-31 represents the hydraulic conductivity for the average matric or pressure potential  $\psi_{avg}$  (cm) in the soil column:

$$\psi_{avg} = (H_{pin} + H_{pout})/2 \quad (VII-32)$$

Hence, the hydraulic conductivity used in Equation VII-31 becomes:

$$K^* = K(\psi_{avg}) \quad (VII-33)$$

#### 7.3.3.1.2 Darcy and Seepage Velocities:

If the volumetric discharge rate  $Q$  (cm<sup>3</sup>/sec) from Darcy's law is divided by the cross-sectional area  $A$  (cm<sup>2</sup>), then the ratio  $Q/A$  has the units of a velocity,  $v_d$  (cm/sec). This "velocity" is called the Darcy velocity or specific discharge:

$$v_d = Q/A = -K\Delta H/\Delta L = -KI \quad (VII-34)$$

where  $I$  (cm/cm) is defined as the hydraulic gradient. However, the Darcy velocity is not the "true" velocity at which the water moves through the pores of a medium. It is both impractical and unnecessary to determine the actual microscopic velocities through the pore spaces. A more useful macroscopic quantity is called the seepage velocity. Since solutes do not migrate across the entire pore space, we need only consider the water filled portion of it. To take this into account, the Darcy velocity  $v_d$  is divided by the volumetric moisture content to yield the seepage velocity,  $v_s$ :

$$v_s = v_d / \theta \quad (\text{VII-35})$$

Since  $\theta$  is less than one, the seepage velocity is greater than the Darcy velocity (usually by a factor of 2 or more). The seepage velocity is also called the average interstitial or pore-water velocity.

For saturated flow, like in Figure VII-17a, the volumetric water content equals the porosity  $p$  (unitless ratio). Upon substitution of  $p$  into Equation VII-35 and  $v_s$  into Equation VII-34, the seepage velocity for saturated conditions becomes:

$$v_s = \frac{-K}{p} \frac{\Delta H}{\Delta L} = -KI/p \quad (\text{VII-36})$$

where  $I$  (cm/cm) is the hydraulic gradient. For unsaturated flow, the seepage velocity is:

$$v_s = \frac{-K}{\theta} \frac{\Delta H}{\Delta L} = -KI/\theta \quad (\text{VII-37})$$

where the hydraulic conductivity  $K$  is now a function of the moisture content  $\theta$ .

In general, the Darcy velocity  $v_d$  is used in the computation of ground water flow problems and the seepage velocity,  $v_s$ , is used in the computation of contaminant or solute transport problems. Great care must be used when obtaining velocity data from published reports since many authors do not state which velocity formulation they are using.

#### 7.3.3.1.3 Applicability of Darcy's Law

Darcy's law is only valid for those conditions in which the flux  $Q$  is a linear function of the hydraulic gradient  $I$  (i.e.,  $\Delta H/\Delta L$ ). This generally corresponds to the condition of laminar flow and when resistance to flow is dominated by viscosity. However, at very high velocities, the flow becomes turbulent and inertial forces become dominant. The Reynolds number  $R_e$  is a dimensionless number that expresses the ratio of the inertial to the viscous forces during flow:

$$R_e = d_s \rho_w v_d / \mu \quad (\text{VII-38})$$

where  $\rho_w$  is the density of water ( $\text{g/cm}^3$ ),  $\mu$  is the viscosity ( $\text{cm}^2/\text{sec}$ ) and  $d_s$  is some characteristic length (cm) representing the intergranular flow channels. Bear (1972) suggests using  $d_{50}$  (i.e., the average or mean grain size diameter) for  $d_s$  but sometimes  $d_{10}$  is used (See Section 7.2.2.2). Values for  $\rho_w$  and  $\mu$  are given in Appendix I.

Darcy's law has been shown experimentally to be valid for those conditions for which the Reynolds number is less than 10 when using  $d_{50}$  (the average grain-size diameter) for  $d_s$ . This covers virtually all natural ground water situations, except perhaps for flow through extremely coarse materials, and in areas of steep hydraulic gradients (gradients greater than 1, such as close to pumping wells). On the other extreme, Darcy's law may also be invalid for extremely low hydraulic gradients and flow through dense clay.

#### 7.3.3.1.4 Methods to Estimate Flow Velocities

There are several ways of estimating the ground water flow velocity. A review of these methods is shown in Table VII-11. The Darcy-based method, as discussed in Sections 7.3.3.1.1 and 7.3.3.1.2, is probably the least expensive and quickest method of estimating flow velocities. From Equation VII-34, the horizontal Darcy velocity  $v_{dh}$  (cm/sec) can be calculated between any two points spaced a distance  $\Delta x$  (cm) apart as:

$$v_{dh} = -K_h \Delta H / \Delta x = -K_h I_h \quad (\text{VII-39})$$

where  $I_h$  (cm/cm) is the horizontal hydraulic gradient,  $\Delta H$  is the hydraulic head change and  $K_h$  (cm/sec) is the horizontal hydraulic conductivity. The vertical Darcy velocity  $v_{dv}$  (cm/sec) can be calculated between any two depths spaced a distance  $\Delta z$  (cm) apart as:

$$v_{dv} = -K_v \Delta H / \Delta z = -K_v I_v \quad (\text{VII-40})$$

where  $I_v$  (cm/cm) is the vertical hydraulic gradient,  $K_v$  (cm/sec) is the vertical hydraulic conductivity and  $\Delta H$  (cm) is the change in hydraulic head across the points of measurement. Note that in the case of saturated flow (confined or unconfined),  $\Delta H$  is simply the difference in water level elevations between the measurement points.

The major disadvantage of using the Darcian method for calculating flow velocities is that the hydraulic conductivity needs to be known. Methods of measuring hydraulic conductivity are given in Section 7.2.5.2.2 but large uncertainties are usually associated with these methods. Despite these uncertainties, Darcy's method is best suited for the screening phase of a ground water study.

TABLE VII-11

## METHODS FOR MEASURING GROUND WATER FLOW VELOCITY

Technique	Advantages	Disadvantages	References
Darcy-based method	inexpensive simple to calculate can measure horizontal or vertical velocity	need to measure hydraulic conductivity separately	Freeze and Cherry (1979) Fetter (1980)
Direct tracer method	simple in principle only travel time needs to be measured	expensive must adjust for dispersion must know direction of flow and approximate velocity to design well sampling program	Knutson (1966) Brown et al. (1972) Gaspar and Oncescu (1972)
Point dilution method	a down-hole method short times needed single observation well is needed	long times are typically required to obtain data can only measure horizontal velocity	Halevy et al. (1967) Drost et al. (1968) Grisak et al. (1977) Klotz et al. (1978)
Flow meter	a down-hole method for directly measuring horizontal velocity quick, real-time method	under development significant interference from well screens and gravel packs does occur	Kerfoot, 1982

### 7.3.3.2 Ground Water Travel Times

The distance traveled by an object moving at a constant velocity is:

$$\Delta l = (\Delta t) (\text{Velocity}) \quad (\text{VII-41})$$

where  $\Delta l$  is the distance traveled and  $\Delta t$  is the time of travel. If the transport of a non-reactive and non-dispersive solute or contaminant is considered, the "velocity" in the above equation becomes equal to the seepage velocity  $v_s$  (which was discussed in Section 7.3.3.1.2). The seepage velocity is used because solutes only travel through the water filled portion of soil pores. The travel time  $\Delta t$  can now be solved from Equation VII-41 to give:

$$\Delta t = \Delta l / v_s \quad (\text{VII-42})$$

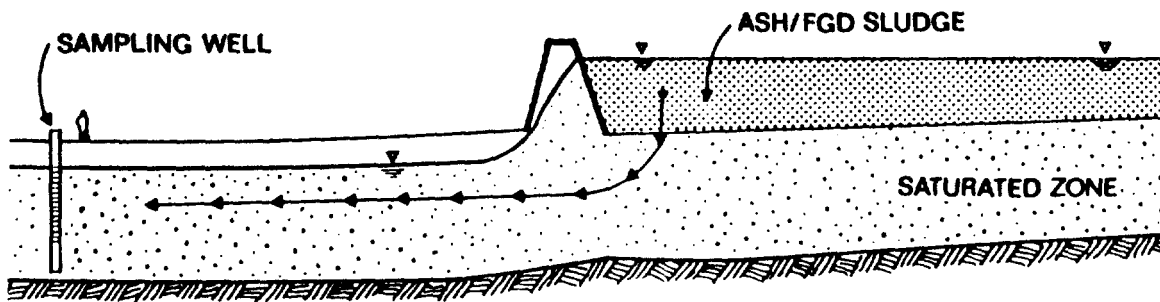
If the seepage velocity is calculated from Darcy's law, then Equation VII-36 can be substituted into Equation VII-42 to yield the travel time for saturated flow conditions:

$$\Delta t = \frac{-p\Delta l}{KI} \quad (\text{VII-43})$$

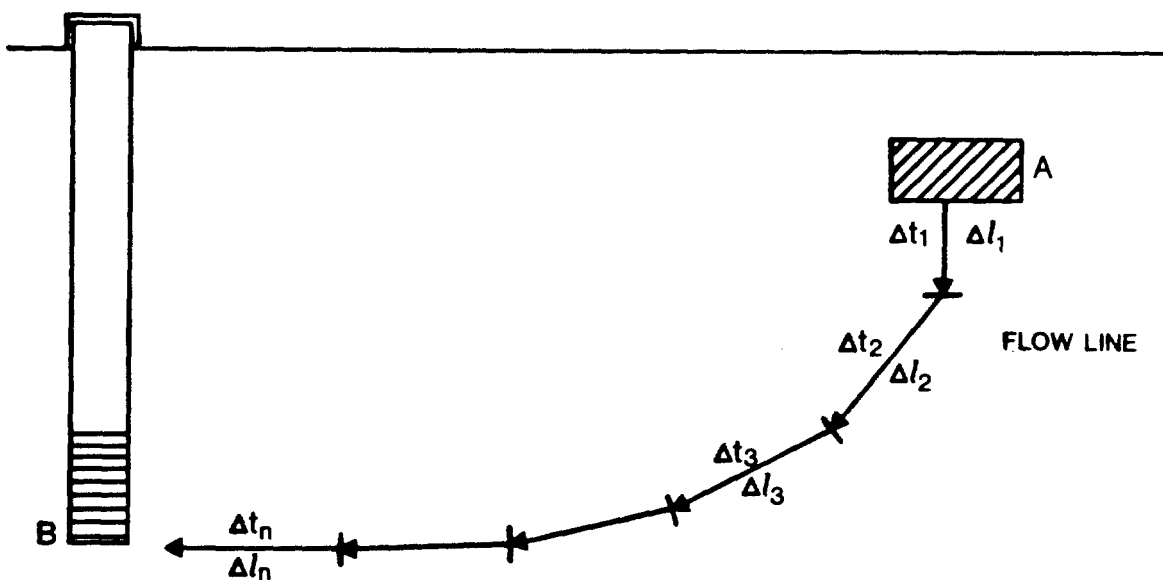
where  $\Delta t$  (sec) is the travel time,  $\Delta l$  (cm) is the travel distance,  $p$  (unitless ratio) is the porosity,  $K$  (cm/sec) is the hydraulic conductivity and  $I$  (cm/cm) is the hydraulic gradient. Estimated values of porosity are given in Table VII-4 for a variety of geologic materials. Note that the porosity used in Equation VII-43 is to be expressed as a ratio or decimal fraction and not as a percent. For unsaturated flow, the volumetric moisture content  $\theta$  (unitless ratio) is substituted in place of porosity "p" in Equation VII-43.

It should be remembered that travel times computed from Equations VII-42 and VII-43 are for non-reactive and non-dispersive, conservative solutes moving at a constant velocity. Retardation by sorption and attenuation by other solute-soil interactions may substantially decrease the velocity of solute movement and increase the travel time. Conversely, dispersive processes can either substantially increase or decrease the velocity that a portion of the solute molecules move and hence change the travel time. The processes of sorption and dispersion will be discussed in greater detail in Section 7.4.

In many situations, the flow velocity may vary in both direction and magnitude in an aquifer. Variable velocity and/or variable soil properties can easily be incorporated into the calculation of solute travel time by assuming that solute flow is a constant over a series of finite subregions. If these properties vary by less than 20 percent, discretization is not necessary for screening calculations. Figure VII-18



(a)



(b)

FIGURE VI 1-18 SCHEMATIC SHOWING HOW TRAVEL TIME CAN BE CALCULATED FOR SOLUTE TRANSPORT WHEN THE FLOW VELOCITY VARIES: A) ORIGINAL PROBLEM, B) DISCRETIZED REPRESENTATION OF THE FLOW LINE. REFERENCE: TETRA TECH (1984)

shows such a discretization process. Equation VII-43 is applied over each "constant" subregion and then all travel times are summed, such that the total travel time  $T_t$  is:

$$T_t = \sum_{i=1}^n \Delta t_i = - \sum_{i=1}^n \left[ \frac{p \Delta l}{K I} \right]_i \quad (\text{VII-44})$$

where the subscript "i" refers to the i-th subregion and n is the total number of subregions, p (unitless ratio) is the porosity,  $\Delta l$  (cm) is the travel distance, K (cm/sec) is the hydraulic conductivity and I (cm/cm) is the hydraulic gradient. For unsaturated flow, the volumetric moisture content  $\theta$  (unitless ratio) is substituted for porosity p. The parameters p,  $\Delta l$ , K and I can be different for each subregion "i". Obviously, a small number of subregions should be chosen at first, and the number increased as more data become available.

Consider the following example illustrating the computation of travel time for ground water from a holding basin to a nearby river.

#### EXAMPLE VII-2

A buried stream channel is suspected of being beneath the holding basin shown in Figure VII-19. The aquifer underlying the holding basin and the surrounding area is a water table aquifer (unconfined). The hydraulic conductivity measurement from a pump test at well B1 was 0.4 cm/sec and the hydraulic conductivity from a pump test in well B2 was 0.6 cm/sec. The water level elevations in wells B1 and B2 were  $2.82 \times 10^4$  cm and  $2.8140 \times 10^4$  cm, respectively. The estimated porosity is 0.3. Calculate the seepage velocity and travel time for sulfate from the edge of the holding basin to the river using the above data. Assume the sulfate does not interact with the soil.

Consider the following steps:

- 1) Obtain the average hydraulic conductivity from the two pumping tests,

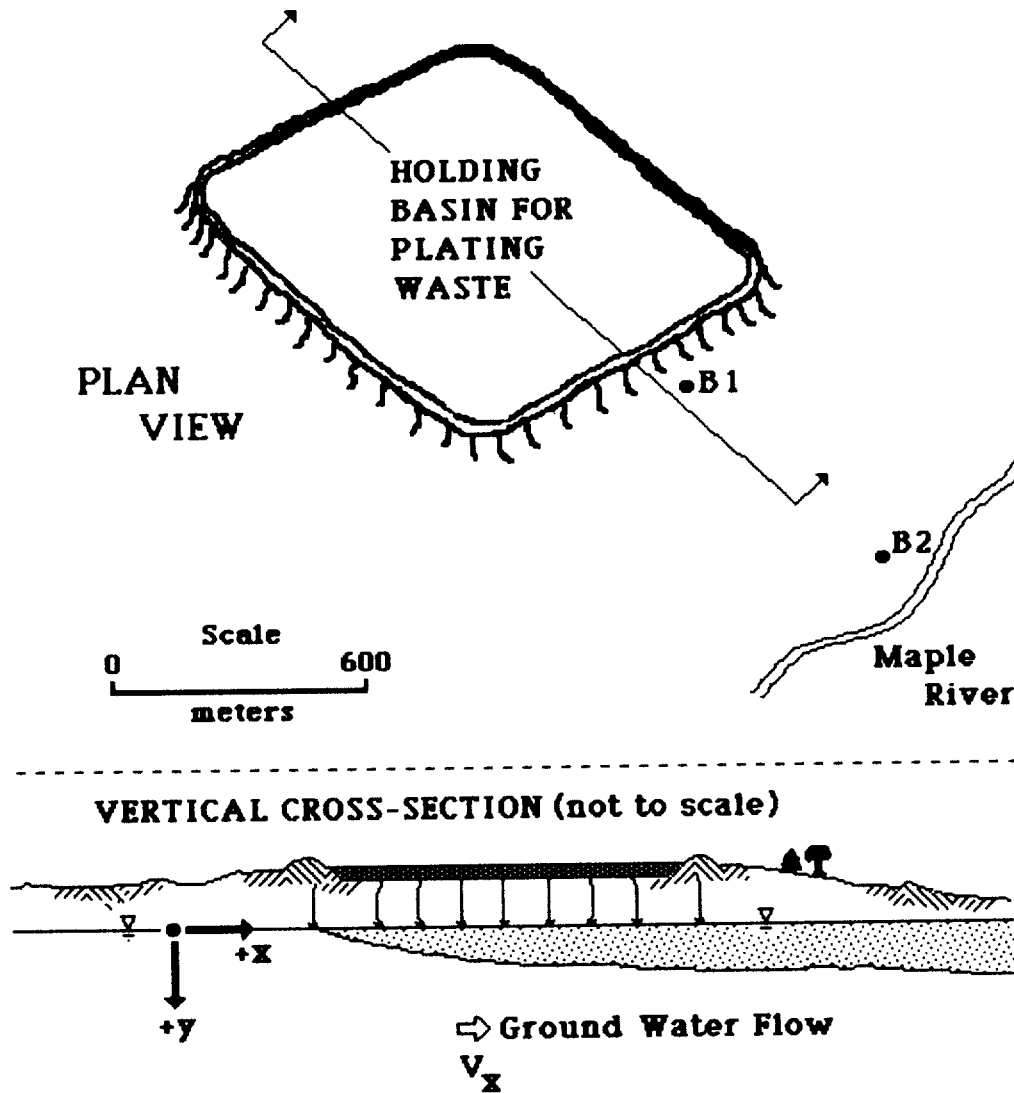
$$K = (0.4 + 0.6)/2 = 0.5 \text{ cm/sec}$$

- 2) Calculate the hydraulic gradient between the basin and the river, where the distance between wells B1 and B2 is  $4 \times 10^4$  cm,

$$I = \frac{\Delta H}{\Delta L} = \frac{(H_1 - H_2)}{\Delta L} = \frac{(2.8200 \times 10^4 - 2.8140 \times 10^4)}{4 \times 10^4}$$

$$= 0.0015 \text{ (cm/cm)}$$





<u>Parameter</u>	<u>Available Data</u>	
	<u>Well No. B1</u>	<u>Well No. B2</u>
H	$2.82 \times 10^4$ cm	$2.814 \times 10^4$ cm
K	0.4 cm/sec	0.6 cm/sec
P	0.3	0.3

FIGURE VII - 19 EXAMPLE PROBLEM: CALCULATION OF TRAVEL TIME FOR SULFATE FROM HOLDING BASIN TO RIVER

3) Calculate the seepage velocity using Equation VII-36,

$$v_s = \frac{KI}{p} = \frac{(0.5)(0.0015)}{(0.3)} = 0.0025 \text{ cm/sec}$$

4) Estimate the travel time to the river using either Equation VII-42 or VII-43, where the distance between the basin and the river is  $6 \times 10^4$  cm,

$$\Delta t = \Delta l / v_s = \frac{(6 \times 10^4)}{(0.0025)} = 2.4 \times 10^7 \text{ sec}$$

or

~~$$\Delta t = \frac{\Delta l}{v_s} = \frac{(0.3)(6 \times 10^4)}{0.0025} = 2.4 \times 10^7 \text{ sec}$$~~

Hence, the travel time for sulfate, from the basin to the river is 280 days or approximately 9 months.

END OF EXAMPLE VII-2

## 7.4 POLLUTANT TRANSPORT PROCESSES

The basis for ground water transport of contaminants is discussed in this section. First, the processes of dispersion and diffusion are reviewed in Section 7.4.1. This section includes both the definition and the estimation of these parameters for the one-dimensional and then the two-dimensional case. Finally, chemical and biological processes that affect contaminant transport are discussed in Section 7.4.2. This section discusses how sorption and rate processes can be represented in screening methods.

### 7.4.1 Dispersion and Diffusion

#### 7.4.1.1 Hydrodynamic Dispersion

Up until this point, the migration of dissolved solutes through porous media was assumed to be only related to the seepage velocity of ground water (see Section 7.3.3). Under this assumption, an injected solute or contaminant would travel through the aquifer by plug flow (e.g., piston-like motion). The concentration profile would resemble a step function. However, experience has shown that solutes do not exhibit true plug flow. Instead, solutes gradually spread out from their initial point of introduction and occupy an ever increasing volume of the aquifer, moving far beyond the region that it would be expected to occupy based on the average seepage velocity alone. This spreading or dispersing phenomenon is called hydrodynamic dispersion.

Hydrodynamic dispersion constitutes a nonsteady, irreversible mixing process. Bear (1972) states that hydrodynamic dispersion is the macroscopic outcome of the

solute's movement due to microscopic, macroscopic and megascopic effects. On the microscopic scale, dispersion is caused by: a) external forces acting on the ground water fluid, b) macroscopic variations in the pore geometry, c) molecular diffusion along solute concentration gradients, and d) variations in the fluid properties, such as density and viscosity.

In addition to inhomogeneity on the microscopic scale (i.e., pores and grains), there may also be inhomogeneity in the hydraulic properties (macroscopic variation). Variations in hydraulic conductivity and porosity introduce irregularities in the seepage velocity with the consequent additional mixing of solute. Finally, over large distances of transport, megascopic or regional variations in the hydrogeologic units or strata are present in the aquifer. The effect of scale on the mechanisms of hydrodynamic dispersion are shown schematically in Figure VII-20. Since the magnitude of dispersion varies significantly with the scale of the physical system, care must be taken to properly define which scale is to be used in any given problem.

The hydrodynamic dispersion coefficient  $D$  (cm<sup>2</sup>/sec) may be mathematically expressed as the sum of two dispersive processes: mechanical dispersion  $D_m$  (cm<sup>2</sup>/sec) and molecular diffusion  $D^*$  (cm<sup>2</sup>/sec). Thus, the sum is:

$$D = D_m + D^* \quad (\text{VII-45})$$

Molecular diffusion  $D^*$  is a microscopic and molecular scale process that results from the random thermal induced motion of the solute molecules within the liquid phase. This process is independent of the advective motion of the ground water and can be of significant importance at low flow velocities and very near solid surfaces. Duursma (1966) reported experimentally determined molecular diffusion coefficients that ranged between  $2 \times 10^{-6}$  and  $6 \times 10^{-6}$  cm<sup>2</sup>/sec for trivalent and monovalent ions (both positive and negative) in fine sand. However, molecular diffusion is generally specified (Sudicky, 1983; Gillham et al., 1984) as:

$$D^* = 1 \times 10^{-6} \text{ cm}^2/\text{sec} \quad (\text{VII-46})$$

Mechanical dispersion  $D_m$  occurs predominately on a macro and megascopic scale and is due to the "mechanical mixing" of the solutes. Such mechanical mixing is caused by: a) variations in the velocity profile across the water filled portions of a pore, b) variations in the channel size of the pores, c) the tortuosity, branching and interfingering of pore channels.

#### 7.4.1.2 One-Dimensional Flow

##### 7.4.1.2.1 Introduction

For one-dimensional flow, mechanical dispersion  $D_m$ (cm<sup>2</sup>/sec) is generally expressed

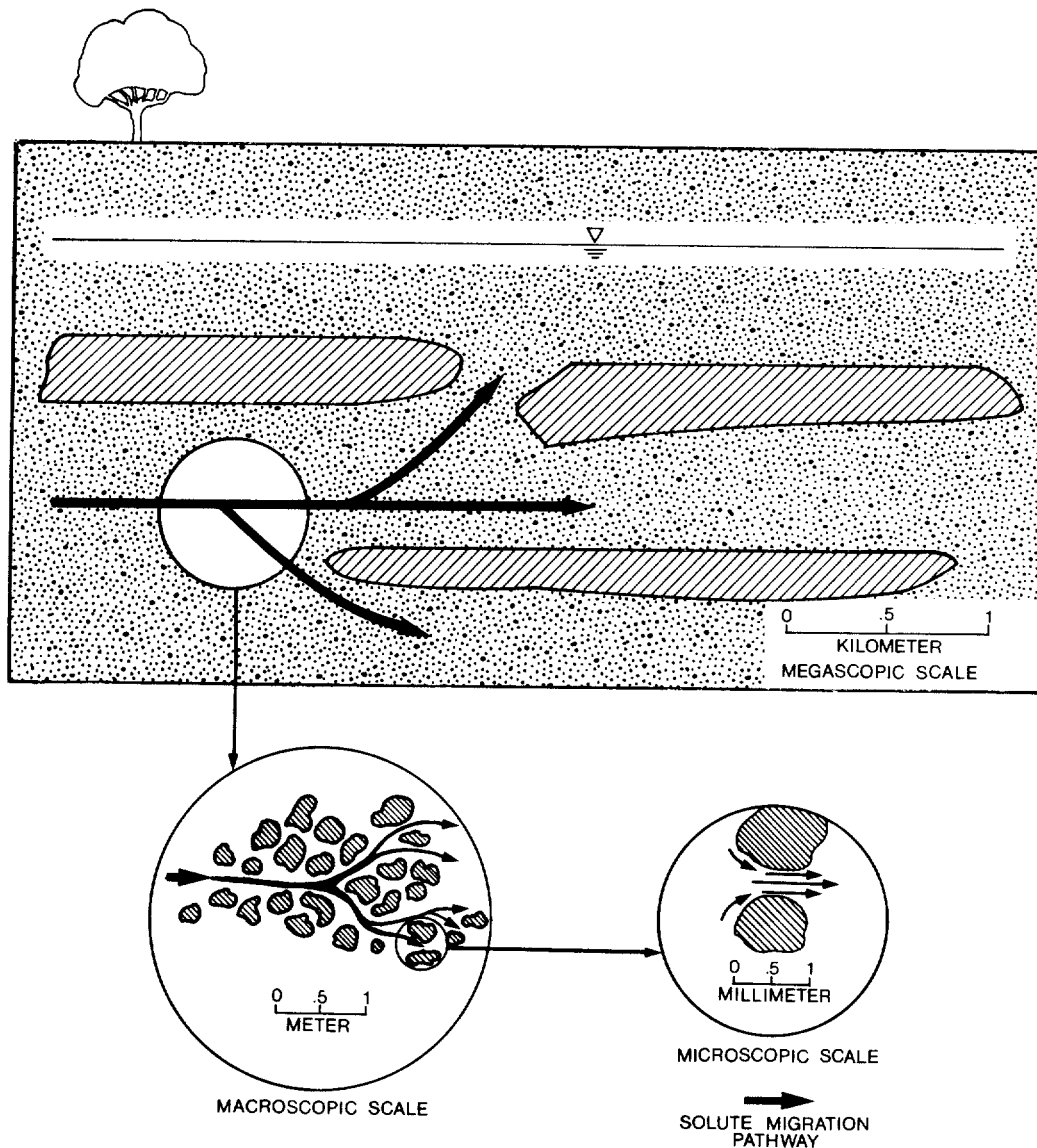


FIGURE VII -20 SCHEMATIC SHOWING THE EFFECT OF SCALE ON HYDRODYNAMIC DISPERSION PROCESSES

as a function of the seepage velocity  $v_s$  (cm/sec) with the relationship:

$$D_m = \alpha_l v_s \quad (\text{VII-47})$$

where  $\alpha_l$  (cm) is the longitudinal dispersivity of the porous medium. Upon substitution of Equation VII-47 into Equation VII-45, the hydrodynamic dispersion coefficient  $D$  (cm<sup>2</sup>/sec) becomes:

$$D = \alpha_l v_s + D^* \quad (\text{VII-48})$$

where the molecular diffusion  $D^*$  ( $\text{cm}^2/\text{sec}$ ) is given by Equation VII-46.

Unfortunately, dispersivity  $\alpha_1$  is not a constant but rather appears to depend on the mean travel distance or scale at which the measurements were taken (Fried, 1975; Pickens and Grisak, 1981 a, b; Sudicky, 1983). For example, laboratory experiments give values of dispersivity in the range of  $10^{-2}$  to 1 cm, while field determined values range from about  $10^3$  to  $10^4$  cm.

#### 7.4.1.2.2 Estimating Longitudinal Dispersivity

A rough estimate of longitudinal dispersivity in saturated porous media may be made by setting  $\alpha_1$  (cm) equal to 10% of the mean travel distance  $\bar{x}$  (cm) (Gelhar and Axness, 1981):

$$\alpha_1 = .1\bar{x} \quad (\text{VII-49})$$

In Figure VII-21, 48 values of longitudinal dispersivity are plotted as a function of scale length of the experiment for saturated porous media (Lallemant-Barres and Peaudecerf, 1978). Note in Figure VII-21 the line predicted by Equation VII-49. Lallemant-Barres and Peaudecerf (1978) concluded that field-scale dispersivity was independent of both the aquifer material and its thickness. In addition, Equation VII-49 and Figure VII-21 suggest that longitudinal dispersivity increases indefinitely with scale length.

More recently, Gelhar et al. (1985) reviewed the available literature and obtained 77 values of longitudinal dispersivity from saturated field studies and 13 values of longitudinal dispersivity from unsaturated field and laboratory studies. The saturated media results are shown in Figure VII-22 and the unsaturated media results in Figure VII-23. These data also show that longitudinal dispersivity increases with scale length. However, a critical evaluation of saturated site data in terms of reliability (as indicated by the size of the circles in Figure VII-22) Ted Gelhar et al. (1985) to suggest that no definite conclusion could be reached concerning scales greater than 100 meters. Longitudinal dispersivity probably approaches asymptotically a constant value for very large or megascopic scale lengths (Gelhar and Axness, 1983; Sudicky, 1983). In addition, the 10 percent rule of thumb expression for longitudinal dispersivity given by Equation VII-49 does not hold in the unsaturated zone. Rough approximations of longitudinal dispersivity for unsaturated flow can be made by using Figure VII-23, where scale means the mean travel distance or simply the distance from the origin of the contaminant.

To estimate longitudinal dispersion, an appropriate distance is determined (typically the distance from the contaminant source to the furthest point of interest). The dispersivity is then selected for the chosen distance from either Equation (VII-44) or Figure VII-22 for the saturated zone or Figure VII-23 for the unsaturated zone.

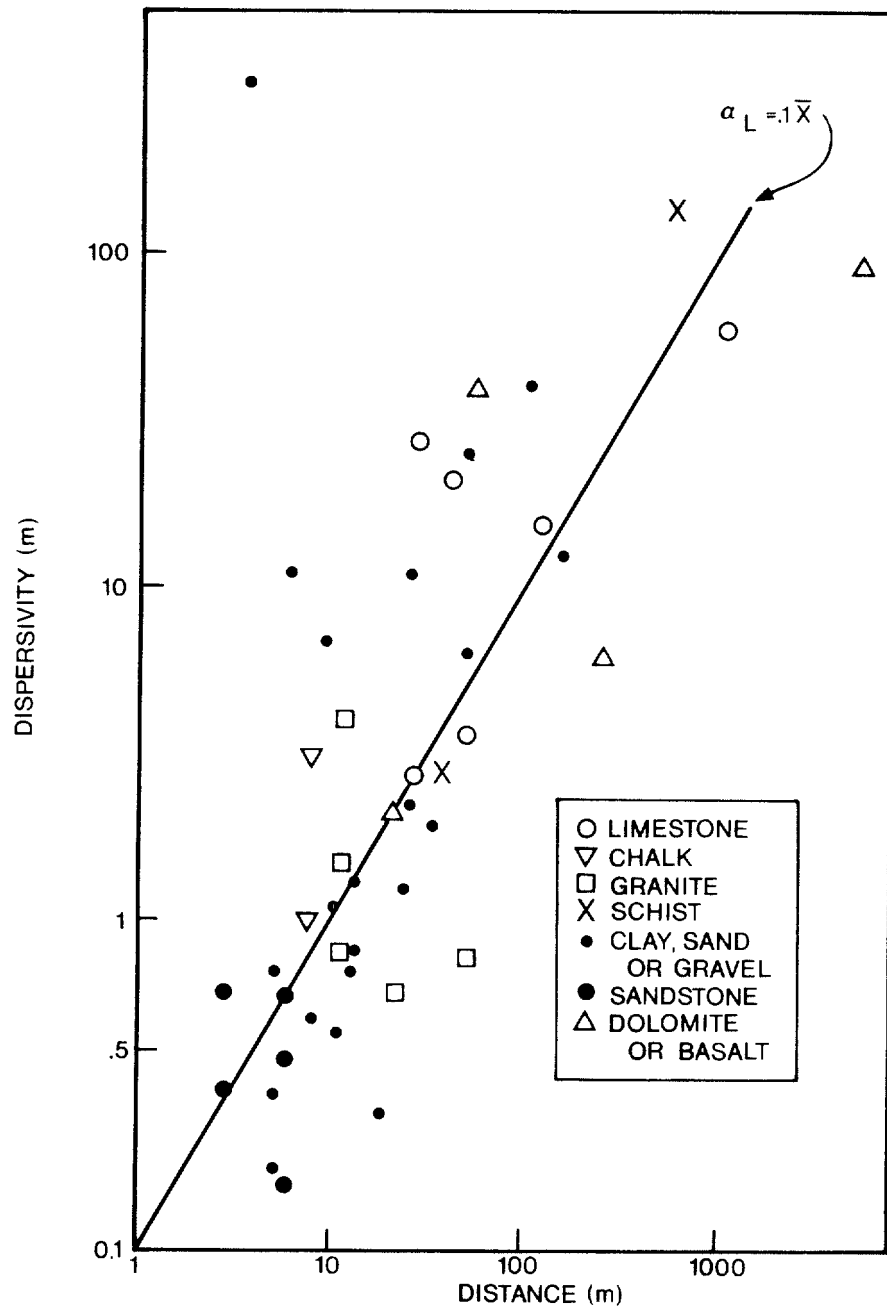


FIGURE VII -21 FIELD MEASURED VALUES OF LONGITUDINAL DISPERSIVITY AS A FUNCTION OF SCALE LENGTH FOR SATURATED POROUS MEDIA. REFERENCE: LALLEMAND-BARRES AND PEAUDECERF (1978)

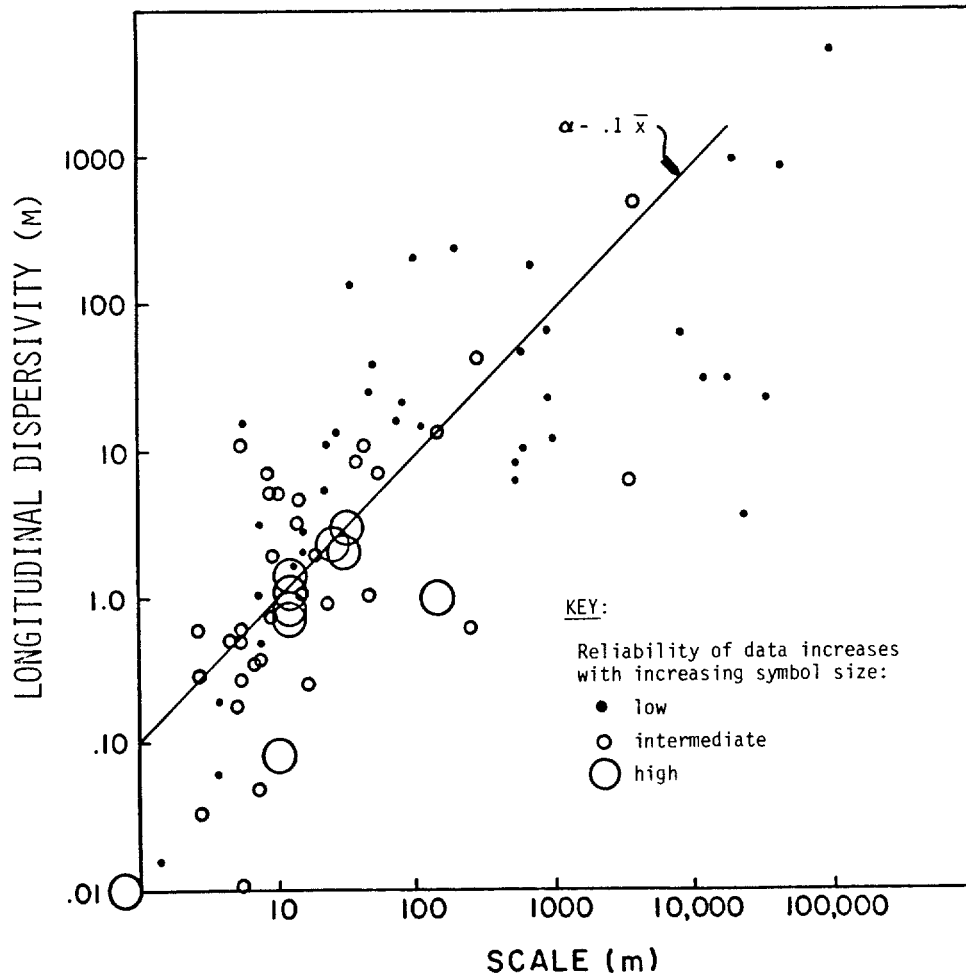


FIGURE VII -22 A PLOT OF LONGITUDINAL DISPERSIVITY VS. SCALE LENGTH FOR SATURATED POROUS MEDIA. REFERENCE: GELHAR ET AL. (1985)

Dispersion is then calculated using Equation (VII-48) or Equation (VII-47) for one-dimensional flow.

#### 7.4.1.2.3 Solute Transport Equation

In order to better visualize the concept of dispersion, a brief discussion is given concerning the equation describing one-dimensional solute transport in ground water flow systems. The partial differential equation describing the one-dimensional, advective-dispersive transport of non-reactive solutes in saturated (or unsaturated), homogeneous porous media is given by:

$$\frac{\partial c}{\partial t} = D \frac{\partial^2 c}{\partial x^2} - v_s \frac{\partial c}{\partial x} \quad (\text{VII-50})$$

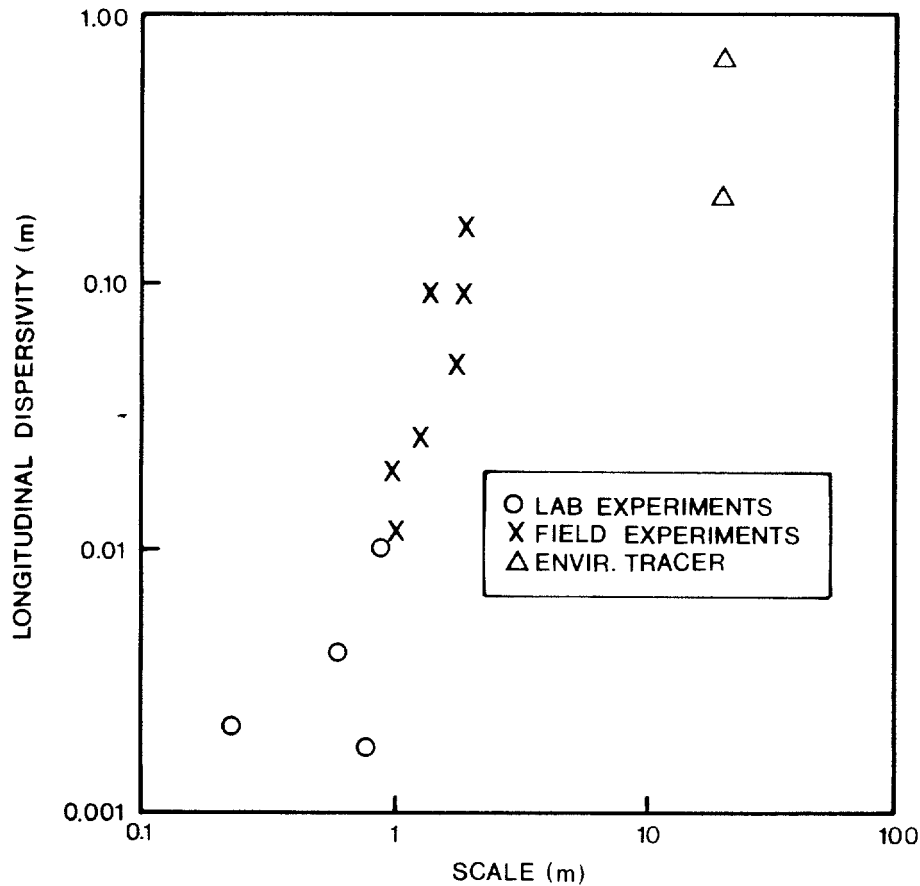


FIGURE VII-23 A PLOT OF LONGITUDINAL DISPERSIVITY VS. SCALE LENGTH FOR UNSATURATED POROUS MEDIA. REFERENCE: GELHAR ET AL. (1985)

where  $c$  (g/ml) is the solute concentration at time  $t$  (day) and distance  $x$  (m),  $D$  ( $m^2/day$ ) is the hydrodynamic dispersion coefficient and  $v_s$  (m/day) is the ground water seepage velocity.

If the aquifer is initially assumed to be solute free and if the  $D$  and  $v_s$  parameters are constant over the distance of interest, then a solution to Equation VII-50 for a step function input (i.e., the initial concentration goes from zero to a value  $c_0$  at  $t = 0$ ) can be obtained (Ogata and Banks, 1961; Ogata, 1970). The analytic solution and a worked out example using an integrated form of Equation VII-50 are given in Section 7.5.4. Note that a constant hydrodynamic dispersion coefficient  $D$  was used when solving Equation VII-50 in Section 7.5.4. Yet, Equation VII-49 and Equation VII-50 indicate that  $D$  is a function of distance or scale. Unfortunately, no simple analytic solution exists for the general case of a spatially varying dispersivity term. Hence, the distance or scale of the problem is used to compute the longitudinal dispersivity.



Consider the analytic solution to Equation VII-50 from Section 7.5.4, shown schematically in Figure VII-24. The solute concentration is plotted as a function of distance in Figure VII-24a at times  $t_1$  and  $t_2$ , where  $t_2$  is greater than  $t_1$ . The solute concentration is plotted as a function of time in Figure VII-24b. The solute concentration versus time plot is also known as a breakthrough curve. Each plot in Figure VII-24 also shows the solution to Equation VII-50 for plug flow (i.e., no dispersion).

A comparison between plug flow and dispersive flow in Figure VII-24 shows an "S" shaped curve when dispersion is considered. As time or distance increases, the S shape flattens out. Remember that solutes in plug flow move at the seepage velocity and as a sharp front. Hence, solutes in dispersive flow are spreading out and the leading portion of the solutes are moving faster than the seepage velocity and the trailing portion are moving slower than the seepage velocity. At the point  $c/c_0 = 0.5$ , the solutes move at a rate approximately equal to the seepage velocity.

In Section 7.3.3.2, the question of travel time was addressed but only for non-reactive, non-dispersive, plug flow. It should now be obvious from the above discussion that ignoring the effect of dispersion can considerably overestimate the travel time of a contaminant. The leading front of a contaminant plume may reach a given location as much as an order of magnitude faster than that predicted by plug or non-dispersive flow. Plug flow only predicts the travel time for the center or centroid of solute mass of the contaminant plume. The travel time estimates given by plug flow in Section 7.3.3.2 are still useful in that it gives a time reference for contaminant transport. What plug flow considerations alone cannot do is to predict time of arrival for the leading edge of a contaminant plume.

Unfortunately, there is no simple, algebraic way to incorporate the effect of dispersion into calculating time of travel and solute concentration profiles. Equation VII-50 has to be solved repeatedly for different times and distances. The example given above plus four other examples of solute transport are discussed with additional detail in Section 7.5.

#### 7.4.1.2.4 Measuring Longitudinal Dispersivity

In Section 7.4.1.2.1, several figures and equations were given as a means of estimating longitudinal dispersivity. These methods of estimation are more than adequate during the screening phase of a ground water project.

A great deal of controversy still exists as to the true meaning of hydrodynamic dispersion, its correct mathematical representation and the proper method to measure it in the field. In Equation VII-49, longitudinal dispersivity was estimated as a linear function of scale distance. However, many other representations are possible (Pickens and Grisak, 1981 a, b). Even stochastic representations are available (Todorovic, 1975; Smith and Schwartz, 1980; Gelhar and Axness, 1983).

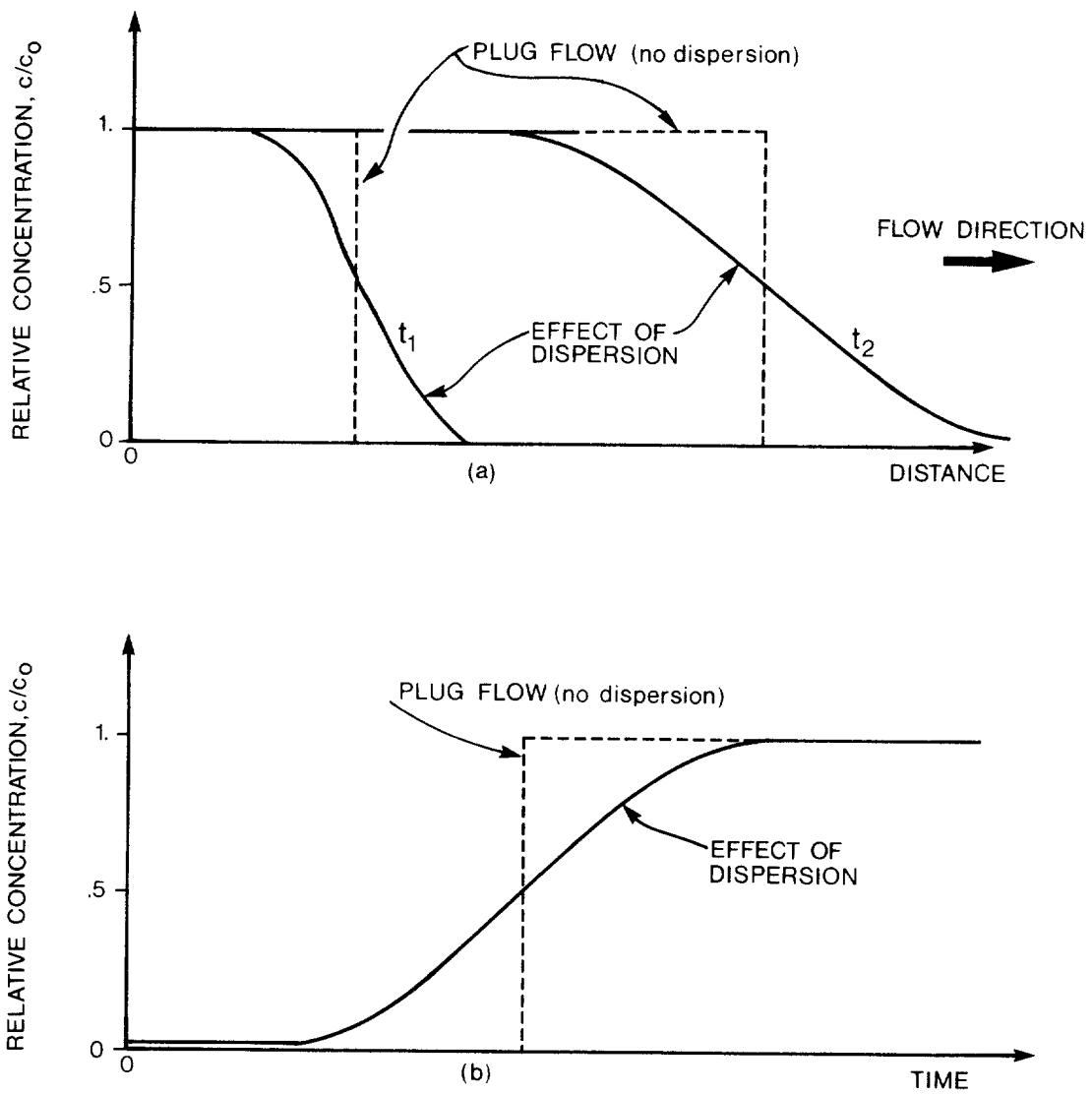


FIGURE VII -24 SCHEMATIC SHOWING THE SOLUTION OF EQUATION VII -50 AND THE EFFECT OF DISPERSION: A) SOLUTE CONCENTRATION AS A FUNCTION OF DISTANCE AT TIMES  $T_1$  AND  $T_2$ , B) SOLUTE CONCENTRATION AS A FUNCTION OF TIME (THE BREAKTHROUGH CURVE)

The typical field method to measure longitudinal dispersivity consists of injecting a tracer into the porous medium and then monitoring the arrival time of the tracer concentrations. The experimental data are then fitted or calibrated (using either an analytical or numerical solution of the dispersion equation) to obtain the longitudinal dispersivity or dispersion coefficients. Many analytical methods of fitting the solute breakthrough curve are available, such as those given by Elprince and Day (1977) and Basak and Murty (1979). An extensive discussion on field methods to determine dispersion coefficients is also given by Fried (1975).

#### 7.4.1.3 Multi-Dimensional Flow

##### 7.4.1.3.1 Introduction

In any real ground water system, the point release of a solute or contaminant into the aquifer will produce an expanding, three-dimensional ellipsoid. The concentration profile of such a plume will be approximately Gaussian in shape in the transverse directions (both across and down). The concentration profile will also be approximately Gaussian in shape along the longitudinal direction if the point release is instantaneous (i.e., a slug or short pulse). The component or contribution of dispersion will generally be greatest along the direction of flow (longitudinal) and less in the transverse directions. The longitudinal direction is implicitly taken to be along the principal direction of ground water flow. The transverse directions  $t$  and  $v$  are perpendicular to the longitudinal but  $t$  (lateral-transverse) is in the same plane as that of ground water flow. The  $v$  or vertical-transverse direction is perpendicular to the  $l$ - $t$  plane but it is not necessarily in the same direction as gravity. The vertical-transverse direction is only along the direction of gravity when the ground water flow is in the horizontal direction.

In a layered, unconsolidated aquifer with horizontal flow, the effect of vertical dispersion will generally be significantly less than from horizontal dispersion. Vertical mixing is a slow process and solute will often remain confined to a narrow horizontal zone in the aquifer. Hence, most analyses, including those of the screening methods, consider one- or two-dimensional analyses of solute transport. If the source of the solute or contaminant is very wide compared to the distance of interest, then one-dimensional analyses (such as is given in Section 7.4.1.2) are adequate.

As in Section 7.4.1.1, the coefficient of hydrodynamic dispersion  $D$  is defined as the linear sum of mechanical dispersion and molecular dispersion  $D^*$ . However, for an anisotropic, three-dimensional medium, Scheidegger (1961) and Bear (1972) define  $D$  as a fourth-rank tensor, containing 81 components. If the coordinate axes are chosen so that they coincide with the principal axes of dispersion, then virtually all of the off-diagonal terms of the tensor are zero.

In a two dimensional, horizontal, isotropic medium, the hydrodynamic dispersion coefficient becomes:

$$\begin{aligned}
 D_{xx} &= \alpha_l v_{sx}^2 / v_s + \alpha_t v_{sy}^2 / v_s + D^* \\
 D_{xy} &= D_{yx} = (\alpha_l - \alpha_t) v_{sx} v_{sy} / v_s \\
 D_{yy} &= \alpha_t v_{sx}^2 / v_s + \alpha_l v_{sy}^2 / v_s + D^*
 \end{aligned}
 \tag{VII-51}$$

where the magnitude of the seepage velocity  $v_s$  (cm/sec) is given by:

$$v_s^2 = v_{sx}^2 + v_{sy}^2
 \tag{VII-52}$$

and where  $D^*$  ( $\text{cm}^2/\text{sec}$ ) is molecular dispersion (see Equation VII-46);  $\alpha_l$  (cm) and  $\alpha_t$  (cm) are the dispersivities in the longitudinal and transverse directions, respectively;  $v_{sx}$  (cm/sec) and  $v_{sy}$  (cm/sec) are the longitudinal and transverse seepage velocity components, respectively;  $D_{xx}$ ,  $D_{yy}$  ( $\text{cm}^2/\text{sec}$ ) are the principal components of the hydrodynamic dispersion term; and  $D_{xy}$ ,  $D_{yx}$  ( $\text{cm}^2/\text{sec}$ ) are the off-diagonal components of the hydrodynamic dispersion term.

If the Cartesian coordinate system is chosen so that the longitudinal (i.e., the x) axis coincides with the direction of the average seepage velocity  $v_s$ , then D reduces to:

$$\begin{aligned}
 D_l &= \alpha_l v_s + D^* \\
 D_t &= \alpha_t v_s + D^*
 \end{aligned}
 \tag{VII-53}$$

where  $D_l$  ( $\text{cm}^2/\text{sec}$ ) and  $D_t$  ( $\text{cm}^2/\text{sec}$ ) are the longitudinal and transverse hydrodynamic dispersion terms, respectively. This orientation of the Cartesian coordinate system is used in most of the problems in Section 7.5. The molecular dispersion term  $D^*$  ( $\text{cm}^2/\text{sec}$ ) ranges in value between  $10^{-6}$  and  $10^{-5} \text{cm}^2/\text{sec}$ . The computation of the seepage velocity  $v_s$  is discussed in Sections 7.3.3.1, the longitudinal dispersivity term  $\alpha_l$  (cm) is given in Section 7.4.1.2.2 and the transverse dispersivity term  $\alpha_t$  (cm) is discussed below.

#### 7.4.1.3.2 Estimating the Transverse Dispersivity Components

Whitaker (1967) predicted that for uniform flow in an isotropic, saturated porous medium, that dispersivity would be dominated by the longitudinal dispersivity component  $\alpha_l$  and that  $\alpha_l$  would be exactly three times the value of the lateral-transverse component  $\alpha_t$ . Hence:

$$\alpha_l / \alpha_t = 3
 \tag{VII-54}$$

The estimate of Equation VII-54 agrees with the field data analyzed recently by Gelhar et al. (1985) for unconsolidated materials. The  $\alpha_l/\alpha_t$  ratio ranged between 2.1 and 5 for alluvial and glacial deposits (sand and gravel), the average being 3.5. The ratio of  $\alpha_l/\alpha_v$  for limestone was 3.2. The vertical transverse component of dispersivity  $\alpha_v$  was generally two orders of magnitude smaller than that of the horizontal components. The  $\alpha_l/\alpha_v$  ratio ranged between 30 and 860 for alluvial/glacial deposits, the average being 400 (Gelhar et al. , 1985).

The dispersivity components can be estimated for screening purposes as follows:

a) use the 10 percent rule of thumb from Equation VII-49 to estimate the longitudinal  $\alpha_l$  component for saturated media and Figure VII-23 for unsaturated media, b) then use either Equation VII-54 or the above ratios to estimate the transverse dispersivities  $\alpha_t$  and/or  $\alpha_v$ .

#### 7.4.1.3.3 Alternative Dispersion Formulations

Before leaving this section on dispersion, one additional comment should be made concerning spatial variability. In both the one-dimensional and two-dimensional representations of solute transport, it is conveniently assumed that the seepage velocity  $v_s$  could be averaged and expressed as a constant. However, the seepage velocity may have substantial variations in space. Consider Figure VII-25 which schematically shows how the horizontal seepage velocity  $v_s(z)$  may vary dramatically with depth. Such stratification or variations are quite common in aquifers and are caused by the variations in the hydraulic conductivity and porosity in the medium (Sudicky et al., 1983; Gillham et al., 1984). Recently, several researchers such as Molz et al. (1983), Sudicky (1983), Gillham et al. (1984), etc. have suggested that the primary physical mechanism that causes the spreading of solute in the longitudinal direction is due to the vertical variation in the seepage velocity  $v_s(z)$ . Hence, they argue that the phenomenon of scale-dependent dispersivity and hydrodynamic dispersion is an artifact. They suggest that more emphasis should be placed on the accurate determination of hydraulic conductivity and aquifer inhomogeneities.

Artifact or not, the use of hydraulic dispersion algorithms is currently the only practical method, short of direct measurement, to account for dispersive solute transport. Those who are in the screening phase of a ground water project are unlikely to have access to a detailed survey of the hydraulic conductivity and seepage velocities of the aquifer. The analytic and heuristic methods presented here and in Section 7.5 are the best that are currently available.

#### 7.4.2 Chemical and Biological Processes Affecting Pollutant Transport

Pollutants in ground water can be affected by a number of chemical and biological processes as shown in Figure VII-26. Volatilization generally does not have to be considered in ground water screening problems unless the pollutant is within a few inches of the land surface and the media is highly permeable. Of the remaining

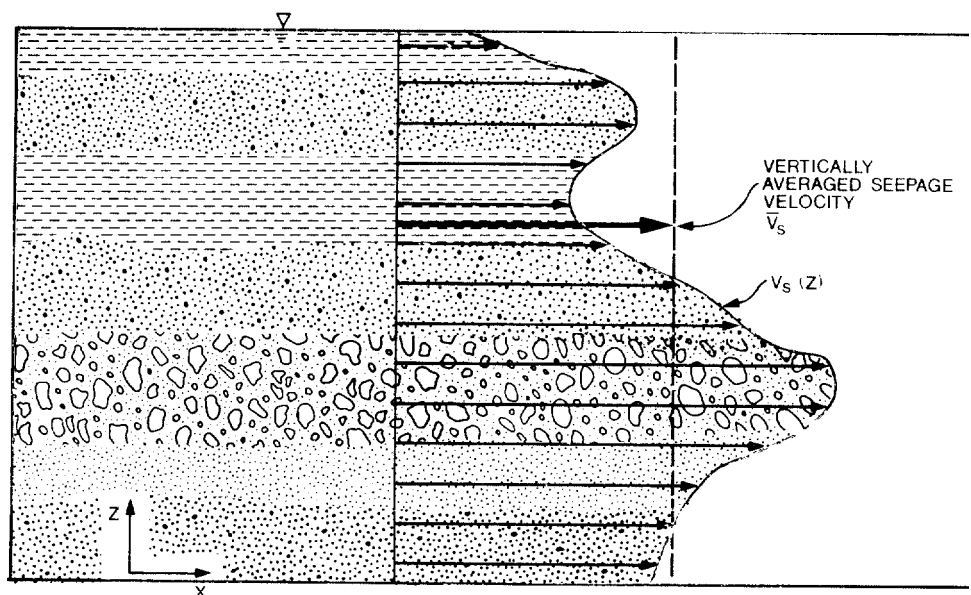


FIGURE VII -25 SCHEMATIC SHOWING HYPOTHETICAL VERTICAL VARIATION IN THE GROUND WATER FLOW VELOCITY

processes shown in Figure VII-26, some can be incorporated directly into the analytical methods to be presented later in this chapter. These processes are sorption-desorption and ion-exchange, hydrolysis, and biodegradation.

Other chemical processes can be considered separately from the analytical methods. Processes which can be evaluated include acid-base reactions, speciation, complexation, oxidation-reduction reactions and precipitation-dissolution. For example, to determine if sorption is important and if so, an appropriate coefficient, the metal speciation must be determined for the pH and redox conditions present in the ground water. This can be done based on Eh-pH diagrams or equilibrium geochemical models. At this point, the transport of the metals can be estimated using the analytical methods discussed in Section 7.5. Next, the extent of precipitation-dissolution can be determined using methods similar to those described in Chapter 4 of this manual. If the calculations show that some metal could precipitate, the transport calculations can be revised using the new dissolved concentration. In most surface and ground waters, revised transport calculations will not be necessary because sorption is the dominant process at typical metal concentrations. However, within a waste material and immediately downgradient of it, metal concentrations can be high so solubility limits should be checked.

#### 7.4.2.1 Sorption

Sorption can be defined as the accumulation of a chemical in the boundary region of the soil-water interface. Sorption-desorption processes are an important

# GEOHYDROCHEMICAL PROCESSES

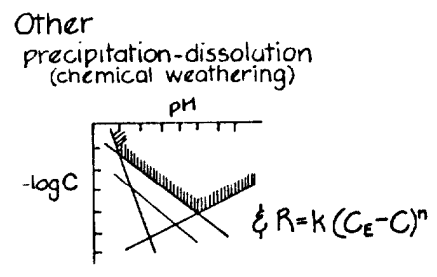
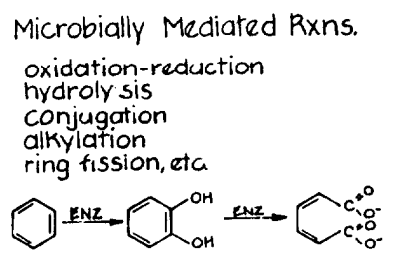
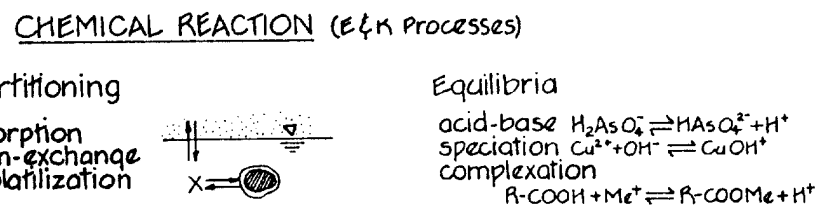
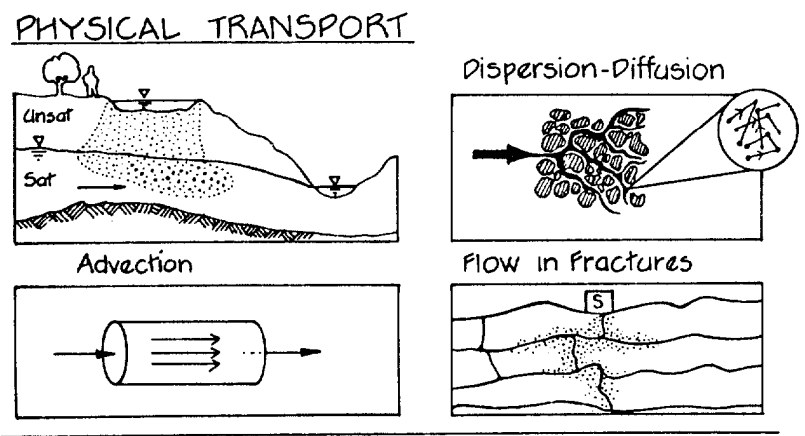


FIGURE VII-26 MAJOR EQUILIBRIUM AND RATE PROCESSES IN NATURAL WATERS. REFERENCE: SCIENCE APPLICATIONS, 1982

determinant of pollutant behavior in the subsurface environment. Because of the much higher solid to liquid ratios in ground waters than in surface waters, the concentration of even a moderately-sorbed pollutant can decrease significantly with distance as it migrates in the ground water. In addition to decreasing the aqueous concentration, there are several other implications of sorption. Volatilization, even in the uppermost soil layers, is diminished. Rates of reactions such as microbial degradation can be different for the adsorbed pollutant and the portion remaining in solution. Unlike in surface waters where the adsorbed pollutant may still be advected

downstream associated with suspended sediment, in ground water the adsorbed pollutant is not usually transported by advection or dispersion (the solid phase is immobile.) However, when the concentration gradient changes, the pollutant can be desorbed over time at the same or a different rate than it was sorbed onto the soil particles. This has important implications for handling waste disposal problems in that when "clean" water flushes an aquifer which previously contained water contaminated with metals or organic chemicals, the concentrations of the pollutants may remain relatively high until the reservoir of adsorbed pollutants has been depleted. In one case of high TCE contamination, the downgradient concentration was predicted to be 80 percent of the existing level even after the aquifer was flushed once with distilled water.

#### 7.4.2.1.1 Retardation Factor

If sorption is modeled as a linear, equilibrium process, it can be incorporated into the analytical methods presented in Section 7.5 as a retardation factor. This factor is defined as follows:

$$R_d = 1 + (K_d \rho_b / p) \quad \text{(VII-55)}$$

where

- $R_d$  = retardation factor (unitless)
- $K_d$  = distribution coefficient (ml/g)
- $\rho_b$  = bulk density (g/ml)
- $p$  = porosity (decimal fraction).

The term,  $K_d$  is used in most ground water literature, but it is synonymous with  $K_p$ , the partition coefficient, which is more common in chemical and surface water literature. If a pollutant is not sorbed, the retardation factor equals 1 which shows that the pollutant moves at the same speed as the ground water. If the retardation factor is greater than 1, say 2, the pollutant will move half as fast as the water. Typical values for bulk density and porosity for different types of soil materials were included in Table VII-2 and VII-4, respectively.

The  $K_d$  term is an empirical coefficient for a specific constituent under a particular set of conditions. For linear, equilibrium sorption,  $K_d$  can be measured in the laboratory as:

$$K_d = [s]/[c] \quad \text{(VII-56)}$$



where  $K_d$  = distribution coefficient, ml/g  
 [S] = concentration of pollutant sorbed on soil, g/g  
 [C] = concentration of pollutant in solution, g/ml.

$K_d$  may be a function of the concentration of the sorbing chemical species itself, the concentration of any competing species (usually major ions affect trace constituents but not vice-versa), concentrations of any competing species present (e.g., Cl, organics), pH of solution, the amount and type of adsorbent (e.g., clays, iron oxides, aluminum oxides), and the amount of organic matter associated with the solid phase. Figure VII-27 shows the effect of pH and organic matter on typical adsorption curves. When obtaining values for a pollutant of interest, these and other factors should be as similar as possible to the conditions in the problem being addressed. Selected  $K_d$  values for metals have been included in Chapter 4. Available values for Al, Sb, As, Ba, Be, B, Cd, Cr, Cu, F, Fe, Pb, Mn, Hg, Mo, Ni, Se, Na,  $SO_4$ , V, and Zn have been compiled from the literature for a variety of conditions (Rai and Zachara, 1984). The values are reported along with characteristics of the adsorbent (i.e., type of material, cation exchange capacity, and surface area), concentration of species of interest, and solution characteristics (i.e., composition, molar concentration of adsorbing species and pH).

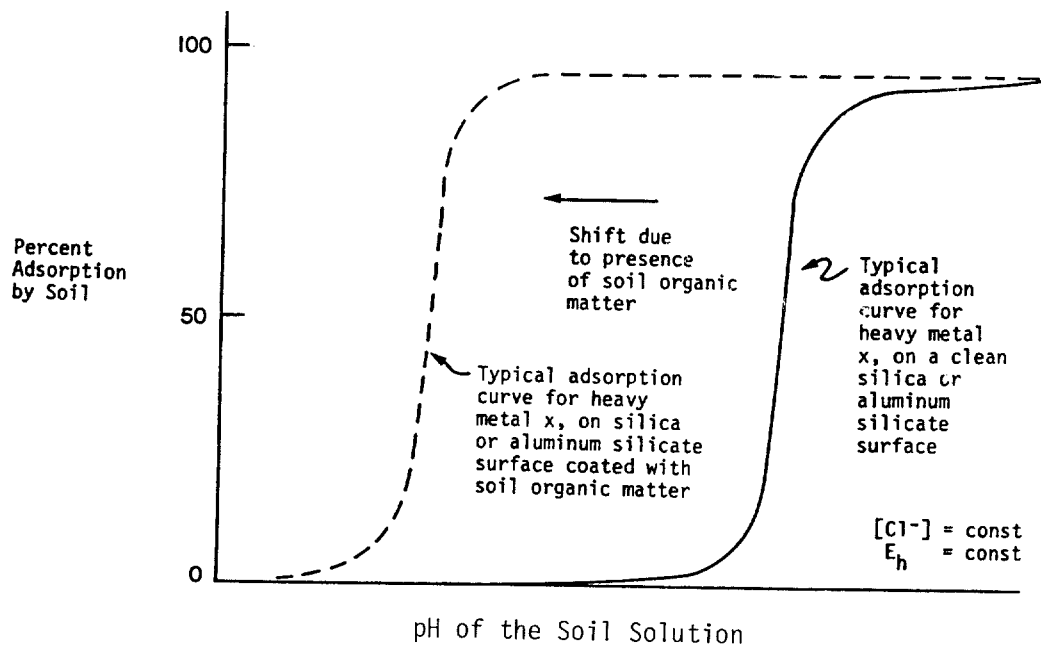
For organic chemicals, the adsorption coefficients are usually referred to as partition coefficients  $K_p$ . The partition coefficient can be calculated from the octanol-water partition coefficient  $K_{ow}$  (unitless) and estimates of the organic fraction of sand and silt plus clay (see Section 2.3.2). The octanol-water partition coefficient can also be calculated from volatility data using an empirical relationship. Typical values for volatility and  $K_{ow}$  are included in Tables II-5 through II-9 for the 129 priority pollutants. Additional data on pesticides including EDB and DBCP are included in Zalkin *et al.* (1984) and Bowman and Saris (1983). Partition coefficients and sorption in general are discussed in more detail in Section 2.3.2.

----- EXAMPLE PROBLEM VII-3 -----

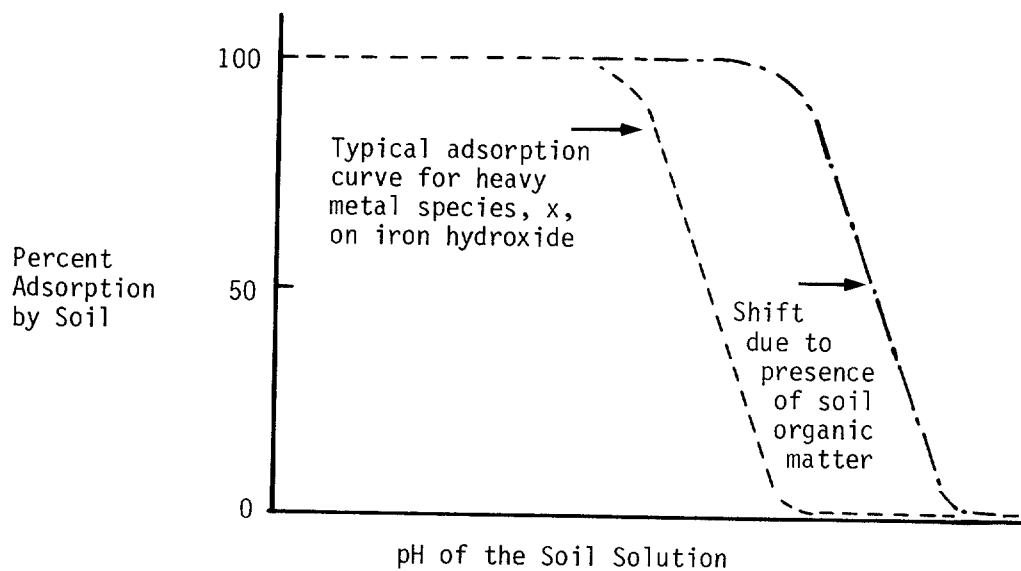
Calculate the retardation factor for anthracene in a silty-clay formation where the organic carbon content of the silty-clay is about 0.01.

From Table II-9, the octanol-water partition coefficient is found to be 28,000 (unitless). The organic carbon partition coefficient is first estimated from Equation 11-18 as follows:

$$\begin{aligned} K_{OC} &= 0.63 K_{ow} \\ &= (0.63)(28,000) \\ &= 17,640 \text{ ml/g} \end{aligned}$$



a) Generalized Heavy Metal Adsorption Curve for Cationic Species (e.g.,  $\text{CuOH}^+$ )



b) Generalized Heavy Metal Adsorption Curve for Anionic Species (e.g.,  $\text{CrO}_4^{2-}$ )

FIGURE VII-27 HYPOTHETICAL ADSORPTION CURVES FOR A) CATIONS AND B) ANIONS SHOWING EFFECT OF pH AND ORGANIC MATTER

where the conversion coefficient 0.63 has units of ml/g.

The partition coefficient,  $K_p$ , is calculated next using Equation 11-17 as follows:

$$K_p = K_{oc} \left[ 0.2(1-f)X_{oc}^s + fX_{oc}^f \right]$$

where

$$f = \frac{\text{mass of silt and clay}}{\text{mass of silt, clay and sand}} \quad (0 \leq f \leq 1)$$

$$X_{oc}^s = \text{organic fraction of sand} \quad (0 \leq X_{oc}^s \leq 0.1)$$

$$X_{oc}^f = \text{organic fraction of silt-clay} \quad (0 \leq X_{oc}^f \leq 0.1)$$

Substituting the above data yields the following expression:

$$\begin{aligned} K_p &= 17,640 [0.2(1-1)0 + 1(0.01)] \\ &= 176 \text{ ml/g} \end{aligned}$$

Finally, the retardation factor is calculated as follows using Equation VII-55, where the bulk density and porosity of this formation are 1.6 g/ml and 0.3 (unitless), respectively:

$$\begin{aligned} R_d &= 1 + \frac{K_p \rho_b}{p} \\ &= 1 + \frac{(176 \text{ ml/g})(1.6 \text{ g/ml})}{0.3} \\ &= 940 \end{aligned}$$

The relative amounts of anthracene in the dissolved and sorbed phases can be estimated using a modified form of Equation 11-22 as follows:

$$\frac{c}{c_t} = \frac{c}{(c + s\rho_b/p)} = \frac{1}{R_d}$$

where  $c$  = total dissolved pollutant concentration

$$c_t = c + s\rho_b/p$$

$s$  = mass of sorbed pollutant per unit mass of soil

$R_d$  = retardation factor

hence,

$$\frac{c}{c_t} = \frac{1}{940} = 0.001$$

Thus, 0.1 percent of the anthracene is in the dissolved phase and the rest is associated with the solid phase.

----- END OF EXAMPLE PROBLEM VII-3 -----

#### 7.4.2.1.2 Effect of Sorption on Seepage Velocity and Travel Time

A solute subject to sorption will travel at the following average velocity:

$$v_s^* = v_s / R_d \quad \text{(VII-57)}$$

where  $v_s^*$  (cm/sec) is the velocity of the solute,  $v_s$  (cm/sec) is the seepage velocity of the ground water and  $R_d$  (unitless) is the retardation factor accounting for sorption. Since the retardation factor  $R_d$  is equal to one for no sorption and is greater than one with sorption, the solute velocity  $v_s^*$  will always be less than or equal to that of the seepage velocity.

Ground water travel time  $\Delta t$  was defined in Section 7.3.3.2 as the average time that it takes ground water to travel a specified distance. In the case of a solute subject to linear, equilibrium sorption, its travel time will be:

$$\Delta t^* = R_d \Delta t \quad \text{(VII-58)}$$

where  $\Delta t^*$  (sec) is the travel time of the solute,  $\Delta t$  (sec) is the travel time of ground water and  $R_d$  (unitless) is the retardation factor accounting for sorption. Hence, the travel time of a solute will be greater than or equal to that of the ground water. (An insignificant exception may exist for solutes like chloride, which because of anion exclusion by negatively charged soils, may move slightly faster than the ground water itself.)

#### 7.4.2.2 Other Processes

Processes such as biodegradation and hydrolysis can be represented in some of the analytical methods by first-order decay rates. The actual rate constant used should be the sum of the individual first order decay rate for the specific pollutant.

Hydrolysis rates are given in Section 2.5.3 for organic chemicals. Biodegradation is presented in Section 2.5.1. Biodegradation for some compounds may be more important in ground waters than in surface waters due to the slow velocities, and hence long travel

times, and the common occurrence of anoxic conditions. Figure VII-28 shows the degradation of tetrachlorethylene and the resulting products of the series of dehydrochlorination reactions which occur under anoxic conditions. Biodegradation rates in ground water for selected organic chemicals are available from Wood *et al.*, 1981 and Wilson and McNabb, 1981.

## 7.5 METHODS FOR PREDICTING THE FATE AND TRANSPORT OF CONVENTIONAL AND TOXIC POLLUTANTS

### 7.5.1 Introduction to Analytical Methods

In this section, five analytical models are presented which can be used to predict the extent of contamination in ground water. A summary of these models is given in Table VII-12. For each model, the types of contaminant sources, flow situations, source release characteristics and spatial dimensions are briefly described. A discussion of the assumptions and the mathematical expression for each model is given in Figures VII-29 to VII-33. Finally, a more complete presentation of the derivation and use of each model, plus one or more worked out examples or applications are given in Sections 7.5.2 to 7.5.6. Each model has been programmed for solution on micro-computers (Mills *et al.*, 1985).

Obviously, there exist far more than five analytical models that describe ground water contamination. These five were chosen because they represent many of the typical ground water contamination problems for which solutions could be obtained with hand-held calculators. A more comprehensive collection of one-dimensional analytical transport models is given by van Genuchten and Alves (1982) and multiple-dimension analytical models by Yeh (1981) but these are primarily suitable for solution with large desk-top or main-frame computers. The models chosen in this section are relatively simple to use, yet are powerful in their range of applications.

Analytical methods allow prediction of contaminant concentrations in the aquifer at given times and locations as a result of an individual contaminant source. The simplest methods are based on the theory of flow to a pumping well (see Section 7.5.2). Most analytical methods, however, involve solving some form of the equation of flow in porous media. The complexity of the solutions varies greatly, depending on the number of dimensions included and the simplifying assumptions made. The equations range from simple, one-dimensional advective-transport equations to those simulating contaminant dispersion, diffusion, sorption and decay in two dimensions.

Analytical techniques are based on a number of simplifying assumptions. A key to using and interpreting the results of these methods appropriately, therefore, is understanding the assumptions which need to be made about the aquifer system and the various hydrogeologic parameters. Common assumptions include steady and uniform ground water flow in the saturated zone, aquifer isotropy (equal hydraulic conductivity in all directions), and constant contaminant concentration or mass loading rate from the contaminant source.

The reliability of the predictions generated depends on the inherent limitations

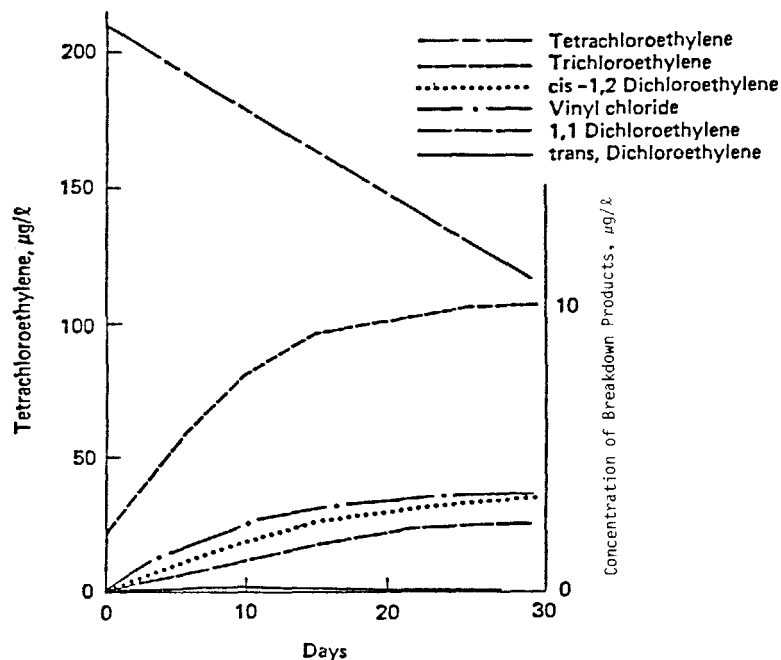


FIGURE VII -28 DEHYDROCHLORINATION RATE OF TETRACHLOROETHYLENE AND THE PRODUCTION RATE OF ITS DECHLORINATION PRODUCTS (AFTER WOOD ET AL . , 1981)

of the equations used, the assumptions made, the data used, and the complexity of field conditions. It is critical for the user to understand how reasonable the assumptions of a particular technique are for the aquifer and site being examined. For example, a technique assuming aquifer isotropy may not be well suited for predicting contaminant transport through an aquifer with a well-developed fracture system. In addition, mathematical constraints due to functions used in the algorithms sometimes limit the usefulness of the analytical techniques, restricting them to relatively narrow ranges of input values. Predictions for a number of times and locations in the aquifer can be used to detect aberrant values stemming from those mathematical factors.

Solving the flow and transport equations of analytical methods requires a limited amount of field data. Typically, these data needs include:

- Contaminant concentration (or mass loading rate) at the source
- Effective porosity of the aquifer
- Aquifer thickness
- Soil bulk density
- Ground water velocity
- Hydraulic conductivity
- Dispersion coefficients in longitudinal and transverse directions
- Distribution coefficient ( $K_d$ ) or retardation factor ( $R_d$ )
- Solute decay rate constants, if appropriate.

TABLE VII-12  
SUMMARY OF SOLUTION METHODS

Solution Method	Contaminant Source	Contaminant Release	Spatial Dimensions and Coordinate System
Section 7.5.2 Figure VII-29	Migration of contaminant to pumping well	continuous and constant	1-D radial
Section 7.5.3 Figure VII-30	Migration of contaminant from injection well	continuous and constant	1-D radial
Section 7.5.4 Figure VII-31	Migration of contaminant from surface to ground water table, such as from: spills or dumping, leaky ponds or tanks, landfills, surface sites or deposits	continuous or intermittent release with a constant or exponential source strength	1-D cartesian
Section 7.5.5 Figure VII-32	Migration of contaminant in saturated zone, such as from: leaky ponds or tanks, spills, landfills	slug	2-D cartesian
Section 7.5.6 Figure VII-33	Migration of contaminant in saturated zone, such as from: leaky ponds or tanks, spills, landfills, surface sites or deposits	continuous or intermittent release with a constant source strength	2-D cartesian

Techniques specifically for wells also require well pumping or injection rate and duration of the pumping/injection period.

Despite some limitations, the analytical techniques are extremely useful in the assessment of aquifer contamination from point sources. Once the necessary input data are collected, contaminant prediction can be performed quickly and easily. The algorithms can be programmed on hand-held calculators or micro-computers. Once they are programmed, contaminant predictions for a number of times and locations can be generated quickly. In this way, maps of potential aquifer contamination can be prepared. When numerical modeling of a site is being considered, use of analytical calculations can indicate whether there is sufficient contamination potential to justify a major modeling effort and, if so, where the data collection efforts for the model should be concentrated.

Given their ability to address many types of problems, their relative ease of application and low cost, analytical techniques offer potential uses for a variety of

CONTAMINANT TRANSFER TO DEEP WELLS  
(SEE SECTION 7.5.2)

Reference: Phillips and Gelhar (1978)

Objective: Compute concentration as a function of time in a deep well drawing water downward or upwards from a contaminated aquifer or layer.

Assumptions:

- uniform, radial flow in saturated media
- no dispersion
- no adsorption or decay of contaminant
- screened interval of well is short (screen-length/depth ratio less than 1/5)
- screen interval is located considerably below or above the base of the contaminant zone

Equation: 
$$\frac{c}{c_0} = \left(1 - T^{-1/3}\right)/2$$

where

$$T = \frac{3Qt}{4\pi H^3 pB} \quad \text{or} \quad t = T \left( \frac{4\pi H^3 pB}{3Q} \right)$$

and

- $c_0$  = average concentration of the contaminated layer (mg/l)
- $c$  = concentration at well screen (mg/l)
- $Q$  = pumping rate of well ( $m^3/day$ )
- $t$  = time (day)
- $H$  = distance from contaminated layer to center of screen (m)
- $p$  = porosity (unitless)
- $B$  = anisotropy ratio =  $K_x/K_z$  (unitless)
- $K_x, K_z$  = saturated hydraulic conductivity in the horizontal and vertical directions, respectively (m/day)

FIGURE VII-29 SUMMARY OF MODEL DESCRIBING CONTAMINANT TRANSFER  
TO DEEP WELLS



SOLUTE INJECTION WELLS: RADIAL FLOW  
(SEE SECTION 7.5.3)

References: Hoopes and Harleman (1967), Tang and Babu (1979)

Objective: To determine contaminant concentrations for a given time and location from a continuously discharging, fully penetrating injection well. Regional flow is negligible compared to flow induced by injection well.

Assumptions:

- uniform, radial flow in a confined aquifer
- contaminant enters the aquifer as a line source over the saturated thickness of the aquifer at  $r = r_0$
- linear equilibrium adsorption of contaminant
- first-order decay of the contaminant
- concentration of contaminant at well is constant

$$c(r,t) = c_0 \frac{\operatorname{erfc}(a)}{\operatorname{erfc}(a_0)} \exp\left(\frac{-kR_d(r^2-r_0^2)}{2A}\right)$$

where

$$a = \frac{(r^2/2 - At/R_d)R_d}{\left(\frac{4}{3}\alpha r^3 + \frac{D^* r^4}{A}\right)^{1/2}}, \quad a_0 = \frac{(r_0^2/2 - At/R_d)R_d}{\left(\frac{4}{3}\alpha r_0^3 + D^* \frac{r_0^4}{A}\right)^{1/2}}$$

- $r$  = radial distance from center of well (meters)
- $r_0$  = radius of well casing (meters)
- $t$  = time (days)
- $\alpha$  = dispersivity of aquifer (meters)
- $A$  =  $Q/(2nbp)$
- $D^*$  = molecular diffusion coefficient ( $m^2/day$ )
- $c$  = contaminant concentration in the aquifer (mg/l)
- $c_0$  = contaminant concentration in the injection well (mg/l)
- $Q$  = volumetric rate of injection by the well ( $m^3/day$ )
- $b$  = saturated thickness of the aquifer (meters)
- $p$  = porosity of the aquifer (unitless)
- $R_d$  = retardation coefficient for linear adsorption (unitless)
- $k$  = total decay rate constant for the contaminant (1/day)

FIGURE VII-30 SUMMARY OF MODEL DESCRIBING RADIAL FLOW FROM AN INJECTION WELL

CONTAMINANT RELEASE ON THE SURFACE WITH 1-D VERTICAL, DOWNWARD TRANSPORT  
(SEE SECTION 7.5.4)

Reference: van Genuchten and Alves (1982)

Objective: Compute solute concentration as a function of time and distance for a continuous surface contaminant release with subsequent vertical, downward transport.

- Assumptions:
- uniform, steady, vertical, downward flow
  - first-order-decay and-linear, equilibrium adsorption of the contaminant in the aquifer
  - constant or first-order decay of the contaminant source at the land surface
  - one-dimensional transport in unsaturated or saturated media

$$c(x,t) = \frac{c_0}{2} \left\{ \exp\left(\frac{v_s x}{2D} - \gamma t\right) e^{-2ab} \operatorname{erfc}\left(-a\sqrt{t} + \frac{b}{\sqrt{t}}\right) + e^{2ab} \operatorname{erfc}\left(a\sqrt{t} + \frac{b}{\sqrt{t}}\right) \right\}$$

where

$$a = \sqrt{k - \gamma + \frac{v_s^2}{R_d 4D}} \quad b = \frac{x}{2} \sqrt{\frac{R_d}{D}}$$

$c_0$  = initial concentration of the contaminant source (mg/l)

$c$  = concentration of the contaminant at a specified time and depth (mg/l)

$v_s$  = seepage velocity, positive vertically downward (m/day)

$D$  = dispersion coefficient in the vertical direction ( $m^2/day$ )

$x$  = vertical distance, positive downwards (m)

$R_d$  = retardation coefficient for linear adsorption (unitless)

$k$  = total decay rate constant for the contaminant in the aquifer (1/day)

$\gamma$  = decay rate of the contaminant source at the land surface (1/day)

FIGURE VII-31 SUMMARY OF MODEL DESCRIBING ONE-DIMENSIONAL,  
VERTICALLY DOWNWARD TRANSPORT OF A CONTAMINANT  
RELEASED ON THE SURFACE

TWO-DIMENSIONAL HORIZONTAL FLOW WITH A SLUG SOURCE  
(SEE SECTION 7.5.5)

Reference: Wilson and Miller (1978)

Objective: To determine contaminant concentration for a given time and location for an instantaneous discharge from a fully penetrating line source. Contaminant transport is dominated by regional flow.

Assumptions:

- uniform, steady regional flow in the x direction
- contaminant enters the aquifer over the full saturated thickness of the aquifer at  $x = 0, y = 0$
- linear, equilibrium adsorption of the contaminant
- decay of the contaminant in the aquifer is first-order
- mass loading rate of contaminant is instantaneous

$$c(x,y,t) = \frac{c_0 Q'}{b4\pi p t (D_x D_y)^{1/2}} \exp\left(-kt - \frac{(xR_d - v_x t)^2}{4D_x t R_d} - \frac{(yR_d)^2}{4D_y t R_d}\right)$$

where

$c_0$  = initial concentration of discharged contaminant (mg/l)  
 $Q'$  = volume of contaminant being discharged ( $m^3$ )  
 $b$  = aquifer saturated thickness (m)  
 $p$  = porosity (unitless)  
 $t$  = time (days)  
 $D_x, D_y$  = dispersion coefficients ( $m^2/day$ )  
 $v_x$  = seepage velocity of the regional flow (m/day)  
 $x, y$  = spatial coordinates (m)  
 $k$  = total decay rate constant for the contaminant (1/day)  
 $R_d$  = retardation coefficient for linear adsorption (unitless)

FIGURE VII-32 SUMMARY OF MODEL DESCRIBING TWO-DIMENSIONAL  
HORIZONTAL FLOW WITH A SLUG SOURCE

TWO-DIMENSIONAL HORIZONTAL FLOW WITH CONTINUOUS SOLUTE LINE SOURCES  
(SEE SECTION 7.5.6)

Reference: Wilson and Miller (1978)

Objective: To determine contaminant concentration for a given time and location from a continuously discharging, fully penetrating line source. Contaminant transport is dominated by the regional flow.

Assumptions:

- uniform, steady regional flow in the x direction
- contaminant enters the aquifer over the full saturated thickness of the aquifer at  $x = 0, y = 0$
- linear, equilibrium adsorption of the contaminant
- decay of the contaminant in the aquifer is first-order
- mass loading rate of contaminant is continuous and constant over the time period of interest

$$c(x,y,t) = \frac{c_0 Q}{4\pi p b (D_x D_y)} \exp\left(\frac{v_x x}{2D_x}\right) W\left(u, \frac{r}{B}\right)$$

where

$W(\cdot)$  = the leaky well function of Hantush

$B$  =  $2D_x/v_x$  (m)

$r = \left(\alpha \left(x^2 + y^2 \frac{D_x}{D_y}\right)\right)^{1/2}$  (m)

$u = \frac{r^2 R_d}{4\alpha D_x t}$  (unitless)

$\alpha = 1 + 2BR_d k/v_x$  (unitless)

$Q$  = volumetric rate of discharge of the line source ( $m^3/day$ )

$t$  = time (days)

$(x,y)$  = spatial coordinates (m)

$D_x, D_y$  = dispersion coefficients ( $m^2/day$ )

$v_x$  = seepage velocity of the regional flow (m/day)

$p$  = porosity of the aquifer (unitless)

$b$  = saturated thickness of the aquifer (m)

$k$  = total decay rate constant for the contaminant (1/day)

$R_d$  = retardation coefficient for linear adsorption (unitless)

$c_0$  = concentration of contaminant being discharged (mg/l)

FIGURE VII-33 SUMMARY OF MODEL DESCRIBING TWO-DIMENSIONAL  
HORIZONTAL FLOW WITH CONTINUOUS SOLUTE LINE  
SOURCES

ground water management activities. Analytical techniques can be used to predict the migration of plumes and to determine the extent of contaminant mixing in ground water. Four specific questions can be addressed: (1) In what direction will a contaminant plume travel and how will its shape change as it travels? (2) To what extent will concentrations of contaminants be reduced as a result of dispersion, sorption and decay? (3) How far will the plume migrate over time? (4) Where should wells to monitor the plume's movement be located?

Other applications of analytical methods include estimating "worst case" concentrations at a site as a conservative estimate of a site's hazard, guiding the collection and analysis of field data to test hypotheses, checking the results of more sophisticated numerical models, determining design requirements for pump tests and tracer studies, and designing and evaluating the effectiveness of plume control options. Because analytical techniques are relatively quick and inexpensive to apply, they are useful in many phases of ground water activities--facility siting and permitting, site inspection and enforcement, monitoring, estimating the extent and significance of known contamination, and evaluating plume management options. A reliable "worst case" evaluation of a known ground water contamination problem may show that the site poses little near-term risk to the public and that a low-level monitoring program is an appropriate management strategy. Alternatively, an evaluation may indicate significant health or environmental risks, in which case intensive monitoring and/or use of a sophisticated numerical model may be warranted.

An overall summary of analytical methods is given below:

- Provide quantitative estimates of potential contamination at a specific location and time
- Require limited field data
- Predictions can be made quickly using hand calculators
- Require simplifying assumptions
- Cannot handle complex field conditions.

In the remaining portion of Section 7.5, the five analytical models are presented along with worked out examples of their use.

### 7.5.2 Contaminant Transport to Deep Wells

Many regions of the country obtain their freshwater supply from deep well systems. However, many of these deep wells are now in jeopardy because of the contamination of shallow ground water aquifers from cesspools, septic tanks and overuse of crop and lawn fertilizers. Subsurface sanitary disposal systems discharge wastewaters high in nitrogen and bacteria to the unsaturated zone. Nitrogen and pesticides from fertilizers and herbicides may migrate to the saturated zone where water-supply wells may intercept them. Our objective is to predict the increase in contaminant concentration at a water supply well and to determine how long it would take for a

specified concentration to be reached. Phillips and Gelhar (1978) presented an equation for solving these types of problems. The Phillips and Gelhar equation is appropriate when the well is either far below the existing contaminant zone or far above the contaminant zone. One other restriction is that the length of the well screen must be less than about one-fifth of the well depth. The flow to the well can then be represented as three-dimensional radial flow as shown in Figure VII-34.

For the example shown in the figure, there is an unbounded radial flow system with a contamination zone initially a distance H above the center of the well screen. The equation to represent the movement of the contamination zone is based on fluid displacement in a homogeneous anisotropic porous medium. The effects of dispersion are not included in Phillips and Gelhar's equation. However, Hoopes and Harleman (1965) have shown that dispersion is a secondary effect in such local flow systems.

The analytic solution for the contaminant concentration at the well screen as a function of time is given by:

$$c(t) = (c_0(1 - T^{-1/3}))/2 \quad (\text{VII-59})$$

where

$$T = \frac{3Qt}{4\pi H^3 pB} \quad (\text{VII-60})$$

or

$$t = \frac{4\pi H^3 pB}{3Q} T \quad (\text{VII-61})$$

and where

- c(t) = concentration at the well (mg/l)
- c<sub>0</sub> = average concentration of the contaminated zone (mg/l)
- Q = constant pumping rate of the well (m<sup>3</sup>/day)
- t = time (day)
- T = dimensionless time (unitless)
- H = distance from the contaminated zone to the center of the screened interval of the well (m)
- p = effective porosity of the saturated portion of the aquifer (unitless-decimal fraction)
- B = anisotropy ratio of the aquifer = K<sub>x</sub>/K<sub>z</sub> (unitless)
- K<sub>x</sub>, K<sub>z</sub> = saturated hydraulic conductivity in the horizontal and vertical directions, respectively (m/day)

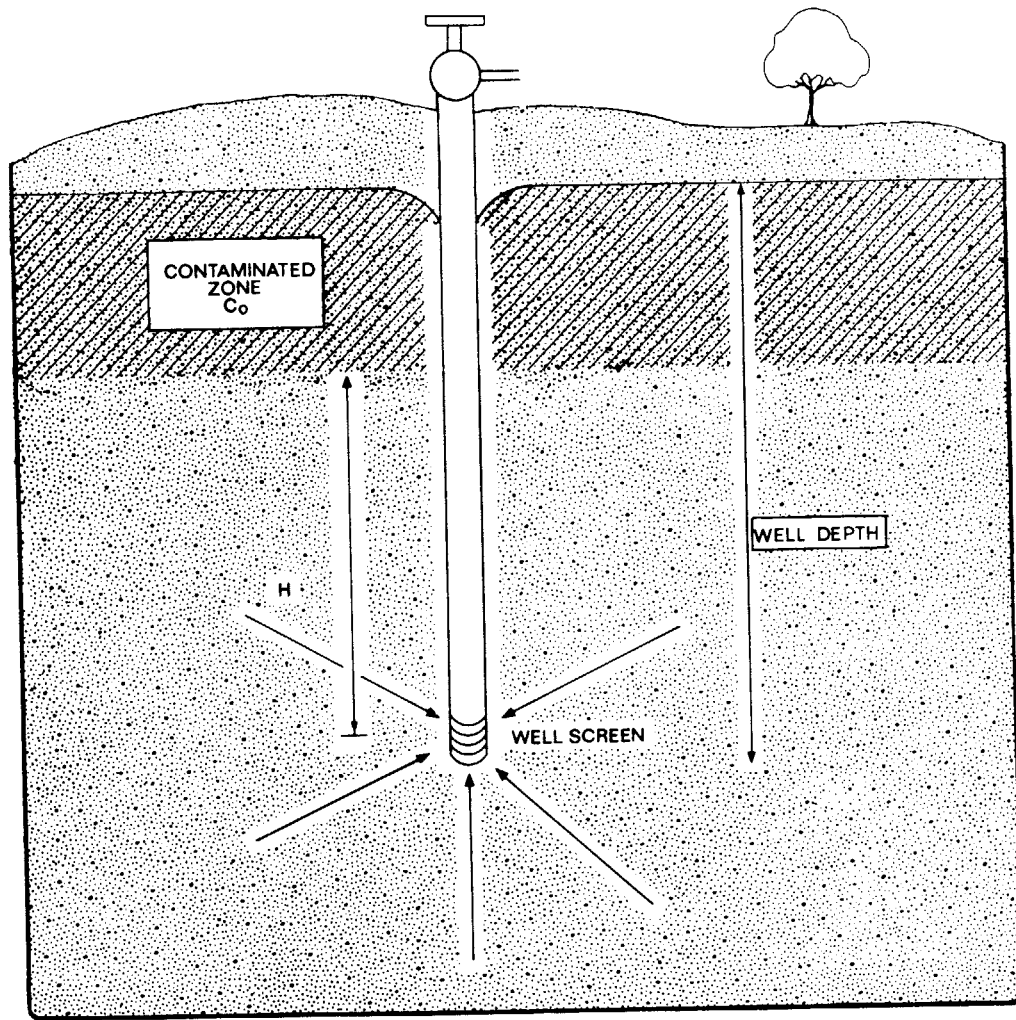


FIGURE VII-34 SCHEMATIC OF FLOW TO A WELL BENEATH A CONTAMINATED ZONE

Equation VII-59 has been solved for various values of  $T$ . The results are shown in Figure VII-35. Equation VII-60 and VII-61 can be solved to answer several questions:

- When will shallow contaminated ground water reach a deep pumping well?
- When will the percentage of the contaminant concentration in the well exceed a given value, say 20 percent?
- What is the effect of changing the pumping rate?

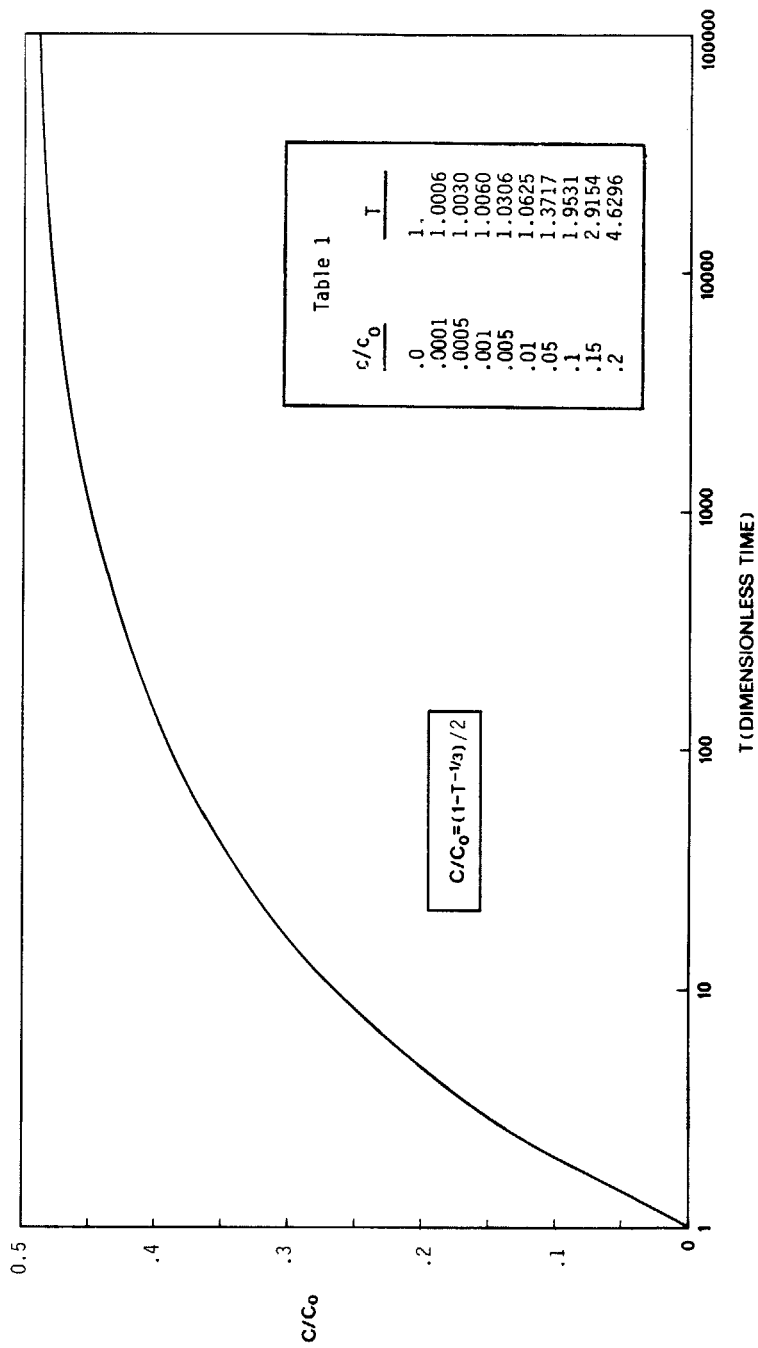


FIGURE VII-35 NORMALIZED SOLUTE CONCENTRATION VS. DIMENSIONLESS TIME



The nitrate concentration in a town's ground water has been increasing for the last several years. The following information is available. A schematic of the problem is shown in Figure VII-36.

The aquifer is unconfined with fine to medium grained quartz sand deposited originally as sand dunes. The storage coefficient is about 0.2 and the ratio of the horizontal to the vertical hydraulic conductivity is 10. This anisotropy is caused by localized cementation and horizontal bedding in the dunes. The municipal well is pumping 3000 m<sup>3</sup>/day. The lower tip of the municipal well screen is located 50 meters below the surface of the land. The well is screened over 4 meters. Analysis of the water samples showed that the municipal well had a nitrate-nitrogen concentration of 7.2 mg/l on January 1, 1984. A series of shallow monitoring wells indicated that the upper part of the aquifer has an average concentration of 26 mg/l of nitrate-nitrogen and that the zone of contamination extends down to 20 meters below the surface of the land.

The city council wants to know when the nitrate-nitrogen concentration in the community well will equal or exceed 10 mg/l (the primary drinking water standard).

The steps required to answer this question are given below:

1. Determine the current dimensionless time,  $T_0$ , where  $c/c_0 =$

$$(1 - T_0^{-1/3})/2 = 7.2/26 = 0.28$$

From Figure VII-35 we find that  $T_0 = 11.7$ .

2. Determine the dimensionless time when the well concentration equals 10 mg/l:

$$c/c_0 = (1 - T_{10}^{-1/3})/2 = 10./26 = 0.38$$

From Figure VII-35 we find that  $T_{10} = 72.3$ .

3. Real time is related to dimensionless time by Equation VII-61:

$$t = T \left( \frac{4\pi H^3 \rho B}{3Q} \right)$$

Hence, the estimated time when the concentration at the pumping well will reach 10 mg/l is given by the difference between  $t_{10}$  and  $t_0$ :

$$t_{10} - t_0 = (T_{10} - T_0) \frac{4\pi H^3 \rho B}{3Q}$$

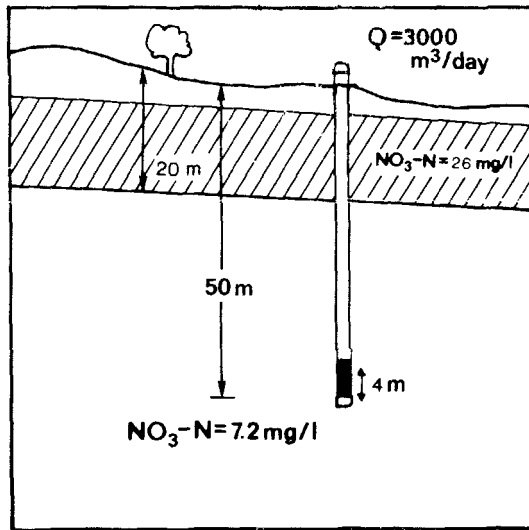


FIGURE V11-36 SCHEMATIC OF EXAMPLE PROBLEM FOR  $t_{10}$ -LOW TO WELL FROM A SHALLOW CONTAMINATED ZONE

4. Calculate  $H$  and then substitute  $H$ ,  $p$ ,  $B$ ,  $Q$ ,  $T_0$  and  $T_{10}$  into the above equation. Note that  $H$  and  $Q$  must be expressed in the same units. Also note that  $H$  is measured as the distance between the center of the well screen and the bottom of the contamination zone. In this example,  $H = (50-20-4/2) = 28$  meters. The data can now be tabulated as follows:

$$\begin{array}{ll}
 H = 28 \text{ meters} & p = 0.2 \\
 B = 10 & Q = 3000 \text{ m}^3/\text{day}
 \end{array}$$

Substituting the above data into the expression for  $t_{10}-t_0$ , results in the following:

$$(t_{10}-t_0) = (72.3-11.7) \frac{(4\pi(28)^3(0.2)(10))}{$$

$$= 3715 \text{ days} = 10.2 \text{ years}$$

Hence, the concentration of nitrate-nitrogen is expected to reach 10 mg/l in the municipal well in about ten years.

--- END OF EXAMPLE PROBLEM VII-4 ---

### 7.5.3 Solute Injection Wells: Radial Flow

Because of the interest in underground injection, the following analyses will be presented to show how injection wells can be modeled analytically. With the model given below, the concentration of solute from an injection well can be predicted as a function of time and space. This information can then be used to estimate the impact of an injection well on the ground water quality. A schematic view of a typical injection well is given in Figure VII-37.

Both shallow and deep wells have been used for injection of waste into subsurface strata. Storm water, spent cooling water, and sewage effluent have been injected through relatively shallow wells. Sometimes these wells are completed in the unsaturated zone; however, they often penetrate the saturated zone and thus contaminants are discharged directly into the ground water. In addition, large volumes of brine produced by chemical industries, geothermal energy production, and other sources have been injected through deep wells into saline-water aquifers. Acids, spent solvents, and plating solutions containing heavy metals have also been injected.

The following assumptions will be made concerning the injection well system to permit the analytical solution given below to be used. A solute with a constant concentration  $c_0$  will be discharged at a constant rate  $Q$  into a homogeneous, non-leaky, isotropic aquifer. The aquifer is assumed to be confined by two parallel, impermeable formations and spaced a distance "b" apart. The injection well is screened over the entire thickness of the confined aquifer. The density and viscosity of the injected solute are the same as those of the native water in the aquifer. There is negligible regional flow in the aquifer and the flow field near the well is dominated by the waste being discharged. A schematic view of the problem is given in Figure VII-37.

The seepage velocity,  $v_s$ , at any specified radius from the well can be computed from the continuity equation:

$$Q = 2\pi r b v_s p \quad (\text{VII-62})$$

where  $Q$  is the volumetric rate of injection by the well ( $\text{m}^3/\text{day}$ ),  $r$  is the radius to a point in the aquifer measured from the center of the well (m),  $b$  is the saturated thickness of the aquifer (m),  $p$  is the porosity of the aquifer (decimal percent, unitless), and  $v_s$  is the radial, seepage velocity of the fluid from the well (m/day).

The seepage velocity can thus be expressed as:

$$v_s = \frac{A}{r} \text{ with } A = Q/(2\pi b p) \quad (\text{VII-63})$$

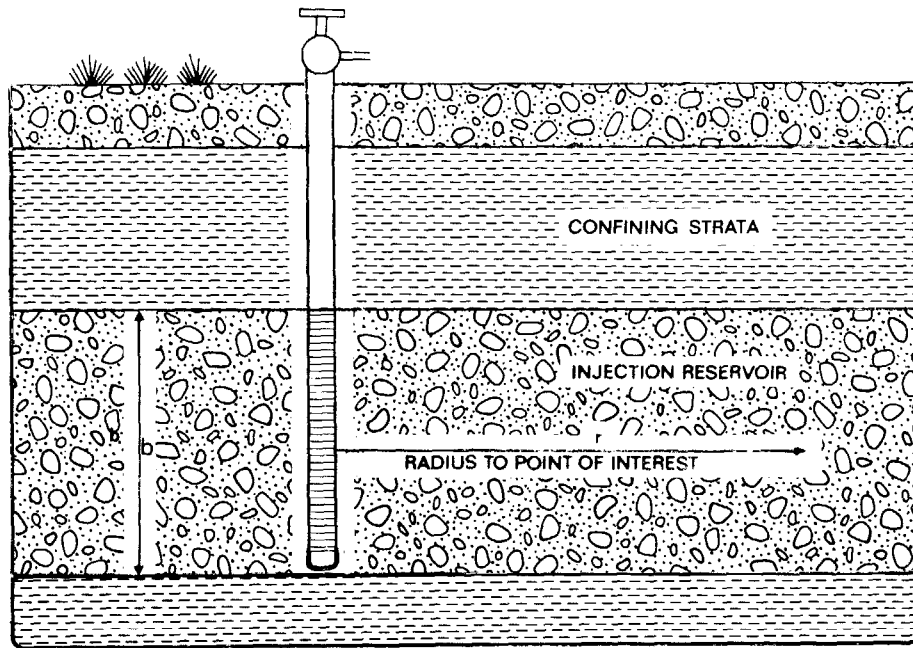


FIGURE VII-37 SCHEMATIC VIEW OF A WELL INJECTING SOLUTE INTO A CONFINED AQUIFER

The governing equation describing the spatial and temporal distribution of a dissolved substance introduced into the saturated zone is:

$$R_d \frac{\partial c}{\partial t} + v_s \frac{\partial c}{\partial r} = \frac{1}{r} \frac{\partial}{\partial r} (D_r r \frac{\partial c}{\partial r}) - kcR_d \quad (\text{VII-64})$$

where  $c$  is the solute concentration (mg/l),  $D_r$  is the radial dispersion coefficient ( $\text{m}^2/\text{day}$ ),  $k$  is the first-order decay rate of the substance (per day), and  $R_d$  is the retardation coefficient for linear, equilibrium adsorption (unitless). The initial concentration in the aquifer is assumed to be zero, the concentration  $c = c_0$  is assumed to be held constant at the well.

If the dispersion coefficient is assumed to vary as a function of the radial seepage velocity, then:

$$D_r = \alpha v_s + D^* \quad (\text{VII-65})$$

where  $\alpha$  is the dispersivity coefficient (m) and  $D^*$  is the molecular diffusion coefficient ( $\text{m}^2/\text{day}$ ).

The general solution to Equation VII-64 can be found by the Laplace transform method to give:

$$c(\rho, \tau) = c_0 \exp \left[ \frac{(\rho - \rho_0)}{2} - k^* \tau \right] \mathcal{L}^{-1} \{ f(s) \} \quad (\text{VII-66})$$

where  $\mathcal{L}^{-1}\{\cdot\}$  is the inverse Laplace transform operator and  $f(s)$  is the Laplace solution to Equation VII-64:

$$f(s) = \frac{1}{(s - k^*)} \frac{A_i \left[ (R_d s)^{-2/3} (R_d \rho s + 1/4) \right]}{A_i \left[ (R_d s)^{-2/3} (R_d \rho_0 s + 1/4) \right]} \quad (\text{VII-67})$$

where  $s$  is the transformed variable of time;  $A_i[\cdot]$  is the Airy function;  $k^*$  is the dimensionless decay rate, where  $k^* = kA\alpha^2$ ;  $\tau$  is the dimensionless time,  $\tau = t/(A\alpha^2)$ ;  $\rho$  is the dimensionless radial distance from the center of the well,  $\rho = r/\alpha$ ; and  $\rho_0$  is the dimensionless radius of the well casing,  $\rho_0 = r_0/\alpha$ .

Equation VII-66 has been solved analytically by Tang and Babu (1979) but their solution involves integrating four different types of Bessel functions of fractional order (order 1/3) over three different integrals. Alternatively, one can numerically compute the Laplace inverse of Equation VII-66 by the Stehfest algorithm (Moench and Ogata, 1981). However, if one uses Equation VII-67 in the numerical inversion, a great deal of care must be used in computing the Airy functions to avoid numerical roundoff problems in the solution.

Because of the difficulties in obtaining numerical values from Equation VII-66, several authors have suggested approximate solutions. The method of Raimondi et al. (1959) assumes that at some distance from the source, the influence of dispersion and diffusion on the concentration distribution are small in comparison to the total dispersion that has taken place up to that point. Thus the spatial gradient on the right-hand side of Equation VII-64 is ignored and is substituted by the temporal gradient:

$$\frac{D_r}{v_s^2} \frac{\partial^2 c}{\partial t^2} \quad (\text{VII-68})$$

The solution to this approximation was originally given by Tang and Babu (1979). Their solution has been modified to allow for retardation and is shown below:

$$c = c_0 \frac{\text{erfc}(a)}{\text{erfc}(a_0)} \exp \left( \frac{-kR_d(r^2 - r_0^2)}{2A} \right) \quad (\text{VII-69})$$

where  $\text{erfc}(\cdot)$  is the complimentary error function (see Appendix J) and

$$a_0 = \frac{\left(\frac{r_0^2}{2} - \frac{At}{R_d}\right) R_d}{\left(\frac{4}{3} \alpha r_0^3 + \frac{D^* r_0^4}{A}\right)^{1/2}} \quad (\text{VII-70})$$

$$a = \frac{\left(\frac{r^2}{2} - \frac{At}{R_d}\right) R_d}{\left(\frac{4}{3} \alpha r^3 + \frac{D^* r^4}{A}\right)^{1/2}} \quad (\text{VII-71})$$

When the radius of the well casing,  $r_0$ , is negligible, then  $\text{erfc}(a_0)$  is set equal to 2 and Equation VII-69 reduces to:

$$c = \frac{c_0}{2} \text{erfc}(a) \exp\left(\frac{-kR_d(r^2 - r_0^2)}{2A}\right) \quad (\text{VII-72})$$

Equation VII-72 is the same as Hoopes and Harleman (1967) when  $k = 0$  (i.e., the exponential term drops out). Equation VII-69 and VII-72 satisfy the boundary conditions  $c = c_0$  at  $r = r_0$  and  $c = 0$  at distances far from the well but they do not satisfy the initial condition  $c = 0$  at  $t = 0$  near the well. Equations VII-69 and VII-72 predict a finite amount of mass in the media at  $t = 0$ . However, Equations VII-69 and VII-72 are approximately true away from the immediate vicinity of the source. Hoopes and Harleman (1965) carried out an extensive series of laboratory investigations in a sand-filled box and concluded that Equations VII-69 and VII-72 are a good approximation of dispersion in radially diverging flow for distances larger than 20 particle diameters from the well.

A table of the complimentary error function is given in Table J-1 of Appendix J.

#### -----EXAMPLE VII-5-----

A local electronic component factory, called "The Chip Works", was recently constructed in town. It produces electronic circuit boards and micro chips. As part of the manufacturing process, various acids are used to etch and plate the electronic circuits. These acids leach various heavy metals, including cadmium from the metal components and hence must be disposed of. Because of the high toxicity of the plating waste, the local sewer authority will not allow The Chip Works to discharge its waste into the domestic sewer line without pretreatment. After much negotiation, it was finally decided to inject the plating waste directly into a deep aquifer. The following analyses were done to determine if solute injection into the aquifer would allow the drinking water standards to be met in the aquifer without pretreating the plating waste.

The sandstone aquifer is about 30 meters thick. It is confined above and below by impermeable shale. The aquifer lies about 300 meters below the surface of the ground. The velocity in the aquifer is negligible. The plating waste is to be injected at a volumetric rate of 550 m<sup>3</sup>/day through a well screened over the entire depth of the aquifer. The casing radius is 0.1 meters. The plating waste contains an average concentration of 50 pg/l of cadmium and has a pH of about 5.5. The dispersivity of the sandstone is about 50 meters, the effective porosity about 0.2 and the molecular diffusion coefficient about 8.7 x 10<sup>-5</sup>

The cadmium concentration is below volatility limits. To be conservative, adsorption is assumed to be negligible, thus the retardation factor is set equal to 1 (see Equation VII-55 of Section 7.4.2.1.1).

The injection well is located in the center of the property of The Chip Works and the nearest property boundary is 450 meters away. The local pollution agency has specified that the cadmium concentration in the aquifer never exceed 10 pg/l at the property boundary. It is known that the background concentration of cadmium is negligible. A series of monitoring wells have been installed at the property boundary to verify compliance. Will the standard be exceeded and if so, when? A schematic of the above problem is given in Figure VII-38. to know when the cadmium concentration will equal or exceed 10 pg/l. be summarized as follows:

$r_o = 0.1 \text{ m}$	$R_d = 1$
$r = 450 \text{ m}$	$k = 0/\text{day}$
$a = 50 \text{ m}$	$b = 30 \text{ m}$
$D^* = 8.7 \times 10^{-5} \text{ m}^2/\text{day}$	$p = 0.2$
$Q = 550 \text{ m}^3/\text{day}$	$c_o = 50 \text{ } \mu\text{g}/\text{l}$

The only missing variable is time,  $t$ , which can be estimated. The well casing radius  $r_o$  is negligible in comparison to the distance of interest,  $r$ , and time is not extremely short (i.e., less than 0.001 days), so Equation VII-72 can be used (i. e.,  $\text{erfc}(a_o) = 2$ ). This expression is first solved for "a":

$$\text{erfc}(a) = 2c/c_o = (2)(10)/50 = 0.4$$

Interpolating the complimentary error function in Table J-1 of Appendix J, one can see that the above corresponds to a value of  $a = 0.59$ . From Equation VII-71, one can solve for time as a function of "a":

$$t = R_d \frac{r^2}{2A} - \frac{a}{A} \left( \frac{4}{3} a r^3 + D^* \frac{r^4}{A} \right)^{1/2} \quad (\text{VII-73})$$

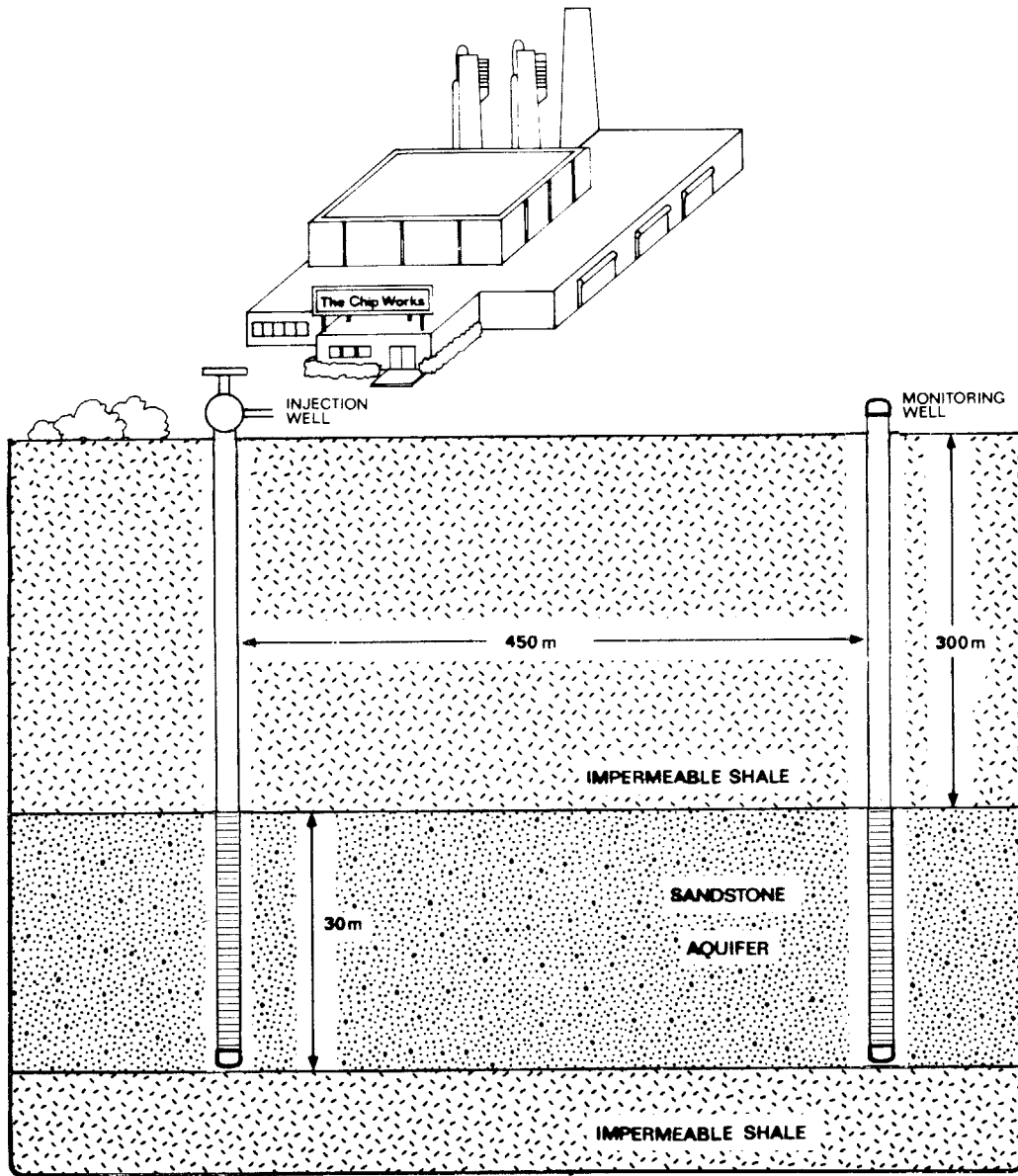


FIGURE VI 1-38 SCHEMATIC OF THE EXAMPLE PROBLEM SHOWING RADIAL FLOW OF PLATING WASTE FROM AN INJECTION WELL



here

$$A = Q / (2\pi bp) \quad (\text{VII-74})$$

Upon substitution of the data into Equations VII-73 and VII-74, we can solve for time,  $t$ . Thus:

$$A = \frac{550}{2\pi(30)(0.2)} = 14.6 \text{ m}^2/\text{day}$$

$$t = \frac{(1)(450)^2}{2(14.6)} - \frac{(0.59)}{(14.6)} \left( \frac{4(50)(450)^3}{3} + (8.7 \times 10^{-5}) \frac{(450)^4}{14.6} \right)^{1/2}$$

$$= 3780 \text{ days or about 10 years}$$

Hence, the cadmium concentration will equal  $10 \mu\text{g/l}$  at the monitoring well after about 10 years of continuous injection. It appears from the calculations that pretreatment of the waste will be necessary prior to disposal.

END OF EXAMPLE VII-5

#### EXAMPLE VII-6

This example problem considers another metal, zinc, which is present in smaller quantities in this waste. Zinc is weakly adsorbed at a pH of 6.0. The adsorption coefficient  $K_d$  for zinc is about 2 ml/g at a pH of 6.0. The bulk density,  $\rho_b$ , of sandstone is 2.3 g/ml. Hence, the retardation factor for linear equilibrium adsorption can be calculated using Equation VII-55.

Calculate the concentration of zinc at the property boundary after 3780 days. Assume the waste has been pretreated to a pH of 6.0. The data can now be summarized as follows:

$$r_o = 0.1 \text{ m}$$

$$r = 450 \text{ m}$$

$$a = 50 \text{ m}$$

$$D^* = 8.7 \times 10^{-5} \text{ m}^2/\text{day}$$

$$K_d = 2 \text{ ml/g}$$

$$k = 0$$

$$\rho_b = 2.3 \text{ g/ml}$$

$$p = 0.2$$

$$Q = 550 \text{ m}^3/\text{day}$$

$$b = 30 \text{ m}$$

$$c_o = 5 \text{ mg/l}$$

$$t = 3780 \text{ days}$$

Step 1. Calculate the retardation coefficient using Equation VII-55:

$$R_d = 1 + \frac{K_d \rho_b}{p} = 1 + \frac{(2)(2.3)}{(0.2)} = 24$$

Step 2. Calculate A using Equation VII-74:

$$A = \frac{Q}{2\pi bp} = \frac{550}{2\pi(30)(0.2)} = 14.6$$

Step 3. Calculate "a" using Equation VII-71:

$$a = \frac{\left(\frac{r^2}{2} - \frac{At}{R_d}\right) R_d}{\left(\frac{4}{3} \alpha r^3 + \frac{A}{A}\right)^{2/2}} = \frac{\left(\frac{(450)^2}{2} - \frac{(14.6)(370)}{(24)}\right) (24)}{\left(\frac{4(50)(450)^3 + (8.7 \times 10^{-5})^5 (450)^4}{(14.6)(6)}\right)^{1/2}} = 30.5 \quad (24)$$

Step 4. Calculate erfc(a) (see Table J-1 of Appendix J):

$$\text{erfc}(a) = \text{erfc}(30.5) = 0$$

Step 5. Calculate c:

$$c = \frac{c_0}{2} \text{erfc}(a) = \frac{(5)(0)}{2} = 0 \text{ mg/l.}$$

Hence, the zinc concentration will be zero at the property boundary after 10 years. The difference between the behavior of cadmium and zinc is due to sorption. Without sorption, cadmium moves with the same velocity as does the injected water (i.e., the seepage velocity  $v_s$ ). With adsorption, zinc moves 24 times slower than the injected water.

END OF EXAMPLE VII-6

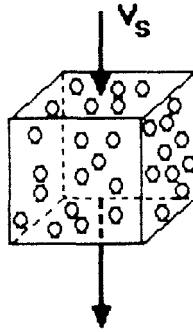
#### 7.5.4 Contaminant Release on the Surface with 1-D Vertical Downward Transport

A surface release of a contaminant can be treated in many instances as a one-dimensional flow problem with the contaminant moving vertically downward through the soil as shown in Figure VII-39. This case can be greatly simplified by considering the velocity, moisture content, retardation and dispersion coefficient as constant over a given depth. If the soil has several distinct layers, calculations can be performed for each layer separately. Flow can occur through either saturated or unsaturated soil, as long as the moisture content is assumed to be a constant throughout the soil.

To understand how the analytical method may be used, the governing equation should be briefly reviewed. The equation describing one-dimensional advective transport with dispersion, adsorption and first-order decay is as follows:

$$R_d \frac{\partial c}{\partial t} = D \frac{\partial^2 c}{\partial x^2} - v_s \frac{\partial c}{\partial x} - kcR_d \quad (\text{VII-75})$$

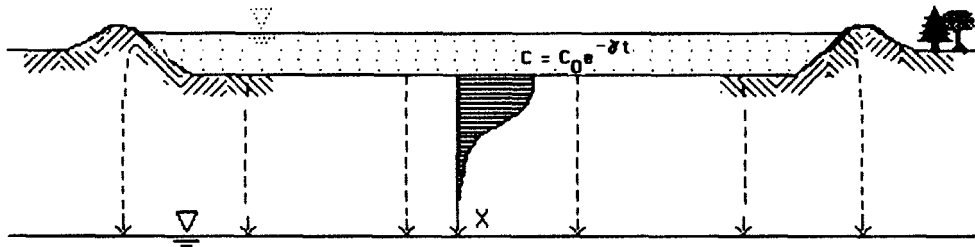
# Mass Transport Equation



$$\left\{ \begin{array}{l} \text{net rate of} \\ \text{mass} \\ \text{accumulation} \end{array} \right\} = \left\{ \begin{array}{l} \text{mass flow} \\ \text{by} \\ \text{dispersion} \end{array} \right\} + \left\{ \begin{array}{l} \text{mass flow} \\ \text{by} \\ \text{advection} \end{array} \right\} - \left\{ \begin{array}{l} \text{mass depletion} \\ \text{by} \\ \text{reactions} \end{array} \right\}$$

$$R_d \frac{\partial c}{\partial t} = D \frac{\partial^2 c}{\partial x^2} - v_s \frac{\partial c}{\partial x} - k c R_d$$

## Waste Pond or Landfill



**Initial condition:**  $c(x, t=0) = 0$

**Boundary Conditions:**  $c(\infty, t) = 0$

$$\frac{\partial c}{\partial x}(\infty, t) = 0$$

FIGURE VI I-39 SCHEMATIC SHOWING EQUATION FOR 1-D VERTICAL TRANSPORT FROM A SURFACE WASTE SOURCE

where

- c = concentration of contaminant in the soil solution (mg/l)
- $v_s$  = seepage velocity, positive downward (velocity of fluid flow through interstices of the soil) (m/day)
- t = time (days)
- x = distance down the soil (positive downward) (m)
- D = dispersion coefficient of the contaminant in solution in the soil ( $m^2$ /day)
- $R_d$  = retardation factor for linear, equilibrium adsorption (unitless)
- k = first-order decay constant of the contaminant in the aquifer (per day)

The terms in Equation VII-75 from left to right represent the time rate of change in the concentration of the contaminant, transport due to dispersion, transport due to advection, and last, a term accounting for adsorption by the soil matrix and chemical reaction (Figure VII-39).

As presented in Equation VII-75, the first-order decay rate, k, assumes that solute in its liquid and solid phases decays at the same rate (i.e.,  $k = k_{\text{liquid}} = k_{\text{solid}}$ ). The liquid phase refers to solute in the aqueous phase and the solid phase refers to solute that has been adsorbed. If the liquid and solid phase decay rates are not the same, the following substitution needs to be made:

$$k = \frac{k_{\text{liquid}} + \frac{k_{\text{solid}} \rho_b K_d}{\theta}}{R_d} \quad (\text{VII-76})$$

where  $K_d$  is the distribution coefficient (unitless) for linear, equilibrium sorption,  $\rho_b$  is the soil bulk density (g/ml) and  $\theta$  is the volumetric moisture content (unitless fraction).

The initial concentration of the contaminant is assumed to be zero in the soil solution:

$$c(x,t) = 0 \quad \text{for } x \geq 0 \text{ and } t = 0$$

At the upper boundary,  $x = 0$ , the concentration of the contaminant (source) is either held constant or allowed to decrease exponentially with a rate constant  $\gamma$  (for a source concentration which does not change with time, set  $\gamma=0$ ):

$$c(x,t) = c_0 e^{-\gamma t} \quad \text{for } x = 0 \text{ and } t > 0$$

At large distances from the upper boundary, both the concentration and the gradient of the concentration become negligible:

$$c, \frac{c}{x} = 0 \quad \text{when } x \text{ is very large and } t > 0$$

Equation VII-75 can be solved with the above initial and boundary conditions by either the integral transform or Laplace transform techniques. A solution is given by van Genuchten and Alves (1982) as:

$$c(x,t) = \frac{c_0}{2} e^{\left(\frac{v_s x}{2D} - \gamma t\right)} \left\{ e^{-2ab} \operatorname{erfc}\left(-a\sqrt{t} + \frac{b}{\sqrt{t}}\right) + e^{2ab} \operatorname{erfc}\left(a\sqrt{t} + \frac{b}{\sqrt{t}}\right) \right\} \quad (\text{VII-77})$$

where

$$a = \sqrt{k - \gamma + \frac{v_s^2}{R_d 4D}} \quad \text{and} \quad b = \frac{x}{2} \sqrt{\frac{R_d}{D}}$$

$\operatorname{erfc}(\cdot)$  = the complimentary error function (Appendix J).

#### EXAMPLE VII-7

A farmhand has just finished spraying a field of potatoes with the insecticide endrin. He then returns the spray rig back to a livestock water well where he washes out the spray tank. After carefully hosing out the inside of the spray tank with fresh water, he opens the tank valve and allows the rinse water to run out on top of the ground. A total of about  $0.5 \text{ m}^3$  of rinse water contaminated with endrin drains and forms a pool about  $10 \text{ m}^2$  in area. This pool takes about four hours to seep into the ground. Upon draining the spray tank, the farmhand drives back to the ranch.

When the farmhand tells the boss of his activities, the boss becomes furious. Apparently, the well used to clean out the spray tank is also used to water the milk cows. If endrin contaminates the well and then the cows, the cows may have to be destroyed. The boss, his son, and the farmhand quickly drive out to the well site. The son has recently completed a course in contaminant transport and wants to try out some of his new knowledge. Along the way, the son explains to his father he thinks a one-dimensional model of contaminant transport with a constant surface concentration would be sufficient to model the spill. The analytical method would predict the contaminant concentration for any depth and time. To use the method, the following parameters would have to be calculated: vertical pore-water velocity, dispersion coefficient and retardation factor for linear, equilibrium adsorption. Upon arriving at the well site, the following information is estimated from well data and their experience in farming the area. A schematic of the example problem is shown in Figure VII-40. Data

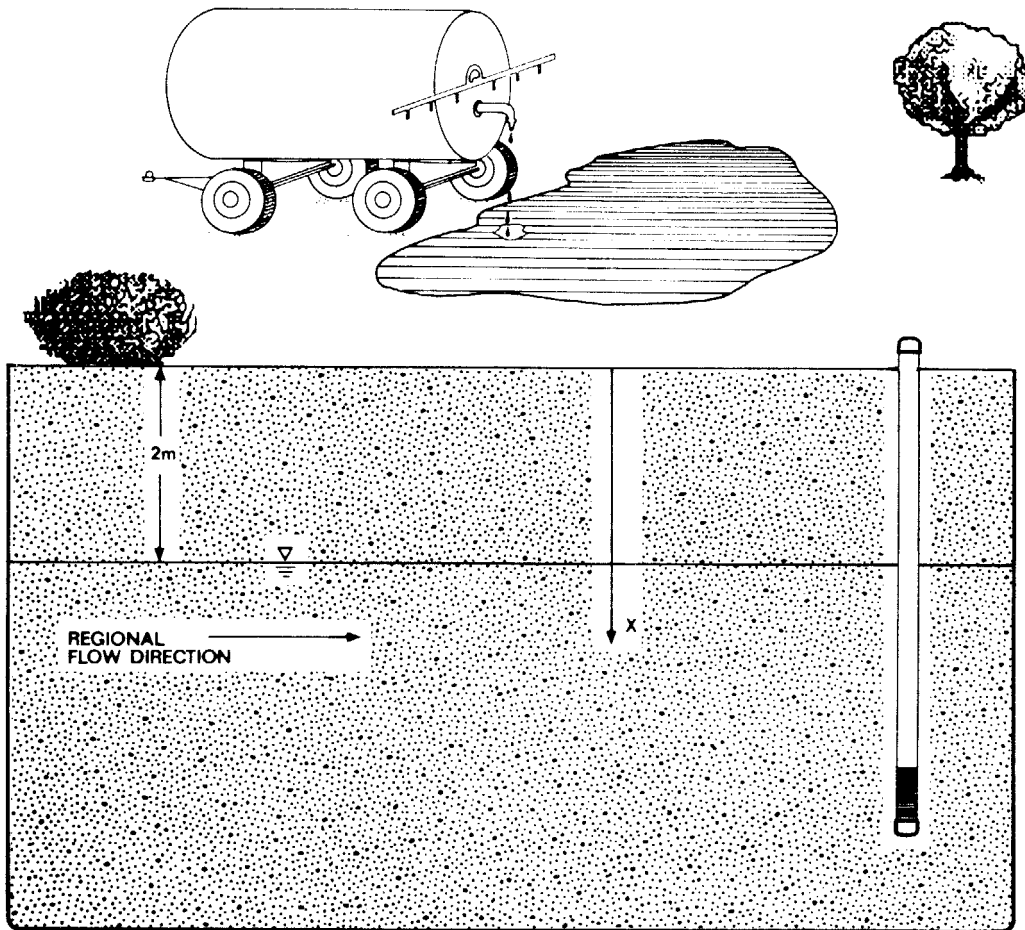


FIGURE VII-40 SCHEMATIC OF EXAMPLE 1-D PROBLEM

are listed below:

Soil type: silty sand with gravel

Soil fraction silt and clay

Percent organic carbon in sand

Percent organic carbon in silt and clay

Soil bulk density

Volumetric moisture content

Dispersivity coefficient

Saturated hydraulic conductivity

Depth to water table

Decay rate in the soil

Decay rate of the source

Time since start of spill

Contaminant

Partition coefficient

$$f = 0.1$$

$$X_{oc}^s = 0$$

$$X_{oc}^f = 0.10$$

$$\rho_b = 1.8 \text{ g/ml}$$

$$\theta = 0.15$$

$$a = 0.22 \text{ meter}$$

$$K_{sat} = 0.5 \text{ m/day}$$

$$x = 2 \text{ meters}$$

$$k = 0/\text{day}$$

$$y = 0/\text{day}$$

$$t = 1 \text{ day}$$

endrin

for endrin in octanol-water

$$K_{ow} = 4 \times 10^5$$

Surface concentration (rinse water)

$$c_o = 200 \text{ ppb}$$

To calculate the retardation factor  $R_d$  for linear, equilibrium adsorption, one must first calculate the partition coefficient  $K_p$  using Equation 11-17 and 11-18:

$$K_p = K_{oc}(0.2(1-f)\chi_{oc}^s + f\chi_{oc}^f)$$

$$K_{oc} = 0.63 K_{ow}$$

$$K_{oc} = (0.63)(4 \times 10^5) = 2.5 \times 10^5 \text{ ml/g}$$

$$K_p = 2.5 \times 10^5 (0.2(1-0.1)(0) + (0.1)(0.1)) = 2500 \text{ ml/g}$$

Therefore,

$$R_d = 1 + \frac{(1.8)(2500)}{0.15} = 30001$$

One next needs to compute the vertical Darcy velocity and then the vertical seepage velocity. For the case of a large spill into unsaturated medium, the following procedure can be used to estimate the Darcy velocity:

$$v_d = \frac{\text{volume of spill}}{(\text{area of spill})(\text{time to completely drain})} \text{ (m/day)} \quad (\text{VII-78})$$

Substitute the above data into Equations VII-35 and VII-78 to get:

$$v_d = \frac{0.5}{(10)(4/24)} = 0.3 \text{ m/day}$$

$$v_s = \frac{0.3}{0.15} = 2 \text{ m/day}$$

To calculate the dispersion coefficient, dispersion is assumed to be a linear function of the seepage velocity and molecular diffusion is considered to be negligible (Equation VII-47). Thus:

$$D = \alpha v_s \text{ (m}^2/\text{day)}$$

where  $\alpha$  is the dispersivity coefficient (meters).

Substituting the data yields:

$$D = (0.22)(2) = .44 \text{ m}^2/\text{day}$$

The concentration of endrin as a function of time and depth can be calculated from Equation VII-77. Upon rearranging terms, Equation VII-77 becomes:

$$c(x,t) = \frac{c_o}{2} e^{-\gamma t} \left( e^{A_1} \text{erfc}(A_2) + e^{A_3} \text{erfc}(A_4) \right) \quad (\text{VII-79})$$

where

$$A_1 = \frac{xv_s}{2D} - 2ab \quad (\text{VII-80})$$

$$A_2 = -a\sqrt{t} + \frac{b}{\sqrt{t}} \quad (\text{VII-81})$$

$$A_3 = \frac{xv_s}{2D} + 2ab \quad (\text{VII-82})$$

$$A_4 = a\sqrt{t} + \frac{b}{\sqrt{t}} \quad (\text{VII-83})$$

and where a and b are as defined previously in Equation VII-77.

For this problem, the concentration of endrin at the water table (i.e.,  $x = 2$  meters) is needed for a time period of one day since the spill started (i.e.,  $t = 1$  day). The data needed for this problem are summarized below:

$D = 0.44 \text{ m}^2/\text{day}$	$c_o = 200 \text{ ppb}$
$v_s = 2 \text{ m/day}$	$R_d = 30001$
$x = 2 \text{ m}$	$k = 0/\text{day}$
$t = 1 \text{ day}$	$\gamma = 0/\text{day}$

Substitute all of the data into Equation VII-79 to get:

$$a = \left( 0 - 0 + \frac{2^2}{30001(4)(0.44)} \right)^{1/2} = 0.009$$

$$b = \frac{2}{2} \left( \frac{30001}{0.44} \right)^{1/2} = 261$$

$$A_1 = \frac{(2)(2)}{(2)(0.44)} - (2)(0.009)(261) = -0.15$$

$$A_2 = -0.009\sqrt{1} + \frac{261}{\sqrt{1}} = 261$$

$$A_3 = \frac{(2)(2)}{(2)(0.44)} + (2)(0.009)(261) = 9.2$$

$$A_4 = 0.009\sqrt{1} + \frac{261}{\sqrt{1}} = 260$$

Hence,



$$c(2,1) = \frac{200}{2} e^{0(1)} \left( e^{-0.15} \operatorname{erfc}(261) + e^{9.2} \operatorname{erfc}(261) \right)$$

but

$$\operatorname{erfc}(261) = 0$$

Thus

$$c(2,1) = 0 \text{ ppb}$$

The model predicted concentration of endrin two meters down and one day after the spill is essentially zero. Why? Because of the extremely high retardation due to adsorption of endrin onto the soil particles.

----- END OF EXAMPLE VII-7 -----

### 7.5.5 Two-Dimensional Horizontal Flow With A Slug Source

The previous three analytical models only considered one-dimensional flow. Methods for two-dimensional flow will now be introduced. The first 2-D model that will be considered calculates the concentration of a contaminant downgradient of the source. The waste is considered to have been instantaneously discharged at a point. The resultant concentration in the aquifer is assumed to be uniform with depth at the point of discharge. The depth of mixing can be less than the full depth of the aquifer if the contaminant is thought to be only in a particular part of an aquifer. Vertical dispersion is usually small as discussed earlier in Section 7.4.1 on dispersion. Hence, only horizontal variations can be considered. Such an instantaneous discharge is also called a slug source and can be caused by leaky ponds or tanks or by spills. Instantaneous means that the duration of the discharge is very short compared to the time since the discharge. An analytical solution will be given below to model this problem. The solution can be used to answer the following questions:

- What is the maximum concentration of contaminants likely to be at a downgradient well?
- When does the concentration of contaminants at a downgradient well exceed a particular value or become negligible?
- At what distance will the concentration of contaminants remain at negligible concentrations?
- What is the approximate areal extent of the contaminant plume?

Before the analytical model can be given, several additional assumptions need to be stated. These are as follows. The saturated thickness of the aquifer is assumed to be uniform and the hydraulic properties of the aquifer are relatively homogeneous. The density and viscosity of the injected solute are the same as those of the native water in the aquifer. The regional flow in the aquifer is uniform and horizontal. The effect of the source on the seepage velocity is assumed to be negligible compared to the uniform regional flow rate.

The mass transport equation governing advection, dispersion, first-order decay and linear, equilibrium adsorption in two dimensions in the aquifer for the above case is:

$$R_d \frac{\partial c}{\partial t} + v_x \frac{\partial c}{\partial x} = D_x \frac{\partial^2 c}{\partial x^2} + D_y \frac{\partial^2 c}{\partial y^2} - kR_d c + m' \frac{\delta(x)\delta(y)\delta(t)}{p} \quad (\text{VII-84})$$

The last term on the right side of Equation VII-84 represents the instantaneous discharge of mass at location  $x=0, y=0$ . The  $\delta(\cdot)$  represents a Dirac delta function and  $m'$  is the strength of the discharge, where  $m' = c_0 Q' / b$  (i.e., the mass of contaminants injected divided by the thickness of the aquifer). A schematic of the problem is shown in Figure VII-41.

As presented in Equation VII-84, the first-order decay rate,  $k$ , assumes that solute in the liquid and solid phases decays at the same rate (i.e.,  $k = k_{\text{liquid}} = k_{\text{solid}}$ ). The liquid phase refers to solute in solution and the solid phase refers to solute that has been adsorbed. If the liquid and solid phase decay rates are not the same, the  $k$  value is corrected using Equation VII-76.

The solution to the equation shown in Equation VII-84, with a zero initial condition and zero gradient at large distances, can be found by means of the integral transform or Laplace transform techniques:

$$c(x,y,t) = \frac{c_0 Q'}{b 4\pi p t (D_x D_y)^{1/2}} \exp \left( -kt - \frac{(xR_d - v_x t)^2}{4D_x t R_d} - \frac{(yR_d)^2}{4D_y t R_d} \right) \quad (\text{VII-85})$$

where

- $c_0$  = initial concentration of contaminant being discharged (mg/l)
- $Q'$  = volume of contaminant being discharged ( $\text{m}^3$ )
- $b$  = saturated thickness of aquifer (m)
- $p$  = effective porosity (decimal percent, unitless)
- $t$  = time (days)
- $D_x, D_y$  = dispersion coefficients in  $x$  and  $y$  directions, respectively ( $\text{m}^2/\text{day}$ )
- $v_x$  = seepage velocity of the regional flow in the  $x$  direction ( $\text{m}/\text{day}$ )
- $x, y$  = location of point of interest (m), where the source is located at  $x=0, y=0$
- $k$  = first-order decay constant of the contaminant in the aquifer (per day)
- $R_d$  = retardation coefficient for linear, equilibrium adsorption (unitless)

Equation VII-85 is similar to the solution presented by Wilson and Miller (1978) but linear, equilibrium adsorption has been added.

The maximum concentration at any specified location occurs at time  $t_{\text{max}}$ . This time is computed as:

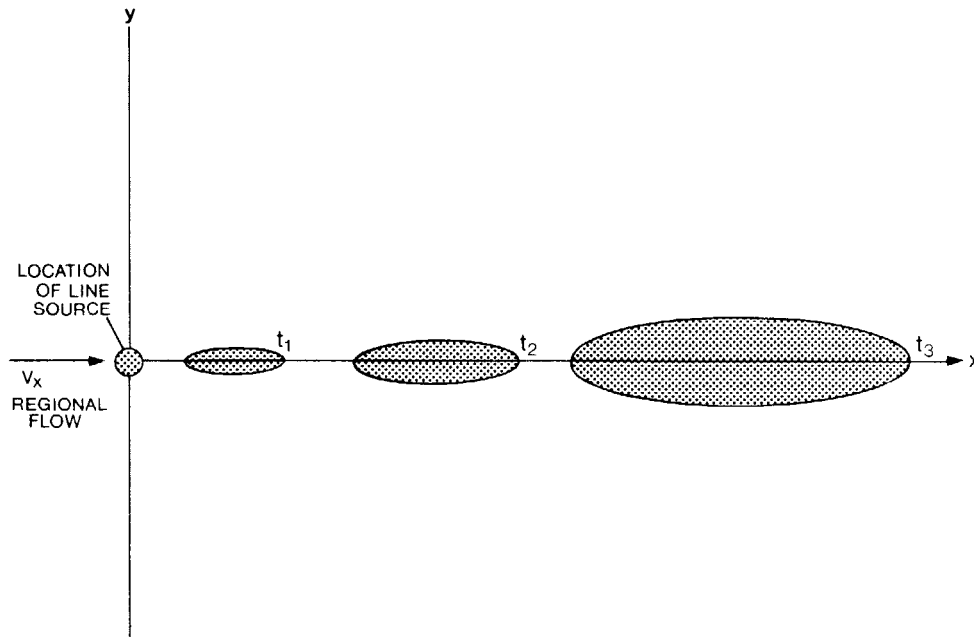


FIGURE VII -41 SCHEMATIC SHOWING A SLUG DISCHARGE OF WASTE INTO A REGIONAL FLOW FIELD

$$t_{\max} = \left( -B + (B^2 - 4AC)^{1/2} \right) / (2A) \quad (\text{VII-86})$$

where

$$A = (k4D_x D_y R_d + v_x^2 D_y) \quad (\text{VII-87})$$

$$B = (4D_x D_y R_d) \quad (\text{VII-88})$$

$$C = - (x^2 R_d^2 D_y + y^2 R_d^2 D_x) \quad (\text{VII-88a})$$

Hence, to calculate the maximum concentration that will occur at a point  $(x, Y)$ , substitute  $t_{\max}$  for  $t$  in Equation VII-85.

----- EXAMPLE VII-8 -----

Consider the problem of an accidental spill inside a chemical warehouse in which a storage drum of chloromethane (methyl chloride) leaks into an industrial sewer. The industrial sewer discharges into an injection well that is screened over the entire saturated thickness of the sandstone aquifer. About  $0.1 \text{ m}^3$  of

chloromethane enters the aquifer at a concentration of 1600 mg/l. The sandstone aquifer has the following properties:

Soil fraction silt and clay	$f = 0.01$
Percent organic carbon in the sand fraction	$X_{oc}^s = 0.01$
Percent organic carbon in the silt and clay fraction	$X_{oc}^f = 0.05$
Soil bulk density	$\rho_b = 2.5 \text{ g/ml}$
Effective porosity	$p = 0.12$
Saturated thickness	$b = 15 \text{ m}$
Dispersion coefficient	$D_x = 4 \text{ m}^2/\text{day}$
	$D_y = 1 \text{ m}^2/\text{day}$
Seepage velocity:	$v_x = 0.3 \text{ m/day}$

In addition, chloromethane has the following adsorption and degradation properties:

Octanol-water partition coefficient	$K_{ow} = 8 \text{ (unitless)}$
Hydrolysis rate (at a pH of 7)	$K_H = 0.0021 \text{ per day}$

At a distance of 35 meters downgradient of the injection well is a domestic supply well. What is the maximum concentration of chloromethane expected to reach the domestic well and when will the maximum concentration occur?

To answer these questions, several parameters have to be computed. Chloromethane undergoes both adsorption and degradation in the aquifer. Adsorption is related to the soil properties as described by Equation 11-17 and 11-18.

Upon substitution of the data into Equations 11-17 and 11-18, one obtains the adsorption coefficient  $K_d$  as shown below:

$$K_{oc} = 0.63(8) = 5 \text{ ml/g}$$

$$K_d = (5)(0.2(1-0.01)(0.01) + (0.01)(0.05)) = 0.012 \text{ ml/g}$$

If we assume adsorption can be described by a linear, equilibrium model, then the retardation coefficient for chloromethane can be computed using Equation VII-55 as shown below:

$$R_d = 1 + \rho_b K_d / p$$

$$R_d = 1 + (2.5)(0.012)/(0.12) = 1.25 \text{ (unitless)}$$

In addition to adsorption, chloromethane in the aqueous phase is subject to hydrolysis. Adsorbed chloromethane does not undergo hydrolysis. The relation between the general degradation rate and the liquid/adsorbed phase rates is given

by Equation VII-76. Thus for this problem,  $k_{\text{liquid}}$  would equal the hydrolysis rate and  $k_{\text{solid}}$  would be zero. Upon substitution of the data into Equation VII-76:

$$k = \frac{0.0021 + \frac{(0)(2.5)(0.012)}{0.12}}{(1.25)} = 0.0017 \text{ per day}$$

All of the soil and chemical properties can now be given for the problem as follows:

$$\begin{array}{ll} x = 35 \text{ m} & c_o = 1600 \text{ mg/l} \\ y = 0 \text{ m} & Q' = 0.1 \text{ m}^3 \\ b = 15 \text{ m} & v_x = 0.3 \text{ m/day} \\ p = 0.12 & \\ R_d = 1.25 & D_x = 4 \text{ m}^2/\text{day} \\ k = 0.0017 \text{ per day} & D_y = 1 \text{ m}^2/\text{day} \end{array}$$

The time at which the maximum concentration occurs can now be computed upon substitution of the above data into Equation VII-86 to VII-89:

$$A = (k4D_x D_y R_d + v_x^2 D_y) = (0.0017)4(4)(1)(1.25) + (0.3)^2(1) = 0.124$$

$$B = (4D_x D_y R_d) = 4(4)(1)(1.25) = 20$$

$$C = -(x^2 D_y + y^2 D_x) R_d^2 = -(35)^2(1) + (0)^2(4)(1.25)^2 = -1914$$

$$t_{\text{max}} = (-B + (B^2 - 4AC)^{1/2})/2A$$

$$= \left( -20 + \left( (20)^2 - 4(.124)(-1914) \right)^{1/2} \right) / (2(.124)) = 67.5 \text{ days}$$

Hence, the maximum concentration will occur at the domestic well 68 days after the spill. The value of the maximum concentration is computed by substituting  $t_{\text{max}}$  and the other data into Equation VII-81:

$$c_{\text{max}} = \frac{c_o Q'}{b4\pi p t_{\text{max}} (D_x D_y)^{1/2}} \exp \left( -kt_{\text{max}} - \frac{(xR_d - v_x t_{\text{max}})^2}{4D_x t_{\text{max}} R_d} - \frac{(yR_d)^2}{4D_y t_{\text{max}} R_d} \right) \quad (\text{VII-89})$$

$$c_{\text{max}} = \frac{(1600)(0.1)}{(15)4\pi(0.12)(67.5)((4)(1))^{1/2}} \exp \left( -(0.0017)(67.5) \right)$$

$$\frac{((35)(1.25) - (0.3)(67.5))^2}{4(4)(67.5)(1.25)} - \frac{((0)(1.25))^2}{4(1)(67.5)(1.25)}$$

$$= (0.0524) \exp(-0.524) = 0.031 \text{ mg/l}$$

Hence, the maximum concentration of chloromethane that will reach the domestic well is 0.031 mg/l or 31  $\mu\text{g/l}$ . This concentration will occur at the domestic well 68 days after the spill.

----- END OF EXAMPLE VII-8 -----

----- EXAMPLE VII-9 -----

Consider a large electric power company that has a coal-burning plant that produces electricity. Its fly ash is deposited as a slurry waste into a large lagoon where the ash is allowed to settle. The lagoon site is above a 2 meter thick water table aquifer that consists of glacial outwash. A layer of impermeable clay lines the bottom of the lagoon. A large river flows nearby.

Next to the lagoon, the electric company has been preparing the ground for another lagoon when a bulldozer accidentally breaches the berm surrounding the lagoon. Very quickly, about 40 m<sup>3</sup> of supernatant spill out and form a pool on top of the ground. The supernatant percolates into the ground after a short time. The greatest concern to the company is the level of boron in the spill water, which had a concentration of about 10 mg/l. They want to know what the maximum concentration of boron will be where the aquifer discharges to the river and when this will occur. The downgradient distance between the spill site and the river is 50 meters.

Since the area of the spill site is very small compared to the area over which the contaminant will travel and since the duration of the spill was short, a slug source model is selected. This model assumes complete vertical mixing of the source in the aquifer. This seems reasonable considering the relative thinness of the glacial outwash aquifer.

After an investigation of the problem, the following information is obtained:

X = 50 m	C <sub>o</sub> = 10 mg/l
Y = 0 m	Q' = 40 m <sup>3</sup>
b = 2 m	v <sub>x</sub> = 2 m/day
p = .15	
R <sub>d</sub> = 17	D <sub>x</sub> = 15 m <sup>3</sup> /day
k = 0/day	D <sub>y</sub> = 5 m <sup>3</sup> /day

Step 1. The time at which the maximum concentration of boron will reach the river,  $t_{\max}$  can now be computed by substituting the above data into Equation VII-86 to VII-89:

$$A = (k4D_x D_y R_d + v_x^2 D_y) = (0)(4)(15)(17) + (2)^2(5) = 20$$

$$B = (4D_x D_y R_d) = (4)(15)(5)(17) = 5100$$

$$C = -(x^2 D_y + y^2 D_x) R_d^2 = -\left((50)^2(5) + (0)^2(15)\right)(17)^2 = -3.61 \times 10^6$$

$$t_{\max} = (-B + (B^2 - 4AC)^{\frac{1}{2}}) / (2A)$$

$$= (-5100 + ((5100)^2 - 4(20)(-3.6 \times 10^6))^{\frac{1}{2}}) / (2(20)) = 316 \text{ days.}$$

Hence, it will take about 320 days for the maximum concentration of boron to reach the river.

Step 2. The value of the maximum concentration of boron that will reach the river is computed by substituting the above data into Equation VII-85:

$$c_{\max} = \frac{c_0 Q'}{b4\pi p t_{\max} (D_x D_y)^{\frac{1}{2}}} \exp(g)$$

where

$$g = \left( -kt_{\max} - \frac{(xR_d - v_x t_{\max})^2}{4D_x t_{\max} R_d} - 4D_y \frac{(yR_d)^2}{t_{\max} R_d} \right)$$

$$g = \left( -(0)(316) - \frac{(50)(17) - (2)(316)}{4(15)(316)(17)} - \frac{((0)(17))^2}{4(5)(316)(17)} \right) = -0.15$$

$$c_{\max} = \frac{(10)(40)\exp(-.15)}{(2)4\pi(.15)(316)((15)(5))^{\frac{1}{2}}} = 0.033 \text{ mg/l}$$

The maximum concentration of boron that will reach the river is about 0.03 mg/l or 30 pg/l.

END OF EXAMPLE VII-9

### 7.5.6 Two-Dimensional Horizontal Flow With Continuous Solute Line Sources

In Section 7.5.5, the problem of an instantaneous waste discharge is considered. In this section, a continuous waste discharge into a homogeneous, isotropic aquifer will be considered. The contaminant is discharged continuously and uniformly with depth into the aquifer. The density and viscosity of the discharged solute are the same as those of the native water in the aquifer. The effect of the discharging solute on the seepage velocity is assumed to be negligible compared to the uniform regional flow rate.

The mass transport equation governing advection, dispersion, first-order decay and linear, equilibrium adsorption in two dimensions in the aquifer is:

$$R_d \frac{\partial c}{\partial t} + v_x \frac{\partial c}{\partial x} = D_x \frac{\partial^2 c}{\partial x^2} + D_y \frac{\partial^2 c}{\partial y^2} - kR_d c + g_L \frac{\delta(x) \delta(y)}{p} \quad (\text{VII-90})$$

The last term on the right-hand side of Equation VII-90 represents the instantaneous discharge of mass by a well screened over the entire depth of the aquifer at location  $X=0, y=0$ . The mixed zone can be set equal to the depth screened, rather than the full depth of the aquifer, if vertical mixing above and below the screened zone is thought to be small. The  $\delta(\cdot)$  is a Dirac delta function and  $g_L$  is the strength of the line source, where  $g_L = c_0 Q/b$ .

As presented in Equation VII-90, the first-order decay rate,  $k$ , assumes that solute in its liquid and solid phases decays at the same rate (i.e.,  $k = k_{\text{liquid}} = k_{\text{solid}}$ ). The liquid phase refers to solute in solution and the solid phase refers to solute that has been adsorbed. If the liquid and solid phase decay rates are not the same, Equation VII-76 needs to be substituted.

The solution to Equation VII-90, with a zero initial concentration and zero gradients at large distances can be found by means of the integral transform or Laplace transform techniques:

$$c(x,y,t) = \frac{c_0 Q}{4\pi p b (D_x D_y)^{1/2}} \exp\left(\frac{v_x x}{2D_x}\right) w\left(u, \frac{r}{B}\right) \quad (\text{VII-91})$$

where

$$\begin{aligned} w(u) &= \text{the leaky well function of Hantush (see Appendix J)} \\ B &= 2D_x/v_x \text{ (m)} \\ r &= (\beta(x^2 + y^2 D_x/D_y))^{1/2} \text{ (m)} \\ u &= \frac{r^2 - R_d}{4\beta D_x t} \text{ (unitless)} \end{aligned}$$



- $\beta$  =  $1 + 2BR_d k/v_x$  (unitless)  
 $Q$  = volumetric rate discharge into the aquifer by the line source ( $m^3/day$ )  
 $t$  = time (days)  
 $(x,y)$  = location of point of interest (m), where the line source is located at  $x=0, y=0$   
 $D_x, D_y$  = dispersion coefficients in the x and y directions, respectively ( $m^2/day$ )  
 $v_x$  = seepage velocity of the regional flow in the x direction (m/day)  
 $p$  = effective porosity of the aquifer (unitless, decimal percent)  
 $b$  = saturated thickness of mixed zone (m)  
 $k$  = first-order decay constant (per day)  
 $R_d$  = retardation coefficient for linear, equilibrium adsorption (unitless)  
 $c_o$  = concentration of contaminant being discharged (mg/l)

Note that Equation VII-91 is similar to the solution presented by Wilson and Miller (1978). However, Equation VII-91 allows for linear, equilibrium adsorption. A schematic representation of Equation VII-91 is shown in Figure VII-42.

The leaky well function of Hantush  $W(u, r/B)$  is discussed in Appendix J. In addition, a table of values (i.e., Table J-3) and several approximations are given for the  $W(\cdot)$  function in Appendix J.

For the special case of steady-state conditions (i.e., large times) and when the ratio  $r/B$  is larger than one (i.e., far from the source), then Equation VII-91 reduces to the following simplified form:

$$c(x,y, \text{steady-state}) = \frac{c_o Q}{b2\pi p} \left( \frac{\pi B}{2D_x D_y r} \right)^{1/2} \exp\left( \frac{v_x x}{2D_x} - \frac{r}{B} \right) \quad (\text{VII-92})$$

#### ----- EXAMPLE VII-10 -----

A small community had water from their municipal well checked for trace organics. To their surprise, they found a concentration of **150  $\mu\text{g/l}$**  of trichloroethylene (TCE). After much investigation, a local environmental organization found the only major user of TCE to be a semi-conductor manufacturing plant. However, the plant was located over 1000 meters away from the site of the municipal well. At first, few could believe that the plant could be the source of the contamination because of the large distance involved. Hence, a blue-ribbon committee was selected to investigate the problem. What follows are the results of the committee's work.

The solvent TCE has been used continuously by the manufacturing plant for the last 25 years as a degreaser for their equipment. All residual TCE is washed

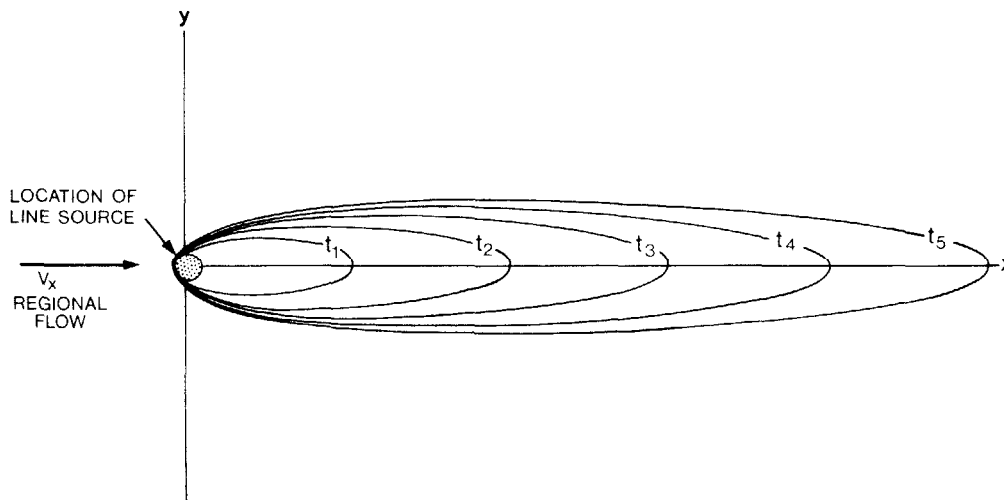


FIGURE VII -42 SCHEMATIC SHOWING A CONTINUOUS DISCHARGE OF WASTE INTO A REGIONAL FLOW FIELD

out of the plant by a large volume of water, which in turn is pumped to a small, unlined pond. The pond receives about  $500 \text{ m}^3$  of TCE contaminated wash water per year and the concentration of TCE in the pond is  $25,000 \text{ } \mu\text{g/l}$ . The wastewater percolates through the bottom of the pond as quickly as it flows in. The depth to the water table is about 2 meters and the underlying aquifer consists of unconsolidated sand. From well logs, observation wells and pumping tests, it was found that the hydraulic conductivity in the unconsolidated sand was  $3640 \text{ m/yr}$ , the effective porosity 0.2, hydraulic gradient in the aquifer  $0.0022 \text{ m/m}$  and saturated thickness of the aquifer 20 meters. The unconsolidated sand is underlain by a thick impermeable clay layer. Dispersion tests showed that the dispersivity along the direction of ground water flow is about 50 m and transverse to the flow about 5 m. The background concentration of TCE upgradient of the plant is below detection.

As a first approximation, the TCE is considered to be vertically mixed in the aquifer. Since the dimensions of the pond are small compared to the travel distance, the analytic solution of Wilson and Miller (1978) can be used to simulate the TCE transport.

In addition to the other information already given, the seepage velocity and dispersion coefficients are needed. The seepage velocity is calculated using Equation VII-36:

$$v_s(\text{seepage}) = (K_{\text{sat}})(\text{hydraulic gradient})/p$$

$$v_x = (3640)(0.0022)/0.2 = 40 \text{ m/yr}$$

Note that the transverse velocity is zero because we have oriented the x axis along the principal flow direction. If hydrodynamic dispersion is assumed to be a linear function of seepage velocity, then dispersion can be computed as follows from Equation VII-53:

$$D_x = \alpha_x v_x = (50)(40) = 2000 \text{ m}^2/\text{yr}$$

$$D_y = \alpha_y v_x = (5)(40) = 200 \text{ m}^2/\text{yr}$$

where  $\alpha_x$  and  $\alpha_y$  are the longitudinal and transverse dispersivities, respectively.

The committee further assumes that there is negligible adsorption of TCE and that degradation (e.g., dehydrochlorination) is zero because of the aerobic conditions. The amount of TCE entering the aquifer through the pond bottom is estimated to have been constant over the past 25 years.

The information for this example can now be tabulated as follows:

$t = 25 \text{ yrs}$	$C_o = 25000 \text{ } \mu\text{g/l}$
$v_x = 40 \text{ m/yr}$	$Q = 500 \text{ m}^3/\text{yr}$
$D_x = 2000 \text{ m}^2/\text{yr}$	$b = 2.0 \text{ m}$
$D_y = 200 \text{ m}^2/\text{yr}$	$p = 0.2$
$x = 1000 \text{ m}$	$R_d = 1$
$y = 0 \text{ m}$	$k = 0 \text{ per yr}$

Determine the concentration of TCE at a distance of 1000 meters from the manufacturing plant after 25 years. This problem is mathematically described by Equation VII-90. Equation VII-91 gives an analytic solution to the problem. To predict the concentration, the committee needs to first evaluate the following terms:

$$B = 2D_x/v_x = (2)(2000)/40 = 100 \text{ m}$$

$$\beta = 1 + 2BR_d k/v_x = 1 + 2(100)(1)(0)/40 = 1$$

$$r = \left( \beta \left( x^2 + y^2 \frac{D_x}{D_y} \right) \right)^{1/2} = \left( (1) \left( (1000)^2 + (0)^2 \left( \frac{2000}{200} \right) \right) \right)^{1/2} = 1000 \text{ m}$$

$$r/B = 1000/100 = 10$$

$$u = \frac{r^2 R_d}{4B D_x t} = \frac{(1000)^2 (1)}{4(1)(2000)(25)} = 5$$

With the above terms, Equation VII-91 can now be evaluated:

$$c(x,y,t) = \frac{c_0 Q}{b4\pi p(D_x D_y)^{1/2}} \exp\left(\frac{v_x x}{2D_x}\right) W\left(u, \frac{r}{B}\right)$$

$$c(1000,0,25) = \frac{(25000)(500)}{(20)4\pi(0.2)((2000)(200))^{1/2}} \exp\left(\frac{(40)(1000)}{2(2000)}\right) W(5,10)$$

$$= (393.2) \exp(10) W(5,10)$$

Unfortunately, the range of parameter values given in Table J-3 of Appendix J does not include the values needed to evaluate the leaky well function of Hantush,  $W(5,10)$ . However, since the  $r/B$  parameter is very large, one can use the Wilson and Miller (1978) approximation to  $W$  given in Appendix J:

$$W(u, r/B) = \left(\frac{\pi B}{2r}\right)^{1/2} \exp\left(-\frac{r}{B}\right) \operatorname{erfc}\left(-\frac{(r/B-2u)}{2\sqrt{u}}\right)$$

$$W(5,10) = \left(\frac{\pi(100)}{2(1000)}\right)^{1/2} \exp(-10) \operatorname{erfc}\left(-\frac{(10-2(5))}{2\sqrt{5}}\right)$$

$$W(5,10) = (0.40) \exp(-10) \operatorname{erfc}(0)$$

but  $\operatorname{erfc}(0) = 1$ , thus

$$W(5,10) = (0.4)(4.54 \times 10^{-5})(1) = 1.82 \times 10^{-5}$$

Therefore, upon substitution of  $W(5,10)$  back into our concentration solution (Equation VII-91):

$$c(1000,0,25) = (393.2)(22026.5)(1.82 \times 10^{-5}) = 158 \mu\text{g/l}$$

If one does not use the Wilson and Miller approximation, the exact solution is **154  $\mu\text{g/l}$** .

As mentioned earlier, a concentration of 150  $\mu\text{g/l}$  of TCE was discovered in the municipal water well. The manufacturing plant appears to be the likely source of the TCE contamination.

----- END OF EXAMPLE VII-10 -----

The previous example showed how the contaminant TCE decreased in concentration with distance and time. Biological and chemical degradation processes were assumed to be negligible. This is true under aerobic conditions for TCE but under anaerobic conditions degradation can take place. It is difficult to provide accurate rates of degradation for field type situations because many variables (e.g., pH, temperature) may affect it. The half life of TCE under anaerobic conditions ranges from 40 to 400 days (Wood et al., 1981). This corresponds to a decay rate of 0.2 to 6 per year.

What is the concentration of TCE at a distance of 1000 m after 25 years if biodegradation at a rate of 0.2 per year is included? The data needed are summarized below:

$t = 25 \text{ yrs}$	$c_0 = 25000 \text{ } \mu\text{g/l}$
$v_x = 40 \text{ m/yr}$	$Q = 500 \text{ m}^3/\text{yr}$
$D_x = 2000 \text{ m}^2/\text{yr}$	$b = 20 \text{ m}$
$D_y = 200 \text{ m}^2/\text{yr}$	$p = 0.2$
$x = 1000 \text{ m}$	$R_d = 1$
$y = 0 \text{ m}$	$k = 0.2 \text{ per yr}$

Step 1. Calculate the following terms in Equation VII-91:

$$B = 2D_x/v_x = 2(2000)/40 = 100$$

$$\beta = 1 + \frac{2BR_d k}{v_x} = 1 + \frac{2(100)(1)(0.2)}{40} = 2$$

$$r = (\beta(x^2 + y^2 D_x/D_y))^{1/2}$$

$$r = (2((1000)^2 + (0)^2(2000)/(200)))^{1/2} = 1414$$

$$r/B = 1414/100 = 14.14$$

$$u = \frac{r^2 R_d}{4\beta D_x t} = \frac{(1414)^2(1)}{4(2)(2000)(25)} = 5$$

Step 2. Is  $r/B$  greater than 1? If so, use the Wilson and Miller (1978) approximation given in Appendix J to evaluate  $W$ , the leaky well function Hantush. If  $r/B$  is less than 1, then use Table J-3 to evaluate  $W$ . For example, to use the Wilson and Miller approximation, proceed as follows. Evaluate the terms:

$$\left(-\frac{(r/B-2u)}{2\sqrt{u}}\right) = -\frac{(14.14-2(5))}{2\sqrt{5}} = -0.93$$

$$\operatorname{erfc}\left(-\frac{(r/B-2u)}{2\sqrt{u}}\right) = \operatorname{erfc}(-0.93) = 1.81$$

Note that  $\operatorname{erfc}(-a) = 2 - \operatorname{erfc}(a) = 2 - 0.188 = 1.81$

$$W(u, r/B) = \left(\frac{\pi B}{2r}\right)^{\frac{1}{2}} \exp\left(-\frac{r}{B}\right) \operatorname{erfc}\left(-\frac{(r/B-2u)}{2\sqrt{u}}\right)$$

$$W(5, 14.14) = \left(\frac{\pi(100)}{2(1414)}\right)^{\frac{1}{2}} \exp(-14.14) (1.81) = 4.36 \times 10^{-7}$$

Step 3. Evaluate the final computation using Equation VII-91:

$$c(x, y, t) = \frac{c_0^0}{4\pi p b (D_x D_y)^{\frac{1}{2}}} \exp\left(\frac{v_x x}{2D_x}\right) W(u, r/B)$$

$$c(1000, 0, 25) = \frac{(25000)(500)}{4\pi(0.2)(20)((2000)(200))^{\frac{1}{2}}} \exp\left(\frac{(40)(1000)}{2(2000)}\right) (4.36 \times 10^{-7})$$

$$c(1000, 0, 25) = 3.8 \mu\text{g/l}$$

With degradation over a 25-year period, the predicted concentration of TCE is decreased from 185  $\mu\text{g/l}$  to 4  $\mu\text{g/l}$ . However, it should be noted that when TCE undergoes degradation by dehydrochlorination, it produces incomplete degradation products (e.g., the two isomers of dichloroethylene) which are also hazardous.

END OF EXAMPLE VII-11

## 7.6 INTERPRETATION OF RESULTS

This section discusses the interpretation of results calculated using the screening methods. Section 7.6.1 reviews water quality criteria which are pertinent to ground water. A brief analysis of uncertainty and methods for quantifying it are given in Section 7.6.2. Finally, Section 7.6.3 provides guidance for determining when more detailed analyses such as those involving numerical computer models are appropriate.

### 7.6.1 Appropriate Reference Criteria

#### 7.6.1.1 Introduction

Federal and state regulations applicable to ground water quality are currently undergoing revision. The trend is toward more regulation at the state level rather

than at the federal level. Pertinent federal laws include the Federal Water Pollution Control Act/Clean Water Act (1972/1977/1982), the Safe Drinking Water Act (1974/1977), the Resource Conservation and Recovery Act (1976/1984), and the Toxic Substances Control Act (1976). The U.S. Environmental Protection Agency recently made public its policy regarding ground water protection in a document referred to as the EPA's Ground Water Protection Strategy (U.S. EPA, 1984). Individual states are also in the process of developing laws and programs related to ground water. For example, Connecticut, Florida, Wisconsin, and New Mexico have ground water classification systems and numerical standards for each classification. Maryland, New Jersey, and New York specify effluent limitations for waste discharges to ground water.

#### 7.6.1.2 Water Quality Standards

The predicted results of the hand calculation methods should be compared to the appropriate standards. The federal standards for drinking water are currently being reviewed (CFR Vol. 48, No. 194, October, 1983). Numerical limits may change and new parameters may be added as shown in Table VII-13. The interim primary drinking water standards are based on human health considerations. The present standards cover ten inorganic chemicals, bacteria, turbidity, organic chemicals and radioactivity.

The interim secondary drinking water standards (Table VII-14) mainly address aesthetic and pragmatic factors rather than public health. The secondary standards cover parameters which affect taste, color, odor and the corrosive properties of water. These standards are not federally enforceable but are considered guidelines for the states.

In addition to the federal drinking water standards, each state may have its own set of water quality standards, which may be equal or more stringent than the federal standards. These regulations may change so it is imperative to check with the local state agencies regarding current values.

The state may specify that standards apply to the ground water at the waste disposal site boundary, at a specified distance downgradient of the site, at a property boundary, or at the point of use. In some states, ground water downgradient of a waste site may have to meet all federal drinking water standards. In addition, if the ground water discharges to a surface water body, surface water standards may apply.

#### 7.6.2 Quantifying Uncertainty

Uncertainty in ground water flow and contaminant transport has been implied throughout this chapter. Part of this uncertainty is due to aquifer heterogeneities and natural variability. Additional uncertainty is introduced by sampling and measurement errors and the assumptions on which the hand calculation methods are based. For numerical models used to compute ground water flow and contaminant transport, uncertainty can also result from the numerical solution techniques.

TABLE VI I -13

## PRIMARY DRINKING WATER STANDARDS

INORGANIC CHEMICALS			
Parameter	Maximum Contaminant Level (mg/l)	Parameters Under Consideration	
Arsenic	0.05	Aluminum	Nickel
Barium	1.0	Antimony	Sodium
Cadmium	0.010	Asbestos	Sulfate
Chromium	0.05	Beryllium	Thallium
Lead	0.05	Copper	Vanadium
Mercury	0.002	Cyanide	Zinc
Nitrate (as N)	10.0	Molybdenum	
Selenium	0.01		
Silver	0.05		
Fluoride	1.4-2.4		

MICROBIOLOGICAL CONTAMINANTS AND TURBIDITY			
Parameter	Maximum Contaminant Level (mg/l)	Parameters Under Consideration	
Total Coliforms	1/100 ml Monthly Average	Giardia, Legionella, Viruses	
	4/100 ml Single Sample	Standard Plate Count (SPC)	
Turbidity	1-5 turbidity units		

ORGANIC CHEMICALS			
Parameter	Maximum Contaminant Level (mg/l)	Parameters Under Consideration	
Endrin	0.002	Aldicarb	Di bromochloropropane (DBCP)
Lindane	0.004	Chlordane	1,2-Dichloropropane
Methoxychlor	0.1	Dalapon	Pentachlorophenol
Toxaphene	0.005	Diquat	Picloram
2,4-D	0.1	Endothal I	Di-noseb
2,4,5-TP Silver	0.01	Glyphosate	Alachlor
Total Trihalomethanes	0.1	Carbofuran	Ethylene dibromide
		1,1,2-Trichloroethane	Epiclorohydrin
		Vydate	Di bromomethane
		Simazine	Toluene
		PAHs	Xylene
		PCBs	Adipates
		Atrazine	Hexachlorocyclopentadiene
		Phthalates	2,3,7,8-TCDF (Dioxin)
		Acrylamide	

RADIOACTIVITY			
Parameter	Maximum Contaminant Level	Parameters under Consideration	
Combined radium 226 and radium 228	5 pCi/l	Uranium	
Gross alpha particle activities	15 pCi/l	Radon	
Beta particle and photon radioactivity from man-made radionuclides	4 millirem/year		

Reference: U.S. EPA (1977a) and Code of Federal Regulations 40 CFR 141.11-141.16 (1982).



TABLE VII-14

## INTERIM SECONDARY DRINKING WATER STANDARDS

Parameter	Maximum Contaminant Level
Chloride	250 mg/l
Color	15 color units
Copper	1 mg/l
MBAS*	0.5 mg/l
Iron	0.3 mg/l
Manganese	0.05 mg/l
Odor	Threshold Odor Number 3
pH	6.5-8.5
Sulfate	250 mg/l
Total Dissolved Solids	500 mg/l
Zinc	5 mg/l
Corrosivity	Non-Corrosive

\*Methylene blue active substances

Reference: U.S. EPA (1977b) and Code of Federal Regulations 40 CFR 143.3 (1982).

#### 7.6.2.1 Sources of Uncertainty

Uncertainty associated with measured values of a parameter may be due to variability of aquifer characteristics, sampling error, and analytical error. The distinction between these sources can be made by collecting replicate samples, splitting them, and performing at least duplicate analyses of the samples. One common sampling design involves collection of four replicates which are then each split four ways. The uncertainty can then be allocated using a 4 x 4 analysis of variance (ANOVA). The quality of laboratory analyses should also be checked by analysis of blanks, standards, and unknowns. Additional discussion of QA/QC procedures is included in Scalf et al. (1981), U.S. EPA (1979b) and (1980).

Uncertainty in the representation of the physical system may also create uncertainty in the parameters used to describe the system. For example, consider the concept of hydrodynamic dispersion which was discussed in Section 7.4.1. Several figures and tables were given to provide estimates for dispersivity, which itself is used to represent the dispersive characteristics of an aquifer. However, current research indicates that dispersion results from variations in the seepage velocity profile. These variations may not be adequately characterized by existing mathematical formulations.

Additional uncertainty and errors can be introduced by mathematical solutions in the form of overshoot, numerical dispersion, truncation and round-off errors. Overshoot and numerical dispersion are the most important errors generated by finite difference and finite element models of contaminant transport. The term overshoot describes the erroneously high values computed near the upstream side of sharp solute fronts (undershoot is the analogous behavior on the downstream side of sharp fronts). Numerical dispersion, which results from the incomplete approximation of the differential equations, can smear a sharp front and thereby produce a solution indicative of a larger dispersion coefficient (Pinder and Gray, 1977). Truncation errors occur when only a finite number of terms are used to represent the original equations describing flow and mass transport. Finally, round-off errors result from the finite accuracy of computer calculations. It should be noted that even analytic solutions can be subject to truncation and round-off errors.

#### 7.6.2.2 Methods of Estimating Uncertainty

The recognition of uncertainty helps put predicted results in perspective. For example, if the time of arrival of a contaminant at a well is 300 + 10 days, then time is available to design a plan of action. However, if our uncertainty analysis predicted a time of arrival of 300 ± 200 days, a plan of action would have to be developed much sooner.

Several methods are available for estimating the uncertainty associated with calculations. Included are sensitivity analysis, variance analysis, interval analysis, and Monte Carlo analysis. Each of these methods is discussed briefly below.

Sensitivity analysis is the process of determining the variation in a model output variable caused by a change in one of the input parameters. This can be done using a mathematical approach or simply by making repeat calculations using different parameter values. The parameters which most influence the results can thereby be identified.

Consider a sensitivity analysis of the seepage velocity  $v_s$  for saturated flow. From Section 7.3.3.1.2, it was shown that the seepage velocity is a function of the hydraulic conductivity  $K$ , the hydraulic gradient  $I$  and the porosity  $p$ . From Equation VII-36 the seepage velocity was shown to be equal to:

$$v_s = -KI/p$$

The total uncertainty in the seepage velocity  $dv_s$  can be expressed as:

$$dv_s = \left(\frac{\partial v_s}{\partial K}\right) dK + \left(\frac{\partial v_s}{\partial I}\right) dI + \left(\frac{\partial v_s}{\partial p}\right) dp \quad (\text{VII-93})$$

where  $(\partial v_s / \partial K)$ ,  $(\partial v_s / \partial I)$  and  $(\partial v_s / \partial p)$  are the sensitivity coefficients and  $dK$ ,  $dI$  and  $dp$  are the uncertainties associated with these parameters (e.g.,  $dK = \pm 1 \times 10^{-5}$  cm/see,

$dI = \pm 0.001$ ,  $dp = \pm 0.05$ ). Upon substitution of Equation VII-36 into Equation VII-93, the uncertainty  $dv_s$  becomes:

$$dv_s = -\left(\frac{I}{p}\right) dK - \left(\frac{K}{p}\right) dI + \left(\frac{KI}{p^2}\right) dp \quad (\text{VII-94})$$

The relative or percent uncertainty is found by dividing Equation VII-94 through by  $v_s$ . Thus upon substitution:

$$\frac{dv_s}{v_s} = \frac{dK}{K} + \frac{dI}{I} - \frac{dp}{p} \quad (\text{VII-95})$$

In the case of the seepage velocity, the uncertainty can be due to  $K$ ,  $I$ , or  $p$ . However, the greatest source of uncertainty is generally the hydraulic conductivity term; its value may vary over several orders of magnitude. The above mathematical procedure for computing the sensitivity analysis can in principal be done for any input parameter but it usually becomes too complicated except for simple expressions. The alternative "brute force" method is to repeatedly perform the calculations, systematically varying the parameters, one at a time and in combinations, to determine how the variations in parameter values affect the predicted result.

Another mathematical technique used to quantify uncertainty is based upon determining how the variance of individual equation terms interact with each other. Consider two variables, called  $X$  and  $Y$ . Let the sum (or difference) of these two variables be called  $Z$ . If  $X$  and  $Y$  are considered as independent random variables, then the variance of  $Z$  can be calculated as:

$$\text{Var}[Z] = \text{Var}[X \pm Y] = \text{Var}[X] + \text{Var}[Y] \quad (\text{VII-96})$$

where  $\text{Var} [ ]$  is the variance of the variable. (An estimate of the variance can be obtained by squaring the standard deviation  $S_x$ .  $S_x$  is defined by Equation VII-22 in Section 7.2.5.4). If  $X$  and  $Y$  are multiplied together to get  $Z$ , then the variance of  $z$  for this product will vary as:

$$\begin{aligned} \text{Var}[Z] &= \text{Var}[XY] \\ &= (E[X])^2 \text{Var}[Y] + (E[Y])^2 \text{Var}[X] + \text{Var}[X] \text{Var}[Y] \end{aligned} \quad (\text{VII-97})$$

where  $E [ ]$  is the expected value of the variable. (An estimate of the expected or mean value is given by Equation VII-23 in Section 7.2.5.4.) If  $Z$  is defined as  $X$  divided by  $Y$ , the variance of  $Z$  for this quotient will vary approximately as:

$$\text{Var}[Z] = \text{Var}[X/Y] \approx \left(\frac{E[X]}{E[Y]}\right)^2 \left(\frac{\text{Var}[X]}{(E[X])^2} + \frac{\text{Var}[Y]}{(E[Y])^2}\right) \quad (\text{VII-98})$$

From the above expressions, it is obvious that if any independent variables have uncertainty associated with them, then the addition, subtraction, multiplication or division of these variables will always increase the variance of the combined variables. However, if the variables are not mutually independent of each other, the effect on the variance is not as clear since covariance terms need to be included in the above equations. Procedures for adding the covariance terms are included in Mood et al. (1974).

Interval analysis (Ross and Faust, 1982) is similar to sensitivity analysis except that likely ranges for the input parameters of interest are chosen and then these values are substituted into the analytical method to provide likely upper and lower bounds for the desired output parameters. For example, the upper bound could be the predicted contaminant concentration in the aquifer at a point 100 ft downgradient of an injection well using as input data a low retardation factor and minimal dispersion. The lower bound could be the predicted contaminant concentration at this same location when the highest retardation factor and dispersion are used in the calculations. When limited field data are available, this approach can provide at least an estimated range for the output parameters.

Monte Carlo analysis involves solving the ground water flow and solute transport equations using randomly chosen values as input parameters. The random values are selected from specified probability density functions (pdf) of key parameters. Typically, 50 to 300 repetitions of the calculations would be performed with different input parameters. Histograms of the predictions are generated and used to calculate the probability of specific events (e.g., number of times that concentration limits will be exceeded or time for a contaminant plume to reach a given well or surface water body.) The principal limitations of this approach are the high cost of doing a large number of calculations, difficulties in estimating the pdf for each of the parameters and the need to include the "worst cases" of interest. The computer program MACRO developed by Kaufman et al. (1980) can be used to calculate pdf's of predicted contaminant concentrations. MACRO works by systematically making repeated model runs with regularly spaced values of the sensitive parameters. This program, however, has only been used for simple cases.

### 7.6.3 Guidelines for Proceeding to More Detailed Analysis

#### 7.6.3.1 Introduction

There are typically four critical questions to be addressed in ground water contamination studies: a) where are the contaminants; b) when will they arrive at a specific location; c) what are the concentrations of the contaminants; and d) what hazards are posed by the contaminants. Answers to these questions provide a concise statement of the information needed to evaluate the environmental consequences of ground water contamination. To address these types of questions, there are three

general types of assessment tools available: site ranking methods, analytical (hand calculation) methods, and numerical models. These tools are useful for different levels of analysis and thus offer complimentary rather than competing uses. Up to this point, the chapter has addressed only the hand calculation methods. The three approaches are briefly compared below:

- Site ranking methods allow initial assessment of a large number of existing ground water contamination problems. With a minimum amount of information and technical expertise, site ranking methods can be used for evaluating the relative hazard posed by a large number of contamination sources. Because site ranking models do not provide quantitative estimates of contaminant concentrations, they will not be discussed further in this chapter. A review of selected ranking methods is included in Summers and Rupp (1982a).
- Analytical (or hand calculation) methods can predict the migration of contaminants in ground water from potential or existing waste sources. As shown in Section 7.5, these techniques are based on simplified representations of the ground water system. The techniques require limited field data and can be applied rapidly with hand calculators.
- Numerical models, like analytical methods, provide site-specific predictions by solving a series of equations. These models can provide greater temporal and spatial resolution. However, using numerical models generally requires large amounts of data and a computer.

Numerical models will be briefly discussed below. A method for determining when numerical models are appropriate is given in Section 7.6.3.3.

#### 7.6.3.2 Numerical Models

Numerical model results can help address the following questions pertinent to ground water contamination problems:

- What is the maximum areal extent of a plume at a given site?
- What is the approximate time for a plume to reach a given well or surface water body?
- What is the maximum concentration of a contaminant that could occur at a given well or in the ground water discharging into a surface water body?
- How much time would be required to flush contaminants from an aquifer?
- What control methods are technically feasible and cost-effective?
- Is it likely that a contaminant plume would form at a candidate waste disposal site?
- Where should monitoring wells be located?

Flow and solute transport models vary in type and complexity depending upon the system being modeled and the extent to which the model attempts to fully represent that system. Modeling contaminant movement in a homogeneous aquifer is significantly less complex than attempting to model movement in a heterogeneous aquifer, such as one with interbedded clay lenses.

Data requirements for ground water flow and solute transport models are given in Table VII-15. The amount of data needed increases with the number of dimensions modeled and the size of the grid system.

Along with the input data shown in Table VII-15, historical water level and ground water quality data are needed to calibrate the model. Model results are usually compared with historical data and refined accordingly--a process known as calibration or history matching. This does not assure that a model will give accurate predictions for the future when conditions may change (e.g., a confined aquifer could have been pumped enough to change it to an unconfined system).

There are many mathematical models available for predicting ground water flow and solute transport in 1, 2, or 3 dimensions. Numerical solution techniques to choose from include finite difference, finite element, integrated finite difference, and method of characteristics. Detailed reviews of numerical models can be found in the following reports: Kincaid et al. (1983), Bachmat et al. (1978), van Genuchten (1978), Oster (1982) and Thomas et al. (1982). In addition, information and copies of publicly available ground water models may be obtained through the International Ground Water Modeling Center (IGWMC) at the Holcomb Research Institute of Butler University. The IGWMC has developed a computerized data base of over 600 models called the Model Annotation Retrieval System or MARS.

#### 7.6.3.3 Model Selection

In this chapter, three different approaches to assessing ground water contamination problems have been briefly discussed, including site ranking, analytical and numerical models. However, the question of which approach to use is as of yet unanswered. Before a method is selected, an assessment should be made of the complexity of the hydrogeologic system, the type of information needed to meet the study objectives, and the present understanding of the aquifer system. Figure VII-43 shows a general sequence for determining whether a numerical model is needed and alternative approaches. Numerical models should be applied when a detailed assessment of the extent and significance of contamination is needed and when adequate funding and trained personnel are available for the required data collection and modeling effort. The steps involved in applying a model are shown in Figure VII-44. As this figure shows, data collection, interpretation and model application ideally should be an iterative process. Analytical methods should be used at each of these feedback points and to check final model results.

## DATA NEEDS FOR NUMERICAL MODELS

---

Flow Models

- areal extent of the aquifer
- grid type and spacing
- aquifer thickness, by node
- boundary conditions and locations of assigned nodes
- hydraulic conductivities (or permeabilities), by node
- specific storage or specific yield
- initial head, by node
- net recharge rate of the aquifer
- the locations and flow rates of system stresses (e.g. pumping wells)
- relationship to surface water, if present
- water level data for model calibration and verification

Solute Transport Models\*

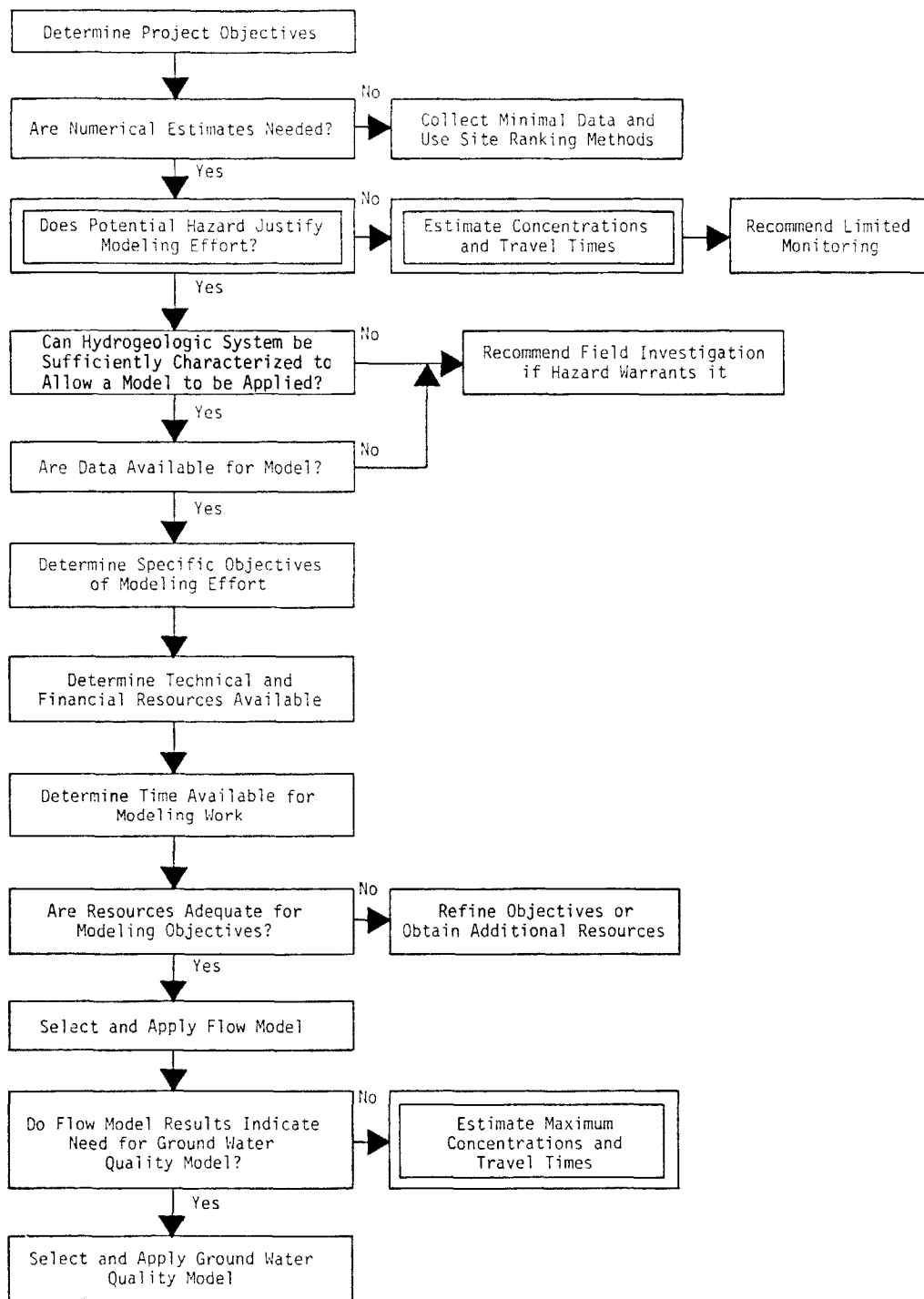
- longitudinal, transverse, and vertical dispersivity coefficients
- bulk density of permeable media
- effective porosity of the aquifer
- initial contaminant concentrations in the aquifer
- concentrations and flow rates of waste sources (these may vary by location and time)
- distribution coefficients or retardation factors for the contaminants of interest
- radioactive or biological decay constants, if appropriate
- concentration data for model calibration and verification

---

\*The flow data are also needed to run solute transport models.

---

The simplest models should be used first to determine sensitive parameters and to identify significant data gaps. Based on the predicted results of the simple models and uncertainty analyses, a decision can then be made as to whether additional data and more complex models are necessary.



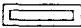
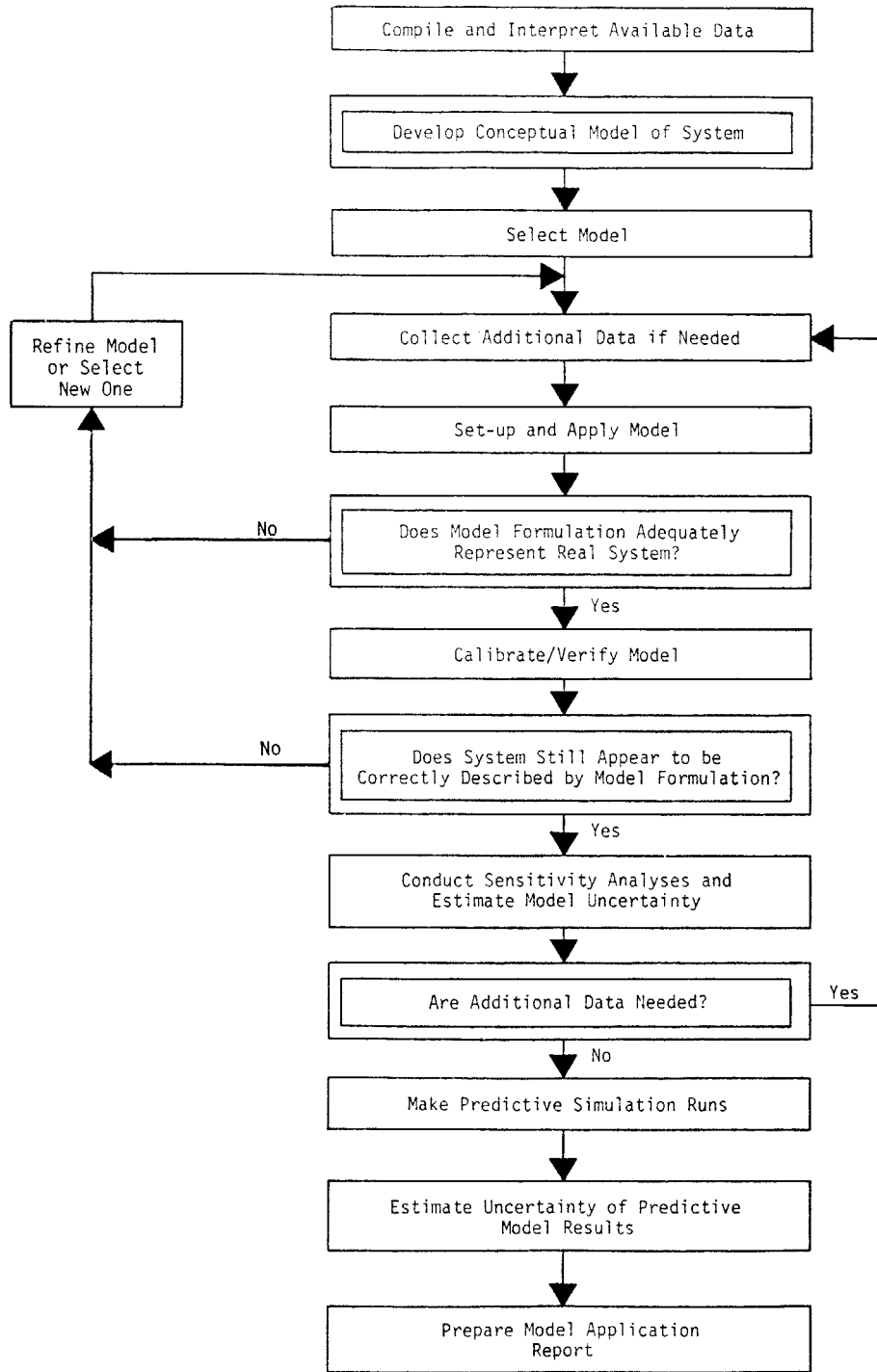
Note: Steps marked with  use analytical techniques.

FIGURE VII-43 GENERAL SEQUENCE TO DETERMINE IF A MODELING EFFORT IS NEEDED, REFERENCE: SUMMERS AND RUPP (1982B)





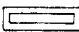
Note: Steps marked with  use analytical techniques.

FIGURE VII-44 STEPS INVOLVED IN MODEL APPLICATION,  
 REFERENCE: SUMMERS AND RUPP (1982B)

## REFERENCES

### References Cited

- Abramowitz, M. and I.A. Stegun. 1964. Handbook of Mathematical Functions with Formulas, Graphs and Mathematical Tables. Applied Mathematics Series No. 55, National Bureau of Standards, 1046 p.
- Bachmat, Y., B. Andrews, D. Holtz and S. Sebastian. 1978. Utilization of Numerical Ground Water Models for Water Resource Management. EPA-600/18-78-012, U.S. EPA, Robert S. Kerr Environmental Research Laboratory, Ada, Oklahoma.
- Basak, P. and V.V. Murty. 1979. Determination of Hydrodynamic Dispersion Coefficients Using "Inverfc". Journal of Hydrology, Volume 41, pp. 43-48.
- Baver, L.D., W.H. Gardner and W.R. Gardner. 1972. Soil Physics, Fourth Edition, John Wiley and Sons, Inc., New York, 498 p.
- Bear, Jacob. 1972. Dynamics of Fluids in Porous Media. American Elsevier Publishing Co., Inc., New York, 764 p.
- Bjerrum, L., J.K. Nash, R.M. Kennard and R.R. Gibson. 1972. Hydraulic Fracturing in Field Permeability Testing. Geotechnique, Volume 22, Number 2.
- Black, C.A. 1965. Methods of Soil Analysis: Part 1, Physical and Mineralogical Properties, Including Statistics of Measurement and Sampling. American Society of Agronomy, Madison, Wisconsin, 770 p.
- Bouwer, H. and R.D. Jackson. 1974. Determining Soil Properties. Drainage for Agriculture, edited by J. van Schilfgaarde. American Society of Agronomy, Madison, Wis., pp. 611-672.
- Bowman, B.T. and W.W. Saris. 1983. Determination of Octanol-Water Partitioning Coefficients of 61 Organophosphorous and Carbonate Insecticides and their Relationship to Respective Water Volubility Values. Journal of Environmental Science and Health, Volume B18, Number 6, pp. 667-683.
- Brady, N.C. 1974. The Nature and Properties of Soils, 8th Edition. MacMillan Publishing Co., Inc., New York, 639 p.
- Braester, C. 1972. Vertical Infiltration at Constant Flux at the Soil Surface. Second Annual Report (Part 1), in: Development of Methods, Tools, and Solutions for Unsaturated Flow with Application to Watershed Hydrology and Other Fields. Technion-Israel Institute of Technology, 48 p.
- Brown, R.H., A.A. Konoplyantsev, J. Ineson and U.S. Kovalovsky. 1972. Ground Water Studies: An International Guide for Research and Practice, Studies and Reports in Hydrology, UNESCO, Volume 7, Number 10, pp. 1-18.
- Campbell, G.S., W.D. Zollinger and S.A. Taylor. 1966. Sample Changer for Thermocouple Psychrometer: Construction and some Applications. Journal of Agronomy, Volume 58, pp. 315-318.
- Cochran, W.G. 1977. Sampling Techniques. John Wiley and Sons, Inc., New York, 413 p.
- Code of Federal Regulations. 1982. Part 141.11-141.16 and Part 143.3. Published by the Office of the Federal Register, U.S. Government Printing Office, Washington, D.C.
- Code of Federal Regulations. 1983. Volume 48, No. 194. Published by the Office of the Federal Register, U.S. Government Printing Office, Washington, D.C.

- Crank, J. 1975. The Mathematics of Diffusion, Second Edition, Clarendon Press, Oxford, 414 p.
- Davis, J.C. 1973. Statistics and Data Analysis in Geology. John Wiley and Sons, New York, 550 p.
- Davis, S.N. and R.J. DeWiest. 1966. Hydrogeology. John Wiley and Sons, Inc., New York, 463 p.
- Davis, S.N. 1969. Porosity and Permeability of Natural Materials. Flow Through Porous Media, ed. R.J.M. DeWiest. Academic Press, New York, pp. 54-89.
- DeWiest, R.M. 1965. Geohydrology. John Wiley and Sons, Inc., New York, 366 p.
- Drost, W., D. Klotz, A. Koch, H. Moser, F. Neumaier and W. Rauert. 1968. Point Dilution Methods of Investigating Ground Water Flow by Means of Radioisotopes. Water Resources Research, Volume 4, pp. 125-146.
- Duursma, E.K. 1966. Molecular Diffusion of Radioisotopes in Interstitial Water of Sediments. International Atomic Energy Agency, Vienna", IAEA SM-72/20.
- Eakin, T.E., D. Price, and J.R. Harrill. 1976. Summary Appraisals of the Nation's Ground Water Resources-Great Basin Region. U.S. Geological Survey Professional Paper 813-G, 37 p.
- Elprince, A.M. and P.R. Day. 1977. Fitting Solute Breakthrough Equations to Data Using Two Adjustable Parameters. Soil Science Society of America Journal, Volume 41, Number 1, pp. 39-41.
- Ferguson, H. and W. Gardner. 1962. Water Content Measurement in Soil Columns by Gamma Ray Absorption. Soil Science Society of America Proceedings, Volume 26, pp. 11-18.
- Fetter, C.W., Jr. 1980. Applied Hydrogeology. Charles E. Merrill Publishing Co., Columbus, Ohio, 488 p.
- Fetter, C.W., Jr. 1981. Determination of the Direction of Ground Water Flow. Ground Water Monitoring Review, Volume 1, Number 3, pp. 28-31.
- Fox, W.E. and D.S. Page-Hanify. 1959. A Method of Determining Bulk Density of Soil. Soil Science, Volume 88, Number 3, pp. 168-171.
- Fox, W.E. 1959. An Instrument for the Determination of Soil Volume. Soil Science, Volume 88, pp. 349-352.
- Freeze, R.A. and J.A. Cherry. 1979. Ground Water. Prentice-Hall, Inc., Englewood Cliffs, N.J., 604 p.
- Fried, J.J. 1975. Groundwater Pollution. Elsevier Scientific Publishing Company, New York, 330 p.
- Gardner, W. and D. Kirkham. 1952. Determination of Soil Moisture by Neutron Scattering. Soil Science, Volume 73, pp. 391-401.
- Gaspar, E. and M. Oncescu. 1972. Radioactive Tracers in Hydrology. American Elsevier, New York, 90 p.
- Gelhar, L.W. and C.J. Axness. 1981. Stochastic Analysis of Macro-Dispersion in Three-Dimensionally Heterogeneous Aquifers. Report No. H-8, Hydraulic Research Program. New Mexico Institute of Mining and Technology, Socorro, New Mexico, 140 p.

- Gelhar, L.W. and C.L. Axness. 1983. Three-Dimensional Stochastic Analysis of Microdispersion. *Water Resources Research*, Volume 19, Number 1, pp. 161-180.
- Gelhar, L.W., A. Mantoglou, C. Welty and K.R. Rehfeldt. 1985. A Review of Field Scale Subsurface Solute Transport Processes Under Saturated and Unsaturated Conditions. Electric Power Research Institute, Palo Alto, California. (In Press.). 107 p.
- Gibson, R.E. 1966. A Note on the Constant Head Test to Measure Soil Permeability In-situ. *Geotechnique*, Volume 16, Number 3.
- Gill, H.E. and J. Vecchioli. 1965. Availability of Ground Water in Morris County, New Jersey, U.S. Geological Survey Special Report 25.
- Gillham, R.W., E.A. Sudicky, J.A. Cherry and E.O. Frind. 1984. An Advection-Diffusion Concept for Solute Transport in Heterogeneous Unconsolidated Geological Deposits. *Water Resources Research*, Volume 20, Number 3, pp. 369-378.
- Golder, H.O. and A.A. Gass. 1963. Field Tests for Determining Permeability of Soil Strata. A.S.T.M. Special Publication 322 (Field Testing of Soils).
- Grisak, G.E., W.F. Merritt and D.W. Williams. 1977. A Fluoride Borehole Dilution Apparatus for Ground Water Velocity Measurements. *Canadian Geotechnique Journal*, Volume 14, pp. 554-561.
- Gurr, C.G. 1962. Use of Gamma Rays in Measuring Water Content and Permeability in Unsaturated Columns of Soil. *Soil Science*, Volume 94, pp. 224-229.
- Guyed, H. 1966. Interpretation of Electric and Gamma Ray Logs in Water Wells. *Well Log Analyst*, January-March.
- Halevy, E., H. Moser, O. Zellhofer and A. Zuber. 1967. Borehole Dilution Techniques: A Critical Review. *Isotopes in Hydrology*. IAEA, Vienna, pp. 531-564.
- Hall, H.N. 1953. Compressibility of Reservoir Rocks. *Transactions AIME*, Volume 198, pp. 309-316.
- Hanson, R.L. 1973. Evaluating the Reliability of Specific Yield Determinations. *Journal of Research of the U.S. Geological Survey*, Volume 1, Number 3, pp. 371-376.
- Hantush, M.S. 1956. Analysis of Data from Pumping Tests in Leaky Aquifers. *Transactions of the American Geophysical Union*, Volume 37, Number 6, pp. 702-714.
- Harleman, D.R., P.F. Mehlhorn and R.R. Rumer. 1963. Dispersion-Permeability Correlation in Porous Media. *Journal of Hydraulics Division of the American Society of Civil Engineering*, Number HY2, Volume 89, pp. 67-85.
- Hillel, D. 1971. *Soil and Water*, Academic Press, New York, 288 p.
- Hoopes, J.A. and D.R.F. Harleman. 1965. Waste Water Recharge and Dispersion in Porous Media, Technical Report Number 75, Hydrodynamic Lab., Massachusetts Institute of Technology, Cambridge, Mass.
- Hoopes, J.A. and D.R.F. Harleman. 1967. Dispersion in Radial Flow from a Recharge Well, *Journal of Geophysical Research*, Volume 72, Number 14, pp. 3595-3607.
- Hough, B.K. 1957. *Basic Soils Engineering*. Ronald Press, New York, 513 p.
- Hvorslev, M.J. 1951. Time Lag and Soil Permeability in Ground Water Observations. *Bulletin Number 36*, U.S. Waterways Experimental Station, Vicksburg.

- Johnson, A. I., R. C. Prill and D. A. Morris. 1963. Specific Yield: Column Drainage and Centrifuge Moisture Content. U.S. Geological Survey Water-Supply Paper 1662-A, 69 p.
- Johnson, A. I. 1967. Specific Yield-Compilation of Specific Yields for Various Materials. U.S. Geological Survey Water-Supply Paper 1662-D, 74 p.
- Jones, O. R. and A. D. Schneider. 1969. Determining Specific Yield of the Ogallala Aquifer by the Neutron Method. Water Resources Research, Volume 5, Number 6, pp. 1267-1272.
- Jumikis, A. R. 1962. Soil Mechanics, D. Van Nostrand Company, Inc., Princeton, N. J.
- Kaufman, A. M., L. L. Edwards and W. J. O'Connell. 1980. A Repository Post-Sealing Risk Analysis using MACRO, in Waste Management '80, Edited by R. G. Post, Arizona Board of Regents, Tucson, pp. 109-123.
- Kemper, W. D. 1959. Estimation of Osmotic Stress in Soil Water from the Electrical Resistance of Finely Porous Ceramic Units. Soil Science, Volume 87, pp. 345-349.
- Kerfoot, W. B. 1982. Comparison of 2-D and 3-D Ground Water Flow Meter Probes in Fully Penetrating Monitoring Wells. Proceedings of the Second National Symposium on Aquifer Restoration and Ground Water Monitoring, May 26-28, 1982, Columbus, Ohio, pp. 264-268.
- Kincaid, C. T., J. T. Morrey, and C. J. Hostetler. 1983. Geohydrochemical Models for Solute Migration. Vol. I EA-3417. Electric Power Research Institute, Palo Alto, CA.
- Kirkham, D. 1964. Soil Physics. Handbook of Applied Hydrology, edited by V. T. Chow. McGraw-Hill, New York, pp. 5.1-5.26.
- Klock, G. O., L. Boersma and L. W. DeBacker. 1969. Pore Size Distributions as Measured by the Mercury Intrusion Method and their Use in Predicting Permeability. Soil Science Society of America Proceedings, Volume 33, Number 1, pp. 12-15.
- Klotz, D., H. Moser and P. Trimborn. 1978. Single-Borehole Techniques: Present Status and Examples of Recent Applications in Isotope Hydrology. Volume 1, International Atomic Energy Agency, pp. 159-179.
- Klute, A. 1965. Laboratory Measurements of Hydraulic Conductivity of Unsaturated Soil. Methods of Soil Analysis, Part I, edited by C. A. Black. American Society of Agronomy, Madison, Wis., pp. 253-261.
- Klute, A. 1972. The Determination of Hydraulic Conductivity and Diffusivity of Unsaturated Soils. Science, Volume 113, Number 4, pp. 264-276.
- Knutson, G. 1966. Tracers for Ground Water Investigations. Ground Water Problems (Proceedings of the International Symposium, Stockholm, Sweden). Pergamon Press, Oxford.
- Krumbein, W. C. and G. D. Monk. 1943. Permeability as a Function of the Size Parameters of Unconsolidated Sand. Transactions of the American Institute of Mineralogy and Meteorology Engineers, Volume 151, pp. 153-163.
- Kruseman, G. P. and N. A. deRidder. 1970. Analysis and Evaluation of Pumping Test Data. International Institute for Land Reclamation and Improvement, Bulletin 11, Wageningen, The Netherlands.
- Lacroix, Y. 1960. Notes on the Determination of Coefficients of Permeability in the Laboratory In-situ. Polytechnic School, Zurich (unpublished).

- Lallemant-Barres, A. and P. Peaudecerf. 1978. Recherche des Relations Entre La Valeur de la Dispersivite Macroscopique D'un Milieu Aquifere, Ses Autres Caracteristiques et Les Conditions de Mesure. Bulletin de Recherches Geologiques et Minières, 2e Serie, Section III, Number 4, Orleans, France.
- Lambe, T.W. 1951. Soil Testing for Engineers. John Wiley and Sons, N.Y., 165 p.
- Lee, D.R. and J.A. Cherry. 1978. A Field Exercise on Ground Water Flow Using Seepage Meters and Mini-Piezometers. Journal of Geology Education, Volume 27, pp. 6-10.
- Liakopoulos, A.C. 1965. Variation of the Permeability Tensor Ellipsoid in Homogeneous Anisotropic Soils. Water Resources Research, Volume 1, Number 1, pp. 135-141.
- Lehman, S.W. 1972. Ground Water Hydraulics, U.S.G.S. Professional Paper Number 708, 70 p.
- Londe, P. 1973. Water Seepage in Rock Slopes. Quarterly Journal of Engineering Geology, Volume 6, Number 1.
- Loudon, A.G., 1952. The Computation of Permeability from Simple Soil Tests. Geotechnique, Volume 3, Number 4.
- Milligan, V. 1976. Field Measurement of Permeability in Soil And Rock. Proceedings of the Conference on In-Situ Measurements of Soil Properties, Volume II, June 1-4, 1975. American Society of Civil Engineers, pp. 3-37.
- Mills, W.B., V. Kwong, L. Mok, and M.D. Unga. 1985. Microcomputer Methods for Toxicants in Ground Waters and Rivers. Presented at National Conference on Environmental Engineering, Boston, Mass.
- Moench, A.F. and A. Ogata. 1981. A Numerical Inversion of the Laplace Transform Solution to Radial Dispersion in a Porous Medium, Water Resources Research, Volume 17, Number 1, pp. 250-252.
- Molz, F.J., O. Guven and J.G. Melville. 1983. An Examination of Scale-Dependent Dispersion Coefficients. Ground Water, Volume 21, Number 6, pp. 715-725.
- Mood, A.M., F.A. Graybill and D.C. Bees. 1974. Introduction to the Theory of Statistics, Third Edition, McGraw-Hill, Inc., New York. 564 p.
- Morris, D.A. and A.I. Johnson. 1967. Summary of Hydrologic and Physical Properties of Rock and Soil Materials, as Analyzed by the Hydrologic Laboratory of the U.S. Geological Survey. 1948-1960, U.S. Geological Survey Water-Supply Paper 1839-D, 42 p.
- Mualem, Y. 1976. A New Model for Predicting the Hydraulic Conductivity of Unsaturated Porous Media. Water Resources Research, Volume 12, Number 3, pp. 513-522.
- Nelson, J.D. and R.C. Ward. 1981. Statistical Considerations and Sampling Techniques for Ground Water Monitoring. Ground Water, Volume 19, Number 6, pp. 617-625.
- Nofziger, D.L. 1978. Errors in Gamma-Ray Measurements of Water Content and Bulk Density in Nonuniform Soils. Soil Science Society of America Proceedings, Volume 42, pp. 845-850.
- Nye, P.H. and P.B. Tinker. 1977. Solute Movement in the Soil-Root System. University of California Press, Berkeley, 342 p.
- Ogata, A. and R.B. Banks. 1961. A Solution of the Differential Equation of Longitudinal Dispersion in Porous Media. U.S. Geological Survey, Professional Paper 411-A. 7 p.
- Ogata, A. 1970. Theory of Dispersion in a Granular Medium. U.S. Geological Survey, Professional Paper 411-1. 134 p.

- Olea, R.A. 1975. Optimum Mapping Techniques Using Regionalized Variable Theory. Number Two Series on Spatial Analysis, Kansas Geological Survey, Lawrence, Kansas, 137 p.
- Oster, C.A. 1982. Review of Ground Water Flow and Transport Models in the Unsaturated Zone. PNL-4427, NUREG/CR-2917, U.S. Nuclear Regulatory Commission, Washington, D.C.
- Pettyjohn, W.A., J.R.L. Studlick, R.C. Bain and J.H. Lehr. 1979. A Ground Water Quality Atlas of the United States. National Demonstration Project, 272 p.
- Phillips, K.J. and L.W. Gelhar. 1978. Contaminant Transport to Deep Wells, Journal of the Hydraulics Division, ASCE, Volume 104, Number HY6, pp. 807-819.
- Pickens, J.F. and G.E. Grisak. 1981a. Scale-Dependent Dispersion in a Stratified Granular Aquifer. Water Resources Research, Volume 17, Number 4, pp. 1191-1211.
- Pickens, J.F. and G.E. Grisak. 1981b. Modeling of Scale-Dependent Dispersion in Hydrogeologic Systems. Water Resources Research, Volume 17, Number 6, pp. 1701-1711.
- Piersol, R.J., L.E. Workman and M.C. Watson. 1940. Porosity, Total Liquid Saturation, and Permeability of Illinois Oil Sands. Illinois Geological Survey Report Investigation 67.
- Pinder, G.F. and W.G. Gray. 1977. Finite Element Simulation in Surface and Subsurface Hydrology. Academic Press, New York, 295 p.
- Rai, D. and J.M. Zachara. 1984. Chemical Attenuation Rates, Coefficients and Constants in Leachate Migration, Volume 1: A Critical Review. Electric Power Research Institute, Report EPRI EA-3356, Volume I, Palo Alto, California, 336 p.
- Raimondi, P.G., H.G. Gradner and C.G. Petrick. 1959. Effect of Pore Structure and Molecular Diffusion on the Mixing of Miscible Liquids Flowing in Porous Media. Paper presented at the American Institute of Chemical Engineers and Society of Petroleum Engineers Joint Symposium on Oil Recovery Methods, San Francisco, Preprint 43.
- Rawls, W.J. and L.E. Asmussen. 1973. Neutron Probe Field Calibration for Soils in the Georgia Coastal Plain. Soil Science, Volume 110, pp. 262-265.
- Reynolds, S.G. 1970a. The Gravimetric Method of Soil Moisture Determination, I, A Study of Equipment and Methodological Problems. Journal of Hydrology, Volume 11, pp. 258-273.
- Reynolds, S.G. 1970b. The Gravimetric Method of Soil Moisture Determination, III, An Examination of Factors Influencing Soil Moisture Variability. Journal of Hydrology, Volume 11, pp. 288-300.
- Rice, R. 1969. A Fast-Response, Field Tensiometer System. Transactions of the American Society of Agricultural Engineering, Volume 12, pp. 48-50.
- Richards, L.A. and G. Ogata. 1961. Psychometric Measurements of Soil Samples Equilibrated on Pressure Membranes. Soil Science Society of America Proceedings, Volume 25, pp. 456-459.
- Richards, L.A. 1965. Physical Condition of Water in Soil. Methods of Soil Analysis, Part 1, Edited by C.A. Black. American Society of Agronomy, Madison, Wis., pp. 128-152.
- Richards, S.J. 1965. Soil Suction Measurements with Tensiometers in Methods of Soil Analysis. Agronomy, Volume 9, pp. 153-163.

- Robinson, V.K. 1974. Low Cost Geophysical Well Logs for Hydrogeological Investigations. Quarterly Journal of Engineering Geology, Volume 7, Number 2.
- Ross, B. and C.R. Faust. 1982. Analysis of Uncertainty in Contaminant Migration Prediction. Report prepared by GeoTrans, Inc., for the U.S. EPA, 33 p.
- Rowe, P.W. 1972. The Relevance of Soil Fabric to Site Investigation Practice. Twelfth Rankine Lecture, Geotechnique, Volume 22, Number 2.
- Sampson, R.J. 1978. SURFACE II Graphics System (revised). Number One Series on Spatial Analysis, Kansas Geological Survey, Lawrence, Kansas, 240 p.
- Scalf, M.R., J.F. McNabb, W.J. Dunlap, R.L. Cosby and J. Fryberger. 1981. Manual of Ground Water Sampling Procedures. U.S. EPA Robert S. Kerr Laboratory and National Water Well Association. 93 p.
- Scheidegger, A.E. 1961. General Theory of Dispersion in Porous Media. Journal of Geophysical Research, Volume 66, Number 10, pp. 3273-3278.
- Schmugge, T.J., T.J. Jackson and H.L. McKin. 1980. Survey of Methods for Soil Moisture Determination. Water Resources Research, Volume 16, Number 6, pp. 961-979.
- Science Applications, Inc. 1982. Planning Workshop on Solute Migration from Utility Solid Wastes. Electric Power Research Institute, Palo Alto, California, Report No. EA-2415, 126 p.
- Selig, E.T., D.C. Wobschall, S. Mansukhani and A. Motiwala. 1975. Capacitance Sensor for Soil Moisture Measurement, Record 532, Transaction of the Reserve Board, Washington, D.C., p. 64.
- Sharp, J.C. 1970. Fluid Flow Through Fissured Media. Ph. D. Thesis, University of London.
- Sherard, J.L., R.J. Woodward, S.F. Gizienski and W.A. Clevenger. 1963. Earth and Earth-Rock Dams. John Wiley and Sons, New York.
- Simmons, C.S. and G.W. Gee. 1981. Simulation of Water Flow and Retention in Earthen Cover Materials Overlying Uranium Mill Tailings. Report Number PNL-3877, Pacific Northwest Laboratory (Battelle), Richland, Washington, 78 p.
- Smith, L. and F.W. Schwartz. 1980. Mass Transport: Part 1, A Stochastic Analysis of Macroscopic Dispersion. Water Resources Research, Volume 16, Number 2, pp. 303-313.
- Stallman, R.W. 1971. Aquifer-Test Design, Observation and Data Analysis. Techniques of Water Resources Investigations of the U.S. Geological Survey, Chapter B1. Government Printing Office, Washington, D.C.
- Sudicky, E.A. 1983. An Advection-Diffusion Theory of Contaminant Transport for Stratified Porous Media. Ph.D. Thesis, University of Waterloo, Waterloo, Ontario, Canada, 203 p.
- Sudicky, E.A., J.A. Cherry and E.O. Frind. 1983. Migration of Contaminants in Groundwater at a Landfill: A Case Study, Part 4. A Natural-Gradient Dispersion Test. Journal of Hydrology, Volume 63, pp. 81-108.
- Summers, K., S. Gherini and C. Chen. 1980. Methodology to Evaluate the Potential for Ground Water Contamination from Geothermal Fluid Releases. EPA Report Number EPA-600/7-80-117, 168 p.
- Summers, K. and G. Rupp. 1982a. Assessment Methods for Predicting Existence and Transport of Ground Water Contamination. Tetra Tech Report. 47 p.



- Summers, K. and G. Rupp. 1982b. Selection and Use of Assessment Methods for Ground Water Contamination. Paper in State, County, Regional and Municipal Jurisdiction of Ground Water Protection: Proceedings of the Sixth National Ground Water Quality Symposium, September 22-24, 1982, Atlanta, GA. p. 209-218.
- Tang, D.H. and D.K. Babu. 1979. Analytical Solution of a Velocity Dependent Dispersion Problem, Water Resources Research, Volume 15, Number 6, pp. 1471-1478.
- Taylor, S.A. and G.L. Ashcroft. 1972. Physical Edaphology, W.H. Freeman and Company, San Francisco, 533 p.
- Terzaghi, K. 1960. Storage Dam Founded on Landslide Debris. Journal of the Boston Society of Civil Engineering. January.
- Tetra Tech. 1977. Stream-Aquifer Model of Carlls River Basin Long Island, New York. 85 p.
- Tetra Tech. 1984a. Ground Water Data Analyses at Utility Waste Disposal Sites. EPRI Research Project RP2283-2. Electric Power Research Institute, Palo Alto, California.
- Tetra Tech. 1984b. Proceedings of First SWES Technology Transfer Seminar on Solute Migration in Ground Water at Utility Waste Disposal Sites. Project Manager-Ishwar P. Muraka. Electric Power Research Institute, Palo Alto, California.
- Thomas, H.E. 1951. Ground Water Regions of the United States.
- Thomas, A. 1963. In-Situ Measurement of Moisture in Soil and Similar Substance by Fringe Capacitance. Journal of Scientific Instrumentation, Volume 43, p. 996.
- Thomas, S.D., B. Ross and J.W. Mercer. 1982. A Summary of Repository Siting Models. NUREG/CR-2782, U.S. Nuclear Regulatory Commission, Washington, D.C.
- Todd, D.K. 1959. Ground Water Hydrology. John Wiley and Sons, Inc., New York, 336 p.
- Todd, D.K. 1980. Ground Water Hydrology, Second Edition. John Wiley and Sons, New York, 535 p.
- Todorovic, P. 1975. A Stochastic Model of Dispersion in a Porous Medium. Water Resources Research, Volume 11, Number 2, pp. 348-354.
- (USBR) United States Department of Interior, Bureau of Reclamation. 1968. Earth Manual, Denver, Colorado.
- U.S. Environmental Protection Agency. 1977a. National Interim Primary Drinking Water Regulations. U.S. Government Printing Office, Washington, D.C.
- U.S. Environmental Protection Agency. 1977b. National Secondary Drinking Water Regulations - Proposed Rules. Federal Register, Volume 42, Number 62.
- U.S. Environmental Protection Agency. 1979a. Draft Report to Congress: Water Supply-Wastewater Treatment Coordination Study. EPA Contract No. 68-01-5033. 375 p.
- U.S. Environmental Protection Agency. 1979b. Handbook for Analytical Quality Control in Water and Wastewater Laboratories, U.S. EPA EMSL Cincinnati, Ohio. EPA Report No. EPA-600/4-79-019.
- U.S. Environmental Protection Agency. 1980. Procedures Manual for Ground Water Monitoring at Solid Waste Disposal Facilities. Report No. SW-611. 2nd Edition. 269 p.
- U.S. Environmental Protection Agency. 1984. Ground Water Protection Strategy. Washington, D.C.

- Vachaud, G., J.M. Royer and J.D. Cooper. 1977. Comparison of Methods of Calibration of a Neutron Probe by Gravimetry on Neutron-Capture Model. Journal of Hydrology, Volume 34, pp. 343-356.
- van Bavel, C.H.M. 1961. Calibration and Characteristics of Two Neutron Moisture Probes. Soil Science Society of America Proceedings, Volume 25, pp. 329-334.
- van Bavel, C.H.M. 1962. Accuracy and Source Strength in Soil Moisture Neutron Probes. Soil Science Society of America Proceedings, Volume 26, p. 405.
- van Everdingen, R.O. 1963. Groundwater Flow-Diagrams in Sections with Exaggerated Vertical Scale. Geological Survey of Canada Paper 63-27, 21 p.
- van Genuchten, M.Th. 1978. Proceedings of the Fourth Annual Hazardous Waste Management Symposium, Southwest Research Institute and U.S. EPA, San Antonio, Texas, March 6-8, 1978.
- van Genuchten, M.Th. 1980. A Closed-Form Equation for Predicting the Hydraulic Conductivity of Unsaturated Soils. Soil Science Society of America Proceedings, Volume 44, pp. 892-898.
- van Genuchten, M.T. and W.J. Alves. 1982. Analytical Solutions of the One-Dimensional Convective-Dispersive Solute Transport Equation. USDA Agricultural Research Service, Technical Bulletin, Number 1661, 149 p.
- Walker, F.C. 1955. Experience in the Evaluation and Treatment of Seepage from Operating Reservoirs. Fifth International Congress on Large Dams, Paris.
- Walton, W.C. 1970. Groundwater Resource Evaluation. McGraw-Hill Book Co., New York, 664 p.
- Weast, R.C. 1969. Handbook of Chemistry and Physics, 50th Edition. The Chemical Rubber Co., Cleveland, Ohio, 2356 p.
- Weeks, E.P. 1969. Determining the Ratio of Horizontal to Vertical Permeability by Aquifer Test Analysis. Water Resources Research, Volume 5, pp. 196-214.
- Whitaker, S. 1967. Diffusion and Dispersion in Porous Media. Journal of the American Institute of Chemical Engineering, Volume 13, Number 3, pp. 420-427.
- Wilkes, P.F. 1974. Permeability Tests in Alluvial Deposits and the Determination of  $K_0$ . Geotechnique, Volume 24, Number 1.
- Williams, T.H.L. 1978. An Automatic Scanning and Recording Tensiometer System. Journal of Hydrology, Volume 39, pp. 175-183.
- Wilson, J.T. and J.F. McNabb. 1981. Biodegradation of Contaminants in the Subsurface. First International Conference on Ground Water Quality Research, October 7-10, 1981, Houston, Texas.
- Wilson, J.L. and P.J. Miller. 1978. Two-Dimensional Plume in Uniform Ground-Water Flow. Journal of the Hydraulic Division, ASCE, Volume 104, Number 4, pp. 503-514.
- Wilson, L.G. 1981. Monitoring in the Vadose Zone, Part 1: Storage Changes. Ground Water Monitoring Review, Volume 1, Number 3, pp. 32-41.
- Wood, P.R., R.F. Lang, I.L. Payan and J. DeMarco. 1981. Anaerobic Transformation, Transport and Removal of Volatile Chlorinated Organics in Ground Water. First International Conference on Ground Water Quality Research, October 7-10, 1981, Houston, Texas.

Yeh, G. 1981. AT123D: Analytical Transient One, Two and Three-Dimensional Simulation of Waste Transport in the Aquifer System. Oak Ridge National Laboratory, ORNL-5602; Publication Number 1439, Environmental Sciences Division, Oak Ridge, Tennessee, 79 p.

Zalkin, F., M. Wilkerson and R.J. Oshima. 1984. Pesticide Movement to Groundwater, Volume II: Pesticide Contamination in the Soil Profile at DBCP, EDB, Simazine and Carbofuran Application Sites. Environmental Hazards Assessment Program, California Department of Food and Agriculture, Sacramento, California, 168 p.

#### Additional References on Ground Water Sampling

Barcelona, M.J., J.A. Helfrich, E.E. Garske, and J.P. Gibb. A Laboratory Evaluation of Ground Water Sampling Mechanisms. Ground Water Monitoring Review. 4: 32-41.

Barcelona, M.J., J.P. Gibb, and R.A. Miller. 1983. A Guide to the Selection of Materials for Monitoring Well Construction and Ground Water Sampling. Illinois State Water Survey Contract. Report 327:78.

Claassen, H.C. 1982. Guidelines and Techniques for Obtaining Water Samples that Accurately Represent the Water Chemistry of an Aquifer. U.S. Geological Survey. Open-File Report 82-1 024, 49 p.

Ford, P.J., P.J. Turina, D.E. Seely. 1983. Characterization of Hazardous Waste Sites--A Methods Manual Vol II Available Sampling Methods. EPA Report No. EPA-600/4-83-040. 215 p.

Gibb, J.P., R.M. Schuller, and R.A. Griffin. 1981. Procedures for the Collection of Representative Water Quality Data from Monitoring Wells. Illinois State Water Survey and Geological Survey. 70 p.

Gillham, R.W., M.J.L. Robin, J.F. Barker, and J.A. Cherry. 1983. Groundwater Monitoring and Sampling Bias. Department of Earth Sciences, University of Waterloo, Ontario. Prepared for American Petroleum Institute. 206 p.

Keely, J.F. 1982. Chemical Time-Series Sampling. Ground Water Monitoring Review. 2: 29-38.

Phillip, J.R. 1957. Evaporation and Moisture and Heat Fields in the Soil. J. Meteorology. Vol. 14, No. 4.

Stolzenburg, T.R., D.G. Nichols, and I. Murarka. 1984. Evaluation of Chemical Changes in Ground Water Samples due to Sampling Mechanism. Electric Power Research Institute, Palo Alto, CA (In Press).

U.S. Environmental Protection Agency. 1983. Ground Water Monitoring Guidance to Owners and Operators of Interim Status Facilities. (Draft). USEPA SW-963.

U.S. Geological Survey. 1980. Ground Water. National Handbook of Recommended Methods for Water Data Acquisition. Chapter 2. Reston, VA.

Appendix A, Monthly Distributor of Rainfall Erosivity Factor R, which appears in the first two editions of this manual, is now out of date and has been deleted.

Appendix B, Methods for Predicting Soil Erodibility Index K, which appears in the first two editions of this manual, is now out of date and has been deleted.

Appendix C, Stream and River Data, which appears in the first two editions of this manual, is now out of date and has been deleted.

## APPENDIX D

### IMPOUNDMENT THERMAL PROFILES

Thermal profile plots are provided (on microfiche in the enclosed envelope for EPA-published manual, or as Part 3, EPA-600/6-82-004c for paper copies purchased from the National Technical Information Service) for a variety of impoundment sizes and geographic locations throughout the United States. The locations are arranged in alphabetical order. Within each location set, the plots are ordered by depth and hydraulic residence time. An index to the plots is provided below, and the modeling approach is described in Appendix F.

	Page
Atlanta, Georgia	
20-ft Initial Maximum Depth . . . . .	D-4
40-ft Initial Maximum Depth . . . . .	D-14
75-ft Initial Maximum Depth . . . . .	D-24
100-ft Initial Maximum Depth . . . . .	D-34
200-ft Initial Maximum Depth . . . . .	D-44
Billings, Montana	
20-ft Initial Maximum Depth . . . . .	D-54
40-ft Initial Maximum Depth . . . . .	D-64
75-ft Initial Maximum Depth . . . . .	D-74
100-ft Initial Maximum Depth . . . . .	D-84
200-ft Initial Maximum Depth . . . . .	D-94
Burlington, Vermont	
20-ft Initial Maximum Depth . . . . .	D-104
40-ft Initial Maximum Depth . . . . .	D-114
75-ft Initial Maximum Depth . . . . .	D-124
100-ft Initial Maximum Depth . . . . .	D-134
200-ft Initial Maximum Depth . . . . .	D-144
Flagstaff, Arizona	
20-ft Initial Maximum Depth . . . . .	D-154
40-ft Initial Maximum Depth . . . . .	D-164
75-ft Initial Maximum Depth . . . . .	D-174
100-ft Initial Maximum Depth . . . . .	D-184
200-ft Initial Maximum Depth . . . . .	D-194

Fresno, California

20-ft Initial Maximum Depth . . . . .	D-204
40-ft Initial Maximum Depth . . . . .	D-214
75-ft Initial Maximum Depth . . . . .	D-224
100-ft Initial Maximum Depth . . . . .	D-234
200-ft Initial Maximum Depth . . . . .	D-244

Minneapolis, Minnesota

20-ft Initial Maximum Depth . . . . .	D-254
40-ft Initial Maximum Depth . . . . .	D-264
75-ft Initial Maximum Depth . . . . .	D-274
100-ft Initial Maximum Depth . . . . .	D-284
200-ft Initial Maximum Depth . . . . .	D-294

Salt Lake City, Utah

20-ft Initial Maximum Depth . . . . .	D-304
40-ft Initial Maximum Depth . . . . .	D-314
75-ft Initial Maximum Depth . . . . .	D-324
100-ft Initial Maximum Depth . . . . .	D-334
200-ft Initial Maximum Depth . . . . .	D-344

San Antonio, Texas

20-ft Initial Maximum Depth . . . . .	D-354
40-ft Initial Maximum Depth . . . . .	D-364
75-ft Initial Maximum Depth . . . . .	D-374
100-ft Initial Maximum Depth . . . . .	D-384
200-ft Initial Maximum Depth . . . . .	D-394

Washington, D.C.

20-ft Initial Maximum Depth . . . . .	D-404
40-ft Initial Maximum Depth . . . . .	D-414
75-ft Initial Maximum Depth . . . . .	D-424
100-ft Initial Maximum Depth . . . . .	D-434
200-ft Initial Maximum Depth . . . . .	D-444

Wichita, Kansas

20-ft Initial Maximum Depth . . . . .	D-454
40-ft Initial Maximum Depth . . . . .	D-464
75-ft Initial Maximum Depth . . . . .	D-474
100-ft Initial Maximum Depth . . . . .	D-484
200-ft Initial Maximum Depth . . . . .	D-494



## APPENDIX E

### MODELING THERMAL STRATIFICATION IN IMPOUNDMENTS

Figure E-1 Comparison of Computed and Observed Temperature Profiles in Kezar Lake

Figure E-2 Comparison of Computed and Observed Temperature Profiles in El Capitan Reservoir

Figure E-3 Log of Eddy Conductivity Versus Log Stability--Hungry Horse Data

## E.1 IMPOUNDMENT THERMAL PROFILE MODEL: BACKGROUND

The model used for computation of impoundment temperature profiles is based on the Lake Ecologic Model originally developed by Chen and Orlob (1975). The model was modified for this application to compute temperature alone. The purpose of the model application was to simulate the effects of mixing, impoundment physical characteristics, hydraulic residence time, and climate on the vertical profiles of temperature.

### Physical Representation

Each configuration simulated was idealized as a number of horizontally mixed layers. Natural vertical mixing is computed by the use of dispersion coefficients in the vertical mass transport equation. Values of the dispersion coefficients for different size lakes were estimated from previous studies (Water Resources Engineers, Inc., 1969).

### Temperature

Temperatures were computed as a function of depth according to Equation (E-1):

$$\bar{v} \frac{\partial T}{\partial t} = \frac{1}{c\rho} \frac{\partial}{\partial z} (A_z D_z \frac{\partial T}{\partial z}) - \frac{\partial}{\partial z} (QT) + \frac{A_s}{c\rho} (\mu - \lambda T) + \frac{\theta}{c\rho} - T \frac{\partial \bar{v}}{\partial t} \quad (E-1)$$

where

- T = the local water temperature
- c = specific heat
- $\rho$  = fluid density
- $A_z$  = cross-sectional area at the fluid element boundary
- t = time
- z = vertical distance
- $D_z$  = the eddy diffusion coefficient in the vertical direction
- Q = advection across the fluid element boundaries
- $A_s$  = cross-sectional area of the surface fluid element
- $\mu, \lambda$  = coefficients describing heat transfer across air-water interface
- $\theta$  = sum of all external additions of heat to fluid volume of fluid element
- $\bar{v}$  = element volume.

### Application/Verification

The model has recently been used in a lake aeration study (Lorenzen and Fast, 1976). In that study, the model was applied to Kezar Lake in New Hampshire and El Capitan Reservoir in California to verify that artificial mixing could be adequately simulated.

Computed temperature profiles were compared to observed values as shown in

Figures E-1 and E-2. The model performance was judged to be good for the intended purpose of providing guidance for further study.

## E. 2 PREPARATION OF THERMAL PROFILES

The thermal profiles in Appendix D of this report were prepared by inputting the selected climatological conditions, inflow rate, impoundment physical conditions, and wind. Of these, only wind warrants special discussion here. The remaining model parameters are discussed in the text of Chapter 5.

### Wind-Induced Mixing and the Eddy Diffusion Coefficient

Figure E-3 is a plot of the eddy conductivity coefficient versus stability. It was used to obtain coefficients for wind mixing for the model runs. The upper envelope represents high wind mixing conditions and the lower envelope represents low wind mixing conditions. Note that the plot in Figure E-3 was developed for this model, and the model was then verified with data from Hungry Horse Reservoir, which is located on the South Fork of the Flathead River in northwestern Montana. Accordingly, the extremes of wind mixing and the effects on impoundment stability are as found for Hungry Horse Reservoir. The coefficients should be applicable elsewhere, however, because the eddy diffusion coefficient is relatively insensitive to climate and location.

The significance of the eddy conductivity coefficient and its implications for wind mixing may be understood by examining an equation describing transport within the system. Mixing implies the transfer of materials or properties within a system from points of high concentration to points of low concentration, and vice versa. For a system which is undergoing forced convection, it has been observed that the time rate of transport,  $F$ , of a property,  $S$ , through the system is proportional (other things being equal) to the rate of change of concentration of this property with distance,  $z$ . In equation form, this rule is expressed as:

$$F = - D \frac{\partial S}{\partial z} \quad (E-2)$$

where

$D$  = coefficient of proportionality.

The mixing process as defined by Equation E-2 is variously called "effective diffusion," "eddy diffusion," or the "diffusion analogy" because it is identical in form to the equation describing the process of molecular diffusion. The difference between the two processes, however, is that for molecular diffusion,  $D$  is constant, while for turbulent transfer,  $D$  is a function of the dynamic character, or the turbulence level, of the system. In general,  $D$  is a temporal and spatial variable, and thus will be referred to here as  $D(z, t)$ . Equation E-2 rewritten for heat flow over the reservoir vertical axis is:

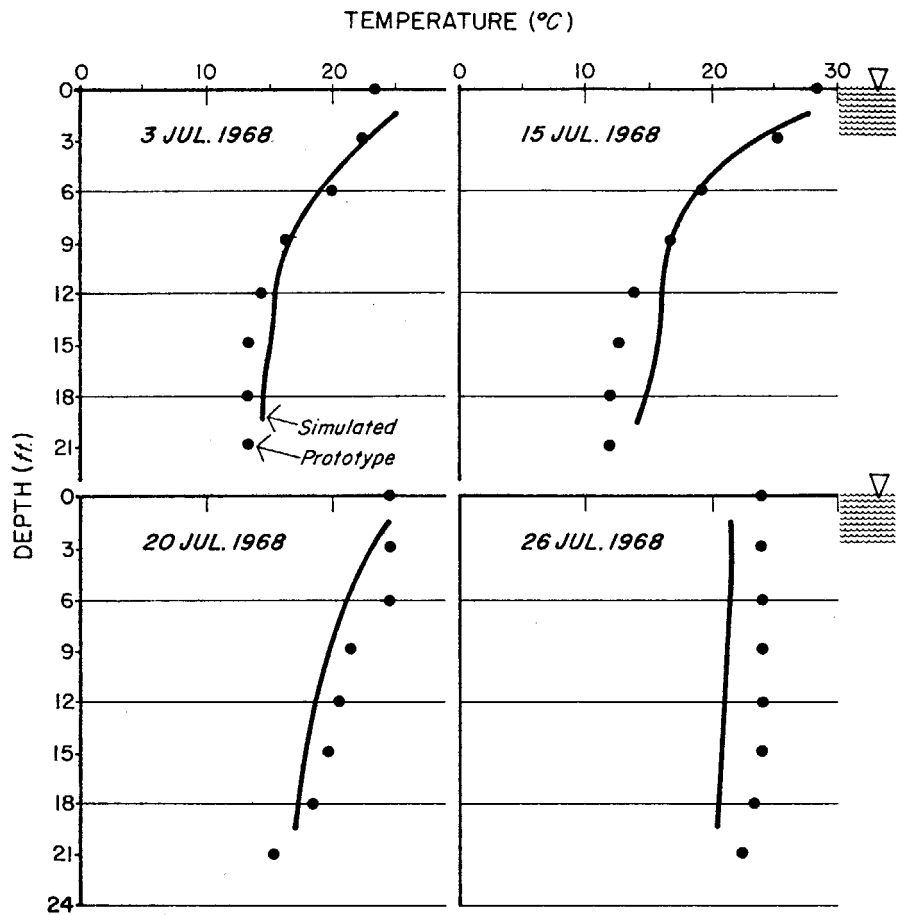
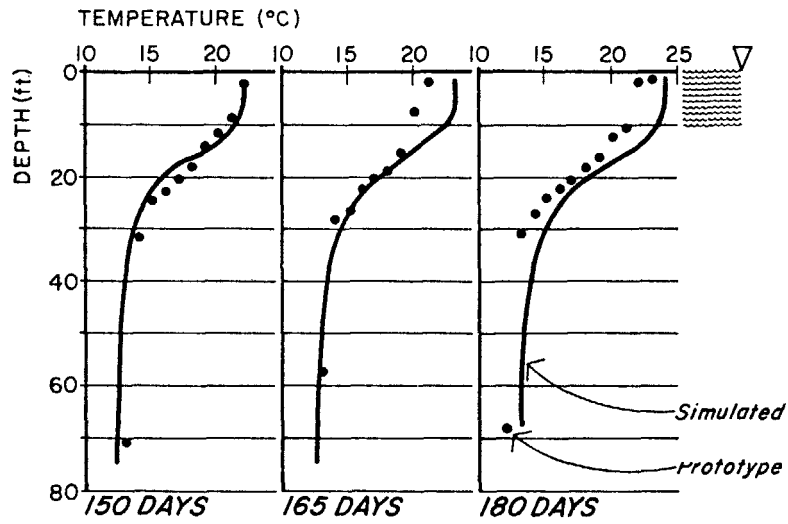


FIGURE E-1 COMPARISON OF COMPUTED AND OBSERVED TEMPERATURE PROFILES IN KEZAR LAKE

**EL CAPITAN 1964 - *NO MIXING***



**EL CAPITAN 1966 - *WITH AERATION***

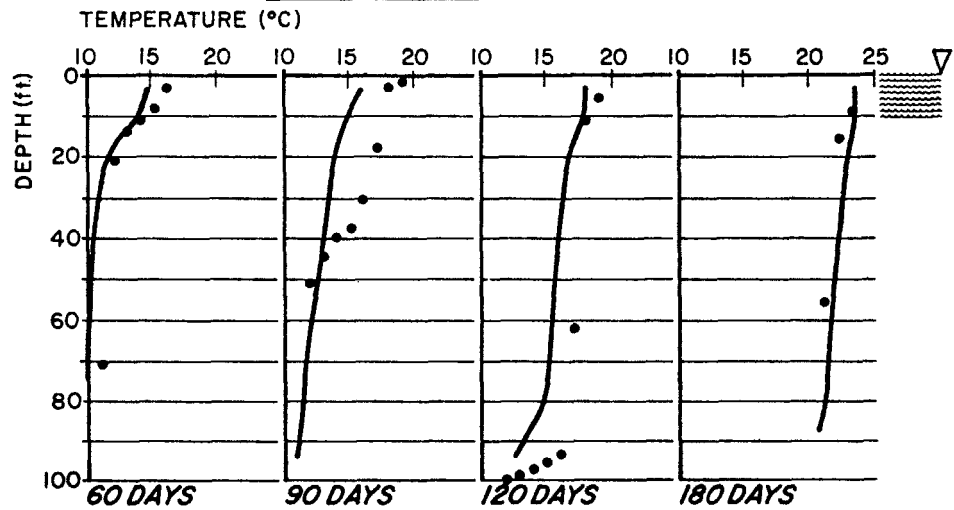


FIGURE E-2      COMPARISON OF COMPUTED AND OBSERVED  
TEMPERATURE PROFILES IN EL CAPITAN  
RESERVOIR

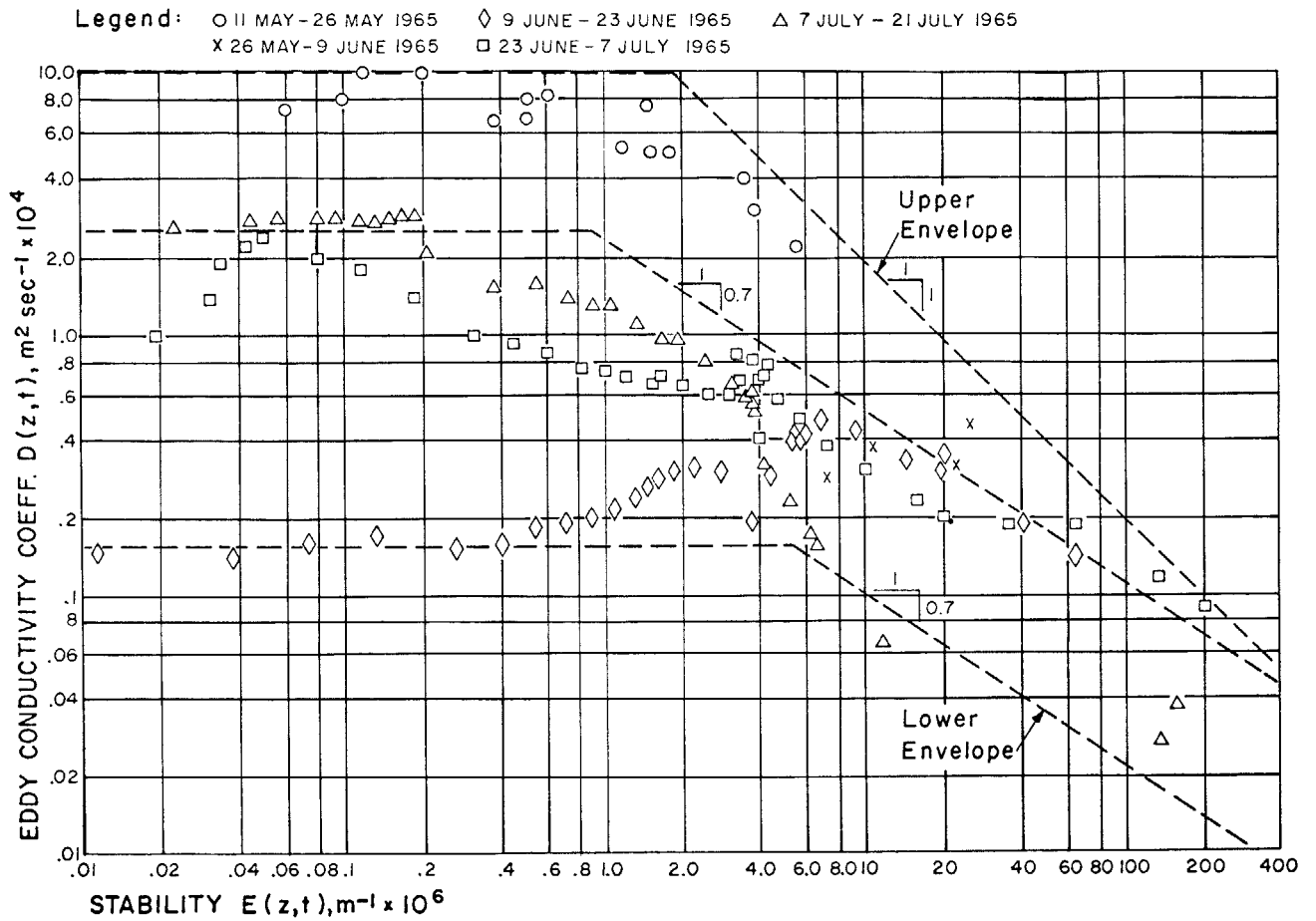


FIGURE E-3 PLOT OF THE EDDY CONDUCTIVITY COEFFICIENT,  $D(z,t)$  VERSUS STABILITY,  $E(z,t)$  FOR HUNGRY HORSE RESERVOIR DATA (AFTER WATER RESOURCES, INC., 1969)

$$H = -\rho c D(z, t) \frac{\partial T}{\partial z} \quad (E-3)$$

where H = heat flux,  $HL^{-2}T^{-1}$   
 ρ = density of water,  $ML^{-3}$   
 c = heat capacity of water,  $HM^{-1}D^{-1}$   
 D(z, t) = coefficient of eddy conductivity,  $L^2T^{-1}$   
 T = temperature, D  
 z = elevation in the reservoir, L  
 t = time T.

From Equation E-3, therefore, it may be seen that the rate of heat flux (H), which describes the rate of energy transfer vertically in an impoundment, is a function of the temperature gradient over depth ( $\frac{\partial T}{\partial z}$ ) and the degree of turbulence (induced by wind and other factors) and is characterized by the eddy diffusion coefficient D(z, t) in the equation. It is this coefficient, D(z, t) which is plotted on the ordinate (stability is on the abscissa) in Figure E-3.

### Surface Heat Flux

The simulation of temperature involves the following steps:

1. The heat transfer at the air-water interface is evaluated for all surface nodes as a function of the meteorological variables and nodal temperatures.
2. The heat input due to shortwave solar radiation is distributed with depth according to the light transmissibility characteristics of the water (which are a function of the suspended particulate).
3. Heat is distributed within the water body by hydrodynamic transport (advection and dispersion) in the same manner as conservative dissolved constituents.

The net rate of heat transfer across the air-water interface is computed according to the following heat budget equation:

$$H = q_{sn} + q_{at} - q_w - q_e \pm q_c \quad (E-4)$$

where

H = net rate of heat transfer ( $Kcal/m^2/sec$ )  
 $q_{sn}$  = net shortwave solar radiation across the air-water interface, including losses by absorption and scattering in the atmosphere, and reflection at the water surface ( $Kcal/m^2/sec$ )  
 $q_{at}$  = atmospheric long wave radiation across the air-water interface ( $Kcal/m^2/sec$ )  
 $q_w$  = long wave back radiation from the water surface to the atmosphere ( $Kcal/m^2/sec$ )

- $a_e$  = evaporative heat loss (Kcal/m<sup>2</sup>/sec)  
 $q_c$  = convective heat exchange between the water surface and the atmosphere (Kcal/m<sup>2</sup>/sec).

The heat transfer terms for long wave back radiation, evaporative heat loss, and convective heat exchange depend on the water temperature in the surface nodes ( $\lambda$  values), while the solar radiation and atmospheric long wave radiation ( $\mu$  values) are independent of water temperature. Algorithms for the various terms of Equation E-2 are used for separate computation and then summed as shown in Equation E-1.

NOTE:

For a more detailed description of the model, its applicability, and the eddy diffusion coefficient, the reader is referred to a report entitled "Mathematical Models for the Prediction of Thermal Energy Changes in Impoundments." (See the list of references at the end of this Appendix.)



## REFERENCES FOR APPENDIX E

- Chen, C.W., and G.T. Orlob. 1975. Ecologic Simulation for Aquatic Environments in Systems Analysis and Simulation in Ecology. Academic Press, New York, San Francisco, and London. III:475-588.
- Lorenzen, M.W., and A. Fast. 1976. A Guide to Aeration/Circulation Techniques for Lake Management. For U.S. Environmental Protection Agency, Corvallis, OR.
- Water Resources Engineers, Inc. 1969. Mathematical Models for the Prediction of Thermal Energy Changes in Impoundments. Water Quality Office, U.S. Environmental Protection Agency, Washington, D.C.

## APPENDIX F

### RESERVOIR SEDIMENT DEPOSITION SURVEYS

Summaries of data from known reliable reservoir sedimentation surveys made in the United States through 1970 are presented in this Appendix, together with an explanation of the summary table. Additional data from surveys made after 1970 are included for some reservoirs. The reservoirs are grouped according to the 79 drainage areas into which the United States is divided in the publication: "River Basin Maps Showing Hydrologic Stations", compiled under the auspices of the Subcommittee on Hydrology, Federal Inter-Agency River Basin Committee. An index map of these drainage areas is shown on page F-78. An index to the surveys is provided below. Appendix F is available on microfiche in the enclosed envelope for the EPA-published manual, or as Part 3, for paper copies purchased from the National Technical Information Service.

Drainage Area	Page
1 St. John Machias, Penobscot, Kennebec, Androscoggin and Presumpscot River Basin	F-6
2 Housatonic, Connecticut, Thames, and Merrimack River Basin	F-6
3 Hudson River Basin and St. Lawrence Drainage in New York	F-6
4 Susquehanna and Delaware River Basins	F-6
5 Potomac, Rappahannock, York, and James River Basins	F-7
6 Chowan, Roanoke, Tar, Neuse, and Cape Fear River Basins	F-7
7 Pee Dee, Santee, and Edisto River Basins	F-8
8 Savannah, Ogeechee, and Altamaha River Basins	F-9
9 Satilla, St. Mary's, St. John's, and Suwannee River Basins	F-9
10 Southern Florida Drainage	F-9
11 Apalachicola and Ocklawaha River Basins	F-9
12 Choctawhatchee, Yellow, Escambia and Alabama River Basins	F-9
13 Tombigbee, Pascagoula, and Pearl River Basins	F-9
14 Lower Mississippi River Basin (Natchez to the Mouth): Calcasieu, Mermentau, and Vermilion River Basins	F-9
15 Lower Mississippi River Basin (Helena to Natchez): Yazoo, Big Black, and Ouachita River Basins	F-10
16 Lower Mississippi River Basin (Chester to Helena): St. Francis River Basin	F-11
17 Ohio River Basin (Madison to Uniontown): Wabash River Basin	F-12
18 Tennessee River Basin (below Hales Bar Dam): Cumberland and Green River Basins	F-13
19 Ohio River Basin (Point Pleasant to Madison): Kanawha, Big Sandy, Licking, Kentucky, Scioto, and Miami River Basins	F-13

Drainage Area	Page
20 Tennessee River Basin (above Hales Bar Dam)	F-15
21 Ohio River Basin (above Point Pleasant) and Lake Erie Drainage	F-17
22 Great Lakes Drainage (in Michigan) and Maumee River Basin	F-20
23 Great Lakes Drainage (in Michigan and Wisconsin)	F-21
24 Mississippi River Basin (Louisiana to Chester): Illinois, Kaskaskia and Meramec River Basins	F-21
25 Upper Mississippi River Basin (Fairmont to Louisiana): Iowa, Skunk, and Des Moines River Basins	F-23
26 Upper Mississippi River Basin (Prairie du Chien to Rock Island) and Lake Michigan Drainage: Rock and Wapsipinicon River Basins	F-23
27 Upper Mississippi River Basin (St. Paul to Prairie du Chien): Wisconsin, Root, Chippewa, and St. Croix River Basins	F-23
28 Upper Mississippi River Basin (above St. Paul)	F-24
29 Lake Superior and Lake of the Woods Area (in Minnesota)	F-24
30 Red River of the North Basin	F-24
31 Missouri River Basin (Nebraska City to Hermann)	F-24
32 Smoky Hill and Lower Republican River Basins	F-26
33 Upper Republican, North Platte River Basins (Fort Laramie to North Platte) and South Platte River Basin (Sublette to North Platte)	F-28
34 North Platte River Basin (above Ft. Laramie) and South Platte River Basin (above Sublette)	F-28
35 Missouri River Basin (above Blair to Nebraska City) and Platte River Basin (below North Platte)	F-29
36 River Basin (Niobrara to above Blair), James, and Big Sioux River Basins	F-31
37 Missouri River Basin (above Pierre to Niobrara): Niobrara and White River Basins	F-32
38 Missouri River Basin (Mobridge to above Pierre): Cheyenne and Belle Fourche River Basins	F-33
39 Missouri River (Williston to Mobridge): Moreau, Grand, Cannonball, Heart, and Little Missouri River Basins	F-34
40 Missouri River Basin (Zortman to Williston): Milk and Musselshell River Basins	F-34
41 Missouri River Basin (above Zortman)	F-34
42 Lower Yellowstone River Basin: Tongue and Power River Basins	F-34
43 Upper Yellowstone River Basin	F-35
44 Arkansas River Basin (Van Buren to Little Rock) and White River Basin	F-35
45 Arkansas River Basin (Tulsa to Van Buren): Grand, Verdigris, and Lower Canadian River Basins	F-36
46 Arkansas River Basin (Garden City to Tulsa): Middle Canadian, Lower Cimarron, and Salt Fork River Basins	F-37
47 Arkansas River Basin (Lamar to Garden City): Upper Cimarron and Upper Canadian River Basins	F-39

Drainage Area	Page
48 Rio Grande Basin (above Espanola) and Arkansas River Basin	F-40
49 Red River Basin (Denisen to Grand Ecore): Little and Sulphur River Basins	F-40
50 Red River Basin (above Denisen)	F-41
51 Sabine, Meches, and Trinity River Basins	F-43
52 Lower Brazes, Lower Colorado, Guadalupe, San Antonio, and Nueces River Basins	F-44
53 Brazes River Basin (South Bend to Washington), Middle, and Colorado River Basins	F-45
54 Upper Brazes and Upper Colorado River Basins	F-47
55 Rio Grande Basin (below Eagle Pass)	F-47
56 Rio Grande Basin (Fort Quitman to Eagle Pass) and Lower Pecos River Basin	F-47
57 Rio Grande Basin (Espanota to Fort Quitman)	F-48
58 Upper Pecos River Basin	F-48
59 Colorado River Basin (below Hoover Dam): Williams and Lower Gila River Basins	F-49
60 Gila River Basin	F-49
61 Little Colorado and San Juan River Basins	F-51
62 Colorado River Basin (Hall's Crossing to Hoover Dam)	F-52
63 Colorado River Basin (above Hall's Crossing): Gunnison, Dolores, and Fremont River Basins	F-52
64 Green River Basin	F-56
65 Great Salt Lake Basin	F-56
66 Sevier River Basin	F-56
67 Great Basin (northwestern part in California, Nevada, and Oregon)	F-57
68 Great Basin: Humboldt, Carson and Truckee River Basins	F-57
69 Great Basin: Owens, Walker, and Mono Lake Drainages	F-57
70 Salton Sea and Southern California Coastal and Great Basin Drainage	F-57
71 San Joaquin and Keen River Basins and Adjacent Coastal Drainage	F-69
72 Sacramento, Eel, and Russian River Basins	F-71
73 Klamath, Rogue, and Umpqua River Basins	F-72
74 Lower Columbia River Basin and Pacific Coast Basins in Northern Oregon	F-73
75 Columbia River Basin (Grand Coulee to Umatilla) and Pacific Coast Drainage in Washington: Yakima, Chelan, and Okanogah River Basins	F-74
76 Columbia River Basin (International Boundary to Grand Coulee) and Pacific Coast Drainage in Washington: Pendorelle, Spokane, Walla Walla, and Lower Snake River Basins	F-75

<u>Drainage Area</u>	<u>Page</u>
77 Columbia River Basin in Canada	F-75
78 Snake River Basin (from Kings Hill to Grande Ronde River)	F-75
79 Snake River Basin (above Kings Hill) and Salmon River Basin	F-77
80 Puerto Rico	F-77

## APPENDIX G

### INITIAL DILUTION TABLES

Appendix G consists of Initial Dilution Tables. Page G-1 provides information for choosing the appropriate table. These follow in numerical order beginning on pp. G-2 through G-101. The Appendix is available on microfiche in the enclosed envelope for the EPA-published manual, or as Part 3 for paper copies purchased from the National Technical Information Service.

APPENDIX H  
EQUIVALENTS OF COMMONLY USED UNITS OF MEASUREMENT

English Unit	Multiplier	SI Unit	English Unit	Multiplier	SI Unit
acre	$\times 4.0468724 \rightarrow$ $+ 2.471 \times 10^{-4} \times$	m <sup>2</sup>	gpd/ft	$\times 0.0124 \rightarrow$ $+ 80.65 \times$	m <sup>3</sup> /day m
acre	$\times 0.405 \rightarrow$ $+ 2.471 \times$	ha*	gpd/sq ft	$\times 0.0408 \rightarrow$ $+ 24.51 \times$	m <sup>3</sup> /day m <sup>2</sup>
acre-ft	$\times 1,233.5 \rightarrow$ $+ 8.11 \times 10^{-4} \times$	m <sup>3</sup>	gpm	$\times 0.0631 \rightarrow$ $+ 15.85 \times$	dm <sup>3</sup> /s
Btu	$\times 1.055 \rightarrow$ $+ 0.9478 \times$	kJ	gpm	$\times 0.0631 \rightarrow$ $+ 15.85 \times$	l*/s
Btu	$\times 0.252 \rightarrow$ $+ 3.968 \times$	kg-cal *	gpm/sq ft	$\times 40.7 \rightarrow$ $+ 0.0245 \times$	l*/min m <sup>2</sup>
Btu/hr/sq ft	$\times 3.158 \rightarrow$ $+ 0.316 \times$	J/s-m <sup>2</sup>	hp	$\times 0.7454 \rightarrow$ $+ 1.341 \times$	kW
Btu/lb	$\times 0.555 \rightarrow$ $+ 1.80 \times$	kg-cal/kg*	hp-hr	$\times 2.684 \rightarrow$ $+ 0.372 \times$	MJ
cfm	$\times 0.028 \rightarrow$ $+ 35.71 \times$	m <sup>3</sup> /min	in.	$\times 2.54 \rightarrow$ $+ 0.3937 \times$	cm
cfs	$\times 1.7 \rightarrow$ $+ 0.588 \times$	m <sup>3</sup> /min	lb/day /acre-ft	$\times 3.68 \rightarrow$ $+ 0.2717 \times$	g/day m <sup>3</sup>
cfs/sq miles	$\times 0.657 \rightarrow$ $+ 1.522 \times$	m <sup>3</sup> /min km <sup>2</sup>	lb/1,000 cu ft	$\times 16.0 \rightarrow$ $+ 0.0625 \times$	g/m <sup>3</sup>
cu ft	$\times 0.028 \rightarrow$ $+ 35.314 \times$	m <sup>3</sup>	lb/day/cu ft	$\times 16 \rightarrow$ $+ 0.0625 \times$	kg/day m <sup>3</sup>
cu ft	$\times 28.32 \rightarrow$ $+ 0.0353 \times$	l*	lb/mil gal	$\times 0.92 \rightarrow$ $+ 8.333 \times$	g/m <sup>3</sup>
cu in.	$\times 16.39 \rightarrow$ $+ 0.061 \times$	cm <sup>3</sup>	mil gal	$\times 3,785 \rightarrow$ $+ 2.64 \times 10^{-4} \times$	m <sup>3</sup>
cu yd	$\times 0.75 \rightarrow$ $+ 1.3709 \times$	m <sup>3</sup>	mgd	$\times 3,785 \rightarrow$ $+ 2.64 \times 10^{-4} \times$	m <sup>3</sup> /day
°F	$0.555(^{\circ}\text{F}-32) \rightarrow$ $+ 1.8(^{\circ}\text{C})+32$	°C	mgd	$\times 0.0438 \rightarrow$ $+ 22.82 \times$	m <sup>3</sup> /s
°C	plus 273 $\rightarrow$ minus 273	K	mile	$\times 1.61 \rightarrow$ $+ 0.621 \times$	km
ft	$\times 0.3048 \rightarrow$ $+ 3.28 \times$	m	ppb	$\times 10^{-3} \rightarrow$ $+ 1,000 \times$	mg/l *
ft-lb	$\times 1.356 \rightarrow$ $+ 0.737 \times$	J	ppm	approximately equal to	mg/l*
gal	$\times 3.785 \rightarrow$ $+ 0.264 \times$	l*	sq ft	$\times 0.0929 \rightarrow$ $+ 10.76 \times$	m <sup>2</sup>
gal	$\times 0.003785 \rightarrow$ $+ 264.2 \times$	m <sup>3</sup>	sq in.	$\times 645.2 \rightarrow$ $+ 0.00155 \times$	mm <sup>2</sup>
gpd/acre	$\times 0.9365 \rightarrow$ $+ 1.068 \times$	m <sup>3</sup> /day km <sup>2</sup>	sq miles	$\times 2.590 \rightarrow$ $+ 0.3861 \times$	km <sup>2</sup>

Other commonly used conversions:

1 MGD = 1.55cfs

$\gamma_{\text{Cp}} = 62.4 \text{ BTU/ft}^3/{}^{\circ}\text{F}$

1 MW =  $3.414 \times 10^6$  BTU/hr

1 BTU = 778 ft-lb

1 BTU = 252 cal

1 Langley/day =  $3.7 \text{ BTU/ft.}^2 / \text{day}$

\* Not an SI unit, but a term commonly used and preferred as a wastewater unit of expression.

## ADDITIONAL AQUIFER PARAMETERS

Physical Properties of Water

The density of a fluid is defined as the mass of fluid per unit volume. The viscosity of a fluid is a measure of the resistance of the fluid to deform when moving. The kinematic viscosity  $\nu$  is defined as the viscosity  $\mu$  divided by the density of the fluid  $\rho_w$ :

$$\nu = \mu / \rho_w$$

Compressibility  $\beta_w$  is the relative change of a unit volume of fluid Per unit increase in pressure. Thus  $\beta_w$  relates the volumetric strain to the stress induced in water by a change in fluid pressure.

Upon examining Table I-1, the viscosity  $\mu$  is most affected by temperature changes and  $\mu$  decreases by about 3 percent per degree Celsius rise in temperature. The properties of water are also a function of pressure, but they are even less sensitive to changes in pressure than to changes in temperature. However, in most situations that are encountered in ground water problems, the physical properties of water are considered as constants.

Particle Density

Particle density,  $\rho_s$  ( $\text{g}/\text{cm}^3$ ), of a soil is defined as the mass of soil solids  $M_s$  (g) divided by the volume of the soil solids  $V_s$  ( $\text{cm}^3$ ):

$$\rho_s = M_s / V_s$$

The particle density for most mineral soils varies between 2.6 and 2.75  $\text{g}/\text{cm}^3$ . Table I-2 gives a list of typical values for various materials. Note that organic matter has a much lower particle density, between 1.2 and 1.5  $\text{g}/\text{cm}^3$ . Thus, surface soils usually have a lower particle density than subsoils.

Sometimes the density of a soil is expressed in terms of the specific gravity. The specific gravity  $G$  (unitless) is equal to the ratio of the particle density  $\rho_s$  ( $\text{g}/\text{cm}^3$ ) of the material to that of water  $\rho_w$  ( $\text{g}/\text{cm}^3$ ) at 4 degrees Celsius and at atmospheric pressure:

$$G = \rho_s / \rho_w$$

However, since the density of water under these conditions is 1  $\text{g}/\text{cm}^3$  (see Table I-2), the specific gravity is numerically (although not dimensionally) equal to the particle density.

The average particle density  $\rho_s$  ( $\text{g}/\text{cm}^3$ ) of a soil can be determined in the laboratory by the picnometer method (i.e., water displacement test) (Fox, 1959; Taylor and Ashcroft, 1972). Typical values for various materials are given in Table VII-3.



TABLE I-1

## PHYSICAL PROPERTIES OF PURE WATER AT ONE ATMOSPHERE

Temperature °C	Density (g/cm <sup>3</sup> )	Viscosity (g/cm sec)	Kinematic Viscosity (cm <sup>2</sup> /sec)	Compressibility (cm sec <sup>2</sup> /g)
0	.99987	.01787	.0179	5.098 x 10 <sup>-11</sup>
4	1.00000	.01567	.0157	4.959 x 10 <sup>-11</sup>
5	.99999	.01519	.0152	4.928 x 10 <sup>-11</sup>
10	.99973	.01307	.0131	4.789 x 10 <sup>-11</sup>
15	.99913	.01139	.0114	4.678 x 10 <sup>-11</sup>
20	.99823	.01002	.01004	4.591 x 10 <sup>-11</sup>
25	.99708	.00890	.00893	4.524 x 10 <sup>-11</sup>
30	.99568	.00798	.00801	4.475 x 10 <sup>-11</sup>
35	.99406	.00719	.00723	4.442 x 10 <sup>-11</sup>

Reference: Weast (1969).

### Specific Yield

Specific yield can be used as an estimate of effective porosity. Specific yield is also used to predict the drawdown of the water table and the local velocity field around a pumping well. It is an essential parameter for the analysis of the performance of a recovery well field.

The specific yield  $S_y$  (unitless) of an unconfined aquifer is a measure of the "water-yielding" capacity of the porous medium. The specific yield is defined as the volume of water that will discharge per unit area of saturated porous medium under a unit drop in hydraulic head. Specific yield can be expressed as either a ratio or as a percentage. That part of the water retained by molecular and surface tension forces in the void spaces of a gravity drained material is known as retained water. The "water-retaining" capacity of porous media is called the specific retention  $S_r$  (unitless). Hence, the porosity of a saturated, unconfined aquifer is equal to the sum of the specific yield and the specific retention:

$$p = S_y + S_r$$

Gravity drainage from most unconfined aquifers is not instantaneous. If the hydraulic conductivity is low, the water-yielding capacity can increase up to the

TABLE I-2

## RANGE AND MEAN VALUES OF PARTICLE DENSITY

Material	Range (g/cm <sup>3</sup> )	Mean <sub>3</sub> (g/cm <sup>3</sup> )
clay	2.51 - 2.77	2.67
silt	2.47 - 2.79	2.62
sand, fine	2.54- 2.77	2.67
sand, medium	2.60 - 2.77	2.66
sand, coarse	2.52 - 2.73	2.65
gravel, fine	2.63 - 2.76	2.68
gravel, medium	2.65 - 2.79	2.71
gravel, coarse	2.64- 2.76	2.69
loess	2.64 - 2.74	2.67
eolian sand	2.63 - 2.70	2.66
till, predominantly clay	2.61 - 2.69	2.65
till, predominantly silt	2.64 - 2.77	2.70
till, predominantly sand	2.63 - 2.73	2.69
till, predominantly gravel	2.67 - 2.78	2.72
glacial drift, predominantly silt	2.70 - 2.73	2.72
glacial drift, predominantly sand	2.65 - 2.75	2.69
glacial drift, predominantly gravel	2.65 - 2.75	2.68
sandstone, fine grained	2.56 - 2.72	2.65
sandstone, medium grained	2.64 - 2.69	2.66
siltstone	2.52 - 2.89	2.65
claystone	2.50- 2.76	2.66
shale	2.47 - 2.83	2.69
limestone	2.68- 2.88	2.75
dolomite	2.64- 2.72	2.69
granite, weathered	2.70 - 2.84	2.74
gabbro, weathered	2.95- 3.09	3.02
basalt	2.95 - 3.15	3.07
schist	2.70 - 2.84	2.79
slate	2.85 - 3.05	2.94

Reference: Morris and Johnson (1967).

TABLE I-3  
RANGE AND MEAN VALUES OF SPECIFIC YIELD

Material <sup>a</sup>	Range (percent)	Mean (percent)
clay	1.1 - 17.6	6
silt	1.1 - 38.6	20
sand, fine	1.0 - 45.9	33
sand, medium	16.2 - 46.2	32
sand, coarse	18.4 - 42.9	30
gravel, fine	12.6 - 39.9	28
gravel, medium	16.9 - 43.5	24
gravel, coarse	13.2 - 25.2	21
loess	14.1 - 22.0	18
eolian sand (dune sand)	32.3 - 46.7	38
till, predominantly silt	0.5 - 13.0	6
till, predominantly sand	1.9 - 31.2	16
till, predominantly gravel	5.1 - 34.2	16
glacial drift, predominantly silt	33.2 - 48.1	40
glacial drift, predominantly sand	29.0 - 48.2	41
sandstone, fine grained	2.1 - 39.6	21
sandstone, medium grained	11.9 - 41.1	27
siltstone	0.9 - 32.7	12
<b>shale<sup>b</sup></b>	0.5 - 5	--
limestone	0.2 - 35.8	14
schist	21.9 - 33.2	26

<sup>a</sup>Reference: Morris and Johnson (1967).

<sup>b</sup>Reference: Walton (1970).

specific yield at a diminishing rate as the time of drainage increases.

Values of specific yield depend on grain size, shape and distribution of pores, compaction of the stratum and time of drainage. The range and mean values of laboratory measured specific yields for various geologic materials are given in Table I-3.

### Specific Storage

The specific storage or elastic storage coefficient  $S_s$  of a confined aquifer is defined as the volume of water released from storage per unit volume of aquifer per unit decline in hydraulic head. This release is due to the compaction of the aquifer's granular skeleton and the expansion of pore water when the water pressure is reduced by pumping.  $S_s$  has the units of  $\text{cm}^{-1}$  and is normally a small quantity ( $1 \times 10^{-5} \text{ cm}^{-1}$  or less). Typical values of specific storage  $S_s$  are given for various geologic materials in Table I-4.

### Storativity

Storativity or storage coefficient,  $S$ , is also defined as the volume of water that is released from storage per unit horizontal area of aquifer per unit decline of hydraulic head. It is a dimensionless quantity. This parameter is obtained in addition to transmissivity from pumping tests. It is used to compute aquifer yields and to compute drawdowns of individual wells.

For confined aquifers, storativity is due to water being released from the compression of the granular skeleton and expansion of the pore water.  $S$  is mathematically defined as the product of the specific storage,  $S_s$  ( $\text{cm}^{-1}$ ) and the aquifer thickness,  $b$  (cm):

$$S = S_s b$$

The value of the storativity for confined aquifers is generally small, falling between the range of 0.00005 and 0.005 (Todd, 1980). Hence, large pressure changes over an extensive area of aquifer are required before substantial water is released.

For unconfined aquifers, storativity is due to the release of water from gravity drainage of voids (i.e., yield) and from the compressibility of the granular skeleton (i.e., elastic storage).

This is mathematically defined as:

$$S = S_y + hS_s$$

where  $S_y$  is the specific yield (dimensionless),  $h$  is the saturated thickness of the water-table aquifer (cm) and  $S_s$  is the specific storage ( $\text{cm}^{-1}$ ). The value of  $S_y$  is usually several orders of magnitude larger than  $hS_s$ , except for fine-grained aquifers where  $S_y$  may approach the value of  $hS_s$ . Storativity  $S$  of unconfined aquifers ranges from 0.01 to 0.30.

TABLE I-4

RANGE OF VALUES FOR COMPRESSIBILITY AND  
SPECIFIC STORAGE OF VARIOUS GEOLOGIC MATERIALS

Material	Specific Storage $S_s$ ( $\text{cm}^{-1}$ )
plastic clay	$2.0 \times 10^{-4} - 2.5 \times 10^{-5}$
stiff clay	$2.5 \times 10^{-5} - 1.3 \times 10^{-5}$
medium-hard clay	$1.3 \times 10^{-5} - 6.9 \times 10^{-6}$
loose sand	$9.8 \times 10^{-6} - 5.1 \times 10^{-6}$
dense sand	$2.1 \times 10^{-6} - 1.3 \times 10^{-6}$
dense sandy gravel	$9.8 \times 10^{-7} - 5.1 \times 10^{-7}$
rock, fissured, jointed	$6.9 \times 10^{-7} - 3.2 \times 10^{-8}$
rock, sound	less than $3.2 \times 10^{-8}$

Reference: Jumi kis (1962) and Walton (1970).

Measuring Specific Yield, Specific Storage and Storativity

Although most field methods determine specific yield directly, most laboratory methods determine specific retention by the centrifuge-moisture method (Johnson et al. 1963), and specific yield  $S_y$  (unitless) is found indirectly by subtracting the specific retention  $S_r$  (unitless) from the porosity  $p$  (unitless):

$$S = p - S_r$$

Other laboratory methods are discussed by Johnson (1967). However, laboratory samples may be disturbed or may not be representative of the aquifer.

Several field methods are available to estimate specific yield, including drawdown tests, recharge tests, the neutron moisture methods and tracer methods. Jones and Schneider (1969) discuss the neutron moisture method and compare it to five other methods for the Ogallala aquifer in Texas. They concluded that pumping and recharge methods underestimate the specific yield by 50% compared to the other methods. Hanson (1973) also concludes that pumping will underestimate the specific yield if the pumping test is done over too short a period of time. However, Todd (1980) believes that methods based on an analysis of the time - drawdown data from well-pumping tests generally give the most reliable results.

Specific storage  $S_s$  is a function of the solid matrix and fluid compressibility. Compressibility can be determined in the laboratory by means of a consolidation

apparatus called a loading cell. Either a fixed-ring or a floating-ring container type loading cell can be used (Hall, 1953; Lambe, 1951). In the field, specific storage is generally measured indirectly as storativity  $S$  by pumping tests. If the saturated thickness  $b$ (cm) of the **confined** aquifer and storativity  $S$  (unitless) are known, then the specific storage  $S_s$  ( $\text{cm}^{-1}$ ) can be solved as shown below:

$$S_s = S/b$$

The contribution of specific storage to storativity in unconfined aquifers is generally negligible.

Storativity can be determined directly from pumping tests of wells and from ground water fluctuations in response to atmospheric pressure or ocean tide variations and river level fluctuations. An extensive discussion of the various types of pumping tests and the procedures for calculating the storativity from them is given by Todd (1980), Walton (1970), and Lehman (1972).

Complimentary Error Function

The complimentary error function (erfc) is defined as follows:

$$\text{erfc}(x) = \frac{2}{\sqrt{\pi}} \int_x^{\infty} e^{-z^2} dz$$

In addition, erfc has the following properties:

$$\text{erfc}(x) = 1 - \text{erf}(x)$$

$$\text{erf}(-x) = -\text{erf}(x)$$

$$\text{erfc}(-x) = 2 - \text{erfc}(x)$$

$$\text{erfc}(0) = 1$$

$$\text{erfc}(\infty) = 0$$

$$\text{erfc}(-\infty) = 2$$

where erf is the error function. A list of the error function and complimentary error function for various values of x are given in Table J-1.

A method for numerically computing erfc is shown in Table J-2.

The following trick should be used when using erfc and exponential functions multiplied together:

$$e^a \cdot \text{erfc}(x) = ?$$

$$\text{when } \begin{array}{l} a \rightarrow \infty \\ x \rightarrow \infty \end{array}$$

Use the following solution:

$$e^a \cdot \text{erfc}(x) = (a_1 t + a_2 t^2 + a_3 t^3 + a_4 t^4 + a_5 t^5) e^{a-x^2}$$

where  $a_1 \dots a_5$  and t are given in Table J-2. Note that the trick is to evaluate the combined exponential argument  $e^{a-x^2}$  rather than  $e^a \cdot e^{-x^2}$ . For example:

$$e^{100} \cdot \text{erfc}(9) = 1.15 \times 10^7$$

$$e^{100} \cdot \text{erfc}(10) = 5.86 \times 10^{-2}$$

$$e^{100} \cdot \text{erfc}(11) = 4.08 \times 10^{-11}$$

TABLE J-1

TABLE OF THE ERROR FUNCTION (erf) AND THE  
COMPLIMENTARY ERROR FUNCTION (erfc)

x	erf(x)	erfc(x)	x	erf(x)	erfc(x)
0	0	1.0	1.1	0.880205	0.119795
0.05	0.056372	0.943628	1.2	0.910314	0.089686
0.1	0.112463	0.887537	1.3	0.934008	0.065992
0.15	0.167996	0.832004	1.4	0.952285	0.047715
0.2	0.222703	0.777297	1.5	0.966105	0.033895,
0.25	0.276326	0.723674	1.6	0.976348	0.0236521
0.3	0.328627	0.671373	1.7	0.983790	0.016210
0.35	0.379382	0.620618	1.8	0.989091	0.010909
0.4	0.428392	0.571608	1.9	0.992790	0.007210
0.45	0.475482	0.524518	2.0	0.995322	0.004678
0.5	0.520500	0.479500	2.1	0.997021	0.002979
0.55	0.563323	0.436677	2.2	0.998137	0.001863
0.6	0.603856	0.396144	2.3	0.998857	0.001143
0.65	0.642029	0.357971	2.4	0.999311	0.000689
0.7	0.677801	0.322199	2.5	0.999593	0.000407
0.75	0.711156	0.288844	2.6	0.999764	0.000236
0.8	0.742101	0.257899	2.7	0.999866	0.000134
0.85	0.770668	0.229332	2.8	0.999925	0.000075
0.9	0.796908	0.203092	2.9	0.999959	0.000041
0.95	0.820891	0.179109	3.0	0.999978	0.000022
1.0	0.842701	0.157299	i n f i n i t e	1.000000	0.000000

$$\text{erfc}(x) = 1 - \text{erf}(x)$$

$$\text{erfc}(-x) = 2 - \text{erfc}(x)$$

$$\text{erf}(-x) = -\text{erf}(x)$$

Reference: Crank (1975).



TABLE J-2

NUMERICAL COMPUTATION OF THE COMPLEMENTARY  
ERROR FUNCTION

$$\operatorname{erfc}(x) = (a_1 t + a_2 t^2 + a_3 t^3 + a_4 t^4 + a_5 t^5) e^{-x^2} + \varepsilon(x)$$

$$\text{Where } t = \frac{1}{(1 + px)}$$

$$\text{error term } |\varepsilon(x)| \leq 1.5 \times 10^{-7}$$

$$\text{and } p = .3275911$$

$$a_1 = .254829592$$

$$a_2 = -.284496736$$

$$a_3 = 1.421413741$$

$$a_4 = -1.453152027$$

$$a_5 = 1.061405429$$

---

Reference: page 299, Eq. 7.1.26 of Abramowitz and Stegun (1964).

---

### Leaky Well Function; of Hantush

The leaky well function of Hantush is defined as follows:

$$W(u, r/B) = \int_u^{\infty} \frac{\exp}{t} \left( -t - \frac{r^2}{4B^2 t} \right) dt$$

where  $W(\cdot)$  has the limits:

$$W(0, r/B) = 2K_0(r/B) \quad (\text{modified Bessel function of zero order})$$

$$W(u, 0) = E_1(u) \quad (\text{exponential integral})$$

$$W(\infty, r/B) = 0$$

$$\exp(\cdot) = \text{exponential function}$$

The leaky well function has been extensively tabulated by Hantush (1956) and is given in Table J-3. For large values of  $r/B$  (i.e.,  $r/B > 1$ ), Wilson and Miller (1978) have developed the following approximation to  $W$ :

TABLE J-3  
 THE LEAKY WELL FUNCTION OF HANTUSH  
 $W(u, r/B)$

$u$	0.01	0.015	0.03	0.05	0.075	0.10	0.15	0.2	0.3	0.4	0.5	0.6	0.7	0.8	0.9	1.0	1.5	2.0	2.5
0.000001	9.4425	8.6319	7.2471	6.2285	5.4228	4.8541	4.0601	3.5054	2.7449	2.2291	1.8488	1.5550	1.3210	1.1307	0.9735	0.8420	0.4276	0.2278	0.1247
0.000005	9.4413	8.6313	7.2471	6.2285	5.4228	4.8541	4.0601	3.5054	2.7449	2.2291	1.8488	1.5550	1.3210	1.1307	0.9735	0.8420	0.4276	0.2278	0.1247
0.00001	9.4176	8.6313	7.2471	6.2285	5.4228	4.8541	4.0601	3.5054	2.7449	2.2291	1.8488	1.5550	1.3210	1.1307	0.9735	0.8420	0.4276	0.2278	0.1247
0.00005	8.9827	8.4533	7.2450	6.2285	5.4228	4.8541	4.0601	3.5054	2.7449	2.2291	1.8488	1.5550	1.3210	1.1307	0.9735	0.8420	0.4276	0.2278	0.1247
0.0001	8.3983	8.1414	7.2122	6.2282	5.4228	4.8541	4.0601	3.5054	2.7449	2.2291	1.8488	1.5550	1.3210	1.1307	0.9735	0.8420	0.4276	0.2278	0.1247
0.0005	6.9750	6.9152	6.6219	6.0921	5.4062	4.8530	4.0691	3.5054	2.7449	2.2291	1.8488	1.5550	1.3210	1.1307	0.9735	0.8420	0.4276	0.2278	0.1247
0.001	6.3069	6.2765	6.1202	5.7965	5.3078	4.8292	4.0695	3.5054	2.7449	2.2291	1.8488	1.5550	1.3210	1.1307	0.9735	0.8420	0.4276	0.2278	0.1247
0.005	4.7212	4.7152	4.6829	4.6084	4.4713	4.2960	3.8821	3.4567	2.7428	2.2290	1.8488	1.5550	1.3210	1.1307	0.9735	0.8420	0.4276	0.2278	0.1247
0.01	4.0356	4.0326	4.0167	3.9795	3.9091	3.8150	3.5725	3.2875	2.7104	2.2253	1.8486	1.5550	1.3210	1.1307	0.9735	0.8420	0.4276	0.2278	0.1247
0.05	2.4675	2.4670	2.4642	2.4576	2.4448	2.4271	2.3776	2.3110	1.9783	1.7075	1.4927	1.2955	1.1210	1.1210	0.9700	0.8409	0.4276	0.2278	0.1247
0.1	1.8227	1.8225	1.8184	1.8128	1.8050	1.7829	1.7527	1.7527	1.6704	1.5644	1.4422	1.3115	1.1791	1.0505	0.9297	0.8190	0.4271	0.2271	0.1178
0.5	0.5598	0.5597	0.5596	0.5594	0.5588	0.5581	0.5561	0.5532	0.5451	0.5344	0.5206	0.5044	0.4860	0.4658	0.4440	0.4210	0.3007	0.1944	0.1174
1.0	0.2194	0.2194	0.2193	0.2193	0.2191	0.2190	0.2186	0.2179	0.2161	0.2135	0.2103	0.2065	0.2020	0.1970	0.1914	0.1855	0.1509	0.1139	0.0803
5.0	0.0011	0.0011	0.0011	0.0011	0.0011	0.0011	0.0011	0.0011	0.0011	0.0011	0.0011	0.0011	0.0011	0.0011	0.0011	0.0011	0.0010	0.0010	0.0009

Reference: Hantush (1956).

$$W(u, r/B) = \left(\frac{\pi B}{2r}\right)^{1/2} \exp\left(-\frac{r}{B}\right) \operatorname{erfc}\left(-\frac{\left(\frac{r}{B} - 2u\right)}{2\sqrt{u}}\right)$$

in which  $\operatorname{erfc}$  is the complementary error function (see Table J-1). This expression for  $w$  is reasonably accurate (within 10 percent) for  $r/B > 1$  and is very accurate (within 1 percent) for  $r/B > 10$ .

Note that at large times (i.e., as  $u$  goes to zero) the leaky well function reduces to the modified Bessel function  $K_0$ :

$$W(0, r/B) = 2K_0(r/B)$$

If  $r/B$  is larger than one, the following approximation for the Bessel function can be made:

$$K_0(r/B) = \left(\frac{\pi B}{2r}\right)^{1/2} \exp\left(-\frac{r}{B}\right)$$





United States  
Environmental Protection  
Agency

Center for Environmental Research  
Information  
Cincinnati OH 45268

Official Business  
Penalty for Private Use, \$300

FOURTH CLASS PERMIT

J. Russell Boulding  
4664 N. Rob's Lane  
Bloomington IN 47401

Please make all necessary changes on the above label,  
detach or copy, and return to the address in the upper  
left-hand corner.

If you do not wish to receive these reports CHECK HERE   
detach, or copy this cover, and return to the address in the  
upper left-hand corner.

EPA/600/6-85/002b

EPA/600/6-85/002c  
September 1985

WATER QUALITY ASSESSMENT:  
A Screening Procedure for Toxic  
and Conventional Pollutants  
(Revised 1985)  
Part III

by

W. B. Mills, J. D. Dean, D. B. Porcella, S. A. Gherini, R. J. M. Hudson,  
W. E. Frick, G. L. Rupp, and G. L. Bowie

Tetra Tech, Incorporated  
Lafayette, California 94549

Contract No. 68-03-2673

Prepared in Cooperation with U.S. EPA's

Center for Water Quality Modeling  
Environmental Research Laboratory  
Athens, Georgia

Monitoring and Data Support Division  
Office of Water Regulations and Standards  
Office of Water  
Washington, D.C.

Technology Transfer  
Center for Environmental Research Information  
Cincinnati, Ohio

ENVIRONMENTAL RESEARCH LABORATORY  
OFFICE OF RESEARCH AND DEVELOPMENT  
U.S. ENVIRONMENTAL PROTECTION AGENCY  
ATHENS, GEORGIA 30613

① 2/1/85

**Blank Page**

---



## APPENDIX F

### RESERVOIR SEDIMENT DEPOSITION SURVEYS

The material in this appendix consists of a reproduction of a bulletin compiled by F. E. Dendy and W. A. Champion, which provides data on rates of sedimentation in U. S. reservoirs.

#### INTRODUCTION

Data from known reliable reservoir sedimentation surveys made in the United States through 1970 are summarized in this bulletin. Additional data from surveys made after 1970 are included for a few reservoirs.

This bulletin supersedes USDA Miscellaneous Publication No. 1143, which was published in May, 1969.<sup>1/</sup> All reservoir surveys reported in Miscellaneous Publication No. 1143 have been repeated in this bulletin. In addition, it includes surveys made before 1965, but not previously reported, and new data on reservoirs surveyed or resurveyed since 1965. The reservoirs are located in all of the 48 conterminous United States, except Florida, and in Puerto Rico. In addition to data on storage reservoirs and ponds, some information on debris basins is included.

A supplement to this bulletin, from which the data were extracted and summarized, contains detailed information about each of the reservoirs

---

<sup>1/</sup> Dendy, F.E. and Champion, W.A., Compilers. Summary of Reservoir Sediment Deposition Surveys Made in the United States Through 1965. U.S. Department of Agriculture Miscellaneous Publication No. 1143, 64 pp., May, 1969. (Cooperative report with the Sedimentation Committee. Water Resources Council).

listed in the summary table. The method used in presenting this information is given on pages F-2, F-3, F-4 and F-5. The supplement has not been distributed with this bulletin because of its bulk and because the detailed information is not of general interest. Copies are available in the offices of the agencies represented on the Sedimentation Committee of the Water Resources Council. Reprints of data sheets for specific reservoirs may be obtained on request from the Director, USDA Sedimentation Laboratory, U.S. Department of Agriculture, Oxford, Miss. 38655. Requests for information not contained in this bulletin or in the supplement should be directed to the agency supplying the data.

The accuracy of the survey data varies greatly. Surveys range from reconnaissance measurements of sediment depth at a few locations to detailed surveys based on closely spaced cross sections or contours. No attempt has been made to classify the surveys according to degree of accuracy.

Information in this bulletin and in the supplement should prove useful to engineers and watershed planning specialists in private and public practice who are concerned with problems of reservoir sedimentation. Engineers, engineering firms and local government agencies who have data on similar reservoir surveys are invited to make this information available to the Sedimentation Committee, WRC, for inclusion in supplements to this publication.

#### EXPLANATION OF THE SUMMARY TABLE

Data in the summary table of this bulletin were obtained from the reservoir sedimentation survey data sheets contained in the supplement. Dashes in columns of the table signify that data were unavailable or that the column is not applicable for the reservoir.

Reservoirs are grouped according to the 79 drainage areas into which the United States has been divided as shown in the publication, "River Basin Maps Showing Hydrologic Stations," compiled under the auspices of the Subcommittee on Hydrology, Federal Inter-Agency River Basin

Committee.<sup>2/</sup> An index map of these drainage areas is shown on page **F-78**. The drainage areas in which the reservoirs are located are shown as subheadings in the summary table. The first of the two numbers identifying a reservoir indicates the drainage basin in which it is located. The second number denotes the particular reservoir in the drainage area and is based upon the order in which the data were prepared. These numbers are the same as those identifying the corresponding survey data sheets in the supplement. When a survey data sheet is revised or when another sheet is prepared with information for additional surveys, the identification number is modified by the addition of letters beginning with a; for example, 13-2, 13-2a, and 13-2b.

Total drainage area includes the reservoir area and the area lying above all upstream dams but generally excludes noncontributing drainage areas lying within the watershed boundary. Where available, the drainage area figure published by the U.S. Geological Survey in Water-Supply Papers is usually used. The net drainage area is the sediment-contributing area and generally excludes the reservoir area and the drainage areas above upstream reservoirs, or other structures which are effective sediment traps.

The first date shown usually corresponds to the beginning of storage when sediment deposition began. However, for some reservoirs the first date represents the date of the contour or range survey made after the reservoir had been in operation for some time.

For most reservoirs, the storage capacity given is the total storage below the level of the crest of an ungated spillway or the top of gates (less gate-height freeboard, if any) of gated spillways. Where capacity values below the spillway crest elevation are given, footnotes are used to explain.

---

<sup>2/</sup> U.S. Inter-Agency Committee on Water Resources, Subcommittee on Hydrology. River Basin Maps Showing Hydrologic Stations. U.S. Dept. Com., Weather Bur., Notes on Hydrol. Activ. Bul. 11, 79 pp., 1961.

The capacity-average annual inflow ratio (C/I ratio) was derived from the reservoir storage capacity and the average annual inflow. Normally the average annual inflow for the entire period of record was used to compute the C/I ratios. This time period may or may not correspond to the period for which sediment accumulation was given. Generally, the C/I ratio was not given if upstream structures controlled 25 percent or more of the drainage area.

The specific weight of deposited sediment is an average or weighted value for the reservoir, determined generally from samples of deposits. In view of the variations with depth and location within the reservoir, specific weight is generally an approximation for the reservoir. The entry is marked by an asterisk where the specific weight is assumed or is calculated from field data or the size-frequency grading of the deposits.

The average annual rate of sediment accumulation (acre-feet and tons per square mile of net drainage area) pertains to sediment deposited in the reservoir below the full pool elevation. Sediment deposited in deltas above full pool level or sediment discharged from the reservoir is not included unless explained by footnote. For reservoirs with more than one survey and where the latest survey indicated an increase in the specific weight of deposited sediment, the annual sediment accumulation rate in tons per square mile was not always computed in the same manner. For some reservoirs, compaction of earlier sediment was considered and in others it was not. All of the deposited sediment was assumed to have been transported into the reservoir by water.

The agency supplying data is shown in the last column of the table. This agency either has the basic data available or has access to it through cooperative arrangements. The symbols used in this column apply to the following agencies:

ARS - Agricultural Research Service	ODW - Ohio Department Natural Resources-- Division of Water
BR - Bureau of Reclamation	
CE - Corps of Engineers	SCS - Soil Conservation Service
FS - Forest Service	
GS - Geological Survey	TVA - Tennessee Valley Authority
IWS - Illinois State Water Survey	

#### FORM FOR REPORTING RESERVOIR SEDIMENTATION

A completed sample of the reservoir sedimentation data sheet from the supplement is shown on pages **F-79** and **F-80**. This sheet is a convenient and standard form for reporting results of reservoir surveys. An invitation is extended to readers, particularly those practicing engineering individually, in engineering firms, or in local government agencies, to prepare sheets covering surveys known to them but not included in this publication. A blank "Reservoir Sedimentation Data" sheet is enclosed as a tear sheet on pages **F-81** and **F-82**. Additional data sheets may be obtained from the department offices listed on the title page or the form may be reproduced if desired. The completed forms may be sent to any one of the agencies represented on the Sedimentation Committee for inclusion in supplements to this bulletin.

SUMMARY OF  
RESERVOIR SEDIMENTATION SURVEYS MADE IN THE UNITED STATES THROUGH 1970

DATA SHEET NUMBER	RESERVOIR	STREAM	NEAREST TOWN	DRAINAGE AREA (SQUARE MILES)		DATE OF SURVEY	PERIOD BETWEEN SURVEYS (YEARS)	STORAGE CAPACITY (ACRE-FT.)	CAPACITY SPECIFIC INFLOW RATIO (ACRE-FT. PER ACRE-FT.)	SPECIFIC WEIGHT (LB. PER CU. FT.)	AVG. ANN. ACCUMULATION PER SQ. MI. AREA FOR PERIOD SHOWN		AGENCY SUPPLYING DATA
				TOTAL	NET						AC.-FT.	TONS	
1-1	Little River Res. #2	Little River	Belfast, Me.	13.9	13.8	1933 Oct. 1969	56	456 341	*0.029 .021	+100	0.15	326	SGS
HOUSTONIC, CONNECTICUT, THAMES, AND MERRIMACK RIVER BASIN													
2-1	Broad Brook	Broad Brook River	Broad Brook, Conn.	5.13		1916 Sept. 1951	35	3,706 1,162		+50	.33	319.4	SGS
2-2	Mountain Street	Trib. of Beaver Brook	Greenfield, Mass.	.8		1905 Sept. 1951	46	1,074.2 1,056.1		+50	.56	609.8	SGS
2-3	Plants Pond	Eightmile Run	Plantville, Conn.	15.76		1850 Sept. 1951	101	1,650.0 84.8		+50	.01	10.9	SGS
2-4	Southington Reservoir	Budd River	Southington, Conn.	1.08		1883 Sept. 1951	68	321.8 314.0		+50	.10	108.9	SGS
2-5	Hallingford	Pine River	Hallingford, Conn.	8.98		1943 Sept. 1951	10	433.4 430.0		+50	.04	43.6	SGS
2-6	West Whately	Ivory Brook	West Whately, Mass.	9.0		1902 Sept. 1951	49	76.7 71.2		+50	.012	13.07	SGS
2-7	Westfield	Moose Mountain Branch	Westfield, Mass.	2.52		1874 Sept. 1951	77	564.8 565.8		+50	.094	102.4	SGS
HUDSON RIVER BASIN AND ST. LAWRENCE DRAINAGE IN NEW YORK													
3-1	Schoharie (Gilboa Dam)	Schoharie Creek	Prattville, N. Y.	311	312.32	1926 Aug. 1950	21.8	63,821 62,702		+60	1/1.66	1/217	SGS
3-2	Englishtown Pond	Weaconk Creek	Englishtown, N. J.	7.2	7.19	1755 May 1955	200	42.3 13.5	.005 .002	+60	.02	26.14	SGS
3-3	Carriage Lake	Hillstone River	Princeton, N. J.	155	47.8	1907 Dec. 1950	42.8	1,256 954		+50	2/1.20	217.8	SGS
3-4	Maplinger	Maplinger Creek	Maplinger Falls, N. Y.	197		1959 Sept. 1900	9.0	3/822 604.4		+50	.01	10.89	SGS
SUSQUEHANNA AND DELAWARE RIVER BASINS													
4-1a	Loch Raven Reservoir	Cunnefer Falls River	Towson, Md.	303	4/219.4	1914 Oct. 1963	59	5/70,169 2/64,813		+60	1/618	1/608	SGS
4-2a	Prentissburg	Roaring Brook	Hartford, Md.	80	77.5	1933 Apr. 1963	18	60,579 60,610		+60	.699	923	SGS
4-3	Griffin	Griffin Creek (Legget)	Seranton, Pa.	3.21	3.04	1888 Sept. 1961	18	59,864 1,971		+60	.391	547	SGS
4-4	Elmhurst	Roaring Brook	Seranton, Pa.	34.85	34.55	1943 May 1943	53	3,746 3,746		+60	.237		SGS
4-5	Lake Williams	Corbous Creek	Tork, Pa.	42.9	42.6	1912 May 1941	51	2,686 2,686		+60	.034		SGS
4-6	William Bridge	Stafford Meadow Brook	Seranton, Pa.	5.0	4.94	1939 Apr. 1951	27	2,232 1,051		+60	.594	421	SGS
4-7a	Adkisson Reservoir	Mintape Run	Bal Air, Md.	45.46	45.35	1943 May 1943	46	896.19 705.32	.025 .019	+60	.022		SGS
4-8a	Palto Dam	Dean Creek	Speacon, N. Y.	.41	.41	1865 July 1955	11	617.06 56.04	.017 .130	+60	.177	459	SGS
4-9a	Pykiss Dam	Roaring Brook	Speacon, N. Y.	.71	.71	1957 Aug. 1966	8.9	55.90 55.60	.129 .128	+60	.170	296	SGS
4-10	Columbia Dam	Paulinus Kill River	Columbia, N. J.	171	171	1955 July 1957	8.9	187.31 186.70	.250 .249	+60	.083	141	SGS
4-10	Columbia Dam	Paulinus Kill River	Columbia, N. J.	171	171	1957 July 1957	70	311.77 244.19	.700 1.119	+60	.130	226.5	SGS

Project No.	Project Name	Location	State	Year	Area (Acres)	Volume (cu ft)	Cost (\$)	Remarks
4-11	Old Glafelter	Spring Grove, Pa.	Pa.	1884	74.3	117.2	---	SGS
4-12	Fallington Reservoir	---do---	Pa.	1929	2.91	10.0	0.034	SGS
4-13	Lake Rushford	---do---	Pa.	1927	---	63.0	---	SGS
4-14	Isedale	Canaan, N. Y.	N. Y.	1929	60.7	28,000	0.669	SGS
4-15	Coatsville	---do---	Pa.	1925	20.0	27,426	0.37	SGS
4-16	Liberty Reservoir	---do---	Pa.	1900	5.0	137	0.03	SGS
4-17	Little Deer No. 1	Wards Chapel, Md.	Md.	1921	164	138,762.4	0.28	SGS
4-18	Mount Morris	Mdonna, Md.	Md.	1921	1,077	138,227.0	0.426	SGS
4-19	Patterson Creek #1	Mount Morris, N. Y.	N. Y.	1921	4.3	338,010	0.25	SGS
4-20	Little Chocanut #2B	Chocanut Center, N. Y.	N. Y.	1921	1.64	335,353	0.20	SGS
5-1a	Lake Barcroft	Tribe of Potomac River	Va.	1915	14.5	87.4	---	SGS
5-2	Pedlar River	---do---	Va.	1938	31.21	9/1,762	0.257	SGS
5-3	Burnt Mill	---do---	Va.	1927	---	1,890	0.728	SGS
5-4b	Greenbelt Lake	---do---	Md.	1920	27.0	1,181	0.134	SGS
5-5	Stanton	---do---	Va.	1925	25	385	0.034	SGS
5-6	Jack	---do---	Va.	1927	337	4,250	0.053	SGS
5-7b	Triadelphia L. (Brighton D.)	---do---	Md.	1922	81.4	12,202,222	0.111	SGS
5-8	Gordon Lake	---do---	Md.	1920	64	20,089	0.20	SGS
5-9	Thomas N. Koon Lake	---do---	Md.	1924	60	19,633	0.72	SGS
5-10	Savage River Dam	---do---	Md.	1924	60	19,045	1.25	SGS
5-11	Rocky Forge	---do---	Md.	1924	60	3,129	1.090	SGS
5-12	South River, Site 26	---do---	Md.	1924	60	7,312	0.036	SGS
5-13	Wild Lake	---do---	Md.	1924	60	20,200	0.643	SGS
6-1	Lake Apex	Apex, N. C.	N. C.	1925	4.0	106	0.19	SGS
6-2	Franklin	Franklin, N. C.	N. C.	1925	1.13	94	---	SGS
6-3	Greenboro (L. Brandt)	Greenboro, N. C.	N. C.	1923	74.1	2,870	0.509	SGS
6-4	High Point	High Point, N. C.	N. C.	1928	62.8	2,610	0.308	SGS

POTOMAC, RAPPAHANNOCK, YORK, AND JAMES RIVER BASINS

10/ Revised 1968.  
 11/ 9 acres-feet raised by dredging.  
 12/ Revised due to movable control gates.  
 13/ Koon Lake, upstream, was built in 1922.  
 14/ Based on total sediment in both Gordon Lake and Koon Lake.  
 15/ Does not include 4.34 acre-feet dredged.  
 16/ Includes 4.34 acre-feet dredged in early spring 1968.  
 17/ Estimated or assumed.

CHOMAN, ROANOKE, TIB, REUSE, AND CAPE FEAR RIVER BASINS

1/ Includes estimated 112 acre-feet passing through Shandaken Tunnel.  
 2/ Includes 103 acre-feet of sediment dredged in 1937-1939.  
 3/ Partial survey covering segments 1-14 for Stony Brook Dam Only.  
 4/ Net sediment contributing area was 299.4 sq. mi. until 1933 when Prettyboy Dam was completed.  
 5/ This area was used in the 1943 calculations.  
 6/ Revised after 1961 survey.  
 7/ Conservation or sediment pool only.  
 8/ Not determined - assumed equal to that determined in 1963.  
 9/ Based on original spillway crest elevation 205 feet m. s. l.  
 10/ Based on original crest elevation 210 feet m. s. l. and assumed crest of 2,300 acre-feet resulting from 1942 addition to top of dam.

SUMMARY OF  
RESERVOIR SEDIMENTATION SURVEYS MADE IN THE UNITED STATES THROUGH 1970

DATA SHEET NUMBER	RESERVOIR	STREAM	NEAREST TOWN	DRAINAGE AREA (SQUARE MILES)		DATE OF SURVEY	PERIOD BETWEEN SURVEYS (YEARS)	STORAGE CAPACITY (ACRE-FT.)	CAPACITY SPECIFIC WEIGHT (DRY) (LB. PER CU. FT.)	AVG. ANN. SEDIMENT ACCUMULATION PER SQ. MI. OF NET DR. AREA FOR PERIOD SHOWN		AGENCY SUPPLYING DATA
				TOTAL	NET					AC.-FT.	TONS	
6-5	Lake Michie	Flat River	Durham, N. C.	167.5	166.7	Apr. 1926	8.75	12,671	---	0.271	---	SCS
6-6	Sanford City	Lick Creek	Sanford, N. C.	3.75	3.73	Feb. 1927	---	12,276	---	.150	---	SCS
6-7	University Lake	Morgan Creek	Chapel Hill, N. C.	30.6	31.3	June 1932	14.33	95	---	---	---	SCS
6-8	Roxboro City Lake	Satterfield Creek	Roxboro, N. C.	7.62	7.52	Apr. 1934	2.9	1,915	---	.728	---	SCS
6-9	Burlington Municipal	Stony Creek	Burlington, N. C.	105.2	105.0	June 1941	17.2	460.3	---	.548	---	SCS
6-10a	Walnut Cove	Dan River	Walnut Cove, N. C.	397	397	Sept. 1929	11.5	1,488	---	.155	21.3	SCS
6-11	John H. Kerr	Roanoke River	South Hill, Va.	7,800	7,391	July 1952	3/9	2,808,600	.001	.214	200	CS
6-12	Phillipott	Smith River	Basett, Va.	212	185.7	Dec. 1951	7.4	2,750,349	.484	1.06	754	CS
						Nov. 1960	8.9	1,964,000	.949	2.06	2,103	CS
PSE DBS, SAINTS, AND EDISTO RIVER BASINS												
7-1	Chester	Sandy River	Chester, S. C.	16.05	15.92	Nov. 1926	---	682	---	---	---	SCS
7-2	Lanoster	Turkey Quarter Creek	Lanoster, S. C.	9.40	9.34	Feb. 1925	11	585	---	.55	---	SCS
7-3a	Spartanburg Municipal	South Phoebe River	Flaggville, S. C.	91.33	90.8	May 1928	13.4	371,506	65.3	.417	593	SCS
						July 1934	16.2	371,199	---	3/612	---	SCS
						Oct. 1947	12.7	372,881	---	3/268	---	SCS
						Oct. 1965	18.6	372,593	---	3/176	---	SCS
7-4	Appalachia	South Tyger River	Greer, S. C.	63.0	62.8	Oct. 1904	18.6	53,109	---	---	---	SCS
7-5	Albemarle City Lake	Long Creek	Albemarle, N. C.	33.0	32.5	July 1934	30	2,500	---	.48	---	SCS
7-6	Cannon Lake	Buffalo Creek	Kannapolis, N. C.	18.0	17.7	Feb. 1924	15.5	1,070	---	.302	---	SCS
7-7	Lake Concord	Chambers & Rose Branch	Kannapolis, N. C.	4.7	4.54	Aug. 1939	1.9	2,600	---	---	---	SCS
						June 1941	10.2	2,574	---	.774	---	SCS
						Mar. 1925	10.2	1,721	---	1.71	---	SCS
						May 1935	10.2	1,822	---	---	---	SCS
						Mar. 1940	18.0	1,163	---	.024	---	SCS
7-8	Entwistle No. 3	Hitchcock Creek	Rosewell, N. C.	168.0	5/18.0	Mar. 1915	48.0	1,104	---	.019	---	SCS
7-9	High Rock	Little River	Troy, N. C.	269	269	Mar. 1940	25.0	976	---	---	---	SCS
7-10	Lake Lee	Jackson River	Salisbury, N. C.	3,930	3,863	Nov. 1927	7.8	289,432	---	.462	---	SCS
7-11	Fee Dee Mfg. Co.	Richardson Creek	Minors, N. C.	50.50	50.34	Apr. 1927	11.1	275,516	---	.302	406	SCS
7-12	Salmon	Hitchcock Creek	Rockingham, N. C.	176	5/25	June 1874	66	652	61.8	---	---	SCS
7-13	Normod L. (Tillery)	Salmon Creek	Minions-Salem, N. C.	27.68	27.26	Mar. 1940	66	464	---	.036	---	SCS
7-14	Lanidom	Fee Dee River	St. Uilead, N. C.	4,600	5/431	Sept. 1939	19.8	3,099	---	.444	367	SCS
7-15	Third Creek Site No. 7	Leonora Creek	Lexington, N. C.	6.75	6.66	July 1928	11.75	136,473	---	.696	---	SCS
						Mar. 1930	11.75	133,162	---	---	---	SCS
						Aug. 1940	4.6	441	45.5	.692	685	SCS
						Mar. 1951	11.1	419	25.5	.299	296	SCS
						Sept. 1962	4.5	948.4	7/62.2	.61	826	SCS
						Mar. 1965	3.0	945.9	7/62.2	.18	244	SCS
						Apr. 1969	4.1	943.1	7/62.2	.14	190	SCS





SUMMARY OF  
RESERVOIR SEDIMENTATION SURVEYS MADE IN THE UNITED STATES THROUGH 1970

DATA SHEET NUMBER	RESERVOIR	STREAM	NEAREST TOWN	DRAINAGE AREA (SQUARE MILES)		DATE OF SURVEY	PERIOD BETWEEN SURVEYS (YEARS)	STORAGE CAPACITY (ACRE-FT.)	CAPACITY INFLOW RATIO (PER ACRE-FT.)	SPECIFIC WEIGHT (DRY) (L.B. PER CU. FT.)	AVG. ANN. SEDIMENT ACCUMULATION		AGENCY SUPPLYING DATA
				TOTAL	NET						AC.-FT.	TONS	
15-1	Lake Hamilton	Ouachita River	Hot Springs, Ark.	1,421	1,413.4	Dec. 1950	19.4	156,315	..50	..	0.11	120	SGS
15-2	Lake Minors	Alum Fork Saurin River	Little Rock, Ark.	43.0	41.3	May 1950	12.6	15,279	..50	..	.37	403	SGS
15-3	O. P. White Pond	Trib. of Chewalla Creek	Holly Springs, Miss.	..	..	Oct. 1947	3.3	34,340	63.65	..	13.1	18,200	SGS
15-4	B. H. Hennesaker Pond	Trib. of Coldwater River	Slayden, Miss.	..	..	Jan. 1947	4.0	12.0	60.09	..	15.3	20,000	SGS
15-5	C. S. Hurdle Pond	Trib. of Coldwater River	Holly Springs, Miss.	..	..	Jan. 1946	4.1	36.4	62.9	..	7.78	10,700	SGS
15-6	Agnes Jones Pond	Trib. of Red Banks Creek	Holly Springs, Miss.	..	..	Oct. 1945	2.3	28.0	67.27	..	12.4	18,200	SGS
15-7	Lee Johnson Pond	Trib. of Red Banks Creek	Holly Springs, Miss.	..	..	Jan. 1945	4.3	17.8	76.13	..	16.6	27,500	SGS
15-8	P. T. Kolesander	Trib. of Coldwater River	Holly Springs, Miss.	..	..	Sept. 1945	2.3	14.8	84.24	..	12.4	22,800	SGS
15-9	Lake Shakkoka	Trib. of Camp Creek	Olive Branch, Miss.	..	..	Jan. 1942	8.5	206	..	..	8.03	10,800	SGS
15-10	Lake Woodland	Trib. of Camp Creek	Olive Branch, Miss.	..	..	Jan. 1941	17.0	396	..	..	5.52	4,800	SGS
15-11	C. L. Patton Pond	Trib. of Red Banks Creek	Warren, Miss.	..	..	Feb. 1941	6.0	94	39.9	..	4.48	6,520	SGS
15-12	G. B. Livingston, Jr., Pond	Trib. of Red Banks Creek	Warren, Miss.	..	..	Feb. 1941	4.0	12.3	66.8	..	6.55	9,040	SGS
15-13	Fletcher Hurdle Pond (North)	Trib. of Bynalia Creek	Victoria, Miss.	..	..	Feb. 1941	4.0	4.61	63.3	..	12.5	17,100	SGS
15-14	Fletcher Hurdle Pond (South)	Trib. of Bynalia Creek	Victoria, Miss.	..	..	Feb. 1941	4.0	5.48	85.1	..	16.8	30,400	SGS
15-15	C. C. Stevenson Pond	Trib. of Cuffass Creek	Holly Springs, Miss.	..	..	Aug. 1948	2.7	6.71	78.8	..	26.0	44,600	SGS
15-16	Gayoso Lake	Trib. of Mississippi River	Horn Lake, Miss.	..	..	Feb. 1942	9.0	53.0	51.85	..	3.13	3,530	SGS
15-17	Ben O. Pettis Pond	Trib. of Toby Tubby Creek	Oxford, Miss.	..	..	Feb. 1946	35.0	1.07	58.72	..	2.39	3,060	SGS
15-18	C. D. Williams Pond	Trib. of Hudson Creek	Oxford, Miss.	..	..	Mar. 1928	23.0	6.70	55.72	..	3.35	4,070	SGS
15-19	R. X. Williams	Trib. of Iacona River	Taylor, Miss.	..	..	Sept. 1946	4.5	2.54	47.74	..	20.5	21,300	SGS
15-20	Henry W. Ramsey Pond	Trib. of Sartor Creek	Oxford, Miss.	..	..	Jan. 1933	18.2	227	41.75	..	2.61	2,370	SGS
15-21	Dr. Bramlett Pond	Trib. of Pumpkin Creek	Batesville, Miss.	..	..	Jan. 1931	11.2	214	*37	..	1.12	913	SGS
15-22	A. S. Kyle Pond	Trib. of Tallahatchie R.	Holly Springs, Miss.	..	..	Mar. 1945	6.0	16.6	52.04	..	3.14	3,560	SGS
15-23	Ben P. Smith Pond	Trib. of Pigeon Roost Cr.	Holly Springs, Miss.	..	..	July 1947	3.7	3.77	67.38	..	1.89	7,100	SGS
15-24	A. L. Redman Pond	Trib. of Arkansas Creek	Arkabutla, Miss.	..	..	Mar. 1945	5.5	30.5	*50	..	1.95	2,120	SGS
15-25	Charles Dockery Pond	Trib. of Hurricane Creek	Eudora, Miss.	..	..	Jan. 1946	5.2	22.0	*44	..	3.60	3,420	SGS
15-26b	Arkabutla Reservoir	Calocheater River	Arkabutla, Miss.	1,000	948	Apr. 1951	6.33	525,300	*695	..	6.27	819	BE
15-27a	W. W. Murphy Pond	Trib. of Jones Creek	Holly Springs, Miss.	..	..	Nov. 1953	2.5	521,540	*695	..	6.27	819	ARS
15-28a	Powerline Dam	East Gause Creek	Oxford, Miss.	..	..	Nov. 1953	4.2	1,222.68	*194	..	6.20	810	ARS
						Sept. 1959	3.3	1,184	*169	..	2/8.4	2/15,465.7	
						Nov. 1963	4.2	1,134	*132	..	2/14.8	2/7,448.8	
						Apr. 1953	2.1	26.26	*133	..	2/3.5	2/6,860.7	
						May 1955	7.0	21.34	..	..	2/5.66	2/8,136.1	
						June 1960	1.66	30.07	..	..	2/5.30	2/8,949.4	
						Aug. 1962	2.15	19.40	..	..	2/7.38	2/2,103.9	

LOWER MISSISSIPPI RIVER BASINS (HELENA TO MATCHEZ)  
Yazoo, Big Black, and Ouachita River Basins

15-29a	Andrew Smith Pond	Trib. of Jones Creek	Holly Springs, Miss.	.327	.300	Nov. 1953	1/22.72	.123	490	2/6.2 2/12.151.2	AMS
15-10a	Sardis Reservoir	Little Tallahatchie River	do	1.545	1.454	Sept. 1957	17.77	*.096	490	2/2.07 2/1.037.6	CS
15-11	End Reservoir	Iocoma River	do	.560	.516	May 1940	1,549.316	.824	460	.687 898	CS
15-22	Grenada Reservoir	Yalobusha River	do	1.320	1.219	May 1961	657.201	1.068	460	.758 729	CS
	do	do	do			July 1952	1,337.400	.969			
	do	do	do			May 1965	1,320,000	.977	460	1.205 1,575	
LOWER MISSISSIPPI RIVER BASIN (CHESTER TO HELENA) St. Francis River Basin											
16-1	Grisham	Lost Creek	Bismark, Mo.	.146	.145	Oct. 1920	24.05	*.077	75.4	1.133 1,860	SC
16-2	Mountain Lake	Trib. of Bluffs Creek	Patterson, Mo.	1.90	1.87	July 1927	17.56	*.063	54.8	.213 254	SCS
16-3	Shepherd Mountain	Trib. of Stouts Creek	Ironton, Mo.	.99	3.96	July 1929	171		64	.338 471	SCS
16-4	Loch Mary	Brown Creek	do	3.81	3.65	July 1939	158		50	.600 784	INS
16-5	Carbondale	Piles Fork	Carbondale, Ill.	3.00	2.77	Dec. 1908	1,184		73.9	3.15 5,070	INS
16-6	Daring Coal Co. Pond	Trib. of Wolf Creek	do	.219	.206	Aug. 1926	1,386		*76	2.64 4,370	INS
16-7	Eldorado	do	Eldorado, Ill.	2.23	1.87	Oct. 1919	89.3		*67	2.18 3,180	INS
16-6	West Rankfort	Wolf Creek	do	4.03	3.75	Oct. 1923	644.4			2.46	INS
16-9	Pineriew (Lower)	Fillis Creek	West Rankfort, Ill.	.63	.07	Aug. 1926	728.0			67.993	SCS
16-10	Pineriew (Middle)	do	do	.56	.06	Aug. 1926	5,168.4			1.43 1,870	SCS
16-11	Pineriew (Upper)	South Fork Jonasa Creek	Farmington, Mo.	.49	.18	July 1919	1,487.8			3.3 4,310	SCS
16-12	Killbuck	do	do	51	51	July 1919	816	*.025	460	.983 825	SCS
16-13a	Mappello	Big Creek	Annapolis, Mo.	1.310	1.206	July 1929	622	*.016	460	.133 174	CS
16-14a	Lake Miller	St. Francis River	Poplar Bluff, Mo.	4.65	4.43	July 1929	625,000	.540		9,4114	
16-15	Flucka Lake	Casey Fork	do	.339		July 1927	624,551	.539		.5705	
16-16	Baker's Lake	Unamed	do	.26	.316	Mar. 1964	613,461	.530			
16-17	Crab Orchard Lake	do	do	.26		Mar. 1964	1,446	.262	34.0	1.20 688	INS
16-18	Marion	do	Marion, Ill.	.26	.25	June 1919	58.1	.267	56.6	1.11 1,368	INS
16-19	Little Grassy Lake	do	do	6.5	6.31	1921	24.0	.143	36.8	.64 512	INS
16-20	Herrin Reservoir No. 1	do	Carbondale, Ill.	1.78	1.60	Aug. 1951	67,320	.611	47.5	1.91 1,976	INS
16-21	Knights of Pythias Lake	do	Marion, Ill.	.33	.32	July 1951	705	.580		.61 458	INS
16-22a	Lake Ashley	do	Carbondale, Ill.	1.24	1.17	July 1951	590	.141	34.5	2.85 2,402	INS
16-23	Christopher	do	Herrin, Ill.	.923	1.70	July 1951	25,741	2,568	27.5	.32 192	INS
	do	do	do			Aug. 1951	178	.155	82.9	1.22 1,671	INS
	do	do	do			Dec. 1925	74.6	.390		.69 692	INS
	do	do	do			Aug. 1921	160	.202		1.01 816.1	INS
	do	do	do			Aug. 1924	383.94	.598			
	do	do	do			July 1960	353.59	.551	37.1	1.01	

1/ Sediment or conservation pool only.  
 2/ Includes sediment within original flow line of reservoir and above conservation pool.  
 3/ Original sediment range surveys.  
 4/ Used as beginning date of sediment deposits.  
 5/ Spillway crest raised from 439 to 441.77 ft. m.s.l. in April 1963. All data computed on basis of 441.77 ft. at spillway elevation.  
 6/ Net sediment volume in 1949 was 120.5 ac.-ft. due to completion of eariler deposits.  
 7/ Dam failed spring 1938, survey conducted July 24, 1939.  
 8/ Original data from topographic survey of 1955-56.  
 9/ Based on incomplete resurvey; 1963 value of 0.57 is more reliable.  
 \* Estimated or assumed.

SUMMARY OF  
RESERVOIR SEDIMENTATION SURVEYS MADE IN THE UNITED STATES THROUGH 1970

DATA SHEET NUMBER	RESERVOIR	STREAM	NEAREST TOWN	DRAINAGE AREA (SQUARE MILES)		DATE OF SURVEY (YEARS)	PERIOD BETWEEN SURVEYS (YEARS)	STORAGE CAPACITY (ACRE-FT.)	CAPACITY SPECIFIC WEIGHT (DRY) (LB. PER CU. FT.)	AVG. ANN. ACCUMULATION PER SQ. MI. AREA FOR PERIOD SHOWN	AGENCY SUPPLYING DATA
				TOTAL	NET						
LOWER MISSISSIPPI RIVER BASIN (CHESTER TO MEMPHIS)											
St. Francis River Basin (Continued)											
16-24	Lake DuQuoin	Reese Creek	DuQuoin, Ill.	10.73	10.35	1917	—	2,003	116	—	IMS
16-25	M. F. Farrell	Trib. of Harper Creek	W. Vernon, Ill.	.519	.512	July 1945	20	1,870	.295	0.64	IMS
16-26a	1788 at Thompsonville	Trib. of Boies Creek	Thompsonville, Ill.	1.799	1.725	June 1960	15	27.4	.079	1.06	IMS
16-27	Lake Johnson City	Lake Creek	Johnson City, Ill.	3.85	3.75	Aug. 1922	34	322.64	.283	.880	IMS
16-28	Valley Outing Club	Andy Creek	Valley, Ill.	2.47	2.37	Aug. 1922	35	394	.165	.59	IMS
16-29	West Parkfort (New)	Stevens Creek	West Parkfort, Ill.	7.622	7.288	Aug. 1922	35	320	.180	.59	IMS
16-30	Lake Reel-Bain (Walker Lake)	Unnamed	Dixon, Ky.	2.05	1.96	July 1926	15	2,528.9	.52	2.41	IMS
16-31	Bough River PIS No. 1	Buffalo Creek	Kingswood, Ky.	2.85	2.85	May 1924	16	617	.228	4.6	SCS
16-32	Oxym Creek PIS #2L	Unnamed Trib. Little Creek	Forest Park, Ky.	.37	.36	June 1920	14.64	396.12	.230	1/50	SCS
16-33	Mad River PIS No. 1a	Antioch Creek	Sharon Grove, Ky.	8.59	8.56	Nov. 1925	5	3,280.80	4.22	1/86	SCS
16-34	Coney Creek PIS #2	Bennet Fork	Cheyville, Ky.	5.77	5.65	May 1920	6.33	1,279.87	.15	75.78	SCS
16-35	Big Ready PIS #1	West Fork	Reedsville, Ky.	6.76	6.69	May 1920	4.5	1,228.4	.33	71.75	SCS
						Apr. 1926	5.4	976.95	1.10	71.58	SCS
						Apr. 1970			1/54	1/92.4	
OHIO RIVER BASIN (MADISON TO UNDFORTW)											
Sabash River Basin											
17-1	Huntingburg (Upper)	Trib. of Patoka River	Huntingburg, Ind.	.67	.63	July 1894	—	117	*.284	—	SCS
17-2a	Oakland City #1	S. Fork Patoka River	Oakland City, Ind.	.52	.40	Sept. 1920	46.3	139	*.229	.617	SCS
17-3	Shafter Lake	Tippecanoe River	Monticello, Ind.	1,700	1,698	Aug. 1925	19.0	2/834.8	*2.116	1.977	SCS
17-4	Spring Mill	Mill Creek	Mitchell, Ind.	15.03	13/5.29	Aug. 1920	24.9	111.0	*.017	2.680	SCS
17-5	Greendale Lake	Connor's Branch	Hamis, Ill.	25.1	25.0	Sept. 1929	17.2	178	*.016	.023	SCS
17-6	Ridge Lake	Trib. of Sabarras River	Charleston, Ill.	1.41	1.38	Sept. 1929	9.9	127	.023	.975	SCS
17-7	Vermilion Lake	Trib. of Vermilion River	Danville, Ill.	267	266	June 1925	6.4	171.9	*.061	1.75	SCS
17-8	Broom Park Lake	Trib. of Haccoon Creek	Piara, Ill.	1.34	1.33	Oct. 1920	25.3	7,438	*.052	1.79	SCS
17-9	Craig & Davidson's Lake	None	Marionville, Ill.	.465	.427	June 1927	—	19.08	.057	.179	SCS
17-10	Greendale Lake	Trib. of Little Creek	Laclede, Ill.	.34	.31	Aug. 1928	12	187.5	.631	.40	SCS
17-11a	ICRE at Blufford	Fouralls Creek	Blufford, Ill.	3.53	3.1-3.9	Aug. 1928	30	175.18	.568	2.46	SCS
17-13	Jones Pond	Trib. of Flat Creek	Oswell, Ind.	.034	.031	June 1924	34	609.70	.273	.218	SCS
17-14a	Oliver Reservoir (New)	Trib. of East Fork	Conerly, Ill.	3.36	3.15	Apr. 1926	1.5	10.6	.723	2.10	SCS
17-15	Pattern Lake	Trib. of Dismal Creek	Edgewood, Ill.	.959	.912	July 1929	6.9	316.75	.516	30.3	SCS
17-16a	Plum Creek No. 15	Little Plum Creek	Taylorville, Ky.	1.03	1.02	Sept. 1926	33	281.09	.658	48.54	SCS
17-17	Plum Creek No. 17	Trib. of Little Plum Creek	—	.56	.55	Apr. 1926	2.5	217.5	.28	.48	SCS
17-18	Steiner Lake	Trib. of Pond Creek	Fairfield, Ill.	3.08	.295	Oct. 1920	1.5	123.7	.256	2.00	SCS
						Oct. 1965	1.5	123.2	.292	3.13	SCS
						June 1960	1.5	48.62	.237	1.15	SCS

Station	Location	Instrument	Date	Area (ac.)	Volume (cu. ft.)	Flow (cfs)	Notes
17-19	Sturgeon's Lake	...	...	...	...	...	...
17-20	Veney Park Lake	...	...	...	...	...	...
17-21	Beaver Lake	...	...	...	...	...	...
17-22	Spottisburgh Lake	...	...	...	...	...	...
17-23	Duglas Mill (Catawba Lake)	...	...	...	...	...	...
18-1	Radnor Lake	...	...	...	...	...	...
18-2a	Lake Tandy	...	...	...	...	...	...
18-1c	Great Hill	...	...	...	...	...	...
18-4c	Contereville	...	...	...	...	...	...
18-5c	Wheeler	...	...	...	...	...	...
18-6c	Wilson	...	...	...	...	...	...
18-7c	Plebsdale Landing	...	...	...	...	...	...
18-8c	...	...	...	...	...	...	...
18-9	Bale Hallow	...	...	...	...	...	...
18-10	Old Hickory	...	...	...	...	...	...
18-11	Wolf Creek (Lake Cumberland)	...	...	...	...	...	...
18-12	Bough River Reservoir	...	...	...	...	...	...
18-13	Upper Green River #5 (Pilot)	...	...	...	...	...	...
19-1	Lake Placid	...	...	...	...	...	...
19-2	Radford	...	...	...	...	...	...
19-3	Eggsummed	...	...	...	...	...	...
19-4	Germantown	...	...	...	...	...	...
19-9	Delight	...	...	...	...	...	...
19-11	...	...	...	...	...	...	...
19-12	...	...	...	...	...	...	...
19-13	...	...	...	...	...	...	...

SEMI-ANNUAL REPORT TO THE BOARD OF WATER RESOURCES, 1956-1957

OHIO RIVER BASIN (POINT PLACANT TO WILSON)

Kenawa, Big Sandy, Licking, Kentucky, Scioto, and Miami River Basins

1955 survey revised.  
 2/ Sedimentation estimates for 1955 are based on corrected instrument surveys of shore line and range locations as used in 1954.  
 3/ The noncontributing drainage area is chiefly closed or plugged limestone sinkholes.  
 4/ In July 1925, in June 1951, spillway elevation was 5 feet lower and capacity was 1,226 ac.-ft.  
 5/ Revised from 228,120 to 272,370 ac.-ft.  
 6/ Contereville dam closed Jan. 14, 1959, reducing sediment contributing area to 5,033 sq. mi.  
 7/ Multiple-use capacity excluding diked areas.

SUMMARY OF  
RESERVOIR SEDIMENTATION SURVEYS MADE IN THE UNITED STATES THROUGH 1970

DATA SHEET NUMBER	RESERVOIR	STREAM	NEAREST TOWN	DRAINAGE AREA (SQUARE MILES)		DATE OF SURVEY	PERIOD BETWEEN SURVEYS (YEARS)	STORAGE CAPACITY (ACRE-FT.)	CAPACITY SPECIFIC WEIGHT (DRY) (LB. PER CU. FT.)	AVG. ANN. SEDIMENT ACCUMULATION PER SQ. MI. OF NET DR. AREA FOR PERIOD SHOWN	AGENCY SUPPLYING DATA
				TOTAL	NET						
19-6	Ohio Cons. Pond No. 73	Blacklick Creek	Columbus, Ohio	24	24	Nov. 1974	1.68	---	0.035	SDS	
19-7	Ohio Cons. Pond No. 74	---	---	27	27	Jan. 1977	2.6	---	0.008	SDS	
19-8a	Lake White	Pelee Creek	Waverly, Ohio	37.4	36.9	Oct. 1975	3.734	---	0.84	OM	
19-8b	---	---	---	---	---	Dec. 1967	12.0	---	1.75	SDS	
19-9	Harrison Lake	Dix River	Harrodsburg, Ky.	4.37	4.31	Aug. 1971	2,796	---	---	SDS	
19-10	Milton	Bank Lick Creek	Milton, Ky.	.25	.24	Oct. 1967	255,706	---	.471	SDS	
19-11	Williamstown	Greasy Creek	Williamstown, Ky.	.47	.47	--- 1970	122	---	.50	SDS	
19-12	Byllsby	New River	Byllsby, Va.	1,310	1,310	Aug. 1972	9,932	---	2.13	SDS	
19-13a	O'Shaughnessy	Seloto River	Dublin, Ohio	988	987	May 1976	3,027	0.08	2,184	OM	
19-13b	---	---	---	---	---	Fall 1974	15,604	0.04	---	OM	
19-14	Decker Lake	Paterson Run	Piqua, Ohio	2.33	2.30	July 1971	115	0.084	91.3	OM	
19-15	Madison Lake	Deer Creek	London, Ohio	57.2	57.0	June 1970	49.0	---	49.0	OM	
19-16	Grant Lake	Stearns Run	Mt. Dear, Ohio	25.25	24.97	June 1970	530.2	---	45.9	OM	
19-17	Calowall Lake	Trib. of Money Creek	Chillicothe, Ohio	31	30	Sept. 1977	7.0	---	49.9	OM	
19-18	Stewart Lake	---	---	---	---	Aug. 1972	3.0	---	2.74	OM	
19-19	Pine Lake	Tar Hollow Creek	Gillespieville, Ohio	2.42	2.40	Sept. 1977	1.6	0.064	86.6	OM	
19-20	Kiser Lake	Wesgate Creek	St. Paris, Ohio	8.73	8.15	Aug. 1972	1,088	0.058	324	OM	
19-21	Everetts Run (Trib. of O'Shaughnessy Res.)	Everetts Run	Dublin, Ohio	13.8	13.7	July 1977	88	0.124	460	OM	
19-22	Allen Lake	Trib. of Silver Creek	Emton, Ohio	.50	.50	Sept. 1969	12	0.130	293	OM	
19-23	Sylvan Lake (Lower)	Trib. of Beaver Creek	Vienna, Ohio	1.85	1.39	Sept. 1971	12.3	---	60	OM	
19-24	Sylvan Lake (Upper)	---	---	.60	.38	Aug. 1971	2.8	---	44.8	OM	
19-25	Rosenman Lake	Trib. of Mad River	Springfield, Ohio	1.59	1.58	Aug. 1971	63	---	95	OM	
19-26	Reynolds Pond	Trib. of Barron Creek	Bidwell, Ohio	.70	.70	Nov. 1973	12.7	---	66.2	OM	
19-27	Mr. Gilend Lake (Upper)	Shaw Creek	Mr. Gilend, Ohio	8.55	5/5.50	Aug. 1970	15	0.034	57.4	OM	
19-28	Seibert Pond	Trib. of Big Walnut Creek	Westerville, Ohio	.82	.82	Oct. 1971	18	0.059	460	OM	
19-29a	Lake Alam	Unnamed	Westerville, Ohio	.81	.70	Sept. 1971	30	---	57.1	OM	
19-29b	Maple Grove Lake	Shaw Creek	Mr. Gilend, Ohio	3.05	3.04	Sept. 1972	50	0.014	64	OM	
19-30	Pond Lick Lake	Pond Lick Run	Friendship, Ohio	2.54	2.53	Sept. 1978	17	0.012	85.2	OM	
19-31	Wolfden Lake	Wolfden Run	---	.60	.60	July 1976	12.3	0.019	96.8	OM	
19-32	Bear Lake	Left Fork Bear Creek	---	.48	.47	July 1975	16.3	0.048	59.92	OM	
19-33	Mulbridge Lake	---	---	.61	.61	July 1976	15.3	0.063	67.02	OM	
19-34	---	---	---	.61	.61	July 1970	13.3	0.053	34.01	OM	

Reservoir No.	Reservoir Name	County	State	Year	Capacity (cu ft)	Volume (cu ft)	Area (sq mi)	Permit No.	Remarks
19-35	Roosevelt Lake	Friendship, Ohio	Ohio	1935	16.38	15.76	10.1	0.088	OM
19-36a	Adair Lake	West Union, Ohio	Ohio	1947	4.45	4.39	218	0.087	OM
19-37	Yonah Lake	Ironton, Ohio	Ohio	1937	10.9	10.7	1,535	0.194	OM
19-38	Flax Lake	Bathbridge, Ohio	Ohio	1937	3.44	3.42	1,465	0.183	OM
19-39	Upper Rocking No. 2	Lancaster, Ohio	Ohio	1936	1.87	1.87	9/86.5		SCS
19-40	Jackson Lake	Oak Hill, Ohio	Ohio	1940	18.8	18.4	7/56.98		OM
19-41	Loraine Lake	Pt. Lewis, Ohio	Ohio	1940	76.7	77.4	4,115		OM
19-42a	Sharon House Reservoir	Sharonville, Ohio	Ohio	1919	4.88	4.82	289		OM
19-43	Coma Lake	Wilington, Ohio	Ohio	1943	49.6	48.5	13,370	3.67	OM
19-44	Havusa Lake	Circleville, Ohio	Ohio	1944	6.60	6.40	2,892	0.671	OM
19-45	Hilleboro	Hillsboro, Ohio	Ohio	1945	.73	.69	279.9		OM
19-46	Dolaney	Dalawara, Ohio	Ohio	1946	381	379	132,480	4.877	OM
19-47	V. Ft. Mill Creek Reservoir (Winton Lake)	Cincinnati, Ohio	Ohio	1947	29.5	28.6	8/12,480	5.32	OM
19-48	Bresh Creek Reservoir	Butlerville, Ind.	Indiana	1948	13.4	13.11	11,207	1.595	SCS
19-49	Whitaker Lake	Liberty, Ind.	Indiana	1949	19.29	19.0	3,990.0	0.279	SCS
19-50	Jisco Lake	Jackson, Ohio	Ohio	1950	1.67	1.58	1,105.6	0.860	OM
19-51	Clark Lake	Vienna, Ohio	Ohio	1951	6.88	6.72	507.3	1.06	OM
19-52	Acton Lake	Oxford, Ohio	Ohio	1952	107.4	106.5	485.2	1.02	OM
19-53	Middle Fork Reservoir	Richmond, Ind.	Indiana	1953	48.14	47.87	9,399	1.31	OM
19-54	Colonial Mine Lake	Boulah, Ky.	Kentucky	1954	1.05	1.00	206.77	0.227	SCS
19-55	W. Strip Mine Lake	Richland, Ky.	Kentucky	1955	.009	.009	193.93	0.214	SCS
20-1b	South Holston	South Fork Holston River	Tennessee	1958	703	691	11/661,888	0.903	TVA
20-2b	Watauga	Watauga River	Tennessee	1964	468	458	657,963	0.903	TVA
20-3b	Boone	South Fork Holston River	Tennessee	1964	1,840	662	570,100	1.154	TVA
20-4b	Port Patrick Henry	South Fork Holston River	Tennessee	1964	1,903	63	568,839	1.151	TVA
20-5a	Sherrake	Holston River	Tennessee	1964	3,428	12/1,477	191,446		TVA

1/ 1951 survey includes several additional ranges. Results of 1947 and 1951 surveys are not directly comparable.  
 2/ Based on total sediment in Washington Mill, Buck, Blydenby, and Fields Reservoirs, total drainage area 1,320 sq. mi.  
 3/ Without 3 ft. flashboards added in 1915.  
 4/ Reservoir damaged by flood in 1914; Sept.-Dec. 1912.  
 5/ 1912 decision for Watauga River.  
 6/ Reservoir partially dredged in March-April 1945. Data on amount of material are unreliable.  
 7/ Actual amounts of sediment probably 10 to 25 percent greater than indicated.  
 8/ Sediment pool only.

RESERVOIR RIVER BASIN (ABOVE HALES BAR DAM)

Reservoir No.	Reservoir Name	County	State	Year	Capacity (cu ft)	Volume (cu ft)	Area (sq mi)	Permit No.	Remarks
20-6	Friendship	Friendship, Ohio	Ohio	1935	16.38	15.76	10.1	0.088	OM
20-7	West Union	West Union, Ohio	Ohio	1947	4.45	4.39	218	0.087	OM
20-8	Ironton	Ironton, Ohio	Ohio	1937	10.9	10.7	1,535	0.194	OM
20-9	Bathbridge	Bathbridge, Ohio	Ohio	1937	3.44	3.42	1,465	0.183	OM
20-10	Lancaster	Lancaster, Ohio	Ohio	1936	1.87	1.87	9/86.5		SCS
20-11	Oak Hill	Oak Hill, Ohio	Ohio	1940	18.8	18.4	7/56.98		OM
20-12	Pt. Lewis	Pt. Lewis, Ohio	Ohio	1940	76.7	77.4	4,115		OM
20-13	Sharonville	Sharonville, Ohio	Ohio	1919	4.88	4.82	289		OM
20-14	Wilington	Wilington, Ohio	Ohio	1943	49.6	48.5	13,370	3.67	OM
20-15	Circleville	Circleville, Ohio	Ohio	1944	6.60	6.40	2,892	0.671	OM
20-16	Hillsboro	Hillsboro, Ohio	Ohio	1945	.73	.69	279.9		OM
20-17	Dalawara	Dalawara, Ohio	Ohio	1946	381	379	132,480	4.877	OM
20-18	Cincinnati	Cincinnati, Ohio	Ohio	1947	29.5	28.6	8/12,480	5.32	OM
20-19	Butlerville	Butlerville, Ind.	Indiana	1948	13.4	13.11	11,207	1.595	SCS
20-20	Liberty	Liberty, Ind.	Indiana	1949	19.29	19.0	3,990.0	0.279	SCS
20-21	Jackson	Jackson, Ohio	Ohio	1950	1.67	1.58	1,105.6	0.860	OM
20-22	Vienna	Vienna, Ohio	Ohio	1951	6.88	6.72	507.3	1.06	OM
20-23	Oxford	Oxford, Ohio	Ohio	1952	107.4	106.5	485.2	1.02	OM
20-24	Richmond	Richmond, Ind.	Indiana	1953	48.14	47.87	9,399	1.31	OM
20-25	Boulah	Boulah, Ky.	Kentucky	1954	1.05	1.00	206.77	0.227	SCS
20-26	Richland	Richland, Ky.	Kentucky	1955	.009	.009	193.93	0.214	SCS

8/ Flood pool elevation 917. Reservoir surveyed to elevation 915.  
 9/ Actual sediment above elevation 915.  
 10/ Revised on basis of topographic maps developed for definite project report and sedimentation range data.  
 11/ 1977 water year included.  
 12/ Multiple-use storage capacity. Reservoir has greater capacity at fullway crest elevation.  
 13/ Sediment contributing area reduced to 3,990 acres by closing of Watauga Dam Dec. 16, 1941; South Holston area reduced to 1,950 acres on Dec. 16, 1942; and Port Patrick Henry on Oct. 27, 1953.  
 14/ Sediment storage included in 1949 survey as sediment contributing area.  
 15/ Estimated or assumed.

SUMMARY OF  
RESERVOIR SEDIMENTATION SURVEYS MADE IN THE UNITED STATES THROUGH 1970

DATA SHEET NUMBER	RESERVOIR	STREAM	NEAREST TOWN	DRAINAGE AREA (SQUARE MILES)		DATE OF SURVEY	PERIOD BETWEEN SURVEYS (YEARS)	STORAGE CAPACITY (ACRE-FT.)	CAPACITY INFLOW RATIO (ACRE-FT. PER ACRE-FT.)	SPECIFIC WEIGHT (LB. PER CU. FT.)	AVG. ANN. ACCUMULATION PER SQ. MI. AREA FOR PERIOD SHOWN	AGENCY SUPPLYING DATA
				TOTAL	NET							
TENNESSEE RIVER BASIN (ABOVE HALES BAR DAM) (Continued)												
20-6d	Molichucky	Molichucky River	Grenville, Tenn.	1,183	1,182	Fall 1943	12.5	3/3,100	50	0.252	TVA	
-do-	-do-	-do-	-do-	-do-	-do-	Feb. 1958	12.5	2/21,750	50	0.252	TVA	
-do-	-do-	-do-	-do-	-do-	-do-	Apr. 1961	12.5	14,450	50	0.252	TVA	
-do-	-do-	-do-	-do-	-do-	-do-	Oct. 1968	12.5	14,600	50	0.252	TVA	
-do-	-do-	-do-	-do-	-do-	-do-	Oct. 1968	12.5	7,760	50	0.252	TVA	
-do-	-do-	-do-	-do-	-do-	-do-	Feb. 1966	2.3	7,470	50	0.252	TVA	
-do-	-do-	-do-	-do-	-do-	-do-	Mar. 1967	2.3	2/3,325	50	0.252	TVA	
-do-	-do-	-do-	-do-	-do-	-do-	Sept. 1970	3.5	2,650	50	0.252	TVA	
20-7c	Douglas	French Broad River	Sterlingville, Tenn.	4,541	2,854	Feb. 1943	6.4	3/1,511,683	55	0.890	TVA	
-do-	-do-	-do-	-do-	-do-	-do-	July 1949	6.4	1,496,712	55	0.890	TVA	
-do-	-do-	-do-	-do-	-do-	-do-	May 1955	5.8	1,500,870	55	0.890	TVA	
-do-	-do-	-do-	-do-	-do-	-do-	June 1967	7.2	1,457,459	55	0.890	TVA	
-do-	-do-	-do-	-do-	-do-	-do-	June 1967	7.2	1,457,459	55	0.890	TVA	
20-8c	Fort Loudoun	Tennessee River	Lenoir City, Tenn.	9,550	1,556	Nov. 1946	4.6	400,945	55	0.890	TVA	
-do-	-do-	-do-	-do-	-do-	-do-	June 1951	4.6	399,414	55	0.890	TVA	
-do-	-do-	-do-	-do-	-do-	-do-	Apr. 1956	4.8	398,060	55	0.890	TVA	
-do-	-do-	-do-	-do-	-do-	-do-	May 1961	5.1	392,711	55	0.890	TVA	
20-9b	Thorpe	W. Fk. Tuckasee River	Glenville, N. C.	36.7	34.4	Feb. 1941	9.6	3/70,700	88	0.888	TVA	
-do-	-do-	-do-	-do-	-do-	-do-	Sept. 1950	9.6	70,337	88	0.888	TVA	
-do-	-do-	-do-	-do-	-do-	-do-	July 1959	10.7	70,337	88	0.888	TVA	
20-10b	Nantahala	Nantahala River	Apopka, N. C.	91	88	Sept. 1950	7.8	138,083	55	0.890	TVA	
-do-	-do-	-do-	-do-	-do-	-do-	July 1958	7.9	137,882	55	0.890	TVA	
20-11c	Fontana	Little Tennessee River	Fontana, N. C.	1,571	1,426	May 1944	10.8	3/1,455,062	55	0.890	TVA	
-do-	-do-	-do-	-do-	-do-	-do-	Mar. 1950	5.4	1,452,385	55	0.890	TVA	
-do-	-do-	-do-	-do-	-do-	-do-	Sept. 1954	4.5	1,450,646	55	0.890	TVA	
-do-	-do-	-do-	-do-	-do-	-do-	June 1959	4.7	1,448,311	55	0.890	TVA	
-do-	-do-	-do-	-do-	-do-	-do-	Oct. 1957	8.5	1,443,692	55	0.890	TVA	
20-12	Chesno	-do-	Sapores, N. C.	1,608	1,607	Sept. 1950	11.8	3/39,030	55	0.890	TVA	
-do-	-do-	-do-	-do-	-do-	-do-	Aug. 1941	10.9	3/35,070	55	0.890	TVA	
20-13b	Caryville	Cove Creek	Caryville, Tenn.	35.98	35.65	Nov. 1936	2.0	4/1,726	62	1.038	TVA	
-do-	-do-	-do-	-do-	-do-	-do-	Nov. 1938	2.0	1,652	62	1.038	TVA	
-do-	-do-	-do-	-do-	-do-	-do-	Jan. 1947	8.2	1,580	62	1.038	TVA	
-do-	-do-	-do-	-do-	-do-	-do-	Mar. 1954	7.1	1,347	62	1.038	TVA	
-do-	-do-	-do-	-do-	-do-	-do-	Aug. 1960	6.4	1,290	62	1.038	TVA	
20-14c	Warri	Clinch River	Norris, Tenn.	2,812	2,823	Mar. 1936	9.3	3/2,051,569	55	0.890	TVA	
-do-	-do-	-do-	-do-	-do-	-do-	June 1946	10.3	2,052,357	55	0.890	TVA	
-do-	-do-	-do-	-do-	-do-	-do-	June 1954	8.0	2,047,357	55	0.890	TVA	
-do-	-do-	-do-	-do-	-do-	-do-	Aug. 1960	6.1	2,044,768	55	0.890	TVA	
20-15c	Matta Bar	Tennessee River	Spring City, Tenn.	17,310	2,925	June 1970	9.8	2,036,324	55	0.890	TVA	
-do-	-do-	-do-	-do-	-do-	-do-	Oct. 1946	-	1,195,229	55	0.890	TVA	
-do-	-do-	-do-	-do-	-do-	-do-	June 1951	4.7	1,193,106	55	0.890	TVA	
-do-	-do-	-do-	-do-	-do-	-do-	Apr. 1956	4.8	1,193,106	55	0.890	TVA	
-do-	-do-	-do-	-do-	-do-	-do-	Apr. 1956	4.8	1,193,106	55	0.890	TVA	
20-16b	Chattahoochee	Hawesee River	Hayesville, N. C.	189	178	Feb. 1942	5.1	242,325	55	0.890	TVA	
-do-	-do-	-do-	-do-	-do-	-do-	Aug. 1949	7.5	242,032	55	0.890	TVA	
-do-	-do-	-do-	-do-	-do-	-do-	Aug. 1954	5.0	241,502	55	0.890	TVA	
-do-	-do-	-do-	-do-	-do-	-do-	Sept. 1960	6.0	240,989	55	0.890	TVA	
20-17b	Mottley	Mottley River	Blairsville, Ga.	214	307	Apr. 1942	4.6	240,516	55	0.890	TVA	
-do-	-do-	-do-	-do-	-do-	-do-	Jan. 1949	7.6	175,665	55	0.890	TVA	
-do-	-do-	-do-	-do-	-do-	-do-	Apr. 1955	7.7	174,529	55	0.890	TVA	
-do-	-do-	-do-	-do-	-do-	-do-	Apr. 1965	6.0	174,327	55	0.890	TVA	
20-18b	Hawesee	Hawesee River	Murphy, N. C.	968	8/599	Apr. 1940	4.0	3/439,741	55	0.890	TVA	
-do-	-do-	-do-	-do-	-do-	-do-	Feb. 1947	7.5	436,009	55	0.890	TVA	
-do-	-do-	-do-	-do-	-do-	-do-	May 1953	5.8	435,686	55	0.890	TVA	
-do-	-do-	-do-	-do-	-do-	-do-	June 1958	5.0	434,243	55	0.890	TVA	
-do-	-do-	-do-	-do-	-do-	-do-	May 1965	6.9	433,568	55	0.890	TVA	
20-19c	Apalachia	-do-	Farmer, Tenn.	1,018	48	Feb. 1943	7.5	28,242	55	0.890	TVA	
-do-	-do-	-do-	-do-	-do-	-do-	Apr. 1949	7.5	27,550	55	0.890	TVA	
-do-	-do-	-do-	-do-	-do-	-do-	Apr. 1960	10.1	27,550	55	0.890	TVA	
-do-	-do-	-do-	-do-	-do-	-do-	May 1965	4.7	27,753	55	0.890	TVA	





SUMMARY OF  
RESERVOIR SEDIMENTATION SURVEYS MADE IN THE UNITED STATES THROUGH 1970

DATA SHEET NUMBER	RESERVOIR	STREAM	NEAREST TOWN	DRAINAGE AREA (SQUARE MILES)		PERIOD BETWEEN SURVEYS (YEARS)	STORAGE CAPACITY (ACRE-FT.)	CAPACITY INFLOW (ACRE-FT. PER ACRE-FT.)	SPECIFIC WEIGHT (DRY) (LB. PER CU. FT.)	AVG. ANN. SEDIMENT ACCUMULATION PER SQ. MI. OF NET DR. AREA FOR PERIOD SHOWN		AGENCY SUPPLYING DATA
				TOTAL	NET					AC.-FT.	TONS	
21-8	Barberton	Wolf Creek	Barberton, Ohio	28.2	28.0	1956 Dec. 1958	2,056	*.101	.55	1.10	1,320	SES
21-9	Buckeye Lake	S. Fork Licking River	Millersport, Ohio	1/59.2	55.1	1959 July 1959	1,688	*.083	.90	.860	937	SES
21-10	Leesville	McClure Creek	Leesville, Ohio	48.0	45.7	1956 Aug. 1956	31,790	*.1159	.90	.087	73	SES
21-11	Munking College	Trib. of Munking River	New Concord, Ohio	.32	.31	1955 Nov. 1955	37,390	*.031	.70	.301	501	SES
21-12	Ohio Cons. Pond No. 22	Trib. of Duck Creek	Marion, Ohio	.05	.05	1958 Oct. 1958	7.01	*.110	.80	4.00	3,485	SES
21-13	Ohio Cons. Pond No. 51	Trib. of Ohio River	---do---	.13	.13	1958 Nov. 1958	15,116	*.152	.60	.977	651	SES
21-14	Ohio Cons. Pond No. 52	---do---	---do---	.17	.16	1958 Nov. 1958	17,95	*.118	.90	1.45	1,577	SES
21-15	Robbins Lake	Ford Creek	Hartford, Ohio	4.47	4.45	1959 Dec. 1959	91.6	*.028	.66	.153	224	SES
21-16	Corleys Lake	Trib. of Toughlohy R.	Uniontown, Pa.	3.00	2.97	1959 June 1959	130	---	.60	.135	176	SES
21-17	Lake Rockwell	Cuyahoga River	Kent, Ohio	305.5	3/224.1	1954 Aug. 1954	7,423	---	.6	.120	120	DM
21-18a	Stony Lake	McClure Creek	Perryville, Ohio	11.75	11.72	1957 Dec. 1957	6,887	---	.65	.319	452	SES
21-19	Tabor Club Lake	Small Br. Munking River	---do---	.55	.54	1953 Dec. 1953	61	*.145	.90	1.36	1,500	SES
21-20	Zanesville Nursery Lake	N. Br. Mount Run	Zanesville, Ohio	2.95	2.93	1956 Dec. 1956	42.6	*.016	.65	.236	462	CE
21-21a	Tionesta	Tionesta Creek	Tionesta, Pa.	478	474	1949 July 1949	72.25	*.032	.65	.203	287	CE
21-22b	Loyalhanna	Loyalhanna Creek	Salisbury, Pa.	290	285	1942 Sept. 1942	132,971	.278	.44	.336	312	CE
21-23b	Mahoning Creek	Mahoning Creek	Dayton, Pa.	360	336	1941 June 1941	5/95,300	.275	.44	.286	272	CE
21-24b	Crooked Creek	Crooked Creek	Ford City, Pa.	277	274	1941 Apr. 1941	91,503	.273	.44	.162	229	CE
21-25a	Tygart River	Tygart River	Grafton, W. Va.	1,184	1,179	1958/59 Feb. 1958/59	71,807	.172	.43	.178	167	CE
21-26a	Toughlohy River	Toughlohy River	Confluence, Pa.	424	428	1943 Oct. 1943	287,700	.174	.65	.075	108	CE
21-27a	Atwood Reservoir	Indian Pt., Conotton Creek	Sherrillsville, Ohio	70	66.2	1949 Apr. 1949	251,121	.406	.65	.341	483	CE
21-28	Babb Pond	Unnamed	Richfield, Ohio	.02	.02	1945 Dec. 1945	49,700	.991	.65	.29	410	SES
21-29	Basom Pond	---do---	Hudson, Ohio	.32	.32	1951 Apr. 1951	475,570	*.019	.60	.15	196	SES
21-30	Christman Pond	---do---	Parma, Ohio	.09	.09	1940 Apr. 1940	3.87	*.015	.60	.281	367	SES
21-31	Schoenbeck Pond	---do---	Richfield, Ohio	.03	.03	1940 Apr. 1940	3.10	*.016	.60	.611	708	SES
21-32	Ticky Pond	---do---	Peninsula, Ohio	.16	.16	1949 Apr. 1949	2.79	*.046	.60	.567	743	SES
21-33b	Lake Hope	Sandy Run	Zaleski, Ohio	9.95	9.75	1949 July 1949	1.26	*.066	.60	.100	131	DM
21-34b	Jefferson Lake	Town Pt. Yellow River	Richman, Ohio	7.52	7.48	1955 Dec. 1955	1,511	*.201	.60	.442	720	DM
						1956 June 1956	1,481	.195	---	---	---	---
						1961 June 1961	1,451	.187	---	---	---	---
							1,56	.07	---	---	---	---
							178	.09	---	---	---	---
							156	.02	---	---	---	---
							34	.022	---	---	---	---
							6	.01	---	---	---	---
							131	.021	---	---	---	---



SUMMARY OF  
RESERVOIR SEDIMENTATION SURVEYS MADE IN THE UNITED STATES THROUGH 1970

DATA SHEET NUMBER	RESERVOIR	STREAM	NEAREST TOWN	DRAINAGE AREA (SQ. MILES)		DATE OF SURVEY	PERIOD BETWEEN SURVEYS (YEARS)	STORAGE CAPACITY (ACRE-FT.)	CAPACITY INFLOR. RATIO (ACRE-FT. PER CU. FT.)	SPECIFIC WEIGHT (LB. PER CU. FT.)	AVG. ANNUAL ACCUMULATION PER SQ. ML. OF NET DR. AREA FOR PERIOD SHOWN		AGENCY SUPPLYING DATA
				TOTAL	NET						AC.-FT.	TONS	
21-57	North Fk. Cowanesque River (EX-106)	White Branch	North Fork, Pa.	3.4	3.3	Aug. 1962	—	654.13	.21	71	3/6.015	1/23.2	SCS
21-58	Salen Fork No. 11A	Warner Hollow	Salen, W. Va.	.287	.287	July 1967	4.9	653.89	.21	460	1.307	1.708	SCS
						Oct. 1956	2	53	.166		1.168	.202	
						Oct. 1958	2	24.05	.165		1.168	.202	
						Nov. 1962	1.58	31.75	.164		1.168	.202	
21-49	Upper Hooking No. 1	Hunters Run	Lancaster, Ohio	1.04	.94	Apr. 1956	—	4.9	.882	71.6	.678	1.057	SCS
						June 1962	6.08	446.13	.875				
GREAT LAKES DRAINAGE (IN MICHIGAN) AND MAUMEE RIVER BASIN													
22-1	Grandy	St. Marys and Wabash River	Galena, Ohio	110	93	1844	—	2/30.175	42.109	65.4	2.64	3.162	SCS
22-2	Spring	Fire of Manistee River	Melliston, Mich.	291	273	Aug. 1962	96	106.60	41.706				SCS
22-3	Galler Pond	Unnamed	Defiance, Ohio	.026	.024	Jan. 1963	41	27	3.003	110.4	.064	154	OM
22-4a	Auglaize R. Power	Auglaize River	—	2,329	2,326	Mar. 1945	9.5	9.4	3.761	45	.92	902	OM
22-5	Eagle Creek	Eagle Creek	—	5.23	5.20	Aug. 1951	6.4	11,600	3.753				OM
22-6	Beutree Creek	Beutree Creek	—	1.94	1.91	1931	39	11,600	.009				OM
22-7	Belt Pond	Unnamed	—	.013	.012	July 1951	39	104	.2109	59	.27	347	OM
22-8	Harrison Lake	Mill Creek	Payette, Ohio	37.2	37.0	Apr. 1947	—	2.6	4.17	52.5	.59	675	OM
22-9	Allardiner Pond	Unnamed	—	.038	.035	July 1951	4.3	981	4.01	73.4	2.75	4,396	OM
22-10	Bugrus No. 2	Trib. of Sandusky River	—	2.94	2.79	June 1949	8.3	929.1	.048	53.2	.20	232	OM
22-11c	Centris Ponds	Trib. of Hoop Creek	—	.13	.13	June 1951	2.1	902.4	.046	53	.34	392	OM
						July 1945	—	5.08	2.39	51.7	1.71	2,001	OM
						July 1949	6.7	24.71	1.25				OM
						Aug. 1949	30	238	1.08	65.4	.28	277	OM
						June 1947	—	9.2	.133				OM
						1951	4	7.9	.114	57.8	2.60	3,270	OM
						1954	3	7.4	.107	49.3	1.36	1,460	OM
						1962	8	6.3	.091				OM
22-12	Skimble Creek	Skimble Creek	Defiance, Ohio	21.6	21.4	1912	—	995	.094	47.8	.36	343	OM
22-13a	Burt Lake	Unnamed	—	.76	.74	July 1951	39	89	3.155				OM
22-14	Kohler Pond	Unnamed	—	.021	.019	Sept. 1951	—	2.4	3.150	37.2	1.13	924	OM
22-15	Van Buren Lake	Rosky Ford Creek	Findlay, Ohio	22.80	22.72	Spring 1939	7.8	2.3	.219	26.1	.53	301	OM
22-16	Norwell Lake	River Raisin	Norwell, Mich.	58.5	25.3	Aug. 1948	9.5	248	.022	53.6	.20	233	OM
22-17	Sharon Hollow	—	—	34.7	25	Nov. 1951	2.8	188	.017	57.9	.31	391	SCS
22-18	Breaklyn Mill Pond	—	—	29.6	6.2	May 1969	100	177.6	.016		.085	43	SCS
22-19	Manchester Power Dam	—	—	6.4	6.4	May 1945	21	269.3	.016	30.1	.11	72	SCS
22-20	Iron Mill Pond	—	—	11.4	5.2	May 1969	23	288.9	.012	43.4	.684	457	SCS
22-21	Phoenix Pond	—	—	56.05	56.05	Aug. 1969	100	259.5	.08	31.5	.20	137	SCS
22-22	Saline River	Saline River	Plymouth, Mich.	73.6	63	Sept. 1969	100	170	.0076	11.8	.0097	8.8	SCS
22-23	Manchester Mill Pond	—	—	17	17	Mar. 1969	31	240.1	.0061	44	.057	54	SCS
22-24	Bridgeway Lake	—	—	7.5	7.5	May 1969	63	10.9	.0036	38	.01	8	SCS
22-25	Franklin Mill Pond	—	—	11.8	7.8	Mar. 1969	41	76.7	.0290	46	.099	97	SCS
22-26	Waterford Pond	—	—	54	54	Apr. 1969	136	9.8	.013	50	.079	66	SCS
						Sept. 1969	100	101	.0039	39	.013	11	SCS

22-27	Teumessah Mill Pond	Poans Creek	Teumessah, Mich.	31.6	26.3	1827	227.8	0.1901	--	--	0.036	--	SCS
22-28	Bellefille Lake	Huron River	Bellefille, Mich.	810	20.3	1929	19,947	0.062	69	2.42	3,637	69	SCS
22-29	Ford Lake	do	Ypsilanti, Mich.	790	11.2	1933	17,926	0.072	81	4.56	8,045	81	SCS
22-30	Barton Pond	do	Ann Arbor, Mich.	708	183	1915	16,085	0.024	39	--	0.055	39	SCS
22-31	Red Mill Pond	Upper Raisin	Teumessah, Mich.	172.9	25.9	1969	2,601	0.068	41.9	1.13	118	41.9	SCS
22-32	H. N. Fry Pond	Squaw Creek	Onsted, Mich.	12.45	12.45	1969	121.3	0.09	--	0.06	--	--	SCS
22-33	Newburgh Lake	Middle Rouge	Plymouth, Mich.	54.3	54.3	1931	667.8	0.026	56.08	0.04	65.96	56.08	SCS
22-34	Lake Adrian	Wolf Creek	Adrian, Mich.	65	59	1942	1,000	0.032	75.1	0.09	147	75.1	SCS

GREAT LAKES DRAINAGE (IN MICHIGAN AND WISCONSIN)

MISSISSIPPI RIVER BASIN (LOUISIANA TO CHESTER) ILLINOIS, KANSAS, AND WYOMING RIVER BASINS

24-1a	Lake Millason (Artic Pond)	Trib. of Honey Creek	Carlinville, Ill.	0.53	0.51	1922	175.6	0.14	46.24	1.18	1,188	46.24	IMS
24-2a	Lake Bloomington	do	do	61	60	1969	6,654	1.980	41.5	0.528	477	41.5	IMS
24-3a	Lake Zephyrville	Honey Creek	Carlinville, Ill.	26.06	25.79	1939	2,903	0.083	40	2.82	243	40	IMS
24-4a	Lake Deatur	Saugeam River	Deatur, Ill.	906	902	1922	19,738	0.098	59.1	0.934	1,200	59.1	SCS
24-5	Shaefer Pond	Trib. of Cahokia Creek	Edwardsville, Ill.	0.87	0.87	1937	20.2	0.087	51.7	0.262	295	51.7	IMS
24-6	Lake Springfield	Sugar and Lack Creeks	Springfield, Ill.	265	258	1921	61,039	0.16	43	2.65	2,890	43	IMS
24-7	Spring Lake	Spring Creek	Macomb, Ill.	20.2	20.1	1927	607	0.07	59.7	0.701	911	59.7	IMS
24-8	Lake Bracken	Brush Creek	Galzburg, Ill.	9.14	8.85	1923	2,881	0.07	52	1.87	2,231	52	SCS
24-9	Pittsfield	Trib. of Panther Creek	Pittsfield, Ill.	1.84	1.77	1925	7,367	0.490	40	3.55	3,090	40	SCS
24-10a	Lake and Dam 25 (Winfield)	Mississippi River	Winfield, Mo.	12,000	--	1929	180,000	0.310	--	--	--	--	CE
24-11a	Mt. Sterling	Trib. of Shelby Creek	Mt. Sterling, Ill.	1.80	1.75	1935	376	0.393	60	2.05	2,679	60	IMS
24-12	Lake Jacksonville	Sandy Creek	Jacksonville, Ill.	10.8	10.1	1931	7,098	1.187	32.5	1.51	1,069	32.5	IMS
24-13	Maumisse Terre Lake	Maumisse Terre Creek	Maumisse Terre, Ill.	32.6	32.2	1932	6,874	0.67	48.2	0.61	610	48.2	IMS
24-14a	Langdon Pond	Langdon Lake	Langdon, Ill.	2.75	2.72	1932	1,216	0.082	41.2	0.38	313	41.2	IMS
24-15a	Franklin Outing Club Lake	Franklin Outing Club Lake	Franklin, Ill.	4.50	4.48	1927	56.8	0.284	31.8	0.78	510	31.8	IMS
24-16	Anderson Lake	Anderson Lake	Anderson, Ill.	0.51	0.60	1925	301	1.382	52.4	1.43	1,632	52.4	IMS
24-17	Waverly City	Waverly City	Waverly, Ill.	3.24	3.16	1922	204	0.863	36.2	1.28	1,009	36.2	IMS
24-18	Whitehall City	Whitehall City	Whitehall, Ill.	0.97	0.92	1922	238.6	0.46	42.4	0.51	509	42.4	IMS
24-19	Roodhouse Park District Lake	Roodhouse Park District Lake	Roodhouse, Ill.	4.51	4.39	1917	408	0.751	43.1	1.02	957	43.1	IMS
24-20	Woodbine Country Club Lake	Woodbine Country Club Lake	Greenfield, Ill.	0.29	0.20	1926	53.9	0.213	42.1	0.50	462	42.1	IMS
24-21	Dale Cole Pond	Dale Cole Pond	Hillview, Ill.	0.21	0.21	1924	67.2	0.521	54.4	1.31	2,144	54.4	IMS
24-22	Seely Pond	Seely Pond	Seely, Ill.	0.093	0.091	1922	56.7	0.460	51.7	1.72	2,012	51.7	IMS
24-23	Seely Pond	Seely Pond	Seely, Ill.	0.093	0.091	1922	56.7	0.460	51.7	1.72	2,012	51.7	IMS

1/ Sediment pool only.  
 2/ Also known as Lake St. Marys.  
 3/ At present spillway elevation (lowered in 1856). In 1944, surface area was 17,603 acres and storage capacity was 220,400 ac.-ft.  
 4/ Capacity and sediment figures include that of several tributary areas including Beebles, Eagle and Sixmile Creeks.  
 5/ Tributary arm of Auglaize River Power Reservoir.  
 6/ All figures subject to readjustment because of minor dredging which occurred in 1953.  
 7/ At present spillway elevation; spillway raised 1.24 ft. in 1944.  
 8/ Estimated or assumed.

SUMMARY OF  
RESERVOIR SEDIMENTATION SURVEYS MADE IN THE UNITED STATES THROUGH 1970

DATA SHEET NUMBER	RESERVOIR	STREAM	NEAREST TOWN	DRAINAGE AREA (SQ. MILES)		DATE OF BETWEEN SURVEY (YEARS)	PERIOD BETWEEN SURVEYS (YEARS)	STORAGE CAPACITY (ACRE-FT.)	CAPACITY (INFL. W/OUT BAYO) (ACRE-FT. PER ACRE-FT.)	SPECIFIC WEIGHT (DIRTY) (LB. PER CU. FT.)	AVG. ANN. SEDIMENT ACCUMULATION PER SQ. MI. OF NET DR. AREA FOR PERIOD SHOWN		AGENCY SUPPLYING DATA
				TOTAL	NET						AC.-FT.	TQIS	
24-24	Vineyard Pond	Unamed	Whitehall, Ill.	0.054	0.052	Jan. 1937	1.58	0.93	36.2	0.33	260	INS	
24-25	Knap	-do-	Springfield, Ill.	3.49	3.43	July 1907	15.6	0.04	98.7	.431	363	INS	
24-26	Archauer Pond	-do-	Riverdon, Ill.	1.586	1.518	Aug. 1932	45	0.09	56.2	1.31	1,603	INS	
24-27	Schmidt Pond	-do-	Chatham, Ill.	1.31	1.30	Aug. 1915	13	0.06	41.2	.22	397	INS	
24-28	Ayers	-do-	Ayers, Ill.	1.43	1.39	Aug. 1906	9	0.05	51.09	.69	766.87	INS	
24-29a	Bodman Reservoir	-do-	Brownswick, Ind.	2.73	2.39	Aug. 1947	52.1	*0.06	56.7	.23	284	INS	
24-30	S & Q R. Lake	-do-	Tallula, Ill.	.85	.84	Sept. 1902	13	0.07	49.3	.39	432	INS	
24-31	Edward Lake	-do-	Gallatin, Ill.	.42	.40	July 1928	90	0.35	66.86	1.72	1,755.47	INS	
24-32	Robison's Lake	-do-	Vandalia, Ill.	.27	.26	Aug. 1943	19.7	0.32	55.66	.93	1,127.33	INS	
24-33	Gloster No. 1	-do-	Elmhurst, Mo.	1.05	1.04	Apr. 1956	16.0	1.11	4.59	.49	---	INS	
24-34	I. C. at Kinmundy	-do-	Kinmundy, Ill.	.618	.581	July 1960	4.3	---	---	---	---	INS	
24-35	Flag Lake	Kaskaskia River	---do---	---	---	July 1952	67	0.10	33.5	.76	564.5	INS	
24-36	Lake Coulterville	Trib. of Cahokia Creek	Englewood, Ill.	.46	.44	June 1928	37	0.60	54.42	1.17	1,386.73	INS	
24-37	Lake Bunker Hill	South Fork Mud Creek	Coulterville, Ill.	1.22	1.18	Aug. 1940	14	0.76	34	.73	541	INS	
24-38	Lake Gillespie	Wood River	Bunker Hill, Ill.	7.19	7.15	Aug. 1934	17	0.93	79.2	.80	1,380	INS	
24-39	Lake Stewart	Dry Fork	Gillespie, Ill.	3.73	3.62	June 1954	17	0.79	37.9	.57	470	INS	
24-40	Lake Staunton	Nashville Creek	Nashville, Ill.	1.39	1.33	July 1936	32	0.376	35.3	1.19	913	INS	
24-41	Neocopin County Lake Club	East Creek	Staunton, Ill.	3.68	3.54	Aug. 1926	19	0.690	28.1	1.09	667	INS	
24-42a	Mine Pond No. 4	Trib. of Hurricane Creek	Carlinville, Ill.	.28	.26	July 1954	28	1.248	37.13	1.76	1,423.32	INS	
24-43	New No. 615e	-do-	Wilsonville, Ill.	3.29	3.23	June 1958	54	1.16	65.34	.70	996	INS	
24-44a	Parsons Lake	Trib. of Indian Creek	White City, Ill.	5.21	5.12	June 1958	20	0.164	52.35	.94	1,071.79	INS	
24-45	Power Farm Ponds	Trib. of Sangamon River	Parsons, Ill.	.85	.84	Aug. 1958	30	0.536	46.2	1.01	1,130	INS	
24-46	Raccoon Lake	Raccoon Creek	Central, Ill.	.668	.666	July 1952	12	4.2	54.9	.36	430	INS	
24-47	Robison Pond	Terra Creek	Jacksonville, Ill.	.314	.304	Sept. 1939	16	0.771	39.7	.47	406	INS	
24-48	Salem City	Trib. of Crooked Creek	Salem, Ill.	4.02	3.90	July 1952	52	0.209	46.8	.70	723.51	INS	
24-49a	Virginia	Job's Creek	Virginia, Ill.	.657	.657	Aug. 1960	48	0.207	40.8	.36	320	INS	
24-50	Walton Club Lake	Long Branch	Michfield, Ill.	2.72	2.67	July 1956	17	0.376	41.0	2.70	2,152	INS	
24-51	Lock and Dam 26	Mississippi River	Alton, Ill.	170.470	---	May 1948	97	187.2	48.4	.73	769.5	CS	
24-52a	Pool No. 22	-do-	Steverson, Mo.	137.800	---	Dec. 1945	15	---	---	---	---	CS	
						Dec. 1946	14	---	---	---	---		
						Oct. 1947	11.5	---	---	---	---		
						July 1948	16.33	---	---	---	---		
						Dec. 1949	15	---	---	---	---		
						Dec. 1969	15	---	---	---	---		
								0.0317	---	---	---		
								0.0318	---	---	---		

UPPER MISSISSIPPI RIVER BASIN (PRAIRIE TO LOUISIANA)  
Iowa, South, and Des Moines River Basins

25-1	Pool No. 13 (Lamb Cooper, Lamb Dam)	Mississippi River	Keosau, Iowa	119.70	1913	479,590				
25-2	Upper Falls	Mississippi River	Keosau, Iowa	11.9	June 1928	370,300				
25-3	Lake O'Brien	Mississippi River	Keosau, Iowa	13.1	June 1928	370,000				
25-4	Carriage	Mississippi River	Keosau, Iowa	13.0	June 1928	312,216				
25-5	McIntosh Creek New Dam	Mississippi River	Keosau, Iowa	13.1	Sept. 1927	660				
25-6	Flax Creek	Mississippi River	Keosau, Iowa	13.0	Sept. 1927	3,625				
25-7	Madley Creek Old Dam	Mississippi River	Keosau, Iowa	2.88	July 1926	112				
25-8	Madley Creek New Dam	Mississippi River	Keosau, Iowa	52.0	Aug. 1929	406.3				
25-9	Elmer Creek Beckling Basin	Mississippi River	Keosau, Iowa	15.24	Dec. 1928	2,400				
25-10	Beaver Basin	Mississippi River	Keosau, Iowa	71.0	Winter 1932	3,000				
25-11	C W D. P & M Res.	Mississippi River	Keosau, Iowa	71.0	Dec. 1928	3,000				
25-12a	Fairfield No. 3	Mississippi River	Keosau, Iowa	66.0	Dec. 1928	2,556				
25-13	Spring Creek	Mississippi River	Keosau, Iowa	31.8	Dec. 1928	2,800				
25-14	Pool No. 16	Mississippi River	Keosau, Iowa	2.44	Dec. 1928	2,290				
25-15	Pool No. 20	Mississippi River	Keosau, Iowa	2.05	Dec. 1928	1,074				
25-16	Blountfield	Mississippi River	Keosau, Iowa	2.11	Dec. 1928	43				
25-17	Pool No. 17	Mississippi River	Keosau, Iowa	99.60	Dec. 1928	25				
25-18	Pool No. 21	Mississippi River	Keosau, Iowa	135.000	Dec. 1928	207				
25-19	Overville	Mississippi River	Keosau, Iowa	3,115	July 1927	166				
26-1a	Pool No. 13	Mississippi River	Rock Island, Ill.	86.900	Mar. 1928	113,370				
26-2	Beaumont Lake (Newsville Lake)	Mississippi River	Rock Island, Ill.	116	Mar. 1928	106,347				
26-3	Pool No. 11	Mississippi River	Rock Island, Ill.	81.600	Mar. 1928	89,850				
27-1	Elk Creek Lake	Elk Creek	San Glair, Wis.	60	Oct. 1927	685				
27-2	Wright Hill Pond	Elk Creek	Elk Creek, Wis.	50.75	June 1927	457				
27-3	Marshall (Davis Lake)	Beaver Creek	Galveston, Wis.	138.6	June 1927	1,617				
27-4	Prattville Lake	Wagonwheel River	Prattville, Mo.	9.900	June 1927	100,000				

UPPER MISSISSIPPI RIVER BASIN (PRAIRIE DU CHIEN TO ROCK ISLAND) AND LAKE MICHIGAN DRAINAGE  
Rock and Wapiti Rivers Basins

26-1a	Pool No. 13	Mississippi River	Rock Island, Ill.	86.900	Mar. 1928	39,432				
26-2	Beaumont Lake (Newsville Lake)	Mississippi River	Rock Island, Ill.	116	Mar. 1928 <td>38,226 <td></td> <td></td> <td></td> <td></td> </td>	38,226 <td></td> <td></td> <td></td> <td></td>				
26-3	Pool No. 11	Mississippi River	Rock Island, Ill.	81.600 <td>Mar. 1928 <td>38,226 <td></td> <td></td> <td></td> <td></td> </td></td>	Mar. 1928 <td>38,226 <td></td> <td></td> <td></td> <td></td> </td>	38,226 <td></td> <td></td> <td></td> <td></td>				
27-1	Elk Creek Lake	Elk Creek	San Glair, Wis.	60	Oct. 1927	685 <td></td> <td></td> <td></td> <td></td>				
27-2	Wright Hill Pond	Elk Creek	Elk Creek, Wis.	50.75	June 1927	457 <td></td> <td></td> <td></td> <td></td>				
27-3	Marshall (Davis Lake)	Beaver Creek	Galveston, Wis.	138.6	June 1927	1,617 <td></td> <td></td> <td></td> <td></td>				
27-4	Prattville Lake	Wagonwheel River	Prattville, Mo.	9.900	June 1927	100,000				

Conservation Pool.  
All X ranges show owner, partially due to removal of borrow material.  
Swilling raised 2.69 ft. in 1942. Original capacity was 285.6 ac-ft. All sedimentation and storage loss data based on higher spillway elevation.  
Excludes 3.8 sq. mi. Mississippi River bottom land.  
Excludes 5.8 sq. mi. Mississippi River bottom land.  
Flow from 6,300 sq. mi. of drainage area passes through power dams, which act as silt traps.  
Estimated or assumed.

SUMMARY OF  
RESERVOIR SEDIMENTATION SURVEYS MADE IN THE UNITED STATES THROUGH 1970

DATA SHEET NUMBER	RESERVOIR	STREAM	NEAREST TOWN	DRAINAGE AREA (SQUARE MILES)		DATE OF SURVEY	PERIOD BETWEEN SURVEYS (YEARS)	STORAGE CAPACITY (ACRE-FT.)	CAPACITY AVG. ANR. INFLOW (ACRE-FT. PER ACRE-FT.)	SPECIFIC WEIGHT (L.B. PER CU. FT.)	AVG. ANR. ACCUMULATION PER SQ. M. OF NET DR. AREA FOR PERIOD SHOWN		AGENCY SUPPLYING DATA
				TOTAL	NET						AC-FT.	TONS	
UPPER MISSISSIPPI RIVER BASIN (ST. PAUL TO FRAZEE DU CHIEN WISCONSIN, ROOT, SHIPPAH, AND ST. JOSEPH RIVER BASIN (CONTINUED))													
27-5	Pool No. 54	Mississippi River	Wadena, Minn.	59,100	--	July 1956	5.6	20,000	--	90	--	--	CE
27-6a	Dike at Wabasha	Trib. of Willow Creek	Princeton, Minn.	1.31	1.29	Mar. 1956	3.4	166.7	474	70	0.31	778	S.J.
27-7	Franklin Farm Pond	Trib. of Spring Creek	Red Wing, Minn.	1.188	1.181	Apr. 1958	4.1	110.5	463	65	1.23	1,743	SCS
27-8	Friehart Farm Pond	Trib. of Zumbro River	Zumbro Falls, Minn.	.269	.268	June 1962	4.1	104.2	1,166	48.5	.52	560	SCS
27-9	Starkweather Farm Pond	Trib. of Coony Creek	Money Creek, Minn.	.231	.230	Sept. 1957	6.8	13.29	2,155	19.09	.96	1,359	SCS
27-10	Mahlfel Farm Pond	Trib. of Zumbro River	Millville, Minn.	.136	.134	July 1955	7.7	18.04	2,277	95	.49	587	SCS
27-11	Hold Farm Pond	Trib. of Crossed Creek	Spring Grove, Minn.	.194	.193	Aug. 1954	6.8	28.10	1,157	90	.33	374	SCS
27-12	Wagon Wheel Dam (East Willow Creek Watershed)	Trib. of Root River	Princeton, Minn.	.456	.433	Oct. 1951	7.3	10.03	1,190	51.86	.331	374	SCS
27-13	E-3 Mankota	Trib. of E.E. Willow Creek	--	3.16	3.10	June 1962	7.7	55.18	431	65	.48	680	SCS
UPPER MISSISSIPPI RIVER BASIN (ABOVE ST. PAUL)													
28	Lake Superior and Lake of the Woods Area (in Minnesota)	--	--	--	--	Mar. 1960	3.83	287.2	314	490	.11	120	SCS
29	--	--	--	--	--	Apr. 1964	4.08	--	314	490	.30	330	SCS
RED RIVER OF THE NORTH BASIN													
30-1	Lake Bronson	Two Rivers	Brown, Minn.	439	438.5	Summer 1950	10	3,792	--	30.94	.088	21.6	SCS
30-2	Prasee	Otter Tail River	Prasee, Minn.	210	24	Oct. 1952	26	153	--	20	.009	12.5	SCS
30-3	Elabon Dam	Trib. of Coony River	Elabon, N. Dak.	1.219	1.188	Oct. 1955	20	120.49	93.54	41	.98	875	SCS
30-4	Boudreau Dam	M. Br. Forest River	Adams, N. Dak.	20.2	14.6	Oct. 1955	22	107.29	2,753	25	.034	16.03	SCS
30-5	Outaouchee Farm Pond	Park River	Adams, N. Dak.	3.755	3.670	Aug. 1957	11	139.6	134	93	.10	76.99	SCS
30-6	Odmar Dam	Trib. of Wild Rice River	Odmar, N. Dak.	.226	.222	May 1956	20	38.70	284	29	.59	372.6	SCS
30-7	Madison Farm Pond	Swan Creek	Neenah, N. Dak.	27.76	27.76	Aug. 1956	17	19.10	2,086	93	.0078	1.95	SCS
30-8	Nepolis Dam	Buffalo Creek	Neenah, N. Dak.	12.16	11.72	June 1958	48	174.40	1,006	93	.042	39.64	SCS
30-9	Meason Sliding Dam	Rush River	Reis, N. Dak.	30.2	30.2	June 1956	44	35.40	284	93	.0098	4.44	SCS
30-10	Melvin Ballerud Farm Pond	Park River	Adams, N. Dak.	1.125	1.121	June 1955	13	14.67	4,412	93	.1579	114.48	SCS
30-11	Wilson WPA Dam	Trib. of Wild Rice River	Millon, N. Dak.	11.375	11.356	May 1954	21	66.59	1,128	93	.0076	51.93	SCS
30-12	Morby Dam	Trib. of Wild Rice River	Harmon, N. Dak.	.183	.183	May 1955	21	46.159	1,197	93	.0076	184.3	SCS
30-13	Raleigh Dam	Dog Tooth Creek	Raleigh, N. Dak.	4.45	4.45	Aug. 1956	22	174.47	925	93	.144	109.8	SCS
30-14	Slone Railroad Reservoir	Park River	Adams, N. Dak.	16.855	16.66	May 1955	14	86.37	1,145	93	.006	18.88	SCS
30-15	White Lake	Trib. of Wild Rice River	Harmon, N. Dak.	37.0	21.05	May 1958	19	1,000.8	1,113	32	.2167	151	CE
30-16	Belchill Dam (Lake Anshabala)	Shogren River	Valley City, N. Dak.	371.979	371.979	June 1958	5.1	76,400	--	90	.0981	194	CE
30-17	Wagon Dam (Park River)	S. Br. Park River	Park River, N. Dak.	29	--	Mar. 1958	5.2	3,362	--	90	.225	441	CE
MISSOURI RIVER BASIN (NEBRASKA CITY TO HEMLOCK)													
31-1	Lake of the Ozarks (Bagnell Dam)	Ozark River	Elkton, Mo.	14,000	13,900	Feb. 1971	--	2,067,223	.299	--	--	--	CE
31-2	Carl Chiquier	Trib. of West Rodaway River	Shannon, Iowa	.146	--	Oct. 1968	17.8	1,972,331	.283	91.3	.464	598	SCS



St.	Location	Area (sq. mi.)	Year	Flow (cfs)	Notes
XI-3	L. R. Puchling	1.05	July 1939	1,100	
XI-4	McDonald Lake	41.9	May 1949	9.8	
XI-5	Douglas Co. Old Ditching Basin	1.62	June 1920	11	
XI-6	Leavenworth Co. State Lake	3.83	June 1937	10.0	
XI-7	Lyon Co. State (Meadow Lake)	2.19	Nov. 1961	16.1	
XI-8	Martin Farm Lake	.18	Nov. 1930	4.0	
XI-9	Rush Lake	8.13	Oct. 1927	6.9	
XI-10	Near	5.15	Apr. 1933	26.4	
XI-11	Lake Kattiba	6.20	July 1932	12.1	
XI-12	Richmond	2.17	July 1939	28	
XI-13	Lampa Farm Pond	.065	Aug. 1948	6.3	
XI-14	E. K. Howell	.909	July 1919	6/6.9	
XI-15	Allerton	1.98	Nov. 1939	25.5	
XI-16	Centerville No. 2	2.70	Nov. 1928	11	
XI-17	Lake of Three Pines	6.15	July 1926	13.6	
XI-18	Douglas Reservoir	.703	Feb. 1932	13.4	
XI-19	Huxley Reservoir	.12	1937	11.37	
XI-20a	Schubeler Reservoir	.188	1936	10.35	
XI-21	Occ	.31	1934	6.23	
XI-22	Dreage	.4	Mar. 1944	8.8	
XI-23	Film	.64	Sept. 1935	11.5	
XI-24	Honey Creek No. 4-2	.278	Oct. 1936	20.7	
XI-25	Honey Creek No. 4-4	.355	Sept. 1939	2.00	
XI-26	Honey Creek No. F-1	1.23	Jan. 1961	1.33	
XI-27	Honey Creek No. E-1	.478	Aug. 1947	1.17	
XI-28	Honey Creek No. I-1	.903	Nov. 1935	2.92	
XI-29	Miller Ranch	.72	Jan. 1961	1.33	
XI-30	Miller	.42	May 1941	16.8	
XI-31	Prairie Lake	1.49	Oct. 1947	4.0	
XI-32	Rybar	.16	Oct. 1915	8.0	
XI-33	Shubert Lake	9.17	Oct. 1949	7.9	
XI-34	Shubert Lake		Jan. 1936	15.5	
XI-35	Shubert Lake		June 1932	1.2	
	Dear Creek Trib. of Remba		Oct. 1933	1.1	
			Apr. 1935	3.15	
			Apr. 1936	1.0	
			Apr. 1938	1.0	
			July 1960	2.3	

✓ Total drainage area (exclusive of closed Berrie Lake Basin with drainage area of 3,940 sq. mi.),  
 ✓ About 2,150 sq. mi. of the total drainage area contribute to the reservoir.  
 ✓ Water supply pool capacity, estimated, 1,300 acre-ft. greater capacity at spillway crest elevation.  
 ✓ Maximum capacity, estimated, 1,300 acre-ft. greater capacity at spillway crest elevation.  
 ✓ Including area of lake and 0.31 sq. mi. above stock pond.

St.	Location	Area (sq. mi.)	Year	Flow (cfs)	Notes
XI-3	Westboro, Mo.	1.05	July 1939	1,100	
XI-4	Springfield, Mo.	41.9	May 1949	9.8	
XI-5	Blair, Kans.	1.62	June 1920	11	
XI-6	Tonganoxie, Kans.	3.83	June 1937	10.0	
XI-7	Reading, Kans.	2.19	Nov. 1961	16.1	
XI-8	Osage, Kans.	.18	Nov. 1930	4.0	
XI-9	Horton, Kans.	8.13	Oct. 1927	6.9	
XI-10	Near	5.15	Apr. 1933	26.4	
XI-11	Clatsa, Kans.	6.20	July 1932	12.1	
XI-12	Richmond, Kans.	2.17	July 1939	28	
XI-13	Tribe of Muddy Creek	.065	Aug. 1948	6.3	
XI-14	Tribe of Tarkio Creek	.909	July 1919	6/6.9	
XI-15	South Charleston River	1.98	Nov. 1939	25.5	
XI-16	Hammond Branch	2.70	Nov. 1928	11	
XI-17	E. Ft. 102 River	6.15	July 1926	13.6	
XI-18	Long Creek	.703	Feb. 1932	13.4	
XI-19	Tribe of Mamba River	.12	1937	11.37	
XI-20a	Long Branch	.188	1936	10.35	
XI-21	Unnamed Trib.	.31	1934	6.23	
XI-22	Occ	.4	Mar. 1944	8.8	
XI-23	Dreage	.64	Sept. 1935	11.5	
XI-24	Honey Creek No. 4-2	.278	Oct. 1936	20.7	
XI-25	Honey Creek No. 4-4	.355	Sept. 1939	2.00	
XI-26	Honey Creek No. F-1	1.23	Jan. 1961	1.33	
XI-27	Honey Creek No. E-1	.478	Aug. 1947	1.17	
XI-28	Honey Creek No. I-1	.903	Nov. 1935	2.92	
XI-29	Miller Ranch	.72	Jan. 1961	1.33	
XI-30	Miller	.42	May 1941	16.8	
XI-31	Prairie Lake	1.49	Oct. 1947	4.0	
XI-32	Rybar	.16	Oct. 1915	8.0	
XI-33	Shubert Lake	9.17	Oct. 1949	7.9	
XI-34	Shubert Lake		Jan. 1936	15.5	
XI-35	Shubert Lake		June 1932	1.2	
	Dear Creek Trib. of Remba		Oct. 1933	1.1	
			Apr. 1935	3.15	
			Apr. 1936	1.0	
			Apr. 1938	1.0	
			July 1960	2.3	

✓ Reservoir silted full Dec. 1934; crest raised June 1937; silted full again Dec. 1940;  
 ✓ crest raised again May 1945; silted full again May 1949. Age computed as 6.7 yr.  
 ✓ Name (-) indicated minor or comparison (limited as negative sediment).  
 ✓ Estimated or assumed.

SUMMARY OF  
RESERVOIR SEDIMENTATION SURVEYS MADE IN THE UNITED STATES THROUGH 1970

DATA SHEET NUMBER	RESERVOIR	STREAM	NEAREST TOWN	DRAINAGE AREA (SQUARE MILES)		DATE OF SURVEY	PERIOD BETWEEN SURVEYS (YEARS)	STORAGE CAPACITY (ACRE-FT.)	CAPACITY INFLOW RATE (ACRE-FT. PER ACRE-FT.)	SPECIFIC WEIGHT (DRY) (L.R. FSR AREA FOR PERIOD SHOWN)	AVG. ANN. SEDIMENT ACCUMULATION PER SQ. MI. OF NET DR. AREA FOR PERIOD SHOWN	AGENCY SUPPLYING DATA
				TOTAL	NET							
MISSOURI RIVER BASIN (NEBRASKA CITY TO HERMAN) (Cont. med)												
31-34	Seton	Unnamed Trib.	Effingham, Kans.	.17	.16	Jan. 1950	--	1/53.2	--	--	--	SCS
31-35	Shirley Pond	--	Effingham, Kans.	--	--	Oct. 1957	7.7	60.86	460	1.88	2,457	SCS
31-36	Trenton	--	Lawrence, Kans.	.18	.18	Nov. 1956	17.7	19.05	86.7	.56	1,057.5	SCS
31-37	Thorne	--	Fairview, Kans.	.18	.18	May 1947	--	1/3.78	62.01	.90	1,201	SCS
31-38b	Unnamed	--	Effingham, Kans.	1.17	1.16	Sept. 1955	8.4	2.42	460	.90	1,176	SCS
	Unnamed	--	Effingham, Kans.	3.78	3.75	Aug. 1957	11	17.7	69	1.44	1,178	ARS
	Unnamed	--	Effingham, Kans.	--	--	Apr. 1951	12.6	212.01	68	.73	807	ARS
	Unnamed	--	Effingham, Kans.	--	--	June 1952	4.3	202.23	68	.76	543	ARS
	Unnamed	--	Effingham, Kans.	--	--	July 1955	6.9	186.07	69.4	.62	1,038	ARS
	Unnamed	--	Effingham, Kans.	--	--	July 1958	6.1	171.52	64.7	.62	611	ARS
	Unnamed	--	Effingham, Kans.	--	--	July 1962	30.0	30.0	55.94	2.081	2,411	ARS
31-39	Higdonville Old City Lake	Trib. of Davis Creek	Higdonville, Mo.	2.78	2.633	Oct. 1950	32.26	32.26	58.74	2.688	3,436	SCS
31-40	Buscher	Trib. of Brush Creek	Lawrence, Kans.	.119	.117	Oct. 1949	13.8	25.55	56.8	.85	1,051	SCS
31-41	Mitchell	Trib. of Washington Creek	Lawrence, Kans.	.61	.58	June 1962	12.67	6.73	42.9	.07	73	SCS
31-42	Unnamed	--	Clinton, Kans.	--	--	Mar. 1962	12.4	6.26	46.7	1.27	1,294	SCS
31-43	Kennedy	Trib. of Marana River	Richland, Kans.	.23	.22	Apr. 1977	63.19	54.27	56.2	2.13	2,609	SCS
31-44	Jett	--	Ruders, Kans.	.123	.122	May 1955	7.1	3/7.32	75	.58	94	SCS
31-45	Lake Jett	--	Manhattan, Kans.	3.20	3.14	Apr. 1956	16.33	37.7	50.7	1.61	1,777	SCS
31-46	Roby	Trib. of Kansas River	Manhattan, Kans.	.284	.280	May 1962	5.9	11.32	41.6	4.57	4,144	ARS
31-47	Callahan Dr. McArthur (C-1)	Trib. of Kamba River	Subota, Kansas	5.623	5.515	Apr. 1967	--	1,017.07	41.6	4.57	4,144	ARS
			Columbia, Mo.	--	--	Aug. 1967	.25	1,030.8	82.2	1.38	2,079	ARS
			Lawrence, Kans.	--	--	July 1967	1.9	97.3	82.2	1.38	2,079	ARS
			Lawrence, Kans.	.83	.82	July 1956	31	19.67	60	.34	444	SCS
31-48	Whitefield	Trib. Marana Des Ognas	Round City, Kans.	.16	.16	July 1967	9.75	18.07	60	1.19	1,555	SCS
31-49	Pool	Trib. Elk Creek	Circularville, Kans.	.28	.27	July 1968	--	16.18	60	1.19	1,555	SCS
31-50	Blucher	Trib. Straight Creek	Holton, Kans.	.23	.23	July 1967	11	54.28	60	1.47	1,921	SCS
31-51	Reamer	--	--	.23	.23	July 1966	12	31.26	60	1.43	1,849	SCS
31-52	Hogers	Big Sugar	Garrett, Kans.	1.17	1.16	July 1956	12	27.3	67	.24	330	SCS
31-53	Lemmo	Trib. of Elm Creek	Garrett, Kans.	.19	.19	June 1967	31	14.1	67	.47	614	SCS
31-54	Elko Dam Reservoir	Trib. Bull Creek	Garrett, Kans.	.77	.77	June 1961	6	6.16	60	.60	614	SCS
31-55	Overhullen Pond	--	Garrett, Kans.	.57	.50	Sept. 1960	10.2	204.3	60	1.88	2,457	SCS
31-56	Richmond Lake	Dry Branch	Edgerton, Kans.	.86	.84	Sept. 1970	10	171.1	65	.77	1,090	SCS
31-57	Hall Pond	Trib. Little Sugar	Richmond, Kans.	.38	.37	July 1975	12	22.08	60	1.07	1,398	SCS
31-58	Johnson Pond	--	Perlinville, Kans.	.94	.93	July 1967	12	44.87	60	.76	993	SCS
			Blue Mound, Kans.	--	--	July 1956	21	24.03	60	.24	313	SCS
			Blue Mound, Kans.	--	--	July 1967	31	17.1	60	.24	313	SCS
SHEET HILL AND LOWER REPUBLICAN RIVER BASINS												
32-1	Ottawa County State Lake	Sand Creek	Stemington, Kans.	20.47	20.26	1959	--	1,001	--	--	--	SCS
32-2	Sherman County State Lake	Saline River	Quincy, Kans.	451	463	Apr. 1957	8.0	930	--	1.38	--	BR
32-3a	Kennett	Shawnee River	Manhattan, Kans.	7,860	3/2,560	Aug. 1968	10.8	146,805	60.5	.0481	96.4	CR
32-3b	Unnamed	Shawnee River	Manhattan, Kans.	--	--	July 1960	11.2	436,300	60.0	.27	294	CR
32-4	Allington Reservoir	Sicly Creek	Beatrice, Mo.	.52	.52	Sept. 1956	20	31.104	65	1.77	2,506	SCS
32-5	Harvard Park Reservoir	Indian Creek	Beatrice, Mo.	.675	.662	Aug. 1947	20.5	14,704	65	1.77	2,506	SCS
32-6	Free Reservoir	Trib. of Little Blue River	Hubbs, Mo.	.175	.171	May 1956	8.75	8.058	65	1.400	1,982	SCS
			Hubbs, Mo.	--	--	July 1956	21	2.301	65	1.566	2,217	SCS



SUMMARY OF  
RESERVOIR SEDIMENTATION SURVEYS MADE IN THE UNITED STATES THROUGH 1970

DATA SHEET NUMBER	RESERVOIR	STREAM	NEAREST TOWN	DRAINAGE AREA (SQ. MILES)		DATE OF SURVEY	PERIOD BETWEEN SURVEYS (YEARS)	STORAGE CAPACITY (ACRE-FT.)	CAPACITY INFL. RATIO (ACRE-FT. PER ACRE-FT.)	SPECIFIC WEIGHT (LB. PER CU. FT.)	AVG. ANNUAL ACCUMULATION PER SQ. MI. AREA FOR PERIOD SHOWN		AGENCY SUPPLYING DATA
				TOTAL	NET						AC.-FT.	TONS	
SHORT HILL AND LOWER REPUBLICAN RIVER BASINS (Continued)													
32-49	Sanger Pond	Trib. S. P. Solomon River	Northland, Kans.	2.53	2.32	Mar. 1974	16.4	322.12	3.59	465	0.65	917	SCS
32-50	Stuebel Pond	Trib. Rose Creek	Munden, Kans.	1.61	1.61	Aug. 1970	10	307.5	3.058	470	.24	343	SCS
32-51	Schroeder Pond	Trib. Mill Creek	Green, Kans.	.73	.67	July 1960	9.6	127.1	1.088	460	.59	767	SCS
32-52	Wals Pond	Trib. Saline River	Ogallah, Kans.	3.93	3.8	Aug. 1958	12	69.32	1.377	460	.12	162	SCS
32-53	Woolhoff Pond	Trib. Fire Creek	Neoplatonville, Kans.	.61	.59	June 1974	16.1	29.05	1.771	465	.48	680	SCS
32-54	Herrington City Lake	Lyness Creek	Herrington, Kans.	17.24	16.93	July 1970	44	2,180	1.68	470	.96	1,465	SCS
UPPER REPUBLICAN, NORTH PLATTE, RIVER BASINS (PT. LIBANIE TO NORTH PLATTE) AND SOUTH PLATTE RIVER BASIN (SUBLETS TO NORTH PLATTE)													
33-1	Wall Creek	Medicine Creek	Wall Creek, Neb.	3715.00	14.89	Oct. 1931	5.6	59	---	465	.66	934	SCS
33-2	Loebart Farm Pond	Trib. of N. Platte River	Gering, Neb.	372.54	2.58	May 1959	12.9	15.64	2.29	573	.208	257	NE
33-3a	Harry Strunk Lake (Medicine Creek Dam)	Medicine Creek	Cambridge, Neb.	656	653	July 1942	8.83	92.817	1.691	---	---	---	---
33-4a	Flanagan Reservoir	Trib. of Republican River	Berkley, Neb.	.900	.497	Dec. 1962	11.17	88.09	1.656	70.4	1.31	2,004	SCS
33-5a	Gallatin Reservoir	Trib. of Beaver Creek	Danberry, Neb.	3.44	3.09	Apr. 1946	10.4	419.5	---	470	.602	918	SCS
33-6	Klein Reservoir	Trib. of Republican River	McCook, Neb.	1.59	1.57	Sept. 1956	10.6-2	381.6	---	470	1.18	1,800	SCS
33-7	Dempsey Pond	Trib. of Bear Gulch Creek	Kearney, Neb.	8.516	.51	June 1949	20	56.0	---	470	1.58	2,409	ARS
33-8a	Redfelt Stock Pond	Unnamed	Julesburg, Colo.	.72	.71	June 1953	4.9	11.10	---	75.6	.447	645	SCS
33-9	Donabala Pond	Trib. Beaver Creek	Atwood, Kans.	1.41	1.4	Nov. 1948	7	22.12	---	80.4	.28	490	SCS
33-10	Frickey Pond	Trib. Salina Creek	Northard, Kans.	3.32	3.28	Aug. 1970	21.8	18.19	---	470	.28	422	SCS
33-11	Walker Pond	Trib. Beaver Creek	Atwood, Kans.	4.78	4.77	Dec. 1958	11.6	63.17	---	460	.24	320	SCS
33-12	Stroud Pond	Trib. Jones Gaugon Creek	Atwood, Kans.	.83	.82	Oct. 1978	21.6	13.62	---	470	.07	109	SCS
33-13	Frankton-Parker M-1 Washed	Mellow Creek	McDonald, Kans.	7.6	7.57	June 1963	11.7	111.25	10.093	470	.96	1,447	SCS
33-14	Bondsgard Stock Pond	Sagecroft Drain	Cardon Road, Colo.	1.5	1.5	Jan. 1967	4	397	21.84	---	---	---	SCS
34-1	Carletonwood	Cherry Creek	Denver, Colo.	167.2	166.9	Aug. 1953	13	3,454	---	---	.099	167	SCS
34-2	Kernwood	North Platte River	Quinn, Wyo.	15,004	675	Mar. 1956	2.25	3,486	---	---	.106	175	SCS
34-3a	Cherry Reservoir	North Platte River	Quinn, Wyo.	15,004	675	June 1958	1.00	9,210	---	---	.711	1,280	NE
34-3b	Cherry Reservoir	North Platte River	Quinn, Wyo.	15,004	675	Feb. 1957	3.83	73,810	---	---	.28	---	---
34-3c	Cherry Reservoir	North Platte River	Quinn, Wyo.	15,004	675	Jan. 1953	2.00	67,840	---	---	.26	---	---
34-3d	Cherry Reservoir	North Platte River	Quinn, Wyo.	15,004	675	Jan. 1953	2.00	65,090	---	---	.20	---	---
34-3e	Cherry Reservoir	North Platte River	Quinn, Wyo.	15,004	675	Feb. 1957	2.00	62,990	---	---	.18	---	---
34-3f	Cherry Reservoir	North Platte River	Quinn, Wyo.	15,004	675	Feb. 1957	2.00	58,430	---	---	.17	---	---
34-3g	Cherry Reservoir	North Platte River	Quinn, Wyo.	15,004	675	Jan. 1944	2.00	56,600	---	---	.17	---	---
34-3h	Cherry Reservoir	North Platte River	Quinn, Wyo.	15,004	675	July 1947	3.00	53,180	---	---	.21	249	---
34-3i	Cherry Reservoir	North Platte River	Quinn, Wyo.	15,004	675	June 1957	5.92	49,150	---	---	.103	107	---
34-3j	Cherry Reservoir	North Platte River	Quinn, Wyo.	15,004	675	June 1966	9.40	44,860	---	---	.0467	---	---
34-3k	Cherry Reservoir	North Platte River	Quinn, Wyo.	15,004	675	Oct. 1960	9.40	42,704	---	---	.186	---	---
34-3l	Cherry Reservoir	North Platte River	Quinn, Wyo.	15,004	675	Sept. 1951	31	77,958	---	---	.025	37.2	---

34-5	Parkfield	North Platte River	Alameda, Wyo.	10,700	5/5,315	Jan 1977	1,094,300	0.1	8/078	2/730
34-6	Sanford	Little River	Law, Wyo.	7,540	7,117	July 1970	1,001,876	45	9/1108	8/753
34-7	Goodland	Little River	Atkinson, Colo.	9,140	9,25	Sept. 1976	1,282,23		37	
34-8	B-3 Elroy Creek	Elroy Creek	Elbert, Colo.	2,92	2,89	July 1976	1,215,2		52	57
34-9	Summit	Osage Creek	Willingham, Colo.	11,7	11,6	Jan 1975	1,107,27		69	109
34-10	Summit	Osage Creek	Willingham, Colo.	11,7	11,6	Jan 1975	1,107,27		69	109
34-11	O-11 Elroy Creek	Elroy Creek	Elbert, Colo.	56	56	Jan 1977	32,30		43	707
34-12	J-13 Elroy Creek	Elroy Creek	Elbert, Colo.	1,07	1,06	July 1976	50,17		69	87
34-13	B-9 Elroy Creek	Elroy Creek	Elbert, Colo.	65	64	July 1975	42,54		69	137
34-13	Slab Canyon	Slab Canyon	Willingham, Colo.	3,15	3,04	July 1977	211,4		69	137
						Feb. 1968	288,3		35	

ROCKWELL RIVER BASIN (ADJUST BASE TO REMARKA CITY) PLAYS RIVER BASIN (BELOW NORTH PLATES)

35-1	Otto Beck	Trib. of Boulder River	Blainville, Iowa	199	197	Sept. 1961	9/6, 28	177	6,41	7,490
35-2	Fred Beck	Trib. of Willow River	Logan, Iowa	100	97	Jan 1961	9/13, 89	296	9,3	13,600
35-3	William Eckhardt	Trib. of Willow River	Elkhart, Iowa	208	204	May 1960	4,61	208	6,41	2,990
35-4	O. R. Rivers Lower Reservoir	Trib. of Upper River	Paulding, Iowa	187	139	May 1969	9,12, 60	139	6,41	2,990
35-5	O. R. Rivers Upper Reservoir	Trib. of Upper River	Paulding, Iowa	187	139	May 1969	9,12, 60	139	6,41	2,990
35-6	Charles Plumb	Trib. of Upper River	Paulding, Iowa	187	139	May 1969	9,12, 60	139	6,41	2,990
35-7	C. T. Gaud	Trib. of Upper River	Paulding, Iowa	187	139	May 1969	9,12, 60	139	6,41	2,990
35-8	Otto Beck	Trib. of Middle Boulder R.	Charles Oak, Iowa	130	127	Apr. 1969	10/2, 8	130	6,375	97,700
35-9	Thomas Hobbs	Trib. of Upper River	Des Moines, Iowa	217	213	Apr. 1969	2,95	217	2,11	2,477
35-10	Fred Hill	Trib. of Willow River	Des Moines, Iowa	217	213	Apr. 1969	2,95	217	2,11	2,477
35-11	Jesse Gresh	Trib. of Upper River	Paulding, Iowa	217	213	Apr. 1969	2,95	217	2,11	2,477
35-12	Sam La Prente	Trib. of Upper River	Paulding, Iowa	155	133	Apr. 1969	1,77	155	6,67	5,797
35-13	James O'Neil Farm Pond	Trib. of L. Roubidoux River	Spretness, Neb.	199	197	Jan. 1975	2,3	199	2,43	3,200
35-14	Polerson Farm Pond	Trib. of Elk Creek	Appomattox, Iowa	186	182	Apr. 1969	7,11	186	2,18	2,180
35-15	Harvey Lager	Trib. of Upper River	Paulding, Iowa	108	106	Apr. 1969	12,07	108	5,5	2,432
35-16	Bernard Mattson	Trib. of Upper River	Paulding, Iowa	100	99	July 1964	8,8	100	6,26	12,778
35-17	William Roper	Trib. of Upper River	Paulding, Iowa	97	95	July 1964	4,4	97	6,26	12,778
35-18	Max Miller No. 1	Trib. of R. Roubidoux R.	Hamonds, Iowa	223	218	Mar. 1961	11,5	223	16,3	39,900
35-19	Max Miller No. 2	Trib. of Upper River	Paulding, Iowa	223	218	Mar. 1961	11,5	223	16,3	39,900
35-20	Harvey Hault	Trib. of Upper River	Paulding, Iowa	336	330	Oct. 1964	3,1	336	3,12	7,200
35-21	Tracy Borch	Trib. of Upper River	Paulding, Iowa	265	258	Mar. 1969	9,4	265	4,95	7,500
35-22	Lois Williams	Trib. of Upper River	Paulding, Iowa	18	18	July 1967	5,9	18	1,38	798
35-23	Ray Farm Pond	Trib. of Upper River	Paulding, Iowa	18	18	July 1967	5,9	18	1,38	798

1/ Basins 25 to 34, m. of noncontiguous drainage.  
 2/ Basins 25 to 34, m. of noncontiguous drainage.  
 3/ Water capacity 1,540 ac-ft. below spillway crest.  
 4/ Water supply pool capacity. Reservoir has greater capacity at spillway crest elevation.  
 5/ Reservoir filled full June 1964.  
 6/ Includes 0.13 ac-ft. of sediment above emergency spillway.  
 7/ Area contained in embankment increases runoff 18.63 c.f.s.

SUMMARY OF  
RESERVOIR SEDIMENTATION SURVEYS MADE IN THE UNITED STATES THROUGH 1970

DATA SHEET NUMBER	RESERVOIR	STREAM	NEAREST TOWN	DRAINAGE AREA (SQ. MILES)		DATE OF SURVEY	PERIOD BETWEEN SURVEYS (YEARS)	STORAGE CAPACITY (ACRE-FT.)	CAPACITY INFLOW RATIO PER ACRE-FT.	SPECIFIC WEIGHT (LB. PER CU. FT.)	AVG. ANNUAL ACCUMULATION OF NET DR. AREA FOR PERIOD SHOWN		AGENCY SUPPLYING DATA	
				TOTAL	NET						AC.-FT.	TONS		
MISSOURI RIVER BASIN (ABOVE BLAIR TO NEBRASKA CITY) PLATTE RIVER BASIN (BELOW NORTH PLATE) (Cont. from)														
35-25	Howe Farm Pond	Trib. of Dead Horse Creek	Loup City, Nebr.	1.80	1.79	Aug. 1948	—	15.6	*.163	—	—	—	SCS	
35-26	Moller Farm Pond	Trib. of Oak Creek	Farwell, Nebr.	.398	.354	Aug. 1949	5	13.9	*.145	.65	.20	.283	SCS	
35-27	Musicka Farm Pond	—	—	.27	.26	Aug. 1949	4	14.39	*.157	.65	.71	1.005	SCS	
35-28	Prather Reservoir	—	Dunbar, Nebr.	.184	.180	Aug. 1952	4	28.04	*.155	.65	2.62	3,700	SCS	
35-29	Cook Reservoir	Trib. of L. Nemaha River	—	.391	.383	1954	5	9.93	—	.65	2.01	2,846	SCS	
35-30a	Ingerson Reservoir No. 1	Trib. of Papillion Creek	Arlington, Nebr.	.211	.209	1952	23	21.1	—	.65	.921	1,504	SCS	
35-31	Ingerson Reservoir No. 2	Turkey Creek	Louisville, Nebr.	.074	.073	1952	5	10.19	—	.65	1.89	2,676	SCS	
35-32	Ingerson Reservoir No. 3	—	—	.335	.331	1957	5	.72	—	.65	1.43	2,004	SCS	
35-33	Kruso Reservoir	—	Elkhorn, Nebr.	.80	.779	1957	2	18.39	—	.65	1.71	2,421	SCS	
35-34	Lugn Reservoir	Unnamed	Douglas, Nebr.	.263	.253	1956	21	61.5	—	.65	2.99	4,233	SCS	
35-35	Bluhner Reservoir	Trib. of L. Nemaha River	Dunbar, Nebr.	.163	.158	1949	11	4.33	—	.65	2.93	4,148	SCS	
35-36	O'Brien Reservoir	South Cedar Creek	Manley, Nebr.	.417	.412	1957	8	10.92	—	.65	2.72	3,491	SCS	
35-37a	O'Neill Reservoir	Trib. of L. Nemaha River	Syracuse, Nebr.	.140	.120	1956	20	22.59	—	.65	1.77	2,506	SCS	
35-38	Pickrell Reservoir No. 1	Russell Creek	Unadilla, Nebr.	.336	.326	1949	21	35.69	—	.65	4.29	6,073	SCS	
35-39	Pickrell Reservoir No. 2	—	—	.102	.100	1954	8	32.35	—	.65	1.27	1,798	SCS	
35-40	Pickrell Reservoir No. 3	—	—	.088	.086	1959	3	2.96	—	.65	.795	1,026	SCS	
35-41	Pollard Reservoir	—	—	.114	.113	1957	18	3.40	—	.65	2.31	3,270	SCS	
35-42	Ross Farm Reservoir	Weping Water Creek	Nebraska, Nebr.	.100	.078	1956	23	7.63	—	.65	.272	.385	SCS	
35-43	Romber Reservoir	H. Fork Little Fox River	Otoe, Nebr.	.077	.074	1948	21	4.38	—	.65	1.55	2,194	SCS	
35-44	Mule Creek #1*	Long Creek	Fort Calhoun, Nebr.	.30	.298	1957	9	6.71	—	.65	2.04	2,888	SCS	
35-45a	Mule Creek #2*	Trib. of Highabotha River	Malvern, Iowa	.188	.177	July 1954	8	4.22	*1.109	.65	3.57	5,054	SCS	
						Sept. 1957	2	43.9	*1.015	71.4	14.63	7,400	SCS	
						Oct. 1957	2	40.2	*1.000	71.4	11.40	18,200	SCS	
						Jan. 1960	1.08	39.6	*.982	72.3	3.11	4,900	SCS	
						Dec. 1960	1.33	38.9	*.922	58.7	2.99	3,800	SCS	
						Jan. 1962	.92	36.5	*.876	60.3	14.50	19,000	SCS	
						Jan. 1963	1.00	34.7	*.877	2/60.3	7.65	11,880	SCS	
						Jan. 1965	1.00	34.9	*.877	2/60.3	4.46	8,110	SCS	
						Jan. 1967	1.00	32.81	*.877	2/60.3	13.99	18,370	SCS	
						Jan. 1968	1.00	30.88	*.828	2/60.3	4/-2.22	—	—	—
						Mar. 1969	1.17	31.37	*.792	5/75.5	4/-2.372	—	—	—
						Aug. 1974	—	55.3	*.684	—	—	—	—	—
						Oct. 1976	—	52.6	*.651	—	—	—	—	—
						Sept. 1957	1.92	51.8	*.641	69.5	2.55	3,900	SCS	
						Oct. 1958	1.08	50.3	*.623	79.2	3.42	4,700	SCS	
						Jan. 1960	1.15	47.6	*.593	55.3	1.55	1,900	SCS	
						Feb. 1962	1.08	45.1	*.558	2/55.3	5.11	6,150	SCS	
						Jan. 1963	.92	43.5	*.538	62.1	4.73	6,400	SCS	
						Jan. 1964	1.00	44.6	*.552	51.8	4/-2.88	—	—	—
						Jan. 1965	1.00	42.7	*.528	51.8	4.92	5,550	SCS	
						Jan. 1966	1.00	36.5	*.452	51.8	16.91	19,080	SCS	
						June 1969	—	39.89	.494	51.8	15.704	—	—	—
						July 1974	2.75	40.89	.50	5/71.64	4/-2.298	—	—	—
35-47b	Mule Creek #3*	—	—	.323	.323	Oct. 1954	2.33	71.8	—	.65	3.28	3,900	SCS	
						Sept. 1957	2.32	69.1	—	.65	15.50	22,300	SCS	



SUMMARY OF  
RESERVOIR SEDIMENTATION SURVEYS MADE IN THE UNITED STATES THROUGH 1970

DATA SHEET NUMBER	RESERVOIR	STREAM	NEAREST TOWN	DRAINAGE AREA (SQUARE MILES)		DATE OF SURVEY	PERIOD BETWEEN SURVEYS (YEARS)	STORAGE CAPACITY (ACRE-FT.)	CAPACITY AVERAGE INFLOW RATIO (ACRE-FT. PER ACRE-FT.)	SPECIFIC HEIGHT (DRT) (LB. PER CU. FT.)	AVERAGE ACCUMULATION PER SQ. MI. OF NET DR. AREA FOR PERIOD SHOWN	AGENCY SUPPLYING DATA
				TOTAL	NET							
RIVER BASIN (MIDBAMA TO ABOVE BLAIR) JAMES AND BIG SIOUX RIVER BASINS (Cont.-med)												
36-9	Thee-old Main	Unnamed	Arthur, Iowa	.483	.442	June 1949	1.01-2	*1.053	72.3	18.1	28,502	SES
	-do-	-do-	-do-	-	-	Aug. 1950	94.0	*.959	72.3	1.36	2,142	
	-do-	-do-	-do-	-	-	May 1951	93.5	*.954	72.3	7.13	11,228	
36-10	Theobald Lateral C.	-do-	-do-	.290	.234	Nov. 1948	37.5	*.735	67.9	7.65	11,313	SES
	-do-	-do-	-do-	-	-	July 1950	34.5	*.676	67.9	1.08	1,597	
	-do-	-do-	-do-	-	-	May 1951	34.3	*.673	67.9	3.60	5,524	
	-do-	-do-	-do-	-	-	May 1952	19.5	*.977	67.9	1.95	2,824	
36-11	Theobald Lateral D.	-do-	-do-	.098	.089	Nov. 1948	18.9	*.985	73.1	1.63	5,780	SES
	-do-	-do-	-do-	-	-	July 1950	18.7	*.970	73.1	2.86	4,540	
	-do-	-do-	-do-	-	-	May 1951	18.6	*.930	73.1	.72	1,146	
	-do-	-do-	-do-	-	-	Oct. 1952	18.6	*.978	73.1	1.35	2,364	
36-12a	Mortenson	-do-	Cherokee, Iowa	1.39	1.37	Oct. 1950	229.0	*.718	77.0	1.35	2,364	SES
36-13	Burlitt	-do-	Alcester, S. Dak.	.234	.234	Nov. 1936	12.84	1.035	77.0	1.35	2,364	SES
36-14b	1/2e Mitchell	-do-	Mitchell, S. Dak.	584	496	Oct. 1928	10,943	.89	946.79	.077	58	SES
	-do-	-do-	-do-	-	-	July 1948	10,380	.47	946.79	.117	119	
	-do-	-do-	-do-	-	-	Aug. 1949	9,798	.48	946.79	.117	119	
	-do-	-do-	-do-	-	-	July 1950	9,176	.48	946.79	.105	121	
36-15	Salem Dam	-do-	Salem, S. Dak.	1.158	1.158	Aug. 1950	12.79	.206	96.0	.80	1,045.44	SES
36-16	Scott No. 2	-do-	Alcester, S. Dak.	.152	.152	Oct. 1936	7.36	.909	96.0	1.52	1,857.2	SES
36-17	Lake Vermillion	-do-	Montrose, S. Dak.	402.9	402.0	Mar. 1959	5,173.7	.277	96.0	1.52	1,857.2	SES
36-19	Vermillion Watershed No. A	-do-	Salem, S. Dak.	.075	.075	June 1964	4,927.5	1.000	96.0	.68	780	SES
36-20	Vermillion Watershed No. B	-do-	Salem, S. Dak.	.237	.237	Nov. 1955	2.87	.834	96.0	.68	780	SES
36-21a	Lake Osagea	-do-	Worthamton, Minn.	17.40	16.27	Nov. 1897	3.06	6.48	96.0	.40	433	SES
	-do-	-do-	-do-	1.85	1.45	Mar. 1963	5,180	2.23	96.0	.67	692	SES
	-do-	-do-	-do-	-	-	Oct. 1964	196.44	2.55	96.0	.26	368	SES
36-22	Richmond Lake	-do-	Aberdeen, S. Dak.	82	73.5	Jan. 1937	179.75	2.33	96.0	.26	368	SES
	-do-	-do-	-do-	-	-	Sept. 1969	9,880.9	7.53	96.0	1.795	2,527	SES
	-do-	-do-	-do-	-	-	Sept. 1969	8,971.08	6.84	96.0	.378	426	SES
MISSOURI RIVER BASIN (ABOVE PIERRE TO MIDBAMA) Niobrara and White River Basins												
37-1a	Elkins Stock Pond No. 1	-do-	Hayes, S. Dak.	.98	.57	May 1907	18.61	-	41.3	.16	144	SES
37-2	Elkins Stock Pond No. 2	-do-	-do-	.33	.33	June 1911	15.78	-	36.6	.136	108	SES
37-3	Land Utilization Project No. 228-1	-do-	Pierre, S. Dak.	.203	.197	June 1937	26.0	-	-	-	-	SES
	-do-	-do-	-do-	-	-	Mar. 1936	16.7	-	-	-	-	SES
37-4	Land Utilization Project No. 228-2	-do-	-do-	.995	.981	July 1945	15.2	-	-	.822	-	SES
	-do-	-do-	-do-	-	-	Mar. 1936	34.0	-	-	-	-	SES
37-5	Land Utilization Project No. 228-4	-do-	-do-	.748	.742	July 1945	29.8	-	-	.458	-	SES
	-do-	-do-	-do-	-	-	May 1936	13.6	-	-	-	-	SES
37-6	Land Utilization Project No. 228-6	-do-	-do-	2.555	2.541	July 1945	9.9	-	-	.539	-	SES
	-do-	-do-	-do-	.166	.163	Apr. 1936	31.8	-	-	-	-	SES
37-7	Land Utilization Project No. 228-13	-do-	-do-	.245	.234	July 1945	25.1	-	-	.285	-	SES
	-do-	-do-	-do-	-	-	Oct. 1936	9.1	-	-	-	-	SES
37-8	Land Utilization Project No. 228-21	-do-	-do-	.514	.511	July 1945	8.3	-	-	.521	-	SES
	-do-	-do-	-do-	-	-	Oct. 1936	28.9	-	-	-	-	SES
37-9	Land Utilization Project No. 228-22	-do-	-do-	.200	.200	July 1945	26.1	-	-	1.389	-	SES
	-do-	-do-	-do-	-	-	Nov. 1936	9.2	-	-	-	-	SES
	-do-	-do-	-do-	-	-	Nov. 1945	6.3	-	-	.200	-	SES



Station	Project	Location	Year	Material	Cost	Notes
37-10	Land Utilization Project No. 228-25	Trib. of Missouri River	Nov. 1957	.147	9.3	
37-11	Land Utilization Project No. 228-31		July 1945 Mar. 1957	.220	8.4 13.5	.799
37-12	Land Utilization Project No. 228-32		July 1945 Mar. 1957	.477	12.3 14.1	.859
37-13	Land Utilization Project No. 228-34		July 1945 June 1957	1.222	12.1 44.3	.508
37-14	Land Utilization Project No. 228-35		July 1945 May 1958	.508	40.0 18.4	.443
37-15	Land Utilization Project No. 243-1		July 1945 Nov. 1957	.108	16.1 2.7	.651
37-16	Land Utilization Project No. 243-2	Unnamed Stream (interior drainage)	July 1945 Nov. 1957	.134	2.0 5.2	.911
37-17	Land Utilization Project No. 243-5	Trib. of Missouri River	July 1945 Nov. 1957	.072	3.0 2.6	2.206
37-18	Land Utilization Project No. 243-6	Trib. of Bad River	July 1945 Nov. 1957	.117	3.2 3.2	.700
37-19	Land Utilization Project No. 243-10	Trib. of Missouri River	July 1945 June 1958	.533	2.8 3.7	.474
37-20	Land Utilization Project No. 243-11		July 1945 July 1958	.339	2.9 4.5	.222
37-21	Harris Reservoir North	Unnamed	July 1945 May 1947	.577	3.9 7.5	.266
37-22	Harris Reservoir South	Unnamed	May 1947 May 1947	11.9	18.6 15.77	.315
37-23	Johnson Reservoir	Unnamed	May 1947 Nov. 1956	.849	16.25 16.25	.025
37-24	Lake Dante	Trib. of Choteau Creek	Nov. 1956 Nov. 1957	2.89	280.73 230.95	.435
37-25	Eggers	Trib. of Missouri River	Oct. 1955 July 1957	10.3	231.0 200.32	.578
MISSOURI RIVER BASIN (BRIDGES TO ABOVE PERCENTAGE)						
Cheyenne and Belle Fourche River Basins						
38-1	Johnson's Stock Pond	Gettysburg, S. Dak.	June 1912	.188	2.56	
38-2	Bartel Stock Pond		June 1912	.609	4.30	.16
38-3a	W-11 (Anderson)	Wals, S. Dak.	June 1937 Nov. 1956	.054	2.80 5.60	.08
38-3b	W-2 (Swenk)		Dec. 1962 Apr. 1967	1.27	5.14 4.51	4.48
38-4a	Augustura Reservoir	Sulphur, S. Dak.	June 1949 June 1949	9.100	10.11 349.9	.65
38-4b	Sturgis Watershed No. 1	Sturgis, S. Dak.	Sept. 1965 Oct. 1965	.339	315.3 138.761	1.38
38-5	Sturgis Watershed No. 2		Oct. 1965	.339	16	1.44
38-6	Sturgis Watershed No. 3		Oct. 1965	.339	56.4	.145
38-7	Sturgis Watershed No. 4		Oct. 1965	.339	92.2	.3
38-8	Sturgis Watershed No. 5		Oct. 1965	.339	92.2	.001
38-9	Sturgis Watershed No. 6		Oct. 1965	.339	92.2	.004
			Oct. 1965	.339	92.2	.252
			Oct. 1965	.339	92.2	.495
			Oct. 1965	.339	92.2	.05
			Oct. 1965	.339	92.2	2.248
			Oct. 1965	.339	92.2	.04
			Oct. 1965	.339	92.2	.076
			Oct. 1965	.339	92.2	.004
			Oct. 1965	.339	92.2	.108
			Oct. 1965	.339	92.2	.404
			Oct. 1965	.339	92.2	.004
			Oct. 1965	.339	92.2	.001
			Oct. 1965	.339	300.77	.011
			Oct. 1965	.339	221.75	.008

1/ 877 ac.-ft. of storage created by dredging.  
 2/ Less than .001. Material removed from Weir Pond facility periodically.  
 3/ Pagsola Reservoir controls about 120 sq. mi.

9.9 ac.-ft. sediment, removed in 1956, not included.  
 Estimated or assumed.

SUMMARY OF  
RESERVOIR SEDIMENTATION SURVEYS MADE IN THE UNITED STATES THROUGH 1970

DATA SHEET NUMBER	RESERVOIR	STREAM	NEAREST TOWN	DRAINAGE AREA (SQ. MILES)		DATE OF BETWEEN SURVEY SURVEYS (YEARS)	PERIOD BETWEEN SURVEYS (YEARS)	STORAGE CAPACITY (ACRE-FT.)	CAPACITY AVG. ANN. INFLOW (ACRE-FT. PER ACRE-FT.)	SPECIFIC WEIGHT (DRY) (L.B. PER CU. FT.)	AVG. ANN. SEDIMENT ACCUMULATION PER SQ. MI. OF NET DR. AREA FOR PERIOD SHOWN		AGENCY SUPPLYING DATA
				TOTAL	NET						AC-FT.	TONS	
MISSOURI RIVER BASIN (BRIDGE TO ABOVE PIERRE) Cheyenne and Belle Fourche River Basins (Continued)													
38-10	Barrel Detention Dam	Unnamed	New Castle, Wyo.	6.15	4.83	Aug. 1968	2.25	154.6	86	1.49	2,799	SCS	
38-11	New Underwood Reservoir	do	New Underwood, S. Dak.	2.97	2.94	Aug. 1955	3	438.1	60	.177	231	SCS	
MISSOURI RIVER BASIN (WILLISTON TO MDRIDGE) Moreau, Grand, Cannonball, Heart, and Little Missouri River Basins													
39-1	Frederick Stock Dam	Louse Creek	Flasher, N. Dak.	1.17	1.17	Aug. 1951	21	1.06	35	.00797	6.07	SCS	
39-2a	Hiddenwood Lake	Hiddenwood Creek	Selby, S. Dak.	31.8	27.2	May 1956	1	864	55	.047	56	SCS	
39-3	Kambloch Reservoir	Trib. of Moreau	Moreau, S. Dak.	2.20	1.97	Sept. 1959	33.3	1,207.78	60	.12	156.8	SCS	
39-4	Clark Reservoir	do	do	3.56	2.56	Aug. 1964	40	389.80	60	.15	196	SCS	
39-5	Neuer Reservoir	do	do	.493	.493	Aug. 1964	15	62.00	60	.30	392	SCS	
39-6	Cole Reservoir	do	do	4.66	3.21	Aug. 1951	13	35.96	60	.29	379	SCS	
39-7	Van Custing Dam	Trib. of Missouri River	Headler, N. Dak.	1.78	1.76	Apr. 1950	27	171.5	60.4	2/1176	3/11.5	SCS	
39-8	Battle Creek Detention Dam	Battle Creek	Hallett, Wyo.	18.44	18.44	Nov. 1967	14.5	167.0	71.4	.104	161.8	SCS	
MISSOURI RIVER BASIN (ZORTMAN TO WILLISTON) Milk and Musselshell River Basins													
40-1	Yellow Water	Yellow Water Creek	Winnett, Mont.	55	54	June 1938	10.3	4,796	32	.32	224	SCS	
40-2	Fort Peck	Missouri River	Fort Peck, Mont.	57,725	3/	Sept. 1948	12.69	19,657,192	56.7	.65	803	CS	
41-1	Anderson Reservoir	Trib. of Pondera Creek	Conrad, Mont.	.156	.156	Oct. 1955	39	8.44	60	.136	163	SCS	
41-2a	Kropp	do	do	.625	.625	Oct. 1900	55	4.70	60	.085	33	SCS	
41-3	Walston	do	do	2.96	2.96	Oct. 1915	40	3.84	60	.122	166	SCS	
MISSOURI RIVER BASIN (ABOVE ZORTMAN)													
LOWER YELLOWSTONE RIVER BASIN Tongue and Fowder River Basins													
42-1a	Baker Lake	Sandstone Creek	Baker, Mont.	5.20	5.01	May 1908	29.1	756	39	1.74	1,478	SCS	
42-2	Tongue River	do	do	1,740	1,734.5	May 1955	18.0	392	45	1.21	1,553	SCS	
42-3	Herring Reservoir	Dry Creek	Miss City, Mont.	6.92	6.92	July 1970	15.2	1,06	40	2.08	1,288	BR	
						May 1959	9.42	72,739	70.5	.188	286.7	SCS	
						Oct. 1948	28	67,300	70	.103	614	SCS	
						Oct. 1941		4.05					
						May 1969		222					

UPPER YELLOWSTONE RIVER BASIN

Station	Location	Area (ac-ft.)	Volume (cu-ft.)	Year	Remarks
43-1b	Buffalo Bill	1,470	1,470	May 1910	
43-2	Big Clin	962	962	Oct. 1954	
43-3	Fraser Draw	27.4	27.4	Oct. 1954	
43-4	East Fork	.81	.81	Nov. 1960	
43-5	West Fork	.38	.38	July 1948	
43-6	Red Spires	5.24	5.24	Oct. 1954	
43-7	Boysen	7,700	7,670	Oct. 1951	
				Aug. 1964	

ARKANSAS RIVER BASIN (VAN BUREN TO LITTLE ROCK) WHITE RIVER BASIN

Station	Location	Area (ac-ft.)	Volume (cu-ft.)	Year	Remarks
44-1a	Lake Bennett	4.16	4.11	June 1935	
44-2	Lake Booneville	2.60	2.57	Mar. 1929	
44-3	Lake Fort Smith	65	64	Feb. 1926	
44-4	Lake Bailey	15.2	15	Sept. 1937	
44-5	Lake Tangren	4,610	4,606	May 1940	
44-6	Miramod	680	672	Aug. 1942	
44-7	North Fork	1,806	1,772	Apr. 1930	
44-8	Cove Lake	10.90	10.66	May 1930	
44-9	Charleston Lake	1.03	.93	Dec. 1937	
44-10	Six Mile Creek No. 2	5.38	5.26	Oct. 1954	
44-11	Six Mile Creek No. 5	1.90	1.81	July 1961	
44-12	Trib. of Hurricane Creek	4.16	3.91	July 1955	

1/ Conservation pool capacity. Reservoir has greater capacity at spillway crest elevation.  
 2/ Includes 0.03 ac.-ft. above crest deposits.  
 3/ 1937-1955, 1977 sq. mi.; 1956-1961=34,692 sq. mi.  
 4/ Supplemental - load inflow was 608 ac.-ft.; suspended - load outflow was 200 ac.-ft. during period. Deposits too small to measure by range survey.

5/ Sediment inflow volume was computed to be 2,350 ac.-ft.; much of this probably settled out over a large area in deposits too thin to be measured accurately by echo sounders.  
 6/ Both sediment and flood pools.  
 7/ Sediment pool only.  
 8/ Estimated or assumed.

SUMMARY OF  
RESERVOIR SEDIMENTATION SURVEYS MADE IN THE UNITED STATES THROUGH 1970

DATA SHEET NUMBER	RESERVOIR	STREAM	NEAREST TOWN	DRAINAGE AREA (SQUARE MILES)		DATE OF SURVEY	PERIOD BETWEEN SURVEYS (YEARS)	STORAGE CAPACITY (ACRE-FT.)	CAPACITY INFLUX RATIO (ACRE-FT. PER ACRE-FT.)	SPECIFIC WEIGHT (DRY) (LB. PER CU. FT.)	AVG. ANN. SEDIMENT ACCUMULATION PER SQ. MI. OF NET DR. AREA FOR PERIOD SHOWN		AGENCY SUPPLYING DATA
				TOTAL	NET						AC-FT.	TONS	
ARKANSAS RIVER BASIN (VAN BUREN TO LITTLE ROCK) WHITE RIVER BASIN (Continued)													
44-13	Dardanelle Reservoir	Arkansas River	Dardanelle, Ark.	11,333	11,333	Oct. 1964	1.08	460,300	2/0532	80	0.628	1,000	CE
44-14	Six Mile Creek Site No. 6	Six Mile Creek	Chilmark, Ark.	4.14	4.07	Apr. 1964	2.36	447,600	2/0532	80	0.321	960	SCS
45-1	Lake Warrington	Trib. of Illinois River	Fayetteville, Ark.	4.06	3.92	July 1937	10.1	1,860	---	---	---	---	SCS
45-2	Wilson	Wilson Creek	---	2.35	2.30	Oct. 1927	---	1,822	---	---	---	---	SCS
45-3	Lake Sapulpa	Buchee Creek	Sapulpa, Okla.	8.72	8.57	June 1940	9.75	517	---	---	23	---	SCS
45-4b	Brown Lake	Peaceable Creek	McAlester, Okla.	20.9	19.9	Dec. 1935	22.5	911	---	---	949	---	SCS
45-5	Lake McAlister	Bull Creek	---	30.7	28.2	Dec. 1946	11.0	842	---	---	732	---	SCS
45-6	Lake Omaliga	Peaceable Creek	McAlester, Okla.	20.9	19.9	May 1943	9.2	4,995	640	94.2	1.83	2,160	SCS
45-7a	Lake Omaliga	Bull Creek	---	30.7	28.2	July 1952	10.75	4,660	597	---	85	743	SCS
45-7b	Shawnee Lake	Duer Creek	Shawnee, Okla.	21.2	18.9	Apr. 1963	22	10,597	580	---	1.43	---	SCS
45-8	Taft Lake	Br. of Pecan Creek	Taft, Okla.	2.3	2.2	Sept. 1927	10	280	---	---	278	---	SCS
45-9	Heweane Lake	Trib. of Deep Rk. Creek	Arenada, Okla.	4.58	4.29	Sept. 1924	14	2,314	---	---	29	---	SCS
45-10	Lake Carlston	Fourche Malins Creek	Wilburton, Okla.	19.8	19.7	Apr. 1950	14	2,148	---	---	3.05	---	SCS
45-11	Holdenville City Lake	Bemore Creek	Holdenville, Okla.	8.95	8.30	July 1947	14	511	---	---	21	---	SCS
45-12	Pretty Water Lake	Pretty Water Creek	---	2.43	2.40	June 1931	18.8	9,844	---	---	5.22	---	SCS
45-13	Greenleaf Lake	Big Greenleaf Creek	Sapulpa, Okla.	81.25	79.84	Apr. 1950	10.75	9,030	---	---	85	---	SCS
45-15	Kirk Lake	Unas	Hudogee, Okla.	2.44	2.36	Dec. 1946	4.7	13,022	---	---	47	---	SCS
45-16	Lowell	Spge. R. & Shoal Creek	Iola, Kans.	2,210.0	2,208.6	Nov. 1927	42	111	---	---	48.10	450	SCS
45-17	Neosho County State Lake (Lake McKinley)	Small Trib. of Neosho River	Baxter Springs, Kans.	3.28	3.24	Sept. 1939	42	69	---	---	4.04	52.3	SCS
45-18	Lake Claremore	Bog Creek	Claremore, Okla.	56.44	55.70	Mar. 1905	34.4	7,580	---	---	74	987	SCS
45-19	Lake Spavinaw	Spavinaw Creek	Spavinaw, Okla.	400.0	397.2	Aug. 1939	12.1	651	---	---	749	835	SCS
45-20	Kemmer Lake	Trib. of Pryors Creek	Chelusa, Okla.	.28	.27	Apr. 1921	8.4	3,929	---	---	51.17	---	SCS
45-21	State Fish Hatchery Lake	Happy Creek	Claremore, Okla.	1.21	1.20	July 1935	11	30,509	---	---	269	---	SCS
45-22	Lake Scarboro	Trib. of Pryor Creek	Claremore, Okla.	3.07	3.04	--- 1923	16	26.5	---	---	35	---	SCS
45-23	Wewoka Lake	Coon Cr. or Spring Cr.	Pryor, Okla.	16.27	15.72	1934	5	34.0	---	---	1.18	---	SCS
45-24	Wetumpka City Lake	Salt Creek	Wetumpka, Okla.	.33	.33	1931	8	123	---	---	46	---	SCS
45-25	Adair	N. Caney River	Sedan, Kans.	.16	.16	July 1939	19.6	2,076	1,028	---	1.51	---	SCS
45-26	Berry	Big Caney River	Cedar Vale, Kans.	.16	.16	Apr. 1954	8.0	4,489	970	---	871.05	---	SCS
						Mar. 1953	7.5	20.9	1,341	---	1.98	---	SCS
						Jan. 1954	23.2	1,898	1,226	---	1.98	---	SCS
						Sept. 1960	20.2	24.8	---	---	28	335	SCS
						Jan. 1958	22.7	21.2	---	---	44	574	SCS

Station	Location	Year	Capacity (cu. ft.)	Original Capacity (cu. ft.)	Rebuilt (Year)	Original Capacity (cu. ft.)	Rebuilt (Year)	Original Capacity (cu. ft.)	Rebuilt (Year)
45-27	Buffalo	1934	51.7	51.7					
45-28a	Foster	1945	34.5	34.5					
45-29	House	1945	48.5	48.5					
45-30	Herbert Miles Pond	1945	477.8	477.8					
45-31	Kahola	1945	10.66	10.66					
45-32	Miller	1945	9.26	9.26					
45-33	Payne Pond	1945	10.59	10.59					
45-34	Shank	1945	6.491	6.491					
45-35	Hulah	1945	5,933.9	5,933.9					
45-36a	Double Creek Site No. 5	1945	21.6	21.6					
45-37	Midren Lake	1945	54.97	54.97					
45-38	Howard City Lake	1945	44.12	44.12					
45-39	Hayburn Reservoir	1945	81.46	81.46					
45-40	Toronto Lake	1945	295,130	295,130					
45-41	Enfelia Lake	1945	292,953	292,953					
45-42	Match	1945	1,109	1,109					
45-43	Mound Valley Experimental Sta.	1945	44.2	44.2					
45-44	Craney	1945	747.36	747.36					
45-45	Scott	1945	54.3	54.3					
45-46	Fletcher	1945	81	81					
45-47	Iesh Pond	1945	363.44	363.44					
45-48	Hess Pond	1945	355.78	355.78					
45-49	Olanhouse	1945	771.0	771.0					
45-50	Sierman	1945	604.7	604.7					
45-51	Hubert	1945	59,650	59,650					
45-52	Merritt Pond	1945	57,270	57,270					
45-53	Big Weverka Site No. 36	1945	192,000	192,000					
45-54	Cane Creek Site No. 11	1945	89	89					
45-55	Big Weverka Site No. 17	1945	3,798,400	3,798,400					
46-1b	Fort Supply Lake	1945	4.74	4.74					
	Wolf Creek	1945	3.54	3.54					
	Fort Supply, Okla.	1945	6.90	6.90					
	Fort Supply, Okla.	1945	5.01	5.01					
	Fort Supply, Okla.	1945	11.8	11.8					
	Fort Supply, Okla.	1945	20.1	20.1					
	Fort Supply, Okla.	1945	15.37	15.37					
	Fort Supply, Okla.	1945	8.72	8.72					
	Fort Supply, Okla.	1945	53.04	53.04					
	Fort Supply, Okla.	1945	29.69	29.69					
	Fort Supply, Okla.	1945	3.8	3.8					
	Fort Supply, Okla.	1945	7.5	7.5					
	Fort Supply, Okla.	1945	16.38	16.38					
	Fort Supply, Okla.	1945	15.0	15.0					
	Fort Supply, Okla.	1945	8.09	8.09					
	Fort Supply, Okla.	1945	4.17	4.17					
	Fort Supply, Okla.	1945	690.3	690.3					
	Fort Supply, Okla.	1945	679.2	679.2					
	Fort Supply, Okla.	1945	2,983.6	2,983.6					
	Fort Supply, Okla.	1945	2,621.3	2,621.3					
	Fort Supply, Okla.	1945	1.36	1.36					
	Fort Supply, Okla.	1945	680.7	680.7					
	Fort Supply, Okla.	1945	5.33	5.33					

ARKANSAS RIVER BASIN (GARRISON CITY TO TULSA)

Middle Canadian, Lower Camarrou, and Salt Fork River Basins

Fort Supply, Okla.

1,735

1,485

Jan. 1943

June 1949

June 1958

Dec. 1969

11.50

6.42

9.0

101,750

100,760

22.21 ac. ml. is probably noncontributing.  
 Based on infillow survey.  
 Original reconnaissance survey.  
 Present ac.-ft. as shown by the two surveys.

Lake drained and dam raised 1977. Original capacity at 1938 crest.  
 Dam broke Apr. 1946; rebuilt Mar. 1946; this period not included.  
 Includes 0.03 ac.-ft. above crest deposits.  
 Estimated or assumed.

SUMMARY OF  
RESERVOIR SEDIMENTATION SURVEYS MADE IN THE UNITED STATES THROUGH 1962

DATA SHEET NUMBER	RESERVOIR	STREAM	NEAREST TOWN	DRAINAGE AREA (SQUARE MILES)		DATE OF SURVEY	PERIOD BETWEEN SURVEYS (YEARS)	STORAGE CAPACITY (ACRE-FT.)	CAPACITY AVG. ANN. INFLOW (ACRE-FT. PER ACRE-FT.)	SPECIFIC WEIGHT (DRY) (LB. PER CU. FT.)	AVG. ANN. SEDIMENT ACCUMULATION PER SQ. MI. OF NET DR. AREA FOR PERIOD SHOWN	AGENCY SUPPLYING DATA
				TOTAL	NET							
46-2a	Great Salt Plains	Salt Pk. of Arkansas River	Jet, Okla.	3,200	3,156	June 1943	—	308,000	1.067	48.6	0.686	OK
46-3	Boomer Lake	Boomer Creek	Skullwater, Okla.	9.13	8.67	Dec. 1949	8.5	292,000	1.011	58.5	1.358	SES
46-4	Bennington's Lake	Chikaskia River	Rago, Kans.	1.42	1.40	Apr. 1925	10.25	2,642	—	60	1.93	SES
46-5	Heade County State Lake (Lake Latrabes)	stump Arroyo	Heade, Kans.	18.00	17.84	Aug. 1929	33	75	—	69.47	2.68	SES
46-6	Lake Medicine	Medicine Lodge Creek	Medicine Lodge, Kans.	1.89	1.84	June 1928	8.8	819	—	60	1.659	SES
46-7	Santa Fe	Indianola Creek	Augusta, Kans.	37.93	37.55	Oct. 1928	11.2	295	—	98.52	3.40	SES
46-8	Outhrie	Trib. of Cottonwood Creek	Outhrie, Okla.	13.30	12.95	May 1937	8.6	1,595	—	58.1	.45	SES
46-9	Gelmer's Stock Pond	Sole d'Ars Creek	Bladwell, Okla.	.31	.31	May 1935	14.5	2,668	—	0	2.42	SES
46-10	Harris Stock Pond	—	—	.22	.21	Sept. 1940	1.0	3.43	—	45	1.0	SES
46-11	Lake Eldorado	Sichel Creek	Eldorado, Kans.	35.1	34.3	Apr. 1928	2.5	1,233	—	65	.489	SES
46-12a	Lake Fryer	Wolf Creek	Perryton, Tex.	108	108	Apr. 1937	9	3,082	—	66	.426	SES
46-13b	Canton Lake	North Canadian River	Canton, Okla.	12,483	12,081	July 1947	7.4	814	.172	—	.16	SES
46-14	Outhrie Municipal Reservoir No. 2	Cottonwood Creek	Outhrie, Okla.	11.63	11.29	May 1949	—	423,500	2.15	70.9	.302	SES
46-15a	Lake Carl Blackwell	Skullwater Creek	Skullwater, Okla.	75.15	70.51	Sept. 1938	20.50	54,326	—	60	2.61	SES
46-16	Lies Pond	Unnamed	Andale, Kans.	3.36	3.36	June 1942	14	20.44	—	94.89	2.38	SES
46-17	London	—	—	.55	.54	June 1936	—	3,632.10	—	85.7	.07	SES
46-18	Hughes No. 1	—	—	.64	.63	Aug. 1942	20	3,632.10	—	72.07	.32	SES
46-19	Perry City Lake	Dow Creek	Perry, Okla.	16.67	16.64	Aug. 1955	13	3,761.50	—	83.5	1.33	SES
46-20	Pottawatomie Pond	Unnamed	Andale, Kans.	.9	.9	Aug. 1929	17.9	3,988	1.311	103.4	1.0	SES
46-21	O. F. Smith Ponds	Trib. of So. Canadian R.	Union City, Okla.	1.80	1.79	Sept. 1945	7	14.87	—	65.4	.22	SES
46-22	Tom Hill Pond	Trib. of Bridge Creek	Tuttle, Okla.	.530	.526	July 1943	14	20.7	.085	—	.112	SES
46-23	Michlaus	Trib. Slough Creek	Haven, Kans.	2.29	2.27	May 1932	11.8	6.43	.071	—	.112	SES
46-24	Therap	—	—	.14	.14	May 1957	35	3,132.6	.04	70	.22	SES
46-25	Kouhoula	Trib. State Creek	Wellington, Kans.	.24	.24	Apr. 1958	7	4.59	—	60	.57	SES
46-26	Mane	Trib. Sand Creek	Heade, Kans.	.24	.24	Oct. 1948	7	9.64	.219	—	.58	SES
46-27	Smith - Lane	Trib. Bluff Creek	Anthony, Kans.	.24	.23	Sept. 1968	19.92	6.95	.158	—	.98	SES
46-28	Merkman	Trib. Little Ark. River	Little River, Kans.	.56	.56	Aug. 1968	31.92	13.50	.56	—	1.00	SES
46-29	Gaul	Trib. Medicine Lodge River	Medicine Lodge, Kans.	.59	.59	Dec. 1968	9.75	66.89	1.86	—	.84	SES
46-30	Schupbach	—	—	.30	.30	Aug. 1955	24.17	10.79	.85	—	.44	SES
46-31	Barrett	Wild Creek	Flora, Kans.	.34	.34	June 1956	13.42	20.29	.70	—	1.23	SES
46-32	Miller	Beaver Creek	Anthony, Kans.	.67	.67	Aug. 1968	12.17	21.91	.61	—	1.18	SES
				1.20	1.20	July 1968	11.35	32.24	.59	—	1.01	SES
				1.20	1.20	Aug. 1959	9	5.26	.63	—	.30	SES
				1.20	1.20	July 1968	9	2.87	.013	—	.30	SES

Reservoir No.	Reservoir Name	Location	Capacity (cu. ft.)	Year	Volume (cu. ft.)	Capacity (cu. ft.)	Volume (cu. ft.)	Capacity (cu. ft.)	Volume (cu. ft.)	Capacity (cu. ft.)	Volume (cu. ft.)
46-33	Roupp	Houston, Kans.	5,47	June 1950	18.12	5,47	18.12	5,47	18.12	5,47	18.12
46-34	Mease	Medicine Lodge, Kans.	3.33	Sept. 1968	1.73	3.33	1.73	3.33	1.73	3.33	1.73
46-35	Benger Pond	Medicine Lodge, Kans.	108.3	Feb. 1961	1.71	108.3	1.71	108.3	1.71	108.3	1.71
46-36	Parle	Jewmore, Kans.	105.19	Aug. 1968	3.0	105.19	3.0	105.19	3.0	105.19	3.0
46-37	Stebert	Jewmore, Kans.	18.55	Mar. 1952	2.2	18.55	2.2	18.55	2.2	18.55	2.2
46-38	Hoop	Dighton, Kans.	12.95	Aug. 1967	2.2	12.95	2.2	12.95	2.2	12.95	2.2
46-39	Harris	Medicine Lodge, Kans.	36.6	Aug. 1967	2.3	36.6	2.3	36.6	2.3	36.6	2.3
46-40	Whitford	Medicine Lodge, Kans.	8.0	June 1952	1.07	8.0	1.07	8.0	1.07	8.0	1.07
46-41	Davis	Medicine Lodge, Kans.	7.15	June 1966	7.27	7.15	7.27	7.15	7.27	7.15	7.27
46-42	Lippold	Medicine Lodge, Kans.	4.0	June 1961	1.97	4.0	1.97	4.0	1.97	4.0	1.97
46-43	Sebes Pond	Medicine Lodge, Kans.	161.4	Oct. 1962	1.98	161.4	1.98	161.4	1.98	161.4	1.98
46-44	Fry	Medicine Lodge, Kans.	160.8	June 1966	1.97	160.8	1.97	160.8	1.97	160.8	1.97
46-45	Burch	Medicine Lodge, Kans.	1.1	June 1966	1.97	1.1	1.97	1.1	1.97	1.1	1.97
46-46	Coberly	Medicine Lodge, Kans.	160.8	June 1966	1.97	160.8	1.97	160.8	1.97	160.8	1.97
46-47	Smith Pond	Medicine Lodge, Kans.	1.1	June 1966	1.97	1.1	1.97	1.1	1.97	1.1	1.97
46-48	Altman	Medicine Lodge, Kans.	1.1	June 1966	1.97	1.1	1.97	1.1	1.97	1.1	1.97
46-49	Rayl	Medicine Lodge, Kans.	1.1	June 1966	1.97	1.1	1.97	1.1	1.97	1.1	1.97
46-50	Lange	Medicine Lodge, Kans.	1.1	June 1966	1.97	1.1	1.97	1.1	1.97	1.1	1.97
46-51	Brodie	Medicine Lodge, Kans.	1.1	June 1966	1.97	1.1	1.97	1.1	1.97	1.1	1.97
46-52	Glen	Medicine Lodge, Kans.	1.1	June 1966	1.97	1.1	1.97	1.1	1.97	1.1	1.97
46-53	Issac	Medicine Lodge, Kans.	1.1	June 1966	1.97	1.1	1.97	1.1	1.97	1.1	1.97
46-54	For	Medicine Lodge, Kans.	1.1	June 1966	1.97	1.1	1.97	1.1	1.97	1.1	1.97
47-2	Conchas Reservoir	Conchas Dam, N. Mex.	6,776	Jan. 1959	7.409	6,776	7.409	6,776	7.409	6,776	7.409
47-3	Reservoir No. 7 and 8	Conchas Dam, N. Mex.	7.409	Jan. 1959	7.409	7.409	7.409	7.409	7.409	7.409	7.409
47-4	Reservoir No. 11	Conchas Dam, N. Mex.	7.409	Jan. 1959	7.409	7.409	7.409	7.409	7.409	7.409	7.409
47-5	Reservoir No. 12	Conchas Dam, N. Mex.	7.409	Jan. 1959	7.409	7.409	7.409	7.409	7.409	7.409	7.409
47-6	Reservoir No. 13	Conchas Dam, N. Mex.	7.409	Jan. 1959	7.409	7.409	7.409	7.409	7.409	7.409	7.409
47-7	Reservoir No. 14	Conchas Dam, N. Mex.	7.409	Jan. 1959	7.409	7.409	7.409	7.409	7.409	7.409	7.409
47-8	Boles	Conchas Dam, N. Mex.	7.409	Jan. 1959	7.409	7.409	7.409	7.409	7.409	7.409	7.409

1/ Excludes 4,642 sq. mi. of watershed not contributed to runoff, 1,735 sq. mi. above Fort Supply Dam, and 25 sq. mi. surface area of Canton Reservoir.  
2/ Includes 2.33 ac.-ft. above crest deposits.  
3/ Water supply pool capacity. Reservoir has greater capacity at spillway crest elevation.  
4/ Includes 0.39 ac.-ft. above crest deposits.  
5/ Spillway eroded 2 ft.  
6/ Capacity based on surface area x 1/3 deepest fill.

7/ During the period 1912-46, a total of 2,435-ac.-ft. capacity was added by reservoir enlargement.  
8/ During the period 1912-46, a total of 126-ac.-ft. capacity was added by reservoir enlargement.  
9/ During the period 1912-46, a total of 692-ac.-ft. capacity was added by reservoir enlargement.  
10/ During the period 1912-46, a total of 600-ac.-ft. capacity was added by reservoir enlargement.  
11/ During the period 1912-46, a total of 246-ac.-ft. capacity was added by reservoir enlargement.  
12/ Estimated or assumed.

SUMMARY OF  
RESERVOIR SEDIMENTATION SURVEYS MADE IN THE UNITED STATES THROUGH 1970

DATA SHEET NUMBER	RESERVOIR	STREAM	NEAREST TOWN	DRAINAGE AREA (SQUARE MILES)		DATE OF SURVEY	PERIOD BETWEEN SURVEYS (YEARS)	STORAGE CAPACITY (ACRE-FT.)	CAPACITY AVERAGE ANNUAL INFLOW RATIO PER ACRE-FT.	SPECIFIC WEIGHT (DRY) (L.B. PER CU. FT.)	AVERAGE ANNUAL ACCUMULATION PER SQ. MI. OF NET DR. AREA FOR PERIOD SHOWN		AGENCY SUPPLYING DATA
				TOTAL	NET						AC-FT.	TONS	
ARKANSAS RIVER BASIN (LAGER TO GARDEN CITY) Upper Cimarron and Upper Canadian River Basins (Continued)													
47-9	Gregory	Trib. Ark. River	Syracuse, Kans.	6.5	6.5	Apr. 1951	—	62.2	1.79	70	—	—	SCS
47-10	Laney	Trib. Cimarron	—	2.78	2.75	June 1967	16.5	135.6	4.6	90	0.11	167	SCS
47-11	Hartshorn	Trib. Little Bear Creek	—	1.90	1.89	June 1966	5.7	133.8	4.5	90	—	120	SCS
47-12	Christian	Trib. Cimarron	—	1.06	1.06	June 1966	16.25	14.6	4.3	97.5	—	310	SCS
47-13	Downing	—	—	.47	.46	June 1966	5	4.5	4.0	97.5	—	229	SCS
47-14	Amerline	Trib. Little Bear Creek	—	3.42	3.40	June 1966	4.8	31.8	6.4	65	—	396	SCS
47-15	Roy Kura	Shirley	—	8.91	8.91	June 1951	23.3	119	3.3	97.5	—	327	SCS
						June 1967	16.5	78.2	1.65	97.0	—	152	SCS
RIO GRANDE BASIN (ABOVE ESPANOLA) AND ARKANSAS RIVER BASIN													
48-1d	John Martin Reservoir (Formerly Canada Res. Proj.)	Arkansas River	Hart, Colo.	178.935	16.102	Apr. 1942	—	701.775	2.47	—	—	—	CE
						July 1942	0.3	690.345	2.43	975.7	—	—	—
						Dec. 1943	1.4	638.590	2.43	975.7	—	124	—
						Sept. 1944	0.7	683.297	2.41	975.7	—	170	—
						May 1948	3.7	671.097	2.38	975.7	—	213	—
						Oct. 1951	3.4	682.870	2.34	975.7	—	346	—
						Aug. 1957	5.7	545.512	2.28	975.7	—	293	—
						Mar. 1962	4.6	642.390	2.26	975.7	—	282	—
						Sept. 1966	4.5	631.121	2.22	975.7	—	242	—
						Aug. 1968	1.9	618.668	2.18	975.7	—	397	—
48-2	Brown Reservoir No. 1	Van Buren Arroyo	Trinidad, Colo.	74.6	74.4	Nov. 1959	39	16.918	—	89.07	—	152	SCS
48-3	Muddy Creek	Muddy Creek, Johnny Creek	Caddo, Colo.	154.2	152.4	Feb. 1959	20	15,227	—	75.25	—	877	SCS
48-4	Horse Creek	Horse Creek	Ordway, Colo.	52.01	47.44	Nov. 1960	39.4	30,738	—	68.36	—	5,515	SCS
48-5	Teller	Turkey Creek	Pueblo, Colo.	78.8	78.5	Mar. 1911	28.9	4,005	—	75.4	—	1,117	SCS
48-6	Chuhara	Oucharas River	Kalsenburg, Colo.	608	608	Feb. 1940	28.9	2,463	—	—	—	—	—
						1912	2	48,274	—	—	—	—	—
						1912	2	31,400	—	—	—	—	—
						1919	2	21,346	—	—	—	—	—
48-7	S-1 Big Sandy Creek Watershed	Big Sandy Creek	Perkon, Colo.	5.4	5.3	May 1962	3	302	—	980	—	2,613	SCS
48-8	Abiquiu Reservoir	Rio Chama	Abiquiu, N. Mex.	2,146	2,127	Apr. 1963	4.58	579,039	1.80	975.7	—	1,072	CE
48-9	Hartshorn Reservoir	Hungerford Hollow	Fowler, Colo.	13.48	13.34	Oct. 1967	60	563	93.9	—	—	—	—
						Mar. 1968	60	527	93.7	—	—	—	—
RED RIVER BASIN (BERNISON TO GRAND DOUBIE) Little and Sulphur River Basins													
49-1a	Lake Creek	Pine Creek	Paris, Tex.	51.6	49.6	Feb. 1923	—	11,487	—	—	—	—	—
						Mar. 1926	13.1	10,755	—	—	—	—	—
						July 1926	19.7	9,864	—	—	—	—	—
49-2a	Lake Gibbons	Trib. of Pine Creek	—	1.46	1.26	Mar. 1900	36	5,134	1.792	—	—	642	SCS
						Mar. 1926	20.3	1,285	1.702	—	—	—	—
						July 1926	20.3	1,285	1.652	—	—	—	—
49-3	Marville	Miss Creek	Marville, Ark.	10.4	10.3	July 1911	10.3	128	—	—	—	—	—
						July 1911	10.3	128	—	—	—	—	—
49-4	Jenkins Pond	Trib. of Landis Creek	Manfield, La.	.35	.32	Sept. 1925	—	137	—	—	—	—	—
49-5	Gordon Country Club Lake	Andis Creek	Paris, Tex.	1.41	1.30	Sept. 1924	29	150	—	—	—	—	—
						June 1929	61.0	598	—	—	—	—	—
49-6	Bayou Bodcau	Bayou Bodcau River	Cotton Valley, La.	683	613	Nov. 1949	—	987,900	1.516	—	—	—	—
						May 1961	11.5	867,900	1.516	—	—	—	—



50-7a	50-8	50-9	50-1	50-2	50-3	50-4	50-5	50-6	50-7	50-8	50-9	50-10	50-11a	50-12b	50-13	50-14a	50-15a	50-16	50-17	50-18	50-19	50-20	50-21	50-22	50-23	50-24a	50-25	
Lake Texarkana	Salpahr River	Salpahr River	Armore, Okla.	Byers, Okla.	Cartier Lake	J. J. Harrison Lake	C. W. Lester Farm Pond No. 1	C. W. Lester Farm Pond No. 2	Santa Rosa Lake	Lake Duncan	Lake Clinton	Belleveue	Altus Reservoir	Lake Texoma (Demison Dam)	Barbour Pond	Barley Creek Site No. 1	Chigley Sandy Site No. 5	Coit Pond No. 1	Dean Pond No. 1	Dean Pond No. 2	George Pond	Hall Pond No. 1	Harrison No. 1	Harrison No. 2	Lake Kemp	Mill Creek No. 17	Murriel Farm Pond	
3,400	3,213	3,400	4,115	2,66	1.81	.88	2.04	.64	336	11.0	23.6	81.5	2,515	39,719	2,110	.68	.39	.0359	.164	.535	.20	.237	.292	2,099	1.41	.031		
Texas, Tex.	Texarkana, Tex.	Texarkana, Tex.	Arkmore, Okla.	Byers, Okla.	Cartier Lake	J. J. Harrison Lake	C. W. Lester Farm Pond No. 1	C. W. Lester Farm Pond No. 2	Santa Rosa Lake	Lake Duncan	Lake Clinton	Belleveue	Altus Reservoir	Lake Texoma (Demison Dam)	Barbour Pond	Barley Creek Site No. 1	Chigley Sandy Site No. 5	Coit Pond No. 1	Dean Pond No. 1	Dean Pond No. 2	George Pond	Hall Pond No. 1	Harrison No. 1	Harrison No. 2	Lake Kemp	Mill Creek No. 17	Murriel Farm Pond	
Sept. 1954	Sept. 1954	Sept. 1954	Dec. 1922	June 1904	Mar. 1949	Mar. 1950	June 1949	June 1949	Jan. 1948	Oct. 1937	Nov. 1938	May 1938	June 1948	July 1953	Apr. 1967	July 1948	Sept. 1955	July 1957	July 1957	Apr. 1959	Apr. 1959	Apr. 1958	Apr. 1958	Apr. 1958	Sept. 1958	July 1959	Aug. 1955	
2,654,300	2,654,300	2,654,300	1,797	507	874	837	42.4	16.3	11,755	5,783	3,981	131	192,842	5,891,000	58.9	41.8	10.28	1.078	1.807	15.8	5.796	13.47	11.242	560,000	481,797	498.45	487.11	6,710
1.15	1.15	1.15	40.7	1.16	1.26	4.59	2.41	1.02	689	63.4	5.275	.64	1.495	1.71	1.71	1.20	1.20	1.20	1.20	1.20	1.20	1.20	1.20	1.20	1.20	1.20	1.20	1.20

RED RIVER BASIN (ARCOPE DEMISON)

1/ Drainage area adjusted to conform with U.S.G.S. published drainage area.  
2/ Off channel reservoir.  
3/ Excludes water and sediment diverted from Arkansas River and Horse Creek.  
4/ Per 100 ac.-ft. water diverted from Ark. River and Horse Cr. Total of 564,918 ac.-ft. diverted to reservoir between 1910 and 1939.  
5/ Little deposition due to dam without, 1930-47. True sediment accumulation rate for 43-yr. period was 0.063 ac.-ft./42-yr.  
6/ Spillway crest was lowered 3 ft. in 1932; capacities are based on present elevation.  
7/ Date of original survey for new dam over deposits placed behind old dam.  
8/ Estimated or assumed.

SUMMARY OF  
RESERVOIR SEDIMENTATION SURVEYS MADE IN THE UNITED STATES THROUGH 1970

DATA SHEET NUMBER	RESERVOIR	STREAM	NEAREST TOWN	DRAINAGE AREA (SQUARE MILES)		PERIOD DATE OF BETWEEN SURVEYS (YEARS)	STORAGE CAPACITY (ACRE-FT.)	CAPACITY SPECIFIC WEIGHT (LB. PER CU. FT.)	AVG. ANN. SEDIMENT ACCUMULATION PER SQ. MI. OF NET DR. AREA FOR PERIOD SHOWN		AGENCY SUPPLYING DATA
				TOTAL	NET				AC.-FT.	TONS	
50-26a	Sabb Creek No. 3	Memphis	Weathercom, Okla.	8.28	8.18	Jan. 1957 Aug. 1960	2,103.1 2,303.3	90	3.34 6.547	SES	
50-27b	Sandstone Site No. 1	Memphis	Weathercom, Okla.	5.33	5.22	Aug. 1953 Apr. 1954	1,781.79 1,553.69	89	1.24 5.31	SES	
50-28b	Sandstone Site No. 3	Memphis	Weathercom, Okla.	.62	.61	Apr. 1954 Aug. 1965	1,380.47 1,344.75	83.15 83.11	7.11 1.36	SES	
50-29a	Sandstone Site No. 5	Memphis	Weathercom, Okla.	3.89	3.84	Apr. 1951 Oct. 1956	1,338.82 1,148.40	83 77.87	2.23 2.79	SES	
50-30b	Sandstone Site No. 6	Memphis	Weathercom, Okla.	6.46	6.24	July 1964 Sept. 1961	1,152.21 1,127.06	80	2.06 1.76	SES	
50-31a	Sandstone Site No. 9	Memphis	Weathercom, Okla.	1.50	1.46	Oct. 1962 Sept. 1967	1,831.22 1,800.52	70.7 72	2.36 2.52	SES	
50-32b	Sandstone Site No. 10a	Memphis	Weathercom, Okla.	2.87	2.80	Oct. 1962 Sept. 1967	1,178.72 1,171.25	75.78 79.4	2.52 2.20	SES	
50-37a	Sandstone Site No. 11	Memphis	Weathercom, Okla.	1.02	1.00	Sept. 1961 July 1966	1,018.8 981.9	79.3 75	1.77 4.16	SES	
50-34b	Sandstone Site No. 16	Memphis	Weathercom, Okla.	11.47	11.28	July 1970 Aug. 1952	2,752.82 4,463.43	75 77.94	2.20 3.04	SES	
50-35b	Sandstone Site No. 16a	Memphis	Weathercom, Okla.	8.78	8.68	July 1957 Sept. 1961	4,184.87 4,038.34	74.85 76	2.73 2.31	SES	
50-36b	Sandstone Site No. 17	Memphis	Weathercom, Okla.	10.13	10.04	Oct. 1954 Aug. 1966	1,987.93 1,979.45	86.6 87.7	1.30 1.34	SES	
50-37a	Sandstone Site No. 22	Memphis	Weathercom, Okla.	2.25	2.20	Oct. 1951 Oct. 1956	1,465.8 1,322.4	70.4 59	2.31 3.53	SES	
50-38	Stickley Pond No. 4	Canadian River	Canadian, Tex.	.171	.171	Sept. 1967 Apr. 1968	15.794 13.943	83	3.63 7.036	SES	
50-39	Stickley Pond No. 6	Canadian River	Canadian, Tex.	.162	.162	Oct. 1965 Apr. 1968	21.055 17.553	83	1.959 1,621.88	SES	
50-40	Wheeler Farm Pond	Canadian River	Canadian, Tex.	.205	.205	Apr. 1968 Jan. 1969	7.353 223.4	85.34 4.33	2.167 4,027.81	SES	
50-41b	Whiteshield Creek Site No. 4	Memphis	Weathercom, Okla.	.62	.60	Jan. 1959 Sept. 1959	207.7 199.6	82.73 75.68	2.19 2.45	SES	
50-42b	Whiteshield Creek Site No. 1	Memphis	Weathercom, Okla.	.97	.95	Aug. 1964 June 1969	199.6 179.9	75.68 75.68	2.45 2.75	SES	
50-43a	Whiteshield Creek Site No. 3	Memphis	Weathercom, Okla.	1.77	1.73	July 1963 July 1966	236.2 229.3	61 61	.63 1.27	SES	
						Mar. 1950 Sept. 1960	587.38 546.24	85	1.16 2.17	SES	
						Aug. 1965	548.66	74	2.05 3.304	SES	

Station	Structure	Location	Year	Capacity	Volume	Remarks
50-44b	Owl Creek No. 1	Owl Creek	Apr. 1949	206.3	65.5	1,527.2
			Oct. 1953	200.0	2.03	3,166.6
			Apr. 1958	194.0	1.29	1,721.1
50-45a	Chigley Sandy Site No. 4	Wambita	Apr. 1955	1,075.3	2.10	2,361
			Nov. 1958	1,054.8	51.61	2,012
			Apr. 1963	1,018.0	51.61	2,012
			July 1969	966.7	2.39	3,454
50-46	Fire Retarding Structure No. 2	Bush Creek	Aug. 1959	655.99		
50-47a	Barnitz No. 14	Barnitz	July 1965	639.60	77.75	2,309
			Nov. 1969	1,644.9	3.87	5,900
			Apr. 1968	1,631.9	.61	877.9
50-48	Sugar Creek Site No. 13	Sugar Creek	Feb. 1964	532.17	82.27	15,499
50-49	Upper Wambita River Site #25	Wambita River	Oct. 1965	503.79	8.65	17,959.9
50-50	Kent Creek Watershed Site #1	Kent Creek	Nov. 1961	1,315.92	91.8	17,959.9
50-51	Bush Creek No. 2	Bush Creek	July 1966	622.01	61	17,959.9
			June 1966	611.63		
			July 1965	606.0		
			Apr. 1969	614.6	77.75	2,309
50-52	Saddle Mountain No. 2	Saddle Mountain Creek	Apr. 1965	771.3	38	2,47
			Apr. 1965	2/-		
			Sept. 1970	751.4	.53	754
51-1	Terrill City Lake	Kings Creek	Oct. 1921	2,219	59.2	3,211
51-2	Lower Benton Lake	Trib. of Elm Creek	Dec. 1949	1,605		
51-3	Burke Meek Lake	Corstons, Tex.	Sept. 1967	201	3.57	
51-4	Lake Dallas	Benton, Tex.	Sept. 1949	92	3.39	
51-5	Lake Halbert	Elm Cr. of Trinity River	Feb. 1928	180,759	53	1,304
51-6	Regonia Lake (Bad Horse)	Elm Creek	Sept. 1958	167,072	53	1,304
51-7	Mountain Creek	Corstons, Tex.	Sept. 1921	8,012	67.4	8,308
51-8	White Rock Lake	White Rock Creek	Sept. 1949	6,657	5.66	
51-9	Grand Salinas	Simmons Branch	Sept. 1969	756		
51-10	Lake Clark	Trib. of Elm Creek	Sept. 1969	659		
51-11	Kemp City	Mountain Creek	Mar. 1957	37,100	3.91	
51-12	Variety Club Boys' Ranch Lake	Dallas, Tex.	Nov. 1946	18,158	1.60	1,708
51-13	Wills Point	White Rock Creek	Apr. 1933	25	35	151
51-14	Bridgeport	White Rock Creek	Apr. 1956	20.9	1.11	905
51-15	Eagle Mountain	White Rock Creek	Oct. 1970	10,743	32	1.11
51-16a	Lake Bels	Simmons Branch	Feb. 1925	531	.82	691
51-17	Mabank City Lake	Grand Salinas	Apr. 1958	509	38.7	
51-18	Wolf Creek	T & P	Apr. 1950	370	61	1,098
51-19	Elkins Lake	Lake Clark	Nov. 1958	328		
51-20		Wambash Creek	Nov. 1958	8.5		
		Emils, Tex.	Dec. 1950	2,295	796	1,098
		Kemp, Tex.	Dec. 1950	2,295	5/2,295	2,851
		Cedar Creek	Apr. 1952	298	4.29	
		Unnamed trib.	Apr. 1952	33	2.2	
		Naglee Creek	Apr. 1950	396		
		West Fork of Trinity River	Sept. 1914	23.6	60.1	3,835
		Bridgeport, Tex.	Apr. 1932	275		
		Fort Worth, Tex.	Apr. 1932	5,792,000		
			Feb. 1943	283,260		
			Mar. 1954	5/21,000		
			Mar. 1959	182,470		
			Mar. 1962	13		
			Apr. 1979	204	1.63	
			Apr. 1926	295		
			Apr. 1939	271	5.51	
			Apr. 1939	222		
			Apr. 1959	20	.46	
			Apr. 1960	896		
			July 1960	612	.72	

1/ Data based upon combined capacities, drainage area, and sediment volumes of all lakes in watershed.

2/ Water supply pool capacity. Does not include exchange or flood storage.

3/ Excludes area above Bridgeport Reservoir which lies upstream from Eagle Mt. Reservoir.

4/ Estimated or assumed.

SUMMARY OF  
RESERVOIR SEDIMENTATION SURVEYS MADE IN THE UNITED STATES THROUGH 1970

DATA SHEET NUMBER	RESERVOIR	STREAM	NEAREST TOWN	DRAINAGE AREA (SQUARE MILES)		DATE OF SURVEY	PERIOD BETWEEN SURVEYS (YEARS)	STORAGE CAPACITY (ACRE-FT.)	CAPACITY AVG. ANN. INFLOW (ACRE-FT. PER AC. FT.)	SPECIFIC WEIGHT (LB. PER CU. FT.)	AVG. ANN. SEDIMENT ACCUMULATION PER SQ. MI. OF NET DR. AREA FOR PERIOD SHOWN	AGENCY SUPPLYING DATA
				TOTAL	NET							
51-21	Murphy Lake	East Fork of Trinity River	Crandall, Tex.	4.09	3.98	Oct. 1922	16.5	397	60	3.94	5,150	SCS
51-22	Loring Lake	Trib. of Herriman Creek	Zwolle, La.	1.05	.95	Sept. 1928	26	663	789	85.08	3,002	SCS
51-23	Kernan City Lake	Cow Creek	Kernan, Tex.	6.42	6.28	Sept. 1954	18.8	630	237	54.49	779	SCS
51-24	Variety Club Lake	Trib. of Trinity River	Bedford, Tex.	.29	.29	July 1942	7.8	38	451	2.21	---	SCS
51-25a	Clear Fk. Watershed Site No. 10.	Trinity River	Weatherford, Tex.	4.30	4.25	May 1950	7.8	33	1.90	---	---	SCS
51-26b	Honey Creek Site No. 11	---	---	---	---	Apr. 1963	7.5	1,430.91	1.84	---	1,682	SCS
51-27b	Honey Creek Site No. 12	---	---	---	---	May 1968	5.1	1,411.04	1.82	---	---	SCS
51-28a	Dawson City Lake	---	---	---	---	Feb. 1952	10.2	1,521.0	1.77	---	---	SCS
51-29	Lake Cherokee	---	---	---	---	Apr. 1962	5.3	1,584.7	1.74	51.9	3,956	SCS
51-30	Lavon Reservoir	---	---	---	---	July 1967	5.3	553.33	1.27	---	---	SCS
51-31a	Site No. 11B Elm Fk. Watershed (Ledisville Dam)	---	---	---	---	Jan. 1965	17.5	475.52	1.09	40.72	3,130	SCS
51-32	Gays-Little Elm Reservoir	---	---	---	---	Apr. 1957	61.0	466	1.126	7.16	5,130	SCS
51-33	Dan B Reservoir	---	---	---	---	Feb. 1956	7.5	390.1	9.02	9.46	6,587	SCS
51-34	Clear Creek Watershed Site No. 2.	---	---	---	---	Sept. 1963	7.5	49,295	4.28	83.12	2,480	SCS
51-35	Upper Lake Fk. Watershed Site 23	---	---	---	---	Oct. 1948	11.5	1,412	1.42	1.37	2,490	SCS
51-36	Lake Amen G. Carter	---	---	---	---	Apr. 1960	11.5	46,705	1.42	1.90	2,197	SCS
51-37	Numbers Creek Site 37	---	---	---	---	Oct. 1953/	0	623,400	1.26	---	---	SCS
51-38	Chambers Creek Site 101-A	---	---	---	---	Oct. 1959	6.0	634,460	1.37	53.1	2,197	SCS
51-39	Clear Fork Watershed Site No. 7.	---	---	---	---	Mar. 1965	1.87	425,598.2	1.33	3,783.3	3,637	SCS
51-40	Denton Creek Watershed Site No. 17.	---	---	---	---	Oct. 1968	5.25	670.0	1.28	87	2,402	SCS
51-41	East Kechi Creek Site No. 1	---	---	---	---	Oct. 1966	5.25	654.6	2.31	1.57	---	SCS
52-1	Lake Corpus Christi	---	---	---	---	---	---	1,016,200	---	---	---	SCS
52-2	Medina Lake	---	---	---	---	---	---	1,002,900	---	---	---	SCS

SABINE, NECHES, AND TRINITY RIVER BASINS (Continued)

LOWER BRAZOS, LOWER COLORADO, GUADALUPE, SAN ANTONIO, AND NICHES RIVER BASINS

Site No.	Location	State	19,313	9/19,350	June 1937	970,010	*.649	1.21	808
52-3	Buchanan	Colorado River			Feb. 1942	954,859			
52-4	Moss Ranch Stock Pond	S. Bull Creek	.07		Feb. 1909	4.7			
52-5	Moss Ranch Stock Pond	M. Bull Creek	.20		Feb. 1903	9.3		.07	
52-6	Reliance	Trib. of Sandy Creek	.15		Feb. 1941	9.1		.021	
52-7	Baker Lake	Trib. of San Antonio River	3.17		Feb. 1915	11.6		.12	
52-8a	Calaveras Creek Site No. 6	Calaveras Creek	7.01		Sept. 1950	251	585	1.90	1,132
52-9	Escondido No. 11	Trib. of Escondido Creek	8.43		Dec. 1956	1,697.82	1.65		706
52-10	Rudder Pond	Trib. of Escondido Creek	1.35		July 1958	2,728.0	2.022	.49	
52-11	Sirdana Lake	Trib. of Escondido Creek	.769		July 1960	2,697.8	1.978	3.79	3,886
52-12	Smith Pond	Trib. of Honda River	.191		Aug. 1951	11.96	.081	.09	
52-13	Thornion Lake	Trib. of Bonito Creek	1.54		Aug. 1953	80.5	1.989		
52-14	Tley Lake	Trib. of Bonito Creek	2.34		Sept. 1955	76.5	1.866	1.12	1,112
52-15	Blackwell Lake	Trib. of Bear Creek	2.76		Apr. 1953	6.41	.361	1.80	1,090
52-16a	Site No. 1 Escondido Creek	Trib. of Escondido Creek	3.01		Aug. 1955	5.60	.315	27.8	
52-17	Cummings Creek Watershed Site No. 6	Trib. Cummings Creek	2.99		Sept. 1952	142.4	.578	1.64	
53-1	Lake Scarborough	Trib. of Jim Ned Creek	10.8		June 1964	14.75	.054		
53-2	Santa Anna Lake	Mid Creek	1.27		Sept. 1954	924.7	2.30	.09	97
53-3	Lake Eugene	Merced Creek	13.76		June 1964	906.2	2.26	.67	3,763
53-4	Lake Merritt	Brown Creek	11.65		July 1969	890.1	2.22	1.12	1,710
53-5	Hubbard City Lake No. 3	Trib. of E. Cottonwood Cr.	.16		Aug. 1958	898.3	.77		
53-6	Hubbard City Lake No. 4	E. Cottonwood Creek	1.40		Sept. 1958	855.2	.77	.22	
53-7a	Rogers Lake	Trib. of Little River	.55		Aug. 1969	894.1	.76	.07	
53-8	Hubbard City Lake No. 1	Trib. E. Cottonwood Creek	.5		May 1923	2,153			
53-9	Hubbard City Lake No. 2	Hubbard, Tex.	.03		May 1940	2,007			
53-10	Hubbard City Lake No. 5	Hubbard, Tex.	.11		May 1923	766			
53-11	Lake Lawn	Hubbard, Tex.	13.0		Apr. 1940	765			
53-12	Lometa	Hubbard, Tex.	4.74		May 1925	1,221			
53-13	Meridian Lake	Hubbard, Tex.	3.30		Sept. 1917	962			
53-14	Miller Lake	Hubbard, Tex.	.41		May 1940	855			
53-15	Ogall Lake	Hubbard, Tex.	.56		May 1949	11/104.5			
53-16	Possum Kingdom Lake	Hubbard, Tex.	12.955		May 1949	90.2			
53-17	Road Crusher	Hubbard, Tex.	16.5		May 1917	318.2			
53-18	Old Santa Anna City Lake	Hubbard, Tex.	.90		May 1949	255.4			

1/ Original capacity from map by stereo photogrammetric methods.  
2/ "Original" or 1945 capacity adjusted in 1961 by range line controls established in 1953 give net. 5% area and capacity.  
3/ Sediment pool only.  
4/ Adjusted for 1957 survey of Lake Dallas.  
5/ Adjusted for Apr. 1963 for detailed range survey in 1952-53-54.  
6/ Determined by USGS Nov. 1961.  
7/ 1951 adjusted data.  
8/ Deposits above Highway 190 bridge only. Not corrected for degradation between highway and dam.

SUMMARY OF  
RESERVOIR SEDIMENTATION SURVEYS MADE IN THE UNITED STATES THROUGH 1970

DATA SHEET NUMBER	RESERVOIR	STREAM	NEAREST TOWN	DRAINAGE AREA (SQUARE MILES)		DATE OF SURVEY	PERIOD BETWEEN SURVEYS (YEARS)	STORAGE CAPACITY (ACRE-FT.)	CAPACITY INFLOW (ACRE-FT. PER PERIOD SHOWS)	SPECIFIC WEIGHT (DRY) (LB. PER CU. FT.)	AVG. ANNUAL ACCUMULATION PER SQ. MI. OF NET DR. AREA FOR PERIOD SHOWS	AGENCY SUPPLYING DATA
				TOTAL	NET							
53-19	Old Coleman City Lake	Home Creek	Coleman, Tex.	0.73	0.69	Nov. 1906	--	289	--	--	SCS	
53-20	Hamilton City Lake	Two Mile Creek	Hamilton, Tex.	12.0	11.9	May 1940	31.6	675	--	0.67	SCS	
53-21	Lake Leon	Leon River	Eastland, Tex.	225	224.7	Mar. 1923	17.75	540	--	.24	SCS	
53-22	Lake Mineral Wells	Rock Creek	Mineral Wells, Tex.	74.4	73.4	Mar. 1941	20.75	1,637	--	.08	SCS	
53-23	Buffalo Tank (Knox Tank)	Trib. of Peasan Bayou	Coleman, Tex.	1.73	1.71	Dec. 1922	19.5	10,741	--	1.19	SCS	
53-24	R. G. Hollingsworth Stock Pond	---	---	2.60	2.58	Feb. 1900	33	33	--	.058	SCS	
53-25	J. S. Wall Stock Pond	Trib. of Brady Creek	Brady, Tex.	.35	.35	Feb. 1927	1.7	14	--	.66	SCS	
53-26	White Tank	Trib. of Peasan Bayou	Brown, Tex.	.80	.80	Mar. 1941	14	12.2	--	.16	SCS	
53-27	Zimmerman Stock Pond (North)	Trib. of Jim Med Creek	Lawn, Tex.	.13	.13	Mar. 1916	4.8	3.6	--	.24	SCS	
53-28	Smith Lake	Rebank Creek	---	1.04	1.01	Feb. 1941	25	102.80	--	.10	SCS	
53-29	Phillipco Lake	Paint Creek	Pioneer, Tex.	9.04	9.00	Aug. 1928	14.6	93	--	.63	SCS	
53-30a	Lake Brownwood	Pecan Bayou (Colo. River)	Brownwood, Tex.	1.544	1.533	Mar. 1925	183	173	--	.07	SCS	
53-31a	Lake Mico (Old)	---	---	271.649	271.645	July 1932	15.9	149,925	1.011	1.011	SCS	
53-32	Lake Edlmann	Flint Creek	Grehan, Tex.	4.2	41.4	Feb. 1924	17.0	6,983	1.144	1.144	SCS	
53-33a	Site No. 3 Cow Bayou	Brasos	Moody, Tex.	1.40	1.32	May 1954	25.25	5,917	1.028	1.028	SCS	
53-34	Cow Bayou No. 4	Forster Creek	Waco, Tex.	5.25	5.20	Apr. 1930	4.9	19,778	1.23	1.23	SCS	
53-35	Deep Creek No. 3	Trib. of Deep Creek	Brady, Tex.	3.42	3.19	Feb. 1927	11.8	3,488	1.08	1.08	SCS	
53-36a	Green Creek No. 1	Green Creek	Dubill, Tex.	3.57	3.38	Dec. 1924	17.0	15,427	1.236	1.236	SCS	
53-37	Silver Lake	N. E. Trib. of Leon River	---	.37	.334	June 1927	5.2	1,351.8	1.144	1.144	SCS	
53-38	Main Res. Deep Creek Site 5	Colorado	Brady, Tex.	2.91	2.72	July 1960	50	114.0	2.296	2.296	SCS	
53-39	Upper Res. Deep Creek Site 5	---	---	2.19	2.18	Aug. 1953	7.9	136.7	4.755	4.755	SCS	
53-40a	Muler Creek Site No. 9	Mid. Colorado River	Bangs, Tex.	4.75	4.55	July 1961	7.9	15.2	1.072	1.072	SCS	
53-41a	Sulphur Creek Site 3	Lampasas River	Lampasas, Tex.	10.81	10.58	June 1965	4.42	734.94	1.053	1.053	SCS	
53-42	Whiting Reservoir	Brasos River	Whiting, Tex.	17.656	17.480	Dec. 1941	5.8	3,224.7	1.6	1.6	SCS	
53-43	Site No. 8 Deep Creek	Dry Fork	Brady, Tex.	4.26	4.02	Apr. 1959	7.4	1,999.900	1.70	1.70	SCS	
53-44	Site No. 10-A Muler Creek	Muler Creek	Bangs, Tex.	15.26	14.59	Sept. 1965	14.8	1,144.89	1.85	1.85	SCS	
53-45	Lake Daniel	Gonzales Creek	Brookridge, Tex.	115	111	Aug. 1949	1.4	3,157.99	.81	.81	SCS	
53-46	Site 9 Lower San Sabo River	Colorado River	San Sabo, Tex.	3.03	2.88	Jan. 1970	21.4	9,515	48	48	SCS	

UPPER BRAZOS AND UPPER COLORADO RIVER BASINS

Site	Location	Capacity (cu ft)	Year	Original Capacity (cu ft)	Adjusted Capacity (cu ft)	Remarks
54-1	Lake Abilene	98.5	1921	10,325	60	SES
54-2	Lake Keworth	3,294	1948	9,786	21	274
54-3	Lake Sweetwater	110	1938	11,485	67.5	SES
54-4	Lake Kirby	44	1938	10,294	67.5	SES
54-5	Lake Throckmorton	11.54	1938	13,287	41	SES
54-6a	Lake Fort Phantom Hill	478	1918	8,133	91	SES
54-7	Mountain Creek	32.00	1934	7,618	31.55	199
54-8	MZ Ranch Pond	1.60	1934	8,133	35.99	SES
54-9	Lake Stamford	360	1935	2,029	53.06	162.17
54-10	Site 18 Valley Cr. Watershed	4.21	1935	2,200	63.6	SES
54-11	Lake Ballinger	210	1935	57,632.35	1.71	760
54-12	Lake Winters	63.14	1935	53,927.57	42.56	210
55-1	Site 6 Olmitos & Garcias Creeks	13.19	1962	719.89	69	SES
56-1a	Cottonwood Detention	2.34	1937	3,872.09	37	137
56-2	Rattlesnake Detention	5.15	1937	2,518.32	39	SES
56-3	Roberts Detention	2.34	1937	1,486.2	40	SES
56-4a	Press Pond	4.65	1937	2,298.11	21.5	SES
56-5	Loney Draw, Site No. 9	2.77	1937	2,252.03	21.4	179.69
56-6	Loney Draw, Site No. 10	8.43	1937	16,129	3.28	SES
56-7	Loney Draw, Site No. 12	4.38	1937	12,154	3.28	SES
56-8	Loney Draw, Site No. 13	1.07	1937	4,687	1.03	SES
56-9	Site No. 1 Diablo Arroyo	20.89	1937	3,221	69.6	112

RIO GRANDE BASIN (LOW EAGLE PASS)

Site	Location	Capacity (cu ft)	Year	Original Capacity (cu ft)	Adjusted Capacity (cu ft)	Remarks
55-1	Site 6 Olmitos & Garcias Creeks	13.19	1962	2,298.11	21.5	SES
56-1a	Cottonwood Detention	2.34	1937	2,298.11	21.4	179.69
56-2	Rattlesnake Detention	5.15	1937	2,252.03	21.4	179.69
56-3	Roberts Detention	2.34	1937	1,486.2	40	SES
56-4a	Press Pond	4.65	1937	2,298.11	21.5	SES
56-5	Loney Draw, Site No. 9	2.77	1937	2,252.03	21.4	179.69
56-6	Loney Draw, Site No. 10	8.43	1937	16,129	3.28	SES
56-7	Loney Draw, Site No. 12	4.38	1937	12,154	3.28	SES
56-8	Loney Draw, Site No. 13	1.07	1937	4,687	1.03	SES
56-9	Site No. 1 Diablo Arroyo	20.89	1937	3,221	69.6	112

1/ Dam was raised 1 ft. in 1928. Capacity at 1928 spillway level.

2/ Latest drainage area by USGS in 1964.

3/ Sediment pool only.

4/ Does not include 8,900 sq. mi. which is considered to be noncontributing to the total 26,606 sq. mi. drainage area.

5/ For the 3,528 sq. mi. area between Possum Kingdom and Winters Dams, excluding 77.8 sq. mi. which is reservoir surface area at elevation 571.

6/ Original storage capacity 2,017,500 ac.-ft. Adjusted in 1963 for detailed range survey in 1951.

7/ Spillway raised 2.3 ft. in Sept. 1948.

8/ Dam was raised 13 ft. in 1961 capacity at 1940 spillway elevation.

9/ Dam has not been certified.

10/ Includes Hanco Watershed but does not include Roberts Watershed.

11/ Estimated or assumed.

SUMMARY OF  
RESERVOIR SEDIMENTATION SURVEYS MADE IN THE UNITED STATES THROUGH 1970

DATA SHEET NUMBER	RESERVOIR	STREAM	NEAREST TOWN	DRAINAGE AREA (SQ. MILES)		DATE OF SURVEY	PERIOD BETWEEN SURVEYS (YEARS)	STORAGE CAPACITY (ACRE-FT.)	CAPACITY (ACRE-FT.)	SPECIFIC WEIGHT (LB. PER CU. FT.)	AVG. ANNUAL ACCUMULATION PER SQ. MI. OF NET DR. AREA FOR PERIOD SURVEYED	AGENCY SUPPLYING DATA
				TOTAL	NET							
RIO GRANDE BASIN (ESPANOLA TO FORT QUINN)												
57-1b	Elephant Butte	Rio Grande River	Elephant Butte, N. Mex.	25,866	25,866	Jan. 1915	—	2,634,800	—	—	—	CS
	-do-	-do-	-do-	—	—	Aug. 1920	3.7	2,768,455	—	—	—	CS
	-do-	-do-	-do-	—	—	Aug. 1925	5.0	2,389,380	—	—	—	CS
	-do-	-do-	-do-	—	—	Apr. 1935	9.7	2,270,300	—	—	—	CS
	-do-	-do-	-do-	—	—	Oct. 1940	5.5	2,219,000	—	—	—	CS
	-do-	-do-	-do-	—	—	Apr. 1947	6.5	2,197,600	—	—	—	CS
	-do-	-do-	-do-	—	—	Feb. 1957	9.7	2,208,780	—	—	—	CS
	-do-	-do-	-do-	—	—	Apr. 1969	12.2	2,137,219	—	—	—	CS
	-do-	-do-	-do-	—	—	Jan. 1978	—	345,872	—	—	—	CS
57-2	Abasco	-do-	Trib. of Conchos, N. Mex.	2,700	3,127	Nov. 1937	19.9	342,990	—	—	—	CS
	-do-	-do-	-do-	93.1	93.1	Feb. 1959	—	4,164	—	—	—	CS
57-3a	Santa Cruz	-do-	Espanola, N. Mex.	—	—	Aug. 1956	27.4	3,758	—	—	—	CS
57-4	Cornfield Wash (1)	-do-	Osbo, N. Mex.	.29	.28	Apr. 1951	—	10.3	—	—	—	CS
57-5	Cornfield Wash (2)	-do-	-do-	.87	.85	Oct. 1960	10.0	54.1	—	—	—	CS
57-6	Cornfield Wash (3)	-do-	-do-	.25	.25	Oct. 1960	10.0	45.1	—	—	—	CS
57-7	Cornfield Wash (4)	-do-	-do-	1.18	1.17	Oct. 1960	10.0	22.1	—	—	—	CS
57-8	Cornfield Wash (5)	-do-	-do-	1.04	1.04	Apr. 1951	—	17.4	—	—	—	CS
57-9	Cornfield Wash (9)	-do-	-do-	.09	.09	Oct. 1960	10.0	3.0	—	—	—	CS
57-10	Cornfield Wash (13)	-do-	-do-	.33	.33	Oct. 1960	10.0	7.4	—	—	—	CS
57-11	Cornfield Wash (15)	-do-	-do-	1.04	1.03	Dec. 1953	—	17.9	—	—	—	CS
57-12	San Luis (1)	-do-	-do-	1.06	1.05	Oct. 1960	10.0	16.3	—	—	—	CS
57-13	San Luis (3)	-do-	-do-	.67	.66	Oct. 1960	10.0	12.0	—	—	—	CS
57-14	Zia Reservoir	-do-	San Felipe, N. Mex.	2.4	2.4	Aug. 1942	—	22.6	—	—	—	CS
57-15a	James Canyon Reservoir	-do-	San Felipe, N. Mex.	1.034	1.034	Oct. 1960	10.0	59.9	—	—	—	CS
57-16	San Luis #2	-do-	Bernalillo, N. Mex.	—	—	Oct. 1953	—	117,213	—	—	—	CS
57-17	Underwood Arroyo	-do-	Bernalillo, N. Mex.	—	—	Jan. 1958	24.25	115,823	—	—	—	CS
57-18	Alamo Arroyo	-do-	Osbo, N. Mex.	—	—	Aug. 1959	57.67	113,874	—	—	—	CS
57-19	Ramones Arroyo	-do-	Osbo, N. Mex.	—	—	Dec. 1965	57.63	112,809	—	—	—	CS
57-20	North Salem Arroyo	-do-	Osbo, N. Mex.	—	—	July 1952	—	53.0	—	—	—	CS
57-21	Roddy Arroyo	-do-	Berry, N. Mex.	—	—	July 1952	—	73.21	—	—	—	CS
	-do-	-do-	-do-	.87	.87	Apr. 1959	—	15.9	—	—	—	CS
	-do-	-do-	-do-	—	—	Aug. 1967	7.8	68.79	—	—	—	CS
	-do-	-do-	-do-	3.15	3.12	Apr. 1962	—	232	—	—	—	CS
	-do-	-do-	-do-	1.17	1.16	Dec. 1968	6.7	160	—	—	—	CS
	-do-	-do-	-do-	—	—	Sept. 1962	—	111	—	—	—	CS
	-do-	-do-	-do-	—	—	Jan. 1969	6.3	37	—	—	—	CS
	-do-	-do-	-do-	3.8	3.8	Oct. 1957	—	204.71	—	—	—	CS
	-do-	-do-	-do-	2.1	2.1	Aug. 1967	10.25	190.62	—	—	—	CS
	-do-	-do-	-do-	—	—	July 1968	—	170.91	—	—	—	CS
	-do-	-do-	-do-	—	—	Aug. 1967	9.1	141.25	—	—	—	CS
UPPER Pecos River Basin												
58-1	Bonita	Bonita Creek, East Gulch	Captlan, N. Mex.	40.0	39.9	June 1931	—	1,130	—	—	—	CS
58-2a	Alamogordo	Pecos River	Pr. Sumner, N. Mex.	4,393	3,749	Sept. 1946	—	156,750	—	—	—	CS
	-do-	-do-	-do-	—	—	Sept. 1946	3.25	146,071	—	—	—	CS
	-do-	-do-	-do-	—	—	Oct. 1943	3.08	130,280	—	—	—	CS
	-do-	-do-	-do-	—	—	Apr. 1944	0.50	132,171	—	—	—	CS
	-do-	-do-	-do-	—	—	Sept. 1964	20.42	110,695	—	—	—	CS
	-do-	-do-	-do-	16,030	1,080	Apr. 1961	31.00	6,633	—	—	—	CS
	-do-	-do-	-do-	—	—	July 1961	—	6,633	—	—	—	CS
	-do-	-do-	-do-	—	—	July 1954	15.25	5,647	—	—	—	CS



Station	Location	Structure	Area	Capacity	Year	Remarks	Notes
58-4a	McMillan (Lake McMillan)	dam	14,950	14,950	1894		
	do	do	do	do	Jan. 1894	91,000	.544
	do	do	do	do	June 1904	73,000	.276
	do	do	do	do	June 1914	6,142	1.80
	do	do	do	do	May 1913	41,500	1.52
	do	do	do	do	June 1925	10,000	1.59
	do	do	do	do	Dec. 1932	7,500	1.53
	do	do	do	do	Jan. 1940	38,655	.017
	do	do	do	do	July 1956	16,500	.146
	do	do	do	do	May 1959	27,994,000	.149
58-5	Upper-Tiempo Site #1	dam	93.92	93.92	1959	4,972.14	8/62.4
	do	do	do	do	Oct. 1959	4,946.54	.69
	do	do	do	do	May 1962	4,896.60	.34
	do	do	do	do	Mar. 1963	4,798.41	1.449
	do	do	do	do	Feb. 1965	4,749.54	.36
58-6	Banovet #7	dam	12	12	1965	10.67	.01
58-7	Banovet #9	dam	.57	.57	1965	7.20	.94
58-8	Banovet #11	dam	.69	.69	1955	4.09	.34
58-9	Banovet #6	dam	.19	.19	1955	10.67	.75
58-10	Pearson #1	dam	.24	.24	1955	1.52	.16
	do	do	do	do	Apr. 1957	2.17	.45
	do	do	do	do	Apr. 1959	1.91	.74
	do	do	do	do	Oct. 1965	6.50	.38
	do	do	do	do	Mar. 1955	5.45	.83
	do	do	do	do	Dec. 1956	4.30	2.75
	do	do	do	do	Jan. 1958	3.62	4.280
	do	do	do	do	Jan. 1959	1.00	2.49
	do	do	do	do	Oct. 1965	6.75	4.130
	do	do	do	do	Oct. 1965	2.55	2.519
58-11	Pearson #9	dam	1.56	1.56	1965	10.92	.45
58-12	Pearson #10	dam	.71	.71	1955	20.19	.74
	do	do	do	do	May 1957	2.17	1.39
	do	do	do	do	Jan. 1958	17.99	2.262
	do	do	do	do	Oct. 1958	7.5	.14
	do	do	do	do	Oct. 1965	7.00	1.241
58-13	Pearson #1B	dam	1.80	1.80	1955	15.60	.31
58-14	Pearson #20	dam	2/16	2/16	1965	10.67	.70
	do	do	do	do	Mar. 1965	6.55	1.442
	do	do	do	do	Oct. 1965	10.58	.46

COLORADO RIVER BASIN (BELOW HOOVER DAM)  
Williams and Lower Gila River Basins

Station	Location	Structure	Area	Capacity	Year	Remarks	Notes
60-1	Agua Fria River	dam	1,450	1,450	1928	184,500	.825
	do	do	do	do	Apr. 1928	176,456	.432
60-2a	Gila River	dam	11,900	11,900	1928	1,266,837	6,054
	do	do	do	do	Feb. 1928	1,232,725	5,870
	do	do	do	do	Mar. 1935	1,200,695	5,882
	do	do	do	do	Jan. 1937	1,209,343	5,780
	do	do	do	do	Jan. 1947	1,170,118	5,592
60-3	Beckler Wash	dam	.69	.69	1926	31.43	1.75
	do	do	do	do	Mar. 1926	1,522,543	1,886
60-4	Salt River & Yonto Creek	dam	5,760	5,760	1927	1,460,140	1,859
	do	do	do	do	May 1927	1,460,140	1,807
	do	do	do	do	Oct. 1916	1,425,813	1,767
	do	do	do	do	Sept. 1925	1,425,813	1,621
	do	do	do	do	Jan. 1925	1,419,013	1,757
	do	do	do	do	Jan. 1939	1,398,430	1,733
	do	do	do	do	Jan. 1946	1,381,990	1,712

1/ Total storage shows a gain of 9,180 ac.-ft. since 1947 survey attributable primarily to compaction.  
 2/ Includes 2,540 sq. mi. in closed basin in San Luis Valley, Colo.  
 3/ Difference between gaging station below Hoover Dam and gaging station below Cahallo Dam.  
 4/ Particulars are between gaging station below Hoover Dam and gaging station below Cahallo Dam.  
 5/ Damoff seasons.  
 6/ Time periods adjusted.  
 7/ Compacted sediment for 1,080 sq. mi.; values for 16,030 sq. mi. are given in appendix summaries.

SUMMARY OF  
RESERVOIR SEDIMENTATION SURVEYS MADE IN THE UNITED STATES THROUGH 1970

DATA SHEET NUMBER	RESERVOIR	STREAM	NEAREST TOWN	DRAINAGE AREA (SQ. MILES)		DATE OF SURVEY	PERIOD BETWEEN SURVEYS (YEARS)	STORAGE CAPACITY (ACRE-FT.)	CAPACITY ANNUAL INFLOW (ACRE-FT. PER YEAR)	SPECIFIC WEIGHT (LB. PER CU. FT.)	AVG. ANNUAL ACCUMULATION PER SQ. MI. OF NET DR. AREA FOR PERIOD SHOWN		AGENCY SUPPLYING DATA
				TOTAL	NET						AC-FT.	TONS	
60-5	Allen	Trib. of Gila River	Thatcher, Ariz.	3/4, 17	4.13	1976	279	2,847	—	—	0.77	—	305
60-6	Mr. B. Tank No. 1	Whiteoak Drain	Douglas, Ariz.	.21	.21	June 1976	253	2,562	—	—	—	—	305
60-7	Mr. B. Tank No. 2	—	—	10.92	10.92	Nov. 1958	2,54	1,116	975	—	.05	81.7	305
60-8	Mr. B. Tank No. 3	—	—	2.48	2.48	Nov. 1958	2,70	1,009	975	—	.008	13.1	305
60-9	Mr. B. Tank No. 4	—	—	.36	.36	Nov. 1958	11.7	0	465	—	.85	1,573	305
60-10	Mr. B. Tank No. 5	—	—	12.3	12.3	Nov. 1958	3.0	.009	990	—	.10	196	305
60-11	Mr. B. Tank No. 6	—	—	5.68	5.68	Nov. 1943	2.7	.005	975	—	.006	9.8	305
60-12	Don Cabesas No. 4	—	—	.6	.6	Nov. 1943	6.0	.312	975	—	.006	9.8	305
60-13a	Don Cabesas No. 5	—	—	.38	.38	Nov. 1943	4.7	.385	990	—	.29	599	305
60-13b	Don Cabesas No. 6	—	—	.2	.2	Nov. 1943	2.8	1,280	990	—	.26	510	305
60-14	Bullhorn	—	—	.9	.9	Oct. 1950	6.8	1,889	985	—	.75	1,388	305
60-15	Bonnetland	—	—	4.80	4.80	June 1960	14.8	1,112	990	—	.78	1,530	305
60-16	Lower Foote Wash	—	—	1.78	1.78	June 1958	5.7	.176	980	—	.13	—	305
60-17	Hagan No. 1	—	—	.38	.38	June 1958	2.7	.064	980	—	.15	261	305
60-18	Hagan No. 2	—	—	21.9	21.9	Feb. 1954	1.3	.108	985	—	.15	278	305
60-19a	Hagan No. 3	—	—	.6	.6	May 1959	6.0	—	975	—	.03	19	305
60-19b	Hagan No. 4	—	—	4.95	4.95	May 1959	1.4	.073	980	—	.06	105	305
60-20	Upper Foote Wash	—	—	.74	.74	Oct. 1954	24.2	.209	980	—	.04	—	305
60-21	Upper Foote Wash	—	—	5.612	5.612	June 1958	3.4	.254	985	—	.23	426	305
60-22	Willow Old Tank	—	—	5.618	5.618	June 1960	1.8	—	985	—	.23	426	305
60-23a	Barklett	—	—	.60	.60	June 1939	162,688	—	—	—	6/154	—	305
60-23b	Burrows	—	—	.33	.33	Feb. 1939	179,440	—	—	—	—	—	305
60-24	Foote Wash Pond #1	—	—	1.09	1.09	Aug. 1942	8,335	7,778,488	—	—	.624	—	305
60-25	Foote Wash Pond #2	—	—	.65	.65	Nov. 1940	13,117	67,900	—	—	.044	—	305
60-26	Williams-Chandler Pond #1	—	—	.51	.51	Jan. 1944	4.9	8/12,630	—	—	.083	—	305
60-27	Williams-Chandler Pond #2	—	—	.44	.44	Nov. 1943	13.1	139,238	—	—	.12	199	305
60-28	Big Horn No. Tank #1	—	—	2/1.60	2/1.60	Jan. 1964	17.10	11,705	76.2	—	.12	190	305
60-29	Big Horn No. Tank #2	—	—	2/1.68	2/1.68	Jan. 1964	6,462	8,864	72.6	—	.12	190	305
60-30	Continental Wash Tank	—	—	1.09	1.09	Jan. 1964	2.10	.197	60	—	.003	43	305
60-31	New Tank	—	—	.65	.65	July 1941	9.33	1,346	60	—	.004	14	305
60-32	West Tank	—	—	.44	.44	July 1941	8.95	1,281	60	—	.004	14	305
60-33	Upper Tadin Tank	—	—	2/1.68	2/1.68	Oct. 1964	21.00	97.83	17.6	—	.11	114	305
60-34	Harrah's No. Tank #1	—	—	1.83	1.83	Oct. 1964	11.46	48.79	90	—	.11	120	305
60-35	Judith Wash Retarding Dam	—	—	1.1	1.1	Oct. 1964	1.37	.209	91.97	—	.09	160	305
60-36	Judith Wash Retarding Dam	—	—	4.60	4.60	May 1964	7.61	.759	71.12	—	.04	158	305
				1.60	1.60	June 1960	10.09	46.31	52.5	—	.13	148.7	305
				.11	.11	Oct. 1964	2.21	8.48	16	—	.015	15	305
				4.57	4.57	Oct. 1964	6.90	11.02	90	—	.18	196	305
				1.60	1.60	Jan. 1964	156.79	91.796	76.9	—	.14	234.5	305
				—	—	July 1964	153.16	91.784	786.3	—	.39	633.2	305



SUMMARY OF  
RESERVOIR SEDIMENTATION SURVEYS MADE IN THE UNITED STATES THROUGH 1970

DATA SHEET NUMBER	RESERVOIR	STREAM	NEAREST TOWN	DRAINAGE AREA (SQUARE MILES)		PERIOD BETWEEN SURVEYS (YEARS)	STORAGE CAPACITY (ACRE-FT.)	CAPACITY (AVG. ANNUAL INFLOW RATIO PER ACRE-FT.)	SPECIFIC WEIGHT (LB. PER CU. FT.)	AVG. ANNUAL SEGMENT ACCUMULATION PER SQ. MI. OF NET DR. AREA FOR PERIOD SURVEY	AGRICULTURE SUPPLYING DATA
				TOTAL	NET						
LITTLE COLORADO AND SAN JUAN RIVER BASINS (Continued)											
61-2a	Millet Swale Reservoir	Trib. of Silver Creek	Taylor, Ariz.	40.0	39.7	June 1959	1,242.0	2.1	67	0.29	00
61-3	Stockyard Tank	Trib. Cottonwood Wash	do	—	—	June 1962	1,259.4	2.0	80	.89	00
61-4	Thomas Tank I	do	Snowflake, Ariz.	.48	.476	June 1966	1,118.5	1.7	—	—	00
61-5	Ellsworth Tank	do	do	.55	.549	May 1963	6.04	4.52	103.6	.17	00
61-6	New Tank	Trib. Snow Low Creek	Taylor, Ariz.	.25	.249	June 1967	3.09	4.36	77.9	.15	00
61-7	West Hill Tank	Trib. Cottonwood Wash	Snowflake, Ariz.	2.45	2.45	Aug. 1968	1.50	4.23	80	.044	00
61-8	Thomas Tank II	Trib. Parkins Spring Drain	Clay Springs, Ariz.	.32	.32	May 1958	10.13	4.15	87.7	.04	00
			do	.10	.10	June 1964	1.39	4.07	93.4	.08	00
			do	.10	.10	July 1968	1.35	4.30	89.3	.10	00
COLORADO RIVER BASIN (HALLS CROSSING TO HOOVER DAM)											
62-1	Lake Mead (Hoover Dam)	Colorado River	Boulder City, Nev.	167,000	167,000	Feb. 1955	31,250,000	2.10	—	—	00
62-2	Brookby Tank	Trib. of Johnson Wash	Frederick, Ariz.	.4	.4	Sept. 1962	29,827,000	2.03	3/65	.620	00
62-3	Riggs Flat Charco	Sandy Canyon Wash	do	57.86	57.83	Sept. 1965	.110	.277	97	3/10	00
62-4	Leroy Judd Tank	Trib. of Kanab Creek	do	.38	.38	Oct. 1956	54.93	1.78	72	.035	00
62-5	Kalabab Indian Reservoir	do	Indian Mound, Ariz.	1.27	1.27	Aug. 1962	36.58	1.19	105.7	.63	00
62-6	James Judd Tank	do	do	57.49	57.49	Oct. 1965	2.287	1.32	87.2	.098	00
62-7	Frog Hollow Detention Res.	Frog Hollow Wash	do	9.2	9.2	Aug. 1965	2.77	—	900	5/12	00
62-8	CCC Pond (West)	Trib. Santa Clara River	St. George, Utah	.03	.03	Mar. 1958	23.0	4.57	90	7/2	00
62-9	CCC Pond (East)	do	do	.32	.32	Apr. 1966	91.0	4.63	92	7/23	00
62-10	Rondo Reservoir Debris Basin #2	Trib. Virginia River	do	.026	.026	Apr. 1964	.12	4.06	90	7/18	00
62-11	Rondo Reservoir Debris Basin #1	do	do	.09	.09	Feb. 1966	81.5	4.53	90	7/15	00
62-12	Illiff Andrea	Trib. Warner Drain	do	1.09	1.08	Feb. 1966	91.0	4.10	90	7/11	00
62-13	Manfred Spindlove	Trib. Fort Peck Wash	do	.85	.84	Jan. 1966	40	42.2	78	7/11	00
62-14	Black Hunkle	Trib. City Creek	do	.59	.58	Mar. 1966	97.0	4.11	87.5	7/11	00
62-15	Little Greasy Pond	do	do	2.3	2.3	Nov. 1963	40	43.2	87.5	7/11	00
62-16	Bill Snow Pond	Trib. Santa Clara River	do	.097	.097	Mar. 1964	92.0	4.2	94	7/10	00
62-17	Magnesian Wash	do	do	.17	.17	June 1966	92.0	4.3	72	7/17	00
COLORADO RIVER BASIN (ABOVE HALLS CROSSING) Dumelon, Dolores and Present River Basins											
63-1	Badger Detention (1A)	Badger Wash	Meek, Colo.	1.53	1.49	May 1957	201.52	3.356	—	—	00
		do	do	—	—	Mar. 1958	199.35	3.300	—	.91	00
		do	do	—	—	Mar. 1959	198.27	3.290	—	2.07	00
		do	do	—	—	Mar. 1961	190.36	3.152	—	1.97	00

Reservoir ID	Reservoir Name	Month	Year	Capacity Increase	Reservoir Raising	Capacity	Reservoir Raising	Capacity	Reservoir Raising	Capacity
63-2	Badger Wash West Twin (2A)	Dec.	1953	.165		6.30		987		6.91
		July	1955		1.6	4.47		679		6.91
		Nov.	1956		1.4	4.47		679		6.91
		Oct.	1957		1.0	3.98		605		2.97
		Nov.	1958		1.0	3.98		605		2.97
		Nov.	1959		1.0	3.65		555		2.00
		Nov.	1961		2.0	2.49		369		3.70
		Dec.	1953	.055		12.90		4,813		2.91
		July	1955		1.6	12.65		4,720		0
		Nov.	1956		1.4	12.65		4,720		0
63-3	Badger Wash Lower Oil Well (3A)	Oct.	1957		1.0	12.55		4,683		1.82
		Nov.	1958		1.0	12.55		4,683		0
		Nov.	1959		1.0	12.55		4,683		0
		Nov.	1961		2.0	12.12		4,601		1.82
		Dec.	1953	.087		3.45		4,522		1.82
		Apr.	1954		2.6	1.76		1,822		2.30
		Oct.	1957		1.0	1.46		1,462		1.46
		Nov.	1959		2.0	1.46		1,462		1.46
		Nov.	1961	.088		16.87		2,986		6.66
		Oct.	1957		2.6	15.87		2,809		5.57
63-4	Bart Basin (11)	Nov.	1959		2.0	15.32		2,712		3.4
		Nov.	1961	.022		2.64		3,77		11.8
		July	1955		1.6	2.64		3,77		0
		Oct.	1957		1.3	2.64		3,77		0
		Nov.	1956		1.0	2.49		3,56		6.82
		Nov.	1958		1.1	2.49		3,56		0
		Nov.	1959		1.0	2.43		3,47		2.73
		Nov.	1961		2.0	2.28		3,26		3.18
		Nov.	1963		1.0	2.05		2,90		2.27
		Nov.	1964		1.0	1.82		2,57		1,900
63-5	MADIA Basin (12)	Nov.	1962		1.0	1.82		2,57		1,900
		Nov.	1963		1.0	1.82		2,57		1,900
		Nov.	1964		1.0	1.82		2,57		1,900
		Nov.	1965		1.0	1.82		2,57		1,900
		Nov.	1966		1.0	1.82		2,57		1,900
		Nov.	1967		1.0	1.82		2,57		1,900
		Nov.	1968		1.0	1.82		2,57		1,900
		Nov.	1969		1.0	1.82		2,57		1,900
		Nov.	1970		1.6	1.60		1,60		10.18
		Oct.	1970		1.6	2.50		3,57		4.45
63-6a	Upper Rankin (1A)	Apr.	1954	.477		27.25		1,854		1.93
		Nov.	1956		2.6	24.85		1,680		2.94
		Oct.	1957		1.0	23.44		1,595		1.24
		Nov.	1959		2.0	22.26		1,514		1.24
		Dec.	1953	.066		8.30		3,81		6.68
		July	1955		1.6	7.59		3,48		0
		Nov.	1956		1.3	7.59		2,56		0
		Nov.	1958		1.0	7.34		3,37		3.78
		Nov.	1959		1.3	7.04		3,23		0
		Nov.	1961		2.0	6.70		3,07		4.55
63-7	Southwest (13)	Nov.	1963		2.0	6.59		3,02		2.73
		Nov.	1964		1.0	6.15		2,80		1,900
		Nov.	1965		1.0	6.15		2,80		1,900
		Nov.	1966		1.0	6.15		2,80		1,900
		Nov.	1967		1.0	6.15		2,80		1,900
		Nov.	1968		1.0	6.15		2,80		1,900
		Nov.	1969		1.0	6.15		2,80		1,900
		Nov.	1970		1.0	6.15		2,80		1,900
		Nov.	1971		1.0	6.15		2,80		1,900
		Nov.	1972		1.0	6.15		2,80		1,900
63-8a	West Twin (2-1)	Dec.	1953	.148		5.54		5,54		7.44
		July	1955		1.6	6.30		1,31		15.44
		Nov.	1956		1.3	4.38		91		15.44
		Oct.	1957		1.0	3.90		81		6.57
		Nov.	1958		1.1	3.90		81		0
		Nov.	1959		1.0	3.15		3,15		1.49
		Nov.	1961		2.0	13.86		2,88		4.22
		Nov.	1963		2.0	13.52		2,80		2.52
		Nov.	1964		1.0	12.59		2,57		7.64
		Nov.	1965		1.0	12.06		2,50		14,966
63-9	West Twin (2-2)	Nov.	1966		1.0	12.10		2,51		2.23
		Nov.	1967		1.0	11.23		2,39		3.85
		Nov.	1968		1.0	10.24		2,09		6.15
		Nov.	1969		1.0	10.64		2,10		14.87
		Nov.	1970		1.0	10.64		2,10		14.87
		Nov.	1971		1.0	10.64		2,10		14.87
		Nov.	1972		1.0	10.64		2,10		14.87
		Nov.	1973		1.0	10.64		2,10		14.87
		Nov.	1974		1.0	10.64		2,10		14.87
		Nov.	1975		1.0	10.64		2,10		14.87

1/ Not adjusted for numerous small reservoirs. Runoff used to compute C/I ratio was not adjusted for upstream diversions.  
2/ Period of measurement from Mar. 1948 - Mar. 1949.  
3/ Based on measured and estimated sediment inflow of 2,000,000 tons in 13.7 yr. period.  
4/ Estimated effective life of pond is 5 yr. 1951 - 1956.  
5/ Reservoir is off main channel. Estimate reservoir intercepts 1/3 of flow and sediment from total drainage area.  
6/ Effective life of reservoir is estimated at 8 yr. storm in 1963 filled reservoir and changed channel course.

7/ Includes deposition above spillway crest level.  
8/ Reservoir cleaned in June 1970.  
9/ Capacity increase.  
10/ Dam and spillway raised in 1959.  
11/ Estimated or assumed.

SUMMARY OF  
RESERVOIR SEDIMENTATION SURVEYS MADE IN THE UNITED STATES THROUGH 1970

DATA SHEET NUMBER	RESERVOIR	STREAM	NEAREST TOWN	DRAINAGE AREA (SQ. MILES)		PERIOD BETWEEN SURVEYS (YEARS)	STORAGE CAPACITY (ACRE-FT.)	CAPACITY INFLOW RATIO (ACRE-FT. PER ACRE-FT.)	SPECIFIC WEIGHT (DRY) (LB. PER CU. FT.)	AVE. ANN. ACCUMULATION PER SQ. MI. OF NET DR. AREA FOR PERIOD SHOWN	AGENCY SUPPLYING DATA						
				TOTAL	NET												
63-10	Oil Well (1-8)	Trib. of Badger Wash	Mack, Colo.	0.059	0.019	Dec. 1953	12.92	5.71	990	7.00	OS						
						July 1955	12.18	5.39	990	0	15,269						
						Nov. 1956	12.18	5.39	990	0	0						
						Oct. 1957	11.90	5.26	990	4.75	9,302						
						Nov. 1958	11.90	5.26	990	0	0						
						Nov. 1959	11.64	5.15	990	4.40	8,638						
						Nov. 1961	11.31	5.00	990	2.71	5,482						
						Nov. 1962	11.25	4.86	990	1.71	3,977						
						Nov. 1963	11.25	4.86	990	1.25	2,859						
						Nov. 1964	10.73	4.75	990	8.14	15,947						
						Nov. 1965	10.82	4.79	990	1/2	1/2						
						Oct. 1967	10.62	4.70	990	3.39	6,643						
						Nov. 1968	10.15	4.49	990	7.96	15,615						
						Nov. 1969	10.15	4.48	990	3.34	564						
						63-11	Windy Point (4-8)			.019	.019	Dec. 1953	4.52	4.42	990	2.38	OS
July 1955	4.31	9.17	990	0	13,427												
Nov. 1956	4.31	9.17	990	0	0												
Oct. 1957	4.19	8.91	990	6.32	12,980												
Nov. 1958	4.19	8.91	990	0	0												
Nov. 1959	4.16	8.85	990	1.58	3,093												
Nov. 1961	4.14	8.80	990	.53	1,032												
Nov. 1962	4.12	8.76	990	.53	1,032												
Nov. 1963	3.89	8.28	990	4.74	10,215												
Nov. 1964	3.89	8.28	990	0	0												
Oct. 1967	3.81	8.11	990	4.21	8,253												
Nov. 1968	3.74	7.96	990	3.68	7,222												
Nov. 1969	3.83	8.15	990	1/2	1/2												
Dec. 1953	8.45	2.14	990	9.50	18,622												
63-12	Tucson (2-8)			.158	.158							July 1955	6.05	1.53	990	0	OS
						Nov. 1956	6.05	1.53	990	0	0						
						Oct. 1957	5.94	1.50	990	.70	1,365						
						Nov. 1958	5.94	1.50	990	0	0						
						Nov. 1959	24.18	6.28	990	2.13	2,840						
						Nov. 1961	24.18	6.12	990	1.96	3,846						
						Nov. 1962	23.89	6.05	990	.95	1,110						
						Nov. 1963	23.45	5.94	990	2.78	3,639						
						Nov. 1964	22.15	5.86	990	1.90	3,178						
						Nov. 1965	22.86	5.79	990	2.34	4,590						
						Oct. 1967	22.12	5.60	990	6.20	12,138						
						Nov. 1968	22.12	5.60	990	1/2	1/2						
						Nov. 1969	8.10	4.60	990	5.42	10,624						
						63-13	North Basin (1-8)			.048	.048	July 1955	7.69	4.37	990	0	OS
												Nov. 1956	7.69	4.37	990	0	0
Oct. 1957	7.98	4.31	990	2.29	4,492												
Nov. 1958	7.98	4.31	990	0	0												
Nov. 1959	7.51	4.27	990	1.46	2,899												
Nov. 1961	7.38	4.19	990	1.46	2,654												
Nov. 1962	7.10	4.03	990	2.92	5,717												
Nov. 1963	7.05	4.00	990	1.06	2,042												
Nov. 1964	6.81	3.87	990	3.87	7,606												
Nov. 1965	6.81	3.87	990	0.63	11,026												
Nov. 1966	6.81	3.87	990	0.64	1,117												
Oct. 1967	6.07	3.12	990	6.07	19,194												
Nov. 1968	6.18	3.51	990	0.80	1,117												
Oct. 1970	6.13	3.48	990	1.04	2,042												



SUMMARY OF  
RESERVOIR SEDIMENTATION SURVEYS MADE IN THE UNITED STATES THROUGH 1970

DATA SHEET NUMBER	RESERVOIR	STREAM	NEAREST TOWN	DRAINAGE AREA (SQ. MILES)		DATE OF SURVEY	PERIOD BETWEEN SURVEYS (YEARS)	STORAGE CAPACITY (ACRE-FT.)	CAPACITY AVERAGE INFLOW RATIO (ACRE-FT. PER ACRE-FT.)	SPECIFIC WEIGHT (DRY) (LB. PER CU. FT.)	AVG. ANNUAL ACCUMULATION OF NET DR. AREA FOR PERIOD SHOWN	AGENCY SUPPLYING DATA
				TOTAL	NET							
COLORADO RIVER BASIN (ABOVE HALLS CROSSING) Gunnison, Dolores and Fremont River Basins (Continued)												
63-19	Lazen Creek Weir	Lazen Creek	Fraser, Colo.	0.48	0.48	Oct. 1955	1.0	--	--	--	10.24	FS
	-do-	-do-	-do-	--	--	Oct. 1956	1.0	--	--	--	17.92	FS
	-do-	-do-	-do-	--	--	Oct. 1957	1.0	--	--	--	21.12	FS
	-do-	-do-	-do-	--	--	Oct. 1958	1.0	--	--	--	3.84	FS
	-do-	-do-	-do-	--	--	Oct. 1959	1.0	--	--	--	3.52	FS
	-do-	-do-	-do-	--	--	Oct. 1960	1.0	--	--	--	0.003	FS
	-do-	-do-	-do-	--	--	Oct. 1961	1.0	--	--	--	0.003	FS
	-do-	-do-	-do-	--	--	Oct. 1962	1.0	--	--	--	8.76	FS
	-do-	-do-	-do-	--	--	Oct. 1963	1.0	--	--	--	2.88	FS
	-do-	-do-	-do-	--	--	Oct. 1964	1.0	--	--	--	5.76	FS
	-do-	-do-	-do-	--	--	Oct. 1965	1.0	--	--	--	0.003	FS
	-do-	-do-	-do-	--	--	Oct. 1966	1.0	--	--	--	2.74	FS
	-do-	-do-	-do-	--	--	Oct. 1967	1.0	--	--	--	1.73	FS
	-do-	-do-	-do-	--	--	Oct. 1968	1.0	--	--	--	0.001	FS
	-do-	-do-	-do-	--	--	Oct. 1969	1.0	--	--	--	1.50	FS
	-do-	-do-	-do-	--	--	Oct. 1970	1.0	--	--	--	4.00	FS
63-20	East St. Louis Creek Weir	East St. Louis Creek	-do-	3.10	3.10	Oct. 1964	1.0	--	--	--	0.002	FS
	-do-	-do-	-do-	--	--	Oct. 1965	1.0	--	--	--	3.45	FS
	-do-	-do-	-do-	--	--	Oct. 1966	1.0	--	--	--	0.002	FS
	-do-	-do-	-do-	--	--	Oct. 1967	1.0	--	--	--	2.16	FS
	-do-	-do-	-do-	--	--	Oct. 1968	1.0	--	--	--	4.20	FS
	-do-	-do-	-do-	--	--	Oct. 1969	1.0	--	--	--	2.90	FS
	-do-	-do-	-do-	--	--	Oct. 1970	1.0	--	--	--	4.25	FS
63-21	Roatcap Wash Weir	Roatcap Wash	Olath, Colo.	11.6	11.5	Dec. 1964	6	829.6	97.0	--	--	SCS
	-do-	-do-	-do-	--	--	Nov. 1970	6	810.0	96.9	--	--	SCS
GREEN RIVER BASIN												
64-1	Duck Park Weir	Ferron Creek	Ferron, Utah	3.56	3.56	Oct. 1962	20	718	93.236	--	--	SCS
64-2	Smith Soda Creek Weir	South Soda Creek	Steamboat Springs, Colo.	3.40	3.40	Oct. 1967	1.0	1,870	93.286	--	--	FS
	-do-	-do-	-do-	--	--	Oct. 1968	1.0	--	--	--	--	FS
	-do-	-do-	-do-	--	--	Oct. 1969	1.0	--	--	--	--	FS
64-3	North Fish Creek Weir	North Fish Creek	-do-	2.24	2.24	Oct. 1968	1.0	--	--	--	--	FS
	-do-	-do-	-do-	--	--	Oct. 1969	1.0	--	--	--	--	FS
64-4	West Walton Creek Weir	Trib. Walton Creek	-do-	1.73	1.73	Oct. 1967	1.0	--	--	--	--	FS
	-do-	-do-	-do-	--	--	Oct. 1968	1.0	--	--	--	--	FS
64-5	Bullwinkle Weir	Trib. Brush Creek	Vernal, Utah	.11	.11	Oct. 1938	30	--	--	--	--	SCS
64-6	Rock Canyon Weir	Rock Canyon	-do-	1.41	1.41	Oct. 1936	22	95.0	91.0	0.06	38.28	SCS
64-7	Miles Haslem Pond	Trib. Steelmaker Draw	-do-	.095	.095	Oct. 1968	22	95.0	91.0	0.06	15.07	SCS
64-8	Neena Reservoir	Trib. Twelve Mile Wash	-do-	.65	.65	Sept. 1962	15	42.0	97.0	0.01	1.4	SCS
	-do-	-do-	-do-	--	--	May 1968	26	98.0	90	0.02	1.02	SCS
GREAT SALT LAKE BASIN												
65-1	East Canyon Weir	East Canyon Creek	Morgan, Utah	144	144	Oct. 1896	58	273,850	98	124	208	BR
65-2	Echo Weir	Weber River	Echo, Utah	732	732	Oct. 1930	24	75,716	97.1	104	161	BR
65-3a	Santaquin Debris Basin	Santaquin Creek	Santaquin, Wash.	17.65	13.5	Oct. 1964	3	964	90	0.06	1.1	SCS
65-3b	Booby Hole Weir	Booby Hole Creek	Koonaham, Utah	5.0	4.9	Oct. 1895	75	607	90	0.02	1.1	SCS



66-2	Indian Creek No. 1	Indian Creek	Beaver, Utah	12.0	11.95	1898	318	--	--	--	.08	503
66-3	Rocky Ford	Beaver River	--do--	5.0	508	Nov. 1910	299	--	--	--	--	503
66-4	Rocky Ford	Sevier River	--do--	9.0	900	Nov. 1910	2,260	--	--	--	--	503
66-5	Skutumpah	Skutumpah Creek	--do--	10.0	9.92	Nov. 1910	2,115	--	--	--	--	503
66-6	Enterprise	Pine Creek	Enterprise, Utah	25.0	23.4	Nov. 1909	667	--	--	--	--	503
66-7	Tanite Meadows	Pole Creek	--do--	7.0	6.9	Nov. 1910	9,000	--	--	--	--	503
66-8	Plute	Sevier River	Parowan, Utah	2.400	2.436	Nov. 1910	2,500	--	--	--	--	503
66-9	Sevier Bridge	Sevier River	Marysville, Utah	5.120	1.089	1910/5	61,010	--	--	--	--	503
66-10	Chalk Creek Debris Basin	Chalk Creek	Hephi, Utah	60.8	60.8	1912	250,000	--	--	--	--	503
66-11a	Fiddlers Canyon Debris Basin	Fiddlers Canyon	Phillmore, Utah	12.6	12.6	July 1916	44,12	0.002	*70	1,112.9	9/75	503
66-12a	Mill Canyon Retarding Structure	Mill Canyon	Cedar City, Utah	19.5	19.5	Nov. 1916	0	0	*75	228.7	7/11	503
			Glenwood, Utah			Dec. 1917	0	0	*70			503
			--do--			Dec. 1917	*15.00		*70	221	9/115	503
			--do--			Dec. 1917	208		*70			503
			--do--			Dec. 1917	*1,431		*70		.38	578

GREAT BASIN (NORTHWESTERN PART IN CALIFORNIA, NEVADA AND GREEN)

GREAT BASIN												
Huboldt, Carson, and Truckee River Basins												
68-1	Willow Creek	Willow Creek	Elko, Nev.	112	111	1924	15,300	--	--	--	--	503
68-2	Elko Summit Reservoir No. 1	(epherical)	--do--	1.25	1.25	Sept. 1917	15,080	0.223	--	--	--	503
68-3	Elko Summit Reservoir No. 2	--do--	--do--	.63	.63	Mar. 1923	7.44	.192	66	6.38	.04	57.5
68-4	Dorsey Creek Reservoir	--do--	--do--	9.16	9.16	Aug. 1945	5.45	.324	66.9	4.96	.05	73
			--do--			Oct. 1952	131	.358	56.9	9/12	8/149	503
			--do--			Sept. 1963	128	.350	--	--	--	503

GREAT BASIN												
Owens, Walker, and Mono Lake Drainages												
69-1	Weber	Walker River	Shurt, Nev.	2,800	2,400	Sept. 1915	13,200	--	--	--	--	503
			--do--			Sept. 1919	12,980	--	--	--	--	503

SALTON SEA AND SOUTHERN CALIFORNIA COASTAL AND GREAT BASIN DRAINAGE												
70-1a	Fullerton Flood-Control Basin	Fullerton Creek	Brea, Calif.	9/5.05	9/4.95	Oct. 1941	753.5	--	--	--	--	503
70-2	Lake Hodges	San Dieguito River	Escondido, Calif.	303	301	Nov. 1944	743.0	--	--	--	--	503
70-3	Railroad Canyon	San Jacinto River	--do--	718	651	Mar. 1962	36,704.5	--	--	--	--	503
70-4	Lake Sherwood	Triunfo Creek	--do--	16	15.7	Jan. 1919	34,789	--	--	--	--	503
70-5	Stone Canyon	Stone Canyon Creek	--do--	1.36	1.16	July 1919	12,218	65	365	517	.365	470
70-6	Bonita Canyon	Bonita Creek	Sawtelle, Calif.	4.00	4.00	Mar. 1916	2,670	60	392	39	.03	39
			Orange, Calif.			Mar. 1921	2,772	60	16	174	.64	677
			--do--			May 1921	7,949	60	2.34	3,058	2.34	503
			--do--			June 1921	205	60	2.63	3,437	2.63	503
			--do--			June 1921	205	60	2.63	3,437	2.63	503

1/ Dam was raised about 6 ft. in 1952.  
2/ Includes above crest deposits.  
3/ Formed by original rock-filled dam 58 feet high, which was subsequently raised in 1900, 1902, and 1916.  
4/ Computed from Siss analysis.  
5/ Original survey made in 1908.  
6/ Basin filled with sediment by one summer flash flood.  
7/ Has no meaning as a large portion of the sediment passed through the basin.  
8/ Includes some deposition above crest of spillway.  
9/ Drainage area and sediment contributing area were increased when Loftus diversion channel was completed on Dec. 21, 1954.  
10/ Based on runoff seasons.  
\* Estimated or assumed.

SUMMARY OF  
RESERVOIR SEDIMENTATION SURVEYS MADE IN THE UNITED STATES THROUGH 1970

DATA SHEET NUMBER	RESERVOIR	STREAM	NEAREST TOWN	DRAINAGE AREA (SQUARE MILES)		DATE OF SURVEY	PERIOD BETWEEN SURVEYS (YEARS)	STORAGE CAPACITY (ACRE-FT.)	CAPACITY INFLOW RATIO (ACRE-FT. PER PERIOD SHOWN)	SPECIFIC WEIGHT (DRY) (LB. PER CU. FT.)	AVG. ANN. SEDIMENT ACCUMULATION PER SQ. MI. OF NET DR. AREA FOR PERIOD SHOWN		AGENCY SUPPLYING DATA
				TOTAL	NET						AC.-FT.	TONS	
70-7	Bonquet Canyon	Bonquet Creek	San Fernando, Calif.	12.6	11.6	Mar. 1934	1/5	36,900	---	40	1.10	98	SCS
70-8a	Chatsworth	Trib. of Los Angeles River	"	5.40	4.45	Apr. 1939	1/5	36,936	---	40	1.10	98	SCS
70-9	Lake Hemet	Trib. of San Jacinto River	Hemet, Calif.	66.0	65.3	June 1939	21	10,077	---	40	1.10	444	SCS
70-10	Laguna	Trib. of Newport Bay	Orange, Calif.	75	72	June 1940	48	11,702	---	40	1.10	1,190	SCS
70-11	San Joaquin	San Joaquin River	Los Angeles, Calif.	1.42	1.30	June 1939	1/2	3,229	---	40	1.10	4,840	SCS
70-12	Palmdale	Antelope Valley River	Palmdale, Calif.	2.64	2.37	June 1939	1/2	7,489	---	40	1.10	710	SCS
70-13b	Little Rock Irrigation Dist.	Little Rock Creek	Palmdale, Calif.	68.0	67.84	Apr. 1934	1/26	7,393	---	40	1.10	185	SCS
70-14c	Live Oak Dam	Live Oak Creek	La Brea, Calif.	2.3	2.3	Mar. 1929	6.5	217	---	40	1.10	2	CE
70-15	Merced	Merced River	Merced, Calif.	112.0	109.4	Mar. 1936	7.0	242	---	40	1.10	31	SCS
70-16b	Prado Flood-Control Reservoir	Santa Ana River	Corona, Calif.	2,233	1,131	Mar. 1936	2.1	228	---	40	1.10	2,90	SCS
70-17	Rockingham Canyon S/	Rockingham Canyon	Arlington, Calif.	11.6	11.5	Mar. 1936	14.5	121	---	40	1.10	21	SCS
70-18c	Hansen Flood-Control Basin	Tulumba Creek	San Fernando, Calif.	167	146	Mar. 1936	14.5	121	---	40	1.10	21	SCS
7-19	Brea F. C. Basin	Brea Creek	Fullerton, Calif.	23.4	23.1	Mar. 1936	4.3	171	1.33	40	1.10	2,813	SCS
70-20c	Ogusall (San Gabriel Dam #2)	San Gabriel River	Abilene, Calif.	39.2	39.0	Apr. 1935	7.5	4,097	---	40	1.10	170	SCS
70-21d	San Gabriel Dam No. 1	San Gabriel River	Abilene, Calif.	203	203	Apr. 1935	8	12,681	---	40	1.10	170	SCS

Station	Location	Year	Capacity (cu ft)	Volume (cu ft)	Remarks				
70-22b	Morris Reservoir	Nov. 1954	1.3	44,013					
		Aug. 1958	4.3	44,614					
		Sept. 1961	3.1	44,366					
		Nov. 1962	1.2	43,642	51				
		Dec. 1965	3.1	42,371	49				
		Apr. 1966	1.3	42,075	51				
		Aug. 1967	1.3	40,697	46				
		Nov. 1967	1.5	38,778	45				
		Mar. 1969	2.5	36,748	42				
		Oct. 1969	4.2	37,822	43				
		Oct. 1970	1.0	41,549	48				
		Jan. 1974	2.1	39,316					
Jan. 1976	2.1	38,692	45						
Feb. 1978	3.1	37,175	43						
Oct. 1978	1.7	36,655	43						
Dec. 1982	1.2	34,843	41						
Nov. 1984	6.8	31,861	39						
Nov. 1984	4.2	31,827	40						
Jan. 1967	6.2	32,961	39						
Oct. 1970	3.8	30,085	35						
Sept. 1972	13.2	47,149	35						
Dec. 1975	2.9	1,373							
Oct. 1978	2.9	1,155							
Nov. 1979	3.0	1,169							
Nov. 1981	1.0	1,071							
Oct. 1983	1.9	1,042							
Nov. 1984	1.0	1,025							
Oct. 1984	9.8	1,025							
Nov. 1961	7.1	785	23						
Apr. 1962	4	729	28						
Apr. 1966	4.3	1,234	49						
Apr. 1967	1.7	1,129	45						
Jan. 1967	1.5	876	34						
Jan. 1967	1.5	716	29						
Nov. 1970	1.75	1,515	47						
Oct. 1979	121	47,148	46						
Jan. 1976	6.25	121	05						
Mar. 1978	2.17	50	02						
Nov. 1979	1.66	76	03						
Oct. 1982	2.92	101	04						
Sept. 1984	1.92	112	05						
Jan. 1982	1.5	112	06						
Sept. 1982	1.67	138	06						
Sept. 1982	9.0	203	09						
May 1966	3.67	125	05						
Oct. 1967	1.41	200	08						
Jan. 1969	1.25	74	03						
Mar. 1969	1.17	42	02						
Nov. 1970	1.66	17,356.3	07						
--- 1985	0	17,356.3							
--- 1987	0	17,398							
Jan. 1981	13	17,190							
Jan. 1990	4.5	47,194							
Sept. 1991	1.7	1,039							
Jan. 1993	3.3	1,053							
Mar. 1998	3.1	969							
Sept. 1993	5.5	953							
Oct. 1994	11.0	951							
Nov. 1961	3.1	880	1.25						
Jan. 1962	3.2	869	1.24						
Aug. 1966	4.7	752	1.14						
Apr. 1967	1.7	692	1.05						
Jan. 1969	1.75	515	.78						
Mar. 1969	1.17	452	.68						
70-23b	San Dimas Wash	211.3							
		2/210.7							
		16.1							
		16.2							
		70-24c	Puddingstone Diversion Dam	19.9					
				10/19.7					
				32.2					
				11/21.0					
				70-25a	Puddingstone Creek	32.2			
						11/21.0			
						4.5			
						4.5			
70-26c	Big Dalton F. C. Basin					4.5			
						4.5			
						4.5			
						4.5			
		4.5							
		4.5							
		4.5							
		4.5							
		4.5							
		4.5							
		4.5							
		4.5							

1/ Based on runoff seasons.  
 2/ Not computed because of record during period.  
 3/ Not operation at various times.  
 4/ Sediment slucied at various times.  
 5/ Equalizing reservoir on Gage Canal System obtaining water from the Santa Ana River.  
 6/ No record of quantities slucied.  
 7/ Includes San Gabriel Dams drainage area 39.2 sq. mi. as sediment is slucied into San Gabriel Dam 1 drainage area.

8/ Storage capacity is regained by sluicing at various times.  
 9/ Includes San Gabriel Dam #1. (Drainage area 203 sq. mi., Sediment slucied into this area.)  
 10/ Includes San Dimas drainage area (16.2 sq. mi.). Sediment slucied into this area.  
 11/ 21.1 sq. mi. controlled by San Dimas, Live Oak Dam, and Puddingstone Diversion Dams.  
 12/ Estimated or assumed.

SUMMARY OF  
RESERVOIR SEDIMENTATION SURVEYS MADE IN THE UNITED STATES THROUGH 1970

DATA SHEET NUMBER	RESERVOIR	STREAM	NEAREST TOWN	DRAINAGE AREA (SQUARE MILES)		DATE OF BETWEEN SURVEY (YEARS)	PERIOD BETWEEN SURVEYS (YEARS)	STORAGE CAPACITY (ACRE-FT.)	CAPACITY SPECIFIC WEIGHT (DRY) (LB. PER CU. FT.)	AVG. ANN. ACCUMULATION PER SQ. MI. OF NET DR. AREA FOR PERIOD SHOWN	AGENCY SUPPLYING DATA
				TOTAL	NET						
70-77c	Big Santa Anita F. C. Basin	Santa Anita Creek	Armadillo, Calif.	10.8	10.8	1923	7.9	171,376	—	3.61	CS
		—	—	—	—	—	—	—	—	—	
		—	—	—	—	—	—	—	—	—	
		—	—	—	—	—	—	—	—	—	
		—	—	—	—	—	—	—	—	—	
		—	—	—	—	—	—	—	—	—	
		—	—	—	—	—	—	—	—	—	
		—	—	—	—	—	—	—	—	—	
		—	—	—	—	—	—	—	—	—	
		—	—	—	—	—	—	—	—	—	
		—	—	—	—	—	—	—	—	—	
		—	—	—	—	—	—	—	—	—	
		—	—	—	—	—	—	—	—	—	
		—	—	—	—	—	—	—	—	—	
		—	—	—	—	—	—	—	—	—	
70-78c	Big Tuljunga F. C. Basin	Big Tuljunga Creek	Sunland, Calif.	82.3	82.2	1931	6.9	176,260	—	2.65	CS
		—	—	—	—	—	—	—	—		
		—	—	—	—	—	—	—	—	—	
		—	—	—	—	—	—	—	—	—	
		—	—	—	—	—	—	—	—	—	
		—	—	—	—	—	—	—	—	—	
		—	—	—	—	—	—	—	—	—	
		—	—	—	—	—	—	—	—	—	
		—	—	—	—	—	—	—	—	—	
		—	—	—	—	—	—	—	—	—	
		—	—	—	—	—	—	—	—	—	
		—	—	—	—	—	—	—	—	—	
		—	—	—	—	—	—	—	—	—	
		—	—	—	—	—	—	—	—	—	
		—	—	—	—	—	—	—	—	—	
70-79b	Devil's Gate F. C. Basin	Arrow Saco River	Pasadena, Calif.	31.9	31.7	1916	13.0	174,601	—	1.11	CS
		—	—	—	—	—	—	—	—		
		—	—	—	—	—	—	—	—	—	
		—	—	—	—	—	—	—	—	—	
		—	—	—	—	—	—	—	—	—	
		—	—	—	—	—	—	—	—	—	
		—	—	—	—	—	—	—	—	—	
		—	—	—	—	—	—	—	—	—	
		—	—	—	—	—	—	—	—	—	
		—	—	—	—	—	—	—	—	—	
		—	—	—	—	—	—	—	—	—	
		—	—	—	—	—	—	—	—	—	
		—	—	—	—	—	—	—	—	—	
		—	—	—	—	—	—	—	—	—	
		—	—	—	—	—	—	—	—	—	
70-90d	Baton (Baton Wash Dam)	Baton Creek	—	9.5	9.4	1926	1.0	179,556	—	1.17	CS
		—	—	—	—	—	—	—	—		
		—	—	—	—	—	—	—	—	—	
		—	—	—	—	—	—	—	—	—	
		—	—	—	—	—	—	—	—	—	
		—	—	—	—	—	—	—	—	—	
		—	—	—	—	—	—	—	—	—	
		—	—	—	—	—	—	—	—	—	
		—	—	—	—	—	—	—	—	—	
		—	—	—	—	—	—	—	—	—	
		—	—	—	—	—	—	—	—	—	
		—	—	—	—	—	—	—	—	—	
		—	—	—	—	—	—	—	—	—	
		—	—	—	—	—	—	—	—	—	
		—	—	—	—	—	—	—	—	—	

70-31c	Picoles F. C. Basin	Picoles Canyon	San Fernando, Calif.	28.2	28.2		1/6,060		
	do	do	do			Oct. 1929	6.3		2.63
	do	do	do			Jan. 1936	5,592		9.47
	do	do	do			Mar. 1942	5,004		1.29
	do	do	do			Apr. 1947	4,771		2.48
	do	do	do			Dec. 1947	4,787		2.97
	do	do	do			Oct. 1954	4,651		6.4
	do	do	do			June 1958	3.9	.83	1.08
	do	do	do			May 1962	4,553	.81	8.40
	do	do	do			Aug. 1966	4,258		8.40
	do	do	do			Mar. 1969	3,811		1.609
	do	do	do			Dec. 1931	25,000		1.619
	do	do	do			Sept. 1938	24,000		1.609
70-32	Santiago	Santiago Creek	Villa Park, Calif.	62.1	62.1	Sept. 1928	14.8		.15
70-33a	Swain F. C. Basin	Swain Creek	Monrovia, Calif.	3.3	3.3	Oct. 1932	6.3		8.18
	do	do	do			May 1938	320		8.03
	do	do	do			May 1941	31.0		2.96
	do	do	do			Dec. 1943	322		3.03
	do	do	do			Mar. 1954	305		.51
	do	do	do			Sept. 1959	5.5		3.03
	do	do	do			May 1962	2.7	.55	1.91
	do	do	do			Aug. 1964	2	.61	5.09
	do	do	do			July 1967	1.9	.28	3.82
	do	do	do			May 1969	2.7	.47	16.39
70-34a	Sierra Madre Debris Dam	Little Santa Anita Creek	Sierra Madre, Calif.	2.39	2.39	Feb. 1930	2.0		.61
	do	do	do			Feb. 1932	2.0		47.4
	do	do	do			Nov. 1939	7.8		34.4
	do	do	do			Jan. 1944	4.1		44.3
	do	do	do			Oct. 1944	8		62.4
	do	do	do			Oct. 1954	12.0		1.00
	do	do	do			Sept. 1969	13.0		2.10
70-35a	Thompson Creek F. C. Basin	Thompson Creek	Claremont, Calif.	3.5	3.5	Sept. 1916	1.0		1.53
	do	do	do			Oct. 1912	5/4.6	3.51	3.26
	do	do	do			Jan. 1943	612	3.11	86
	do	do	do			Sept. 1954	11.7	2.90	1.00
	do	do	do			Jan. 1957	3.3	2.87	.86
	do	do	do			June 1957	1.4	2.89	
	do	do	do			July 1962	2.6	2.91	2.64
	do	do	do			Feb. 1969	4.6	2.71	2.71
70-36a	Wilbur Ave. Debris Basin	Alliso Creek	Northridge, Calif.	8.63	8.63	June 1942	2.0	2.27	8.93
	do	do	do			Sept. 1943	1	1.33	2.37
	do	do	do			Sept. 1944	1	2.72	2.72
	do	do	do			Sept. 1947	3.0		.85
	do	do	do			Sept. 1950	2.0		2.28
	do	do	do			Sept. 1957	5		2.49
	do	do	do			Sept. 1960	3		.60
	do	do	do			Sept. 1962	2		1.29
	do	do	do			Sept. 1965	3		.41
	do	do	do			Sept. 1966	1		3.99
	do	do	do			Sept. 1967	1		2.35
	do	do	do			Sept. 1968	1		2.17
	do	do	do			Sept. 1969	1		2.72
	do	do	do			Sept. 1974	1		4/1.83
	do	do	do			Sept. 1949	1		1.35
	do	do	do			Sept. 1950	1		1.58
	do	do	do			Mar. 1952	1.5		1.75
	do	do	do			Feb. 1956	3.9		1.11
	do	do	do			Sept. 1957	1.6		1.23
	do	do	do			Apr. 1958	1.6		8.97
	do	do	do			Sept. 1959	1.4		2.57

1/ Sediment is removed at various times by sluicing and/or excavation.  
2/ Date normal operation began - Mar. 1927.  
3/ Date normal operation began - June 1927.  
4/ Sedimentation values as computed by Los Angeles County FCD are based on complete water year.  
5/ Storage and surface areas assumed same at time of initial normal operations, Mar. 1928 as in 1916 survey.  
6/ Estimated or assumed.

SUMMARY OF  
RESEK-VIR SEDIMENTATION SURVEYS MADE IN THE UNITED STATES THROUGH 1970

DATA SHEET NUMBER	RESERVOIR	STREAM	NEAREST TOWN	DRAINAGE AREA (SQUARE MILES)		DATE OF SURVEY	PERIOD BETWEEN SURVEYS (YEARS)	STORAGE CAPACITY (ACRE-FT.)	CAPACITY AVG. ANN. INFLOW (ACRE-FT. PER ACRE-FT.)	SPECIFIC WEIGHT (L.B. PER CU. FT.)	AVG. ANN. ACCUMULATION PER SQ. MI. AREA FOR PERIOD SHOWN		AGENCY SUPPLYING DATA
				TOTAL	NET						AC.-FT.	TONS	
70-386	By Day Debris Basin	Ballig Channel	Sierra Madre, Calif.	0.60	0.60	Sept. 1946	1	1/2	---	---	---	370.84	CS
						Sept. 1947	1	---	---	---	---	0	
						Sept. 1948	1	---	---	---	---	0	
						Sept. 1949	1	---	---	---	---	0	
						Sept. 1950	1	---	---	---	---	0	
						Sept. 1952	2	---	---	---	---	.18	
						Sept. 1959	4+8	---	---	---	---	2.08	
						Sept. 1962	2.0	---	---	---	---	8.45	
						Sept. 1964	2.0	---	---	---	---	2.13	
						Sept. 1970	2.0	---	---	---	---	37.58	
						Sept. 1941	5	1.03	---	---	---	0	
						Sept. 1942	1	---	---	---	---	1.06	
70-390	Broad Debris Basin	Broad Canyon Channel	La Canada, Calif.	1.03	1.03	Sept. 1943	1	---	---	---	---	0	CS
						Sept. 1944	1	---	---	---	---	0	
						Sept. 1945	1	---	---	---	---	0	
						Sept. 1947	1	---	---	---	---	0	
						Sept. 1948	1	---	---	---	---	0	
						Sept. 1949	1	---	---	---	---	0	
						Sept. 1950	1	---	---	---	---	1.19	
						Sept. 1952	2	---	---	---	---	1.14	
						Sept. 1954	1	---	---	---	---	2.87	
						Sept. 1956	5	---	---	---	---	27.81	
						Sept. 1970	5	---	---	---	---	37.69	
						70-400	Dunsmuir Debris Basin	Dunsmuir Canyon Channel	Tahoe, Calif.	.64	.64	Sept. 1956	
Sept. 1958	2	---	---	---	---							8.14	
Sept. 1960	2	---	---	---	---							8.74	
Sept. 1961	1	---	---	---	---							10.17	
Sept. 1962	1	---	---	---	---							2.87	
Sept. 1964	1	---	---	---	---							5.6	
Sept. 1965	1	---	---	---	---							3.13	
Sept. 1967	1	---	---	---	---							1.13	
Sept. 1968	1	---	---	---	---							0	
Sept. 1969	1	---	---	---	---							0	
Sept. 1974	2	---	---	---	---							4.07	
Sept. 1979	5	---	---	---	---							3.17	
70-410	Eagle Debris Basin	Eagle Canyon	La Crescenta, Calif.	.61	.61	Sept. 1959	1	---	---	---	---	1.56	CS
						Sept. 1968	2	---	---	---	---	37.12	
						Sept. 1969	1	---	---	---	---	7.00	
						Sept. 1970	11	---	---	---	---	34	
						Sept. 1971	2	---	---	---	---	15.7	
						Sept. 1972	1	---	---	---	---	4.59	
						Sept. 1973	1	---	---	---	---	1.11	
						Sept. 1974	1	---	---	---	---	.19	
						Sept. 1977	1	---	---	---	---	.07	
						Sept. 1989	1	---	---	---	---	0	
						Sept. 1990	1	---	---	---	---	2.66	
						Sept. 1992	2	---	---	---	---	1.02	
70-420	Fair Oaks Debris Basin	Fair Oaks Canyon	Altadena, Calif.	.21	.21	Aug. 1956	3.9	---	---	---	---	2.05	CS
						Sept. 1960	4.1	---	---	---	---	5.28	
						Sept. 1961	1	---	---	---	---	5.87	
						Sept. 1970	4	---	---	---	---	37.64	
						Sept. 1976	1	---	---	---	---	47.6	
						Sept. 1978	2	---	---	---	---	3.9	
						Sept. 1981	3	---	---	---	---	4.2	
						Sept. 1983	2	---	---	---	---	1.71	
						Sept. 1985	1	---	---	---	---	2.06	
						Sept. 1986	1	---	---	---	---	1.95	
						Sept. 1987	1	---	---	---	---	---	

Station	Basin	Location	Date	Capacity (cu ft)	Settlement	Remarks
70-43b	Fern Debris Basin	Fern Canyon	Sept. 1948	1		
			Sept. 1949	1		
			Sept. 1950	0		
			Sept. 1952	2		4.57
			Sept. 1954	4.1		18.05
			Sept. 1958	1.7		4.76
			Sept. 1963	5.2		10.14
			Sept. 1966	3		3.10
			Sept. 1968	2		46.9
			Sept. 1969	1		2/21.2
			Sept. 1976	2	1/	41.3
			Sept. 1978	2		3.30
			Sept. 1981	1		22.0
			Sept. 1983	1		6.17
			Sept. 1984	1		3.07
			Sept. 1985	1		2.77
			Sept. 1987	1		.43
			Sept. 1988	1		0
			Sept. 1989	1		0
			Sept. 1990	1		1.47
			Sept. 1991	1		1.23
70-44c	Gould Debris Basin	Gould Canyon Channel	Sept. 1964	12		16.67
			Sept. 1966	2		11.5
			Sept. 1968	2		24.6
			Sept. 1969	1		2/0
			Sept. 1968	1	1/	0
			Sept. 1972	2		5.32
			June 1975	5.2		3.67
			Sept. 1978	4		9.04
			Sept. 1986	4.0		1.88
			Sept. 1988	2		28.7
			Sept. 1989	1		2/6.99
			70-45a	Haines Debris Basin	Tujunga, Calif.	Sept. 1948
Sept. 1949	2					5.09
Sept. 1941	1					4.22
Sept. 1943	2					2.82
Sept. 1944	1					0
Sept. 1945	1					0
Sept. 1946	1					0
Sept. 1947	1					0
Sept. 1948	1					0
Sept. 1949	1					0
Sept. 1950	1					1.57
May 1952	1.6					2/17.2
70-46c	Hall's Debris Basin	Hall - Beckley Canyon	Sept. 1936	1		31.7
			Sept. 1937	1		7.1
			Sept. 1941	1		12.0
			Sept. 1943	2		17.9
			Sept. 1944	1		6.10
			Sept. 1945	1		2.97
			Sept. 1946	1		1.00
			Sept. 1947	1		2.60
			Sept. 1948	1		---
			Sept. 1950	1		---
			Sept. 1952	2		6.40
			Feb. 1957	4.4		11.03
Sept. 1959	2.6		1.063			
Sept. 1962	3		4.48			
Sept. 1964	2		3.43			
Sept. 1968	4		34.4			
Sept. 1969	1		---			

1/ Capacity of debris basin varies. Debris presented at various times.  
2/ Settlement values as computed by L2750 are based on complete water year.

3/ Drainage area 0.84 sq. mi. to 1945; 1.0659 sq. mi. beginning 1945.

SUMMARY OF  
RESERVOIR SEDIMENTATION SURVEYS MADE IN THE UNITED STATES THROUGH 1970

DATA SHEET NUMBER	RESERVOIR	STREAM	NEAREST TOWN	DRAINAGE AREA (SQ. MILES)		DATE OF SURVEY	PERIOD BETWEEN SURVEYS (YEARS)	STORAGE CAPACITY (ACRE-FT.)	CAPACITY AVERAGE ENFLOW RATIO (ACRE-FT. PER ACRE-FT.)	SPECIFIC WEIGHT (LB. PER CU. FT.)	AVG. ANNUAL ACCUMULATION PER SQ. MI. OF NET DR. AREA FOR PERIOD SHOWN		AGENCY SUPPLYING DATA							
				TOTAL	NET						AC. FT.	TONS								
70-47e	Hay Debris Basin	Hay Canyon Channel	La Canada, Calif.	0.20	0.20	Sept. 1979	2	1/1	---	---	---	2/28.3	CS							
						Sept. 1980	1	---	---	6.30										
						Sept. 1981	1	---	---	1.55										
						Sept. 1982	1	---	---	1.90										
						Sept. 1983	1	---	---	4.75										
						Sept. 1984	1	---	---	1.65										
						Sept. 1985	1	---	---	1.55										
						Sept. 1986	1	---	---	0										
						Sept. 1987	1	---	---	0										
						Sept. 1988	1	---	---	0										
						Sept. 1989	1	---	---	0										
						Sept. 1990	1	---	---	0										
						Sept. 1991	1	---	---	2.30										
						Sept. 1992	2	---	---	3.58										
						Sept. 1993	9	---	---	5.95										
						Sept. 1994	3	---	---	3.25										
						Sept. 1995	4	---	---	11.5										
						Sept. 1996	2	---	---	2/14.7										
						Sept. 1997	1	---	---	3.15										
						70-48e	Las Flores Debris Basin	Las Flores Channel	Alhambra, Calif.	.45	.45	Sept. 1979		1	1/1	---	---	---	---	CS
Sept. 1980	1	---	---	1.15																
Sept. 1981	1	---	---	1.10																
Sept. 1982	1	---	---	1.40																
Sept. 1983	1	---	---	3.71																
Sept. 1984	1	---	---	1.51																
Sept. 1985	1	---	---	1.57																
Sept. 1986	1	---	---	1.57																
Sept. 1987	1	---	---	0																
Sept. 1988	1	---	---	0																
Sept. 1989	1	---	---	0																
Sept. 1990	1	---	---	0																
Sept. 1991	1	---	---	1.27																
Sept. 1992	2	---	---	4.00																
Sept. 1993	3	---	---	2.48																
Sept. 1994	7	---	---	13.18																
Sept. 1995	1	---	---	270.96																
Sept. 1996	1	---	---	17.8																
Sept. 1997	2	---	---	1.51																
70-49d	Lincoln Debris Basin	Lincoln Canyon	---	.70	.70							Sept. 1980	2	1/1	---	---	---	---	CS	
						Sept. 1981	1	---	---	6.48										
						Sept. 1982	2	---	---	2.32										
						Sept. 1983	1	---	---	1.98										
						Sept. 1984	1	---	---	0										
						Sept. 1985	1	---	---	0										
						Sept. 1986	1	---	---	0										
						Sept. 1987	1	---	---	0										
						Sept. 1988	1	---	---	0										
						Sept. 1989	1	---	---	0										
						Sept. 1990	1	---	---	0										
						Sept. 1991	1	---	---	0										
						Sept. 1992	1	---	---	1.82										
						Sept. 1993	1	---	---	1.10										
						Sept. 1994	1	---	---	3.34										
						Sept. 1995	2	---	---	14.20										
						70-50e	Nichols Debris Basin	Nichols Canyon	Hollywood, Calif.	.54	.54	Sept. 1982	5	1/1	---	---	---	---		CS
												Sept. 1983	1	---	---	1.98				
												Sept. 1984	1	---	---	4.48				
												Sept. 1985	1	---	---	2.80				
Sept. 1986	1	---	---	1.15																
Sept. 1987	1	---	---	3.72																
Sept. 1988	1	---	---	1.29																
Sept. 1989	1	---	---	1.80																
Sept. 1990	1	---	---	1.80																
Apr. 1992	1	---	---	5.82																
Feb. 1996	3.6	---	---	1.47																
Sept. 1999	3.6	---	---	1.59																
Sept. 1980	1	---	---	1.08																
Sept. 1986	2	---	---	2.15																
Sept. 1970	2	---	---	2.77																



Station	Basin	Location	Capacity (%)	Excavation (%)	Year	Capacity (%)	Excavation (%)
70-52b	Paradise Debris Basin	La Canada, Calif.	.96	.96	Sept. 1965	1	1
	-do-	-do-			Sept. 1966	1	1
	-do-	-do-			Sept. 1967	1	1
	-do-	-do-			Sept. 1968	1	1
	-do-	-do-			Sept. 1969	1	1
	-do-	-do-			Sept. 1970	1	1
	-do-	-do-			Sept. 1971	1	1
	-do-	-do-			Sept. 1972	1	1
	-do-	-do-			Sept. 1973	1	1
	-do-	-do-			Sept. 1974	1	1
70-52c	Pickens Debris Basin	La Crescenta, Calif.	.58	.58	Apr. 1952	1.4	1.4
	-do-	-do-			Mar. 1956	3.9	3.9
	-do-	-do-			Sept. 1936	1	1
	-do-	-do-			Sept. 1937	1	1
	-do-	-do-			Sept. 1938	1	1
	-do-	-do-			Sept. 1939	1	1
	-do-	-do-			Sept. 1940	1	1
	-do-	-do-			Sept. 1941	1	1
	-do-	-do-			Sept. 1943	2	2
	-do-	-do-			Sept. 1944	1	1
70-53c	Rubio Debris Dam	Altadena, Calif.	1.3	1.3	Sept. 1945	1	1
	-do-	-do-			Sept. 1946	3	3
	-do-	-do-			Sept. 1947	1	1
	-do-	-do-			Sept. 1948	1	1
	-do-	-do-			Sept. 1949	1	1
	-do-	-do-			Sept. 1950	1	1
	-do-	-do-			Sept. 1951	1	1
	-do-	-do-			Sept. 1952	2	2
	-do-	-do-			Apr. 1957	4.7	4.7
	-do-	-do-			Sept. 1966	9.4	9.4
70-54b	Scholl Debris Basin	Glendale, Calif.	.66	.66	Sept. 1969	3	3
	-do-	-do-			Sept. 1970	4	4
	-do-	-do-			Sept. 1971	1	1
	-do-	-do-			Sept. 1972	1	1
	-do-	-do-			Sept. 1973	1	1
	-do-	-do-			Sept. 1974	1	1
	-do-	-do-			Sept. 1975	1	1
	-do-	-do-			Sept. 1976	1	1
	-do-	-do-			Sept. 1977	1	1
	-do-	-do-			Sept. 1978	1	1
70-55a	Shields Debris Basin	La Crescenta, Calif.	.27	.27	Sept. 1978	1	1
	-do-	-do-			Sept. 1979	1	1
	-do-	-do-			Sept. 1980	1	1
	-do-	-do-			Sept. 1981	9	9
	-do-	-do-			Sept. 1982	9	9
	-do-	-do-			Sept. 1983	1	1
	-do-	-do-			Sept. 1984	1	1
	-do-	-do-			Sept. 1985	1	1
	-do-	-do-			Sept. 1986	1	1
	-do-	-do-			Sept. 1987	1	1
70-56c	Shover Debris Basin	Shover Canyon	.23	.23	Sept. 1978	2	2
	-do-	-do-			Sept. 1979	1	1
	-do-	-do-			Sept. 1980	1	1
	-do-	-do-			Sept. 1981	2	2
	-do-	-do-			Sept. 1982	2	2
	-do-	-do-			Sept. 1983	2	2
	-do-	-do-			Sept. 1984	2	2
	-do-	-do-			Sept. 1985	2	2
	-do-	-do-			Sept. 1986	5	5
	-do-	-do-			Sept. 1987	5	5
70-57b	Spart Debris Basin	Monterey, Calif.	.84	.84	Sept. 1967	1	1
	-do-	-do-			Sept. 1968	1	1
	-do-	-do-			Sept. 1969	1	1
	-do-	-do-			Sept. 1970	1	1
	-do-	-do-			Sept. 1971	1.5	1.5
	-do-	-do-			Sept. 1972	1.5	1.5
	-do-	-do-			Sept. 1973	9.5	9.5
	-do-	-do-			Sept. 1974	1	1
	-do-	-do-			Sept. 1975	1	1
	-do-	-do-			Sept. 1976	1	1
70-58b	Stough Debris Basin	Burbank, Calif.	1.65	1.65	Sept. 1943	3	3
	-do-	-do-			Sept. 1944	1	1
	-do-	-do-			Sept. 1945	1	1
	-do-	-do-			Sept. 1946	1	1
	-do-	-do-			Sept. 1947	1	1
	-do-	-do-			Sept. 1948	1	1
	-do-	-do-			Sept. 1949	1	1
	-do-	-do-			Sept. 1950	1	1
	-do-	-do-			Sept. 1951	1	1
	-do-	-do-			Sept. 1952	1	1

1/ Capacity of debris basin varies. Debris excavated at various times. 2/ Sedimentation values as computed by LACFD are based on complete water year.

SUMMARY OF  
RESERVOIR SEDIMENTATION SURVEYS MADE IN THE UNITED STATES THROUGH 1970

DATA SHEET NUMBER	RESERVOIR	STREAM	NEAREST TOWN	DRAINAGE AREA (SQUARE MILES)		DATE OF BETWEEN SURVEY SURVEYS (YEARS)	STORAGE CAPACITY (ACRE-FT.)	CAPACITY AVERAGE INFLOW RATIO (PER ACRE-FT.)	SPECIFIC WEIGHT (LB. PER CU. FT.)	AVERAGE ANNUAL ACCUMULATION PER SQ. MI. OF NET DR. AREA FOR PERIOD SHOWN		AGENCY SUPPLYING DATA
				TOTAL	NET					AC.-FT.	TONS	
70-59b	Sweet Canyon Debris Dam (upper)	Sweet Canyon Channel	Burbank, Calif.	0.44	0.44	Sept. 1942 13	1/1	--	--	2/1.34	--	CS
	do	do	do	--	--	Sept. 1944 2	--	--	--	.84	--	--
	do	do	do	--	--	Sept. 1945 1	--	--	--	.18	--	--
	do	do	do	--	--	Sept. 1946 1	--	--	--	.20	--	--
	do	do	do	--	--	Sept. 1949 4	--	--	--	0	--	--
	do	do	do	--	--	Sept. 1952 2	--	--	--	2.41	--	--
	do	do	do	--	--	Sept. 1959 7	--	--	--	1.68	--	--
	do	do	do	--	--	Sept. 1966 7	--	--	--	7.80	--	--
	do	do	do	--	--	Sept. 1969 3	1/1	--	--	4.20	--	--
	do	do	do	--	--	Sept. 1970 1	--	--	--	2/1.02	--	CS
70-60	Vanalden Debris Basin	Vanalden Channel	Brea, Calif.	1.08	1.08	Sept. 1947 1	--	--	--	--	--	CS
	do	do	do	--	--	Sept. 1948 3	--	--	--	--	--	CS
	do	do	do	15.5	10.0	Sept. 1949 3	1/1	--	--	2/1.83	--	CS
	do	do	do	--	--	Sept. 1943 2	--	--	--	.81	--	--
	do	do	do	--	--	Sept. 1943 2	--	--	--	2.09	--	--
	do	do	do	--	--	Sept. 1944 1	--	--	--	4.27	--	--
	do	do	do	--	--	Sept. 1943 1	--	--	--	.68	--	--
	do	do	do	--	--	Sept. 1943 1	--	--	--	3.71	--	--
	do	do	do	--	--	Sept. 1943 1	--	--	--	0.02	--	--
	do	do	do	--	--	May 1956 2.67	--	--	--	.89	--	--
70-61a	Verdugo Debris Basin	Verdugo Wash	Monrovia, Calif.	--	--	Jan. 1959 2.67	--	--	--	.05	--	--
	do	do	do	--	--	Sept. 1960 1.66	--	--	--	.51	--	--
	do	do	do	--	--	Sept. 1964 4	--	--	--	1.71	--	--
	do	do	do	--	--	Sept. 1966 2	--	--	--	3.11	--	--
	do	do	do	--	--	Sept. 1968 2	--	--	--	3.11	--	--
	do	do	do	--	--	Sept. 1968 2	--	--	--	3.11	--	--
	do	do	do	--	--	Sept. 1968 2	--	--	--	3.11	--	--
	do	do	do	--	--	Sept. 1968 2	1/1	--	--	2/1.63	--	CS
	do	do	do	--	--	Sept. 1967 1	--	--	--	4.86	--	--
	do	do	do	--	--	Sept. 1967 1	--	--	--	1.00	--	--
70-62b	West Debris Basin (lower)	West Canyon	La Graciosa, Calif.	3/1.64	3/1.64	Sept. 1947 1	--	--	--	1.11	--	--
	do	do	do	--	--	Sept. 1948 1	--	--	--	.36	--	--
	do	do	do	--	--	Sept. 1949 1	--	--	--	1.11	--	--
	do	do	do	--	--	Apr. 1952 1.3	--	--	--	6.14	--	--
	do	do	do	--	--	Sept. 1956 4.4	--	--	--	.52	--	--
	do	do	do	--	--	Sept. 1956 2.0	1/1	--	--	2/47.85	--	CS
	do	do	do	--	--	Sept. 1956 1	--	--	--	45.42	--	--
	do	do	do	--	--	Sept. 1957 1	--	--	--	71.05	--	--
	do	do	do	--	--	Sept. 1958 2	--	--	--	2.80	--	--
	do	do	do	--	--	Sept. 1960 1	--	--	--	21.44	--	--
70-63b	West Ravine Debris Basin	West Ravine Canyon	Alladene, Calif.	.25	.25	Sept. 1954 2.0	1/1	--	--	.70	--	--
	do	do	do	--	--	Sept. 1956 1	--	--	--	2/47.85	--	CS
	do	do	do	--	--	Sept. 1957 1	--	--	--	45.42	--	--
	do	do	do	--	--	Sept. 1958 2	--	--	--	71.05	--	--
	do	do	do	--	--	Sept. 1960 1	--	--	--	21.44	--	--
	do	do	do	--	--	Sept. 1962 1	--	--	--	20.20	--	--
	do	do	do	--	--	Sept. 1963 1	--	--	--	6.00	--	--
	do	do	do	--	--	Sept. 1964 1	--	--	--	.80	--	--
	do	do	do	--	--	Sept. 1965 1	--	--	--	1.56	--	--
	do	do	do	--	--	Sept. 1967 1	--	--	--	1.22	--	--
70-64	Dear Creek	Dear Creek	Julian, Calif.	1.6	1.59	Sept. 1948 1	--	--	--	0	--	--
	do	do	do	--	--	Sept. 1949 1	--	--	--	0	--	--
	do	do	do	--	--	Sept. 1950 1	--	--	--	0	--	--
	do	do	do	--	--	Sept. 1952 2	--	--	--	4.76	--	--
	do	do	do	--	--	Sept. 1954 4	--	--	--	1.08	--	--
	do	do	do	--	--	Sept. 1956 8	--	--	--	6.47	--	--
	do	do	do	--	--	Sept. 1958 4	--	--	--	43.2	--	--
	do	do	do	--	--	Sept. 1969 1	14.1	--	--	.11	--	SS
	do	do	do	--	--	Sept. 1970 2	1/1	--	--	2/26.9	--	CS
	do	do	do	--	--	Mar. 1952 8	--	--	--	3/280	--	CS
70-65b	Cook's Canyon	Cook's Canyon	La Graciosa, Calif.	.58	.58	Sept. 1963 9.5	--	--	--	.08	--	--
	do	do	do	--	--	Sept. 1969 8	--	--	--	.08	--	--
	do	do	do	--	--	Dec. 1974 4.8	1/1	--	--	2.6	--	CS
	do	do	do	--	--	Sept. 1959 4.8	1/1	--	--	2.6	--	CS
	do	do	do	--	--	Jan. 1955 4.67	1/1	--	--	2/48.15	--	CS
	do	do	do	--	--	Sept. 1957 2.0	--	--	--	1.42	--	--
	do	do	do	--	--	Sept. 1964 5	--	--	--	6.65	--	--
	do	do	do	--	--	Sept. 1964 5	--	--	--	23.5	--	--
	do	do	do	--	--	Sept. 1969 3	--	--	--		--	--
	do	do	do	--	--	Sept. 1969 3	--	--	--		--	--

Station	Basin	Location	Capacity (cu ft)	Excavated	Notes	Drainage Area (sq. mi.)	Notes	Excavated	Notes
70-66a	Carter Debris Basin	Carter Canyon	0	0	Sierra Madre, Calif.	.12	12	Dec. 1954	2/2.8
			0	0				Sept. 1959	4.8
			0	0				Sept. 1962	21.7
70-66b	Deer Debris Basin	Deer Canyon	0	0	Glendale, Calif.	.59	59	Jan. 1955	4.06
			0	0				Sept. 1959	4.63
			0	0				Sept. 1964	2/55
			0	0				Sept. 1965	2.20
			0	0				Sept. 1966	2/74
			0	0				Sept. 1967	2/19
			0	0				Sept. 1968	19.0
70-70	Floral (Upper) Debris Basin	Floral Canyon	0	0	Sierra Madre, Calif.	.06	6	Sept. 1954	2.4
			0	0				Sept. 1959	5.6
70-71	La Tuna Debris Basin	La Tuna Canyon	0	0	Los Angeles, Calif.	5.34	534	Jan. 1954	2/04
			0	0				July 1957	1.4
			0	0				Sept. 1958	1.2
			0	0				Sept. 1959	1.0
			0	0				Sept. 1960	2.33
			0	0				Sept. 1961	1.0
70-72a	Lanman Debris Basin	Lanman Wash	0	0	Sierra Madre, Calif.	.25	25	Mar. 1954	2/5.44
			0	0				Sept. 1959	5.6
			0	0				Sept. 1962	11.3
			0	0				Sept. 1967	4.8
			0	0				Sept. 1968	20.4
70-73b	Nadbrook Debris Basin	Nadbrook Canyon	0	0	Duarte, Calif.	.25	25	Sept. 1950	2/17.8
			0	0				Mar. 1955	1.2
			0	0				Mar. 1956	3.5
			0	0				Sept. 1959	1.8
			0	0				Sept. 1960	15.8
			0	0				Sept. 1961	2
			0	0				Sept. 1962	2.96
70-74a	Ray No. 1 Debris Basin	Ray Canyon	0	0	San Fernando, Calif.	.70	70	Sept. 1970	2/78
			0	0				Aug. 1953	7.20
			0	0				Sept. 1959	8
			0	0				Sept. 1968	1
			0	0				Sept. 1969	104.0
70-75a	Ray No. 2 Debris Basin	Ray Canyon	0	0	Duarte, Calif.	.09	9	Sept. 1959	2/36
			0	0				Sept. 1965	1.9
			0	0				Sept. 1967	4.5
			0	0				Sept. 1968	28.9
70-76a	McClure Debris Basin	McClure Canyon	0	0	Burbank, Calif.	.62	62	Sept. 1953	2/5.6
			0	0				Sept. 1959	5.8
			0	0				Sept. 1961	2.0
			0	0				Sept. 1965	9.27
			0	0				Sept. 1966	2.0
			0	0				Sept. 1966	4
			0	0				Sept. 1966	10.0
			0	0				Sept. 1967	9.52
70-77	Rendley Debris Basin	Rendley Canyon	0	0	Tulare, Calif.	.58	58	Jan. 1954	2/62
			0	0				Sept. 1959	3.67
			0	0				Sept. 1968	1.5
			0	0				Sept. 1968	11.8
70-78	Baby - Upper Debris Basin	Baby Canyon	0	0	Sierra Madre, Calif.	.21	21	Jan. 1954	2/5.2
			0	0				Sept. 1959	5.8
			0	0				Sept. 1961	2.0
70-79a	Baby - Lower Debris Basin	Baby Canyon	0	0	Sierra Madre, Calif.	.10	10	Dec. 1955	2/2.9
			0	0				Sept. 1959	3.8
			0	0				Sept. 1962	1.0
			0	0				Sept. 1969	12.8
70-80a	Sandpit Debris Dam	Sandpit Creek	0	0	Murveria, Calif.	6.34	634	Jan. 1955	2/4.6
			0	0				Sept. 1959	6.9
			0	0				Sept. 1962	9.82
70-81a	Sierra Madre Villa Debris Basin	Sierra Madre Villa Canyon	0	0	Sierra Madre, Calif.	1.46	146	May 1958	2/34
			0	0				Sept. 1959	16.92
			0	0				Sept. 1968	1.8
70-82a	Splains Debris Basin	Splains Canyon	0	0	Murveria, Calif.	.44	44	Sept. 1970	45.89
			0	0				Dec. 1958	2
			0	0				Sept. 1959	.8
			0	0				Sept. 1962	3
70-83a	Turnball Debris Basin	Turnball Canyon Wash	0	0	Whittier, Calif.	.99	99	Jan. 1953	1.66
			0	0				Sept. 1959	5.32
			0	0				Sept. 1968	6.8
			0	0				Sept. 1968	9
70-84a	Zachau Debris Basin	Zachau Canyon	0	0	Tulare, Calif.	.35	35	Jan. 1956	2/28
			0	0				Sept. 1959	1.33
			0	0				Sept. 1961	10.0
			0	0				Sept. 1961	2/80
			0	0				Sept. 1969	2.37

1/ Capacity of debris basin varies. Debris excavated at various times.  
2/ Sedimentation values computed by Los Angeles County. CE are based on complete water year.  
3/ Drainage area 0.75 sq. mi. through 1947; 0.54 after 1947.  
4/ Estimated or assumed.

SUMMARY OF  
RESERVOIR SEDIMENTATION SURVEYS MADE IN THE UNITED STATES THROUGH 1970

DATA SHEET NUMBER	RESERVOIR	STREAM	NEAREST TOWN	DRAINAGE AREA (SQUARE MILES)		DATE OF BETWEEN SURVEY (YEARS)	STORAGE CAPACITY (ACRE-FT.)	CAPACITY INFLON RATIO (ACRE-FT. PER PERIOD SURVEY)	SPECIFIC WEIGHT (DRY) (L.B. PER CU. FT.)	AVG. ANN. ACCUMULATION PER SQ. MI. OF NET DR. AREA FOR PERIOD SURVEY	AGENCY SUPPLYING DATA
				TOTAL	NET						
70-84a	Hard Debris Basin (Upper)	Hard Canyon	La Graciana, Calif.	0.10	0.10	Nov. 1956	1/2	1.00	276.1	C	
						Sept. 1957			39.3		
						Sept. 1958			17.5		
						Sept. 1959			4		
						Sept. 1967			2.1		
						Sept. 1968			2.9		
70-85	Sepulveda Flood Control Basin	Los Angeles River	Van Nuys, Calif.	132	142	Nov. 1941	16,720	1.00		C	
						Nov. 1944	17,120	1.04			
						Nov. 1945	17,250	1.05			
70-87a	Santa Fe Flood Control Basin	San Gabriel River	Baldwin Park, Calif.	236.0	3/20.54	June 1943	34,670		2.91	C	
						Nov. 1949	34,276		1.51		
						Mar. 1959	33,987		13.32		
						June 1961	33,385		5.72		
						Feb. 1967	32,716				
						Sept. 1968	3/34,916				
70-88a	Ball IV (ORCA)	Ball Creek	Glendora, Calif.	.061	.061	Aug. 1969	32,642	.234	123.0	P	
						Jan. 1966	2,30		1.16		
						Dec. 1966			39.6		
						Oct. 1968			.048		
						Mar. 1969					
						July 1970					
70-89	Ball Debris Basin		Garage Park, Calif.	7.0	7.0	Sept. 1970	1/2		2/7.71	C	
70-90	Carbon Canyon F. C. Basin	Carbon Canyon Creek	Brea, Calif.	19.3	19.3	Sept. 1964	7,093	10.0	2.54	C	
70-91	Chilids Debris Basin	Chilids Canyon	Glendale, Calif.	.31	.31	Sept. 1963	6,615	9.45	2/6.81	C	
70-92	Elmwood Debris Basin	Elmwood Canyon	Burbank, Calif.	.31	.31	Sept. 1966	1/2		2/7.90	C	
70-93	Englewood Debris Basin	Englewood Canyon	Glendora, Calif.	.4	.4	Sept. 1968	1/2		2/10.4	C	
70-94	Farrow Debris Basin	Farrow Canyon	Glendora, Calif.	.43	.43	Sept. 1969	1/2		13.5	C	
70-95	Hook East Debris Basin	Hook Canyon	Arroyo, Calif.	.18	.18	Sept. 1969	1/2		16.3	C	
70-96	Kinnelon Debris Basin	Kinnelon Canyon	Arroyo, Calif.	.20	.20	Sept. 1969	1/2		2/6.7	C	
70-97	Kinnelon - West Debris Basin	Kinnelon Canyon	Arroyo, Calif.	.16	.16	Sept. 1966	1/2		2/10.90	C	
70-98	Little Dalton Debris Basin	Little Dalton	Glendora, Calif.	3.3	3.3	Sept. 1969	1/2		21.65	C	
70-99	Morgan Debris Basin	Morgan Canyon	Arroyo, Calif.	.6	.6	Sept. 1969	1/2		13.4	C	
70-100	San Antonio F. C. Basin	San Antonio Creek	Claremont, Calif.	26.7	26.7	Sept. 1966	1.92		2/2.95	C	
70-101	San Jose Debris Basin	San Jose Canyon	Glendora, Calif.	.28	.28	Sept. 1966	1/2		7.45	C	
70-102	San Jose Debris Basin (Lower)	San Jose Canyon	Glendora, Calif.	.65	.65	Sept. 1966	1/2		2/11.1	C	
70-103	Santa Anita Debris Basin	Santa Anita Creek	Arroyo, Calif.	1.7	1.7	Sept. 1967	1/2		2/5.58	C	
70-104	Wilson Debris Basin	Wilson Canyon	Arroyo, Calif.	2.58	2.58	Sept. 1968	1/2		2/11.1	C	
						June 1969			30.0		
						Sept. 1967			2/11.23		

70-105	70-106	71-1	71-2	71-3	71-4a	71-5	71-6	71-7	71-8	71-9	71-10	71-11	71-12	71-13	71-14	71-15	71-16	71-17	71-18a	71-19	71-20	71-21	71-22	71-23	71-24a	71-25	71-26	71-27a	71-28a	71-29a	71-30
Wildwood Debris Basin	Winery Debris Basin	Upper Crystal Springs	Atascadero Park Lake	Hawkins	Salinas	Copperopolis	Crows Valley	Jarvis	Don Pedro	Bonhoefer	Glimore	Humboldt	La Grange	Lyonne	McCarthy	Pardee	Salt Springs Valley	Upper Bear River	Woods Pond	St. Mary's	Black Hills	Lakewood	Contra Costa Country Club	Burdett Pond	C. C. Anderson Pond	Upper Walker Keller Pond	F. J. Healy Pond	Low Higgins Pond	Sonsa	Crowley	North Fork
Midwood Creek	Winery Canyon	Laguna Creek	Atascadero Creek	R. Ft. Los Viboras Creek	Salinas River	Penny Creek	R. Ft. San Joaquin River	Shaw Creek	Tuolumne River	Merced River	Trib. of Norman Slough	Tim Rile Creek	Tuolumne River	S. Ft. Stanislaus River	Trib. of Johnny Creek	Hokulume River	Rock Creek	Bear River	Sycamore Creek	Walnut Creek	Green Valley Creek	Walnut Creek	Orayson Creek	North Creek			Alhambra Creek	North Creek			
Marshall, Calif.	La Crescenta, Calif.	San Francisco, Calif.	Atascadero, Calif.	Hollister, Calif.	Santa Margarita, Calif.	Copperopolis, Calif.	Madras, Calif.	Stockton, Calif.	Hollister, Calif.	Merced, Calif.	Bellota, Calif.	Fresno, Calif.	Hollister, Calif.	Tuolumne, Calif.	San Andreas, Calif.	Lodi, Calif.	San Andreas, Calif.	Pleasantville, Calif.	Danville, Calif.	Walnut Creek, Calif.	Danville, Calif.	Concord, Calif.	Fishers, Calif.	Brentwood, Calif.						Hollister, Calif.	
		13.3	1.0	4.04	111	2.06	14.5	7.87	1.001	1.027	5.01	24.2	1.501	6/40.0	.35	2/387	20.3	28.5	.30	3.11	.76	.75	.20	.033	.083	.027	.045	.202	.319	.619	66.2
		12.0	1.0	4.01	110	2.01	52.7	7.62	986.5	1,022.4	4.32	24.1	5/1.501	39.7	.32	383.5	18.4	28.2	.30	2.97	.76	.74	.20	.033	.083	.027	.045	.199	.267	.613	66.0
		12.0	1.0	4.01	110	2.01	52.7	7.62	986.5	1,022.4	4.32	24.1	5/1.501	39.7	.32	383.5	18.4	28.2	.30	2.97	.76	.74	.20	.033	.083	.027	.045	.199	.267	.613	66.0
		12.0	1.0	4.01	110	2.01	52.7	7.62	986.5	1,022.4	4.32	24.1	5/1.501	39.7	.32	383.5	18.4	28.2	.30	2.97	.76	.74	.20	.033	.083	.027	.045	.199	.267	.613	66.0
		12.0	1.0	4.01	110	2.01	52.7	7.62	986.5	1,022.4	4.32	24.1	5/1.501	39.7	.32	383.5	18.4	28.2	.30	2.97	.76	.74	.20	.033	.083	.027	.045	.199	.267	.613	66.0
		12.0	1.0	4.01	110	2.01	52.7	7.62	986.5	1,022.4	4.32	24.1	5/1.501	39.7	.32	383.5	18.4	28.2	.30	2.97	.76	.74	.20	.033	.083	.027	.045	.199	.267	.613	66.0
		12.0	1.0	4.01	110	2.01	52.7	7.62	986.5	1,022.4	4.32	24.1	5/1.501	39.7	.32	383.5	18.4	28.2	.30	2.97	.76	.74	.20	.033	.083	.027	.045	.199	.267	.613	66.0
		12.0	1.0	4.01	110	2.01	52.7	7.62	986.5	1,022.4	4.32	24.1	5/1.501	39.7	.32	383.5	18.4	28.2	.30	2.97	.76	.74	.20	.033	.083	.027	.045	.199	.267	.613	66.0
		12.0	1.0	4.01	110	2.01	52.7	7.62	986.5	1,022.4	4.32	24.1	5/1.501	39.7	.32	383.5	18.4	28.2	.30	2.97	.76	.74	.20	.033	.083	.027	.045	.199	.267	.613	66.0
		12.0	1.0	4.01	110	2.01	52.7	7.62	986.5	1,022.4	4.32	24.1	5/1.501	39.7	.32	383.5	18.4	28.2	.30	2.97	.76	.74	.20	.033	.083	.027	.045	.199	.267	.613	66.0
		12.0	1.0	4.01	110	2.01	52.7	7.62	986.5	1,022.4	4.32	24.1	5/1.501	39.7	.32	383.5	18.4	28.2	.30	2.97	.76	.74	.20	.033	.083	.027	.045	.199	.267	.613	66.0
		12.0	1.0	4.01	110	2.01	52.7	7.62	986.5	1,022.4	4.32	24.1	5/1.501	39.7	.32	383.5	18.4	28.2	.30	2.97	.76	.74	.20	.033	.083	.027	.045	.199	.267	.613	66.0
		12.0	1.0	4.01	110	2.01	52.7	7.62	986.5	1,022.4	4.32	24.1	5/1.501	39.7	.32	383.5	18.4	28.2	.30	2.97	.76	.74	.20	.033	.083	.027	.045	.199	.267	.613	66.0
		12.0	1.0	4.01	110	2.01	52.7	7.62	986.5	1,022.4	4.32	24.1	5/1.501	39.7	.32	383.5	18.4	28.2	.30	2.97	.76	.74	.20	.033	.083	.027	.045	.199	.267	.613	66.0
		12.0	1.0	4.01	110	2.01	52.7	7.62	986.5	1,022.4	4.32	24.1	5/1.501	39.7	.32	383.5	18.4	28.2	.30	2.97	.76	.74	.20	.033	.083	.027	.045	.199	.267	.613	66.0
		12.0	1.0	4.01	110	2.01	52.7	7.62	986.5	1,022.4	4.32	24.1	5/1.501	39.7	.32	383.5	18.4	28.2	.30	2.97	.76	.74	.20	.033	.083	.027	.045	.199	.267	.613	66.0
		12.0	1.0	4.01	110	2.01	52.7	7.62	986.5	1,022.4	4.32	24.1	5/1.501	39.7	.32	383.5	18.4	28.2	.30	2.97	.76	.74	.20	.033	.083	.027	.045	.199	.267	.613	66.0
		12.0	1.0	4.01	110	2.01	52.7	7.62	986.5	1,022.4	4.32	24.1	5/1.501	39.7	.32	383.5	18.4	28.2	.30	2.97	.76	.74	.20	.033	.083	.027	.045	.199	.267	.613	66.0
		12.0	1.0	4.01	110	2.01	52.7	7.62	986.5	1,022.4	4.32	24.1	5/1.501	39.7	.32	383.5	18.4	28.2	.30	2.97	.76	.74	.20	.033	.083	.027	.045	.199	.267	.613	66.0
		12.0	1.0	4.01	110	2.01	52.7	7.62	986.5	1,022.4	4.32	24.1	5/1.501	39.7	.32	383.5	18.4	28.2	.30	2.97	.76	.74	.20	.033	.083	.027	.045	.199	.267	.613	66.0
		12.0	1.0	4.01	110	2.01	52.7	7.62	986.5	1,022.4	4.32	24.1	5/1.501	39.7	.32	383.5	18.4	28.2	.30	2.97	.76	.74	.20	.033	.083	.027	.045	.199	.267	.613	66.0
		12.0	1.0	4.01	110	2.01	52.7	7.62	986.5	1,022.4	4.32	24.1	5/1.501	39.7	.32	383.5	18.4	28.2	.30	2.97	.76	.74	.20	.033	.083	.027	.045	.199	.267	.613	66.0
		12.0	1.0	4.01	110	2.01	52.7	7.62	986.5	1,022.4	4.32	24.1	5/1.501	39.7	.32	383.5	18.4	28.2	.30	2.97	.76	.74	.20	.033	.083	.027	.045	.199	.267	.613	66.0
		12.0	1.0	4.01	110	2.01	52.7	7.62	986.5	1,022.4	4.32	24.1	5/1.501	39.7	.32	383.5	18.4	28.2	.30	2.97	.76	.74	.20	.033	.083	.027	.045	.199	.267	.613	66.0
		12.0	1.0	4.01	110	2.01	52.7	7.62	986.5	1,022.4	4.32	24.1	5/1.501	39.7	.32	383.5	18.4	28.2	.30	2.97	.76	.74	.20	.033	.083	.027	.045	.199	.267	.613	66.0
		12.0	1.0	4.01	110	2.01	52.7	7.62	986.5	1,022.4	4.32	24.1	5/1.501	39.7	.32	383.5	18.4	28.2	.30	2.97	.76	.74	.20	.033	.083	.027	.045	.199	.267	.613	66.0
		12.0	1.0	4.01	110	2.01	52.7	7.62	986.5	1,022.4	4.32	24.1	5/1.501	39.7	.32	383.5	18.4	28.2	.30	2.97	.76	.74	.20	.033	.083	.027	.045	.199	.267	.613	66.0
		12.0	1.0	4.01	110	2.01	52.7	7.62	986.5	1,022.4	4.32	24.1	5/1.501	39.7	.32	383.5	18.4	28.2	.30	2.97	.76	.74	.20	.033	.083	.027	.045	.199	.267	.613	66.0
		12.0	1.0	4.01	110	2.01	52.7	7.62	986.5	1,022.4	4.32	24.1	5/1.501	39.7	.32	383.5	18.4	28.2	.30	2.97	.76	.74	.20	.033	.083	.027	.045	.199	.267	.613	66.0
		12.0	1.0	4.01	110	2.01	52.7	7.62	986.5	1,022.4	4.32	24.1	5/1.501	39.7	.32	383.5	18.4	28.2	.30	2.97	.76	.74	.20	.033	.083	.027	.045	.199	.267	.613	66.0
		12.0	1.0	4.01	110	2.01	52.7	7.62	986.5	1,022.4	4.32	24.1	5/1.501	39.7	.32	383.5	18.4	28.2	.30	2.97	.76	.74	.20	.033	.083	.027	.045	.199	.267	.613	66.0
		12.0	1.0	4.01	110	2.01	52.7	7.62	986.5	1,022.4	4.32	24.1	5/1.501	39.7	.32	383.5	18.4	28.2	.30	2.97	.76	.74	.20	.033	.083	.027	.045	.199	.267	.613	66.0
		12.0	1.0	4.01	110	2.01	52.7	7.62	986.5	1,022.4	4.32	24.1	5/1.501	39.7	.32	383.5	18.4	28.2	.30	2.97	.76	.74	.20	.033	.083	.027	.045	.199	.267	.613	66.0
		12.0	1.0	4.01	110	2.01	52.7	7.62	986.5	1,022.4	4.32	24.1	5/1.501	39.7	.32	383.5	18.4	28.2	.30	2.97	.76	.74	.20	.033	.083	.027	.045	.199	.267	.613	66.0
		12.0	1.0	4.01	110	2.01	52.7	7.62	986.5	1,022.4	4.32	24.1	5/1.501	39.7	.32	383.5	18.4	28.2	.30	2.97	.76	.74	.20	.033	.083	.027	.045	.199	.267	.613	66.0
		12.0	1.0	4.01	110	2.01	52.7	7.62	986.5	1,022.4	4.32	24.1	5/1.501	39.7	.32	383.5	18.4	28.2	.30	2.97	.76	.74	.20	.033	.083	.027	.045	.199	.267	.613	66.0
		12.0	1.0	4.01	110	2.01	52.7	7.62</																							

SUMMARY OF  
RESERVOIR SEDIMENTATION SURVEYS MADE IN THE UNITED STATES THROUGH 1970

DATA SHEET NUMBER	RESERVOIR	STREAM	NEAREST TOWN	DRAINAGE AREA (SQ. MILES)		DATE OF SURVEY	PERIOD BETWEEN SURVEYS (YEARS)	STORAGE CAPACITY (ACRE-FT.)	CAPACITY SPECIFIC INFLOW RATIO (ACRE-FT. PER CU. FT.)	AVG. ANN. SEDIMENT ACCUMULATION PER SQ. MI. OF NET DR. AREA FOR PERIOD SHOWN	AGENCY SUPPLYING DATA
				TOTAL	NET						
71-31a	Teakettle Reservoir No. 1	Teakettle Creek	Fresno, Calif.	0.77	0.77	Fall 1948	1.0	0.39	---	0.0271	FS
						Fall 1948	10.0	.18	---		
						Fall 1951	3.0	.602	---		
						Fall 1955	4.0	0	---		
						Fall 1956	---	2/.352	---		
						Fall 1957	1.0	---	---		
						Fall 1959	1.0	---	---		
						Fall 1960	1.0	---	---		
						Fall 1961	1.0	---	---		
						Fall 1962	1.0	---	---		
						Fall 1963	1.0	---	---		
						Fall 1964	1.0	---	---		
						Fall 1965	1.0	---	---		
						Fall 1968	1.0	---	---		
						71-32a	Teakettle Reservoir No. 2a	---	---	.273	
Fall 1948	7.0	.068	---								
Fall 1951	3.0	.084	---								
Fall 1955	1.0	.039	---								
Fall 1956	---	.023	---								
Fall 1957	1.0	2/.065	---								
Fall 1958	1.0	---	---								
Fall 1959	4.0	---	---								
Fall 1960	1.0	---	---								
Fall 1961	1.0	---	---								
Fall 1962	1.0	---	---								
Fall 1963	1.0	---	---								
Fall 1964	1.0	---	---								
Fall 1965	1.0	---	---								
71-33a	Teakettle Reservoir No. 2	---	---	.847	.847						Fall 1948
						Fall 1951	3.0	.021	---		
						Fall 1955	4.0	.022	---		
						Fall 1956	---	2/.303	---		
						Fall 1957	1.0	---	---		
						Fall 1958	1.0	---	---		
						Fall 1959	1.0	---	---		
						Fall 1960	1.0	---	---		
						Fall 1961	1.0	---	---		
						Fall 1962	1.0	---	---		
						Fall 1963	1.0	---	---		
						Fall 1964	1.0	---	---		
						Fall 1965	1.0	---	---		
						Fall 1968	1.0	---	---		
						71-34a	Teakettle Reservoir No. 3	---	---	.856	.856
Fall 1941	3.0	.127	---								
Fall 1948	7.0	.109	---								
Fall 1951/3	3.0	.060	---								
Fall 1956	---	.007	---								
Fall 1957	1.0	2/.117	---								
Fall 1958	1.0	---	---								
Fall 1959	1.0	---	---								
Fall 1960	1.0	---	---								
Fall 1961	1.0	---	---								
Fall 1962	1.0	---	---								
Fall 1963	1.0	---	---								
Fall 1964	1.0	---	---								
Fall 1965	1.0	---	---								
71-35	Teakettle No. 7	---	---	.091	.091						
						Fall 1957	19.0	.181	.129	---	
						Fall 1958	1.0	.178	.127	---	
						Fall 1959	1.0	.162	.130	---	
						Fall 1960	1.0	.178	.127	---	
						Fall 1961	1.0	.162	.130	---	
						Fall 1962	1.0	.178	.127	---	
						Fall 1963	1.0	.162	.130	---	
						Fall 1964	1.0	.178	.127	---	
						Fall 1965	1.0	.162	.130	---	
						Fall 1966	1.0	.178	.127	---	
						Fall 1967	1.0	.162	.130	---	
						Fall 1968	1.0	.178	.127	---	
						Fall 1969	1.0	.162	.130	---	

Station	Location	Reservoir	Capacity	Year	Capacity	Year	Capacity	Year	Capacity	Year	Capacity	Year	Capacity
71-36	Pine Flat	Kings River	1,542	1952	1,013,000	1952	54	1952	54	1952	54	1952	54
71-37	Salinas Boys Ranch	Salinas	1,133	1956	1,011,950	1956	39	1956	39	1956	39	1956	39
71-38	Roy Alexander	San Joaquin	205	1951	1,011,950	1951	23	1951	23	1951	23	1951	23
71-39	Gibraltar	Santa Ynez	216	1954	1,011,950	1954	10	1954	10	1954	10	1954	10
71-40	Santa Felicia	Piru	425	1955	1,011,950	1955	58	1955	58	1955	58	1955	58
71-41	Success Lake	Tule River	393	1955	1,011,950	1955	90	1955	90	1955	90	1955	90
71-42	Isabella Reservoir	Kern River	2,074	1957	1,011,950	1957	100	1957	100	1957	100	1957	100
71-43	Lake Kaweah (Terminal Dam)	Kaweah River	560	1957	1,011,950	1957	106	1957	106	1957	106	1957	106
71-44	Cachuma	Santa Ynez River	117	1953	1,011,950	1953	19	1953	19	1953	19	1953	19

Station	Location	Reservoir	Capacity	Year	Capacity	Year	Capacity	Year	Capacity	Year	Capacity	Year	Capacity
72-1a	Ridgewood (Walker)	Walker Creek	5.7	1930	113	1930	10	1930	10	1930	10	1930	10
72-2a	Morris	Davis Creek	5.1	1927	113	1927	12	1927	12	1927	12	1927	12
72-3	Big Canyon	Big Canyon	5.50	1934	113	1934	24	1934	24	1934	24	1934	24
72-4	Budget	Trib. of Cosumnes River	3.12	1935	113	1935	46	1935	46	1935	46	1935	46
72-5	Bullards Bar	North Yuba River	480	1919	113	1919	31	1919	31	1919	31	1919	31
72-6	Combe (Van Gelsan)	Bear River	130	1935	113	1935	70	1935	70	1935	70	1935	70
72-7b	East Park	Little Stony Creek	11/100.5	1935	113	1935	70	1935	70	1935	70	1935	70
72-8	Faulk Lake (False Lake)	N. Fr. Jenny Creek	.71	1851	113	1851	130	1851	130	1851	130	1851	130
72-9	Catbed	Trib. of Burch Creek	.31	1915	113	1915	182	1915	182	1915	182	1915	182
72-10	Magnolia	Little Butte Creek	11/8.23	1918	113	1918	148	1918	148	1918	148	1918	148
72-11b	Stony Gorge	Stony Creek	15/199	1920	113	1920	29	1920	29	1920	29	1920	29
72-12	Misselbeck	N. Fr. Cottonwood Creek	12.0	1920	113	1920	75	1920	75	1920	75	1920	75
72-13	Lake Pillsbury (Scott Dam)	Sal River	283	1921	113	1921	248	1921	248	1921	248	1921	248
72-14	Oakcreek (Bar 49)	Maxwell Creek	.71	1953	113	1953	46	1953	46	1953	46	1953	46
72-15	Milliken	Milliken Creek	10.5	1924	113	1924	181.4	1924	181.4	1924	181.4	1924	181.4
72-16a	Onion Creek No. 1	Onion Creek, trib. of Amer. River	.19	1937	113	1937	.039	1937	.039	1937	.039	1937	.039
72-17	Onion Creek No. 2	Onion Creek	.48	1957	113	1957	.074	1957	.074	1957	.074	1957	.074
72-18	Onion Creek No. 3	Onion Creek	.65	1960	113	1960	.067	1960	.067	1960	.067	1960	.067

1/ Overtopped by sediment, no measurements taken in 1956; sediment removed down to original reservoir bottom.  
 2/ Sediment removed in summer 1956 - no measurements taken.  
 3/ Last data for which significant data are available; reservoir inoperative until 1956 when sediment was removed.  
 4/ Sediment not applicable to watershed as a whole.  
 5/ Period of abnormal operation. Represents 0.3 year of sediment accumulation behind partially closed gates and 1.5 years of sediment depletion with wide open gates. Sediment value is residue at end of period.  
 6/ Represents sedimentation for 3 full runoff years because no significant inflow occurred from Oct. 1, 1953, to Feb. 13, 1954, or from Oct. 1, 1956, to Nov. 15, 1956.  
 7/ Original capacity determined from 1964 survey.  
 8/ Effective drainage area prior to 1931 was 210 sq. mi. Thereafter 202.2 sq. mi.  
 9/

SACRAMENTO, EEL AND RUSSIAN RIVER BASINS

10/ Data at elevation 708 (limit of 8-7-49 survey). Spillway crest elevation 750 ft.  
 11/ Natural drainage area. Flow diverted into the reservoir from Stony Gorge drainage basin after 1914.  
 12/ Spillway elevation (flashboard crest elevation 30,000); 1:35 Water-Supply Paper 1798-F.  
 13/ Based on the natural drainage area.  
 14/ Excluding 3 sq. mi. above P. G. & E. Canal.  
 15/ The natural drainage area less area above East Park Reservoir. Flow diverted from the basin to East Park Reservoir after 1914.  
 16/ U. S. Bureau of Reclamation capacity curve (3-31-45); USGS Water-Supply Papers 1535 Part 11, 1798-F.  
 17/ Water treatment loss - treated as 0 gal/h.  
 18/ Estimated or assumed.

SUMMARY OF  
RESERVOIR SEDIMENTATION SURVEYS MADE IN THE UNITED STATES THROUGH 1970

DATA SHEET NUMBER	RESERVOIR	STREAM	NEAREST TOWN	DRAINAGE AREA (SQ. MILES)		PERIOD BETWEEN SURVEYS (YEARS)	STORAGE CAPACITY (ACRE-FT.)	CAPACITY AVG. ANN. INFLOW RATIO PER ACRE-FT.	SPECIFIC WEIGHT (DRY) (LB. PER CU. FT.)	AVG. ARR. SEDIMENT ACCUMULATION PER SQ. MI. OF NET DR. AREA FOR PERIOD SHOWN	AGENCY SUPPLYING DATA
				TOTAL	NET						
SACRAMENTO, EEL AND MISSISSIPPI RIVER BASINS (continued)											
72-19a	Orion Creek No. 5	Orion Creek, trib. of Amer. River	Soda Springs, Calif.	0.39	0.39	1957	0.177	0.098		PS	
						1958	1.0	.087	0.1248		
						1959	1.0	.033	.0256		
						1960	1.0	.035	.1790		
72-20a	Orion Creek No. 7			.80	.80	1958		.0754		PS	
						1959	1.0	.0723	.0069		
						1960	1.0	.020	.0010	SCS	
72-21	Leo Reservoir	Trib. of Dry Creek	Copeland, Calif.	.038	.038	Aug. 1963/	1/10	.0605	2.97	4,269	SCS
						Oct. 1965/	1/21	.50	.52	796	SCS
72-22	Rasal Hill			.175	.175	Oct. 1963/	21.04	.077	.69	1,186	SCS
						Oct. 1965/	1/54	.85	.98	1,359	SCS
72-23	Babe Wood			1.69	1.68	Oct. 1963/	46.76	.092	.98	1,359	SCS
						Nov. 1965/	2/17	.88	.75	1,350	PS
72-24	Mission	Trib. of Santa Rosa Creek	Santa Rosa, Calif.	.187	.184	Nov. 1964/	16.62	.088			
						Nov. 1966/	3/6	.010			
72-25	Leo Reservoir	Serp. Oaks Creek	Healdsburg, Calif.	.594	.592	Oct. 1963/	4.0	.077			
						Oct. 1965/					
72-26a	Casper Creek - South Fork	Casper Creek	Casper, Calif.	1.63	1.63	Fall 1962			.04		
						Summer 1963	.80		.028		
						Summer 1964	1.0		.039		
						Summer 1965	1.0		.119		
						Summer 1966	1.0		.068		
						Summer 1967	1.0		.073		
						Summer 1968	1.0		.077		
						Summer 1969	1.0		.242		
						Summer 1970	1.0		.141		
72-27a	Casper Creek - North Fork		Fort Bragg, Calif.	1.92	1.92	Fall 1962			.079		PS
						Summer 1963	.78		.043		
						Summer 1964	1.0		.425		
						Summer 1965	1.0		.674		
						Summer 1966	1.0		.077		
						Summer 1967	1.0		.242		
						Summer 1968	1.0		.141		
						Summer 1969	1.0		.11		SCS
						July 1970	13		.40		SCS
72-28	McOle	Virgin Creek	Fort Bragg, Calif.	.084	.083	July 1964/	7.3	.11			
						July 1967	7.07	.11			
72-29	Lady Creek		Palo, Calif.	.666	.663	Aug. 1953/	26.94	.098			
						Aug. 1955/	31.78	.186	.94	1,372	SCS
72-30	Appleton	Unnamed	Healdsburg, Calif.	.146	.143	Aug. 1967/	24.24	.182			
						Aug. 1967	24.24	.182	.37	475	SCS
72-31	M. S. Wilson	Bourne Gulch	Oakdale, Calif.	.285	.283	July 1952/	14.06	.060			
						July 1967	13.02	.077	.24	314	SCS
KUMATHI, HOODE, AND UREQUA RIVER BASINS											
73-1	Emigrant Gap	Emigrant Creek	Ashland, Oreg.	61.6	61.2	Oct. 1924					SCS
						Oct. 1963	7,300		.24		
73-2	Coyote Creek #1	Trib. South Umpqua River	Tiller, Oreg.	.267	.267	June 1965	7,019	.000			PS
						Aug. 1966			.0052		
						Aug. 1967	1.12		.0005		
						Aug. 1968	1.0		.0016		
						July 1969	.94		.0022		
						July 1970	.98		.0019		PS
73-3	Coyote Creek #2			.264	.264	Aug. 1965	7,012	.00004			
						Aug. 1966	1.11		.0031		
						Aug. 1967	1.0		.0009		
						Aug. 1968	1.0		.0006		
						July 1969	.94		.0002		
						July 1970	.98		.0004		
73-4	Coyote Creek #3			.192	.192	June 1965	7,011	.000			PS
						Aug. 1966	1.11		.0047		
						Aug. 1967	1.0		.002		
						Aug. 1968	1.0		.0025		
						July 1969	.94		.003		
						July 1970	.98		.0077		



74-5	Coyote Creek #4	Trib. South Umpqua River	Tiller, Ore.	188	188	June 1965	1.11	2/	PS
74-1	Condit (White Salmon)	White Salmon River	Underwood, Wash.	337	337	Aug. 1936	23	g/1,081	SCS
74-2	Lake Harriet (Oak Grove)	Trib. of Clackamas River	Portland, Ore.	126	126	Aug. 1924	24	1,054	SCS
74-3	McKay	McKay Creek	Pendleton, Ore.	184	184	July 1945	19.75	73,737	SCS
74-4	Cottage Grove	Coast Fk. Willamette River	Cottage Grove, Ore.	102	102	Oct. 1942	5.1	33,000	CE
74-5a	Luther Claypool Pond	Trib. of Beaver Creek	Post, Ore.	1.09	1.09	Dec. 1947	3.79	32,873	SCS
74-6	Paul Jaeger No. 1 Pond	Trib. of John Day River	Condon, Ore.	.625	.624	Oct. 1951	5	3.59	SCS
74-7	Paul Jaeger No. 2 Pond	Trib. of Rock Creek	Condon, Ore.	.668	.667	Oct. 1951	8	1.40	SCS
74-8a	Paul Jaeger No. 3 Pond	Trib. of John Day River	Condon, Ore.	.250	.249	Oct. 1951	5	2.45	SCS
74-9	J. M. Wilson Pond	Trib. of Deschutes River	Moro, Ore.	1.40	1.50	Oct. 1946	5	2.81	SCS
74-10	Willard Barnett Pond	Buck Creek	Kent, Ore.	.210	.209	Oct. 1951	10	1.91	SCS
74-11	Arthur Schmidt Pond	Trib. of Buck Creek	Shaniko, Ore.	.115	.114	Oct. 1951	10	2.41	SCS
74-12	Rock Creek Improvement Co.	Trib. of White River	Shaniko, Ore.	5.62	5.60	Oct. 1951	11	2.00	SCS
74-13	Vernon Christ Pond	Five Mile Creek	Dufur, Ore.	.089	.088	Oct. 1944	10	3.97	SCS
74-14	Mill J. Martin Pond	Hill Creek	The Dalles, Ore.	.070	.069	Oct. 1951	7	2.72	SCS
74-15	Hunt Livestock Co. Pond	Trib. of Buck Creek	Shaniko, Ore.	.050	.050	Oct. 1951	9	2.25	SCS
74-16	Gold Springs	Gold Springs Canyon	Gold Springs, Ore.	186	186	Feb. 1908	43	49,709	CE
74-17	Dorena	Row River	Cottage Grove, Ore.	265	262	Oct. 1949	8.9	44,688	FS
74-18	H. J. Andrews #1	Trib. Blue River	Blue River, Ore.	.37	.37	Sept. 1952	1.05	77,180	FS
74-19	H. J. Andrews #2	Blue River	Blue River, Ore.	.233	.233	Aug. 1947	92	77,180	FS
74-20	H. J. Andrews #3	Blue River	Blue River, Ore.	.391	.391	Aug. 1947	92	77,180	FS

1/ Original capacity determined by 1965 survey.  
 2/ Original capacity determined from 1964 survey. Capacity shown is for an elevation 4 ft. below spillway crest.  
 3/ Original capacity determined from 1965 survey. Total capacity with flashboards = 9.21 ac.-ft.  
 4/ From one disturbance and two undisturbed sample.  
 5/ Original capacity determined from 1967 survey.

6/ Based on original topographic survey; believed to be unreliable.  
 7/ Sediment measured 5 feet in 1977.  
 8/ Built in 1948. Reservoir was thoroughly cleaned in 1945.  
 9/ Estimated or assumed.

SUMMARY OF  
RESERVOIR SEDIMENTATION SURVEYS MADE IN THE UNITED STATES THROUGH 1970

DATA SHEET NUMBER	RESERVOIR	STREAM	NEAREST TOWN	DRAINAGE AREA (SQUARE MILES)		DATE OF SURVEY	PERIOD BETWEEN SURVEYS (YEARS)	STORAGE CAPACITY (ACRE-FT.)	CAPACITY AVG. ANN. INFLOW RATIO (ACRE-FT. PER ACRE-FT.)	SPECIFIC WEIGHT (LB. PER CU. FT.)	AVG. ANN. SEDIMENT ACCUMULATION PER SQ. MI. OF NET DR. AREA FOR PERIOD SHOWN	AGENCY SUPPLYING DATA
				TOTAL	NET							
75-1	Diablo	Shadet River	Ballingus, Wash.	1,100	1,100	July 1940	6	89,220	--	--	SCS	
75-2	High Valley Ranch #1 Pond	Wenas Creek	Fakem, Wash.	4.11	4.10	July 1939	6	88,862	--	0.054	SCS	
75-3	High Valley Ranch #2 Pond	--	Ellensburg, Wash.	.184	.184	Oct. 1941	12	7.63	*70	.02	30.49	
75-4	High Valley Ranch #3 Pond	--	--	.312	.312	Oct. 1941	11	1.53	*70	.04	61.0	
75-5	Henry Clark Pond	Eye Grass Creek	--	6.47	6.47	Oct. 1951	11	2.38	*70	.03	46.0	
75-6	Goffin Sheep Co. Pond	Hogies River	Yakima, Wash.	.482	.480	Oct. 1946	5	2.63	*70	.01	15.24	
75-7	Fox Creek	Fox	Ackerman, Wash.	1.82	1.82	Summer 1965	12	2.47	*70	.027	41.16	
75-8	Burns	Burns	--	2.18	2.18	Summer 1967	1	1/	110	.0076	18.4	
75-9	McGree	McGree	--	1.985	1.985	Summer 1967	1	1/	110	.0076	18.4	
75-10	Crabtree	Trib. White	Auburn, Wash.	.475	.11	May 1967	1	6.92	110	.0165	39.7	
75-11	Llewellyn	Trib. Goose	Wilbur, Wash.	1.25	1.25	July 1957	3	17.52	*60	1.65	2,156	
75-12	Schwab	No name	Ritzville, Wash.	4.15	4.15	May 1959	10	8.42	*80	.73	1,272	
75-13	Rex Lyle	--	--	.71	.71	June 1969	10	0	*80	.09	156.8	
75-14	Schoesler	--	--	.31	.31	June 1969	10	1.66	*80	.155	270	
75-15	John Janda (TU 80, BLK. 81)	--	Mass Lake, Wash.	.092	.092	Sept. 1970	18	0	*80	.40	696.8	
75-16	Shaffer	--	--	.756	.756	June 1958	12	2/	*60	.28	366	
75-17	Sam Spiced No. 1	--	--	.17	.17	Nov. 1969	1	2/	*60	.73	954	
75-18	Sam Spiced No. 2	--	--	.80	.80	Sept. 1970	1	2/	*60	.52	680	
75-19	Sheffels	--	Wilbur, Wash.	4.77	4.77	Apr. 1963	6	5.1	*70	.15	289	
75-20	Teledy	Trib. Crab	Edwall, Wash.	2.26	2.26	Apr. 1957	7	13.43	*80	.85	1,480	
75-21	Terwilliger (TU 273, BLK. 1)	No name	Warren, Wash.	.05	.05	Apr. 1968	1	2/	*60	1.4	1,429	
75-22	Roby	Goose Creek	Davenport, Wash.	4.10	3.85	Dec. 1968	1	22.91	*70	8.6	11,238	
						Apr. 1969	30	2.56		.175	266	

COLUMBIA RIVER BASIN (GRAND COULES TO UMATILLA) AND PACIFIC COAST DRAINAGE IN WASHINGTON  
Yakima, Chelan, and Okanogan River Basins

COLUMBIA RIVER BASIN (INTERNATIONAL BOUNDARY TO GRAND CANYON) AND PACIFIC COAST DRAINAGE IN WASHINGTON  
 Pendergill, Spokane, Walla Walla, and Lower Snake River Basins

76-1	Mrs. Meigs No. 1 Pond	Austin Creek	Amotin, Wash.	1,129	Sept. 1945	1.45	90	-.31	473	905
76-2	Mrs. Meigs No. 2 Pond	Trib. of Austin Creek	Amotin, Wash.	218	Sept. 1945	1.23	90	-.31	473	905
76-3a	Leaker Reservoir No. 1 Pond	Austin Creek E. & S. Fork	Amotin, Wash.	101	Sept. 1945	2.54	90	-.27	4,116	905
76-4	Leaker Reservoir No. 2 Pond	Austin Creek	Amotin, Wash.	125	Sept. 1945	1.15	90	-.70	1,067	905
76-5	Don Holt Pond	Letah Creek	Waverly, Wash.	110	Sept. 1945	1.21	90	-.12	181	905
76-6	Ray T. Wood Pond	Trib. of Clearwater River	Leadsom, Idaho	014	Oct. 1941	2.20	90	5.38	4,202	905
76-7	El Comstock Pond	Clearwater River	Drofling, Idaho	021	Sept. 1945	2.12	90	4.20	6,409	905
76-8	Midway Reservoir Pond	Malheur River	Men Pierce, Idaho	015	Sept. 1945	4.40	90	2.14	3,265	905
76-9	Henry Eastman Pond	Palouse River	Prichard, Idaho	021	Sept. 1943	2.71	90	1.20	1,690	905
76-10	George McCall Pond	Clearwater River	Prichard, Idaho	043	Sept. 1941	2.52	90	-.19	290	905
76-11a	Johnston Reservoir Pond	Clearwater River	Prichard, Idaho	014	Sept. 1943	2.41	90	2.0	3,090	905
76-12	El Calloway Pond	Clearwater River	Prichard, Idaho	014	Sept. 1943	4.97	90	-.64	976	905
76-13	A. K. Yeady Pond	Clearwater River	Prichard, Idaho	014	Sept. 1941	1.25	90	-.64	976	905
76-14	Walla Walla River Ave Railway Reservoir	Walla Walla River	Walla Walla, Wash.	1,760	Apr. 1953	9,688	90	-.64	976	905
76-15	Main Fork Horse Creek	Horse Creek	Elk City, Idaho	6.51	Nov. 1956	7,277	90	-.024	4.8	95
76-16	East Fork Horse Creek	East Fork Horse Creek	Elk City, Idaho	5.56	Nov. 1956	5,507	90	-.024	12.9	95

COLUMBIA RIVER BASIN IN CANADA

77-	Snake River Basin (From King Hill to Orange Grove River)	Snake River Basin (From King Hill to Orange Grove River)	Snake River Basin (From King Hill to Orange Grove River)	Snake River Basin (From King Hill to Orange Grove River)	Snake River Basin (From King Hill to Orange Grove River)	Snake River Basin (From King Hill to Orange Grove River)	Snake River Basin (From King Hill to Orange Grove River)	Snake River Basin (From King Hill to Orange Grove River)	Snake River Basin (From King Hill to Orange Grove River)	Snake River Basin (From King Hill to Orange Grove River)
77-1	Orchard	Indian Creek	Boise, Idaho	43	June 1947	4,737	90	-.01	4.8	905
77-2	Black Canyon	Payette River	Boise, Idaho	2,750	June 1924	4,668	90	-.132	1.1	905
77-3	Pinnacle Wall	Blaine's Creek	Boise, Idaho	916	June 1945	37,659	90	-.063	173.3	905
77-4	Arrowhead-Boise Project	Boise River	Boise, Idaho	2,211	June 1945	7,897	90	-.109	173.3	905
77-5	Lady Anderson Pond	Wester River	Cambridge, Idaho	631	Aug. 1945	271,250	90	-.136	207	905
77-6	Wilson Branch Pond	Trib. of Wester River	Boise, Idaho	436	Sept. 1951	100,67	90	-.259	395	905

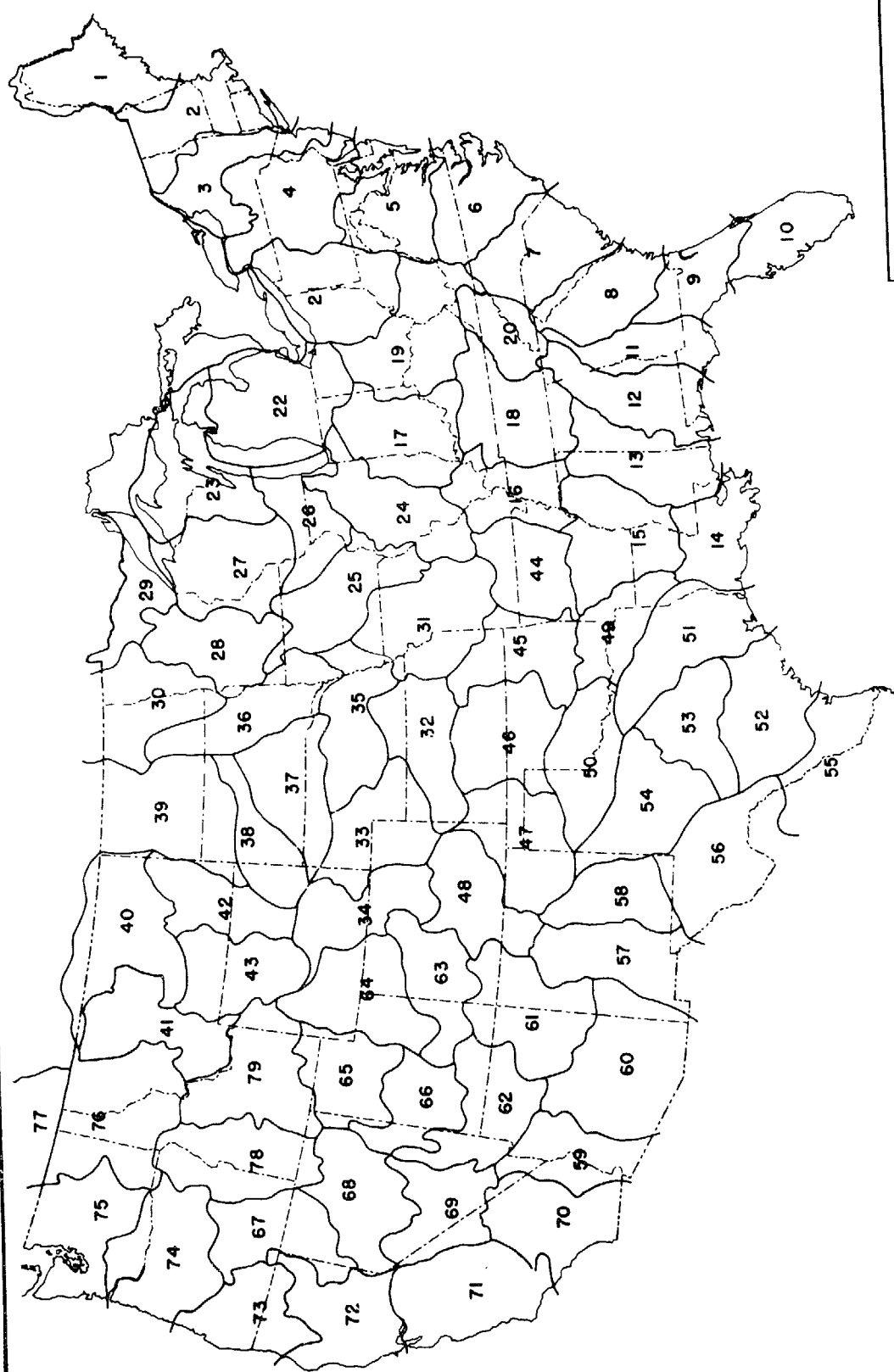
1/ Sediment measured and removed periodically.  
 2/ Desilting structure for return irrigation water.  
 3/ Built 1941. Reservoir was thoroughly cleaned in 1945.  
 4/ Includes above crest deposits within original flow lines.  
 5/ Does not include drainage area above Payette Lakes.  
 6/ Estimated or assumed.

SUMMARY OF  
RESERVOIR SEDIMENTATION SURVEYS MADE IN THE UNITED STATES THROUGH 1970

DATA SHEET NUMBER	RESERVOIR	STREAM	NEAREST TOWN	DRAINAGE AREA (SQUARE MILES)		DATE OF SURVEY	PERIOD BETWEEN SURVEYS (YEARS)	STORAGE CAPACITY (ACRE-FT.)	CAPACITY/AVG. ANN. INFLOW RATIO PER ACRE-FT.	SPECIFIC WEIGHT (DRY) (LB. PER CU. FT.)	AVG. ANN. SEDIMENT ACCUMULATION PER SQ. MI. OF NET DR. AREA FOR PERIOD SHOWN	AC.-FT. TONS	AGENCY SUPPLYING DATA
				TOTAL	NET								
78-7	M. B. Muninger Pond	Trib. of Westar River	Cambridge, Idaho	0.543	0.438	Aug. 1951	8	17.58	—	970	0.240	366	SCS
78-8	Miller Smead Pond	Little Willow Creek	Payette, Idaho	.218	.217	Sept. 1951	6	2.90	—	970	.147	224	SCS
78-9	Twin Puddles Pond	Trib. of Boise River	Boise, Idaho	1.61	1.61	Sept. 1941	10	7.82	—	970	.02	30.49	SCS
78-10	Lambkin Pond	—	Mountain Home, Idaho	.193	.191	Sept. 1941	10	4.54	—	970	.05	76.23	SCS
78-11	Mad Springs Pond	—	—	1.07	1.06	Sept. 1951	12	11.83	—	970	.03	15.73	SCS
78-12	J. J. Galton Pond	Trib. of Powder River	Keating, Oregon	.484	.483	Oct. 1951	12	.84	—	970	.04	51.0	SCS
78-13	Hawkins Pond No. 1	Trib. of Clover Creek	Westfall, Oregon	.12	.12	May 1952	4	1.52	—	—	.079	—	SCS
78-14	Hawkins Pond No. 2	—	—	.27	.27	May 1952	4	6.54	—	—	.17	—	SCS
78-15a	Rhysom	Wharton Creek	—	14.0	—	May 1956	4	6.78	—	—	.18	—	SCS
78-16	Sal Creek Sediment Dam	Trib. Silver Creek	Cascade, Idaho	.098	.098	Aug. 1965	8	31.708	—	—	.002	—	PS
78-17	Control Creek Sediment Dam	—	—	.775	.775	June 1966	1.0	—	—	—	.002	—	PS
78-18	Cabin Creek Sediment Dam	—	—	.40	.40	July 1967	.97	—	—	—	.002	—	PS
78-19	Ditch Creek Sediment Dam	—	—	.41	.41	Sept. 1965	.75	—	—	—	.006	—	PS
78-20	—	—	—	.75	.75	Aug. 1966	.80	—	—	—	.003	—	PS
78-21	—	—	—	.47	.47	July 1965	.21	—	—	—	.0017	—	PS



**INDEX OF  
RIVER BASIN MAPS**



*Index number corresponds to first of two numbers  
in summary table, which appear in column headed  
"Data Sheet No."*

# RESERVOIR SEDIMENT DATA SUMMARY

CONCHAS RESERVOIR  
NAME OF RESERVOIR

47-1b  
DATA SHEET NO.

DAM	1. OWNER <u>Corn of Engineers</u>			2. STREAM <u>Canadian and Conchas</u>			3. STATE <u>New Mexico</u>									
	4. SEC. <u>33</u> TWP. <u>14N</u> RANGE <u>26E</u>			5. NEAREST P. O. <u>Conchas Dam</u>			6. COUNTY <u>San Miguel</u>									
RESERVOIR	7. LAT <u>35° 24' 10"</u> LONG <u>104° 11' 25"</u>			8. TOP OF DAM ELEVATION <u>4240</u>			9. SPILLWAY CREST ELEV. <u>4201 1/2</u>									
	10. STORAGE ALLOCATION		11. ELEVATION TOP OF POOL		12. ORIGINAL SURFACE AREA, ACRES		13. ORIGINAL CAPACITY, ACRE-Feet		14. GROSS STORAGE, ACRE-Feet							
	a. FLOOD CONTROL		4,218		13,715		201,834		601,112							
	b. MULTIPLE USE								15. DATE STORAGE BEGAN							
	c. POWER								1 Jan. 1939							
	d. WATER SUPPLY								16. DATE NORMAL OPER. BEGAN							
	e. IRRIGATION								Jan. 1939							
	f. CONSERVATION		4,201		10,073		296,412		399,278							
g. INACTIVE		4,155		8,520		102,866		102,866								
WATERSHED	17. LENGTH OF RESERVOIR <u>Canadian 23 2/3</u> MILES				AV. WIDTH OF RESERVOIR <u>4200 Contour 0.75</u> MILES											
	18. TOTAL DRAINAGE AREA <u>7,409</u> SQ. MI.				22. MEAN ANNUAL PRECIPITATION <u>15.2 3/4</u> INCHES											
	19. NET SEDIMENT CONTRIBUTING AREA <u>6,976</u> SQ. MI.				23. MEAN ANNUAL RUNOFF <u>0.4884 3/4 (65.6)</u> INCHES											
	20. LENGTH <u>100</u> MILES AV. WIDTH <u>73</u> MILES				24. MEAN ANNUAL RUNOFF <u>192,200 (65.6)</u> AC.-F.T.											
21. MAX. ELEV. <u>13,000</u>		MIN. ELEV. <u>4,074</u>		25. ANNUAL TEMP MEAN <u>49°</u> RANGE <u>20-75 3/4</u>												
SURVEY DATA	26. DATE OF SURVEY <u>5/</u>		27. PERIOD YEARS		28. ACCL. YEARS		29. TYPE OF SURVEY		30 NO. OF RANGES OR CONTOUR INT.		31. SURFACE AREA, ACRES		32. CAPACITY, ACRE-Feet		33. C/I. RATIO, AC.-FT. PER AC.-FT.	
	Jan. 1939		1.4		1.4		Contour		10 feet		13,715		601,112		3.18	
	May 1940		2.1		3.4		Range		14 ranges		599,712		585,112		3.12	
	June 1942		.4		3.8		Range		24 ranges		581,112		576,756		3.04	
	Nov. 1942		1.9		5.7		Range		28 ranges		13,349		581,112		3.02	
	Oct. 1944		4.3		10.1		Contour		10 feet		13,552		576,756		3.00	
	Feb. 1949		14.7		24.83		Contour		10 feet		13,677		566,163		2.95	
	Oct. 1963		6.92		31.75		Range (D)		45 ranges		13,664		550,796		2.87	
	Oct. 1970						Contour		5 feet		13,664		528,951		2.75	
	26. DATE OF SURVEY <u>5/</u>		34. PERIOD ANNUAL PRECIPITATION		35. PERIOD WATER INFLOW, ACRE-Feet				36. WATER INFL. TO DATE, AC.-FT.							
		Inches		a. MEAN ANNUAL		b. MAX. ANNUAL		c. PERIOD TOTAL		a. MEAN ANNUAL		b. TOTAL TO DATE				
May 1940		14.26		72,700		1,059,699		101,780		72,700		101,780				
June 1942		22.40		859,780				1,805,540		560,980		1,907,320				
Nov. 1942		12.50		1,079,980				431,990		615,607		2,339,310				
Oct. 1944		14.32		143,750		1,168,350		273,130		458,320		2,612,440				
Feb. 1949		13.88		120,500		158,858		518,140		309,960		3,130,580				
Oct. 1963		13.01		144,340		336,514		2,121,850		211,790		5,252,430				
Oct. 1970		12.04		157,100		394,190		1,087,100		199,870		6,339,530				
26. DATE OF SURVEY <u>5/</u>		37. PERIOD CAPACITY LOSS, ACRE-Feet				38. TOTAL SED. DEPOSITS TO DATE, ACRE-Feet										
		a. PERIOD TOTAL		b. AV. ANNUAL		c. PER SQ. MI.-YEAR		a. TOTAL TO DATE		b. AV. ANNUAL		c. PER SQ. MI.-YEAR				
May 1940		1,400		6,952		0.996		1,400		1,000		0.143				
June 1942		14,600						16,000		4,710		.875				
Nov. 1942		4,000						20,000		5,260		.754				
Oct. 1944		4,356		2,290		.328		24,356		4,370		.612				
Feb. 1949		10,593		2,460		.353		34,949		3,460		.496				
Oct. 1963		15,364		1,045		.150		50,313		2,080		.291				
Oct. 1970		21,848		3,157		.453		72,161		2,273		.326				
26. DATE OF SURVEY <u>5/</u>		39. AV DRY WGT., LBS. PER CU. FT.		40 SED. DEP., TONS PER SQ. MI.-YR.		41. STORAGE LOSS, PCT.		42. SED. INFLOW, PPM								
		a. PERIOD		b. TOTAL TO DATE		a. AV. ANN.		b. TOT. TO DATE		a. PERIOD		b. TOT. TO DATE				
May 1940		75.7*		236		0.17		0.23		16,687		16,687				
June 1942		75.7		1,113		.78		2.66		9,810		10,177				
Nov. 1942		75.7		1,243		.88		3.33		11,233		10,372				
Oct. 1944		75.7		541		.71		4.05		19,346		11,810				
Feb. 1949		75.7		581		.58		5.81		24,302		13,548				
Oct. 1963		75.7		247		.34		8.37		8,748		11,621				
Oct. 1970		75.7		746		.38		12.00		24,376		13,808				

\*Estimated

26. DATE OF SURVEY	43. DEPTH DESIGNATION RANGE IN FEET BELOW, AND ABOVE, CREST ELEVATION										
	178-128	128-108	108-88	88-68	68-58	58-48	48-28	28-28	28-Crest	Crest-17	17-29
	PERCENT OF TOTAL SEDIMENT LOCATED WITHIN DEPTH DESIGNATION										
May 1940											
June 1942											
Nov. 1942											
Oct. 1944	16	4	7	10	6	10	15	16	16		
Feb. 1949	13	4	5	9	5	7	11	14	14	16	2
Oct. 1963	9	9	8	15	9	11	13	11	8	7	
Oct. 1970	3	7	12	10	5	6	8	11	33	4	1

26. DATE OF SURVEY	44. REACH DESIGNATION PERCENT OF TOTAL ORIGINAL LENGTH OF RESERVOIR														
	0-10	10-20	20-30	30-40	40-50	50-60	60-70	70-80	80-90	90-100	-105	-110	-115	-120	-125
	PERCENT OF TOTAL SEDIMENT LOCATED WITHIN REACH DESIGNATION														
May 1940 <sup>6/</sup>	114	23	3	-26	-16	2									
	30	22	7	10	18	18									
June 1942	6	3	4	4	22	14	27	18	2						
	20	21	-12	12	13	27	5	14							
Nov. 1942	6	2	5	8	16	16	23	16	2						
	-1	0	1	2	19	57	5	14	3						

45. RANGE IN RESERVOIR OPERATION							
WATER YEAR	MAX. ELEV.	MIN. ELEV.	INFLOW, AC.-FT.	WATER YEAR	MAX. ELEV.	MIN. ELEV.	INFLOW, AC.-FT.
1947	4,202.46	4,199.00	129,330	1959	4,200.38	4,193.40	112,820
1948	4,201.46	4,195.63	154,700	1960	4,199.37	4,192.68	131,520
1949	4,200.97	4,192.50	153,280	1961	4,201.75	4,196.55	216,440
1950	4,198.59	4,185.85	131,410	1962	4,201.13	4,193.02	119,280
1951	4,194.68	4,184.24	106,770	1963	4,193.01	4,178.16	76,510
1952	4,184.15	4,168.23	125,930	1964	4,178.58	4,166.05	31,060
1953	4,176.16	4,162.07	107,950	1965	4,201.83	4,157.61	394,190
1954	4,173.22	4,155.80	32,030	1966	4,200.77	4,192.25	108,660
1955	4,190.37	4,157.10	297,760	1967	4,195.35	4,185.79	142,740
1956	4,189.98	4,173.19	51,680	1968	4,193.13	4,183.51	113,130
1957	4,175.40	4,163.80	129,930	1969	4,193.65	4,180.65	192,830
1958	4,201.82	4,173.97	336,510	1970	4,197.55	4,189.30	105,630

46. ELEVATION-AREA-CAPACITY DATA								
ELEVATION	AREA	CAPACITY	ELEVATION	AREA	CAPACITY	ELEVATION	AREA	CAPACITY
4,230	16,380	709,353	4,180	5,513	173,912	4,110	311	1,299
4,220	14,110	514,000	4,170	4,323	125,102	4,100	2	24
4,218	13,664	488,000	4,160	3,394	86,519	4,090	1	9
4,210	11,845	408,166	4,150	2,642	56,348	4,080		2
4,201	9,692	330,124	4,140	1,959	33,495	4,070	0	0
4,200	9,463	320,546	4,130	1,323	17,170	4,060	0	0
4,190	7,290	237,119	4,120	797	6,690			

47. REMARKS AND REFERENCES

1/ Emergency Spillway Crest at 4218.  
2/ Conchas 13.8 miles.  
3/ From climatic Atlas dated June 1968.  
4/ This figure affected by water taken out above reservoir for irrigation.  
5/ Totals computed to end of each month shown.  
6/ Only dates computed.

48. AGENCY MAKING SURVEY	Albuquerque District Corps of Engineers	50. DATE	May 1970
49. AGENCY SUPPLYING DATA	Corps of Engineers		

April 1965



**RESERVOIR SEDIMENT  
DATA SUMMARY**

NAME OF RESERVOIR \_\_\_\_\_

DATA SHEET NO. \_\_\_\_\_

<b>DAM</b>	1. OWNER			2. STREAM			3. STATE							
	4 SEC.		TWP.		RANGE		5. NEAREST P. O.			6. COUNTY				
	7 LAT.			" LONG.			8. TOP OF DAM ELEVATION			9. SPILLWAY CREST ELEV.				
<b>RESERVOIR</b>	10. STORAGE ALLOCATION		11. ELEVATION TOP OF POOL		12. ORIGINAL SURFACE AREA, ACRES		13. ORIGINAL CAPACITY, ACRE-FEET		14. GROSS STORAGE, ACRE-FEET		15. DATE STORAGE BEGAN			
	a. FLOOD CONTROL													
	b. MULTIPLE USE													
	c. POWER													
	d. WATER SUPPLY										16. DATE NORMAL OPER. BEGAN			
	e. IRRIGATION													
	f. CONSERVATION													
g. INACTIVE														
<b>WATERSHED</b>	17. LENGTH OF RESERVOIR				MILES		AV. WIDTH OF RESERVOIR				MILES			
	18. TOTAL DRAINAGE AREA				SQ. MI.		22. MEAN ANNUAL PRECIPITATION				INCHES			
	19. NET SEDIMENT CONTRIBUTING AREA				SQ. MI.		23. MEAN ANNUAL RUNOFF				INCHES			
	20. LENGTH		MILES		AV. WIDTH		MILES		24. MEAN ANNUAL RUNOFF				AC.-FT.	
	21. MAX. ELEV.			MIN. ELEV.			25. ANNUAL TEMP: MEAN						RANGE	
<b>SURVEY DATA</b>	26. DATE OF SURVEY		27. PERIOD YEARS	28. ACCL. YEARS	29. TYPE OF SURVEY		30. NO. OF RANGES OR CONTOUR INT.		31. SURFACE AREA, ACRES		32. CAPACITY, ACRE-FEET		33. C/I. RATIO, AC.-FT. PER AC.-FT.	
	26. DATE OF SURVEY		34. PERIOD ANNUAL PRECIPITATION		35. PERIOD WATER INFLOW, ACRE-FEET			36. WATER INFL. TO DATE, AC.-FT.						
					a. MEAN ANNUAL	b. MAX. ANNUAL	c. PERIOD TOTAL		a. MEAN ANNUAL	b. TOTAL TO DATE				
	26. DATE OF SURVEY		37. PERIOD CAPACITY LOSS, ACRE-FEET				38. TOTAL SED. DEPOSITS TO DATE, ACRE-FEET							
			a. PERIOD TOTAL		b. AV. ANNUAL	c. PER SQ. MI.-YEAR	a. TOTAL TO DATE		b. AV. ANNUAL	c. PER SQ. MI.-YEAR				
	26. DATE OF SURVEY		39. AV. DRY WGT., LBS. PER CU. FT.		40. SED. DEP., TONS PER SQ. MI.-YR.		41. STORAGE LOSS, PCT.		42. SED. INFLOW, PPM					
			a. PERIOD		b. TOTAL TO DATE	a. AV. ANN.	b. TOT. TO DATE	a. PERIOD	b. TOT. TO DATE					

26. DATE OF SURVEY	43. DEPTH DESIGNATION RANGE IN FEET BELOW, AND ABOVE, CREST ELEVATION														
	PERCENT OF TOTAL SEDIMENT LOCATED WITHIN DEPTH DESIGNATION														
26. DATE OF SURVEY	44. REACH DESIGNATION PERCENT OF TOTAL ORIGINAL LENGTH OF RESERVOIR														
	0-10	10-20	20-30	30-40	40-50	50-60	60-70	70-80	80-90	90-100	-105	-110	-115	-120	-125
	PERCENT OF TOTAL SEDIMENT LOCATED WITHIN REACH DESIGNATION														
45. RANGE IN RESERVOIR OPERATION															
WATER YEAR	MAX. ELEV.	MIN. ELEV.	INFLOW, AC. FT.	WATER YEAR	MAX. ELEV.	MIN. ELEV.	INFLOW, AC. FT.								
46. ELEVATION-AREA-CAPACITY DATA															
ELEVATION	AREA	CAPACITY	ELEVATION	AREA	CAPACITY	ELEVATION	AREA	CAPACITY							
47. REMARKS AND REFERENCES															
48. AGENCY MAKING SURVEY															
49. AGENCY SUPPLYING DATA															
50. DATE _____															

REFERENCES FOR APPENDIX F

Miscellaneous Publication No. 1266, U.S. Department of Agriculture,  
Sedimentation Laboratory, Oxford, Mississippi, July, 1973.



APPENDIX G  
INITIAL DILUTION TABLES

The Tables are ordered as follows:

<u>Tables</u>	<u>Port Spacing (PS) (Diameters)</u>
<u>N<sub>1</sub></u>	
1-20	2
21-40	5
41-60	10
61-80	25
81-100	1000 (effluent from each port acts as a single plume)

<u>Tables</u>	<u>Current Velocity to Effluent Velocity Ratio (k)</u>
<u>N<sub>2</sub></u>	
1-5	0.1
6-10	0.05
11-15	0.02
16-20	0.00 (no current)

<u>Tables</u>	<u>Composite Stratification Parameter (SP)</u>
<u>N<sub>3</sub></u>	
1	200 (high stratification)
2	500
3	2000
4	10000
5	infinity (no stratification)

After finding N<sub>1</sub>, N<sub>2</sub>, and N<sub>3</sub> the appropriate Table number is:

$$N_1 + N_2 + N_3 - 2$$

TABLE 1

DIFFUSER PLUME DILUTION  
 PORT SPACING = 2 DIAMETERS, STABILITY STRATIFICATION PARAMETER = 200  
 CURRENT TO EFFLUENT RATIO = 0.10

RISE(DIA)	DENSIMETRIC FROUDE NUMBER					
	1	3	10	30	100	1000
1	T)					
	M)	1.9	2.2( 0.4) 2.7	2.1( 0.0) 4.3	2.1( 0.0) 7.0	2.1( 0.0) 13.0
2	T)					
	M)	2.7	3.3	5.1	8.5	15.8
3	T)					
	M)	3.5	3.8	5.7	9.5	17.9
4	T)					
	M)	4.3( 3.7)				
5	T)					
	M)	4.5	4.2	6.2	10.3	19.6
7	T)					
	M)	5.4	4.7	6.7	11.1	21.1
9	T)					
	M)	7.0	5.6	7.7	12.6	23.6
12	T)					
	M)	8.5	6.6	8.6	13.8	26.0 27.1( 10.0)
15	T)					
	M)	10.7	7.8	9.9	15.8	29.4
20	T)					
	M)	12.8	9.2	11.2	17.6 18.1( 15.9)	33.6
25	T)					
	M)	16.1	11.3	13.6	21.0	
33	T)					
	M)	16.9( 21.3)	13.5( 25.0)	14.3( 21.7)		
33	T)					
	M)	19.2		16.2		
33	T)					
	M)		17.5			

DI. AT MAX REAL  
 OR PERMITTED RISE 35.3( 31.0) 26.8( 36.6) 23.0( 32.5) 25.6( 24.8) 37.2( 16.2) 104.0( 5.8)

TABLE 2

DIFFUSER PLUME DILUTION  
 PORT SPACING = 2 DIAMETERS, STABILITY STRATIFICATION PARAMETER = 500  
 CURRENT TO EFFLUENT RATIO = 0.10

WISE(DIA)	DENSIMETRIC FROUDE NUMBER					
	1	3	10	30	100	1000
1	1.9	2.2( 0.4) 2.7	2.1( 0.0) 4.3	2.1( 0.0) 7.0	2.1( 0.0) 12.9	2.1( 0.0) 48.1
2	2.7	3.3	5.1	8.4	15.8	60.1
3	3.6	3.8	5.7	9.5	17.7	68.5
4	4.3( 3.8) 4.5	4.2	6.2	10.3	19.4	75.5
5	5.4	4.7	6.7	11.1	20.8	81.5
7	7.0	5.6	7.6	12.5	23.3	93.0 94.3( 7.3)
9	8.5	6.6	8.5	13.7	25.3	104.0
12	10.9	7.8	9.8	15.5	28.0	
15	13.1	9.2	11.0	17.3	30.7 35.0( 20.2)	
20	16.7	11.4	13.0	20.0		
25	20.3	13.6	15.0	22.8 25.6( 30.0)	39.4	
33	25.5 26.5( 34.8)	16.9	18.5 21.4( 39.2)	27.5		
42	30.7	20.8 21.0( 42.6)	22.9	33.4		
54		26.5	32.2			

DIL AT MAX REAL  
 OR PERMITTED WISE 59.3( 50.2) 44.9( 61.0) 36.8( 56.8) 37.0( 45.6) 48.3( 31.9) 131.0( 11.7)

TABLE 3

DIFFUSER PLUME DILUTION  
 PORT SPACING = 2 DIAMETERS, STABILITY STRATIFICATION PARAMETER = 2000  
 CURRENT TO EFFLUENT RATIO = 0.10

RISE(DIA)	DENSIMETRIC FROUDE NUMBER					
	1	3	10	30	100	1000
1	1.9	2.2( 0.4) 2.7	2.1( 0.0) 4.3	2.1( 0.0) 7.0	2.1( 0.0) 12.9	2.1( 0.0) 48.1
2	2.7	3.3	5.1	8.4	15.8	59.7
3	3.6	3.8	5.7	9.5	17.7	67.6
4	4.3( 3.8) 4.5	4.2	6.2	10.3	19.3	74.0
5	5.4	4.7	6.7	11.0	20.7	79.8
7	7.0	5.6	7.6	12.4	23.1	89.2
9	8.6	6.6	8.5	13.6	25.1	96.9
12	10.9	7.9	9.7	15.3	27.7	107.0
15	13.2	9.2	10.9	17.0	30.0	116.0
20	17.0	11.4	12.8	19.7	33.9	131.0 132.0( 20.7)
25	20.8	13.6	14.7	22.3	37.5	145.0
33	26.7	17.0	17.8	26.3	42.8	176.0
42	33.1	21.0	21.3	31.1	48.8 56.1( 53.4)	
54	41.6	26.2	25.8	37.3	56.7	
70	52.0 52.6( 71.3)	32.9 41.3( 90.3)	32.7 41.1( 89.4)	45.9 47.1( 72.5)	67.2	
90	63.2		41.6	57.8		
115		53.1	59.6			

OIL AT MAX REAL  
 OR PERMITTED RISE 125.0(102.0) 96.1(128.0) 76.2(125.0) 69.5(106.0) 78.7( 82.7) 184.0( 33.4)



TABLE 4

DIFFUSER PLUME DILUTION  
 PORT SPACING = 2 DIAMETERS, STABILITY STRATIFICATION PARAMETER = 10000  
 CURRENT TO EFFLUENT RATIO = 0.10

		DENSIMETRIC FROUDE NUMBER					
		1	3	10	30	100	1000
1	: T)						
	: M)	1.9	2.2( 0.4)	2.1( 0.0)	2.1( 0.0)	2.1( 0.0)	2.1( 0.0)
2	: T)						
	: M)	2.7	2.7	4.3	7.0	12.9	48.1
3	: T)						
	: M)	2.7	3.3	5.1	8.4	15.8	59.7
4	: T)						
	: M)	3.6	3.8	5.7	9.5	17.7	67.6
5	: T)						
	: M)	4.3( 3.8)	4.2	6.2	10.3	19.3	74.0
7	: T)						
	: M)	5.4	4.7	6.7	11.0	20.7	79.3
9	: T)						
	: M)	7.0	5.6	7.6	12.4	22.9	88.0
12	: T)						
	: M)	8.6	6.6	8.5	13.6	24.9	95.6
15	: T)						
	: M)	10.9	7.9	9.7	15.3	27.7	105.0
20	: T)						
	: M)	13.3	9.2	10.9	17.0	30.0	113.0
25	: T)						
	: M)	17.0	11.4	12.8	19.7	33.6	125.0
33	: T)						
	: M)	21.0	13.6	14.7	22.2	37.2	135.0
42	: T)						
	: M)	27.1	17.1	17.6	26.2	42.5	149.0
54	: T)						
	: M)	33.8	21.1	21.0	30.5	48.1	163.0
70	: T)						
	: M)	42.8	26.3	25.3	36.5	55.3	180.0
90	: T)						
	: M)	54.9	33.3	31.1	44.0	64.7	200.0( 6R.9)
115	: T)						
	: M)	69.3	41.9	38.3	53.8	76.0	228.0
148	: T)						
	: M)	87.0	52.6	47.5	66.2	90.4	
190	: T)						
	: M)	109.0	66.5	60.1	82.9	109.0	
244	: T)						
	: M)	117.0(161.0)			101.0(182.0)	117.0(150.0)	
244	: T)						
	: M)	133.0	83.9	77.5	106.0	133.0	
244	: T)						
	: M)		91.5(209.0)	90.4(217.0)			
244	: T)						
	: M)		107.0	107.0	140.0		

DIL AT MAX REAL  
 OR PERMITTED RISE 225.0(232.0) 224.0(293.0) 176.0(297.0) 152.0(260.0) 155.0(224.0) 244.0( 99.9)

TABLE 5

DIFFUSER PLUME DILUTION  
 PORT SPACING = 2 DIAMETERS, STABILITY STRATIFICATION PARAMETER = INFINITE  
 CURRENT TO EFFLUENT RATIO = 0.10

RISE(DIA)	DENSIMETRIC FROUDE NUMBER					
	1	3	10	30	100	1000
1	1.9	2.2[ 0.4] 2.7	2.1[ 0.0] 4.3	2.1[ 0.0] 7.0	2.1[ 0.0] 12.9	2.1[ 0.0] 48.1
2	2.7	3.3	5.1	8.4	15.8	59.3
3	3.6	3.8	5.7	9.5	17.7	67.6
4	4.3[ 3.8] 4.5	4.2	6.2	10.3	19.3	74.0
5	5.4	4.7	6.7	11.0	20.7	79.3
7	7.0	5.6	7.6	12.4	22.9	88.0
9	8.6	6.6	8.5	13.6	24.9	95.6
12	10.9	7.9	9.7	15.3	27.7	105.0
15	13.3	9.2	10.9	17.0	30.0	113.0
20	17.1	11.4	12.8	19.6	33.6	124.0
25	21.0	13.6	14.6	22.2	37.0	133.0
33	27.1	17.1	17.6	26.2	42.2	147.0
42	34.0	21.1	20.8	30.5	47.8	159.0
54	43.1	26.3	25.1	36.2	54.9	174.0
70	55.3	33.3	30.9	43.7	64.4	191.0
90	71.0	42.2	38.0	53.0	75.5	210.0
115	89.6	53.0	46.8	64.5	89.2	232.0
148	115.0	67.5	58.3	79.5	107.0	
190	147.0	85.8	73.0	98.8	130.0	
244	188.0	109.0	92.0	123.0	158.0	

DIL AT MAX REAL  
 OR PERMITTED RISE 231.0(300.0) 134.0(301.0) 111.0(300.0) 149.0(300.0) 188.0(301.0) 257.0(147.0)

TABLE 6

DIFFUSER PLUME DILUTION  
 PORT SPACING = 2 DIAMETERS, STABILITY STRATIFICATION PARAMETER = 200  
 CURRENT TO EFFLUENT RATIO = 0.05

RISE(DIA)	DENSIMETRIC FROUDE NUMBER					
	1	3	10	30	100	1000
1	1.9	2.1( 0.4) 2.6	2.1( 0.0) 4.0	2.1( 0.0) 6.3	2.1( 0.0) 10.9	2.1( 0.0) 36.5
2	2.7	3.2	4.6	7.4	13.0	44.9
3	3.6	3.6	5.1	8.1	14.5	51.2
4	4.2( 3.7) 4.5	4.0	5.5	8.8	15.7	56.5 59.3( 4.6)
5	5.4	4.4	5.8	9.3	16.7	61.8
7	6.9	5.1	6.4	10.2	18.5	74.0
9	8.4	5.9	7.0	11.0	20.0 22.2( 12.1)	
12	10.4	7.0	7.7	12.0		
15	12.5	8.1	8.5	13.0 14.2( 18.8)	24.2	
20	15.6 16.5( 21.6)	9.8	9.7	14.6		
25	18.4	11.4 12.1( 27.2)	10.9 11.1( 25.9)	16.5		
33		13.8	13.0			

DIL AT MAX REAL  
 OR PERMITTED RISE 29.4( 31.7) 20.4( 40.7) 17.0( 40.3) 19.6( 30.5) 29.9( 19.6) 81.1( 7.4)

TABLE 7

DIFFUSER PLUME DILUTION  
 PORT SPACING = 2 DIAMETERS, STABILITY STRATIFICATION PARAMETER = 500  
 CURRENT TO EFFLUENT RATIO = 0.05

RISE(DIA)	DENSIMETRIC FROUDE NUMBER					
	1	3	10	30	100	1000
1	1.9	2.1( 0.4) 2.6	2.1( 0.0) 4.0	2.1( 0.0) 6.3	2.1( 0.0) 10.9	2.1( 0.0) 36.5
2	2.7	3.2	4.6	7.4	13.0	44.6
3	3.6	3.6	5.1	8.1	14.4	50.2
4	4.3( 3.7) 4.5	4.0	5.5	8.8	15.6	54.9
5	5.4	4.4	5.8	9.3	16.6	59.3
7	6.9	5.2	6.4	10.1	18.2	66.2
9	8.4	5.9	7.0	10.9	19.7	72.4 73.5( 9.3)
12	10.6	7.0	7.7	11.9	21.4	82.7
15	12.7	8.1	8.4	12.7	23.1	
20	16.2	9.9	9.6	14.1	25.4 27.5( 24.5)	
25	19.6	11.7	10.7	15.6	27.8	
33	24.6 25.8( 35.4)	14.4	12.5	17.6 18.9( 37.8)	31.7	
42	29.4	17.4 18.6( 46.3)	14.4 15.9( 48.6)	20.1		
54		21.0	17.3	24.2		
70			22.8			

DIL AT MAX REAL  
 OR PERMITTED RISE 50.6( 51.5) 34.8( 68.1) 26.9( 73.2) 27.2( 59.1) 37.4( 39.8) 101.0( 15.0)

TABLE 8

DIFFUSER PLUME DILUTION  
 PORT SPACING = 2 DIAMETERS, STABILITY STRATIFICATION PARAMETER = 2000  
 CURRENT TO EFFLUENT RATIO = 0.05

RISE(DIA)	DENSIMETRIC FROUDE NUMBER					
	1	3	10	30	100	1000
1	1.9	2.1( 0.4) 2.6	2.1( 0.0) 4.0	2.1( 0.0) 6.3	2.1( 0.0) 10.9	2.1( 0.0) 36.5
2	2.7	3.2	4.6	7.4	13.0	44.3
3	3.6	3.6	5.1	8.1	14.4	49.8
4	4.3( 3.7) 4.5	4.0	5.5	8.7	15.6	54.5
5	5.4	4.4	5.8	9.3	16.6	58.0
7	6.9	5.2	6.4	10.1	18.1	64.4
9	8.5	6.0	6.9	10.9	19.4	69.5
12	10.6	7.1	7.7	11.8	21.1	76.6
15	12.8	8.2	8.4	12.6	22.6	82.3
20	16.4	10.1	9.5	14.0	24.8	91.3
25	20.1	11.9	10.6	15.2	26.7	99.4 101.0( 26.5)
33	25.8	14.8	12.4	17.1	29.6	112.0
42	32.0	18.0	14.3	19.2	32.7	131.0
54	39.0	22.3	16.8	21.9	36.7 41.4( 68.8)	
70	49.6 51.1( 72.6)	27.7	20.2	25.3	41.8	
90	60.0	34.3 36.7( 98.7)	24.4 29.6(115.0)	30.1 31.9( 98.1)	48.7	
115		41.5		36.7		
140			37.9			

OIL AT MAX PEAL  
 OR PERMITTED RISE 112.0(105.0) 77.9(143.0) 58.3(167.0) 51.0(147.0) 58.0(109.0) 140.0( 43.3)

TABLE 9

DIFFUSER PLUME DILUTION  
 PORT SPACING = 2 DIAMETERS, STABILITY STRATIFICATION PARAMETER = 10000  
 CURRENT TO EFFLUENT RATIO = 0.05

		DENSIMETRIC FROUDE NUMBER					
		1	3	10	30	100	1000
1	: T)		2.1( 0.4)	2.1( 0.0)	2.1( 0.0)	2.1( 0.0)	2.1( 0.0)
	: M)	1.9	2.6	4.0	6.3	10.9	36.2
2	: T)		3.2	4.6	7.4	13.0	44.3
	: M)	2.7					
3	: T)		3.6	5.3	8.1	14.4	49.8
	: M)	3.6					
4	: T)		4.3( 3.7)	5.5	8.7	15.6	54.1
	: M)	4.5	4.0				
5	: T)		4.4	5.8	9.3	16.4	58.0
	: M)	5.4					
7	: T)		5.2	6.4	10.1	18.1	63.9
	: M)	6.9					
9	: T)		6.0	6.9	10.6	19.4	69.0
	: M)	9.5					
12	: T)		7.1	7.7	11.8	21.1	75.5
	: M)	10.7					
15	: T)		8.2	8.4	12.6	22.5	80.8
	: M)	12.9					
20	: T)		10.1	9.5	13.9	24.6	88.6
	: M)	16.6					
25	: T)		11.9	10.6	15.1	26.5	95.4
	: M)	20.2					
33	: T)		14.6	12.4	17.0	29.2	105.0
	: M)	26.0					
42	: T)		18.2	14.3	18.9	32.2	113.0
	: M)	32.7					
54	: T)		22.6	16.8	21.4	36.0	124.0
	: M)	41.3					
70	: T)		28.4	20.2	24.6	40.4	136.0
	: M)	52.7					151.0( 69.8)
90	: T)		35.7	24.4	28.6	46.1	151.0
	: M)	66.6					
115	: T)		44.6	29.4	33.5	53.0	170.0
	: M)	83.1					
148	: T)		55.8	36.4	40.0	62.1	
	: M)	104.0					
190	: T)		69.6	44.9	48.5	74.0	
	: M)	114.0(165.0)					
244	: T)		81.4(229.0)	55.8	60.4	77.7(204.0)	
	: M)	127.0					
244	: T)		85.9	64.0(285.0)	66.0(267.0)	89.8	
	: M)						

DIL AT MAX HEAL  
 OR PERMITTED RISE 185.0(239.0) 101.0(300.0) 67.3(300.0) 75.7(301.0) 108.0(300.0) 191.0(138.0)

TABLE 10

DIFFUSER PLUME DILUTION  
 PORT SPACING = 2 DIAMETERS, STABILITY STRATIFICATION PARAMETER = INFINITE  
 CURRENT TO EFFLUENT RATIO = 0.05

RISE(DIA)	DENSIMETRIC FROUDE NUMBER					
	1	3	10	30	100	1000
1	1.9	2.1( 0.4) 2.6	2.1( 0.0) 4.0	2.1( 0.0) 6.3	2.1( 0.0) 10.9	2.1( 0.0) 36.2
2	2.7	3.2	4.6	7.4	13.0	44.3
3	3.6	3.6	5.1	8.1	14.4	49.8
4	4.3( 3.7) 4.5	4.0	5.5	8.7	15.6	54.1
5	5.4	4.4	5.8	9.3	16.4	58.0
7	6.9	5.2	6.4	10.1	18.1	63.9
9	8.5	6.0	6.9	10.8	19.4	69.0
12	10.7	7.1	7.7	11.8	21.1	75.0
15	12.9	8.2	8.4	12.6	22.5	80.8
20	16.6	10.1	9.5	13.9	24.6	88.2
25	20.2	11.9	10.6	15.1	26.5	94.5
33	26.2	14.9	12.4	16.9	29.2	103.0
42	32.7	18.2	14.3	18.9	32.2	112.0
54	41.6	22.6	16.8	21.4	35.7	121.0
70	53.0	28.6	20.2	24.6	40.3	132.0
90	68.1	36.0	24.4	28.4	45.7	144.0
115	86.3	45.2	29.6	33.1	52.2	156.0
148	110.0	57.5	36.5	39.1	60.9	172.0
190	141.0	73.0	45.1	46.8	71.3	189.0
244	180.0	92.7	56.3	56.5	84.8	

DIL AT MAX REAL  
 OR PERMITTED RISE 221.0(300.0) 113.0(301.0) 67.8(300.0) 66.5(301.0) 98.4(301.0) 201.0(221.0)

TABLE 11

DIFFUSER PLUME DILUTION  
 PORT SPACING = 2 DIAMETERS, STABILITY STRATIFICATION PARAMETER = 200  
 CURRENT TO EFFLUENT RATIO = 0.02

RISE(DIA)	DENSIMETRIC FROUDE NUMBER					
	1	3	10	30	100	1000
1	1.9	2.1( 0.4) 2.6	2.0( 0.0) 3.8	2.0( 0.0) 5.8	2.0( 0.0) 9.7	2.0( 0.0) 27.6
2	2.7	3.1	4.4	6.7	11.2	33.3
3	3.6	3.5	4.8	7.4	12.4	37.2
4	4.2( 3.7) 4.5	3.9	5.1	7.8	13.3	40.5
5	5.3	4.3	5.4	8.3	13.9	43.4 45.5( 5.8)
7	6.8	5.0	6.0	8.9	15.2	48.8
9	8.2	5.7	6.4	9.5	16.2	55.7
12	10.3	6.7	7.0	10.3	17.6 18.5( 14.2)	
15	12.2	7.7	7.6	10.9	18.9	
20	15.3 16.2( 21.9)	9.3	8.5	12.0 12.2( 21.4)	21.1	
25	17.9	10.9 11.6( 28.0)	9.3 9.9( 28.3)	13.0		
33		13.0	10.6	14.8		
42		15.5	12.2			

OIL AT MAX REAL OR PERMITTED RISE 24.0( 32.1) 16.6( 42.2) 13.5( 45.1) 16.0( 35.2) 24.1( 23.2) 60.7( 9.5)



TABLE 12

DIFFUSER PLUME DILUTION  
 PORT SPACING = 2 DIAMETERS, STABILITY STRATIFICATION PARAMETER = 500  
 CURRENT TO EFFLUENT RATIO = 0.02

		DENSIMETRIC FROUDE NUMBER					
		1	3	10	30	100	1000
1	: T)		2.1( 0.4)	2.0( 0.0)	2.0( 0.0)	2.0( 0.0)	2.0( 0.0)
	: M)	1.9	2.6	3.8	5.8	9.7	27.8
2	: T)		3.1	4.4	6.7	11.2	33.1
	: M)	2.7					
3	: T)		3.5	4.8	7.4	12.3	36.7
	: M)	3.6					
4	: T)	4.2( 3.7)					
	: M)	4.5	3.9	5.1	7.8	13.2	39.6
5	: T)		4.3	5.4	8.2	13.9	42.2
	: M)	5.4					
7	: T)		5.0	6.0	8.9	15.0	46.5
	: M)	6.9					
9	: T)		5.7	6.4	9.5	16.0	50.2
	: M)	8.4					55.3( 12.1)
12	: T)		6.8	7.0	10.2	17.3	
	: M)	10.4					
15	: T)		7.8	7.6	10.8	18.2	60.4
	: M)	12.6					
20	: T)		9.5	8.5	11.7	19.8	
	: M)	15.9					
25	: T)		11.2	9.3	12.5	21.1	
	: M)	19.2				22.3( 29.6)	
33	: T)	23.9	13.7	10.6	13.6	23.2	
	: M)	25.5( 35.8)					
42	: T)		16.5	12.0	14.9	25.8	
	: M)	28.6	18.0( 47.8)	13.8( 54.0)	15.1( 44.2)		
54	: T)		19.7		16.5		
	: M)						
70	: T)		23.5	16.2	19.5		
	: M)						

DEL AT MAX REAL OR PERMITTED RISE 40.5( 52.2) 27.4( 70.8) 19.9( 83.6) 20.5( 71.6) 29.3( 48.4) 73.9( 19.6)

TABLE 13

DIFFUSER PLUME DILUTION  
 PORT SPACING = 2 DIAMETERS, STABILITY STRATIFICATION PARAMETER = 2000  
 CURRENT TO EFFLUENT RATIO = 0.02

RISE(DIA)	DENSIMETRIC FROUDE NUMBER					
	1	3	10	30	100	1000
1	1.9	2.1( 0.4) 2.6	2.0( 0.0) 3.8	2.0( 0.0) 5.8	2.0( 0.0) 9.7	2.0( 0.0) 27.8
2	2.7	3.1	4.4	6.7	11.2	33.1
3	3.6	3.5	4.8	7.4	12.3	36.7
4	4.2( 3.7) 4.5	3.9	5.1	7.8	13.2	39.4
5	5.4	4.3	5.4	8.2	13.8	41.9
7	6.9	5.0	5.9	8.9	15.0	45.9
9	8.4	5.7	6.4	9.5	15.9	49.1
12	10.5	6.8	7.0	10.1	17.0	53.0
15	12.6	7.8	7.6	10.7	18.0	56.8
20	16.2	9.6	8.5	11.6	19.4	61.8
25	19.7	11.3	9.3	12.3	20.5	66.4
33	25.3	14.0	10.7	13.4	22.2	72.9 74.5( 35.4)
42	31.3	17.1	12.2	14.5	23.8	80.0
54	39.1	21.1	14.1	15.9	25.6	91.1
70	48.6 50.3( 73.6)	26.2	16.7	17.6	28.0 30.3( 87.0)	
90	58.4	32.2 35.4(102.0)	19.7	19.7	30.8	
115		38.9	23.4 25.3(129.0)	22.2 23.1(124.0)	34.4	
146		47.2	27.8	25.7		
190			34.7	32.6		

DIL AT MAX PEAK  
 OR PERMITTED RISE 93.0(107.0) 61.3(149.0) 41.1(194.0) 34.5(194.0) 41.2(143.0) 101.0( 58.2)

TABLE 14

DIFFUSER PLUME DILUTION  
 PORT SPACING = 2 DIAMETERS, STABILITY STRATIFICATION PARAMETER = 10000  
 CURRENT TO EFFLUENT RATIO = 0.02

RISE(DIA)	DENSIMETRIC FROUDE NUMBER					
	1	3	10	30	100	1000
1	1.9	2.1[ 0.4] 2.6	2.0[ 0.0] 3.8	2.0[ 0.0] 5.8	2.0[ 0.0] 9.7	2.0[ 0.0] 27.8
2	2.7	3.1	4.4	6.7	11.2	33.1
3	3.6	3.5	4.8	7.4	12.3	36.5
4	4.2[ 3.7] 4.5	3.9	5.1	7.8	13.2	39.4
5	5.4	4.3	5.4	8.2	13.8	41.6
7	6.9	5.0	5.9	8.9	14.9	45.5
9	8.4	5.7	6.4	9.5	15.9	48.8
12	10.6	6.8	7.0	10.1	17.0	52.7
15	12.7	7.8	7.6	10.7	18.0	56.1
20	16.3	9.6	8.5	11.6	19.3	60.8
25	19.8	11.4	9.3	12.3	20.4	64.5
33	25.4	14.1	10.7	13.4	22.0	70.1
42	31.8	17.3	12.2	14.4	23.5	75.2
54	40.2	21.4	14.2	15.8	25.2	81.2
70	51.2	26.9	16.9	17.4	27.2	88.2
90	64.8	33.8	20.1	19.4	29.6	96.1
115	81.1	42.2	24.1	21.8	32.2	105.0 107.0(123.0)
148	101.0 112.0(167.0)	52.8	29.4	25.1	35.6	116.0
190	123.0	65.8 78.6(236.0)	35.9	29.0	39.7	134.0
244		80.9	43.9	34.0	45.0 49.6(289.0)	

DIL AT MAX FEEL  
 OR PERMITTED RISE 161.0(243.0) 93.8(300.0) 51.7(300.0) 39.1(301.0) 50.8(301.0) 140.0(199.0)

TABLE 15

DIFFUSER PLUME DILUTION  
 PORT SPACING = 2 DIAMETERS, STABILITY STRATIFICATION PARAMETER = INFINITE  
 CURRENT TO EFFLUENT RATIO = 0.02

RISE(DIA)	DENSIMETRIC FROUDE NUMBFR					
	1	3	10	30	100	1000
1	1.9	2.1( 0.4)	2.0( 0.0)	2.0( 0.0)	2.0( 0.0)	2.0( 0.0)
2	2.7	3.1	4.4	6.7	11.2	33.1
3	3.6	3.5	4.8	7.4	12.3	36.5
4	4.2( 3.7)	3.9	5.1	7.8	13.2	39.4
5	5.4	4.3	5.4	8.2	13.8	41.6
7	6.9	5.0	5.9	8.9	14.9	45.5
9	8.4	5.7	6.4	9.5	15.9	48.8
12	10.6	6.8	7.0	10.1	17.0	52.7
15	12.7	7.8	7.6	10.7	18.0	55.7
20	16.3	9.6	8.5	11.6	19.3	60.5
25	19.8	11.4	9.3	12.3	20.4	64.2
33	25.6	14.1	10.7	13.4	22.0	69.5
42	32.0	17.3	12.2	14.4	23.4	74.4
54	40.5	21.5	14.2	15.7	25.1	80.0
70	51.9	27.1	16.9	17.4	27.1	86.4
90	66.2	34.0	20.2	19.4	29.2	93.1
115	84.1	42.8	24.4	21.8	31.8	100.0
148	108.0	54.3	29.8	25.0	35.1	109.0
190	137.0	69.0	36.6	29.0	38.7	117.0
244	175.0	87.7	45.6	34.0	43.3	128.0

DIL. AT MAX REAR,  
 OR PERMITTED RISE 215.0(301.0) 107.0(300.0) 54.7(301.0) 39.2(301.0) 47.9(302.0) 137.0(300.0)

TABLE 16

DIFFUSER PLUME DILUTION  
 PORT SPACING = 2 DIAMETERS, STABILITY STRATIFICATION PARAMETER = 200  
 CURRENT TO EFFLUENT RATIO = 0.00

		DENSIMETRIC FROUDE NUMBER					
		1	3	10	30	100	1000
1	: T)						
	: M)		2.1( 0.4)	2.0( 0.0)	2.0( 0.0)	2.0( 0.0)	2.0( 0.0)
2	: T)	1.9	2.6	3.7	5.6	8.8	22.2
	: M)						
3	: T)	2.7	3.0	4.2	6.3	10.1	25.4
	: M)						
4	: T)	3.6	3.5	4.6	6.9	11.0	27.8
	: M)	4.2( 3.6)					
5	: T)	4.5	3.8	4.9	7.3	11.7	29.6
	: M)						
7	: T)	5.3	4.2	5.2	7.6	12.3	31.1
	: M)						
9	: T)	6.8	4.9	5.7	8.2	13.2	33.8
	: M)						34.0( 7.3)
12	: T)	8.2	5.6	6.1	8.7	13.9	36.2
	: M)						
15	: T)	10.2	6.6	6.6	9.3	14.9	40.8
	: M)						
20	: T)	12.1	7.5	7.1	9.8	15.8	
	: M)					15.9( 15.8)	
25	: T)	15.1	9.0	8.0	10.6	17.0	
	: M)	16.1( 22.0)			11.0( 23.2)		
33	: T)	17.6	10.5	8.7	11.3	18.7	
	: M)		11.3( 28.4)	9.3( 29.4)			
42	: T)		12.5	9.8	12.4		
	: M)						
	: T)		14.1	10.8			
	: M)						

DIL AT MAX REFL  
 OR PERMITTED RISE 20.1( 32.3) 14.2( 43.2) 11.6( 47.8) 13.8( 38.8) 19.9( 26.7) 42.8( 12.4)

TABLE 17

DIFFUSER PLUME DILUTION  
 PORT SPACING = 2 DIAMETERS, STABILITY STRATIFICATION PARAMETER = 500  
 CURRENT TO EFFLUENT RATIO = 0.00

RISE (DIA)	DENSIMETRIC FROUDE NUMBER					
	1	3	10	30	100	1000
1	1.9	2.1( 0.4) 2.6	2.0( 0.0) 3.7	2.0( 0.0) 5.6	2.0( 0.0) 8.8	2.0( 0.0) 22.2
2	2.7	3.0	4.2	6.3	10.1	25.4
3	3.6	3.5	4.6	6.9	11.0	27.7
4	4.2( 3.6) 4.5	3.8	4.9	7.3	11.6	29.2
5	5.4	4.2	5.2	7.6	12.2	30.7
7	6.8	4.9	5.6	8.2	13.1	32.9
9	8.3	5.6	6.1	8.6	13.7	34.8
12	10.3	6.6	6.6	9.2	14.6	37.2
15	12.4	7.6	7.1	9.7	15.3	39.3 39.8( 15.8)
20	15.7	9.2	8.0	10.4	16.4	42.6
25	18.9	10.8	8.7	11.1	17.3	46.5
33	23.6 25.1( 35.9)	13.3	9.9	12.0	18.5 18.6( 33.8)	
42	28.2	15.9 17.5( 48.4)	11.2	12.8 13.5( 48.9)	19.8	
54		18.9	12.7 13.0( 56.5)	14.0	21.9	
70		21.8	14.6	15.3		

DIL AT MAX REAL OR PERMITTED RISE 31.5( 52.6) 22.0( 72.5) 16.3( 89.0) 16.8( 80.4) 23.3( 57.1) 49.7( 26.7)

TABLE 18

DIFFUSER PLUME DILUTION  
 PORT SPACING = 2 DIAMETERS, STABILITY STRATIFICATION PARAMETER = 2000  
 CURRENT TO EFFLUENT RATIO = 0.00

RISE(DIA)	DENSIMETRIC FPOUDE NUMBER					
	1	3	10	30	100	1000
1	1.9	2.1( 0.4) 2.6	2.0( 0.0) 3.7	2.0( 0.0) 5.6	2.0( 0.0) 8.8	2.0( 0.0) 22.0
2	2.7	3.0	4.2	6.3	10.1	25.4
3	3.6	3.5	4.6	6.9	11.0	27.5
4	4.2( 3.7) 4.5	3.8	4.9	7.3	11.6	29.2
5	5.4	4.2	5.2	7.6	12.1	30.5
7	6.8	4.9	5.6	8.2	13.0	32.7
9	8.3	5.6	6.0	8.6	13.7	34.3
12	10.4	6.6	6.6	9.2	14.5	36.5
15	12.6	7.6	7.1	9.7	15.2	38.2
20	16.0	9.3	8.0	10.3	16.2	40.6
25	19.4	10.9	8.8	10.9	16.9	42.6
33	24.9	13.6	10.0	11.8	18.0	45.2
42	30.7	16.6	11.3	12.7	19.1	47.9 49.9( 49.4)
54	38.3	20.4	13.1	13.7	20.2	51.2
70	47.7 49.9( 74.4)	25.3	15.3	15.0	21.5	55.4
90	57.3	31.1 34.6(104.0)	18.1	16.6	22.9 23.9(104.0)	
115		37.3	21.4 23.9(136.0)	18.4 19.8(138.0)	24.6	
146		43.2	25.2	20.5	26.7	
190			29.0	22.9		

DIL AT MAX PFAL  
 OR PERMITTED RISE 62.5(108.0) 43.4(153.0) 29.9(207.0) 24.9(225.0) 30.0(179.0) 62.7( 84.6)

TABLE 19

DIFFUSER PLUME DILUTION  
 PORT SPACING = 2 DIAMETERS, STABILITY STRATIFICATION PARAMETER = 10000  
 CURRENT TO EFFLUENT RATIO = 0.00

RISE(DIA)	DENSIMETRIC FROUDE NUMBER					
	1	3	10	30	100	1000
1	1.9	2.1( 0.4) 2.6	2.0( 0.0) 3.7	2.0( 0.0) 5.6	2.0( 0.0) 8.8	2.0( 0.0) 22.0
2	2.7	3.0	4.2	6.3	10.1	25.3
3	3.6	3.5	4.6	6.6	11.0	27.5
4	4.2( 3.7) 4.5	3.8	4.9	7.3	11.6	29.0
5	5.4	4.2	5.2	7.6	12.1	30.5
7	6.9	4.9	5.6	8.2	13.0	32.7
9	8.3	5.6	6.0	8.6	13.6	34.3
12	10.5	6.6	6.6	9.2	14.5	36.2
15	12.6	7.6	7.1	9.7	15.1	38.0
20	16.1	9.3	8.0	10.3	16.1	40.2
25	19.6	11.0	8.8	10.9	16.9	42.0
33	25.1	13.7	10.0	11.8	17.9	44.5
42	31.3	16.7	11.4	12.6	18.9	46.8
54	39.6	20.7	13.2	13.7	19.9	49.2
70	50.5	26.0	15.6	15.0	21.2	52.0
90	63.9	32.7	18.5	16.7	22.5	54.8
115	79.7	40.8	22.3	18.5	23.9	58.0
148	99.6 111.0(169.0)	50.9	27.1	20.9	25.6	61.5 65.1(187.0)
190	121.0	63.4 76.9(240.0)	32.9	23.9	27.5	65.4
244	139.0	77.8	40.2	27.6	29.8	70.3

OIL AT MAX FEAL  
 OR PERMITTED RISE 139.0(245.0) 90.2(300.0) 47.4(300.0) 31.7(301.0) 31.9(302.0) 76.2(300.0)



TABLE 20

DIFFUSER PLUME DILUTION  
 PORT SPACING = 2 DIAMETERS, STABILITY STRATIFICATION PARAMETER = INFINITE  
 CURRENT TO EFFLUENT RATIO = 0.00

		DENSIMETRIC FROUDE NUMBER					
		1	3	10	30	100	1000
RISE(DIA)	: M]		2.1( 0.4)	2.0( 0.0)	2.0( 0.0)	2.0( 0.0)	2.0( 0.0)
1	: M]	1.9	2.6	3.7	5.6	8.8	22.0
2	: M]	2.7	3.0	4.2	6.3	10.1	25.3
3	: M]	3.6	3.5	4.6	6.9	11.0	27.5
4	: M]	4.2( 3.7)	3.8	4.9	7.3	11.6	29.0
5	: M]	5.4	4.2	5.2	7.6	12.1	30.5
7	: M]	6.9	4.9	5.6	8.2	13.0	32.7
9	: M]	8.3	5.6	6.0	8.6	13.6	34.3
12	: M]	10.5	6.6	6.6	9.2	14.5	36.2
15	: M]	12.6	7.6	7.1	9.7	15.1	38.0
20	: M]	16.1	9.3	8.0	10.3	16.1	40.2
25	: M]	19.6	11.0	8.8	10.9	16.9	42.0
33	: M]	25.3	13.7	10.0	11.8	17.9	44.4
42	: M]	31.5	16.8	11.4	12.6	18.9	46.5
54	: M]	39.9	20.8	13.2	13.7	19.9	48.9
70	: M]	51.2	26.2	15.7	15.0	21.1	51.5
90	: M]	65.3	32.9	18.6	16.7	22.4	54.2
115	: M]	82.5	41.3	22.5	18.5	23.8	56.9
148	: M]	106.0	52.5	27.5	21.0	25.5	59.9
190	: M]	135.0	66.6	33.8	24.1	27.3	63.0
244	: M]	173.0	84.7	41.8	28.1	29.5	66.2

DIL AT MAX REAL  
 OR PERMITTED RISE 212.0(301.0) 103.0(301.0) 50.2(301.0) 32.1(301.0) 31.7(301.0) 69.1(301.0)

TABLE 21

DIFFUSER PLUME DILUTION  
 PORT SPACING = 5 DIAMETERS, STABILITY STRATIFICATION PARAMETER = 200  
 CUPRENT TO EFFLUENT RATIO = 0.10

		DENSIMETRIC FROUDE NUMBER					
		1	3	10	30	100	1000
1	: T)						
	: M)			6.3( 1.0)	6.2( 0.1)	6.2( 0.0)	6.2( 0.0)
	: T)	1.9	2.8	6.4	11.8	22.2	85.6
	: M)						
2	: T)						
	: M)						110.0
	: T)	2.7	3.7	8.2	14.4	27.3	117.0( 2.4)
	: M)						
3	: T)						
	: M)						131.0
	: T)	3.5	4.6	9.6	16.4	31.1	
	: M)						
4	: T)						
	: M)						
	: T)	4.5	5.6	10.9	18.2	34.3	
	: M)						
5	: T)						
	: M)						37.3
	: T)	5.5	6.6	12.0	20.0	37.3	
	: M)					41.6( 6.6)	
7	: T)						
	: M)						
	: T)	8.1	8.8	14.4	23.3	42.8	
	: M)						
9	: T)						
	: M)						48.5
	: T)	10.8	9.1( 7.3)	16.8	26.3	48.5	
	: M)		11.0		28.4( 10.3)		
12	: T)						
	: M)						
	: T)	15.4	14.0	20.4	31.3		
	: M)			23.1( 14.2)			
15	: T)						
	: M)						
	: T)	18.1( 13.7)	17.0	24.4	36.7		
	: M)	20.3	20.4( 18.3)				
20	: T)						
	: M)						
	: T)	23.9( 17.7)	22.5	33.1			
	: M)	26.9					
25	: T)						
	: M)						
	: T)		34.1				
	: M)						

DIL AT MAX REAL  
 OR PERMITTED RISE 52.7( 24.4) 41.3( 25.6) 35.9( 20.8) 40.0( 16.0) 57.5( 10.6) 163.0( 3.8)

TABLE 22

DIFFUSER PLUME DILUTION  
 PORT SPACING = 5 DIAMETERS, STABILITY STRATIFICATION PARAMETER = 500  
 CURRENT TO EFFLUENT RATIO = 0.10

		DENSIMETRIC FROUDE NUMBER					
		1	3	10	30	100	1000
RISE(DIA)	: T)						
	: M)			6.3( 1.0)	6.2( 0.1)	6.2( 0.0)	6.2( 0.0)
1	: T)	1.9	2.8	6.4	11.7	22.2	85.0
	: M)						
2	: T)	2.7	3.7	8.2	14.3	27.1	107.0
	: M)						
3	: T)	3.6	4.6	9.6	16.3	30.9	123.0
	: M)						
4	: T)	4.5	5.6	10.8	18.1	33.8	137.0
	: M)						146.0( 4.7)
5	: T)	5.6	6.6	12.0	19.8	36.5	150.0
	: M)						
7	: T)	8.1	8.1	14.2	22.9	41.3	180.0
	: M)						
9	: T)	10.9	9.3( 7.5)	16.4	26.0	45.9	
	: M)		10.9				
12	: T)	15.6	14.0	19.7	30.3	51.9	
	: M)					54.2( 13.1)	
15	: T)	19.6( 14.3)	17.0	23.1	34.8	58.4	
	: M)	20.8			40.5( 19.1)		
20	: T)	28.2	21.9	28.8	41.9	70.5	
	: M)			35.0( 24.9)			
25	: T)	35.0	26.7	35.2	49.8		
	: M)	37.8( 27.3)	31.8( 30.0)				
33	: T)	44.9	35.3	48.8			
	: M)						

DIL AT MAX REAL  
 OR PERMITTED RISE 87.4( 37.9) 68.4( 41.7) 56.6( 35.8) 58.1( 29.1) 75.2( 20.7) 204.0( 7.6)

TABLE 23

DIFFUSER PLUME DILUTION  
 PORT SPACING = 5 DIAMETERS, STABILITY STRATIFICATION PARAMETER = 2000  
 CURRENT TO EFFLUENT RATIO = 0.10

PISE(DIA)	DENSIMETRIC FROUDE NUMBER					
	1	3	10	30	100	1000
1	1.9	2.8	6.3( 1.0) 6.4	6.2( 0.1) 11.7	5.2( 0.0) 22.0	6.2( 0.0) 84.4
2	2.7	3.7	8.2	14.3	27.1	105.0
3	3.6	4.6	9.5	16.3	30.7	120.0
4	4.5	5.6	10.8	18.1	33.6	132.0
5	5.6	6.6	12.0	19.7	36.2	143.0
7	8.1	8.7	14.2	22.8	40.8	161.0
9	10.9	9.4( 7.6) 10.9	16.3	25.8	44.9	176.0
12	15.7	14.0	19.4	30.0	50.5	197.0 206.0( 13.3)
15	20.2( 14.6) 21.0	17.0	22.5	34.0	56.1	217.0
20	28.8	21.8	27.7	40.8	64.4	257.0
25	36.2	26.7	32.7	47.5	73.0	
33	47.5	34.3	41.0	58.4	85.7 88.1( 34.6)	
42	59.7 74.0( 53.2)	42.8	51.2	70.5 75.4( 45.6)	101.0	
54	75.2	54.5 62.6( 62.3)	66.2 68.1( 55.4)	87.8		
70	95.2	71.5	93.7			

DIL AT MAX REAL  
 OR PERMITTED RISE 181.0( 75.0) 143.0( 85.9) 114.0( 77.5) 109.0( 66.7) 123.0( 53.1) 288.0( 21.5)

TABLE 24

DIFFUSER PLUME DILUTION  
 PORT SPACING = 5 DIAMETERS, STABILITY STRATIFICATION PARAMETER = 10000  
 CURRENT TO EFFLUENT RATIO = 0.10

RISE(DIA)	DENSIMETRIC FROUDE NUMBER					
	1	3	10	30	100	1000
1	1.9	2.8	6.3( 1.0) 6.4	6.2( 0.1) 11.7	6.2( 0.0) 22.0	6.2( 0.0) 84.4
2	2.7	3.7	8.2	14.3	27.1	105.0
3	3.6	4.6	9.5	16.3	30.7	119.0
4	4.5	5.6	10.8	18.3	33.6	131.0
5	5.6	6.6	12.0	19.7	36.2	141.0
7	8.1	8.7	14.1	22.8	40.8	157.0
9	10.9	9.5( 7.7) 10.9	16.3	25.6	44.9	171.0
12	15.7	14.0	19.4	29.8	50.5	189.0
15	20.4( 14.7) 21.1	17.0	22.5	34.0	55.7	204.0
20	29.0	21.8	27.5	40.5	63.9	227.0
25	36.5	26.7	32.2	47.1	71.9	247.0
33	48.5	34.3	40.2	57.6	84.4	276.0
42	61.3	42.8	48.8	69.0	97.5	305.0 312.0( 44.2)
54	78.7	54.2	60.9	84.4	115.0	345.0
70	101.0	69.5	77.1	105.0	138.0	
90	123.0	88.2	98.6	131.0 162.0(113.0)	166.0 173.0( 95.3)	
115	160.0 164.0(118.0)	112.0 138.0(142.0)	128.0 152.0(132.0)	165.0	202.0	
148	200.0	145.0	177.0	212.0		
190		241.0				

DIL AT MAX FEAL  
 OR PERMITTED RISE 257.0(166.0) 318.0(195.0) 256.0(191.0) 232.0(161.0) 237.0(139.0) 351.0( 55.8)

TABLE 25

DIFFUSER PLUME DILUTION  
 PORT SPACING = 5 DIAMETERS, STABILITY STRATIFICATION PARAMETER = INFINITE  
 CURRENT TO EFFLUENT RATIO = 0.10

RISE(DIA)	DENSIMETRIC FROUDE NUMBER					
	1	3	10	30	100	1000
1	1.9	2.8	6.3( 1.0) 6.4	6.2( 0.1) 11.7	6.2( 0.0) 22.0	6.2( 0.0) 84.4
2	2.7	3.7	8.2	14.3	27.1	105.0
3	3.6	4.6	9.5	16.3	30.7	119.0
4	4.5	5.6	10.8	18.0	33.6	131.0
5	5.6	6.6	12.0	19.7	36.2	141.0
7	8.1	8.7	14.1	22.8	40.8	157.0
9	10.9	9.5( 7.7) 10.9	16.3	25.6	44.6	170.0
12	15.7	14.0	19.4	29.8	50.2	188.0
15	20.5( 14.7) 21.1	17.0	22.3	33.8	55.7	203.0
20	29.0	21.8	27.3	40.5	63.9	223.0
25	36.7	26.7	32.2	47.1	71.4	242.0
33	48.5	34.3	39.9	57.2	83.8	267.0
42	61.8	42.8	48.5	68.5	96.7	291.0
54	79.3	54.1	60.1	83.8	114.0	320.0
70	103.0	69.5	75.0	104.0	136.0	355.0
90	132.0	88.2	93.8	128.0	164.0	
115	169.0	112.0	117.0	159.0	198.0	
148	216.0	143.0	149.0	200.0	242.0	
190	277.0	183.0	188.0	251.0	297.0	
244		234.0	239.0			

DIL AT MAX PFAI.  
 OR PERMITTED RISE 333.0(228.0) 286.0(299.0) 284.0(294.0) 312.0(240.0) 315.0(204.0) 362.0( 73.4)

TABLE 26

DIFFUSER PLUME DILUTION  
 PORT SPACING = 5 DIAMETERS, STABILITY STRATIFICATION PARAMETER = 200  
 CURRENT TO EFFLUENT RATIO = 0.05

RISE(DIA)	DENSIMETRIC FROUDE NUMBER						
	1	3	10	30	100	1000	
1	1.9	2.8	5.7( 0.9) 5.8	5.6( 0.1) 9.9	5.6( 0.0) 17.6	5.6( 0.0) 62.2	
2	2.7	3.6	7.1	11.8	21.3	77.6 90.4( 3.0)	
3	3.6	4.4	8.0	13.2	23.7		
4	4.6	5.1	8.7	14.2	26.0	103.0	
5	5.6	6.0	9.4	15.2	28.0		
7	8.1	7.6	10.6	16.9	31.3 33.1( 8.1)		
9	10.8	9.2( 8.9) 9.4	11.8	18.6	34.5		
12	15.4	11.7	13.5	21.0 21.6( 12.8)	40.2		
15	18.0( 13.7) 20.0 23.4( 17.9)	13.8	15.1 16.7( 17.7)	23.4			
20	25.6	17.2 17.3( 20.3)	18.3	28.6			
25		20.4	22.3				

DIL AT MAX REAL OR PERMITTED RISE 44.2( 25.0) 31.1( 29.6) 26.3( 27.1) 29.9( 20.4) 45.1( 13.2) 124.0( 4.9)

TABLE 27

DIFFUSER PLUME DILUTION  
 PORT SPACING = 5 DIAMETERS, STABILITY STRATIFICATION PARAMETER = 500  
 CURRENT TO EFFLUENT RATIO = 0.05

		DENSIMETRIC FROUDE NUMBER					
		1	3	10	30	100	1000
RISE(DIA)	: T)						
	: M)						
1	: T)	1.9	2.8	5.7( 0.9)	5.6( 0.1)	5.6( 0.0)	5.6( 0.0)
	: M)			5.8	9.9	17.6	61.8
2	: T)	2.7	3.6	7.1	11.8	21.3	76.6
	: M)						
3	: T)	3.6	4.4	8.0	13.1	23.7	87.4
	: M)						
4	: T)	4.6	5.1	8.7	14.1	25.8	96.3
	: M)						
5	: T)	5.7	6.0	9.3	15.1	27.7	104.0
	: M)						112.0( 6.1)
7	: T)	8.1	7.6	10.6	16.8	30.7	119.0
	: M)						
9	: T)	10.9	9.4	11.6	18.2	33.3	137.0
	: M)						
12	: T)	15.5	9.5( 9.1)	13.3	20.4	36.7	
	: M)		11.8				
15	: T)	19.4( 14.3)		14.8		40.2	
	: M)	20.7	14.0			41.6( 16.4)	
20	: T)	27.5	17.5	17.4	25.8	45.8	
	: M)				29.2( 25.0)		
25	: T)	33.6	21.0	20.0	29.4	52.6	
	: M)	36.2( 27.5)		24.1( 32.7)			
33	: T)	41.8	26.0	24.2	35.5		
	: M)		26.5( 33.9)				
42	: T)		31.8	30.5			
	: M)						

DIL AT MAX REAL  
 OR PERMITTED RISE 74.4( 39.0) 52.7( 48.9) 42.0( 48.7) 42.4( 38.7) 57.2( 26.4) 154.0( 9.8)



TABLE 28

DIFFUSER PLUME DILUTION  
 PORT SPACING = 5 DIAMETERS, STABILITY STRATIFICATION PARAMETER = 2000  
 CURRENT TO EFFLUENT RATIO = 0.05

RISE(DIA)	DENSIMETRIC FROUDE NUMBER					
	1	3	10	30	100	1000
1	1.9	2.8	5.7( 0.9) 5.8	5.6( 0.1) 9.9	5.6( 0.0) 17.6	5.6( 0.0) 61.8
2	2.7	3.6	7.1	11.8	21.1	76.0
3	3.6	4.4	8.0	13.1	23.6	86.1
4	4.6	5.1	8.7	14.1	25.6	93.6
5	5.7	6.0	9.3	15.0	27.5	101.0
7	8.1	7.6	10.5	16.7	30.3	112.0
9	10.9	9.4	11.6	18.1	32.7	123.0
12	15.6	9.6( 9.3) 11.9	13.2	20.2	36.0	136.0
15	20.1( 14.6) 21.0	14.1	14.7	22.2	39.1	147.0 156.0( 17.5)
20	28.4	17.8	17.1	25.3	43.7	166.0
25	35.2	21.3	19.6	28.2	48.1	187.0
33	45.9	26.9	23.4	32.9	54.5	
42	56.8	33.1	27.8	38.3	62.0 64.3( 44.9)	
54	70.7 71.0( 54.5)	41.0	33.6	45.5 51.6( 63.4)	72.1	
70	85.6	51.0 51.6( 71.1)	41.6 45.2( 77.2)	56.3	88.2	
90		63.2	53.1	74.4		

DIL AT MAX REFL  
 OR PERMITTED RISE 160.0( 77.9) 116.0(102.0) 89.7(110.0) 79.4( 93.6) 90.3( 70.6) 216.0( 28.2)

TABLE 29

DIFFUSER PLUME DILUTION  
 PORT SPACING = 5 DIAMETERS, STABILITY STRATIFICATION PARAMETER = 10000  
 CURRENT TO EFFLUENT RATIO = 0.05

RISE(DIA)	DENSIMETRIC FPOUDE NUMBER					
	1	3	10	30	100	1000
1	1.9	2.8	5.7( 0.9) 5.8	5.6( 0.1) 9.9	5.6( 0.0) 17.6	5.6( 0.0) 61.8
2	2.7	3.6	7.1	11.8	21.1	75.5
3	3.6	4.4	8.0	13.1	23.6	85.6
4	4.6	5.1	8.7	14.1	25.6	93.6
5	5.7	6.0	9.3	15.0	27.3	100.0
7	8.1	7.6	10.5	16.7	30.3	111.0
9	10.9	9.4	11.6	18.1	32.7	120.0
12	15.7	9.7( 9.3) 11.9	13.2	20.1	35.7	132.0
15	20.4( 14.7) 21.0	14.1	14.7	22.0	38.8	142.0
20	28.6	17.9	17.1	25.1	43.1	157.0
25	35.7	21.4	19.6	27.8	47.5	169.0
33	46.8	27.1	23.4	32.4	53.8	187.0
42	58.8	33.6	27.7	37.2	60.5	204.0
54	75.0	41.9	33.1	43.7	69.4	226.0 233.0( 58.3)
70	95.6	53.0	40.8	52.3	80.7	254.0
90	120.0	66.5	49.8	62.9	94.9	
115	150.0 156.0(121.0)	83.4	61.6	76.9	113.0 124.0(130.0)	
148	182.0	104.0 114.0(165.0)	77.3 98.0(190.0)	97.0 109.0(166.0)	137.0	
190		129.0	98.3	127.0	169.0	
244			140.0			

DIL AT MAX REAL OR PERMITTED WISE 209.0(173.0) 262.0(235.0) 214.0(265.0) 177.0(237.0) 175.0(196.0) 276.0( 81.1)

TABLE 30

DIFFUSER PLUME DILUTION  
 PORT SPACING = 5 DIAMETERS, STABILITY STRATIFICATION PARAMETER = INFINITE  
 CURRENT TO EFFLUENT RATIO = 0.05

		DENSIMETRIC FROUDE NUMBER					
		1	3	10	30	100	1000
RISE(DIA)	: M]			5.7[ 0.9]	5.6[ 0.1]	5.6[ 0.0]	5.0[ 0.0]
1	: M]	1.9	2.8	5.8	9.9	17.6	61.8
2	: M]	2.7	3.6	7.1	11.8	21.1	75.5
3	: M]	3.6	4.4	8.0	13.1	23.6	85.6
4	: M]	4.6	5.1	8.7	14.1	25.6	93.0
5	: M]	5.7	6.0	9.3	15.0	27.3	99.6
7	: M]	8.1	7.6	10.5	16.7	30.3	111.0
9	: M]	10.9	9.4	11.6	18.1	32.7	120.0
12	: M]	15.7	9.7[ 9.3]	13.2	20.1	35.7	131.0
15	: M]	20.4[ 14.7]	11.9	14.6	22.0	38.8	141.0
20	: M]	21.0	14.1	17.1	25.1	43.1	155.0
25	: M]	28.6	17.9	19.6	27.8	47.1	166.0
33	: M]	35.7	21.4	23.3	32.2	53.4	183.0
42	: M]	47.1	27.3	27.5	37.0	60.1	198.0
54	: M]	59.3	33.6	33.1	43.4	69.0	216.0
70	: M]	76.0	42.2	40.5	51.2	80.2	237.0
90	: M]	98.3	53.4	49.8	61.5	93.7	260.0
115	: M]	125.0	67.6	61.5	73.6	110.0	
148	: M]	160.0	85.5	76.6	90.0	132.0	
190	: M]	204.0	109.0	95.7	110.0	159.0	
244	: M]	262.0	138.0	120.0	136.0	194.0	

DIL AT MAX REAL  
 OR PERMITTED RISE 325.0(237.0) 216.0(300.0) 146.0(301.0) 163.0(300.0) 229.0(300.0) 286.0(114.0)

TABLE 31

DIFFUSER PLUME DILUTION  
 PORT SPACING = 5 DIAMETERS, STABILITY STRATIFICATION PARAMETER = 200  
 CURRENT TO EFFLUENT RATIO = 0.02

RISE(DIA)	DENSIMETRIC FROUDE NUMBER					
	1	3	10	30	100	1000
1	: T)					
	: M)	1.9	2.7	5.3( 0.9) 5.5	5.3( 0.1) 6.9	5.3( 0.0) 14.7
2	: T)					
	: M)	2.7	3.6	6.6	10.3	17.3
3	: T)					
	: M)	3.6	4.3	7.3	11.2	19.0
4	: T)					
	: M)	4.6	5.1	7.9	12.0	20.5
5	: T)					
	: M)	5.7	5.9	8.4	12.7	21.7
7	: T)					
	: M)	8.1	7.5	9.3	13.8	23.9
9	: T)					
	: M)	10.8	9.1( 8.9) 9.2	10.1	14.8	25.8
12	: T)					
	: M)	15.2	11.3	11.2	16.1 17.4( 15.2)	28.4
15	: T)					
	: M)	18.0( 13.7) 19.8	13.3	12.2		31.8
20	: T)					
	: M)	23.1( 17.8)		13.8( 20.1)		
25	: T)					
	: M)	25.3	16.1 16.5( 20.8)		19.6	
25	: T)					
	: M)	29.5	18.6	15.5		

DIL AT MAX REAL  
 OR PERMITTED RISE 35.8( 25.1) 24.2( 30.9) 19.4( 32.1) 23.0( 24.8) 34.9( 16.2) 90.3( 6.5)

TABLE 32

DIFFUSER PLUME DILUTION  
 PORT SPACING = 5 DIAMETERS, STABILITY STRATIFICATION PARAMETER = 500  
 CURRENT TO EFFLUENT RATIO = 0.02

RISE(DIA)	DENSIMETRIC PROUDE NUMBER					
	1	3	10	30	100	1000
1	1.9	2.7	5.3( 0.9) 5.5	5.3( 0.1) 8.8	5.3( 0.0) 14.7	5.3( 0.0) 44.3
2	2.7	3.6	6.6	10.3	17.3	53.4
3	3.6	4.3	7.3	11.2	19.0	59.7
4	4.6	5.1	7.8	12.0	20.4	65.3
5	5.7	5.9	8.4	12.6	21.5	69.5
7	8.1	7.5	9.2	13.7	23.4	77.6 82.1( 8.2)
9	10.9	9.2	10.0	14.6	25.1	85.5
12	15.5	9.3( 9.2) 11.5	11.1	15.8	27.3	97.9
15	19.4( 14.3) 20.5	13.6	12.1	16.9	29.0	
20	27.3	16.7	13.7	18.5	32.0 32.2( 20.6)	
25	33.1 35.7( 27.6)	19.7	15.4	20.0 21.7( 31.0)	34.8	
33	40.9	24.3 25.1( 34.9)	17.8 19.3( 38.4)	22.5	41.0	
42		28.6	20.4	25.4		
54			24.3			

DIL AT MAX REAL  
 OR PERMITTED RISE 60.6( 39.4) 40.2( 51.4) 29.2( 59.5) 30.0( 50.0) 42.7( 33.6) 111.0( 13.3)

TABLE 33

DIFFUSER PLUME DILUTION  
 PORT SPACING = 5 DIAMETERS, STABILITY STRATIFICATION PARAMETER = 2000  
 CURRENT TO EFFLUENT RATION = 0.02

RISE(DIA)	DENSIMETRIC FROUDE NUMBER					
	1	3	10	30	100	1000
1	1.9	2.7	5.3( 0.9) 5.5	5.3( 0.1) 8.8	5.3( 0.0) 14.7	5.3( 0.0) 44.3
2	2.7	3.6	6.6	10.3	17.3	53.0
3	3.6	4.3	7.3	11.2	18.9	59.3
4	4.6	5.1	7.8	12.0	20.2	64.4
5	5.7	5.9	8.4	12.6	21.4	68.5
7	8.1	7.5	9.2	13.6	23.3	75.5
9	10.9	9.2	10.0	14.5	24.7	80.9
12	15.6	9.5( 9.3) 11.6	11.1	15.7	26.7	88.3
15	20.1( 14.6) 20.8	13.6	12.1	16.7	28.4	95.2
20	28.2	17.0	13.7	18.1	30.9	105.0 112.0( 23.8)
25	34.8	20.2	15.3	19.6	32.9	114.0
33	44.9	25.4	17.9	21.5	35.8	129.0
42	55.7	30.9	20.7	23.7	39.0	
54	68.8 69.5( 54.9)	38.0	24.2	26.5	43.1 44.8( 59.7)	
70	82.8	47.0 48.9( 74.1)	29.0	30.2 33.8( 65.4)	48.4	
90		56.3	34.5 35.3( 93.1)	35.0	56.3	
115			41.3	42.2		

DIL AT 4X REAL  
 OR PERMITTED RISE 136.0( 79.1) 90.1(108.0) 61.5(139.0) 52.7(133.0) 61.9( 97.2) 152.0( 39.0)

TABLE 34

DIFFUSER PLUME DILUTION  
 PORT SPACING = 5 DIAMETERS, STABILITY STRATIFICATION PARAMETER = 10000  
 CURRENT TO EFFLUENT RATIO = 0.02

		DENSIMETRIC FROUDE NUMBER					
		1	3	10	30	100	1000
1	: T)			5.3( 0.9)	5.3( 0.1)	5.3( 0.0)	5.3( 0.0)
	: M)	1.9	2.7	5.5	8.8	14.7	44.3
2	: T)						
	: M)	2.7	3.6	6.6	10.3	17.3	53.0
3	: T)						
	: M)	3.6	4.3	7.3	11.2	18.9	59.3
4	: T)						
	: M)	4.6	5.1	7.8	12.0	20.2	63.9
5	: T)						
	: M)	5.7	5.9	8.4	12.6	21.4	68.1
7	: T)						
	: M)	8.1	7.5	9.2	13.6	23.3	75.0
9	: T)						
	: M)	10.9	9.2	10.0	14.5	24.7	80.4
12	: T)						
	: M)	15.6	9.5( 3.3) 11.6	11.1	15.7	26.7	87.2
15	: T)						
	: M)	20.2( 14.6) 21.0	13.7	12.1	16.7	28.2	93.1
20	: T)						
	: M)	28.4	17.1	13.7	18.1	30.7	102.0
25	: T)						
	: M)	35.2	20.4	15.5	19.4	32.7	109.0
33	: T)						
	: M)	45.9	25.6	18.0	21.4	35.4	119.0
42	: T)						
	: M)	57.6	31.5	20.8	23.4	38.1	128.0
54	: T)						
	: M)	73.5	39.4	24.6	26.2	41.6	140.0
70	: T)						
	: M)	93.0	49.5	29.6	29.6	46.0	153.0 163.0( 81.6)
90	: T)						
	: M)	117.0	61.7	35.7	33.7	51.2	170.0
115	: T)						
	: M)	145.0 153.0(123.0)	77.0	43.3	39.0	57.5	192.0
140	: T)						
	: M)	176.0	95.5 108.0(171.0)	52.9	45.8	65.8	
190	: T)						
	: M)		117.0	64.7 76.0(232.0)	54.4	76.8 77.2(192.0)	
244	: T)						
	: M)		139.0	79.2	65.7 66.2(247.0)	92.8	

DIL AT MAX REAR  
 OR PERMITTED RISE 194.0(176.0) 191.0(249.0) 93.7(300.0) 79.2(300.0) 115.0(296.0) 201.0(124.0)

TABLE 35

DIFFUSER PLUME DILUTION  
 PORT SPACING = 5 DIAMETERS, STABILITY STRATIFICATION PARAMETER = INFINITE  
 CURRENT TO EFFLUENT RATIO = 0.02

RISE(DIA)	DENSIMETRIC FROUDE NUMBER					
	1	3	10	30	100	1000
1	1.9	2.7	5.3( 0.9) 5.5	5.3( 0.1) 8.8	5.3( 0.0) 14.7	5.3( 0.0) 44.3
2	2.7	3.6	6.6	10.3	17.3	53.0
3	3.6	4.3	7.3	11.2	18.9	59.3
4	4.6	5.1	7.8	12.0	20.2	63.9
5	5.7	5.9	8.4	12.6	21.4	68.1
7	8.1	7.5	9.2	13.6	23.3	74.5
9	10.9	9.2	10.0	14.5	24.7	79.8
12	15.7	9.5( 9.4) 11.6	11.1	15.7	26.7	86.6
15	20.4( 14.7) 21.0	13.7	12.1	16.7	28.2	92.6
20	28.4	17.1	13.7	18.1	30.5	101.0
25	35.5	20.5	15.5	19.4	32.4	108.0
33	46.2	25.8	18.0	21.4	35.2	117.0
42	58.4	31.8	20.8	23.4	37.9	126.0
54	74.0	39.6	24.6	26.2	41.5	136.0
70	95.6	50.2	29.6	29.4	45.5	148.0
90	122.0	63.1	36.0	33.6	50.5	160.0
115	154.0	79.2	43.7	38.7	56.3	173.0
148	198.0	101.0	54.1	45.4	63.6	189.0
190	253.0	128.0	67.3	53.9	72.5	207.0
244		163.0	83.9	64.5	83.4	

DIL AT MAX REAL  
 OR PERMITTED RISE 321.0(242.0) 200.0(300.0) 101.0(300.0) 75.7(301.0) 94.6(300.0) 208.0(194.0)



TABLE 36

DIFFUSER PLUME DILUTION  
 PORT SPACING = 5 DIAMETERS, STABILITY STRATIFICATION PARAMETER = 200  
 CURRENT TO EFFLUENT RATIO = 0.00

RISE(DIA)	DENSIMETRIC FROUDE NUMBER					
	1	3	10	30	100	1000
1	1.9	2.7	5.1( 0.9) 5.3	5.0( 0.1) 8.2	5.0( 0.0) 12.9	5.0( 0.0) 32.0
2	2.7	3.5	6.2	9.3	14.8	37.0
3	3.6	4.3	6.9	10.1	16.0	40.5
4	4.6	5.0	7.4	10.7	17.0	43.1
5	5.7	5.8	7.8	11.2	17.9	45.5 46.5( 5.5)
7	8.1	7.4	8.6	12.1	19.2	50.2
9	10.8	9.0( 8.9) 9.1	9.3	12.8	20.4 21.7( 11.8)	56.2
12	15.2	11.2	10.3	13.7	21.9	
15	18.0( 13.7) 19.8 23.1( 17.9)	13.0	11.1	14.6 15.0( 16.9)	23.4	
20	25.1	15.7 16.1( 21.1)	12.5 12.8( 21.6)	15.9		
25	28.3	17.9	13.6	17.2		
33			15.4			

DIL AT MAX REAL OR PERMITTED RISE 28.3( 25.2) 19.8( 31.5) 16.0( 34.7) 18.8( 28.3) 27.0( 19.6) 58.0( 9.1)

TABLE 37

DIFFUSER PLUME DILUTION  
 PORT SPACING = 5 DIAMETERS, STABILITY STRATIFICATION PARAMETER = 500  
 CURRENT TO EFFLUENT RATIO = 0.00

RISE(DIA)	DENSIMETRIC FROUDE NUMBER					
	1	3	10	30	100	1000
1	: T)					
	: M)			5.1( 0.9)	5.0( 0.1)	5.0( 0.0)
2	: T)	1.9	2.7	5.3	8.2	12.9
	: M)					32.0
3	: T)	2.7	3.5	6.2	9.3	14.7
	: M)					36.7
4	: T)	3.6	4.3	6.9	10.1	16.0
	: M)					39.9
5	: T)	4.6	5.0	7.4	10.7	16.9
	: M)					42.5
7	: T)	5.7	5.8	7.8	11.2	17.7
	: M)					44.6
9	: T)	8.1	7.4	8.6	12.0	19.0
	: M)					47.8
12	: T)	10.9	9.1	9.3	12.7	20.0
	: M)		9.2( 9.1)			50.8
15	: T)	15.5	11.3	10.3	13.5	21.3
	: M)					53.9( 11.6)
20	: T)	19.3( 14.2)				
	: M)	20.5	13.3	11.2	14.3	22.5
25	: T)	27.1	16.3	12.6	15.5	24.0
	: M)					25.2( 24.7)
33	: T)	32.9	19.2	13.9	16.4	25.4
	: M)	35.5( 27.7)				
42	: T)	40.3	23.4	16.0	17.9	27.5
	: M)		24.4( 35.3)	17.8( 40.9)	18.2( 35.3)	
54	: T)		27.4	18.1	19.4	
	: M)					
	: T)			20.5	21.4	
	: M)					

DIL AT MAX REAL OR PERMITTED RISE 43.8( 39.6) 30.3( 52.6) 22.2( 64.8) 22.8( 58.9) 31.6( 41.9) 67.5( 19.6)

TABLE 38

DIFFUSER PLUME DILUTION  
 PORT SPACING = 5 DIAMETERS, STABILITY STRATIFICATION PARAMETER = 2000  
 CURRENT TO EFFLUENT RATIO = 0.00

RISE(DIA)	DENSIMETRIC FROUDE NUMBER					
	1	3	10	30	100	1000
1	1.9	2.7	5.1( 0.9) 5.3	5.0( 0.1) 8.2	5.0( 0.0) 12.9	5.0( 0.0) 32.0
2	2.7	3.5	6.2	9.3	14.7	36.7
3	3.6	4.3	6.9	10.1	16.0	39.6
4	4.6	5.0	7.4	10.7	16.9	42.2
5	5.7	5.8	7.8	11.2	17.6	44.0
7	8.1	7.4	8.6	12.0	18.9	47.1
9	10.9	9.1	9.3	12.6	19.8	49.8
12	15.6	9.4( 9.3) 11.4	10.3	13.5	21.1	52.7
15	20.1( 14.6) 20.8	13.5	11.2	14.2	22.2	55.4
20	28.0	16.7	12.6	15.3	23.4	58.7
25	34.5	19.8	14.0	16.3	24.7	61.8
33	44.6	24.6	16.2	17.8	26.3	66.1 67.7( 36.4)
42	54.9	29.8	18.8	19.2	27.7	70.5
54	67.8 68.5( 55.1)	36.7	21.9	21.0	29.5	76.5
70	81.1	45.1 47.5( 75.6)	25.8	23.1	31.7 32.5( 77.2)	
90		53.7	30.6 32.5( 99.3)	25.7 27.0(101.0)	34.0	
115			35.8	28.6	37.1	
148			40.4	31.9		

OID AT MAX PFAL  
 OR PERMITTED RISE 85.6( 79.9) 59.2(111.0) 40.7(151.0) 33.8(165.0) 40.7(131.0) 85.0( 62.3)

TABLE 39

DIFFUSER PLUME DILUTION  
 PORT SPACING = 5 DIAMETERS, STABILITY STRATIFICATION PARAMETER = 10000  
 CURRENT TO EFFLUENT RATIO = 0.00

RISE(DIA)	DENSIMETRIC FROUDE NUMBER					
	1	3	10	30	100	1000
1	1.9	2.7	5.1( 0.9) 5.3	5.0( 0.1) 8.2	5.0( 0.0) 12.9	5.0( 0.0) 31.8
2	2.7	3.5	6.2	9.3	14.7	36.5
3	3.6	4.3	6.9	10.1	16.0	39.6
4	4.6	5.0	7.4	10.7	16.9	41.9
5	5.7	5.8	7.8	11.2	17.6	44.0
7	8.1	7.4	8.6	12.0	18.9	47.1
9	10.9	9.1	9.3	12.6	19.8	49.5
12	15.6	9.4( 9.3) 11.4	10.3	13.5	21.1	52.4
15	20.2( 14.6) 21.0	13.5	11.2	14.2	22.0	54.8
20	28.2	16.7	12.6	15.3	23.4	58.0
25	35.0	20.0	14.1	16.2	24.5	60.7
33	45.5	24.9	16.3	17.6	26.0	64.4
42	56.8	30.5	18.9	19.2	27.4	67.7
54	71.9	37.8	22.2	21.0	29.1	71.2
70	91.8	47.5	26.5	23.3	31.0	75.3
90	115.0	59.2	32.0	25.9	33.0	79.7
115	142.0 151.0(124.0)	73.4	38.6	29.3	35.3	84.5 88.3(137.0)
148	172.0	91.2 105.0(176.0)	47.1	33.5	37.9	90.1
190		111.0	57.5	38.7	41.1	97.1
244		129.0	69.6 70.3(248.0)	45.1 51.1(300.0)	44.8 46.8(270.0)	

DIL AT MAX PEAK  
 OR PERMITTED RISE 189.0(179.0) 131.0(257.0) 80.3(300.0) 51.2(301.0) 48.3(300.0) 107.0(234.0)

TABLE 40

DIFFUSER PLUME DILUTION  
 PORT SPACING = 5 DIAMETERS, STABILITY STRATIFICATION PARAMETER = INFINITE  
 CURRENT TO EFFLUENT RATIO = 0.00

RISF(DIA)	DENSIMETRIC FROUDE NUMBER					
	1	3	10	30	100	1000
1	1.9	2.7	5.1[ 0.9]	5.0[ 0.1]	5.0[ 0.0]	5.0[ 0.0]
2	2.7	3.5	6.2	9.3	14.7	36.5
3	3.6	4.3	6.9	10.1	16.0	39.6
4	4.6	5.0	7.4	10.7	16.9	41.9
5	5.7	5.8	7.8	11.2	17.6	44.0
7	8.1	7.4	8.6	12.0	18.9	46.8
9	10.9	9.1	9.3	12.6	19.8	49.5
12	15.7	9.4[ 9.3]	10.3	13.5	21.0	52.4
15	20.4[ 14.7]	11.4	11.2	14.2	22.0	54.8
20	28.2	13.5	12.6	15.3	23.4	57.7
25	35.0	16.8	14.1	16.2	24.5	60.4
33	45.9	20.0	16.3	17.6	26.0	63.9
42	57.6	24.9	18.9	19.2	27.4	67.1
54	72.9	30.7	22.3	21.0	29.0	70.5
70	93.6	38.0	26.7	23.3	30.8	74.3
90	120.0	48.1	32.2	26.0	32.8	78.1
115	152.0	60.5	39.4	29.5	35.1	82.1
148	194.0	75.7	48.5	34.0	37.7	86.3
190	248.0	96.1	60.0	39.6	40.9	90.9
244	318.0	122.0	75.1	46.8	44.6	95.6

DIL AT MAX REAR  
 OR PERMITTED RISE 318.0(245.0) 190.0(301.0) 90.6(301.0) 54.2(301.0) 48.3(300.0) 99.8(300.0)

TABLE 43

DIFFUSER PLUME DILUTION  
 PORT SPACING = 10 DIAMETERS, STABILITY STRATIFICATION PARAMETER = 2000  
 CURRENT TO EFFLUENT RATIO = 0.10

RISE(DIA)	DENSIMETRIC FROUDE NUMBER					
	1	3	10	30	100	1000
1	1.9	2.8	6.4	15.9( 0.91) 16.3	15.9( 0.11) 34.3	15.9( 0.01) 131.0
2	2.7	3.7	8.8	21.3	42.2	164.0
3	3.6	4.6	11.0	25.1	47.8	189.0
4	4.5	5.6	13.4	28.4	53.0	208.0
5	5.6	6.6	15.9	31.5	57.2	224.0
7	8.1	8.7	16.8( 5.4) 20.8	37.5	65.3	254.0
9	10.9	11.2	25.4	43.4	72.9	283.0 289.0( 9.5)
12	15.7	15.5	32.2	51.6	83.2	324.0
15	21.1	20.4	39.1	60.1	93.6	381.0
20	31.5	28.6( 19.2) 30.3	50.2	73.5	110.0 124.0( 24.5)	
25	44.0	39.9	61.8	87.4 107.0( 32.1)	126.0	
33	59.7( 30.7) 66.2	54.9	81.5 99.7( 39.8)	109.0	152.0	
42	88.0 97.9( 46.4)	72.5 87.4( 49.4)	107.0	136.0		
54	115.0	99.0	150.0			

DIL AT MAX PEAK  
 OR PERMITTED RISE 241.0( 62.5) 192.0( 66.0) 156.0( 55.2) 153.0( 47.3) 174.0( 37.7) 404.0( 15.3)

TABLE 44

DIFFUSER PLUME DILUTION  
 PORT SPACING = 10 DIAMETERS, STABILITY STRATIFICATION PARAMETER = 10000  
 CURRENT TO EFFLUENT RATIO = 0.10

RISE(DIA)	DENSIMETRIC FROUDE NUMBER					
	1	3	10	30	100	1000
1	1.9	2.8	6.4	15.9( 0.9) 16.3	15.9( 0.1) 34.0	15.9( 0.0) 131.0
2	2.7	3.7	8.8	21.3	42.2	163.0
3	3.6	4.6	11.0	25.1	47.8	186.0
4	4.5	5.6	13.4	28.4	52.7	205.0
5	5.6	6.6	15.9	31.5	57.2	221.0
7	8.1	8.7	16.8( 5.4) 20.8	37.5	65.3	248.0
9	10.9	11.2	25.4	43.1	72.4	271.0
12	15.7	15.5	32.2	51.6	82.6	299.0
15	21.1	20.4	38.6	59.7	92.3	325.0
20	31.8	29.0( 19.5) 30.3	49.5	72.9	108.0	363.0
25	44.0	39.9	60.1	86.1	124.0	398.0 439.0( 31.5)
33	63.5( 31.8) 67.1	54.5	77.6	108.0	146.0	449.0
42	91.1	71.0	97.6	131.0	173.0	
54	121.0	93.0	124.0	163.0	207.0 245.0( 67.7)	
70	158.0	122.0	162.0	204.0 231.0( 79.7)	252.0	
90	204.0 216.0( 95.7)	159.0 194.0(107.0)	216.0 221.0( 91.7)	259.0	309.0	
115	260.0	213.0	299.0			

DIL AT MAX PEAK  
 OR PERMITTED RISE 310.0(128.0) 327.0(142.0) 331.0(123.0) 313.0(109.0) 320.0( 93.8) 456.0( 34.1)

TABLE 45

DIFFUSER PLUME DILUTION  
 PORT SPACING = 10 DIAMETERS, STABILITY STRATIFICATION PARAMETER = INFINITE  
 CURRENT TO EFFLUENT RATIO = 0.10

RISE(DIA)	DENSIMETRIC FPOUDE NUMBER					
	1	3	10	30	100	1000
1	1.9	2.8	6.4	15.9( 0.9) 16.3	15.9( 0.1) 34.0	15.9( 0.0) 131.0
2	2.7	3.7	8.8	21.3	42.2	163.0
3	3.6	4.6	11.0	25.1	47.8	186.0
4	4.5	5.6	13.4	28.4	52.7	205.0
5	5.6	6.6	15.9	31.5	57.2	220.0
7	8.1	8.7	16.8( 5.4) 20.8	37.5	64.8	246.0
9	10.9	11.2	25.4	43.1	72.4	268.0
12	15.7	15.3	32.0	51.6	82.6	296.0
15	21.1	20.4	38.6	59.7	92.3	320.0
20	31.8	29.2( 19.6) 30.3	49.1	72.9	108.0	354.0
25	44.3	39.9	60.1	86.1	123.0	383.0
33	64.8( 32.2) 67.6	54.5	76.6	107.0	146.0	425.0
42	91.7	71.0	95.6	130.0	171.0	
51	123.0	92.3	121.0	161.0	205.0	
70	162.0	121.0	154.0	202.0	249.0	
90	212.0	156.0	196.0	252.0	303.0	
115	273.0	201.0	247.0	315.0	369.0	
148	354.0	259.0	316.0	398.0		
190		333.0				

DIL AT MAX REAR  
 OR PERMITTED RISE 397.0(166.0) 356.0(203.0) 376.0(177.0) 400.0(149.0) 400.0(127.0) 464.0( 41.7)



TABLE 46

DIFFUSER PLUME DILUTION  
 PORT SPACING = 10 DIAMETERS, STABILITY STRATIFICATION PARAMETER = 200  
 CURRENT TO EFFLUENT RATIO = 0.05

		DENSIMETRIC FROUDE NUMBER					
		1	3	10	30	100	1000
RISE (DIA)	: T)						
	: M)						
1	: T)	1.9	2.8	5.9	12.6( 0.8)	12.6( 0.1)	12.6( 0.0)
	: M)				13.6	26.2	94.9
2	: T)	2.7	3.6	7.5	16.9	32.0	121.0
	: M)						124.0( 2.2)
3	: T)	3.6	4.4	9.1	19.2	36.0	145.0
	: M)						
4	: T)	4.6	5.1	10.3	21.1	39.6	
	: M)						
5	: T)	5.6	6.0	11.7	22.8	42.8	
	: M)					45.5( 5.9)	
7	: T)	8.1	7.6	14.0( 6.8)	26.2	49.1	
	: M)			14.3			
9	: T)	10.8	9.4	16.8	29.2	56.5	
	: M)				29.8( 9.4)		
12	: T)	15.4	12.3	20.3	34.3		
	: M)			22.9( 14.3)			
15	: T)	20.3	15.5	23.9			
	: M)	24.9( 17.7)	20.5( 19.2)				
20	: T)	29.3	21.7	32.7			
	: M)						
25	: T)	33.4( 22.4)	22.6( 20.7)				
	: M)		28.9				

DIL AT MAX REAL  
 OR PERMITTED RISE 54.2( 24.0) 41.6( 26.6) 36.6( 21.1) 41.6( 14.9) 62.0( 9.6) 172.0( 3.5)

TABLE 47

DIFFUSER PLUME DILUTION  
 PORT SPACING = 10 DIAMETERS, STABILITY STRATIFICATION PARAMETER = 500  
 CURRENT TO EFFLUENT RATIO = 0.05

RISE (DIA)	DENSIMETRIC FROUDE NUMBER						
	1	3	10	30	100	1000	
1	T)						
	M)	1.9	2.8	5.9	12.6( 0.8) 13.5	12.6( 0.1) 26.2	12.6( 0.0) 94.3
2	T)	2.7	3.6	7.6	16.9	31.8	117.0
	M)						
3	T)	3.6	4.4	9.0	19.0	35.7	134.0
	M)						
4	T)	4.6	5.1	10.3	21.0	38.8	150.0
	M)						155.0( 4.4)
5	T)	5.7	6.0	11.6	22.6	41.9	164.0
	M)						
7	T)	8.1	7.6	14.2( 7.1)	25.6	46.8	205.0
	M)						
9	T)	10.9	9.4	16.6	28.6	51.6	
	M)					57.6( 11.9)	
12	T)	15.5	12.3	19.7	32.9	58.0	
	M)						
15	T)	20.8	15.6	22.9	37.0	64.8	
	M)				41.3( 18.1)		
20	T)	30.7	21.6	28.0	44.3		
	M)			33.8( 25.2)			
25	T)	41.3	27.1( 24.0)		52.6		
	M)	44.0( 26.2)	28.4				
33	T)	47.5( 27.8)	34.5( 30.1)				
	M)	56.5	38.0	46.2			

DIL AT MAX FEAL  
 OR PERMITTED RISE 98.4( 35.3) 72.4( 41.4) 58.7( 36.4) 59.5( 27.9) 79.3( 19.1) 215.0( 7.1)

TABLE 48

DIFFUSER PLUME DILUTION  
 PORT SPACING = 10 DIAMETERS, STABILITY STRATIFICATION PARAMETER = 2000  
 CURRENT TO EFFLUENT RATIO = 0.05

RISE(DIA)	DENSIMETRIC FROUDE NUMBER					
	1	3	10	30	100	1000
1	1.9	2.8	5.9	12.7( 0.8) 13.5	12.6( 0.1) 26.2	12.6( 0.0) 93.6
2	2.7	3.6	7.6	16.8	31.5	115.0
3	3.6	4.4	9.0	19.0	35.5	131.0
4	4.6	5.1	10.3	20.8	38.6	144.0
5	5.7	6.0	11.6	22.5	41.3	155.0
7	8.1	7.6	14.1	25.4	46.2	174.0
9	10.9	9.4	14.3( 7.2) 16.4	28.2	50.2	191.0
12	15.6	12.3	19.6	32.2	56.1	214.0 217.0( 12.6)
15	21.0	15.6	22.5	36.0	61.8	236.0
20	31.3	21.7	27.3	42.2	70.0	287.0
25	43.1	28.6	32.0	48.5	78.7 90.6( 32.4)	
33	60.1( 31.6) 64.0	30.1( 26.0) 39.4	39.6	58.4	92.0	
42	82.7 92.4( 47.3)	50.2	48.5	70.5 73.9( 44.7)	107.0	
54	104.0	64.0 68.7( 58.5)	60.9 64.0( 56.7)	88.3		
70		81.8	84.0			

DIL AT MAX RIAL  
 OR PERMITTED RISE 213.0( 65.2) 157.0( 81.4) 123.0( 79.9) 111.0( 66.0) 127.0( 50.6) 302.0( 20.3)

TABLE 49

DIFFUSER PLUME DILUTION  
 PORT SPACING = 10 DIAMETERS, STABILITY STRATIFICATION PARAMETER = 10000  
 CURRENT TO EFFLUENT RATIO = 0.05

RISE(DIA)	DENSIMETRIC FROUDE NUMBER					
	1	3	10	30	100	1000
1	1.9	2.8	5.9	12.7( 0.8) 13.5	12.6( 0.1) 26.2	12.6( 0.0) 93.6
2	2.7	3.6	7.6	16.8	31.5	115.0
3	3.6	4.4	9.0	19.0	35.5	131.0
4	4.6	5.1	10.3	20.8	38.6	143.0
5	5.7	6.0	11.6	22.5	41.3	153.0
7	8.1	7.6	14.0	25.4	45.9	171.0
9	10.9	9.4	14.3( 7.2) 16.3	28.2	50.2	185.0
12	15.7	12.3	19.6	32.0	55.7	204.0
15	21.0	15.6	22.5	35.7	60.9	220.0
20	31.3	21.7	27.3	41.9	69.5	244.0
25	43.4	28.8	31.8	47.8	77.1	265.0
33	63.9( 32.6) 85.3	30.9( 26.5) 39.6	39.1	56.8	89.1	295.0 326.0( 41.8)
42	87.4	50.9	47.5	67.6	103.0	326.0
54	114.0	65.3	58.0	81.5	120.0	
70	147.0	84.3	72.9	100.0	143.0	
90	185.0 201.0( 99.1)	107.0	91.0	125.0 158.0(115.0)	172.0 175.0( 92.6)	
115	227.0	135.0 151.0(129.0)	116.0 140.0(138.0)		208.0	
148		172.0	153.0	211.0		

DIL AT MAX PEAK  
 OR PERMITTED RISE 259.0(136.0) 294.0(180.0) 284.0(189.0) 240.0(163.0) 239.0(135.0) 361.0( 51.8)

TABLE 50

DIFFUSER PLUME DILUTION  
 PORT SPACING = 10 DIAMETERS, STABILITY STRATIFICATION PARAMETER = INFINITE  
 CURRENT TO EFFLUENT RATIO = 0.05

RISE(DIA)	DENSIMETRIC FROUDE NUMBER					
	1	3	10	30	100	1000
1	1.9	2.8	5.9	12.7( 0.8) 13.5	12.6( 0.1) 26.2	12.6( 0.0) 93.6
2	2.7	3.6	7.6	16.8	31.5	115.0
3	3.6	4.4	9.0	19.0	35.5	131.0
4	4.6	5.1	10.3	20.8	38.6	143.0
5	5.7	6.0	11.6	22.5	41.3	153.0
7	8.1	7.6	14.0	25.4	45.9	170.0
9	10.9	9.4	14.3( 7.3) 16.3	28.2	50.2	184.0
12	15.7	12.3	19.6	32.0	55.7	202.0
15	21.1	15.6	22.5	35.7	60.9	218.0
20	31.5	21.7	27.1	41.9	69.0	240.0
25	43.4	28.8	31.8	47.5	77.1	259.0
33	64.8( 32.8)	31.1( 26.6)	39.1	56.8	89.2	284.0
42	88.0	51.2	47.1	66.7	102.0	310.0
54	116.0	65.7	57.6	79.8	119.0	339.0
70	152.0	85.6	71.9	97.2	141.0	
90	196.0	109.0	89.4	119.0	168.0	
115	251.0	140.0	111.0	146.0	201.0	
148	324.0	179.0	141.0	181.0	245.0	
190		229.0	177.0	226.0	300.0	
244		294.0	224.0	283.0		

DIL AT MAX REAL  
 OR PERMITTED RISE 382.0(174.0) 310.0(258.0) 273.0(300.0) 295.0(256.0) 312.0(200.0) 370.0( 67.5)

TABLE 51

DIFFUSER PLUME DILUTION  
 PORT SPACING = 10 DIAMETERS, STABILITY STRATIFICATION PARAMETER = 200  
 CURRENT TO EFFLUENT RATIO = 0.02

RISE(DIA)	DENSIMETRIC FROUDE NUMBER					
	1	3	10	30	100	1000
1	1.9	2.7	5.5	11.1( 0.8) 11.7	11.0( 0.1) 20.8	11.0( 0.0) 64.8
2	2.7	3.6	7.1	14.1	24.6	79.8 90.4( 2.9)
3	3.6	4.3	8.2	15.7	27.1	91.7
4	4.6	5.1	9.3	16.9	29.4	104.0
5	5.7	5.9	10.2	17.9	31.3	
7	8.1	7.5	12.0	19.7	34.8 35.2( 7.4)	
9	10.8	9.2	12.8( 8.0) 13.6	21.3 22.9( 11.4)	38.0	
12	15.2	12.0	15.6	23.4	44.7	
15	20.3 24.8( 17.6)	14.9 19.7( 19.6)	17.4 19.3( 16.5)	25.8		
20	29.0	20.1	20.4			
25	32.9( 22.4)	22.0( 21.8) 24.9	24.9			

DIL AT MAX REAL OR PERMITTED RISE 44.1( 24.0) 32.0( 27.7) 26.1( 25.4) 30.7( 18.8) 46.7( 12.2) 123.0( 4.8)

TABLE 52

DIFFUSER PLUME DILUTION  
 PORT SPACING = 10 DIAMETERS, STABILITY STRATIFICATION PARAMETER = 500  
 CURRENT TO EFFLUENT RATIO = 0.02

		DENSIMETRIC FROUDE NUMBER					
		1	3	10	30	100	1000
RISF (DIA)	: T)						
	: M)						
1	: T)	1.9	2.7	5.5	11.1( 0.8)	11.0( 0.1)	11.0( 0.0)
	: M)				11.7	20.8	64.4
2	: T)	2.7	3.6	7.1	14.1	24.4	78.2
	: M)						
3	: T)	3.6	4.3	8.2	15.7	26.9	88.6
	: M)						
4	: T)	4.6	5.1	9.3	16.8	29.0	96.9
	: M)						
5	: T)	5.7	5.9	10.2	17.7	30.7	105.0
	: M)						111.0( 6.0)
7	: T)	8.1	7.5	11.9	19.4	33.8	118.0
	: M)						
9	: T)	10.9	9.2	13.2( 8.6)	20.8	36.2	135.0
	: M)			13.5			
12	: T)	15.5	12.0	15.6	22.8	39.6	
	: M)						
15	: T)	20.7	15.1	17.4	24.4	42.8	
	: M)					43.1( 15.4)	
20	: T)	30.5	20.7	20.1	27.3	48.0	
	: M)				29.0( 23.3)		
25	: T)	41.3	26.9( 25.2)	22.8	30.1	56.2	
	: M)	43.7( 26.2)	32.7( 30.9)	25.5( 30.1)			
33	: T)	47.5( 27.9)					
	: M)	55.2	34.5	27.1	35.4		
42	: T)		41.5	32.4			
	: M)						

DIL AT MAX REAR  
 OR PERMITTED RISF 81.4( 35.6) 54.6( 43.6) 40.0( 46.1) 40.7( 37.5) 57.7( 25.1) 152.0( 9.8)

TABLE 53

DIFFUSER PLUME DILUTION  
 PORT SPACING = 10 DIAMETERS, STABILITY STRATIFICATION PARAMETER = 2000  
 CURRENT TO EFFLUENT RATIO = 0.02

RISE(DIA)	DENSIMETRIC FROUDE NUMBER					
	1	3	10	30	100	1000
1	1.9	2.7	5.5	11.1( 0.8) 11.7	11.0( 0.1) 20.7	11.0( 0.0) 63.9
2	2.7	3.6	7.1	14.1	24.4	77.6
3	3.6	4.3	8.2	15.6	26.9	87.3
4	4.6	5.1	9.3	16.8	28.8	94.9
5	5.7	5.9	10.1	17.7	30.5	101.0
7	8.1	7.5	11.9	19.3	33.3	112.0
9	10.9	9.2	13.4( 8.9) 13.5	20.7	35.7	121.0
12	15.6	12.0	15.5	22.5	38.6	134.0
15	21.0	15.1	17.3	24.1	41.3	144.0 152.0( 17.4)
20	31.1	21.0	20.2	26.5	45.2	162.0
25	42.8	27.5	22.9	28.8	48.7	181.0
33	59.7( 31.5) 63.5	29.8( 26.9) 37.0	27.3	32.4	53.9	
42	82.1 90.8( 47.3)	46.2	31.8	36.5	60.1 61.5( 44.4)	
54	101.0	57.6 63.4( 61.1)	37.8	41.8 46.5( 64.1)	68.1	
70		70.4	45.6 46.4( 71.7)	49.7	81.7	
90			55.5	62.6		

DIL AT MAX REAR  
 OR PERMITTED RISE 184.0( 66.0) 122.0( 87.2) 85.1(106.0) 73.5( 97.9) 85.3( 71.5) 209.0( 28.6)



TABLE 54

DIFFUSER PLUME DILUTION  
 PORT SPACING = 10 DIAMETERS, STABILITY STRATIFICATION PARAMETER = 10000  
 CURRENT TO EFFLUENT RATIO = 0.02

		DENSIMETRIC FROUDE NUMBER					
		1	3	10	30	100	1000
1	: T)						
	: M)	1.9	2.7	5.5	11.1( 0.8)	11.0( 0.1)	11.0( 0.0)
2	: T)				11.7	20.7	63.9
	: M)	2.7	3.6	7.1	14.1	24.4	77.6
3	: T)						
	: M)	3.6	4.3	8.2	15.6	26.9	86.7
4	: T)						
	: M)	4.6	5.1	9.3	16.8	28.8	94.3
5	: T)						
	: M)	5.7	5.9	10.1	17.7	30.5	100.0
7	: T)						
	: M)	8.1	7.5	11.9	19.3	33.3	111.0
9	: T)						
	: M)	10.9	9.2	13.4( 8.9)	13.5	20.7	35.5
12	: T)						
	: M)	15.6	12.0	15.5	22.3	38.3	130.0
15	: T)						
	: M)	21.0	15.2	17.3	23.9	41.0	139.0
20	: T)						
	: M)	31.3	21.0	20.2	26.3	44.6	153.0
25	: T)						
	: M)	43.4	27.5	27.9	28.6	47.8	164.0
33	: T)						
	: M)	63.5( 32.5)	30.9( 27.5)	27.3	32.2	53.0	180.0
42	: T)						
	: M)	86.1	47.5	32.0	36.0	57.9	196.0
54	: T)						
	: M)	112.0	60.5	38.3	40.8	64.6	216.0
70	: T)						
	: M)	143.0	76.6	46.5	47.0	73.0	224.0( 59.7)
90	: T)						
	: M)	179.0	96.1	56.7	54.7	83.5	241.0
115	: T)						
	: M)	196.0(100.0)					
148	: T)						
	: M)	219.0	119.0	69.2	64.7	96.7	109.0(139.0)
190	: T)						
	: M)		137.0(136.0)				
244	: T)						
	: M)		147.0	85.3	77.6	115.0	
244	: T)						
	: M)			99.4(178.0)	91.9(182.0)		
244	: T)						
	: M)		176.0	105.0	95.9	142.0	
244	: T)						
	: M)			135.0	133.0		

DIL AT MAX REAR OR PERMITTED WISE 245.0(138.0) 200.0(197.0) 214.0(259.0) 172.0(264.0) 160.0(212.0) 264.0( 83.7)

TABLE 55

DIFFUSER PLUME DILUTION  
 PORT SPACING = 10 DIAMETERS, STABILITY STRATIFICATION PARAMETER = INFINITE  
 CURRENT TO EFFLUENT RATIO = 0.02

RISE (DIA)	DENSIMETRIC FROUDE NUMBER					
	1	3	10	30	100	1000
1	1.9	2.7	5.5	11.1( 0.8) 11.7	11.0( 0.1) 20.7	11.0( 0.0) 63.9
2	2.7	3.6	7.1	14.1	24.4	77.6
3	3.6	4.3	8.2	15.6	26.9	86.7
4	4.6	5.1	9.3	16.7	28.8	94.3
5	5.7	5.9	10.1	17.7	30.5	100.0
7	8.1	7.5	11.9	19.3	33.1	111.0
9	10.9	9.2	13.5( 9.1)	20.5	35.5	119.0
12	15.7	12.0	15.5	22.3	38.3	130.0
15	21.0	15.2	17.3	23.9	40.8	138.0
20	31.3	21.1	20.2	26.3	44.6	151.0
25	43.4	27.7	22.9	28.6	47.8	162.0
33	64.8( 32.8) 65.7	31.1( 27.6) 37.8	27.3	32.0	52.8	176.0
42	97.3	47.8	32.2	35.7	57.7	190.0
54	114.0	60.9	38.6	40.5	64.0	206.0
70	144.0	78.2	46.8	46.8	72.0	225.0
90	191.0	99.0	57.2	54.2	81.5	245.0
115	244.0	125.0	70.3	63.7	93.1	268.0
148	314.0	160.0	87.6	75.7	108.0	
190		204.0	110.0	91.2	126.0	
244		260.0	137.0	111.0	149.0	

DIL AT MAX REAL  
 OR PERMITTED RISE 375.0(178.0) 295.0(278.0) 166.0(301.0) 131.0(300.0) 173.0(300.0) 271.0(119.0)

TABLE 56

DIFFUSER PLUME DILUTION  
 PORT SPACING = 10 DIAMETERS, STABILITY STRATIFICATION PARAMETER = 200  
 CURRENT TO EFFLUENT RATIO = 0.00

RISE (DIA)	DENSIMETRIC FROUDE NUMBER					
	1	3	10	30	100	1000
1	: T)					
	: M)				10.1( 0.9)	10.1( 0.1)
2	: T)	1.9	2.7	5.3	10.6	17.3
	: M)					42.5
3	: T)	2.7	3.5	6.7	12.5	19.8
	: M)					49.1
4	: T)	3.6	4.3	7.8	13.6	21.5
	: M)					53.8
5	: T)	4.6	5.0	8.7	14.4	22.8
	: M)					57.6
7	: T)	5.7	5.8	9.6	15.2	23.9
	: M)					60.9
9	: T)	8.1	7.4	11.2	16.4	25.8
	: M)					27.5( 9.2)
12	: T)	10.8	9.1	12.1( 8.3)	17.4	
	: M)			12.6		
15	: T)	15.2	11.8	14.3	18.8	29.8
	: M)				19.3( 13.4)	
20	: T)	20.3	14.7	15.8	20.0	32.8
	: M)	24.8( 17.7)	19.6( 19.8)	16.8( 17.5)		
25	: T)	28.8	19.8	17.9	22.1	
	: M)	32.9( 22.5)	21.9( 22.0)			
	: T)		24.1	19.6		
	: M)					

DIL AT MAX FEAL  
 OR PERMITTED RISE 34.1( 24.1) 25.4( 20.1) 20.7( 27.6) 23.9( 22.2) 34.3( 15.4) 73.3( 7.1)

TABLE 57

DIFFUSER PLUME DILUTION  
 PORT SPACING = 10 DIAMETERS, STABILITY STRATIFICATION PARAMETER = 500  
 CURRENT TO EFFLUENT RATIO = 0.00

RISE (DIA)	DENSIMETRIC FROUDE NUMBER					
	1	3	10	30	100	1000
1	1.9	2.7	5.3	10.1( 0.9) 10.6	10.1( 0.1) 17.3	10.1( 0.0) 42.2
2	2.7	3.5	6.7	12.5	19.7	48.5
3	3.6	4.3	7.7	13.5	21.4	53.0
4	4.6	5.0	8.7	14.4	22.6	56.1
5	5.7	5.8	9.5	15.1	23.7	58.8
7	8.1	7.4	11.2	16.2	25.4	63.5
9	10.9	9.1	12.5( 8.8) 12.6	17.3	26.7	67.8( 9.2)
12	15.5	11.9	14.4	18.5	28.4	73.6
15	20.7	14.9	16.0	19.6	30.0 31.9( 19.4)	81.0
20	30.5	20.5	18.3	21.1	32.2	
25	41.1 43.7( 26.2) 47.2( 27.8)	26.5 32.2( 31.2) 26.7( 25.3)	20.4 23.1( 32.1)	22.6 23.2( 27.6)	34.3	
33	54.6	33.8	23.4	24.7	39.4	
42		38.9	26.3	27.0		

DIL AT MAX REAL  
 OR PERMITTED RISE 56.4( 35.6) 39.5( 44.2) 28.6( 50.7) 29.0( 46.3) 40.0( 33.1) 85.1( 15.6)

TABLE 58

DIFFUSER PLUME DILUTION  
 PORT SPACING = 10 DIAMETERS, STABILITY STRATIFICATION PARAMETER = 2000  
 CURRENT TO EFFLUENT RATIO = 0.00

		DENSIMETRIC FROUDE NUMBER					
		1	3	10	30	100	1000
1	: T)						
	: M)	1.9	2.7	5.3	10.1( 0.9)	10.1( 0.1)	10.1( 0.0)
2	: T)						
	: M)	2.7	3.5	6.7	12.4	19.7	48.5
3	: T)						
	: M)	3.6	4.3	7.7	13.5	21.4	52.7
4	: T)						
	: M)	4.6	5.0	8.7	14.4	22.6	55.7
5	: T)						
	: M)	5.7	5.8	9.5	15.0	23.6	58.4
7	: T)						
	: M)	8.1	7.4	11.1	16.2	25.3	62.2
9	: T)						
	: M)	10.9	9.1	12.6( 9.1)	17.1	26.5	65.5
12	: T)						
	: M)	15.6	12.0	14.4	18.4	28.0	70.0
15	: T)						
	: M)	21.0	15.0	16.1	19.4	29.4	73.3
20	: T)						
	: M)	31.1	20.8	18.5	21.0	31.2	78.0
25	: T)						
	: M)	42.8	27.1	20.8	22.3	32.9	82.3
33	: T)						
	: M)	59.3( 31.5)	29.8( 27.1)	24.4	24.4	35.0	85.2( 28.7)
42	: T)						
	: M)	63.5	36.5	28.2	26.5	37.1	95.7
54	: T)						
	: M)	81.5	45.2	33.1	29.2	39.7	
70	: T)						
	: M)	90.4( 47.6)	61.4( 61.6)	39.2	32.5	42.7	
90	: T)						
	: M)	99.9	67.4	41.6( 77.3)	34.2( 80.0)	46.6	
115	: T)						
	: M)			51.3	40.1		

DIL AT MAX FEAL  
 OR PERMITTED FISE: 111.0( 66.4) 76.0( 89.3) 51.7(118.0) 42.8(130.0) 51.3(104.0) 107.0( 49.5)

TABLE 59

DIFFUSER PLUME DILUTION  
 PORT SPACING = 10 DIAMETERS, STABILITY STRATIFICATION PARAMETER = 10000  
 CURRENT TO EFFLUENT RATIO = 0.00

RISE(DIA)	DENSIMETRIC FROUDE NUMBER					
	1	3	10	30	100	1000
1	1.9	2.7	5.3	10.1[ 0.9] 10.6	10.1[ 0.1] 17.3	10.1[ 0.0] 42.2
2	2.7	3.5	6.7	12.4	19.7	48.5
3	3.6	4.3	7.7	13.5	21.3	52.3
4	4.6	5.0	8.7	14.4	22.5	55.7
5	5.7	5.8	9.5	15.0	23.6	58.0
7	8.1	7.4	11.1	16.2	25.1	62.2
9	10.9	9.1	12.6	17.1	26.5	65.1
12	15.6	12.0	12.7[ 9.2] 14.5	18.4	28.0	69.3
15	21.0	15.0	16.1	19.4	29.2	72.3
20	31.3	20.8	18.6	21.0	31.0	76.6
25	43.4	27.3	21.0	22.3	32.5	80.2
33	63.5[ 32.5] 65.3	30.7[ 27.5] 37.2	24.8	24.4	34.6	84.9
42	85.6	46.5	28.8	26.5	36.6	89.4
54	110.0	58.4	34.0	29.2	38.8	94.4
70	141.0	73.9	41.0	32.8	41.6	100.0
90	176.0 193.0(101.0)	92.2	49.5	37.0	44.4	106.0 111.0(109.0)
115	214.0	114.0 133.0(140.0)	59.8	42.1	47.6	113.0
144		139.0	72.6	48.6	51.6	122.0
190		163.0	87.6 88.9(194.0)	56.5 64.6(237.0)	56.2 59.0(218.0)	
244			104.0	65.7	61.5	

DIL AT MAX REAL  
 OR PERMITTED RISE 239.0(140.0) 166.0(203.0) 112.0(290.0) 73.9(300.0) 66.6(300.0) 132.0(180.0)

TABLE 60

DIFFUSER PLUME DILUTION  
 PORT SPACING = 10 DIAMETERS, STABILITY STRATIFICATION PARAMETER = INFINITE  
 CURRENT TO EFFLUENT RATIO = 0.00

		DENSIMETRIC FROUDE NUMBER					
		1	3	10	30	100	1000
RISE(DIA)	: M]				10.1[ 0.9]	10.1[ 0.1]	10.1[ 0.0]
	: M]	1.9	2.7	5.3	10.6	17.3	42.2
2	: M]	2.7	3.5	6.7	12.4	19.7	48.5
3	: M]	3.6	4.3	7.7	13.5	21.3	52.3
4	: M]	4.6	5.0	8.7	14.4	22.5	55.7
5	: M]	5.7	5.8	9.5	15.0	23.6	58.0
7	: M]	8.1	7.4	11.1	16.2	25.1	62.2
9	: M]	10.9	9.1	12.6	17.1	26.3	65.1
12	: M]	15.7	12.0	12.7[ 9.2]	18.4	28.0	68.9
15	: M]	21.0	15.0	16.1	19.3	29.2	72.0
20	: M]	31.3	20.8	18.6	21.0	31.0	76.3
25	: M]	43.4	27.3	21.0	22.3	32.6	79.9
33	: M]	64.8[ 32.9]	30.9[ 27.6]	24.7	24.4	34.6	84.5
42	: M]	86.7	47.1	28.8	26.5	36.5	88.6
54	: M]	113.0	59.3	34.3	29.2	38.8	93.1
70	: M]	146.0	75.5	41.3	32.9	41.3	98.1
90	: M]	188.0	95.0	50.2	37.3	44.2	103.0
115	: M]	239.0	120.0	61.3	42.5	47.4	108.0
148	: M]	306.0	152.0	76.0	49.5	51.3	114.0
190	: M]		193.0	94.3	50.5	55.9	120.0
244	: M]		246.0	118.0	69.9	61.6	126.0

DIL AT MAX REAL  
 OR PERMITTED RTSE 371.0(180.0) 288.0(287.0) 143.0(301.0) 81.8(300.0) 67.2(300.0) 132.0(300.0)

TABLE 61

DIFFUSER PLUME DILUTION  
 PORT SPACING = 25 DIAMETERS, STABILITY STRATIFICATION PARAMETER = 200  
 CURRENT TO EFFLUENT RATIO = 0.10

RISE (DIA)	DENSIMETRIC FROUDE NUMBER					
	1	3	10	30	100	1000
1	1.9	2.8	6.4	16.4	51.6	71.0( 0.0)
2	2.7	3.7	8.8	23.3	71.0( 1.9)	258.0
3	3.5	4.6	11.1	29.4	88.6	261.0( 1.1)
4	4.5	5.6	13.5	35.7	92.3( 3.3)	
5	5.6	6.6	16.1	42.2	103.0	
7	8.1	8.8	22.2	57.2	53.0( 6.5)	
9	10.8	11.3	29.6	71.5( 8.6)	75.5	
12	15.4	15.8	44.9	38.0( 10.8)		
15	20.5	21.4				
20	25.5( 17.6)	26.2( 17.0)				
	30.7	37.3				

OIL AT MAX REAL  
 OR PERMITTED RISE 67.2( 23.4) 63.3( 22.2) 60.1( 14.7) 83.2( 9.4) 128.0( 5.1) 361.0( 1.7)



TABLE 62

DIFFUSER PLUME DILUTION  
 PORT SPACING = 25 DIAMETERS, STABILITY STRATIFICATION PARAMETER = 500  
 CURRENT TO EFFLUENT RATIO = 0.10

RISE(DIA)	DENSIMETRIC FROUDE NUMBER					
	1	3	10	30	100	1000
1	1.9	2.8	6.4	16.4	51.2	71.0( 0.0)
2	2.7	3.7	8.8	23.1	71.0( 2.0)	249.0
3	3.6	4.6	11.0	29.0	86.1	319.0
4	4.5	5.6	13.4	35.2	97.6	326.0( 2.1)
5	5.6	6.6	16.0	41.3	108.0	390.0
7	8.1	8.8	21.7	54.9	121.0( 6.2)	130.0
9	10.9	11.2	28.6	70.0	153.0	
12	15.6	15.6	41.6	85.0( 11.0)		
15	21.0	20.7	58.0	71.5( 9.2)		
20	31.1	31.3	69.5( 16.7)	93.0		
25	43.1	46.5	73.5( 17.3)	117.0		
33	72.5	82.7( 30.5)	94.3			
	90.5( 33.7)					

DIL AT MAX REAR  
 OR PERMITTED RISE 126.0( 34.0) 118.0( 32.3) 114.0( 22.1) 125.0( 15.7) 168.0( 9.6) 452.0( 3.4)

TABLE 63

DIFFUSER PLUME DILUTION  
 PORT SPACING = 25 DIAMETERS, STABILITY STRATIFICATION PARAMETER = 2000  
 CURRENT TO EFFLUENT RATIO = 0.10

RISE(DIA)	DENSIMETRIC FROUDE NUMBER					
	1	3	10	30	100	1000
1	1.9	2.8	6.4	16.4	50.9	71.0( 0.0) 245.0
2	2.7	3.7	8.8	22.9	71.0( 2.0)	306.0
3	3.6	4.6	11.0	29.0	85.0	352.0
4	4.5	5.6	13.4	35.0	96.2	391.0
5	5.6	6.6	15.9	41.0	106.0	425.0 458.0( 6.0)
7	8.1	8.7	21.5	54.2	124.0	492.0
9	10.9	11.2	28.2	68.5	142.0	573.0
12	15.7	15.5	40.2	71.4( 9.4) 90.4	166.0	
15	21.1	20.4	55.3	111.0	191.0 197.0( 15.8)	
20	31.5	30.5	75.5( 18.4) 86.2	146.0 166.0( 23.1)	232.0	
25	44.0	42.8	119.0 155.0( 30.5)	181.0		
33	67.1	69.5	174.0			
42	98.3	109.0( 41.2) 114.0				
54	112.0( 45.5)	129.0( 44.4)				
	157.0	239.0				
	159.0( 54.4)					

DIL AT MAX REAL  
 (OR PERMITTED RISE 312.0( 58.3) 270.0( 55.1) 236.0( 40.6) 238.0( 32.7) 275.0( 24.1) 617.0( 9.6)

TABLE 64

DIFFUSER PLUME DILUTION  
 PORT SPACING = 25 DIAMETERS, STABILITY STRATIFICATION PARAMETER = 10000  
 CURRENT TO EFFLUENT RATIO = 0.10

RISE(DIA)	DENSIMETRIC FROUDE NUMBER					
	1	3	10	30	100	1000
1	1.9	2.8	6.4	16.4	50.9	71.0( 0.0) 244.0
2	2.7	3.7	8.8	22.9	71.0( 2.0)	304.0
3	3.6	4.6	11.0	29.0	84.4	347.0
4	4.5	5.6	13.4	35.0	95.6	380.0
5	5.6	6.6	15.9	41.0	105.0	411.0
7	8.1	8.7	21.5	54.1	124.0	461.0
9	10.9	11.2	28.0	68.1	141.0	505.0
12	15.7	15.5	39.9	71.4( 9.5) 89.8	164.0	563.0
15	21.1	20.4	54.5	111.0	187.0	615.0
20	31.8	30.3	76.0( 18.7) 84.4	144.0	225.0	
25	44.0	42.5	115.0	177.0	261.0	
33	67.6	67.1	164.0	230.0	317.0	
42	99.0	103.0	219.0	289.0	381.0	
54	150.0	124.0( 46.1) 163.0	297.0	364.0( 53.2) 369.0	387.0( 43.0)	
70	234.0	244.0	408.0			
90	309.0( 83.7) 247.0( 72.4)	318.0( 82.4)				
	343.0	379.0				

DIL AT MAX REAL  
 OR PERMITTED RISE 447.0(103.0) 510.0( 99.9) 462.0( 77.1) 453.0( 66.5) 461.0( 53.4) 629.0( 15.9)

TABLE 65

DIFFUSER PLUME DILUTION  
 PORT SPACING = 25 DIAMETERS, STABILITY STRATIFICATION PARAMETER = INFINITE  
 CURRENT TO EFFLUENT RATIO = 0.10

RISE(DIA)	DENSIMETRIC FROUDE NUMBER					
	1	3	10	30	100	1000
1	1.9	2.8	6.4	16.4	50.9	71.0( 0.0)
2	2.7	3.7	8.8	22.9	71.0( 2.0)	244.0
3	3.6	4.6	11.0	28.8	84.4	302.0
4	4.5	5.6	13.4	34.8	95.6	345.0
5	5.6	6.6	15.9	41.0	105.0	378.0
7	8.1	8.7	21.4	53.8	124.0	407.0
9	10.9	11.2	28.0	68.1	140.0	456.0
12	15.7	15.3	39.9	71.4( 9.5)	164.0	497.0
15	21.1	20.4	54.1	89.8	187.0	550.0
20	31.8	30.3	76.6( 18.9)	110.0	223.0	595.0
25	44.3	42.2	83.8	144.0	259.0	
33	67.6	66.7	114.0	177.0	315.0	
42	99.6	102.0	162.0	228.0	377.0	
54	151.0	129.0( 47.7)	215.0	287.0	458.0	
70	234.0	160.0	284.0	364.0		
90	289.0( 79.2)	232.0	378.0	468.0		
115	352.0	321.0	495.0			
	487.0	431.0				

DIL AT MAX REAL  
 OR PERMITTED RISE 535.0(124.0) 487.0(128.0) 528.0( 95.9) 541.0( 81.6) 536.0( 65.9) 633.0( 17.9)

TABLE 66

DIFFUSER PLUME DILUTION  
 PORT SPACING = 25 DIAMETERS, STABILITY STRATIFICATION PARAMETER = 200  
 CURRENT TO EFFLUENT RATIO = 0.05

RISE(DIA)	DENSIMETRIC FROUDE NUMBER					
	1	3	10	30	100	1000
1	1.9	2.8	5.9	13.7	40.5	44.9( 0.0) 172.0
2	2.7	3.6	7.6	18.6	44.9( 1.3) 54.5	195.0( 1.4) 232.0
3	3.6	4.4	9.1	22.5	63.5 71.0( 4.0)	
4	4.6	5.1	10.3	26.2	71.5	
5	5.6	6.0	11.7	29.8	78.7	
7	8.1	7.6	14.3	37.8 41.3( 7.8)		
9	10.8	9.4	17.3	45.2( 8.7) 46.8		
12	15.4	12.3	22.3 26.0( 13.8)			
15	20.3 24.9( 17.7)	15.5 20.5( 19.2)	29.0	45.6( 19.1)		
20	29.3	21.7				
25	49.2( 23.9)	30.9 45.6( 26.4)				

DIL AT MAX REFL  
 OR PERMITTED RISE 56.1( 23.9) 46.2( 26.4) 48.5( 19.4) 62.6( 11.7) 97.2( 6.4) 269.0( 2.3)

TABLE 67

DIFFUSER PLUME DILUTION  
 PORT SPACING = 25 DIAMETERS, STABILITY STRATIFICATION PARAMETER = 500  
 CURRENT TO EFFLUENT RATIO = 0.05

RISE(DIA)	DENSIMETRIC FROUDE NUMBER					
	1	3	10	30	100	1000
1	1.9	2.8	5.9	13.7	40.2	44.9( 0.0) 169.0
2	2.7	3.6	7.6	18.5	44.9( 1.3) 53.8	214.0 242.0( 2.8)
3	3.6	4.4	9.0	22.3	62.2	249.0
4	4.6	5.1	10.3	25.8	69.0	289.0
5	5.7	6.0	11.6	29.4	75.0	
7	8.1	7.6	14.2	36.5	86.2 90.4( 7.4)	
9	10.9	9.4	16.9	44.3	56.9	
12	15.5	12.3	21.4	45.5( 9.4) 55.7 62.6( 13.9)	116.0	
15	20.8	15.6	26.5	67.1		
20	30.7	21.6	37.3 45.2( 22.8) 51.2( 24.6) 53.1	89.2		
25	41.3 44.0( 26.2)	28.6 36.2( 29.9)				
33	59.6 71.2( 34.9)	42.2 61.0( 38.7)				

DIL AT MAX REAL  
 OR PERMITTED RISE 108.0( 35.1) 89.1( 39.9) 84.4( 30.7) 91.6( 20.2) 124.0( 12.4) 335.0( 4.5)

TABLE 68

DIFFUSER PLUME DILUTION  
 PORT SPACING = 25 DIAMETERS, STABILITY STRATIFICATION PARAMETER = 2000  
 CURRENT TO EFFLUENT RATIO = 0.05

RISE(DIA)	DENSIMETRIC FROUDE NUMBER					
	1	3	10	30	100	1000
1	1.9	2.8	5.9	13.7	39.9	44.9( 0.0)
2	2.7	3.6	7.6	18.5	44.9( 1.3)	168.0
3	3.6	4.4	9.0	22.2	53.4	208.0
4	4.6	5.1	10.3	25.6	61.3	237.0
5	5.7	6.0	11.6	29.0	68.1	261.0
7	8.1	7.6	14.1	36.0	74.0	282.0
9	10.9	9.4	16.7	43.4	83.8	320.0
12	15.6	12.3	21.0	45.9( 9.7)	93.6	339.0( 8.0)
15	21.0	15.6	25.8	54.2	107.0	357.0
20	31.3	21.7	35.0	64.4	119.0	420.0
25	43.1	28.6	45.9	80.9	140.0	143.0( 20.9)
33	64.4	41.6	57.2( 29.3)	97.6	160.0	118.0( 30.8)
42	91.1	58.9	67.6	118.0( 30.8)	126.0	160.0
54	130.0	87.4	93.6	102.0( 44.5)	161.0	105.0( 46.4)
70	143.0( 57.7)	88.6( 54.6)	99.7( 58.5)	144.0	167.0	143.0( 57.7)

DIL AT MAX REAR  
 (OR PERMITTED RISE 274.0( 61.2) 222.0( 71.0) 183.0( 59.0) 173.0( 44.3) 200.0( 32.4) 471.0( 13.0)

TABLE 69

DIFFUSER PLUME DILUTION  
 PORT SPACING = 25 DIAMETERS, STABILITY STRATIFICATION PARAMETER = 10000  
 CURRENT TO EFFLUENT RATIO = 0.05

RISE(DIA)	DENSIMETRIC FRONTS NUMBER					
	1	3	10	30	100	1000
1	1.9	2.8	5.9	13.7	39.9	44.9( 0.0)
2	2.7	3.6	7.6	18.5	44.9( 1.3)	53.4
3	3.6	4.4	9.0	22.2	61.3	234.0
4	4.6	5.1	10.3	25.6	67.6	258.0
5	5.7	6.0	11.6	29.0	73.5	277.0
7	8.1	7.6	14.0	36.0	83.2	309.0
9	10.9	9.4	16.7	43.1	92.3	337.0
12	15.7	12.3	21.0	45.9( 9.8)	53.8	105.0
15	21.0	15.6	25.6	63.9	118.0	404.0
20	31.3	21.7	34.5	79.8	137.0	451.0
25	43.4	28.8	44.9	95.6	156.0	495.0
33	65.3	41.6	59.7( 31.1)	64.8	121.0	185.0
42	94.3	58.8	87.4	149.0	217.0	
54	139.0	86.2	117.0	188.0	260.0	277.0( 58.8)
70	205.0	130.0( 69.8)	157.0	241.0	318.0	
90	279.0( 87.3)	131.0	215.0	255.0( 74.2)		
115	248.0( 79.5)	184.0	223.0(105.0)	232.0( 95.2)		
	290.0	249.0	326.0			

DIL AT MAX REAL OR PERMITTED RISE 361.0(111.0) 375.0(136.0) 388.0(123.0) 350.0( 99.6) 353.0( 79.7) 506.0( 26.4)



TABLE 70

DIFFUSER PLUME DILUTION  
 PORT SPACING = 25 DIAMETERS, STABILITY STRATIFICATION PARAMETER = INFINITE  
 CURRENT TO EFFLUENT RATIO = 0.05

RISE(DIA)	DENSIMETRIC FROUDE NUMBER					
	1	3	10	30	100	1000
1	1.9	2.8	5.9	13.7	39.9	44.9[ 0.0]
2	2.7	3.6	7.6	18.5	44.9[ 1.3]	168.0
3	3.6	4.4	9.0	22.2	53.4	206.0
4	4.6	5.1	10.3	25.6	61.3	234.0
5	5.7	6.0	11.6	29.0	67.6	256.0
7	8.1	7.6	14.0	36.0	73.5	275.0
9	10.9	9.4	16.7	43.1	83.2	306.0
12	15.7	12.3	21.0	45.9[ 9.8]	92.3	333.0
15	21.1	15.6	25.4	53.8	105.0	366.0
20	31.5	21.7	34.3	63.5	117.0	396.0
25	43.4	28.8	44.6	79.8	136.0	436.0
33	65.7	41.9	60.5[ 31.6]	94.9	155.0	472.0
42	94.9	59.3	64.4	119.0	183.0	
54	141.0	86.1	86.1	147.0	215.0	
70	212.0	131.0	114.0	183.0	257.0	
90	299.0[ 87.0]	139.0[ 72.9]	151.0	231.0	310.0	
115	316.0	187.0	196.0	290.0	378.0	
148	429.0	252.0	251.0	365.0		
		337.0	326.0			

DIL. AT MAX REAL  
 OR PERMITTED RISE 503.0(132.0) 408.0(176.0) 386.0(175.0) 422.0(135.0) 428.0(105.0) 512.0( 31.4)

TABLE 71

DIFFUSER PLUME DILUTION  
 PORT SPACING = 25 DIAMETERS, STABILITY STRATIFICATION PARAMETER = 200  
 CURRENT TO EFFLUENT RATIO = 0.02

RISE(DIA)	DENSIMETRIC FROUDE NUMBER					
	1	3	10	30	100	1000
1	: T)					
	: M)					32.0( 0.0)
2	: T)	1.9	2.7	5.5	11.9	30.5
	: M)					111.0
3	: T)					138.0( 2.0)
	: M)	2.7	3.6	7.1	15.5	32.0( 1.1)
4	: T)					140.0
	: M)	3.6	4.3	8.2	18.2	44.3
5	: T)					171.0
	: M)	4.6	5.1	9.3	20.5	48.5
7	: T)					
	: M)	5.7	5.9	10.2	22.6	52.7
9	: T)					53.0( 5.2)
	: M)	8.1	7.5	12.0	26.5	60.5
12	: T)					
	: M)	10.8	9.2	13.7	30.5	
15	: T)					31.5( 9.5)
	: M)	15.2	12.0	16.2	32.9( 10.2)	36.7
20	: T)					
	: M)	20.3	14.9	19.0		
25	: T)	24.8( 17.6)	19.7( 19.6)	19.8( 16.0)		
	: M)	29.0	20.1	24.4		
30	: T)					
	: M)	39.3( 24.0)		32.5( 23.7)		
35	: T)					
	: M)		25.6			
40	: T)					
	: M)		33.4( 27.5)			

DIL AT MAX REAL  
 OR PERMITTED RISE 45.5( 24.0) 34.8( 27.6) 33.3( 23.8) 45.0( 14.7) 70.4( 8.3) 187.0( 3.2)

TABLE 72

DIFFUSER PLUME DILUTION  
 PORT SPACING = 25 DIAMETERS, STABILITY STRATIFICATION PARAMETER = 500  
 CURRENT TO EFFLUENT RATIO = 0.02

RISE(DIA)	DENSIMETRIC FROUDE NUMBER					
	1	3	10	30	100	1000
1	1.9	2.7	5.5	11.9	30.5	32.0( 0.0) 109.0
2	2.7	3.6	7.1	15.5	32.0( 1.1) 38.8	134.0
3	3.6	4.3	8.2	18.1	43.7	153.0 169.0( 4.0)
4	4.6	5.1	9.3	20.4	47.5	170.0
5	5.7	5.9	10.2	22.3	50.9	188.0
7	8.1	7.5	11.9	25.8	56.5	
9	10.9	9.2	13.5	29.2	61.8 64.8( 10.4)	
12	15.5	12.0	16.0	33.6( 11.6) 34.3	69.0	
15	20.7	15.1	18.5	38.8 42.8( 17.9)	77.2	
20	30.5	20.7	22.9	46.2		
25	41.3 43.7( 26.2)	26.9 34.1( 30.7)	27.9 30.9( 28.1)	54.8		
33	58.4	37.3	37.0			
42	64.1( 35.1)	50.0( 41.3) 57.5	40.8( 35.5)			

OIL AT MAX REAL OR PERMITTED RISE 90.0( 35.3) 66.5( 42.1) 56.3( 40.3) 61.8( 27.3) 87.3( 16.9) 231.0( 6.5)

TABLE 73

DIFFUSER PLUME DILUTION  
 PORT SPACING = 25 DIAMETERS, STABILITY STRATIFICATION PARAMETER = 2000  
 CURRENT TO EFFLUENT RATIO = 0.02

RISE (DIA)	DENSIMETRIC FROUDE NUMBER					
	1	3	10	30	100	1000
1	1.9	2.7	5.5	11.9	30.5	32.0( 0.01) 109.0
2	2.7	3.6	7.1	15.3	32.0( 1.1) 38.6	132.0
3	3.6	4.3	8.2	18.0	43.4	149.0
4	4.6	5.1	9.3	20.2	47.1	163.0
5	5.7	5.9	10.1	22.2	50.2	175.0
7	8.1	7.5	11.9	25.6	55.7	195.0
9	10.9	9.2	13.5	28.8	60.1	213.0 233.0( 11.5)
12	15.6	12.0	15.9	33.3	65.7	238.0
15	21.0	15.1	18.4	34.0( 12.5) 37.5	71.4	264.0
20	31.1	21.0	22.6	43.7	80.0	
25	42.8	27.5	27.3	49.5	88.3 95.2( 29.4)	
33	64.0	38.8	35.2	58.4	101.0	
42	90.4 104.0( 46.4)	53.4	45.5	69.0 72.2( 44.7)	118.0	
54	127.0	74.5 79.8( 57.0)	54.5( 49.4) 60.1 66.6( 59.7)	85.7		
70	139.0( 58.1)	94.6( 65.0)	103.0	79.4		

DIL. AT MAX REAL  
 OR PERMITTED RISE 244.0( 61.6) 175.0( 76.7) 130.0( 82.7) 115.0( 66.3) 132.0( 46.8) 321.0( 18.8)

TABLE 74

DIFFUSER PLUME DILUTION  
 PORT SPACING = 25 DIAMETERS, STABILITY STRATIFICATION PARAMETER = 10000  
 CURRENT TO EFFLUENT RATIO = 0.02

RISE(DIA)	DENSIMETRIC FROUDE NUMBER					
	1	3	10	30	100	1000
1	1.9	2.7	5.5	11.9	30.5	32.0( 0.0) 108.0
2	2.7	3.6	7.1	15.3	32.0( 1.1) 38.6	132.0
3	3.6	4.3	8.2	18.0	43.4	148.0
4	4.6	5.1	9.3	20.2	47.1	162.0
5	5.7	5.9	10.1	22.2	50.2	172.0
7	8.1	7.5	11.9	25.4	55.3	191.0
9	10.9	9.2	13.5	28.6	59.7	207.0
12	15.6	12.0	15.9	33.1	65.3	226.0
15	21.0	15.2	18.4	34.0( 12.7) 37.2	70.5	244.0
20	31.3	21.0	22.6	43.1	78.2	268.0
25	43.4	27.5	27.1	48.5	85.7	291.0
33	65.3	39.4	35.2	56.8	97.6	323.0 345.0( 39.1)
42	94.3	54.5	45.2	65.7	110.0	356.0
54	138.0	77.6	60.1	77.4	126.0	
70	204.0 276.0( 87.3)	112.0	61.3( 55.1) 79.3	93.2	148.0 175.0( 89.1)	
90	246.0( 79.5) 285.0	131.0( 78.2) 156.0	101.0	114.0	176.0	
115		194.0(112.0) 199.0	128.0	141.0	215.0	
148		248.0	146.0(133.0) 163.0	147.0(120.0) 191.0		

DIL. AT MAX REAL OR PERMITTED RISE 340.0(112.0) 259.0(152.0) 295.0(185.0) 258.0(170.0) 241.0(131.0) 374.0( 46.7)

TABLE 75

DIFFUSER PLUME DILUTION  
 PORT SPACING = 25 DIAMETERS, STABILITY STRATIFICATION PARAMETER = INFINITE  
 CURRENT TO EFFLUENT RATIO = 0.02

RISE(DIA)	DENSIMETRIC FROUDE NUMBER					
	1	3	10	30	100	1000
1	1.9	2.7	5.5	11.9	30.5	32.0 [ 0.01 ]
2	2.7	3.6	7.1	15.3	32.0 [ 1.1 ]	108.0
3	3.6	4.3	8.2	18.0	38.6	131.0
4	4.6	5.1	9.3	20.2	43.4	148.0
5	5.7	5.9	10.1	22.2	47.1	161.0
7	8.1	7.5	11.9	25.4	50.2	172.0
9	10.9	9.2	13.5	28.6	55.3	190.0
12	15.7	12.0	15.9	33.1	59.3	205.0
15	21.0	15.2	18.2	34.3 [ 12.9 ]	65.3	225.0
20	31.3	21.1	22.6	37.2	70.0	241.0
25	43.4	27.7	27.1	43.1	78.2	264.0
33	65.7	39.4	35.0	48.5	85.3	283.0
42	94.9	54.9	45.2	56.4	96.4	310.0
54	140.0	78.2	60.1	65.3	109.0	336.0
70	211.0	114.0	63.1 [ 56.4 ]	76.5	124.0	367.0
90	297.0 [ 86.9 ]	144.0 [ 81.9 ]	79.8	91.4	144.0	
115	314.0	163.0	103.0	110.0	169.0	
148	423.0	217.0	129.0	132.0	199.0	
190		283.0	166.0	161.0	239.0	
244		367.0	211.0	198.0	288.0	
			269.0	245.0		

DIL AT MAX REAL  
 OR PERMITTED RISE 496.0(133.0) 375.0(194.0) 298.0(272.0) 273.0(276.0) 295.0(196.0) 380.0( 59.8)

TABLE 76

DIFFUSER PLUME DILUTION  
 PORT SPACING = 25 DIAMETERS, STABILITY STRATIFICATION PARAMETER = 200  
 CURRENT TO EFFLUENT RATIO = 0.00

RISE(DIA)	DENSIMETRIC FROUDE NUMBER					
	1	3	10	30	100	1000
1	1.9	2.7	5.3	10.6	23.6	25.1( 0.0) 62.2
2	2.7	3.5	6.7	13.5	25.3( 1.2) 28.8	71.9
3	3.6	4.3	7.8	15.5	31.5	79.3 79.8( 3.2)
4	4.6	5.0	8.7	17.1	33.8	85.6
5	5.7	5.8	9.6	18.6	35.5 38.3( 6.9)	93.5
7	8.1	7.4	11.2	21.3	38.6	
9	10.8	9.1	12.7	23.7 26.0( 11.0) 26.5( 11.5)	41.5	
12	15.2	11.8	14.9	27.1		
15	20.3 24.8( 17.7)	14.7 19.6( 19.8)	17.3 18.5( 16.8)	29.8		
20	28.8	19.8	21.0			
25	34.9( 24.1)	24.9	25.0			
		27.4( 27.9)	25.7( 25.5)			

DIL AT MAX HEAD  
 OR PERMITTED RISE 34.9( 24.0) 27.5( 27.8) 26.0( 25.6) 33.3( 17.5) 47.3( 11.3) 99.9( 5.3)

TABLE 77

DIFFUSER PLUME DILUTION  
 PORT SPACING = 25 DIAMETERS, STABILITY STRATIFICATION PARAMETER = 500  
 CURRENT TO EFFLUENT RATIO = 0.00

RISE(DIA)	DENSIMETRIC FROUDE NUMBER					
	1	3	10	30	100	1000
1	1.9	2.7	5.3	10.6	23.6	25.1( 0.0) 61.8
2	2.7	3.5	6.7	13.4	25.3( 1.3) 28.6	71.0
3	3.6	4.3	7.7	15.5	31.3	77.1
4	4.6	5.0	8.7	17.0	33.3	82.1
5	5.7	5.8	9.5	18.5	35.0	86.1 92.5( 6.7)
7	8.1	7.4	11.2	21.0	37.8	93.5
9	10.9	9.1	12.6	23.1	39.9	101.0
12	15.5	11.9	14.9	26.2	42.6 44.3( 14.3)	
15	20.7	14.9	17.1	27.5( 13.5) 28.6	45.0	
20	30.5	20.5	21.0	32.0 32.7( 21.5)	48.9	
25	41.1 43.7( 26.2)	26.5 33.8( 30.9)	24.8 28.4( 29.7)	34.6		
33	58.0	36.8	31.1	38.6		
42	61.4( 35.2)	46.8( 41.8)	35.9( 39.2)	47.0 37.6		

DIL AT MAX REAL  
 OR PERMITTED RISE 61.5( 35.3) 47.2( 42.6) 38.6( 43.9) 40.5( 34.7) 54.9( 24.1) 116.0( 11.4)



TABLE 78

DIFFUSER PLUME DILUTION  
 PORT SPACING = 25 DIAMETERS, STABILITY STRATIFICATION PARAMETER = 2000  
 CURRENT TO EFFLUENT RATIO = 0.00

RISE(DIA)	DENSIMETRIC FROUDE NUMBER					
	1	3	10	30	100	1000
1	1.9	2.7	5.3	10.6	23.4	25.1( 0.0) 61.8
2	2.7	3.5	6.7	13.4	25.3( 1.3) 28.6	70.5
3	3.6	4.3	7.7	15.3	31.3	76.6
4	4.6	5.0	8.7	17.0	33.1	80.9
5	5.7	5.8	9.5	18.4	34.8	84.4
7	8.1	7.4	11.1	20.8	37.2	90.5
9	10.9	9.1	12.6	22.9	39.1	95.4
12	15.6	12.0	14.8	25.8	41.6	102.0
15	21.0	15.0	17.1	28.2( 15.0) 28.4	43.7	107.0
20	31.1	20.8	21.0	31.8	46.5	114.0 116.0( 21.1)
25	42.8	27.1	25.1	34.3	48.9	121.0
33	64.0	38.6	31.8	38.3	52.3	134.0
42	90.4 104.0( 46.4)	53.0	40.2	41.9	55.6 56.3( 44.1)	
54	127.0	74.0 79.3( 57.3)	52.0 59.3( 63.4)	46.7 48.1( 58.3)	59.8	
70	138.0( 58.2)	93.6( 65.3)	53.0( 55.4)			
90		99.7	63.7	52.1	65.7	
			72.6	57.7		

DIL AT MAX REAL  
 OR PERMITTED RISE 143.0( 61.8) 105.0( 77.6) 73.1( 92.2) 59.4( 94.3) 70.2( 75.3) 145.0( 36.3)

TABLE 79

DIFFUSER PLUME DILUTION  
 PORT SPACING = 25 DIAMETERS, STABILITY STRATIFICATION PARAMETER = 10000  
 CURRENT TO EFFLUENT RATIO = 0.00

RISE(DIA)	DENSIMETRIC FROUDE NUMBER					
	1	3	10	30	100	1000
1	1.9	2.7	5.3	10.6	23.4	25.1( 0.0) 61.3
2	2.7	3.5	6.7	13.4	25.3( 1.3) 28.6	70.5
3	3.6	4.3	7.7	15.3	31.3	76.0
4	4.6	5.0	8.7	17.0	33.1	80.4
5	5.7	5.8	9.5	18.4	34.8	84.4
7	8.1	7.4	11.1	20.8	37.2	90.0
9	10.9	9.1	12.6	22.9	39.1	94.5
12	15.6	12.0	14.8	25.6	41.3	100.0
15	21.0	15.0	17.1	28.2	43.5	105.0
20	31.3	20.8	21.0	28.6( 15.6) 31.5	46.2	111.0
25	43.4	27.3	25.1	34.3	48.2	116.0
33	65.3	39.1	32.0	38.3	51.4	123.0
42	94.3	54.2	40.5	42.5	54.4	130.0
54	138.0	76.6	53.0	47.4	58.0	137.0
70	204.0 275.0( 87.4)	111.0	60.9( 61.3) 69.5	53.8	62.1	146.0 151.0( 80.5)
90	246.0( 79.5) 283.0	131.0( 78.7) 154.0	86.2	61.7	66.7	156.0
115		189.0(113.0)	105.0	70.7	72.1	168.0
148		192.0	125.0(146.0)	81.9	78.5	
190		228.0	126.0	89.0(171.0)	80.6(160.0)	
244			148.0	94.6	86.0	
				107.0	94.9	

DIL AT MAX RFAL  
 OR PERMITTED RISE 334.0(112.0) 232.0(154.0) 154.0(213.0) 111.0(267.0) 99.9(267.0) 173.0(123.0)

TABLE 80

DIFFUSER PLUME DILUTION  
 PORT SPACING = 25 DIAMETERS, STABILITY STRATIFICATION PARAMETER = INFINITE  
 CURRENT TO EFFLUENT RATIO = 0.00

RISE(DIA)	DENSIMETRIC FROUDE NUMBER					
	1	3	10	30	100	1000
1	1.9	2.7	5.3	10.6	23.4	25.1( 0.0)
2	2.7	3.5	6.7	13.4	25.3( 1.3)	61.3
3	3.6	4.3	7.7	15.3	28.6	70.5
4	4.6	5.0	8.7	17.0	31.3	76.0
5	5.7	5.8	9.5	18.4	33.1	80.4
7	8.1	7.4	11.1	20.8	34.8	84.4
9	10.9	9.1	12.6	22.9	37.2	90.0
12	15.7	12.0	14.8	25.6	39.1	94.5
15	21.0	15.0	17.1	28.2	41.3	99.9
20	31.3	20.8	21.0	28.6( 15.6)	43.2	104.0
25	43.4	27.3	25.1	31.5	45.9	111.0
33	65.7	39.1	32.0	34.3	48.2	116.0
42	94.9	54.1	40.8	38.3	51.3	122.0
51	140.0	77.6	53.4	42.5	54.1	128.0
70	211.0	114.0	63.5( 63.1)	47.7	57.7	135.0
90	297.0( 86.9)	143.0( 81.9)	70.5	54.3	61.7	142.0
115	313.0	162.0	88.6	62.4	66.3	149.0
148	419.0	212.0	110.0	72.7	71.6	157.0
190		274.0	138.0	85.5	78.3	165.0
244		351.0	172.0	102.0	86.4	
			216.0	123.0	96.3	

DIL AT MAX REAL  
 OR PERMITTED RISE 491.0(133.0) 363.0(197.0) 262.0(300.0) 145.0(301.0) 106.0(301.0) 174.0(191.0)

TABLE 81

DIFFUSER PLUME DILUTION  
 PORT SPACING = 1000 DIAMETERS, STABILITY STRATIFICATION PARAMETER = 200  
 CURRENT TO EFFLUENT RATIO = 0.10

RISE(DIA)	DENSIMETRIC FROUDE NUMBER					
	1	3	10	30	100	1000
1	1.9	2.8	6.4	16.4	51.6	436.0( 0.7)
2	2.7	3.7	8.8	23.3	73.5	
3	3.5	4.6	11.1	29.4	93.0	
4	4.5	5.6	13.5	35.7	114.0	96.9( 3.2)
5	5.6	6.6	16.1	42.2		
7	8.1	8.8	22.2	57.2	53.0( 6.5)	
9	10.8	11.3	29.6	76.1		
12	15.4	15.8	44.9			38.0( 10.8)
15	20.5	21.4				
20	25.5( 17.6)	26.2( 17.0)				
	30.7	37.3				

DIL AT MAX REAL  
 OR PERMITTED RISE 67.2( 23.4) 63.3( 22.2) 66.1( 14.7) 84.7( 9.4) 152.0( 4.9) 684.0( 1.1)

TABLE 82

DIFFUSER PLUME DILUTION  
 PORT SPACING = 1000 DIAMETERS, STABILITY STRATIFICATION PARAMETER = 500  
 CURRENT TO EFFLUENT RATIO = 0.10

RISE(DIA)	DENSIMETRIC FROUDE NUMBER					
	1	3	10	30	100	1000
1	1.9	2.8	6.4	16.4	51.2	497.0 592.0( 1.3)
2	2.7	3.7	8.8	23.1	71.9	893.0
3	3.6	4.6	11.0	29.0	89.2	
4	4.5	5.6	13.4	35.2	105.0	
5	5.6	6.6	16.0	41.3	122.0 136.0( 5.9)	
7	8.1	8.8	21.7	54.9	156.0	
9	10.9	11.2	28.6	70.0 86.2( 11.0)		
12	15.6	15.6	41.6	96.3		
15	21.0	20.7	58.0 69.5( 16.7)	129.0		
20	31.1	31.3	97.0			
25	43.1 45.6( 26.0)	46.5 48.8( 25.6)				
33	72.5					

DIL AT MAX REAL  
 OR PERMITTED RISE 128.0( 34.0) 121.0( 32.3) 120.0( 22.0) 138.0( 15.4) 215.0( 8.8) 929.0( 2.0)

TABLE 83

DIFFUSER PLUME DILUTION  
 PORT SPACING = 1000 DIAMETERS, STABILITY STRATIFICATION PARAMETER = 2000  
 CURRENT TO EFFLUENT RATIO = 0.10

RISE(DIA)	DENSIMETRIC FROUDE NUMBER					
	1	3	10	30	100	1000
1	1.9	2.8	6.4	16.4	50.9	477.0
2	2.7	3.7	8.8	22.9	71.0	689.0
3	3.6	4.6	11.0	29.0	87.3	867.0 929.0( 3.4)
4	4.5	5.6	13.4	35.0	102.0	
5	5.6	6.6	15.9	41.0	117.0	
7	8.1	8.7	21.5	54.2	147.0	
9	10.9	11.2	28.2	68.5	176.0	
12	15.7	15.5	40.2	92.3	224.0 254.0( 13.8)	
15	21.1	20.4	55.3	120.0	277.0	
20	31.5	30.5	86.8	173.0 197.0( 22.0)		
25	44.0	42.8	129.0 178.0( 29.8)	236.0		
33	67.1	69.5	218.0			
42	98.3 112.0( 45.5)	114.0 132.0( 44.3)				
54	157.0	303.0				

DIL AT MAX REAL  
 OR PERMITTED RISE 326.0( 58.2) 310.0( 54.2) 297.0( 38.1) 314.0( 29.8) 402.0( 20.0) 974.0( 3.6)

TABLE 84

DIFFUSER PLUME DILUTION  
 PORT SPACING = 1000 DIAMETERS, STABILITY STRATIFICATION PARAMETER = 10000  
 CURRENT TO EFFLUENT RATIO = 0.10

		DENSIMETRIC FROUDE NUMMR					
		1	3	10	30	100	1000
1	: T)						
	: M)	1.9	2.8	6.4	16.4	50.9	474.0
2	: T)						
	: M)	2.7	3.7	8.8	22.9	71.0	670.0
3	: T)						
	: M)	3.6	4.6	11.0	29.0	87.3	819.0
4	: T)						
	: M)	4.5	5.6	13.4	35.0	102.0	954.0
5	: T)						
	: M)	5.6	6.6	15.9	41.0	116.0	
7	: T)						
	: M)	8.1	8.7	21.5	54.1	145.0	
9	: T)						
	: M)	10.9	11.2	28.0	68.1	173.0	
12	: T)						
	: M)	15.7	15.5	39.9	91.7	218.0	
15	: T)						
	: M)	21.1	20.4	54.5	118.0	265.0	
20	: T)						
	: M)	31.8	30.3	85.0	170.0	351.0	
25	: T)						
	: M)	44.0	42.5	124.0	230.0	444.0	
33	: T)						
	: M)	67.6	67.1	203.0	344.0	613.0	
42	: T)						
	: M)	99.0	103.0	319.0	500.0		
54	: T)						
	: M)	150.0	171.0	525.0( 54.1)	544.0( 44.4)		
70	: T)						
	: M)	234.0	317.0				
90	: T)						
	: M)	322.0( 83.6)	432.0( 77.8)				
90	: T)						
	: M)	375.0					

DIL AT MAX REAL  
 OR PERMITTED RISE 546.0(101.0) 720.0( 88.9) 671.0( 61.0) 668.0( 50.4) 690.0( 36.2) 974.0( 4.2)

TABLE 85

DIFFUSER PLUME DILUTION  
 PORT SPACING = 1000 DIAMETERS, STABILITY STRATIFICATION PARAMETER = INFINITE  
 CURRENT TO EFFLUENT RATIO = 0.10

RISE(DIA)	DENSIMETRIC FROUDE NUMBER					
	1	3	10	30	100	1000
1	1.9	2.8	6.4	16.4	50.9	474.0
2	2.7	3.7	8.8	22.9	71.0	666.0
3	3.6	4.6	11.0	28.8	86.7	813.0
4	4.5	5.6	13.4	34.8	102.0	934.0
5	5.6	6.6	15.9	41.0	116.0	
7	8.1	9.7	21.4	53.8	144.0	
9	10.9	11.2	28.0	68.1	172.0	
12	15.7	15.3	39.9	91.7	217.0	
15	21.1	20.4	54.1	118.0	263.0	
20	31.8	30.3	84.4	170.0	347.0	
25	44.3	42.2	123.0	229.0	438.0	
33	67.6	66.7	199.0	342.0	601.0	
42	99.6	102.0	311.0	492.0		
54	151.0	164.0	501.0	737.0		
70	234.0	278.0				
90	363.0	481.0				
115	563.0					

DIL AT MAX REAL  
 OR PERMITTED RISE 620.0(121.0) 730.0(108.0) 795.0( 68.6) 794.0( 56.6) 787.0( 41.2) 974.0( 4.4)



TABLE 86

DIFFUSER PLUME DILUTION  
 PORT SPACING = 1000 DIAMETERS, STABILITY STRATIFICATION PARAMETER = 200  
 CURRENT TO EFFLUENT RATIO = 0.05

RISE(DIA)	DFNSIMETRIC FROUDE NUMBER					
	1	3	10	30	100	1000
1	1.9	2.8	5.9	13.7	40.5	364.0( 0.9)
2	2.7	3.6	7.6	18.6	56.8	407.0
3	3.6	4.4	9.1	22.5	71.0	81.5( 3.8)
4	4.6	5.1	10.3	26.2	84.4	
5	5.6	6.0	11.7	29.8	100.0	
7	8.1	7.6	14.3	37.8		
9	10.8	9.4	17.3	46.8		
12	15.4	12.3	22.3	26.0( 13.8)		
15	20.3	15.5	29.0			
20	24.9( 17.7)	20.5( 19.2)				
25	29.3	21.7				
		30.9				

DIL AT MAX REAL  
 OR PERMITTED RISE 56.5( 23.9) 46.2( 26.4) 48.9( 19.4) 66.7( 11.6) 127.0( 5.8) 571.0( 1.3)

TABLE 87

DIFFUSER PLUME DILUTION  
 PORT SPACING = 1000 DIAMETERS, STABILITY STRATIFICATION PARAMETER = 500  
 CURRENT TO EFFLUENT RATIO = 0.05

RISF(DIA)	DENSIMETRIC FROUDE NUMBER					
	1	3	10	30	100	1000
1	1.9	2.8	5.9	13.7	40.2	374.0
2	2.7	3.6	7.6	18.5	56.1	491.0( 1.6)
3	3.6	4.4	9.0	22.3	68.5	583.0
4	4.6	5.1	10.3	25.8	79.8	
5	5.7	6.0	11.6	29.4	90.4	
7	8.1	7.6	14.2	36.5	112.0( 7.0)	
9	10.9	9.4	16.9	44.3	137.0	
12	15.5	12.3	21.4	57.2	65.8( 13.7)	
15	20.8	15.6	26.5	73.0		
20	30.7	21.6	37.3	45.2( 22.8)		
25	41.3	28.6	53.1			
33	44.0( 26.2)	36.2( 29.9)				
	59.6	42.2				

DIL AT MAX REAL  
 OR PERMITTED RISE 109.0( 35.1) 91.4( 39.9) 90.9( 30.5) 108.0( 19.5) 176.0( 10.6) 770.0( 2.4)

TABLE 88

DIFFUSER PLUME DILUTION  
 PORT SPACING = 1000 DIAMETERS, STABILITY STRATIFICATION PARAMETER = 2000  
 CURRENT TO EFFLUENT RATIO = 0.05

RISE(DIA)	DENSIMETRIC FROUDE NUMBER					
	1	3	10	30	100	1000
1	1.9	2.8	5.9	13.7	39.9	364.0
2	2.7	3.6	7.6	18.5	55.7	519.0
3	3.6	4.4	9.0	22.2	67.5	647.0
4	4.6	5.1	10.3	25.6	78.2	770.0 774.0( 4.1)
5	5.7	6.0	11.6	29.0	88.0	906.0
7	8.1	7.6	14.1	36.0	107.0	
9	10.9	9.4	16.7	43.4	126.0	
12	15.6	12.3	21.0	55.3	155.0	
15	21.0	15.6	25.8	68.5	186.0 205.0( 16.8)	
20	31.3	21.7	35.0	94.9	244.0	
25	43.1	28.6	45.9	125.0 150.0( 28.5)		
33	64.4	41.6	69.0	187.0		
42	91.1 105.0( 46.4)	58.9	108.0 117.0( 43.7)			
54	130.0	87.4 88.6( 54.6)	214.0			
70		208.0				

DIL AT MAX REAL  
 OR PERMITTED RISE 285.0( 61.1) 245.0( 70.5) 236.0( 55.4) 247.0( 38.5) 324.0( 24.4) 914.0( 5.1)

TABLE 89

DIFFUSER PLUME DILUTION  
 PORT SPACING = 1000 DIAMETERS, STABILITY STRATIFICATION PARAMETER = 10000  
 CURRENT TO EFFLUENT RATIO = 0.05

RISE(CIA)	DENSIMETRIC FROUDE NUMBER					
	1	3	10	30	100	1000
1	1.9	2.8	5.9	13.7	39.9	362.0
2	2.7	3.6	7.6	18.5	55.3	508.0
3	3.6	4.4	9.0	22.2	67.1	621.0
4	4.6	5.1	10.3	25.6	77.6	719.0
5	5.7	6.0	11.6	29.0	87.3	807.0
7	8.1	7.6	14.0	36.0	106.0	
9	10.9	9.4	16.7	43.1	124.0	
12	15.7	12.3	21.0	54.9	152.0	
15	21.0	15.6	25.6	67.6	180.0	
20	31.3	21.7	34.5	92.3	230.0	
25	43.4	28.8	44.9	122.0	285.0	
33	65.3	41.6	65.3	177.0	382.0 486.0( 40.6)	
42	94.3	58.8	94.9	254.0	506.0	
54	139.0	86.2	148.0	379.0 426.0( 57.9)		
70	205.0 285.0( 87.2)	131.0	256.0 374.0( 81.7)			
90	299.0	201.0 258.0(103.0)	492.0			
115		332.0				

DIL AT MAX REAL OR PERMITTED RISE 410.0(109.0) 558.0(127.0) 602.0( 96.1) 577.0( 69.0) 598.0( 48.0) 914.0( 6.4)

TABLE 90

DIFFUSER PLUME DILUTION  
 PORT SPACING = 1000 DIAMETERS, STABILITY STRATIFICATION PARAMETER = INFINITE  
 CURRENT TO EFFLUENT RATIO = 0.05

RISE (DIA)	DENSIMETRIC FROUDE NUMBER					
	1	3	10	30	100	1000
1	1.9	2.8	5.9	13.7	39.9	362.0
2	2.7	3.6	7.6	18.5	55.3	508.0
3	3.6	4.4	9.0	22.2	67.1	617.0
4	4.6	5.1	10.3	25.6	77.6	710.0
5	5.7	6.0	11.6	29.0	87.3	791.0
7	8.1	7.6	14.0	36.0	105.0	
9	10.9	9.4	16.7	43.1	124.0	
12	15.7	12.3	21.0	54.5	151.0	
15	21.1	15.6	25.4	67.6	180.0	
20	31.5	21.7	34.3	92.3	229.0	
25	43.4	28.8	44.6	121.0	282.0	
33	65.7	41.9	64.4	175.0	376.0	
42	94.9	59.3	92.3	249.0	493.0	
54	141.0	86.1	141.0	367.0	670.0	
70	212.0	131.0	227.0	564.0		
90	317.0	199.0	379.0			
115	470.0	302.0	637.0			
148		476.0				

OIL AT MAX REAR  
 OR PERMITTED RISE 571.0(130.0) 551.0(160.0) 689.0(119.0) 717.0( 80.7) 708.0( 56.5) 914.0( 6.7)

TABLE 91

DIFFUSER PLUME DILUTION  
 PORT SPACING = 1000 DIAMETERS, STABILITY STRATIFICATION PARAMETER = 200  
 CURRENT TO EFFLUENT RATIO = 0.02

		DENSIMETRIC FROUDE NUMBER					
		1	3	10	30	100	1000
1	: T)						
	: M)						
2	: T)	1.9	2.7	5.5	11.9	30.5	265.0
	: M)						282.0( 1.1)
3	: T)	2.7	3.6	7.1	15.5	41.6	
	: M)						
4	: T)	3.6	4.3	8.2	18.2	50.5	
	: M)						
5	: T)	4.6	5.1	9.3	20.5	58.4	
	: M)					64.0( 4.7)	
7	: T)	5.7	5.9	10.2	22.6	66.7	
	: M)						
9	: T)	8.1	7.5	12.0	26.5	89.8	
	: M)						
12	: T)	10.8	9.2	13.7	30.5		
	: M)				31.5( 9.5)		
15	: T)	15.2	12.0	16.2	37.5		
	: M)						
20	: T)	20.3	14.9	19.0			
	: M)	24.8( 17.6)	19.7( 19.6)	19.8( 16.0)			
25	: T)	29.0	20.1	24.4			
	: M)						
	: T)		25.6				
	: M)						

DIL AT MAX REAL  
 OR PERMITTED RISE 45.8( 24.0) 34.8( 27.6) 33.5( 23.8) 49.2( 14.5) 99.7( 7.2) 439.0( 1.7)

TABLE 92

DIFFUSER PLUME DILUTION  
 PORT SPACING = 1000 DIAMETERS, STABILITY STRATIFICATION PARAMETER = 500  
 CURRENT TO EFFLUENT RATIO = 0.02

RISE(DIA)	DENSIMETRIC FROUDE NUMBER					
	1	3	10	30	100	1000
1	1.9	2.7	5.5	11.9	30.5	254.0
2	2.7	3.6	7.1	15.5	41.0	374.0 380.0( 2.1)
3	3.6	4.3	8.2	18.1	49.1	528.0
4	4.6	5.1	9.3	20.4	56.5	
5	5.7	5.9	10.2	22.3	63.1	
7	8.1	7.5	11.9	25.8	75.0 86.2( 8.9)	
9	10.9	9.2	13.5	29.2	87.4	
12	15.5	12.0	16.0	34.3	109.0	
15	20.7	15.1	18.5	39.6 44.9( 17.7)		
20	30.5	20.7	22.9	50.2		
25	41.3 43.7( 26.2)	26.9 34.1( 30.7)	27.9 30.9( 28.1)	65.8		
33	58.4	37.3	37.0			
42		58.3				

DIL AT MAX REAL  
 OR PERMITTED RISE 90.6( 35.3) 67.9( 42.1) 59.1( 40.2) 74.4( 26.3) 135.0( 13.5) 594.0( 3.1)

TABLE 93

DIFFUSER PLUME DILUTION  
 PORT SPACING = 1000 DIAMETERS, STABILITY STRATIFICATION PARAMETER = 2000  
 CURRENT TO EFFLUENT RATIO = 0.02

RISF(DIA)	DENSIMETRIC FROUDE NUMBER					
	1	3	10	30	100	1000
1	1.9	2.7	5.5	11.9	30.5	249.0
2	2.7	3.6	7.1	15.3	40.8	352.0
3	3.6	4.3	8.2	18.0	48.8	433.0
4	4.6	5.1	9.3	20.2	55.7	508.0
5	5.7	5.9	10.1	22.2	61.3	578.0
7	8.1	7.5	11.9	25.6	71.9	594.0( 5.2)
9	10.9	9.2	13.5	28.8	82.1	744.0
12	15.6	12.0	15.9	33.3	96.3	
15	21.0	15.1	18.4	38.0	111.0	
20	31.1	21.0	22.6	46.2	137.0	149.0( 22.2)
25	42.8	27.5	27.3	54.9	166.0	
33	64.0	38.8	35.2	71.0		91.7( 41.1)
42	90.4	53.4	45.5	94.9		
54	104.0( 46.4)	74.5	60.9	147.0		
70	127.0	79.8( 57.0)	69.0( 59.5)			
		105.0	89.2			

DIL AT MAX REAL  
 OR PERMITTED RISE 251.0( 61.6) 190.0( 76.4) 160.0( 80.1) 170.0( 56.8) 238.0( 32.7) 807.0( 7.5)



TABLE 94

DIFFUSER PLUME DILUTION  
 PORT SPACING = 1000 DIAMETERS, STABILITY STRATIFICATION PARAMETER = 10000  
 CURRENT TO EFFLUENT RATIO = 0.02

RISE(DIA)	DENSIMETRIC FROUDE NUMBER					
	1	3	10	30	100	1000
1	1.9	2.7	5.5	11.9	30.5	249.0
2	2.7	3.6	7.1	15.3	40.8	347.0
3	3.6	4.3	8.2	18.0	48.8	421.0
4	4.6	5.1	9.3	20.2	55.3	487.0
5	5.7	5.9	10.1	22.2	60.9	545.0
7	8.1	7.5	11.9	25.4	71.4	644.0
9	10.9	9.2	13.5	28.6	80.9	735.0
12	15.6	12.0	15.9	33.1	94.9	
15	21.0	15.2	18.4	37.5	108.0	
20	31.3	21.0	22.6	45.2	131.0	
25	43.4	27.5	27.1	53.4	156.0	
33	65.3	39.4	35.2	67.6	199.0	
42	94.3	54.5	45.2	86.1	252.0	
54	138.0	77.6	60.1	115.0	334.0	
70	204.0	112.0	83.2	165.0	466.0	
90	295.0	162.0	118.0	257.0		
115	292.0(87.2)	216.0(110.0)	171.0	461.0	347.0(55.8)	
148		229.0	193.0(124.0)	293.0		

AT MAX REAL  
 PERMITTED RISE 384.0(110.0) 337.0(144.0) 470.0(158.0) 467.0(116.0) 478.0( 71.3) 807.0( 10.7)

TABLE 95

DIFFUSER PLUME DILUTION  
 PORT SPACING = 1000 DIAMETERS, STABILITY STRATIFICATION PARAMETER = INFINITE  
 CURRENT TO EFFLUENT RATIO = 0.02

RISE(DIA)	DENSIMETRIC FROUDE NUMBER					
	1	3	10	30	100	1000
1	1.9	2.7	5.5	11.9	30.5	249.0
2	2.7	3.6	7.1	15.3	40.8	347.0
3	3.6	4.3	8.2	18.0	48.5	421.0
4	4.6	5.1	9.3	20.2	55.3	484.0
5	5.7	5.9	10.1	22.2	60.9	539.0
7	8.1	7.5	11.9	25.4	71.4	632.0
9	10.9	9.2	13.5	28.6	80.9	712.0
12	15.7	12.0	15.9	33.1	94.3	
15	21.0	15.2	18.2	37.5	108.0	
20	31.3	21.1	22.6	45.2	131.0	
25	43.4	27.7	27.1	53.0	154.0	
33	65.7	39.4	35.0	66.7	195.0	
42	94.9	54.9	45.2	84.4	245.0	
54	140.0	78.2	60.1	111.0	320.0	
70	211.0	114.0	83.2	154.0	435.0	
90	316.0	167.0	117.0	221.0		
115	468.0	243.0	166.0	328.0		
148		360.0	247.0	512.0		
190			371.0			

DIL AT MAX REAL  
 OR PERMITTED RISE 570.0(130.0) 486.0(179.0) 460.0(216.0) 565.0(156.0) 598.0( 89.6) 807.0( 11.7)

TABLE 96

DIFFUSER PLUME DILUTION  
 PORT SPACING = 1000 DIAMETERS, STABILITY STRATIFICATION PARAMETER = 200  
 CURRENT TO EFFLUENT RATIO = 0.00

RISE (DIA)	DENSIMETRIC FROUDE NUMBER					
	1	3	10	30	100	1000
1	1.9	2.7	5.3	10.6	23.6	111.0 144.0( 2.0)
2	2.7	3.5	6.7	13.5	29.8	146.0
3	3.6	4.3	7.8	15.5	34.5	187.0
4	4.6	5.0	8.7	17.1	38.6	
5	5.7	5.8	9.6	18.6	41.9 45.5( 6.1)	
7	8.1	7.4	11.2	21.3	48.8	
9	10.8	9.1	12.7	23.7 26.0( 11.0)	56.9	
12	15.2	11.8	14.9	27.3		
15	20.3 24.8( 17.7)	14.7 19.6( 19.8)	17.3 18.5( 16.8)	30.9		
20	28.8	19.8	21.0			
25		24.9	25.0			

DIL. AT MAX REAL OR PERMITTED RISE 34.9( 24.0) 27.5( 27.8) 26.1( 25.6) 36.6( 17.3) 64.3( 9.8) 203.0( 3.1)

TABLE 97

DIFFUSER PLUME DILUTION  
 PORT SPACING = 1000 DIAMETERS, STABILITY STRATIFICATION PARAMETER = 500  
 CURRENT TO EFFLUENT RATIO = 0.00

RISE(DIA)	DENSIMETRIC FROUDE NUMBER					
	1	3	10	30	100	1000
1	1.9	2.7	5.3	10.6	23.6	110.0
2	2.7	3.5	6.7	13.4	29.6	140.0
3	3.6	4.3	7.7	15.5	34.0	163.0 181.0( 3.9)
4	4.6	5.0	8.7	17.0	37.8	185.0
5	5.7	5.8	9.5	18.5	40.8	206.0
7	8.1	7.4	11.2	21.0	46.2	
9	10.9	9.1	12.6	23.1	50.9 57.6( 12.1)	
12	15.5	11.9	14.9	26.2		
15	20.7	14.9	17.1	28.8	64.4	
20	30.5	20.5	21.0	33.3 34.3( 21.3)		
25	41.1 43.7( 26.2)	26.5 33.8( 30.9)	24.8 28.4( 29.7)	37.8		
33	58.0	36.8	31.1	46.7		
42		47.0	38.1			

DTL AT MAX REAL OR PERMITTED RISE 61.6( 35.3) 47.5( 42.6) 40.0( 43.9) 48.2( 33.3) 81.1( 19.4) 255.0( 6.2)

TABLE 98

DIFFUSER PLUME DILUTION  
 PORT SPACING = 1000 DIAMETERS, STABILITY STRATIFICATION PARAMETER = 2000  
 CURRENT TO EFFLUENT RATIO = 0.00

RISE (DIA)	DENSIMETRIC FROUDE NUMBER					
	1	3	10	30	100	1000
1	1.9	2.7	5.3	10.6	23.4	109.0
2	2.7	3.5	6.7	13.4	29.6	138.0
3	3.6	4.3	7.7	15.3	34.0	159.0
4	4.6	5.0	8.7	17.0	37.5	175.0
5	5.7	5.8	9.5	18.4	40.5	190.0
7	8.1	7.4	11.1	20.8	45.2	213.0
9	10.9	9.1	12.6	22.9	49.5	236.0 255.0( 10.8)
12	15.6	12.0	14.8	25.8	54.9	267.0
15	21.0	15.0	17.1	28.4	59.7	302.0
20	31.1	20.8	21.0	32.4	66.6	
25	42.8	27.1	25.1	36.2	73.1	
33	64.0	38.6	31.8	42.2	82.8 83.6( 33.8)	
42	90.4 104.0( 46.4)	53.0	40.2	49.1 57.8( 54.1)	93.8	
54	127.0	74.0 79.3( 57.3)	52.0 60.9( 63.3)			
70		102.0	68.1	69.8		

DIL AT MAX REAL  
 OP PERMITTED RISE 146.0( 61.7) 111.0( 77.3) 85.8( 89.6) 81.5( 82.4) 117.0( 53.7) 359.0( 17.4)

TABLE 99

DIFFUSER PLUME DILUTION  
 PORT SPACING = 1000 DIAMETERS, STABILITY STRATIFICATION PARAMETER = 10000  
 CURRENT TO EFFLUENT RATIO = 0.00

RISE(DIA)	DENSIMETRIC FROUDE NUMBER					
	1	3	10	30	100	1000
1	1.9	2.7	5.3	10.6	23.4	109.0
2	2.7	3.5	6.7	13.4	29.6	137.0
3	3.6	4.3	7.7	15.3	33.8	157.0
4	4.6	5.0	8.7	17.0	37.2	173.0
5	5.7	5.8	9.5	18.4	40.2	186.0
7	8.1	7.4	11.1	20.8	45.2	208.0
9	10.9	9.1	12.6	22.9	49.1	228.0
12	15.6	12.0	14.8	25.6	54.5	251.0
15	21.0	15.0	17.1	28.2	58.8	272.0
20	31.3	20.8	21.0	32.2	65.7	302.0
25	43.4	27.3	25.1	36.0	71.2	328.0
33	65.3	39.1	32.0	41.9	79.3	367.0 381.0( 36.0)
42	94.3	54.2	40.5	48.8	88.0	
54	138.0	76.6	53.0	58.0	98.3	
70	204.0 282.0( 87.3)	111.0	71.4	70.4	112.0	
90	295.0	160.0 215.0(111.0)	96.8	87.0	127.0 139.0(106.0)	
115		228.0	131.0 160.0(135.0)	109.0 130.0(130.0)	147.0	
148			179.0	138.0	173.0	
190				174.0		

DIL AT MAX PEAL  
 OR PERMITTED RISE 381.0(110.0) 298.0(145.0) 225.0(184.0) 183.0(201.0) 187.0(162.0) 407.0( 41.5)

TABLE 100

DIFFUSER PLUME DILUTION  
 PORT SPACING = 1000 DIAMETERS, STABILITY STRATIFICATION PARAMETER = INFINITE  
 CURRENT TO EFFLUENT RATIO = 0.00

RISE(DIA)	DENSIMETRIC FROUDE NUMBER					
	1	3	10	30	100	1000
1	1.9	2.7	5.3	10.6	23.4	108.0
2	2.7	3.5	6.7	13.4	29.6	137.0
3	3.6	4.3	7.7	15.3	33.8	156.0
4	4.6	5.0	8.7	17.0	37.2	172.0
5	5.7	5.8	9.5	18.4	40.2	186.0
7	8.1	7.4	11.1	20.8	45.2	208.0
9	10.9	9.1	12.6	22.9	49.1	226.0
12	15.7	12.0	14.8	25.6	54.1	248.0
15	21.0	15.0	17.1	28.2	58.8	268.0
20	31.3	20.8	21.0	32.2	65.3	295.0
25	43.4	27.3	25.1	36.0	70.8	318.0
33	65.7	39.1	32.0	41.9	79.1	348.0
42	94.9	54.1	40.8	48.8	87.2	378.0
54	140.0	77.6	53.4	58.0	97.3	
70	211.0	114.0	71.9	70.5	110.0	
90	315.0	165.0	99.0	87.5	125.0	
115	468.0	242.0	136.0	111.0	143.0	
148		357.0	193.0	144.0	168.0	
190			276.0	191.0	200.0	
244			400.0	259.0	244.0	

DIL AT MAX REAL  
 OR PERMITTED RISE 569.0(130.0) 485.0(180.0) 402.0(245.0) 329.0(294.0) 248.0(250.0) 407.0( 52.5)

*Handwritten signature and date*

**Blank Page**



